Process Metallurgy 7B

SOLVENT EXTRACTION 1990

Part B

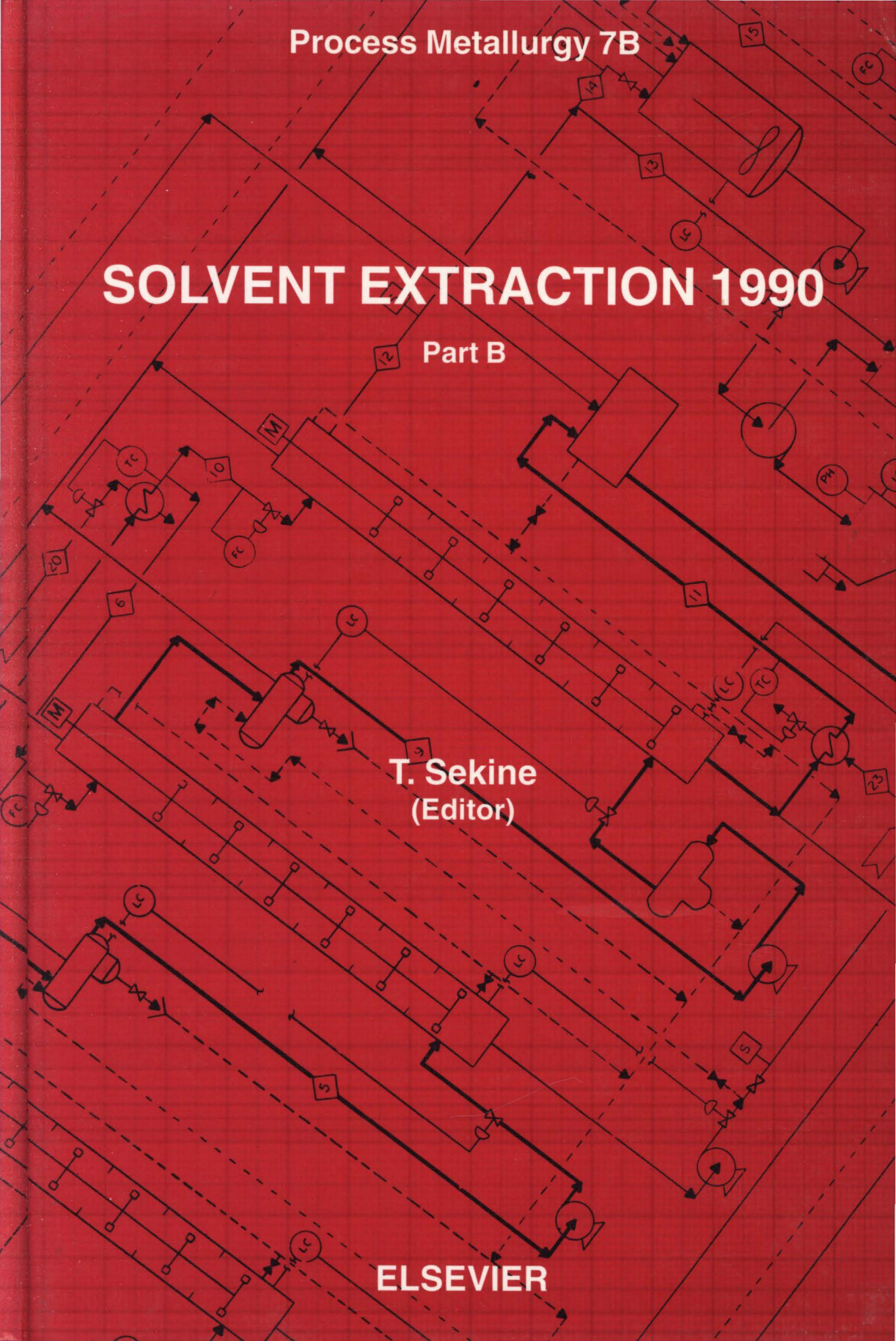

T. Sekine
(Editor)

ELSEVIER

Process Metallurgy 7B

SOLVENT EXTRACTION 1990

Process Metallurgy
Advisory Editor: G.M. Ritcey

1
G.M. RITCEY and A.W. ASHBROOK
Solvent Extraction: Principles and Applications to Process Metallurgy, Part I and Part II

2
P.A. WRIGHT
Extractive Metallurgy of Tin (Second, completely revised edition)

3
I.H. WARREN (Editor)
Application of Polarization Measurements in the Control of Metal Deposition

4
R.W. LAWRENCE, R.M.R. BRANION and H.G. EBNER (Editors)
Fundamental and Applied Biohydrometallurgy

5
A.E. TORMA and I.H. GUNDILER (Editors)
Precious and Rare Metal Technologies

6
G.M. RITCEY
Tailings Management

7
T. SEKINE (Editor)
Solvent Extraction 1990, Part A and Part B

Process Metallurgy 7B

SOLVENT EXTRACTION 1990

PROCEEDINGS OF THE INTERNATIONAL SOLVENT EXTRACTION CONFERENCE (ISEC '90)

PART B

Edited by

T. SEKINE

Department of Chemistry, Science University of Tokyo, 1-3 Kagurazaka, Shinjuku-ku, Tokyo, Japan

Assisted by

S. KUSAKABE
Department of Chemistry, Science University of Tokyo, 1-3 Kagurazaka, Shinjuku-ku, Tokyo, Japan

ELSEVIER
Amsterdam — London — New York — Tokyo 1992

ELSEVIER SCIENCE PUBLISHERS B.V.
Sara Burgerhartstraat 25
P.O. Box 211, 1000 AE Amsterdam, Netherlands

Distributors for the United States and Canada:

ELSEVIER SCIENCE PUBLISHING COMPANY INC.
655, Avenue of the Americas
New York, NY 10010, U.S.A.

Library of Congress Cataloging-in-Publication Data

International Solvent Extraction Conference (1990 : Kyoto, Japan)
Solvent extraction 1990 : proceedings of the International Solvent Extraction Conference (ISEC '90) / edited by T. Sekine, assisted by S. Kusakabe.
p. cm. -- (Process metallurgy ; 7)
Includes bibiographical references and index.
ISBN 0-444-88677-X (part A) (sold as 2 v. set only)
1. Solvent extraction--Congresses. I. Sekine, Tatsuya, 1932- II. Kusakabe, S. (Satoshi), 1941- . III. Title. IV. Series.
TP156.E8I518 1990
660'.284248--dc20 91-26291
CIP

ISBN 0-444-88677-X (A+B)

© 1992 Elsevier Science Publishers B.V. All rights reserved

No part of this publication may be reproduced, stored in a retrieval system or transmitted in any form or by any means, electronic, mechanical, photocopying, recording or otherwise, without the prior written permission of the Publisher, Elsevier Science Publishers B.V., Permissions Department, P.O. Box 521, 1000 AM Amsterdam, Netherlands.

Special regulations for readers in the USA – This publication has been registered with the Copyright Clearance Center Inc. (CCC), Salem, Massachusetts. Information can be obtained from the CCC about conditions under which photocopies of parts of this publication may be made in the USA. All other copyright questions, including photocopying outside of the USA, should be referred to the Publisher.

No responsibility is assumed by the Publisher for any injury and/or damage to persons or property as a matter of products liability, negligence or otherwise, or from any use or operation of any methods, products, instructions or ideas contained in the material herein.

This book is printed on acid-free paper.

Printed in The Netherlands

CONTENTS

PART A

Preface

Introduction

Organization of Conference

List of Sponsors

Papers

Plenary Lectures 1

1. Fundamentals of Solvent Extraction 61

2. Extractants and Diluents 297

3. Analytical Chemistry and Environmental Science 441

4. Nuclear Fuel Cycles 539

5. Kinetics and Interfacial Phenomena 765

6. Metal Extraction (Precious and Rare Metals) 883

PART B

7. Hydrometallurgy 1099

8. Simulation, Modelling and Control 1223

9. Equipment and Equipment Design 1313

10. Liquid Membranes 1459

11. Supercritical and New Extraction Systems 1661

12. Special Applications: Petrochemicals, Biotechnology 1737

Author Index 1917

PART A

Plenary Lectures

Solvent extraction and membrane processes in the treatment of metalliferous effluents and wastes
FLETT,D.S. 1

Liquid-liquid extraction for protein separations
HATTON,T.A. 23

Emulsion liquid membranes for waste water treatment
DRAXLER,J.;MARR,R. 37

Analytical separations based on ion-pair extraction principle - design of reagents and systems
YOTSUYANAGI,T. 49

1. Fundamentals of Solvent Extraction

Solvation and hydration in solvent extraction
CHOPPIN,G.R. 61

Role of the interface in solvent extraction processes
FREISER,H. 69

Model interfacial system for solvent extraction studies
ZHOU,NAI-FU;NEUMAN,R.D. 75

Effects of temperature on the solvent extraction of divalent metal complexes with 8-quinolinol and its derivatives
YAMADA,E.;NAKAYAMA,E. 81

Extraction of europium(III) by triphenylarsine oxide mixed with some related chelating agents in benzene from nitrate medium
ALY,H.F.;KHALIFA,S.M.;ZAKAREIA,N.;NOFAL,M. 87

Carboxylic acids as synergists in lanthanoid(III) extraction with β-diketones
HASEGAWA,Y.;YAMADA,Y.;WATANABE,T.;IKEUCHI,H.;TOMINAGA,T. 93

New approach to description of complex formation in solvent extraction systems; solvation and hydration contributions into extraction constant
ROZEN,A.M. 99

Extraction of rare earths by naphthenic acid and structure of the extracted complex
HUANG,CHUN-HUI;LIU,HE-PING;LI,BIAO-GUO;XU,GUANG-XIAN 105

Solvent extraction equilibrium of cadmium(II) bromide complexes with 4-methyl-2-pentanone in the presence of tetrabutylammonium ions
MURAI,R.;NAKAYAMA,H.;OHYAMA,Y.;SEKINE,T. 111

Equilibria in the $Ni(NO_3)_2$-LIX63/n-hexane extraction system
SAVASTANO,C.A.;PEREZ DE ORTIZ,E.S.;OSSEO-ASARE,K. 117

Thermodynamic study on the solvent extraction of perchlorates of uni-charged cation with trioctylphosphine oxide in hexane
KUSAKABE,S.;ABE,S.;SEKINE,T. 123

Fluid dynamics of pulsed sieve-plate extraction columns
LORENZ,M.;VOGELPOHL,A. 129

On the mechanism of cobalt extraction from chloride solutions using tri-iso-octylammonium chloride
NOIROT,P.A.;SAOUD,M.;DEBREUILLE-GRESSE,M.F.;WOZNIAK,M. 135

Solubility of fatty acid methyl esters in water
KATO,S.;MATSUDA,M.;NAGAHAMA,K. 141

Extraction of divalent metals with mono(2,4,4-trimethylpentyl) phosphinic acid
MARTINEZ,M.;MIRALLES,N.;SASTRE,A.;HERRANZ,C. 147

Substituent effects on dimerization of copper(II) carboxylates in extraction of copper(II) with mono-substituted benzoic acids
YAMADA,H.;MIZUTA,M. 153

Preparation and characterization of macroporus resins impregnated with organophosphorous compounds
CORTINA,J.L.;MIRALLES,N.;AGUILAR,M.;SASTRE,A. 159

Comparison of aggregates formed by acidic organophosphorus extractants and metals (Ni and Co) in solvent extraction
ZHOU,NAI-FU;WU,JINGUANG;SARATHY,P.K.;LIU,FUAN;NEUMAN,R.D. 165

Comparison between liquid-liquid extraction and impregnated resin systems. The extraction of Au(III) from chloride media by tri-n-dodecylammonium chloride
VILLAESCUSA,I.;AGUILAR,M.;DE PABLO,J.;VALIENTE,M.;SALVADÓ,V. 171

Solvent extraction of phosphorous acid from plating bath solution
MISHIMA,K.;NAGATANI,M.;ARAI,Y. 177

Neptunium(VII) extraction from alkaline media
ROZEN,A.M.;NIKIFOROV,A.S.;KARTASHEVA,N.A.;NIKOLOTOVA,Z.J.;
TANANAEV,J.G. 183

Solution structure of synergistic lanthanoid dibutylphosphate complexes
TAKAHASHI,T.;SUZUKI,Y.;YAMASAKI,A. 189

W/o microemulsions formed by acidic extractants and effect of lanthanides
WU,JINGUANG;LIU,FUAN;YU,ZHI-JIAN;ZHOU,NAI-FU;NEUMAN,R.D. 195

Extraction of nickel from nitrate media with di(2-ethylhexyl) phosphoric acid under high loading conditions
PARK,SANG JOON;NEUMAN,R.D. 201

Extraction of mono and polynuclear complexes of zinc(II) with di(2-ethylhexyl)phosphoric acid
KUNZMANN,M.W.;KOLARIK,Z. 207

Difference in mechanism of solvent extraction of iron(III) and chromium(III) with several β-diketones into 4-methyl-2-pentanone
INABA,K.;SEKINE,T. 213

Diluent influence on the extraction of divalent cobalt by thenoyltrifluoroacetone, dibenzo-18-crown-6 and their mixtures from perchlorate aqueous medium
KHALIFA,S.M.;SHEHATA,F.;ALY,H.F. 219

Study of solvent extraction process by ion-transfer polarography at the liquid/liquid interface
YOSHIDA,Z.;AOYAGI,H.;TACHIKAWA,E.;KIHARA,S. 225

Ion transfer of some metal ions across the liquid-liquid interface facilitated by ion carrier compounds
MASUDA,Y.;KATANO,H.;SEKIDO,E. 231

Polyenergetic conjugation of kinetic factors in synergistic solvent extraction processes
MEHANDJIEV,M.R.;MEHANDJIEV,M.M. 237

Extraction of 12-tungstatosilicic acid and 12-tungstatophosphoric acid by petroleum sulfoxide
LI,DA-REN;SU,YUAN-FU 243

Extraction of europium(III) by 8-hydroxyquinoline and some related amines in chloroform from nitrate medium
KHALIFA,S.M.;ALY,H.F.;EL-DESSOUKY,S. 249

New method of electrolyte activity coefficient determination from extraction data
VLASOV,V.S.;ROZEN,A.M. 255

Investigation of uranyl and thorium nitrate complex formation with TBP by high resolution NMR method
ROZEN,A.M.;NIKIFOROV,A.S.;KARTASHEVA,N.A.;NEUMOEV,N.V.;
MARKOV,V.S.;YUSHMANOV,V.E.;SHKARIN,P.YU. 261

Mass transfer on freely suspended single droplets measured by scintillation quenching and single-photon counting-technique
RHEIN,H.B.;STENNS,M.;SCHÜGERL,K. 267

Investigation on the extraction behavior of carboxyl crown ethers for uranyl ions
ZHU,LIN;CHEN,SHAO-JIN;LIU,ZHONG-QUN;CHEN,WEN-JUN 273

Polymerization and solvation of rare-earth di-(2-ethylhexyl) phosphates
TRIFONOV,YU.I.;LEGIN,E.K.;SUGLOBOV,D.N. 279

The influence of extractants and diluents on the extraction of actinoids in the systems with high content of uranyl nitrate
ZILBERMAN,B.YA.;FEDOROV,YU.S. 285

Thermodynamic aspects of changes in electron-donor ability of halogenacetate-ions and extraction equilibria
BALUEV,A.V. 291

2. Extractants and Diluents

New extractants for the nuclear hydro-metallurgy
MUSIKAS,C. 297

Adduct formation properties of some polydentate phosphine oxides in the synergistic extraction of metals with 4-acyl-5-pyrazolone derivatives
UMETANI,S.;KIHARA,S.;MATSUI,M. 309

Extraction and separation of metal ions with n-alkylcarbonyl-n-phenylhydroxylamines
HARAGUCHI,K.;OGATA,T.;NAKAGAWA,K.;YAMAZAKI,Y.;SAITOH,T.;KAMIDATE,T.;WATANABE,H. 315

Rational design of organic solvent extractants
YUAN,CHENGYE;LI,SHUSEN;YUAN,SHENGANG;HU,W.H. 321

Experimental study of the influence of diluent characteristics on performance in metal extraction
YOUNG,J.W.;FAWDRY,G.P.;BOSMAN,R.J. 327

New aspects in extraction by acid-base couple extractants
EYAL,A.M.;ARBEL-HADDAD,M.;BRESSLER,E. 333

Effect of temperature and acidity on various phosphorus containing extractants
BEYAD,M.H.;LYMAN,D.E.;ZARNEGAR,B.M. 339

Extraction of anionic metal complexes and organic anions by use of dicationic anion-exchange extractants
OHKI,A.;TAKAGI,M.;MAEDA,S. 345

Solvent extraction of mercury(II) with novel types of sulfur-containing extractants
BABA,Y.;INOUE,K.;YOSHIZUKA,K.;YASUKAWA,R.;TAZAKI,M. 351

TUCS: a new class of aqueous complexing agents for use in solvent extraction processes
HORWITZ,E.P.;DIAMOND,H.;GATRONE,R.C.;NASH,K.L.;RICKERT,P.G. 357

Solvent extraction of aqueous metal picrates with (3m+n)-crown-m (m=4-12, n=0-4) and the related glymes
OUCHI,M.;INOUE,Y.;LIU,YU.;HAKUSHI,T. 363

The solvent extraction of some divalent transition metals with n-pentafluorobenzoylphenylhydroxylamine
FUJINAGA,K. 369

Studies on the structural analysis of components of petroleum sulfoxides
LONG,TIWU;GU,GUOBANG;WU,QUIZHI;LI,YANLI 375

Performance of two new nil aromatic diluents in the recovery of copper, uranium and rare earths
SHELLEY,P.;QUAN,C. 381

Influence of diluents on extraction of fluorine from wet phosphoric acid with trioctylamine
TIAN,HENG-SHUI;WANG,XIANG-TIAN;SU,YUAN-FU 387

Effect of nitric acid on tributylphosphate hydrolysis
SINEGRIBOVA,O.A.;LANIN,V.P.;CHIKIRDA,N.M.;SAVIN,A.V. 393

Evaluation of index on degradation degree of Purex solvent
AOSE,S.;ICHIGE,Y.;OKAMOTO,F.;TOGASHI,A.;HAYASHI,S. 399

Lanthanoide extraction by organophosphoric acid in various organic solvents
IMAI,M.;SAEKI,N.;URUSHIYAMA,S.;SHIMIZU,M. 405

Extraction of pentavalent vanadium from acid solutions by n-decanol: dilution studies
RAKIB,M.;STAMBOULI,M.;DURAND,G.;CHESNE,A. 411

Advance in actinides separations by solvent extraction. Research and applications
MUSIKAS,C.;CONDAMINES,N.;CUILLERDIER,C. 417

Two synergic pairs for the extraction of ammoniacal Ni
PENNER,L.R.;RUSSEL,J.H.;CAMPBELL,M.J. 423

Extraction of lower carboxylic acids from aqueous solution by tri-n-octylamine with diluents
CHEN,FUMING;TANAKA,H.;NAKA,Y.;O'SHIMA,E. 429

A new liquid phosphine oxide for the recovery of acetic acid from sulfite pulping liquors
PFÜLLER,P. 435

3. Analytical Chemistry and Environmental Science

Factors affecting selectivity of synergistic extraction
AKAIWA,H. 441

Multistage liquid-liquid extraction separation of inorganic ions using a planet centrifuge
SPIVAKOV,B.YA.;MARYUTINA,T.A.;ZOLOTOV,YU.A. 451

Preconcentration and determination of a trace amount of lithium in water as its thenoyltrifluoroacetone complex with tributyl phosphate by means of solvent extraction and flame photometry
OOKA,N.;HONJO,T.;TERADA,K. 457

Extraction-spectrophotometric determination of copper(II) with thiophenealdehyde-4-phenyl-3-thiosemicarbazone
NISHIOKA,H.;MIKI,R.;UESUGI,K. 463

Solvent extraction separation of thorium, uranium(VI), zirconium and hafnium with crown ethers
DEORKAR,N.V.;KHOPKAR,S.M. 467

Hydrolysis studies of Tm using solvent extraction techniques
ENGKVIST,I.;ALBINSSON,Y.;MIN,YI 473

Extractive recovery of p-nitrophenol from its mother liquor and recirculation to production
TETZLAFF,H.;RITTNER,S. 479

Solvent extraction of molybdenum(VI)-catechol derivative chelates with and without malachite green
MOTOMIZU,S.;OSHIMA,M.;MAEDA,Y. 485

SISAK - a solvent extraction technique for nuclear and chemical studies of exotic radionuclides
SKARNEMARK,G.;SKÅLBERG,M.;ALSTAD,J.;BAUER,G.;HABERBERGER,F.;
KAFFRELL,N.;ROGOWSKI,J.;TRAUTMANN,N. 491

Application of laser induced photoacoustic spectroscopy system to the determination of transuranic elements
KIHARA,T.;FUJINE,S.;MATSUI,T.;KITAMORI,T.;MAEDA,M.;
SAKAGAMI,M. 497

A structural consideration of ionic species and solvents for ion-pair extraction
KASAHARA,I.;TAGUCHI,S.;GOTO,K. 503

Determination of gold in environmental samples by using extraction methods
DMITRIEV,S.N.;SHISHKINA,T.V.;ZHURAVLEVA,E.L.;SHISHKIN,S.V.;
GERBISH,SH. 509

Liquid-liquid distribution of Cu(II), at trace level, between aqueous and organic solutions containing MIAMP
PEREZ TRUJILLO,J.P.;BORGES,T.M.;ARIAS,J.J.;VALIENTE,M. 515

Solvent extraction separation of alkaline earth metal ions in sodium perchlorate media at various temperatures
KOMATSU,Y. 521

Correlation and prognosing the distribution coefficients of phenol compounds in different extractive systems
KORENMAN,JA.I.;SELMANCHUK,N.N.;KRJUKOV,A.I.;DANILOV,V.N.; SUKHANOV,P.T.;ERMOLAJEVA,T.N.;TALDYKINA,S.N. 527

Extraction of dithiocarboxylates of platinum metals
MEŽARAUPS,G.;JANSONS,E.;GARNAKA,Z. 533

4. Nuclear Fuel Cycles

The use of solvent extraction in the nuclear fuel cycle, forty years of progress
CHESNE,A.;GERMAIN,M. 539

The development of a three-cycle chemical flowsheet to reprocess oxide nuclear fuel
DENNISS,I.S.;PHILLIPS,C. 549

Progress in the development of a one-cycle Purex process (Impurex)
PETRICH,G.;BLEYL,H.-J.;ERTEL,D.;GALLA,U.;GOLDACKER,H.;RÖMER,J.; SCHMIEDER,H.;SCHÖN,J. 555

Behaviour of technetium in the extraction with tributyl phosphate in the Purex process
KOLARIK,Z.;PETRICH,G.;BLEYL,H.-J. 561

Development of a centrifugal contactor
TAKEDA,H.;KAWATA,T.;UEDA,S.;SHIMIZU,R.;NEMOTO,S.;HAYASHI,S. 567

Electrochemical operations in extractive separation of uranium and plutonium in centrifugal contactors
RENARD,E.V.;PAVLOVICH,V.B.;SHKLYAR,L.I.;NEUMOEV,N.V.; NEROSIN,N.A.;SMETANIN,E.YA.;KOROTKOV,I.A.;GLASUNOV,N.V.; KLYGUIN,V.A.;ANISIMOV,V.I. 573

Characteristics and behaviour of interface sludges formed in the first extraction cycles of the Purex process
GUE,J.P.;PHILIPPE,M.;MASSON,M. 579

Separation of neptunium from high-level waste by extraction with diisodecyl phosphoric acid
MORITA,Y.;TANI,S.;KUBOTA,M. 585

Separation of actinides and lanthanides from nuclear power reactor fuel reprocessing waste solution by DHDECMP
ZHAO,HUGEN;FU,LICHUN;WEI,XIUFANG;LIU,SUYING;YE,GUOAN;YE,YUXING;
YANG,XUEXIAN;YANG,LIUCHENG;JIANG,JINCAI 591

A new reagent for uranium-plutonium partitioning
GERMAIN,M.;GILLET,B.;PASQUIOU,J.Y. 597

Application of salt-free technology to the Purex process for FBR fuel reprocessing
OZAWA,M.;TAMURA,N.;YAMAMOTO,R.;KAWATA,T.;HAYASHI,S. 603

Operating experience of centrifugal contactors used in a third plutonium purification cycle at the Marcoule Reprocessing Plant
BRESCHET,C.A.;DELAFONTAINE,G.L.;COSTE,J.A. 609

Extraction dynamics of pulsed column in the Purex process
HONMA,S.;KOGA,J.;MATSUMOTO,S. 615

Impurity carry-over in liquid-liquid extraction contactors
JENKINS,J.A.;ARM,S.T.;MYERS,P.E.;PARTRIDGE,B.A. 621

Axial temperature profiles in a pulsed column for Purex process
TSUKADA,T.;TAKAHASHI,K.;YOKOYAMA,H. 627

U/Pu separation in the Purex process: experimental comparision of different procedures
GALLA,U.;SCHÖN,J.;SCHMIEDER,H. 633

Development of electro-reduction pulse column
YAMAMOTO,T.;NEMOTO,S.;TAKEDA,H.;HAYASHI,S. 639

Electrochemical reduction of uranium in organic and aqueous mixed phases
KIM,KWANG-WOOK;SHIN,YOUNG-JOON;YOO,JAE-HYUNG;PARK,HYUN-SOO;
KIM,J.D. 645

Scrubbing effect of tritium and ruthenium from irradiated organic solvent
FUJINE,S.;UCHIYAMA,G.;MAEDA,M.;BAUTZ,H.;STIEGLITZ,L. 651

Results of ^{106}Ru and ^{95}Zr decontamination studies in the co-decontamination cycle of the Tokai Reprocessing Plant
YAMANA,H.;OMORI,E.;MIURA,N.;KOMATSU,H. 657

Interphase mass transfer coefficient of neptunyl ion in the Purex system
SUYITNO;FUJINE,S.;MAEDA,M.;FUMOTO,H.;SUZUKI,A. 663

Study of the complexes of Np(V) with some organic ligands by solvent extraction
TOCHIYAMA,O.;INOUE,Y.;NARITA,S. 669

Process study on neptunium separation using salt-free reductive reagent
UCHIYAMA,G.;HOTOKU,S.;KIHARA,T.;FUJINE,S.;MAEDA,M. 675

A study on the interfacial crud formation in the Purex process
IDEGAMI,A.;SUGAI,H.;TANAKA,C.;OZAWA,M.;KISHIMOTO,Y.;HAYAHSI,S. 681

Study on hydrodynamics of pulsed plate columns by computer code DYNAC
NABESHIMA,M.;TANAKA,C. 687

Reaction model for the extraction of uranium(VI) from nitric acid and hydrochloric acid solutions with bis(2-ethylhexyl) phosphoric acid
HUANG,CHING-TSVEN;SHIEH,MU-CHANG;HUANG,TING-CHIA 693

Study on accumulation of U(IV) in extraction-scrub culumns of 30 vol% TBP-n.dodecane-U(VI)-HNO_3 system
KUBO,N.;TACHIMORI,S.;USUDA,S.;AMI,N.;WAKAMATSU,S.;SATO,M. 699

Conceptual study for a computer-aided extraction-status diagnostic system for the Pu-U partition cycle of the Tokai Reprocessing Plant
IWABUCHI,H.;SASAKI,K.;KOYAMA,K.;YAMANA,H. 705

Separation of the actinides Pa, Th, U, Np and TPE including Md by extraction methods
GORSKI,B.;GLEISBERG,B.;NAM,N.T.P. 711

Application of centrifugal partition chromatography to separation of actinides and lanthanides in TBP extraction system
USUDA,S.;ABE,H.;TACHIMORI,S.;TAKEISHI,H.;MURAYAMA,W. 717

Applications of extraction chromatography in the bifunctional extractant-nitric acid system for separation of actinides in nuclear fuel cycle
KIMURA,T.;AKATSU,J. 723

Purification of uranium from zirconium using mixer-settler unit
EL-SOUROUGY,M.R.;IBRAHIM,A.;ALY,H.F. 729

Performance of the feed-rate control system for the uranous nitrate solution operated in Tokai Reprocessing Plant
WATAHIKI,M.;HIRANO,H.;YOSHINARI,T.;ONDA,N.;YAMANA,H. 735

The removal of thorium isotopes from a waste acidic liquor
ECCLES,H.;FAWCETT,P.;GREENWOOD,H.;RUSHTON,A. 741

Purex process improvements for the UP3 spent fuel reprocessing plant at la Hague, France
FOURNIER,W.;HUGELMANN,D.;DALVERNY,G.;BERNARD,C.;MIQUEL,P.; LEUDET,A. 747

Extractants for actinides
NIKIFOROV,A.S.;ROZEN,A.M. 753

The behavior of decomposition products of hydrazine in Purex process
ZILBERMAN,B.YA.;LELYUK,G.A.;MASHKIN,A.N.;FEDOROV,YU.S. 759

5. Kinetics and Interfacial Phenomena

Interfacial phenomena in extraction systems
SZYMANOWSKI,J. 765

Interfacial reaction in metal extraction with chelating agents
HARADA,M.;KISHIDA,M.;MIYAKE,Y. 777

Role of interface in the kinetics of synergic extraction of nickel(II)-dithizone-1,10-phenanthroline complex
WATARAI,H.;SASAKI,K.;TAKAHASHI,K. 783

Gallium/aluminum separation from sulfate solutions by solvent extraction using D2EHPA
MIHAYLOV,I.;DISTIN,P.A. 787

Studies on mechanism of extraction of iron(III) from sulfate solution and stripping with sulfuric acid by FT-IR and laser light scattering spectrometry I. HDEHP or RNH_2 as extractant with octane as diluent
LIU,HUIZHOU;YU,SHUQIU;CHEN,JIAYONG;WENG,SHIFU;WU,JINGUANG 793

On determination of rate processes in extraction from concentration measurements of diffusing species
KANKI,T.;ASANO,T.;TOMITA,A.;IGUCHI,T. 799

Extraction kinetics of holmium(III) and yttrium(III) with D2EHPA in membrane extractor using a hollow fiber
YOSHIZUKA,K.;SAKAMOTO,Y.;BABA,Y.;INOUE,K.;NAKASHIO,F. 805

A kinetic study on the extraction of erbium(III) from hydrochloric acid solutions with HEH/EHP
YUE,SANTANG;LI,DEQIAN 811

Equilibrium and kinetics of copper extraction from acidic sulphate solutions with 1-(2'-hydroxy-5'-nonylphenyl)-1-ethanone (e)-oxime and 1-(2'-hydroxy-5-methylphenyl)-1-decanone (e)-oxime
SZYMANOWSKI,J.;KRZYZANOWSKA,E.;CIERPISZEWSKI,R.;PROCHASKA,K. 817

Synergistic extraction of metal ion with LIX63 in microemulsion system
MIYAKE,Y.;NAKATA,Y.;SUZUKI,T.;TERAMOTO,M. 823

Extraction of palladium in aqueous hydrochloric acid solution with tri-n-octylamine in toluene
KAWANO,Y.;ODA,M.;YOSHIZUKA,K.;KONDO,K.;NAKASHIO,F. 829

Interfacial mass transfer on small drops
MAS,C.;FRANZ,G.;VON AMMON,R. 835

Effect of interfacial tension gradient on momentum and mass transfer through a moving interface of single drops
HIRATA,A.;NISHIZAWA,S.;OKANO,Y. 841

Two phase kinetics of the solubulization in reversed micelles
PLUCINSKI,P.;NITSCH,W. 847

Studies on mechanism of extraction of iron(III) from sulfate solutions and stripping with sulfuric acid by FT-IR and laser light scattering spectrometry II. HDEHP and RNH_2 as extractant with octane as diluent
LIU,HUIZHOU;YU,SHUQIU;CHEN,JIAYONG;WU,PEIQIANG;ZHOU,ZUKANG 853

A model for the rate of two phase nitration of some highly reactive aromatic hydrocarbons
SOHRABI,M. 859

A model for the mononitration of chlorobenzene in a liquid-liquid contactor
KAGHAZCHI,T. 865

Emulsion and accumulation at aqueous/organic interface of mixer-settlers
GONDA,K.;YASU,S. 871

Coalescence of an emulsion in a packed bed (I). Selecting the packed fibre
DAI,XING;SHI,YAJUN 877

6. Metal Extraction (Precious and Rare Metals)

Solvent extraction processes for the separation of the rare-earth metals
PRESTON,J.S.;DU PREEZ,A.C. 883

Solvent extraction of lanthanoid(III) with a macrocyclic crown ether and halogenated carboxylic acids
IMURA,H.;SAMI,T.M.;SUZUKI,N. 895

Stripping rare earth from its loaded di(2-ethylhexyl)-phosphate complex by oxalic acid
HUNG,TSUNG-MIN;HORNG,JIIN-SHIUNG;HOH,YING-CHU;LEE,CHAU-JEN 901

Studies on the extraction of ReO_4^- by use of crown ethers
JEWAD,S.K.;AL-MURAB,S.R.;JALHOOM,M.G. 907

Solvent extraction of mercury(II) from hydrochloric acid solutions
SATO,T.;ISHIKAWA,I.;SATO,K. 913

The pecularities of molybdenum(VI) and vanadium(V) extraction by lipophilic quaternary ammonium salts
BAL,Y.;COTE,G.;BAUER,D. 919

Synergistic extraction of rhodium with 2-mercaptobenzothiazole and tri-n-octylamine
HWANG,RAN;CHUNG,KOO-SOON 925

Solvent extraction of palladium(II) and platinum(IV) with amino- and amido-carboxylic acids
YOSHIZUKA,K.;BABA,Y.;INOUE,K.;WADA,F.;MATSUDA,T. 931

The separation of rare earth elements by the porous resin impregnated with 2-ethylhexyl hydrogen 2-ethylhexylphosphonate
WAKUI,Y.;MATSUNAGA,H.;SUZUKI,T.M. 937

Silver extraction from photographic fixing solutions
STENSTRÖM,S. 943

Mechanism of gallium extraction by tri-n-octylamine
ABISHEVA,Z.S.;BLAIDA,I.A.;PONOMAREVA,E.I.;KASYMOVA,A.S. 949

Rhenium extraction by tri-n-octylammonium hydrosulphate
ZAGORODNYAYA,A.N.;PONOMAREVA,E.I.;ABISHEVA,Z.S.;TARASOVA,E.G. 955

The high efficiency separation of iridium from rhodium by solvent extraction using a mono n-substituted amide
GRANT,R.A.;BURNHAM,R.F.;COLLARD,S. 961

Extraction of lanthanide ions with benzoyltrifluoroacetone-tri-n-butylphosphate:synergism and antagonism
D'OLIESLAGER,W.;SANNEN,L. 967

Extraction mechanism of Ga with 2-bromodecanoic acid
SHONO,A.;SATO,M.;IMAISHI,N.;HOZAWA,M. 973

Equilibrium and mechanism of extraction of gold, palladium and platinum by 2-hydroxy-4-sec.octyloxyl-benzophenoxime
MA,HENGLI;YUAN,CHENGYE 979

Extraction of titanium(IV) from hydrochloric acid solutions by acid organophosphorus compounds
SATO,T.;SATO,K. 985

Diluent effect on the heat change in solvent extraction of divalent copper, zinc and cadmium and uranium(VI) from hydrochloric acid solutions by high-molecular weight amines
SATO,T.;KUWAHARA,M.;SATO,K. 991

Extraction of lanthanum(III) and yttrium(III) from aqueous thiocyanate solutions by neutral organophosphorus compounds
SATO,T.;SATO,K. 997

Separation of neodymium from its concentrate using 20% saponified di-(2-ethylhexyl)phosphoric acid in kerosene as an extractant
THAKUR,N.V.;JAYAWANT,D.V.;KOPPIKER,K.S. 1003

Solvent extraction of palladium(II) from aqueous chloride media with LIX 63
DHASKALI,G.;PAREAU,D.;CHESNE,A.;DURAND,G. 1009

Separation and purification of vanadium and molybdenum by solvent extraction and subsequent reductive stripping
HIRAI,T.;KOMASAWA,I. 1015

Extraction of Sc, Y, and lanthanoids by quaternary ammonium salts
GORSKI,B.;GORSKI,N.;BEER,M. 1021

Extraction and separation of tungsten with 3-hydroxy-2-methyl-1-(4-tolyl)-4-pyridone
TAMHINA,B.;BRAJENOVIĆ,N. 1027

Extractions of precious metal ions with tris(2,6-di-methoxyphenyl)phosphine and its derivatives from hydrochloric acid solutions
MATSUSHITA,T.;YAMASHOJI,Y.;TANAKA,M.;SHONO,T. 1033

A study of the extraction kinetics of lanthanum(III) with primary amine N1923 sulfate
SUN,DUCHENG;LI,DEQIAN 1039

Synergic extraction of cadmium(II) from thiocyanide with primary amine N1923 and DBBP
LI,DEQIAN;ZI,XIAOHONG;WANG,ZHONGHUI;MA,GENXIANG 1045

Extraction of scandium(III) from nitrate-thiocyanate solutions with primary amine N1923
MA,GENXIANG;LI,DEQIAN 1051

Synergistic extraction of zinc thiocyanate with primary amine N1923 and TBP
MA,GENXIANG;GAO,LIJUAN;LI,DEQIAN 1057

Synergistic extraction of zinc(II) and cadmium(II) with di-(1-methylheptyl) methyl phosphonate and primary amine N1923
HAN,SHUMIN;MA,GENXIANG;LI,DEQIAN 1063

Problems in the separation of rare earths from HCl leached Monazite solution
RITCEY,G.M.;LEVINS,D.M. 1069

Extraction of rare earth elements with p-(1,1,3,3-tetramethylbutyl)phenyl 2-ethylhexyl phosphoric acid
MORI,K.;ADACHI,K.;KANEKO,T. 1075

Solvent extraction of rare-earth metals by carboxylic acids
DU PREEZ,A.C.;PRESTON,J.S. 1081

Solvent extraction of palladium by pyridine carboxylic esters
BURGESS,A.;DALTON,R.F. 1087

Solvent extraction separation of uranium(VI) with dibenzo-24-crown-8 from hydrochloric acid media
MOHITE,B.S.;PATIL,J.M. 1093

PART B

7. Hydrometallurgy

The production of high value particles in solvent extraction media
DEMOPOULOS,G.P. 1099

Solvent extraction separation of Nb and Ta at MHO: potentialities of Cyanex® 923 versus MIBK
HAESEBROEK,G.;VLIEGEN,J.;DE SCHEPPER,A. 1115

Metals recovery from a garbage incinerator
BART,H.-J.;DRAXLER,J.;MARR,R. 1121

Solvent extraction of silver from chloride solution by Cyanex 471X
ABE,Y.;FLETT,D.S. 1127

Application of liquid extraction to production of extra pure magnesium oxide
BUMBÁLEK,V.;HAMAN,J. 1133

Solvent extraction of arsenic from sodium tungstate solutions
SZILASSY,I.;VADASDI,K. 1139

Acorga CLX50 - a pyridine carboxylic ester based extractant for the solvent extraction of copper from chloride leach solutions
DALTON,R.F.;BURGESS,A. 1145

Mixed solvent extraction - annular chromatographic systems for f-element separation and purification
NAVRATIL,J.D.;MURPHY,A.;SUN,D. 1151

Application of Pitzer's equations to the analysis of extraction equilibria of Cu(II) from hydrochloric acid solutions with hydroxyoximes under practical conditions
TANAKA,M. 1157

New production method of metallic oxide and metal powders - application of solvent extraction technique
SANO,M.;SHIBATA,J.;NISHIMURA,S. 1163

Extraction of metal ions from mixed aqueous-organic media with liquid-liquid extraction and ion exchange resin
SHIBATA,J.;SANO,M.;NISHIMURA,S. 1169

Recovery of zinc and manganese from waste batteries by liquid-liquid extraction
STEINER,L.;XING,MIAOLIN;HARTLAND,S. 1175

Recovery and purification of iron from acidic high iron-bearing effuluent by solvent extraction with secondary amine
HO,KUNG-LIANG;CHIU,TAI-MING;HOH,YING-CHU 1181

Extraction of iron from chloride solutions by binary extractants (carboxylates of tertiary amines)
FLEITLICH,I.YU.;LUBOSHNIKOVA,K.S.;KHOL'KIN,A.I.;PASHKOV,G.L.; SERGEEV,V.V.;KULMUCHAMEDOV,G.K.;MÜHL,P.;GALANTSEVA,T.V.; ZELENTSOVA,L.V. 1187

On application of solvent extraction and chelating ion-exchange resin for purification of copper electrolytes
SHIBAYAMA,R.;NAGAI,T. 1193

Recovery of rare metals from coal fly ash
TSUBOI,I.;KASAI,S.;YAMAMOTO,T.;KOMASAWA,I.;KUNUGITA,E. 1199

Improvement of removing arsenic from copper electrolyte with solvent extraction
YANG,JIAOYONG;LIU,DAXING;ZHAN,HUIFANG;JIANG,KAIXI 1205

Solvent extraction of zinc from hypersaline brine
BYESEDA,J.J.;WARREN,K.W. 1211

Recovery of gallium from hydrochloric acid solutions by emulsion liquid membranes
KIRGIOS,J.;DEGENER,W.;SCHÜGERL,K. 1217

8. Simulation, Modelling and Control

Relative contribution of axial dispersion on the performance of liquid extraction columns
MIYAUCHI,T. 1223

How to fit a simulator to a real liquid-liquid extraction plant
GRINBAUM,B.;ANGEL,S.A. 1235

The simulation of interacting liquid-liquid dispersions
- a new algorithm and its potentiality
GUIMARÃES,M.M.L.;CRUZ-PINTO,J.J.C.;REGUEIRAS,P.F.R.;
MADUREIRA,C.M.N. 1241

Simulation and control of a multistage stirred cell column
extractor
KIROU,V.I.;TSOURIS,C.;TAVLARIDES,L.L. 1247

A study on the drop size distribution and the holdup in a
rotating impeller extraction column
LEE,YONG-KUK;KIM,CHUL 1253

Performance of extraction columns filled with regular packing
STEINER,L.;NEDUNGADI,K.;HARTLAND,S. 1259

The effects of mass transfer on drop breakage in rotating disc
contactors
CAUWENBERG,V.;MESSEMAEKERS,C.;VAN ROMPAY,P.;SLATER,M.J. 1265

Operation of a pulsed sieve-plate extraction column with
an extreme phase flow ratio
RAUSCHER,H.;BLASS,E. 1271

Application of kinetic models to contactor design
SAEED,M.T.;PEREZ DE ORTIZ,E.S. 1277

Operation and simulation of a liquid-liquid-extraction column
HUFNAGL,H.;BLASS,E.;KIENLE,A. 1283

An application of expert system techniques to the operation of
solvent extraction processes
MILLS,A.L.;HARRISON,J.W. 1289

Studies on dynamic process of three-outlet fractional
extraction in five-component system
LI,BIAO-GUO;GAO,SONG;YAN,CHUN-HUA;LI,HUI;XU,GUANG-XIAN 1295

Experimental determination of the residence time distribution
of the drop phase in a pulsed perforated plate extraction column
SCHMIDT,H.;PFEFF,M.;PRÖLL,TH.;MÜLLER,U. 1301

Mass transfer and drop size in liquid-liquid Cu extraction with LIX 84N in motionless mixers
WOLF,D.;SEMBIRA,A.;MERCHUK,J.C. 1307

9. Equipment and Equipment Design

Contacting and separation equipment-the electrical alternative
BAILES,P.J. 1313

Multiple upcomer aromatics extraction trays
RESETARITS,M.R.;YONEYAMA,K. 1327

Considerations for scaling up agitated extraction columns
KARR,A.E.;CUSACK,R.W. 1333

Apparatus selection and design in solvent extraction
BART,H.-J.;MARR,R. 1339

The hydrodynamic performance of pulsed perforated-plate columns
LOGSDAIL,D.H.;JENKINS,J.A.;ROBINSON,K.S. 1345

Axial mixing of liquid-liquid-solid system in open turbine rotating disc contactor (OTRDC)
CHEN,XIAO-XIANG;SU,YUAN-FU 1351

Interfacial area of liquid-liquid dispersion in a mixer-settler extraction column
TAKAHASHI,K.;TAKEUCHI,H. 1357

Mass transfer to freely moving drops
TEMOS,J.;PRATT,H.R.C.;STEVENS,G.W. 1363

Hydrodynamics and mass transfer of a sieve plate column for liquid-liquid extraction
ZHU,SHENLIN;YE,GUIQIN;KE,JIAXIONG;ZHANG,BAOQING;FEI,WEIYANG 1369

Hydrodynamic and mass transfer characteristics of a spray column with vertical parallel plate electrodes
YAMAGUCHI,M.;YOSHIYASU,S.;IMAI,T.;KUNIMASA,H.;KATAYAMA,T. 1375

Study on mass transfer characteristics in an annular pulsed sieve plate extraction column
QIN,WEI;DAI,YOUYUAN;LEI,XIA;WANG,JIADING 1381

The H-0.3 centrifuge for small-scale fast solvent extraction procedures
SKARNEMARK,G.;SKÅLBERG,M.;ALSTAD,J. 1387

Phase inversion in mixer settlers
GODFREY,J.C.;FRAUX,A.;REEVE,R.N. 1393

The design and performance of an extraction column with an adjustable working capacity
HABERLAND,K. 1399

Some experience on energy saving for a large Scheibel extraction column system
LO,T.C. 1405

Design factors affecting the performance of electrostatic coalescers
BAILES,P.J.;LARKAI,S.K.L. 1411

The electrodynamic contactor for extraction
WARREN,K.W.;BYESEDA,J.J. 1417

Criteria for the design of plate separators for the separation of droplets from liquids
ROMMEL,W.;BLASS,E. 1423

Laser transmission technique for hold-up measurements in agitated tank
ABID,K.H.;GODFREY,J.C. 1429

Formation of uniformly-sized emulsions by means of applied electrostatic field
SATO,M. 1435

Formation of single charged drops from a laminar liquid jet in electric fields
HIBIKI,T.;YAMAGUCHI,M.;KATAYAMA,T. 1441

Computer-assisted selection of equipment for liquid-liquid extraction
GOETTERT,W.;BLASS,E. 1447

Breakage and coalescence rates of droplets in Karr columns
FAN,ZHENG;WANG,DIANXIA;LI,XIMING 1453

10. Liquid Membranes

New surfactants for metal extraction by liquid surfactant membranes
NAKASHIO,F.;GOTO,M.;KONDO,K. 1459

Retardation of the transport of Eu(III) through supported di(2-ethylhexyl)phosphoric acid-kerosene liquid membrane
HUNG,TSUNG-MIN;LEE,CHAU-JEN 1469

Modelling and application of a pilot-scale supported liquid membrane unit for uranyl nitrate extraction
HOFMAN,D.L.;CRAIG,W.M.;SMIT,J.J. 1475

Recovery of uranium(VI) from wet process sulfuric acid by an emulsion-type liquid membrane technique
HIRATO,T.;KOYAMA,K.;AWAKURA,Y.;MAJIMA,H. 1481

Leakage suppressing of w/o emulsion using high viscous solvent
OKAZAKI,S.;IMAI,M.;SHIMIZU,M. 1487

Membrane extraction of actinides
MYASOYEDOV,B.F.;NOVIKOV,A.P.;MIKHEEVA,M.N. 1493

Transport of lanthanoids through liquid membranes containing D2EHPA as a carrier
HIRASHIMA,Y.;KOHRI,S.;ADACHI,G. 1499

Study of a palladium mass accelerate transfer through a solid supported liquid membrane containing Kelex100
ANTICÓ,E.;HIDALGO,M.;MASANA,A.;SALVADÓ,V.;MUÑOZ,M.;VALIENTE,M. 1505

A phosphine sulfide system for the solvent extraction and liquid membrane process of gold(III)
SALVADÓ,V.;HIDALGO,M.;MASANA,A.;MUÑOZ,M.;VALIENTE,M.;
MUHAMMED,M. 1511

Separation of alkali metal cations by polymer-supported liquid membranes using ionizable crown ethers
STRZELBICKI,J.;STRZELBICKA,B.;LUBBOCH,E.;BARTSCH,R.A. 1517

Crown ethers in separation of alkali metal cations
STRZELBICKI,J.;STRZELBICKA,B.;SCHÜGERL,K.;BARTSCH,R.A. 1523

Separation of cobalt and nickel ions with 2-ethylhexyl phosphonic acid mono-2-ethylhexyl ester dissolved in kerosene
HUANG,TING-CHIA;TSAI,TEH-HUA 1529

Supported liquid membranes for chromate recovery. Experimental study
ALONSO,A.I.;ORTIZ,M.I.;IRABIEN,A. 1535

Mathematical modelling of phenol recovery using supported liquid membranes
URTIAGA,A.M.;ORTIZ,M.I.;IRABIEN,A. 1539

Separation of cadmium from zinc in a chloride media by a supported liquid membrane
HOH,YING-CHU;LIN,CHUNG-YUN;HUNG,TSUNG-MIN;CHIU,TAI-MING 1543

FTIR-ATR and solvent extraction studies on potentiometric responses of neutral carrier type liquid membranes
SUGAWARA,M.;LIN,XIAO-MING;UMEZAWA,K.;SHRIADAH,M.M.A.;
NISHIZAWA,S.;UMEZAWA,Y. 1549

Potentiometric response of synergistic extractive liquid membranes
ITOH,Y.;AKAIWA,H.;SUGAWARA,M.;UMEZAWA,Y. 1555

Separation of rhenium and molybdenum by liquid surfactant membranes
STRZELBICKI,J.;DEGENER,W.;SCHÜGERL,K. 1561

Extraction of uranium from heap leaching solutions by liquid surfactant membranes
HARTMANN,D.;PAREAU,D.;CHESNE,A.;DURAND,G. 1567

Separation of gold from its hydrochloric solution with the liquid surfactant membranes
YAN,NIAN-XI;SHI,YAJUN;SU,YUAN-FU 1573

Recovery of chromium(VI) from sulfuric acid solution by liquid surfactant membrane
MORI,Y.;TANIGAKI,M.;EGUCHI,W.(THE LATE) 1579

Membrane behaviour in chromate recovery using emulsion liquid membranes
SALAZAR,E.;ORTIZ,M.I.;IRABIEN,A. 1585

Highly selective separation of organic solutes by aqueous liquid surfactant membranes
ULBRICH,M.;MARR,R.;DRAXLER,J. 1589

Newly developed way to improve separation selectivity in liquid membrane permeation for hydrocarbon separation
EGASHIRA,R.;KAWASAKI,J. 1595

Energy requirement for liquid membrane process to separate binary hydrocarbon mixtures
KAWASAKI,J.;PUAJINDANETR,S.;EGASHIRA,R. 1601

Modeling of mass transport with simultaneous diffusion and chemical reaction in liquid membrane systems
YOO,JAE-HYUNG;PARK,HYUN-SOO;SUH,IN-SUK 1607

The effects of w/o emulsion properties in electrostatic demulsification kinetics
HANO,T.;OHTAKE,T.;MATSUMOTO,M.;HORI,F.;NAKASHIO,F. 1613

Immobilized enzymes in liquid membrane permeation productseparation and productbrushing in biotechnology
PREITSCHOPF,W.;MARR,R. 1619

Membrane transport of alkali metals by crown ethers
MURAI,T.;NAKAMURA,K.;NISHIYAMA,S.;TSURUYA,S.;MASAI,M. 1625

Rare earth recovery using pseudo liquid membranes
GU,ZHONGMAO;NAVRATIL,J.D.;CHENG,HANYING 1631

Membrane extraction for separation of long-chain unsaturated fatty acids
MATSUBA,Y.;KITAMURA,Y.;TAKAHASHI,T. 1637

Affinity separation of protein by gel-matrix membrane
KURAHASHI,H.;IMAI,M.;SHIMIZU,M. 1643

Enzyme-like catalytic behaviors of the enantioselective hydrolysis in liquid membrane systems
UEOKA,R.;MATSUMOTO,Y.;GOTO,K.;KATO,Y. 1649

Study on the swelling of emulsion liquid membrane
LI,WEIXUAN;DAI,XING;SHI,YAJUN 1655

11. Supercritical and New Extraction Systems

Extraction of xanthines from cocoa nut shells with carbon dioxide
BRUNNER,G.;ZWIEFELHOFER,U.;SIMON,A. 1661

Chromatographic measurement of vapor-liquid equilibrium ratios of organic solvents in supercritical CO_2 + poly(vinyl acetate) system
HATTORI,K.;WANG,NING-HE;TAKISHIMA,S.;MASUOKA,H. 1671

Application of liquid-liquid extraction of lanthanoid elements to centrifugal partition chromatography
AKIBA,K.;ISHIBASHI,Y.;NAKAMURA,S. 1677

Utilization of third-phase-formation in solvent extraction systems employing amine extractants
HARTL,J.;MARR,R. 1683

High pressure phase behavior for binary mixtures of indole, pyrazine, pyrimidine, and quinoxaline with CO_2, C_2H_4, C_2H_6, and CHF_3
YAMAMOTO,S.;OHGAKI,K.;KATAYAMA,T. 1689

Correlation of solubilities of coal liquefaction products in supercritical carbon dioxide and solubility enhancements using equation of state
IWAI,Y.;YAMAMOTO,H.;SHIMIZU,T.;ARAI,Y. 1695

Supercritical extraction of alcohol from aqueous solution using only carbon dioxide
SUZUKI,T.;TSUGE,N.;NAGAHAMA,K. 1701

Separation of polyunsaturated fatty acid from vegitable oil by supercritical fluid extraction and chromatography
IKAWA,N.;FURUTA,S.;FUKUZATO,R.;IMANISHI,N.;KAWANA,H.;
MITSUIKI,M.;SUZUKI,H. 1707

Supercritical fluid extraction of flavours from milkfat
DE HAAN,A.B.;DE GRAAUW,J.;SCHAAP,J.E.;BADINGS,H.T. 1713

Debindering from molded fine ceramics by supercritical carbon dioxide
TAKISHIMA,S.;NAGASAKI,H.;MASUOKA,H.;MUKAI,Y.;SAKAI,T. 1719

New homogeneous liquid-liquid extraction by phase separation and phase transformation with fluorocarbon surfactant and quaternary ammonium salt
IGARASHI,S.;YOTSUYANAGI,T. 1725

Dividing into layers as extraction method. On the example of some salt-water systems
SCHWARTZ,J.M.;KURSINA,M.M. 1731

12. Special Applications: Petrochemicals, Biotechnology

Hollow fiber for liquid-liquid extractions
WICKSRAMASINGHE,S.R.;SEMMENS,M.J.;CUSSLER,E.L. 1737

Extraction of amino acids and peptides by reversed micelles
FURUSAKI,S.;KISHI,K. 1749

Solubilization of cells in organic solvents by reverse micelles
PFAMMATTER,N.;FAMIGLIETTI,M.;HOCHKÖPPLER,A.;LUISI,P.L. 1755

Separation and concentration of proteins with liquid-liquid extraction using reversed micelles
NISHIKI,T.;SATO,I.;KATAOKA,T. 1761

Bioselective aqueous two-phase partition - Relative merits of polymer and particle derivatives
HUDDLESTON,J.G.;LYDDIATT,A.;KUBOI,R.;SUZUKA,R.;WANG,W.-H.; KOMASAWA,I. 1767

Extraction of penicillin acylase using PEG/K_3PO_4 aqueous two-phase system
SHEN,ZHONG-YAO;RONG,GUO;BO,LU 1773

Immunoaffinity partition of a protein in aqueous two phase system
SUGA,K.;SHIOYA,S.;HIRASAWA,T. 1779

Recovery of aspartic acid from aqueous solutions by extraction with TOMAC in xylene
HANDOJO,L.;DEGENER,W.;SCHÜGERL,K. 1785

Regeneration of carboxylic acid extracts
KING,C.J.;STARR,J.N.;POOLE,L.J.;TAMADA,J.A. 1791

Reactive-extraction of L-phenylalanine from an enzymatic solution
BART,H.-J.;MARR,R.;BAUER,U.;REISINGER,H. 1797

Extraction of amino acid with organophosphorus extractant
TERAMOTO,M.;MIYAKE,Y.;MATSUYAMA,H.;NARA,H. 1803

A new separation process of chloroacetic acids by extraction
TETZLAFF,H.;RITTNER,S. 1809

Protein extraction by reverse micelles
LESER,M.E.;MARCOZZI,G.;CASELLI,M.;LUISI,P.L. 1815

Measurement and correlation of phase equilibria of aqueous two-phase systems and partition coefficients of enzymes
FURUYA,T.;NAKADA,K.;IWAI,Y.;ARAI,Y.;TAKEUCHI,K. 1821

Characteristics of enzymatic NAD^+-recycling reaction in microcapsule of liquid-surfactant membrane
KATO,K.;YAMASAKI,N.;NAKASHIMA,Y. 1827

Phase equilibria of three aqueous two-phase systems
KATO,M.;YAMAGUCHI,M.;KIUCHI,T.;ITO,S.;NAKAMURA,M. 1833

Transport of proteins through reversed micellar solution layer as a liquid membrane
KINUGASA,T.;TANAHASHI,S.;TAKAHASHI,K.;TAKEUCHI,H. 1839

Protein extraction by reversed micelles using new surfactants
GOTO,M.;KONDO,K.;NAKASHIO,F. 1845

Separation of proteins using affinity aqueous two-phase extraction in PEG/salt systems
WANG,W.-H.;KUBOI,R.;KOMASAWA,I. 1851

Hydrophobic effect on partition of biopolymers in aqueous two-phase extraction systems with salts
KUBOI,R.;TANAKA,H.;KOMASAWA,I. 1857

Separation of biopolymers with reverse micellar bulk liquid membranes
KUBOI,R.;MORI,Y.;YAMADA,Y.;KOMASAWA,I.;LUISI,P.L. 1863

Phase inversion behaviour of aqueous two-phase systems
MOORE,I.P.T.;GILCHRIST,A.;HAWTIN,J.;NIENOW,A.W.;KUBOI,R.;
KOMASAWA,I. 1869

Protein transport between aqueous phase and micellar organic phase using self-assembled amphiphiles
ICHIKAWA,S.;IMAI,M.;URUSHIYAMA,S.;SHIMIZU,M. 1875

Separation and enrichment of amino acids with liquid surfactant membrane
HANO,T.;OHTAKE,T.;MATSUMOTO,M.;KITAYAMA,D.;HORI,F.;NAKASHIO,F. 1881

Application of liquid membrane technique to the recovery of fermented organic acids
HANO,T.;MATSUMOTO,M.;OHTAKE,T.;SASAKI,K.;HORI,F.;KAWANO,Y. 1887

Methods for characterization the hydrodynamic behaviour of fermenter broths in liquid-liquid extractors
JOB,C.;BLASS,E. 1893

A use of liquid emulsion membrane for the optical isomer separation of amino acid
HA,HEUNG YONG;HONG,SEONG-AHN 1899

Recovery of low-molecular biological products from aqueous mixtures by carrier extraction
SCHÜGERL,K.;BRANDES,A.;DEGENER,W.;VON FRIELING,P.;HANDOJO,L. 1905

Separation of mixture of vinyltrimethylsilane and tetrahydrofuran by extraction
BORISOVA,I.A.;SOKOLOV,N.M.;VATSKOVA,V.G.;GORBUNOV,A.I. 1911

7. HYDROMETALLURGY

Solvent Extraction 1990, T. Sekine (Editor)

© 1992 Elsevier Science Publishers B.V. All rights reserved

THE PRODUCTION OF HIGH VALUE PARTICLES IN SOLVENT EXTRACTION MEDIA

G.P. DEMOPOULOS
Department of Metallurgical Engineering
McGill University, Montreal, Quebec, Canada H3A 2A7

ABSTRACT

In this paper the potential of using solvent extraction media as reaction environment for the production of metallic and other inorganic particles is examined. The subject is examined from the synthesis of advanced inorganic materials point of view. Research data drawn from our own laboratory work or from the technical literature is reviewed and specific precipitation systems are described. Emphasis is given to identifying the underlying factors which govern the formation of particles in solution and control ultimately their size and morphology. Particle nucleation, growth and anti-aggregation mechanisms are discussed in relation to the physicochemical parameters of the reaction environment. In particular two reaction environments are considered:
(i) precipitation directly in the organic solvent and
(ii) precipitation within the water pools of an aqueous-in-organic solvent dispersion.

INTRODUCTION

The integration of solvent extraction technology to hydrometallurgical processing has been one of the most successful stories in the non-ferrous metal extraction industry. Undoubtedly further applications of solvent extraction (SX) to large scale metallurgical operations are possible as is for example the case of Fe(III) removal from zinc process liquors (Demopoulos and Pouskouleli, 1989). However the undisputed strength and future of SX lies mostly with by-product recovery, i.e. the treatment of complex matrix liquors for the recovery of low volume but high value inorganic substances. Metals like Ga, Ge, In, rare earths and PGMs are examples which fit in this category. The ability of SX to separate and prepare purified precursor solutions for the recovery of these high value by-products impacts directly with the growing importance of advanced materials market. At least 100 papers are presented in this conference which deal in fact with the recovery of elements (common base and nuclear metals are excluded) which are already used or are investigated for use in advanced materials applications.

Apart, however, from this "purification" role solvent extraction plays, there exists the distinct possibility solvent extraction media to be used for the "in-situ" preparation of high-value powders suitable for the fabrication of advanced materials. In this unconventional solvent extraction approach the in-

organic species after transfer from the aqueous feed liquor to the immiscible organic phase (extraction) is precipitated out of the solvent by a controlled treatment in a separate reaction vessel. It is the object of this paper to examine the precipitation phenomena which govern the formation of particles in solvent extraction media and relate the latter to the synthesis of inorganic particulate materials.

2 APPLICATIONS TO CONVENTIONAL METALLURGICAL OPERATIONS

The concept of direct recovery of metal values from organic solvents via a precipitation-stripping route is not new. In the past, various solvent-based precipitation methods have been proposed to either simplify the process flowsheet or alternatively to effect stripping from an "inert" metal-loaded organic solvent. All these methods are summarized in Table 1. Among them only two have attained commercial status. The first one is the precipitation of gold from dibutyl carbitol using an aqueous oxalic acid solution (Barnes and Edwards, 1982):

TABLE 1

Summary of solvent-based precipitation methods

Method	Precipitant	Phase System*	Products	Ref.
Reduction	gaseous (H_2) aqueous ($H_2C_2O_4$)	S/G S/A	metals	Demopoulos 1985 Barnes 1982
Hydrolysis	H_2O	S/A	oxides, hydroxides	Monhemius 1985 Doyle 1985
Crystallization	aqueous (H_2S, CO_2, F^-)	S/A	sulphides, carbonates, fluorides	Distin 1988 Watanabe 1986
Electrodeposition	e^-	S/A	metals	Wan 1986

*S: solvent, G: gas, A: aqueous

$$\overline{2R_2OH^+AuCl_4^-} + 3H_2C_2O_4 \rightarrow 2Au\downarrow + 6CO_2 + 8HCl + \overline{2R_2O} \quad (1)$$

The other industrial application took place in Japan and it involves the precipitation of a complex $(NH_4)_3FeF_6$ salt from iron(III)-loaded D2EPA solvents (Watanabe et al, 1986):

$$\overline{FeR_3} + 3NH_4HF_2 \rightarrow (NH_4)_3FeF_6\downarrow + 3\overline{HR} \quad (2)$$

Hydrolytic stripping of Fe(III)-Versatic acid has been tested at a pilot-plant level as a possible iron removal process for the zinc industry (Monhemius and

Thorsen, 1980; Collier et al, 1986):

$$\overline{FeV_3} + 3H_2O \rightarrow Fe_2O_3\downarrow + 3\overline{HV} \quad (3)$$

Finally, of industrial relevance is the direct electrolysis of gold from alkyl phosphorus esters loaded with $AuCN_2^-$ using an organic-in-aqueous electrolyte dispersion which was described recently by Wan and Miller (1986):

$$\overline{R_3PONa^+AuCN_2^-} + e^- \rightarrow Au\downarrow + \overline{R_3PO} + Na^+ + 2CN^- \quad (4)$$

The other methods, namely hydrogen reduction (Demopoulos and Distin, 1985 a) sulphide stripping (Quon and Distin, 1988; Distin et al, 1988) and crystallization stripping (Shibata et al 1988) could prove useful in solving problems related to conventional metallurgical circuits as well. However, it is in the synthesis of materials field that the above precipitation stripping methods have the greatest potential for industrial application.

3 BASIC CONSIDERATIONS

In the development of solvent-based precipitation methods consideration should be given to the following three critical areas:

(i) the stability, recycling and reproducible performance of the solvent

(ii) the properties of the precipitated compounds: purity, composition, physical form, particle size distribution, morphology and filterability. In reference to the latter, organic losses due to extensive adsorption have to be contained, if eventually implementation of the process is to be pursued. It is worthy to note at this point that hydrolytic precipitation of Fe_2O_3 from Versatic solvents is apparently associated with solid/solvent separation problems (Collier et al, 1986) while this is not the case with the well grown and easily filterable crystals of $(NH_4)_3FeF_6$ (Watanabe et al, 1986).

(iii) the design of the precipitation reactor and the integration of the precipitation unit operation to the overall process scheme. In this respect, aspects like agitation regime, particle collection - washing-handling, solvent recovery-recycling, reagent compatibility etc. have to be carefully assessed.

In this paper the focus is on identifying the factors which influence the properties of the produced precipitates (item (ii) above).

3.1 Solvent stability

Both thermal and chemical stability considerations are of primary importance. Solvent extraction reagents are not designed for high temperature applications and various degradation mechanisms might be triggered upon temperature eleva-

tion which can render the solvent unsuitable for reuse. Possible degradation mechanisms are hydrolysis (acid attack), hydrogenolysis (destructive hydrogenation), oxidation (high valence metal ions) and pyrolysis (thermal decomposition). It is through experimentation that the extent of stability of a particular extractant can be established and via design of long-term stability tests to incorporate all the "ingredients" of a real system (re: catalytic effects of product, dissolved species, protons etc.). So far the most extensive stability studies involving commercial solvent extraction reagents have been made in conjunction with the hydrogen precipitation method (Demopoulos and Distin, 1985). Thus for example in connection with this reaction system, long chain alcohols (decanol) were found to inhibit hydrogenation of the hydroxyquinoline (HQ) nucleus of Kelex 100 and render the latter stable even after 40 recycles at 325°C/4140kPaP_{H_2} in the presence of well known hydrogenation catalysts (Cu, Ni, Co). This is not the case however when palladium powders are produced (Demopoulos, 1986). On the other hand the protonation of the N heteroatom of HQ via acid extraction has an accelerating effect on the unwanted hydrogenation. Moreover the reactivity (or instability) can be influenced by the type of substituent groups carried by the extractant as is for example the case of hydroxyoximes (Demopoulos and Distin, 1985a). Of relevance to the stability of the extractant is the oxidation of the latter by the extracted metal species. This type of intramolecular redox reaction was discussed in ISEC'88 (Demopoulos 1988). If reversible in nature this redox mechanism can be exploited for the preparation of powders (Demopoulos, 1986; Muhl et al., 1990).

3.2 Products

The produced solids can be: fine metal particles (precious metals, Cu, Ni, Co) suitable for electronic and catalyst applications (Demopoulos and Pouskouleli, 1988, Mamoory et al., 1990); alloy powders for magnetic applications; composite powders (deposition of metal films on non-metallic substrates); oxide powders for ceramic applications (Doyle and Ye, 1987), or other precursor compounds like carbonates, oxalates (Shibata et al., 1988; Yoon and Doyle, 1989) sulphides etc. These powders can be used as they are or after pretreatment. Since the physicochemical properties of the starting building powders largely influence the performance of the final fabricated material, understanding and controlling the phenomena which govern the formation of particles in SX media becomes of critical importance.

3.3 Particle formation phenomena

The shape and the size of the produced particles are the outcome of a complex interplay of nucleation, growth and aggregation phenomena. Nucleation is preceded by the formation of a precursor ("activated") complex. If the

latter forms in solution, homogeneous nucleation prevails (an important prerequisite if fine particles are to be prepared) as opposed to heterogeneous nucleation (and growth) which takes place on the surface of a seed particle or even on the walls of the reactor. Separation of the homogeneous nucleation and heterogeneous growth stages and regulation of the two rates as it is predicted by the LaMer diagram (Sugimoto, 1987) is necessary if optimun particle size control is to be achieved. Depending on the rate and the extent of the nucleation stage the ultimate size distribution of the particulare product is determined. Extensive overlapping of the nucleation/growth stages results in a rather wide size distribution and loss of size control. For example in the case of copper powder production from Kelex 100 by H_2 reduction (Mamoory et al., 1990) a self-induced homogeneous nucleation stage precedes (in the absence of H_2) the heterogeneous precipitation stage (H_2 action).

In addition to controlling the nucleation process the prevention of aggregation (or coagulation) of the newly-formed particles is equally important from the standpoint of size control. Van der Waals attraction forces are responsible for aggregation, while electrostatic repulsion forces arising from the double layers surrounding the particles act against coagulation. The latter forces operate only in an aqueous environment. The electrostatic repulsion forces can have some bearing on particle stabilization (dispersion) if mixed aqueous/organic media are employed but it is mainly stabilization arising from the long-chain surfactant molecules present in the organic solvent that dominates (Napper, 1970; Tadros, 1984). Total coverage of the newly formed particles by adsorbed layers of surfactants prevents particle coagulation. By using two surfactants an enhancement in steric stabilization is obtained. Thus in the case of Cu/Kelex 100/H_2, decanol and tertiary carboxylic acids are used simultaneously for optimal particle size control (Mamoory et al., 1990) There is always a delicate balance between stabilization and flocculation. The latter is favoured in the case of fractional coverage. Thus the ratio of surfactant (modifier/extractant) concentration to total particle population is critical as it is the presence of water in the system. For a particle stabilized in an organic medium the presence of trace amounts of water has a catastrophic (agglomerating) effect (Lyklema, 1968). Temperature plays an equally important role in particle dispersion this being dependent on the nature of the steric stabilization process, i.e. "entropic" vs. "enthalphic" (Gregory, 1978). The former dominates in organic media and thus heating favours stabilization as opposed to the enthalpic type that dominates in aqueous media and results in flocculation when heating is applied.

4 REACTION SYSTEMS-DESIGN PARAMETERS

On the basis of the phenomena identified above the reaction environment of

two distinctly different precipitation systems is analysed next. The two reaction systems are differentiated according to the site of precipitation (= particle formation): (1) precipitation occuring in the organic solvent and (2) precipitation occuring in the aqueous phase.

4.1 Precipitation in solvent

The best studied system in this category is H_2 reduction:

$$\overline{MAn} + n/2H_2 \rightarrow M + n\overline{HA} \qquad (5)$$

According to the electrochemical theory, metal couples (M^{n+}/M), whose reduction potential lies above that of H_2 (H^+/H_2), can in principle be precipitated For reactive metals, like Mo, V, W, U the respective low valence oxides can be precipitated by the action of H_2. In an organic medium the hydrogen reduction potential (e_{H^+/H_2}) moves towards more negative values due to the combined effect of lack of free protons and increased H_2 solubility (P_{H_2}*):

$$e_{H^+/H_2} = -\frac{RT}{2F} \ln \frac{P^*_{H_2}}{\alpha^2_{H^+}} \qquad (6)$$

On the other hand due to complexation, the metal reduction potential assumes lower values, the extent of this potential lowering effect being dependent on the stability of the complex. Depending on the relative magnitude of these two potential changing factors a more favourable or less favourable precipitation system can result in comparison to precipitation from ionic solutions. Thus Cu precipitation is more readily done in carboxylic acid solvents than in aqueous sulphate solutions while at the same time precipitation in hydroxyquinoline solvents is considerably less readily accomplished (higher reduction temperatures are required) (Demopoulos and Distin, 1985a). But in addition to modifying the precipitation driving force, complexation has a direct impact on the nucleation mechanism as well.

Hydrogen activation-nucleation. Molecular hydrogen is a highly inert reactant. For reduction to occur, homogeneous or heterogeneous catalytic activation of hydrogen is necessary. The dissolved metal species itself (homogeneous) or the precipitated metal (heterogeneous) can act as catalysts to hydrogen activation. The form of hydrogen activation impacts directly on the nucleation mechanism and thereby to the overall character of the precipitation system. Thus homogeneous activation becomes practically synonymous with predominantly homogeneous precipitation. Cu precipitation from Versatic solvents is believed to be associated with homogeneous activation:

Heterolytic splitting

$$\overline{\overline{CuV_2}} + H_2 \xrightarrow{slow} \overline{\overline{CuHV}} + \overline{HV} \quad (7)$$

Cu(II) reduction to Cu(I)

$$\overline{\overline{CuHV}} + \overline{\overline{CuV_2}} \xrightarrow{fast} \overline{2CuV} + \overline{HV} \quad (8)$$

Formation of copper particles can be effected by further hydrogen reduction of $\overline{CuV}$ (van der Zeeuw and Gandon, 1975) or alternatively via the following disproportionation reaction:

$$\overline{2CuV} \rightleftarrows Cu\downarrow + \overline{CuV_2} \quad (9)$$

Disproportionation reactions are excellent routes towards preparing fine and narrow sized particles (Sasaki and Nagai, 1989; Sutherland et al., 1990).

A predominantly homogeneous precipitation system (neglecting aggregation at this point) tends to be associated with the production of very fine closely-sized particles. Copper particles produced from Versatic solvents are in fact of colloidal dimensions (« 1 μm) (Burkin 1974 and Distin 1987). The homogeneous catalytic activity of Cu(II) is greatly reduced upon formation of chelate complexes. Thus practically no homogeneous activity is exhibited by $\overline{CuL_2}$ (where L: Kelex anion) resulting in a predominantly heterogeneous precipitation system. It is through the separate self-induced formation of copper nuclei before the introduction of H_2 that makes possible the production of closely sized particles here.

The presence of water (accidental transfer or deliberate addition) can have profound effects on the precipitation mechanism and the properties of the powder. Filtration of the organic solvent to remove traces of water was found to be essential in ensuring the production of uniformly grown particles in the system Cu/Kelex 100/H_2 (Mamoory et al., 1990). The role of NH_3 in increasing the apparent particle size of copper powders produced from Versatic solvents (Burkin, 1974) might be linked to water transfer in the system as well. Water entering the system along NH_3 would cause agglomeration by disrupting the particle-versatic solvent stabilizing forces. Additionally a loss in the stabilizing power of the versatic solvent could have been the outcome of the prevalence of the salt form rather than the acid form of Versatic. Also particle aggregation due to the presence of an aqueous microphase (2 v/0) is believed to have been responsible for the rather coarse powder production in the case of hydrogen reduction of gold from dibutyl carbitol solvents despite the predominantly homogeneous nature of the system (Li & Distin1984):

$$2\ \overline{R_2OH^+AuCl_4^-} + 3H_2 \rightarrow 2Au\downarrow + 2\overline{R_2O} + 8HCl \qquad (10)$$

But water, in addition to affecting particle aggregation, can be responsible as well for triggering side reactions. This is particularly true when metal precipitation is attempted from an outer sphere configuration. Solvents loaded via outer-sphere complexation (basic and solvating extractants) tend to extract water along with the acid due to hydration of proton ($H_9O_4^+$) and microemulsion formation. Thus upon heating water can react. This may have been the case of tungsten oxide powder ($WO_{2.9}$)production by hydrogen reduction of a quaternary amine (Aliquat 336) described recently by Wang Chen et al (1989). No reduction of tungsten (VI), $\overline{(R_4N^+)_2WO_4^{2-}}$, seems to have taken place. Alternatively the presence of water in association with a shift in equilibrium due to temperature elevation (ion-pair forming systems being exothermic) appears to have been responsible for the formation of $WO_{2.9}$. Other side reactions like intramolecular redox coupling (Demopoulos, 1988) or polymerization (ageing) of the loaded organic solvent (Monhemius et al, 1984; Demopoulos and Distin,(1985b) have to be taken into account as well.

4.2 Precipitation in aqueous microphase

In this system precipitation takes place within an aqueous microphase dispersed in the continuous organic solvent. The aqueous microphase is formed via either transference of water in the organic solvent during metal extraction or via the deliberate external addition of water (as for example in the case of hydrolytic stripping (Doyle and Ye, 1987) or crystallization stripping (Shibata et al., 1988). The aqueous microphase consists of reverse micelles or W/O microemulsions. It is due to the surfactant (amphiphilic) character of most of the solvent extraction reagents (extractants and/or modifiers) that water is encapsulated in the form of tiny water pools (Fig. 1).

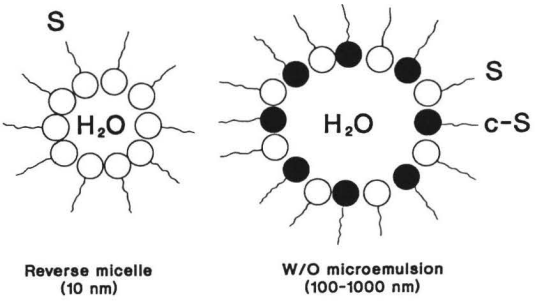

Fig. 1. Forms of water encapsulation in organic solvent.

The formation and "catalytic" role of reverse micelles and microemulsions in enhancing solvent extraction rates has been documented (Fourré et al.,

1983; Gaonkar and Neuman, 1987; Osseo-Asare, 1988). Reverse micelles are formed by the aggregation of polar surfactant molecules (like long-chain alcohols or organic acids) while W/O microemulsions form via the cooperative action of two surfactant molecules. Typical surfactants are salts of long-chain organic acids and protonated amines. The typical cooperative surfactant is a long-chain alcohol. All these surfactant molecules are common ingredients of a solvent extraction system and their impact on the particle formation process starts now to be better understood. The stability, size and composition of the formed aqueous microdrops influence ultimately the properties of the precipitated powders.

Emulsion-based precipitation systems are already being investigated as a promising synthesis route for metalic, ceramic and other inorganic particles (Boutonnet et al., 1982; Langevin, 1984; Fendler, 1987; Lianos and Thomas, 1987; Kanai et al., 1988; Rinn and Schmidt, 1988; Celikkaya and Akinc, 1988). In these systems, the general approach is to prepare an aqueous microphase by mixing the organic surfactant medium with the metal-bearing aqueous solution (O/A > 20) and then to add an aqueous-soluble precipitant to effect precipitation inside the aqueous pools of the emulsion. For microemulsion-based precipitation systems using solvent extraction media the difference is that the metal-bearing phase is the organic solvent but precipitation still takes place inside the dispersed aqueous microphase. So, the reaction scheme is as follows:

(i) Interfacial mass transfer (stripping)

$$\overline{MXL} + S(aq) \overset{K_s, k_s}{\rightleftarrows} MX(aq) + \overline{L} \qquad (11)$$

(ii) Homogeneous precipitation

$$MX(aq) + P(aq) \overset{K_p, k_p}{\rightleftarrows} M \text{ or } MP\downarrow + X(aq) \qquad (12)$$

where S and P are stripping and precipitating agents respectively and K_s, K_p, k_s and k_p are the respective equilibrium and rate constants. The precipitant can be a base to cause hydroxide formation, H_2S or NaHS to produce sulphide semiconductors, CO_2 or $NaHCO_3$ to produce carbonates, H_2 to produce metals, $H_2C_2O_4$ or $Na_2C_2O_4$ to form oxalates, $NaBH_4$ to form borides etc. A good control of the relative magnitude of K_s, K_p (functions of temperature and activities) and k_s, k_p is important in optimizing complex precipitation systems. With $k_p > k_s$ formation of monodisperse particles is to be favoured. Of equal importance in obtaining monodisperse particles is the stability (enhanced by the proper choice of surfactants) and size of the water pools and the steric stabilization imparted to the newly formed particles by the surfactant

molecules. A simplified graphical representation of the events leading to fine particle formation in a W/O microemulsion environment is presented in Fig. 2. The case of lanthanum carbonate precipitation by bubbling CO_2 in a loaded carboxylate solvent (HV) saturated with dispersed stabilized water microdrops is depicted.

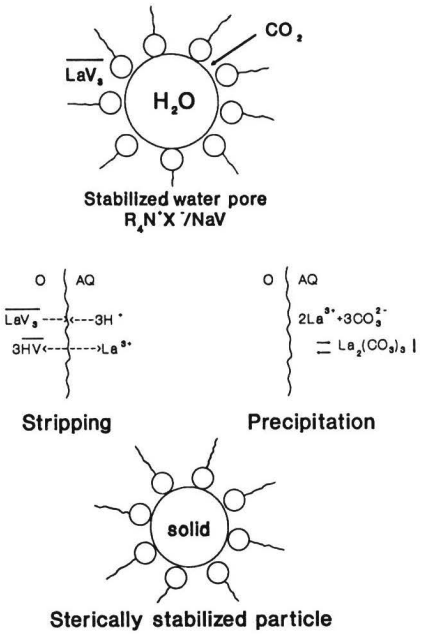

Fig. 2. A schematic representation of precipitation in a W/O microemulsion environment.

5 DISCUSSION OF SELECTED CASES

5.1 Precipitation in solvent

The chemistry of copper powder precipitation from Kelex 100-Decanol-kerosene solvents by H_2 reduction has been described previously (Demopoulos and Distin, 1985b). Recently this system has been under further investigation aiming at optimizing the properties of precipitated powders. Preparation of very fine spherical particles with narrow size distribution suitable for thick film applications has been the target of our studies (Mamoory et al., 1990). The powder is now practically free of agglomerates consisting of smooth and closely-sized particles (0.5 - 1.5 μm; surface area 1 m^2/g). Control of particle size was achieved (i) via the separation of the nucleation (self-induced disproportionation) and growth (heterogeneous H_2 activation) stages and (ii) via steric stabilization generated by the co-action of decanol and Versatic 10. High H_2 pressure was also found to be important in ensuring uniform particle growth via complete coverage of copper nuclei by chemisorbed hydrogen.

Precipitation of palladium powders by H_2 reduction of loaded Kelex 100 or Lix 26 solvents has been studied (Demopoulos, 1986) in the temperature range of 95 to 125°C. The precipitation kinetic curves are characterized by an initial induction period (varying from 30 min to 5 min) during which no metal forms followed by rapid and complete (< 5 ppm left in solution) precipitation. The induction period is attributed to the extremely stable chelate, PdL_2, which effectively cancels the catalytic activity of Pd^{2+}:

$$\overline{PdL_2} + H_2 \xrightarrow{\text{very slow}} \overline{PdHL} + \overline{HL} \qquad (13)$$

As soon as $\overline{PdHL}$ forms (the "activated" complex) further reduction to Pd metal takes place, the overall process giving very fine ($\sim$ 0.4μm) uniform particles. However $\overline{PdHL}$ (and Pd(H)) will not reduce only $\overline{PdL_2}$ but will attack as well the organic substrate (the nucleus of 8-HQ) causing degradation via the breakage of the heteroring as it was determined by loading tests (Table 2) and GC-MS analysis. Kelex 100 showed overall the best performance.

TABLE 2

Loss of loading capacity due to hydrogenolysis of HQ in the presence of palladium as a function of reduction time.

Solvent	T (°C)	P_{H_2} (psi)	Pd^0 (g/L)	% Loss of Loading Capacity 2	4	8	24 hrs
5v/O Lix 26	95	400	5	7	40	60	> 90
5v/O Kelex 100	115	400	5	0	20	40	65

Recently, iron alloy powders were prepared in our laboratory by hydrogen reduction of Fe(III)-Versatic 10 solvents. The reduction tests were carried out in the presence of seed powder (Cu, Ni, or Fe) at 270°C, 400 psi H_2 and 100 min. Examination of the precipitates by SEM and X-ray microanalysis showed deposition not to have taken on the surface of the seed but rather by coprecipitation. Alloy particle formation is envisaged to occur via seed dissolution (another side reaction!) followed by co-precipitation:

$$2\,\overline{FeV_3} + M \rightarrow 2\overline{FeV_2} + \overline{MV_2} \qquad (14)$$

$$\overline{FeV_2.MV_2} + 2H_2 \rightarrow FeM\downarrow + 4\overline{HV} \qquad (15)$$

where M: Cu or Ni.

Mixed complex formation $\overline{FeV_2.MV_2}$, is assumed to precede reduction due to magnetic interaction forces (Doyle and Monhemius, 1985). The distinctly different powder morphology (fine particles for FeCu vs. flakes for FeNi) is attributed to the activation mechanism of H_2 (i.e. homogeneous for Cu and heterogeneous for Ni).

5.2 Precipitation in aqueous microphase

Gold powder can be produced by extraction of Au(III) from chloride solutions using substituted 8-hydroxyquinolines via ion-pair formation (ΔH^o=-14kcal/mol) and subsequent hydrothermal treatment of the loaded organic solvent (Demopoulos et al., 1990). Typical precipitation curves are shown in Fig. 3 for various solvent/water ratios. The precipitation involves intramolecular reduction of Au(III) to Au(I), interphase transfer of Au(I) from the organic

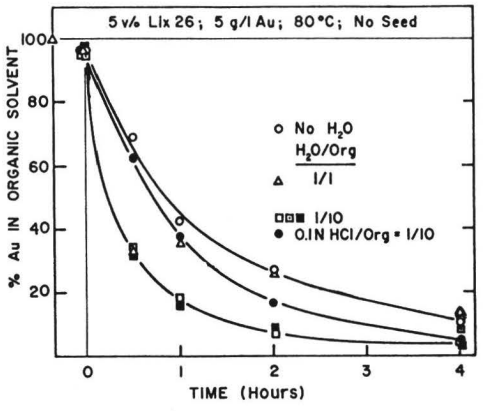

Fig. 3. Precipitation of Au from Lix 26-isodecanol-Solvesso 150/H_2O mixtures by intramolecular reduction.

to the aqueous phase and disproportionation of Au(I)(Demopoulos, 1988). Fig. 3 shows that even with no water addition precipitation still takes place. Analysis of the water content of the organic solvent showed to be as high as 1 v/O and this level to depend on the degree of acid extracted. Apparently a w/O microemulsion forms under these circumstances with $\overline{H_2L^+Cl^-}$ acting as the surfactant (HL: Kelex 100 or Lix 26) and isodecanol as the co-surfactant. The study showed that the higher the acid content of the solvent (i.e. the higher the concentration of $\overline{H_2L^+Cl^-}$ the higher the purity of the powder will be, this being associated with the stability of the microemulsion. However there is an upper optimum limit of aqueous acidity which if exceeded results in the production of contaminated product due to back-transfer and disproportionation of Au(I) in the organic periphery of the aqueous microphase. Large volume of water has the undesirable effect of diluting the acid content and thus imparting destabilization on the microemulsion.

The impact of solvent composition on the powder morphology of gold was investigated in a series of ambient temperature tests involving mixing the solvent (loaded at 50% of its theoretical capacity) with distilled water (A/O=1) followed by quiescent long time storage. Various particle morphologies were obtained. Some of these results are summarized in Table 3.

TABLE 3

The impact of solvent composition on gold powder morphology produced by intramolecular reduction and disproportionation.

Solvent	Product
5v/O HQ 10v/O isodecanol Solvesso 150	Mixture of spherical particles (partially aggregated), platelets (triangular and hexagonal) and worm-like crystallites
5v/O HQ 95v/O isodecanol	Mixture of spherical particles and platelets
near 100% HQ (isolated as third phase)	Mostly discrete spherical particles with a few platelets
100% isodecanol	Mixture of spherical particles (partially aggregated) and well grown (almost perfect) polyhedron crystals

Apart from metallic particles the production of particulate inorganic compounds using mixed aqueous/organic media has been attempted. Of great interest in this regard is the work of Professors Nishimura and Doyle in Japan and USA respectively. Shibata et al. (1988) in their work involving precipitation of basic carbonates of nickel from Versatic acid solvents found an excess of HV or use of $NaHCO_3$ instead of CO_2 to increase the average size of the particles. This effect could be linked to the formation of w/O microemulsions arising from the cooperation of V^- (ligand anion) and 2-ethylhexanol used as modifier). Enlarged and more stable water pools apparently allowed for further particle growth. The alteration of the nucleation mechanism (from homogeneous to heterogeneous) via adduct complex formation could have been another contributing factor in the case of excess HV. Microemulsion phenomena can be thought to have played a role in the case of $\overline{CuV_2/ROH/R_3N}/CO_2(aq)$ as well (Sano et al., 1988). The addition of R_3N apparently accelerated the stripping process (eq. 11) by increasing the interfacial area due to microemulsion formation ($R_3NH^+HCO_3^-$ - surfactant and ROH - cosurfactant). Fine spherical particles rather than "rings" were obtained due to the stabilizing effect the amine had on the water pools and the localized supersaturation environment created in the pools which accelerated the homogeneous precipitation rate.

Yoon and Doyle (1989) investigated the production of rare earth oxalate powders from mixed carboxylate/aqueous media (O/A = 5) emulsified with the use of commercial surfactants. Interfacial stripping (eq. 11) followed by homogeneous precipitation (eq. 12) of the oxalate powder within the aqueous microphase was postulated as the plausible particle path. The authors found particle morphologies to depend on the type of emulsion (w/O or O/w). In the case of O/w the small volume of the continuous aqueous phase (O/A = 5) was apparently in the form of thin films surrounding the solvent droplets. As a result of this, elongated and thin particles were produced. On the other hand the compartmentalization of the aqueous phase into tiny droplets dispersed within the continuous organic phase (w/O configuration) gave rise fo the formation of very fine equiaxed particles.

6. CONCLUDING REMARKS

Solvent extraction media are to continue to play an indispensable role in the recovery of low mass-high value by-products. Since many of these high value elements are essential ingredients in the synthesis of advanced materials, possibilities exist for the integration of solvent extraction with precipitation of inorganic powders. To make substantial progress though towards the realization of this new role of SX, the fundamental particle formation phenomena (nucleation-growth-aggregation) will have to be studied and correlated to the interfacial (particle-solvent and solvent-aqueous) and kinetic properties of

the reaction environment. In this paper a number of critical physicochemical factors which directly influence the properties of the powders were identified and discussed. With the growing importance of advanced materials, the type of SX research reviewed here is expected to be further augmented. The integration of conventional hydrometallurgical separations to the preparation of materials is an exciting challenge.

7 REFERENCES

Barnes, J.E. and Edwards, J.D., 1982. Solvent extraction at Inco's Acton precious metals refinery. Chemistry and Industry, 10: 151-155.

Boutonnet, M., Kizling, J. Stenius, P. and Maine, G., 1982. The preparation of monodisperse colloidal metal particles from microemulsions, Colloids and Surf. 5: 209-225.

Burkin, A.R., 1974. Physical chemistry of metal production by reduction of loaded organic solvents by hydrogen, In: Proc. The Physical Chemistry of Process Metallurgy, IMM, London, pp 43-47.

Celikkaya, A. and Akinc, M., 1988. Synthesis and characterization of yttria powders by emulsion precipitation, In: G.L. Messing (ed.) Ceramic Transactions, The American Ceramic Soc., Westerville, Ohio, Vol. 1: 110-118.

Collier, D., Henry, R., Lehmann, R., Pietsch, H.B. and Rathge, G., 1986. The versatic acid process - a solution to the iron problem in the zinc industry? In: J.E. Dutrizac and A.J. Monhemius, Iron Control in Hydrometallurgy, Ellis Horwood, Chichester, U.K. pp 297-311.

Demopoulos, G.P., 1986. Direct recovery of gold-precious metals from loaded organics with hydrogen, Contract Report, CANMET, Energy Mines and Resources Canada, Ottawa, 51 p.

Demopoulos, G.P., 1988. Intramolecular redox reactions in metal extraction systems, In: Proc. ISEC'88, USSR Academy of Sciences, Moscow, Vol. III: 302-305.

Demopoulos, G.P. and Distin, P.A., 1985a. Pressure hydrogen stripping in solvent extraction, Journal of Metals, 37: 46-52.

Demopoulos, G.P. and Distin, P.A., 1985b. Direct copper precipitation from a loaded chelating extractant by pressure hydrogen stripping, Metall. Trans. B, 16B: 13-22.

Demopoulos, G.P., Kelebek, S. and Pouskouleli, G., 1990. Preparation of gold powders by solvent extraction and intramolecular reduction , McGill University, Montreal, Quebec, in preparation.

Demopoulos, G.P. and Pouskouleli, G., 1988. Hydrochemical preparation of fine precious metal powders, Journal of Metals, 40: 46-50.

Demopoulos, G.P. and Pouskouleli, G., 1989. Solvent extraction of Iron(III) from acid sulphate solutions by mono(2-ethyl hexyl) phosphoric acid. Can. Metall. Quarterly, 28: 13-18.

Distin, P.A., 1987. Hydrogen stripping in copper solvent extraction In: W.C. Cooper (ed.) Copper 87, Universidad de Chile, Santiago, Vol. 3: 323-336.

Distin, P.A., Desantis, D. and Mihaylov, I., 1988. Fine particles production in solvent extraction, In: A.J. Plumpton (ed.), Production and Processing of Fine Particles, Pergamon Press, Toronto, pp 651-661.

Doyle, M.F. and Ye, W., 1987. ZrO_2 powders from ziroconium(IV) carboxylates, Journal of Metals, 39: 34-37.

Doyle-Garner, M.F. and Monhemius, A.J., 1985. Hydrolytic stripping of versatic acid solutions containing iron and other metals, Minerals and Metall. Proc., 2: 47-51.

Fendler, J.H., 1987. Atomic and molecular clusters in membrane mimetic chemistry, Chem. Rev., 87: 877-899.

Fourré, P., Bauer, D. and Leverle, J., 1983. Microemulsions in the extraction of gallium with 7-(1-ethenyl-3,3,5,5-tetramethyl hexyl)-8-quinolinol from aluminate solutions, Anal. Chem., 55:662-667.

Gaonkar, A.G. and Neuman, R.D., 1987. Interfacial activity, extractant selectivity, and reversed micellization in hydrometallurgical liquid/liquid extraction systems, J. Coll. Interf. Sci., 119: 251-161.

Gregory, J., 1978. Effects of polymers on colloid stability, In: K.J. Ives (ed.) The Scientific Basis of Flocculation, Sijthoff and Noordhoff, The Netherlands, pp 101-130.

Kanai, T., Rhine,W.E. and Bowen, H.K., 1988. Preparation of 2 ZrO_2.Yb_2O_3 by emulsion techniques, In: G.L. Messing (ed.) Ceramic Transactions, The American Ceramic Soc., Westerville, Ohio, Vol. 1: 119-126.

Langevin, D., 1984. Technological relevance of microemulsions and reverse micelles in apolar media, In: P.L. Luisi and B.E. Straub (eds.) Reverse Micelles, Plenum Press, New York, pp 287-305.

Lianos, P. and Thomas, J.K., 1987. Small CdS particles in inverted micelles, J. Coll. Interf. Sci., 117: 505-512.

Li, R.X. and Distin, P.A., 1984. Gold reduction from dibutyl carbitol with use of hydrogen, In: Proc. Mineral Processing and Extractive Metallurgy (China), IMM, London, pp 235-243.

Lyklema, J., 1968. Principles of the stability of lyophobic colloidal dispersion in non-aqueous media, Adv. Colloid. Interf. Sci., 2: 65-114.

Mamoory, R.S., Drew, R.A.L. and Demopoulos, G.P., 1990. Preparation and characterization of fine copper powders derived by reaction of metal-organic precursor complexes with hydrogen, In: 29th Ann. Conf. of Metallurgists, CIM, Hamilton, Ontario.

Monhemius, A.J., 1985. The precipitation of metal values from cationic extractants. In: L.F. Haughton (ed.), Proc. Int. Conf. Min. Sci. Tech. Mintek 50, Randburg, South Africa, Vol. 2: 599-609.

Monhemius, A.J., Teixeira, L.A.C. and Thorsen, G., 1984. The precipitation of hematite from iron-loaded versatic acid solutions by hydrolytic stripping, In: R.G. Bautista (ed.), Hydrometallurgical Process Fundamentals, Plenum, New York, pp 647-661.

Monhemius, A.J. and Thorsen, G., 1980. The application of hydrolytic stripping to the iron problem in hydrometallurgy, In: Proc. ISEC'80, University of Liege, Liege, Belgium, Vol. 3, paper no. 80-91.

Muhl, P., Gloe, K., Besald, J., Shaffrath, W. and Behr, G., 1990. Fine copper powders from organic complex compounds as conductor material for thick-film applications - preparation and sintering properties, Metall (W. Germany), 44: 273-278.

Napper, D.H., 1970. Colloid stability, Ind. Eng. Chem. Proc. Develop., 9: 467-477.

Osseo-Asare, K., 1988. Enhanced solvent extraction with water-in-oil microemulsions, Sep. Sci. Techn., 23: 1269-1284.

Quon, K. and Distin, P.A., 1988. Sulphide stripping in solvent extraction, In: Proc. ISEC'88, USSR Academy of Sciences, Moscow, Vol. IV: 255-258.

Rinn, G. and Schmidt, H., 1988. Preparation of Y-doped zirconia by emulsion technique, In: H. Hausner (ed.) Ceramic Powder Processing Science, Deutsche Keramische Gessellschaft, pp 221-228.

Sano, J., Ohashi, N., Shibata, J. and Nishimura, S., 1988. Crystallization stripping of Cu from the organic phase containing versatic acid 10 under the pressurized carbon dioxide, In: Proc. Symp. on Solv. Extr., Tokyo, pp 199-204.

Sasaki, H. and Nagai, T., 1989. Studies on the production of fine copper powder by hydrogen reduction of copper sulphate solution, Metall. Rev. MMIJ, 6: 128-138.

Shibata, J., Sano, M. and Nishimura, S., 1988. Application of solvent extraction to inorganic synthesis - production of nickel carbonate, nickel oxide, nickel and nickel-cobalt powders, Metall. Rev. MMIJ, 5: 1-9.

Sugimoto, T., 1987. Preparation of monodispersed colloidal particles, Adv. Coll Interf. Science, 28: 65-108.

Sutherland, B.R., Ramsden, J.B. and Bolton, G.L., 1990. The characterization and application of very fine copper powders produced in aqueous media, In: V.E. Lakshmanan (ed.), SME, Littleton, Co, pp 109-115.

Tadros, T.F., 1984. Suspensions, In: T.F. Tadros (ed.), Surfactants, Academic Press, pp 197-220.

Wan, R.Y. and Miller, J.D., 1986. Solvation extraction and electrodeposition of gold from cyanide solutions, Journal of Metals, 38: 35-40.

Wang, C., Tang, X., Cai, Y. and Wu, Q., 1989. Direct preparation of blue tungsten oxide by reduction of loaded organic extractant with hydrogen, In: M.H.I. Baird and S.Vijayan (eds.), Proc. 2nd Int'l Conf. on Separations Sci. and Techn., CSChE, Ottawa, Canada, Vol. 1: 380-386.

Watanabe, T., Hoshino, M. Uchino, K., Nakazato, Y. and Nishimura, S., 1986. A new recovery process for stainless steel liquors with an iron removal process using solvent extraction, In: J.E. Dutrizac and A.J. Monhemius, (eds.), Iron Control in Hydrometallurgy, Ellis Horwood, Chichester, U.K., pp 549-570.

Yoon, J.H. and Doyle, F.M., 1989. Precipitation of rare-earth powders from aqueous solutions and emulsions, In: F.M. Doyle, (ed.), Innovations in Materials Processing Using Aqueous, Colloid and Surface Chemistry, TMS, Warendale, Pa, pp 195-211.

van der Zeeuw, A.J. and Gandon, L., 1975. Study of the hydrogenation of the versatic acid salts of copper, nickel and cobalt. In: G.A. Davies and J.B. Scuffham (eds.) Hydrometallurgy, IChEng., London, Symposium Series No. 42: 11.1-9.

Solvent Extraction 1990, T. Sekine (Editor)

© 1992 Elsevier Science Publishers B.V. All rights reserved

SOLVENT EXTRACTION SEPARATION OF Nb AND Ta AT MHO : POTENTIALITIES OF CYANEX® 923 VERSUS MIBK.

G. HAESEBROEK, J. VLIEGEN, A. DE SCHEPPER
MHO a division of ACEC-UM, Research department - 2430 Olen - Belgium.

ABSTRACT

Since 1963, MHO is running an industrial solvent extraction unit in its Hoboken plant for the extraction and separation of Niobium and Tantalum from concentrated HF - H_2SO_4 solutions with MIBK. The flowsheet of this production unit is shown. An alternative process with Cyanex® 923 i.o. MIBK as extractant has been developed through a lab scale test program. The development work as well as the resulting flowsheet are discussed. Eventually both processes are compared.

INTRODUCTION

MIBK is a very effective extractant for the recovery of Nb and Ta from mixed HF-H_2SO_4 solutions. MIBK is used since 1963 at MHO for this application. The actual industrial flowsheet is presented in fig. 1. Although this process gives satisfactory recovery yields and pure end products, it suffers from the drawbacks inherent to MIBK : low flashpoint (fire risks), high vapor pressure (smell) and high solubility of MIBK in aqueous phases (solvent losses).

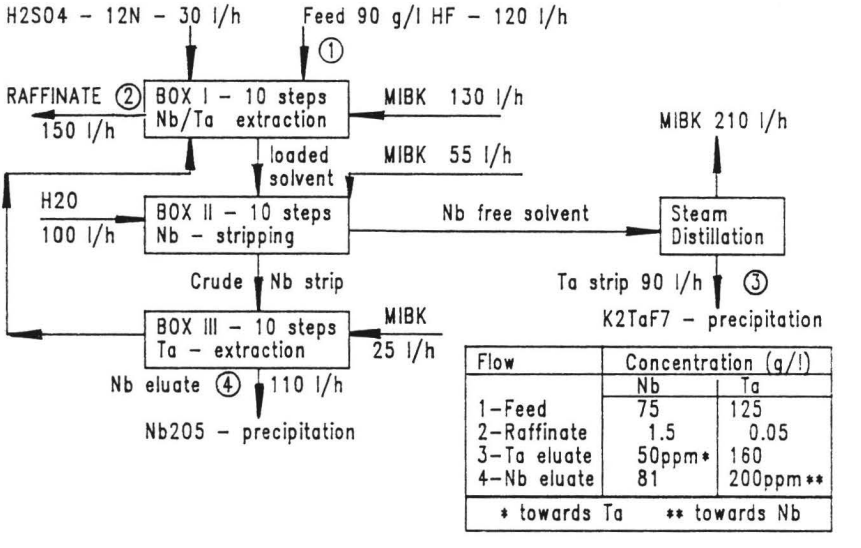

Flow	Concentration (g/l)	
	Nb	Ta
1-Feed	75	125
2-Raffinate	1.5	0.05
3-Ta eluate	50ppm*	160
4-Nb eluate	81	200ppm**

* towards Ta ** towards Nb

Fig. 1. Existing process : SX Nb/Ta with MIBK.

Therefore MHO decided to investigate other potential extractants having none of these inconveniences.

1 SELECTION OF AN ALTERNATIVE EXTRACTANT

Several commercially available extractants were tested for their Nb and Ta extraction efficiencies. The most promising solvents are compared with MIBK in figure 2. As can be seen, Cyanex ® 923 and Alamine ® 336 seem to be competitive with MIBK. From comparative Nb stripping experiments we learned that Cyanex ® 923 gives better Nb/Ta separation yields than Alamine 336. Therefore we focused the further work solely on Cyanex ® 923.

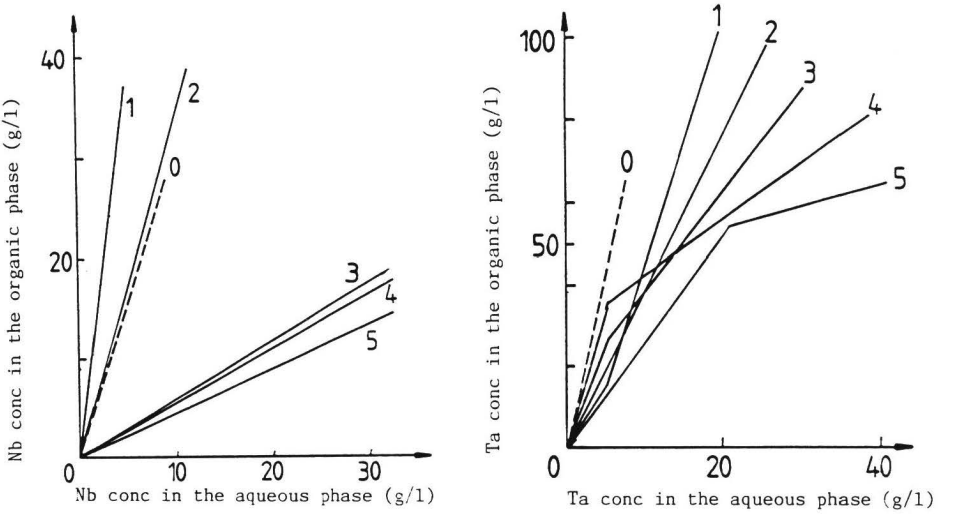

Fig. 2. Comparison of different extractants for the simultaneous extraction of Nb and Ta. Feed : 77 g/l Nb, 125 g/l Ta, 90 g/l HF. O/A : 1/1 - 20°C - 10 min. contact. (0) MIBK (1) Cyanex ® 923 (2) Alamine 336 (50% in Solvesso 150) (3) Aliquat 336 (40% in 20% ID and 40% Escaid 120) (4) Hostarex PO 212 (5) TBP.

2 DEVELOPMENT OF THE Nb - Ta SEPARATION PROCESS WITH CYANEX ® 923

2.1. Simultaneous extraction of Niobium and Tantalum

The study was started with undiluted Cyanex ® 923 as extractant. However the density of this solvent loaded with Niobium and Tantalum is so high that

in the following Nb stripping stages, the washed solvent behaves as the heavy phase and moves to the bottom of the settling device.

In order to avoid this unwanted behaviour we tried to limit the density of the organic phase by adding diluents. A solvent with 25 vol. % of Escaid 120 and 75 vol. % of Cyanex ® 923 gave satisfactory results. We used this solvent composition for the further experiments.

Extraction equilibrium is reached within about 5 minutes. An increase in temperature from 20 °C to 50 °C improves the Nb and Ta extraction yields with about 6 to 8%. The addition of H_2SO_4 to the feed solution has a limited effect on the extraction curves. An optimum mixture contains 90 g/l HF and 50 g/l H_2SO_4.

The stability of Cyanex ® 923 in contact with this feed solution at room temperature is very good. After 1000 hours of contact we detected neither degradation products (G.C. analysis) nor a change in the loading capacity of the solvent phase.

2.2. Selective stripping of Niobium

TABLE 1

Selective stripping of Niobium versus Tantalum from Cyanex 923.

Strip solution	(Nb) $\frac{A}{g/l}$	K_D Nb	(Ta) $\frac{A}{g/l}$	(Nb/Ta) A
H_2O	14.40	1.03	<0.20	>72
H_2SO_4 10 g/l	13.0	1.25	<0.20	>65
H_2SO_4 50 g/l	9.70	2.01	0.60	16.20
HF 10 g/l	18.20	0.60	0.50	36.40
HF 50 g/l	19.80	0.48	1.30	15.20
HF 10 g/l - H_2SO_4 10 g/l	15.30	0.91	0.30	51.0

Conditions : Solvent : 75 vol. % Cyanex 923 - 25 vol. % Escaid 120
29.2 g/l Nb - 55.2 g/l Ta
O/A ratio : 1/1 ; T = 20 °C ; contact time 10 min. ; 1 step.

The data in table 1 show that a 10 g/l HF solution is a good compromise considering Nb stripping yield and Ta/Nb selectivity. Unfortunately, as it is the case with MIBK, too much Ta is stripped together with Nb in order to obtain a sufficiently pure Nb eluate. With the actual flowsheet in mind, we checked if Tantalum could be selectively extracted from the crude Nb strip solution with an organic bleed stream. Shake-out tests with O/A-ratios ranging from 1/10 to 1/20 showed that this was a successful way to get a Ta-free Nb strip solution.

The stripping of Nb with a 10 g/l HF solution was further studied.

Stripping curves with varying operating conditions were determined. In the range 20 - 50 °C, the operating temperature has no effect on the chemical behaviour. In all cases an equilibrium is reached within a 5 minutes contact time.

2.3. Stripping of Tantalum

Steam distillation as performed for the stripping of Ta from loaded MIBK is not feasible while the boiling point of Cyanex® 923 is too high. The stripping power of aqueous solutions of different reagents was checked. Hydroxides (KOH, NaOH, NH_4OH) had to be rejected due to the limited solubility of Tantalum even with overstoechiometric amounts of reagent. NH_4F solutions gave more promising results. The effect of the NH_4F concentration was checked in the range 1 to 5 M. The optimal results were obtained with 2 M NH_4F solutions. At higher concentrations, the distribution coefficient increases while at lower concentrations Ta precipitation occurs. A typical stripping isotherm is shown in fig. 3. Tantalum can easily be separated from the pregnant strip by neutralisation with KOH up to pH 8. The produced K_2TaF_7 precipitate is suitable for metal recovery. NH_3 can be recovered from the filtrate and recycled for NH_4F preparation.

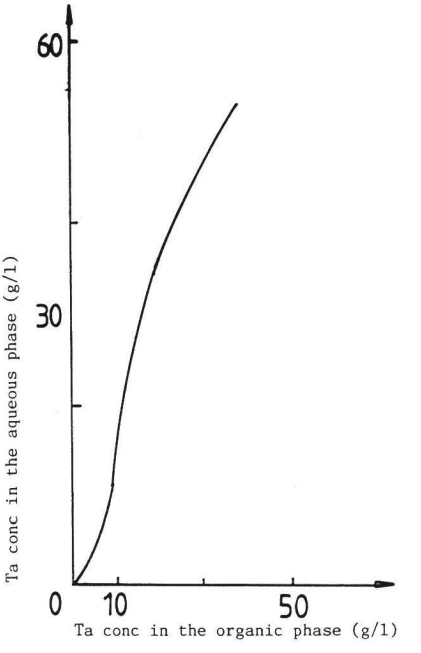

Fig. 3. Stripping of Ta from Cyanex 923 with a 2 M NH_4F solution.
Solvent : 75% Cyanex® 923 - 25% Escaid 120 - 80 g/l Ta.
O/A = 1/1 - 1/2, 50 °C, 5 min. contact.

3 TENTATIVE FLOWSHEET FOR THE SEPARATION OF Nb AND Ta WITH CYANEX ® 923

From the optimal isotherms generated in the shake-out tests, we derived a tentative flowsheet.

In this work, we made the following assumptions :

a) The solvent existing of 75 vol. % Cyanex ® 923 and 25 vol. % Escaid 120 would initially be loaded up to 0,8 mole Nb + Ta/1.

b) A scrub section could be necessary to reduce physical entrainment of feed solution with the loaded solvent.

c) After Ta stripping, the stripped solvent could have to be conditioned in order to maintain an optimum acid balance in the extraction.

This leads to the flowsheet shown below which could be used as a basis for further continuous tests.

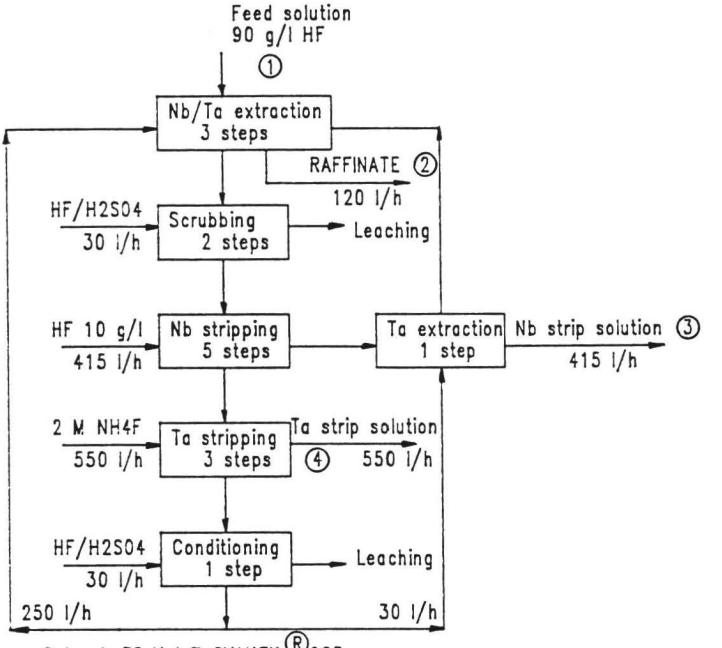

FLOW	Concentration (g/l)	
	Nb	Ta
1-Feed solution	81.7	130
2-Barren raffinate	0.02	0.02
3-Nb strip solution	21.7	0.005
4-Ta strip solution	50ppm vs Ta	27.2

Fig. 4. New process : SX Nb/Ta with Cyanex ® 923.

4 CONCLUSIONS

Cyanex® 923 is a suitable alternative for MIBK for the simultaneous extraction and successive selective stripping of Niobium and Tantalum. It allows high recovery yields and separation factors leading to end products of good quality. The Cyanex® 923 containing solvent has the advantage over MIBK of a high flash point, a low vapor pressure and a low solubility in aqueous phases. This reduces fire risks and solvent losses, improves operators' comfort and lowers operating costs.

When comparing the actual and the new flowsheet one however sees that the process based on Cyanex® 923 needs substantially higher flowrates of organic and aqueous strip solutions. Also the lower solubility of the solvent in the aqueous phases will probably necessitate the installation of an activated carbon treatment section for both strip solutions. These elements will have a detrimental effect on capital costs.

Eventually the choice between Cyanex® 923 and MIBK will be determined by an accurate comparison between the overall economics of both processes for a given application.

In the case of MHO, continuous tests should have to be performed to get all necessary data. This has not been done because the decision was taken to stop the treatment of Nb-Ta bearing raw material.

5 ACKNOWLEDGMENT

The authors wish to thank the Management of MHO for giving the permission to publish this paper and all people of MHO involved in this study and in the preparation of the paper.

6 REFERENCES

C.K. Gupta, Int. Met. Rev., 1984, 29(6) : Extractive metallurgy of niobium, tantalum and vanadium, p. 405-444.

R. Hahn, H.J. Ketelsdorf, Erzmetall, 1984, 3719 : Herstellung von Rein - Niob, p. 444-448.

Ishimatsu Kazuhiko et al., Japan. Kokai, 1972, 7719 : Niobium and tantalum separation, p. 172.

T.H. Tunley et al., Nath. Indust. Metal., Republ. S. Afr. Rep., 1976 : The extraction and separation of Nb and Ta by liquid liquid extraction using tri-n-butyl-phosphate, p. 1154-1175.

Solvent Extraction 1990, T. Sekine (Editor)

© 1992 Elsevier Science Publishers B.V. All rights reserved

METALS RECOVERY FROM A GARBAGE INCINERATOR

H.-J. BART, J. DRAXLER and R. MARR
Institut für Thermische Verfahrenstechnik und Umwelttechnik, Technische Universität Graz, Inffeldgasse 25, A-8010 Graz (Austria)

ABSTRACT

Incineration processes act as possible source of heavy metals when leaching the slags and filter ashes with the washing waters of the flue gas. Detailed laboratory and pilot work on the recovery of heavy metals by the use of liquid ion exchangers is reported. A cost comparison in regard to a conventional precipitation plant gives a picture of the economics.

INTRODUCTION

Garbage incineration processes have environmental problem areas derived from their heavy metal content and gaseous reaction products. The latter problem is nowadays solved with a flue gas purification unit. The problem remaining is the heavy metals. When looking on the distribution of heavy metals in an incineration plant one finds three sources. The solid ones are slags and flue dusts and the liquid one is the effluent from the gas scrubber. The slags and ashes can be leached with the sour scrub solution (pH ≈ 1.5). The resulting metal concentrations are given in Tab. 1. As can be seen, the key element is zinc. According to Bart (1988) the extraction of Zn looks promising with the monothio phosphoric acid. Ca as the main component of acidic scrub solution (saturated $CaCO_3$/CaSQ-solution) will not be extracted.

TABLE 1

Heavy metals in the acid scrubbing solution after solids leaching

	mg/l
Zn	300 - 600
Pb	10 - 20
Cd	1 - 20
Cu	10 - 20
Hg	< 0.1
As	< 1
Cr	< 3
Ni	< 5
Al	40 - 100
Fe	0 - 40

PILOT OPERATION EXTRACTION

The plant was operated on varying throughputs from 50 to 200 l/h for two months. A two stage extraction circuit and a one stage stripping with sulphuric acid followed by a stage with the stronger hydrochloric acid proved to be satisfactory. Some starting problems came from the high entrainment (about 1 %) of strip-solution in the organic phase caused by a stage with the simple design of the pilot Denver (reg. Trademark) mixer-settlers. The high content of about 20 g/l Zn in the stripping solution was transferred to the raffinate extraction stage with the organic phase due to entrainment. The Zn concentrate was diluted and found in the raffinate. After installation of an aqueous scrub step between stripping and extraction sections (after 20.6. in Fig. 1) the acidic zinc solution containing the entrained stripping phase could be drained from the organic phase.

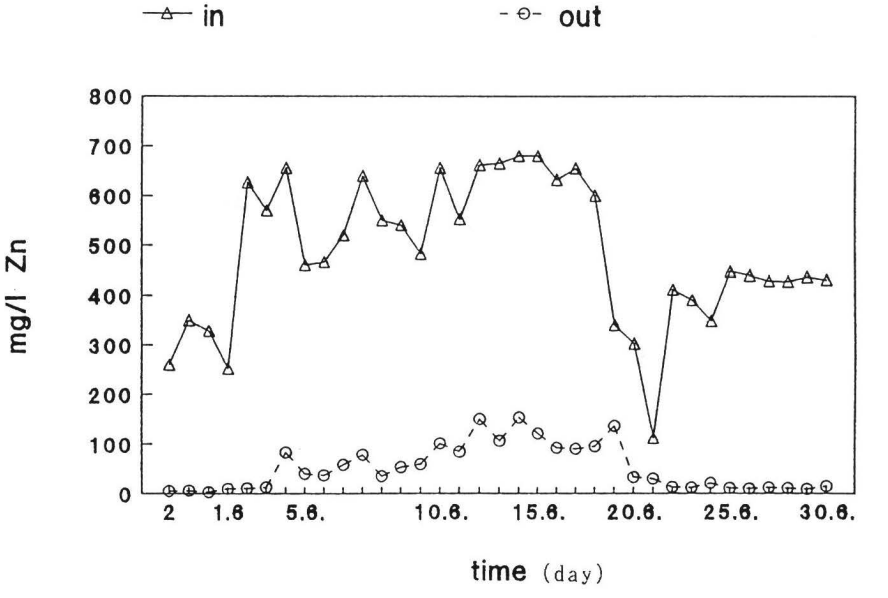

Fig. 1. Pilot plant Zn raffinate values

Typical plant results of the end of the pilot period are given in Table 2. As can be seen, the better extractable elements like Cu, Pb and Cd were always extracted to levels smaller 1 mg/l. Zn raffinate values came down after the modification of the pilot plant schema to the range of 9 to 20 mg/l which was thought to be satisfactory. Lower levels can be achieved with additional mixer settlers or better with pH-adjustment since the raffinate-pH of about 1.7 is extreme low.

TABLE 2

Solvent extraction pilot plant results

mg/l	Zn	Cu	Pb	Cd	acidity
feed	447	13	40	21	pH = 3.4
raff.	11	<0.1	<0.5	<0.2	pH = 1.7
strip.	19450	0.9	3.3	12.4	1.5 M H_2SO_4
strip.	640	1570	142	1090	7 M HCl

The data from the stripping section are of potential interest for recycling. In the first stripper with sulphuric acid mainly Zn is recovered. In the second stripper with hydrochloric acid the rest, like Cu and Cd, is removed. The only problem in the reextraction circuit is the occurrence of suspended solids in both mixer settlers. This is $PbSO_4$ as well as $PbCl_2$ which is extremly insoluble when stripped from the organic phase. The only advantage is, that these salts are rather heavy in weight and can be found at the bottom of the settler and not in the boundary layer. However, with this selective stripping operation two different product qualities can be obtained, where the Zn fraction is directly usable in a Zn electrowinning plant.

LIQUID MEMBRANE PERMEATION

An alternative to solvent extraction is the use of liquid membranes as described by Draxler (1986). The liquid membrane pilot plant operation was done in parallel to the solvent extraction circuit at same throughputs. The flow schema is shown in Fig. 2. The stripping phase I of the emulsion is sulphuric acid. Thus the product after emulsion splitting is zinc sulphate with some solid Pb. The pure organic phase from the splitter is scrubbed with hydrochloric acid similar to the solvent extraction circuit before reused.

Zinc concentrations at the bottom and top of the column are given in Fig. 3. The raffinate values are rather high which came from difficulties of the initial layout of the column length. The assumption was, that the metal leaching section will bring a Zn feed of about 150 mg/l. Due to an increase in the efficiency of that section, which was also piloted in parallel, the Zn feed was about 400 to 600 mg/l. The primary column length of 4 m was obviously too short to solve this problem. The raffinate levels stayed at average 200 mg/l, since there was no reconstruction of the column during the pilot period. A repetition of these pilot experiments in a column 6 m in height should bring satisfying results.

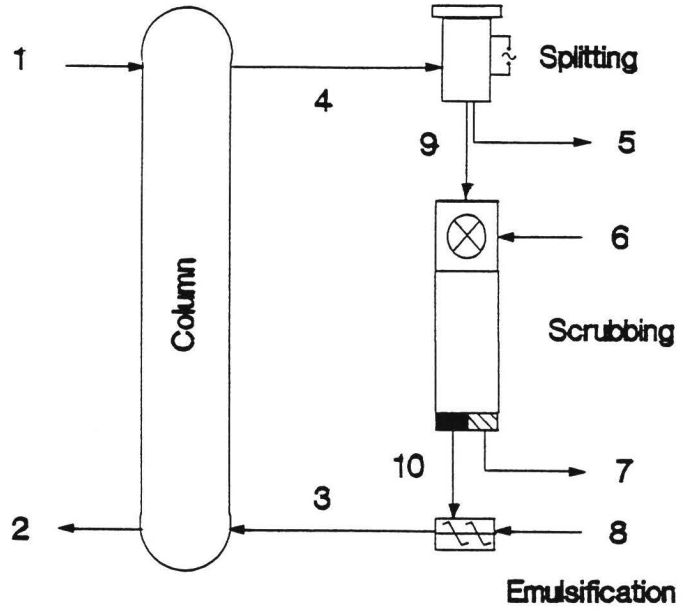

Fig. 2. Flowsheet of the liquid membrane pilot plant (1 feed, 2 raffinate, 3 fresh emulsion, 4 loaded emulsion, 5 sulphuric acid product, 6 hydrochloric acid, 7 hydrochloric acid product, 8 sulphuric acid, 9 org. phase, 10 purified org. phase)

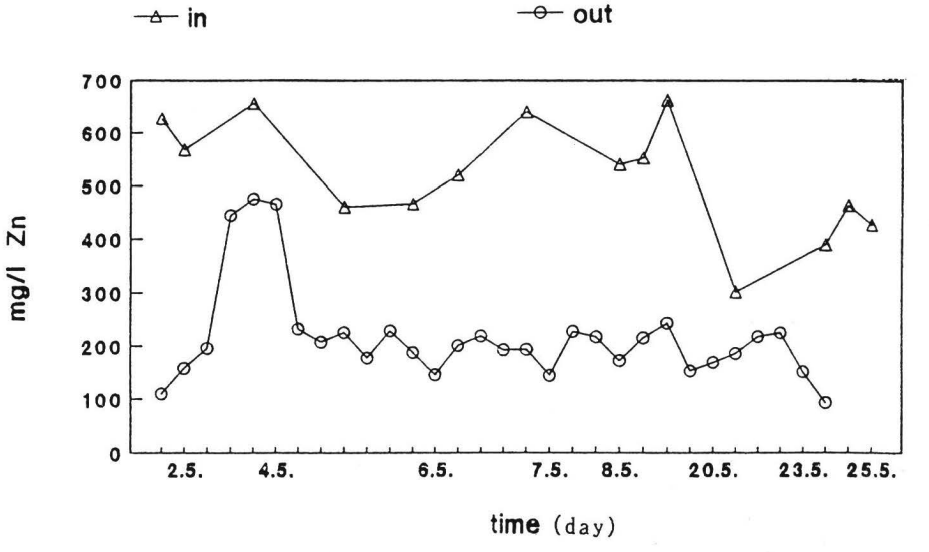

Fig. 3 Liquid membrane permeation pilot plant results

CONCLUSIONS

The pilot plant operations have proved the technical feasibility of liquid ion exchange techniques for metal recovery at a garbage incineration plant. A standard technique for metal recovery is precipitation, so a cost calculation was made for comparison. In order to compare technical equivalent recovery grades, a hydroxid precipitation must be followed by a sulphid precipitation.

The main disadvantages of this plant are in the disposal problems of the residues since there is no possibility directly to reuse the heavy metals. The deposit contains, as main component filtration aids which enlarge (as further disadvantage) the deposit volume.

TABLE 3

Cost comparison for heavy metal recovery at a waste incineration plant (solvent extraction, liquid membrane permeation and precipitation)

Mio. AS	SX	LMP	Pcpt.
investment	15.0	13.0	6.0
depreciation (15 years, 8%)	1.60	1.38	0.64
raw & process materials	0.93	0.88	2.02
energy	0.20	0.20	0.27
maintenance	0.30	0.26	0.12
insurance	0.30	0.26	0.12
returns (e.g.Zn)	0.80	0.80	–
landfill disposal	0.08	0.08	2.50
operating costs total	2.61	2.26	5.67
costs per Mg waste (in AS/Mg)	10.4	9.0	22.7

The calculation was done for an incineration plant (power about 100 MW_{th}) with a throughput of garbage of 250.000 Mg/a at 8000 h/a. The conclusions from Table 3 are evident. The investment costs of a precipitation plant are at least half that of SX or LMP. The operating costs are similar and even better with SX and LMP, without regarding returns and landfill disposal costs. However, actual landfill disposal costs in Austria of 5000 AS/Mg cannot be neglected and contribute markedly to the operating

costs of the precipitation plant. Materials costs are very high, too. This is after Marr (1988) due to the large quantity of $FeCl_3$ and polyelectrolyte needed. This is the reason why the overall costs per ton garbage are twice as high as with SX and LMP.

ACKNOWLEDGEMENT

The authors wish to acknowledge the help of "F. Zechner, SGP/VA Energie- und Umwelttechnik", and the "Christian Doppler Ges.", Vienna, which make this work possible.

REFERENCES

Bart, H.-J., Draxler, J. and Marr, R., 1990. Chem. Engng. and Technology, submitted.

Draxler, J. and Marr R., 1986. Chem. Engng. Process. 20, 319-329.

Marr, R. and Draxler, J., 1988. Chem.-Ing.Techn. 60, No. 5, 348-359.

Solvent Extraction 1990, T. Sekine (Editor)

© 1992 Elsevier Science Publishers B.V. All rights reserved

SOLVENT EXTRACTION OF SILVER FROM CHLORIDE SOLUTIONS BY CYANEX 471X

Y. ABE, Nippon Mining Co. Ltd, Japan and D.S. FLETT, Warren Spring Laboratory, Stevenage, U.K.

ABSTRACT
The solvent extraction of silver from chloride solutions by Cyanex 471X (American Cyanamid) was studied to determine the nature of the extracted species and to examine selective recovery of silver from the major components of complex sulphide ore chloride leach liquors. Silver was extracted as a solvated Ag Cl species. Little extraction selectivity occurred for silver over cuprous copper but good selectivity was found over cupric copper, zinc and lead. Silver can readily be stripped from the organic phase with sodium thiosulphate fixer solution.

INTRODUCTION

Chloride hydrometallurgy is of considerable interest for the treatment of bulk flotation concentrates of complex Cu/Pb/Zn/Ag sulphide ores although as yet no commercial plants are in operation. The recovery of precious metals from such bulk flotation concentrates is a very important economic factor. (Collins & Flett, 1990). In such processes, chloride based oxidative leaching ensures silver dissolution as an anionic chloro-species. In the proposed flowsheets (Campbell & Ritcey 1981; Andersson et al 1980; Danielsson et al, 1983) if the copper concentration in the leach liquor is low then silver is co-cemented with copper, and if the copper concentration is high then silver is recovered as part of the cathode product. Thus further refining has to take place before a pure silver product is recoverable.

While it is known that silver is readily extracted from sulphate or nitrate liquors by sulphur containing extractants (Rickelton & Robertson, 1984; Cattrall et al 1978; Hitchcock et al 1983) no systematic work has ever been done on its extraction from chloride media although Beutier & Bunzynski (1986) have reported silver extraction from chloride liquors. It was therefore decided to study the extraction of silver from chloride media with the American Cyanamid reagent Cyanex 471X (tri-isobutyl phosphine sulphide).

2 EXPERIMENTAL

Cyanex 471X was purified by dissolving it in 75 v/o propane-2 ol/25 v/o deionised water (100 g/400 ml) heating to 40°C, filtering and then allowing the filtrate to cool. This gave white needle crystals at 67% yield. The product was dissolved in Escaid 110 as a 0.5 M solution with either 5 v/o DEHPA

(Rickelton & Robertson 1984) or 5 v/o isodecanol as modifier.

Silver chloride solution was prepared by dissolution of precipitated Ag Cl in NaCl, or HCl or mixed NaCl/HCl solutions as appropriate. Cuprous chloride solutions were prepared by similar dissolution of AR CuCl. Other metal chlorides were made up as necessary. Fixer solution (Rickelton & Robertson 1984) was used to strip silver from the loaded organic phases.

3 RESULTS

3.1 Silver Extraction

The results of silver extraction tests for varying silver, acidity and chloride concentration are shown in fig. 1. The results all fall on a common curve which is linear above 2 M chloride with a slope of -3.6. The constancy of distribution from NaCl and HCl suggested that HCl was not extracted by Cyanex 471X and this was confirmed by shake out tests.

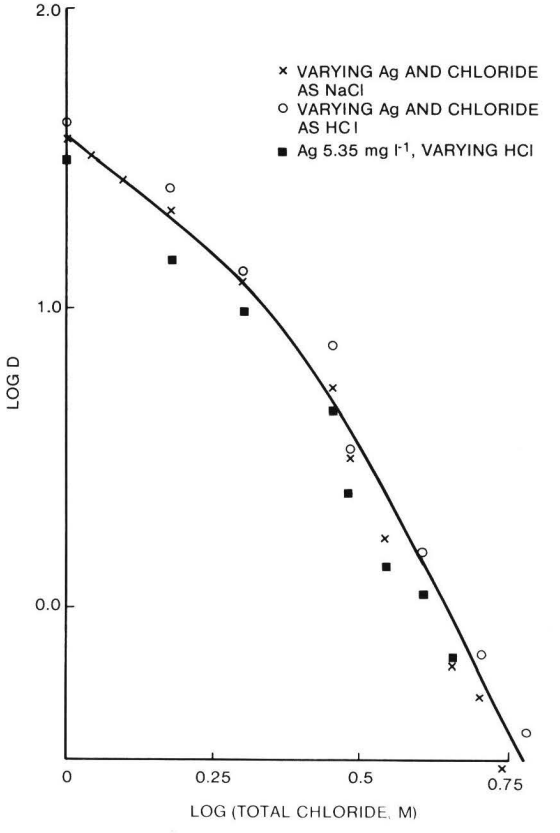

Fig. 1. Silver Extraction With CYANEX 471X: Effect of Silver and Chloride Ion Concentrations.

The effect of varying Cyanex 471X at constant Ag and chloride concentrations is shown in fig. 2. This log plot gave a straight line of slope approx. 2 indicating a Cyanex 471X:Ag ratio of 2:1. As the Ag:Cl ratio in the organic phase was determined to be 1:1 therefore the stoichiometry of the extracted species is $(\text{Cyanex 471X})_2\text{AgCl}$. This explains the negative effect of increasing chloride ion as formation of non-extractable anionic silver species in the aqueous phase will decrease the extraction.

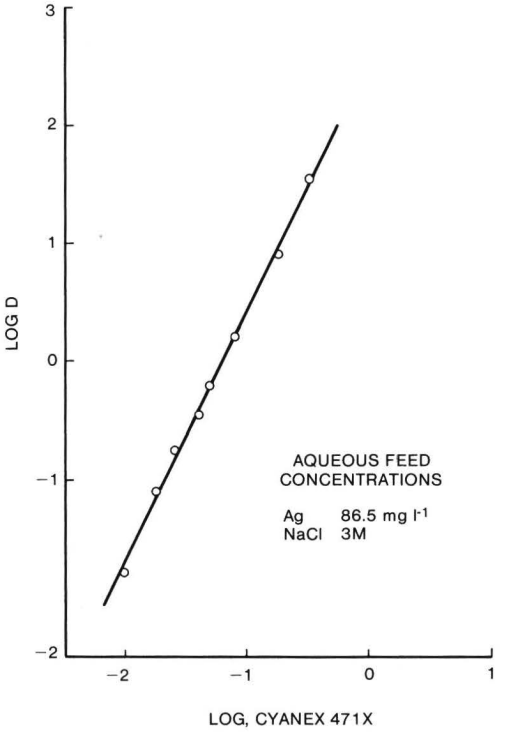

Fig. 2. Silver Extract with CYANEX 471X: Effect of Extractant Concentration.

The effect of changing the modifier from DEHPA to isodecanol is shown in fig. 3 which shows good agreement between the two systems at D values less than 100.

3.2 Extraction of copper

Work with the cuprous system was difficult due to oxidation to cupric even under nitrogen but as cupric chloride was not significantly extracted by Cyanex 471X (D values $< 10^{-1}$ even at 5M HCl) then copper in the organic phase was assumed to be cuprous. The variation of Cu(1) extraction with chloride concentration and comparison with silver extraction (data from fig. 1) is shown in fig. 4. The results show that copper extraction also decreases with

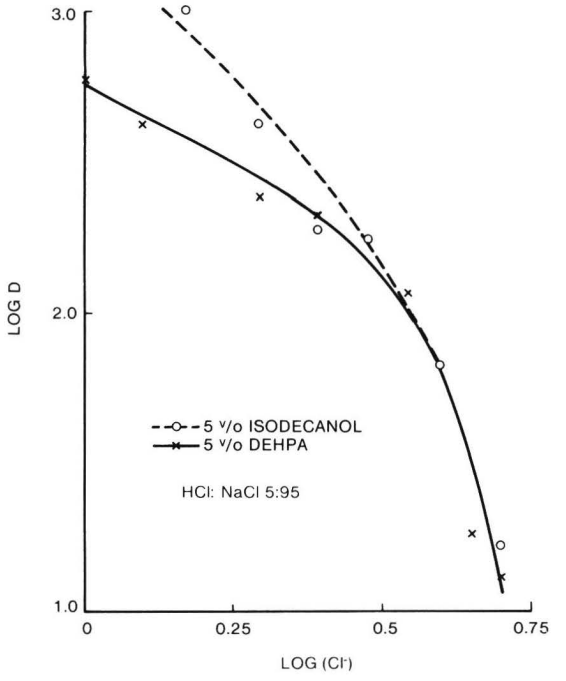

Fig. 3. Extraction of Silver with CYANEX 471X: Effect of Modifier on Silver Extractant.

increasing chloride concentration and that Cyanex 471X extracts copper more strongly than silver. Unlike silver, copper extraction for unknown reasons seems to be lower from HCl than NaCl.

3.3 Extraction of silver in the presence of Cu II, Zn II and Pb II

Neither zinc nor lead were extracted by Cyanex 471X and neither had any measurable effect on silver extraction. The effect of cupric ions on silver extraction is shown in fig. 5. which shows that increasing copper (II) concentration increased the extraction of silver.

4 DISCUSSION AND CONCLUSIONS

The results of this study show that silver is well extracted by Cyanex 471X from chloride solutions as an AgCl disolvate but that the degree of extraction decreases with increasing chloride concentration. As Cu(1) is more strongly extracted than Ag I, then Cyanex 471X is of less interest as a silver extractant for cuprous chloride hydrometallurgy circuits. However selective silver removal from cupric leach liquors as produced in the CUPREX Metal Extraction Process (Dalton et al 1987) is quite possible and no interference need be anticipated from zinc or lead. However such leach liquors contain other

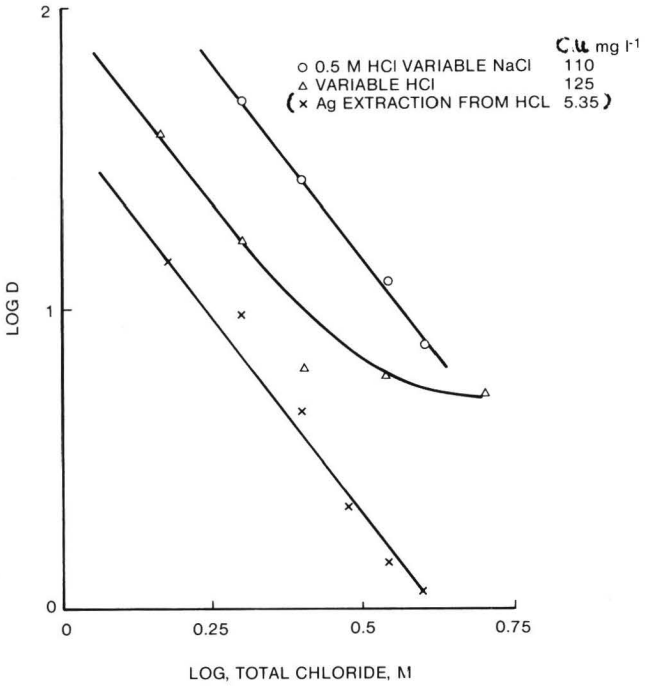

Fig. 4. Extraction of Cu (1) by CYANEX 471X: Effect of Chloride Concentration.

impurities such as bismuth, mercury, arsenic etc. Although not studied here information from the literature (Cattrall et al 1978; Hitchcock et al 1963) suggests that bismuth and mercury in particular will also be extracted by Cyanex 471X. Extraction of arsenic is considered to be unlikely.

REFERENCES

Anderson, E; Boe, G.H., Danielssen, T. and Finne, P.M., 1980. Production of base metals from complex sulphide concentrates by the ferric chloride route in small continuous pilot plant. In: Complex Sulphide Ores, IMM London. pp 186-192.

Beutier, D. and Bunzynski, J.P., 1986. Iron elimination by oxygen in acid cuprous chloride solution: the case of the Minemet Process. In: Iron Control in Hydrometallurgy. J.E. Dutrizac and A.J. Monhemius (Editors). Ellis Horwood Ltd. pp 640-656.

Campbell, M.C. and Ritcey, G.M., 1981. Application of chloride metallurgy to base-metal sulphide and uranium ores at CANMET. In: Extraction Metallurgy '81, IMM London. pp 76-90.

Cattrall, R.W., Martin, A.A. and Tribuzio, S., 1978. The solvent extraction of copper, silver, gold and mercury by some trialkyl monothio phosphate and trialkyl phosphine sulphides and the attempted use of these reagents in coated wire ion-selective electrodes. J. inorg. nucl. Chem. 40, 687-690.

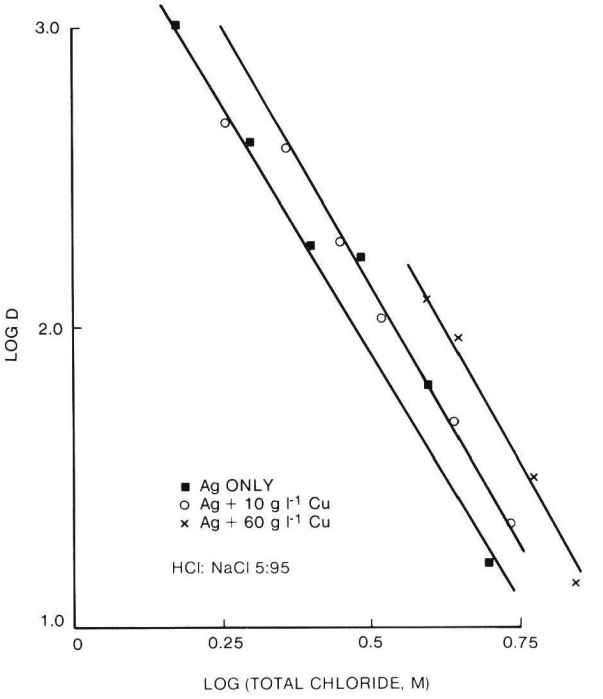

Fig. 5. Extraction of Silver by CYANEX 471X: Effect of Cu (1) on Silver Extraction.

Collins, D.N. and Flett, D.S., 1990. The role of chloride hydrometallurgy in the processing of complex sulphide ores - In: Sulphide Ores. P.M.J. Gray (Editor) IMM London, in preparation.

Dalton, R.F., Hermana, E. and Hoffmann, B., 1987. The CUPREX process - a new chloride-based hydrometallurgical process for the recovery of copper from sulphidic ores. In: Separation Processes in Hydrometallurgy. G.A. Davies (Editor) Ellis Horwood Ltd. pp 466-476.

Danielssen, G.H., Boe, G.M. and Finne, P.M., 1983. Extraction of cupric chloride from iron chloride leach liquors. In: Proc. Int. Conf. ISEC '83 Denver, Colorado, USA. p 536.

Hitchcock, R.B., Dean, J.A. and Handley, T.H., 1963. Tri-n-butyl phosphine sulfide as an organic extractant. Anal. Chem. 35(2) 254-255.

Rickelton, W.A. and Robertson, A.J., 1984. The selective recovery of silver by solvent extraction with tri isobutylphosphine sulphide. Paper presented at SME-AIME Fall Meeting, Denver, Colorado, USA. Preprint No. 84-357.

Solvent Extraction 1990, T. Sekine (Editor)

© 1992 Elsevier Science Publishers B.V. All rights reserved

APPLICATION OF LIQUID EXTRACTION TO PRODUCTION OF EXTRA PURE MAGNESIUM OXIDE

V.BUMBÁLEK and J.HAMAN (1)
Ore Research Institute Mníšek pod Brdy, Czechoslovakia
(1) Research Institute of Chemical Equipment,Prague,Czechoslovakia

ABSTRACT

A process for purifying magnesium chloride solution from calcium ions by liquid-liquid extraction using a solution of di-2-ethyl hexyl phosphoric acid in organic solvents has been developed for the processes of production of extra-pure magnesium oxide. This process as verified in laboratory, model and pilot scale is realized, at present, in Slovak Magnesite Works,Hačava, in a plant being erected with capacity of 26,000 tpa of MgO. This process is generally usable for all technologies using chloride solutions. It enables to recover refined magnesium chloride solution having concentration up to 400 $MgCl_2$ per litre with $CaCl_2$ content less than 50 mg per litre.

INTRODUCTION

Predominant percentage of magnesium oxide production pertains to production from sea water (1). Among a series of other technologies being viable in principle, processes based on thermal decomposition of magnesium chloride have been brought to industrial-scale realization (2,3). Waste magnesium chloride solution from production of chlorides /Dead Sea Periclase, Israel; Kali Kombinat, GDR/ are used as feedstock or these technologies are based on natural magnesite using Aman /HCl/ process /Magnohrom, Yugoslavia; Veitscher, Austria/. The advantage of these processes is the possibility to attain higher quality /MgO content 99 %/ even from waste materials, a disadvantage is higher energy demand /by 7 to 10 GJ per 1 t MgO/ in comparison with MgO production from sea water.

The energy demand of these processes is increased by the necessity to wash out calcium ions /in common with Na and K ions if they are present/ from magnesium oxide obtained by thermal splitting of magnesium chloride.

Aiming at decrease of energy demand of the process and increase of the grade of the obtained MgO, a process enabling to eliminate washing of the decomposition magnesium oxide, a modified HCl process has been developed and verified in the Ore Research Institute. This has been enabled by introduction of technological

sections of de-alkalization of the feedstock (4) and, especially, development of magnesium chloride solution de-calcification before thermal splitting using liquid-liquid extraction (5). This process is, at present, realized in Slovak Magnesite Works, Hačava, with capacity of 26,000 t of MgO sinter per year and will be put in operation in the first half-year of 1991. The MgO grade will exceed 99.5 % containing less than 0.05 % CaO.

Technological flowsheet of the process is seen from Fig. 1. The filtered $MgCl_2$ solution having concentration of approx.400 g $MgCl_2$ per litre with up to 18 g $CaCl_2$ per litre is refined by liquid-liquid extraction using 40 % solution of di-2-ethyl hexyl phosphoric acid in the solvents Escaid 110. The refined solution having concentration of $CaCl_2$ under 50 mg per litre is thermally decomposed and MgO can be finalized as light MgO or, after previous treatment, briquetted and sintered. The organic phase is stripped with hydrochloric acid and recycled into the extraction process. Re-extract /$CaCl_2$solution with small $MgCl_2$ content/ is subjected to the carbonatation process wherein $MgCl_2$ /l/ and $CaCO_3$ /s/ are formed under addition of active MgO and gaseous CO_2. The $MgCl_2$ solution is recycled into the leaching section.

Among a series of further processes for production of synthetic magnesium oxide which have been developed in research and verified at various stages, nitrate technology (6), formate technology (7), sulfite technology (8), bicarbonate technology (9) and others, technologies based on ammonium chloride decomposition by caustic magnesite, e.g. modified method of soda production (10) Sulmag process (11) or chloride-carbonate technology of the Ore Research Institute seem to be the most promising for industrial-scale realization. They have some advantages in comparison with technologies based on thermal decomposition of magnesium chloride - they do not work with aggressive medium /HCl/ and they are not limited by the properties of pyrolytic MgO.

The chloride-carbonate technology of the Ore Research Institute seems to be best elaborated and attains the best results. The flowsheet of this technology is seen from Fig. 2. The new steps in this technology are liquid-liguid extraction with di-2-ethyl hexyl phosphoric acid, stripping of organic phase, carbonatation of reextract and pressure precipitation of $MgCO_3$ anhydrous magnesium carbonate (12). The chloride-carbonate technology enables to produce MgO grade better than 99.9 % at lower energy

Fig.1 Flowsheet of the modified HCl process

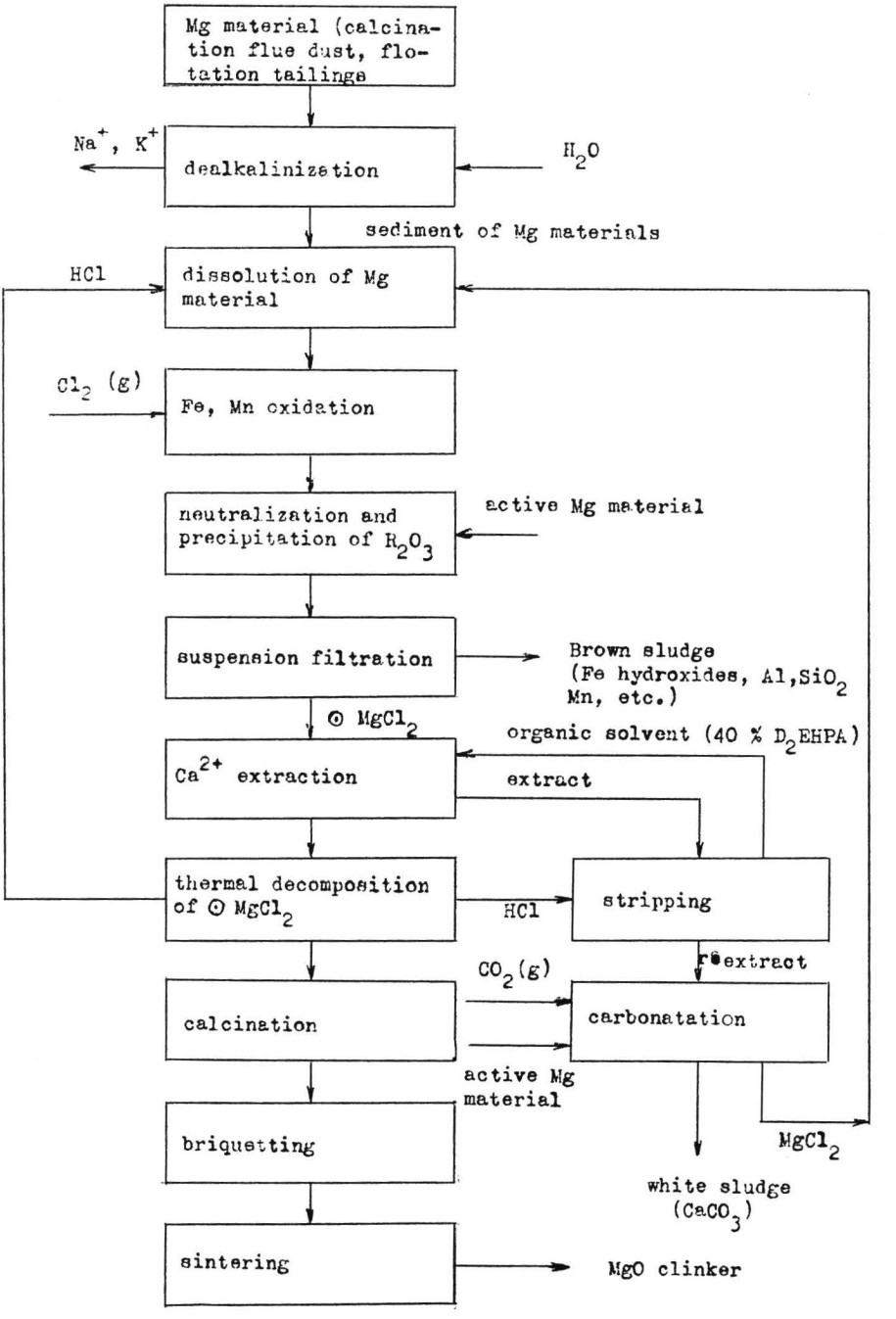

demand than 30 GJ/t MgO.

TECHNOLOGY OF CALCIUM AND MAGNESIUM SEPARATION FROM CONCENTRATED CHLORIDE SOLUTIONS

Extraction of calcium and simultaneously extracted magnesium /denoted as Me^{+2}/ with di-2-ethyl hexyl phosphoric acid /HX/ Bumbálek et al./ proceeds according to the summary relationship

$$(Me^{+2})_{aq} + /(n+2)HX_{org} \rightleftharpoons /MeX_2(HX)_n/_{org} + (2H^+)_{aq} \qquad (1)$$

The course of reaction depends primary on concentration of H^+ ions in the aqueous phase. The equilibrium measurements (13) taken at $MgCl_2$ content up to 5 M have shown that the concentration range of H^+ ions between 10^{-2} and 10^{-3} is suitable for calcium separation while re-extraction of both cations into the aqueous phase occurs in the strong acid region. At decreasing concentration of H^+ ions, approximately from the value of 10^{-1} M, calcium begins to be extracted and magnesium in a substantially lesser degree. However, magnesium extraction increases monotonously due to many times higher magnesium content in the aqueous phase at further decrease in concentration of H^+ ions while extraction of calcium is suppressed by magnesium extraction at further drop, approx. under 10^{-3} M of H^+ ions, and the distribution coefficient as well as the selectivity of calcium separation decrease.

A problem of realization of multistage separation of calcium is (H^+) control at the individual stages. H^+ ions liberated by extraction can be neutralized, e.g. by MgO addition into the aqueous phase at the stages, but the control is very difficult. Totally, up to 0.5 M H^+ ions are liberated during the operation, their concentration at the individual stages, however, must be kept at the value of around 10^{-3} M. Therefore, D_2EHPA partially saturated with magnesium was used and calcium separation proceeded according to the mechanism of ion exchange

$$(Ca^{+2})_{aq} + (MgX_2)_{org} \rightleftharpoons (CaX_2)_{org} + (Mg^{+2})_{aq} \qquad (2)$$

For extract stripping, approx. 5 M of HCl solution is preferably used which is prepared in the section of thermal decomposition of $MgCl_2$.

Technological parameters of calcium separation have been found in an equilibrium countercurrent multistage cascade consisting of shaken flaks and a system of mixers and separating funnels. The process has been verified in pilot scale. The volume of mixers

Fig. No. 2: Flowsheet of chloride-carbonate technology of MgO production

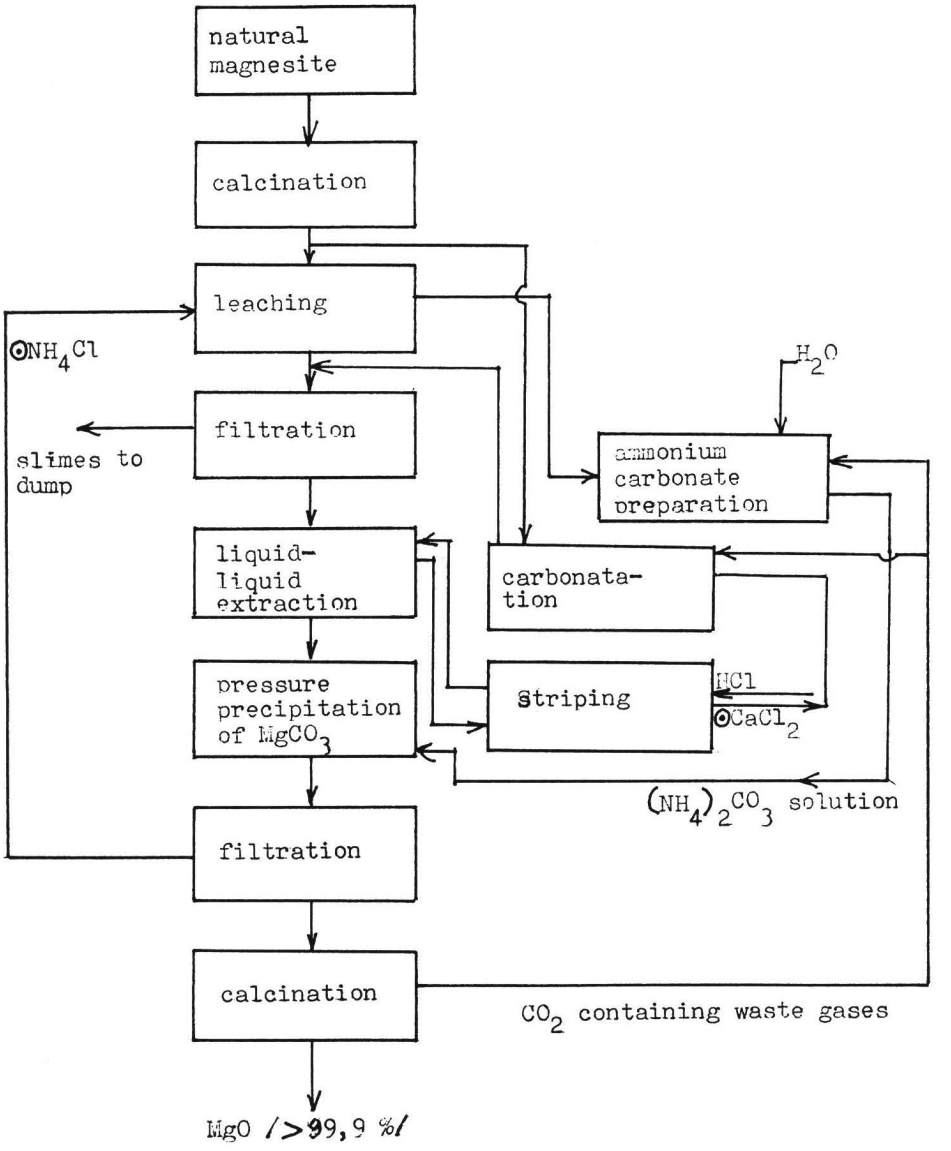

was 7.5 dm^3, the settlers had surface area 9.2 dm^2. These tests aimed mainly at obtention of data for suggestion of an industrial--scale equipment (14).

CONCLUSIONS

1. A method for separation of magnesium and calcium ions generally applicable for chloride solutions has been developed.
2. The developed process enables to produce MgO sinter with grade of + 99.5 % with energy demand less then 32 GJ per ton of sinter. The technology will be put in operation in 1991.
3. Original chloride-carbonate technology using liquid-liguid extraction has been developed which enables to produce MgO of 99.9 % grade in industrial scale.

REFERENCES

(1) Annual Mining Review, 1982, 119-121
(2) Jedlička, H., Herstellung von Magnesiumoxid nach dem Ruthner HC - Verfahren, Andritz-Ruthner, Austria
(3) Jedlička, H. Neue Anwendungen des Sprühröstverfahrens in der Chlorid-Nassmetallurgie, ibid.
(4) Pliešovský, J. et al, Method for decreasing the content of alkalies in magnesium oxide, Czechoslovak Patent 222,888 /in Czech/
(5) Bumbálek,V. et al, Method for decalcification of chloride samples, Czechoslovak Patent 227,703 /in Czech/
(6) Najmr, S.,Nitrate technology of production of extra-pure magnesium oxide, Proceedings Prospects of Development of Mg Compounds in Czechoslovakia, 1980, Vinné
(7) Zikmund, M., Otherspecific technologies of pure MgO production, Proceedings Prospects of Development of MgO compounds in Czechoslovakia, 1980, Vinné
(8) Najmr, S., Sulfite method for MgO production. Research Report of the Ore Research Institute, 1990
(9) US patent 2,458,847 /1949/
(10) Šturc, J., Complex use of East-Slovak raw materials for MgO production, Proceedings Prospects of Development of MgO Compounds in Czechoslovakia, 1980, Vinné
(11) Ainscow, S., Technischer Rundschau Sulzer 1/1986
(12) Bumbálek, V. et al, Method of recovery of anhydrous magnesium carbonate, Czechoslovak Patent 265,971 /in Czech/
(13) Jakubec,K. et al, Separation of calcium from concentrated magnesium chloride solutions by solvent extraction with di(2-ethylhexyl) phosphoric acid, Hydrometallurgy, 17 (1986) 15-26
(14) Haman, J. et al, Development of solvent extraction process for separation of calcium from concentrated magnesium chloride solutions, paper VI.36 presented at the 8th International Congress CHISA 84, Prague, 1984

Solvent Extraction 1990, T. Sekine (Editor)

© 1992 Elsevier Science Publishers B.V. All rights reserved

SOLVENT EXTRACTION OF ARSENIC FROM SODIUM TUNGSTATE SOLUTIONS

I. SZILASSY and K. VADASDI
Research Institute for Technical Physics of the Hungarian Academy of Sciences
P.O. Box 76, H-1325 Budapest (Hungary)

ABSTRACT

The separation of arsenic from sodium tungstate solutions is an important step of all processes producing ammonium paratungstate /APT/ from ores. Due to the stable heteropoly-acid formation between arsenate and tungstate ions only separation methods functioning in alkaline media can be used. We have observed the possibility of the selective arsenic extraction in the presence of tungstate ions in alkaline media using a traditional, commercially available extractant.

INTRODUCTION

The separation of arsenic impurity is an important step in the hydrometallurgy of tungsten. It has been observed many years ago, that certain impurities at 10 ppm level strongly influence the reduction of ammoniumparatungstate (APT) with hydrogen. Among these impurities the arsenic plays an outstanding role since it diminishes the grain-size of tungsten powder product, which is an undesirable effect for most of the applications of the powder (Millner, 1961). At the same time the arsenic is a natural companion of the tungsten ores (Yih, 1979).

The typical processing of tungsten ores to ammoniumparatungstate involves the following steps:

1. Leaching of the ore with Na_2CO_3 or NaOH and thus dissolving the tungsten content in the form of Na_2WO_4.
2. Removing of Mo, As, P, Si impurities from the Na_2WO_4 solution by precipitating them with Al and Mg salts and Na_2S.
3. Transforming the Na_2WO_4 solution with amine containing LIX reagent to ammonium-tungstate solution.
4. Crystallizing the solid ammoniumparatungstate salt from the ammonium-tungstate solution.

The removal of arsenic is an important step in the production of APT (Benesovsky, 1979). According to the traditional industrial method, the arsenic is removed with the P, Si impurities in the form of ammonium magnesium arsenate precipitate. The precipitate coprecipitates a substantial amount of tungsten, resulting tungsten loss. Some arsenic is coprecipitated in the form of arsenic sulfide during the precipitation of Mo impurity. Other methods, for example adsorption of arsenic impurities on a freshly precipitated ferric hydroxide, extraction of arsenic in the form of heteropolyacids, or volatilizing of As_2O_3

during the roasting of tungsten ore have been published, although their practical efficiency is questionable.

2 EXPERIMENTS AND RESULTS

Our study to find a new process for the removal of As was initiated by our general environment preserving process for producing APT (Vadasdi, 1985). This basic process was invented many years ago and since then we have developed a small size production plant. Our process basically follows the LIX process, but before the solvent extraction step we recover the sodium hydroxide from the sodium tungstate solution with the help of electrodialysis. The recovered sodium hydroxide is reused for leaching. The incorporation of electrodialysis into the LIX process and its coupling with the purification steps of Na_2WO_4 required certain modifications. It can be understood that precipitates are undesirable in a membrane technology.

We wanted to replace the molybdenum precipitation method, which worked in acidic pH range around pH 2-3, with another method working in alkaline pH region. Trying to replace the molybdenum precipitation method, we had to study the behaviour of As as well. The industrial solvent extraction of As is not a widely developed field. There are only a few methods published or patented, mostly for the purification of electrolytic copper refining circuits (Baradel, 1986; Guerriero, 1985; Marr, 1983; Takahashi, 1976). We did not try to apply these methods because their operating range is acidic. In acidic pH ranges the tungsten forms extremely stable heteropolyacid compounds with the arsenic, for example

$[AsW_9O_{33}]^{9-}$, $[AsW_{11}O_{39}]^{7-}$, $[AsW_{12}O_{40}]^{3-}$, $[As_2W_{18}O_{62}]^{6-}$, $[As_2W_{19}O_{67}]^{4-}$, $[As_2W_{21}O_{69}(H_2O)]^{6-}$.

These are very stable polymeric aggregates, much more stable than the usual chelate or ion association species. Therefore, the acidic extracting methods did not show great promise. In alkaline pH range the heteropolyacids are usually decomposed and therefore the separation is not hindered by this means.

A Mo extraction method has been proposed in the literature in alkaline pH ranges (MacInnis, 1981a,b). This method, invented by GE scientists, is based on the selective extraction of thiomolybdenum species by quaternary amines in the presence of great excess of tungsten. When we tested the extraction of molybdenum with Aliquat 336 we tested the behaviour of As as well.

Fig. 1 shows our measurements. The molybdenum is extracted well between pH 8-10. Neither in this publication nor in other literature we could find anything about of As under such circumstances. The As is extracted well with a narrower extraction range but with a remarkable efficiency.

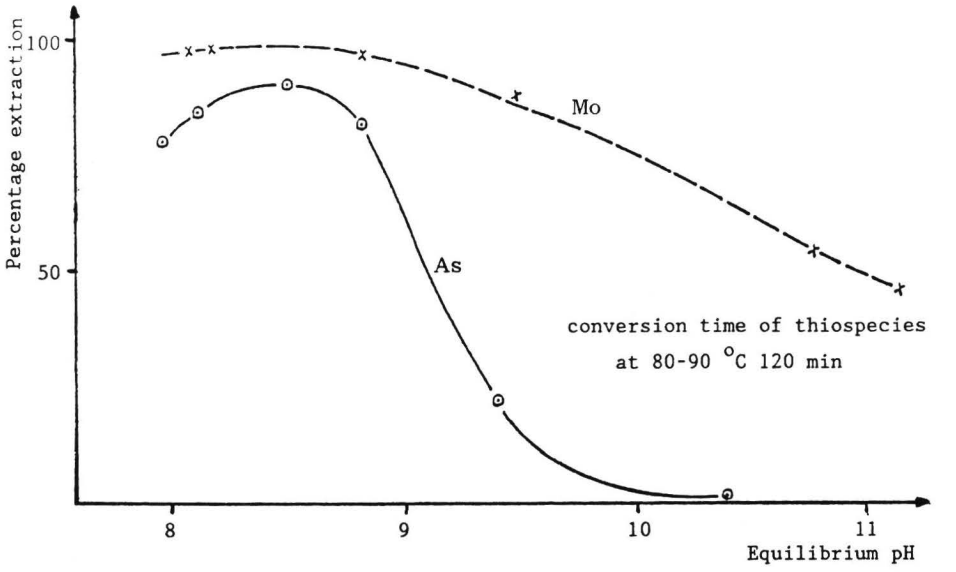

Fig. 1. Extraction of thiocomplexes of As and Mo by Aliquat 336.

Table 1 shows the extraction of As from a synthetic solution having a composition of 100 g/dm^3 W, 100 mg/dm^3 As at pH 8.5. This is the maximum extraction of As.

TABLE 1

Effect of sulfide ion concentration on the extraction of As and W.

Amount of S^{2-} ion as $NaHS.H_2O$	Extn. of As (%)	Extn. of W (%)
1x stoich. amount	80	3
2x stoich. amount	95	5
3x stoich. amount	95	4
4x stoich. amount	97	8

Table 2 compares the extracting capacibilities of different types of industrially available primary, secondary, tertiary and quaternary amines at pH 8.5. It should be noted that we have used an aromatic Shellsol base solvent, 5 % decanol and 5 % of amine in each cases. Phase ratio is 1:1.
Though the distribution coefficient of the quaternary amine is the highest, the other amine types can also come to role in the practical application since the quaternary Aliquat is the amine having tungsten extracting ability at higher pH ranges, above pH 4, which means that its selectivity is not the best.

Fig. 2 shows the extraction of thioarsenate species by Aliquat 336. We can understand that the formation of thiospecies is not an instant process.

TABLE 2

Extraction of thioarsenates by various amine extractants.

Type of extractant	Extraction of As (%)
Primene JM-T	83
Amberlite LA-1	75
Alamine 336	84
Aliquat 336	91

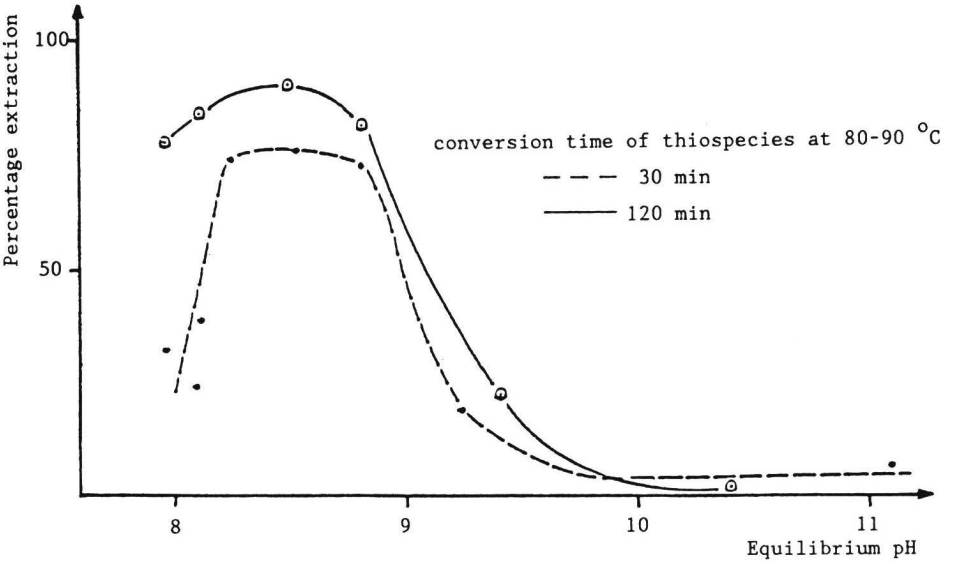

Fig. 2. Extraction of thioarsenate species by Aliquat 336.

Table 3 shows the difficulties of the stripping of As from the organic phase. Stripping is possible only in the presence of oxidizing agents with satisfactory efficiency. This means that the sulphur content of the extracted thiospecies should be oxidized to sulfate during the stripping.

On the basis of these and other similar experiments we have tested and optimised the process capable of removing As contamination from Na_2WO_4 solution on our continuous laboratory mixer-settler equipment (Szilassy, 1990).

TABLE 3

Stripping of As from the organic solution in the absence of oxidizing agent

Reagens			Stripped of As (%) (5 min., 1 stage)
NaOH-NaCl	(1-1 mol/dm^3)	25 °C	31-40
NaOH	(5 mol/dm^3)	25 °C	30-40
NaOH	(5 mol/dm^3)	50 °C	30-40
Na_2CO_3	(2 mol/dm^3)	25 °C	12-19
$(NH_4)_2SO_4$-NH_4OH	(3 mol/dm^3)	25 °C	28-50

Stripping of As from the organic solution in the presence of oxidizing agent

Oxidizing agent	Conc. (mol/dm^3)	Nonoxidizing agent	Conc. (mol/dm^3)	Stripped of As (%) (5 min., 1 stage)
NaOCl	1.26	NaOH pH ~ 13	-	76
NaOCl	0.63	NaOH pH ~ 13	-	72
NaOCl	0.32	NaOH pH ~ 13	-	80
NaOCl	0.16	NaOH pH ~ 13	-	76
H_2O_2	1	-	-	6
-	-	NaOH-NaCl	1-1	90
H_2O_2	1	NaOH pH ~ 11	-	71
-	-	NaOH-NaCl	1-1	27

3 CONCLUSION

The main advantages of our arsenic extraction method:

Better efficiency in the arsenic removal.

Carrier free collection of the arsenic in the form of reprocessable W, Mo, As concentrate.

Economic processing of low quality raw materials.

The simple possibility of coupling with recovery process of NaOH by electrodialysis.

4 REFERENCES

Baradel, A., Guerriero, R., Meregalli, L. and Vittadini, I., 1986. ISEC '86, München, Proc. Vol. II pp. 401-7.

Benesovsky, F., 1979. Gmelin Handbuch der Anorganischen Chemie Ergänzungsband A 1. In: K. Swars (Editor), Springer-Verlag, Berlin, pp. 44-6.

Guerriero, R., Veronese, G., Baradel, A. and Rivola, L., 1985. Process for the separation of arsenic from acidic solutions containing it. UK Patent Application GB 2 151 220 A.

MacInnis, M.B. and Kim, T.K., 1981. Method for removing molybdenum from tungstate solutions by solvent extraction. United States Patent 4,278,642.

MacInnis, M.B. and Kim, T.K., 1981. Separating molybdenum values from an aqueous solution containing tungsten by solvent extraction. United States Patent 4,288,413.

Marr, R., Bart, H.J. and Wachter, R., 1983. Verfahren zum Abtrennen von Arsen aus einem Kupferelektrolyten. European Patent EP 0 106 118 A1.

Millner, T., Neugebauer, J. and Imre, L., 1961. Festkörperphyzik. Akad. Verlag, Berlin, pp. 227-33.

Szilassy, I., Vadasdi, K., Sümeghy, L., Árvay, P. and Oláh, R., 1990. Process for removing arsenic from alkaline tungstate solutions. Patent Pending.
Takahashi, M., Itoh, E., Urawa, S. and Nagai, T., 1976. Verfahren zur Entfernung von Arsen aus einer Arsen zusammen mit Kupfer enthaltenden Lösung. German Patent DT 26 03 874 A1.
Vadasdi, K., Oláh, R., Szilassy, I. and Jeszenszky, A., 1985. 11th Intern. Plansee Seminar, Reutte, Proc. Vol. I pp. 77-89.
Yih, S.W.H. and Wang, C.T., 1979. Tungsten, Plenum Press, New York.

Solvent Extraction 1990, T. Sekine (Editor)

© 1992 Elsevier Science Publishers B.V. All rights reserved

ACORGA CLX50 - A PYRIDINE CARBOXYLIC ESTER BASED EXTRACTANT FOR THE SOLVENT EXTRACTION OF COPPER FROM CHLORIDE LEACH SOLUTIONS

RAYMOND F.DALTON AND ARTHUR BURGESS
Imperial Chemical Industries Plc, Colours and Fine Chemicals P.O. Box 42, Hexagon House, Blackley, Manchester M9 3DA, UK,
RAYMOND PRICE, Consultant for Nerco Minerals Co. Vancouver, Washington USA,
ENRIQUE HERMANA, Technicas Reunidas S.A., Madrid, Spain.

ABSTRACT
The past two decades have seen great interest in the development of chloride based hydrometallurgical process for the recovery of metals from sulphide ores. Until recently however, utilisation of chloride processes for the production of copper has been inhibited by their inability to produce pure copper directly without the need for further refining. The reagent Acorga CLX50 has been developed specifically to overcome this problem by enabling the solvent extraction of copper from chloride leach solutions without the need for pH adjustment and with very high selectivity over other metals and metalloids. Extraction of copper is favoured by a high chloride ion concentration and stripping is effected by contacting with hot water. The utility of the reagent has now been demonstrated by its use in a successful long term pilot plant operation of The CUPREX Metal Extraction Process, a new chloride based process for the recovery of copper from sulphide ores.

INTRODUCTION

ACORGA CLX50 is a commercial formulation of development reagents referred to in earlier publications (Dalton, Price et al 1983,1984) as DS5443 or CLX20. It is based on a formulation of the active constituent of these earlier extractants which is a diester of pyridine 3,5- dicarboxylic acid. The reagent was developed primarily in order to provide a solvent extraction step in chloride based hydrometallurgical processes for copper and thus facilitate their production of a pure copper product. Earlier work (Dalton et al 1984), characterised this extractant in the context of its use for the extraction of copper from chloride solutions by reference to the important "S" properties of an ideal solvent extraction reagent a summary of which are given below.

STRENGTH	- Ideal, with high metal recoveries and facile stripping.
SELECTIVITY	- Highly selective for copper over other metals and metalloids.
SOLUBILITY	- Extractant and its copper complex are highly soluble in kerosene.
SPEED	- Very fast rates of extraction and stripping.
SEPARATION	- Rapid, clean phase separations.
STABILITY	- Reagent has very high stability in aggressive chloride systems.
SYSTEM	- Good integration with the rest of the metal extraction process.

ACORGA CLX50 is ideally suited for the extraction of copper from chloride media since the loading and stripping operations are governed by chloride ion concentration in the aqueous phase. It is capable of transferring large amounts of copper in the cupric oxidation state with no need for pH adjustment and with very high selectivity over a wide range of metals and metalloids.

EXTRACTION BEHAVIOUR OF ACORGA CLX50

In a recent study we have used slope analysis techniques to investigate the dependence of the copper distribution (D) on aqueous chloride ion activity [Cl^-] estimated from mean ionic activity coefficient data, and the free ligand concentration [L] in the organic phase. Plots of log D as a function of log[Cl^-] and log[L] are linear over a considerable concentration range with slopes of 2 (+/- 0.2) and are indicative of a relationship:

$$\log D = \log K + 2\log[Cl^-] + 2\log[L],$$

thus confirming that extraction behaviour is in accord with equation (1)

$$Cu^{2+}_{(AQ)} + 2Cl^-_{(AQ)} + 2L_{(ORG)} \longrightarrow L_2CuCl_{2(ORG)} \quad .....(1)$$

The large deviations from ideal solution behaviour that result in exceptionally high activity coefficients in strong chloride solutions are of benefit in giving high copper extraction distributions at high chloride ion concentrations. The extraction equilibria of copper by ACORGA CLX50 are also quite sensitive to temperature. Thus, extraction at ambient temperature (25^oC) and at the high chloride ion concentrations encountered in chloride leach solutions gives high copper recoveries. Stripping with water at 60-65^oC, however, facilitates the attainment of very concentrated pregnant copper electrolyte solutions (> 100g/l Cu) with a completely stripped organic phase.

THE CUPREX METAL EXTRACTION PROCESS

The practical utility of ACORGA CLX50 has now been demonstrated by its use in a successful large scale pilot plant operation of the CUPREX Metal Extraction Process (CMEP), a new chloride based hydrometallurgical process for the recovery of copper from sulphide ore concentrates (Dalton, Price, Hermana and Hoffmann 1987). The process has been developed by a Joint Venture partnership between Imperial Chemical Industries Plc, Nerco Minerals Company of the USA and the Spanish engineering Company Tecnicas Reunidas S.A. It incorporates several novel steps to overcome the major problems associated with earlier chloride based processes, including a solvent extraction step using Acorga CLX 50 to produce a pure, highly concentrated cupric chloride electrolyte from which copper is electrowon in a membrane divided (METCLOR) cell developed by Tecnicas Reunidas. This results in a very pure copper product equivalent to that produced by conventional electrorefining. The mild leaching conditions employed facilitate the recovery of valuable by- and co-products such as sulphur, molybdenite and gold. Silver if present in the concentrates is leached and may be recovered by cementation. The technical viability and robustness of the process have now been clearly demonstrated by a series of trials carried out over a period of one year in a one ton per day (ore concentrate) pilot plant located at the research centre of Tecnicas Reunidas S.A. near Madrid, Spain.

FIG.1. THE CUPREX METAL EXTRACTION PROCESS

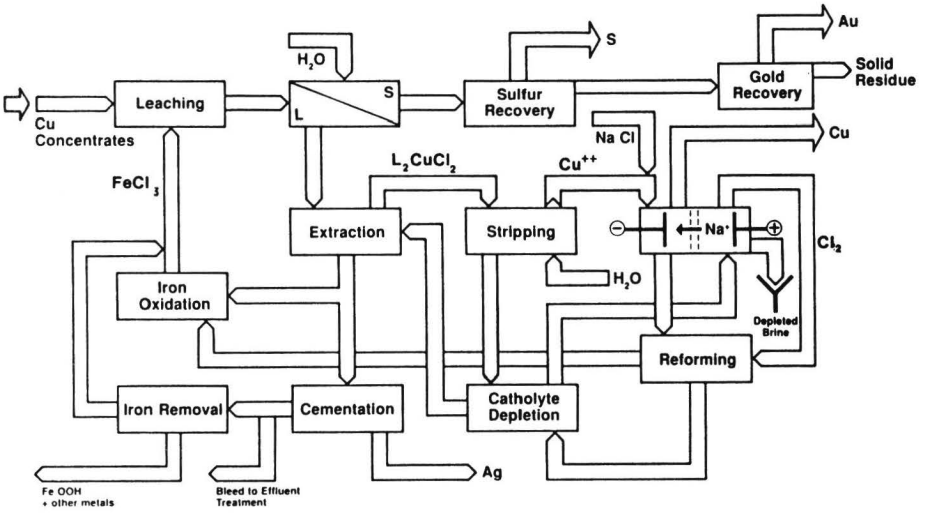

The CUPREX Metal Extraction Process flowsheet is shown in Fig.1 above. Concentrate is leached at atmospheric pressure with ferric chloride solution at about 95°C to produce a solution in which all the copper is in the divalent oxidation state (equation 2) and with the liberation of elemental sulphur.

$$CuFeS_2 + 4FeCl_3 \longrightarrow CuCl_2 + 5FeCl_2 + S \quad .....(2)$$

The reaction mixture is then cooled and passed to a thickener and filtration. The clarified pregnant liquor containing approximately 25 g/l copper, 120 g/l iron, minor amounts of impurities, mainly zinc, lead and silver, and 5.5 to 6 molar in chloride ion is then sent to the extraction stage of the solvent extraction circuit.

The solvent extraction circuit used in the pilot plant operation comprised 2 Extraction, 2 Scrub, 4 Strip and 2 Depletion stages and employed a 50^{v}/o solution of the reagent Acorga CLX50 in Escaid 100. Its function should be viewed with respect to Fig.2 which shows diagramatically how it is integrated with the rest of the CUPREX Metal Extraction Process. In essence the functions of the various parts of the solvent extraction circuit are as follows.

i) **Extraction** to isolate copper from the leach liquor with high selectivity over other metals.

ii) **Stripping** to provide a pure, highly concentrated cupric chloride electrolyte as well as regenerating the extractant solution.

iii) **Depletion** to remove copper from the spent catholyte so that the resulting pure brine solution can be used as anolyte.

FIG.2. CMEP SOLVENT EXTRACTION - ELECTROWINNING CIRCUIT

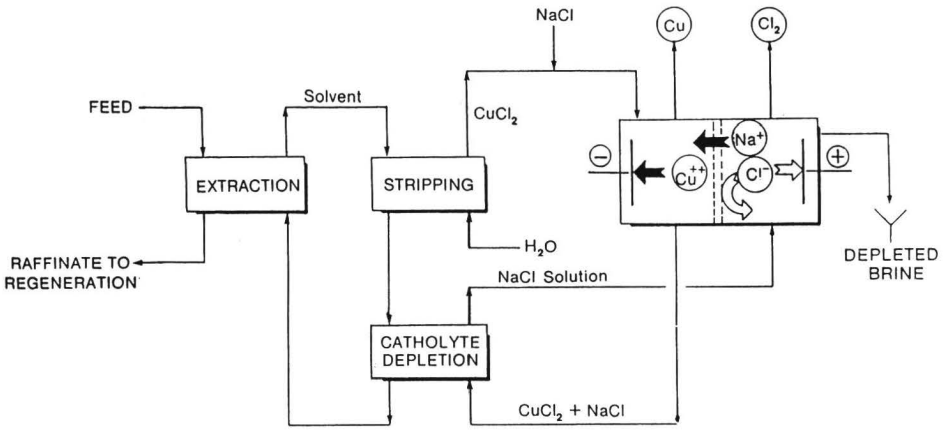

In the Pilot plant operations the extraction section consistently produced raffinates containing less than 0.5g/l copper. The loaded organic then passed to two stages of scrubbing where it was contacted at high organic to aqueous phase ratio with a bleed taken from the spent anolyte (approximately 3 molar sodium chloride solution). This is essential to remove entrained aqueous which contains high concentrations of impurities, e.g. 120g/l of iron.

The scrubbed organic passed to stripping where it was stripped by contact with 5 g/l hydrochloric acid at 60 - 65^{o}C. The small amount of acid is required merely to prevent precipitation of basic salts such as copper oxychloride. In the pilot plant operations the stripping stage consistently produced advanced aqueous electrolytes containing up to 110 g/l copper and a completely barren organic.

In the Depletion section copper in the reformed spent catholyte is reduced from approximately 10 gl^{-1} to less than 0.1 gl^{-1} by contact with regenerated extractant solution with which it is contacted at high O/A ratio. The organic solvent, now containing a relatively small amount of copper returns to the extraction stage of the solvent extraction circuit.

The chloride ion content of the aqueous extract obtained from stripping is increased by the addition of sodium chloride to enhance its conductivity and to minimise the possibility of precipitation of cuprous chloride on reduction. It is then fed to the cathode compartment of the METCLOR electrowinning cell.

This is a two compartment cell in which anode and cathode are separated by NAFION ion exchange membrane. A granular copper product is produced at the titanium cathodes and is removed continuously from the cells, washed, and dried. Chlorine gas is produced at the anode and collected for reuse in the process. The spent catholyte which contains copper in the cuprous and cupric oxidation states plus the added sodium chloride is sent to the reforming stage.

In the reforming stage some chlorine is used to oxidise monovalent copper in the spent catholyte to the divalent oxidation state to facilitate its removal in the depletion stage of the solvent extraction circuit. The copper-depleted aqueous brine solution is fed to the electrolysis cell as anolyte.

Excess iron in the leach raffinate resulting from leaching of chalcopyrite is removed as goethite in a pressure oxidation stage simultaneously regenerating part of the leachant (equation 3). The remainder of the leachant is regenerated using chlorine from the electrolysis stage (equation 4).

$$6FeCl_2 + 1.5O_2 + H_2O \text{ ----> } 2FeO(OH) + 4FeCl_3 \quad .....(3)$$

$$2FeCl_2 + Cl_2 \text{ ----> } 2FeCl_3 \quad .....(4)$$

In the demonstration plant copper in the scrubbing and washing liquors was precipitated as copper sulphide and returned to the leaching stage. Other metal cations were precipitated by a combination of liming and sulphide treatment to produce environmentally acceptable solid and liquid effluents.

Any silver present in the original concentrate is leached and reports in the raffinate from the solvent extraction stage. Since the copper concentration in this solution is very low recovery of silver by zinc dust cementation is a practical proposition.

SUMMARY OF PILOT PLANT EXPERIENCE

All of the steps in the CUPREX Metal Extraction process comprising leaching, solvent extraction, electrowinning, leachant regeneration, and treatment of liquid effluents have been tested in the continuous pilot plant operations at the Torrejon facility of Tecnicas Reunidas S.A. The plant, with a capacity of 0.3 tonne copper per day was operated on a continuous 24 hour per day basis during a series of trials, each of which lasted up to three weeks. The plant was highly automated and contained as much on line instrumentation as would be required in a commercial scale plant. A single stage leaching operation was used comprising five reactors arranged in series. Leach efficiencies of greater than 97% were obtained with a residence time of 9 to 10hrs at 95-100^{o}C leading to an overall copper recovery in the process of greater than 96%.

The solvent extraction circuit proved to be robust, relatively insensitive to fluctuations in conditions and consistently produced a very pure cupric chloride electrolyte. No signs of either decomposition or deterioration in the performance of the extraction reagent were detected during the entire period of operations.

Electrowinning operated well with copper being electrowon at a current efficiency greater than 94% and current density of 1.5 kA/m^2. Mean Power consumption in the cells during the Demonstration plant trials was 2.6 KWhr per Kg copper produced. Optimisation of solution composition and electrowinning conditions produced a coarse granular copper product which could be readily washed free of chloride and other contaminants. Analysis of numerous samples taken throughout the trials showed the copper to be of cathode quality with very low levels of contaminants. A typical analysis of impurities in copper produced from a chalcopyrite concentrate from the South West USA is given below. All concentrations are in parts per million (ppm); n.d. indicates not detected.

Al	Sb	As	Bi	Cd	Cr	Co	Fe	Pb	Mg	Mn	Ni	Se	Ag	Te	Zn
0.32	3.7	0.3	nd	0.05	nd	0.7	3.2	nd	3.7	0.36	nd	nd	0.5	0.5	nd

No problems were encountered in the depletion and regeneration stages and excess iron was successfully removed from the extraction raffinate as a filterable goethite precipitate.

SUMMARY

In summary the pilot trial demonstrated the mutual compatibility of the four main sections of the CUPREX Metal Extraction Process: leaching, solvent extraction, electrowinning and leachant regeneration. Inevitably problems were encountered but satisfactory solutions were found and implemented during the course of the demonstration plant operations. Possibly the most important result to emerge from the pilot operation was the ability of the CUPREX Metal extraction process to produce copper of a quality matching that of the highest standards in the industry when operating under optimum conditions overall.

Long operating experience and analysis of the pilot plant data leads us to conclude that the technical and economic viability of the CMEP has been clearly demonstrated and that it may prove to be particularly attractive in a number of situations.

REFERENCES

R.F.Dalton, R.Price, and P.M.Quan, Novel solvent extractants for chloride leach systems. International Solvent Extraction Conference, Denver, Colorado, USA, Aug 26-Set 2, 1983.

R.F.Dalton, R.Price, P.M.Quan, and B.Townson, Novel solvent extractants for copper from chloride leach solutions derived from sulphide ores. Reagents in the Minerals Industry, 1984, 181. IMM London.

R.F.Dalton, R.Price, E.Hermana, and B.Hoffmann. The CUPREX Process - A New Chloride Based Hydrometallurgical Process for the Recovery of copper from Sulphidic Ores. "Separation processes in Hydrometallurgy" pp 466-476. Ed. G.A.Davies, Pub. by Ellis Horwood for SCI London. (Paper presented at International symposium, UMIST Manchester July, 1987.and at the Western Mining Congress, Denver, USA. Feb 1987.)

NOTE The word ACORGA is a registered trade mark of ACORGA Ltd., a wholly owned subsidiary of Imperial Chemical Industries Plc.

Solvent Extraction 1990, T. Sekine (Editor)

© 1992 Elsevier Science Publishers B.V. All rights reserved

MIXED SOLVENT EXTRACTION-ANNULAR CHROMATOGRAPHIC SYSTEMS FOR F-ELEMENT SEPARATION AND PURIFICATION

J.D. NAVRATIL*, A. MURPHY and D. SUN
Department of Mineral Processing and Extractive Metallurgy, The University of New South Wales, P. O. Box 1, Kensington NSW 2033 Australia

ABSTRACT

Neutral bifunctional organophosphorous solvent extractants (such as carbamoylmethylphosphonates and carbamoylmethylphosphine oxides) strongly extract lanthanides and actinides and do not extract more than 40 other elements from mineral acids. Because of their excellent properties they have been found useful for f-element recovery and purification processes. A brief overview of these reagents will be given. A discussion of recent work using these reagents with monofunctional extractants on supports in an annular chromatograph for rare earth recovery and separation will also be presented.

SOLVENT EXTRACTION

Although solvent extraction technology had its beginning more than 100 years ago, it owes a significant amount of its present prominence as a separation technique to its successful application with actinide elements. Solvent extraction plays a vital role in actinide, as well as lanthanide element, separation, recovery and purification. The use of thorium, uranium and plutonium and other actinides in nuclear energy programs has led to the rapid development of many new solvent extraction processes that display simplicity, selectivity and speed.

The scientific literature abounds with articles on new solvent extractants (Lo, 1983). While many of the reagents are only of academic interest, several types of extractants show promise in improving f-element recovery, separation or purification. In the last decade there has been much interest in the potential application of certain neutral and acidic bifunctional organophosphorous compounds in actinide separations. Triggering

---

*Present address: Chemical Waste Management, Inc., Geneva Research Center, 1950 S. Batavia Ave., Geneva, IL 60134-3310 USA.

this interest is the ability of some carbamoylmethylenephosphorous (CMP) and carbamoylmethylenephosphine oxide compounds to extract trivalent actinides from strong nitric acid solutions, a property which distinguishes them from monofunctional organophosphorous compounds (Schulz, 1984).

Because CMP strongly extracts actinides and lanthanides, and does not extract more than 40 other elements from 5-7 M nitric acid, the extractant, for example, has been found useful for an americium recovery and purification process (Yamada, 1982). In the process, dihexyl-N,N-diethylcarbamoylmethylphosphonate (DHDECMP) is sorbed on a non-ionic macroreticular resin and used in an extraction chromatography mode. The process effectively separates and purifies americium from impurities such as aluminum, calcium, chloride, copper, fluoride, iron, lead, magnesium, plutonium, potassium, sodium and zinc.

Using solvent extractants sorbed onto a solid (extraction chromatography) is well known. The technique combines the attractive properties of solvent extraction (high selectivity, fast rates, high loading capacities, etc.) with the advantages of column adsorption and ion exchange (applicability to the treatment of very dilute solution, ease of liquid/solid phase separation associated with lack of serious problems, such as crud formations and solvent losses into the aqueous phase, ease of handling and simplicity of equipment, etc.)

Recently some additional advantages have been reported using the technique for actinide recovery (Muscatello, 1986). The system uses solid supports, such as styrene divinylbenzene beads, polyurethane foam, activated carbon, etc., loaded with a solid solvent extractant, such as octylphenyl-N,N-diisobutylcarbamoyl methylphosphine oxide (CMPO) or trioctylphosphine oxide (TOPO). The extractant (without diluent) is equilibrated with the support at a temperature just slightly above the melting point of the extractant. In addition to efficient sorption of ionic actinide species, polymeric species of plutonium (IV) are also effectively removed from aqueous mineral acid solutions by the solid extractant-solid support. The actinide loaded material is removed

from the column and incinerated, leaving the plutonium in the residue for further recovery.

The advantages of the technique are as follows: (1) The CMPO or TOPO removes actinides in all oxidation states as well as actinide polymers. (2) The purity of the extractant is not critical since no back extraction step is needed. Thus acid hydrolysis or radiation damage to the reagent should not be a problem, and solvent clean-up steps and solvent pollution problems are eliminated. (3) No diluent is needed, only an inexpensive and combustible support material. (4) The process yields high recoveries and has a high concentration factor.

We have recently applied the above reagents and extraction chromatography techniques for the recovery and separation of rare earths. We are using DHDECMP-D2EHPA mixtures on solid supports in conjunction with an annular chromatograph. The following will briefly review this device.

2 ANNULAR CHROMATOGRAPHY

The large-scale and difficult separation of rare earths and trivalent actinide elements would greatly benefit from an improved continuous chromatographic operational device. Truly continuous, multi-component chromatographic separations may be achieved by means of the annular chromatograph. This section briefly reviews the annular chromatograph, its description, operation, applications and potential use for f-element separation and purification.

The development of large-scale chromatographic processes has been biased toward the batch-mode until recently when a number of alternative continuous systems were introduced. "Continuous" refers to any configuration which uses continuous feed introduction; the system utilizes the available mass transfer area, offers constant product quality, and does not require product recycling, resulting in higher throughputs. The separation and purification of f-elements would greatly benefit from an improved continuous chromatographic operational device such as the annular chromatograph.

Martin (1949) was the first to consider an annular chromatograph

rotating with respect to fixed continuous feed and product streams, and later Giddings (1962) reported that a larger capacity is theoretically possible in an annular device with the same resolution as a conventional column. A semicontinuous chromatographic unit consisting of an assembly of 100 conventional columns was reported by Dinelli (1962). Since 1974, various versions of a truly continuous annular chromatographic apparatus have been constructed and tested by workers at Oak Ridge National Laboratory (Scott, 1976; Canon, 1978; Begovich, 1983). The applications for metals separation of their equipment as well as those of other workers are summarized in Table 1.

Table 1. Summary of applications of annular chromatography

Components separated	Reference
Blue dextran/Co	Sisson (1987)
Al/Fe	Canon (1980)
Ca/Sr	Moskvin (1975)
Cu/Ni/Co	Canon (1980), Begovich (1982)
Fe/Cr	Byers (1988)
Hf/Zr	Begovich (1983)
Hg/Cd/Cu	Moskvin (1975)
Rare earths	Navratil (1988)

The apparatus consists of an annular bed of adsorbent or ion exchange material, packed in the space between two concentric cylinders. Traditionally the column is slowly rotated while feed and eluent solutions are continuously fed to the top of the annular bed, whereas in the design of Navratil (1989), the feed nozzle and product collectors are rotated (see Figure 1). With time helical component bands develop from the feed point and the slopes depend on the distribution coefficient, eluent velocity and rotational speed. At steady state the component bands form helices between the top and bottom of the column. The portion of the bed adsorbent bed which is not receiving feed is being eluted or regenerated.

The inherent advantages of the annular chromatograph are:

1) Completely continuous
2) Cross-current operation
3) Separates multicomponent mixtures

4) Simple-no timing equipment required

The practical limitations are:

1) Three-dimensional dispersive effects occur in annular bed
2) Need for high pressure or very large-scale operation
3) Compatibility of materials of construction with feed and eluent.

Work has been initiated at The University of New South Wales involving the development, demonstration and modeling of the improved annular device for the separation and purification of rare earths. The annular bed contains Amberlite XAD-4 loaded with a mixture of DHDECMP and D2HEPA. Initial tests have shown that the system has an advantage in relation to resolution and capacity compared to using the supported extractants alone.

3 REFERENCES

Begovich, J.M.,Ph.D. dissertation, The University of Tennessee, Knoxville, 1982.

Begovich, J.M. and Sisson, W.G., Hydrometall. 10, 1983, 11.

Begovich, J.M., Byers, C.H., and Sisson, W.G., Sep. Sci. Technol., 18, 1983, 1167.

Byers, C.H., Sission, W.G., and DeCarli, J.P., Presented at IEX '88, Cambridge, U.K., 1988.

Canon, R.M. and Sisson, W.G., J. Liq. Chromatogr. 1, 1978, 427.

Canon, R.M., Begovich, J.M., and Sisson, W.G., Sep. Sci. Technol.,15, 1980, 655.

Dinelli, D., Polezzo, S., and Taramasso, M., J. Chromatogr. 7, 1962, 477.

Giddings, J.C., Anal. Chem., 34, 1962, 37.

Lo, T.C., Baird, M.H.I., and Hanson, C., Handbook of Solvent Extraction, Wiley, New York, 1983.

Martin, A.J.P., Discuss. Faraday Soc. 7, 1949, 332.

Muscatello, A.C., Navratil, J.D. and Saba, M.T., Actinide Recovery Process, U. S. Patent 4,683,124, July 28, 1986.

Moskvin, L.N., Mozzhukhin, A.V., and Tsaritsyna, L.G., Zhur. Anal. Khim.,30, 1975, 39.

Navratil, J.D., Proceedings of Chemeca 88, Institution of Engineers, Australia, 1988,481.

Navratil, J.D., Proceedings of Eighth Australian Biotechnology Conference, UNISEARCH, Kensington, NSW, 1989, 203.

Schulz, W.W., and Navratil J.D., Sep. Sci. Technol, 19, 1984, 927.

Scott, C.D., Spence, R.D., and Sisson, W.G., J. Chromatogr., 126, 1976, 381.

Sisson, W.G., Begovich, J.M., Byers, C.H., and Scott, C.D., ACS National Meeting, New Orleans, LA, 1987.

Yamada, W.I., Martella, L.L., and Navratil, J.D., J. Less-Common Met., 86, 1982, 211.

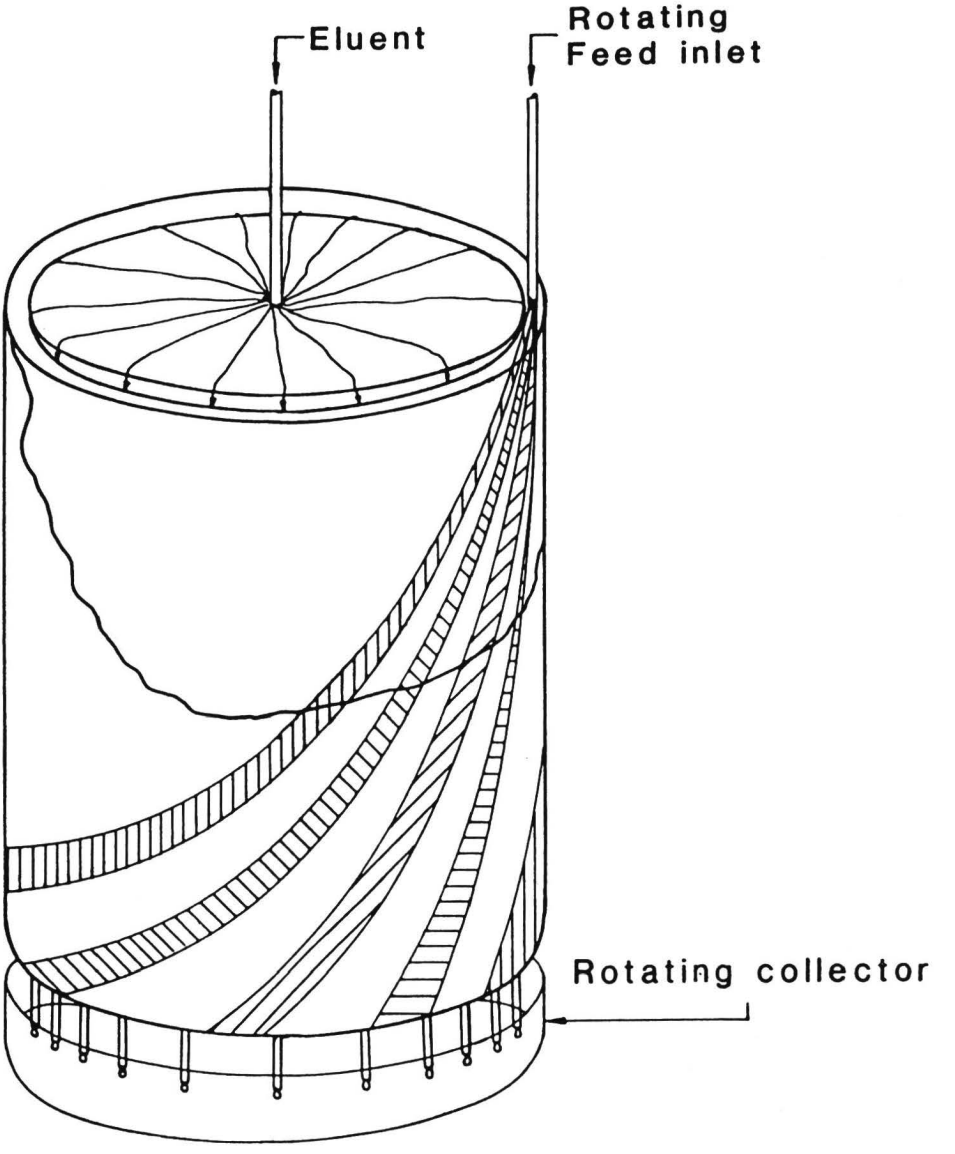

Figure 1. Simplified schematic of the annular chromatograph with rotating feed nozzle and solute collectors.

Solvent Extraction 1990, T. Sekine (Editor)

© 1992 Elsevier Science Publishers B.V. All rights reserved

APPLICATION OF PITZER'S EQUATIONS TO THE ANALYSIS OF EXTRACTION EQUILIBRIA OF Cu(II) FROM HYDROCHLORIC ACID SOLUTIONS WITH HYDROXYOXIMES UNDER PRACTICAL CONDITIONS

Mikiya TANAKA
National Research Institute for Pollution and Resources, MITI, 16-3, Onogawa, Tsukuba 305, Japan

ABSTRACT
Tanaka, M., 1990. Application of Pitzer's equations to the analysis of extraction equilibria of Cu(II) from hydrochloric acid solutions with hydroxyoximes under practical conditions.

Equilibrium distribution ratios of Cu(II) in the extraction from HCl solutions have been measured at 298 K under the initial aqueous Cu(II) concentration of 0.1 mol·dm^{-3} using LIX65N and SME529 as extractants and n-heptane and xylene as diluents. In a comparison with literature data, Pitzer's equations have been found to offer reliable estimates for the activity ratios, $a(H^+)^2/a(Cu^{2+})$, under the experimental conditions. The nonlinear least-squares analysis of the extraction data employing Pitzer's equations enables the simultaneous determination of the extraction and the aggregation constants which can be used for accurate distribution predictions.

1 INTRODUCTION

A chemically based correlation of extraction behavior under hydrometallurgically practical conditions has been hindered by the nonideality in aqueous and organic phases. However, semiempirical equations for thermodynamic properties of concentrated and mixed electrolytes developed by Pitzer (1979) are very attractive in handling this difficulty as far as the aqueous phase is concerned. The present author has already applied these equations to the modeling of Cu(II) extraction equilibrium systems from acidic solutions with Acorga P-5100 and demonstrated the usefulness of the model to predict the extraction behaviors under practical conditions (Tanaka,1990a,b,c). As an extension of our previous studies, this paper has dual purposes; first, to investigate the reliability of the activity ratios, $a(H^+)^2/a(Cu^{2+})$, in the solution system of HCl-$CuCl_2$-H_2O estimated by Pitzer's equations by a comparison with literature data; and second, to present a method for the analysis of equilibrium data of the Cu(II) extraction with β-hydroxyoxime extractants under practical conditions.

2 EXPERIMENTAL

2.1 Preparation of working solutions

LIX65N and SME529, respectively supplied by Henkel Corp. and Shell Chemical

Co., Ltd. were used without further purification from a practical standpoint. These were dissolved into reagent grade n-heptane and xylene to prepare 5, 10, and 20 vol% organic working solutions. The active hydroxyoxime contents were determined by an ultimate copper-loading at the pH range from 6 to 9.

A stock solution of copper chloride was prepared by dissolving $CuCl_2 \cdot 2H_2O$, (reagent grade) into water. Aqueous working solutions were prepared by mixing appropriate amounts of the stock solution and of a hydrochloric acid solution of an appropriate concentration titrated by a sodium hydroxide standard solution. The concentration of Cu(II) in the working solutions is 0.1 $mol \cdot dm^{-3}$ and those of HCl range from 1.00×10^{-2} to 1.00 $mol \cdot dm^{-3}$.

2.2 Extraction and analysis

The extraction procedure and the method of Cu determination were described elsewhere (Tanaka, 1990b). The relative deviation of the mass balance of Cu concentrations before and after the extraction was 1.9% at the maximum, and the relative deviations for 89% of the data were less than 1.0%. The distribution ratio was calculated from the copper concentrations in both phases. The hydrogen ion concentration was calculated by the mass balance equation.

3 METHOD FOR NUMERICAL ANALYSIS

The stoichiometric relation of the extraction of Cu(II) with β-hydroxyoxime extractants is well-known (e.g. Tanaka 1990a,b). The apparent extraction constant, K_e, is defined in the same manner as in our previous studies (Tanaka, 1990a,b); namely, activity coefficients of the organic phase species are assumed to be constant while changes in activity coefficients of the aqueous phase species are taken into account. Thus, the following equation can be derived:

$$\log [a(H^+)^2/a(Cu^{2+})] = 2\log [\overline{HR}] - \log [\overline{CuR_2}] + \log K_e \qquad (1)$$

Here, superscripts represent the organic phase species. The left part of eqn. (1) can be calculated using Pitzer's equations and equilibrium molalities of the ions in the aqueous phase. The detail of Pitzer's equations for the activity coefficient is explained elsewhere; thus, only the expression for the activity coefficient ratio, $\gamma(H^+)^2/\gamma(Cu^{2+})$, is described here:

$$\begin{aligned} \ln [\gamma(H^+)^2/\gamma(Cu^{2+})] = {} & -2f^{\gamma} + 2m_{Cl}[(2B_{HCl} - B_{CuCl}) + m_{Cl}(2C_{HCl} - C_{CuCl}) \\ & - (m_H B'_{HCl} + m_{Cu} B'_{CuCl})] - (m_H - 2m_{Cu})[2(^{S}\theta_{HCu} + {}^{E}\theta_{HCu}) + m_{Cl}\psi_{HCuCl}] \\ & - 2m_H m_{Cu} \theta'_{HCu} \end{aligned} \qquad (2)$$

Symbols of f^{γ}, B, C, $^{S}\theta$, $^{E}\theta$, θ', and ψ have the same meanings as those in the

series of Pitzer's publications. Note that throughout this paper stoichiometric activity coefficients are used with respect to the aqueous phase species. Single salt parameters needed in the calculation were taken from Pitzer et al. (1973) for HCl and from Downes et al. (1976) for $CuCl_2$. Since equilibrium data are taken in molarity, conversion of molarity to molality is carried out by estimating the excess volume of the aqueous phase also by Pitzer's equations detailed by Connaughton et al.(1989). Single salt parameters needed in the calculation were taken from Pogue et al. (1988) for $CuCl_2$ and were determined by the least-squares method from the density data (Washburn, 1928) for HCl. Mixing coefficients, $\theta_{HCu}{}^{V}$ and $\psi_{HCuCl}{}^{V}$, were neglected.

The leading term on the right part in eqn. (1) can be calculated by the successive aggregation model proposed by Whewell et al. (1977). This model gives the following expression for $[\overline{HR}]$:

$$[\overline{HR}] = [2K_s[\overline{HR}]_T + 1 - 4K_s[\overline{CuR_2}] - (4K_s[\overline{HR}]_T + 1 - 8K_s[\overline{CuR_2}])^{1/2}]/[2([\overline{HR}]_T - 2[\overline{CuR_2}])K_s{}^2] \quad (3)$$

where K_s is the stepwise aggregation constant.

Consequently, K_e and K_s are determined by the nonlinear least-squares method regarding the left part in eqn. (1) as the observed value and $[\overline{CuR_2}]$ as the abscissa. The Gauss-Newton method in SALS (Nakagawa et al., 1980) is used as a least-squares program.

4 RESULTS AND DISCUSSION

Majima et al. (1988) calculated mean activity coefficients of solutes in the solution system of $HCl-CuCl_2-H_2O$ at 298 K by the McKay-Perring method based on water activities measured by themselves. Their study enables the check of the accuracy of Pitzer's equations for this solution system. Thus, $a(H^+)^2/a(Cu^{2+})$ in this solution system are compared in Fig. 1. The solid curves include the contribution from $^{E}\theta$ which is the ionic strength dependent term (Pitzer, 1983), while the broken curves do not. Values of $^{S}\theta_{HCu}$ and ψ_{HCuCl} , which are ionic independent constants, are taken to be zero in both cases. This figure demonstrates that coincidence between the calculated and the observed values are very good in a relatively dilute region and is substantially improved by the consideration of $^{E}\theta$. The correlation coefficients, r, and the root mean squares of the residuals in log $[a(H^+)^2/a(Cu^{2+})]$, rms, in the region of $m(CuCl_2)$ = 0.2 $(mol \cdot kg^{-1})$ and $m(HCl) \leq 1.4$ $(mol \cdot kg^{-1})$, which is the nearest to our extraction experiment, are calculated as $r^2 = 0.99994$, rms = 0.052 (without $^{E}\theta$) and $r^2 = 0.99999$, rms = 0.020 (with $^{E}\theta$). A trial for determining $^{S}\theta_{HCu}$ and ψ_{HCuCl} by the least-squares method from water activity data (Awakura et al., 1987) showed that the obtained values were accompanied with large uncertainties

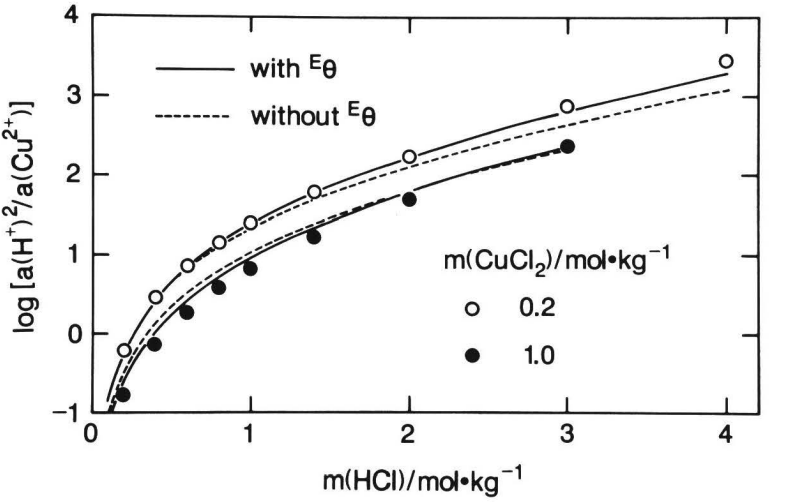

Fig. 1 Log $[a(H^+)^2/a(Cu^{2+})]$ as a function of m(HCl) in the solution system of $HCl-CuCl_2-H_2O$.

and values of zero were included in these uncertainties for both $^{S}\theta_{HCu}$ and ψ_{HCuCl}. We decided, therefore, in the following activity calculation, to include $^{E}\theta$ and to set $^{S}\theta_{HCu}$ and ψ_{HCuCl} at zero.

The experimental results of the extraction are shown in Fig. 2 as log D vs. - log $[H^+]$ plots. From these data, unknown constants are determined and listed in Table 1 together with r^2 and rms in log D when these constants are used. The detailed procedure for the calculation of log D was described in Tanaka (1990c). As seen in this table, very good agreement between the observed and the calculated log D values are obtained, which is also visualized in Fig. 2 where the log D values calculated by using the obtained equilibrium constants are depicted by the solid curves.

Table 1 shows that the values of K_e and K_s for n-heptane are much higher than those for xylene. This is generally accepted and is ascribed to the difference of hydrogen bonding capabilities between these diluents. The K_s value of 3.5 $dm^3 \cdot mol^{-1}$ by Whewell et al. (1979) for LIX64N in Escaid 100 is intermediate between our values for LIX65N in n-heptane and in xylene, which is reasonable if we take into account that Escaid 100 contains ca. 20% of aromatic compounds.

Our previous result for Acorga P-5100 (Tanaka, 1988) and the present results show that aggregating tendency increases in the sequence: P-5100 < SME529 < LIX65N. This is in agreement with VPO results by Whewell et al. (1977) although our values are significantly lower than theirs. This discrepancy seems to be mainly due to the effects of impurities (nonylphenol and kerosene in the received extractants) in our study.

Furst et al. (1988) and Haung (1989) independently parametarized for the

calculation of free activity coefficients in the solution system of HCl-$CuCl_2$-H_2O by Pitzer's equations. Although the use of free activity coefficients has some merits, numerous parameters are required in the calculation. On the contrary, the use of stoichiometric coefficients reduces the number of

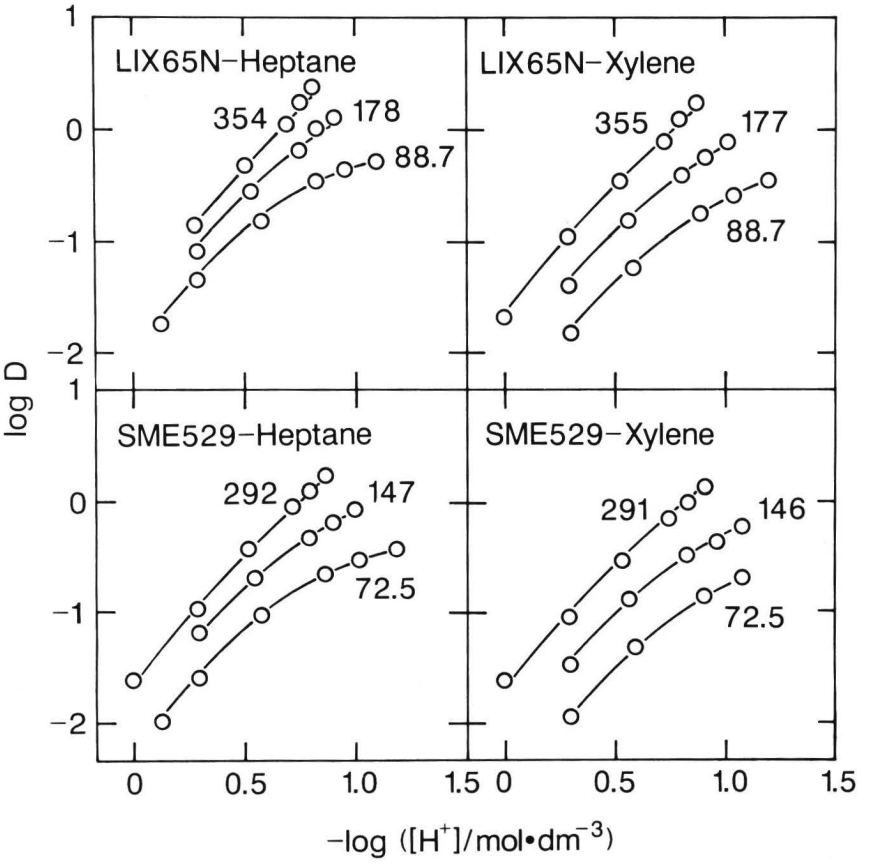

Fig. 2 Relationship between log D and -log [H^+] in the various extraction systems. Numerals in the figure denote total oxime concentrations (mol·m^{-3}).

TABLE 1 Results of the numerical analysis.

Extractant	Diluent	log (K_e/dm^3·mol^{-1})	K_s/dm^3·mol^{-1}	r^2	rms
LIX65N	n-heptane	1.54 ± 0.05	9.1 ± 1.0	0.9992	0.036
LIX65N	xylene	0.43 ± 0.02	1.3 ± 0.1	0.9994	0.019
SME529	n-heptane	1.18 ± 0.03	5.4 ± 0.4	0.9989	0.025
SME529	xylene	0.39 ± 0.03	0.9 ± 0.1	0.9983	0.027

parameters and still offers reliable estimates in our exprimental conditions as seen in Fig. 1.

We considered the difference between molarity and molality. This difference is almost negligible in the present aqueous solutions as shown in Tanaka (1990a); however, if the ionic strength is increased by the presence of other salts, such a neglect produces significant deviations of predicted log D values from the observed values (Tanaka, 1990c). Thus, for the rigorous treatment, we incorporate the excess volume estimation into the present approach.

In conclusion, we have found that Pitzer's equations offer reliable estimates of $a(H^+)^2/a(Cu^{2+})$ under the present experimental conditions, and that the method presented here for the numerical analysis of the extraction data enables the simultaneous determination of K_e and K_s values which can be used for accurate distribution predictions.

5 ACKNOWLEDGMENTS

The author wishes to thank Mr. Y. Kurihara of Kokan Mining Co., Ltd. for his experimental assistance. The author also wishes to thank Henkel Corp. and Shell Chemical Co., Ltd. for the samples of the extractants.

6 REFERENCES

Awakura,Y., Kawasaki,Y., Uno,A., Sato,K. and Majima,H., 1987. Hydrometallurgy, 19: 137-157.
Connaughton,L.M., Millero,F.J. and Pitzer,K.S., 1989. J.Solution Chem., 18: 1007-1017.
Downes,C.J. and Pitzer,K.S., 1976. J.Solution Chem., 5: 389-398.
Furst,W., Hachimi,S. and Renon,H., 1988. J.Solution Chem., 17: 953-965.
Haung,H.-H., 1989. J.Solution Chem., 18: 1069-1084.
Majima,H. and Awakura,Y., 1988. Metall.Trans.B., 19B: 347-354.
Nakagawa,T. and Oyanagi,Y., 1980. In: K.Matsushita (Editor), Recent Developments in Statistical Inference and Data Analysis. North Holland, Amsterdam, pp.221-225.
Pitzer,K.S., 1979. In: R.M.Pytkowicz (Editor), Activity Coefficients in Electrolyte Solutions.I. CRC Press, Boca Raton, Fla., pp.157-208.
Pitzer,K.S., 1983. J.Phys.Chem., 87: 2360-2364.
Pitzer,K.S. and Mayorga,G., 1973. J.Phys.Chem. 77: 2300-2308.
Pogue,R. and Atkinson,G., 1988. J.Chem.Eng.Data, 33: 370-376.
Tanaka,M., 1988. J.Min.Met.Inst.Japan, 104: 395-401(in Japanese, with English abstract). English translation, 1990. Metall.Rev.MMIJ 7(1): 13-30.
Tanaka,M., 1990a. Hydrometallurgy 24: 317-331.
Tanaka,M., 1990b. Mater.Trans.JIM, 31: 409-414.
Tanaka,M., 1990c. In: Proc.Spring Meeting Min.Mater.Processing Inst. Japan, pp.389-390 (in Japanese).
Washburn,E.W. (Editor), 1928. International Critical Tables, Vol.III. McGraw-Hill, New York. p.54.
Whewell,R.J. and Hughes,M.A., 1979. Hydrometallurgy, 4: 109-124.
Whewell,R.J., Hughes,M.A. and Hanson,C., 1977. In: Proc.Int.Solvent Extraction Conference ISEC 77: 185-192.

Solvent Extraction 1990, T. Sekine (Editor)

© 1992 Elsevier Science Publishers B.V. All rights reserved

NEW PRODUCTION METHOD OF METALLIC OXIDE AND METAL POWDERS - APPLICATION OF SOLVENT EXTRACTION TECHNIQUE -

M. SANO, J. SHIBATA AND S. NISHIMURA
Department of Chemical Engineering, Faculty of Engineering, Kansai University, Yamate-cho 3-3-35, Suita, Osaka 564, (JAPAN)

ABSTRACT
Sano, M., Shibata J. and Nishimura S., 1990. New production method of metallic oxide and metal powders. - Application of solvent extraction technique -.

Crystallization-stripping under the pressurized CO_2 at various combinations of extractants such as VA10, SNA-180, DP-8R and PC-88A and metals such as Ag, Cu, Co, Ni, Zn and Nd were carried out to expand the applicable extraction systems.

The metal loaded in VA10 and SNA-180 can be recovered as metal carbonates. The reaction depends on CO_2 pressure, extractant concentration and metal concentration in the organic phase. The crystallized products can be converted to metallic oxide by roasting in air and changed to metal by a thermal decomposition in hydrogen atmosphere.

INTRODUCTION

The conventional solvent extraction process used in hydrometallurgy consists of three stages; extraction, scrubbing and stripping. The metal values in an organic phase is transferred to an aqueous phase at the stripping stage and subsequently recovered as a metal by electrowinning. Recently, new stripping methods have been developed, in which the stripping and recovery of metal are accomplished at one stage.

The crystallization-stripping under the pressurized CO_2 is one of these stripping methods in which the metal values in an organic phase are recovered as fine metal carbonate powders (1-5). The reaction significantly relates to the back-extractabilty of metal ion and the solubility of metal carbonate. The extraction system which can be applied to this stripping method is a limited extent owing to the reverse tendency between the back-extractability and solubility in increasing pH.

The metal carbonates except for rare earths can be easily converted to metallic oxide and metal powders by a thermal decomposition at the lower temperature in air and hydrogen atmosphere, respectively. The application of this stripping technique to a new production process of fine metallic oxide and metal powders consisting of solvent extraction, crystallization-stripping and thermal decomposition is proposed.

In order to expand the extraction systems applicable to this stripping method, the works have been carried out at many combinations of extractants

and metals. The examined extraction systems were Versatic acid 10, SNA-180, DP-8R and PC-88A as extractants and Ag, Cu, Co, Ni, Zn and Nd as metals. The crystallized products were converted to the metallic oxide and metal powders by roasting in air and hydrogen atmosphere, respectively.

2 REAGENTS AND PROCEDURE

The extractants used were mainly Versatic acid 10(Shell Chemical, 98%, Carboxylic acid, abbreviated as VA10), and additionally SNA-180(Koei Chemical, 98%, Naphthenic acid), DP-8R(Daihachi Chem. Ind., 99%, Di-2-ethylhexyl phosphoric acid) and PC-88A(Daihachi Chem. Ind., 97%, 2-ethylhexyl phosphonic acid 2-ethylhexyl ester). These were diluted in kerosene or Solvesso 150 (Esso, high-aromaticity) and 2-ethylhexanol was added in the organic phase in order to modify the separability of liquid-liquid and/or liquid-solid. The metal loaded organic solutions were prepared by contacting the above organic phase with the aqueous solutions containing metal ions which were supplied as Ag, Cu, Co and Ni nitrates and Zn sulphate and Nd chloride.

The metal loaded organic solution and the strip solution such as water or sodium bicarbonate solution were poured into an autoclave and then stirred under the pressurized CO_2 of 0.5~ 2.0 MPa. The products were outpoured through the sampling tube and then were centrifugal separated as the organic and aqueous phases and the crystallized products. The metal concentrations in feed(Cm_f) and organic(Cm_o) and aqueous (Cm_a) phases after the operation were measured by an atomic absorption spectrophotometry. The stripping and crystallization percentages were defined as follows;

$$\text{Stripping}(\%) = (Cm_f - Cm_o)\ 100/Cm_f,$$
$$\text{Crystallization}(\%) = (Cm_f - Cm_o - Cm_a)\ 100/Cm_f.$$

The crystallized products were filtrated by a paper filter of Toyo No.5C and washed with ethanol or acetone in order to remove the organic contamination. The crystallized products were supplied to a thermal analysis and roasted by an electric furnace in air and hydrogen atmosphere to convert to the fine metallic oxide and metal powders. The crystallized and roasted products were identified by a X-ray diffraction analysis. The shape and particle size distribution of these powders were measured by a SEM photograph and a centrifugal sedimentation method, respectively.

3 RESULTS AND DISCUSSION

3.1 Crystallization-stripping

Crystallization-stripping under the pressurized CO_2 gas was carried out at various combinations of extractant and metal. The obtained results are shown in Table 1. The extractants employed in the works are mainly VA10 and addi-

tionally SNA-180, DP-8R and PC-88A. Most of the examined metals can be back-extracted in the pH range of more than 3.9 which is the pH value measured in CO_2 saturated water. The solubilities of these metal carbonates are small enough to precipitate in water.

From the table, it is found that the metal values loaded in carboxylic acid extractants can be stripped and crystallized with high stripping and crystallization percentages by contacting with water or sodium bicarbonate solution under the pressurized CO_2 gas and recovered as metal carbonates or basic metal carbonates. The reaction rates of metals except Cu are relatively rapid and within one hour reach more than 90% of the crystallization percentage obtained at the equilibrium. The reaction of Cu proceeds more slowly through two crystallization steps, in which malachite forms at the beginning, followed by an azurite production. On the other hand, in the case of the phosphorus acid extractant, the metal values in organic phase can be slightly stripped and precipitated.

Table 1 Crystallization-stripping under the pressurized CO_2 at various combinations of extractant and metal.
Conditions ; 0.5mol/dm^3 extractant, at room temp., and O/A ratio = 1, Metal concn.(0.1mol/dm^3 Ag,Cu,Zn and 0.15mol/dm^3 Co,Ni and 0.05 mol/dm^3 Nd)

Extraction system	Strip agent (mol/dm^3)	Pco_2 (MPa)	Time (h)	Str. (%)	Cry. (%)	Crystallized product
Ag-VA10	0.8 $NaHCO_3$	1.5	1	87	87	Ag_2CO_3
Cu-VA10	water	2.0	5	49	48	$Cu_2CO_3(OH)_2$
	water	2.0	8	95	95	$Cu_3(OH)_2(CO_3)_2$
Co-VA10	water	1.5	1	89	77	$CoCO_3$
	0.8 $NaHCO_3$	1.5	1	88	86	$CoCO_3$
Ni-VA10	water	1.5	1	88	78	$Ni(CO_3)2Ni(OH)_24H_2O$
	0.8 $NaHCO_3$	1.5	1	92	91	$Ni(CO_3)2Ni(OH)_24H_2O$
Zn-VA10	water	2.0	1	93	89	$ZnCO_3$
Nd-VA10	water	2.0	0.33	98	96	$Nd_2(CO_3)_38H_2O$
Co-SNA-180	0.8 $NaHCO_3$	2.0	1	71	69	$CoCO_3$
Co-DP-8R	0.8 $NaHCO_3$	2.0	1	8	6	green solution
Co-PC-88A	0.8 $NaHCO_3$	2.0	1	3	2	green solution
Ni-PC-88A	0.8 $NaHCO_3$	2.0	1	2	0	-

The crystallization-stripping of Ni loaded in VA10 were carried out at various conditions. Figure 1 shows the crystallization of Ni as a function of time. The reaction depends on the CO_2 pressure, metal concentration and extractant concentration in the organic phase. The crystallization percentage increases with the increase in CO_2 pressure and metal concentration and the decrease in extractant concentration. The use of sodium bicarbonate solution as a strip reagent enhances the percentage of crystallization. The results of other metals have almost similar tendency to that of Ni.

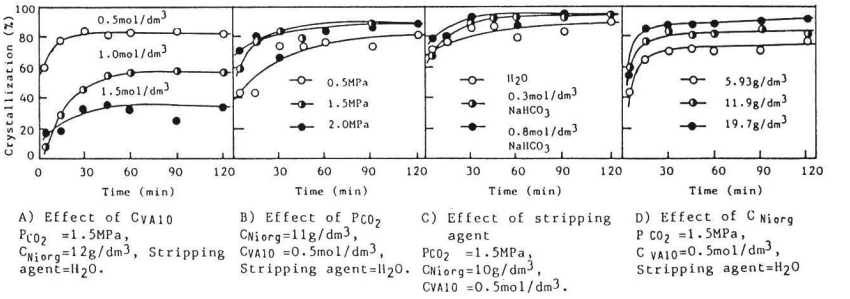

A) Effect of C_{VA10} P_{CO_2} =1.5MPa, C_{Niorg}=12g/dm^3, Stripping agent=H_2O.

B) Effect of P_{CO_2} C_{Niorg}=11g/dm^3, C_{VA10} =0.5mol/dm^3, Stripping agent=H_2O.

C) Effect of stripping agent P_{CO_2} =1.5MPa, C_{Niorg}=10g/dm^3, C_{VA10} =0.5mol/dm^3.

D) Effect of C_{Niorg} P_{CO_2} =1.5MPa, C_{VA10}=0.5mol/dm^3, Stripping agent=H_2O

Fig.1 Effects of various factors on the crystallization-stripping of Ni.

3.2 Thermal decomposition

The thermal analyses of crystallized products were carried out. The obtained results are shown in Fig. 2. The thermal decomposition properties of the crystallized products are very important to convert them to metallic oxide and metal powders. The most of carbonates except Nd can be converted to the metallic oxide and metal powders at the low temperature less than 573K by a thermal decomposition in air and hydrogen atmosphere, respectively.

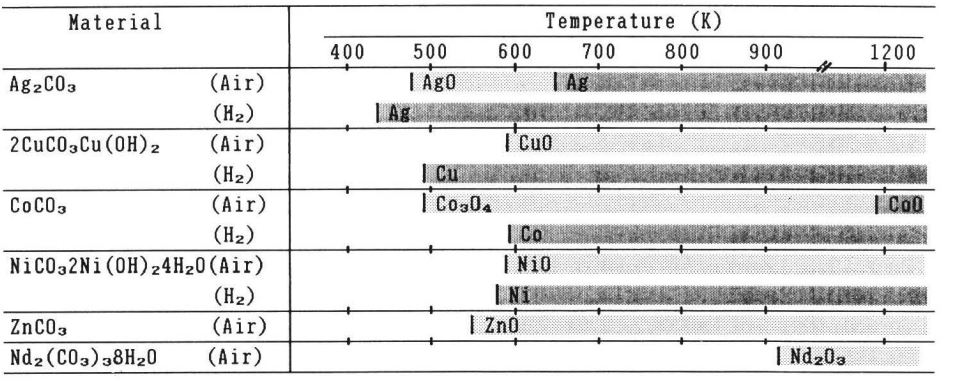

Fig. 2 The thermal decomposition properties of metal carbonates.

Figure 3 shows the effect of temperature on the particle size of the products roasted in air and hydrogen atmosphere in the case of Ni. The original material has the mean particle diameter of about 0.59 μm. The particle size of oxide powder roasted in the temperature range of 573 to 973K is about 0.3 μm and increases with an increase in temperatures above 973K. The particle size of metal powders roasted at 573K is about 4 μm because of sintering at about 573K and significantly enlarges with an increase in temperature.

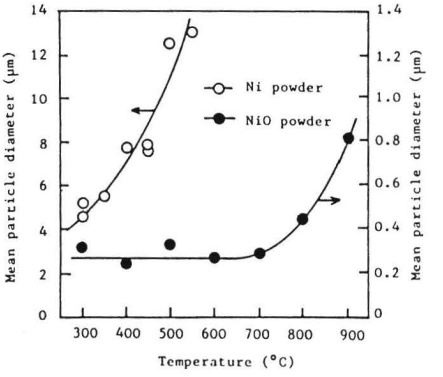

Fig. 3 Relationship between roasting temperature and particle size.

SEM photographs of the crystallized and roasted products of Cu are shown in Fig. 4. The different particle shapes of metal carbonates produced under the various conditions are observed from the figure. If Alamine 336 are added in the organic phase, the particle shape of the products becomes fine and spherical. Changing of the phase ratio and extractant concentration significantly influences the particle size of the product. Roasting the crystallized product in air at the lower temperature, in most case, the product changes to the metallic oxide powder with the same shape as the original particle but with a smaller particle size. The considerable sintering among the particles occurs when the crystallized product is roasted in hydrogen atmosphere.

4. CONCLUSION

The crystallization-stripping under the pressurized CO_2 was examined for many combinations of extractants and metals. The crystallized products were converted to metallic oxide and metal powders by a thermal decomposition in air and hydrogen atmosphere. The obtained results are described as follows.

1. The extraction system which this stripping method is applicable to is limited to the combinations of carboxylic acids such as VA10 and SNA-180 and the metals which are back-extractable in the pH range of more than 3.9.

2. The reaction depends on CO_2 pressure, metal concentration and extractant concentration in the organic phase and also the use of $NaHCO_3$ as a strip solution enhances the percentage of crystallization.

3. The crystallized products by this method are metal carbonate powders, and most of the products except for Nd are converted to metallic oxide and metal powders by a thermal decomposition in air and hydrogen atmosphere at the low temperature less than 573K.

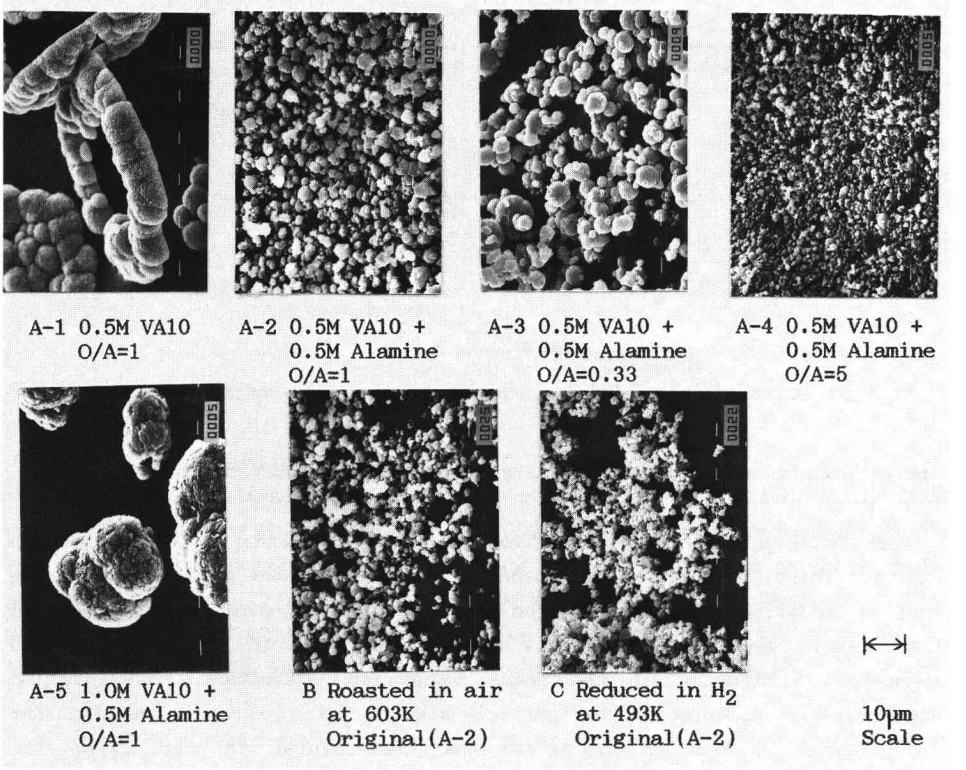

Fig. 4 SEM photographs of the crystallized and thermal decomposed products. A-1 to A-5 are the crystallized products from 0.1 mol/dm^3 Cu loaded VA10 under 2.0 MPa of Pco_2 at room temprature, B and C are the roasted products in air and H_2, respectively.

5. REFERENCE

1) Okuda, A., Shibata, J., Sano, M. and Nishimura, S., 1986. Production of fine metal and metal oxide powders by the liquid phase chemical reaction applying solvent extraction. J. Mining and Metall. Inst. Japan., 102: 869-874.

2) Shibata, J., Okuda, A., Sano, M. and Nishimura, S., 1986. Crystallization stripping of Ni-loaded Versatic Acid with the aqueous solution containing carbon dioxide. J. Mining and Metall. Inst. Japan., 104: 97-102.

3) Shibata, J., Kinoshita, T., Sano, M. and Nishimura, S., 1987. Crystalliza tion-stripping of silver and nickel loaded Versatic Acid 10 with the aqueous solution containing carbon dioxide. Proc. Symp. Sol. Extr. Japan., : 239-244.

4) Sano, M., Ohashi, N., Shibata, J. and Nishimura, S., 1988. Crystallization stripping of Cu from the organic phase containing Versatic Acid under the pressurized carbon dioxide. Proc. Symp. Sol. Extr. Japan.,:199-204.

5) Kitade, H., Sano, M., Shibata, J. and Nishimura, S., 1990. Crystallization stripping of Zn-loaded Versatic Acid 10 under the pressurised CO_2 gas. Spring meeting Inst. Mining and Materials Process. Inst. Japan., :387-388.

EXTRACTION OF METAL IONS FROM MIXED AQUEOUS-ORGANIC MEDIA WITH LIQUID-LIQUID EXTRACTION AND ION EXCHANGE RESIN

J. SHIBATA, M. SANO AND S. NISHIMURA
Department of Chemical Engineering, Faculty of Engineering, Kansai University, Yamate-cho 3-3-35, Suita, Osaka 564, (JAPAN)

ABSTRACT
Shibata, J., Sano, M. and Nishimura S., 1990. Extraction of metal ions from mixed aqueous-organic media with liquid-liquid extraction and ion exchange resin.

Extraction of metal ions from the aqueous-organic solution containing dimethyl formanide (DMF), dimethyl sulfoxide (DHSO) and acetonitrile (AN) was investigated by using solvent extraction and ion exchange resin. The polar phase was a three component solution of metal salt, non-aqueous solvent and water. The extracted metal ions were Cu, Ni, Co(II) and Mg.
The extraction behaviors may be explained by the solvation ability of non-aqueous solvents and other interactions.

INTRODUCTION

Solvent extraction and ion exchange resin have been a well established process for separation and recovery of Cu, Ni, Co, Ga, In, rare earths etc. However, such separations sometimes may require extraction stages as many as 15-20 stages in solvent extraction and a special eluant in a resin process. Consequently, various methods have been investigated in order to improve the separation between metals: i) adding a second extractant to the organic phase containing a main extractant, which is sometimes called a synergistic effect (1-2), ii) adding a complexing agent such as EDTA and acetylacetone to an aqueous phase (3-4) and iii) adding a non-aqueous solvent such as acetonitrile and dimethy formamide to an aqueous phase (5-6).

Recently, a new leaching process for metal oxides has been reported by Gill et al. (7), in which dimethyl sulfoxide and acetonitrile are used in the presence of sulphur dioxide. Solvent extraction and ion exchange may be applied to the separation and recovery of metal elements from such leach solutions.

In the present work, the extraction properties of various metal ions from the mixed aqueous-organic solution containing dimethyl sulfoxide, dimethyl formamide and acetonitrile were investigated by using solvent extraction and ion exchange resin.

2 REAGENTS

The extractant used was di-2-ethylhexylphophoric acid supplied by Daihachi Chem. Ind. Co., Ltd. (DP-8R, 97.6% purity, abbreviated as D2EHPA henceforth).

D2EHPA was diluted at 0.5kmol/m^3 in n-hexane without a purification. The resins used were Amberlite IR-120B (cation exchange type) and Unitika UR-50 (chelating type). Acetonitrile, dimethyl sulfoxide and dimethyl formamide (abbreviated as AN, DMSO and DMF, respectively) were added to an aqueous phase at various concentrations. Metal ions used for this purpose were Cu, Ni, Co(II) and Mg. Metal ions were added to the aqueous-organic solution at 1.0kg/m^3 as metal chlorides.

3 RESULTS AND DISCUSSION

3.1 Extraction by D2EHPA

In a solvent extraction process, volume change of both aqueous and organic phases is a most important problem as is dissolution of an extractant and diluent into the aqueous phase. Table 1 shows volume change in the extraction from the aqueous-organic solution containing DMSO, DMF and AN. It is recognized that volume change strongly depends on the nature of the non-aqueous solvent and the nature of the diluent, whereas it is independent of the sort of metal ions and the aqueous pH. Diluents markedly affect the volume change. When a binary solution of D2EHPA and toluene is used, volume change is large and the volume of the organic phase increases irrespective of the type of non-aqueous solvents. On the other hand, the volume change is small when n-hexane is used as a diluent.

Table 1 Volume change in extraction from mixed aqueous-organic media.

Solvent	Diluent	Vol% of non-aqueous solvent in polar phase			
		30%	50%	70%	90%
		Volume ratio (V_{org}/V_{aq}) after extraction			
DMF	toluene	a	1.102	1.208	b
	n-hexane	a	a	0.985	0.924
DMSO	toluene	a	a	1.015	1.067
	n-hexane	a	a	0.975	0.956
AN	toluene	1.423	2.242	-----	-----
	n-hexane	a	a	a	0.975

a: no volume change
b: completely miscible

The extraction of metal ions with D2EHPA diluted in n-hexane was investigated from the aqueous-organic solution containing 0~90 vol% AN, DMF and DMSO. The acidity or alkalinity is kept constant for all extraction experiments of an individual metal ion. Namely, the acidity or alkalinity is adjusted so as to obtain the extraction from 10 to 90 %. The extraction properties of Cu and Mg are shown in Figs. 1 and 2, respectively.

Figure 1 shows extraction of Cu as a function of the concentration of DMSO, DMF and AN. The extraction of Cu exhibits almost the same behavior in the presence of DMSO and DMF. When the amount of DMSO and DMF is less than 50 vol%, the extraction of Cu increases with an increase in the concentra-

tion. Then, the extraction decreases with addition more than 50 vol%. The extraction remarkably decreases in the presence of 90 vol% of DMSO and DMF. When AN is added to an aqueous phase, the extraction of Cu slightly decreases with an incerase in the amount.

The extraction behaviors of Ni and Co(II) in the presence of DMSO, DMF and AN exhibit almost the same tendency as the extraction of Cu by adding non-aqueous solvents.

Extraction of Mg is shown in Fig. 2. The extraction of Mg increases with an increase in the mole fraction of DMSO and DMF. The extraction of Mg tends to decrease slightly by adding AN as same as those of other metals. Although the results shown in Figs. 1 and 2 are obtained by using n-hexane as a diluent, similar extraction behaviors are observed in the use of toluene.

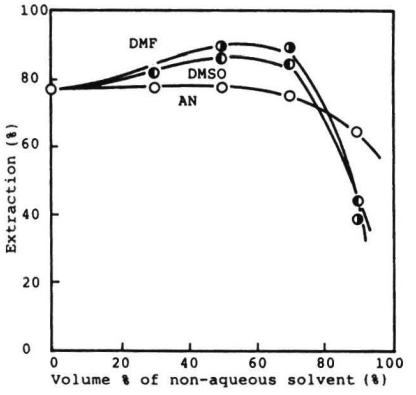

Fig. 1 Extraction of Cu with 0.5 kmol/m^3 D2EHPA diluted in n-hexane at constant initial NaOH conc.(0.018kmol/m^3).

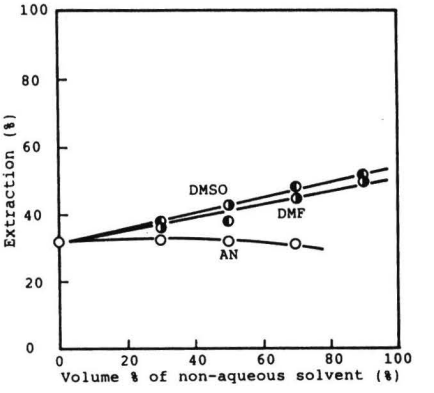

Fig. 2 Extraction of Mg with 0.5 kmol/m^3 D2EHPA diluted in n-hexane at constant initial NaOH conc.(0.018kmol/m^3).

Non-aqueous solvents such as DMSO, DMF and AN may give rise to the following effects on the extraction of metal ions: i) non-aqueous solvents solvate to cations in the polar phase to decrease the activity of cations (8), which suppresses the extraction of metal ions, ii) the extractant and non-aqueous solvents dissolved in the organic phase interact to decrease the activity of the extractant, which may suppress the extraction of metal ions, iii) the non-aqueous solvent dissolved in the organic phase takes part in the formation of the extracted species, which may increase the extraction of metal ions, and iv) the distribution ratio of the extractant and extracted species may decrease, which leads to extraction suppression.

3.2 Extraction by ion exchange resin and chelating resin

An uptake of metal ions such as Cu, Ni, Co and Mg with ion exchange and

chelating resins was measured as a function of time. Polar phases containing metal ions were water, 80 vol% AN, 80 vol% DMF and 80 vol% DMSO. The equilibrium state of uptake is attained within 1 hour for any metal ion, when water and 80 vol% AN are used as a polar phase. If 80 vol% DMF is used, however, the time required for equilibrium is almost 17~26 hours. In the case of 80 vol% DMSO, 41~96 hours are required for the equilibrium uptake. It is considered that the addition of non-aqueous solvents such as DMF and DMSO changes the dissolved state of metal ions and as a result an ionic radius is larger due to the solvation to metal ions. The longer equilibrium time mentioned above is considered to be due to the slower diffusion rate of metal ions inside resins. When Unitika UR-50 is used instead of Amberlite IR-120B, the uptake speed is remarkably reduced by an addition of DMF and DMSO in the polar phase.

The relation between percentage uptake of metal ions and added amount of non-aqueous solvents was studied for Amberlite IR-120B and Unitika UR-50. The results are shown in Figs. 3~6. Figure 3 shows the relation between equilibrium uptake of Cu and added amount of non-aqueous solvents for Amberlite IR-120B. Behaviors for DMF and DMSO are very similar, and the uptake of Cu decreases with an increase in the added amount. The addition of AN does not almost affect the uptake of metal ions. The uptake of Mg with Amberlite IR-120B is shown in Fig. 4. Any non-aqueous solvent does not cause an extreme decrease in uptake of Mg. Figure 5 and 6 show the uptake of Ni and Mg with Unitika UR-50, respectively. The addition of DMF and DMSO decreases uptake of Ni, while AN increases uptake of Ni by the addition. The uptake of Mg is increased by the addition of AN and DMF, whereas it is decreased at an addition of DMSO as high as 80 vol%.

Non-aqueous solvents may give rise to the following effect on the uptake of metal ions; i) non-aqueous solvents solvate to metal ions to decrease the

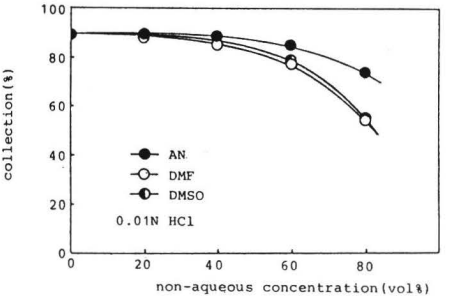

Fig. 3 Effect of non-aqueous concentration on collection of Cu with Amberlite IR-120B.

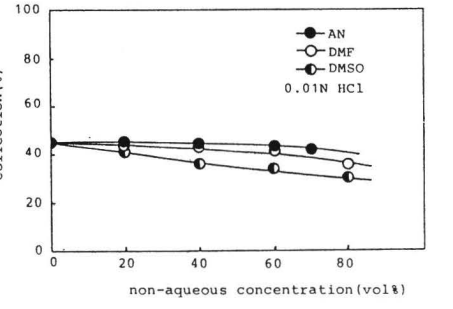

Fig. 4 Effect of non-aqueous concentration on collection of Mg with Amberlite IR-120B.

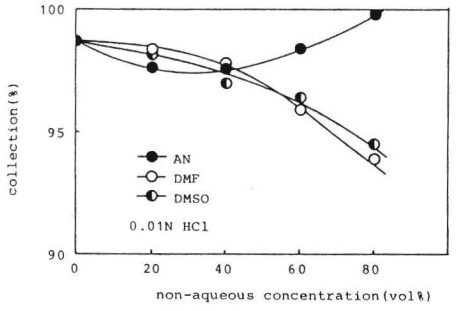

Fig. 5 Effect of non-aqueous concentration on collection of Ni with UR-50.

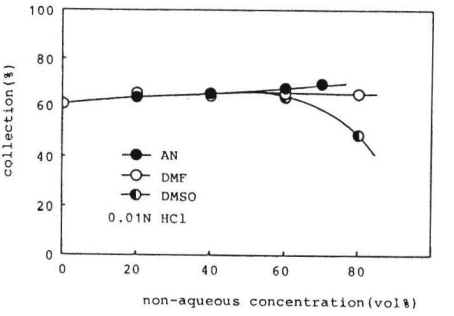

Fig. 6 Effect of non-aqueous concentration on collection of Mg with UR-50.

activity of metal ions, which increases the time required for equilibrium uptake and suppresses the uptake of metal ions, ii) non-aqueous solvents decreases an dielectric constant of the polar phase, which causes the stabilization of ion-pair formation and chelating formation.

3.3 Discussion

Donor number and transfer free energy of metal ions from water to DMSO and DMF can indicate whether the non-aqueous solvent can displace water from the solvation sheath of metal ions. When the donor number is large, it means that the solvent has a strong solvation ability to metal ions. The donor number of non-aqueous solvents used in this work is given in Table 2 with some physical and chemical properties (5). Some instances of transfer free energy of metal ions from water to non-aqueous solvents are shown in Table 3 (10). When the transfer free energy is a large negative value, the metal ion is solvated strongly by the non-aqueous solvent and is stable in the solvent. According to Table 2, the donor numbers of DMSO and DMF are larger than that of water, which means that DMSO and DMF can solvate to metal ions more strongly than water in the aqueous-organic solution. Acetonitrile has a

Table 2 Some physical and chemical properties of the non-aqueous solvents and water.

Solvent	Molecular weight	Density at 298K (g/cm^3)	Dielectric constant at 298 K	Dipole moment (10^{-30}Cm)	Donor number	Accepter number
DMF	73.10	0.944	36.71	12.86	26.6	16.0
DMSO	78.14	1.096	46.60	---	29.8	19.3
AN	41.05	0.777	35.95	13.06	14.1	18.9
Water	18.01	0.997	78.54	6.47	18.0	54.8

Table 3 Free energies of transfer(ΔG_{tr}/kJmol^{-1}) of some ions from water to non-aqueous solvents.

Ion	$H_2O \longrightarrow$DMF	$H_2O \longrightarrow$DMSO	$H_2O \longrightarrow$AN
Na^+	-9.6	-13.4	15.1
Ag^+	-20.8	-34.8	-23.2
Cu^{2+}	-18	-49	59
Zn^{2+}	-30	-45	69
Cl^-	48.3	40.8	42.1
CN^-	40	35	35
NO_3^-	----	----	21

smaller donor number than water, and the tendency of solvation to metal ions is considered to be insignificant. Such difference of solvation ability among solvents can be also confirmed by the value of free energy given in Table 3. Chemical properties of DMSO and DMF, the donor number and transfer free energy, seem to correspond to a remarkable decrease in extraction and uptake of Cu, Ni and Co(II). It is reported by Muir that activities of many metal ions decrease with the addition of non-aqueous solvents (8). Although the transfer free energy of Mg has not been measured, the results in Fig. 2 suggest that non-aqueous solvents solvate Mg poorly.

At present, we can not throughly explain the extraction and uptake behaviors of metal ions in the presence of non-aqueous solvents, but it is considered that some of factors mentioned here may take part in the extraction and uptake of metal ions.

5 REFERENCE

1) Preston, J.S., 1982. Hydrometallurgy, 9: 115-133.

2) Shibata, J., Sano, M., Ohmori H. and Nishimura S., 1987. Japan Inst. Metals, 51: 749-754.

3) Zheng, Q. and Fan, H., 1986. Hydrometallurgy, 16: 263-270.

4) Harder, H. and Chaberek, S., 1959. J. Inorg. Nucl. Chem., 11: 197-209.

5) Muir, D.M. and Parker, A.J., 1983. Hydrometallurgy: J.D. Miller and K. Osseo-Assare (Editors), AIME, New York, pp.341-356.

6) Ohmori, H., Shibata, J., Sano, M. and Nishimura, S., 1987. Japan Inst. Metals, 51: 645-650.

7) Gill, J.B., Goodall, D.C. and Jeffreys, B., 1985. Hydrometallurgy, 13: 221-226.

8) Muir, D.M., 1985. Extraction Metallurgy '85, IMM London, pp.65-91.

9) Gutmann, V., 1968. Coordination Chemistry in Non-Aqueous Solutions, Springer-Verlag, Vienna, New York.

10)Marcus, M., 1983. Pure and Appl. Chem., 55: 977-1021.

Solvent Extraction 1990, T. Sekine (Editor)

© 1992 Elsevier Science Publishers B.V. All rights reserved

RECOVERY OF ZINC AND MANGANESE FROM WASTE BATTERIES BY LIQUID -LIQUID EXTRACTION.

L. STEINER, XING MIAOLIN and S. HARTLAND
Department of industrial chemistry,
Swiss Federal Institute of Technology, 8092 Zurich, Switzerland.

ABSTRACT
A process for the safe disposal of small batteries is being developed in Switzerland to decrease environmental pollution by heavy metals. Using conventional means of disintegration, washing, screening and thermal treatment some 60 % of the original material weight may be eliminated. The rest is a black powder consisting mostly of carbon and metal oxides from which zinc and manganese may be recovered by extraction with Cyanex 301 reagent.

INTRODUCTION

About 5000 tons of small batteries are discarded every year in Switzerland. If they are disposed of together with other household garbage through incineration, some 1000 t of manganese, 600 t zinc, 10 t mercury and 1 t of cadmium are released into the environment each year. For a small and densely populated country this represents such an amount of unacceptable pollution that the federal bureau for environmental protection has originated a research project to enable a safe disposal of spent batteries within the country. The investigation was carried out in the Swiss Federal Institute of Technology by the AFIF-group (1987) The basic layout of the procedure is shown in Fig.1.

The collected material is first screened to remove the small button cells which must be treated separately because of their high mercury content. The rest is disintegrated, washed and wet-screened. The coarse fraction consists of a mixture of metal scrap, paper and plastics. The light materials are separated in a hydrocyclone, dried and incinerated. The metals are acceptable for smelting plants after magnetic separation.

The fine fraction from the screening is first heated to remove the mercury. The rest is a fine black powder containing about 40% manganese, 20% zinc, up to 15% carbon and small amounts of copper and iron. It cannot be dumped in a normal landfill without first removing the zinc. In the original study either fractional

electrolysis or high temperature sublimation were proposed for this purpose but difficulties were encountered with both these alternatives. Steiner et al. (1988) attempted a separation by hydrometallurgy using DEHPA to extract both zinc and manganese which were then separated by multistage scrubbing. The separation worked on a small scale but operation of a continuous pilot-plant was difficult because of the fine pH control required. Therefore, alternative reagents were sought to enable separation directly from the leach.

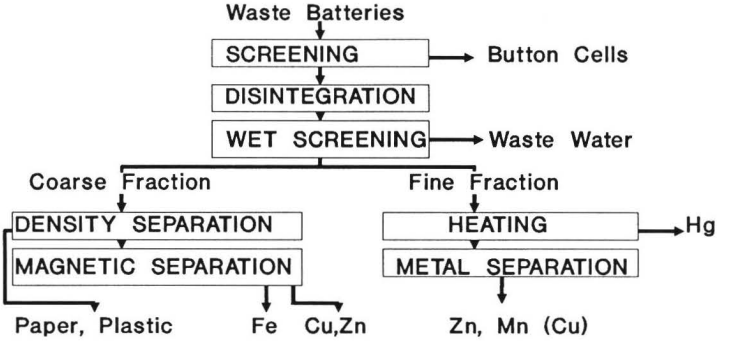

Fig. 1: Treatment of spent small batteries by the AFIF process (1987).

SOLVENT SELECTION

Cyanex 301 (abbreviated C301) manufactured by American Cyanamid Company in New Jersey, U.S.A. consists mainly of bis(2,4,4-trimethylpentyl)dithiophosphinic acid with the formula given in Fig. 2. Its solution in organic diluents exchanges the hydrogen from the SH group for metallic cations from aqueous solutions. Being a very strong acid, some metals (including Zn) are extracted at extremely low pH values.

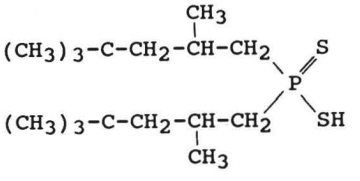

Fig. 2: Structure of the active component of Cyanex 301

Working with proton donating reagents (such as C301 or DEHPA) at reasonable concentrations of dissolved metals (over 10 g/l) the extraction is connected with a considerable decrease of the pH-value. This could be balanced by neutralization but large amounts of useless amonia or sodium sulfate would be produced and disposed off. With C301 zinc is transfered to organic phase at any pH so that no neutralization is necessary. The remaining water phase contains sulfuric acid in such a concentration that it may be recycled to dissolve more raw material. This is an essential advantage over other possible extractants as the environmental requirements on the process are very strict. C301 was therefore selected despite difficulties encountered when stripping metals back into the aqueous phase.

DISSOLUTION

The raw material for the extraction experiments is the fine fraction from Fig. 1. Some 85% of it is easily dissolved in diluted sulfuric acid. The rest consisting mostly of carbon and silicates is insoluble even in mixtures of nitric and hydrochloric acids, and contains only traces of heavy metals. It may be filtered and disposed off by incineration.

The filtration (or decantation) is easy if all manganese has been dissolved, otherwise the slurry clogs the filters and the process becomes slow. Attempts to remove the carbon by heating the material to 750 ^{o}C resulted in brown powder which, however, did not dissolve in sulfuric acid. Melting with sodium bisulfate removed the carbon, the rest was 70% water-soluble but the insoluble part still contained heavy metals. Therefore, simple leaching of original material with diluted sulfuric acid, filtration and burning of the residue is considered the simplest possibility available.

A quantitative study of the leaching process has shown that the dissolution is sufficiently fast even with 0.1N acid. As shown in Fig. 3. about 1 ml of concentrated sulfuric acid per gram of powder must be used to dissolve all metals which is slightly above the stoichiometric ratio. The ratio of zinc to manganese in the leach increases with the amount of acid indicating that manganese is dissolved before zinc.

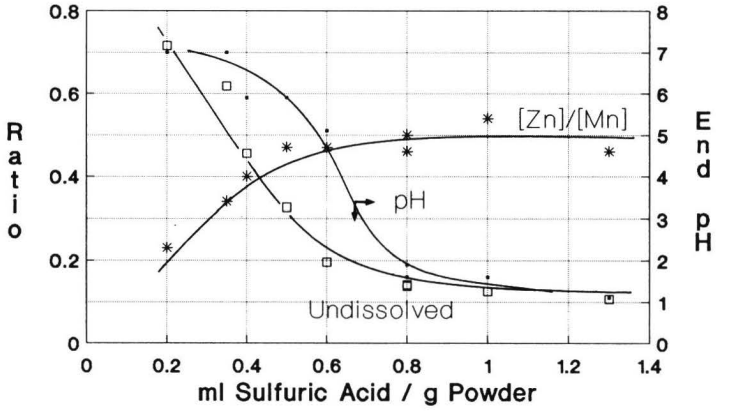

Fig. 3: Dissolution of raw material in sulfuric acid.

EXTRACTION

With C301 zinc and copper are extracted quantitatively even at pH values close to zero (i.e. from normal acids), the process being very fast. The characteristic dark color of the loaded extractant develops in seconds, the pH stabilising in about a minute. Manganese is not extracted until the pH increases well above two so the reagent is well suited for the specific separation. The extractability of iron depends on its valency, Fe^{++} being more readily extracted than Fe^{+++}. The extraction of manganese and trivalent iron is shown in Fig. 4. Maintaining a pH slightly above unity during the extraction process, practically pure manganese remains in the aqueous phase.

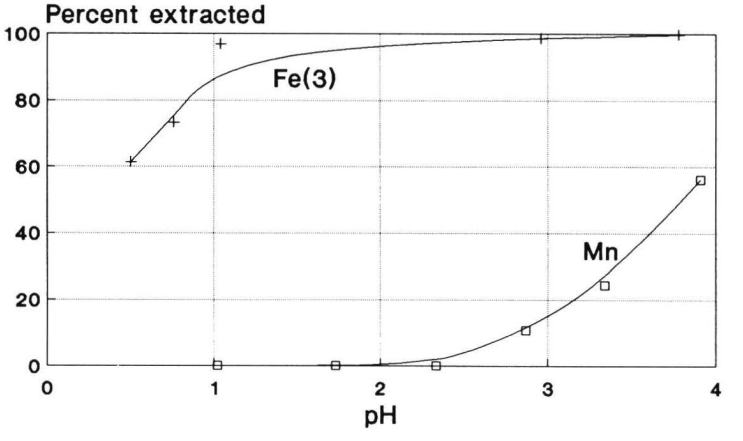

Fig. 4: Extraction of iron and manganese by C301.
A/O = 1, ca 0.5N solutions, C301 in toluene.

An experiment has been carried out repeatedly dissolving portions of the raw material in the same aqueous phase, extracting with C301 and adding concentrated acid to sulfatize the newly added manganese. After 10 repetitions the zinc and manganese concentrations in the aqueous phase were 0.006 and 14.1 g/l respectively. After a time manganese sulfate crystalised from the solution in pure form. Fig. 5 shows the linear increase of manganese concentration during the experiment.

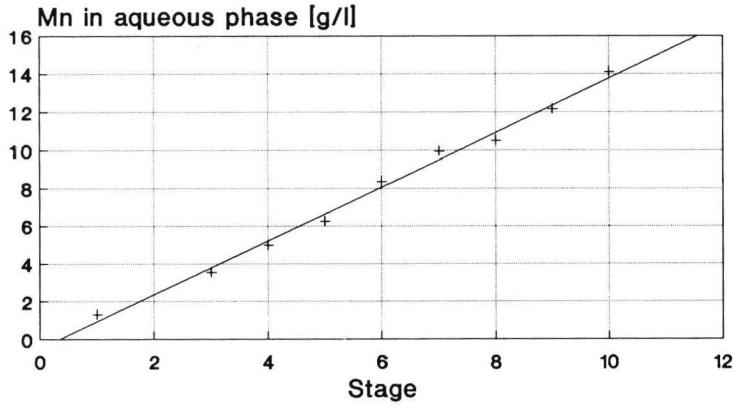

Fig. 5: Repeated extraction of battery powder with C301. Increase of Mn concentration in aqueous phase.

STRIPPING

Contrary to the extraction the reverse process is very tedious and sometimes impossible. With zinc the stripping is manageable but a multistage operation is necessary. In an experiment contacting the zinc-saturated solution of C301 five times with 30% sulfuric acid, the Zn concentration in the aqueous phase decreased from 12.2 to 0.38 g/l in the first and fifth stages respectively. Copper is not stripped at all, its concentration in the aqueous phase remaining in the ppm range even if hot 30% sulfuric acid is used. Striping of iron again depends on its valency. It is in any case more difficult than zinc, practically impossible with Fe^{++}. Some experimental results for Zn and Fe are collected in Fig. 6.

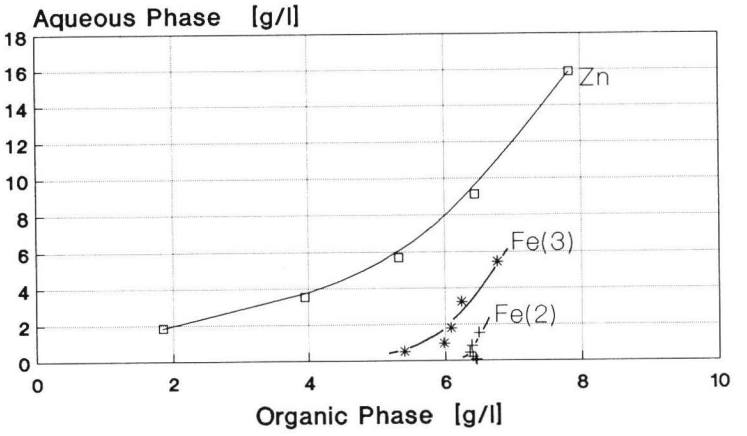

Fig. 6: Stripping of Zinc and iron from C301.
30% H_2SO_4, ca 0.5N solutions of C301 in toluene.

DISCUSSION

Using C301 for the separation of zinc and manganese from spent batteries, single stage extraction and multiple stage stripping are necessary. Copper must be removed by a selective extractant before the solution is contacted with C301. This is possible using LIX reagents, performing the dissolution so that the pH of the aqueous phase before extraction is about two. By the following C301 treatment the pH would decrease below one so the manganese would remain safely in the water phase which may be recycled until the Mn concentration increases to a desired value.

Without special treatment iron would accumulate in the C301 solution as most of it is present as unstrippable Fe^{++}. This would decrease the activity of the extractant which would have to be replaced periodically. With magnetic separation of the raw material before solution, loss of the extractant would not be severe. However, removal or masking of iron before the C301 extraction would be feasible and a suitable solvent is being sought.

REFERENCES

1. Bohac P., Aufbereitungsverfahren für Kleinbatterien.
AFIF Report, ETH Zurich 1987.
2. Steiner L, Xing M.L., Hartland S., Application of solvent extraction in metal recovery from waste batteries.
Proc. 1st Conf. on Hydrometallurgy p. 399, Beiing 1988.

Solvent Extraction 1990, T. Sekine (Editor)

© 1992 Elsevier Science Publishers B.V. All rights reserved

RECOVERY AND PURIFICATION OF IRON FROM ACIDIC HIGH IRON-BEARING EFFLUENT BY SOLVENT EXTRACTION WITH SECONDARY AMINE

KUNG-LIANG HO, TAI-MING CHIU AND YING-CHU HOH

Chemical Engineering Division, Institute of Nuclear Energy Research,
P.O. Box 3-7, Lung-Tan, Taiwan, R.O.C.

ABSTRACT
KUNG-LIANG HO, TAI-MING CHIU AND YING-CHU HOH, 1990. Recovery and purification of iron from acidic high iron-bearing effluent by solvent extraction with secondary amine. ISEC'90

A process, including pre-treatment, oxidation, extraction, stripping, reduction and post-treatment, for the recovery and purification of iron from acidic high iron-bearing effluent was proposed.

It was found that very high purity iron-containing solution can be obtained from high iron-bearing effluent by solvent extraction with secondary amine in a mixture of xylene and S-100. Deionized water was employed as the stripping agent. The results indicated that 90% of the iron in the effluent can be recovered. In the stripped solution, the impurities such as Si, Ca, Al were less than 1 mg/L, and Mn, Cr, Ni were less than 5 mg/L.

1 INTRODUCTION

In Japan, solvent extraction procedure has been applied to the recovery of iron and acids from spent pickling solutions (Watanabe et al., 1986). The iron removal from aluminium sulfate solutions by amine Priemene 81R has been studied by Alguacil et al.(1986,1987). The selective removal of iron from ferrochromium leach liquors using the secondary amine Amberlite LA-2 has been reported by Preston (1984). The various options that have been investigated or used industrially to remove iron from leach liquors have been thoroughly reviewed by Ritcey (1986).

Iron oxide is widely used as a base material of ferrite products in the electronic industry. High purity iron oxide is essential to processing the high resolution and vertical recording media. Some industrial spent acidic solutions contain high concentration of iron as well as various trace impurities such as Si, Ca, Al, Mn, Cr, Ni, etc. The purpose of this study was to investigate the extraction of iron from spent acidic solution containing high concentration of iron by using various commercial extractants. A continuous extraction and stripping scheme for iron purification and recovery was proposed for the most effective organic extractants.

2 EXPERIMENTAL

2.1 Materials

LA-2 was supplied by Rhom & Hass Co. The experimental molecular weight was around 370. The acid binding capacity determined by titration was 2.2 meq./ml at 26 ^{o}C. Kerosene and S-100 were provided by China Petroleum Corporation. TBP was supplied by Union Carbide and pretreated by caustic soda and collected by distillation. D2EHPA was obtained from Union Carbide and had a purity of greater than 96%. Kelex 100 was obtained from Ashland Company and Alamine 336 & Aliquat 336 were obtained from Henkel Chemical Company. All other chemicals were reagent grade. Synthetic solutions were prepared by dissolving ferric chloride in distilled water and adjusting the acidity by hydrochloric acid for testing the characteristics of the extractants.

2.2 Extractant selection

Several commercially available extractants, diluted in various diluents, were examined by shake-out test for the ability to extract iron from the spent acidic solution. In shake-out test, aliquots of organic and aqueous solutions of 20 ml were introduced into 60 ml separatory funnels and shaked mechanically for 15 minutes at room temperature. After the phases had separated, samples were taken and the metal concentration in both phases as well as acidity were analyzed.

2.3 Continuous multistage operation

The performance of multistage separation was conducted by a bench scale mixer-settler. The box-type mixer-settler was made of plexiglas. The system, as shown in Fig.1, comprised of filtration process, ten extraction stages, two oil

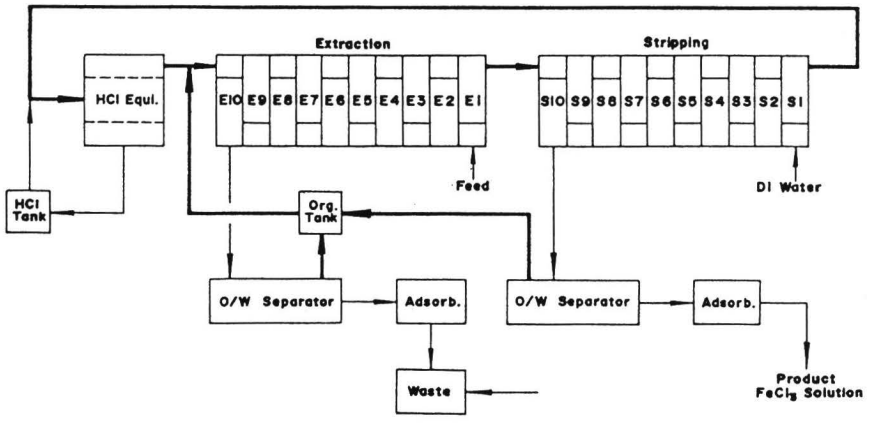

Figure 1 Extraction and stripping system flow diagram

and water separators, ten stripping stages, one acid pretreatment unit, and one active carbon adsorption unit. The system had a maximum flow rate of 700 ml/min, with mixing and settling volumes 1.4 and 7.2 liters, respectively. The real spent acidic solution obtained from local industry was also adopted in the bench scale mixer-settler tests.

2.4 Analysis

The iron concentration in the aqueous phase was determined by using a Metroham E636 Autotitrator with potassium dichromate as the standard solution. The acidity was also titrated by the same instrument with standard sodium hydroxide solution and while potassium oxalate was added as the masking agent. The impurities in the aqueous solution were determined either by atomic absorption or induction coupled plasma emission spectroscopy. The metal concentration and the loading capacity of the organic phase were checked by stripping the loaded organic phase with 0.01M HCl solution and analyzed in the same way as for the aqueous samples.

3 RESULTS AND DISCUSSION

3.1 Extractant selection

The extractant screen tests were conducted with several commercially available extractants including carboxylic acids, organophosphoric acids, amines and oximes by shake-out tests. The diluents used were kerosene and toluene. The test results indicated that TBP and amines give better results. The spent acidic solution contains various trace impurities such as Ca, Al, Si, Mn, Cr and Ni. The extractant should have higher rejection for the impurities in order to obtain very high purity iron-bearing solution. The efficiencies of impurity removal by TBP and amines in toluene indicated that amines have a very good separation efficiency for the impurities mentioned above. Therefore, amines were selected for further study.

The batch simulation counter-current extraction was carried out for evaluating the extraction performance of amines. The results were shown in Table 1. It was found that quaternary and tertiary amines extract iron easily but strip with much difficult. It was also found that secondary amine LA-2 has the most desirable results. More than 93% of the feed iron concentration could be recovered by 6 extraction and 7 stripping stages. Therefore, LA-2 was used for continouous bench scale mixer-settler tests.

TABLE 1

Comparison of the extraction and stripping efficiencies of 20% amine extractants in toluene with batch simulation counter-current extraction method

	Aliquat 336	Alamine 336	Alamine 336	Alamine 336	LA-2
Process	8E8S	3E3S	3E7S	8E8S	6E7S
Extraction, %	96	60	96	95	99
Stripping, %	8	43	78.8	39	93

3.2 Diluent selection

The diluent plays an important role in an extraction process. Chang et al.(1986) pointed that the efficiecncy of iron extraction with aliquot 336 is relatively higher using kerosene as diluent than toluene and the opposite is true for stripping. The low solubility of iron-extractant complex in extractant/kerosene solution concludes that kerosene is not a good diluent. The solubility of iron-extractant can be improved by adding a modifier such as isododecanol into the organic phase. However, it may result in an increase in settling time as well as the loss of isododecanol, and therefore, a decreasing in extraction efficiency may result. The effect of diluent on the extraction of Fe(III) by LA-2 was carried out by batch counter-current extraction. The test results indicated that toluene, xylene, and a mixture of xylene and S-100 are good as a diluent. Toluene was abandoned due to its toxicity and bad smell. It was visually observed that the phase separation time is relatively longer when using S-100 as diluent than xylene. However, the cost of xylene is relatively higher than S-100. Therefore, a mixture of xylene and S-100 was selected as the diluent.

The extraction isotherm for the extraction of iron(III) from 0.5M hydrochloric acid by 30% LA-2 in S-100 was shown in Fig. 2. It indicated that, for a feed solution containing 130 g/L of iron, nine theoretical stages are necessary to remove 95% of the feed iron content for an O/A ratio 5. Figure 3 shows the stripping isotherm of Fe(III) by deionized water from 30 % LA-2/ 15% xylene / 55% S-100.

3.3 Continuous bench scale mixer-settler tests

The organic phase used in the continuous bench scale mixer-settler tests was the mixture of 30% LA-2, 15% xylene and 55% S-100. The organic phase after equilibrated with 2M HCl was pumped from stage E10 (as shown in Fig. 1) to stage S6 at 250 ml/min. The aqueous feed containing 70 g/L of iron(III) entered stage E1 at 50 ml/min. The loaded organic phase was stripped by deionized water. The stripped organic phase was recycled back to stage E10. The iron

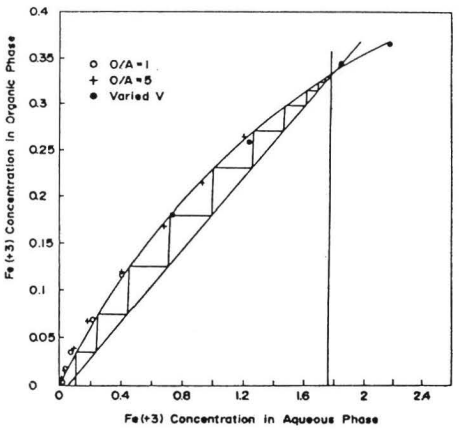

Fig. 2 Extraction isotherm for Fe(+3) extracted by 30 % LA-2 in 55 % S-100 and 15 % xylene

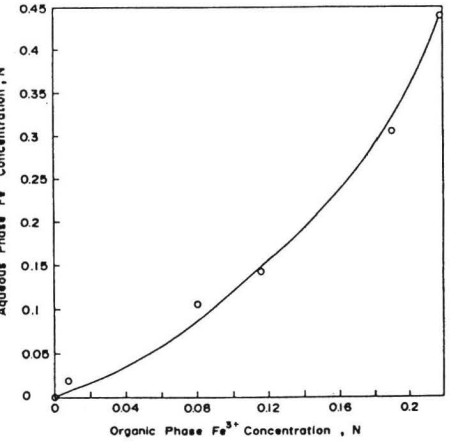

Fig. 3 Stripping isotherm of Fe^{3+} by deionized water from 30 % LA-2/15 % xylene/55 % S-100

extraction and stripping efficiencies were 99% and 73%, respectively. It was inferred that the six stripping stages are not enough. The iron(III) concentration in the raffinate as a function of operating time was shown in Fig. 4. It indicated that the system reaches the steady state after 15 hours. In a further study, synthetic iron(III) solution was adopted as the aqueous feed. The iron concentration in the feed solution was 130 g/L. The flow rate of aqueous phase was 58 ml/min. The organic phase entered into S10 at 290 ml/min. The test result was found that the extraction efficiency is about 87% and the stripping efficiency is more than 99%. It was also found that the

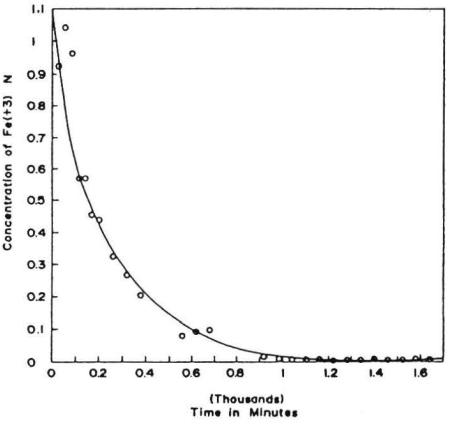

Fig. 4 The outlet Fe^{3+} concentration from E10 as a function of operating time

concentrations of impurity such as Ca, Si and Al are all less than 1 mg/L and Mn, Ni and Cr are all less than 5 mg/L. During the tests, it was found that an oil-water separator between extraction and stripping stages is required in order to reduce the aqueous phase entrainment as it may result in higher concentration of impurities in the stripped solution.

4 CONCLUSIONS

The following conclusions can be drawn from this work:

1) Very high purity of iron-bearing solution can be obtained from spent acidic solution containing high iron concentration by solvent extraction with LA-2 in mixture of xylene and S-100.
2) The contents of impurity such as Ca, Si and Al in the stripped solution were all less than 1 mg/L and the contents of Mn, Ni and Cr in the stripped solution were all less than 5 mg/L.

5 REFERENCES

Alguacil, F.J., S. Amen and A. Luis, 1986, in Chemical Separations , edited by C.J. King and J.D. Navratil, Vol. II, Litarvan Literature, Denver, pp. 285-297

Alguacil, F.J., S. Amen and A. Luis, 1987, Hydrometallurgy, Vol. 18, pp.65-92

Chang, C.C., T.M. Chiu, Y.C. Hoh and W.K. Wang, 1986, Hydrometallurgy, Vol.17, pp.1-13

Mahi, P., and N.T. Bailey, 1985, Chemistry and Industry, Jan. 7, pp.18-21

Preston, J.S., 1984, MINTEK 50, pp.611

Ritcey, G.M., 1986, in Iron Control in Hydrometallurgy , edited by J.E.Dutrizac and A.J. Monhemius, Ellis Horwood Limited., pp.247-281

Ritcey, G.M., and A.W. Ashbrook, 1984, Solvent Extraction: Principles and Applications to Process Metallurgy, Part I, Elsevier Science Publishers B.V., Netherlands

Sekine, T., and Hasegawa, Y., 1977, Solvent Extraction Chemistry , Marcel Dekker Inc., New York, pp.218

Watanabe, T., M.Hoshino, K. Uchino, Y. Nakazato and S. Nishimura,1986, in Iron Control in Hydrometallurgy, edited by J.E. Dutrizac and A.J. Monhemius, Ellis Horwood Limited., pp. 549-570

Solvent Extraction 1990, T. Sekine (Editor)

© 1992 Elsevier Science Publishers B.V. All rights reserved

EXTRACTION OF IRON FROM CHLORIDE SOLUTIONS WITH BINARY EXTRACTANTS (CARBOXYLATES OF TERTIARY AMINES)

*I.Yu.FLEITLICH, *K.S.LUBOSHNIKOVA, *A.I.KHOL'KIN, *G.L.PASHKOV, **V.V.SERGEEV, **G.K.KULMUCHAMEDOV, ***P.MUHL, **T.V.GALANTSEVA, **L.V.ZELENTSOVA
*Institute of Chemistry and Chemical Technology of Siberian Branch of the Academy of Science, Krasnoyarsk, USSR, **Institute "Hydrotsvetmet", Novosibirsk, USSR, ***Central Institute of Solid State Physics and Material Research of GDR Academy of Sciences, Dresden, GDR

ABSTRACT

Extraction of iron from chloride solutions of various compositions with trialkylamine carboxylates (TAAC) in monocarboxylic acids as solvents has been studied. It has been shown that these binary extractants can be effectively used for purification of solutions from iron. Extraction may be carried out at temperature range from 20 to 90°C using preferably straight-chain carboxylic acids as solvents.

INTRODUCTION

The problem of purification of chloride solutions from iron can be effectively solved using tertiary amine salts as extractants (Shmidt, 1970). Earlier we have reported about extractive properties of trioctylamine-alkylphenolates and trioctylamine-carboxylates binary mixtures for this purpose. Extraction equilibrium in that case can be expressed as following:

$$H^+_{(a)} + FeCl^-_{4(a)} + R_3NHA_{(o)} \rightleftharpoons R_3NHFeCl_{4(o)} + HA_{(o)} \qquad (1)$$

where R_3NHA - binary extractant, R_3N - trialkylamine (TAA), HA - alkylphenol or monocarboxylic acid.

The data for extraction of Fe(III) with TAAC in carboxylic acids as solvents have been reported in present communication in contrast to previous work (Khol'kin et al., 1988) where kerosene as a solvent was mainly used.

Carboxylic acids as solvents have some advantages in comparison with kerosene, namely:

(1) the excess of HA shifts the reaction equilibrium to the left (eqn.1) providing more effective stripping of iron;

(2) it is no necessity to use modifier to avoid the forming

of two organic layers;

(3) this process can be easily made fire-safe and explosion-proof owing to the higher ignition points of carboxylic acids which enables us to carry out extraction at the temperature more than 50°C.

REAGENTS

Straight-chain monocarboxylic acids, caprylic acid and its technical analogue such as mixture of synthetic fatty acids C_7-C_9 (SFA) and also α-branched carboxylic acids (VIC) C_5-C_9 and trialkylamine with alkyls C_7-C_9 have been used as components of organic phase.

RESULTS AND DISCUSSION

Chloride solutions after leaching of non-bauxite raw material have a high temperature (more than 90°C) and contain 40-55 $g \cdot dm^{-3}$ of Al(III), 1.0-10.0 $g \cdot dm^{-3}$ of Fe(III) and 170-230 $g \cdot dm^{-3}$ of chloride-ion. To decrease power expense, extraction without any cooling seems to be reasonable.

One can see (fig.1) that temperature rise enhances iron ext-

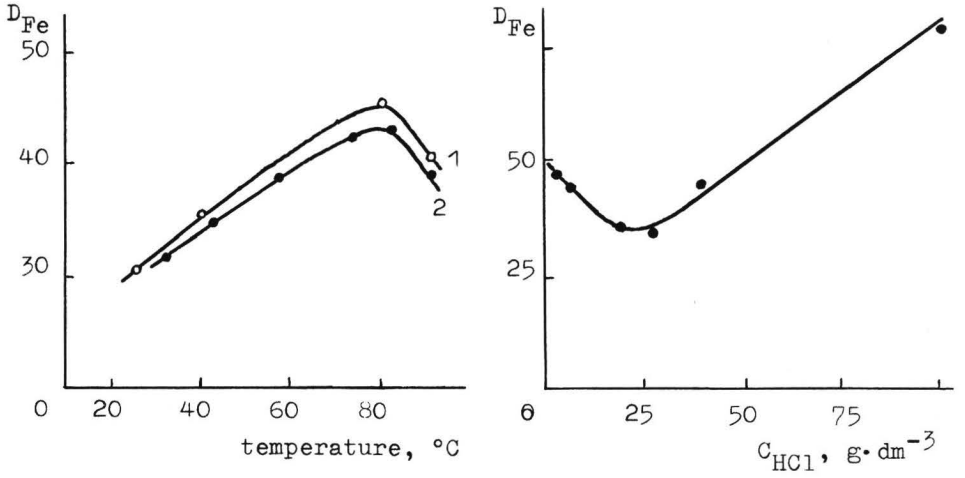

Fig.1. Effect of temperature on iron extraction by 0.3 M TAAC in: 1 - VIC; 2 - caprulic acid. Initial concentration, $g \cdot dm^{-3}$: Al-54.0; Fe-9.5; HCl-40. Contact time - 3 min.

Fig.2. Effect of hydrochloric acid concentration on iron extraction by 0.3M TAA α-monoalkylcarboxylate in VIC at 80°C. Initial concentration, $g \cdot dm^{-3}$: Al-54.0; Fe-10.0; Cl^- -215÷315. Contact time - 3 min.

raction, however, distribution coefficients (D_{Fe}) slightly decrease at temperature above 80°C. This enhancement is possibly due to both the dehydration of the ions and the increase in stability constants $K_{FeCl_4^-}$ and, as consequence, the growing of iron tetrachloride-anion amount in aqueous phase. Decrease in D_{Fe} may be attributed to the high-temperature hydrolysis processes. Dependence of D_{Fe} on concentration of hydrochloric acid is shown in fig.2. Such unusual shape of the curve is conditioned by altering iron extraction as cations with carboxylic acids to its anion-exchange extraction with binary extraction while the concentration of hydrochloric acid has been risen. To prevent from hydrolysis proceeding, acid concentration has to be not less than 30 $g \cdot dm^{-3}$, and temperature below 80°C and time of phase contact about one minute are needed (previous experiences showed such short time to be sufficient to complete the extraction).

Extraction isotherms of iron from leach solutions with 0.3M solutions of TAAC in carboxylic acids with diverse structures have been obtained. As shown in fig.3 iron extraction is independent of structures of carboxylic acids investigated. Iron concentration in the aqueous phase can be reduced from 10 to 0.01 $g \cdot dm^{-3}$ after two stages of extraction.

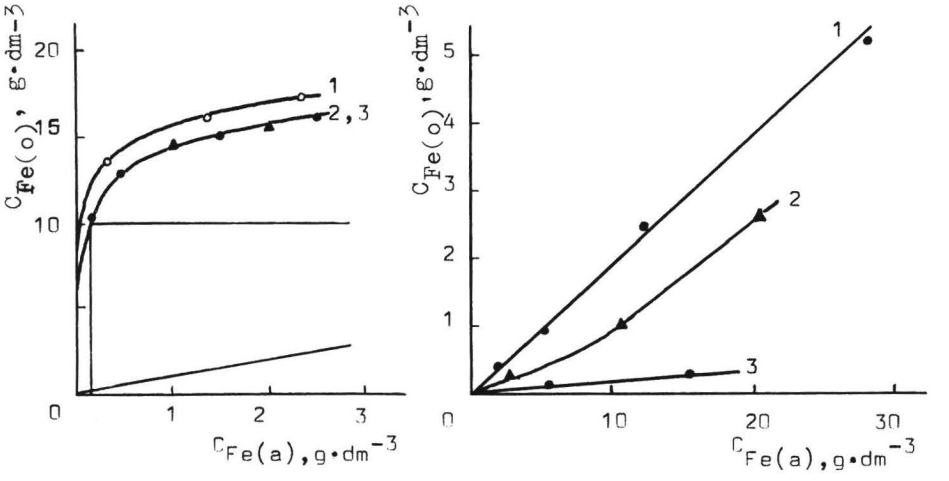

Fig.3. Isotherms of iron extraction by 0.3M TAAC in various solvents at 80°C: 1 (o) - TAA α-monoalkylcarboxylate in VIC; 2 (▲) - TAA caprylate in caprylic acid; 3 (•) - TAA caprylate in SFA. Initial concentrations, $g \cdot dm^{-3}$: Al-54.0; HCl-40.0.

Fig.4. Isotherms of iron stripping from 0.3M TAA α-monoalkylcarboxylate in VIC at different temperatures: 1 - 80°C; 2 - 50°C; 3 - 20°C. Concentration of HCl - 10 $g \cdot dm^{-3}$.

Dilute solutions of hydrochloric acid (about 15 g·dm^{-3}) were used for stripping of iron. It is clear (fig.4) that temperature reducing enhances stripping of iron, but on the other hand it is expedient to conduct the stripping at the temperature below 50°C to curtail the power expense. Stripping isotherms from 0.3M solutions of TAAC in carboxylic acids of various structures are presented in fig.5. Iron stripping is evidently much better for systems with straight-chain acids (curves 2 and 3) compared with branched ones (curve 1). More effective stripping in the former case is concerned both with larger stability of R_3NHA salt when it is consisting of the smaller organic anion (A^-) and with larger concentration of carboxylic acids in comparison with one for branched acids (eqn.1). In optimal conditions (curves 2 and 3) iron stripping requires 2 or 3 stages resulting in rather iron-containig solutions (from 50 to 60 g·dm^{-3} of Fe (III)).

Thus, taking account of both the similar extraction values for various systems and the better stripping values for systems with straight-chain carboxylic acids, one should consider the latter being reasonable for purification of solutions from iron. It is necessary to mark the fine stratification of the phases at high temperature in all cases.

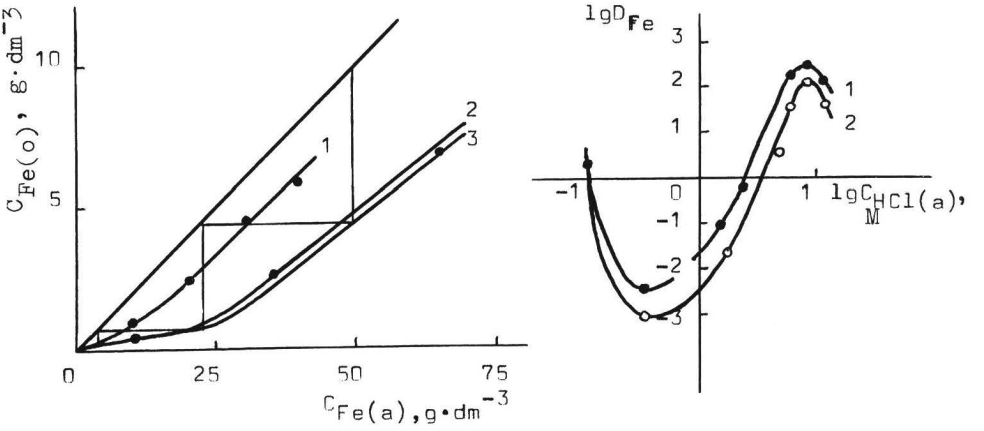

Fig.5. Isotherms of iron stripping from 0.3M TAAC in carboxylic acids at 50°C: 1 - TAA α-monoalkylcarboxylate in VIC; 2 - TAA caprylate in caprylic acid; 3 - TAAC in SFA. Concentration of HCl - 20 g·dm^{-3}.

Fig.6. Dependence of iron extraction by TAA caprylates in caprylic acid on HCl concentration: 1 - 0.3M solution of R_3NHA; 2 - 0.2M solution of R_3NHA. Initial iron concentration - 4.4 g·dm^{-3}.

Purification of cobalt solutions has been performed under normal conditions (at 25°C) and 0.2M TAAC in SFA has been used. Chloride-ion concentration in aqueous phase is desirable to be not less than 150 $g \cdot dm^{-3}$. The laboratory data obtained were confirmed by results of pilot-plant tests made using mixer-settler equipment. Iron extraction from solutions containing $g \cdot dm^{-3}$: Co-120; Ni-12.9; Fe-5.0; Cu-2.2 and HCl-15 has been shown to proceed almost entirely yielding residual iron concentration not more than 0.005 $g \cdot dm^{-3}$. Another metals are hardly extracted from the solutions above. Iron stripping was made by hydrochloric acid (10-15 $g \cdot dm^{-3}$) and concentrated solutions containing Fe (III) from 45 to 50 $g \cdot dm^{-3}$ were obtained.

Using TAAC for extraction process is able to solve the problem of purification of pickling liquors from iron. From fig.6 one can see that iron will be effectually extracted by 0.2-0.3M solutions of TAA caprylate in caprylic acid if hydrochloric acid concentration is more than 5.0 $mol \cdot dm^{-3}$. The minimum on the curve similar to one obtained in Al(III) extraction study is concerned with altering the extraction mechanism from cation-exchange type to anion-exchange one for the extraction of metal-chloride complexes. The maximum observed is dealt with the existence of competing reaction between chloride- and $FeCl_4^-$ - anions with alkylammonium cation. Extraction isotherm shows possibility to purify hydrochloric acid solutions from iron in 3-4 stages of extraction.

It should be noted extraction efficiency reduces in a series $Al^{3+} > Co^{2+} > Na^+ > H^+$ that corresponds to these cations hydration energies.

CONCLUSIONS

(1) rise of the temperature from 20 to 50°C enhances iron extraction and reduces its stripping in systems with TAAC in carboxylic acid;

(2) increase in hydrochloric acid concentration results in change of cation-exchange mechanism to anion-exchange one;

(3) use of the systems with straight-chain acids is preferable to the systems with branched acids due to much better iron stripping for the former;

Thus, such systems may be effectually used for purification

of chloride-containing solutions from iron.

REFERENCES

Shmidt, V.S., 1970. Extraction by amines. Atomizdat, Moscow, pp. 242-243.

Khol'kin, A.I., Fleitlich, I.Yu., Luboshnikova, K.S., Pashkov, G. L.,Kulmuchamedov, G.K., Zelentsova, L.V., Muhl, P., Gloe, K., 1988. Proc.Intern.Solv.Extr.Conf., ISEC'88, Moscow, pp. 263-265.

Solvent Extraction 1990, T. Sekine (Editor)

© 1992 Elsevier Science Publishers B.V. All rights reserved

ON APPLICATION OF SOLVENT EXTRACTION AND CHELATING ION-EXCHANGE RESIN FOR PURIFICATION OF COPPER ELECTROLYTES

R. SHIBAYAMA and T. NAGAI
Dept. of Metallurgical Engineering, Hokkaido Univ., Sapporo, 060 Japan.

ABSTRACT
Shibayama, R. and Nagai, T., 1990. On application of solvent extraction and chelating ion-exchange resin for purification of copper electrolytes. Proc. ISEC '90

A global flowsheet for purification of copper electrolytes is drawn on the basis of processes developed in this laboratory. They are: solvent extraction of As with TBP; chelating ion-exchange adsorption of Sb, Bi and Fe; hydrogen reduction of excess copper in an autoclave; also some relational techniques in order to support the aforesaid processes. Brief explanations of respective processes are given.

1. INTRODUCTION

In electrorefining of copper, some accumulative impurities must be removed from the electrolytes, in order to keep the copper quality and the electric efficiency. The major impurities are As, Sb, Bi and Ni. The minors are Fe, Zn, alkaline- and alkaline earth-metals, etc. Also, excess copper ion in electrolytes is removed at electrowinning cells in the tankhouse. Conventional purification process is shown in Fig. 1, which is energy consuming and, in addition, is accompanied with evolution of toxic arsine gas.

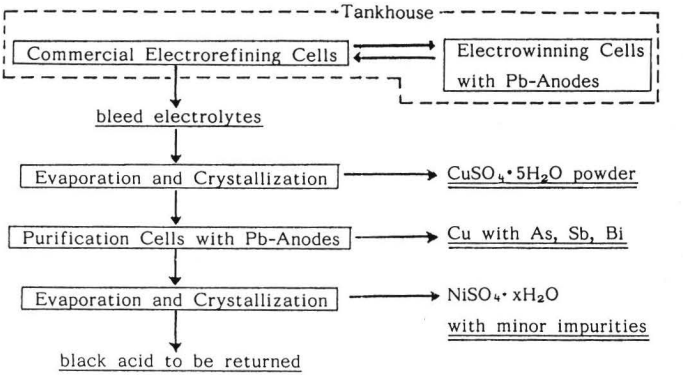

Fig. 1. Flowsheet of conventional purification process.

Since 1974, studies on the purification process have been continued in this laboratory. The purpose of this paper is to describe our conclusive flowsheet of the purification processes for copper electrolytes at this moment. One of the processes developed has been operated in Japanese copper refineries.

2. THE PROPOSED PROCESS

Several processes on purification of copper electrolytes have been developed in this laboratory. On the basis of these processes, a global flow-sheet for the purification of copper electrolytes is illustrated in Fig. 2.

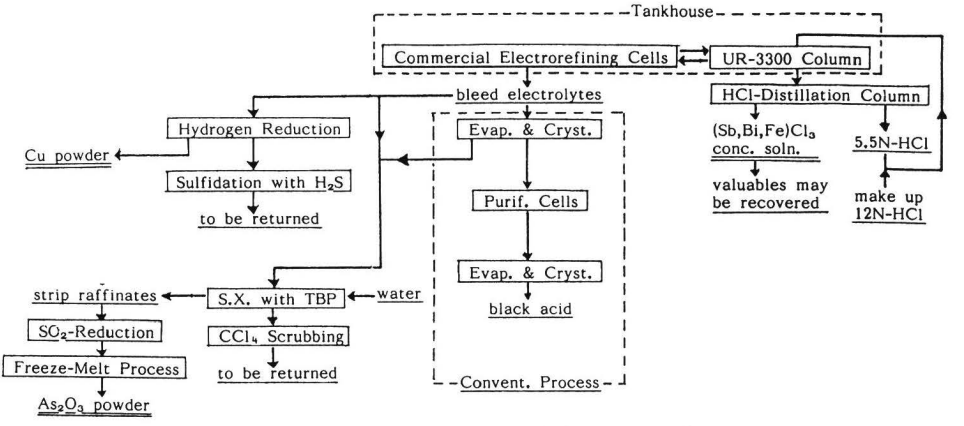

Fig. 2. A global flowsheet of the proposed process.

2.1 Solvent extraction of arsenic with TBP from bleed stream.

While the extraction of arsenic from some sulfuric acid solutions had been reported by Tserekova et al.(1970), the first information on selective extraction of the arsenic from copper electrolytes with TBP was released from this laboratory (Nagai et al., 1976). Examples of experimental results are shown in Fig. 3 and 4 in a form of flow-diagram with arsenic concentrations. About 80-90% of arsenic could be removed in this manner. The extraction efficiency was high, when a) sulfuric acid concentration was high such as in the mother liquor from copper sulfate plant(about 400g/l), and b) extraction temperature was lower than 20°C. Phase sepa-

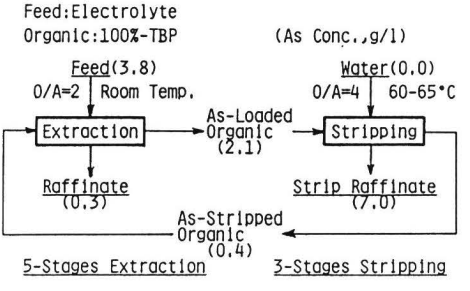

Fig. 3. Flow-diagram of As-extraction from copper electrolyte.

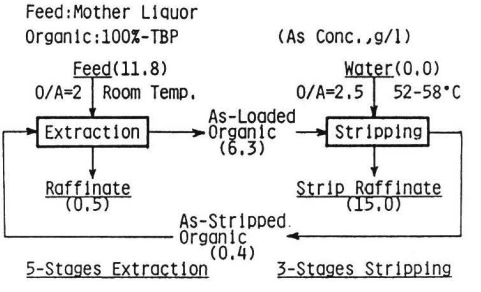

Fig. 4. Flow-diagram of As-extraction from mother liquor of copper sulfate plant.

ration was good at extraction stages and not good at stripping stages. However, somewhat better phase separation at stripping stages was made at higher temperature than 50°C.

TBP in the raffinates was rather high, so that the raffinates could not be returned to commercial cells, directly. The scrubbing of the raffinates with carbon tetra-chloride was confirmed to be effective for removal of TBP, as the carbon tetra-chloride extracted the TBP in the both forms of emulsion and of solution (Kanoh et al., 1982a). The stripped solutions contained 10-20g/l As(as acid arsenate) and 50-250g/l sulfuric acid. To obtain As_2O_3-powder from this solution, the SO_2-reduction of arsenate, followed by "Freeze-Melt process", was also studied(Nagai et al., 1977).

A similar solvent extraction process was also developed at the Metallurgie Hoboken-Overpelt at almost the same time and has been successfully operated in the company(De Schepper, 1979).

2.2 Direct removal of Sb, Bi and Fe from copper electrolytes with chelating ion-exchange resin, UR-3300(Unitika Ltd.).

The resin is characterized by methylene amino-phosphonic acid as the active group. Examples of experimental results are shown in Figs. 5 and 6. The resin selectively adsorbed Sb, Bi and ferric iron, directly from the copper electrolytes at commercial operation temperature of 60°C, which contain 45g/l Cu and 200g/l H_2SO_4. This suggests that the resin column should be applied in circulating stream of electrolytes within the tankhouse, rather than in the bleed stream from the tankhouse operation. After passing the resin column, the electrolytes can be returned without any change of temperature or compositions, except the removal of Sb, Bi and Fe (Kanoh and Nagai, 1983).

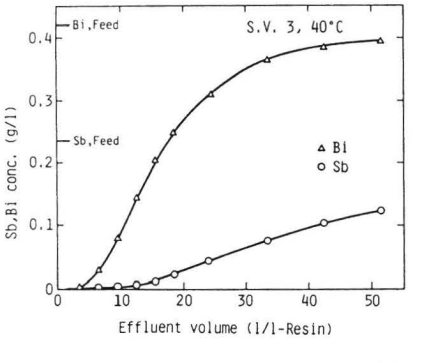

Fig. 5. Column adsorption test with UR-3300(30ml) for Sb and Bi.

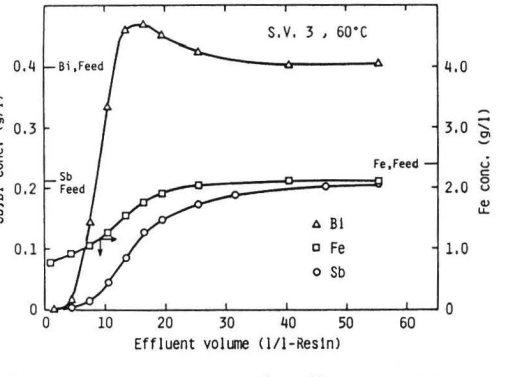

Fig. 6. The same test, but Fe was added and at 60°C.

Our proposal was accepted and has been extended by engineers both in the Tamano refinery, Hibi Kyodo Smelting Co. Ltd. and in the Research and Develop-

ment Center, Unitika Ltd. In order to regenerate the eluant(6N-HCl), they have developed a joint-system of an eluates-distillation column with the adsorption resin column. By means of the distillation, both the azeotropic aqueous solution of ca. 5.5N-HCl and the highly concentrated liquor of the impurities, from which valuables may be recovered, were obtained. Since 1985, the "Tamano Chalating Resin Process" has been intermittently operated, only when the Sb-level in the electrolytes exceeded some normal range of control(Oda et al., 1986).

The chelating ion-exchange resin process has been operated also at the Nikko refinery, Furukawa Elec. Ind. Ltd., in order to remove the accumulative iron in mother liquor of the copper sulfate plant. In this case, the eluates can be reuse at the elution of the UR-3300 column, after passing a strong anion-exchange resin column. The resin is simply regenerated with water(Shirakawa and Suzuki, 1988).

2.3 Copper-catalyzed SO_2-reductive elution of ferric iron from the resin.

Majima et al.(1985) reported SO_2-reductive stripping of ferric iron from D2EHPA with sulfuric acid solution. If the elution of the resin could be made with sulfuric acid solution, the purification system may be operated without any contamination of chloride ion.

Under conditions similar to that applied by Majima et al.(1985), the reductive elution tests were carried out. However, the ferric iron in the chelating resin was rather difficult to elute, especially with dilute sulfuric acid. This suggests the stronger adsorption of the resin than in the case of solvent extraction with D2EHPA. However, by means of the addition of copper sulfate to the sulfuric acid solution and at elevated temperature of 60°C, the SO_2-reductive elution of the ferric iron from the resin was accelerated. Results are shown in Table 1.

Table 1. Elution of UR-3300 with 33-bed volumes and S.V.=6.

Temperature	20°C		60°C	
H_2SO_4	50g/l	200g/l	50g/l	200g/l
acid only	44.9%	60.8%	58.9%	67.9%
acid+SO_2	52.4	68.0	79.2	89.5
acid+SO_2+Cu(10g/l)	57.4	69.9	91.7	98.2
acid+SO_2+Cu(20g/l)	60.0	72.8	94.2	99.7
acid+SO_2+Cu(40g/l)	58.3	70.3	93.7	99.3

2.4 Hydrogen reduction of copper electrolyte.

Instead of the electrowinning of copper with insoluble anodes, the hydrogen reduction of copper in an autoclave was studied to remove the excess copper. Bismuth ion in the electrolytes accelerates the reduction rates, especially in high acidic range more than 100g/l H_2SO_4, and leads the reaction to completion. However, in order to obtain a good powder, the hydrogen reduction must be stopped before

80% of copper was reduced. The copper powders, thus obtained, were pure, mainly consisted of fine single crystallines of 2-10μ, and exhibited a high oxidation resistivity, also. An example of analysis of the powder is shown in Table 2. Such powder may have various new usages, hence, additional values(Togashi and Nagai, 1983).

To remove the impurities in the liquor after the hydrogen reduction, sulfidation of the liquor with hydrogen sulfide was also studied (Kanoh et al., 1982b).

Table 2. Analysis of copper powder.

Impurities in copper (ppm)		
As	Sb	Bi
0.30	0.25	0.54

3. DISCUSSION AND CONCLUSION

In cases of copper refineries in Japan, total volume of the bleed electrolytes from a tankhouse in a month is nearly the same as that of whole electrolytes in the tankhouse. The rate of bleed stream is determined by one impurity which tends to exceed some normal range of control. Usually, the impurity has been the arsenic for a long time. However, the bleeding-rate determining impurity may change from one to another, e.g., from arsenic to antimony, according to the change of the raw materials and to the progress of techniques in the refineries.

In the case of the arsenic is the impurity, the rate of bleed stream to the conventional purification process can be calculated by the equation;

$$V(m^3/d)=\frac{\text{Anode dissolved(t/d)x(As\% in anodes)x(1 − Ratio of As into anode slime)}}{\text{As conc. in bleed(t/m}^3\text{)x(Removal\% of As at purification cells)}}$$

If the solvent extraction process or the chelating ion-exchange resin process was applied to the bleeding-rate determining impurity, the next one determines the bleeding-rate, and so on. However, because of these processes are highly selective, the removal of nickel and the minor impurities should be left in charge of the conventional purification process.

According to the recent operation data of Japanese refineries, the rate of the bleed stream can be reduced to about one-fourth, if As, Sb and Bi are removed by these processes. When the bleed steam is fixed at a rate enough to remove the impurities in usual tankhouse operations, the allowance for the impurity level in anode copper increases, and the more complex ores can be treated at the smelter. This is the case of Tamano smelter and the allowance of Sb contents in anode copper was nearly doubled with the process.

4. ACKNOWLEDGEMENT

The authors express our thanks to the Nippon Mining Co. Ltd., the Mitsui Metal Mining Co. Ltd. and the Unitika Ltd., for their technical and financial supports given on these studies.

5. REFERENCES

De Schepper, A., 1979. Extraction of arsenic from copper electrolytes by solvent extraction. Paper presented at meeting, Soc. Chem. Ind.(London); also in De Schepper, A., 1985. MHO solvent extraction process for removal of arsenic from Olen copper tankhouse bleed. in "Extraction Metallurgy '85 ", pp. 951-965.

Kanoh, G., Togashi, R. and Nagai, T., 1982a. Removal and recovery of TBP in a raffinate by carbon tetrachloride-scrubbing. Proc. Symp. on S.X. 1982, pp. 41.

Kanoh, G., Togashi, R. and Nagai, T., 1982b. Purification of copper electrolytes by means of a combination of solvent extraction, hydrogen reduction and sulfidation. Proc. Symp. in Fall Meeting(Kitakyushu), Min. Met. Inst. Japan, K-8, pp. 24-27.(in Japanese)

Kanoh, G. and Nagai, T., 1983. Purification of copper electrolytes including solvent extraction. Preprint Annual Meeting, MMIJ, pp. 185-6.(in Japanese); also in Kanoh, G. and Nagai, T., 1983. Removal of antimony, bismuth and iron in copper electrolyte by a chelating resin. Proc. Symp. on Solvent Extraction 1983, pp. 147-154.

Majima, H., Izaki, T. and Sanuki, S., 1985. Reductive stripping of Fe-loaded D2EHPA with the aqueous solutions containing sulfur dioxide. Metal. Trans., 16B: 187-194.

Nagai, T., Yamazaki, N. and Kobayashi, M., 1976. Purification of copper electrolytes by solvent extraction. Proc. Symp. in Fall Meeting(Muroran), MMIJ, L-1, pp. 1-4.(in Japanese); also in Nagai, T., et al. 1985. Removal of arsenic from spent copper electrolyte by solvent extraction with TBP. J. Min. Met. Inst. Japan, 101: 537-542.(in Japanese); Totsuka, T., Sasaki, K. and Nagai, T., 1986. Fundamental studies on purification of copper electrolyte. Met. Rev. MMIJ, 3: No. 2, 146-154.

Nagai, T., Kobayashi, M. and Higashioka, K., 1977. Manufacture of arsenic tri-oxide by wet process. Proc. Symp. in Fall Meeting(Fukuoka), MMIJ, G-6, pp. 23-26.(in Japanese); also in Higashioka, K. and Nagai, T., 1978. On a treatment of arsenic containing solutions. Proc. Symp. in Fall Meeting(Morioka), MMIJ, P-1, pp. 1-4.(in Japanese)

Oda, Y., Hashiuchi, M., Katoh, T. and Yonekawa, H., 1986. Tamano chelating resin adsorption process. Met. Rev. MMIJ, 3: No. 2, 155-163.

Shirakawa, R. and Suzuki, H., 1988(Nov.). An example of iron removal process with a chelating ion-exchange resin. Proc. 69-Committee, GAKUSHIN. p.76.(in Japanese)

Togashi, R. and Nagai, T., 1983. Hydrogen reduction of spent copper electrolyte. Hydrometallurgy, 11: 149-163.

Tserekova, A. M., Giganov, G. P., Kolomina, G. K. and Fokina, V. I., 1970. Tri-butyl phosphate extraction of arsenic(V) from sulfuric acid solutions. Sb. Nauch. Tr., Vses. Nauch-Issled. Gornomet, Inst. Tsvet. Metal., 19: 119-124.(in Russian)

Solvent Extraction 1990, T. Sekine (Editor)

© 1992 Elsevier Science Publishers B.V. All rights reserved

RECOVERY OF RARE METALS FROM COAL FLY ASH

I. TSUBOI, S. KASAI, T. YAMAMOTO, I. KOMASAWA and E. KUNUGITA*
Department of Chemical Engineering, *Department of Information and Computer Sciences, Faculty of Engineering Science, Osaka University, Toyonaka 560(Japan)

ABSTRACT

A process has been developed to recover several rare metals such as Li, B, V and Ga from coal fly ash. The process consists of three serial operations; two-stage leaching with H_2SO_4 of different concentrations in series; concentrating of rare metals in the leach liquor with functional resins; and purification of each metal by solvent extraction.

Li and B could be leached with dilute acid, the other undesirable transition metals being left in the residue. The two metals were then concentrated, respectively, with λ-MnO_2 and glucamic type resin, followed by purifcation by solvent extraction, employing a mixture of LIX51 and TOPO, and 2-ethyl-1,3-hexanediol.

Ga and V were leached with 1.5 mol/l H_2SO_4 from the solid residue of the first leaching, and both were then concentrated with iminodiacetic type functional resin. The two metals were isolated and purified by solvent extraction employing TOMAC or D2EHPA.

INTRODUCTION

There has been a significant increase in the use of and demand for rare metals in the modern chemical and electronics industries. Recovery of the trace rare metals from the coal fly ash is likely to be very prospective since the amount of the ash generated has been increasing. This industrial waste will be upgraded as one of the resources for the rare metals. In this work, the recovery of Li, B, Ga and V from the ash is investigated and a process for the recovery is proposed.

2 EXPERIMENTAL

2.1 Reagents

Fly ash, marketed as a cement additive by Kanden Kako Co., Ltd., was used. The functional resin for the adsorption of Li is λ-MnO_2 (HMnO) synthesized following the procedure of Hunter[1] and Ooi et al[4]. The commercial functional resins used are DIAION CRB-02 (Mitsubishi Chemical Industrial Co., Ltd.) and UNICELLEX UR-50 (Unitika Ltd.). The extractants used are α-perfluoroalkanoyl-m-dodecylacetophenone (LIX51, Henkel Corp.), tri-n-octylphospine oxide (TOPO, Dojin Seiyaku Co., Ltd.), 2-ethyl-1,3-hexanediol (EHD, Wako Pure Chemicals Industry Ltd.), tri-n-octylmethylammonium chloride (TOMAC, Koei Chemicals Co., Ltd. as KEX-L-84) and di(2-ethylhexyl)phosphoric acid (D2EHPA, Daihachi Chemicals Industry Co., Ltd. as DP-8R). LIX51 and TOPO were diluted in xylene

to 0.10 mol/l and 0.13 mol/l, respectively in a mixed state. EHD was diluted in xylene to 0.50 mol/l. TOMAC was purified following the procedure of Sato and Watanabe[6] and diluted in xylene to 0.10 mol/l. Kerosene solution of 0.30 mol/l of D2EHPA was used, to which 0.07 mol/l of tri-n-butylphosphate was added as a modifier.

2.2 Procedures

(1) Total analysis of fly ash constituents Measurements of element contents except B in fly ash were carried out following the method recommended by Sato[5], using HF and HCl. The concentration of metals in the resulting aqueous solution obtained was measured by an inductively coupled argon plasma emission spectrophotometry and a flame emission spectrophotometry.

(2) Leaching of metals from fly ash Pure water and H_2SO_4 of various concentrations were used as leachants for metals. Leaching was carried out by means of agitating 40 g fly ash and 80 ml leachant at each reflux temperature for 3 hr. The leach liquor thus obtained was filtered to remove solid residues.

(3) Selective adsorption of metals with functional resins The column operation was conducted using a column of 1.0 cm in diameter and 40 cm of effective height and actual fly ash leach liquor. The height was 16 cm for the Li adsorption. The pregnant leach liquor was fed on the top of the column. The elution of metals adsorbed was effected with various eluents.

(4) Purification of metals by solvent extraction For the extraction of metals, equal volumes of an organic and aqueous solution were equilibrated at 25 C. Loaded organic samples were stripped and the resulting aqueous samples were analyzed for the metal concentrations.

3 RESULTS AND DISCUSSION

3.1 Constituents of fly ash The results of total analysis of the fly ash are summarized in Table 1. The major constituents in this fly ash are Si, Al, Fe, Na, Mg, K and Ti. The contents of rare metals such as B and Ga are seen to be greater than base metals such as Cu, Pb and Zn.

3.2 Leaching of metals from fly ash The components in the resulting solutions with H_2SO_4 of various concentrations are shown in Table 2. The concentrations of metals have a tendency to increase with the concentration of the acid used.

Two-stage leaching was employed. Dilute H_2SO_4 of 0.18 mol/l was selected as the first-stage leachant, since it gives a weak alkaline liquor from which Li and B can be adsorbed by the resins without any pretreatment. H_2SO_4 of 1.5 mol/l was selected as the second-stage leachant, since the dissolution of Ga attains nearly the maximum.

TABLE 1 Constituents of fly ash

TABLE 2 Components of the fly ash leach liquors at reflux temperature for 3 hr

[μg/g-ash]

Al	50000	Mo	3.2
As	8.4	Na	13000
B	1200	Nd	280
Ba	1100	Ni	140
Be	7.7	P	1600
Ca	1500	Pb	130
Co	65	Rb	67
Cr	120	Si	420000
Cu	72	Sm	120
Fe	35000	Sr	1300
Ga	230	Ta	66
In	520	Ti	6600
K	9400	V	340
Li	1400	Y	39
Mg	10000	Zn	180
Mn	260	Zr	330

[μg/g-ash]

Leachant	Water	H_2SO_4			
Conc.[mol/l]	-	0.18	0.5	0.9	1.8	3.6
pH	12.5	9.1	3.1	2.6	-	-
Al	0	0	4200	7200	46000	46000
B	280	700	1000	1100	1200	940
Ca	2800	1800	15	20	30	5.0
Fe	0	0	560	5000	18000	11000
Ga	0	0	0	0.4	15.4	19
K	110	62	2.6	8.0	3200	4400
Li	9.8	10	20	32	60	70
Mg	0	0	2200	1600	3800	4000
Na	520	500	520	780	980	5000
Ti	0	0	0	0	2800	2800
V	0	0	24	38	50	160

3.3 Recovery of Lithium Separation and concentration of Li from leach liquor were carried out by λ-MnO_2 column operation, flow rate being 3.0 l/l-resin hr. The break through capacity of Li ion was obtained 0.92 g/l-resin. But other metal ions were also adsorbed significantly. Therefore, two-stage elution was followed[3]. One mol/l NH_4NO_3 was used as the first eluent, which eluted and removed the adsorbed metal ions except Li. Li was, then, eluted and concentrated with 0.1 mol/l HNO_3.

The resulting eluate liquor contained some impurities such as Na, K, Mg, Ca, and Mn. The purification of Li was performed by solvent extraction employing a mixture of two extractants, LIX51 and TOPO[2]. The effect of equilibrium pH on the extraction is shown in Fig.1, where E denotes the fraction extracted. Based on these results, extraction was carried out at equilibrium pH 8.2 at which Mn had been precipitated and removed prior to the extraction. Loaded organic phase was scrubbed with $1x10^{-3}$mol/l HCl to remove the co-extracted Na and K. Li was then stripped with $1x10^{-2}$mol/l HCl, Mg and Ca being left in the organic phase.

3.4 Recovery of Boron

The resin, CRB-02 which has a functional group of a glucamic type, gives a full play to its maximum ability in the range of neutral to mild alkaline condition. The separation and concentration of B by adsorption were carried out using the solution which had been passed through the column for the Li adsorption as a feed solution. When 3 l/l-resin of flow rate was employed, the break through capacity was obtained 3.0 g/l-resin. Concentration of B into the eluate liquor was effected with 1.0 mol/l H_2SO_4. Eighty seven percent of B was recovered and the B concentration was raised to 3.6 g/l.

The eluate liquor contained some impurities such as Ca, Mg and Na. These were separated by solvent extraction with EHD. The effect of proton concentration on the extraction of B and Ca is shown in Fig.2. Extracted fraction of B from the aqueous solution exceeds 95 % in the range of high acidity to neutral condition. Ca is not extracted, except at high alkaline condition. The stripping was completed with 1.0 mol/l NaOH, forming borax, $Na_2B_4O_7 \cdot 10H_2O$, which was then recovered from the solution by crystallization.

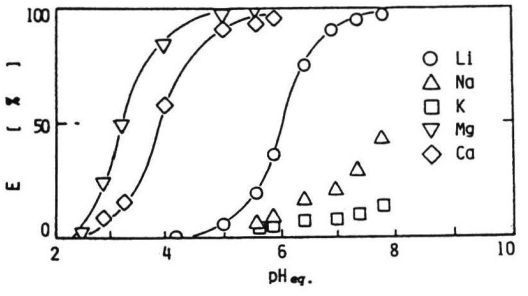

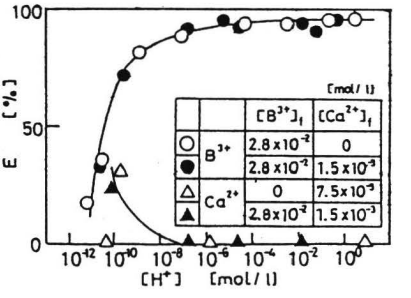

Fig. 1. Extraction of various alkali and alkaline earth metals with a mixed extractant of 0.1 mol/l LIX51 and 0.13 mol/l TOPO in kerosene.

Fig. 2. Effect of pH on extraction of borate ion and calcium with 0.5 mol/l 2-ethyl-1,3-hexanediol.

3.5 Recovery of Gallium and Vanadium

The effect of pH on the affinities of the functional resin, UR-50, for Ga(III), V(IV), Fe(II), Fe(III) and Al(III) were examined by batch operation. The adsorption of metals except Fe(II) increases with pH. The feasible maximum value of pH for the actual leach liquor is 2.5, since Ga starts to precipitate as its hydroxide at this pH. The adsorption of Fe can be prevented by reducing it from Fe(III) to Fe(II), and, thus, selective adsorption of Ga and V over Fe is feasible.

The second leach liquor obtained by 1.5 mol/l H_2SO_4 was treated by column operation. Na_2S and NaOH were added to the leach liquor for reduction of Fe and for pH adjustment to 2.5, respectively, prior to the column operation. Ninety five percent of Ga ion and 81 % of V in the feed solution were adsorbed, flow rate being 1.0 l/l-resin hr. The elution was effected with 1.5 mol/l H_2SO_4. The concentration of Ga and V in the eluate were 140 mg/l and 2800 mg/l, respectively. The Ga concentration, 140 mg/l, was not yet enough, and a re-concentration of the eluate was performed. The resulting eluate by 3.0 mol/l HCl contained 4000 mg/l Ga and 26000 mg/l V. The concentration of proton in the eluate liquors was about 2.0 mol/l.

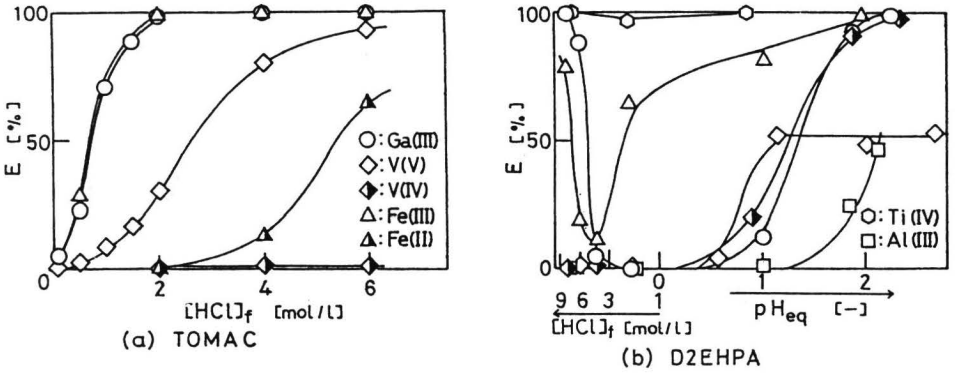

Fig. 3. Effect of proton concentration on extraction of metal ions with TOMAC(a) and D2EHPA(b).

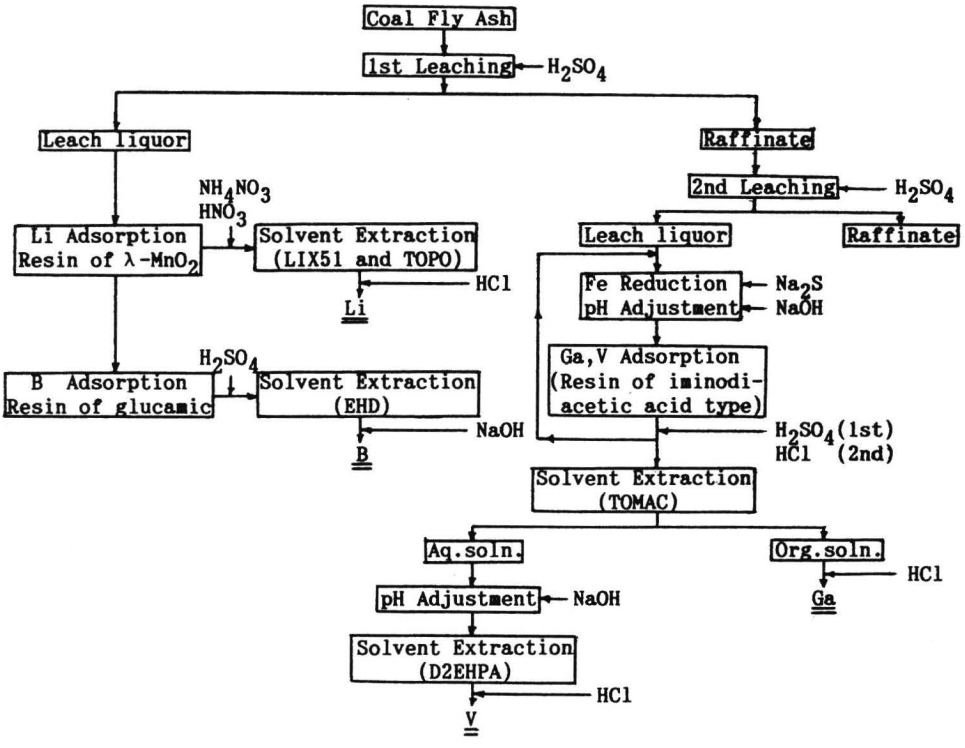

Fig. 4. Flow-chart of a process for the recovery of Li, B, Ga and V from coal fly ash.

The solvent extraction techniques with TOMAC and D2EHPA were employed for the separation and purification of Ga and V, since the resulting eluate liquors still contained such impurities as Al, Fe and Ti. The effects of proton concentration in the chloride system on the extraction of related metals are shown in Figs.3(a) and (b). Although the Fe ion was trivalent in the eluate, it was readily reduced to divalent by adding Na_2S, whereas the V ion in the eluate seemed to exhibit four valences from the color of the solution.

Based on these results of the extraction behavior of the extractants as well as the proton concentration of the actual eluate liquor, the following process was employed for the purification and isolation of Ga and V. Na_2S was at first added to the eluate to reduce Fe(III). The eluate was then contacted with TOMAC for the extraction of Ga. The stripping was effected with 0.1 mol/l HCl. To the raffinate solution NaOH was added to raise pH to around 2.0 and V was extracted with D2EHPA. The stripping was effected with 2.0 mol/l HCl. For the regeneration of D2EHPA, the organic solution was contacted with 2.0 mol/l $(NH_4)_2CO_3$ to remove Ti[7]. More than 90 % of Ga in the eluate was recovered with purity of 96.6 %. The V purity was 94.8 %. The final process is summarized in Fig.4.

4 CONCLUSIONS

An experimental study to recover and purify Li, B, Ga and V from coal fly ash was made with the following results.

(1) Several rare metal values are found to be contained in coal fly ash from the total analysis of its constituent. The ash was leached with H_2SO_4 of two different concentrations, 0.18 and 1.5 mol/l, in series.

(2) From first-stage leach liquor, Li and B were separated and concentrated by selective adsorption with λ-MnO_2 ion exchanger and glucamic functional resin, respectively. They were purified by solvent extraction, respectively, with the mixture of LIX51 and TOPO, and EHD.

(3) From second-stage leach liquor, both Ga and V were separated and concentrated together with an iminodiacetic chelating resin. Eluate liquor was concentrated again, and they were finally purified by solvent extraction with TOMAC and D2EHPA, respectively.

5 REFERENCES

(1)Hunter, J.: J. Solid State Chem., 39, 142(1981)
(2)Kunugita, E., J. H. Kim and I. Komasawa: Kagaku Kogaku Ronbunshu, 15, 504(1989)
(3)Idem: Ibid., 16(5) (1990) in press
(4)Ooi, K., Y. Miyai and S. Katoh: Sep. Sci. Technol., 21, 755(1986)
(5)Sato, K.: Energy and Environment Laboratory Report, No.283051(1984)
(6)Sato, T. and M. Watanabe: Anal. Chim. Acta, 49, 463(1970)
(7)Tsuboi, I., J. Ingham and E. Kunugita: J. Chem. Eng. Japan(1990) in press

Solvent Extraction 1990, T. Sekine (Editor)

© 1992 Elsevier Science Publishers B.V. All rights reserved

IMPROVEMENT OF REMOVING ARSENIC FROM COPPER ELECTROLYTE WITH SOLVENT EXTRACTION

YANG JIAOYONG, LIU DAXING, ZHAN HUIFANG, JIANG KAIXI
Beijing General Research Institute of Mining and Metallurgy, Beijing 100044, Peopie's Republic of China.

ABSTRACT

This paper describes an improved process of removing arsenic from copper electrolyte by solvent extraction. The solvent is 40% TBP and 10% P204 in kerosene. This solvent system has higher extraction capacity in a higher acidic solution(150~200g/lH_2SO_4). Arsenic can be loaded into the organic phase up to a concentration of 13g/l.

A new solvent extraction/bicupric arsenic(SX/BCA) process is being operated commercially at Shilu Copper Company in Guang dong Province, China. The plant incorporates five extraction stages, one scrubbing stage, and three stripping stages to produce a low-acid arsenic-bearing stripping liquor which can be used to produce bicupric arsenate. This product is emplyed in making arsenical timber preservatives CCA or ACA.

INTRODUCTION

In the process of copper electrolytic refining, about 70% arsenic contained in copper anodes dissolves into electrolyte, and accumulates gradually in it. Because of the approach of the standard electric potentials of copper and arsenic, arsenic will deposit on cathodes if arsenic in electrolyte increases to certain amount. This would disgrace electrolytic copper. So it is important to control the arsenic content in electrolyte.

The conventional method for removing arsenic from copper electrolyte is electrodeposition. The shortcomings of this method are:

i) high energy consumption, which accounts for 6~8% of total energy consumption of electrolytic refining;

ii) the risk to produce the noxious gas H_3As when copper content in electrolyte is less than 0.5g/l;

iii) high copper content and high arsenic content in blackcopper, which is returned to smelting process for further treatment, and in which partial arsenic recycles between smelting and refining, and useful arsenic product can not be obtained.

Solvent extraction (SX) to remove arsenic from copper electolytic has been developed in recent years. Most of the extractants are TBP. [1 - 8].

The advantages of removing arsenic by SX from copper electolyte are:

i) that arsenic products (white arseic or BCA) can be directly yielded which avoids arsenic dispersion in interim-products and interim-product storage;

ii) that the process does not produce the noxious gas H_3As, Does not pollute environment, and does not endanger operators'health;

iii) that the process saves energy, which consumes 8% of electricity less than the conventional method.

Since 1985, Beijing General Research Institute of Mining and Metallurgy has developed the research work on removing arsenic from copper electrolyte using solvent extraction. A commercial plant was built up in Shilu Copper Company, China. Its capacity was 100 ton bicupric arsenate per year. The plant was put into operation in 1987. Figure 1 shows the flow sheet of the plant.

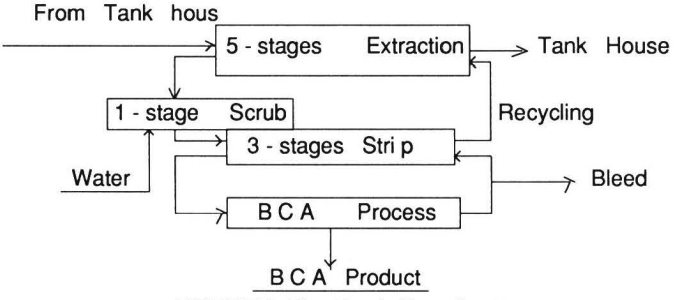

FIGURE 1. Plant basic flow sheet

THE CHOICE OF EXTRACTION SYSTEM

TABLE 1. The influence of various additives on TBP removing arsenic

No.	system of solvent extraction	phase separation time (min.)	As in organic phase (g/l)
1	50%TBP+kerosene	1.0	0.92
2	50%TBP+5%N263+kerosene	1.0	1.34
3	50%TBP+10%N263+kerosene	1.0	1.73
4	50%TBP+10%P204+kerosene	1.0	2.10
5	50%TBP+10%P507+kerosene	1.0	1.60
6	50%TBP+10%iso-octyl alcohol+kerosene	2.0	0.66
7	50%TBP+10%sec-octyl alcohol+kerosene	1.0	0.79
8	50%TBP+10%V911+kerosene	1.0	0.59
9	50%TBP+10%naphthenic acid+kerosene	1.0	0.88

Conditions: 1. The composition of copper electrolyte: Cu 40g/l, As 6.38g, H_2SO_4 200g/l.
2. The ratio of phase: 1, room temperature, mixing time: 10 minutes, stripping liquor: 60 °C water; phase ratio of stripping: 1.

It is known that arsenic loading into TBP solvent is affected greatly by the sulphuric acid

concentration in aqueous solution. Usually, copper electrolyte contains 160~200g/l sulphuric acid. At such a concentration of sulphuric acid,the arsenic loading of organic phase is not high enough. Therefore, the influence of additives on TBP removing arsenic has been studied.

The additvies can be classified as alcohols, phosphinic acids, neutral phosphate esters, tertiary-carboxylix acids, and quadri-amines. The organic phase of the tests useis 50%TBP and various additives in kerosene. The test results are given in Table 1.

The test results show that among various additives, P204 and N263 has obvious synergistic effect on the extraction arsenic. The further results are shown in Table 2.

TABLE 2. The influence of P204 and N263 on TBP removing arsenic (O/A=1)

No.	system of solvent extraction	phase separation time (min.)	composition of organic phase (g/1)	
			As	H_2SO_4
1	40%TBP+10%P204+kerosene	0.5	1.42	1.76
2	45%TBP+10%P204+kerosene	0.5	1.38	2.12
3	50%TBP+5%P204+kerosene	5	1.34	2.58
4	50%TBP+10%P204+kerosene	9	2.10	2.98
5	60%TBP+10%P204+kerosene	13	2.30	4.98
6	50%TBP+5%N263+kerosene	>10	0.64	7.90
7	50%TAB+10%N263+kerosene	>10	1.42	12.10

The test results show that addition P204 into TBP has more adventages such as:

i) That arsenic loading of organic phase is 30% higher than that of organic phase of addition N263, i.e. P204 has better synergism;

ii) Faster phase separation rate;

iii) That organic phase contains less sulphuric acid, which is advantageous to the following processes.

Test results also show that arsenic loading of organic phase increases with the increase of TBP concentration; but the higher TBP concentration, the slower phase separation rate is, and the more sulphuric acid is extracted into organic phase.

Considering both arsenic loading and phase separation rate, we chose the solvent extractant of 45%TBP+10%P204+kerosene.

INFLUENCE OF VARIOUS FACTORS ON ARSENIC LOADING

The influence of sulphuric acid concentration in copper electrolyte, temperature and additive P204 is shown in Figure 2 and Figure 3, respectively.

The mixing time testwork indicates that this system has rather rapid rate of solvent extraction; solvent extraction reactions reach equilibrium in 5 minutes.

It can been known from the McCabe - Theile figure of arsenic extraction that in order to decrease the arsenic content in raffinate to less than 1g/l, five extraction stages are necessary.

THE PRACTICAL ORERATION

1. The process designing

The copper anode produced by Shilu Copper Company contains very high arsenic (As 0.7% on the average). The commercial removing arsenic unit by SX has been operating normally since its beginning operation at the end of 1987.

The organic phase is 45% TBP+ 10% P204 in kerosene. The plant incorporates in total nine stages: five extraction stages, one scrubbing stage, and three stripping stages. The raffinate and stripping liquor flow through oil-water separators. The stripping liquor recycles until its arsenic content reaches above 30g/l, and then is pumped to the bicupric arsenate (BCA) process. The raffinate is returned to copper electrolysis through activated charcoal absorption for removing organism.

2. The influence of arsenic content in electrolyte

Arsenic content in electrolyte affects greatly as loading of organic phase. When sulphuric acid concentration and phase ratio are constant, the higher arsenic content of electrolyte, the higher arsenic loading organic phase has. See Table 3.

TABLE 3. The relationship between arsenic concentration of electrolyte and arsenic loading of organic phase

No	the composition of electrolyte(g/l)		As content of organic phase
	As	H_2SO_4	(g/l)
1	58.59	200	11.83
2	39.06	200	7.93
3	29.29	200	6.65
4	14.65	200	3.94
5	7.32	200	1.60

TABLE 4. The typical composition of all liquors in practical process (g/l)

component	As	Cu	Fe	Sb	Bi	H_2SO_4
electrolyte	40～50	40～50	2～2.5	1.0～1.2	0.02～0.05	170～200
raffinate	20～25	39～43	2～2.5	1.0～1.2	0.02～0.05	170～200
scrubbing liquor	50～55	0.5～0.8	trace	0.5～0.8	0.04±	25～30
stripping liquor	30～40	0.05～0.007	0.002～0.003	0.02～0.04	<0.001	<1

Because the SX process was set up into operation oone year after electrolytic refining production, arsenic content of electrolyte reached more than 40g/l. The organic phase of fifth stage contains 11～13g/l arsenic. When the phase flow ratio O/A is 3, the arsenic extraction ratio may reach 50%. The typical composition of all liquors in practical process is in Table 4.

From Table 4, it can be seen that stripping liquor contains very little H_2SO_4. The scrubbing stage can wash out more than 90% H_2SO_4 from loading organic phase.

3. The influence of TBP on copper electrolysis and its elimination

The influence of TBP in the raffinate on cathodic copper is investigated. Tests show that when TBP in electrolyte is more than 0.6g/l, the surficial form of electrolytic copper is affected; the surface loses metallic luster, becomes gloomy, and appears organic burn. Tests show that activated charcoal has a good role in absorbing organism of the raffinate. Therefore, in the practical process, the raffinate flows through an activated charcoal column to remove the trace organism, quality of electrolytic copper can be ensured.

4. The manufacture of BCA

The stripping liquor containing more than 30g/l arsenic is pumped into three reaction tanks with mechanical stirring. It is mixed with copper sulphate and neutralized, meanwhile the reaction temperature is controlled. Thus the blue filterable BCA is obtained. The typical composition of BCA is given in Table 5.

TABLE 5. The typical composition of BCA*

component	As	Cu	Fe	Sb	Bi	Ca	Mg	Na_2O
wt%	28~32	28~32	<0.02	0.01~0.03	<0.001	<0.1	<0.05	<5

*The compostion is based on the dried BCA.

The molecular formula of BCA is $Cu_5As_4O_{15}$.9H2O.

5. The treatment of waste water

The BCA filter liquor contains about 0.03~0.1g/l arsenic. This water and other waste water (e.g. water gathered on floors) are mixed with lime and iron salt; the terminate pH is about7. The reaction time is 20~30 minutes. In this way, arsenic in waste water is reduced to less than 0.5 ppm.

CONCLUSION

Removing arsenic using SX not only produces directly commercial product of arsenic, but also eliminates the risk of producing noxious gas H_3As. The process has a good operation condition, less energy consumption. It has obvious advantages, and is suitable for removing arsenic from high arsenic anode electrolysis. When other parameters are kept constant, P204 addition into TBP, arsenic loading of organic phase may increase to more than 13g/l. The commercial plant of removing arsenic with SX has been operating normally since its beginning operation at the end of 1987. Product-BCA are used as raw material in the manufacture of timber preservatives (CCA, ACA).

REFERENCES

[1] Tserekova A. M., et al, Gornomet. Inst. Tsvet Metal, No 19,119~124, 1970
[2] Cutmone J.P., Proc. Regional Meeting, The Aust. I.MM. North west Queensland Branch, August, 1974
[3] Demirkiran A., M. Phil. Thesis, Department of Mining and Mineral Aciences, The university of leeds, 1978
[4] Nagai T.et al,J. MMIJ, 100, 537-542, 1985.
[5] Baradele A., et al, J. M. Feb. 32~37 1986
[6] Schepper, A. D., "Extractive Metallurgy", 167~188, 1985
[7] O'Kane J., "Extractive Metallurgy", 951~965, 1985
[8] Keith R. S., E/MJ 52~55 Dec. 1987

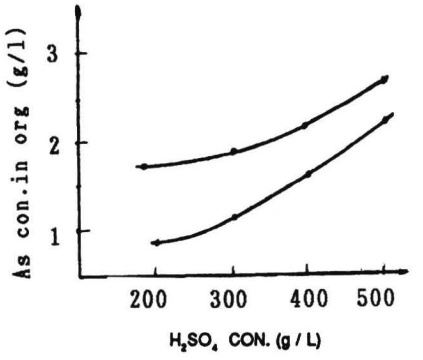

FIGURE 2. The influence of additive P204 and H_2SO_4 concentration in aqueous phase on arsenic loading (O /A=1,20°C)

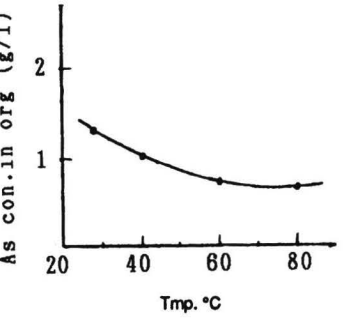

FIGURE 3. The influence of temperature on arsenic loading

Solvent Extraction 1990, T. Sekine (Editor)

© 1992 Elsevier Science Publishers B.V. All rights reserved

SOLVENT EXTRACTION OF ZINC FROM HYPERSALINE BRINE

J.J. Byeseda and K.W. Warren
NATCO, P.O. Box 1710, Tulsa, OK 74101 USA

ABSTRACT

This report summarizes development of a process for recovering metals from Imperial Valley (California) geothermal brine. The process exploits the fact that some brines in the Imperial Valley contain enough dissolved metals to qualify as ore deposits. A process is described that can selectively extract zinc from brine solutions (United States Patent Number 4,624,704). The reagent system separates zinc from brine nearly saturated with sodium and calcium chloride, even in the presence of other metals like iron, lead and manganese. Equilibrium data is presented for brine obtained from a flowing geothermal well in the Imperial Valley. We operated a laboratory mixer-settler pilot plant to obtain information on process characteristics. This data is presented, with insights about operation of a full-scale system. A mathematical model simulating design and operation of the mixer-settler system was developed. The following data is required to operate the model: equilibrium data, mechanical and process design assumptions, and assumptions related to the cost of equipment and operation. This model designs the process and auxiliary equipment, estimates plant cost, and evaluates the economics for a zinc recovery project. The behavior of the pilot plant correlates with predictions of the simulator. The economic calculations indicate that as the brine flow approaches 4000 gpm, a venture that incorporates zinc recovery using this technology will be profitable.

1 INTRODUCTION

Power can be produced from either vapor or liquid dominated reservoir systems. The well-head fluid from a vapor-dominated geothermal resource is essentially pure steam, which is fed directly to a power plant turbine. Unfortunately only a small fraction of the geothermal resource exists in vapor dominated reservoir systems. Many reservoirs containing fluid suitable for electric power production are liquid-dominated (hydrothermal) where the reservoir contains water as a superheated liquid phase. When the pressure is decreased, a fraction of the liquid vaporizes and can be used to drive a turbine. This arrangement is called a flash-steam power plant. The United States geothermal industry is actively developing several geothermal areas for electric power production. The Geysers (near San Francisco, CA) is a vapor-dominated resource that has been producing electricity since 1960. The Imperial Valley (near San Diego, CA) has liquid-dominated geothermal resources and a large area contains brine with unusually high total dissolved solids (more than 20% by weight salt). The term hypersaline is usually applied to these brines which are located under an area about 16 miles wide and 25 miles long extending southeast from the edge of the Salton Sea. This hypersaline brine offers a great opportunity for metal/mineral recovery ventures.

Although there has been a recognition that mineral recovery can potentially improve the overall economics of a power generation project, no commercial mineral recovery plants have been built in the Imperial Valley. Our work shows that solvent extraction for zinc recovery is a technically viable option, and our economic analysis indicates the technology can be the basis of a profitable venture.

2 PROCESS DEVELOPMENT CRITERIA

Table 1 shows Michels' summary of the best available data for the composition of Imperial Valley hypersaline brine. The large values for the standard deviations in these data illustrate the necessity of obtaining data from a well near the proposed site for the metal recovery operation. Michels used this data to analyze the economic potential for recovering several components in this hypothetical hypersaline brine. Table 1 also shows his calculations of potential mineral recovery based on treating the reject brine flow from a 50 MW power plant. The work done by Michels narrows the focus for process development for metal recovery from Imperial Valley hypersaline brine.

TABLE 1 (after Michels)

Hypersaline brine composition and mineral recovery from 50 MW power plant reject brine

Specie	# wells	Avg Conc wppm	Std Dev wppm	Market Form	Rec Frac	Product Tons/yr	Value $/Ton	Value MM $
Na	7	57900	11300	NaCl	0.9	2880000	50	144 (e)
Ca	7	27500	9800	$CaCl_2$ (a)	0.8	3300000	32	106 (e)
K	7	15400	5300	KCl (b)	0.8	494000	60	30 (e)
Fe	7	2050	1420	$Fe(OH)_3$	0.9	79000	120	10 (e)
Mn	6	1280	340	MnO_2	0.8	34300	175	6 (f)
Ba	6	810	860	$BaSO_4$	0.9	10900	100	1
Zn	6	770	350	Zn	0.8	12600	860	11
Sr	5	750	620	$SrSO_4$ (c)	0.4	11600	640	7 (e)
Mg	7	740	870					
B	6	380	120	H_3BO_3	0.05	2300	550	1 (e)
Li	7	300	130	Li_2CO_3	0.6	2800	2800	56 (e)
Pb	6	130	80	Pb	0.95	2400	300	0.7
Cu	4	4	3	Cu	0.5	1300	1300	0.03
Ag	2	0.9	0.1	Ag	0.5	10	9 (d)	2.5
Cl	7	160000	32000					
Br	3	50	60	Br_2	0.1	64	600	0.04
Power							$.06/ kwh	21

(a) 38% liquid (c) requires conversion to $SrCO_3$ (e) inadequate market
(b) fertilizer grade (d) per Troy ounce (f) unknown marketability

3 PROCESS DEVELOPMENT

3.1 Laboratory and Field Data - Solvent Development

We evaluated a large number of reagent formulations for metal recovery using a synthetic hypersaline brine prepared from the chloride salt of each metal and distilled water. The pH was adjusted to 4-5 using hydrochloric acid to simulate the typical acidity of post-flash brine. Table 2 shows equilibrium results for the organic reagent formulation

(described in U.S. Patent 4,624,704) that was very selective for Zn using hypersaline brine obtained from a flowing well in the Imperial Valley. Two cases are shown: data obtained with brine taken directly from a flowing well and for brine shipped to our lab. The data show our formulation selectively recovers zinc even when iron is present in the feed brine. The experimental errors for the brine concentrations are relative values in %; those reported for the recovery (%) are absolute ones. These numbers give one a feel for the uncertainty in the removal efficiency for each metal. We found that the data obtained using synthetic brine was similar to that obtained using brine from the well. Thus one can use synthetic brine for preliminary determination of equilibrium data and for lab-scale pilot plant operation

TABLE 2

Equilibrium data for metal recovery obtained using brine from an Imperial Valley well

Metal	Brine Concentration (a)				Recovery (a)		Brine Concentration (b)				Recovery (b)	
	Initial wppm	% Error	Final wppm	% Error	%	Error ±	Initial wppm	% Error	Final wppm	% Error	%	Error ±
Na	63163	0.8	64276	0.2	-1.8	0.8	59481	1.7	60794	0.2	-1.8	1.7
Ca	34059	1.3	35243	1.3	-3.5	1.9	32608	2.8	33042	1.5	-1.3	3.2
K	20152	1.1	20460	0.3	-1.5	1.2	17023	1.7	17501	0.2	-2.8	1.7
Fe	2691	2.1	2674	1.5	0.6	2.6	2324	1.8	2278	1.2	2.0	2.1
Mn	1767	1.7	1740	0.7	1.6	1.9	1705	1.3	1709	0.6	-0.2	1.4
Zn	743	1.7	98	3.3	86.9	2.3	714	1.6	101	2.4	85.9	2.2
Sr	687	0.9	709	0.9	-3.3	1.3	592	3.3	595	1.1	-0.6	3.5
Ba	333	4.3	352	3.2	-5.7	5.5	263	5.4	267	4.2	-1.7	6.9
Li	304	0.5	311	0.3	-2.1	0.6	252	1.3	260	0.3	-3.2	1.3
Pb	91	6.3	89	5.5	3.1	8.2	157	14.6	147	7.6	6.1	16.3
Mg	136	0.6	138	0.6	-1.8	0.8	110	2.2	112	0.1	-2.2	2.2

(a) Lab test data, using stabilized brine. Reagent formulation SA-410. Aqueous/Organic Ratio = 3:1. Contact temperature = 150 °F.
(b) Field test data, using brine from flowing well. Reagent formulation SA-410. Aqueous/Organic ratio = 3:1. Contact temperature = 160 °F.
(c) All metal concentration data were obtained using a Perkin-Elmer Model 460 atomic absorption spectrophotometer.

3.2 Strip Chemistry Development

Once the organic reagent has contacted the feed brine, the metal must be stripped from the organic phase into an aqueous phase from which the metal can be recovered. We found that a solution of sodium sulfate at 10-20 wt% was effective at stripping zinc from the organic phase. The sodium sulfate solution has three process advantages:

1) It is insensitive to changes in the pH and to chloride concentration, so that close monitoring of the solution composition is not required.

2) It allows use of a straightforward process for production of zinc in a marketable form: precipitation or electrowinning of zinc is feasible from this strip solution.

3) It is non-corrosive, so that process components to handle the solution will be relatively uncomplicated and inexpensive.

3.3 Pilot Plant Operation

The pilot has mixer sections with about 100 ml capacity, and settler sections of about 500 ml. Three independent circuits are included in the system. Figure 1 illustrates the arrangement of the system and the process flows. The extraction circuit (E1) contacts the brine, which contains about 800 mg/l zinc, with the organic reagent formulation. The extraction mechanism appears to be exchange of a chloro-zinc complex from the brine with chloride ions bound to the active component of the organic formulation. The zinc-rich organic phase then flows to a surge tank before being pumped to the strip circuit (S1 & S2) where it contacts the sodium sulfate strip brine. In a commercial operation the strip solution would be recycled to the strip circuit after recovery of a zinc product. For the operation of the pilot plant, fresh strip solution was supplied continuously, while the zinc-rich strippant was collected for analysis.

In the strip section (S1 &S2), sulfate anions displace the chloro-zinc complex from the organic reagent. The zinc is concentrated into this flow stream by a factor of 10-20 times the original concentration in the inlet geothermal brine. The strip solution flow is considerably smaller than the organic flow in order to maximize the concentration of zinc in the strip solution. In order to maintain an aqueous continuous dispersion in the strip circuit mixers, the strip solution is recycled around each mixer-settler. If the solution is recycled back to the strip section after zinc product recovery, chloride anions will accumulate in the circuit. The experiments done on strip chemistry indicate that the strip solution can accommodate a high concentration of chloride without adversely affecting zinc removal. Since evaporation of water from sodium sulfate solution causes crystallization of sodium chloride, it should be possible to maintain purity of the stripping solution without undue waste of sodium sulfate.

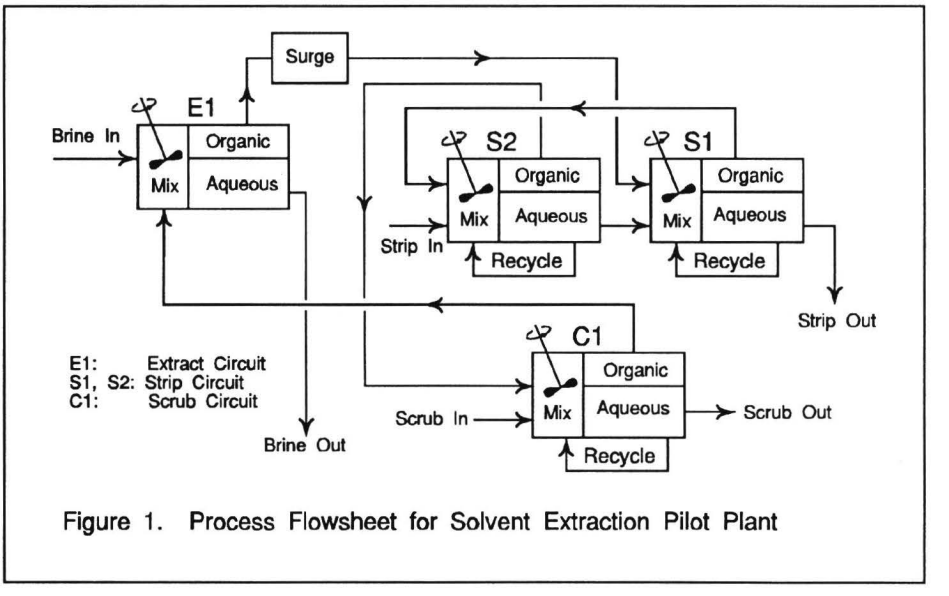

Figure 1. Process Flowsheet for Solvent Extraction Pilot Plant

The organic phase flows to a scrub circuit (C1) after removal of zinc in the stripping circuit to displace the sulfate anions from the reagent. Sodium chloride was found effective

for this purpose. We operated the pilot plant scrub circuit using a 10 wt% solution of sodium chloride. Removal of the sulfate anions from the organic prevents precipitation of barium sulfate in the extract circuit which would cause problems in the brine injection wells.

The pilot plant was operated using the active reagent at 10 vol% along with 10 vol% of a C9-C11 alcohol mixture as a phase modifier. The phase modifier prevents the formation of multiple organic phases at high metal loading. All runs were performed using a synthetic Imperial Valley hypersaline brine. The following conditions were used:

Inlet brine flow	21 ml/min	Scrub solution circulation	21 ml/min
Organic circulation	7 ml/min	Temperature	170 °F
Strip brine flow	2 ml/min	NaCl concentration (scrub)	10 wt%
Strip recycle flow	19 ml/min	Na_2SO_4 concentration (strip)	10 wt%

The solvent extraction pilot was able to decrease the zinc concentration in the inlet brine from 800 mg/l to 25-50 mg/l. The strip solution contained zinc at 6000-7000 mg/l. The plant continued to operate at this efficiency for 351 hours before we observed two organic phases in the extraction section, along with degradation in the zinc extraction: after another 150 hours of operation a sludge had begun to accumulate in the extraction circuit. When we shut down the plant to investigate, the problem appeared to stem from thermal degradation of the reagent formulation. The active component of the organic phase has an upper temperature limit of about 170 °F for continuous operation. While we were not operating the process above this limit, we used electric immersion heaters for temperature control in the pilot plant. The skin temperature at the immersion heater surface is approximately 200-220 °F. We confirmed this phenomenon by using an immersion heater to maintain one sample of the organic phase and brine at 170 °F, and another sample on a hot plate set at the same temperature. No degradation was seen in the organic phase on the hot plate.

4 PROCESS SIMULATION, DESIGN AND ECONOMICS

A computer model has been developed to simulate the behavior of our solvent extraction technology for zinc recovery. The code was written using Microsoft Fortran and implemented on an IBM PC. The model uses data on the extraction and stripping properties of the reagent formulation to predict the zinc recovery for a given set of plant operating conditions. The simulator estimates cost of building and operating the plant , and calculates estimated profitability of the project. We tested the simulator using data from the pilot plant and found the results were in agreement. Thus we can use the program to experiment with various operating conditions. The results shown on Table 3 represent an optimum design for recovering the maximum amount of zinc for the minimum capital and operating costs when processing a brine flow of 4000 gpm, which corresponds to the reject brine flow from a 50-75 MW flash steam power plant. The information displayed consists of some output obtained from the simulator package. The simulator "experiments" revealed that there is an advantage to using the active reagent at 20 vol%. Extraction and stripping isotherms were measured at this strength and incorporated into the model. The economic data in Table 3 demonstrate the potential profit for a zinc recovery venture from Imperial Valley hypersaline brine. This analysis assumes no recovery of NaCl or Na_2SO_4 ; if crystallizers were added to the scrub and strip circuits, total consumption of both chemicals could be reduced by 75-90%.

TABLE 3 Simulator design, performance, and economics results for 4000 gpm brine flow

			Flows (gpm)		Aqueous (mg/l)		Organic (mg/l)	
	Zn (Ton/yr)	Stages	Aqueous	Organic	Zn In	Zn Out	Zn In	Zn Out
Extract	6100	1	4000	800	800	27	2767	6630
Strip	6100	2	350	800	0	8830	6630	2767

PARAMETER		EXTRACT SECTION	SCRUB SECTION	STRIP SECTION
A:O :	actual	5.0	0.01	0.44
	effective	5.0	1.3	1.3
Mix tank:	residence	2.00 min	2.00 min	2.00 min
	volume	9600 gal	3680 gal.	3680 gal.
	dimensions(ft)	12.3 X 12.3 X 9.5	8.4 X 8.4 X 8	8.4 X 8.4 X 8
	mixer	100 HP	50.00 HP	50.00 HP
Settler:	residence	15 min	15.00 min	15.00 min
	volume	72000 gal	27600 gal.	27600 gal
	dimensions(ft)	92.2 X 12.3 X 9.5	62.9 X 8.4 X 8.0	62.9 X 8.4 X 8.0
	recycle pump	0 HP	15.00 HP	10.00 HP
Solvent loss		89553 gpy	45 gpy	7836 gpy
Sludge production		680 gpy	680 gpy	1360 gpy

Installed Equipment Costs

Mixer/settler system	$ 1129921
Brine feed tank	$ 159200
Solvent storage tank	$ 65339
Rich solvent surge tank	$ 117175
Strip solution storage tank	$ 112401
Strip solution surge tank	$ 71354
Scrub solution storage tank	$ 73989
Scrub solution recycle tank	$ 7901
Brine cooler	$ 437257
Brine filter	$ 102962
Brine feed pump & spare	$ 31590
Extract stage recycle pump	$ 0
Stripping stage recycle pump	$ 17041
Scrub stage recycle pump	$ 14616
Solvent transfer pump	$ 6232
Solvent feed pump and spare	$ 12464
Strip solution pump & spare	$ 7225
Strip solution transfer pump	$ 7225
Scrub solution pump & spare	$ 5994
Scrub recycle pump & spare	$ 2997
Sludge processing equipment	$ 226677
Installed Equipment Costs	$ 2609563
Other Capital Costs	
Site development	$ 2000000
Auxiliary systems	$ 2000000
Chemical inventory	$ 603644
Indirect costs	$ 1982869
Total Capital Cost	$ 9196075

Annual Costs and Revenue

Labor	$ 320000
Electricity	$ 76663
Chemicals	
-Solvent	$ 511526
-Na_2SO_4	$ 223927
-NaCl	$ 165402
Maintenance	$ 260956
Total Operating Costs	$ 1558474
Zinc Revenues	$ 9149635
Gross Profit	$ 7591161
IRR on Investment =	59.7 %
ChE Plant Cost Index	390.5
Unit costs: Solvent	$ 5.25 per gal
NaCl	$ 25.00 per ton
Na_2SO_4	$ 25.00 per ton
Zinc	$ .75 per lb
Electricity	$ .040 per kWh
Labor: --wages per person	$ 40000.00 /yr
--# of personnel	8.
Operating factor	.90
Project life	10 yr
Effective tax rate	.50
Investment tax credit	.10
Indirect cost fraction	.30
Maintenance fraction	.10
ACRS depreciation--fraction	.95

5 REFERENCE

Michels, D.M., Symposium on Hydrothermal Alteration and Geothermal Brine Chemistry,Processing, and Mineral Recovery, Geothermal Resources Council, June 5-6 1985, Sheraton, Palm Springs, CA

Solvent Extraction 1990, T. Sekine (Editor)

© 1992 Elsevier Science Publishers B.V. All rights reserved

RECOVERY OF GALLIUM FROM HYDROCHLORIC ACID SOLUTIONS BY EMULSION LIQUID MEMBRANES

J. KIRGIOS, W. DEGENER, K. SCHÜGERL
Institut für Technische Chemie, Universität Hannover, Callinstr. 3, D-3000 Hannover, F.R.G.

ABSTRACT

The extraction of gallium from 6n HCl solutions is investigated with water as the inner phase, LA-2 in kerosene as the membrane phase, and Paranox 100 as surfactant. The equilibrium, stoichiometry, and kinetics of the reaction are evaluated and the extraction is modelled. Under optimal conditions, complete extraction is attained in a single-stage equipment.

INTRODUCTION

Gallium is a widespread element, however its content in minerals is very low (e.g., in germanite 1.5% Ga). Since the liquid membrane technique is especially suitable for the recovery of metals at low concentrations, this method was investigated for Ga-recovery from dilute solutions.

2 MATERIALS AND METHODS

EXSOL 200/240 (Esso Chemie) was used as solvent phase, AMBERLITE LA-2 (N-lauryl-N-trialkylmethylamine) (Rohm and Haas) as carrier, PARANOX 100 (ECA 4360) (Esso Chemie) as surfactant. Ga-analysis was performed by AAS (Type A 370, Perkin Elmer) in a graphite oven (HGA 400), with a sampling automat (Model AS 40), and interface (RS 232 C). Since in high HCl-concentrations the extinction of Ga depends decisively on the HCl-concentration, the sample was diluted to a HCl-concentration below 0.01- 0.06 mmol/l. The analysis was merely impaired by alkaline and alkaline earth metals. Ga was extracted as $HGaCl_4$ by ether from a 6 mol/l HCl solution and, thus, was separated from the alkaline and alkaline earth metals for analysis. In our investigations, the Ga-extraction was performed by means of HCl-solutions at pH 0 to 2, at which it prevailed as tetrachloro-complex.

3 RESULTS

Equilibrium

Fig. 1 shows the degree of extraction of 600 ppm Ga from 6 n HCL with 11 mmol/l anion exchangers. The best back-extraction with water was achieved from the LA-2-complex. Therefore, this carrier was employed for the Ga-recovery. The back-extraction was carried out with different solutions. Since water gave a satisfactory degree of extraction, it was used for back-extraction in these investigations. The extraction and back-extraction with water are given by the following equations:

$$GaCl_{4w}^{-} + H_w^{+} + R_2NH_{org} = R_2NH_2GaCl_{4,org} \qquad (1a)$$

$$R_2NH_2GaCl_{4,org} = R_2NH_{org} + GA_w^{3+} + H_w^{+} + Cl_w^{-} , \qquad (1b)$$

where indices org and w denote the organic and aqueous phases.

The equilibrium constant K of the extraction is defined as

$$K = \frac{K_{eq}}{G} = \frac{(AHX_{org})}{(X_w^{-})\,(A_{org})^{n}\,(H_w^{+})}, \qquad (2)$$

where X = gallium-tetrachloro-complex ($GaCl_4$),
A = carrier LA-2 (R_2NH)
AHX = carrier-metal-complex
n = stoichiometric factor

$$G = \frac{(g_{AHX})}{(g_X^{-})\,(g_A)^{n}\,(g_H^{+})} , \qquad (3)$$

g are the activity coefficients of the components.

The stoichiometric factor n = 1 and the equilibrium constant K = 103.8 $(mol/l)^{-2}$.

The distribution coefficient D is defined as

$$D = \frac{(X_{org})}{(X^{-}_w)} \qquad (4)$$

Above 6 mol/l, D was constant. The degree of extraction E = 100% at pH < 1, above this value it diminished. At pH 1.8, it decreased to 50%.

Extraction in the three-phase system

A small glass beaker was put into a larger one. The 600 ml Ga-solution (165 ppm Ga in 44 mmol/l HCl) was put into the large beaker and stirred by a magnetic stirrer, the 100 ml stripping phase (distilled water) was filled into the small beaker stirred by an impeller. Both of them were topped with a 100-ml membrane phase (Exsol D with 2 vol% LA-2), which was stirred with the two-stage impeller as well. The concentrations of Ga and the pH-values were determined in the three phases as a function of time. On account of the small (9.62 cm^2 inner, 27.23 cm^2 outer) liquid/liquid interfaces, the concentrations varied only slowly. Fig. 2 shows a typical result. At t = 23 h, the Ga-concentration in the membrane phase attained a maximum. The pH in the inner phase quickly dropped to 1.5. The Ge-extraction was not influenced by the presence of copper and zink, which are not extracted under these conditions. The coextraction of HCl was slight (65 mmol/l after 193 h).

Emulsion liquid membrane

The stripping phase (e.g., distilled water) was emulgated in the membrane phase by IKA Ultra-Turrax TO 18/10 at 10.000 rpm for 4 minutes. The emulsion was added to the continuous phase at low stirrer speed. Below 200 rpm, the extraction rate was very low; at 250 rpm, the extraction was completed within 4 minutes. At the same time, the Cl^-ion concentration increased to 1.4 mol/l in the stripping phase. At higher stirrer speeds and after longer times, the Ga-concentration increased in the continuous phase because of the liquid membrane leakage. The presence of copper and zinc in the continuous phase, which were practically not extracted, did not impair the Ga-extraction. The selectivity of the gallium extraction was better than 99%. The emulsion had to be broken in order to recover the gallium from the stripping phase.

The breaking of the emulsion was carried out by electrocoalescence at 20 kV and 50 cycles within 13 minutes.

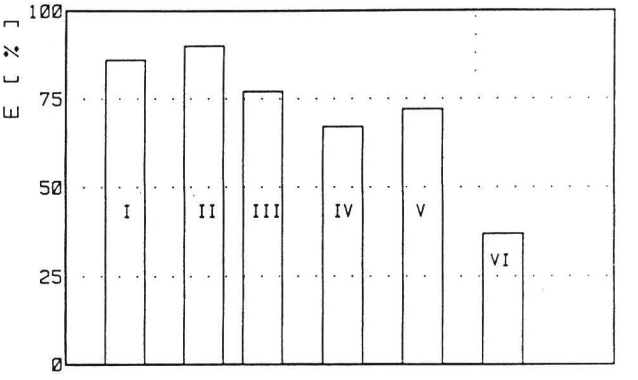

Fig. 1 Gallium degree of extraction E with different carriers
I. LA-2, II. HOSTAREX A-327, III. F-2562, IV. 14 R 3020, V. SO 3020, VI O - 020.

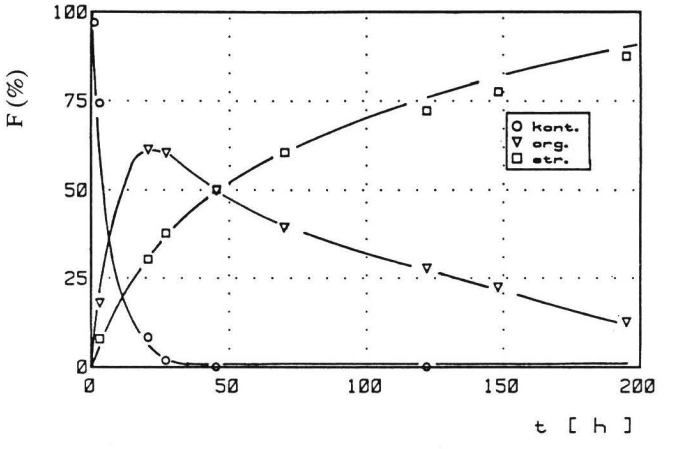

Fig. 2 Relative gallium concentration F as a function of time t in a three-phase reactor

O feed phase (6 n HCl)

▽ membrane phase

□ stripping phase (water)

Modelling of the gallium extraction by liquid membrane emulsion

The model (Völkel, Halwachs, and Schügerl, J. of Membrane Sci., 1980, 6: pp. 19-31) assumes that the mass transfer resistances in the inner and outer phases can be neglected. The mass transfer is controlled by the adsorption rate

$$-j_{ads} = -\frac{1}{a}\frac{dC_X}{dt} = k_{ads}\, C_X\, C_A\, C_H\,, \tag{5}$$

the desorption rate

$$-J_{des} = \frac{1}{a}\frac{dC_{AHX}}{dt} = k_{des}\, C_{AHX}\,, \tag{6}$$

and the diffusion through the membrane phase

$$j_{diff} = -\frac{1}{a}\frac{dC_X}{dt} = k_L\, C_{AHX}\,, \tag{7}$$

where j_{ads}, j_{des}, j_{diff}, are the mass fluxes of gallium by adsorption, desorption and diffusion, H = protons, C = concentrations of the components, a=specific interfacial area, k_{ads}, k_{des}, and k_L are the coefficients of adsorption, desorption and mass transfer. Under steady state with some manipulations (Kirgios, dissertation, University of Hannover, 1987) and integration, the following relationship was obtained:

$$t = \frac{1}{k_L a\, C_{Ao}}\left((C_{Xo}-C_X) + \frac{\ln C_X - \ln C_{Xo}}{K\, C_H} \right), \tag{8}$$

where C_{Ao} is the total carrier concenration,
C_{Xo} the intitial concentration of X (at t = 0)
C_X the concentration of X at t, and
$K = k_{ads}/k_{des}$

Figure 3 compares the calculated and measured gallium concentrations with respect to its initial concentrations as a function of the extraction time for two different carrier concentrations. The agreement is satisfactory. At high stirrer speeds and at higher extraction times, the agreement is not satisfactory any

longer because of the leakage, the change of the emulsion consistence (aging), and the back-extraction of $GaCl_4^-$, which are not taken into account by the model.

CONCLUSION

Gallium can be selectively extracted from 6 n HCl solution by LA-2 carrier in Exsol membrane and with water as the stripping phase in presence of copper and zinc by liquid membrane emulsion in a single-stage extraction unit within a few minutes.

It can be recovered from the stripping phase by electrocoalescence within a short time.

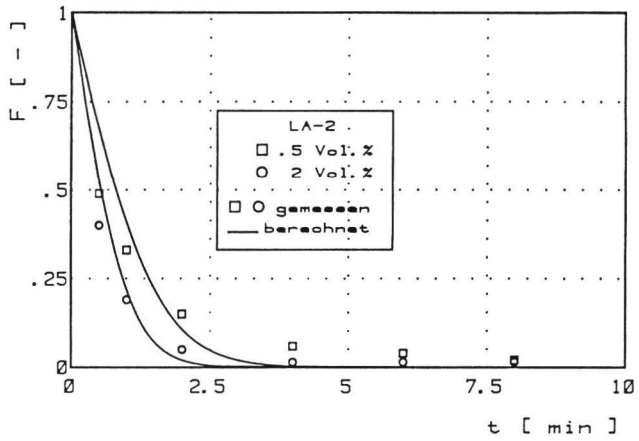

Fig. 3 Comparison of measured (symbols) and calculated (curve) relative gallium concentration F in the continuous phase as a function of time t. Emulsion liquid membrane with 0.5 vol% (□) and 2 vol% (O) LA-2 in the membrane phase

8. SIMULATION, MODELLING AND CONTROL

Solvent Extraction 1990, T. Sekine (Editor)

© 1992 Elsevier Science Publishers B.V. All rights reserved

RELATIVE CONTRIBUTION OF AXIAL DISPERSION ON THE PERFORMANCE OF LIQUID EXTRACTION COLUMNS

TERUKATSU MIYAUCHI
Department of Industrial Chemistry, Science University of Tokyo
1-3 Kagurazaka, Shinjuku-Ku, Tokyo 162, JAPAN

ABSTRACT
Terukatsu Miyauchi, 1990. Relative contribution of axial dispersion on the performance of liquid extraction columns

Early development has been reviewed for the theories and modelling to evaluate the effect of axial dispersion on the performance of solvent extraction columns. These include the diffusion model, the backflow model and the convective model. The concept of equilibrium dispersion model is extended. Possible future approaches have been discussed.

In two-phase counterflow operations such as absorption, extraction, and column crystallization, longitudinal dispersion (or axial mixing) has an undesirable effect on equipment performance, especially if a high degree of completion is needed. In 1950 Geankoplis and Hixon found a concentration jump of the continuous phase at the phase inlet and none at the phase outlet of a spray extraction column (Fig.1, dotted curve). This jump is considered mainly to come from axial dispersion prevailing in the continuous phase of the column. Early development of the theories on axial dispersion in two-phase flow will be reviewed first, and some discussions will be given later.

1. Early development of the theories on axial dispersion:

There are three kinds of modellings. These are a diffusion (or dispersion) model, a backflow model, and a convective (or forward mixing; sometimes velocity distribution) model.

1.1. Diffusion model

The diffusion model for axial dispersion in differential columns has been studied by Miyauchi (1957), Sleicher (1959), Miyauchi and Vermeulen (1963a), Rod (1964), and Hartland and Mecklenburgh (1966).

(a) Properties of general solution: The equations of mass transfer in differential columns with axial dispersion are as follows:

$$d^2X/dZ^2 - P_xBdX/dZ - P_xB \cdot N_{ox}(X-Y) = 0 \quad (1)$$

$$d^2Y/dZ^2 + P_yBdY/dZ + P_yB \cdot N_{ox}(X-Y) = 0 \quad (2)$$

where P_xB (= U_xL/E_x) and P_yB (= U_yL/E_y) are column Péclet numbers for the X-phase and Y-phase respectively. N_{ox} (= $k_{ox}aL/U_x$) is the true number of transfer units based on the X-phase; Λ (= mU_x/U_y) is the extraction factor; and Z (= z/L) is the dimensionless distance along the column with L, the total column length. The solutions to Equations 1 and 2 are

$$X = A_1 + A_2e^{\lambda_2 Z} + A_3e^{\lambda_3 Z} + A_4e^{\lambda_4 Z} \quad (3)$$

for the X-phase and a similar solution for the Y-phase (Miyauchi 1957, Miyauchi and Vermeulen 1963). The λ_j are the roots of the auxiliary equation:

$$\lambda_j = \alpha/3 + 2\sqrt{p}\cos[u/3 + 2(j-2)\pi/3] \quad (4)$$

where α and $\sqrt{p}$ are linear functions of the column length, L. In consequence, the term, λ_jZ (= $(\lambda_j/L)z$) is independent of L. The u in Equation 4 is determined as an angle between 0 and π, such that

$$\cos u = q/p^{3/2} \quad (5)$$

where the $q/p^{3/2}$ is a complicated function of the four dimensionless parameters of P_xB, P_yB, N_{ox} and Λ, but is independent of L.

Figure 2 shows calculated concentration distribution in an extraction column. The concentration jump $\overline{AB}$ is observed at the phase inlet in conformity with Figure 1. Figure 3 illustrates the local accumulation and depletion of transferring material in the X-phase.

(b) Equilibrium diffusion model: One of the special cases studied is that of the equilibrium diffusion model (Miyauchi 1957, Miyauchi and Vermeulen 1963a) defined as N_{ox}(= $k_{ox}aL/U_x$) $\to \infty$, for which the solutions are extremely simple. Fig. 4 shows how the X- and Y-phase concentrations approach with each other, when N_{ox} is increased. In the extreme of $N_{ox} \to \infty$ (with $\Lambda \neq 1$), cos u $\to 0$ (Equation 5) and the solution, Equation 3, is reduced to well known Colburn equation as follows:

$$X_{Z=1} = \frac{1 - \Lambda}{\exp\left[(1 - \Lambda)\, N_{oxp}\right] - \Lambda} \tag{6}$$

where

$$N_{oxp} = L/H_{oxp} = \ln \Lambda/(\Lambda - 1) + P_{oy}B \tag{7}$$

$$1/P_{oy}B = \Lambda/P_xB + 1/P_yB \tag{8}$$

When two-phases move in piston flow, N_{oxp} in Equations 6 and 7 is equal to the true NTU, i.e., N_{ox}. For $\Lambda = 1$ the relations are further simplified. Fig. 5 illustrates how the maximum extent of completion is limited by axial dispersion.

(c) Addition relation for H_{oxp}: For chromatography operations, Van Deemter et al. (1956) developed an addition relation for column HETP. An addition relation for HTU for the two-phase counterflow has been developed as follows (Miyauchi and Vermeulen 1960, 1963).

The behaviour of N_{oxp} in the two limiting cases of mass transfer controlling and of longitudinal dispersion controlling is consistent with the addition of reciprocals,

$$1/N_{oxp} = 1/N_{ox} + 1/N_{oxD} \tag{9}$$

where N_{oxD} is the "number of over-all dispersion units" referred to the X-phase. If every term in Equation 9 is multiplied by the column height L, the quotinent $H_{ox} = L/N_{ox}$ is the customary true HTU. $H_{oxp} = L/N_{oxp}$ becomes the apparent HTU; and $H_{oxD} = L/N_{oxD}$ is "height of overall dispersion unit". Thus,

$$H_{oxp} = H_{ox} + H_{oxD} \tag{10}$$

For a finite N_{ox}, N_{oxD} is different from Equation 7 which is for $N_{ox} \to \infty$. An ultimately obtained N_{oxD} is as follows:

$$N_{oxD} = \ln \Lambda/(\Lambda - 1) + (PB)_y \tag{11}$$

$$1/(PB)_y = \Lambda/f_xP_xB + 1/f_yP_yB \tag{12}$$

where f_x and f_y are the correction factors of order unity when Λ is in around unity.

Equations 6, 9 and 11 give an algebraic calculation method of $X_{z=1}$, which is less exact, but much easier. Also, the addition relation, Equation 10, makes it possible to separate H_{ox} and H_{oxD} by utilizing experimentally measured H_{oxp} obtained under various flow rates (Miyauchi, 1972). Figure 6 shows such an example when applied to the data taken by a 4.1 cm dia. RDC (Vermijs and Kramers, 1954), where acetic acid was extracted from the continuous X-phase (MIBK) to the dispersed Y-phase (water). In this example, a small size RDC is governed by mass transfer.

Figure 7 is an example to see the relative contribution of H_{ox} and H_{oxD} when a RDC is scaled up or scaled down, keeping similarity in column geometry and in drop dispersion (water-AcCOOH-MIBK; mass transfer from continuous aqueous X-phase to dispersed MIBK Y-phase)(Miyauchi 1972). A large diameter RDC in this example is seen to be governed by axial dispersion.

The addition relation for HTU was also studied by Stemerding and Zuiderweg (1963). Sleicher (1959) presented a correlation of N_{ox}/N_{oxp}. A graphical method to solve Equations 1 and 2 owes to Rod (1964).

1.2. Back-flow model

Axial mixing effects in agitated countercurrent equipments may be described by the back-flow model which assumes back flow, superimposed on the net flows through a column, with perfectly mixed stages in cascade (Figure 8). Exchange of material between two adjacent stages is due to net flows $\bar{F}_x$ and $\bar{F}_y$ of main streams and an additional backflow, F, of the mixed phases, which occures in each direction and is the sum of individual-phase backflows of F_x and F_y. Thus, the total flows between adjacent stages are $(\bar{F}_x + F_x + F_y)$ and $(\bar{F}_y + F_y + F_x)$. For the limiting case of $F(= F_x + F_y) \to 0$, this system reduced to a staged model. For another limiting case, with $n_p \gg 1$ under a given column length L, the system reduces to the diffusion model.

Sherwood and Jenny (1935) utilized a similar concept to treat the effect of entrainment on tray efficiency. The model was applied to a mixer-settler extractor with interstage entrainment (Sleicher, 1960). Miyauchi and Vermeulen (1963b) studied the model to relate the differential extractors with those staged. Procházka and Landau (1963) introduced the concept of stage efficiency. Hartland and Mecklenburgh (1966) presented a thorough study on the diffusion model and the back-flow model. Essential character of the back-flow model is a "lumped parameter system", and is convenient for numerical computation (for example, Mecklenburgh and Hartland, 1975, and Ricker et al., 1981). The purpose of our studying the back-flow model was dual (Miyauchi and Vermeulen 1963b), i.e., firstly, under what conditions the diffusion model may be applicable to the staged extraction columns, and secondly under what restrictions the dispersed phase (liquid droplets) may be treated as a second continuous phase.

a. Conversion relation: The material balance and rate equation taken for the jth stage are written down for the back-flow model. Next, a finite difference expression for the diffusion model, Equations 1 and 2, is written down by using lowest order central differences. These two expressions are compared with each other and the following conversion relation has been obtained.

$$1/P_iB = 1/2n_p + \alpha_i/n_p \ , \ (i = x \text{ or } y) \tag{13}$$

$$\lim_{n_p \gg 1}(P_iB) = n_p/\alpha_i \tag{13a}$$

A working conversion relation for an extraction column with finite number of stages is

$$1/P_iB = (1/2 + \alpha_i)/(n_p - 1)\ f_T \tag{14}$$

where f_T is a correction factor of order unity.

The conversion relations have been applied to correlate the axial dispersion coefficients of staged columns with stage height L_0 and operating conditions. For example, Equation 13 transforms to

$$E_i = (1/2)\ \bar{F}_iL_o + F_iL_o \tag{15}$$

The continuous-phase back flow (= F_c) is reported to change in complicated manner with the net flow rate of $\bar{F}_c$ or $\bar{F}_p$ (Ingham 1972).

b. Properties of the dispersed phase:

When there is no coalescence and redispersion of droplets in a given stage the concentration of each droplets is different, depending on the time it has been in the stage, its size, and its entering concentration. Applying the concept of residence time distribution (RTD) for each droplet, it has been shown that the dispersed phase for noncoalescing systems may be treated as a second continuous phase if drop sizes are uniform and the distribution coefficient, holdup, and mass transfer coefficient are constant. This suggests that each drop-size group in a polydispersed system may be treated as a continuous phase. If some coalescence and redispersion do occure, as has been observed for agitated systems (Vermeulen et al. 1955, Madden and Damerell 1957, McFerrin and Davison 1971, Tavlarides and Stamatoudis 1981) and for extraction columns (Komasawa and Ingham 1978, Garg and Pratt 1984, Hamilton and Pratt 1984, Dimitrova Al Khani et al. 1989), it may be possible to relax some of the restrictions above stated.

2. Discussion

Tow topics of the convective model and the equilibrium diffusion model will be discussed in what follows.

2.1. Equilibrium diffusion model

A question was once raised by Pratt (1971) for the equilibrium diffusion model, Equations 6 - 8. The question is also related to the basic structure of the diffusion model itself. The point is that, for N_{ox} (= $k_{ox}aL/U_x$) $\gg$ 1, the condition can arise in two ways, with L = ∞, $k_{ox}a$ finite, or with $k_{ox}a$ = ∞, L finite, and the results can be shown to differ for the two cases. Based on this, he concluded that N_{ox} and B(= L/d_p) - i.e., $k_{ox}a$ and L - should be treated as separate parameters. Figure 9 shows X and Y, computed from Equations 3-5, for two columns of length L_o (finite) and L $\to \infty$ (in this case, N_{ox}, P_xB and P_yB $\to \infty$ for finite $k_{ox}a$, U_x/E_x and U_y/E_y respectively). Obviously, X_∞ for L $\to \infty$, i.e., $N_{ox} \to \infty$ is not equal to Y_∞. Also there is a concentration jump at the phase inlet for L $\to \infty$, i.e., infinite P_xB and P_yB. For these, the ultimate conditions to satisfy the equilibrium diffusion model have turned out that the two conditions of $N_{ox} \gg 1$ (not $k_{ox}a \to \infty$) and $N_{ox}/P_{oy}B \gg 1$ provide the satisfactory conditions. The same is true for the back-flow model solution (Pratt 1976). With these two conditions, the diffusion model solution shows no contradiction any more. There are several applications of the equilibrium diffusion model. Recently, the model is utilized to analyse the performance of a column crystallizer, where heat and mass transfer takes place simultaneously and the equilibrium relationship is non-linear.

2.2. Convective model

Drops in an agitated column are usually polydispersed (Olney 1964). Large droplets travel faster than small ones, thus causing RTD of droplets. Larger drops tend to leave the column earlier with incomplete extraction. This may decrease the extent of extraction when compared with the case of uniformly dispersed droplets. Apparent axial dispersion as a result of nonuniform distribution of drop velocity is called the convective (or velocity distribution) model. The concept of the model was first formulated by Olney (1964).

$$E_D \frac{d^2\bar{x}}{dz^2} - \int_\ell \varepsilon_D u_D(\ell) \frac{dx(\ell)}{dz} f(\ell)\, d\ell - \Psi = 0 \qquad (16)$$

$$E_c \frac{d^2y}{dz^2} + U_c \frac{dy}{dz} + \Psi = 0 \qquad (17)$$

where $\Psi = 6\,\varepsilon_D \int_{\ell} \frac{K_D(\ell)}{\ell} [\,x(\ell) - my\,]\, f(\ell)\, d\ell$.

The fractional holdup $d\varepsilon_D$ of the drop-size range, $\ell \sim \ell + d\ell$, is given by $\varepsilon_D f(\ell) d\ell$, with ε_D, the mean holdup.

The diffusive part of drop motion is included in E_D, the axial dispersion coefficient of the dispersed phase. When coalescence and redispersion take place, formulation by the population balance equations is most suitable (Dimitrova Al Khani et al. 1988, 1989). Under steady mass transfer, this formulation leads to Equations 16 and 17 with appropriate approximation. Rod (1966) studied relationships for the effective HTU in polydisperse systems, including the effect of back and forward mixing on mass transfer. Many studies have followed since then (Misek and Marek 1970, Chartres and Korchinsky 1975, Korchinsky and Cruz-Pinto 1979, Cruz-Pinto and Korchinsky 1980, Zhang et al. 1985, Aufderheide and Vogelpohl 1986, Houghton et al. 1988).

The properties of axial dispersion for the dispersed phase is not always obvious. Equations 16 and 17 suggest that the equations may be solved if the RTD of the drop phase is split into two parts of convection and diffusion. The convective part comes from the relative velocity difference of polydispersed drops. Hence, the normalized RTD does not change with column length. In contrast, column Péclet number determined from the normalized RTD for the diffusive part is proportional to the column length (Fig. 10), as has been suggested previously (Levenspiel and Fitzgerald 1983, Miyauchi 1957). This distinct difference in the performance of the convective and diffusive parts seems to be useful to identify the two mechanisms. Main drawback may be the difficulty in obtaining an accurate RTD-curve and the axial distribution of drop-holdup. The diffusive part consists of three mechanisms - i.e., the equalization of radial concentration difference of drops by Taylor dispersion (Houghton et al. 1988), interstage mixing (back-flow) of drops, and Taylor diffusion by continuous movement (Taylor 1922). The first mechanism depends on the rate of mass transfer and the rate of coalescence and redispersion of drops. As for coalescence and redispersion of drops in extraction columns, the study by Komasawa and Ingham (1978) is suggestive. If the rate of mass transfer is high, Equations 16 and 17 lead to the equilibrium diffusion model, and the influence of the convective model disappears. Figure 11 shows an example of the RTD for drops (Zhang et al. 1985) for 10 cm dia. RDC. Figure 12 illustrates a correlation of the RTD of drops by Olney (1964) for 15 cm dia. RDC. The contribution of diffusive part is seen considerable in medium to high rotation speed range in these examples.

NOTATION

a = specific surface area of drops per unit column volume, cm^2/cc

B = L/d_o, dimensionless

d_o = length characteristic of equipment, cm

E_i = superficial longitudinal dispersion coefficient of ith-phase, cm^2/sec

$f(\ell)$ = drop-size distribution function, 1/cm

F_i = superficial backflow velocity of ith-phase, cm/sec

$\bar{F}_i$ = superficial net velocity of ith-phase, cm/sec

H_{oxp} = L/N_{oxp}, overall HTU based on x-phase, cm

H_{ox} = L/N_{ox}, true overall HTU based on x-phase, cm

H_{oxD} = L/N_{oxD}, overall height of dispersion units based on x-phase, cm

k_{ox} = overall coeff. of mass transfer based on x-phase, cm/sec

ℓ = drop diameter, cm

L = effective column lentgh, cm

L_o = stage height, cm

m = dx^*/dy, solute partition coeff., dimensionless

n_p = total number of stages in series

N_{oxp} = overall NTU based on x-phase, piston flow value, dimensionless

N_{ox} = $k_{ox}aL/U_x$, true NTU based on x-phase, dimensionless

N_{oxD} = overall number of dispersion units, Equations 7 and 9, dimensionless

P_i = $U_i d_o/E_i$, local Péclet number, dimensionless

P_iB = U_iL/E_i, column Péclet number of i-th phase, dimensionless

$u_D(\ell)$ = linear axial velocity of a drop, with size ℓ, relative to the wall, cm/sec

U_i = superficial velocity of ith-phase, cm/sec

x = conc. of solute in x-phase, mol/cc

$\bar{x}$ = mean droop conc. averaged cross-sectionally, mol/cc-drop phase

$x(\ell)$ = solute conc. of a drop with size ℓ, mol/cc-drop

$X = \dfrac{x - my^1}{x^0 - my^1}$, dimensionless

y = conc. of solute in y-phase, mol/cc

$Y = \dfrac{my - my^1}{x^0 - my^1}$, dimensionless

z = axial distance meas'ed from x-phase inlet, cm

Z = z/L, dimensionless

α_i = $F_i/\bar{F}_i$, backflow ratio of ith-phase, dimensionless

ε_D = mean fractional holdup of the dispersed phase

Λ = mU_x/U_y, capacity ratio, dimensionless

Subscripts

C,D = continuous or dispersed phase
i = designates phase concerned, either x or y, and either C or D
o = over-all
x,y = x or y phase

Superscripts

* = equilibrium
o = feed-inlet end, outside column
1 = feed-outlet end, outside column

REFERENCES

Aufderheide E. and Vogelpohl A., Chem. Eng. Sci. 1986 41 1747

Chartres R.H. and Korchinsky W.J., Trans. Instn Chem. Engrs 1975 53 247

Cruz-Pinto J.J.C. and Korchinsky W.J., Chem. Eng. Sci. 1980 35 2213

Dimitrova Al Khani S., Gourdon C. and Casamatta G., Ind. Eng. Chem. Res. 1988 27 329

Dimitrova Al Khani S., Gourdon C. and Casammata G., Chem. Eng. Sci. 1989 44 1295

Geankoplis C.J. and Hixon A.N., Ind. Eng. Chem. 1950 42 1141

Garg M.O. and Pratt H.R.C., AIChE Journal 1984 30 432

Hamilton J.A. and Pratt H.R.C., AIChE Journal 1984 30 442

Hartland S. and Mecklenburgh J.C., Chem. Eng. Sci. 1966 21 1209

Houghton P.A., Madurawe R.U. and T.A. Hatton, Chem. Eng. Sci. 1988 43 617

Ingham J., Trans. Instn Chem. Engrs 1972 50 372

Komasawa I. and Ingham J., Chem. Eng. Sci. 1978 33 479

Korchinsky W.J. and Azimzadeh-Khatayloo S., Chem. Eng. Sci. 1976 31 871

Levenspiel O. and T.J. Fitzgerald, Chem. Eng. Sci. 1983 38 489

Madden A.J. and Damerell G.L., AIChE Journal 1962 8 233

Mecklenburgh J.C. and Hartland S., "The Theory of Backmixing" Wiley-Interscience, N.Y. (1975)

McFerrin A.R. and Davison R.R., AIChE Journal 1971 17 1021

Misek T. and Marek J., Brit. Chem. Eng. 1970 15 202

Miyauchi T., Univ. Calif. Radiation Lab. Rept UCRL 3911 Aug. 1957

Miyauchi T., McMullen A.K. and Vermeulen T., UCRL 3911 Rev. Mar. 1960

Miyauchi T. and Vermeulen T., Ind. Eng. Chem. Fundam. 1963a 2 113

Miyauchi T. and Vermeulen T., Ind. Eng. Chem. Fundam. 1963b 2 304

Miyauchi T., Textbook for Continuing Education Lectures at Tokyo, Soc. Chem. Eng'rs, Japan p72-93 (1972)

Olney R.B., AIChE Journal 1964 10 827

Pratt H.R.C., Ind. Eng. Chem. Fundam. 1971 10 170

Pratt H.R.C., Ind. Eng. Chem., Process Des. Dev. 1976 15 544

Procházka J. and Landau J., Coll. Czechoslov. Chem. Commun. 1963 20 1927

Ricker N.L., Nakashio F. and C.J. King, AIChE Journal 1981 27 277

Rod V., Brit. Chem. Eng. 1964 9 300

Rod V., Brit. Chem. Eng. 1966 11 483

Sherwood T.K. and Jenny F.J., Ind, Eng. Chem. 1935 27 265

Sleicher C.A.Jr., AIChE Journal 1959 5 145

Sleicher C.A.Jr., AIChE Journal 1960 6 529

Stemerding S. and Zuiderweg F.J., The Chemical Engineer 1963 May CE 156

Tavlarides L.L. and Stamatoudis M., "Advances in Chemical Engineering", Academic Press, 11 199-273 (1981)

Taylor G.I., Proc. London Math. Soc. 1922 (2) 20 196; Ref. to Goldstein S., "Modern Development in Fluid Dynamics" Vol.1 p217 (1938), Dover Pub. Inc., N.Y. (1964)

Van Deemter J.J., Zuiderweg F.J. and Klinkenberg A., Chem. Eng. Sci. 1956 5 271

Vermeulen T., Williams G.M. and Langlois G.E., Chem. Eng. Progr. 1955 51 85

Vermijs H.J.A. and Kramers H., Chem. Eng. Sci. 1954 3 55

Zhang S.H., Yu S.C., Zhou C. and Su Y.F., Can. J. Chem. Eng. 1985 63 212

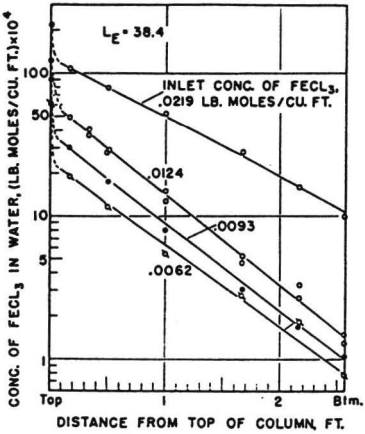

Figure 1. Effect of Inlet Concentration of Ferric Chloride in Water Phase

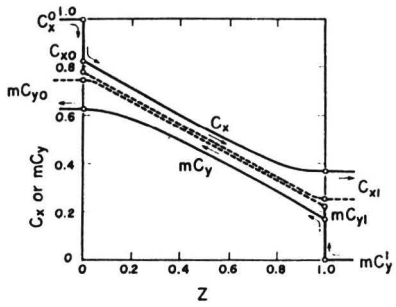

Figure 4. Concentration distribution
$P_xB = P_yB = 4$
$\Lambda = 1$
—— $N_{ox} = 5$
- - - $N_{ox} = 100$

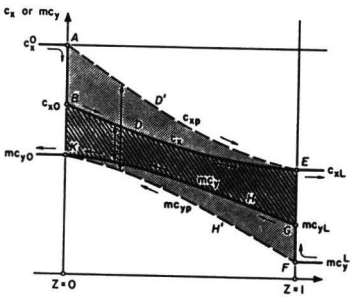

Fig. 2. Concentration distribution in an extractor. Curve ABDE, actual distribution of c_x; curve FGHK, same for c_y. Curve AD'E, apparent distribution of c_x assuming piston flow; curve FH'K, same for c_y.

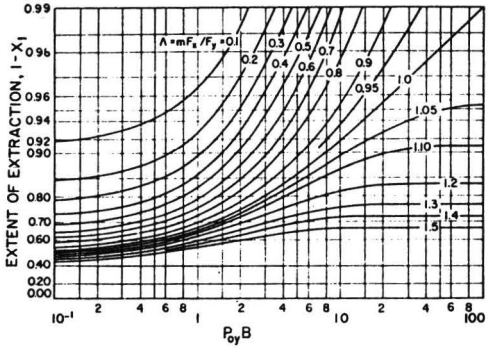

Figure 5. Limiting extent of approach to completion for $N_{ox} \rightarrow \infty$

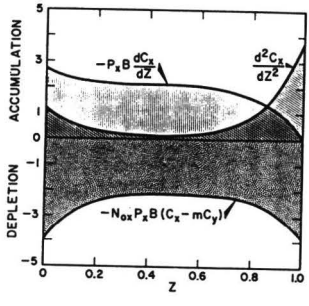

Fig. 3. Local accumulation and depletion of transferring material in X stream ($P_xB = P_yB = 4$, $N_{ox} = 5$, $\Lambda = 1$).

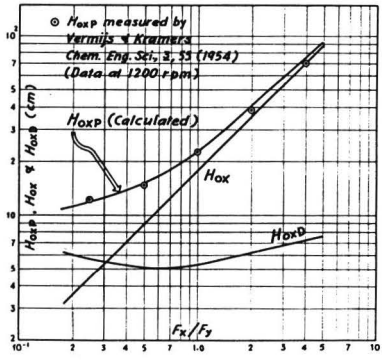

Fig.6 Three kinds of HTU (4.1cm dia. RDC)

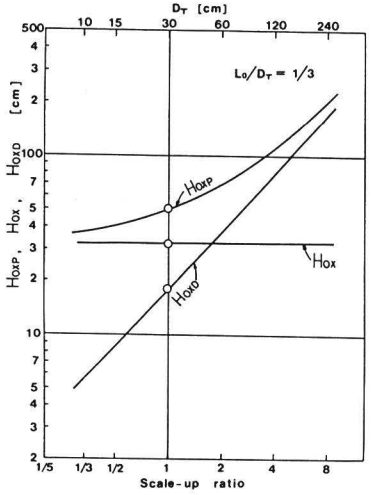

Fig.7 Change of HTU for RDC by scale-up or scale-down

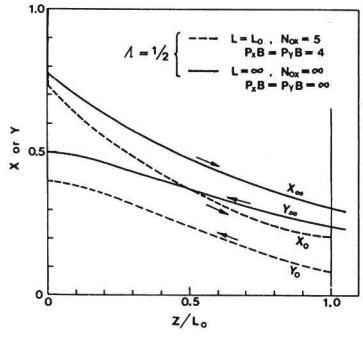

Fig.9 Effect of column length ($L=L_o$ and $L=\infty$) on the concentrations, X and Y

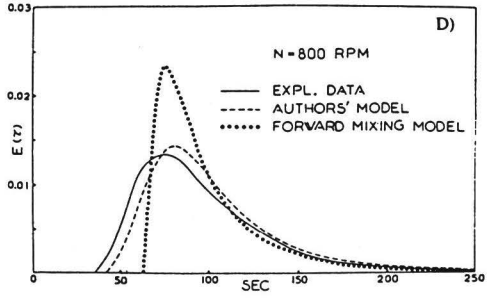

Figure 11 – (A, B, C, D) Overall age distribution of dispersed phase.

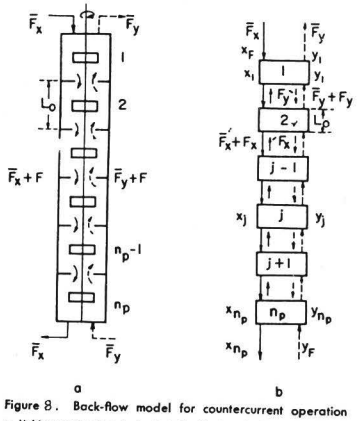

Figure 8. Back-flow model for countercurrent operation a. Multicompartment contactor b. Indentification of flows, with internal flow $F = F_x + F_y$

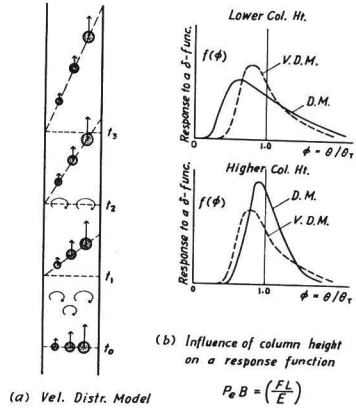

Fig.10 Convective model and RTD

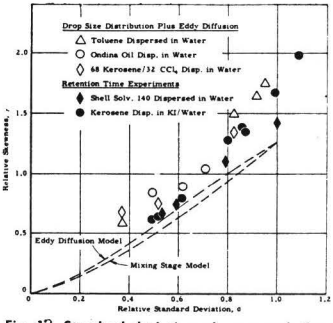

Fig. 12. Standard deviation, skewness relations.

Solvent Extraction 1990, T. Sekine (Editor)

© 1992 Elsevier Science Publishers B.V. All rights reserved

HOW TO FIT A SIMULATOR TO A REAL LIQUID-LIQUID EXTRACTION PLANT

B. GRINBAUM and S.A. ANGEL

IMI(TAMI) Institute for Research and Development,P.O.Box 313, Haifa 31002 (Israel)

ABSTRACT

Grinbaum, B. and Angel, S.A., 1990. How to fit a simulator to a real liquid-liquid extraction plant.
J. Title

As a part of the development at IMI(TAMI) of the technology of production of inorganic salts and acids from aqueous solutions by extraction, a steady-state simulator of these processes was prepared. It performed well during the stages of process development, design and optimization. But when installed in the industrial plant, the results predicted by it varied from the real ones, so that a modification of the simulator was necessary.

The main problems were: partial mass transfer (non-ideal stages), backmixing caused by entrainment and decrease in solvent's activity (i.e. equilibrium coefficient) due to contamination or change in the concentration of the active ingredients.

The influence of the entrainment is introduced directly to the mathematical model. Deviations in the composition of the solvent are taken into account while calculating the liquid-liquid equilibrium coefficient.The difference between the theoretical and real concentration of the extracted species in the solvent is expressed through **stage efficiency coefficient.** Either the **Murphree Efficiency** or the **Mass Transfer Factor (MTF)** are used.

The entrainment is measured directly in every stage. The composition of the solvent is checked analytically. The stage efficiency coefficient is calculated periodically from plant data. All the data are fed as input to the simulator.

All the modifications mentioned above were applied to the $CaBr_2$-by-extraction plant by the Dead Sea. Without them the simulator failed to give a good description of the plant. With the modifications the simulator is used successfully for follow-up and optimization. For this case the MTF was found to be superior to the Murphree coefficient.

1. INTRODUCTION

Steady-state computer simulators of extraction processes have been known for quite a long time (Tsuboka and Katayamu,1976), and were found to be useful tool in the development, simulation and supervisory control of various liquid-liquid extraction processes.

At IMI(TAMI) the technology of production of inorganic salts and acids from aqueous solutions by extraction of ions into an organic solvent and stripping them back to water was developed and has been implemented in a number of

plants, using mainly mixer-settlers . Its principles are given by Lo at al. (1983, pp. 825-838).

As a part of the development, a steady-state simulator of these processes was developed. It performed well during the stages of process development, design and optimization, and saved a lot of experimental work in the pilot plant. But when installed in the industrial plant, the results predicted by it varied from the real ones, so that a modification of the simulator was necessary.

Part of the problems are specific to the inorganic processes, while the other are common to all extraction processes which are using mixer-settlers.

The inorganic extraction processes have two features, which disable them from using the common simulators:

a. Non-standard equilibrium equations

Unlike in organic processes, no general model for liquid-liquid equilibria can be derived. The extraction mechanism varies from one process to another, according to type of solvent (alcoholic, anionic, cationic or mixed-ion) and extracted components (salts or acids). So, for every process, or at least a group of processes, a special liquid-liquid-equilibrium (LLE) model must be derived and incorporated into the simulator.

b. Non-ideal behavior of stages due to entrainment

Entrainment of one phase in the other one occurs, to some extent, in every multistage process. As the entrainment usually does not exceed a few percent, its backmixing influence is not crucial. In inorganic extraction processes, the phase ratio solvent-aqueous is sometimes very high, and may exceed 40. In such a case, entrainment of 1% aqueous phase in solvent means that about 40%(!) of the aqueous phase is backmixed. The entrainment can vary from one stage to another, and for reliable solution the influence of the entrainment must be included in the mass balances and a good approximation of the entrainment on every stage must be known.

2. PRINCIPLES OF THE EXTRACTION PROCESS

The process is carried out in 2-4 batteries: extraction, washing and optionally purification and stripping (in some organic processes the washing battery is substituted by a distillation column). Each battery consists of stirred reactors (mixers) and liquid-liquid separators (settlers), the number and type of which is determined by the process and design considerations. Every mixer may get a feed and/or a reflux stream.

The overall rate of the process is determined by two main factors: interphase mass transfer and phase separation. In many cases, full liquid-liquid equilibrium is not achieved, because the residence time is not long enough to complete the mass transfer under the existing operational conditions. In a mixer-settler plant, the mass transfer depends on mixing characteristics, phase ratio, concentration gradient etc. Phase separation is usually slower than the mass transfer, and its quality is a function of the residence time in the settler.

2.1 Mathematical Model of the Process

From the modeling point of view, a mixer-settler unit is treated as one equilibrium stage, and the entire plant is just one long battery, with a few feed and product streams, and with the solvent recycled in a closed loop.

The basic steady-state mass balance model of an extraction plant is well known for many years (Tsuboka and Katayamu, 1976; Kehat and Gitis 1982). It consists, for every stage, on total and component mass balances and on liquid-liquid equilibrium equations.

The variables, whose values are calculated by the model, are:concentration of all components in both phases, flow of both phases from the stage and flow of product streams.

The numerical solution of the model is quite efficient, and, as found by Grinbaum at al. (submitted for publication), no convergence problems occur.

2.2 Liquid-Liquid Equilibrium Equations.

As stated earlier, these equations are based on theoretical considerations, if available, or on experimental results otherwise. In both cases, their accuracy, in describing a real plant, may be not sufficient.

Their general form is:

$$y_i^* = f(\bar{x}, T, P, \bar{C}) \qquad (1)$$

where:

- y^* - concentration of component in solvent at equilibrium (kmole/kg).
- $\bar{x}$ - vector of all compositions in the aqueous phase
- T - temperature (°K)
- P - pressure (kPa).

$\dot{C}$ - vector of the concentration of active ingredients and contaminates in the solvent (kmole/kg).

3. STAGE EFFICIENCY

Stage efficiency is defined by:

$$y_{i,j} = y^{*}_{i,j}\,\eta \qquad (2)$$

where η - stage efficiency (fraction).

The proper estimation of the efficiency of stages is of utmost importance in all the multistage processes. In many cases the assumption of equilibrium with respect to mass transfer is not reasonable, and the composition of one liquid phase is not related to the second liquid phase simply by thermodynamic K values. The subject was dealt with lately for distillation by Seader (1989).

The common way to express efficiency in distillation is through Murphree efficiency or Holland's vaporization efficiency. Both approaches can be utilized for liquid-liquid extraction.

3.1 Murphree Efficiency

$$\eta = \frac{y_j - y_{j-1}}{y^{*}_j - y_{j-1}} \qquad (3)$$

where:

y^{*}_j - concentration of the component on stage j in the solvent at equilibrium (kmole/kg)

For inorganic extraction processes the Murphree efficiency has two serious disadvantages:

1. In numerous processes the concentration profile over the battery does not change monotonically, but passes through a maximum [1]. This may cause η values to vary strongly in the vicinity of this maximum.

2. In certain stages high mass transfer may occur, which results in a very low concentration of the component in the solvent (this happens mainly in the first stages of the washing and purification batteries). For such a case, the above efficiency definition is not convenient, as can be illustrated by the following example :

The equilibrium concentration of a component in the washed solvent is about 0.02% weight, while its concentration obtained in the plant is 0.05%. The component concentration in solvent on the second stage is 0.5%. From

eq.3 η=0.94, i.e. an efficient stage. On the other hand, the actual concentration is 2.5 times its equilibrium value -a significant factor in plant's operation.

3.2 Mass Transfer Factor (MTF)

To overcome the problems mentioned above, the expression of Mass Transfer Factor (MTF) was introduced. It is defined as:

$$MTF = y_{i,j} / y^{*}_{i,j} \qquad (4)$$

and may be seen as the equivalent of Holland's vaporization efficiency for extraction.
This factor is more readily incorporated into computer algorithms than is the Murphree efficiency, and is more readily obtained from experimental data.
The definition in eq. 4 is purely empirical, and unlike the Murphree efficiency gives no clue about the real amount of mass transfer. It is also more sensitive to deviations from the steady state. Yet, in some cases it is more convenient and effective for practical calculations, as it describes directly the connection between theoretical and actual concentrations in the solvent (see example above). Note that for numerical purposes there is no restriction on the value of η, and it may be greater than one.
Eqs. 1 and 2 may be merged together, to yield:

$$y_{i,j} = f(\dot{x}, T, P, \dot{C})\eta \qquad (5)$$

η is calculated by either eq. 3 or 4.

4. RESULTS

A simulator with all the fitting devices, was installed in the $CaBr_2$-by-extraction plant.In this process $CaBr_2$ is extracted from the
Dead Sea brine, which contains mainly Mg^{++}, Ca^{++} and Cl^{-} ions, and about 0.8% Br^{-} . The plant consists of three batteries:

1. Extraction, where a mixture of Ca^{++}, Mg^{++}, Cl^{-} and Br^{-} is extracted to the washed solvent.
2. Purification, where most of the Mg^{++} and Cl^{-} in the solvent are replaced by Ca^{++} and Br^{-}.
3. Washing, where the resulting $CaBr_2$ is washed by water, to yield the final product.

The equilibrium equations, evaluated by Gai (1986), are highly non-linear and quite complex. They take into consideration deviations in solvent's composition.

The correction data for the plant are the concentrations of the various ingredients of the solvent and of some contaminates.

For every stage the following data may be added: the MTF's for Br^- and Cl^- (there may be quite a large difference between both of them), the entrainment of aqueous phase from the settler and the temperature in the mixer.

4.1 Verification of the results

Data obtained in the Pilot Plant in IMI(TAMI) and in the demonstration plant by the Dead Sea were compared with these calculated by the simulator.

Data from the Pilot Plant were close to those obtained by the simulator *without any correction:* the deviation between the calculated and measured concentrations was about 10% - within the experimental and analytical error.

For data from the demonstration plant the fit was rather poor:

Without the correction for stage efficiency (MTF), solvent composition and entrainment, the deviation between calculated and measured profile of concentrations in the plant changed from 15% under optimal operating conditions (just after the start-up) to 50% in especially cold days (when the mass transfer goes down and the entrainment goes up).

When the correction factors were introduced, the simulation results were found to be within the experimental and analytical accuracy of the plant results (±5%), with random deviations.

The values of the entrainment are updated on a daily basis, while the MTF and solvent composition are updated periodically. Any misfit between the results in the field and those predicted by the simulator shows that something happened in one or more stages, and a careful study of the results helps to locate the problem without an excessive troubleshooting.

An attempt to use the Murphree efficiency for this process failed. Due to the shape of the profile of the concentrations, numerical problems were encountered, and the results obtained were less reliable than those with MTF.

5. REFERENCES

Gai, J.E., 1986. Internal IMI(TAMI) Report 03508/R3 (unpubl.), 25 pp.

Grinbaum, B., 1986. Internal IMI(TAMI) Report 03508/R6 (unpubl). 28 pp.

Kehat,E., Gitis,B., 1982. Simulation of extraction column, I&EC Fund., 21,214

Lo,T. C., Baird,M.H., Hanson,C. (eds.), 1983. Handbook of solvent extraction, Wiley, N.Y. pp. 825-838

Seader, D.J., 1989. The rate based approach for modeling staged separations, CEP 85, 10, 41

Tsuboka,T., Katayamu,T., 1976. J. Chem. Eng. Japan, 91, 40

Solvent Extraction 1990, T. Sekine (Editor)

© 1992 Elsevier Science Publishers B.V. All rights reserved

THE SIMULATION OF INTERACTING LIQUID-LIQUID DISPERSIONS - A NEW ALGORITHM AND ITS POTENTIALITY

M.M.L. GUIMARÃES[@,#], J.J.C. CRUZ-PINTO[#], P.F.R. REGUEIRAS[&] and C.M.N. MADUREIRA[&]
[@]ISEP, 4200 Porto, [#]CQPA (INIC)/U.Minho, 4700 Braga, [&]FEUP/U. Porto, 4000 Porto (PORTUGAL)

ABSTRACT

A survey is given of the authors' latest work on the simulation of interacting liquid-liquid dispersions undergoing mass transfer in a stirred tank contactor, at steady state. A presentation is made of an analytical (moment generating function) and a direct (Monte-Carlo) simulation technique. This Monte-Carlo technique is entirely new in the chemical engineering field, is free from any assumption of statistical independence of the drop properties, and is intrinsically able to reveal and describe the fine structure and behaviour of the dispersion.

1 INTRODUCTION

The simulation of interacting liquid-liquid dispersions undergoing mass transfer and/or chemical reactions is a major chemical engineering problem in a variety of fields, which has not yet been satisfactorilly solved. The difficulties do not exclusively lie on the experimental validation of the models and of their predictions, but are still rooted on their inability to describe the real nature of the dispersion, namely its full trivariate structure - i.e. the existence of a broad and complex distribution of drop volumes (v), solute or reactant concentrations (c) and ages (τ - time since last interaction or entry into the contactor).

It is now widely known and understood the importance of creating and maintaining a sufficiently large interfacial area to ensure fast mass transfer between the phases, which is normally obtained by means of more or less intense agitation. This agitation almost always results in an interacting behaviour of the dispersed phase drops, through frequent breakage and coalescence.

In addition to the most obvious effects that an interacting drop behaviour may have upon the overall interfacial area, other important effects are the frequent renewal of the interface, and the decreases in the solute or reactant concentration differences, both within each of the drops and among different drop sizes of the dispersion. This causes significant changes in the mass transfer fluxes and in the reaction rates; in the case of multicomponent mass transfer and/or reactions, not just the yield but also the selectivity may be significantly affected. Another effect, which is still more difficult to account for, is the possible increase in the local mass transfer rates during the actual drop interaction events.

This communication describes the results of the authors' recent work in the

simulation of a liquid-liquid dispersion undergoing mass transfer (continuous to dispersed phase) in a stirred tank contactor, at steady state. Different operating conditions and drop mass transfer activities were considered, but no allowance was made for any acceleration of mass transfer during the drop interactions.

Previous work on the general development of drop interaction models and on the main features of previous solution algorithms has been already thoroughly described by various authors - (Ross, 1971; Coulaloglou, 1975; Cruz-Pinto, 1979; Ramkrishna, 1981, 1985; Guimarães and Cruz-Pinto, 1988; Guimarães, 1989; Guimarães *et. al.*, 1990) - and does not need to be reviewed here.

2 THE TWO MAIN SIMULATION APPROACHES

2.1 The Analytical, Moment Generating Function, Method

The properties of an interacting liquid-liquid dispersion may be described by the number density of drops within each size, concentration and age fraction, $f(v,c,\tau)$, which obeys the well-known Liouville's equation (see Guimarães and Cruz-Pinto, 1988). Bayens (1967) developed an elegant solution method, based on the use of the multidimensional Laplace transform of $f(v,c,\tau)$, also called moment generating function, which he used to predict the behaviour of a dispersion where an instantaneous binary breakage followed each binary coalescence.

The most striking feature of the method is its ability to yield any of the moments of the trivariate distribution of the drop properties, by means of adequate differentiations of the distributions' transform (Bayens, 1967; Bayens and Laurence, 1969; Guimarães and Cruz-Pinto, 1988 and Guimarães, 1989). In every case to date, to reasonably simplify the analytical manipulations, the drop properties v, c and τ had to be assumed as statistically independent, i.e.

$$f(v\,,\,c\,,\,\tau) \;=\; f_v(v) \cdot f_c(c) \cdot f_\tau(\tau) \qquad (1)$$

With this simplification, the marginal drop volume distribution may be directly obtained, whereas the other two marginal distributions may then be characterized by their moments. Actually, as the variance of the drop age marginal distribution may be easily proved to be the square of its average for any drop interaction and mass transfer mechanism (Guimarães, 1989), the resulting age distribution is a simple negative exponential, i.e.

$$f_\tau(\tau) \;=\; (1/\bar{\tau}) \cdot \exp(-\,\tau/\bar{\tau}) \qquad (2)$$

However, one should recognize that the assumption of statistical independence needed in this type of approach may be a crude representation of the behaviour, particularly when the drop interaction frequency is low and/or the contact time is short. Also, no attempt had been made at combining this method with more realistic

descriptions of the drop interacting behaviour (Ross, 1971; Coulaloglou, 1975).

A very detailed description of the authors' work on the moment generating function method is given elsewhere (Guimarães and Cruz-Pinto, 1988).

2.2 The Direct Simulation, Monte-Carlo, Method

The Monte-Carlo simulation method is a powerful tool for predicting the *microscopic* behaviour of a complex physical system, such as a liquid-liquid dispersion.For the discretization of the simulation time, two techniques have been devised: the early and relatively wasteful *time slicing* or *periodic sampling* technique (Spielman and Levenspiel, 1965; Zeitlin and Tavlarides, 1972; Hsia and Tavlarides, 1980; Rod and Misek, 1982) and the more economical *critical event* technique (Shah *et al.*, 1977; Bapat, 1982; Bapat *et al.*, 1983; Hsia and Tavlarides, 1983). With this latest technique, the simulation time steps are statistically adjusted to the actual dispersion behaviour, so that within each of them at least one drop event (breakage, coalescence or exit) does occur.

So, most typical previous simulations (see Shah *et al.*, 1977 and Bapat *et al.*, 1983) involved (a) generating a quiescence interval, based on the overall frequency of drop events, (b) identifying the type of event that occurs, (c) identifying the drops taking part in the event, through adequate sampling procedures of their properties (v, c and τ), and (d) identifying the properties of the daughter drops, in the case of a breakage event. The procedure is thoroughly discussed in the above and other references (Guimarães, 1989; Guimarães *et al.*, 1990), and constitutes a significant computational burden, especially because of the complete drop property updates needed before (to account for mass transfer and/or reaction) and after the interaction events.

As a result, and in order to keep the computational burden to within reasonable bounds, previous authors adopted oversimplified sampling schemes to select drops from within the dispersion (very often equivalent to assuming that v, c and τ are statiscally independent) and/or had to drastically reduce the precision of their description of the dispersed phase (too low number of drop size and concentration classes), thus impairing the accuracy of their algorithms. Also, previous works generally show a lack of statistical validation of the attainment of steady state.

3 A NEW CONCEPT OF MONTE-CARLO SIMULATION ALGORITHM

The Monte-Carlo algorithm developed by the authors contrasts with previous algorithms in that its basic simulation entity is not a single drop drawn from the whole population or a sample, but rather a single point (called *Bastenaire's point*) having a uniform probability of belonging to any volume element of the dispersed phase; this point is at all times characterized by the properties of the drop to which it belongs, but these are drawn from the actual *trivariate* property distribution

(more exactly from its three bivariate marginal distributions - $f_{v\tau}(v,\tau)$, $f_{c\tau}(c,\tau)$ and $f_{vc}(v,c)$), without the need to keep track of a large number of drops. The number of size, concentration and age fractions were 100 each.

The usual procedure was used to generate the times at which the Bastenaire's point may be involved in breakage, coalescence or exit events. The volume, v', of one of the drops resulting from the breakage of a drop of volume v is drawn from

$$\int_0^{v'} \beta(v'|v)\, dv'$$ [see Guimarães and Cruz-Pinto, 1988, equation (11b)], and

the point is taken to follow one of the daughter drops with a probability proportional to their volumes. In the case of a coalescence, the volume of the other drop involved, v*, is drawn from

$$\int_0^{v^*} \int_0^{c_{max}} f_{vc}(v,c)\, dc\, dv,$$ while its concentration, c*, is obtained from

$$\int_0^{c^*} f(c|v^*)\, dc,$$ with $f(c|v^*)$ obtained by sectioning $f_{vc}(v,c)$ at $v = v^*$,

followed by renormalization. This is the exact procedure needed to ensure that any statistical dependence that may exist or arise between v, c and τ is constantly accounted for.

Rigid and oscillating drop mass transfer mechanisms have been considered in this work. Typically, 30 000 Bastenaire's points were needed to simulate the attainment of the vessel's steady state. This was ascertained by performing chi-square tests on the predicted outlet dispersion property distribution against that of the vessel's contents, and also through means stability analysis.

4 RESULTS AND MAIN CONCLUSIONS

Fig. 1 (a) shows some of the drop age predictions by both simulation methods, for rigid drops, and Fig. 1 (b) illustrates a set of the chi-square tests made to validate the results; the attainment of the steady state is beyond doubt ($\chi^2 \leq 1$).

As expected, predicted drop ages strongly decrease with mixing intensity, and increased with residence time; this increase, however, is only significant at low agitation rates, due to the overriding effect of higher breakage and coalescence frequencies at higher agitation rates (Guimarães *et al.*, 1990).

The Monte-Carlo algorithm predicted drop ages which are up to 16% higher than its analytical, moment generating function, alternative. In contrast, the average drop sizes (that determine the interfacial area) and the average solute concentrations are almost identical (average differences of .059% and .96%,

respectively). These negligible differences predicted in the more relevant variables indicate that the much faster analytical method is a sufficiently accurate alternative for the low levels of statistical interdependence prevailing here (Guimarães, 1989).

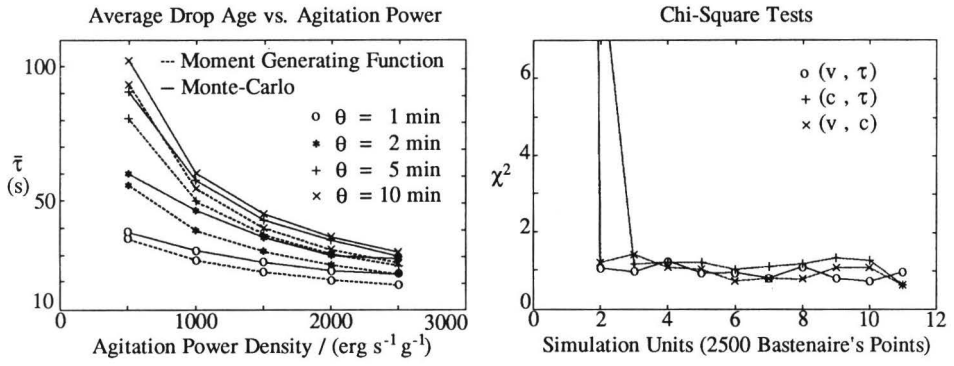

Fig. 1. (a) Predicted average drop ages for various residence times and agitation power densities. (b) Sample chi-square test results for the three bivariate marginal distributions.

In Fig.2, one can see a graphical representation of some the predicted bivariate marginal (v,τ) and (c,τ) distributions, for rigid drop mass transfer behaviour. This type of information is, to our knowledge, entirely new.

It is clearly seen that there is a dominance of the average feed drop size, which slowly attenuates at longer residence times; there is also a clear second peak at $\sim \bar{v}_{feed}/2$, due to the assumed binary breakage. These diagrams and the corresponding isoprobability curves (Guimarães, 1989) show two distinct perpendicular ridges, and so the statistical dependence between drop volumes (v) and ages (τ) is low, which is also confirmed by the low values for the corresponding mean quadratic contingencies (Guimarães, 1989).

On the other hand, the bivariate marginal (c,τ) distribution shows an obvious curved ridge, which is dominant at θ = .5 min, and corresponds to the drops that exit the vessel after very few interactions; their ages are equal to their residence times, and increase simultaneously with the solute concentration, thus giving rise to a significant statistical dependence between c and τ. The relative spread of the ridge along the c-axis is the direct result of the different mass transfer activities of the various drop sizes in the feed (a normal size distribution has been assumed). So, for the residence times and mixing intensities assumed here, it may be concluded that the variables v, c and τ are not totally independent (i.e. Eq. 1 is not valid), although

$$f(v, c, \tau) \approx f_V(v) \cdot f_{c\tau}(c, \tau) \qquad (3)$$

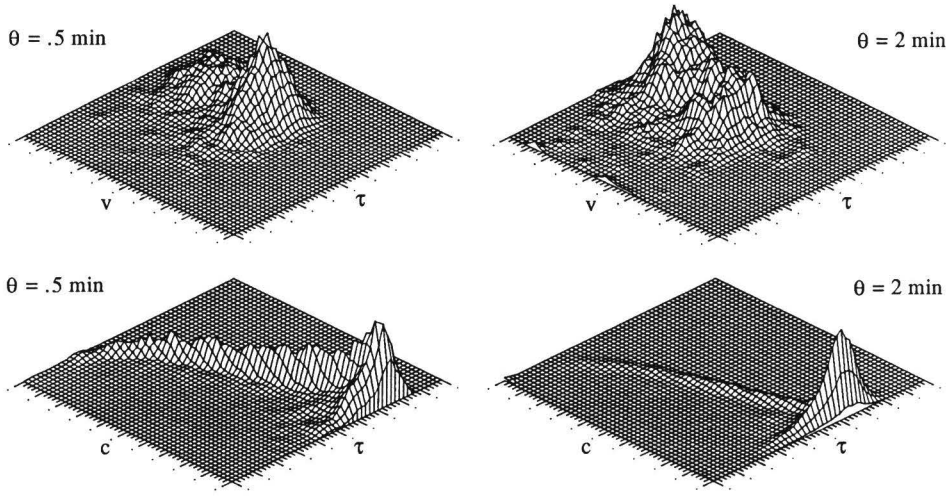

Fig. 2. Tridimensional diagrams showing typical changes of the drop property distribution with residence time, for low intensity of agitation ($\dot{\varepsilon}$ = 500 erg s^{-1} g^{-1}).

Guimarães (1990) has also proved that the differences reported between the moment generating function and the Monte-Carlo results - average drop ages and concentrations, and overall extraction efficiencies - are statistically significant and can definitely be correlated with the level of variable interdependence, as measured by the mean quadratic contingency.

5 REFERENCES

Bapat, P.M, 1982. Ph.D. Thesis, Illinois Institute of Technology, Chicago, U.S.A.
Bapat, P.M., Tavlarides, L.L. and Smith, G.W., 1983. Chem. Engng Sci., 38: 2003.
Bastenaire, F., 1965. Rev. Ind. Min 45: 39.
Bayens, C.A., 1967. Ph.D. Thesis, John Hopkins University, Baltimore, U.S.A..
Bayens, C.A. and Laurence, R.L., 1969. Ind. Engng Chem. Fundam., 8: 71.
Coulaloglou, C.A., 1975. Ph.D. Thesis, Illinois Institute of Technology, Chicago, U.S.A..
Cruz-Pinto, J.J.C., 1979. Ph.D. Thesis, The Victoria University of Manchester, Manchester, United Kingdom.
Guimarães, M.M.L. and Cruz-Pinto, J.J.C., 1988. Comput. chem. Engng, 12: 1075.
Guimarães, M.M.L., 1989. Doctoral Thesis, Universidade do Minho, Centro de Química Pura e Aplicada (INIC), Braga, Portugal.
Guimarães, M.M.L., Regueiras, P.F.R. and Cruz-Pinto, J.J.C., 1990. Comput. chem. Engng., 14: 139.
Hsia, M.A. and Tavlarides, L.L., 1980. Chem. Engng J., 20: 225.
Hsia, M.A. and Tavlarides, L.L., 1983. Chem. Engng J., 26: 189.
Ramkrishna, D., 1981. Chem. Engng Sci., 36: 1203.
Ramkrishna, D., 1985. Rev. Chem. Engng, 3: 49.
Rod, V. and Misek, T., 1982. Trans. IChemE, 60: 48.
Ross, S.L., 1971. Ph.D. Thesis, University of Michigan, U.S.A.
Shah, B.H., Ramkrishna, D. and Borwanker, 1977. Chem. Engng Sci., 32: 1419; AIChE Jl, 23: 897.
Spielman, L.A. and Levenspiel, O., 1965. Chem. Engng Sci., 20: 247.
Zeitlin, M.A., and Tavlarides, L.L., 1972. Can. J. Chem. Engng, 50: 207.

Solvent Extraction 1990, T. Sekine (Editor)

© 1992 Elsevier Science Publishers B.V. All rights reserved

SIMULATION AND CONTROL OF A MULTISTAGE STIRRED CELL COLUMN EXTRACTOR

V.I. Kirou, C. Tsouris and L.L. Tavlarides
Department of Chemical Engineering and Materials Science
Syracuse University, Syracuse, NY 13244 U.S.A.

1. Stochastic Simulation of Dispersed Phase Holdup and Drop Size Distribution Profiles in a Mixer Column Contactor

The accurate prediction of dispersed phase holdup and drop size distribution profiles in column contactors has been a major research problem in liquid extraction over the last 40 years. In this work, a stochastic simulation is formulated for the prediction of the above quantities in a mixer column (Kirou, 1990). The dispersed phase in each of the stages of the contactor is represented by an ensemble of drops. In each ensemble, the dispersed phase dynamics is taken into account quantitatively by considering (a) the dispersed phase breakage and coalescence, and (b) the macroscopic flow patterns of the continuous phase in order to estimate the droplet movement between stages. The framework required to incorporate mass transfer process is also presented and includes a stagewise flow model for the continuous phase and the interphase mass transport balances. Although the simulation is developed for a specific contactor, it can be easily extended to represent other types of contactors provided that appropriate event frequencies are available.

Figure 1 shows the essential details of the simulation. The simulation time advances according to a poisson pattern. First, it is decided whether a feed event should occur in the first stage. Feed activities are performed deterministically, i.e., at regular time intervals. Then, a breakage, coalescence, or exit event is performed in a stage according to the probability of the individual drops and of the ensemble of the drops. After the execution of the event, the affected frequencies are updated, and the procedure is repeated. In the case of mass transfer, during the interval of quiescence, i.e., during the time between events, mass transfer is performed between the droplets and the continuous phase as dictated by the mass transfer equations. The implementation of the simulation requires knowledge of the droplet event frequencies, i.e., the breakage, coalescence and exit frequencies. In this work, the phenomenological models developed by Coulaloglou and Tavlarides (1977) are used for breakage and coalescence. The exit frequency is obtained by a model that accounts for the peculiarities of the investigated mixer column. The model is based on a probabilistic approach and is formulated in terms of operating conditions, physical properties of the system, and geometric characteristics of the contactor. The basic premise of the model is that the drops move inside the stages of the column following the circulating patterns of the continuous phase. During this movement the drops are exposed to the region which is located in the free area between adjacent stages, called the critical region. Once in the critical region, a drop has a probability to exit in the adjacent stage. Thus, the exit frequency is obtained by calculating the probability of exposure in the

critical region and the conditional probability of exit from the critical region to an adjacent stage. The latter probability depends on the time of exposure in the critical region and on the time required for penetration through the critical region.

In order to investigate the effect of the initialization parameters on the computational demands of the simulation and on the accuracy of the simulated results, several computer experiments were performed. For the performed experiments, it is found that the initial stage of the simulation affects the path of the simulated results towards the steady state but not the steady state. Figure 2 shows the evolution of the mean holdup for two runs with different initial holdup values. One run is initialized with 0.03 and the other with 0.20 holdup at every stage. Each ensemble has 600 microns mean diameter. It can be observed that the time average values of the holdup after 1000 seconds are very close, indicating the independence of the simulated results from the initial stage. The effect of the initial number of drops was also investigated.

Runs with small initial samples (e.g., 100/stage) reduce drastically the computational demands without affecting the estimated mean holdup and the Sauter mean diameter values. These runs required only 2-5 hours cpu on a common mainframe machine (vax 8820).

Figures 3 and 4 show comparisons between simulated results and experimental measurements for the holdup and Sauter mean diameter profiles. The experimental system is toluene(disp)/water(cont.) mutually equilibrated. The experiments were performed in a 7-stage mixer column described elsewhere (Kirou et al., 1988; Tsouris et al., 1990a). In the range of the operating conditions dispersed phase flowrate 0.12-0.36 L/min, continuous phase flowrate of 0.72-1.6 L/min, agitation 160-200 rpm, the mean values of holdup a_{32} are predicted with 27% and 7% relative error, respectively, for the comparisons. Furthermore, simulation of the dynamics of the mean holdup is found in agreement with experimental results when the final steady state is predicted accurately.

REFERENCES

Coulaloglou, C.A. and L.L. Tavlarides, Chem. Eng. Sci., 32, 1289 (1977).

Kirou, V.I., "Stochastic Simulation of Dispersed Phase Holdup and Drop Size Distribution Profiles in a Mixer Column Contactor", Ph.D. Dissertation, Syracuse University, Syracuse, NY, 1990.

Kirou, V.I., J.C. Bonnet and L.L. Tavlarides, AIChE J., 34, 283-292 (1988).

Tsouris, C., L.L. Tavlarides and J.C. Bonnet, "Application of the Ultrasonic Technique for Real-Time Holdup Monitoring for the Control of Extraction Columns", Chem. Eng. Sci., in press 1990.

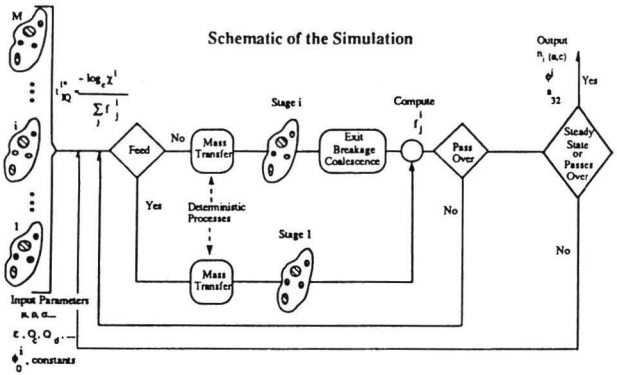

Figure 1 Schematic Indicating the Basic Steps of the Simulation

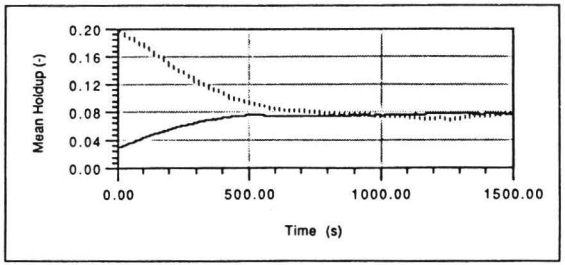

— 3 % ; 400 drops ··· 20 % ; 800 drops

(Qc=1200 L/min; Qd=120 L/min; 180 rpm)

Figure 2 Holdup Evolution as Function of Initial Holdup Values. The initial holdup value affects the path towards the steady state but not the steady state itself.

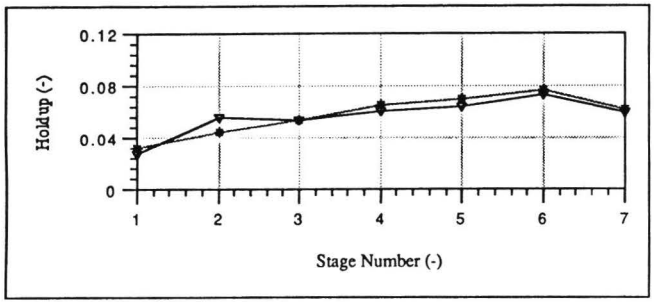

Simulated Experimental (this work)

(Qc=1200 mL/min; Qd=120mL/min; 160rpm)

Figure 3 Holdup Profile Comparison I. Simulated holdup values closely agree with experimental results.

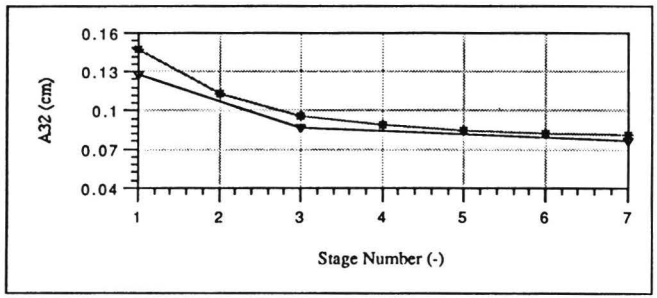

Simulated Experimental (Kirou et al.,1988)

(Qc=1200 mL/min; Qd=120mL/min; 160rpm)

Figure 4 Comparison of a_{32} profile I. As in the case of the holdup profile, close agreement is observed between experimental and simulated values.

2. Control of the Dispersed Phase Holdup in Multistage Column Extractors

It has been reported by many investigators that the optimum performance of extraction columns occurs at conditions near flooding (Oldshue and Rushton, 1952). Predicting the holdup at such conditions, as shown by Tsouris et al. (1990a) is not an easy task. Le Lann et al. (1986) and Najim et al. (1987) used a flooding detection technique to control holdup at suboptimal conditions. Camurdan et al. (1990) controlled holdup within 70% of the flooding holdup. In this study, an ultrasonic technique (Fig. 1) is used (Tsouris et al., 1990a) to monitor and control the holdup very close to flooding, by inspection of the holdup profiles (Fig. 2).

The process has been modeled by a first-order-plus-dead-time transfer function. Agitation speed has been used as the manipulated variable, whereas flow rates as the disturbance variable. Adaptive gain scheduling and nonadaptive controllers were designed to provide first-order closed-loop response (Smith and Corripio, 1985 p. 237). The final form of the controller was the following PI form:

$$G_c = \frac{\tau}{K(\lambda+\theta)} \left(1 + \frac{1}{\tau s}\right) \qquad (1)$$

where $\tau/K(\lambda+\theta)$ is the gain, τ, K, θ the open-loop time constant, gain and dead time, respectively; λ is the closed-loop time constant and is treated as a design parameter. Adaptation of the controller parameters with operating conditions is suggested to overcome nonlinearities (Taylor et al., 1982). The performance of the controller is demonstrated in Figs. 3-6.

By inspecting the holdup profiles at certain periods of time and imposing the flooding criteria reported by Tsouris et al. (1990b), one can control the mean holdup very close to flooding, as shown in Figs. 7 and 8. The flooding criteria used here are $\phi_1 > \phi_2 > \phi_3 > \phi_4$ and $\phi_1 - \phi_2 > \phi_2 - \phi_3$. In Fig. 7, the column was operated at 20% holdup until 700s. Then the set point moved to 45% which is in the flooding region. The flooding criteria were satisfied around 1800s (see holdup profile with squares in Fig. 8), and therefore, the set point was automatically reduced by 10% of the previous value. The same procedure is followed until the holdup profile is acceptable. By requesting the maximum holdup to occur in the first stage, one can impose lower bounds in the mean holdup, as shown in Fig. 7. In this case, the mean holdup was controlled within 93% of the flooding holdup.

REFERENCES

Camurdan, M.C., P.A. Taylor and M.H.I Baird, Can. J. Chem. Eng. (1990) in press.

Le Lann, M.V., K. Najim and G. Casamatta, Chem. Eng. Commun., 48, 237-253 (1986).

Najim, K., M.V. Le Lann, and G. Casamatta, Chem. Eng. Sci., 42, 1619-1628 (1987).

Oldshue, J.Y. and J.M. Rushton, Chem. Eng. Prog., 48, 297-306 (1952).

Smith, C.A. and A.B. Corripio, "Principles and Practice of Automatic Process Control", J. Wiley & Sons (1985).

Taylor, P.A., M.H.I. Baird and I. Kusuma, Can. J. Chem. Eng., 60, 556-565 (1982).

Tsouris, C., L.L. Tavlarides and J.C. Bonnet, "Application of the Ultrasonic Technique for Real-Time Holdup Monitoring for the Control of Extraction Columns", Chem. Eng. Sci., (1990a), in press.

Tsouris, C., R. Ferreira and L.L. Tavlarides, "Characterization of Hydrodynamic Parameters in a Multistage Column Contactor", Can. J. Chem. Eng. (1990b), in press.

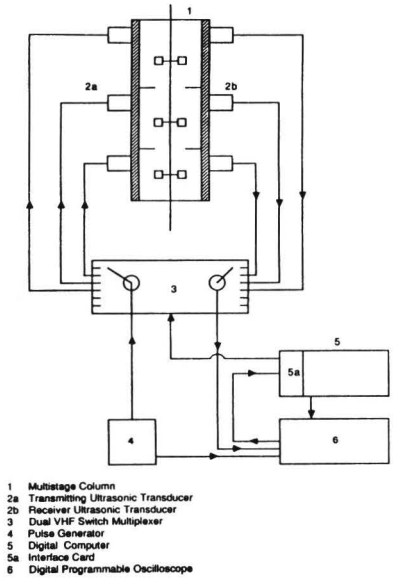

Fig. 1: Schematic of data acquisition

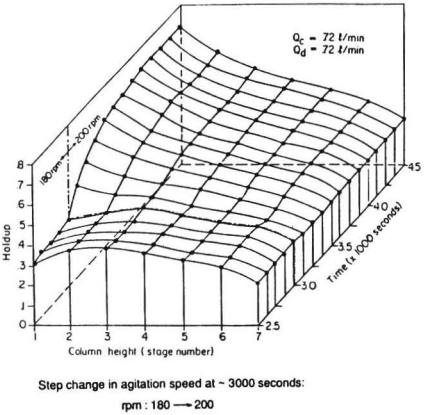

Fig. 2: Transient holdup profiles

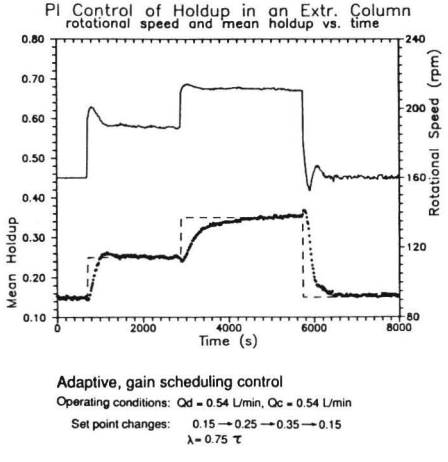

Fig. 3: Servo-control of mean holdup

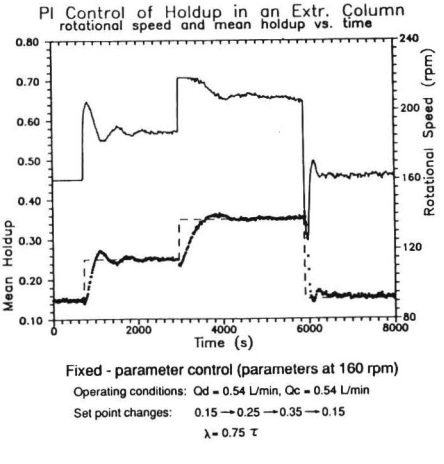

Fig. 4: Servo-control of mean holdup

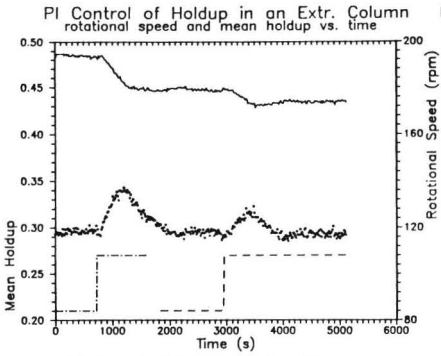

Fig. 5: Regulatory-control of mean holdup

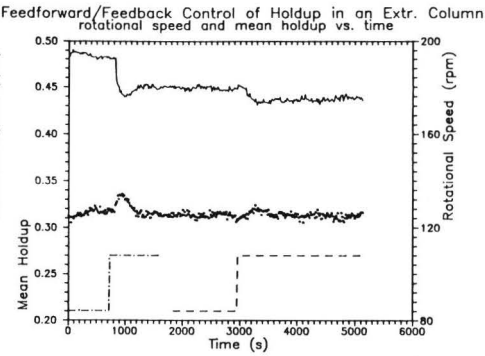

Fig. 6: Regulatory-control of mean holdup

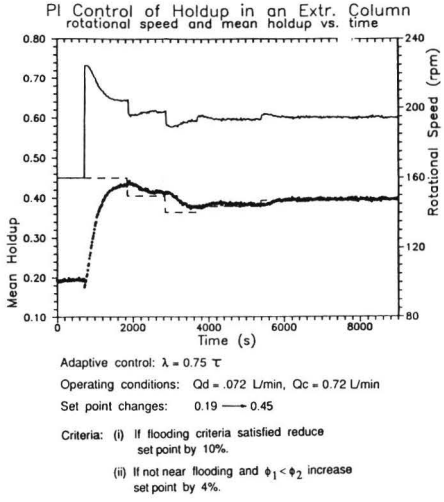

Fig. 7: Holdup control of near flooding

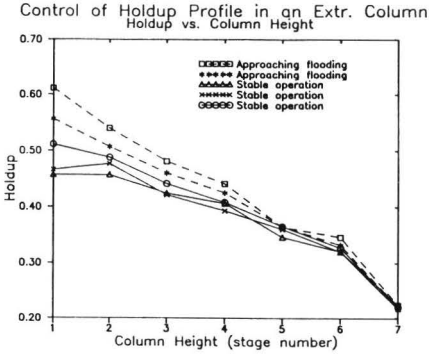

Fig. 8: Holdup profiles near flooding and at stable operation

Solvent Extraction 1990, T. Sekine (Editor)

© 1992 Elsevier Science Publishers B.V. All rights reserved

A STUDY ON THE DROP SIZE DISTRIBUTION AND THE HOLDUP IN A ROTATING IMPELLER EXTRACTION COLUMN

Y.K. LEE and C. KIM*

Energy Department, Research Institute of Industrial Science and Technology, #31 Hyoja-Dong San, 790-330, Pohang(Korea)
Chemical Engineering Department, Ajou University, #5 Wonchon-Dong San, 440-749, Suwon(Korea)*

ABSTRACT

A stagewise hydrodynamic model, applying drop population balance equations derived from the model for the breakage and coalescence of the drops in a countercurrent flow liquid-liquid extraction system, was developed to predict the drop size distribution and the holdup of the dispersed phase in a rotating impeller extraction column.

The local values of the dispersed phase holdup were measured where the drop size distributions were obtained by taking photographs of the dispersions.

The solutions of the model equations, a set of nonlinear integro-differential equations, were obtained by preforming computer simulation and the optimum parameter values were determined.

The drop size distribution and the holdup in a rotating impeller extraction column predicted by the model were in good agreement with the experimental results.

1. INTRODUCTION

Liquid-liquid extraction is widely used in the chemical industry. In a number of extraction processes several types of equipment are employed, such as impeller columns, rotating disc columns, reciprocating plate columns, pulse columns, spray columns, and constant flow stirred tank contactors.

In each equipment one liquid phase of limited mutual solubility is contacted by dipersing the other liquid phase in the form of droplets. A relatively large specific contacting area of each is phase in required for the high efficiency of the countercurrent liquid-liquid extractor. For this objective appropriate design of dispersed phase contacting equipment should be based on the knowledge of the drop size distributions and the dynamics of the drop. The breakage and coalescence of drops greatly affect the interfacial area, concentration driving forces, and extraction efficiencies. The mass transfer rate has been obtained mainly from data based on the above and can be calculated by introducing the drop population balance equation.

The objectives of this work are to develop a more adequate model of the hydrodynamics, applying drop population balance equations for predicting the drop size distribution in a countercurrent flow liquid-liquid extraction column and to obtain

experimental data on a rotating impeller column, in order to compare the calculated results with the experimental data.

2. Theoretical development

The basic hydrodynamic equation for liquid-liquid countercurrent flow is expressed in terms of the overall phase flow rates as follows:

$$\frac{U_C}{C_R(1-\phi)} + \frac{U_D}{C_R\phi} = U_S \tag{1}$$

Applying individual drop size fraction of size d_i to it, a form of that equation becomes

$$\frac{U_C}{C_R(1-\phi)} + U_{D,i} = U_{S,i} \tag{2}$$

where $U_{D,i}$ is the rise velocity and $U_{S,i}$ is the velocity of the same drop(with diameter d_i) relative to the continuous phase.

If the dispersed phase static volume fraction of drops of size d_i is f_i, then equation(2) may be summed overall drop size fraction. Thus

$$(C_R\sum_i f_i U_{S,i})^2 + \phi^2(U_C - U_D - C_R\sum_i f_i U_{S,i})\phi + U_D = O \tag{3}$$

This equation may be solved iteratively for the holdup, flow rates, and drop size distribution data.

In this work a modified stagewise column model is considered. It is assumed that a section of the column is regarded as a constant flow stirred tank contactor and an isotropic field of turbulence applies within each section and further assume that the dispersed phase holdup is uniform within each section and drops move upward only at the boundary of the each section.

In this column those assumptions will be applied to each of the sections although there must exist at least some non-uniformities. To get the drop size distribution in a column a set of non linear integro-differential equations for one section is developed.

$$NA(v) = [n_0 a(v) + \int_v^{v_{max}} \lambda(v',v)v(v')g(v')NA(v')dv'$$

$$+ \int_0^{v/2} \lambda(v-v',v')h(v-v',v')NA(v-v')NA(v-v')dv]/[f(v)+g(v)+w(v)] \tag{4}$$

where $f(v) = f(Q,v)$, $w(v) = w(NA(v'),h,\lambda)$

The various functions, that is, $g(v)$, $b(v,v')$,$h(v,v')$ and $\lambda(v,v')$ appearing in the above equations should be obtained before the solution is made.

Analytical solutions of the integro-differential equation are not known, but a

numerical solution can be obtained by reduction with an integration formula.

It is considered that four functions cannot be applied to other dispersion systems without changing the values of the five parameters, because of the different characteristics of each system. Thus optimum values must be found for the five parameters to obtain minimum differences between the experimental and calculated results. For this purpose a nonlinear regression method is used.

3. Experimental

Detailed design of the experimental apparatus used in the present works has been described in the literature. The main column had an inside diameter of 6.5 cm and 30 sections of which working height was 210 cm.

The main aim of the experiment was to obtain the drop size distribution data and the holdup in the countercurrent extraction column. Experiments were performed with odorless kerosene for the dispersed phase and distilled water for the continuous phase.

The experimental column was initially filled with distilled water and the water flow rate was set at the disired level. The agitator was then started with its speed adjsted at the proper RPM. Opening the organic outlet line from the column, the organic feed pump was then started and the rate was increased gradually to the desired level. The agitator speed was checked at regular intervals using a tachometer. Flow rates were checked periodically during the course of experiments. The column was operated at the experimental settings until steady state conditions were established.

Drop size data were obtained photographically in this work. Detailed description of the photographic method can be found elsewhere in the literature. Holdup measurements were made when two phases had been completely seperated after the solenoid valves were shut off in order to stop the flows. Local holdups were measured for three selected sections with sample probes.

4. Results and discussion

Using the experimentally obtained local drop size distributions and the dipersed phase holdup measured, the local holdups with respect to column heights were calculated. The calculated holdups were subject to the constraint that the overall predicted value of the holdup agreed with the experimental average value. Typical data for the experimental and the calculated holdups are shown in Fig.1. It was found that holdups at the dispersed phase depend largely on the dispersed phase flow rate.

The drop size distribution and average drop size(d_{32}) were calculated by using the procedure described in theoretical development. In this work the rigid sphere assumption was adapted to overcome the non-uniformities. The typical data for the drop size distribution are depicted in Fig.2. It was found that the drop size distribution in a rotating impeller extraction column generally shows a unimodal form and the drop size gradually decreases as the column height increases under the same operating condition. This is believed to occur because the drops break up further during agitation as they

move up the column while the dynamic equilibrium between the breakage and the coalescence is maintained.

It is also observed that the narrow profile of the drop size distribution takes place and the variance decreases at higher impeller speed. The drop size increases with the phase flows and decreases as the column height increases. Also an increase in impeller speed caused a considerable decrease in the drop size.

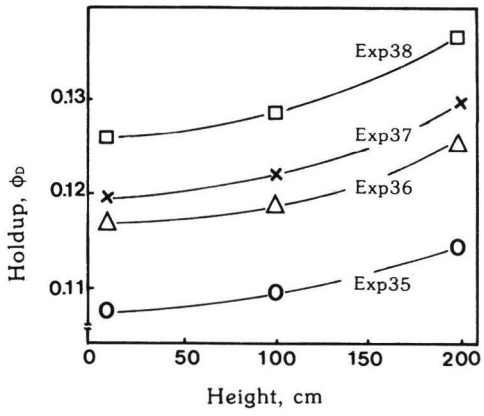

FIG. 1. AXIAL DISTRIBUTION OF HOLDUP, EXP 35-38.

Besides assuming binary, and homogeneous, drop breakage and coalescence, the model used in this work was developed for a local isotropic turbulent field, where drop breakage and coalescence were assumed to be the results of turbulent fluctuation at the drop surface.

The possibility that the basic hydrodynamics and drop population balance equations do not accurately represent the experimental behavior of the dispersion may not be neglected and leaves a subject for further study.

However at the present stage, as direct experimental data for the rotating impeller column are not available, this model can be useful to predict the holdup and the drop size distribution.

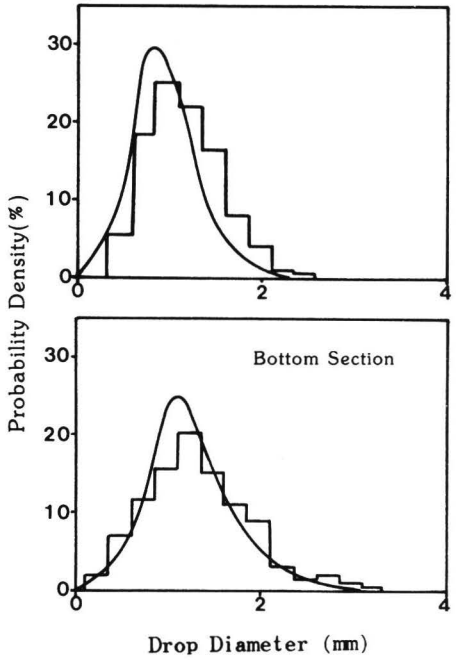

FIG. 2. DROP SIZE DISTRIBUTIONS FOR EACH SECTION, EXP 130

5. Conclusion

A stagewise hydrodynamic model, applying drop population balance equations derived from models for the breakage and coalescence of the drops in a contercurrent flow liquid-liquid extraction system, was developed to predict the drop size distribution and the holdup of the dispersed phase in a rotating impeller extraction column. To obtain the solution of a set of nonlinear integro-differential equation, computer simulation was performed using the backward iteration scheme.

Experiments were conducted using the kerosene-water system and the data for the holdup and the drop size distribution were obtained.

By comparing the results of simulations and those of the experiments the optimum values of the parameters in the model equations were obtained.

The drop size distribution and the holdup in a rotating impeller extraction column predicted by the model were in good agreement with the experimental results.

6. References

Coulaloglou, C.A. and Tavlarides, L.L., 1977, Description of Interaction Processes in Agitated Liquid-Liquid Dispersions. Chem Engr Sci., 32: 1289-1297

Cruz-Pinto, J.J.C. and Korchinsky, W.J., 1981. Drop Breakage in Countercurrent Flow Liquid-Liquid Extraction Columns. Chem Engr Sci., 36: 687-694

Gayler, R.,Roberts, N.W. and Pratt, H.R.C., 1953. Liquid-Liquid Extraction: Part IV. A Further Study of Holdup in Packed Columns. Trans Instn Chem Engrs., 31: 69-77

Jeon, Y.M., 1984. A Drop Population Balance Model for Mass Transfer in Liquid-Liquid Dispersion System. Ph.D. Thesis, KAIST

Korchinsky, W.J. and Azimzadeh-Khatayloo, S., 1976. An Improved Stagewise Model of Countercurrent Flow Liquid-Liquid Extractors. Chem Engr Sci., 31: 871-875

Landau, J and Houlihan,R., 1974. Throughput of Rotating Disc Contactor: a Review. The Can Jour of Chem Engr., 52: 338-344

Lee, Y.K., 1988. A Study on the Drop Population Balance Phenomena in a Rotating Impeller Extraction Column. Ph.D. Thesis, Ajou University

Olney, R.B., 1964. Droplet Chartacteristics in a Countercurrent contactor. AIChE J.,10: 827-835

Sovova, H.,1983. A Model of Dispersion Hydrodynamics in a Vibrating Plate Extractor. Chem Engr Sci., 38: 1863-1872

Valentas, K.J., Bilous, O. and Amundson, N.R.,1966. Analysis of Breakage in Dispersed Phase System. I & EC Fund., 5:271-279

Solvent Extraction 1990, T. Sekine (Editor)

© 1992 Elsevier Science Publishers B.V. All rights reserved

PERFORMANCE OF EXTRACTION COLUMNS FILLED WITH REGULAR PACKING

Ladislav STEINER, Kishore NEDUNGADI and Stanley HARTLAND
Swiss Federal Institute of Technology, Department of Industrial and Engineering Chemistry, 8092 Zürich, Switzerland.

ABSTRACT

A pilot plant size extraction column filled with regular SMV Sulzer packing has been built and operated with different liquid systems. In comparison to conventional (random) packings extremely large specific throughputs and good efficiency were observed. The column behaves more like a spray column but without bulk circulation; backmixing is reduced to acceptable levels and mass transfer rates are higher. Measured concentration profiles were well predicted by computer simulation using a lumped parameter model assuming noncoalescing drops passing through a cascade of well mixed stages with backmixing.

INTRODUCTION

Regular packings were derived from static mixing elements used for homogenisation of single-phase fluids. They established themselves especially in gas-liquid transfer operations such as absorption or distillation. Recently, their applicability has been extended also to liquid-liquid systems, extraction columns being now available up to very large diameters. Their main advantages are that they work at high phase throughputs, do not contain moving parts, and do not need any energy input. Disadvantages are lower transfer rate (compared to columns with intensive agitation), the fact that the packing must be preferably wetted by the continuous phase, and a limited selection of suitable packings for corrosive liquids. Obviously, they are not universally applicable but represent an interesting alternative for many bulk processes with large throughputs and easy separation.

EXPERIMENT

A column with a diameter of 70 mm and a height of 3.5 m was constructed from QVF technical glass. The packed section was 3.17 m long and consisted of 15 standard elements of Sulzer's

stainless-steel packing SMV. Holes 25 mm in diameter were erroded through the middle of the elements to enable photography and insertion of probes used to monitor the column performance. A distributor with 109 precisely cut stainless tubes (1mm ID, 25 mm long) was placed 250 mm under the lower end of the packed section to guarantee defined inlet conditions. A supply system with four 400 l tanks enabled the column to be operated at the steady-state for several hours. The same equipment and distributor were used previously by Ugarcic (1981) in his investigation of a spray column. Water and toluene were respectively the continuous and dispersed phases, acetone, ethanol and methyl-isopropyl ketone being used as solutes.

As in our earlier studies concentration profiles were measured using special probes along the column height, together with hold-up, drop size and backmixing in both phases. Some probes and techniques were newly developed to suit the special conditions encountered in this type of column.

MODEL SELECTION

To achieve good efficiency and large throughputs, the column should be constructed of materials wetted preferably with the continuous phase and the transfer direction should be selected so that coalescence between the drops is suppressed. Under these conditions the drop size distribution is narrow and the mean diameter remains practically constant along the column height. The numerous vertical channels in the packing suppress bulk circulation so that practically identical hydrodynamic conditions are established in columns of different diameter. To simulate this performance on a computer, models which consider the behaviour of individual drops in spray columns are more realistic than those based on backmixing which assume constant radial homogenisation of both phases. In the simplest case the drops are represented by a mean diameter, and it is assumed that they move in plug flow through a series of well mixed stages filled with the continuous phase. To characterise axial mixing backflow of the continuous phase is considered. The mass balance for a typical stage is then

$$(1+f)(X_{n+1}-X_n)+f(X_{n-1}-X_n) = (L/H)(Y_n-Y_{n-1}) \qquad (1)$$

The concentration inside the drops is calculated from Newman's function (1931) replacing the molecular diffusivity by an

empirical coefficient as described by Steiner (1986) who also derived an empirical equation for the effective diffusivity in spray columns:

$$R = (5.56(10^{-5})[2Re\mu_c/(\mu_c+\mu_d)]^{1.42}\ Bo^{0.12}\ Sc_d^{0.67}\ (1-e) \qquad (2)$$

The same parameter may also be obtained by integrating Handlos and Baron's (1957) definition of eddy diffusivity in turbulent drops:

$$R = d_D v_s/(3072 D_d(1+\mu_d/\mu_c)) \qquad (3)$$

With Newman's equation the concentration change inside the drops is calculated directly without first evaluating a (constant) mass transfer coefficient. The resistance in the continuous phase is taken into consideration as it influences the Eigen values of the Newman's function. However, with the system used in this work transfer resistance inside drops is much more important than that outside.
For simulation of concentration profiles from first principles the following parameters are necessary:

Holdup: Kumar et al. (1980) published the following equation for the slip velocity in spray columns which correlated available literature data:

$$v_s = [2.725(\rho_c-\rho_d)d_D g/\rho_c\ ((1-e)/(1+e^{1/3}))^{1.834}]^{1/2} \qquad (4)$$

Combining eq. (4) with the definition of slip velocity the hold-up may be calculated.

Backmixing: Horvath et al. (1978) showed that the equation of Zheleznyak and Landau (1973) is applicable for spray columns with medium hold-up and in the absence of bulk circulation:

$$E_c = 6.6(\mu_c/\rho_c)Re_h^{0.987}\ e^{0.814\bar{\mu}3.89} \qquad (5)$$

where $Re_h = \dfrac{\rho_c v_s d_{col}(1-e)}{\mu_c[1.5e(d_{col}/d_D)+1]}$ and $\bar{\mu} = \dfrac{\mu_c+\mu_d}{(2/3)\mu_c+\mu_d}$

Transfer rate: For the continuous phase equations published by Steiner (1986) are applicable. In the dispersed phase effective diffusivity should be calculated and used in the Newman's equation.

RESULTS

The slip velocities evaluated from known phase throughputs and measured mean hold-ups are compared to those predicted by eq. (4) in Fig.1. Agreement is good, the measured values being slightly higher than those predicted.

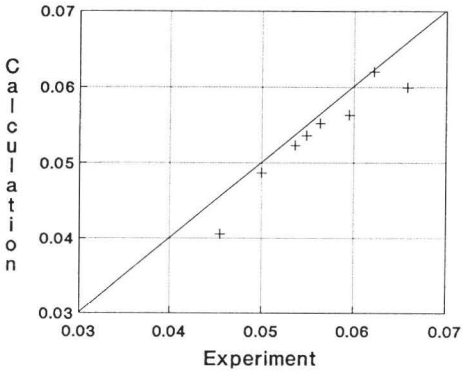

Fig. 1: Comparison of measured slip velocity to eq. (4) of Kumar et al. (1980)

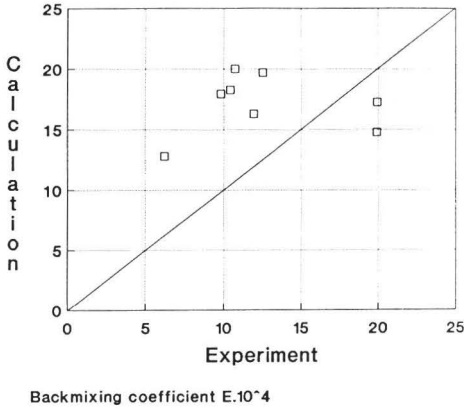

Fig. 2: Comparison of measured backmixing coefficients in continuous phase to eq. (5) of Zheleznyak and Landau(1973)

Fig. 2 shows that backmixing coefficients calculated from eq. (5) are usually higher than those observed. However, given the low sensitivity of the concentration profiles to the value of the backmixing coefficient, a rough estimation is sufficient for the purpose of profile simulation.

Working with high phase throughputs the drops were formed in the jetting regime so mass transfer during formation was negligible.

Therefore, the effective diffusivity was evaluated by single--parameter optimisation, varying its value until the sum of the deviations from both exit concentrations and in 8 intermediate positions (for each phase) was minimised. An example of such a best fitting profile is in Fig. 3. The mean deviations were very low, typically under 0.0004 (in concentration units), and the trends are well reproduced, even in the dispersed phase just after drop release. This is not possible with a constant transfer coefficient or when a simple backmixing model is used.

The results of the optimisation are collected in Fig.4 where lines for eq. (2) and (3) are also shown. The experimental values are considerably above those predicted by eq. (2) derived for spray columns and sometimes even above eq. (3) of Handlos and Baron. As the purity of the systems was about the same as in our previous work on spray columns, it obviously was the packing which caused the enhancement.

If values from eq.(3) are used for profile generation instead of the optimised ones, the mean deviation increases only marginally. Well fitting profiles may therefore be calculated from common equations available in the literature.

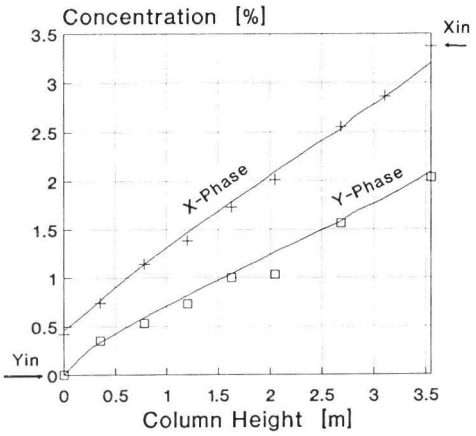

Fig. 3: Example of optimised concentration profiles in a column with organised packing. Water, toluene and acetone, total loading 75.2 m^3/m^2h.

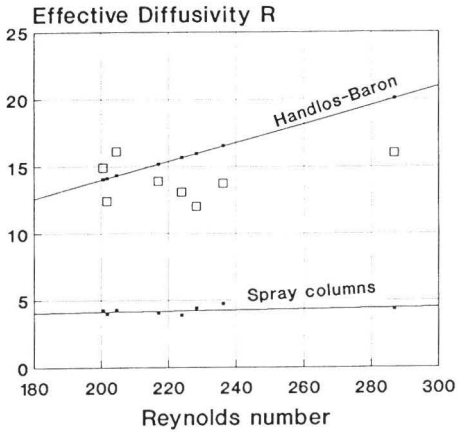

Fig. 4: Comparison of values of effective diffusivity optimised from the concentration profiles and calculated from equations (2) and (3).

CONCLUSIONS

When working with a column filled with organised packing under clean conditions the hydrodynamic regime is similar to the one found in spray columns. Hold-up and backmixing coefficient may be predicted from corresponding equations but the mass transfer rate is higher. The effective diffusivity is close to the one obtained from Handlos and Baron's derivation.

Even a simple model assuming plug flow of dispersed phase through a cascade of backmixed stages filled with continuous phase realistically simulates the concentration profiles. Reasonable prediction of separation performance is then possible without any experimental data.

SYMBOLS

Bo	Bond number $(=\rho_c-\rho_d)gd_D^2/\sigma$	R	effective diffusivity
d_D	drop diameter	Re	Reynolds number
e	hold-up	Sc	Schmidt number
E_c	eddy diffusivity (cont.)	v_s	slip velocity
f	backflow coefficient	X	concentration, heavy ph.
g	gravity acceleration	Y	concentration, light ph.
H	throughput, heavy phase	ρ	density
L	throughput, light phase	μ	viscosity
		σ	interphase tension

REFERENCES

Handlos A.E., Baron J.T., AICHE J. 1957, 3, 127.
Horvath M., Steiner L., Hartland S., Can.J.Ch.Eng. 1978,56,9.
Kumar A., Vohra D., Hartland S., Can.J.Ch.Eng. 1980, 58,154.
Newman A.B., Trans.A.I.Ch.E. 1931, 27, 203.
Steiner L., C.E.Sci. 1986, 41, 1979.
Ugarcic M. Diss. ETH No. 6825, Zurich 1981.
Zheleznyak A.S., Landau A.M. Th.Osn.Kh.Tech. 1973, 7, 577.

Solvent Extraction 1990, T. Sekine (Editor)

© 1992 Elsevier Science Publishers B.V. All rights reserved

THE EFFECTS OF MASS TRANSFER ON DROP BREAKAGE IN ROTATING DISC CONTACTORS

V. CAUWENBERG*, C. MESSEMAEKERS*, P. VAN ROMPAY*, M.J. SLATER†
* Department of Chemical Engineering, Catholic University of Leuven, Belgium
† Department of Chemical Engineering, University of Bradford, UK.

ABSTRACT

The breakage probability has been measured for single liquid drops in a non-flowing continuous phase in a rotating disc contactor. It has been found that correlation of breakage probability with a modified Weber number is physically realistic. For conditions of mass transfer, the use of an appropriate interfacial tension correlates results with the same equation as for no mass transfer. Interfacial solute concentrations should be used to find interfacial tension. Steady-state mass transfer experiments or theoretical calculations will give the interfacial tension data required.

INTRODUCTION

A knowledge of drop size distributions in liquid-liquid extraction columns is required for proper interpretation of behaviour and for design work. Drop breakage and coalescence phenomena have to be studied, and the influence of the mass transfer process established. Drop population balances can be written when breakage and coalescence rate functions are available. This note concerns breakage rates only in a rotating disc contactor (RDC) and in particular the use of an appropriate value of interfacial tension during mass transfer. No difference in the breakage process should be observable according to direction of mass transfer if the interfacial tension is properly accounted for (Kleczek et al., 1989).

2 EXPERIMENTAL WORK

Experiments on single solvent drops in water or a water/ethylene glycol mixture were carried out in an RDC of 152mm diameter with 13 stages. The continuous phase was non-flowing and solvent phase was pumped to one of several glass capillary tubes or needles to form a stream of widely-spaced uniform drops of a variety of sizes depending on capillary diameter (Bahmanyar et al., 1990). The capillary was adjusted so that rising drops just missed the first rotor edge at zero rotor speed. At least 300 drops were observed in each run and the number fraction which broke at the first rotor was determined by eye (breakage probability, p). Drops only broke at the rotor edge. This was done at various rotor speeds for a variety of

systems with a wide range of physical properties (Table 1). Phases were presaturated with each other. Some experiments were carried out with mass transfer, in both directions.

Materials of construction were glass, stainless steel and p.t.f.e. and the equipment was thoroughly cleaned with acetone and distilled water between sets of experiments.

The interfacial tension values were measured with a Kruss K8551 Tensiometer (du Nouy ring); for cases of mass transfer the phases were brought together in a cell and the determination made quickly. It is accepted that this is not ideal and a continuous flow cell with steady-state mass transfer is now being used to obtain better data.

Typical experimental data are given in Figure 1. Values of the breakage fraction, p, less than 0.05 tend not to be very reproducible. At rotor speeds which are high relative to the critical speed at which no drops break, drops tend to move further away from the rotor edge and breakage is lessened. The experimental observations are sensitive to drop position relative to rotor edge (Bahmanyar and Slater, 1990).

3 CORRELATION OF RESULTS

The correlation of breakage probability is based on a particle Weber number $We_p = \rho_c \epsilon^{2/3} d^{5/3}/\gamma$ derived from Kolmogoroff's theory of local (at rotor edge) isotropic turbulence. The power per unit mass, ϵ, is determined using equations given by Misek and Marek (1970) for power input per disc;

$$\text{For } Re_D < 6 \times 10^4 \qquad P = 23.1\ (\rho_c N^3 D_R^5)(\rho_c N D_R^2/\mu_c)^{-0.568} \tag{1}$$

$$\text{For } Re_D > 6 \times 10^4 \qquad P = 0.261\ (\rho_c N^3 D_R^5)(\rho_c N D_R^2/\mu_c)^{-0.155} \tag{2}$$

(note misprints of constants in original paper)

Hence, for $Re_D < 6 \times 10^4$

$$We_p = C_1\ (\rho_c^{0.62} N^{1.62} \mu_c^{0.38} D_R^{2.58} d^{1.67}/\gamma\ D_c^{1.33} H_c^{0.67}) \tag{3}$$

and for $Re_D > 6 \times 10^4$

$$We_p = C_2\ (\rho_c^{0.90} N^{1.90} \mu_c^{0.10} D_R^{3.13} d^{1.67}/\gamma\ D_c^{1.33} H_c^{0.67}) \tag{4}$$

The ratio of breakage fraction , p, to fraction not breaking, (1-p), is considered to be a function of a Weber number which is a ratio of applied stress to forces resisting breakage. To take account of assumed zero breakage at a critical rotor speed, N_{CR}, (obtained by extrapolation), we propose the correlation

$$p/(1-p) = a\,[We_p - We_{pCR}]^b = a\,We_m^b = 9.67\,We_m^{1.01} \text{ for } Re_D < 6x10^4 \qquad (5)$$

The correlation shown in Figure 2 is for data with and without mass transfer. The deviations are large because in some systems it is difficult to estimate N_{CR} by extrapolation, drop position relative to the rotor tends to depend on rotor speed, and interfacial tension during mass transfer needs to be more accurately measured. There is regular deviation from Eq.(5) according to interfacial tension values which needs to be explained. The data for the toluene systems are well-behaved and Figure 3 shows clearly that the influence of physical properties and of interfacial tension during mass transfer can be satisfactorily described by Eq.(5).

4 DISCUSSION

The linear dependence of the ratio $p/(1-p)$ on We_m is very encouraging, supporting a realistic physical interpretation of breakage. In previous work (Bahmanyar and Slater, 1990, and Bahmanyar et al., 1990) the modified Weber number was defined as $We_m = \rho_c\, d\, D_R^2\, (N^2 - N_{CR}^2)/\gamma$ (ratio of drop kinetic energy to drop surface energy) which is close to Equations (3) and (4) but probably over-simplistic. Nevertheless this modified Weber number correlates data as well as Eq.(5). The dependence of breakage on rotor diameter and column dimensions can now be tested more carefully using Eq.(5).

The measurement of interfacial tension during steady state mass transfer is being carried out now with a du Nouy ring tensiometer and a flow cell. Estimates of interfacial concentrations can be made using the ratio of film mass transfer coefficients and a plot of interfacial tension against an (equilibrium value) interfacial solute concentration can be drawn up. Initial data agree moderately well with batch equilibrium experimental data. The flow effects in the cell are small but interfacial contaminants might influence flow cell and batch results differently.

The work of Fu et al. (1986) has been used to predict interfacial tensions for ternary systems with good results (Figure 4). Thus making the reasonable assumption that the interfacial tension for estimated interfacial concentrations is the value required in correlations for drop breakage, then experimental measurements might be dispensed with in calculations of drop sizes produced when the breakage process is dominant.

5 CONCLUSIONS

The process of single drop breakage in an RDC is not yet clearly understood. Experimental work is rendered difficult because drop path

changes with drop size, physical properties and rotor speed. However, a physically realistic dependence of drop breakage probability on a modified Weber number has been established. The use of the proper value of interfacial tension correlates breakage data for either direction of mass transfer. It is now possible to consider the influence of the mass transfer process on drop breakage via the changing interfacial solute concentrations, dependent on knowing film mass transfer coefficients.

6 SYMBOLS

d	drop diameter	m
D_C	column diameter	m
D_R	rotor diameter	m
H_C	compartment height	m
N	rotor speed	s^{-1}
N_{CR}	critical rotor speed for p=0	s^{-1}
P	power input per rotor disk	W
$p(d)$	breakage probability of a drop of diameter d	-
Re_D	Reynolds number (ρ_c N D_R^2/μ_c)	-
We_p	Weber number (ρ_c $\epsilon^{2/3}d^{5/3}/\gamma$)	-
ϵ	energy dissipation per unit mass	m^2/s^3
μ_c	dynamic viscosity of continuous phase	Pa.s
ρ_c	density of continuous phase	kg/m^3
γ	interfacial tension	N/m

7 REFERENCES

Bahmanyar, H., Chang-Kakoti, D.K., Garro, L., Liang, T-B and Slater, M.J., 1990, Trans. I. Chem. E., "Mass transfer from single drops in rotating disc, pulsed sieve plate and packed liquid-liquid extraction columns", Vol. 68, Part A, 74-83.

Bahmanyar, H. and Slater, M.J., 1990, "Studies of drop-breaking in liquid-liquid systems in a rotating disc contactor - Part 1"; Chem. Eng. Technol., In Press.

Fu, J., Li, B. and Wang, Z., 1986, "Estimation of fluid-fluid interfacial tensions of multicomponent mixtures", Chem. Eng. Sci., Vol.41, No.10, 2673-2679.

Kleczek, F., Cauwenberg, V. and Van Rompay, P., 1989, "Effect of mass transfer on droplet size in liquid-liquid dispersions", Chem. Eng. Technol., Vol.12, 395-399.

Misek, T. and Marek, J., 1970, "Asymmetric rotating disc extractor", British Chem. Eng., Vol.15, 202.

No mass transfer	ρ_c	ρ_d	μ_c	μ_d	γ
water - toluene	996	886	1.016e-3	0.610e-3	28.37e-3
water+ethyleneglycol - toluene	1008	886	2.397e-3	0.610e-3	18.43e-3
water - n-Butylacetate	996	879	1.016e-3	0.732e-3	12.08e-3
water - MIBK	996	803	1.016e-3	0.602e-3	10.16e-3
water - n-Hexane	996	660	1.016e-3	0.335e-3	41.97e-3
water - 1-octanol	996	827	1.016e-3	8.802e-3	7.62e-3
water - toluene+oil	996	882	1.016e-3	1.482e-3	17.60e-3
water - toluene+oil	996	897	1.016e-3	3.454e-3	18.00e-3
Solute transfer from dispersed to continuous phase					
water - toluene+MIPK	996	864	1.016e-3	0.610e-3	24.60e-3
water - n-Butylacetate+MIPK	996	877	1.016e-3	0.732e-3	11.56e-3
water - MIBK+acetic acid	996	812	1.016e-3	0.602e-3	7.96e-3
water - n-Hexane+acetic acid	996	687	1.016e-3	0.346e-3	32.73e-3
Solute transfer from continuous to dispersed phase					
water+acetic acid - toluene	998	886	1.016e-3	0.610e-3	22.53e-3
water+acetic acid - MIBK	998	803	1.016e-3	0.602e-3	7.50e-3

Table 1 : Physical properties of the systems used

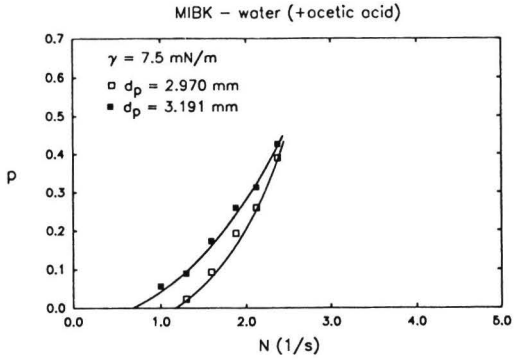

Fig. 1a

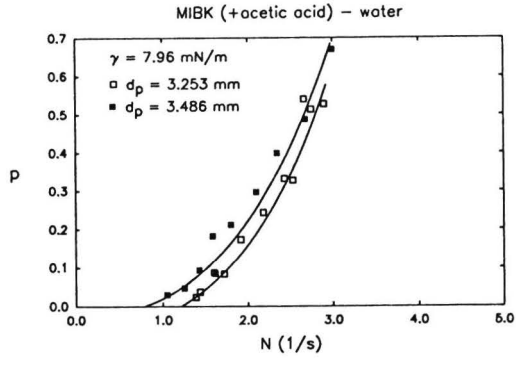

Fig. 1b

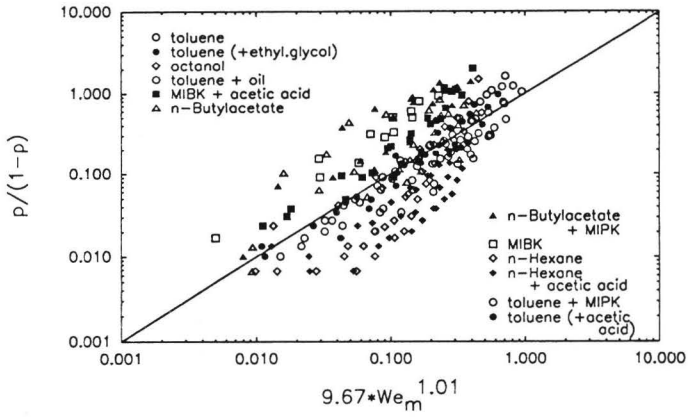

Fig. 2

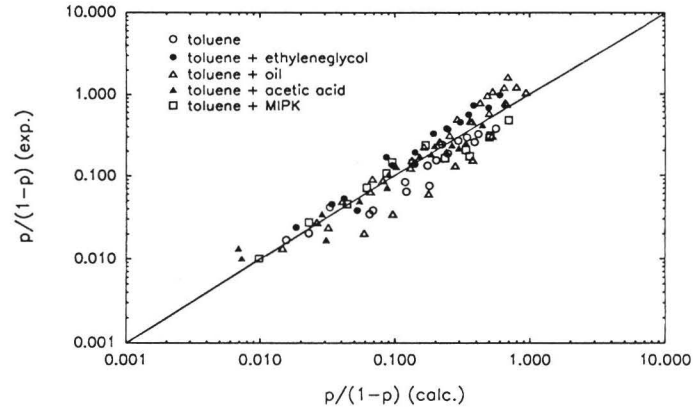

Fig. 3

Water + Hexane + Acetic acid

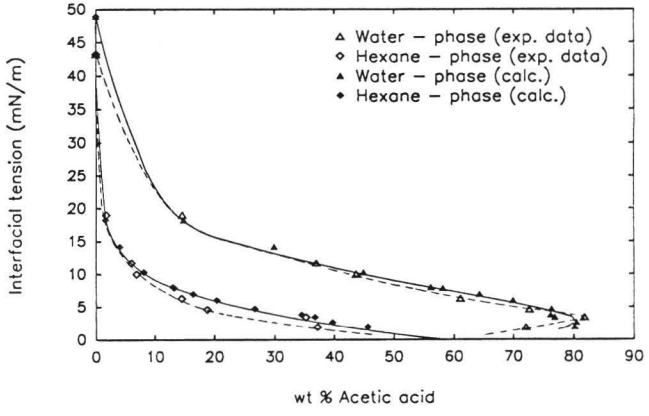

Fig. 4

Solvent Extraction 1990, T. Sekine (Editor)

© 1992 Elsevier Science Publishers B.V. All rights reserved

OPERATION OF A PULSED SIEVE-PLATE EXTRACTION COLUMN WITH AN EXTREME PHASE FLOW RATIO

H. RAUSCHER and E. BLAß
Lehrstuhl A für Verfahrenstechnik, Technische Universität München, Arcisstraße 21, 8000 München 2, Germany

Abstract

A liquid-liquid extraction test stand for experiments with an extreme phase flow ratio and physical data for a new standard test system of medium interfacial tension are presented. Experiments are carried out to describe fluiddynamics and mass transfer in the column. The results show reasons for the observed decay of the extraction efficiency and made basic data available to describe column behaviour with a forward mixing model.

1. INTRODUCTION

Many material systems in liquid-liquid extraction show an extreme phase equilibrium coefficient. In state of equilibrium the transfer component enriches one phase much more than the other. If the extractor shall be worked near the optimum operating point, the extraction factor $\lambda=1$ ought to be achieved. The extraction factor

$$\lambda = \frac{x_{org}}{x_{aqu}} \cdot \frac{m_{org}}{m_{aqu}}$$

is the product of a concentration ratio and the flow ratio between extract phase and raffinate phase. The concentration ratio depends on the material system and describes the slope of the balance line. If its value is high, it is necessary to reduce the volumetric flow ratio to get an extraction factor equaling one.
Compared to operating conditions with equal volumetric flow rates a decay of the separation performance is observed which can not described by the dispersion model. Measurements were carried out for the purpose of quantifying the reduction of the separation performance and trying to find an explanation for it.

2. Pilot plant and material system

A pulsed sieve plate extraction column of a diameter of 50 mm and an active column height of 3.5 m was used as a pilot plant. The sieve plates showed holes of a diameter of 3mm and a superficial free area of 23%. For the purpose of recording the hydrodynamic processes in the column, probes were installed (Fig. 1) for the determination of the drop size (marked as DSD in the figure), of the holdup (marked as holdup in the figure) and for the distribution of the residence time (marked as photomultiplier or conductivity in the figure). For the determination of mass transfer samples of the phases were taken at five points in the active part of the column. Hence, together with the concentrations of the inlet and outlet, the axial concentration profile for each phase is based on seven measuring points.

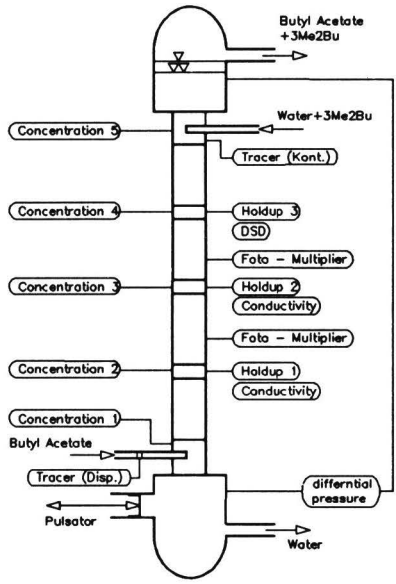

Fig. 1 Extraction pilot plant and measuring technique

As material system to be tested the EFCE suggested the combination of Water-3 Methyl-2-Butanone as raffinate phase and n-Butyl Acetate as solvent phase. All experiments were carried out with dispersed organic phase, hence, mass transfer takes place from the continuous to the dispersed phase. In the range of 5 mass-% the distribution balance of the transfer component shows an almost linear progression with the gradient of 13. That means that an extraction factor of 1 requires a flow rate of the watery phase which is 13 times higher than the organic phase.

3. Results

During the series of tests for the determination of the separation performance the operation parameters, i.e. pulsation intensity and load, were varied within a great range.

The measured drop size is the most important hydrodynamic parameter of a dispersion, since it has considerable influence on the

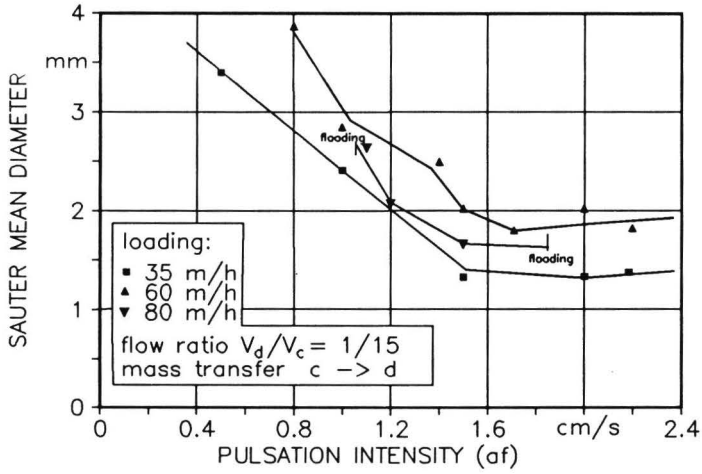

Fig. 2 Sauter drop diameter versus pulsation intensity

interfacial area available for mass transfer. The Sauter diameter being plotted versus the pulsation intensity (Fig. 2) shows clearly that no further reduction of the medium drop diameter is possible by increasing the energy supply, once the pulsation intensity has exceeded $16 \cdot 10^{-3}$ m/s. If the little influence of the total load is neglected, the Sauter diameter can be evaluated by equation

$$d_{32} = 0.41 \frac{\sigma^{0.6}}{\rho_c^{0.6}} \xi_m^{-0.267} \quad \textit{and}$$

$$\xi_m = \frac{\pi^2}{2} \frac{1-\phi^2}{H_p C_0^2 \phi^2} (af)^3$$

which is based on the turbulence theory.

In the case of extreme distribution coefficients the width of the drop size distributions (Fig.3) is strongly influenced by pulsa-

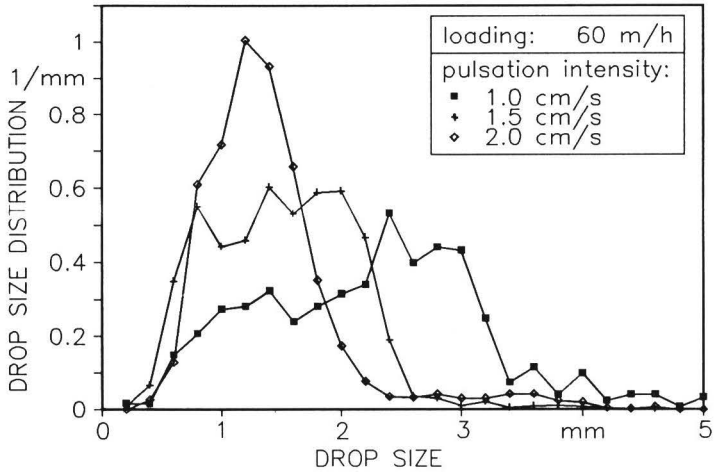

Fig. 3 Influence of pulsation intensity on the width of the drop size distribution

tion intensity. If pulsation intensity is weak the drop size distributions are wide. An increase of pulsation intensity leads to narrower drop size distributions, at the same time a shifting to the left side takes place, i.e. towards the smaller drops.

The specific interfacial area can be determined by the Sauter drop diameter and the holdup measured in the experiments. Due to the low holdup only small specific areas can be obtained. An increase of the total load leads to a considerable enlargement of the interfacial area and thus to an improvement of mass transfer. However, these operating points are quite near to the flooding point of the extractor and are avoided in practical work if possible.

The separation performance of the extractor can be evaluated with the concept of the equivalent height. Separation performance at first remains on an almost constant level, if pulsation intensity is low. There are about 0.4 theoretical stages per meter obtained. Separation performance increases linear to the flooding point, when pulsation intensity exceeds 1.3 cm/s. In that region a maximum of 1.2 stages per meter was obtained.

The axial dispersion model is frequently applied for the calculation of the course of the concentrations in the two phases, if

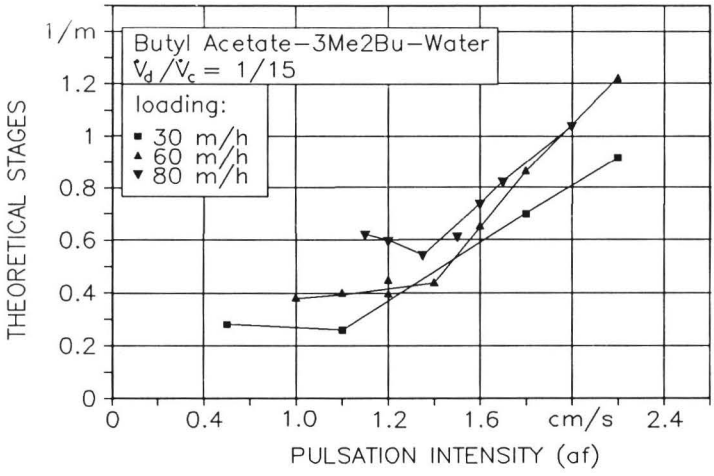

Fig. 4 Mass transfer coefficient evaluated from measured concentration curves

processes of axial mixing shall be considered for the assessment of the separation performance of the extractor. In a comparison between measured and calculated concentration curves a mass transfer coefficient can be found which allows an optimum agreement between model calculation and reality. The obtained mass transfer coefficient is a measure for the separation performance of the extractor. It is plotted in Fig. 4 versus the pulsation intensity. It shows that for low pulsation intensities only low mass transfer coefficients are obtained. This contradicts the theoretical considerations which predict high mass transfer coefficients for the large drop diameters presented here.

The drop size distributions shown in Fig. 3 may provide an explanation. If pulsation intensities are low and the phase flow ratios extreme, the drop size distributions are wide. The share of fast rising large drops, which transports the main part of the dispersed phase through the extractor, contributes little to mass transport, due to its short residence time. Since the dispersion model always underlies uniform drop size distributions, this effect is not taken into consideration. In an optimalization this leads to a diminution of the mass transfer coefficient.

3. Summary

Due to the low holdup only small specific interfacial areas are available for mass transfer, if liquid-liquid extractors are operated with extreme phase flow ratios. The width of the drop size distribution is more strongly influenced by pulsation intensity than this has been known for the operation with the phase ratio equal one. Especially when pulsation intensities are low, wide drop size distributions appear, which cause a considerable reduction of the separation performance. Therefore, for the predetermination of the separation performance only models of columns should be used which explicitly take into consideration the influence of drop size distribution on mass transfer.

4. Symbols

a	amplitude	m
C_0	coefficient =0.6	
d_{32}	Sauter drop diameter	m
f	frequency	1/s
m	mass flow	kg/s
x	concentration	kg/kg
ρ_c	density of continuos phase	kg/m^3
ϕ	fractional free area	-
σ	interfacial tension	N/m

5. Acknowledgement

Financial support of the "Arbeitsgemeinschaft Industrieller Forschungsvereinigungen (AIF)" is gratefully acknowledged.

Solvent Extraction 1990, T. Sekine (Editor)

© 1992 Elsevier Science Publishers B.V. All rights reserved

APPLICATION OF KINETIC MODELS TO CONTACTOR DESIGN

M. T. SAEED* AND E. S. PEREZ DE ORTIZ
Department of Chemical Engineering, Imperial College, London, SW7, U.K..
* PCSIR Laboratories, Ferozepur Road, Lahore–16, Pakistan

ABSTRACT

A kinetic model of the extraction of zinc by di(2ethylhexyl) phosphoric acid (DEHPA), which includes the extraction and stripping reactions as well as the mass transfer coefficients of the species involved in the process, is used in the calculation of the height of a continuous countercurrent contactor. These results are compared with contactor heights estimated with an interfacial equilibrium model over a wide range of operating conditions. It is shown that heights calculated with the equilibrium model can be set up to an order of magnitude lower than the heights estimated with the kinetic model. The relative values of these heights vary with concentrations and operating conditions.

Results simulated with the kinetic model are in good agreement with experimental determinations in a small spray column.

INTRODUCTION

Continuous liquid–liquid contactors are usually designed assuming interfacial equilibrium. In the case of mass transfer with chemical reaction, this assumption is only valid when the reaction is very fast with respect to the mass transfer rate.

However, there are numerous liquid–liquid metal extraction reactions which have been reported to be intermediate or slow and are controlled by both chemical reaction and mass transfer parameters (mixed control). In this case, the extraction flux is affected by both chemical and mass transfer resistances and the assumption of interfacial equilibrium may not be applicable.

In this paper, the kinetic model of the extraction of zinc by di(2–ethylhexyl) phosphoric acid (abbreviated as DEHPA in the text and H_2A_2 in the equations) in n–heptane is used in the design of a continuous countercurrent contactor and a comparison is made with results obtained using the equilibrium model. Predicted heights are also compared with experimental results obtained in a spray column.

HEIGHT OF A CONTINUOUS COUNTERCURRENT CONTACTOR

At steady state, constant flow rates and neglecting backmixing, the height, H, of a countercurrent continuous contactor is estimated from a mass balance for the zinc ion.

$$H = L_d \int_1^2 dC_{zo} / [R_z\, a_c\, (1 - \phi)\,] \tag{1}$$

In order to integrate this equation, a mathematical expression for R_z as a function of zinc concentration is required.

ZINC INTERFACIAL FLUX

Murthy [1] studied the extraction equilibrium for the zinc–DEHPA system and reported that two complexes of zinc–DEHPA are formed in n–heptane according to the stoichiometry of the reactions.

$$Zn^{2+} + 1.5\ H_2A_2 \rightleftharpoons Zn\ A_2.HA + 2H^+ \tag{2}$$

$$Zn^{2+} + 2.0\ H_2A_2 \rightleftharpoons Zn\ A_2.H_2\ A_2 + 2H^+ \tag{3}$$

where bars indicate the species in organic phase and $H_2\ A_2$ is DEHPA in dimer form. He also reported that reactions 2 and 3 take place at the interface.

Kinetic Model

The following kinetic model was proposed based on extraction and stripping studies conducted in a constant interfacial area cell [2, 3, 4].

$$R_{zk} = k_I\,(C_{za} - R_{zk}/K_{za})\,(a_o - R_{zk}/K_D)/(C_H + 2R_{zk}/K_H) - k_I'\,(C_{zo} + R_{zk}/K_{zo})$$

$$(C_H + 2R_{zk}/K_H) \,/\, [(a_o - 1.8\ R_{zk}/K_D) + 0.05\,(a_o - 1.8\ R_{zk}/K_D)^{\frac{1}{2}}] \tag{4}$$

This gives R_{zk} in terms of bulk concentrations of the species involved, individual mass transfer coefficients and the specific reaction rate constants for the extraction and stripping reactions (k_I and k_I').

Equilibrium Model

The equilibrium conditions for interfacial reactions 2 and 3 are given by [1]

$$(C_{zoi}/C_{zai})_{eq} = K_{E1}\,(a_{oi}\ 1.5/C_{Hi}{}^2)_{eq} + K_{E2}\,(a_{oi}{}^2/C_{Hi}{}^2)_{eq} \tag{5}$$

where subscript i indicates interfacial values. Assuming interfacial equilibrium [5] and combining equation 5 with the equations for the fluxes of the different species, the following expression is obtained in terms of bulk concentrations

$$(C_{zo} + R_{ze}/K_{zo})/(C_{za} - R_{ZE}/K_{za}) = k_{E1}\,(a_o - 1.8\,R_{ze}/K_D)\,1.5/\,(C_H + 2R_{ze}/K_H)^2 +$$

$$k_{E2}\,(a_o - R_{ze}/k_D)^2/(C_H + 2R_{ZE}/K_H)^2 \qquad (6)$$

Equations 4 and 6 were solved for R_z by using subroutines [6] for polynominal equations. In all cases considered, there was only one real root for positive interfacial concentrations.

COMPARISON OF SIMULATED RESULTS

A computer programme was written to perform the numerical integration of equation 1 using the interfacial fluxes given by the kinetic and equilibrium models (equations 4 and 6).

Figures 1 and 2 show the effect of concentrations and mass transfer coefficients on the ratio between the contactor heights obtained using the two models. It can be seen that the equilibrium model predicts smaller contactor heights at most investigated conditions. As zinc or DEHPA concentrations are increased at constant mass transfer coefficients as shown in Figure 1 the heights calculated with the two models become closer. The same effect is observed when the values of the mass transfer coefficients are reduced at constant concentrations as show in Figure 2. In both cases this is due to a relative increase in the mass transfer resistances with respect to the rate of chemical reaction which allows the reactions to get closer to equilibrium

EXPERIMENTAL

In order to test the models experiments were performed in a glass spray column of 1.4 m effective height and 0.05 m diameter with five sampling points. Two flat windows, one at the top and the other at the bottom, allow for the dispersion to be photographed with a cine camera. The column was operated in a semi–batch mode, i.e. the continuous aqueous phase was kept stagnant, and the dispersed phase was not recirculated. Concentrations and operating conditions are given in Table 1. Thirty runs were performed at wide ranges of concentrations of zinc and DEHPA and disperse phase flow rate. Table 1 gives the conditions for three of these runs for a DEHPA concentration of 0.075 M.

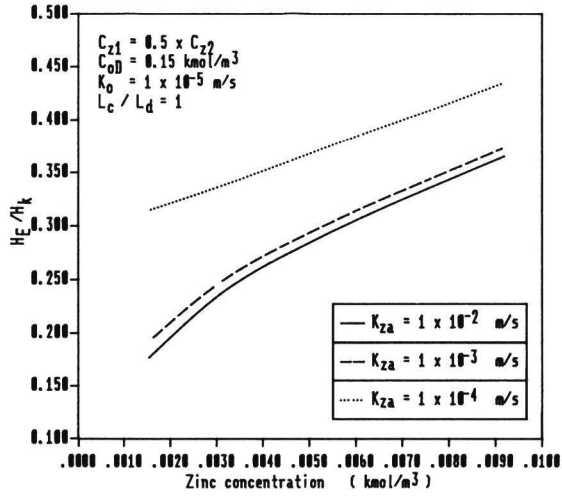

Figure 1 Effect of zinc concentration on the ratio of contactor heights.

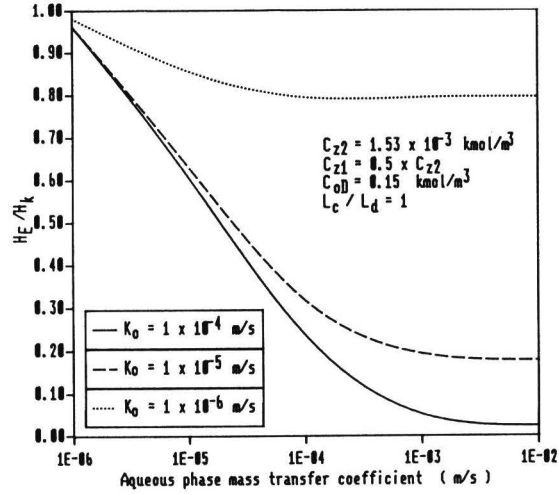

Figure 2 Effect of aqueous phase mass transfer coefficients on the ratio of contactor heights.

COMPARISON OF EXPERIMENTAL AND PREDICTED RESULTS

Predicted heights were estimated using equation 1 for inlet and outlet dispersed phase zinc concentrations measured in the experimental runs. Mass transfer coefficients for the continuous and dispersed phases were estimated using correlations reported in the literature [7 and 8]. Calculated heights by using both models are given in Table 1. It can be seen that while the kinetic model gives good estimates of the column height the equilibrium model underestimates it substantially. The fact that the heights predicted with the kinetic model are in all cases higher than the height of the column suggests that the estimated values for the mass transfer coefficients may be low.

TABLE 1
Examples of experimental and predicted results. (Experimental height = 1.4m)

$C_{za} \times 10^2$	pH	$(R_{z,exp}$	R_{zk}	$R_{zE})\times 10^7$	H_k	H_E
0.32	2.50	0.88	0.61	4.19	2.0	0.29
0.10	2.71	0.40	0.31	1.70	1.84	0.33
1.99	2.40	1.91	1.50	10.8	1.78	0.25

CONCLUSIONS

From the simulated results, it can be concluded that for extraction with a slow to intermediate chemical reaction, the contactor height could be underestimated by up to one order of magnitude if the equilibrium rather than the kinetic model is used in the design equation. The heights calculated with the two models become closer when the system approaches the conditions of diffusion control. Experimental results confirm the applicability of the kinetic model over a wide range of conditions.

Acknowledgement

One of the authors (M. T. Saeed) wish to thank the Ministry of Science and Technology, Pakistan for provision of scholarship and CVCP of the Universities of the United Kingdom for providing an ORS award for partial remission of tuition fees.

NOMENCLATURE

a_c	Specific interfacial area	m^{-1}

a_o	Activity of DEHPA (based on dimer conc.)	$kmol/m^3$
C	Concentration	$kmol/m^3$
H	Contactor height	m
k_I	Chemical reaction rate constant for extraction based on interfacial area	m/s
k_I'	Chemical reaction rate constant for stripping based on interfacial area	m/s
K	Mass transfer coefficient	m/s
K_{E1}	Equilibrium constant for reaction 2	$kmol^{1/2}\ m^{3/2}$
K_{E2}	Equilibrium constant for reaction 3	–
L_d	Disperse phase volumetric flow rate per unit contactor cross–sectional area	m/s
R	Interfacial flux	$kmol/m^2s$

Subscripts

1	Inlet	f	Forward
2	Outlet	H	Hydrogen ion
a	Aqueous phase	i	Interfacial value
D	DEHPA	k	Kinetic model
eq	Equilibrium value	o	Organic phase
E	Equilibrium model	z	Zinc ion

REFERENCES

1. Murthy, C. V. R., Ph.D. Thesis, University of London, (1987)
2. Murthy, C. V. R. and Perez de Ortiz, E. S., ISEC (1986)
3. Ajawin, L. A., Perez de Ortiz, E. S. and Sawistowski, H., ISEC 80–112 (1980)
4. Ajawin, L. A., Demetriou, J., Perez de Ortiz, E. S., and Sawistowski, H., IChemE Symposium Series No. 88, 183 (1984)
5. Chapman, T. W., Caban, R. and Tunison, M. E., AIChE Symp. Series, No. 153, V. 71, 128 (175)
6. The NAG Library Imperial College
7. Angelo, J. B., Lightfoot, E. N., and Howard, D. W., AIChE J. 12, 751, (1966)
8. Garner, F. H., Foord, A., and Tayeban, M., J. Appl. Chem., 9, 315, (1959)

Solvent Extraction 1990, T. Sekine (Editor)

© 1992 Elsevier Science Publishers B.V. All rights reserved

OPERATION AND SIMULATION OF A LIQUID-LIQUID EXTRACTION COLUMN

H.HUFNAGL, E.BLASS, A.KIENLE
Lehrstuhl A für Verfahrenstechnik
Technische Universität München
Arcisstrasse 21, 8000 München 2, West-Germany

ABSTRACT

The dynamic behavior of a liquid-liquid extraction column influenced by disturbances was investigated experimentally. The results fueled the modelling of a dynamic simulation program, which provides a satisfactory calculation of the non steady-state behavior of the apparatus. The experimental and calculated results are discussed in an example.

1. INTRODUCTION

No one denies the importance of steady-state simulation programs for the design and calculation of process engineering apparati. The benefits of simulation programs are undoubted and, due to rapid advancing computer facilities, their importance is still increasing in industrial practice. However, sole knowledge on steady-state performance cannot solve all the problems encountered with design and calculation of chemical apparati or plants. During their operation the apparati are subject to various time dependent factors, i.e. incoming disturbances, start-up and shut-down processes, load modifications, etc.. For the solution of such problems, data on the dynamic behavior of the apparatus are required as foundation for the design calculations and control system synthesis. Best operability for a user is given by providing the data about the dynamic behavior in shape of a dynamic simulation program. Whereas in case of rectification columns sophisticated dynamic simulation programs already exist, only few publications devoted to the dynamic behavior of liquid-liquid extraction columns are known. However, today's demands for energy-saving separation procedures meet in liquid-liquid extraction separation processes a fine solution, but also application in biochemical engineering, metal-extraction or waste water treatment opens new promising possibilities.

2. PILOT PLANT

An agitated liquid-liquid extraction column was used for the experimental investigation on the dynamic behavior. Fig. 1 shows the pilot column (type Kühni, dk=150mm) together with its measurement technique. The experimental investigations were carried out with the material system toluene-acetone-water recommended by the EFCE.

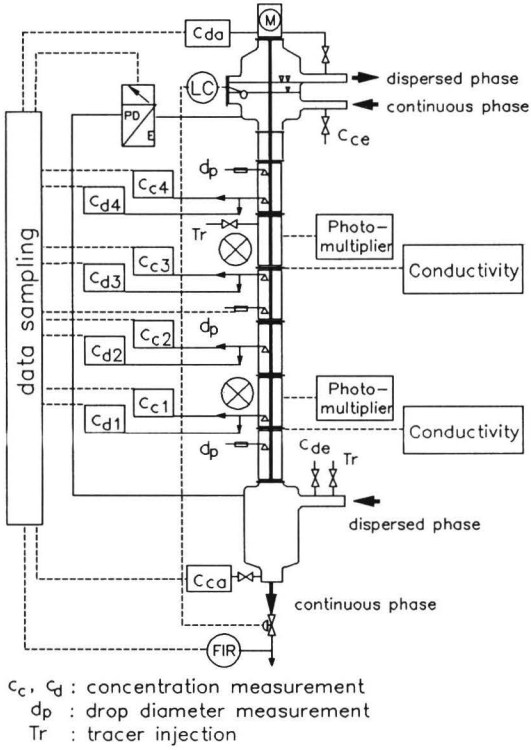

Fig. 1: Pilot pant and measuring technique

The transient responses of raffinate phase concentrations are measured cuntinuously at six different column heights. The probes in the active column section are numbered in ascending order. Additionally, all decisive fluiddynamic variables are recorded. Hold-up is measured by differential pressure, drop size with the aid of a photoelectric suction probe and distribution parameters with customary tracer-dispersion measurements.

3. EXPERIMENTAL MEASUREMENTS

For the experimental investigation of the dynamic behavior, the extractor first is operated at a steady-state operation point. Then the system is stimulated by feeding step changes to distinct input parameters. The resulting transitions of all decisive state variables are shown in Fig. 2 . The system was stimulated by a 40% step rise of the feed volumetric flow rate. The upper diagram lists the changes in raffinate concentrations, where Δc_c repre-

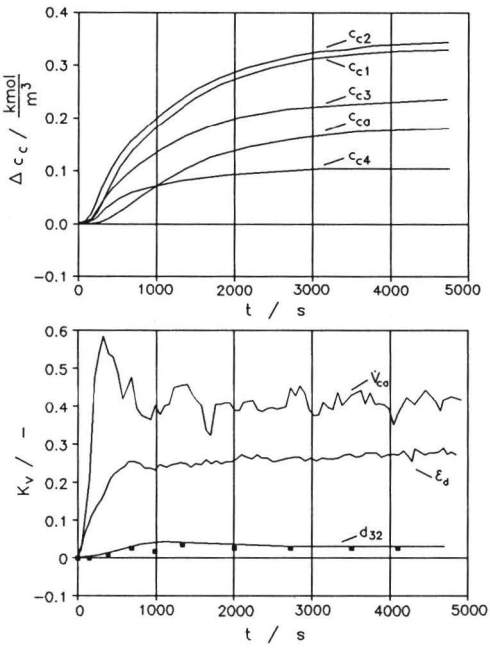

Fig. 2: Experimental dynamic behavior after a step change in feed flow rate of +40%

sents the difference between the actual value and the value right before the access of the disturbance. The curves are labelled in accordance to the specifications in Fig. 1.

The effects of the incoming disturbance can first be observed at the probes located at the bottom of the column c_{c1} and c_{c2}. The probes above succeed with increasing delay and decreasing amplitude. Due to the enclosed volume in the column's bottom chamber, the outcoming raffinate concentration c_{ca} shows a considerably higher dead-time and retardation compared to all other measuring points.

The diagram below lists the transitions of drop size, holdup and raffinate output flow rate in standardized, dimensionless form. While the considered disturbance only leads to a moderate increase of the mean drop diameter, the holdup manifests a more significant increase of about 27%. The behavior of the holdup proved to be the most sensitive hydrodynamic variable for all other experiments as well. The leaving raffinate flow rate is affected by the interface controller in the upper separation chamber. The increase of the holdup caused by the disturbance of the volumetric flow rate is compensated by an additional outflow of heavy phase to keep the interface at a constant level. Thus, the raffinate flow sways over the 40%-level, which will be held at the new steady-state operation point right after the access of the disturbance. The transitions of the hydrodynamic variables approach to their new steady-state after about 1000 sec. Hence, the

steady-state is obtained much earlier than in the concentration curves.

4. SIMULATION MODULE

The project's main objective was to develope a simulation module for the calculation of the dynamic behavior of the extraction column. The formulation of the process describing equations is based on the dispersion model as a physically, equation oriented model, which employs all experimentally investigated variables. The dispersion model offers several advantages. Various connections between input and output variables can be inspected, without having to change or modify the mathematical system. In addition, simulation calculations need not to be restricted to a closer neighbourhood of a steady-state operation point. A mass transfer balance of the transferred component at a differential column section leads to the following partial differential equations:

continuous phase:

$$\frac{dc_c}{dt} = \frac{v_c}{1-\varepsilon_d} \cdot \frac{\partial c_c}{\partial h} + D_{ax,c} \frac{\partial^2 c_c}{\partial h^2} - \beta_{od} \frac{a_e}{1-\varepsilon_d} (c_d^* - c_d)$$

dispersed phase:

$$\frac{dc_d}{dt} = - \frac{v_d}{\varepsilon_d} \cdot \frac{\partial c_d}{\partial h} + D_{ax,d} \frac{\partial^2 c_d}{\partial h^2} + \beta_{od} \frac{a_e}{\varepsilon_d} (c_d^* - c_d)$$

For the calculation of the hydrodynamic and mass transfer kinetic variables, which appear in this equations, further mathematical correlations are to be added. The variables were determined experimentally within a large operating range. Then, suitable correlations were chosen from the literature to fit the collected data best. Using mathematical correlations, which only describe the steady-state, in dynamic calculations is only applicable, if the fluiddynamic variables approach to their new steady-state much faster than the concentrations. According to Fig. 2 this assumption obviously is justified.

The volumes enclosed in the two separation chambers and in the tubes leadig to and from the chambers are taken into consi-

deration in the simulation by establishing dead-time or mixer elements in the simulation module. Hence these storage elements, which have quite an influence on the dynamic behavior, are taken into account as well.

Finally a comprehensive equation system of differential- and algebraic equations is obtained, which was combined to a simulation module. The simulation module was installed in the dynamic simulator DIVA, developed at the TU-Stuttgart with Prof. Gilles in charge. Various simulation runs were carried out, revealing generally good agreement beween calculation and experiment, but also indicating some characteristic deviations in some cases. One example is to be presented next.

5. SIMULATION RESULTS

Fig. 3 shows the simulated transient behavior of the state-variables discussed before. According to the application of steady-state correlations for the calculation of hydrodynamic variables, those manifest a steep ramp right after the access of the disturbance. In their further course, modifications due to a shift in the concentration profile occur. In our example, the increase of the feed volumetric flow rate leads to a rise in the concentration profile. The increase of the concentrations results in a drop of the interface tension, beeing the reason for a slight decrease of the drop size and thus increasing the holdup.

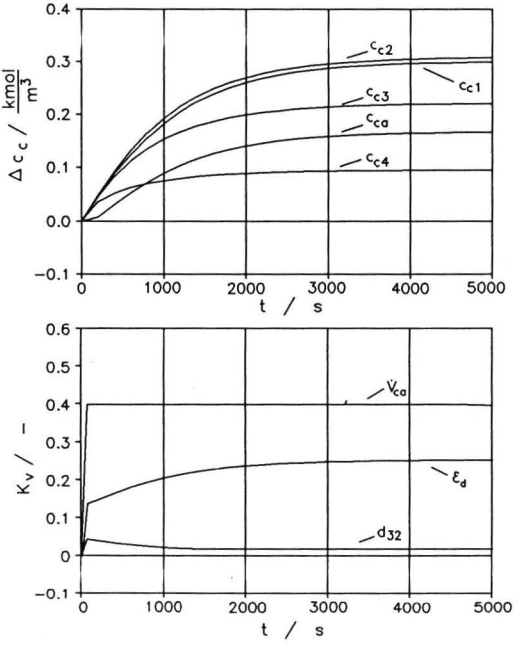

Fig. 3: Simulated dynamic behovior after a step change in feed flow rate of + 40%

On condition that the hydrodynamic varia-

bles change practically abruptly to their new values, the calculated concentration transients start without delay and with maximum slope. The real system (Fig. 2), however, shows a distinct dead-time and more retardation right after the access of the disturbance. Still, simulation and experiment agree well with each other; the concentration changes, which increase towards the bottom of the column, are correctly interpreted in the program. Slight deviations between the simulated and experimental steady-state values cannot be avoided due to the scattering of measured values.

6. SUMMARY

The dynamic behavior of a stirred liquid-liquid-extraction column was investigated experimentally. The results lead to the development of a dynamic simulation module based on the dispersion model for the calculation of the non steady-state performance of the apparatus. The result is, that despite of using steady-state relationships for the calculation of the hydrodynamic variables, simulation and experiment agree well with each other.

7. SYMBOLS

a_e	spezific mass transfer area	m^{-1}
c	concentration	$kmol/m^3$
d_{32}	Sauter mean diameter	m
D_{ax}	dispersion coefficient	m^2/s
h	height	m
t	time	s
v	superficial velosity	m/s
$\dot{V}_{ca}$	output raffinate flow rate	m^3/s
β_{od}	mass transfer coefficient	m/s
ε_d	dispersed phase holdup	

SUBSCRIPTS

c	continuous
d	dispersed

Solvent Extraction 1990, T. Sekine (Editor)

© 1992 Elsevier Science Publishers B.V. All rights reserved

AN APPLICATION OF EXPERT SYSTEM TECHNIQUES TO THE OPERATION OF SOLVENT EXTRACTION PROCESSES

A.L. MILLS and J.W. HARRISON
Process Services Division, AEA Fuel Services, Harwell Laboratory, Didcot, Oxon, OX11 ORA, (United Kingdom)

INTRODUCTION

The possibility of developing a computer based Expert System to assist operators in the control of liquid-liquid extraction plant and processes has been examined.

By considering possible process faults 1, 2, 3 or more at a time "consequence" tables may be developed which can then be used directly or in reverse to determine from a "consequence" the cause of a fault.

Certain multiple faults can cancel each other out and may not be apparent to an operator.

The present paper indicates the method to develop the Expert System.

EXPERT SYSTEM - BASIS

A number of assumptions have been made without which it is not possible to consider operating any plant or process:

(i) The plant and process are assumed to have been correctly designed and, given the correct skills both plant and process are operable.

(ii) The operators are trained and competent.

(iii) The process design has taken into account tolerances with respect to input feed flows and concentrations.

(iv) Suitable instrumentation is available and installed to detect 'fault' conditions.

(v) The operation of the total process is such that:-
"correct inputs + correct operating conditions = correct products (and waste streams)".

Using the plant layout shown in Figure 1 as a model and assuming the PUREX process with only ONE solute it is possible to define a series of 'what if' questions and to postulate the consequences of such questions. Table 1 lists a selection of such questions assuming that only one parameter at a time is at fault. It will also be seen from Table 1 that a single input parameter fault can sometimes have more than one consequence.

TABLE 1
Response of system to changes in input parameters considered one at a time

Input Parameter	Change from set value	Possible effect	Reason
Aqueous scrub flow	+	Loss of solutes to raffinates, fission product DFs increased	Pinch in scrub section
	−	Fission product DFs decreased	Insufficient/Inefficient scrubbing
Aqueous scrub acidity	+	Poor DF_{Zr}; improved DF_{Ru}	High acid favours DF_{Ru}
	+	Possible loss of solutes to aqueous raffinate	Change in extraction conditions below feed plate
	−	Poor DF_{Ru}; improved DF_{Zr}	Low acid favours DF_{Zr}
	−	Possible loss of solutes to aqueous raffinate	Change in extraction conditions below feed plate
Aqueous feed flow	+	Loss of solutes to aqueous raffinate, solvent product solute concentration high, fission product DFs high	S/A flow rate in extraction section low, incomplete extraction of solutes, high solvent loading
	+	Loss of throughput	Contactor flooding
	−	Low solute levels in aqueous raffinate, low solvent product loading, poor fission product DFs	S/A flow ratio in extraction section high, low solvent loading causes poor DFs
Aqueous feed acidity	+	Possible loss of solutes to aqueous raffinate	High acid has changed extraction conditions for solutes
	+	Poor DF_{Zr}; improved DF_{Ru}	High acid favours DF_{Ru}
	−	Possible loss of solutes to aqueous raffinate	Low acid has changed extraction conditions for solutes
	−	Poor DF_{Ru}; improved DF_{Zr}	Low acid favours DF_{Zr}
Solute (1) concentration	+	Loss of solute to aqueous raffinate, loss of other solutes to raffinate, improved fission product DFs	Solvent saturated with solute (1); other solutes displaced to aqueous raffinate
	−	Low solute levels in aqueous raffinates, low solvent product loading, poor fission product DFs	Required solvent product not attained due to insufficient solute
Solute (1) valence	incorrect	Loss of solute (1) to aqueous raffinate, low solvent product loading, poor fission product DFs	Incorrect valence for effective extraction
Organic phase flow	+	Solvent product concentration low, fission product DFs low, low solute levels in aqueous raffinate	S/A flow ratio in extraction and in scrub section high. Excess extractant present
	+	Loss of throughput	Contactor flooding
	−	High solvent product concentration, fission product DFs high, solute loss to aqueous raffinate	S/A flow ratio in extraction section low, insufficient extractant present
Extractant concentration	+	Fission product DFs low	Excess "free" extractant, low 'relative' solvent loading
	−	Fission product DFs high, solute loss to aqueous raffinate	High solvent saturation, insufficient extractant for extraction
Organic phase acidity	+	Unlikely to be any perceived effect unless extraction section requires all available stages for solute extraction	Stripping of acid occurs before extraction of solutes.
	−		Extraction of acid occurs before extraction of solutes.

Table 2 considers the situations where a single 'fault' can have multiple causes. A loss of solute to the aqueous raffinate in a two solute system can have at least 8 initiating causes and each initiating cause can have one or more other (or secondary) effect. The examples given could be extended to tertiary effects in some instances.

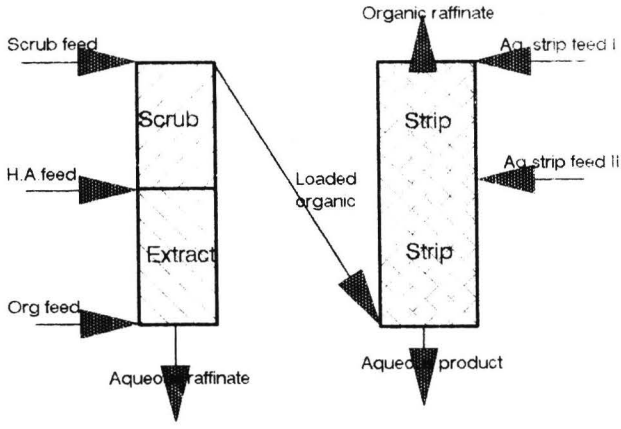

Fig 1 The process model

In indicating a possible cause related to an observed effect the operator needs to know the probability of such a cause. In the example given in Table 2 an examination of operating plant records shows that the possibility of the extractant concentration (TBP) being low and outside its tolerance limit is low but of the possible causes listed high HA feed acidity or solute concentration are the most likely errors.

However, and not shown in the table, an even more likely reason for the observed effect is that the HA feed acidity and solute concentrations are all high but within tolerance, the extractant concentration is low but within tolerance. The combination of these factors gives rise to the observed effect.

TABLE 2

Example of effects with possible multiple causes

Observed or primary effect	Possible cause	Other or secondary effects
DF(Zr) low & DF(Ru) high	Aq scrub H high? or Aq Feed H high?	Possible solute loss to raffs.
Loss of solute to Aq raff.	Aq scrub flow high? or	DF(FPs) high?
	HA feed flow high? or	DF(FPs) high; SP concs high
	HA feed acidity high? or	DF(Ru) high; DF(Zr) low?
	HA feed acidity low? or	DF(Zr) high; DF(Ru)low?
	HA feed solute 1 conc high?	DF(FPs) high?
	HA feed solute 2 conc high?	DF(FPs) high?
	Organic feed flow low? or	DF(FPs) high; SP concs high
	Extractant conc low?	DF(FPs) high?

This situation could arise if the process designer had not fully considered every possible combination of error and tolerance band limits.

It is now becoming clear that the operator could usefully be supplied with sets of operational tolerances relating to which and how many inputs are simultaneously at fault.

Table 3 presents a further sequence of faults which singly could have an observable effect on the process but in combination could cancel out such effects causing the process to give the correct product (and waste streams) but to operate at a non-standard throughput.

TABLE 3

Multiple errors which cancel each other out

Error*	Consequence
HA feed, solute 1 concn) high, and)	No effect observed in this contactor because the higher extractant flow and concentration results in an intolerance solute loading and acceptable decontamination factors.
HA feed, solute 2 concn) high, and)	
Extractant concn) high, and)	There could be incomplete stripping in the subsequent contactor.
Extractant flow high	

(*All items can be within their individual tolerance bands.)

An operator might find such a situation acceptable until one of the faults in combination is rectified or fails further or another fault occurs. In this latter case the operator now has three faults giving rise to a multiplicity of consequences the causes of which might only be obvious to a very experienced operator.

It is clear from the above that extensions to two or more simultaneous faults and their consequences are necessary to totally define all possible faults and the combination of faults.

Thus far the work has been purely qualitative. A fault has been identified and the cause of the fault has been sought. In order to correct the fault it would be necessary to recompute part or all of the process flowsheet and to reset the plant operating conditions.

In addition to considering the 'local' effect of a fault, any changes in flowsheet or operating parameters may have consequences for downstream or upstream processes, hence it will be necessary for the operator to consider the total effect of any proposed changes.

The flowsheet development computing suite REPROCX, Harrison et al (1986) may be used to examine flowsheet changes and their consequences. By using the appropriate REPROCX options such calculations may be made across the whole plant very rapidly.

THE EXPERT SYSTEM UNDER DEVELOPMENT

In considering the process model, Figure 1, it has been assumed that the flowsheet has been calculated by any suitable means, say by REPROCX and that all the input flows and compositions have appropriate tolerances. In this work column contactors are shown merely for convenience but the work relates to any contactor type.

Any contactor, mixer settler, pulse column or centrifugal contactor has certain operational parameters that have to be fulfilled and incorporated into the flowsheet calculation. During plant operation these parameters e.g. pulse amplitude and frequency if pulse columns are used, have to be monitored.

In the example based on Figure 1 it would be necessary to monitor the composition of the organic product from the extraction contactor for heavy metal loading, acidity and fission product content. The aqueous raffinate heavy metal loading and acidity is also required but if the example represents the highly active cycle, knowledge of the fission product content of this stream is of little value for plant control purposes.

The heavy metal content and acidity of both the aqueous product and the organic raffinate from the strip contactor and the volumes of all streams leaving a contactor are also required.

Because of volumetric hold-up in contactors and of variable transit time for transients or changes in input to a contactor to become manifest at the contactor output points, the monitoring of product (and raffinate) streams has to be such that the operator uses data integrated over periods of time related to the response time of the contactor.

The process is then started and monitored. The data in Tables 1 to 3 are then used to identify process faults.

Table 1 considers the response of the system to changes in input parameters considered one at a time. The table also gives the operator the reason why, if a change from set value occurs, a given response is obtained. The table has been extended, but this is not shown here, to indicate the action the operator should consider in order to rectify the "fault" assuming that the required initial flowsheet conditions cannot be restored. Such action would generally require a recomputation of the flowsheet for the contactor involved but the necessity of having to recompute all of the

downstream flowsheet must not be overlooked. An alternative course of action would be to recompute the upstream flowsheet such that this "new" flowsheet would "fit" the fault conditions. The application of Tables 2 and 3 is similar.

The speed with which REPROCX can handle a complete plant calculation is of use to the operator in such circumstances.

THE EXPERT SYSTEM SHELL

The data discussed above and presented as examples only in Tables 1, 2 and 3 are being expanded to cover all possible combination of 'faults' and consequences for the process shown in Figure 1.

These data have then to be programmed into a suitable 'Expert System' shell as a series of 'rules'.

At the present time no particular commercially available shell has been identified as being totally suitable, the requirements for the shell must include the following:

It must be simply programmed, preferably by inputting statements/rules in English and not in some form of computer language;

It must be possible for the user to expand and change the rules as experience with both the Expert System and the Process is gained;

The Expert System must be capable of accepting as input measurements from plant equipment, comparing these measurements with 'nett' values and also computing rates of change of input as functions of time. These inputs must then be available to indicate (in English) which parameters are incorrect and then the System should be self assessing in order to inform the operator of a fault and of the prognosis.

The operator should be able to access a computational system such as REPROCX via the Expert System in order to make flowsheet calculations. Having made such a calculation the operator then has to interrogate the Expert System to ask "what if" type questions.

Any shell should be available for use on a dedicated PC which can also act as a terminal to a main frame computer for the flowsheet calculations.

FUTURE WORK

In addition to the completion of the logic tables for multiple 'faults' an analysis of plant operating data is in progress in order to identify the frequency of a given fault so that a "weighting" can be given to faults listed in the Expert System.

REFERENCE

Harrison, J.W., Mills, A.L. and Wilkins, M., Proc. ISEC 1986.
REPROCX - A reprocessing flowsheet computational system.

Solvent Extraction 1990, T. Sekine (Editor)

© 1992 Elsevier Science Publishers B.V. All rights reserved

STUDIES ON DYNAMIC PROCESS OF THREE-OUTLET FRACTIONAL EXTRACTION IN FIVE-COMPONENT SYSTEM

Biao-Guo Li, Song Gao, Chun-Hua Yan, Hui Li, Guang-Xian Xu
Research Center of Rare Earth Chemistry, Peking University, Beijing 100871 (China)

1 INTRODUCTION

Most extraction systems for separating rare earths have two characters: the number of components is more than three or four and the separation factors between the neighboring components are rather small. Because of this, the number of stages necessary to obtain pure products is usually quite large. In order to establish a new extraction process, it will usually take a lot of time to do laboratory experiments and to run pilot plants before actual industrial production. Even though this tedious process is taken, the extraction process parameters are not optimized at all.

In recent years, a new method for treating the dynamic processes of three or four component extraction systems have been studied by Biao-Guo Li et al. (1985a,b) and Chun-hua Yan et al. (1989). Meanwhile, the three-outlet process, a novel method for separation of multi-component rare earths by cascade extraction technology, is advanced by Biao-Guo Li et al. (1985c). In order to simulate multi-component systems more naturally and get a new optimized extraction process in short time, a dynamic program has been established in this paper. This program is applicable to five-component three-outlet systems using saponified acid extractants such as D2EHPA, HEH(EHP), DBP, DOP, DDPA, OPPA, naphthenic acid, etc. It can simulate the so-called "funnel method" experiment of laboratory practice of the system from starting to steady state.

2 DESIGN OF THE PROGRAM

Based on the previous report (Biao-Guo Li et al., 1985a,b), a program has been designed as follows:

2.1 Input parameters:

KSW, KI, PKB, PKC, PKD, G,
FA, FB, FC, FD, BTAB, BTBC, BTCD, BTDE,
S, PANM, PBI, PC1, RA, RC, I, N, M

where KSW=selection of feed solution; KI=selection of position of the third outlet; PKB, PKC and PKD=selection of separation mode; G=ratio of the number of transfers to the number of

total stages which is the direct ratio time; FA, FB, FC, FD and FE=molar fraction of every component in the feed; BTAB, BTBC and BTCD, BTDE=separation factors; S=extractive amount when entered feed amount equals 1 molar; PANM, PBI and PC1=purities of three products; RA and RC=yields of A and C; I=the stage in which the third product is drawn; N=stage number of extraction section; M=stage number of stripping section.

2.2 Calculation parameters:

(a) Molar fractions of three outlets: FAP, FBP, FCP

when I<N,

$$FAP=FA\cdot RA/PANM \quad (1)$$

$$FBP=[FA+FC-FAP\cdot PANM-(1-FAP)\cdot PC1]/(1-PBI-PC1) \quad (2)$$

$$FCP=1-FAP-FBP \quad (3)$$

when I>N,

$$FCP=FC\cdot RC/PC1 \quad (4)$$

$$FBP=[PANM\cdot PC1+(PC1-PANM)\cdot FC\cdot RC-(1-FB)\cdot PC1]/(PC1\cdot(PANM+PBI-1)) \quad (5)$$

$$FAP=1-FBP-FCP \quad (6)$$

(b) Minimum extraction amount S_{min}

The formula for calculating S_{min} was reported by Biao-Guo Li et al.(1985c).

2.3 Extractor-filling mode

All stages of the extractor are filled with feed solution.

2.4 Simulation of establishment of cascade equilibrium

When the system reaches extraction cascade equilibrium, the fractions of each component in both aqueous and organic phases in every stage XA, ..., XE, YA, ..., YE must satisfy the following equations:

$$BTAB=(YA\cdot XB)/(YB\cdot XA) \quad (7)$$

$$BTBC=(YB\cdot XC)/(YC\cdot XB) \quad (8)$$

$$BTCD=(YC\cdot XD)/(YD\cdot XC) \quad (9)$$

$$BTDE=(YD\cdot XE)/(YE\cdot XD) \quad (10)$$

$$MA=XA+YA \quad (11)$$

$$MB=XB+YB \quad (12)$$

$$MC=XC+YC \quad (13)$$

$$MD=XD+YD \quad (14)$$

$$ME=XE+YE \quad (15)$$

$$M=XA+XB+XC+XD+XE$$

$$M=YA+YB+YC+YD+YE \quad (16)$$

The set of equations was solved by using Newton Method.

2.5 Simulation of mass balance

The basis for mass balance is that the amount of the feed added must equal the sum of the three products during the dynamic process.

2.6 Output information

The information can be given by computer as a function of G in the following aspects:

(a) The average accumulations of A, B, C, D and E.

$$DSW(X)=(\sum_{i}^{n+m} MX_i)/(N+M) \quad (X=A, ..., E) \tag{17}$$

where MX_i is the sum of the mass contents of the aqueous and the organic phases of X in the stage i.

(b) The mass balance degree of A, B, C, D and E.

The mass balance degree of component X is defined as:

DXY(X)=(the total outlet amount of component X)/(input amount of component X in the feed)

(c) The purities of extract, raffinate and the third outlet.

(d) The composition of each stage in both the aqueous and the organic phases at any moment during the dynamic process.

(e) The highest purity and its position of intermediate component B, C and D.

3 ILLUSTRATIVE EXAMPLE AND RESULTS

For a certain extraction separation system, the molfractions of each component in feed are: FA=0.130, FB=0.025, FC=0.350, FD=0.052, FE=0.443; the separation factors are: BTAB=2.00, BTBC=2.70, BTCD=1.50, BTDE=2.00; the required purities of three products are: PANM=0.999, PBI=0.60, PC1=0.999; the yield of component C, RC=0.999; separation mode is: EDC/B/A. The corresponding countercurrent extraction parameters are calculated as follows by another program which is applicable to design steady state parameters:

S=1.00, W=0.885, N=13, I=19, M=18

Using above extraction parameters, the computer simulation of the dynamic process was made.

Figure 1 to figure 6 show the results of calculation.

Figure 1 and 2 show the accumulation or drain of every component. From Fig. 1, component A and B trend towards accumulation while component C, D and E drain. The amount of intermediate component B is always more than that of at the beginning time. Figure 2 shows the variation of mass balance with G for each component, it also shows increase or decrease for each component during the dynamic process.

From Figure 3, it can be seen that the purities of extract and raffinate will not increase monotonously with the increase of G, and both purities will not reach the required purities at the same time.

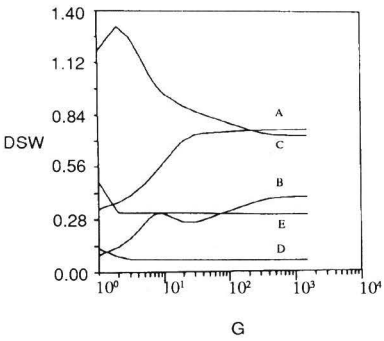

Fig.1 Variation of average accumulations of A, B, C, D and E with G

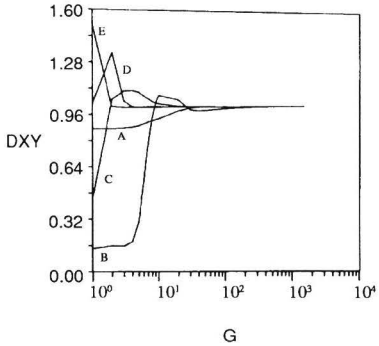

Fig.2 Mass balance degree as function of G

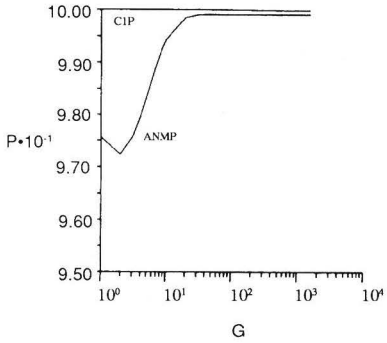

Fig.3 Purities of extract and raffinate as function of G

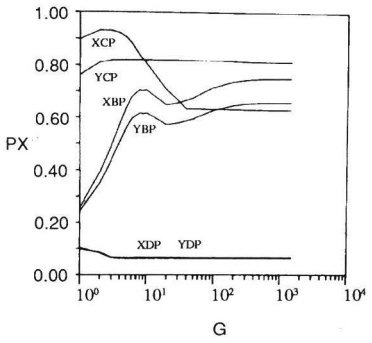

Fig.4 Highest purities of intermediate components as function of G

As shown in Figure 4, the highest purity of intermediate component B increases with the increase of G. Figure 5 shows big difference in composition of the third outlet stage between starting and steady state.

The stage-wise distribution of each component in the aqueous phase at the steady state is shown in Figure 6.

When G>500, the system is near the steady state of purity and mass distribution for each component. In a word, designed quality indexes are reached. This indicates that the parameters given by the steady state calculation program are suitable for the system.

Many extraction systems with various separation factors, feed compositions and different grades of purities and yields for three products have been designed and simulated by this program. Some of these have been verified in industrial scale, and the results obtained from industrial experiments are in satisfactory agreement with the calculations.

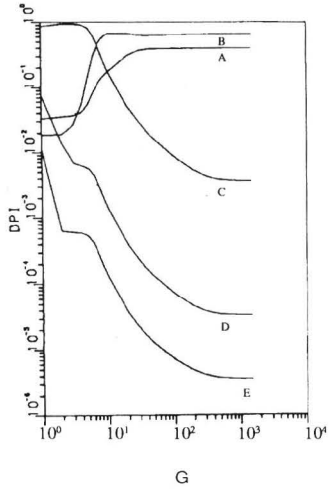

Fig.5 Variation of composition of the third outlet stage in aqueous with G

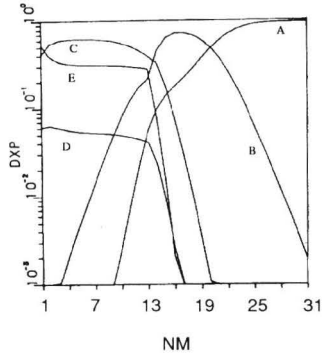

Fig 6. Distribution of each component in aqueous at steady state

4 REFERENCES

Biao-Guo Li, Jun-Ran Li, Chun-Hua Yan and Guang-Xian Xu, 1985, Rare Metals (China), 4(3), 17-23.

Biao-Guo Li, Chun-Hua Yan, Shu-Ping Qiao and Guang-Xian Xu, 1985, Journal of the Chinese Rare Earth Society, 3(3), 20-26.

Biao-Guo Li, Chun-Hua Yan, Shu-Ping Qiao and Guang-Xian Xu, 1985, Proceedings of the 1st National conference on Solvent Extraction (China), pp. 165, Beijing.

Chun-Hua Yan, Song Gao, Hui Li, Biao-Guo Li and Guang-Xian Xu, 1989, Proceedings of 2nd International Conference on Separations Science and Technology, pp. 553-556, Hamilton, Canada.

* Project Supported by National Science Foundation of China

Solvent Extraction 1990, T. Sekine (Editor)
© 1992 Elsevier Science Publishers B.V. All rights reserved

EXPERIMENTAL DETERMINATION OF THE RESIDENCE TIME DISTRIBUTION OF THE DROP PHASE IN A PULSED PERFORATED PLATE EXTRACTION COLUMN

H. SCHMIDT, M. PFEFF*, Th. PRÖLL*, U. MÜLLER
Kernforschungszentrum Karlsruhe, Institut für Reaktorbauelemente,
P.O. Box 36 40, 7500 Karlsruhe 1, FRG
*Universität Karlsruhe (TH), P.O. Box 69 80, 7500 Karlsruhe 1, FRG

ABSTRACT

The new approaches of two phase liquid-liquid column extractor modeling account for drop-drop interactions and local transport processes. This events are time oriented, and therefore the residence time distribution of the drop phase is of interest.

Experiments are being carried out with fluids of matched refractive indices. The parameters investigated are: the volumetric flow rates, the pulsation, the geometry and spacing of plates, and the physical properties of different material systems. The results of dimensional analysis show the residence time of drops of different size as a function of the dimensionless groups.

INTRODUCTION

The calculation of extractor length and apparatus scale-up in multistage liquid-liquid extractors has yet to be satisfactorily executed despite the fact that global models have been used.

In the last decade modeling of extraction columns has been initiated which accounts for the stochastic droplet interaction processes of breakage and coalescence, the liquid flow patterns, and the interphase mass transport [1,2,3]. These approaches attempt to calculate the drop population and the drop rate processes in each consecutive stage of the extractor. The drops which are present in a polydisperse form and their dispersion undergo entrance, exit, breakage and coalescence events which are drop size and time oriented (Fig. 1). Hence for the numerical execution of the simulation process the dispersed phase residence time distributions are required for the calculation of the drop rate events.

Very recently, results of a Monte Carlo simulation technique were reported for a continuous flow stirred column contactor [4]. The results of the simulation which accounts for the drop processes mentioned above showed good agreement with the experimental holdup and drop size profiles. There are different approaches in modeling the drop rate processes in reciprocating column extractors. For example the velocity of drops in a vibrating plate column extractor is derived from the terminal rise velocity of drops in a stagnant continuous phase [5]. Whereas the authors in [6] use the characteristic drop velocity correlation of [7] to calculate the drop rate processes in a pulsed-

plate extraction column, and in [8] the slip velocity correlation of [9] is applied to split the velocity of drops into different size classes.

In this work the residence time behavior of individual drops of distinct drop sizes is investigated under variation of the influencing parameters s.a. physical properties, operational and geometric parameters in order to put the calculation of drop rate processes on a more reliable basis.

EXPERIMENTS

The experiments are carried out in a pulsed perforated plate extraction column. The length of the cartridge is 1400 mm the inner tube diameter is 38 mm (Fig. 2). The perforated plates are of stainless steel with cylindrical holes in the aqueous phase continuous mode of operation. In the organic phase continuous, aqueous phase dispersed mode of operation the cartridge is PTFE-coated, to meet the condition of good wettability of the plates by the continuous phase and repel of the drop phase.

The two fluids are part of the reciprocating countercurrent flow and are mutually saturated and of matched refractive indices. Hence, it is not possible to distinguish between drop- and continuous phase. Colored drops are added into the system through an immersed capillary tube. These variable sized drops are distinguishable in the presence of the other drops and their motion is recorded on video tape (Fig. 3). The physical properties of the material systems used in the experiments are shown in Table 1 and the governing parameters investigated are listed in Table 2.

RESULTS

The drop size distributions as a function of the governing parameters are determined from photographs using a semi-automatic optical particle analyzer and an IBM computer scan. For this purpose the material systems are shifted out of the matched refractive index mode by a slight decrease of the Glycerine concentration in the aqueous phase. No noticeable change in the physical properties is observed.

A typical result obtained under these conditions is shown in Fig. 4. The range of the drop diameter observed reaches from drops smaller than 0.1 mm to drops of close to 2 mm in diameter. The maximum number density is found to be in the small drop diameter range whereas medium sized and large sized drops significantly contribute to the volume density. This indicates the minor importance of the small drops on the transportation processes, and as a result of this leads to the classification into three drop size classes for which the residence time behavior is investigated. In the cases of extended drop size ranges caused by altered operation conditions a fourth large scale drop size class is added to be investigated.

The dispersed phase holdup ε is determined by the use of the sampling and phase separation technique. Fig. 5 illustrates the local holdup as a function of the total throughput in dependence of the tractional free area of plates, and the mode of operation. It is clearly seen that there exists a strong dependence of the holdup on the

total flux, the flow rate ratio, and the mode of operation, and only a minor influence on the geometry of plates. In Fig. 6 the influence of the pulsation and the material systems are presented and show a strong dependency on the pulsation energy (A·f) put into the system and on the physical properties, mainly in the densities of the fluids being involved.

Both entities, drop size and holdup of the dispersed phase are important for the understanding and the interpretation of the results of the drop residence time measurements. The definition for the measured variable: residence time t_j is given in Fig. 7, showing also the micro and macro scale eddies being part of the general flow pattern of the drop phase in a schematic scale. The mean residence time of drops of a certain size class d_j is obtained from video tape recordings by taking a minimum of 20 single individual drops d_i into account, and more typically upwards of 50.

The figures 8,9, and 10 show actual values of t_j in number and their variations with the parameters under investigation. The main general results are as follows:

- the mean residence time of drops strongly depends on the drop size;
- the volumetric flow rates, the pulsation, and the physical properties of the fluids are of significant influence;
- the mean residence time of drops depends on the geometry of the plates to a minor extent.

EVALUATION

The experimental findings are subjected to a dimensional analysis by applying the Buckingham π-Theorem. With the three basic units: mass, length, and time, and by taking the physical properties, geometric parameters, operational variables, and inner parameters into account the following set of dimensionless groups is obtained.

$$t_j\,\omega = f\left(Re;\, We;\, Ar,\, Str;\, E\ddot{o};\, \frac{\dot{V}_d}{\dot{V}_c};\, \frac{h_R}{A};\, \frac{\Delta\mu}{\mu_c}\right) \tag{1}$$

in which each of the numbers Re and We are combinations of two π-numbers.

The functional relationship between the experimental findings and the dimensionless groups results in a correlation equation for the residence time t_j of drop size class j:

$$t_j = \frac{A^{1,21}\,\omega^{3,03}\,\dot{V}_c^{1,36}\,\rho_c^{0,54}\,\mu_c^{0,18}\,\sigma^{1,1}\,d_0^{7,77}}{d_j^{5,52}\,\dot{V}_d^{3,01}\,\Delta\rho^{1,18}\,\Delta\mu^{0,64}\,g^{2,06}\,h_R^{1,17}} \tag{2}$$

The reliability of the correlation is good for the set of results obtained with constant pulse stroke (A = 15 mm) and fixed plate spacing (h_R = 50 mm). The mean error band width for small sized drops is ± 9%, for medium size ± 5,6%, and for large drops ± 15%. Taking all experimental data sets into account the deviations are located within the ± 30% margin, in some few cases however exceeding this margin.

A test of the t_j values can be obtained by comparing the experimental results on holdup and calculated holdup results. The calculation is based on the experimentally determined volume density distribution and the residence time distribution of drops. In Fig. 11 the calculated holdup is plotted against the holdup determined by sampling. The plot is divided into the three operational flow regimes experimentally investigated: mixer-setter -, dispersion -, and unstable mode of operation. The results reasonably fit a ± 30% error band, plotted in dashed lines. The deviations in the mixer-setter regime could be explained by a measuring fault of the sampling technique, due to the strong inhomogenity of the dispersed and continuous phase characterizing this mode of operation.

SUMMARY

The results obtained show a complex correlation for the residence time of drops as a function of the governing parameters. The two inner parameters drop size and drop residence time are linked together; the resulting entity is the holdup.

The drop size distribution is strongly influenced by the material system and the energy input. The drop residence time is governed by the operational and geometric variables.

This investigation indicates that simple correlations derived from the unhindered motion of rising drops will not lead to satisfactory results. To overcome this situation additional experimental investigations are required to account for the actual physical events.

SYMBOLS:

A	pulse stroke; pulsation amplitude
V	volume
$\dot{V}$	volume flow rate
d	diameter
$d_0 = \frac{d_p}{\varepsilon_p}$	specific diameter of holes
f	frequency
g	gravity
h	height
t	time
Δ	difference
ε	holdup; fractional free area
μ	viscosity
ρ	density
σ	interfacial tension
ω	$= 2\pi f$

Subscripts

c	continuous phase
d	dispersed phase
j	size class
t	total
P	plate
R	compartment

DIMENSIONLESS GROUPS:

$$Re = \frac{A\omega d_0 \rho_c}{\mu_c}$$ Reynolds number

$$We = \frac{(A\omega)^2 \rho_c d_j}{\sigma}$$ Weber number

$$Ar = \frac{\rho_c \Delta\rho g d_j^3}{\mu^2}$$ Archimedes number

$$Str = \frac{\omega d_0^3}{\dot{V}_d}$$ Strouhal number

$$Eö = \frac{\rho_c g d_j^2}{\sigma}$$ Eötvös number

REFERENCES

[1] Bapat, P.M., Tavlarides, L.L., Smith, G.W., 1983. Chem. Eng. Science, Vol. 88, Nr. 12, pp. 2003-2013.

[2] Cruz-Pinto, J.J.C., Korchinsky, W.J., 1980. Chem.Eng. Science, Vo. 35, p. 2213

[3] Casamatta, G., 1981. Thesis, L'Institut National Polytechnique de Toulose.

[4] Tsouris, C., Ferreira, R., C.C. Tavlarides., Can. J. of Chem. Eng. (to be published).

[5] Sovová, H., 1983. Chem. Eng. Science, Vol. 38, No. 11, pp 1863-1872

[6] Garg, M.O., Pratt, H.R.C., 1984. AIChE Journal, Vol. 30, No. 3.

[7] Thornton, J.D., 1957. Trans. Inst. Chem. Eng., 35, p. 316

[8] Laso, M., Steiner, L., Hartland,S., 1984. 8th Int. Congress of Chem. Engineering, Chem. Equipment, Design and Automation (CHISA), Praha, CSFR.

[9] Kumar, A., Vohra, D.K., Hartland, S., 1980. Can. J. Chem. Engng., No. 58, pp. 154-159

TABLES

Table 1:

Material System I:
organic phase: 28 % vol. TBP / 72 % vol. n-Heptane
aqueous phase: 45 % vol. 0,5 m HNO_3 / 55 % vol. Glycerol

Material System II:
organic phase: Silicone
aqueous phase: 40,6 % vol. dem H_2O / 4,5 % vol. HNO_3 / 54,9 % vol.Glycerol

	Material System I		Material System II	
T = 20° mutually saturated	organic phase	aqueous phase	organic phase	aqueous phase
Density, kg/l	0,765	1,127	0,9167	1,134
Viscosity, 10^{-3} Pa x s	0,895	4,89	5	4,89
Difference in Density, kg/l	0,362		0,221	
Difference in Viscosity, 10^{-3} Pa x s	3,995		0,11	
Interfacial Tension, 10^{-3} N/m	10,04		32,7	
Refractive Index	1,396		1,396	

Table 2:

Parameters Investigated:

throughput:	- volumetric flow rate $\dot{V}_c$, $\dot{V}_d$, - flow rate ratio $\dot{V}_d/\dot{V}_c$
pulsation:	- frequency of pulsation f, - pulse stroke A
cartridge:	- fractional free area of plates ε_p by variation of the hole diameter d_p - spacing of plates h_R
mode of operation:	- aqueous phase continuous/organic phase dispersed mode - organic phase continuous/aqueous phase dispersed mode
material system:	- large differences in density and viscosity, System I - small differences in density and viscosity, System II

FIGURES

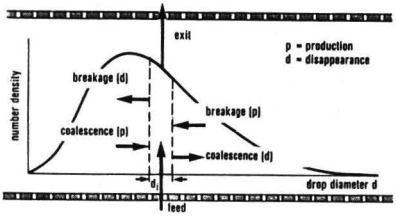

Fig. 1 Balance about a Drop Size Class d_j

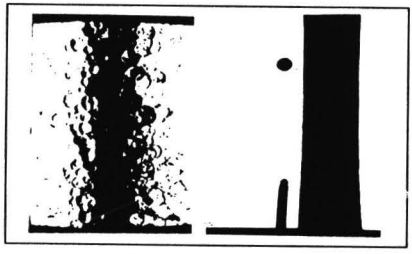

Fig. 3 Fluids of Non Matched and Matched Refractive Indices

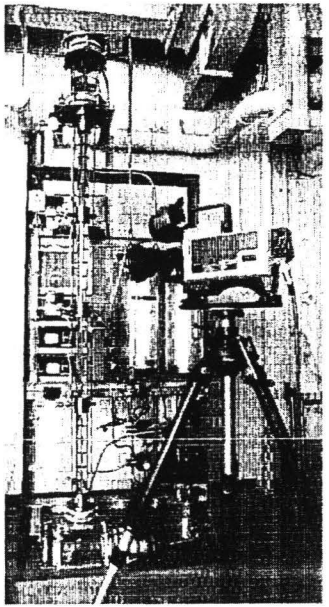

Fig. 2 Experimental Setup

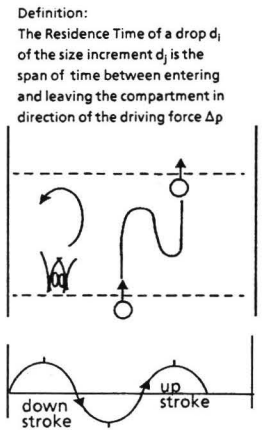

Fig. 7 Definition and Basic Flow Patterns

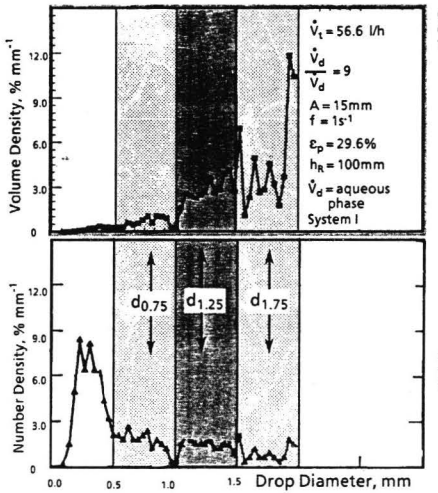

Fig. 4 Drop Density Distribution

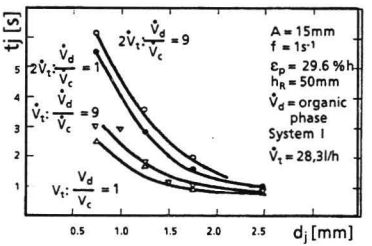

Fig. 8 $t_j = f$ (volumetric flow rates, flow rate ratio)

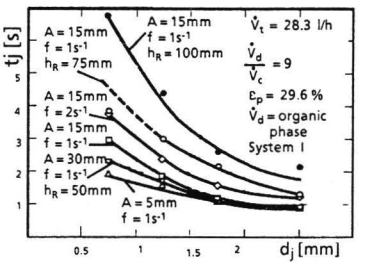

Fig. 9 $t_j = f$ (pulsation, plate spacing)

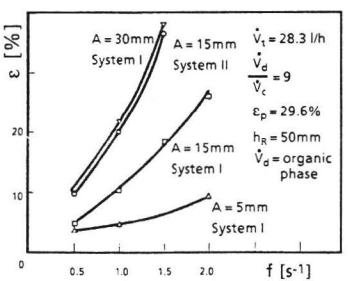

Fig. 6 ε = f (pulsation, material system)

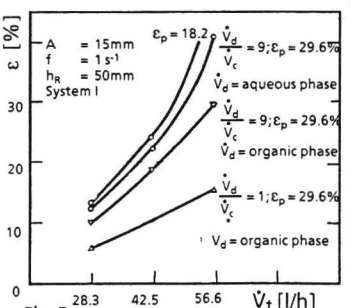

Fig. 5
ε = f (volumetric flow rates, fractional free area of plates, mode of operation)

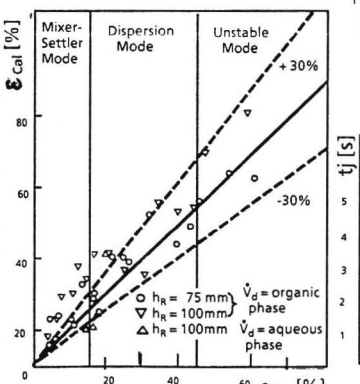

Fig. 11 Comparison of Measured and Calculated Holdup

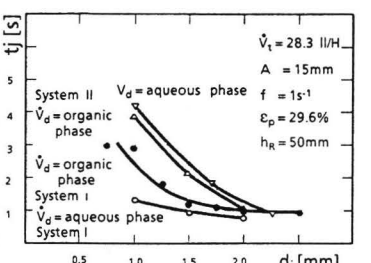

Fig. 10 $t_j = f$ (material system, mode of operation)

Solvent Extraction 1990, T. Sekine (Editor)

© 1992 Elsevier Science Publishers B.V. All rights reserved

MASS TRANSFER AND DROP SIZE IN LIQUID-LIQUID CU EXTRACTION WITH LIX 84N IN MOTIONLESS MIXERS

D. WOLF, A. SEMBIRA AND J.C. MERCHUK
Department of Chemical Engineering, Ben Gurion University of the Negev,
Beer-Sheva, Israel

ABSTRACT

Data of drop size and mass transfer in the extraction of Cu from an aqueous solution into a solution of LIX 84N in kerosene for several lengths of motionless mixers of the Sulzer type SMV-4 and 3/4" diameter is presented. Previous data obtained with same static mixers and other types of mixers will also be presented for background and comparison purposes.

INTRODUCTION AND CHARACTERISTICS OF MOTIONLESS MIXERS

Conventional mixer-settlers require large amounts of solvent and ground areas mainly caused by the generation of small droplets by the impeller blade and thus slow separation of phases. The use of motionless mixers in lieu of mixers-settlers provides an interesting alternative.

The experimental system used for the study of the static mixer characteristics and performance is found elsewhere (Sembira et al. 1986). Data obtained with the Koch mixer of 10 mixing elements and an agitated vessel show that the increase in flow rates increases significantly the efficiency for the Koch mixer while for the mixing vessel the efficiency decreases (Merchuk et al. 1980a). Thus at high flow rates, the motionless mixer would be superior from the efficiency point of view. Also, the residence time in the motionless mixer is two orders of magnitude smaller than that in the stirred vessel and thus great savings are achieved in solvent inventory and ground area. Calculations showed that the energy input is about the same for both devices at practical operating conditions.

It was also found that the efficiency of extraction with motionless mixers could be correlated with the energy input into the system, measured as pressure drop. Diagrams of the dispersion bands for the Koch type motionless mixers vs. flow rates for concentrations of LIX 64N of 5% and 10% and for an organic to aqueous phase ratio of 1:1, 2.5:1 and 4:1 were presented by Merchuk et al. (1980b). They showed that the velocity of the liquid flowing through the motionless mixer determines the characteristics of the dispersion rather than the residence time in the mixer. The difference between the extraction efficiencies and settling times obtained with phase ratios O/A of 1:1 and 2.5:1, confirmed the importance of whether the organic or the aqueous phase is continuous (Merchuk et al., 1980a,b).

A comparison was made between the settling process for organic and aqueous

continuous dispersions, where data of dispersion band height versus time are presented for the same flow rates, LIX 64N concentrations (10%), and phase ratio 1:1 for a 10 mixing unit Koch motionless mixer and for a tube 18.5 cm long packed with polypropylene saddles. The profiles of dispersion are straight lines, implying that the settling velocity of a given dispersion is independent of the height. Data published on dispersions generated in conventional mixers (Paynter et al., 1970) show an exponential type profile that may be attributed to a wide range of drop sizes. The straight profiles obtained with static mixers may be attributed to a narrow range of drop sizes, and this concurs with the experimental findings of Middleman (1974) and Streiff (1977). The above results indicate the importance of drop size and phase inversion phenomena.

DROP SIZE AND DROP SIZE DISTRIBUTION

For the study of drop size an electro-resistivity method was developed and described by Sembira et al. (1986), based on the technique used by Neal and Bankoft (1963). A mathematical analysis of the measuring system allowed to express the local dispersed-phase hold-up ϕ which is equal to C_w and the Sauter mean diameter D_{32} as:

$$D_{32} = 1.5((C_w \cdot V)/C_N) \tag{1}$$

where: C_w = the cumulative pulse width per unit time, C_N = the numer of pulses per unit time, and V = linear velocity of the dispersion.

The results obtained for water/kerosene with Sulzer motionless mixers of the type SMV-4 and 3/4" diameter of stainless steel and teflon coated internals with 14 mixing elements lead to the following correlations within the intervals of Reynolds number and Weber number at the appropriate powers: (Sembira et al., 1986).

$$0.9 > We^{-0.5}\, Re^{0.15} > 0.35 \tag{2}$$

For mixing elements made of SS316:

$$D_{32}/d_h = 0.047 + 0.197\, We^{-0.5}\, Re^{0.15} \tag{3}$$

and for Teflon-coated mixing elements:

$$D_{32}/d_h = -0.3 + 0.91\, We^{-0.5}\, Re^{0.15} \tag{4}$$

For water/kerosene with $CuSO_4$ in the aqueous phase and with LIX 84N in the organic phase the correlation for teflon was found to be:

$$D_{32}/d_h = -0.08 + 0.44\, We^{-0.5}\, Re^{0.15} \tag{5}$$

where d_h = hydraulic diameter of mixer.

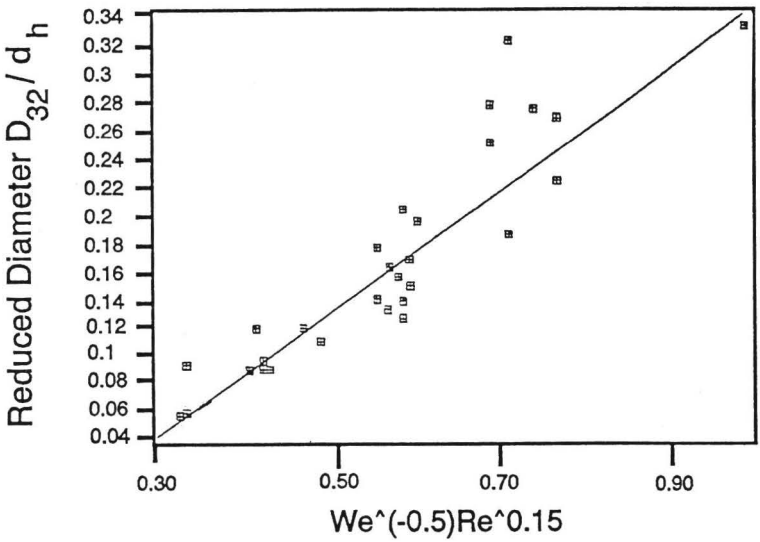

Fig. 1. Reduced drop diameter obtained for both 5 and 8 teflon coated Sulzer static mixer elements and with Lit 84N in the kerosene phase.

The correlation given in Equation 5 and shown on Figure 1 for 5 and 8 mixing elements is in-between the two correlations, Equations 3 and 4.

Another way of presenting the data is of drop diameters versus the average velocity of the fluid in the mixer calculated as the flow rate divided by the cross section for flow. The cross section area is taking into account the porosity which is 87%. The droplet diameter decreases almost exponentionally with increase of fluid velocity. Analyzing these results one can deduce that in addition to the material, the length of the static mixer and the surface tension of the fluids affect the droplets diameter. The correlations obtained for the drop size can be used for the determination of the K_{Lw} in the range of the experimental results obtained.

Drop size diameters measured from photographs showed that at high liquid velocities the drop size distribution is normal (Sembira et al. 1986). Also, the higher the velocity of the dispersion, the narrower the spectrum of drop sizes obtained. This is parallel to the findings reported by Luhning and Sawistowski (1971). In their case which was a stirred vessel, the velocity of agitation is the variable which corresponds to the fluid velocity in a static mixer.

The Sauter mean diameter obtained here is close to the results reported by Streiff (1977) as long as stainless-steel internals are used. The results indicate that at low flow rates of the dispersion, the mechanism of drop coalescence and dispersion is affected strongly by the nature of the surface of the mixing elements.

PHASE INVERSION

The effect of the hydrophobicity of the surface elements led to the study of the phenomenon of phase inversion in motionless mixers by Tidhar et al. (1986) as some of the experimental results could be explained on this basis. Different mixing elements gave different results as obtained when ϕ is plotted versus the velocity V.

A thermodynamic analysis of the system before and after phase inversion, assuming that the total energy of the system does not change, allowed the derivation of the following general expression for the organic volumetric fraction at phase inversion conditions:

$$\phi = 0.5 + C\, We^{-0.5}\, Re^{0.15}(d_h a)\cos\theta \qquad (6)$$

where a = motionless mixer area per unit volume, C = constant, θ = contact angle, and ϕ = organic phase volume fraction.

Experimental data for three different liquid-liquid systems, and internal surface of stainless steel and Teflon were published by Tidhar et al. (1986). These experiments led to the important observations as described in the conclusions of their paper.

EFFICIENCIES OF EXTRACTION BY SULZER TYPE STATIC MIXERS

As part of the characterization of the Sulzer static mixers we studied the effect of flow rates, organic to aqueous phase ratio and length of static mixer on the efficiency of extraction of Cu from aqueous solutions by LIX 84N in kerosene. LIX 84N is the trade name for 2-hydroxy-5-nonylacetophenone oxime. Like other extraction reagents from the LIX family, LIX 84N forms with the Cu cation a water insoluble complex as per the following equation:

$$2\, RH_{org} + Cu^{2+}_{ag} \rightleftharpoons R_2Cu_{org} + 2H^{+}_{ag} \qquad (7)$$

The concentration of Cu in the water was 2 gr/lit and the LIX 84N was 5% in the kerosene. The length of the static mixer was changed by adding modular elements of packing. The concentrations of Cu were measured by a Spectrophotometer. The efficiency was calculated in the usual way as follows:

$$E_t = [(C_o - C)/(C_o - C_e)]\, x\ 100 \qquad (8)$$

where C_o = initial concentration of Cu, C = concentration of Cu at exit of mixer and C_e = equilibrium concentration of Cu.

First, the effect of flow rate and length of static mixer on the efficiency was studied. Efficiencies of extraction of Cu by LIX 84N in kerosene as a function of total flow rate of aqueous and organic phases is given in Figure 2 for an O/A ratio of 2:1. One can see that the efficiencies increase with increase of total flow rates. This is probably since the increases

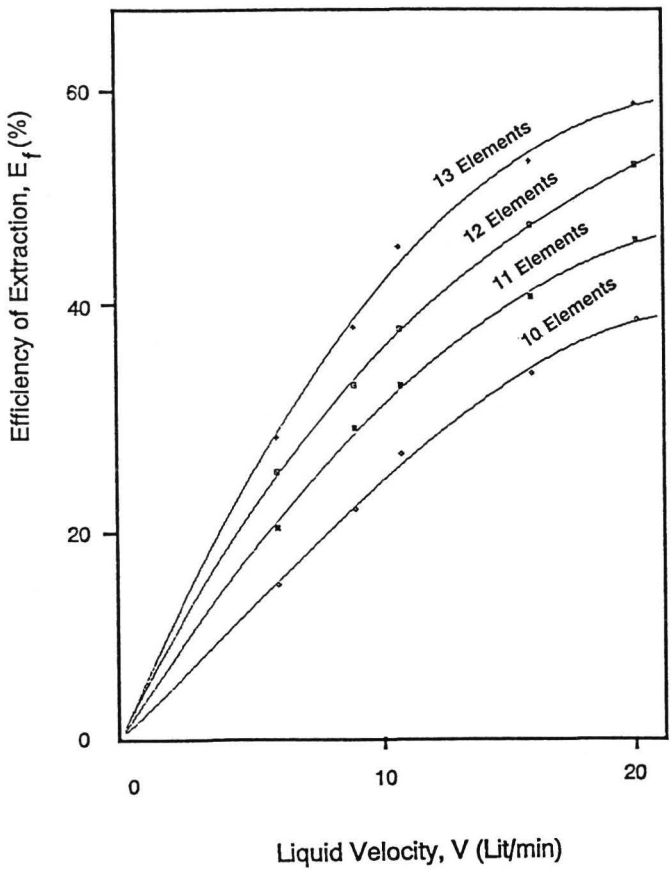

Fig. 2. Efficiency of extraction versus liquid velocity in teflon coated Sulzer static mixer elements and O/A ratio of 2:1.

in flow rate increases the dispersion of the two phases. The increase in the efficiency eventually levels off as the flow rate reaches levels of maximum dispersion. The transition from laminar flow to turbulent flow is around a flow rate of 12 lit/min. On Figure 2 one can also see that an increase in length of the static mixer increases the efficiency due to increased dispersion obtained. Experiments with O/A ratio of 1:1 and several other O/A ratios gave similar results and also a higher O/A ratio gives higher efficiencies. This can be explained by our previous work, where we found that at O/A ratios of 1:1 the continuous phase was always the aqueous phase while at a ratio of O/A of 2:1 the organic phase was continuous

until around 8 mixing elements and only afterwards there was a phase change to the aqueous phase as the continuous one. Thus, it appears that there is better mass transfer when the aqueous phase is the continuous phase.

One additional objective was to obtain values of the mass-transfer coefficient K_L for the static mixers studied. Due to the non-linearity of the equilibrium data between the aqueous phase and the organic phase of the concentration of Cu and due to the different average diameter of the droplets obtained under the operating conditions of these experiments the exact calculations of the K_L could not be ready for this presentation. However, approximate values were calculated using the correlations obtained for the system kerosene/water (Sembira et al. 1986) and assuming linearity of the equilibrium data. These data will be reported as soon as exact equilibrium data is available and applied in the calculations.

CONCLUSION

From our studies on static mixers we can conclude that the static mixer is an important unit operation in the liquid-liquid extraction process and has interesting characteristics. So far we have studied the aspects of dispersion, phase change, mass transfer rates and efficiencies of extraction. The experimental results proved that additional work on the performance of static mixers is warranted and is indeed being continued.

ACKNOWLEDGEMENT

The help of the following students in the experimental work is gratefully acknowledged: S. Lasri, D. Dzvili, H. Stinmarder, I. Fistiner and A. Mezamer-Tov.

References

Luhning, R.W., and Sawistowski, H., 1971, I.S.E.C., Session 5A, Paper 136-51.
Merchuk, J.C., Shai, R., and Wolf, D., 1980a, Ind. Eng. Chem. Proc. Des. Dev., 19, 91.
Merchuk, J.C., Wolf, D., Shai, R., and White, D.H., 1980b, Ind. Eng. Chem. Proc. Des. Dev., 19, 522.
Middleman, S., 1974, Ind. Engng. Chem. Proc. Des. Dev., 13, 78.
Neal, L.G., and Bankoff, S.G., 1973, A.I.Ch.E., 9, 490.
Paynter, J.C., Tunkey, T.K., and Birch, C.P., 1970, National Inst. Metallurgy, Johannesburg, S.A. Research Report 940.
Sembira, A., Merchuk, J.C., and Wolf, D., 1986, Chem. Eng. Sci., 41, 445.
Sembira, A., Merchuk, J.C. and Wolf, D., 1988, Chem. Eng. Sci., 43, 373.
Streiff, F., 1977, Sulzer Techn. Rev., 3, 108.
Tidhar, M., Merchuk, J.C., Sembira, A., and Wolf, D., 1986, Chem. Eng. Sci., 41, 457.

9. EQUIPMENT AND EQUIPMENT DESIGN

Solvent Extraction 1990, T. Sekine (Editor)

© 1992 Elsevier Science Publishers B.V. All rights reserved

CONTACTING AND SEPARATION EQUIPMENT - THE ELECTRICAL ALTERNATIVE

P. J. BAILES
Department of Chemical Engineering, University of Bradford, Bradford, West Yorks., BD7 1DP, UK

ABSTRACT

Present understanding of the way in which electric fields can be used to improve equipment performance is based upon a few fundamental observations. Thus, drops forming in an electric field are subject to additional forces that can result in drop rupture or the formation of smaller than usual drops. Conversely, when in close proximity to each other, or with the bulk interface, drops can be made to coalesce very rapidly in the presence of an electric field. In other circumstances drops may be accelerated through the continuous phase whilst exhibiting vigorous internal circulation and enhanced mass transfer rates. These observations either singly or combined have formed the foundation for several recent investigations which are reviewed. An essential precondition that must be satisfied before electric fields can be properly applied is that the continuous phase liquid must be electrically insulating in character. This ensures that sufficient field may be established to have the desired effect on the dispersed phase, which must be relatively conducting.

The technology is appropriate for breaking emulsion liquid membranes, hydrometallurgical solvent extraction of metals and crude oil dehydration and desalting.

INTRODUCTION

Solvent extraction involves the intimate contact of two immiscible or partially miscible liquids and their subsequent separation. The first process, if it is to be efficient, requires large numbers of drops to be created; the second process requires the recombination of drops to form a separated bulk liquid. Designers of solvent extraction equipment strive to achieve high rates of drop break-up and coalescence to maximise mass transfer performance. The wide variety of equipment that is available today bears testimony to the different approaches that have been adopted. Almost without exception these designs rely on improvements brought about by mechanical means. However, this situation is now beginning to change as increasing attention is focussed on the direct use of electric fields as a means of securing better performance in certain applications.

There are two areas of application where electric fields are uniquely effective. One concerns crude oil dehydration, the other refers to the splitting of liquid membrane emulsions. In both cases the use of electrically augmented phase separation offers definite commercial and environmental benefits over competing technology. In particular, successful commercial exploitation of electric fields as a means of

promoting the removal of the multitude of stable micro-droplets of brine present in crude oil reaching the well-head, has been in progress for most of this century. This experience is undoubtedly an important precursor to wider acceptance of the role that electric fields can play in chemical engineering unit operations, not least solvent extraction.

Developments within the oil industry are leading to an increasing need for off-shore production platforms where there are enormous savings to be made by improving the performance and thereby reducing the size and weight of platform separation equipment; there are also great incentives to move towards automated procedures. Increasingly the industry is having to cope with emulsions where the crude oil is both exceptionally viscous and has a density close to that of water (e.g. Eocene oils). This combination of factors makes gravity separation very slow and as such can greatly increase the size of separator needed for a given flow of oil. As oil fields go through their productive life the water content of the emulsion produced at the well-head increases dramatically. The outcome may be an emulsion containing 60% water that must be treated on an off-shore rig to give oil containing at most 2% water and possibly a good deal less, depending upon pipeline requirements.

These changing demands are sure to impinge on the design of oil field electric treaters in a way that is of interest to the designers of solvent extraction equipment for reasons that will now be considered.

CRUDE OIL DEHYDRATION AND LIQUID MEMBRANE EMULSION SPLITTING

Crude oil dehydration is not a solvent extraction operation but both processes have in common, a requirement for liquid phase separation. The fact that crude oil operations involve rather stable water-in-oil emulsions at elevated temperatures was considered, in the past, sufficient reason to differentiate between the two processes as far as phase separation equipment was concerned. However, by embracing liquid membrane emulsion technology, the subject of solvent extraction has at the same time, expanded to include an interest in breaking stable water-in-oil emulsions, this being essential in order to recover the internal phase. The stabilising surface active agents are natural in origin in the case of crude oil, and deliberately introduced in the liquid membrane process. In either event, the result is that the natural rate of phase disengagement is far too slow and must be accelerated to give equipment of acceptable size. Thus, the relative positions of solvent extraction and crude oil dehydration with regard to their phase separation requirements has changed. They are now closer together. Further evidence for this is seen in the trend towards higher water content crude oil emulsions and the fact that

liquid membrane emulsions also contain substantial water fractions.

Chemical demulsifiers have a role in crude oil dehydration but their use does represent a cost to the process and there are environmental consequences. In contrast, the addition of a demulsifier to break a water-in-oil liquid membrane emulsion is prohibited, because subsequent extractions depend upon the ability to re-create a stable membrane emulsion using the organic phase recycled from the separator. The presence of any demulsifier at this stage would obviously have a destabilising effect. It seems certain therefore, if liquid membrane technology is to form the basis of continuous processes designed to clean up aqueous effluent streams, and if crude oil production from off-shore and sub-sea locations is to expand, that there will be a demand for non-invasive, non-polluting, emulsion breaking technology that can cope with high water content emulsions. Within these constraints, the use of electric fields offers a bright prospect particularly as new methods of avoiding short-circuiting problems between the electrodes when treating water-rich emulsions, are now available.

ELECTRICALLY AUGMENTED PHASE SEPARATION

Practical evidence obtained with crude oil/water separations has shown that almost any type of high voltage field will promote to some extent the separation of water-in-oil emulsions. The mechanisms whereby this can occur are not clearly understood except, that if a large potential gradient can be established and maintained in the continuous phase of a liquid-liquid emulsion, it causes very fine drops to grow by coalescence with each other to a point where they fall out of the continuous phase under the action of gravity. The technique is specific for water-in-oil emulsions rather than the inverse, since it requires the continous phase to be relatively insulating in character.

F. G. Cottrell, who is much more famous for his pioneering work on gas cleaning by electrostatic precipitation, was granted the first patents on the process of electrical coalescence (Cottrell, 1911; Cottrell and Speed, 1911); although the subject had been studied much earlier (Rayleigh, 1879). It was believed by Cottrell and several other early workers that drops in the presence of either DC or AC fields grew in size as a result of chain formation and coalescence. Thus Cottrell and Speed (1911) observed that when a high voltage was applied between two fine wire electrodes immersed in a thin layer of emulsion spread on a microscope slide, the water drops formed chains extending from one electrode to the other. Coalescence of adjacent globules in each chain followed and the drops nearest the electrodes became larger as new drops were acquired by the chain. Cottrell

was of the opinion that under the influence of AC fields, charged water drops would also vibrate and thereby rupture the enveloping oil films to the benefit of the coalescence process. Certainly it has become the preferred practice in crude oil dehydrators to use two electrodes within the emulsion, one being electrically earthed, the other being AC energised.

Gradually it became apparent that in addition to chain formation there were several other electrical effects which might prevail under certain circumstances. Waterman (1965) used the term "electrofining" to encompass all the known mechanisms for coalescence in DC fields. It involved electrophoresis, DC induced dipole coalescence, random collision of oppositely charged drops moving in opposite directions, and collisions due to differences in velocity of movement of different sized drops in the same direction. Systems exemplifying electrofining invariably had an oil phase of very low electrical conductivity such as kerosene or gas condensate, and a very low hold-up of dispersed phase. The various mechanisms have provided a basis for the theoretical work of others and each mechanism has been substantiated by experiment as may be seen from Table 1.

Factors such as form and magnitude of electric field, fractional volumetric hold-up of dispersed phase, electrode geometry, and electrode insulation, determine which mechanism will dominate. This realisation has led to an astonishing number of patents, many of which represent simple variations on the basic theme. In order to illustrate the manner in which progress has been made, the salient points arising in a selection of patents from the past sixty years or so, are given in Table 2. The driving force underlying most of this work was the desire to circumvent current leakage so that high potential gradients could be employed even with wet emulsions. The nature of this difficulty is well described in a paper by Hsu and Li (1985). Essentially the problem arises if a single chain of water drops happens to extend from one electrode to the other or if, for any other reason, a very low resistance path should develop between the electrodes. As a result of this, current can flow freely between the electrodes, sparking often occurs, and unless the emulsion is relatively dry (e.g. < 1% water) or the applied voltage is limited, this causes a total loss of the coalescing force between the electrodes. It is this castastrophic effect upon coalescence that is of so much concern in the drive to devise current limiting designs, rather than the more obvious benefit of reduced power consumption. In recent years there has been an upsurge of interest in electrode insulation as a means of preventing this collapse of the electric field over the entire electrode and in different forms its use is now being proposed for crude oil desalting applications

TABLE 1

Charged drop coalescence - mechanisms and models

Mechanism	Model/Experimental Verification
Random collision	Sjoblem and Goren, 1966; Prestridge, 1973; Sadek and Hendricks, 1974
Induced-dipole coalescence	Waterman, 1965; Williams and Bailey, 1983; Yamaguchi *et al*, 1985, 1987
Electrophoresis	Seibert and Brady, 1919; Waterman, 1965; Turner, 1967
Pearl chaining	Pearce, 1954; Taylor, 1986; Ise *et al*, 1989

TABLE 2

A selection of electrical coalescence patents in chronological order

Year	Inventor(s)	Patented innovation
1926	de Brey	Pulsating DC fields of high voltage, bare metal electrodes
1936	Dillon	Pulsating AC fields with a capacitor in the external circuit, bare metal electrodes
1936	Heinrich	Unidirectional voltage pulses of 10 μs or less with a maximum mark:space ratio of 1:10; bare metal electrodes
1944	Wolfe	Pulsating AC fields or very high frequency AC with a dielectric layer interposed between the two electrodes and a number of capacitors in the external circuit
1945	Deutsch	Pulsating DC with a bare metal energised electrode and an insulation coating on the earthed electrode
1958	Stenzel	Emulsion treating by uniform AC fields followed by pulsed DC (half wave rectified AC) to give two electric treating zones; bare metal electrodes
1973	Prestridge	Emulsion treated first by AC then by fluctuating unidirectional field using only one power source to generate both fields
1977	Richards and Clark	AC field applied by insulation coated high voltage electrode
1986	Bailes and Larkai	Pulsed DC applied by insulation coated high voltage electrode

(Bailes and Larkai, 1984; Prestridge and Johnson, 1987, 1989).

The great advantage of using a high voltage electrode that is completely coated in a layer of insulating material, is that the insulation layer localises the ill-effects of any short-circuit caused by the mass of conducting drops. Thus the field is automatically almost fully sustained in the event that a local conducting path occurs. The disadvantage is that the insulation coating serves to raise the level of the applied voltage required to produce the same effective field in the emulsion. The essence of the problem may be seen by representing the system as a two layer condenser as shown in Figure 1.

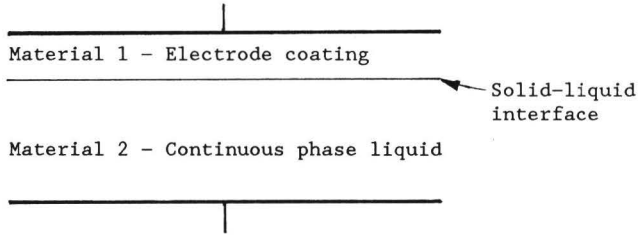

Figure 1 Two layer condenser

In such a system the field distribution that immediately follows the sudden application of a DC field is governed by the electrostatic requirement of equal dielectric displacement (surface charge density) in the two layers, thus:

$$D_1 = D_2 \quad \text{or} \quad E_1/E_2 = \epsilon_2/\epsilon_1 \tag{1}$$

Thereafter there appears a surface charge at the interface and hence a discontinuity in the dielectric displacement such that ultimately the relation between the fields in the two layers is dictated by the requirement for conduction current continuity, that is:

$$E_1/E_2 = \kappa_2/\kappa_1 \tag{2}$$

Typical values for the relative permittivities and electrical conductivities would be as follows:

$$\epsilon_1 = 3.5,\ \epsilon_2 = 1.32 \text{ and } \kappa_1 = 3.16 \times 10^{-13},\ \kappa_2 = 4.00 \times 10^{-9} \text{ S m}^{-1}$$

thus, initially, $E_1/E_2 = 0.38$ and finally, $E_1/E_2 = 1.27 \times 10^4$.
It is immediately apparent that resetting to the initial condition

maximises the field in the oil layer. This is the reason why pulsed DC is so effective when used with an insulation coating on the high voltage electrode. It also explains why continuous DC does not promote very much coalescence when used with insulation coated electrodes, a fact that has been reported by others (Richards and Clark, 1977).

The benefit of using high voltage pulsed DC in conjunction with a thin coating of insulating material on the high voltage electrode, may be seen in Figure 2. The ability of the system to continue operating even though the gap between the electrodes may be bridged by water is clearly evident from Figure 2b where both electrodes dip into the same water. Figure 2a depicts the dispersion with no electric field applied; Figure 2b shows the effect of applying a pulsed high voltage field between the high voltage electrode, which comprises a thin-walled plastic tube filled with electrolyte in contact with the curved HV supply wire, and an earthed metal rod. It is apparent that the field causes ripples at the bulk liquid interface and drop size increases through coalescence as the dispersion flows down between the electrodes.

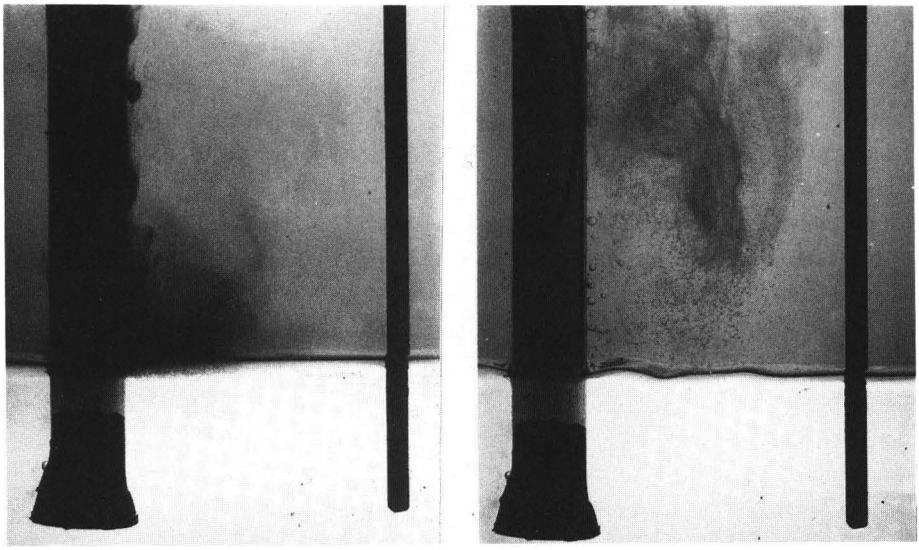

(a) (b)

Figure 2 (a) Normal coalescence (b) Electrostatic coalescence

Experimental work (Bailes and Larkai, 1982) has shown in practice that the use of pulsed DC and insulation coated electrodes does not always cause an increase in coalescence as the pulsation frequency is increased. There is invariably an optimum pulsation frequency at which coalescence is maximised. A variety of causes for this has been identified, thus: the electrostatic coalescer is an element in the RC of an electrical circuit and when a pulsed voltage is applied it responds accordingly (Joos and Snaddon, 1985); the achievable polarisation of the organic molecules present in the continuous phase has an influence and makes it desirable to break different emulsions with differing electric fields (Hautermann *et al*, 1989); and the relative permittivity of the emulsion is a function of its water content and it affects the frequency response of the system (Sherman, 1968).

For ease of photography, Figure 2 refers to a solvent extraction system in which water is dispersed in an organic phase of Acorga P5100 diluted with kerosene. This is not an emulsion and is not very challenging as far as phase separation is concerned. However, it should be noted that experience has shown pulsed DC to be very effective with liquid membrane emulsions (Kataoka and Nishiki, 1986; Yan *et al*, 1987). Several investigators have reported the use of AC fields with insulation coating (Hsu *et al*, 1983; Fujinawa *et al*, 1984; Hano *et al*, 1988; Feng *et al*, 1988; Goto *et al*, 1989; Hauertmann *et al*, 1989). Not surprisingly, in view of equation (1) it is found that the use of AC fields also affords a means of developing a field in the emulsion when there is an intervening layer of insulation. Interestingly, these workers report that there is an advantage in stirring the emulsion during the electrical treatment.

An alternative to fixing the nature of the electrode insulation and finding the pulsation frequency at which the effective field is a maximum, is to keep the applied voltage constant and change the electrode coating. Hsu, Li and Hucal (1983), test a number of different insulation coatings on this basis and conclude that, in order to get best results with liquid membrane emulsions, the coating should be hydrophobic and have a relative permittivity of at least three and preferably greater. This finding is again in keeping with expectations based upon equation (1).

Phase separation applications for electric fields in solvent extraction are, of course, not limited to liquid membrane processes. There is ample evidence that electric fields can be used to advantage in conventional hydrometallurgical solvent extractions. This is particularly true where stagewise equipment is used. Here it is necessary to repeatedly separate the two liquid phases and the gravity settlers must be designed to

give a holding time in keeping with the rate of phase disengagement. Consequently, for systems that are naturally slow to separate, large settlers are required and liquid inventories are proportionately increased. By comparison with liquid membrane emulsions, solvent extraction dispersions are unstable and separate easily, nevertheless phase separation rates can be greatly improved by the use of electric fields. For example, field tests at Ranchers' Bluebird copper mine in Arizona have shown that electrostatic coalescence vessels can be used at ten times the liquid loading rates of conventional separators (Warren *et al*, 1978). Similar tests at the United Nuclear Church Rock Mill in the US have shown for amine extraction of uranium, electrostatic coalescer operation at six times the conventional loading rate (Prestridge *et al*, 1983). The speed with which electrostatic coalescence can occur in solvent extraction dispersions is indicated in Figure 3.

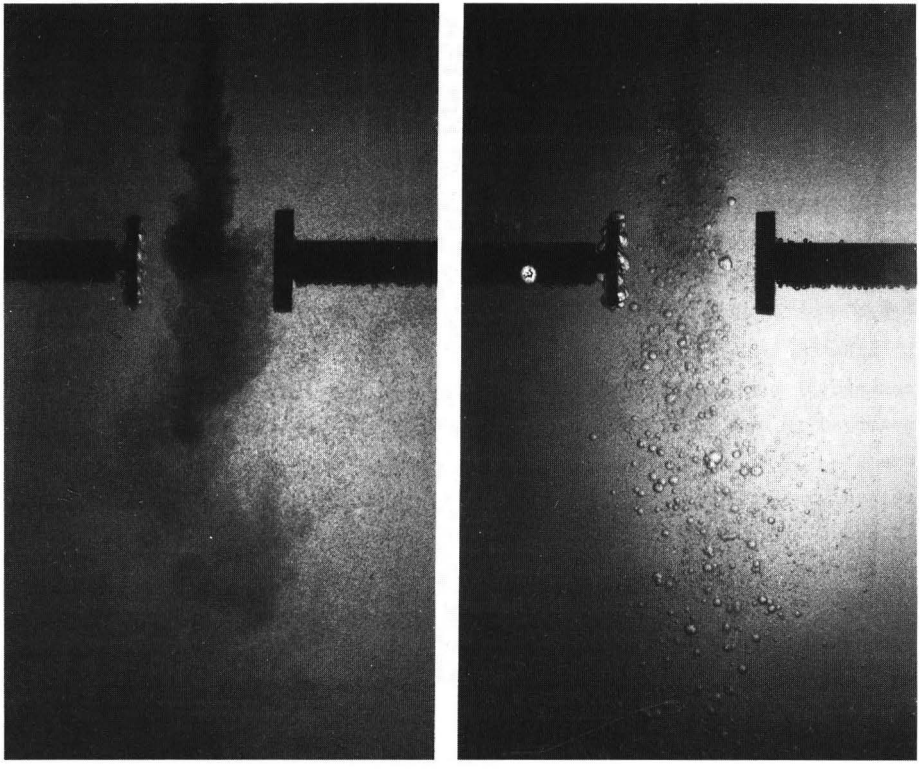

(a) (b)

Figure 3 The effect of an electric field on a flow of dispersion

A dispersion of water drops in LIX 64N diluted with kerosene is shown passing between parallel electrodes 3.3 cm apart. Figure 3a depicts the situation with no electric field applied to the jet of dispersion. Figure 3b shows what happens when a DC voltage of 4 kV pulsed at 10 Hz, is applied to the PTFE coated right-hand electrode of the pair, with the bare netal left-hand electrode earthed.

ELECTRICALLY AUGMENTED LIQUID CONTACTING

It is well recognised that inter-drop coalescence is a factor in liquid-liquid contacting operations, insofar as it occurs in the mixing process as part of the drop coalescence-redispersion cycle. This leads to the idea that electrically enhanced coalescence can be used to improve mixing performance. A counter-current liquid-liquid extraction column designed to allow simultaneous use of high voltage fields and high shear mixing, to promote coalescence and redispersion respectively has been tested in the laboratory (Bailes and Stitt, 1987). Measurements, with cumene transferring from kerosene into a dispersed phase which was composed of a 50/50 mixture of N-methyl pyrrolidone and ethylene glycol, reveal substantial improvements in mass transfer rates are possible by matching increases in impeller speed and applied voltage to create more intense coalescence-redispersion cycles.

The concept of liquid-liquid contacting by means of vigorous mechanical agitation, balanced by electrostatic coalescence, is one which can be put into practical form so that high hold-up dispersions are just as readily dealt with as dilute mixtures. This is not true of many other ideas for augmenting mass transfer by the use of electric fields. The problem so often facing the equipment designer is how to reproduce on a commercial scale with realistic throughputs, the mass transfer enhancement observed in the laboratory with single drops or a dilute dispersion. For example, it is known that single drops formed at a metal nozzle, which is raised to a high potential, detach prematurely carrying a free charge (Stewart and Thornton, 1967; Takamatsu *et al*, 1982). These drops can be accelerated in the presence of a DC field through an insulating immiscible organic liquid and as a result of the increased turbulence within and around the drops they exhibit enhanced mass transfer performance (Bailes and Thornton, 1971; Chang and Berg, 1985; Vu and Carleson, 1986). Attempts to employ this knowledge in a practical contactor have been dogged by the difficulty of reproducing the single drop behaviour in a situation where there are numerous nozzles and a respectable hold-up of charged drops. Inherent problems of space charge between the electrodes, drop screening

effects and electrical tracking down the walls and along aqueous filled pipes, all pose difficulties that remain to be solved. Meanwhile, in the laboratory, work with single charged drops continues to give useful results. Thus, Weatherley describes the electrical enhancement of microencapsulation reactions (Murray and Weatherley, 1989) and reports on the extraction of ethanol from charged drops of fermentation liquor (Laughland *et al*, 1987).

The formation of single charged drops or indeed a spray of charged drops does not have to be accomplished at a nozzle. It is feasible to disperse a conducting liquid directly into an insulating liquid from the plane interface between the two bulk phases by means of a DC field perpendicular to the interface. Yoshida *et al*, 1988, have developed a novel inclined plate contactor based upon this idea but again there seems to be a problem in getting sufficient hold-up fraction of the drops formed.

A number of different electrically augmented liquid-liquid contactors have been designed around the simple gravity spray column. Yamaguchi *et al* (1988) report tests on a spray column with four vertical rod electrodes arranged equidistant from each other on the inner wall of a column made from acrylic resin. DC energisation in this case causes coalescence, redispersion and motion of the drops in such a way that mass transfer is significantly enhanced, although the dispersed phase hold-up fraction is somewhat disappointing. The authors attribute this to the weak electric field at the core of the column not producing the requisite redispersion. In contrast, Warren and Prestridge (1979, 1980) deliberately ensure in their column design (see Figure 4) that the dispersed phase is first exposed to a very high potential gradient, which causes drop break-up, and subsequently to a lower field strength, which promotes drop coalescence.

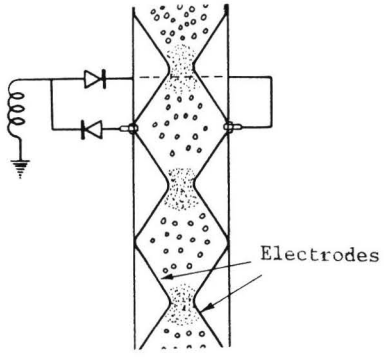

Figure 4 Extraction column with electrically induced droplet break-up and coalescence

The electrodes are shown as being energised by means by Prestridge's dual polarity circuit (Prestridge, 1973, 1974). Also feasible is the application of AC to one electrode with the other at earth potential. The drawback with the design is that when sufficient voltage is applied to the electrodes to cause satisfactory mixing, the polar fluids accumulate within the mixing zone, ultimately forming a conductive path, which allows arcing or short-circuiting to occur between the electrodes. One answer to this problem is to modulate the strength of the electric field so that time is provided for coalesced polar drops to gravitate from the mixing zone. Prestridge and Johnson (1986) describe this approach and show the advantage of a modified multistage device in the context of crude oil desalting but it is equally applicable to solvent extraction applications.

CONCLUSIONS

It is clear from the foregoing, that there is considerable interest in the application of electric fields to enhance rates of liquid phase separation in solvent extraction and emulsion liquid membrane processes. In these applications, and in the area of crude oil dehydration, there is a demand for new electrical technology to cope with high water content emulsions. Also foreseen are developments in mixing by means of electric fields, which could lead to novel forms of liquid-liquid contactor.

NOMENCLATURE

D electric displacment

E electric field intensity

ϵ relative permittivity

κ electrical conductivity

REFERENCES

Bailes, P. J. and Thornton, J. D., 1971. Proceedings Int. Solvent Extr. Conf., 2:1431.

Bailes, P. J. and Larkai, S. K. L., 1982. Trans. I.Chem.E., 60:(2) 115.

Bailes, P. J. and Larkai, S. K. L., 1984. Chem. Eng. Res. Des., 62:(1) 33.

Bailes, P. J. and Larkai, S. K. L., 1986. US Patent 4 601 834, July.

Bailes, P. J. and Stitt, E. H., 1987. Chem. Eng. Res. Des., 65:(11),514.

Chang, L. S. and Berg, J. C., 1985. A.I.Ch.E. Journal, 31:(1), 149.

Cottrell, F. G., 1911. US Patent 987 114, March.

Cottrell, F. G. and Speed, J. B., 1911. US Patent 987 115, March.

de Brey, J. H. C., 1926. US Patent 1 570 209, January.

Deutsch, W., 1945. US Patent 2 382 697, August.

Dillon, L., 1936. US Patent 2 038 479, April.

Feng, Z., Wang, X. and Zhang, X. *et al*, 1988. Water Treatment, 3:320.

Fujinawa, K., Morishita, M., Hozawa, M., Imaishi, N. and Ino, H., 1984. J. Chem. Eng. Japan, 17:(6), 632.

Goto, M., Irie, J., Kondo, K. and Nakashio, F., 1989.
J. Chem. Eng. Japan, 22:(4), 401.
Hano, T., Ohtake, T. and Takagi, K., 1988.
J. Chem. Eng. Japan, 21:(4), 345.
Hauertmann, H.B., Degener, W. and Schügerl, K., 1989.
Separation Science and Technology, 24:(3 & 4), 253.
Heinrich, R., 1936. US Patent 2 000 018, May.
Hsu, E. C. and Li, N. N., 1985. Separation Science and Technology,
20: (2 & 3), 115.
Hsu, E. C., Li, N. N. and Hucal, T., 1983. US Patent 4 415 426,
November.
Ise, T., Yamaguchi, M. and Katayama, T., 1989.
Kagaku Kogaku Ronbunshu, 15:(6), 1087.
Joos, F. M. and Snaddon, R. W. L., 1985. Chem. Eng. Res. Des.,
63:(9), 305.
Kataoka, T. and Nishiki, T., 1986. J. Chem. Eng. Japan, 12:16.
Laughland, G. J., Millar, M. K. and Weatherley, L. R., 1987.
I.Chem.E Symposium Series No. 103, 263.
Murray, K. R. and Weatherley, L. R., 1989. Personal communication.
Pearce, C. A. R., 1954. Brit. J. of Appl. Phys., 5: (April), 136.
Prestridge, F. L., 1973. US Patent 3 772 180, November.
Prestridge, F. L., 1974. US Patent 3 847 775, November.
Prestridge, F. L. and Johnson, C., 1986. US Patent 4 606 801, August.
Prestridge, F. L., Johnson, B.C. and Sublette, K. L., 1983
Transactions of Society of Mining Engineers at AIME, 274: 1959.
Rayleigh Lord, 1879. Proc. Roy. Soc., A28, 406.
Richards, K. J. and Clark, D. R., 1977. US Patent 4 039 404, August.
Sadek, S. E. and Hendricks, C. D., 1974. Ind. Eng. Chem. Fund.,
13:(2), 139.
Seibert, F. M. and Brady, J. D., 1919. US Patent 1 290 369, January.
Sherman, P., 1968. Emulsion Science. Academic Press, London and
New York
Sjobolm, G. L. and Goren, S. L., 1966. Ind. Eng. Chem. Fund.,
5:(4), 519.
Stenzel, R. W., 1958. US Patent 2 855 356, October
Takamatsu, T., Yamaguchi, M. and Katayama, T., 1982.
J. Chem. Eng. Japan, 15:(5), 349.
Taylor, S. E., 1986. AIChE Spring National Meeting, New Orleans,
6-10 April, Paper No. 93C.
Turner, D. W., 1967. US Patent 3 342 720.
Vu, N. and Carleson, T.E., 1986. A.I.Ch.E. Journal, 32:(10), 1739.
Warren, K. W. and Prestridge, F. L., 1979. US Patent 4 161 439, July.
Warren, K. W. and Prestridge, F. L., 1980. US Patent 4 204 934, May.
Warren, K. W., Prestridge, F. L. and Sinclair, B. A., 1978.
Mining Engineering, 30:(4), 355.
Waterman, L. C., 1965. Chem. Eng. Progress, 61: 10, 51.
Williams, T. J. and Bailey, A. G., 1983. Proceedings of Electrostatics
1983, (Oxford), Inst. Phys. Conf. Ser. No. 66, 39.
Wolfe, K. M., 1944. US Patent 2 364 118.
Yamaguchi, M., Kobayashi, A. and Katayama, T., 1985.
Kagaku Kogaku Ronbunshu, 11:599.
Yamaguchi, M., Sugaya, H. and Katayama, T., 1988.
J. Chem. Eng. Japan, 21:(2), 179.
Yamaguchi, M., Kobayashi, A., Ohbori, K. and Katayama, T., 1987.
International Chemical Engineering 27:(3), 506.
Yan, Z., Li, S., Yu, Y. and Zhang, X., 1987. Desalination, 62:323.
Yoshida, F., Yamaguchi, M. and Katayama, T., 1988.
J. Chem. Eng. Japan, 21:(2), 123.

Solvent Extraction 1990, T. Sekine (Editor)

© 1992 Elsevier Science Publishers B.V. All rights reserved

MULTIPLE UPCOMER AROMATICS EXTRACTION TRAYS

M. R. RESETARITS and K. YONEYAMA
UOP, P.O. Box 44, Tonawanda, New York 14150 (USA) and
UOP, Toranomon Mori Bldg. No. 45, 1-5, Toranomon
5-Chome, Minato-Ku, Tokyo 105 (Japan)

ABSTRACT

Liquid-liquid extraction has historically been the preferred route for the recovery of aromatics from a C_6-C_8 hydrocarbon stream. UOP's Sulfolane, TETRA, and CAROM processes have been popular choices of many petrochemical companies. Each of these processes employs a different extractive solvent. None require agitation in the liquid-liquid contactor. The TETRA and CAROM processes have often employed UOP Multiple Upcomer (MU) Trays in that contactor.

UOP MU Trays are similar in many ways to UOP's Multiple Downcomer (MD) Trays for high pressure distillation columns. MU Trays were developed along similar lines including the use of bench apparatuses, hydraulic models, pilot plants, and industrial experience. To date, MU Trays have already been employed in eight full-scale liquid-liquid contactors. Half of those experiences were revamp experiences.

Like MD Trays, MU Trays maximize the utilization of a column's cross-sectional area for heavy and light phase traffic. In grass-roots applications, a column's diameter is reduced; in revamp applications, a column's capacity is increased. Additionally, MU Trays are designed to virtually eliminate heavy phase upwards entrainment and light phase downwards backmixing. Their efficiency is high.

This paper describes UOP Multiple Upcomer Liquid-Liquid Extraction Trays, including their development and the petrochemical industries' experiences with them in grass-roots and revamp applications.

1 INTRODUCTION

Hydrocarbon streams containing C_6, C_7, and C_8 compounds often contain high percentages of aromatic compounds like benzene, toluene, and xylenes. These streams come from pyrolysis and reformate units. It is sometimes desirable to recover the aromatic compounds from their non-aromatic counterparts. It is impracticable to achieve such a separation via distillation (specifically, a series of distillations). Usually, the required recovery can be achieved with liquid-liquid extraction. Several liquid solvents are available; UOP's TETRA, CAROM and Sulfolane Processes are often employed. With all of these high-capacity, high-selectivity processes, the interfacial tension between the heavy-phase solvent and the light-phase hydrocarbon feed is low (i.e., less than 15 dynes per centimeter). With low-surface-tension liquid-liquid systems, agitation/rotation is not required to achieve efficient mass transfer between the phases. Trays suffice to bring the phases into intimate contact with a large interfacial mass transfer area. Agitation/rotation is, in fact, detrimental to the separation of the phases that preferably occurs between contact stages.

2 DISCUSSION

2.1 Tray Description

The UOP Multiple Upcomer (MU) Extraction Tray was specifically developed for dearomatization processes like the TETRA, CAROM, and Sulfolane processes where the heavy phase liquid is the more voluminous of the two liquid phases. It was invented (1) employing many of the same concepts that have made UOP's Multiple Downcomer (MD) Distillation Trays so successful in highly-liquid-loaded vapor-liquid contacting services (2,3,4).

As their name states, all MU Trays employ a multiplicity of upcomers. For example, a liquid-liquid extractor having a diameter of 8 feet might have 3, 4, or 5 upcomers, depending on the relative volume of the light liquid phase. In the case of the MU Tray, the upcomers are specifically designed to support the trays, thus no additional support beams are required.

On an MU Tray, the heavy liquid phase is the dispersed phase. The tray decks employ perforations that are dimpled/nozzled in the downwards direction. This dimpling assures the uniformity of the heavy phase droplets. Mass transfer occurs as these droplets fall through the cross-flowing light liquid phase. When the droplets reach the tray below the tray from which they originated, they coalesce in a coalescence layer before being redispersed. On conventional extraction trays this coalescence is often incomplete and light phase backmixing occurs as the light phase passes downwards through the deck perforations.

The light liquid phase progresses up the column in a snake-like fashion. Upcomers allow the light phase to pass through the trays. Upcomers consist of settling boxes, pressure drop plates, and chimneys. The velocity in the settling boxes is purposely low to prevent the entrainment of heavy phase droplets up the tower. The pressure drop plates also prevent the heavy phase droplets from ascending through the upcomers. Additionally, the light phase pressure drop they create, act to back up the heavy phase coalescence bands on the tray decks. With additional back-up, the heavy phase residence time is increased, complete heavy phase coalescence occurs, and light phase downwards backmixing is eliminated. Chimneys reside above the pressure drop plates. These chimneys are purposely narrow to allow more contact time between the two liquid phases. Hats on the tops of the chimneys prevent heavy phase droplets from falling into the upcomers.

The capacity of UOP MU Trays is high because

1. The upcomers (alone) support the trays
2. The chimneys are narrow
3. The chimney hats are located at the tops of the chimneys rather than beneath the decks of the above tray

The efficiency of MU Trays is high because

1. Heavy phase droplets are small and uniform
2. Light phase downwards backmixing is eliminated
3. Heavy phase upwards entrainment is eliminated

Proof of these claims has been obtained from bench, pilot plant, and industrial experience.

2.2 Tray Development

The UOP MU Tray was first conceived in 1974. At that time, development work began simultaneously across three fronts - desk engineering, bench apparatus experimentation, and pilot plant operation. Desk-type development work addressed the hydraulics and the mass transfer. The literature was searched for applicable correlations especially regarding the following:

1. Droplet size distribution
2. Coalescence layer thicknesses (or coalescence times)
3. Mass transfer resistances
4. Liquid diffusion coefficients (diffusivities)

Pressure balances yielded equations that could be employed to calculate the total back-up of heavy phase on the tray decks as a function of the pressure drop plate designs.

Laboratory efforts in support of the development of MU Trays were intensive and included the following:

1. A 2-inch diameter droplet apparatus in Tonawanda, New York
2. A liquid diffusivity cell also in Tonawanda, New York
3. A 4-inch pilot plant column (associated with a complete TETRA/CAROM-Process pilot plant unit) in Tarrytown, New York
4. A 12-inch diameter pilot plant column residing alongside a 15-foot diameter industrial TETRA extractor in Taft, Louisiana.

The 12-inch Louisiana column was employed intermittently over a 3 year period to check the results of the desk-type development work. That column was heavily instrumented and included back-lit sight glasses and assorted sampling taps. Heavy phase entrainment rates were measurable with the sampling taps. One of the more surprising findings of the 12-inch pilot plant work was that the column failed to function, except at very low feed rates, with the pressure drop plates removed. It was hypothesized that high heavy phase entrainment and high light phase backmixing yielded flooding (or stacking). On the other hand, consistent with theory, tray efficiency was found to be a strong function of feed aromaticity - up to the point where the feed aromaticity was so high that the column emulsified or "went single phase".

2.3 Industrial Experience

Before too long, UOP Multiple Upcomer (MU) Extraction Trays will have been employed in eleven columns (as is shown in TABLE 1).

TABLE 1

UOP MULTIPLE UPCOMER EXTRACTION TRAYS EXPERIENCE LIST

PROJECT	YEAR	AROMATICS %	DIAM, MM	REVAMP
TETRA - Ontario	1975	80-90	2438	N
TETRA - Africa	1976	30-40	2100	N
TETRA - Texas	1977	30-50	2438	R
TETRA - Louisiana	1978	85-92	4572	R
TETRA - Texas	1980	40-60	3962	R
TETRA - Ontario	1981	78	3048	N
TETRA - Ohio	1982	42	3962	N
CAROM - Texas	1988	71	2591	R
CAROM - Texas	1991	44-61	2438	N
SULFOLANE - Far East	1991	72-90	1524	R
		1991	1830	R

The Louisiana experience has already been documented (5). Roughly half of the experiences involved new (grass-roots) vessels. The remaining experiences involved revamps where conventional extraction trays were removed and replaced.

Some of the experiences of Table 1 were associated with solvent change-outs. The Texas revamp of 1977 was comprised of

1. The replacement of a Udex-type cosolvent consisting of diethylene glycol and dipropylene glycol with tetraethylene glycol and UOP's TETRA process
2. The replacement of conventional extraction trays with MU Trays in the liquid-liquid extractor
3. The replacement of conventional 4-pass valve trays with MD Trays in the liquid-vapor stripper as exhibited in TABLE 2 as follows:

TABLE 2

TEXAS 1977 MU REVAMP EXPERIENCE

	ORIGINAL	REVAMP
Solvent	DEG/DPG	TETRA
Extraction Trays	Conventional	Multiple Upcomer
Stripper Trays	Conventional	Multiple Downcomer
Feed Rate, kg/hr	27,900	59,300
Feed Aromaticity, %	39	30
Product Rate, kg/hr	12,100	19,000

As a result of that work, the aromatics production rate of the Texas unit was increased by at least 50% even with a decreased feed aromaticity.

2.4 The Future

Work is presently underway to qualify the utilization of UOP Multiple Upcomer Trays in other liquid-liquid extraction processes requiring high tray capacities and efficiencies.

In lube oil processes, for example, lubricating oils are treated in liquid-liquid contactors to effect dearomatizations and, by so doing, improve their thermal viscosity indicies. UOP Multiple Downcomer (MD) Trays could be employed in the associated vapor-liquid contacting vessels. MU and MD Trays could be employed to reduce investment costs by reducing the sizes (diameters and heights) of columns being planned for construction.

3 SUMMARY

The development of the UOP Multiple Upcomer (MU) Liquid-Liquid Extraction Tray began fifteen years ago. Appreciable industrial experience has been acquired as the development of that tray has progressed.

4 REFERENCES

1. Forte, P. and Somekh, G.S., Liquid-Liquid Contacting Systems, U.S. Patent 4,247,521.
2. Resetarits, M.R., Agnello, J., Lockett, M.J., and Kirkpatrick, H.L., Retraying Increases C3 Splitter Column Capacity, Oil & Gas Journal, June 6, 1988, 54-59.
3. Lockett, M.J. and Wisz, M.W., Use of MD Trays to Increase Column Capacity, European Federation of Chemical Engineering, Winterthur, Switzerland, June, 1983.
4. Kirkpatrick, R.D., MD Trays Can Provide Savings in Propylene Purification, Oil & Gas Journal, April 3, 1978, 72-83.
5. Resetarits, M.R. and Prevost, R.J., Energy Conservation in an Aromatics Production Unit, International Chemical Engineering Jubilee Symposium, London, England, 1982.

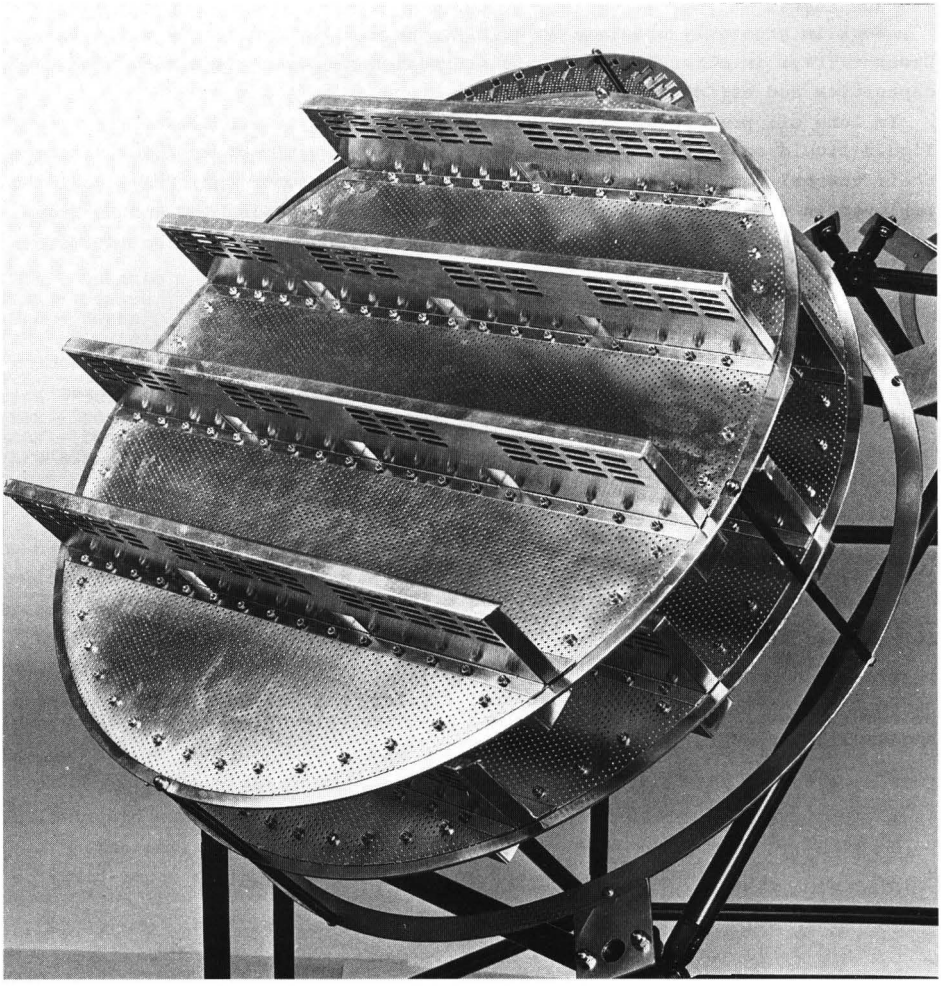

Solvent Extraction 1990, T. Sekine (Editor)

© 1992 Elsevier Science Publishers B.V. All rights reserved

CONSIDERATIONS FOR SCALING UP AGITATED EXTRACTION COLUMNS

A.E. KARR and R.W. CUSACK
Otto H. York Company, Inc.
Parsippany, New Jersey, USA

ABSTRACT

Designing an agitated extraction column from basic principles without obtaining pilot scale data is risky. Theoretical calculations are unreliable because of coalescence effects, variations in physical properties and flow rates along the length of the column, and especially contamination in commercial systems. Wetting phenomena, the presence of solids, the tendency to form emulsions, and density gradients in the continuous phase are additional factors that dictate the need for pilot scale testing. The pilot scale column performance should be optimized with respect to volumetric efficiency and arrangement of the column internals. Empirical scale-up procedures are presented for three types of agitated extraction columns.

INTRODUCTION

The main purpose of this brief paper is to provide the reader with some practical insights into how to approach the job of designing and scaling up an agitated extraction column.

In a previous paper Karr (1985) pointed out that designing an extraction column from basic principles without pilot scale test work is very risky. The reasons given were:

(a) The degree of coalescence and interfacial turbulence effects in commercial systems cannot be predicted accurately.

(b) Physical properties and flow rates may vary throughout the column which greatly complicates calculations.

(c) Most commercial systems are contaminated, frequently by surface active components.

(d) Reliable axial mixing data for the dispersed and continuous phases in large diameter columns are not usually available.

In connection with (c) above, Karr et al (1990) found that different types of equipment are affected differently by trace contaminants.

2 OTHER CONSIDERATIONS

2.1 Wetting

Normally one would select a material of construction that would be wet preferentially by the continuous phase. However, depending on the degree of

wetting and also on economics, there may be exceptions to this rule.

2.2 Solids

Some columns can handle solids better than others. The Reciprocating Plate Extraction Column (RPEC) handles solids very well because of the large open area (55-60%), large holes (15 mm), and all the plates including the baffle plates are in motion.

2.3 Emulsions

Some types of columns can handle systems that tend to emulsify better than others. Again, the RPEC is ideally suited for systems that tend to emulsify because of the uniform mixing over the cross-sectional area of the column. That type of mixing produces a more uniform drop size than columns with rotating impellers. Karr et al (1980) has shown that the RPEC can handle systems that tend to emulsify.

2.4 Density Gradient of Continuous Phase

There is not a single report in the literature of the effect of density gradients in the continuous phase on axial mixing. In a poster at ISEC '90, Holmes et al (1990) presented data that showed a major deleterious effect of unfavorable density gradients on axial mixing.

3 PREPARATION FOR DOING THE TESTS

If we have to do tests before designing an extraction column, how does one go about preparing to carry out the pilot scale tests?

3.1 Clean Equipment

First of all, the equipment used must be as clean as possible and not in the least reactive with feed and solvent.

3.2 Plant Feeds

If possible, actual plant or pilot plant feed and solvent should be used.

3.3 Equilibria Data as Function of Temperature

The equilibria data should be determined experimentally, preferable at more than one temperature. As shown by Karr et al (1988), operating an extraction column at elevated temperatures may give better results than at lower temperatures because the effect of higher rates of mass transfer surpasses the effect of possible lower distribution coefficients.

3.4 Diameter of Test Column

The diameter of the column to be selected depends upon the type of column, and the projected diameter of the production column. The RPEC has been scaled up from 25 and 50 mm to 1-2/3 m. York Scheibel and RDC Columns are frequently scaled up from 75 mm diameter columns. Some columns require 150 mm diameters for scale up. The advantage of the smaller diameter test column is that less material can be employed, an important economic and safety consideration.

3.5 Height of Test Column

The active height of the test column selected will of course depend on the number of theoretical stages required and the expected value of optimum HETS. For various reasons, there is always some uncertainty about the optimum HETS. Therefore, ideally, some flexibility in the active height of the column should be provided. This can be done by providing feed connections along the length of the column.

3.6 Arrangement of Internals

If the physical properties of the system are expected to vary along the length of the column due to appreciable concentration changes, then the drop size and holdup will vary along the length of the column more than they normally do. In that case, ideally, one should vary the degree of mixing along the length of the column. The goal is to make the tendency for the column to flood equal everywhere along the column length. As shown by Karr (1980), in the RPEC this is usually done by varying plate spacing but it can also be done by varying the open area in the plates. In columns with rotating impellers, it can be done by varying the diameter of the impellers along the length of the column.

4 DOING THE TESTS

The data to be obtained in the test column will depend to some degree on the type of agitated column employed and the scale-up procedure recommended by the manufacturer of the equipment. The minimum data required for the optimum scale-up of the York-Scheibel Column, RDC Column, and the Karr RPEC are as follows:

4.1 HETS is determined as a function of RPM or SPM at at least three values of throughput and at a solvent to feed ratio that was preselected based on economic considerations. In small diameter columns of 25 to 75 mm the minimum value of HETS will generally occur close to the flood point, which should be determined. The curves in Fig. 1 are typical plots of HETS versus RPM or SPM

at different total throughputs. For systems with relatively high interfacial tension, these curves may exhibit a minimum value prior to the flood point.

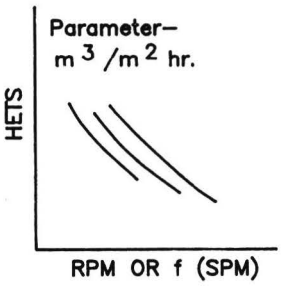

Fig.1 Effect of RPM or SPM on HETS

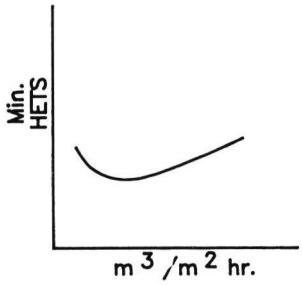

Fig.2 Effect of throughput on minimum HETS

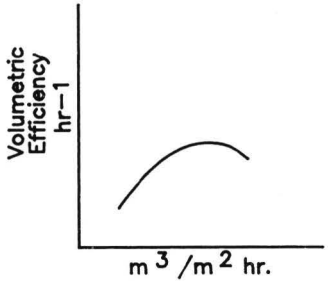

Fig.3 Effect of throughput on volumetric efficiency

4.2 A plot is made of the minimum value of HETS as a function of throughput as shown in Fig. 2. At low throughputs as throughput increases the minimum value of HETS will decrease. However, at higher throughputs the minimum HETS will increase as throughputs increase.

4.3 The optimum volumetric efficiency is plotted against total throughput as shown in Fig. 3. Volumetric efficiency is defined as follows:

$$\text{Volumetric Efficiency} = \frac{\text{Total Throughput}}{\text{HETS}} \qquad (1)$$

$$= \frac{m^3/m^2hr}{m} = \frac{1}{hr}$$

The volumetric efficiency is inversely proportional to the volume of column required to do a given extraction job.

As shown in Fig. 3, if sufficient data are obtained the volumetric efficiency will pass through a maximum. The conditions corresponding to the maximum value of volumetric efficiency represents the optimum performance of the test column.

5 APPROACHES TO DESIGN AND SCALE-UP

There are basically three approaches to the design and scale-up of agitated extraction columns as follows:

a. Theoretical based on physical properties

b. Semi theoretical

- Simulate hydrodynamics of test unit and
- Estimate effect of axial mixing on HTU

c. Empirical based on pilot scale tests

As mentioned at the outset, the first approach is risky. The second procedure would be less risky if one could really simulate the hydrodynamics accurately and could predict axial mixing accurately.

The third procedure is easy to use and in experienced hands it is probably as accurate as the other approaches. This is borne out by the essentially perfect success rate we have had in employing the scale-up procedures for the agitated extraction columns presented in the next section.

6 SCALE-UP PROCEDURES

The following are the scale-up procedures for the three agitated columns marketed by the Otto H. York Company, Inc.

6.1 Karr Reciprocating Plate Column

As previously shown by Karr (1985) in production scale columns, there is a minimum in the HETS versus f curve and this minimum occurs at a lower value of f than the flooding value of f. The minimum is due to increased axial mixing in the production column.

The object of the scale-up procedure is to predict the minimum in the HETS versus f curve for the production column.

The scale-up procedure is as follows:

a. Data are obtained in a 25, 50 or 75 mm diameter column. The diameter selected is frequently determined by the availability of feed materials. Most scale-ups have been done directly from the 25 mm column.

b. The optimum performance of the pilot column is determined. The criterion for optimum performance is maximum volumetric efficiency in a column having optimum plate spacing.

c. When scaling up from the pilot data, the following parameters are held constant: plate spacing, stroke length and throughput per unit cross-sectional area.

d. The expected minimum HETS in the large diameter column is calculated from the following equation:

$$\frac{(HETS)_2}{(HETS)_1} = \left(\frac{D_2}{D_1}\right)^{0.38} \qquad (2)$$

The 0.38 exponent was determined for a high interfacial tension system. Somewhat lower exponents were determined for a low interfacial tension system. The 0.38 exponent is used for reasons of conservatism.

e. The reciprocating speed required for minimum HETS is calculated from Eq. 3.

$$\frac{(SPM)_2}{(SPM)_1} = \frac{f_2}{f_1} = \left(\frac{D_1}{D_2}\right)^{0.14} \qquad (3)$$

f. Baffle plates suitable in design and spacing are provided. By using these exponents, since the power per unit volume varies as the cube of the reciprocating speed, Karr (1985) has shown that the power per unit of cross-sectional area or per unit of throughput is the same for both the test column and the production column. However, the power to the production column is provided in a more gentle fashion over a greater height of column.

6.2 York-Scheibel Baffle Column

(a) Data are obtained in a 75 mm diameter column and the data are optimized with respect to volumetric efficiency.

(b) On scaling up, the throughput per unit of cross-sectional area is increased by a factor of 3 to 5 depending on whether the total throughput in the 75 mm column is $8m^3/m^2$ hr or $2m^3/m^2$ hr.

(c) The number of actual stages is the same as that in the test column but the height of each stage is increased as follows:

$$\frac{H_2}{H_1} = \left(\frac{D_2}{D_1}\right)^{0.7} \tag{4}$$

(d) The power per unit of throughput is the same as in the test column.

6.3 RDC Column

(a) Data are obtained in a 75 mm diameter column and the data are optimized with respect to volumetric efficiency.

(b) On scaling up the throughput per unit of cross-sectional area is 70 to 80% of the selected throughput in the 75 mm column.

(c) The number of actual stages is the same as that in the test column but the height of each stage is increased as follows:

$$\frac{H_2}{H_1} = \left(\frac{D_2}{D_1}\right)^{0.5} \tag{5}$$

(d) The power per unit of stage volume is the same as in the test column.

REFERENCES

Holmes, T.L., Karr, A.E. and Baird, M.H.I., "Effect of Density Gradient in Continuous Phase on Axial Mixing", Poster at ISEC '90, Kyoto, Japan.

Karr, A.E., "Design, Scale-up and Applications of the Reciprocating Plate Extraction Column", Separation Science and Tech 15 (4), 877 (1980).

Karr, A.E. "Amplification of the Scale-up Procedure for the Reciprocating Plate Extraction Column", AIChE J. 31 (4), 690 (1985).

Karr, A.E. and Ramanujam, S., "Scale-up and Performance of 5 ft. (1.52 m) Diameter Reciprocating Plate Extraction Column", Solvent Extr and Ion Exch 6 (2), 221 (1988).

Karr, A.E., Gebert, W. and Wang, M., "Extraction of Whole Fermentation Broth with Karr Reciprocating Plate Extraction Column", Can. J. Chem. Eng., 58, 299 (1980).

Karr, A.E., Holmes, T.L. and Cusack, R.W., "Effect of Trace Contaminants on Performance of Agitated Extraction Equipment", accepted for publication in "Solvent Extraction and Ion Exchange" June or July, (1990).

Solvent Extraction 1990, T. Sekine (Editor)

© 1992 Elsevier Science Publishers B.V. All rights reserved

APPARATUS SELECTION AND DESIGN IN SOLVENT EXTRACTION

H.-J. BART and R. MARR
Institut für Thermische Verfahrenstechnik und Umwelttechnik, Technische Universität Graz, Inffeldgasse 25, A-8010 Graz (Austria)

ABSTRACT

Different rate controlling processes will dominate the mass transfer in solvent extraction when chemical reactions are involved. The design and selection of a specific apparatus is then under certain limitations. These restrictions can be expressed into some rules which will be discussed in detail with copper extraction.

INTRODUCTION

The traditional apparatus in solvent extraction is the mixer-settler. This is why its lay-out and scale-up is easy. In complex extraction circuits, including scrubbing and stripping stages with different solutions, a very flexible arrangement is possible. The situation changes when high throughputs and a multistage operation favours columns. Neglecting the use of centrifuges for special applications (low density differences etc.) it isn't quite clear at which certain point a column or mixer-settler should favourably be used.

The analysis in the following is only considering mass transfer effects and their impact on design and selection. Further aspects, like costs, safety etc., contribute then markedly to the final apparatus selection.

RESULTS AND DISCUSSION

The mass transfer through the interphase in extraction systems with chemical reactions (e.g. for metals extraction), may be formulated as shown in Fig. 1 according to the two film model of Whitmann (1923).

The mass transfer from this picture can be controlled either through the chemical reaction or the physical mass transfer or both, respectively. In analogy to gas-solid reactions this behaviour can be compared with the Damköhler II number. Since ion exchanger and solute are considered as insoluble in the other phase, the Da_{II} number is better to use than the Hatta number (Bart 1988). The Da_{II} number relates diffusion and reaction as follows:

$$Da_{II} = \frac{\dot{n}_R}{\dot{n}_D} = \frac{k_F\ (Me)^{b-1}\ (RH)^c}{k_{Me}\ \ (H)^d} \qquad (2)$$

when $$\dot{n}_D = k_{Me}\ (Me - Me_i) \qquad (3)$$

and interfacial concentrations are neglegible ($Me_i \approx 0$) and

$$\dot{n}_R = k_F \frac{(Me)^b\ (RH)^c}{(H)^d} \qquad (4)$$

which is an often used expression for forward reaction in solvent extraction (see Proceed. ISEC '77).

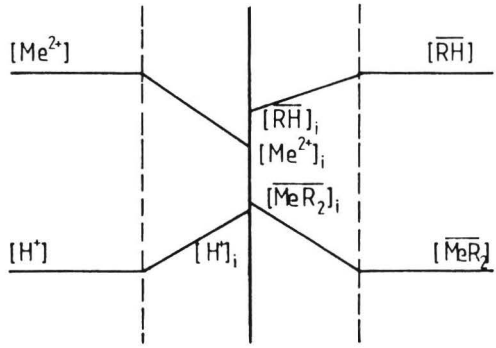

Fig. 1. Mass transfer at the interphase
$Me^{2+} + 2\ RH \leftrightarrow MeR_2 + 2\ H^+$ (1)

A Da_{II} number higher than unity (e.g. » 10) says diffusion is dominating, a small one (e.g. « 0.1) says reaction controls.

With the knowledge of k_F (experimentally detectable, see Nitsch 1978) and k_{Me} (calculated from a Sh-number) the controlling mechanism becomes evident. This was done for copper extraction in Tab. 1.

Figs. 2,3 and 4 show the profiles in the kinetic, mixed and diffusion regime in a mixer-settler cascade. As was expected, calculation with reaction alone in the diffusion regime and vice versa, gives wrong results. An additional calculation was done for infinite residence time which models a 100 percent efficient extraction stage. The diffence to the other profiles is obvious, which were calculated with a three minutes residence time as usual in copper extraction.

The same situations arise, if a column calculation is done under the same aspects as discussed above (see Figs.5 and 6).

TABLE 1

Da_{II} numbers for copper extraction at different concentrations

regime:	kinetic	mixed	diffusion
$(Me)_o$	0.002	0.018	0.157
$(RH)_o$	0.090	0.090	0.400
$(H)_o$	0.100	0.010	0.001
$(MeR_2)_o$	0.000	0.000	0.000
$Da_{II,Me}$	0.12	1.20	53.3

CONCLUSIONS

The Da_{II} number proves to be a good criteria for the simplification of a calculation procedure. With slow reaction rates (Da_{II} «) the use of mixer-settlers should be favoured. This is common practice, since long residence times are difficult to achieve in columns. The usual lay-out of a mixer-settler is then done in a McCabe Thiele like operating diagram. The lay-out doesn't consider much on mass transfer effects and is therefore always overdesigned in the residence time of the mixer.

Processes in the diffusion regime (Da_{II} ») are improved by large concentration differences. Here countercurrent columns give then benefits in comparison to mixer-settlers. The decision to change from mixer-settler operation to column operation is only bent to the Da_{II} number. Thus the Da_{II} number gives information for the apparatus selection.

In contrast to simple physical systems, the dominating regime in reactive ones can switch from the physical to the chemical. At low concentrations usually the chemical regime dominates (see Tab. 1).

At such a situation it then might be useful to reduce e.g. half of the column length and add a mixer-settler in series, to obtain the same extraction results at lower costs. The lay-out of an apparatus in reactive systems is more complex than in pure physical ones (Bart et al. 1988). Realizing a dominating regime with the help of the Da_{II} number, it is then possible to reduce the system equations. The apparatus is then treated either as a conventional extractor or as a chemical reactor.

ACKNOWLEDGMENTS

The authors want to thank the "Österreichischen Fonds zur Förderung der wissenschaftlichen Forschung", Vienna and the "Christian Doppler Ges.", Vienna, which makes this work possible.

REFERENCES

Bart, H.-J., Bauer, A., Lorbach, D., Marr, R., 1988. Chem.-Ing.Techn. 60, No. 3, 169-179.

Bart, H.-J., 1988. Habilitationsschrift. dbv-Verlag, Graz.

Bart, H.-J., Marr, R. and Bauer, A., 1989. Chem.-Ing. Techn. 61, No. 12, 941-948.

Nitsch, W. and Kruis, B., 1978. J. Inorg. Nucl. Chem. 40, 857/864.

Proceed. ISEC 77, 1979. Ch. 5 Mass Transfer. CIM Spec. Vol. 21, Montreal, 184 ff.

Whitman, W.G., 1923. Chem. Met. Eng. 29, 147.

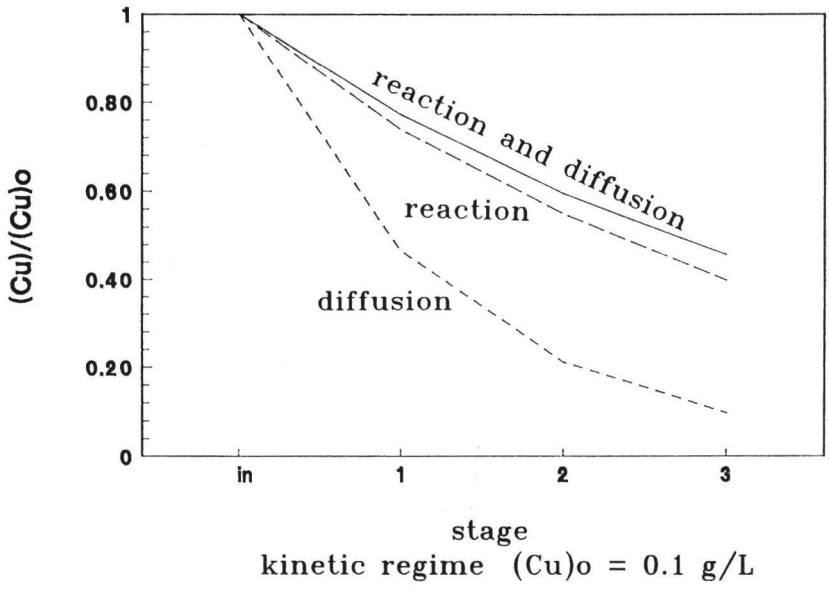

Fig. 2. Mixer Settler (kinetic regime)

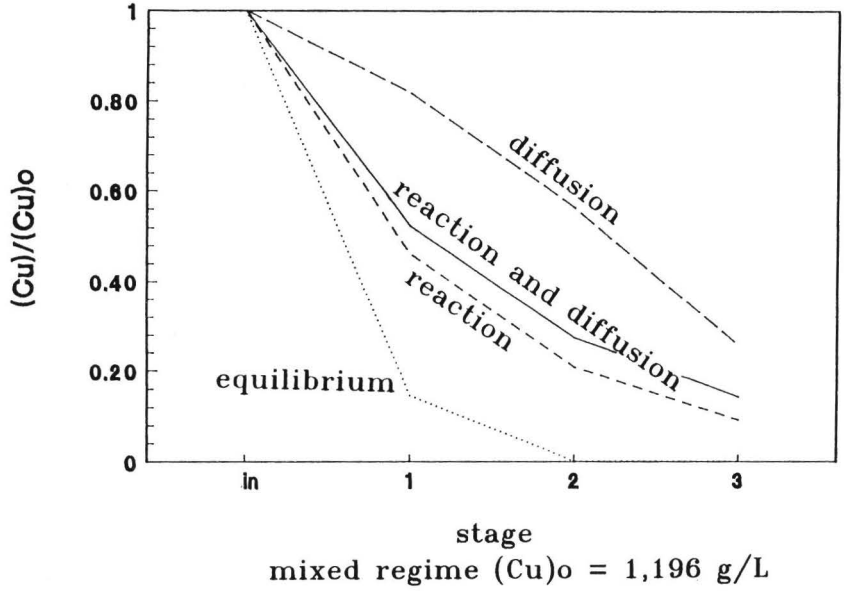

Fig. 3. Mixer settler (mixed regime)

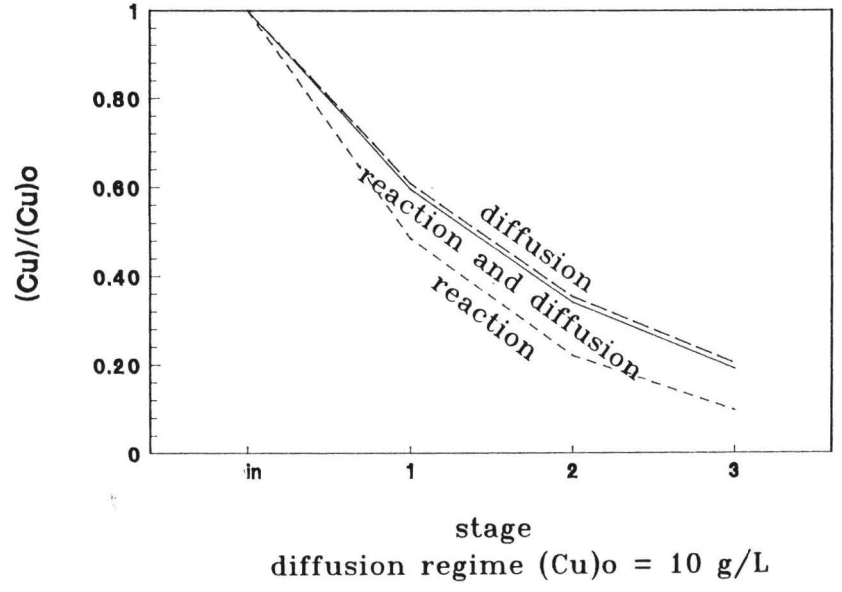

Fig. 4. Mixer Settler (diffusion regime)

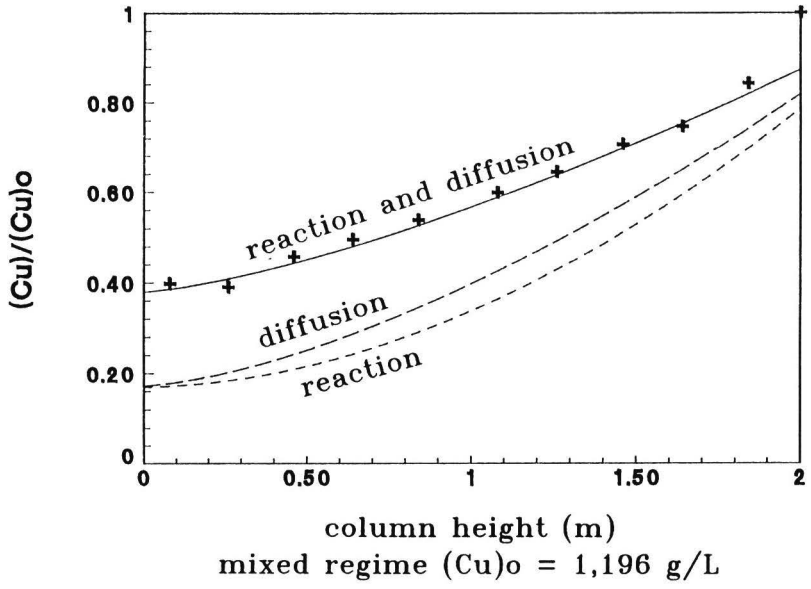

Fig. 5. Column (mixed regime)

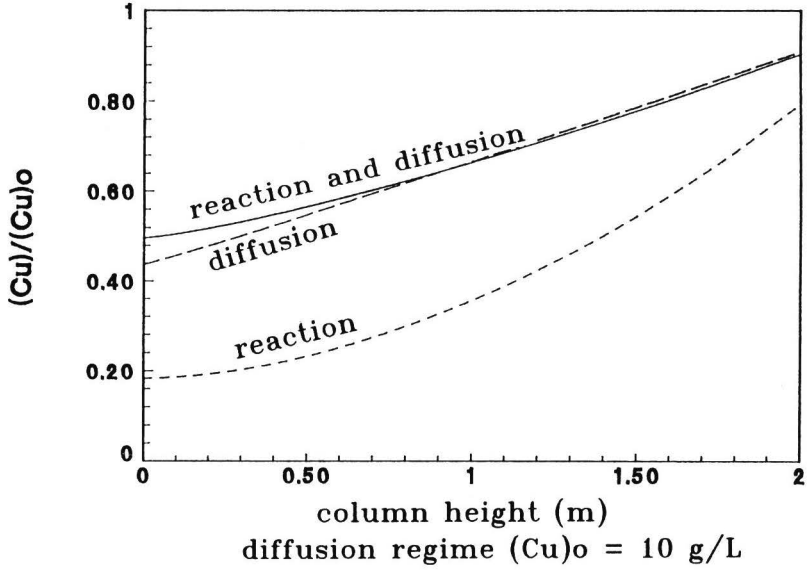

Fig. 6. Column (diffusion regime)

Solvent Extraction 1990, T. Sekine (Editor)

© 1992 Elsevier Science Publishers B.V. All rights reserved

THE HYDRODYNAMIC PERFORMANCE OF PULSED PERFORATED-PLATE COLUMNS

D.H.Logsdail,J.A.Jenkins,K.S.Robinson - AEA Technology,Harwell Laboratory,Oxfordshire, U.K.

Abstract

Pulsed perforated-plate column operation depends on the extent to which the plates are wetted by the dispersed phase and plate wetting depends on the physical properties of the process solutions and the surface characteristics of the plates.Experiments have demonstrated that high volumetric throughputs can be achieved in pulsed columns when the dispersed phase tends to wet the plates, but the drops are large and non-uniform in shape and size. However, when the plates are not wetted by the dispersed phase the throughputs are much lower, but the drops are smaller and uniform in shape and size.
An example of severe plate wetting occurs in the extract/scrub compound column for the extraction of uranium by TBP/odourless kerosene. With the aqueous phase dispersed the plates near the feed point become wetted by the aqueous phase and a foam-like dispersion accumulates between the plates causing phase inversion and flooding.

INTRODUCTION

Changes in the wetting behaviour of the plates in pulsed columns markedly affect maximum volumetric throughputs(Charvillat,1984; Larner,1964; Schmidt,1983).

High volumetric throughputs can be achieved in pulsed columns when the dispersed phase tends to wet the plates, but the drops are large and non-uniform in shape and size. When the plates are not wetted by the dispersed phase the throughputs are much lower but, the drops are smaller and uniform in shape and size.

A particular example of plate wetting occurs in the extract/scrub compound column during the extraction of U by TBP/OK. Plates near the feed point become wetted by the aqueous phase and a foam-like dispersion accumulates between the plates followed by premature flooding.

2 FLOODING DATA FOR HYDROPHILIC AND HYDROPHOBIC PLATES

Floodpoint measurements have been made in a 50mm diameter test column fitted with stainless steel nozzle plates and identical plates coated with a thin layer of PTFE. With the coated plates the drops were spherical and uniform in size (Fig. 1a) whereas, with the uncoated plates the drops were irregular in shape and size(Fig. 1b) .

The marked differences in flooding throughput for both uncoated and coated

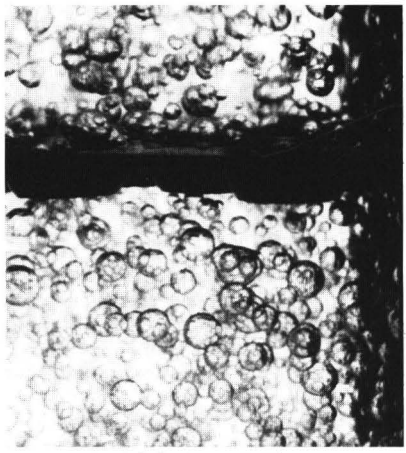

(a) Coated Plate

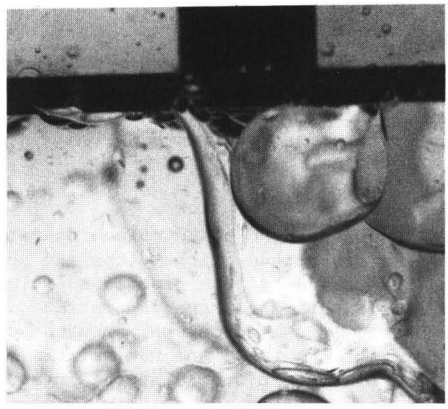

(b) Uncoated Plate

Figure 1 Contrasting dispersions in pulsed plate columns

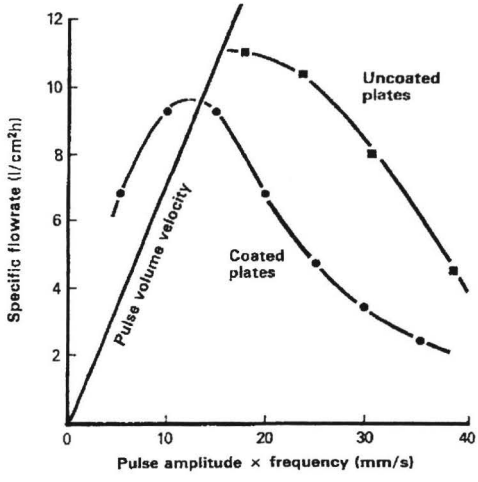

Figure 2 Flooding throughputs for coated and uncoated plates

plates are clearly shown in Fig. 2. For the hydrophilic uncoated plates the throughputs are high and the peak in the curve flat; for the hydrophobic coated plates the throughputs are much lower and the peak much sharper and occurs at a lower amplitude-frequency product.

These results indicate that the reduction in throughput with time observed in pulsed plate columns is probably due to the plates changing in character from hydrophilic to hydrophobic.

If, in plant operation, the plates are found to ''age'' and become hydrophobic there is scope to reduce the pulse amplitude-frequency product to re-establish an adequate margin between the normal operating condition and the floodpoint.

3 Compound Extract-Scrub Column Performance

A particular example of severe plate wetting occurs in the extract/scrub compound column for the extraction of U from HNO_3 solution by TBP/OK. With the aqueous phase dispersed the stainless-steel nozzle plates near the feed point become wetted by the aqueous phase, large balloon-like drops form and a foam-like dispersion accumulates between the plates causing phase inversion and flooding.

Experiments have been undertaken to gain a better understanding of this phenomenon. Simple beaker tests have been carried out in an attempt to simulate column conditions and to observe the dispersion behaviour under carefully controlled conditions. The beaker tests were followed by experiments in a short pulsed column operated under simulated scrub conditions.

3.1 *Beaker Tests* - equal volumes of aqueous and organic phases were mixed in a small glass beaker by a standard pulsed column nozzle plate, which was moved up and down through the interface to simulate pulsing. The appearance of the dispersion was observed for 15 minutes after mixing was begun, at the end of which time the liquids generally had reached chemical equilibrium. The observations are summarised in Table 1.

Table 1 Results of Beaker Tests at Ambient Temperature

Experiment	Aqueous Phase	Solvent Phase	Initial Mixing [first 5 min.] Solvent continuous phase appearance	Comments
Pilot Plant Liquids(1)				
a	Scrub	Unloaded	Clear	Wide drop-size distribution
b	U feed	Unloaded	Cloudy	Wide drop-size distribution
c	Scrub	U-loaded [from (b)]	Clear	'Frog-spawn' distribution
d	Scrub	Unloaded	Clear	Wide drop-size distribution
e	U feed	Unloaded	Clear	Wide drop-size distribution
f	Scrub	U-loaded [from (e)]	Clear	'Frog-spawn' distribution
Pure Reagents(1)				
g	U feed	Unloaded	Cloudy	Emulsified after 11 mins.
h	Scrub	U-loaded	Cloudy	'Frogspawn' dispersion

Notes; 1)Scrub-3M HNO3, U feed- ~200g/l & 3M HNO3, Solvent - 20% TBP/OK

Generally, the appearance of the dispersions was similar to that observed in an extraction/scrub column. For example, the liquids in the simulated scrub, with U-loaded solvent, tended to produce 'frog-spawn' sticking to the plate or large pendular drops ''ballooning'' from the plate. Photographs illustrating the difference between a good dispersion and one giving 'frog-spawn' adhering to the plate are shown in Fig. 3.

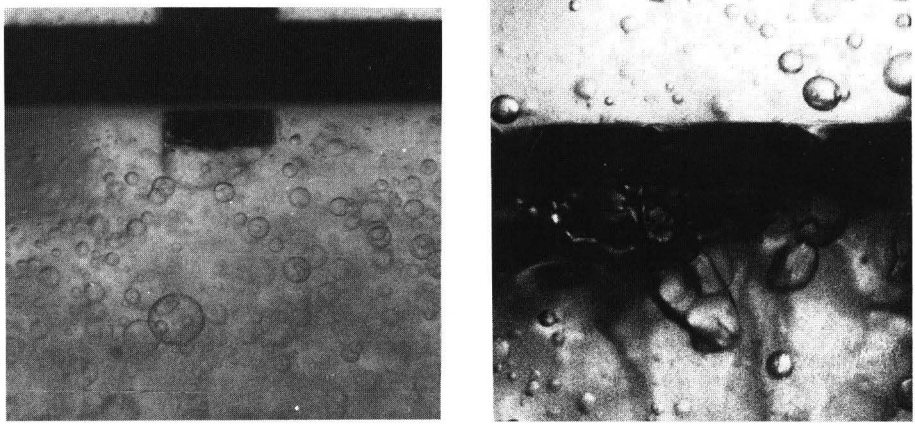

(a) Good dispersion (b) Frog-spawn type dispersion

Figure 3 Different dispersions observed during beaker tests

Because the poor phase dispersion was found to be due to a plate wetting phenomena the effect of increasing the temperature on the type of dispersion formed was examined. Increasing the temperature changes the physical properties of the solutions, particularly the interfacial tension and viscosity, and these in turn affect the extent of plate wetting. The results of these experiments are shown in Table 2 and indicate that the 'frog-spawn' type behaviour is eliminated during scrubbing of U-loaded solvent by operating at temperatures > 35°C.

Table 2 Effect of Increased Temperature on Scrub System

Expts [total]	Temp (C)	Number of Experiments				
		Appearance of cont. solvent phase during initial mixing		Appearance of dispersion		
		Clear	Cloudy	Discrete Spheres	Ballooning from plate	'Frogspawn'
10	35	10	0	0	10	0
6	65	6	0	2	4	0

3.2 *Pulsed Column Tests* - as temperature affected the disperson behaviour in the beaker tests, the scrub process was simulated at different temperatures in a 50mm diameter test column. Experiments at ambient temperature showed that initially, with no U present in the solvent phase the drops of scrub acid passed freely through the plates. However, as the U concentration in the solvent increased the dispersion deteriorated, with 'ballooning' from the plates and eventually, when the full U loading was reached,'frogspawn' which adhered to the plates. At 35°C an increase in drop size occurred when the U-loading in the solvent reached its full value, but there was no evidence of 'frogpawn'. At 65°C the dispersion appeared much better than at 35°C.

4 OPERATING CONDITIONS

These observations indicate that the poor dispersion observed in the scrub process is in fact drops of solvent encapsulated by thin aqueous films within the bulk solvent. Similarly, the large balloon like drops also observed are believed to be solvent held in a large film of aqueous phase. These drops settle only very slowly since they have a density close to that of the bulk solvent.

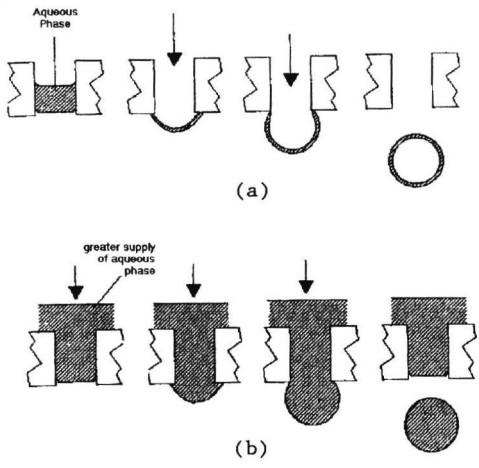

Figure 4 Suggested mechanisms of drop formation

This type of behaviour requires a dynamic analysis of pulsing conditions but, the sequence of events for the formation of such a dispersion is suggested in Fig. 4(a). Qualitative reasoning suggests that the factors which lead to the formation of balloon-like drops and 'frog-spawn' are;

* preferential wetting of plates
* small holes bridged by the aqueous phase
* low density difference and high interfacial tension
* low flowrate ratio

The qualitative relevance of the latter is shown in Fig. 4(b). In contrast to the conditions described in Fig. 4(a) the dispersed phase flow through the plate holes is sufficient for discrete drops of dispersed phase to be formed. Hence, depending on the combination of phase physical properties, flows, plate wetting behaviour and pulsing conditions a system could operate in either of these two modes, one giving a good dispersion, the other leading to flooding.

Experiments with stainless-steel sieve plates have demonstrated that there is a boundary of operating conditions beyond which this poor dispersion behaviour does not occur.

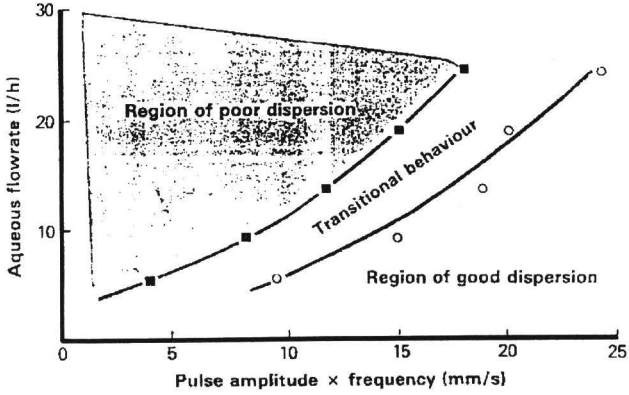

Figure 5 Operating boundaries with stainless steel sieve plates.

Such a boundary is shown in Fig. 5. Here, both high amplitude-frequency product and low aqueous phase flow are required to avoid the region of poor dispersion.

A theoretical model has been developed based on these experiments for designing a plate which minimises, or even eliminates the envelope of operating conditions which gives poor dispersion behaviour.

5 CONCLUSIONS

The nature of the dispersion generated in pulsed plate columns depends largely on the wetting properties of the plates.

With hydrophilc plates and the aqueous phase dispersed the drops are irregular in shape and size whereas, with hydrophobic plates the drops are spherical and uniform in size.

The agglomeration of drops into 'frog-spawn' does not occur during the scrubbing of U-loaded solvent with 3M HNO_3 at temperatures >35°C.

A boundary of operating conditions for pulsed columns with hydrophilic plates can be defined beyond which poor phase dispersion can be prevented.

For long term plant operation with the aqueous phase dispersed pulsed plate columns should be designed on the basis that, either; the plates behave with hydrophobic characteristics,or,the operating pulse conditions are within the region of good phase dispersion

REFERENCES

Charvillat,J.P., et al, 1984; I.Chem.E.Symposium Series
Larner,G.S. and Logsdail,D.H. 1964: UKAEA Report AERE-R 4409
Schmidt,H., 1983; Separation Science and Technology, 18, pp.1595-1616

Solvent Extraction 1990, T. Sekine (Editor)

© 1992 Elsevier Science Publishers B.V. All rights reserved

AXIAL MIXING OF LIQUID-LIQUID-SOLID SYSTEM IN OPEN TURBINE ROTATING DISC CONTACTOR (OTRDC)

CHEN, Xiao-Xiang and SU, Yuan-Fu (Y.F. SU)
Chemical Engineering Research Centre
East China Institute of Chemical Technology, Shanghai 200237, CHINA

ABSTRACT
Experiments were carried out in the open turbine rotating disc contactor using quartz particles, tap water (continuous phase) and kerosene (dispersed phase). Correlations for predicting backflow ratio of each phase have been given. In comparison with liquid-liquid system, it has been found that (1) the presence of solid particles results in smaller dispersed phase but larger continuous phase axial mixing; (2) the solid phase axial mixing is mainly determined by the particle size distribution and rotor speed.

1 INTRODUCTION

The rotating disc contactors (RDC) are notable for their wide application in various industries. It is said that the RDC can be applied to systems containing some solid. However, when it handles systems with high content of suspended solid, an appreciable amount of the particles is observed to deposit on the stator rings. Therefore, the rotators have been modified by welding three narrow strips to the lower surface of each rotating disc, as first suggested by one of the present authors, so that the stirring intensity may be enhanced and column can be used for liquid-liquid-solid system with high solid particle content as well as liquid-liquid system. This modified column is named open turbine rotating disc contactor (OTRDC).

The previous study emphasizing on the hydrodynamics of liquid-liquid and liquid-liquid-solid systems were reported by Zhu (1989) at ACHEMASIA, October, 1989 in Peking, China. The present work deals with the axial mixing of liquid-liquid-solid system in OTRDC.

2 EXPERIMENTAL

2.1 Apparatus

The column used can be referred to the paper reported at ACHEMASIA (1989). The various column geometries are summarized in Table 1. Where D_T is the column diameter, D_S stator ring opening, D_R rotor diameter, H_T compartment height, b strip width, N total stage number.

TABLE 1 Column dimensions

Unit	D_T, m	D_S, m	D_R, m	H_T, m	b, m	N
A	0.152	0.090	0.084	0.050	0.006	35
B	0.152	0.105	0.084	0.075	0.006	24
C	0.152	0.090	0.084	0.075	0.006	24

2.2 System used

Quartz particles were used as solid phase, tap water and kerosene as continuous and dispersed phases respectively. Two kinds of quartz particles which had average diameters of 0.184×10^{-3} and 0.225×10^{-3} m were used in experiments. Their terminal settling velocities in water are 0.0276 and 0.0413 m/s. The density of quartz particles is 2659 kg/m^3 and kerosene 795.8 kg/m^3. The ratio of solid to continuous phase varied from 0.15 to 0.30 (by weight).

2.3 Measurements

The column was first filled with water which was set at the desired flow rate. At the same time the solid feed screw and the rotating discs were started and maintained at proper values. Quartz particles were first mixed with water in the mixer and then introduced to the top of column.

The light phase was introduced gratually at the bottom of the column and its flow rate was finally set at a desired value. After the steady state had been attained, a pulse of tracer was injected to determine the axial mixing. The measuring technique for continuous phase and dispersed phase axial mixings offered no difficulty and could be referred to the method of Zhu (1984). Marble particles which had the same size distribution of quartz particles were used as tracer for the solid phase. Its density is 2651 kg/m^3 and approximately equals to that of quartz. The tracer was injected at the top inlet of the column and samples were withdrawn at regular intervals beneath the bottom compartment. The sample was decomposed with HCl and the excess acid was determined by titration with NaOH. Thus, the residence time distribution (RTD) curve of the particle could be obtained.

At the end of each run, the dispersed phase hold-up value was obtained by displacement method. The solid particles were withdrawn from the bottom of column dried and weighed so as to get the solid phase hold-up value.

3 RESULTS AND DISCUSSIONS

As the OTRDC is partially compartmentalized it can be well represented by the backflow cell model. In this case the axial mixing in each phase may be evaluated by the interstage backflow ratio f. The backflow model equation is

$$dC_i/d\theta = N\left[f(C_{i-1}+C_{i+1}-2C_i) + (C_{i-1}-C_i)\right], \quad i = 1, 2, \ldots\ldots N \qquad (1)$$

B.C. $(1+f)C_1 = fC_2 + C_0$

$C_N = C_{N-1}$

$C_i = 0, \quad i \neq 1 \quad \text{at} \quad \theta = 0$

where C is the tracer concentration, θ dimensionless time, i stage number and starts from top of the column, N total stage number. The general solution of the model equation is

$$\sigma^2 = (1+2f)/N - 2f(1+f)\left\{1-\left[f/(1+f)\right]^N\right\}/N^2 \qquad (2)$$

where σ^2 is the standard deviation (Mecklenburgh et al., 1975). Following these principles, backflow ratio f can be obtained by comparison of the experimental RTD curve with that calculated from the model equation.

3.1 Continuous phase axial mixing

The dependence of backflow ratio f_c on the rotor speed N_R is shown in Figure 1. The difference between the values of f_c for liquid-liquid-solid system (see two upper curves) and those for liquid-liquid system (the lowest curve) is obvious. All experimental points of the former are greater than those of the latter because of the interaction between the motions of particles and the continuous phase which may be entrained by the eddies formed in the wakes of particles or may be carried with the particles as films around them, so as to increase the forward mixing in the continuous phase. Within the experimental range of N_R, the value f_c

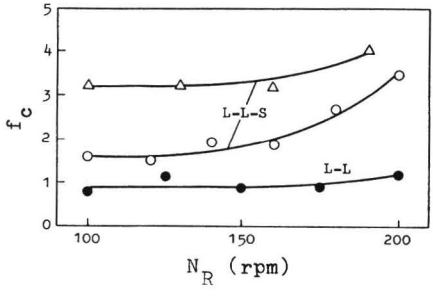

	H_T m	U_c 10^{-3}m/s	U_d 10^{-3}m/s	U_s 10^{-3}m/s
△	0.050	5.51	2.76	0.321
○	0.075	4.96	1.65	0.280
●	0.075	4.96	1.65	-

Fig. 1 Continuous phase axial mixing

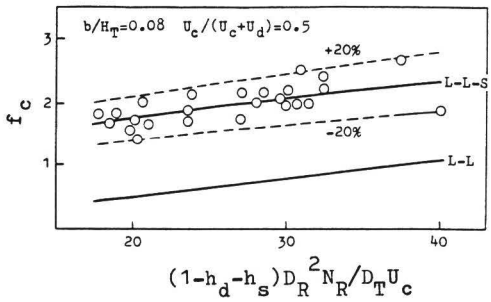

Fig. 2 Correlation of continuous phase axial mixing

for the liquid-liquid system changes little, while that for the liquid-liquid-solid system increases with increasing rotor speed. From experiments it has been found that f_c is dependent not only on the rotor speed and column geometry but also on the values U_c, U_d and U_s (the superficial velocity of each phase). Using optimization method to correlate 60 raw data obtained in the liquid-liquid-solid experiments, and empirical expression for the continuous phase backflow ratio f_c is as follows:

$$f_c = 38.2(b/H_T)^{1.54}\left[U_c/(U_c+U_d)\right]^{0.57}\left[D_R^2 N_R(1-h_d-h_s)/D_T U_c\right]^{0.4} \qquad (3)$$

where h_d and h_s are dispersed phase hold-up and solid phase hold-up respectively.

Figure 2 gives the comparison between the experimental data and the calculated values for liquid-liquid-solid system. The line representing the liquid-liquid system given by Zhu (1989) is also shown.

3.2 Dispersed phase axial mixing

From Figure 3 it seems that at low rotor speed, the dispersed phase backflow ratio f_d is almost independent of the rotor speed, and then drops slightly as the rotor speed further increases. It may be attributed to the observed phenomena that the range of drop size becomes even narrower at high rotor speed than at low. This characteristic of OTRDC is in good agreement with the previous study on liquid-liquid system (Zhu, 1989). The experiments also reveal that f_d decreases with increasing U_s (Figure 4), but increases with increasing U_c (Figure 3). The explanation for the latter case may be due to high entrainment of small drops at high value of U_c.

In comparison with liquid-liquid system, the dispersed phase axial mixing of liquid-liquid-solid system is apparently small under the same operating conditions (Figure 3). It is probably due to the presence of solid particles which enhance stirring intensity and result in a rela-

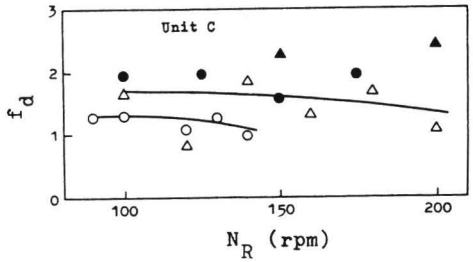

	U_c 10^{-3}m/s	U_d 10^{-3}m/s	U_s 10^{-3}m/s
△	4.96	1.65	0.280
○	3.31	3.31	0.194
▲	4.96	1.65	-
●	3.31	3.31	-

Fig. 3 Dispersed phase axial mixing

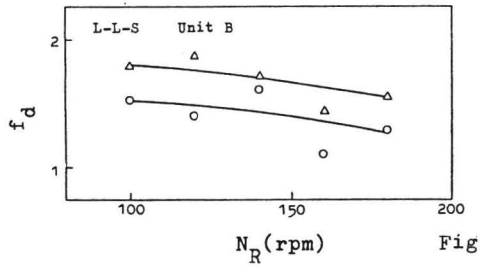

	U_c 10^{-3}m/s	U_d 10^{-3}m/s	U_s 10^{-3}m/s
○	3.31	3.31	0.321
△	3.31	3.31	0.194

Fig. 4 Dispersed phase axial mixing

tively narrow spectrum of drop size. It also accounts for the experimental results that f_d falls as the superficial velocity of solid phase U_s increases.

Experimental values were treated by similar manner to that used in the continuous phase axial mixing. The backflow ratio f_d can be expressed as

$$f_d = 16.39(b/H_T)^{0.95}\left[(D_s^2-D_A^2)/D_T^2\right]^{0.44}(U_c/U_s)^{0.25}(D_R N_R h_d/U_d)^{-0.15} \quad (4)$$

where D_A is the shaft diameter.

3.3 Solid phase axial mixing

Figure 5 shows the effect of rotor speed on the solid phase backflow ratio. When the rotor speed is low, the deposition of a certain portion of particles on the stator rings has been observed and led to much longer residence time of these particles than the average. Therefore, f_s also appears high. However, with increasing rotor speed, the particles can be kept in suspension and pass through the column freely. As a result, the value of f_s decreases rapidly and approaches a constant value. It can be also seen from Figure 5 that the values of f_s for the particles of different sizes differ from each other, the upper curve $d_m = 0.225\times10^{-3}$m and the lower for $d_m = 0.184\times10^{-3}$m. Therefore, it appears reasonable to

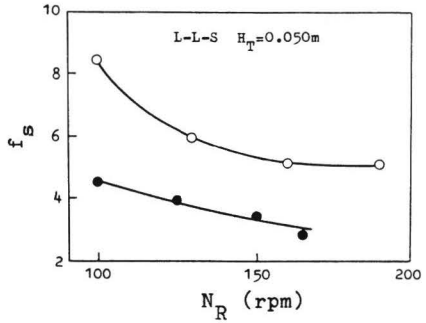

	d_m 10^{-4}m	U_c 10^{-3}m/s	U_d 10^{-3}m/s	U_s 10^{-3}m/s
o	2.25	3.31	3.31	0.280
●	1.84	3.31	3.31	0.280

Fig. 5 Solid phase axial mixing

say that fine particles will be easily "fluidized" by the action of rotors. From experiments U_s and U_d have no significant influence on f_s. The solid phase axial mixing is determined mainly by column geometries and the rotor speed as well as the nature and size distribution of the particles.

From the experimental data the solid phase axial mixing may be correlated by following equation:

$$f_s = 0.012(b/H_T)^{-2.46}\left[(D_s^2-D_A^2)/D_T^2\right]^{-2.03}(U_t/D_R N_R)^{0.85} \qquad (5)$$

where U_t is the terminal settling velocity and comprises the influence of particle size.

4 CONCLUSION

When quartz particles are used as solid phase in liquid-liquid-solid system, it seems appropriate to use marble particles impulse technique to estimate the solid phase axial mixing during the operation of OTRDC. But the model, which treats the behaviour of the solid particles as though it were a continum, is only a rough approximation to the actual behaviour.

The presence of solid particles will result in larger continuous phase but smaller dispersed phase axial mixings than for the liquid-liquid system. The rotor speed and particle size distribution are the predominant factors which influence the solid phase axial mixing.

5 REFERENCES

MECKLENBURGH, J.C. and S. HARTLAND, 1975, The Theory of Backmixing, p.53, John Wiley & Sons.

ZHU, F.G., X.D. NI, Y.C. ZHOU, S.C. YU and Y.F. SU, 1984, AIChE Symposium Series, No. 238, p.115, Vol.80.

ZHU, J.W., 1989, Ph.D. Thesis, East China Institute of Chemical Technology, Shanghai, CHINA.

ZHU, J.W., X.K. ZHOU, X.X. CHEN and Y.F. SU, 1989, ACHEMASIA'89, p.124.

Solvent Extraction 1990, T. Sekine (Editor)

© 1992 Elsevier Science Publishers B.V. All rights reserved

INTERFACIAL AREA OF LIQUID-LIQUID DISPERSION IN A MIXER-SETTLER EXTRACTION COLUMUN

K. Takahashi and H. Takeuchi
Depertment of Chemical Engineering, Nagoya University, Nagoya 464-01(Japan)

ABSTRACT

Holdups and drop sizes in a stirred liquid-liquid dispersion were measured in a single-stage mixer-settler column having a lifter turbine impeller and the downspouts. From the holdup profile in the vertical direction in the mixer, a simple model was developed to predict the dispersed phase holdup. The model parameters were correlated with the agitation speed, the interfacial tension and the density difference between phases. Sauter mean diameter of the dispersed droplets was correlated with Weber number and the mean residence time of dispersed phase. Dropsize distribution had two peaks and the peak fraction of smaller drop increased with the mean residence time of dispersed phase.

INTRODUCTION

Many types of extraction column have been reported, and new devices have been developed to improve the throughput and the extraction efficiency. The agitation with impellers is useful for obtaining large interfacial area. As the agitation speed increases, however, the countercurrent operation becomes difficult and the stage efficiency drops because of back-mixing. Enhancement of the drop coalescence between the compartments is useful for the improvement of the throughput and the stage efficiency (Steiner et al., 1984; Caubinger et al., 1983; Bailes et al., 1987). In mixer-settler columns, the dispersed phase is coalesced more completely and high stage efficiency can be achieved (Horvath et al., 1985). To elucidate the extraction behavior in the mixer-settler column, the interfacial area in the mixer as well as the mass transfer characteristics must be known. In the present work, the holdup and the drop size of dispersed phase were investigated in a single-stage mixer-settler column having a lifter turbine impeller and the downspouts.

1. EXPERIMENTAL

Experimental apparatus used in this work is shown in Fig.1, which gives two sectional views. This apparatus corresponds to one stage of the mixer-settler column, and consists of two parts: a lower mixer and an upper settler. A 6-blade lifter turbine (LT) is installed in the mixer. Aqueous phase (continuous phase) is led to the bottom of the mixer through two pipes and is discharged from the bottom of the settler through two other pipes (downspouts). Organic phase (dispersed phase) is also introduced from the bottom of the mixer and is

drawn from the top of the settler. A liquid sample was drawn from the mixer with a syringe and the volume of organic phase as well as the total amount of the liquid sample was measured to determine the holdup of the dispersed phase. Drop sizes were measured by photography through the vessel wall. A small mirror reflecting the light from a stroboscope was located at the level of impeller and 4cm distance from vessel axis by the same way as Imai et al. (1984). The magnification of photograph was between 22 and 60.

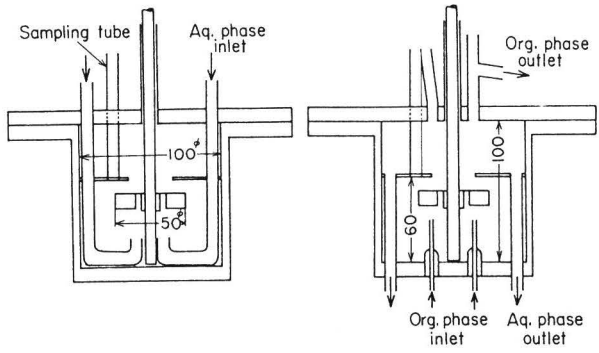

Fig.1 Sectional views of experimental apparatus cut by two axial planes at right angles to each other

The organic phase used in the experiments was tributyl phosphate(TBP)-n-heptane solution or cyclohexane; the aqueous phase was deionized water. For TBP-n-heptane solution, the interfacial tension, γ, against water reduces remarkably in the presence of a small amount of TBP, while the density, ρ, increases linearly with TBP concentration. All the experiments were carried out at room temperature of 25 ± 1°C.

2 RESULTS and DISCUSSION

2.1 Dispersed-phase Holdup in Mixer

Local holdup, ϕ, of the dispersed phase in the mixer is shown in Fig.2 against the vertical distance, H, from the bottom of the mixer. The value of ϕ below the LT impeller varies little with H (circulating zone), but decreases suddenly near the lower end of the impeller (diffusion zone) and becomes constant above the impeller (free rising zone).

Since there is no circulating flow above the LT impeller, the motion of drops would follow a free rising pattern and the holdup may be expressed in a similar way as a spray column. When the

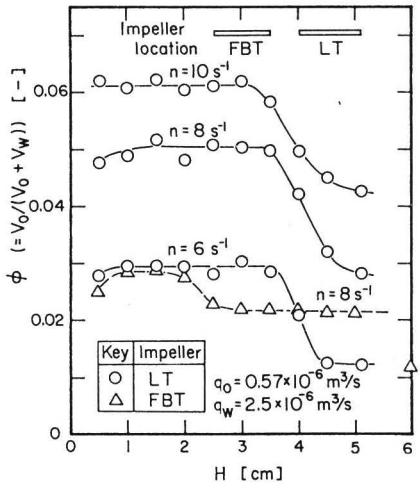

Fig.2 Holdup profile of dispersed phase in vertical direction of mixer

dispersed and the continuous phases flow cocurrently through the mixer, the relative velocity, v_r, between phases is given by

$$v_r = [(q_o/\phi^u) - \{q_w/(1 - \phi^u)\}]/A \quad (1)$$

where A is the cross-sectional area of flow pass around the impeller, ϕ^u the holdup above the impeller, q_o and q_w the flow rates of organic and aqueous phases, respectively. The value of v_r calculated with ϕ^u obtained experimentally was hardly affected by q_o and q_w, being correlated as follows.

$$v_r = 0.00029(3.3\Delta\rho\gamma)^a; \quad a = 0.2 + 13/(n^{1.65}) \quad (2)$$

where $\Delta\rho$ is the density difference between organic and aqueous phases, n the agitation speed.

Circulating flow exists below LT impeller, and both the dispersed and the continuous phases flow out through the space around the impeller. The holdup, ϕ^L, below the impeller may be dependent on the discharge mode of the dispersed phase from the circulating zone. Diffusional transfer of dispersed phase depending on the holdup gradient near the lower end of the impeller may be expected as well as the discharge by axial flow, and the discharge rate of the dispersed phase can be expressed as

$$q_o = (q_o + q_w)\,\phi^L + KA(\phi^L - \phi^U) \quad (3)$$

where K is the transfer coefficient. The value of K varied little with the flow rate or TBP concentration in organic phase, and was correlated by

$$K = 0.043 + 260/(n^7) \quad (4)$$

For $n > 7\ s^{-1}$, K was independent of n. This might result from that the increase in the dispersion coefficient with n was compensated with the increase in the diffusion distance as can be seen in Fig.2. At low agitation speed, large drops may leave the ciculating zone by buoyancy. As a result, K increased with the decrease in n.

Holdups below and above the impeller are derived from Eqs.(1) and (3) as follows.

$$\phi^L = (q_o + KA\phi^U)/(q_o + q_w + KA) \quad (5)$$

$$\phi^U = (b - \sqrt{b^2 - Av_r q_o})/Av_r \; ; \; b = q_o + q_w + Av_r \quad (6)$$

The values of ϕ^L for cyclohexane-water system were calculated from Eqs.(5) and (6) with v_r and K given by Eqs.(2) and (4), respectively, and were compared with the experimental results in Fig.3. The effects of flow rates q_o and q_w on

the holdup are well explained by Eqs.(5) and (6). Details about the dispersed phase holdup were given in a previous paper (Takahashi et al., 1990)

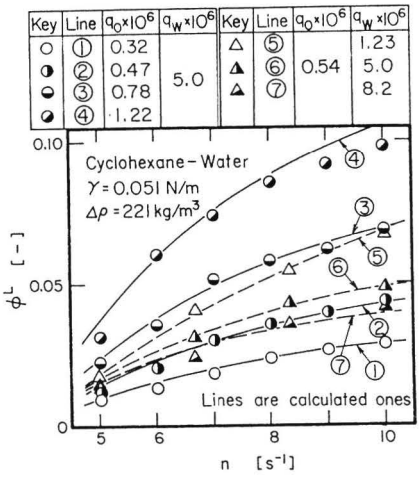

Fig.3 Comparison of calculated holdup with experimental one

2.2. Drop Sizes

(i) Sauter mean diameter. For the organic phase of TBP-n-heptane solution, Sauter mean diameters, d_{32}, of dispersed drops are plotted against n in Fig.4. Points for each concentration of TBP are on a straight line of the slope - 1.9. As the increase in the TBP concentration, d_{32} decreases because of the decrease in the interfacial tension. In Fig.5, values of $d_{32} \cdot n^{1.9}$ are plotted against γ ; the slope is 0.96. Since the absolute value of the slope in Fig.4 is just twice of that in Fig.5, d_{32} can be correlated with Weber number, We ($=D_i^3 n^2 \rho/\gamma$), as follows.

$$d_{32}/D_i = 1.00\ W_e^{-0.95} \qquad (7)$$

where D_i is the impeller diameter. The dependency on We is close to that obtained for the batch stirred vessel by Konno et al. (1987). The value of d_{32}/D_i in the present work, however, is about three times larger than that for the batch stirred vessel, because the residence time of the dispersed phase was very short in comparison with the experiments of the batch stirred vessel.

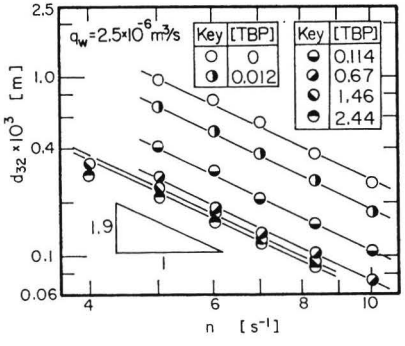

Fig.4 Sauter mean diameter of dispersed drops against agitation speed

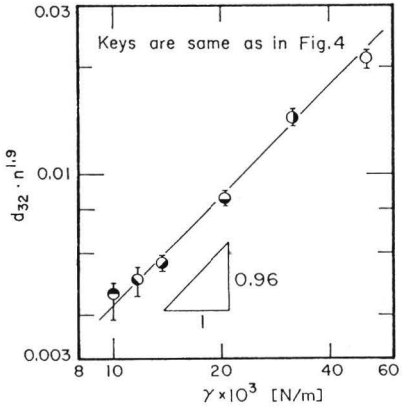

Fig.5 Effect of interfacial tension on Sauter mean diameter

As the value of q_w increses, the holdup of the dispersed phase decreased as shown in Fig.3, i.e., the mean residence time $\bar{\theta}_o$, of the organic phase below the impeller in the mixer became small. Figure 6 shows the effect of q_w on d_{32} and the broken line represents $\bar{\theta}_o$ calculated from ϕ^L given by Eq.(5). From these results the following relation, which was the same as with the relation between the drop size and the agitation time in the batch stirred vessel (Skelland et al., 1981, Konno et al., 1983), was derived

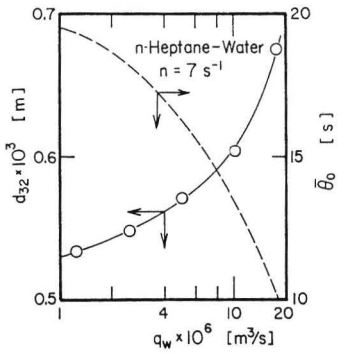

Fig.6 Effect of aqueous flow rate on Sauter mean diameter

$$d_{32} \propto \bar{\theta}_o^{-0.36} \qquad (8)$$

Since ϕ^L (i.e, $\bar{\theta}_o$) varied with n or TBP concentration in the organic phase, d_{32} in Fig.4 might be affected with $\bar{\theta}_o$. The correlation of Eg.(7) was modified by use of Eq.(8) as follows.

$$d_{32}/D_i = 0.86We^{-0.72}\,\bar{\theta}_o^{-0.36} \qquad (9)$$

The absolute value of dependency of the We became smaller than that in Eq.(7), and it is larger than 0.6 obtained by many investigators for the batch stirred vessel (Coulalouglou et al., 1976).

(ii) Drop size distribution.

Volumetric drop size distributions are shown in Fig.7. For the case of small n, two peaks are observed in the distribution. When the distribution was divided into two single peak distributions under the assumption that the first distribution (for small drops) was symmetric, the first one was given by a normal distribution and the second one by a logarithmic normal distribution. The fractions, F_{V2}, of the second distribution are given against $\bar{\theta}_o$ in Fig.8. The value of $\bar{\theta}_o$ was varied using three methods: by changing TBP concentration in the organic phase, n

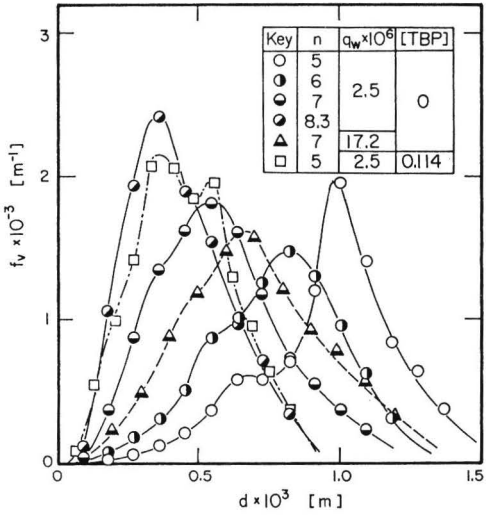

Fig.7 Volumetric drop size distribution

or q_w. In any case F_{V2} decreased with $\bar{\theta}_o$, that is, the fraction of the first distribution increased with the holdup ϕ^L. This indicates that the drops of the first distribution may be the circulating ones because the increase in the circulating drops results in the increase of ϕ^L. The drops of the second distribution may be generated by the initial breakage of the inlet organic phase.

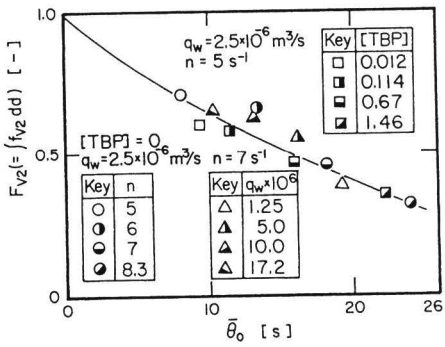

Fig.8 Fraction of second peak in drop size distribution against mean residence time of organic phase

CONCLUSION

Large difference of the dispersed phase holdups between above and below the lifer turbine impeller has been obserbed in the mixer-settler column. The holdups were expressed by a simple model (Eqs.(1) and (3)). Drop size varies with the agitation speed, the interfacial tension and the residence time of dispersed phase; it was correlated by Eq.(9). Two peaks appeared in the drop size distribution and the fraction of the first peak increased with the mean residence time of dispersed phase.

REFERENCES

Bailes,P.J. and Stitt,E.H.,1987. Column liquid contacting with vigorous agitation balanced by electrostatic coalescence. Chem. Eng. Res. Des., 65: 514-523

Caubinger,W., Husung,G. and Marr,R.,1983. Operating behaviour of the self-stabilizing high performance extractor "SHE". Ger. Chem. Eng.,6:74-79

Coulalouglou,C.A. and Tavlarides,L.L., 1986. Drop size distributions and coalescence frequencies of liquid-liquid dispersion in flow vessels. AIChE J., 22: 289-297

Horvath,M. and Hartland,S.,1985. Mixer-settler-Extraction column: mass transfer efficiency and entrainment. Ind. Eng. Chem. Process. Des. Dev., 24:1220-1225

Imai,M. and Furusaki,S.,1984. Sauter mean drop size of W/O/W emulsions in agitated vessele. Kagakukogaku Ronbunshu, 6: 707-713

Konno,M., Aoki,M. and Saito,S.,1983. Scale effect on breakup process in liquid-liquid agitated tanks. J. Chem. Eng. Japan, 16: 312-319

Konno,M. and Saito,S.,1987. Correlation of drop sizes in liquid-liquid agitation at low dispersed phase volume fractions. J. Chem. Eng. Japan, 20, 533-535

Skelland,A.H.P. and Lee,J.M.,1981. Drop size and contiuuous-phase mass transfer in agitated vessels. AIChE J., 27: 99-111

Steiner,L., Fisher,E. and Hartland,S.,1984. Performance of a liquid-liquid extraction column with enhanced coalescence lattice. AIChE Symp. Ser.,80, No.238:130-138

Takahashi,K. and Takeuchi,H.,1990. Holdup of dispersed phase in a mixer-settler extraction. J. Chem. Eng. Japan. 23: 12-17:

Solvent Extraction 1990, T. Sekine (Editor)
© 1992 Elsevier Science Publishers B.V. All rights reserved

MASS TRANSFER TO FREELY MOVING DROPS

J.TEMOS, H.R.C. PRATT and G.W.STEVENS
Department of Chemical Engineering, University of Melbourne, Parkville Victoria 3052 (Australia)

ABSTRACT
Overall mass transfer coefficients for individual droplets have been obtained for the MIBK/HAC/water system in a "single file" droplet column. Dispersed phase film coefficients were also obtained for the presaturated MIBK/water system using tritiated water as solute. Results indicate that for the systems studied, the coefficient is initially strongly time dependant, decreasing from a high value and becoming relatively constant after the drop traverses a distance of 15 to 30cm; this is several times the distance required to attain the terminal velocity. The results show that useful data can only be obtained from single file columns by conducting experiments over a full range of heights.

INTRODUCTION

The prediction of mass transfer coefficients for single drops has been investigated by many workers; however, their conclusions are often conflicting and a high degree of uncertainty exists. This is due to the difficulty of quantifying the hydrodynamics and related phenomena as well as the mechanisms of the mass transfer process itself.

With systems for which the drop phase is the controlling resistance, three models exist. For internally stagnant drops where mass transfer is by pure molecular diffusion, the model of Newman (1931) applies. Kronig and Brink (1950) developed a model (henceforth termed "KB model") for diffusion in laminar circulating drops where the streamlines are those described by Hadamard. Handlos and Baron (1957) extended this model ("HB model") to turbulent circulating drops where mass transfer takes place within internal circular toroidal streamlines. Most investigations have found that stagnant drops can be represented by the Newman model. For Reynolds numbers of less than about 20, the KB model has been used with limited success. For higher Reynolds number ranges, the coefficients have mostly been found to lie between those given by the KB and HB models.

For systems where the continuous phase is the controlling resistance, much of the data have been correlated using an equation developed on the basis of dimensional analysis, of the form

$$Sh = A + B\ Re^{m}Sc^{n} \qquad (1)$$

In general m is found to be about 1/2 and n about 1/3, with A strongly negative for circulating drops; for noncirculating drops, however, as

obtained when a surfactant is present, the value of A approaches 2 as for solid spheres (Thorsen and Terjesen, 1962). The theoretical models that have been developed apply only at the extremes of the Reynolds number range, i.e. Re<<1 (creeping flow) and Re>>1.In the intermediate range of Reynolds number, no theoretical models have been able to explain the available data with any degree of reliability and much work remains to be done in this area.

The basic problem therefore lies in the interpretation of the experimental data. Too often, the hydrodynamics of the two phases are not well characterized and there is no real way of determining whether a certain model will apply for a given set of conditions. Further, it is difficult to characterize the degree of contamination by surface active agents, the effect of which is usually a reduction in the mass transfer rate. Although in most experimental work efforts are made to keep equipment and materials clean, the best that can really be hoped for is a minimization of contaminants. Also, the influence of Marangoni effects in causing interfacial oscillation gives cause for concern as no satisfactory theory is available to predict their existence and their net effect on the mass transfer.

Finally, in many experimental investigations it has been assumed that the mass transfer coefficient during free rise or fall is constant. This is generally not the case, as the rate of penetration into the drop is a function of the time of contact. This means that experimental data has to be carefully interpreted to avoid incorrect conclusions being reached.

This paper examines the problems in interpreting data from single file droplet columns. Data are presented for experiments with binary systems comprising MIBK/H_2O in which the organic phase was saturated with water containing tritium, and for the ternary MIBK/HAc/H_2O system with acetic acid as the transferring solute.

2 EXPERIMENTAL

2.1 Equipment

The column containing the stationary continuous phase was a 38mm i.d. QVF glass section, with a base consisting of a s.s. plate clamped with a Teflon gasket in between. A range of drop sizes was investigated by interchanging nozzles of differing diameters.

The dispersed phase was contained in a microburette connected to a constant head device to provide a constant flowrate to the nozzle. An infrared detector was used to monitor drop formation; the inlet flow was adjusted using a micrometer valve in the feed line to maintain a constant formation time.

After passing through the column, the drops coalesced in an inverted funnel whose position could be varied in the column. A small interface

was maintained just below the neck of the funnel by controlling the rate of removal of the coalesced phase with a valve. For a ternary system all the dispersed phase was removed for analysis. Typically, over 1000 drops passed through the column for the ternary system and about 5 to 7 ml was collected separately for analysis. The drop size was determined from the number of drops registered by a chart recorder and the volume of the dispersed phase collected; the latter was then compared with the volume entering the column. Acetic acid was determined by titrating with 0.1 M NaOH using phenolphthalein as the indicator. It was found that the composition of the continuous phase did not change significantly during the course of a run.

With the systems containing radioactive tracers, the first 1 to 2 ml of sample were discarded, after which, about 3 ml of dispersed phase was collected as sample. The samples were analyzed for tritium in a Packard Tricarb 2000CA Liquid Scintillation Analyzer.

The drop velocities were measured using two other infrared detectors spaced 30 to 40 cm apart, with the lower detector about 30 cm above the nozzle. When the drop paths deviated appreciably from the vertical, they were timed using a stopwatch. The velocity of the drops were based on a minimum of 10 to 20 measurements.

The experiments were conducted at ambient temperature and the recorded data covers a temperature range of about 17-25°C. The temperature on any one day of an experiment, where only one drop size was investigated, varied only by ±1°C.

2.2 Materials Used

(i) Non-radioactive system. The MIBK and acetic acid were of analytical grade quality. Distilled water was used throughout. Prior to an experiment, the MIBK and water were mutually saturated and separated, and the acetic acid subsequently added to the relevant phase. The starting concentration of acid used was about 5 wt% in either phase.

(ii) Radioactive system. Tritiated water was obtained from Amersham Chemicals. The continuous water phase was inactive and was saturated with MIBK, while the dispersed MIBK phase was saturated with tritiated water. Thus transfer of the active material took place from the dispersed to the continuous phase. At the end of each run, the continuous phase was discarded and fresh material used.

3 RESULTS

The mass transfer process is represented by the following differential mass balance on a drop.

$$dN_a = V_d\, dC_d = k_{od}\, a\, (C_{d,eq} - C_d)\, dt \qquad (2)$$

Integration over the path length gives

$$\mathrm{Ln}\left(\frac{C_{d,eq} - C_{d,F}}{C_{d,eq} - C_{d,h}}\right) = \frac{6k_{od}}{v_D.d}h \qquad (3)$$

A similar result is obtained for the case of transfer from the dispersed to continuous phase. In each case, the logarithmic term is plotted against the height, h. The gradient at any point of the resulting curve is directly related to the mass transfer coefficient.

Figure 2 shows data for the ternary system with transfer from the continuous to dispersed phase. At the lower heights (<30 cm), the line is curved, indicating a high initial coefficient which decreases with height until it becomes effectively constant. Similar behaviour is shown in Figure 3 for the radioactive system, in which the transfer is from the dispersed to the continuous phase. For the ternary system with transfer from the dispersed to continuous phase (Figure 1), the plot is essentially linear over all heights, indicating a constant mass transfer coefficient. Figure 4 shows a typical plot along with model predictions for the dispersed phase coefficient. The extended HB model with four eigen values was used as described by Korchinsky and Cruz-Pinto (1979). For the KB model, the eigen values as given by Johnson and Hamielec (1960) were used, with diffusivities calculated using the Wilke and Chang (1955) correlation.

4 DISCUSSION

The variation in the mass transfer coefficient can be explained by considering the motion of a drop. As the drops begin to form, the interfacial area increases and solute is transferred. On detachment from the nozzle, the initial movement is unstable. During rise, the circulation patterns inside the drop begin to develop and the boundary layers are set up. Eventually, after the initial transients have died away, the droplets attain a stable hydrodynamic configuration and rise in a straight path. The drops, however, reach their terminal velocity in the first 10cm of rise, less than the distance required for the initial instabilities to disappear.

For transfer from the continuous to the dispersed phase with the ternary system, the high initial rate of mass transfer appears to be due to the high flux of acetic acid into the drop, as well as transfer of MIBK out of the drop and H_2O into the drop. This was found by comparing the inlet and outlet diameter of the drops. The outlet diameter was found to be constant for all heights, but was always greater than the inlet diameter.

The data obtained for the radioactive tracer showed similar trends.

In this case, there was no net transfer of material as the two phases were saturated and only radioactive solute was transferred. These experiments eliminated the troubling Marangoni effect so that the mass transfer mechanism was purely diffusional. It was found, in general, that the results for spherical circulating drops did lie somewhere between the HB and the KB models.

For transfer of acetic acid from dispersed into continuous phase, the mass transfer coefficient was found to be high and constant. This suggests that oscillation of the droplet interface was occurring. The droplet motion was also non-linear with an appreciable horizontal component throughout.

In conclusion, useful data from single file droplet columns can only be obtained if experiments are conducted over a full range of heights. The often used method of selecting two heights to measure a mass transfer coefficient can lead to incorrect values of the coefficient.

5 NOMENCLATURE

a = interfacial area, cm^2.
$C_{d,eq}$ = concentration of solute in dispersed phase in equilibrium with concentration of solute in continuous phase, g cm^{-3}.
$C_{d,F}$ = concentration of solute in dispersed phase feed, g cm^{-3}.
$C_{d,h}$ = concentration of solute in dispersed phase at height h, g cm^{-3}.
D = diffusion coefficient, $cm^2\ s^{-1}$.
d = droplet diameter, cm.
k_{od} = overall mass transfer coefficient based on dispersed phase, cms^{-1}.
N_a = mass flux of component A, g $s^{-1}\ cm^{-2}$.
t = time, s.
v_d = droplet velocity, cm s^{-1}.
V_d = droplet volume, cm^3.
A,B,m and n = constants in Equation (1).
Re = Reynolds number, $d\ v_d\rho_c/\mu_c$.
Sc = Schmidt number, $\mu_c/\rho_c D$.
Sh = Sherwood number, $k_{od}d/D$.

6 REFERENCES

Handlos, A.E. and Baron, T., 1957. A.I.Ch.E.J., 3:127-136.
Johnson, A.I. and Hamielec, A.E., 1960. A.I.Ch.E.J., 6:145-149.
Korchinsky, W.J. and Cruz-Pinto, J.J.C., 1979. Chem. Eng. Sci., 34:551-561.
Kronig, R. and Brink, J.C., 1950. Appl. Sci. Res., A2:142-154.
Newman, A.B., 1931. Trans. A.I.Ch.E.J., 27:310-333.
Thorsen, G. and Terjesen, S.G., 1962. Chem. Eng. Sci., 17:137-148.
Wilke, C.R. and Chang, P., 1955. A.I.Ch.E.J., 1:264-270.

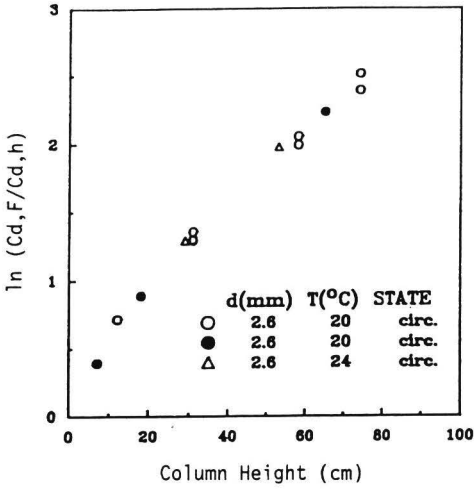

Fig 1: Plot of extend of extraction versus column height for MIBK/Acetic acid/water with transfer from dispersed to continuous phase.

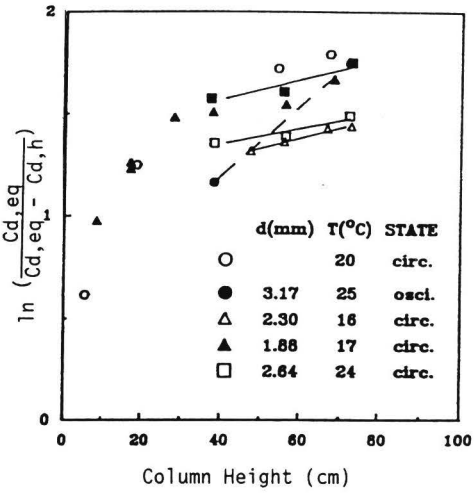

Fig 2: Plot of extent of extraction versus column height for MIBK/Acetic acid/water with transfer from continuous to dispersed phase.

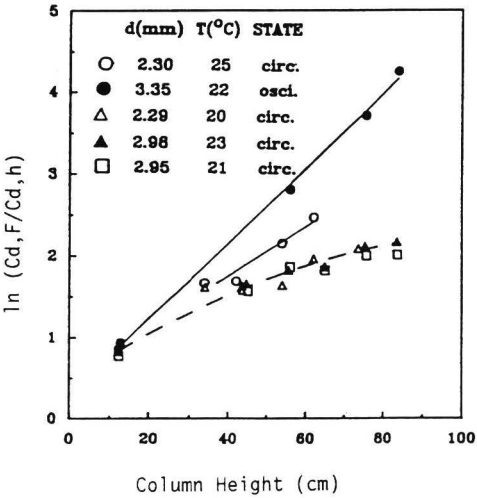

Fig 3: Plot of extent of extraction versus column height for MIBK/Water with tritiated water as the solute.

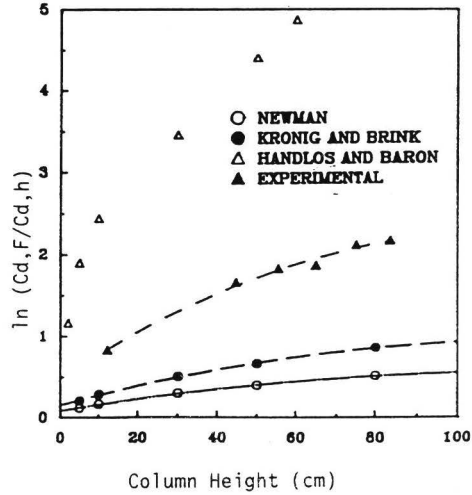

Fig 4: Plot of extent of extraction versus column height for MIBK/Water with tritiated water and model predictions.

Solvent Extraction 1990, T. Sekine (Editor)

© 1992 Elsevier Science Publishers B.V. All rights reserved

HYDRODYNAMICS AND MASS TRANSFER OF A SIEVE PLATE COLUMN FOR LIQUID LIQUID EXTRACTION

Zhu Shenlin, Ye Guiqin, Ke Jiaxiong, Zhang Baoqing, Fei Weiyang
Dept. of Chem. Eng. Tsinghua University, Beijing, 100084, China

ABSTRACT

A systematic study on hydrodynamics and mass transfer of the sieve plate extraction column had been carried out in a 100 mm diameter column with 7 mm hole diameter. The experimental system was 30% TBP(Kerosene as diluent)/Acetic acid/Water and the acetic acid was extracted from the continuous organic phase to dispersed water phase. The Murphree stage efficiency, drop size distribution and dispersed phase hold up were measured simultaneously. An improved hydrodynamic model was proposed. Then, the Overall stage efficiencies were evaluated based on the single oscillating drop mass transfer mechanism. A new procedure for estimating the tray efficiency based on developed correlations had been suggested to design and simulate aromatics extraction column.

INTRODUCTION

The separation of aromatic hydrocarbons from multicomponent hydrocarbon feedstock such as reformed naphtha is considered an important commercial process and is carried out by liquid-liquid extraction. The excellent performance of Sulfolane as a solvent has been demonstrated by many commercial units(Fandary et al, 1989) Because of the high capacity and low cost, the sieve plate extraction column is widely used in the Solfolane process. However, the data of hydrodynamics and interphase mass transfer coefficient in the sieve plate column are still lacking, especially in case of the large hole sieve plate and heavy dispersed phase.This work devotes to study the hydrodynamics and mass transfer of the sieve plate column. Attempts are made to correlate the Murphree stage efficiency against mass transfer of single drop. The nonspherical, oscillating drop mass transfer model(Angelo et al, 1966, Rose and Kintner, 1966) was applied to evaluate the dispersed phase mass transfer coefficient. These estimated overall efficiencies have been compared with results obtained from experiments. Good agreement have been obtained in majority of the experiments. This paper is aimed at developing reliabe models for describing the performance of aromatics extraction columns. It is shown that these models would be useful in the design and simulation of Sulfolane extraction process. It would appear reasonable to assume that the basic principles applying to models for conventional extraction sieve tray columns.

2 EXPERIMENTS

2.1 Description of equipment

The flow diagram of experimental equipment is shown in Fig.1.
Light and heavy phases are fed into the column from feed tanks by centrifugal pumps. After counter current contact they flowed back into their storage tanks. Flow rates are reguated carefully by adjustable valves. The rotameters are used to measure the flow rates. The column is made of hard glass equipped with stainless steel sieve plates.The geometry of the column are listed in table 1.

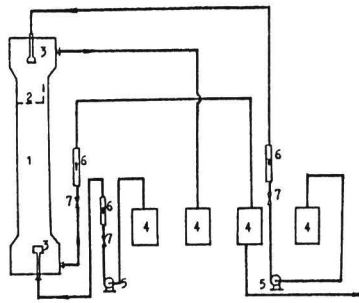

Fig. 1. Flow diagram of experimental equipment
1. glass column, 2. tray cartridge, 3. liquid distributor, 4. feed tanks,
5. centrifugal pumps 6. rotameters, 7. adjustable valves

TABLE 1

Dimension of sieve plate extraction column

inside diameter	0.1m	area holes/area column	7%
effective height	1.0m	area upcomer/area column	10%
tray spacing	0.225m	upcomer height	0.055m
hole diameter	0.007m		

2.2 System studied

Because the interfacial tension is very important for mass transfer efficiency, the 30% Tributyl Phosphate (TBP) in Kerosene/Acetic acid/Water system is used to simulate Sulfolane-hydrocabons system. It's physical properties at 20°C are listed in table 2.

TABLE 2

Physcial properties for system tested

	continuous phase	dispersed phase
density(kg/m^3)	837	997
viscosity(Pa·s)	1.72×10^{-3}	0.94×10^{-3}
diffusivity(m^2/s)	7.8×10^{-10}	1.04×10^{-9}
interfacial tension(N/m)		9.29×10^{-3}

2.3 Experimental methed

As the direction of mass transfer is from organic phase to water, Acetic acid is added to the solvent to prepare the feed solution. Preliminary experiments have shown that steadystate concentration gradients are set up only when the column contents are displaced at least five times, and hence the column was operated under given conditions, more than 30 minutes before sampling. Fresh water was used for every run. Acetic acid concentration in the inlet and outlet streams was determined by titrating a known volume with 0.1N sodium hydroxide solution, using phenol-phthalein as indicator.

The mean drop sizes were determined by direct photography. The camera was Canon-

F1 equipped extension tube, with an exposure1/1000 S. Prints of the photographs taken were enlarged and the drop size and size distribution estimated using microcomputer system. The dispersed phase hold-up was measured by volumetric replacement method.

3 MATHEMATICAL MODEL AND CALCULATION

3.1 Equilibrium data

The equilibrium distribution of acetic acid in water and 30% TBP was measured at 20°C. The data obtained are represented by following equation:

$$Y^*/X = 1.37X + 1.79 \tag{1}$$

When the concentrations of both phases are low, the equilibrium concentration of the acetic acid in water is assumed to be linearly dependent on the raffinate. Then, the equation (1) could be simplified as:

$$Y^* = mX = 1.79X \tag{2}$$

3.2 Mass transfer models

The mass transfer in a separation stage is characterized by the Murphree stage efficiency of dispersed phase:

$$E_{md} = (Y_{n+1} - Y_n)/(Y^*_{n+1} - Y_n) \tag{3}$$

It is influenced by the mean drop size, the residence time of two phases, the mass transfer coefficient and degree of mixing between two phases. In the simplest case of a completely mixed continouus phase the Murphree stage efficiency can be calculated from the contributions of the different contact zones in a separation stage. According to the following zones in each stage could be distinguished liquid jetting, droplet formation, droplet movement and droplet coalescence (Schulz and Pilhofer, 1982, Rocha and Fair, 1986).

When the definition of Murphree stage efficiency is used to a material balance in n-th stage, the general form of the proposed model can be obtained.

$$E_{md} = \frac{1.1K_{fd}A_f + K_{rd}A_r}{Q_d + 0.5K_{rd}A_r + 0.1K_{fd}A_f} \tag{4}$$

However, different authors recommend different approach to calculate the individual mass transfer coefficients which are used for calculating the overall coefficients K_{id}.

$$1/K_{id} = 1/k_{id} + m/k_i \qquad i = f, r \tag{5}$$

For computation of the mass transfer coefficient in droplet formation, the modified Higbie penetration model(Nakaike, 1983) has been found useful. For the stationary droplet movement, Steiner model (Steiner, 1986) is adopted as the mass transfer model for outside of droplets.

The choice of the computational method for the mass transfer coefficient on the inside of the droplets depends on the flow conditions i.e., the Reynolds number Re. Droplet oscillation commences in regimes of Reynolds number 200. This work has demonstrated that best agreement is generally observed with oscillating drop correlations. Therefore the correlation developed by rose and Kintner (1966) for single oscillating drops has been applied to predict the mass transfer coefficient of the dispersed single drop.

4 RESULTS AND DISCUSSIONS

4.1 Hold-up of dispersed phase and characteristic velocity

The slip velocity under countercurrent flow conditions is defined as the sum of linear

velocities of the dispersed and continuous phase. Thus for a sieve plate column:

$$u_s = u_d/x + u_c/(1-x) \tag{6}$$

Experimental work has shown that the slip velocity could be correlated with the characteristic velocity by following simple equation

$$u_s = u_0(1-x) \tag{7}$$

The data of this investigation can be tentatively correlated as

$$u_s = u_0(1-x) = 1.81\left(\frac{\sigma\Delta\rho g}{\rho_c^2}\right)^{\frac{1}{4}}(1-x) \tag{8}$$

Experimental results indicate that the characteristic velocity u_0 is not affected to the velocity of the dispersed at the perforation of 7 mm hole size. This result is similar to the relation found by Laddha et al (1976).

4.2 Drop size distribution

It is necessary to ascertain the drop size and size distribution in order to assess its mass transfer performance. The typical drop size distribution curves are shown in Fig. 2.

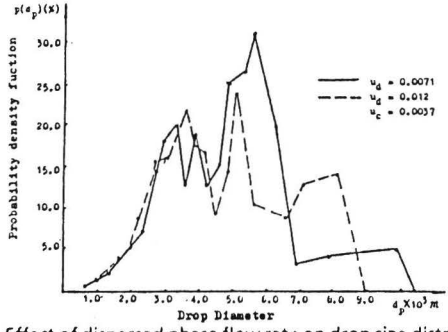

Fig. 2 Effect of dispersed phase flow rate on drop size distribution

At both of low and high superficial velocities the drop sizes spread over a very wide range and curves show a number of peaks. The drop size distribution could be plotted vs the cumulative drop volume(Fig. 3). It is clear from Fig. 3 that the volume fraction of drop in the oscillating drop regime has more than 90% of the drop population. Hence it is assumed that the majority of drops under operating conditions could be described

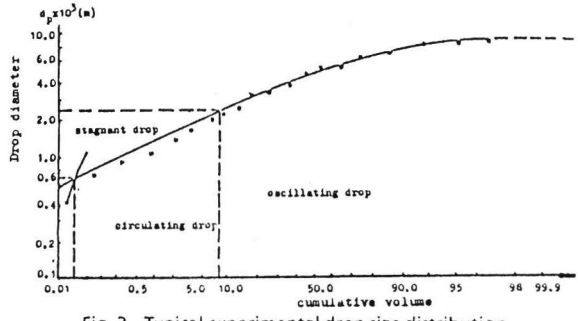

Fig. 3 Typical experimental drop size distribution

by the oscillating model. the Sauter mean drop size is obtained from the statistics of a large number of drops. In this work the experimental $d_{3,2}$ were compared with Seiberti's correlation (1986).

$$d_{3,2} = 1.15K\left(\frac{\upsilon}{\Delta\rho g}\right)^{\frac{1}{2}} \tag{9}$$

It is found the K value of Seibert's equation should equal to 1.50–1.75.

4.3 Mass transfer results

Murphree stage efficiency E_{md} were evaluated using definition in equation (3). In order to study the effect of flow rates on the mass transfer coefficient, both the flow rates of organic and water phase were varied over a wide range. The effect is shown in Fig. 4. It is evident from Fig. 4 that the E_{md} is increased slightly with the dispersed flow rate. This is due to the increase of drop number which increased the interfacial area and also to the vigorous turbulence inside the column. Fig. 4 shows that at a particular dispersed phase rate, The values of E_{md} are almost constant indicating litle dependency on the continous phase flow rate.

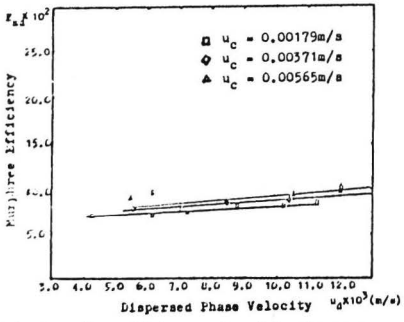

Fig. 4 Effect of Dispersed and Continuous Phase flow rate on Murphree efficiency

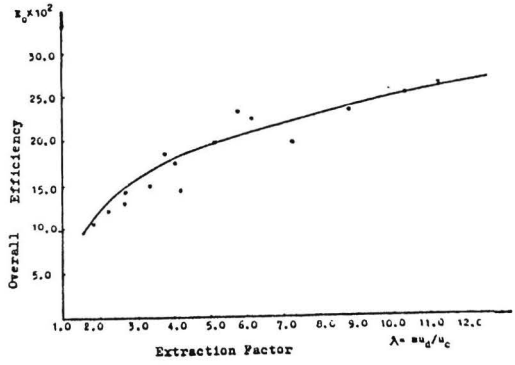

Fig. 5 Effect of extraction factor on Overall stage efficiency

The average Overall efficiencies E_0, are plotted against the extraction factor (mu_d/u_c) (in Fig. 5) which shows that E_0 increases with extraction factor and the variation is linear for larger extraction factor. As m is a constant for given system any variation in the extraction factor is due only to the variation in the flow rates of either phase, u_d and u_c. It is found from Fig. 5 that the calculated results by presented models in this work are good agreement with the majority of the experimental data. The models selected in this work are different from those published by Rocha et al (1986). This set of models is composed of individual models for predicting hydraulic parameters, mass transfer coefficients and Murphree and Overall efficiencies. For the system studied, the model generally underpredicted Overall efficiencies but provided a reasonably good fit to the data within ±15%. Nevertheless, the applicability of the models appears to be clear, especially since the general trend efficiency underprediction in a pilotscale column such as the one used in this work can be beneficial to the use the model for commercial column.

5 CONCLUSIONS

On the basis of the present investigation the following may be concluded:

(1) The fundamental equation of flow characteristics for the sieve-plate extraction column should be expressed as:

$$u_s = u_d/x + u_c/(1-x) = 1.81\left(\frac{\sigma\Delta\rho g}{\rho_c^2}\right)^{\frac{1}{4}}$$

(2) It is known from drop size distribution that the oscillating droplets in drop population are exceed 90% in proportion to the volume fraction. The sauter mean diameter of drop, $d_{3,2}$ is related to the physical properties of the system. the expression found in this work is

$$d_{3,2} = 1.15K\left(\frac{\sigma}{\Delta\rho g}\right)^{\frac{1}{2}} \quad K = 1.50 - 1.75$$

(3) In connection with single drop mass transfer, overall efficiency can be predicted from the mass transfer model of oscillating drop. Predicted overall efficiencies are close to the majority of the experimental values with deviation within ±15%.

(4) The correlation obtained in this work can be used to simulation and design of sieve plate column in aromatics extraction process. More work should be carried out with different testing system to prove further the conclusions obtained in this work.

NOMENCLATURE

A = interfacial area, m^2
d_0 = hole diameter, m
d_p = drop diameter, m
D = diffusion coefficient, m^2/s
E_{md} = murphree stage efficiency
E_0 = overall tray efficiency
g = accelearation due to gravity, $9.8 m/s^2$
h_c = heihgt of the coalesced layer, m
H_t = plate spacing, m
K_{td} = overall mass transfer coefficient, m/s
m = distribution coefficent
Q = volumetric flow, m^3/s
Re = Reynolds number
u = superficial velocity of phase, m/s
u_s = slip velocity, m/s
u_0 = characteristic velocity, m/s
x = operation hold up
X = mass fraction solute in organic phase
Y = mass fraction solute in water phase

Greek synbols

$\Delta\rho$ = phase density difference, kg/m^3
λ = extraction factor (mu_d/u_c)
σ = interfacial tension, N/m
ρ = density, kg/m^3
μ = viscosity, Pa·s

Subscripts

c = continuous phase
d = dispersed phase
f = formation
r = rise (or fall)

REFERENCES

Angelo, J.B., E. N. Lightfoot and D.W. Howard, AIChE J. 1966, 12, 751.
Fandary, M.S.h., G.S. Aly and M.A. Fahim, Solvent Extraction and Ion Exchange, 1989 , 7, 677.
Laddha, g.S., N. Prabhu., Indian Journal of Technology, 1976, 14,55.
Nakaike, Y. and T. Tadaki, Kagaku Kogaku Ronbunshu, 1983, 9, 135.
Rocha, J.A., and J. r. Fair., Ind. Eng. Chem. process Des. Dev. 1986, 25, 862.
Rose, P.M., and R. C. Kintner, AIChE J., 1966, 12, 530
Schulz, L., and T. Pilhofer, Inter. Chem. Eng. 1982, 22, 61.
Steiner, L., Chem. Eng. Sci, 1986, 8, 1979.
Seibert, A. f., Ph. D. Dissertation, The University of Texas at Austin, 1986.

Solvent Extraction 1990, T. Sekine (Editor)

© 1992 Elsevier Science Publishers B.V. All rights reserved

HYDRODYNAMIC AND MASS TRANSFER CHARACTERISTICS OF A SPRAY COLUMN WITH VERTICAL PARALLEL PLATE ELECTRODES

Manabu YAMAGUCHI, Satoshi YOSHIYASU, Tsuneo IMAI, Hideyuki KUNIMASA, and Takashi KATAYAMA
Department of Chemical Engineering, OSAKA UNIVERSITY, Toyonaka 560, Japan

ABSTRACT

A spray liquid-liquid extractor with vertical plate electrodes was devised. The population behavior of dispersed drops in a d.c. electric field was studied on dispersed phase holdup, drop velocity and drop size distribution and axial mixing of continuous phase by using the system of water drops in cyclohexane. Mass transfer efficiency of iodine from the dispersed phase into the continuous phase was also measured. The axial mixing and the mass transfer were effectively improved with the applied voltage. Simulation of the present column efficiency was carried out by using a modified dispersion model.

INTRODUCTION

Novel liquid extractors equipped with electrodes have been developed/5-7/; one/7/ was an "inclined electrostatic liquid-liquid contactor" equipped with a plate electrode with notched flash-boards and the other/5,6/ was a "spray column" equipped with vertical four rod electrodes. It was /5-7/ that their extractors had some favorable characteristics for liquid dispersion, mixing of the liquid phases, phase separation and others, but dispersed phase holdup was low. In the present study, a spray column equipped with vertical parallel plate electrodes was designed to improve the dispersed phase holdup and liquid dispersion of previous extractors. The electrohydrodynamics and the mass transfer characteristics of the column were investigated.

EXPERIMENTAL

1.1 Experimental apparatus

Figure 1 shows a schematic diagram of the experimental apparatus, which is essentially the same as shown in the previous study/5/ except the arrangement of the electrodes and its shape. They influence significantly electrohydrodynamic behavior of the drops, such as coalescence, redispersion and motion of the drops. The test column ② was made of transparent acrylic resin and, 90 mm inner dia. and 380 mm high, had a cross section(B-B) shown in the figure. Two copper plate electrodes ④ ⑤ coated by a thin layer of teflon, 270 mm long, 60 mm wide and 2 mm thick, were installed vertically along the inner wall of the column and were faced apart 67 mm each other. One of the electrodes ④ was connected to a high-voltage generator ⑮ and the other ⑤ was grounded.

The upper part ① of the column was equipped with a distributor having 25 pieces of stainless hypodermic tubing (0.5 mm i.d.) for supply of the dispersed phase. The lower part ③ of the column was equipped with a distributor having two sets of 15 holes (3 mm dia.) each for supply of the continuous phase ⑦ and a tracer liquid phase ⑧, respectively, and with an outlet for the dispersed phase ⑥ . Arrangement of the distributor holes was devised to feed the continuous liquid phase uniformly into the column. When dispersed phase holdup was measured, the lower part was exchanged with a phase collector.

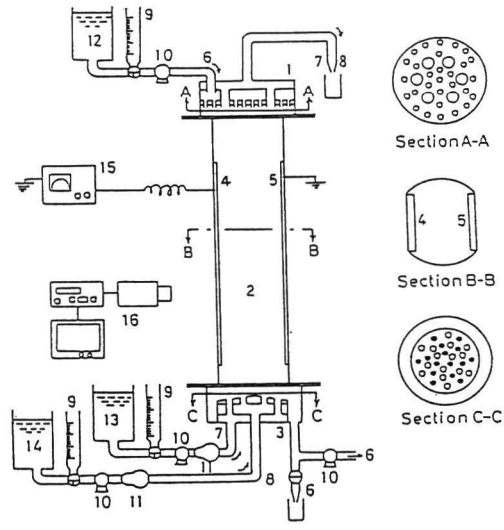

Fig. 1. Experimental apparatus.

1.2 Experimental procedure

Hydrodynamic; A dispersed phase and a continuous phase, respectively, were fed from the upper and lower distributors ① ③ to the column ② by roller pumps ⑩. Both phases were contacted in a two-phase flow countercurrently and a specified voltage was applied. After a steady state flow of the phases was kept under the applied voltage, the feeding of the phases was stopped and simultaneously the voltage was cut off. The holdup was determined by measuring the volume of the dispersed phase settled in the collector. The moving behavior and velocity of the drops, and its diameter were determined by using a camera and a T.V. system ⑯.

Axial mixing of continuous phase; Axial mixing of continuous phase was examined by the pulse injection technique of a tracer/1,6/. The continuous phase at the outlet ⑦ of the column was sampled at a specified interval and iodine of the tracer was analyzed by iodometry/6/.

Mass transfer; Effect of applied voltage on extraction efficiency, in which iodine was extracted from a population of charged drop phase into the continuous phase was examined for various applied voltages. Iodine as a transfer material was used to evaluate mass transfer rate in the dispersed phase because the distribution coefficient of iodine between the dispersed and

continuous phases was 0.015. The experimental procedure was the same as described in the previous study/6/. The physical properties of liquids used are listed in Table 1.

RESULTS AND DISCUSSION

Hydrodynamic; The water drops had induced electric charge or after

TABLE 1 Physical properties of liquids(20°C)

	density [kg/m^3]	interfacial tension [mN/m]	viscosity [mPa·s]	dielectric constant [-]
Cyclohexane	779	-	0.98	2.02
Water	998	47.7	1.0	80.1

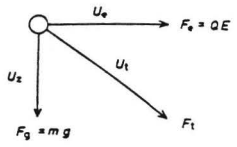

Fig. 2. Force and velocity components.

contacting with the electrodes they received true electric charges. With increasing of the applied voltage the drops behaved from smooth falling motion to violent zigzag motion with the drop coalescence-redispersion cycle. The velocity of a charged drop was estimated as follows. The components of force acting on the drop and those of velocity of the drop are shown in Fig. 2, and their relations are given as follows,

$$F_t = (F_e^2 + F_g^2)^{1/2}, \quad F_g = \pi (\rho_d - \rho_c) g d_e^3/6 \qquad (1),(2)$$

where F_t, F_e and F_g are resulting, electric and gravitational forces[N], respectively. $(\rho_d - \rho_c)$ is density difference between the dispersed and continuous phases[kg/m^3]. d_e is drop diameter[m]. If a drop are assumed to receive maximum electric charge/4/, the electric force acting on the drop is given by Eq.(3).

$$F_e = 1.12\pi \varepsilon_c \varepsilon_0 d_e^2 (E_p/l)^2. \qquad (3)$$

$$U_e = (F_e/F_t)U_t, \quad U_z = (F_g/F_t)U_t \qquad (4),(5)$$

where ε_c and ε_0 are dielectric constant[-] and permittivity of vacuum[F/m], respectively. E_p and l are applied voltage[V] and electrode gap[m], respectively. U_t, U_e and U_z are resulting, electric and gravitational components of drop velocity[m/s], respectively. A relation between F_t-value and U_t-value is given with drag coefficient as a parameter as follows.

$$F_t = C_D \rho_c U_t^2 \pi d_e^2/8 \qquad (6)$$

where C_D is drag coefficient[-] acting on the drop. An example of experimental results is shown in Fig. 3, in which each of components of the drop velocity is

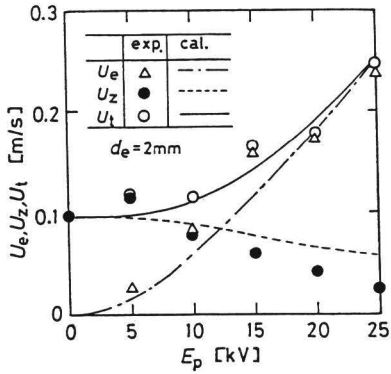

Fig. 3. Velocity components of a water drop falling through cyclohexane in the electric field.

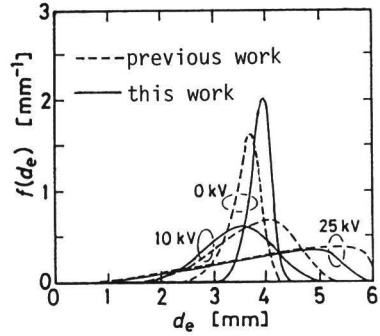

Fig. 4. Drop size distribution in electric field.

plotted against the applied voltage(E_p) for drop size of d_e=2 mm in the presence of an ensemble of the drops. The U_e(△)- and U_t(○)-values increase with applied voltage, while the U_z (●) -value decreases with applied voltage. The experimental data agree satisfactorily with the calculated values which are presented as the lines, which are calculated by Eqs.(1)-(6).

Drop size distribution; Experimental results of drop size distribution{$f(d_e)$} are shown in Fig. 4 for typical applied voltages. The lines in the figure are the values calculated by using the Mugele-Evans distribution function/3/, in which the parameters were obtained by the method of least-squares so as to fit experimental data. The dotted and solid lines show results of previous column and present one, respectively. As shown in the figure, there is little difference between both results.

Dispersed phase holdup; Figure 5 shows experimental relations between dispersed phase holdup(ϕ) and applied voltage(E_p) for various feed rates (U_d) of dispersed phase. In the low feed rate of dispersed phase, the holdup increased in proportion to the applied voltage. This is due to a following reason. Frequency of coalescence between the drops was low because of low holdup fraction and zigzag and spiral motion of the drops became more active with the voltage. As a result, the U_z values decreased and their residence time increased. On the other hand, in the high feed rate the effect of the applied voltage on the holdup was much different from that in the low feed rate. That is, with increasing applied voltage the holdup first decreased and then began to increase. This tendency was roughly the same as observed in the previous column. However, as shown in the figure, present holdup was somewhat higher than previous one.

Axial mixing of continuous phase; The experimental axial dispersion coefficient (E_o) was calculated by the diffusion model/2/. Their results are shown in Fig. 6. The coefficient decreased significantly with the voltage. It means that the forward axial mixing of the continuous phase is depressed and radial mixing of the phase is promoted because zigzag motion of the drops becomes violent more and more with applied voltage. This fact was confirmed by

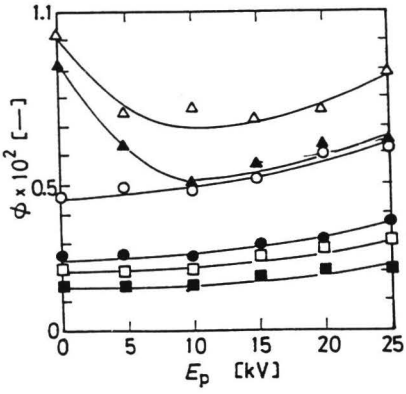

Fig. 5. Effect of applied voltage on dispersed phase holdup. this work,△,○,□, U_d=0.051,0.032,0.016cm/s; previous work, ▲,●,■, U_d=0.046,0.029,0.014cm/s.

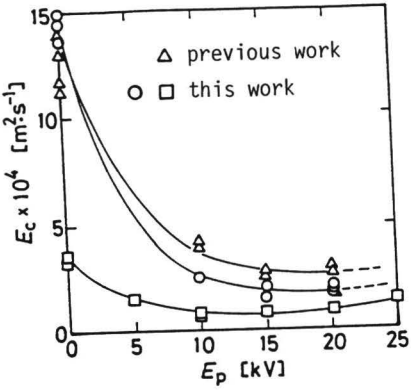

Fig. 6. Effect of applied voltage on axial dispersion coefficient of continuous phase. ○,U_d=0.032cm/s,U_c=0.118cm/s; □,U_d=0.016cm/s,U_c=0.062cm/s; △,U_d=0.029cm/s,U_c=0.098cm/s.

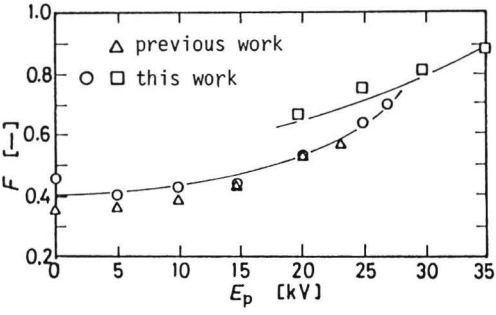

Fig. 7. Effect of applied voltage on extraction efficiency. ○,□, U_d=0.0077, 0.016cm/s, U_c=0.059cm/s; △,U_d=0.029, U_c=0.098cm/s.

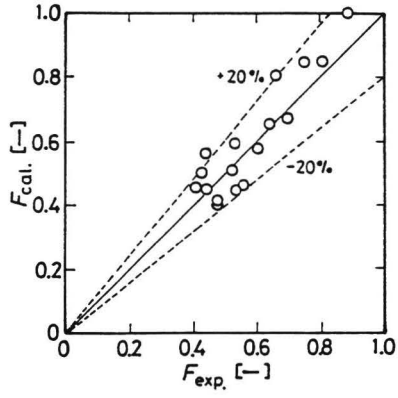

Fig. 8. Comparison between experimental extraction efficiencies and calculated ones by modified dispersion model.

movement of the tracer.

Mass transfer; Experimental extraction efficiency($F=(C_{d,i}-C_{d,o})/(C_{d,i}-C^*)$) is plotted against the applied voltage(E_p) in Fig. 7. The present column was possible to be operated up to higher applied voltage and higher efficiency was obtained.

Simulation of column efficiency; In order to establish design procedure of column, simulation of column efficiency is very important. The simulation was carried out by using the modified dispersion model/6/. The calculation procedure was the same as used in the previous study. The comparison between experimental values(F_{exp}) and simulated ones(F_{cal}) is shown in Fig. 8. As shown in the figure, experimental efficiencies are simulated satisfactorily with the model. However, it is evident that the model includes some unreasonable assumptions. That is, the drop coalescence and redispersion cycle in the field is not taken into account and its effect on efficiency results in low evaluation. On the other hand, the drops without the cycle can be estimated to have high velocity and its effect on efficiency results in high evaluation. As a result, both of them may set off a merit against a fault.

CONCLUSION

1) In comparison with the previous column, the present column was improved on dispersed phase holdup and axial mixing of the continuous phase. Predictions of various factors for present column design can be easier than those for previous one because of uniformity in the electric field.

2) The coalescence and redispersion behavior of the drops in present column was essentially the same as that in a column with agitator. The behavior could be easily controlled by means of an applied voltage.

3) The mass transfer efficiency increased effectively with the applied voltage.

4) Simulation of the present column efficiency was almost possible, but much more fundamental information about coalescence and redispersion of the drops have to be accumulated.

REFERENCES

1)Hozawa,M., Konno,H., Tadaki,T. and Maeda,S., 1970. Kagaku Kogaku, 34, 533
2)Hozawa,M., Konno,H., Tadaki,T. and Maeda,S., 1971. Kagaku Kogaku, 35, 351
3)Mugele,R.A. and Evans,H.D., 1951, IEC., 43, 1731
4)Takamatsu,T., Hashimoto,Y., Yamaguchi,M. and Katayama,T., 1981. J. Chem. Eng. Japan, 14, 178
5)Yamaguchi,M., Sugaya,H. and Katayama,T., 1988. J. Chem. Eng. Japan, 21, 179
6)Yamaguchi,M., Sugaya,H. and Katayama,T., 1989. J. Chem. Eng. Japan, 22, 25
7)Yoshida,F., Yamaguchi,M. and Katayama,T., 1988. J. Chem. Eng. Japan, 21, 123

ACKNOWLEDGEMENT

This study was partially supported by a Financial Aid to Research Grant from the Asahi Glass Foundation for Industrial Technology.

Solvent Extraction 1990, T. Sekine (Editor)

© 1992 Elsevier Science Publishers B.V. All rights reserved

STUDY ON MASS TRANSFER CHARACTERISTICS IN AN ANNULAR PULSED SIEVE PLATE EXTRACTION COLUMN

Qin Wei , Dai Youyuan , Lei Xia , WangJiading.
Tsinghua University
Beijing People's Republic of China

ABSTRACT

Mass transfer characteristics was studied in an annular pulsed sieve plate extraction column with H_2O– HNO_3 –30%TBP system. The fractional hold-up of dispersed (organic) phase and the steady state solute concentration profiles were measured. The " true" height of tranfer unit , diffusional height of transfer unit and apparent height of tranfer unit were estimated from the diffusion model by fitting the measured concentration profile. Results show that mass tranfer efficiency of annular column is equivalent to that of the circular column with the same cross section. And Hocd of the annular column is less than the circular one . And Ec in the annular column is only 40% of that of the circular one. Ec obtained in the mass transfer process is apparently less than that from the no mass transfer process.

INTRODUCTION

The new configuration of pulsed sieve plate extraction column with an annular cross section was suggested to meet the requirment of increase in volumetric throughput in processing of irradiated nuclear fuels. Kendall recommanded this type of column in the early 70's [1] , Benedict [2] studied on the flooding velocity and mass transfer characteristics of this kind of column in 1980. In 1986 [3] Schmidt gave the behavior of two-phase flow and axial mixing. Since 1985 the authors have been engaged in the research of flow behavior[4] and axial mixing characteristics. This paper is a continuation of the aforementioned work–the research of mass transfer.

1. MODELLING

Many mathematical models have been brought about to describe the behavior of mass transfer in extraction column, and diffusion model has come into widespread use. The method proposed by Miyauchi and Vermeulen [6] in cartridge design in the existence of axial mixing — Hocp = Hocd + Hoc , was selected in this paper. Hoc, the "true" height of transfer unit , axial diffusion coefficients of two-phase Ec and Ed , were calculated with the measured concentration profile[7]. Hocd , the diffusional height of transfer unit, was valued with the approximate method suggested by Miyauchi[6].

2. EXPERIMENT

The experimental column is made of glass tube of 0.05m i. d. with a stainless steel pipe of 0.03m o. d. , thus the cross-section area of the annular space just equals to that of a circular column of 0.04m i. d. , while the width of the annular passage is only 0.01m. Sieve plates , having holes 0.03m in diameter and 23% free area , are mounted on the central tube with spacing of 0.05m. This configuration is equivalent to the "standard" cartridge of a conventional circular column . The total height of the sieve plate cartridge is 1.0m. Air pulse of sinusoidal wave was used throughout the tests.

Water - HNO_3-30% TBP (in kerosene) with water as continuous phase was used for study of mass transfer behavior in the direction from continuous phase to dispersed phase. The fractional hold-up of dispersed phase and the steady state concentration profiles were measured in several different operational conditions. The physical property of the experimental system and the range of operational conditions are showed in table 1, table 2 respectively.

Table 1. Operation conditions

A(m)	f(1/s)	Superficial Velocity	
		Uc(m/s)	Ud(m/s)
0.01 — 0.024	1.17 — 2.33	0.0012 — 0.0017	0.0012 — 0.0053

Tbale 2. Physical properties of experimental system

dispersed phase	continuous phase	viscosity (cp)		density (g/cm^3)		σ (dyn/cm)
		μ_d	μ_c	ρ_d	ρ_c	
30% TBP	H_2O (HNO_3)	1.800	0.900	0.830	1.040	10.8

3. RESULT AND DISCUSSION

3.1 Influence of operational condition on the mass transfer behavior

(i) Effect of the energy input

Fig.1 showed the effect of the energy input on Hoc. Hoc decreases with the increase of energy input. The increase of pulse intensity not only improves the extent of contact of the two-phase but also increases the fractional hold-up. And the "true" overall mass transfer coefficient increases.

Hocd increases with the increase of energy input, which is showed in Figure 2. The fact may be explained by the flow characteristics that axial mixing in continuous phase increases with the increase of turbulance intensity resulted from the input energy in emulsion region. The drop sizes are smaller , then the continuous phase

entrains the dispersed phase. Therefore , when the energy input increases , axial mixing in dispersed phase will increase also.

(ii) Effect of the rate ratio

The effect of the two-phase flow rate ratio on Hoc and Hocd is shown in Figure 3. In the range of operational conditions , when the rate ratio increases , fractional hold-up in dispersed phase and specific interfacial area , a, increase , consequently , Hoc decreases.

Hocd decreases with the increase of the rate ratio , it is generally believed that when the fractional hold-up increases due to increasing the rate ratio , the axial mixing coefficient in continuous phase will increase slightly , but Hocd will decrease. It is in accordance with that of the circular pulsed sieve plate extraction column [7].

(iii) Influence of flow rate

The experimental results showed that flow rate effects on Hoc and Hocd. Hoc increases and Hocd decreases with the increase of flow rate. This tendency is in accordance with that in circular pulsed sieve plate extraction column.

3.2 CORRELATION OF Hoc , Hocd IN ANNULAR PULSED SIEVE PLATE EXTRACTION COLUMN

Inertia force model of pulsed condition by Ziolkowski [8] was adopted for Hoc. The parameter of f^3A^2/Uc expresses the energy input for Hoc, and the parameter fA expresses the energy input for Hocd.

Empirical equations were obtained by regression of 40 sets of experimental data as follows:

$$Hoc = 0.668\,(f^3A^2/Uc)^{-0.226}\,(Uc/Ud)^{0.928}$$

$$Hocd = 0.1886\,(fA/Uc)^{0.33}\,(Uc/Ud)^{1.34}$$

plots of Hoc , Hocd (evaluated) vs. the value (calaculated) in Fig. 4 and Fig. 5 indicate the relative errors are less than 20% respectively.

3.3 COMPARISON OF MASS TRANSFER BEHAVIOR BETWEEN ANNULAR PULSED SLEVE PLATE EXTRACTION COLUMN AND CIRCULAR ONE

The comparisons of mass transfer behavior Hoc and Hocd between the two configurations were carried out in the same operation system and cross-section in Fig.6 and Fig.7 . The results showed that Hoc in annular type corresponds to that in circular type , and Hocd in annular type is less than that of circular one.

It is obvious that Hoc in pulsed column is concerned with the operational region and Hoc operated in larger frequency and smaller amplitude is less than that operated in smaller frequency and larger amplitude. The auther's experiment covers the region of literature [7] , [9] , therefore , the values of Hoc vary between their values.

Hoc is the functions of overall mass transfer coefficient based on continuous phase Koc and a , based on the diffusion model. Kod is evaluated by Handlos-Baron internal circle model in the emulsion region of $Re > 10$ in pulsed sieve plate extraction column [9]. When the conclusion of flow characteristics by Schmidt was used, it can be showed that Hoc in annular type is equal to the one in circular type and Kod in annular pulsed sieve plate extraction column can be evaluated with Handlos-Baron model and Koc can be computed with Kod and solute distribution coefficients in Fig.9.

Hocd is the parameter of axial mixing. In fact, the cartridge of annular type restrains the axial mixing [5]. Ec in annular type is equal to 40 percent of the Ec in circular type. Ed in two kinds of cartridges are nearly equal , therefore , Hocd is less in annular type.

Hocp is the important parameter, which stands for the mass transfer behavior. The results of comparison of Hocp in the two kinds of cartridges indicated that Hocp in annular column is less than that in circular column due to the correspond Hoc and the less Hocd. (Fig.8)

This is an advantage for the equipment design , which decreases the height of column , and the annular pulsed sieve plate extraction column will find a good application.

3.4 FORECAST OF THE DESIGN FOR ANNULAR PULSED SIEVE PLATE EXTRACTION COLUMN

(i) The diameter of column and annular space

The research of the flow characteristics in annular pulsed sieve plate extraction column indicated that the flooding velocity decreased with the decrease of the ratio of annular space to the diameter. But when annular space is constant , and diameter increases , the cross-section area increases, consequently , this cartridge has a maximum throughput in processing of irradiated nuclear fuel , which annular space is the parameter of critical safety.

(ii) The height of column

The height of column is decided by Hocp, or Hoc and Hocd for the separation condition given.

Hoc may be calculated with the Handlos-Baron model.

Hocd may be evaluated with the method by Miyauchi , but Ec and Ed are sensitive , it is difficult to measure accurately Ec and Ed in the presence of mass transfer. In general , the values of Ec and Ed in absence of mass transfer are used in engineering design. In this paper , Ec in mass transfer system is compared with that in absence of mass transfer (Fig.10). Result shows Ec in mass transfer system is less. Therefore the height of column used Ec in absence of mass transfer is rational.

In brief, mass transfer efficiency of annular pulsed extraction column is

equivalent to that of the circular pulsed sieve plate column with the same cross section, and Hocd of the annular column is less than that of the circular one.

The authors gratefully acknowledge the support of K. C. Wong education foundation, HongKong.

4. NOTATION

A: Pulsed amplitude , m.
a: Specific interfacial area , m^2/m^3.
Ec: Axial diffusion coefficient in continuous phase , m^2/sec.
Ed: Axial diffusion coefficient in dispersed phase , m^2/sec.
f: Frequency of pulsation , 1/ sec.
Hoc: "True" overall height of transfer unit based on continuous phase , m.
Hocd: Height of overall dispersion unit based on continuous phase , m.
Hocp: "Apparent" overall height of transfer unit based on continuous phase , m.
Koc: Overall mass transfer coefficient based on continuous phase , m/sec.
Kod: Overall mass transfer coefficient based on dispersed phase , m/sec.
R: Flow rate ratio , R = Ud/Uc
Uc: Flow rate of continuous phase , m/sec.
Ud: Flow rate of dispersed phase , m/sec.
Us: Slip velocity between two phase , m/sec.
x: Fractional hold-up of dispersed phase.

5. REFERENCES

[1] Kendall , Jack B. et al. , U. S. Patent 3 , 854 , 176 (1974).
[2] Benedict , G. E. , Sep. Sci. Tech. 15(4) , 945 (1980).
[3] Schmidt , H. , ISEC–86 , 1 , 405 (1986).
[4] Qin Wei , et al. , ICHM'88 247.
[5] Qin Wei , et al. , Chinese J. of Nucls , Sci & Eng. 10 , 47 (1990).
[6] T. Miyauchi , T. Vermeulen , I & EC. , Funds , 2 , 304 (1963).
[7] Lei Xia , et al. , J. of Chem. , Ind & Chem. 4 , 368 (1982).
[8] Ziolkowski , Z. et al. , Inz. Chem. , 4(1) , 163 (1974).
[9] Qian Yu , Doctorate dissertation Tsinghua Univ. Beijing China (1987).

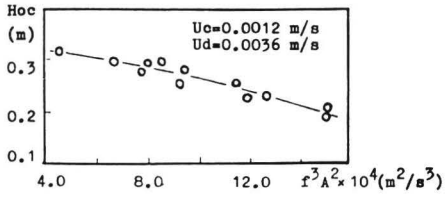

Fig.1 Effect of the energy input on Hoc.

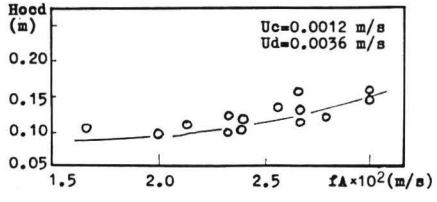

Fig.2 Effect of the energy input on Hocd.

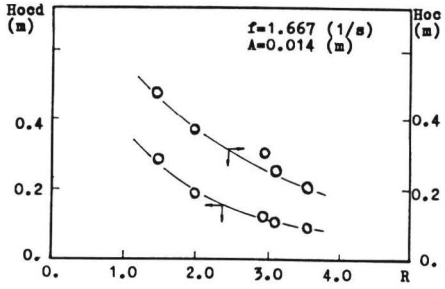

Fig.3 Effect of flow rate ratio on Hoc , Hocd.

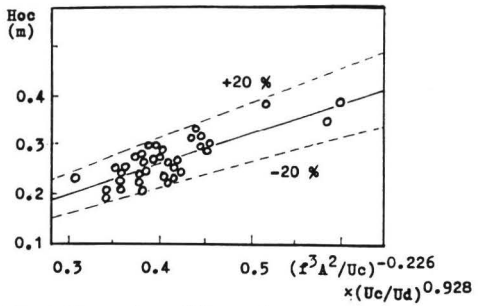

Fig.4 Comparison of Hoc evaluated and calculated.

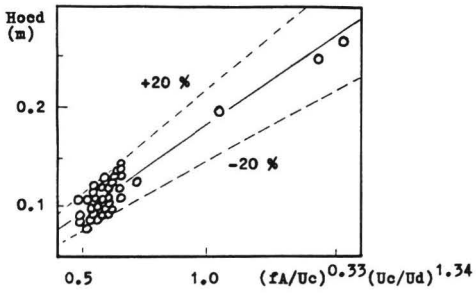

Fig.5 Comparison of Hocd evaluated and calculated.

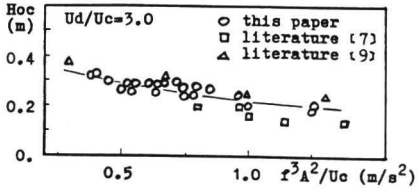

Fig.6 Comparison of Hoc in annular column and in circular column.

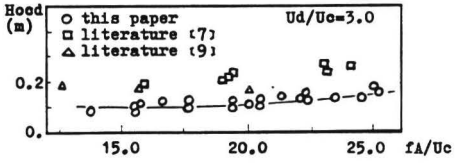

Fig.7 Comparison of Hocd in annular column and in circular column.

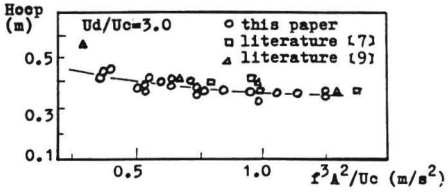

Fig.8 Comparison of Hocp in annular column and in circular column.

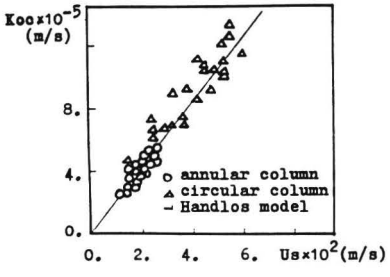

Fig.9 Comparison of Koc evaluated and calculated

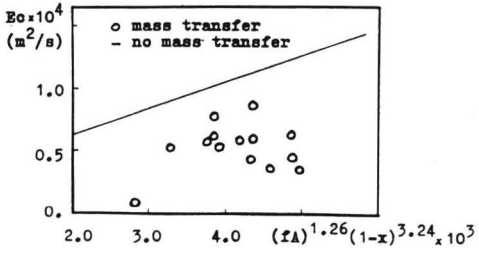

Fig.10 Comparison of Ec in mass tranfer and in no mass tranfer.

Solvent Extraction 1990, T. Sekine (Editor)

© 1992 Elsevier Science Publishers B.V. All rights reserved

THE H-0.3 CENTRIFUGE FOR SMALL-SCALE FAST SOLVENT EXTRACTION PROCEDURES

G. SKARNEMARK, M. SKÅLBERG
Department of Nuclear Chemistry, Chalmers University of Technology, S-412 96 Göteborg, Sweden

J. ALSTAD
Department of Chemistry, University of Oslo, N-0315 Oslo, Norway

ABSTRACT

A small centrifuge for rapid and efficient separation of a mixture of two liquid phases is presented. The hold-up volume of the rotating bowl is 0.3 mL, and the maximum flowrate about 3 mL/s per phase, corresponding to a shortest hold-up time of ~50 ms. The properties of the centrifuge and its applications to fast separations in solvent extraction research and nuclear science are briefly discussed.

INTRODUCTION

Two decades ago a laboratory centrifugal separator (the H-33 centrifuge) was introduced and built into the AKUFVE flow system for measurements of metal distribution ratios (Reinhardt and Rydberg 1969). A few years later the centrifuge was successfully applied to fast chemical separations (the SISAK 1 system) for studies of short-lived radioactive nuclides (Aronsson et al 1974). About 10 years ago, the centrifuge was found to be too slow for this application, and therefore the H-10 centrifuge (Rydberg et al 1980) was developed and built into the new SISAK 2 equipment (Skarnemark et al 1980). It is also frequently used in AKUFVE units (Albinsson et al 1988). Recently there was a need for a SISAK equipment with much lower flowrates combined with an even shorter hold-up time, and therefore we developed a new version of the centrifuge, H-0.3. This centrifuge is now used in a compact SISAK equipment called SISAK 3 (Persson et al 1989). It has also been used for studies of distribution ratios and solvent extraction kinetics in connection with the development of chemical separation procedures for the transactinide elements. The H-centrifuge models are presented in Table 1.

2 TECHNICAL DESCRIPTION

2.1 The H-0.3 liquid-liquid centrifuge design

A cut-away drawing of the H-0.3 centrifuge is shown in Fig. 1. The mixture of the two phases enters centrally and is accelerated to the speed of rotation in the inlet chamber. After ac

Table 1. H-centrifuges used in SISAK systems

Type:	H-33	H-10	H-0.3
Volume, mL	120	12	0.3
Maximum flowrate (ml/s per phase)	25	15	3.3
Bowl diameter, mm	110	54	35
Speed of rotation, rpm	15000	18000	35000

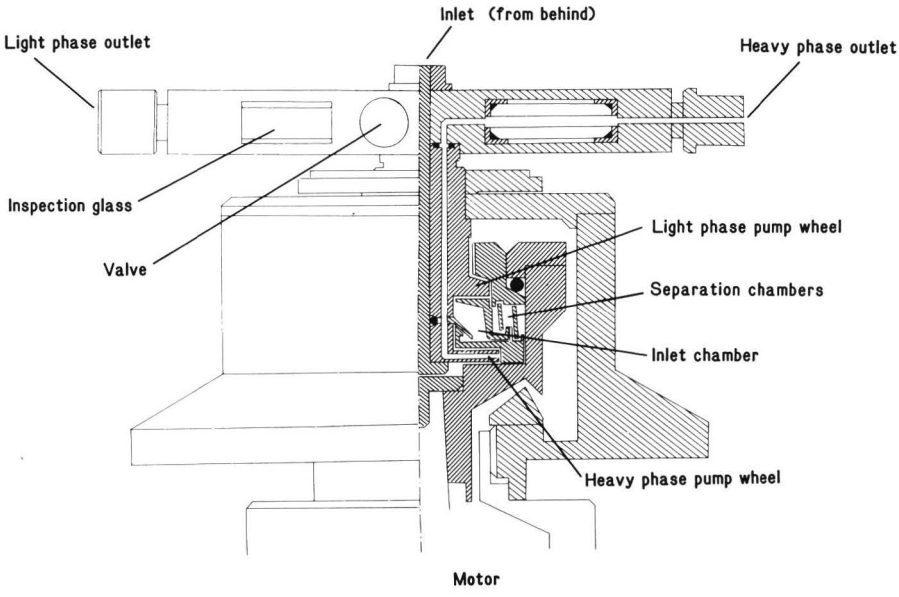

Fig. 1. The H-0.3 centrifuge

celeration, the mixture is forced into the separation volume which contains four small chambers symmetrically arranged around the axis of rotation and totally isolated from each other. In these separation chambers the mixture has a zig-zag motion imposed by the peripheral partition walls and interspersed baffle ridges. The separated phases are discharged (the light phase from the upper collecting chamber, the heavy phase from the lower one) by stationary pump wheels which are individually designed to provide the appropriate pressure and avoid excessive frothing of the liquids. The outlets are equipped with valves, the purpose of which is to maintain a proper

pressure balance in the centrifuge. By adjusting the valves the liquid-liquid interface can be moved until both outgoing phases are free from entrainments of the opposite phase.

It should be mentioned that the new centrifuge is not just a scaled-down version of the older models, but a new construction. The main difference is that the separation chambers, seen from above, are not longer formed as sectors covering almost the whole area of the centrifuge, but consist of four sets of slightly elliptical holes with only about 2 mm^2 area each. This makes the liquid volume much smaller without making it necessary to decrease the radius (and thus the centrifugal force) too much. The tube to the inlet chamber and the tubes from the outlet chambers have also been re-designed to prevent any extra hold-up time caused by cavities containing stationary liquid.

2.2 The motor arrangement

The H-0.3 centrifuge is driven by a 3-phase asynchronous motor powered by an AC current of continuously variable frequency (30-750 Hz). The speed is 25-35,000 rpm at normal running conditions. The centrifuge bowl is fixed directly on to the motor shaft which is mounted on ball bearings. The upper bearing (close to the bowl) is elastically journalled in O-rings in order to allow the shaft and the bowl to rotate around its center-of-gravity. The arrangement decreases the need for balancing of the centrifuge rotor, and it strongly reduces the influence of critical speeds of rotation. The bearings are water-cooled to extend the life-time.

2.3 Choice of materials

The centrifuges are made of palladium passivated titanium, which makes them resistant to most solutions except hydrofluoric acid, strong sulfuric acid and strong hydrochloric acid. The use of metal instead of a plastic material decreases problems caused by sorption on the surfaces inside the centrifuge. The valves are made of PVDF (a teflon type plastic), and the O-ring seals of viton or rubber.

3 OPERATIONAL PERFORMANCE

The flow capacity and phase purity of the centrifuge were tested using an arrangement where two phases were mixed, fed into the centrifuge and then collected. The phase purity was first checked ocularly; from earlier centrifuge tests we know that phase impurities of $\geq 0.1\%$ show up as a white cloudiness in the impure phase. In some cases the phase purity was also checked by adding a radioactive tracer that stays either in the aqueous or in the organic phase. The organic phases tested yielded organic/aqueous density ratios from 0.8 to 1.59. In all cases good phase

separation could be obtained from flowrates less than 0.1 mL/s per phase up to about 3.3 mL/s per phase. The optimal speed of rotation was 25-35,000 rpm depending on the flowrate.

3.1 Hold-up time

When developing an equipment for isolation of short-lived species it is important to know how fast they can pass through a separation step. The transmission of pertechnetate has therefore been investigated using injection of radioactive tracer as a pulse in the aqueous feed. This was performed in two types of experiments.

In the first one a shot of 50 - 100 μL $^{99m}TcO_4^-$ solution from a syringe was given to the aqueous phase ahead of the centrifuge inlet. The pulse passed a detector at the inlet and outlet of the centrifuge, and the time of transmission was measured by a detection system with a multichannel analyzer operating in the multiscaling mode.

In a second experiment the radioactive pulse was generated by a reactor operated in the pulse mode. The fission products from a ^{239}Pu target were transported from the irradiation position in the reactor by a KCl/N_2 gas-jet system (Stender et al 1980) to a degassing unit in which they were transferred to an aqueous phase. The aqueous phase with the radioactive pulse was then mixed with the organic phase at the inlet of the centrifuge. After phase separation in the centrifuge the organic phase passed a detector measuring the extracted short-lived Tc activity. In this case the multiscaling operation of the multichannel analyzer and the neutron pulse in the reactor were started simultaneously, whereby an overall transmission time could be measured. The experiment is outlined in more details elsewhere (Persson et al 1989).

In the first type of experiment, the transmission time was calculated as a function of the fraction of the total activity passing the detector after the centrifuge. For comparison of various runs the times are given at 50% transmission of the activity. In a series of runs with a flowrate range of 1.0 - 3.3 mL/s and without extractant in the organic phase the transmission times were 0.2 - 0.3 s. In the runs with extractant in the organic phase and at flowrates $\geq$1 mL/s the times were 0.3 - 0.7 s. The latter is comparable with the results from the second type of experiments although the time could not be evaluated in a similar way.

4 APPLICATIONS

4.1 Studies of short-lived nuclides.

The H-0.3 centrifuge was primarily developed as a part of a new SISAK equipment intended to combine low flowrates with a short hold-up time. The low flowrates are necessary when studying nuclides decaying by α-emission, e.g. the transactinide elements. In this case we intend to feed the effluent from the centrifuge directly into a very thin cell facing a PIPS (Passivated

Implanted Planar Silicon) detector for α-spectroscopy.

So far the new centrifuge has been successfully used for nuclear decay studies of the fission product ^{113}Ru, with a half-life of only 0.80 s. Studies of transactinide elements are in progress.

4.2 Solvent extraction studies.

When developing separation procedures e.g. for the transactinide elements one has to consider the short phase contact time available in the SISAK system. These contact times, 20-50 ms at normal running conditions, make most literature data unsatisfactory, because published partition data usually refer to equilibrium conditions. We are therefore, as part of the development of separation procedures for elements 104 and 105, performing a study of the extraction of the 104/105 homologs Zr, Hf, Nb, Ta and Pa with tertiary amines or HDEHP (bis-2-ethylhexyl-orthophosphoric acid) as extractants. The extraction of the trivalent actinide homologs La, Gd and Lu as well as Np has also been investigated. The study is not yet finished, but the first results show that acceptable yields ($D \geq 10$) can be obtained also at these short contact times. The amines give partition coefficients comparable to those obtained at equilibrium conditions, while values obtained with HDEHP are significantly lower.

5 ACKNOWLEDGEMENT

The authors want to thank Professor J.O. Liljenzin for valuable discussions and his interest in this work.

6 REFERENCES

Albinsson, Y., Ohlsson, L.-E., Persson, H., Rydberg, J., 1988. App. Radiat. Isot. 39: 113

Aronsson, P.O., Johansson, B.E., Rydberg, J., Skarnemark, G., Alstad, J., Bergersen, B., Kvåle, E., Skarestad, M., 1974. J. inorg. nucl. Chem. 36: 2397

Persson, H., Skarnemark, G., Skålberg, M., Alstad, J., Liljenzin, J.O., Bauer, G., Haberberger, F., Kaffrell, N., Rogowski, J., Trautmann, N., 1989. Radiochim. Acta 48: 177

Reinhardt, H., Rydberg, J., 1969. Acta Chem. Scand. 23: 2773

Rydberg, J., Aronsson, P.O., Persson, H., Selme, A., Skarnemark, G., 1980. Hydrometallurgy 5: 273

Skarnemark, G., Aronsson, P.O., Brodén, K., Rydberg, J., Björnstad, T., Kaffrell, N., Stender, E., Trautmann, N., 1980. Nucl. Instrum. Methods 171: 323

Stender, E., Trautmann, N., Herrmann, G., 1980. Radiochem. Radioanal. Letters 42: 291

Solvent Extraction 1990, T. Sekine (Editor)

© 1992 Elsevier Science Publishers B.V. All rights reserved

PHASE INVERSION IN MIXER SETTLERS

J.C. GODFREY and A. FRAUX, University of Bradford, Bradford, BD7 1DP, U.K.
R.N. REEVE, Sunderland Polytechnic, Sunderland, SR2 7EE, U.K.

ABSTRACT

The phenomenon of phase inversion is one of the major causes of operating problems in industrial mixer-settler equipment. However, although the avoidance of inversion is one of the most important design criteria, the study of inversion has not attracted as much research attention as other aspects of liquid-liquid mixing. In this presentation inversion and related problems in industrial mixer-settlers will be discussed and laboratory studies of inversion reviewed.

INTRODUCTION

In liquid-liquid processes contacting of the two phases is often achieved in agitated tanks with one phase present as drops and the other as the continuum. The drop size is usually small, $d<0.5mm$, and the drops are usually well distributed throughout the tank at a volume fraction equal to the flow ratio. As there are many processes where the desired dispersion is not the "natural" dispersion there has long been as interest in which phase will become dispersed for various startup conditions, combinations of physical properties, etc. However, a successful startup does not necessarily guarantee that the preferred dispersion will be maintained and the spontaneous exchange of roles between dispersed and continuous phases, phase inversion, has also been the subject of industrial and academic study for some time. Thus, from the point of view of the preferred dispersion, there are two major considerations: startup and phase inversion.

1.1 Startup

In most startup procedures the creation of the desired dispersed phase is achieved by presenting it as the minority phase. Once dispersed the drop phase will have a degree of stability which allows the volume fraction of the dispersed phase to be increased above the initial, minority phase, starting condition to an operating value usually of the order of 50%.

In batch operations startup can often be achieved by locating the impeller in the desired continuous phase. Provided that the flow pattern generated is of a suitable form, a thin stream of the desired dispersed phase is drawn through the continuous phase and dispersed by the impeller. Research has been conducted to explore preferred dispersed phase characteristics where the impeller position is not used to favour one

phase, e.g. Gaggero et al., and also where steps are taken to minimize the effect of impeller location, e.g. McClarey and Mansoori.

1.2 Phase inversion

Once a dispersion has been generated it has a certain degree of stability and the volume fraction of the dispersed phase can be increased, in some cases to very high values perhaps in excess of 90%. Eventually a volume fraction is reached where inversion occurs, the drop phase becoming the continuous phase and vice versa. For well mixed conditions this process does not seem to be very impeller speed dependent for most systems. It is interesting that for systems where the maximum volume fraction is impeller speed dependent, e.g. Quinn and Sigloh, the observation of the relationship between volume fraction and impeller speed remains the same regardless of which is chosen as the experimental variable.

Both phases may be studied for their behaviour as the dispersed phase and thus two phase inversion boundaries may be defined. Between these two boundaries, the ambivalent region, either phase may be the dispersed phase depending on the startup procedure. A number of attempts have been made to analyse the characteristics of the two phase inversion boundaries in terms of physical properties. Selker and Sleicher considered the influence of the viscosity ratio, Luhning and Sawistowski defined a Weber number, Clarke and Sawistowski investigated drop size, Quinn and Sigloh investigated mixing effects, Watanabe and Takenchi viscosity ratio. Attempts have also been made to model the relationship between phase boundaries and impeller speed but without much evident success. Arashmid and Jeffreys have investigated a collision and coalescence model.

Laboratory studies suggest that the batch systems show considerable potential for stability and resistance to phase inversion at a range of moderate phase ratios. Some data has also been presented for continuous systems, e.g. Rowden et al, which shows a large ambivalent region. Similar results have been demonstrated for batch and continuous systems, e.g. Guilinger et al. On this basis it would not seem that stable operation of batch or continuous liquid-liquid mixers with a preferred dispersion would present problems. However, this is not the case, with many reports of phase inversion problems in continuous liquid-liquid extraction plant and of startup problems in batch liquid-liquid reaction processes.

In the operation of mixer-settler plant successful startup is achieved with the preferred dispersed phase and a period of stable operation follows. The nature of the problem is that inversion occurs some time

after startup, perhaps initiated by a small change in plant operating conditions but not certainly so. To obtain long periods of stable operation it is often found necessary to run at flow ratios which give an excess of continuous phase, a requirement which would not be considered necessary by reference to the ambivalence region characteristic.

In batch processes problems have been reported in establishing or maintaining the preferred dispersed phase. For some systems the required dispersion is established only to invert a short time later, with the delay time between startup and inversion being very dependent on operating conditions, e.g. Gilchrist et al.

In both batch and continuous systems there is the question of the distribution of the dispersed and continuous phases and the possibility of considerable variations in local volume fractions. For continuous processes there is the additional complication that the volume fraction in the mixer differs from that intended - as nominally specified from the flow ratio - and usually deficient in light, probably organic, phase. Thus the possibility exists for both batch and continuous systems, that phase inversion may be related to local variations in volume fraction due to insufficient agitation.

2. EXPERIMENTAL

2.1 Copper Extraction

One of our first studies was to look at the stability of the combination : acidic copper sulphate solution/LIX64N in Escaid diluent. The measurements were conducted with and without mass transfer, which made little difference, in a Rushton turbine agitated continuous flow tank of square cross-section and approximately 3½ litres in volume. Both aqueous and organic drop dispersions were very stable, volume fractions in excess of 90% being recorded for both dispersions. As the mixer was constructed from perspex (Plexiglas) which is organic wetted it was argued that there could be some element of surface effect stabilizing the 'more difficult' organic continuous dispersion, especially in the relatively small 3½ litre mixer, e.g. Guilinger et al. To explore this a larger (27 litre) mixer was built to the same design but the stability characteristics were unchanged. A stainless steel base was later fitted to the larger mixer to provide a substantial area of aqueous wetted surface where aqueous drops might collect. However, there was no detectable influence on stability characteristics. The possibility of effects due to particulate matter in plant operation was also considered, Godfrey and Gledhill, tests were conducted with particulate matter added to the aqueous phase and, although

some interesting effects were observed, the stability of the systems was not significantly changed.

2.2 Cumene/water system

The possible influence of large density difference was examined in a small semi-batch mixer of 3 litres, using a baffled cylinder geometry and a large turbine impeller (D_i/D_t = 2/3). The liquid- liquid system used was cumene (isopropylbenzene)/water with the alternatives of pure water and high concentrations of sodium nitrate being used to examine the effects of large aqueous phase density. However, the results obtained for the two different aqueous phase densities showed little difference, and with little effect of impeller speed. Organic drop dispersions in excess of 95% volume fraction were obtained and the maximum volume fraction for aqueous drop dispersions were of the order of 60%.

Measurements were also made for the cumene/water system in a continuous flow, pump-mix, agitated tank. The mixer was of square cross section, fabricated from glass and stainless steel and had a volume of 21.5 litres. Various impeller combinations were used, principally a centrally located impeller with draught-tube (similar to the Davy design) or bottom located impeller (similar to the 'General Mills' design). The results were broadly similar to those obtained from the semi-batch experiments - i.e. organic drop dispersions of 90% volume fraction, aqueous drop dispersions of 60% volume fraction and higher depending on experimental conditions. The use of a solute (iso butyric acid) to reduce interfacial tension produced a shift in both limiting volume fractions, maximum organic volume fraction being reduced to 80% or less, maximum aqueous volume fraction increasing to 70% or more.

2.3 Operating Conditions

For the pump-mix geometry changes of total throughput rate or impeller to draught tube clearance have little effect on the phase stability characteristics of the cumene/water system. The main operating variable to have real influence on phase stability is impeller speed, particularly at the lower end of the impeller speed range.

In the well mixed regime where average mixer volume fraction (X_V) is close to the nominal flow ratio value (X_F) impeller speed only appears to influence the maximum volume fraction of aqueous dispersed phase, maximum value falling as impeller speed falls. However at low impeller speeds, where a well mixed regime cannot be assumed, light phase volume fractions are such that $X_V < X_F$. Some observations of inversion under these conditions

suggest that the contents of the mixer may be regarded as consisting of a moderately well mixed dispersion region in the vicinity of the impeller with stagnant regions of both organic and aqueous phase far from the impeller. At inversion the volume fraction in the dispersion region approximates that determined from well mixed condition studies but with the mixer (X_V) and flow (X_F) values being quite different.

2.4 Mixer Design

Amongst the various impellers studied it has been noted that change of impeller design can expand the width of the ambivalence region or cause a shift of the ambivalence region on the volume fraction - impeller speed plot without changing the width of the region. These observations refer to behaviour in the well mixed regime with different characteristics being observed at low impeller speeds.

For lower impeller speeds in the conventional bottom inlet/top outlet pump mix design the low impeller speed characteristics of different impellers are very different. Under these conditions aqueous continuity is generally the more stable condition and the maintenance of organic continuity is difficult. Inversion usually comes about when the energy input falls to a value below which organic continuity can only be maintained at high volume fractions. It appears that the limiting levels of energy input can be very different for different impellers, initial values covering a range as wide as 200W/m^3 at one extreme to 5000W/m^3 at the other.

3. DISCUSSION

Simple batch liquid-liquid mixing often looks very complicated. At startup the impeller circulates the phase in which it is located and draws in and disperses the second phase. The location of the impeller and the volume fraction of the two liquids (and therefore the position of the interface) nearly always govern which will be the dispersed phase. The flow generated by the impeller needs to be considered and if the impeller is very near the interface then anything can happen.

For either batch or semi-batch experiments inadequate levels of agitation may leave unmixed regions of one or both phases. It has been shown, e.g. Hemrajani, that the requirements for 'complete' mixing differ very considerably in terms of impeller speed and power consumption for different impellers and different baffle configurations. This aspect of liquid-liquid mixing is, as yet, relatively poorly documented but can be

seen as one aspect of the influence of impeller and vessel geometry on phase inversion.

In continually operated mixers the simplest characteristic, under well mixed conditions, is of the existence of two phase boundaries, which show a small degree of impeller speed dependence, and which delineate an ambivalent region. However, at impeller speeds less than those required to establish a well mixed condition, many complications arise. The contents of the tank are no longer uniform and there is also the possibility of unmixed volumes of either continuous or dispersed phases, or both. The volume fraction in the tank will differ from the flow ratio value and, on the basis of these many characteristics, seemingly premature inversion can occur. In addition, inversion in continuous flow systems is usually preceded by an increase in entrainment levels leaving the settler. This increase in entrainment is occasionally interpreted as evidence of overmixing and the impeller speed reduced, thus hastening inversion.

It seems that many aspects of phase inversion may be interpreted by consideration of the quality of mixing in liquid-liquid systems. Data currently available suggests that the mixing characteristics of different impellers and vessel geometries can be very different and sometimes in a a complex way. This may explain some of the complicated observations made of phase inversion.

REFERENCES

M Arashmid, G V Jeffreys : AIChEJ 26 (1), 51-55, 1980.
S I Clarke, H Sawistowski : Trans IChE 56 50-55, 1978.
M Gaggero, E Arato, P Costa, G Lodi : 6th European Conference on Mixing, 1988.
A Gilchrist, K N Dyster, I P T Moore, A W Nienow: Chem. Eng. Sci., 44 (10), 2381-4, 1989.
J C Godfrey, J Gledhill : ISEC '83.
T R Guilinger, A K Grislingas, O Erga : Ind.Eng.Chem. Res. 27 (6) 978-982, 1988.
R R Hemrajani : 5th European Conference on Mixing, 63-80, 1985.
R W Luhning, H Sawistowski : ISEC '71, 873, 1971.
M J McClarey, G H Mansoori : AIChE Symp. Series 74 (173) 134-139, 1978.
J A Quinn, D B Sigloh : CanJChemEng 41 15-18, 1963.
M Rehakova, V Rod : Coll Czech Chem Comm 44 340, 1979.
G A Rowden, J B Scuffham, G C I Warwick, G A Davies : IChE Sym.Series 42.
A H Selker, C A Sleicher : CanJChemEng 43 298-301, 1965.
K Watanabe, T Takenchi Kagaku Kogaku Ronbunshu 7 538-540, 1981.

Solvent Extraction 1990, T. Sekine (Editor)

© 1992 Elsevier Science Publishers B.V. All rights reserved

THE DESIGN AND PERFORMANCE OF AN EXTRACTION COLUMN WITH AN ADJUSTABLE WORKING CAPACITY

K. Haberland

Wiederaufarbeitungsanlage Karlsruhe Betriebsgesellschaft mbH
Postfach 12 63, 7514 Eggenstein-Leopoldshafen (FRG)

ABSTRACT
Newly developed column cartridges allow the adjustment of the column to different loading ranges, without changing the plates themselves, thus changing the operating characteristics. Comparative pilot plant studies of uranium extraction have been carried out under identical conditions using the uranylnitrate/tributyl-phospate-system of the purex-process. Column design and the results obtained are presented.

INTRODUCTION

The choice of extractor design is essentially governed by four factors: physical properties, insensibility to interface phenomena (wetting), number of theoretical stages and throughput. However some operational aspects are of equal importance, for example flexibility with respect to load fluctuations and product quality. As the column diameter becomes larger an aggravation of channeling tendencies brings with it increasing HETS values resulting in an increasing column length /1/. Furthermore with increasing working time the hazard of wetting occurs and mass transfer will be jeopardized /2/. Continued development work indicated increased assurance of adequate performance and/or an increase in the versability of pulsed columns /3/.

The newly developed column cartridge aims towards the extension of the range of operability /4/.

Design features

The new cartridge geometry consists of slot hole plates rather than sieve or nozzle plates, Fig. 1. If the slots of the new plates are arranged, for example at 90° to each other, the countercurrent flow of the liquid phases will be frequently forced to alter its flow pattern on its way through the extraction column, thus breaking up any possible channeling.

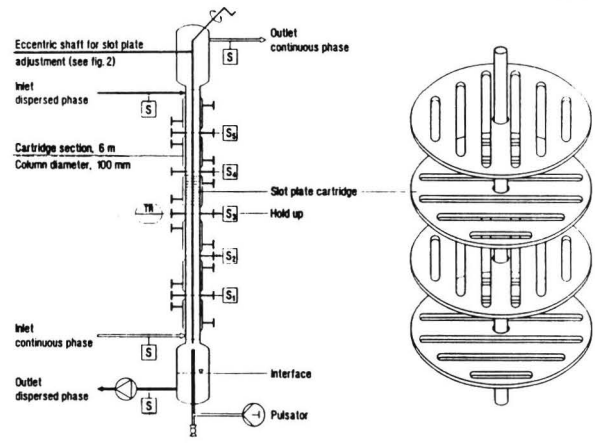

Fig. 1 Schematic Sketch of Pilot Plant Column with Slot Plate Cartridge

The projection of such a cartridge reduces the slot holes to square holes. In the neighbourhood of the above cartridge different operating conditions are obtained by turning various slot plates against each other. Depending on the plate spacing, hole size and free area will be varied and therefore, as an additional parameter, the working capacity becomes adjustable. Fig. 2 shows such an assembled cartridge.

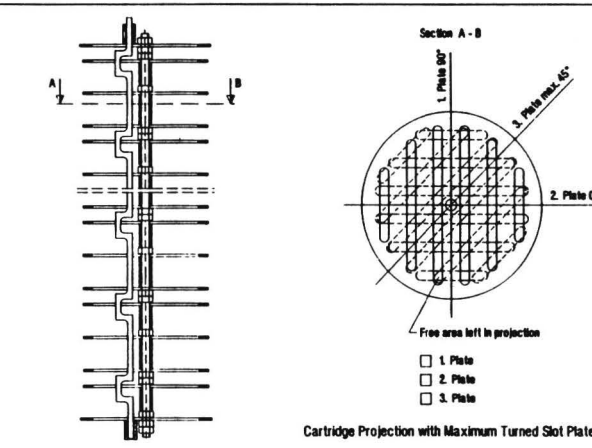

Fig. 2 Construction of Cartridge Section with Adjustable Slot Plates

With the help of an eccentric shaft next to the centre rod it is possible to turn every third slotplate to a different angle and therefore transform the projected free area from outside the column.

Experimental results

Slotplates of the design indicated in Fig. 1 and 2 were successfully tested for solvent extraction of uranium using the uranylnitrate/tributylphosphate-system of the purex-process. The organic was the continuous phase,

masstransfer: d → c

phase ratio: $\dot{V}_d/\dot{V}_c = 0.5$

gradient of density: $\Delta\rho = 0.55$ g/ml

interface tension: $\sigma = 13.4$ dyn/cm

Stainless steel slotplates in a 90° arrangement to each other with 25 % free area and 25 mm plate-to-plate spacing were employed. In addition pivotally attached slotplates were fitted in the upper plate section at a cartridge-length of 2 m approximately. The effect of adjustable slotplates on flooding characteristics is shown in Fig. 3. At a pulse frequency of 60 cycles/min. and a slotplate position of 90° a maximum loading range of 550 l/h has been obtained. By turning every third plate to a 45° position, the free area will be reduced thus reducing the actual flooding capacity to 220 l/h. In this case the adjustable plates had been installed with 1 mm spacing to the fixed ones.

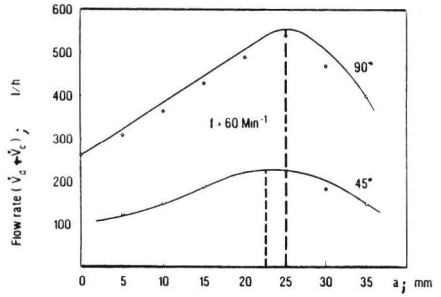

Fig. 3 Maximum Loading Range as a Function of Slot Plate Position

If the adjustable plates were installed with 10 mm spacing the maximum loading range remained unchanged with 550 l/h total throughput even at the 45° position. Because of the plate spacing the free area had been changed in the "projection" of the cartridge only. But the flow vector across the column-axis was increased resulting in an increased operating hold-up. Fig. 4 compares the hold-up-behaviour at both plate positions in steady-state operation. As the interfacial area, which also determines the mode of mass transfer, is a function of both the hold-up and the dropsize the Sauter mean diameter is of special interest. Fig. 5 shows a typical dropsize distribution measured for a 90° degree slotplate position, where d_{32} = 2.3 mm.

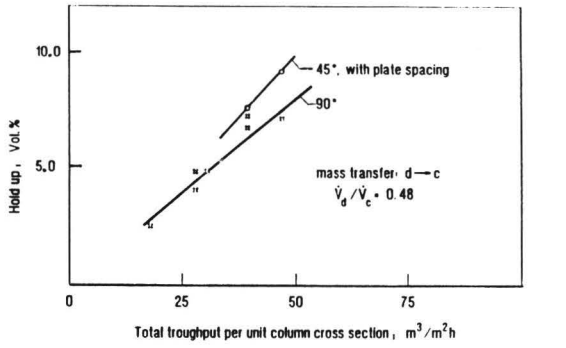

Fig. 4 Comparison of Measured Hold up Behaviour

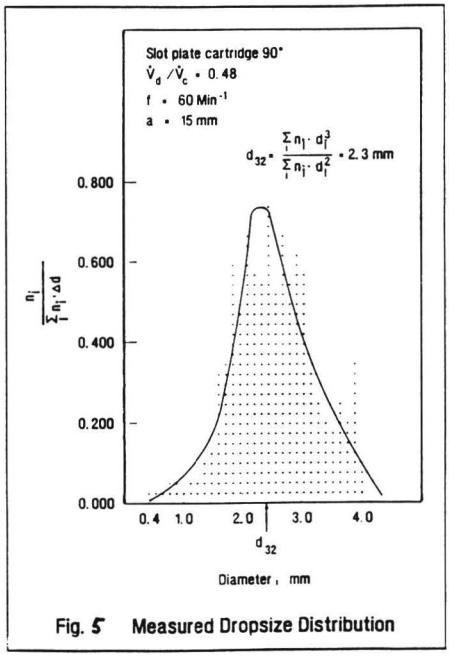

Fig. 5 Measured Dropsize Distribution

Due to the geometric design of the slotplates the dropformation is completed within the turbulent flow region via pressure and shearing forces rather than being formed directly from holes of sieve plates for example. This different mechanism minimizes the influence of plate-wetting on dropformation.

Fig. 6 compares the slotplates with other types of equipment in terms of separation efficiency obtained by taking concentration profiles along the column. It should be noted, that all measurements shown in Fig. 6 were carried out with the same system of physical properties and under identical conditions.

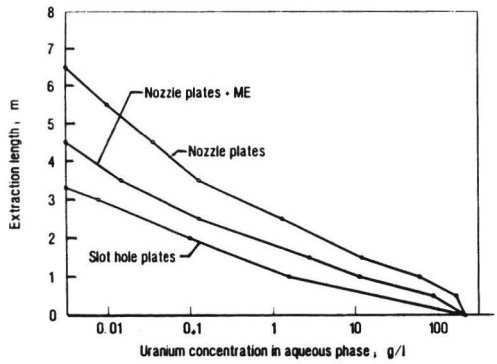

Fig. 6 Comparison of Column Internals regarding Separation Efficiency

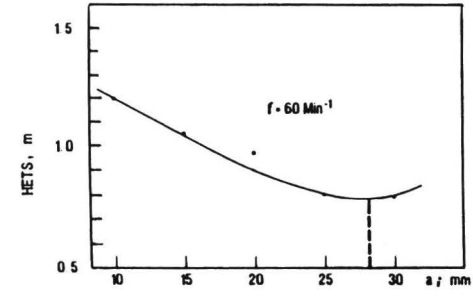

Fig. 7 Effect of Pulse Amplitude on Separation Efficiency

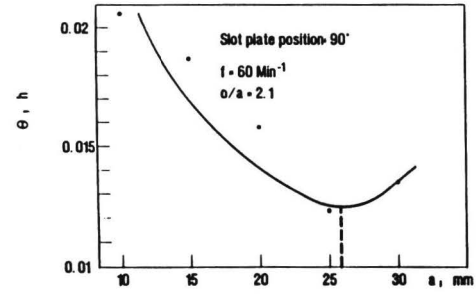

Fig. 8 Characteristic Value of Residence Time for One Theoretical Stage

The excellent performance obtained with slotplates may be related to improved flow characteristics which led to a rather extensive mass transfer immediately below the aqueous feed. The required extraction length of the column is markedly decreased compared with nozzles plates. Due to the very intensive radial mixing HETS values decreased rapidly as the pulse amplitude was increased, Fig. 7. The basis for column layout is the loading range and HETS values. The relationship

$$\theta = \frac{\text{HETS} \cdot m^2}{(\dot{V}_d + \dot{V}_c)_{max}}$$

characterizes the minimum residence time for one theoretical stage, Fig. 8. The smaller the characteristic value "θ" the smaller the necessary column volume. Therefore the minimum indicates the optimum operating level.

Conclusions

Using the diagram shown in Fig. 9 it becomes clear that the main advantage of the adjustable slotplate-cartridge is the large range of loadings in which the separation remains high. This cartridge provides a multipurpose extraction column with a high degree of flexibility, so that the same column can be used for different processes or operation modes and also when the loading varies with time. Due to the plate design an easy and appropriate scale-up is possible. Furthermore the introduced cartridge may be an attractive alternate to the present sieve or nozzle plate cartridges.

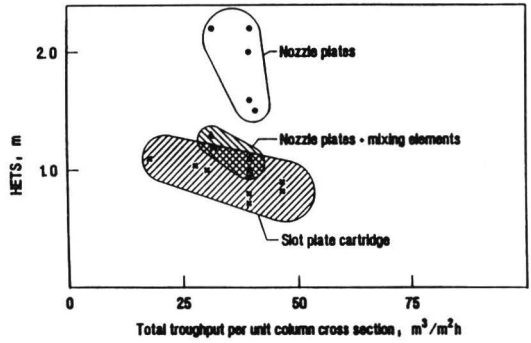

Fig. 9 Comparison of Performance of Different Column Internals

References

/1/ H. Zimmermann et. al., Untersuchungen an mit Düsenböden ausgerüsteten pulsierten Siebboden-Extraktionskolonnen im industriellen Maßstab einer Wiederaufarbeitungsanlage,
Chem.-Ing.-Techn. 57 (1985) Nr. 6, S. 540-541

/2/ I. Chem.E. Symposium Serie-No. 88, p. 311-312, 1984

/3/ E. Blaß et. al., Fortschritte auf dem Gebiet der Flüssig-/Flüssig-Extraktion,
Chem.-Ing.-Techn. 57 (1985) Nr. 7, S. 565-581

/4/ K. Haberland, Stoffaustauschkolonne mit von außen verstellbarem Arbeitsbereich,
Patent registered P 39 26 974.4, 1989

Solvent Extraction 1990, T. Sekine (Editor)

© 1992 Elsevier Science Publishers B.V. All rights reserved

SOME EXPERIENCE OF ENERGY SAVING FOR A LARGE SCHEIBEL EXTRACTION COLUMN SYSTEM

T. C. LO
Chemical Engineering Development Department, Hoffmann-La Roche Inc.
340 Kingsland Street, Nutley, New Jersey U.S.A.

ABSTRACT

Three large Scheibel extraction columns were used for recovery and purification of an intermediate compound in a fine chemical plant. The plant was designed in 1970 when the oil price at that time was relatively low (US$3/barrel). Escalation in the price of oil (US$34/barrel) in mid '70's caused a great concern on the energy consumption for this process in the plant. It was soon realized that the major energy consumption was in the solvent recovery system. A development program led to a modified process scheme.

In the original scheme, the continuous extraction process employed two agitated 1.75 M (5'9") multistage Scheibel extraction columns which operated in parallel. The extract from these two columns was combined with the extract from a reaction liquor extraction column, which was fed to a first effective evaporator. In the modified process scheme, the continuous extraction process is operated in the same manner as that described above in the original process scheme except the extract from the second Scheibel extraction column was used as solvent feed to the 1st Scheibel extractor. The total cost saving was calculated to be $600,000/yr at 1982 US dollars. The initial cost for modifications of the plant was minimal, and the project was highly cost-effective and well justified.

INTRODUCTION

Three large Scheibel extraction columns (2,3,4,5) are used for recovery and purification of an intermediate compound in a fine chemical plant. The plant was designed in 1970 when the oil price at that time was relatively low (US$3/barrel). Escalation in the price of oil (US$34/barrel) in mid 1970 caused a great concern on the energy consumption for this process in the plant (3). It soon found that the major consumption of energy was in the solvent recovery system. A development program was initiated to reduce steam consumption in the solvent recovery.

Original Process Scheme. Figure 1 shows original process scheme. The continuous extraction process for an aqueous feed employs two agitated 1.75 M (5'9") diameter, 27-stage Scheibel extraction column (Position #1A and 1B). The extracts from these columns are combined with the solvent distillates from the 2nd effect evaporator (Position #5) and the stripper (Position #7), and the extract from the reaction liquor extraction column (Position #2, Scheibel column, 1.45 m (4'-9") diameter, 33-stage). The combined stream was fed to

the lst effect evaporator (Position #3) at a rate of 24.3 cu.ft./min. The pure solvent distillate rate was 21.3 cu.ft./min.

Modified Process Scheme. Figure 2 shows the modified process flow diagram. The continuous extraction process is operated in the same manner as that described above in the original process except for slight differences in the column operating parameters. The distillate from the 2nd effect evaporator and stripper are combined with the extract, 11.4 cu. ft./min from the the second Scheibel extraction column (Position #2). The combined solvent, containing ∿3% organic intermediate compound, is then used as a solvent feed to the lst Scheibel extraction column (Position #1). The extract from the column is fed to the lst effect evaporator at a rate of 14.8 cu.ft./min. as compared with 24.3 cu.ft./min. in the original process scheme, a reduction of 9.6 cu.ft./min. (40%) of solvent-organic that need not be processed. The distillate rate of recovered pure solvent is 11.4 cu.ft./min. as compared with 21.3 cu.ft./min. before the process was modified. Therefore, the energy required to evaporate 10 cu.ft./min. of solvent is saved. Because the extract feed rate to the first-effect evaporator was dramatically reduced, only one solvent recovery train was needed instead of two trains which were operated in parallel. Thus, the solvent losses and operating costs are substantially reduced.

Piloting Experiments. A series of pilot-plant experiments were performed using a jacketed 71 mm (2.8") diameter, 27 stage Scheibel extraction column, to determine process feasibility and develop scale-up data for the aqueous feed extraction column (Position #1). Results indicated that the extraction efficiency was satisfactory and the data could be scaled up with confidence (2,5). Hence, the process modification was implemented in the plant in 1982, and the plant has been performing satisfactory and smoothly ever since.

Cost Saving. Table 1 shows that the estimated saving in steam amounts to $400,000/yr (1982). An additional cost saving of $110,000 can also be realized from the improvement of intermediate product recovery. The solvent usage will be reduced from 32,888 to 19,652 cu.ft./day (reduction of 40%). The cost saving from the operation and by reducing solvent loss was estimated to be $93,000/yr. The total cost savings were calculated to be $600,000/yr at 1982 dollars. As it can be evidenced from Figures 1 and 2, the cost for modifications of the plant was minimal (∿$50,000). Therefore, the project was highly cost-effective and well-justified.

TABLE 1

Cost Saving for an Extraction System

	Before Modification	After Modification
1st effect evaporator, solvent distillate, cu.ft./min.	21.3	11.8
Heat duty, millions BTU/hr.	15.3	8.0
Annual steam cost savings*	-	$400,000
Extraction efficiency	97%	99%
Cost Savings for improvement of product recovery per year	-	$110,000
Cost savings by eliminating labor, maintenance, etc. on 2nd train	0	$ 5,000
Steam savings by using vacuum-ring pumps	-	$ 13,000
Potential saving of solvent	-	$ 75,000
Total estimated cost saving/yr.		$600,000

* Based on a nominal steam cost of $6.50/1,000 lb (1982).

REFERENCES

1. Hanson, C., paper on "Solvent Extraction--An Economically Competitive Process" in Chemical Engineering, May 1979.
2. Lo, T. C., Section 1.10 on "Commercial Liquid-Liquid Extraction Equipment" in Schweitzer (ed.), Handbook of Separation Techniques for Chemical Engineers, McGraw-Hill (First Edition, 1979, Second Edition, 1988).
3. Lo, T. C., "Recent Development in Commercial Extractors", presented at Engineering Foundation Conference on Mixing Research at Rindge, New Hampshire, August 1975, The Engineering Foundation, New York, N.Y.
4. Scheibel, E.G., Chapter 13.3, "Scheibel Column" in Lo, T. C., Baird, M.H.I., and Hanson, C. (Editors), Handbook of Solvent Extraction, Wiley-Interscience (1983).
5. Technical note on "Scale-Up Procedure for a Scheibel Extraction Column" (71 Pages), U.S. Department of Energy DOE/MC/1654-1420 (DE83013576), prepared by Radian Corporation (1983).

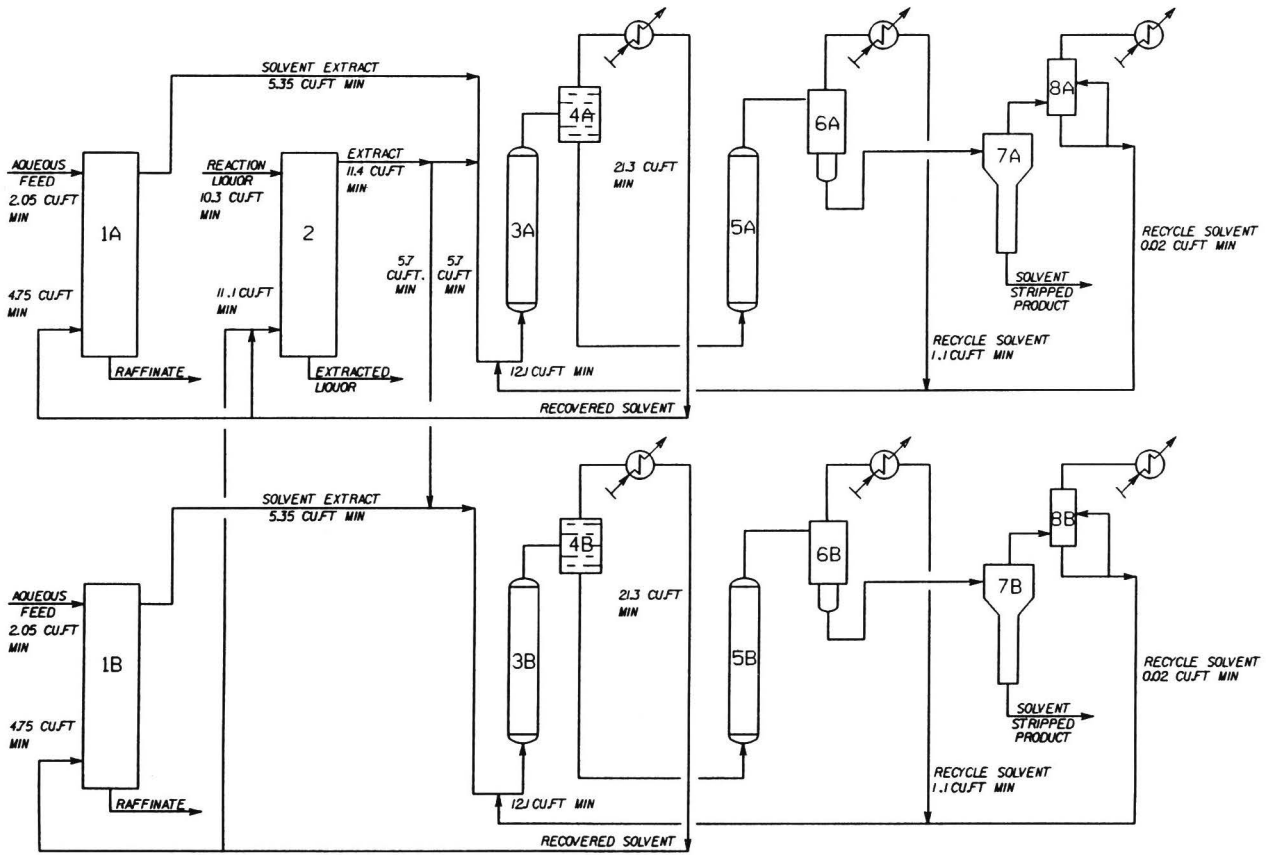

FIGURE 1

SCHEMATIC FLOW DIAGRAM FOR AN EXTRACTION SYSTEM BEFORE MODIFICATION:

1A/1B - SCHEIBEL EXTRACTOR (5'-9" Ø X 18'-27 STAGES), 2 - SCHEIBEL EXTRACTOR (4'-9" Ø X 22'-33 STAGES), 3A/B - 1ST EFFECT EVAPORATOR, 4A/B - BUBBLE CAP TRAY TOWER, 5A/B - SECOND EFFECT EVAPORATOR, 6A/B - SEPARATOR, 7A/B - STRIPPER, 8A/B - SCRUBBER.

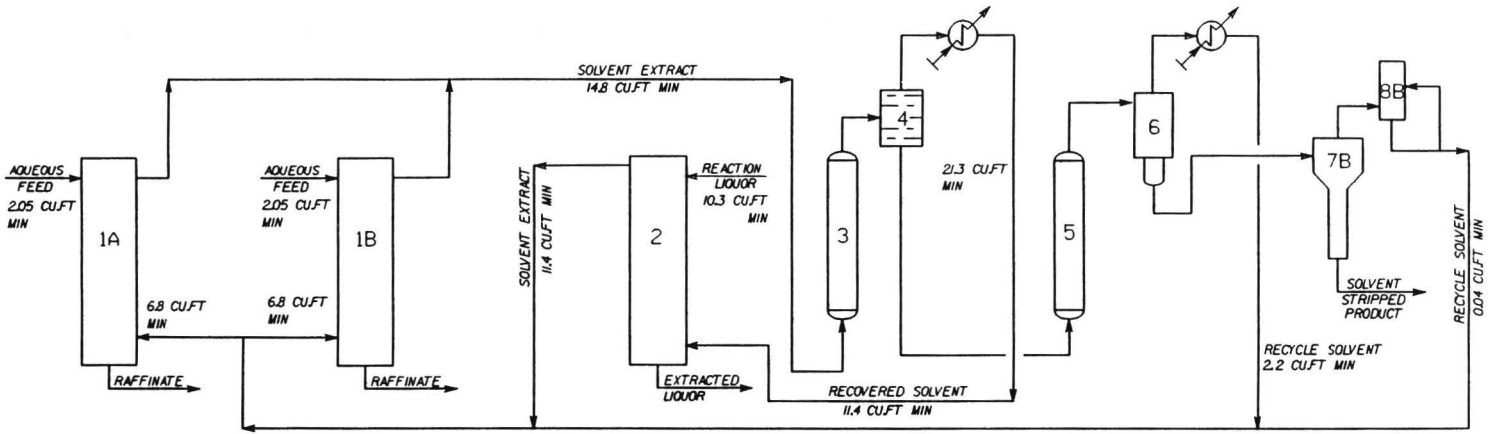

FIGURE 2

SCHEMATIC FLOW DIAGRAM FOR AN EXTRACTION SYSTEM AFTER MODIFICATION:

1A/1B - SCHEIBEL EXTRACTOR (5'-9" Ø X 18'-27 STAGES), 2 - SCHEIBEL EXTRACTOR (4'-9" Ø X 22'-33 STAGES), 3 - IST EFFECT EVAPORATOR, 4 - BUBBLE CAP TRAY TOWER, 5 - SECOND EFFECT EVAPORATOR, 6 - SEPARATOR, 7 - STRIPPER, 8 - SCRUBBER.

Solvent Extraction 1990, T. Sekine (Editor)

© 1992 Elsevier Science Publishers B.V. All rights reserved

DESIGN FACTORS AFFECTING THE PERFORMANCE OF ELECTROSTATIC COALESCERS

P. J. BAILES* and S. K. L. LARKAI**
*Department of Chemical Engineering, University of Bradford, W. Yorks., UK
** RHM Research & Engineering Ltd., High Wycombe, Bucks., HP12 3QR, UK

Abstract

Measurements of entrainment in the effluent phases from six specially-designed continuous flow electrostatic coalescers are reported for a range of applied voltages and pulsation frequencies. A convergent flat electrode geometry is shown to give extremely rapid and effective phase separation of the water-in-oil dispersion used in the tests.

SCOPE OF THE INVESTIGATION

Previous work by the authors[1,2] has established that pulsed DC applied to a water-in-oil dispersion by means of an electrode coated with a thin layer of insulating material promotes coalescence between the droplets. The purpose of the present study was to find out whether attention to electrode geometry and other design aspects of a coalescer could significantly improve its phase separation performance. This necessitated the fabrication of a number of test coalescers and required a suitable experiment for assessing their performance. The liquid-liquid system chosen for the practical work was distilled water - Escaid 100 kerosene containing 5% Acorga P5100 with the phases mutually saturated. The relative permittivity and electrical conductivity of the continuous phase were 1.9 and 8.9 x 10^{-9} S m^{-1} respectively.

The basic experiment consisted of creating a water-in-oil dispersion on a continuous basis and passing the dispersion through the test coalescer where the field was applied. The principal performance criterion was taken to be the level of entrainment in the coalescer organic effluent stream. Thus, aqueous entrainment (a/o) was determined in all experiments. Measurements of organic entrainment were also made in many experiments.

EXPERIMENTAL EQUIPMENT AND ANALYTICAL PROCEDURES

The dispersion was created in a fully baffled cube-shaped perspex mixing vessel of side 341 mm internally. Agitation was accomplished by means of a 6-bladed Rushton turbine impeller 115 mm diameter and driven at a constant speed of 400 min^{-1} by a Buddeberg pneumatic motor. For all the experiments the phase ratio of dispersed phase: continuous phase was 1:1 and unless stated otherwise the total flow rate was 10.0 l min^{-1}.

Experiments were carried out at a temperature of 25° ± 1°C.

The electrical requirements were met by Brandenburg high voltage generators. For pulsed DC, a Brandenburg (0-30 kV, 2mA) generator was connected via a decoupling resistance to a purpose-built valve modulator unit and the load (in parallel). The valve was under the control of a Philips (model PM5131) function generator. In this way high voltage pulses approximating to a square wave with a mark:space ratio of unity were generated for the experimental work at frequencies up to 60 Hz. An oscilloscope with a suitable voltage divider was used to measure the voltage applied to the coalescer.

Aqueous entrainment was measured by sonicating a sample of the organic stream leaving a coalescer and analysing a sub-sample for its water content by means of Karl Fischer titration. This figure was corrected for the presence of dissolved water and any existing traces of entrained water by subtracting the water content of the organic feed.

Organic entrainment was quantified by treating samples of the aqueous effluent stream from a coalescer with a known amount of freon to extract the entrained organic. The freon layer was subsequently analysed by infra-red spectrophotometry to find the amount of organic phase liquid. This analysis was carried out conveniently using an Horiba Oil Content Analyzer Model OCMA-220.

COALESCER DESIGN, RESULTS AND DISCUSSION

Six horizontal flow electrostatic coalescers were tested and these represented three basically different designs, that is, parallel plate, converging plate and concentric electrode geometries.

Parallel plate electrostatic coalescers Mk I and Mk II

The two units were constructed from perspex sheet, each was essentially a rectangular duct 400 mm long with a divergent inlet section (80 mm long) to distribute the incoming dispersion. The high voltage was applied to a metal sheet electrode convering the 6 mm thick perspex top of the duct. The earth electrode was formed by the settled aqueous phase which accumulated in the coalescer during operation and which was parallel to the high voltage electrode.

The difference between the Mk I and Mk II coalescers lay in the design of the entry and exit regions and in the cross-sectional dimensions of the duct (100 mm wide x 40 mm deep for Mk I and 50 mm wide x 80 mm deep for Mk II). In the Mk I coalescer a perforated plate across the entrance to the rectangular duct was used to distribute the dispersion over the entire flow cross-section of the duct. Whereas in the Mk II version, the perforated plate was replaced with one having holes only in the top half so as to

distribute all the flow directly into the electric field region. In addition, a flow deflection plate was installed on the lower half of the upstream side of the distributor plate.

The aqueous entrainment levels in the organic leaving the Mk 1 unit are given in Table 1. For a constant applied voltage of 18.7 kV it was found that there was a single optimum pulsation frequency at which aqueous entrainment was minimised. The lowest field assisted value of a/o entrainment was 1,250 ppm at 8 Hz. The o/a entrainment was observed to be always at a high level. Similar experiments with the Mk II electrostatic coalescer showed a great improvement in the clarity of the aqueous phase and confirmed that the distributor design had a very beneficial effect on o/a entrainment. This is corroborated by the measurements (see Table 1). There is no evidence of pulsation frequency significantly affecting entrainment in the aqueous phase. Tests at 18.7 kV and 24.5 kV on the Mk II unit gave minimum a/o entrainment values at a frequency of 20 Hz. At frequencies above and below this optimum the a/o entrainment levels were much higher.

TABLE 1 **Effect of pulsation frequency on entrainment**

	Mk I	Mk II			Mk III			HCEC
	a/o (ppm)	a/o (ppm)		o/a (ppm)	a/o (ppm)		o/a (ppm)	a/o (ppm)
f (Hz)	18.7 kV	18.7 kV	24.5 kV	18.7 kV	13.9 kV	18.7 kV	13.9 kV	18.7 kV
1.0	10,400	32,810	16,650	100	1,210	900	80	3,300
2.0	8,200	23,330	11,410	100	740	340	-	2,770
4.0	-	15,880	7,520	100	530	220	70	3,570
6.0	3,540	8,830	1,200	80	440	120	75	-
8.0	1,250	7,160	990	120	370	100	70	3,730
10.0	1,300	5,640	520	100	360	90	-	-
15.0	-	5,260	-	-	900	450	-	-
20.0	1,910	4,510	440	100	1,080	620	60	-
30.0	3,060	4,670	500	100	1,600	860	70	-
40.0	-	4,920	1,110	100	2,060	1,020	70	4,010
50.0	4,710	6,750	1,200	150	2,760	1,970	60	4,260
60.0	-	-	-	-	3,010	2,060	60	5,650

Converging plate electrostatic coalescers Mk III, Mk IV and Mk V

An effort to exploit the above findings led to the Mk III-Mk V electrostatic coalescers which were designed so that the electric field strength across the flow path was greater at the exit from the duct than it was at the entrance. This was achieved, as previously, in a duct of 400 mm

length and with the same constant cross-sectional area. These requirements meant that the top and bottom plates of the duct converged towards the exit, while the sides of the duct converged towards the duct entrance. The internal dimensions of the three ducts were 100 mm wide x 40 mm deep at the inlet and 200 mm wide x 20 mm deep at the exit. All had the same distributor arrangement as used in the Mk II electrostatic coalescer, supplemented by a perspex block on the downstream side of the lower half of the distributor plate. This served to displace the aqueous layer that would normally collect in that region and prevented the incoming current of primary dispersion from mixing with, and being partially incorporated into, the bulk aqueous phase. For the majority of the experiments, the nominal residence time of the dispersion was of the order of 11.4 sec. Sampling ports were located near the exit end of the coalescer and individual exit pipes were used to convey the separated phases from the unit.

The high voltage electrode covered the top of the Mk III coalescer in a manner similar to the Mk I and Mk II designs. However, the electrode arrangement for the Mk IV unit was different. Here there were three sheet electrodes each the full width of the coalescer top and 80 mm long but separated from the next by a 40 mm gap. They were energised by a single high voltage source so that the dispersion would experience three electric field zones in succession as it progressed along the duct. The Mk V coalescer employed a different electrode arrangement altogether. In this case the first 250 mm length of duct had an electrode on the outside surface of the duct top in the usual manner, thereafter, a second sheet electrode was fitted to the inside surface of the duct top. The latter arrangement gave an uncoated electrode 100 mm long in contact with the organic phase as it moved toward the exit of the duct. The two electrodes were energised from separate sources so that they could be operated under different conditions of voltage and frequency.

The benefits of the graduated field and the further modification of the entrance region are evident from Table 1. The main advantage of the Mk III version is that away from the optimum frequency region it managed to hold the aqueous entrainment in a much narrower range than the Mk II unit. It seems that because the field increased along the flow path of the electrostatic coalescer it enabled the entrainment to be reduced at those frequencies where the results would have been otherwise poor.

Further experiments on the Mk III electrostatic coalescer revealed that for applied voltages above 22.5 kV the a/o entrainment values begin to increase. This was probably due to redispersion of the aqueous phase caused by the induced charge exceeding the Rayleigh stability limit for the drops. The ability of the Mk III unit to cope with higher and lower total

throughputs was also examined. At 10 Hz and 18.7 kV, total throughputs (1 min^{-1}) of 6.0, 8.0, 10.0, 12.0 and 14.0 gave a/o entrainment values (ppm) of 70, 80, 90, 510 and 740, respectively.

Results for the Mk IV electrostatic coalescer were disappointing. It was hoped that alternately exposing the dispersion to a field region and a "zero-field" region, as it flowed along the coalescer, would obviate the problem of redispersion at higher voltages since drops would be afforded time for charge relaxation. In the event, it was found that redispersion at voltages near 22.5 kV was prevented but for applied voltages below this level, the entrainment was much higher than for the Mk III version (see Table 2). This finding was attributed to the fact that the total residence time of the dispersion in the electric field was less in the Mk IV electrostatic coalescer.

The Mk V electrostatic coalescer was designed to couple together the advantage of a coated electrode for treating a water rich "wet" dispersion with the advantage of the high fields associated with the bare electrode for removing fine drops from a dilute "dry" dispersion. This arrangement was tested with a variety of voltage and frequency permutations for the uncoated electrode with the conditions for the coated electrode being fixed throughout at 18.7 kV and 10 Hz. The detailed results are presented elsewhere[3], however, it is sufficient to note that trials, using a range of pulsation frequencies for the uncoated electrode showed an optimum frequency of 50 Hz. It is clear from the data in Table 2 that very low levels of entrainment were attainable using either continuous DC or pulsed DC at 50 Hz. Unquestionably the coated-uncoated electrode system allowed a/o and o/a entrainment to be reduced to much lower levels than those obtained with the fully coated electrode systems.

TABLE 2 **Effect of voltage upon entrainment**
(coated electrode frequency 10 Hz)

	Mk IV	Mk V (coated electrode voltage 18.7 kV)			
V (kV)		Continuous DC		Pulsed DC at 50 Hz	
	a/o (ppm)	a/o (ppm)	o/a (ppm)	a/o (ppm)	o/a (ppm)
9.3	–	60	50	50	–
13.9	1,640	20	40	20	–
18.7	410	10	60	10	–
22.5	320	< 5	40	< 5	–
24.5	120				–

Experiments at two higher total throughputs using a continuous DC voltage at the uncoated electrode of 22.5 kV gave a/o entrainment values (ppm) of 140 and 560 for throughputs (1 min^{-1}) of 12.0 and 14.0 respectively.

Horizontal concentric electrode coalescer (HCEC)

This apparatus comprised a horizontally disposed cylindrical glass vessel 140 mm diameter and 300 mm long having closed ends fitted with openings to allow for the introduction and removal of fluids and to permit electrode connections to be made. A glass baffle attached to the end of the axially located dispersion inlet port ensured even distribution of dispersion around the entire circumference of the vessel. The earth electrode was a flexible stainless steel plate 200 mm long and spring-fitted to the inner wall of the vessel. The high voltage electrode was a stainless steel rod 250 mm long and covered with 0.3 mm wall thickness PTFE tubing. It was mounted on the axis of the cylindrical vessel. At the vessel end, opposite the dispersion inlet, two pipes ensured removal of the separated phases.

The data given in Table 1 show that this device had an optimum frequency of 2.0 Hz and exhibited high levels of entrainment. The hydrodynamics within the coalescer were poor and performance was markedly inferior to the flat electrode geometries.

CONCLUSIONS

The study shows that the performance of an electrostatic coalescer depends very much upon its design. In particular, the results reveal that the entrance region exerts a critical influence on entrainment in both phases and the performance of each geometry can be optimised by careful choice of applied electric field. A design giving horizontal flow under coated and non-coated flat electrodes in series, was capable of delivering effluent a/o and o/a entrainment values as low as 5 ppm and 40 ppm, respectively, 11.4 seconds after leaving the mixer.

REFERENCES

1. Bailes, P. J. and Larkai, S. K. L., 1981. Trans I Chem E., 59: (4), 229
2. Bailes, P. J. and Larkai, S. K. L., 1982. Trans I Chem E., 60: (2), 115
3. Bailes, P. J. and Larkai, S. K. L., Science and Engineering Research Council Report - 1988. Grant No. GR/C 88703.

ACKNOWLEDGEMENT

Financial assistance from the Science and Engineering Research Council is gratefully acknowledged.

Solvent Extraction 1990, T. Sekine (Editor)

© 1992 Elsevier Science Publishers B.V. All rights reserved

THE ELECTRODYNAMIC CONTACTOR FOR EXTRACTION

Kenneth W. Warren and J.J. Byeseda
NATCO, P.O. Box 1710, Tulsa, OK 74101 USA

ABSTRACT

Electrostatic fields are commonly used to coalesce fine water droplets in oil-continuous emulsions. Soluble salts are removed from the organic phase by first mixing the hydrocarbon with fresh water. The resulting mixture of finely dispersed water drops is then separated using high voltage electrostatic energy. Several stages of mixing and separation (using multiple vessels) may be required in order to achieve the desired mass transfer efficiency. The Electrodynamic Contactor uses electrostatic energy for both mixing and separation of the phases. Countercurrent flow of the aqueous and organic phases enables the attainment of the equivalent of several theoretical stages within one vessel. Data generated in the removal of soluble salts from crude petroleum may be applied in the design of other two-phase solvent extraction processes.

INTRODUCTION

The removal of soluble of salts from petroleum is a special case of liquid/liquid extraction utilizing intimate contact followed by phase separation to achieve mass transfer from the feed stream to a second stream consisting of an immiscible phase. It differs from conventional two phase liquid extraction in that the feed stream is a heterogeneous dispersion rather than a solution, and the material to be extracted consists primarily of liquid dispersed in the feed rather than solutes. There are sufficient parallels between petroleum desalting and normal solvent extraction processes to enable one to readily utilize developments in one field as steps to process improvements in the other.

Any extraction process may be divided into three steps: (1) Intimate contact between the two immiscible phases, (2) Coalescence or growth of the drops of the dispersed phase, and (3) Separation of the phases, usually by sedimentation. Contact is most often secured by a variety of mechanically driven mixing schemes followed by retention time to allow gravity induced phase separation.

Coalescence is the agglomeration of drops of the dispersed phase to a size sufficient for removal by sedimentation. It is a multistage process consisting of coagulation, a chemical process in which the surface forces stabilizing the dispersion are reduced to allow droplet collisions to occur, and flocculation in which drops combine into larger drops. It is essential to note that droplet growth cannot proceed until the stabilizing forces are small enough to permit drop collisions. Flocculation may also be promoted chemically, although the introduction of additional chemical species in a closed loop process may be undesirable. Therefore, electroflocculation produced by the application of electric fields to the dispersion is to be preferred as long as operating considerations permit the maintenance of organic phase continuous dispersions.

Sedimentation in a solvent extraction process relies upon retention time within a quiescent zone to allow the flocculated drops to settle out of the continuous phase. This is accomplished in the settler section of a typical mixer/settler. Although elevated temperatures can aid sedimentation by reducing the continuous phase viscosity and often increasing the density differential between the two phases, the range of available temperatures in a conventional mixer/settler is limited. The sedimentation velocity is given by the following:

$$V = \frac{(1.36)(10^{-6})gr^2(\rho_w - \rho_o)}{\eta} \quad (1)$$

where V = Sedimentation Velocity (m sec^{-1})
ρ_w = Specific Gravity of Dispersed Phase
ρ_o = Specific Gravity of Continuous Phase
g = Gravitation Constant
r = Drop Radius (m)
η = Viscosity (centipoise)

The importance of the drop size, differential density, and viscosity are readily apparent. Although augmentation of the gravitational field is possible, due to operational constraints, this approach is of limited application.

2. RESOLUTION OF EMULSIONS BY ELECTRIC FIELDS

2.1 AC Fields

Design considerations for solvent extraction systems assume that a properly coagulated mixture is to be processed. Therefore, design emphasis is placed on the flocculation and sedimentation device.

The oldest commercially applied electroflocculation technology utilizes the application of high voltage alternating current (AC) fields to the water-in-oil emulsion. Due to the dipolar nature of the water molecules, these molecules tend to align themselves with an electrical field. As the molecules within a drop become aligned with the field, the drop itself becomes distorted into an ellipsoidal shape. A collection of such drops consists of ellipsoids aligned with the field such that the charged end of one drop is adjacent to the oppositely charged end of its neighbor. An electrical attraction thus arises between adjacent drops. The attractive force between adjacent drops of equal size may be expressed as follows:

$$F = \frac{24\epsilon_0 \epsilon E^2 r^6}{(d+2r)^4} \quad (2)$$

where F = Electrostatic Force between Drops (N)
ϵ = Dielectric Constant of Continuous Phase
ϵ_0 = Permittivity of Free Space
d = Interdrop Distance (m)

Although this force is significant, particularly at close range, it rises and falls with the oscillating AC field and reverses itself at a rate twice that of the frequency of the applied

field.[1] Thus there is little opportunity for drop movement, and coalescence is limited to drops which are very close together. AC flocculation is particularly effective in assisting condensation of the hindered settling zone which develops at the oil/water interface as large water drops settle but are unable to penetrate the interfacial surface. An additional benefit realized as a result of the oscillatory deformation of the dispersed drops is the rupture of stabilizing films of suspended solids, semisoluble organic fractions, and other debris which collect at the drop surface and hinder interaction between drops which would otherwise coalesce.[2]

2.2 DC Fields

The use of direct current (DC) fields in electroflocculation has several beneficial effects. The dispersed water drops still experience the attraction expressed in Equation (2), but in a steady, unidirectional field, attraction results in migration. Therefore, coalescence effects dependent on drop proximity are greatly enhanced. Migration ultimately results in movement of drops to one of the electrodes where they assume a net charge of the same polarity as the contacted electrode. In an array of oppositely charged electrodes, the charged drops are then accelerated toward an oppositely charged electrode. This results in drops of opposite charge flowing counter-current to each other with a large increase in electrically induced flocculation.

A problem encountered in any metal/electrolyte system in the presence of an electrical current is corrosion. In an AC system, the rapid directional change in the current results in reversal of the electrolytic reactions before diffusion of the reaction products away from the electrolytic cell makes these reactions irreversible. In a DC system, the electrolytic reactions are continuous, and corrosion of the metallic components can become a serious problem.

2.3 Combination AC/DC Fields

The benefits of both AC and DC fields can be obtained by an electrical arrangement which places a DC field across adjacent electrodes constructed of corrosion resistant material while maintaining an AC field between these electrodes and electrical ground. (Figure 1) [3,4] The containment vessel and the water layer are maintained at ground potential, so the corrosion inhibiting effects of the AC field are found at the vessel wall, and the AC field induced condensation of the hindered settling zone occurs at the oil/water interface. Between the electrodes, the DC induced migration of water droplets and enhanced electroflocculation result in greater droplet growth.

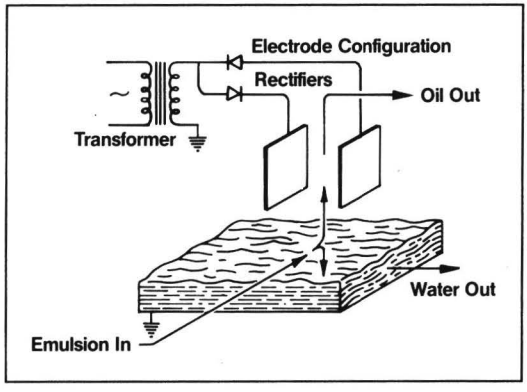

Figure 1 Dual Polarity™ Coalescer

3. DROP SIZE CONTROL BY THE ELECTRIC FIELD

It has been recognized that an equilibrium drop size is reached in an electroflocculation device which is dependent upon field strength with smaller drops occurring at higher field strength.[5] Examination of Equation (2) also indicates that electroflocculation of small drops requires a high electric field gradient in order to achieve significant coalescence. Thus the field strength necessary to reduce the remnant water content of an organic stream may produce an equilibrium drop size not well suited to sedimentation.

There are two approaches for avoiding this compromise. One is time varying control of field strength [6], and the other is control of field strength over a segment of the treating space.[7,8] In the first, the field strength is subjected to a periodic variation which coalesces small droplets in a strong field, and then allows drop growth in a declining field. Since the drops are settling as this occurs, the small droplets which settle slowly are subjected to repeated cycles while large drops fall out of the affected zone during periods of low field strength.

In the second case, the treating zone field strength is varied along its vertical axis by using resistive electrodes to generate the field.[9] Again, the larger drops migrate downward into the zone of lower field strength which results in further growth. In practice, both methods may be applied simultaneously.[10]

Just as declining field strength can enhance drop growth, increasing field strength can produce drop dispersion or electrostatic mixing. [11,12,13] Several mechanisms contribute to this effect. (a) Increasing migration velocity at high field strength leads to increased hydrodynamic shear resulting in drop deformation and division. (b) If the field strength is oscillating at a frequency near the resonant frequency of the drops, unstable oscillations resulting in drop shatter are produced. [14,15,16] (c) Drop charge of sufficient magnitude has been shown to produce electrostatic instability leading to drop shattering. It should be noted in each of these mechanisms that the forces leading to dispersion are largely confined to the dispersed phase with minimum power expenditure on movement of the continuous phase. The resonant frequency technique, called the Emulsion Phase Contactor, is now being commercially developed for solvent extraction applications.

4. APPLICATION DATA

4.1 Salt Extraction from Petroleum

Electrostatic mixing in which the voltage is periodically modulated between dispersion voltage and coalescing voltage has been applied in the extraction of soluble salts from petroleum. Performance in such a system consists of two factors: mass transfer and phase separation. These factors are shown for a light petroleum (specific gravity 0.845), similar to the diluents in commercial hydrometallurgical installations, in Figures 2 and 3. Figure 2 illustrates the mass transfer of soluble salts from the petroleum to the aqueous phase. Note that two parallel commercial installations are included. The average inlet salt concentration is 56.1 ppm while the average outlet concentrations are 2.69 ppm for Unit #1 and 2.20 ppm for Unit #2. Salt was analyzed as soluble chloride and reported as equivalent sodium chloride. In each case, the outlet values approach the limits of analytical accuracy for the methods used (titrimetry).

Phase separation performance is shown in Figure 3. Inlet water concentration was

effectively five percent since that was the amount of water added. Unit #1 had an average effluent water content of 0.06% while Unit #2 had an average of 0.11%. Phase separation efficiencies were 98.8% for Unit #1 and 97.8% for Unit #2. These data represent a single physical contact stage operated at a flux of between 1.2 and 1.5 gpm ft^{-1}.

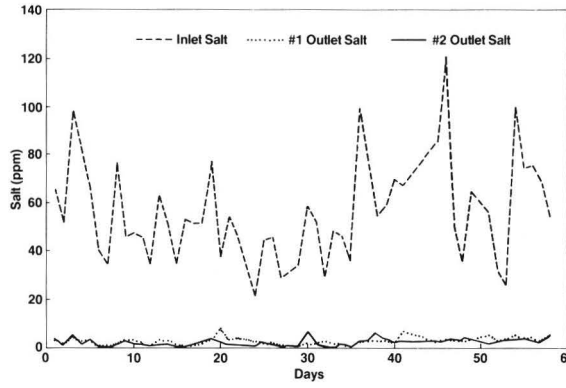

Figure 2 Salt Extraction Performance

4.2 Extraction of Organic Acid

Data from Oak Ridge National Laboratory using the resonant frequency technique[17] have demonstrated the effectiveness of the electrostatic contactor as compared to conventional techniques. Data for the transfer of acetic acid between water and methyl isobutyl ketone in the Emulsion Phase Contactor were compared with published mass transfer data on this system in a York-Scheibel column and a Podbielniak centrifugal contactor. The Emulsion Phase Contactor produced 1.71 theoretical stages per centimeter of column compared to 0.10 stages per cm for the York-Scheibel column and 0.17 stages per cm for the Podbielniak.

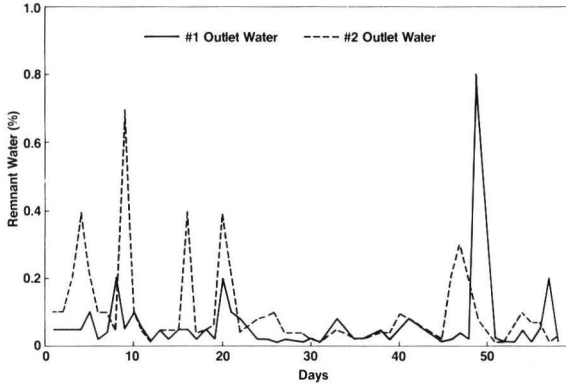

Figure 3 Phase Separation Performance

4.3 Removal of Water from Alcohol/Ketone/Ester Solvent

Samples of a solvent used in a wash process in an ester plant consisting of a blend of oxygenated organic compounds were tested for susceptibility to electrostatic phase separation. The samples were saturated with the aqueous phase in a blender and allowed to settle. The resulting emulsion contained 1.1% aqueous phase in the form of a fine haze after settling. Electrostatic treatment of these emulsions consistently produced phase separation with an organic phase containing less than 0.1% by weight of water.

4.4 Removal of Water from Lanthanide Extraction Solvent

Samples of a solvent from a lanthanide extraction operation using an aliphatic organic acid in a kerosene diluent were also tested for phase separation by electrostatic fields. Water was added to the samples as received to a concentration of 10%. After agitation, the samples were subjected to electrostatic separation. The water content dropped

rapidly to between 0.05 and 0.1% and continued to drop to trace quantities within five minutes.

5. CONCLUSIONS

Electrostatic processes have proved their merit in phase separation and mass transfer in liquid/liquid extraction systems in both pilot and commercial scale installations. Although phase separation is the more commercially advanced application, rapid developments in electrostatically enhanced mass transfer promise great benefits to solvent extraction operators in the form of more compact equipment, reduced energy requirements, higher purity products, and the increased environmental safeguards inherent in closed systems.

6. REFERENCES

1. Burris, D. R.: "Dual Polarity Oil Dehydration," Petroleum Engineer International (August 1977).
2. Brown, A. H. and Hanson, C.: "The Effect of Oscillating Electric Fields on the Coalescence of Liquid Drops," Chem. Eng. Sci. 23, 841 (1968).
3. Prestridge, F. L.: "Electric Treater," U. S. Pat. 3,772,180.
4. Prestridge, F. L.: "Process for Electrical Coalescing of Water," U. S. Pat. 3,847,775.
5. Bailes, P. J.: "Solvent Extraction in an Electrostatic Field," I&EC Process Design and Development 20, 564-570 (July 1981).
6. Prestridge, F. L., Schuetz, A. A., and Wheeler, H. L.: "Voltage Control System for an Electrostatic Oil Treater," U. S. Pat. 4,400,253.
7. Prestridge, F. L.: "Method and Apparatus for Separation of Fluids with an Electric Field," U. S. Pat. 4,126,537.
8. Prestridge, F. L. and Longwell, R. L.: "Separation of Emulsions with an Electric Field," U. S. Pat. 4,308,127.
9. Prestridge, F. L. and Johnson, B. C.: "Distributed Charge Composite Electrodes and Desalting System," U. S. Pat. 4,702,815.
10. Warren, K. W. and Prestridge, F. L.: "Crude Oil Desalting by Counterflow Electrostatic Mixing," National Petroleum Refiners Association 1988 Annual Meeting, AM-88-78, San Antonio, Texas (March 1988).
11. Warren, K. W. and Prestridge, F. L.: "Apparatus for Application of Electrostatic Fields to Mixing and Separating Fluids," U. S. Pat. 4,161,439.
12. Warren, K. W. and Prestridge, F. L.: "Process for Application of Electrostatic Fields to Mixing and Separating Fluids," U. S. Pat. 4,204,934.
13. Johnson, B. C. and Prestridge, F. L.: "Electrostatic Mixer/Separator" U. S. Pat. 4,606,801.
14. Basaran, O. A. and Scriven, L. E.: "Axisymmetric Shapes and Stability of Isolated Charged Drops," Phys, Fluids A 5, 795-798 (May 1989).
15. Basaran, O. A. and Scriven, L. E.: "Axisymmetric Shapes and Stability of Charged Drops in an External Electric Field," Phys. Fluids A 5, 799-809 (May 1989).
16. Scott, T. C. and Wham, R. M.: "Surface Area Generation and Droplet Size Control in Solvent Extraction Systems Utilizing High Intensity Electric Fields," U. S. Pat. 4,767,515.
17. Scott, T. C. and Wham, R. M.: "An Electrically Driven Multistage Countercurrent Solvent Extraction Device: The Emulsion Phase Contactor," Industrial and Engineering Chemistry Research 28, 94 (1989).

Solvent Extraction 1990, T. Sekine (Editor)

© 1992 Elsevier Science Publishers B.V. All rights reserved

CRITERIA FOR THE DESIGN OF PLATE SEPARATORS FOR THE SEPARATION OF DROPLETS FROM LIQUIDS

W.Rommel and E.Blass
Lehrstuhl A fuer Verfahrenstechnik, Technical University Munich
Arcisstr. 21, D-8000 Muenchen 2 (FRG)

ABSTRACT

Rommel, W. and Blass, E., 1990. Criteria for the Design of Plate Separators for the Separation of Droplets from Liquids. Preprints of ISEC'90, Kyoto (Japan)

The paper presents criteria for the estimative design of plate separators which have been deduced from experiments with droplet swarms. The criteria require the knowledge of the physical properties of the dispersion to be separated and its volumetric flow rate only. They allow the estimation of the area of the plates and the optimum load of the settler.

1 INTRODUCTION

Plate packages are frequently used as coalescing aids for the separation of disperse liquid-liquid systems even at high numbers of droplets per unit volume. They shorten the sedimentation pathes of the droplets and enlarge the interfacial area at which the droplets can coalesce. The coalescence of droplet swarms leads to the formation of thin liquid films of drop phase which flow off the inclined plates towards the hydrostatic pressure head. Following droplets reach these trickling films, are subsequently drawn with them for a certain distance until they coalesce with the film. A constant renewal of the interface at the actual points of coalescence results. The interfacial adsorption of surfactants which hinders the process of coalescence is avoided, the reason being the tensid molecules are swept away by the trickling film. Fig. 1, for example, shows a horizontal gravity settler with two inclined plate packages as coalescing aids. Meon (1988, 1989) developed a criterion from single droplet studies which allows the estimation of the optimum operating range of a plate separator. In addition to the physical properties and the operating parameters this criterion requires the knowledge of the drop size or the drop size distribution of the dispersion to be separated. In the stadium of the settlers design this kind of information is normally not available. In the following a new criterion is reported which requires no information on the drop size. It was deduced from many empirical data.

2 EXPERIMENTS ON DROPLET SWARM COALESCENCE AT INCLINED PLATES

2.1 Pilot Plant

A pilot plant was constructed which allows the simulation of the processes between two plates of a plate separator. The main component of the pilot plant is an inclinable flow channel with glass walls and a length of 1 m. The upper plate of the channel is made of PTFE which is wetted

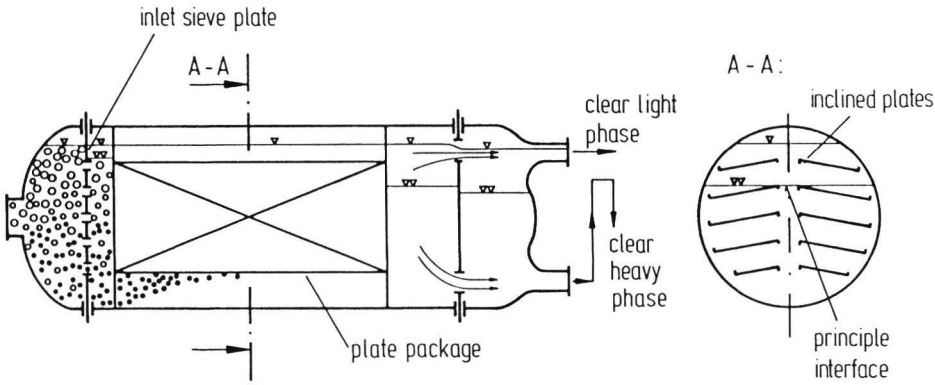

Fig. 1: Example for a gravity settler with inclined plate packages for the separation of liquid-liquid dispersions

well by the drop phase. Inside the channel a second plate with variable distance from the upper plate is located. This construction renders possible the evaluation of the influence of the plate inclination and the plate distance. The plate area cannot be varied in the experiments. Therefore the volumetric flow rates of the dispersed phase $\dot{V}_d$ are related to the plate width b_P. The resulting values (named "load of dispersed phase" $\dot{V}_d/b_P$) evaluate implicitely the plate width as influencing parameter. The plate length l_P is considered to be no determining parameter, since Meon (1989) showed that already short plates are sufficient within the range of optimum working conditions.

2.2 Aimed Parameters

For the practical use of plate separators the "degree of separation" is of the highest interest. It is defined:

$$E(x_i) = \frac{\dot{V}_d - \dot{V}_{P,i}}{\dot{V}_d} \tag{1}$$

2.3 Measuring technique

For the evaluation of the degree of separation the volumetric flow rate of not coalesced drops at the measuring point is to be measured. There was no standard measuring technique available at the beginning of this work. Therefore we developed first a photographic technique, which was very time consuming, and later on an electronic technique based on the numerical evaluation of scan patterns (Rommel, 1990). Besides the degree of separation both techniques deliver the drops size distributions, too.

2.3 Measuring Results

The results reported in the following are drawn from the material system toluene(d)/water, but meanwhile we could confirm them with two other testing systems (see Rommel, 1990).

(i) Degree of separation of polydispersed droplet swarms. Fig. 2 illustrates the degree of separation for toluene(d)/water at the position $x = 585\ mm$ and polydispersed swarms with a mean Sauter diameter of $4.15 \pm 0.25\ mm$. The adjustment of the mean Sauter diameter independent from the volumetric flow rate was achieved by a special dispersion method, which this paper does not report on. Two regions of different separation behaviour can be recognized. Left of the

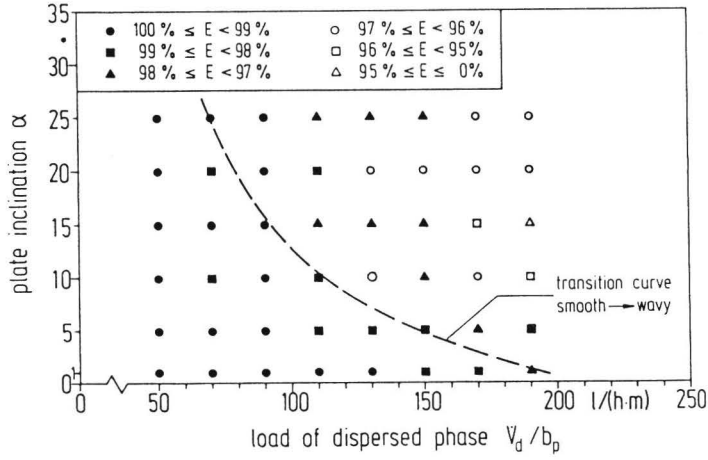

Fig. 2: Points of similar values of the degree of separation for toluene(d)/water

plotted boundary line degrees of separation of more than 99% can be achived. On the other side of the line the degrees of separation decrease significantly. The maximum load of dispersed phase can be operated at an inclination of 1^o. But from the practical point of view it is well known that plate separators are operated at a plate inclination of about 15^o. Our results show that at this inclination the maximum degrees of separation are about 50% lower. Indeed our experiments have been carried out with highly pure liquids which can be hardly expected in praxi. Technical liquids are always more or less contaminated. The fouling susceptibility of plate separators decreases with increasing plate inclination because of the resulting higher flow velocity between the plates. For practical application the lower load of dispersed phase in the case of a higher plate inclination can be compensated by a higher plate area. For the conditions reported in this paper the operation of a plate separator with a plate inclination of 15^o at a load of dispersed phase of 90 $l/(hm)$ would be appropriate.

It can be ascertained that if one succeeds in modelling the boundary line refered to before, it is possible to predetermine the optimum operating range and the required plate area without knowing anything about the drop size and without any experiment.

(ii) Surfactant influence on the degree of separation. Fig. 3 compares the degrees of separation of the pure liquid system toluene(d)/water with the ones of a system contaminated with the surfactant sodium-dodecyl-sulfate (SDS). The black symbols mark the pure liquid system with a surface tension of 34 mN/m and the blank ones the liquid system with a concentration of 0.2 g/l

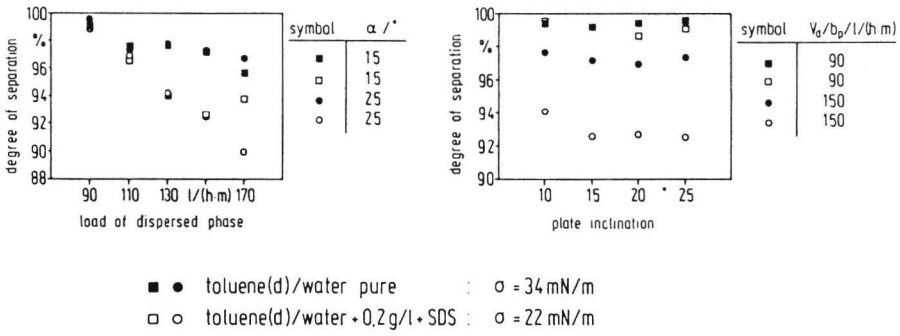

Fig. 3: Surfactant influence on the degree of separation of toluene(d)/water

of SDS and a surface tension of 22 mN/m. There is no significant difference between the two liquid systems at a load of dispersed phase of 90 $l/(hm)$ considered to be optimum before. But an increase of the load leads to a strong drop of the degree of separation of the contaminated system compared to the pure one. It is evident that in this case the negative effect of the surfactants can no longer be compensated by the plate effect.

(iii) Modelling of the boundary line. We found that the line which limits the optimum operation region plotted in Fig. 2 closely corresponds with the transition from smooth to wavy film flow between the plates. This fact is not only valid for toluene(d)/water but we also could establish it for n-amyl alcohol(d)/water and butyl acetate(d)/water. Fig. 4 shows the boundary lines for these three liquid test systems depending on the plate inclination and the load of dispersed phase.

Plotting the film-Reynolds number versus the liquid number of these boundary lines leads to the merging of the lines to points, as is illustrated in Fig. 5. The onflowed plate width b_P serves as significant length in the Reynolds number for the film. The thickness of the trickling film can be calculated by a simple equation (Rommel, 1988):

$$\delta_R = k_\delta \sqrt[3]{\frac{3\dot{V}_d \eta_d}{b_P g \Delta\rho \sin\alpha}} \tag{2}$$

with

$$k_\delta = \frac{1 + \eta_d/\eta_c}{0.97 + \eta_d/\eta_c} \tag{3}$$

Finally a regression delivers the interrelation between Re_R and $K_{F,d}$ at the transition from smooth to wavy film flow:

$$Re_R = 80.0\ K_{F,d}^{0.19} \tag{4}$$

which is not only a measure for the transition of the flow regime but also a limiting criterion for the optimum operation of a plate separator.

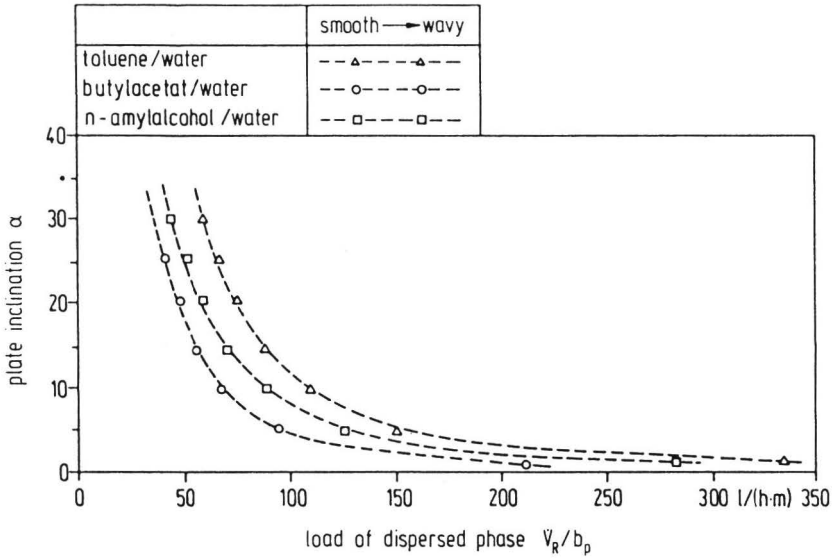

Fig. 4: Boundary lines for the transition from smooth to wavy film flow between the plates

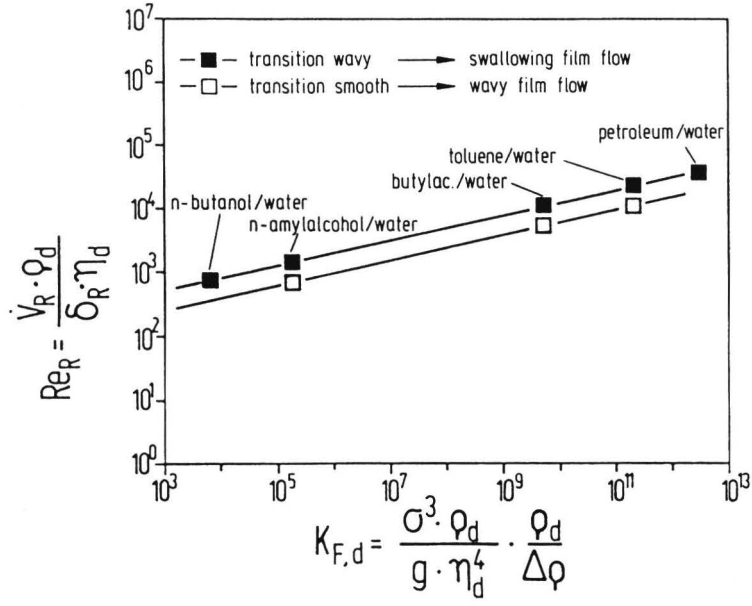

Fig. 5: Dimensionless form of the boundary lines for the transition from smooth to wavy film flow between the plates

3 DESIGN CRITERION

The reported limiting criterion allows to estimate the required plate area when the volumetric flow rate of the dispersed phase is given or to evaluate the maximum flow rate of the dispersed phase in case the plate area or plate number is given. But it does not render possible

- the optimation of the plate inclination and
- the predetermination of the degree of separation.

Further experiments, which are not reported in this paper, show that the absolute value of the degree of separation is determined by the phenomenon of the so-called partial coalescence. Since in many cases, e.g. in environmental protection techniques, the degree of separation should be next to 100% our future work will focuss on the partial coalescence.

4 SYMBOLS

b_P	m	plate width
g	m/s^2	gravity acceleration
k_δ	$-$	correction constant for the film thickness
l_P	m	plate length
$\dot{V}_d$	$l/(hm)$	volumetric flow rate of dispersed phase
$\dot{V}_{P,i}$	$l/(hm)$	drop flow rate
α	^{o}	plate inclination
ρ_i	kg/m^3	density of phase i
η_i	$Pa\ s$	viscosity of phase i

5 REFERENCES

Meon, W.,1989 Ein Beitrag zur Koaleszenz einzelner Tropfen in Schwerkraftabscheidern mit Platteneinbauten. Doctoral thesis, Technical University Munich.

Meon, W.and Blass, E., 1988 Fundamental research on drop coalescence at inclined plates. Procceedings of ISEC'88, Moscow, pp. 136-139.

Rommel, W., 1990 Tropfenabscheidung in Schwerkraftapparaten mit Platteneinbauten. Doctoral thesis, Technical University Munich.

Rommel, W. and Blass, E., 1988 Die Stroemung zweier nicht mischbarer Fluessigkeiten und von mitschwimmenden Tropfen zwischen parallelen geneigten Platten. Chem.-Ing.-Tech., 11: pp. 916-917.

5 ACKNOWLEDGEMENT

Financial support of this work by means of the Deutsche Forschungsgemeinschaft (DFG) is gratefully acknowledged.

Solvent Extraction 1990, T. Sekine (Editor)
© 1992 Elsevier Science Publishers B.V. All rights reserved

LASER TRANSMISSION TECHNIQUE FOR HOLD-UP MEASUREMENTS IN AGITATED TANK

K. H. ABID and J. G. GODFREY
Chemical Engineering Department, Bradford University.

ABSTRACT

A technique has been developed for measuring dispersed phase hold-up in an agitated tank. Hold-up was determined as a function of laser transmission in a coloured dispersion after the refractive index of the continuous phase was modified to match the refractive index of the dispersed phase. This technique is designed to study the effect of impeller speeds on hold-up in a system free of hydrodynamic disturbance. The technique can be applied to study hold-up variation with the mixer height.

1-INTRODUCTION

The quality of liquid-liquid dispersion in an operating mixer can be assessed by the dynamic dispersed phase hold-up. Several measurement techniques are available for hold-up measurements but have limitations. The nature of dispersion is disturbed either by sampling[7] or by inserting a probe, e.g., electroresistivity[3] or ultrasonic[2] . Further, investigations of local hold-up variation require many radial measurements in order to characterize the system by an radial average value. Tavlarides[8] investigated these problems by measuring the hold-up using two acoustic transducers positioned outside the mixer wall and facing each other. The hold-up was measured as a function of the time difference of ultrasonic waves in both phases. This technique becomes an accurate when the time difference becomes small. In column contactors, a pressure method[5] was used for vibrating plate extractor. It shows a limitation due to the density differences. In packed columns a light transmission has been used[1] but, although the system was not complicated by motion of impeller or plates poor results was reported. However, the principles need to be clarfied. In this paper a technique for hold-up measurements is presented using laser transmission in a system with an impeller agitation.

2-BASIS OF THE TECHNIQUE

For the experimental arrangement shown in Figure (1) a plane of dispersed drops of spherical shape and a range of sizes is

illuminated by a parallel light beam. Light scattering takes place because the refractive index of the drop phase is different from the refractive index of the continuous media. If we define a field **P** which is far enough from the dispersion plane and neglect the multiscattering effect then **P** only receives forward travelling light[4] The fraction of light received by **P** is a function of the interfacial area[6].

If we refer to the refractive index of the continuous phase and the dispersed phase by X_c and X_d respectively:

(i) $X_c << X_d$ field **P** received only the parallel light which dose not strike any drop

(ii) $X_c \longrightarrow X_d$ only small fraction of light is scattered

(iii) $X_c/X_d=1$ no scattering takes place.

The general rule is that the scattering pattern of the dispersion is expressed by $X_c/X_d=1+E$ and $X_c/X_d=1-E$,where **E** represents any fractional number. If the refractive index of the continuous phase is modified until **E** becomes zero then the scattering pattern in both phases becomes identical and consequently all the incident rays are received by the field **P**. Now, if the dispersed phase is coloured then the transmission light to **P** is only function to the dispersed phase hold-up since the coloured drops absorb a fraction of incident light. In this free scattering coloured dispersion the transmitted light is a function of the dye concentration and the quantity of dispersion.

3-EXPERIMENTAL

3.1 Laser set-up

Figure (2) shows the set-up of the laser transmission technique and the associated equipment. A 10 mW HeNe laser was used in conjunction with 10 times magnifying beam expander to give a beam width equal to 6.9 mm. The field **P** of Figure 1 is a photo detector which has the same diameter of the laser band. The laser band penetrated the dispersion in the gap half way between the impeller tip and the tank wall.

3.2 Mixing equipment

The mixing tank was designed according to the standard configuration given by Rushton and Oldshue[9] . The tank was a glass cylinder with 153 mm in I.D.and 153 mm in height. The impeller was turbine with 51 mm in diameter, located at 51 mm off the bottom. The mixing tank was operated without an air-liquid interface. The jacket box was made of perspex. The temperature was well controlled with the aid of refrigerated circulator which was capable to keep the temperature as required, 25.5°C.

3.3 Liquid-liquid system

n-Octanol was used as a dispersed phase in 11.5% volume fraction. Sucrose was chosen as a matching refractive index agent for the water phase. The materials were of technical grade, and the water was purified to remove particles. The water-sucrose solution showed a Newtonian behavior, with a viscosity of 15.3 cP. The solvent phase viscosity was 7.0 cP. The refractive index for both phases was 1.4251.

3.4 Procedure

At first, the mixer was carefully cleaned then both phases were charged separately, beginning with the heavy phase, after they were equilibrated. The air bubbles generated during the filling process were removed through two openings on the top plate of the mixer; this was carried out by moving the impeller to a position near to the top plate and it was revolved at low speed. After the condition of matched refractive index was achieved the dispersed phase was coloured with an oil soluble green dye with a concentration equal to 0.005 w/v. The dye is not surface active.

4-RESULT AND DISCUSSION

4.1 Mixture refractive index

Figure (3) shows the effect of refractive index ratio (X_c/X_d) on laser transmission. The data was generated from a transparent dispersion under uncompleted mixing condition. The refractive index of continuous phase was changed each time by injecting a

volume of water under the top layer of the dispersed phase. The experiments showed that **E** is in the order of 10^{-4} which was very difficult to determine precisely, therefore the matching refractive index was established when 100% laser transmition was achieved.

4.2 The critical temperature

It was necessary to investigate the effect of temperature on laser transmission. The experimental results shown a type of normal distribution behavior, see Figure (4). As change of 1°C may give an error of the order of 25%, therefore precise temperature control was needed. As a consequence, during all the experiments, the temperature was successfully controlled within 0.01 °C. Changing the impeller speeds at the critical temperature (100% transmission) did not show effect on transmission percent. This confirms that the transmission is not a function of the drop size.

4.3 Hold-up and laser transmission

A calibration diagram was constructed to show the relationship between the hold-up and laser transmission at nearly spatially homogeneous dispersion. An exponential curve describes the transmission characteristic and a regression analysis shows a some deviation at the both ends of the curve. This is in agreement with Beers-Lambert law for light absorption in a single phase where the light absorption shows different behavior from the exponential model at low and high dye concentration.

4.4 Effect of impeller speeds on hold-up

Typical data is shown in Figure (5). A situation of incomplete dispersion, a layer of dispersed phase could be recognized, was found when the impeller speeds less than 600 rpm. Investigations of local hold-up with respect to mixer height were carried out by locating the laser in four different position and no significant variation of hold-up was seen.

5-CONCLUSION

A laser transmission technique is proposed for the measurements of dispersed phase hold-up in a turbulently agitated

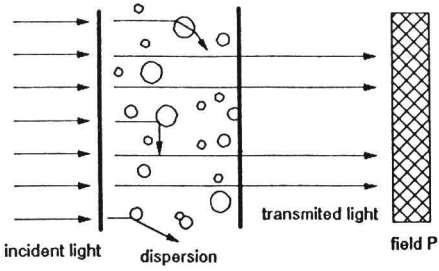

Fig. 1. Incident light distribution across dispersion plane

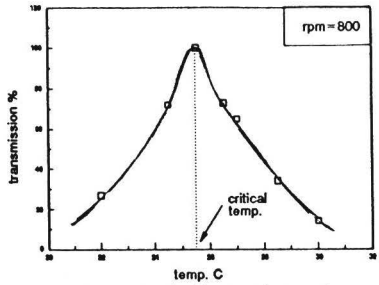

Fig. 4. Effect of temperature on laser transmission

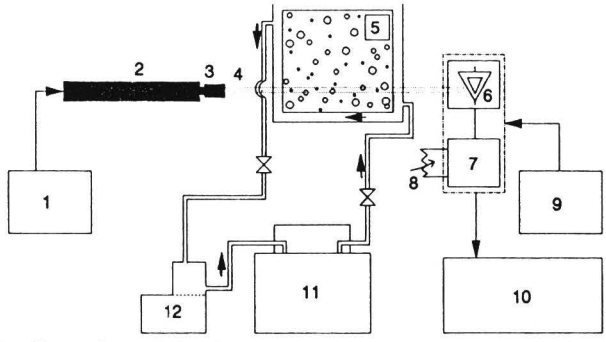

Fig. 2. Experimental set-up

Keys

1. laser power supply
2. HeNe laser
3. beam expander
4. laser band
5. dispersion
6. photo detector
7. amplifier
8. gain
9. power supply
10. output terminal
11. refregerator
12. refractometer

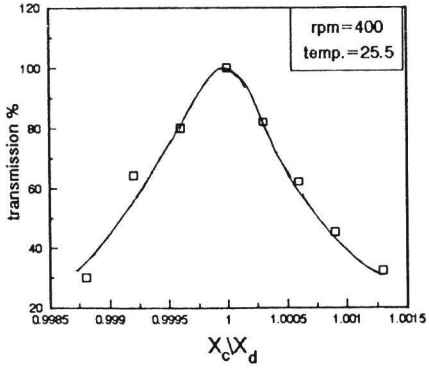

Fig. 3. Effect of refractive index ratio on laser transmission

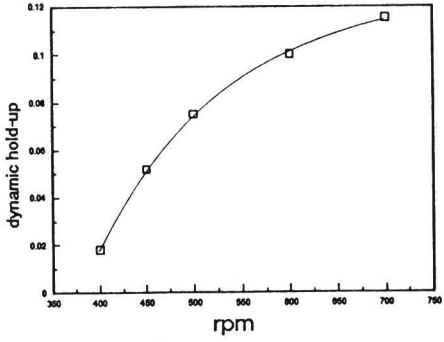

Fig. 5. Effect of impeller speed on dispersion process

liquid-liquid dispersion. The measurements can be made free from any hydrodynamic disturbance and is characterized by an average radial value. The technique is now being applied to a pilot scale pump-mix system.

6-REFERENCE

1. Burdett, J.D., Webb, D.R. and Davies, G.A., Chem.Eng. Sci., **36**, 1951, (1981).
2. Halicek, A. and Sovava, H., Coll. Czech. Chem. Commun., **49**,379, (1984).
3. Hoffer, M.S. and Resnick, W.,Chem. Eng. Sci., **30**, 437, (1975).
4. Hulst, H.C. van dee, Light Scattering by Small Particals, Wiley New York, (1981).
5. Jiricy,V. and Prochazka, J., Chem.Eng. Sci., **36**, 2237, (1980).
6. McLaughlin, C.M. and Rushton, J.H., AIChE J., **19**, No. 4, 817,(1973).
7. Mylnek, Y. and Resnick, W., AIChE J., 18, 122, (1972).
8. Tavlarides,L.L., Schmidt, H., Stamatovic,M. and Bont,C.J., Conference on Nuclaer Fuel Reprocessing and Waste Managment, Paris, 387, (1987).
9. Rushto n , J.H. and Oldshue, J.Y., Chem.Eng. Progr., **55**, 181, (1959)

Solvent Extraction 1990, T. Sekine (Editor)

© 1992 Elsevier Science Publishers B.V. All rights reserved

FORMATION OF UNIFORMLY-SIZED EMULSIONS BY MEANS OF APPLIED ELECTROSTATIC FIELD.

MASAYUKI SATO
Department of Biological and Chemical Engineering, Gunma University, 1-5-1 Tenjin-cho, Kiryu, Gunma, 376 Japan

ABSTRACT
Sato, Masayuki, 1990. Formation of uniformly-sized emulsions by means of applied electrostatic field.
Uniformly-sized O/W emulsions were produced by means of applied electrostatic field in the diameter range from 1 to 300 μm. Essentially uniform emulsions were obtained using ac voltage from 30 to 300 μm in diameter within a synchronous region which was determined by the ac voltage, frequency and other parameters. On the other hand, cloudy droplets of 0.9 μm average diameter having very sharp size distribution were formed under applied dc voltage. The present methods have many advantages over the prevalent methods such as: (1) droplets have a uniform diameter and easily controllable due to ac frequency change; (2) electrically insulating liquid can be emulsified in water medium; (3) droplets can be produced directly in immiscible liquid.

1 INTRODUCTION

In highly advanced industrial processes, uniformly-sized emulsions (including uniformly-sized solid particles) have become desirable for various purposes. The size of the particles produced by prevalent methods usually have a widely spread frequency distribution represented by a log normal function. It is possible to reduce the size distribution range by the application of electrical or mechanical vibration to the liquid dispersion system. The author previously reported the electrical method to produce essentially uniform gas bubbles in liquid, droplets in gaseous media and droplets in immiscible liquid in "synchronization" with the applied ac frequency.

Uniformly-sized emulsions can be widely utilized in the following purposes of: (a) liquid-liquid extraction processes (easy to break emulsions after extraction, easy to decide operative conditions and equipment design); (b) packed bed for liquid chromatography, separators for large scale liquid crystal displays, standard particles for size distribution measurement, etc., (after polymerization in immiscible liquids or vaporization of solvent from the polymer solution droplets).

In the present paper, the author proposes new valuable methods for producing uniformly-sized emulsions directly in the immiscible liquid (distilled water in this case) by means of applied ac or dc potential in the diameter rage from 1 to 300μm.

2 PREVIOUS WORKS

There are some trials to produce uniformly-sized liquid droplets in gaseous media in utilization of mechanical vibration or electrical force to the laminar liquid jet. They were applied mainly to the ink-jet printing system. When one would try to produce emulsions taking the uniform liquid droplets suspended in air into the immiscible liquid, the droplets will coalesce with each other or fly away with the air flow. So, it could be desirable to produce emulsions directly within the liquid medium.

An interesting phenomena was reported, where smaller sized uniform emulsions can be obtained when a multiple laminar liquid jet issuing from a nozzle (for example, monomer liquid jet is surrounded with distilled water) is disintegrated in synchronization with the applied ac frequency into uniformly-sized concentric drops, and then dripped into distilled water (Sakai et al., 1989). However, there have been almost no trials for the direct production of uniform emulsions.

The author reported on the production of uniformly-sized gas bubbles from a single capillary nozzle in liquid media with an applied ac field (Sato et al., 1980, 1981 and 1983). The bubbles were detached from the nozzle tip when the applied ac potential reached a certain level in its positive and/or negative peak. Similar phenomena were observed for the formation of liquid drops in gaseous or immiscible liquid media (Sato, 1984). Mechanism of the liquid dispersion in immiscible liquid into uniform droplets in synchronously with an ac potential as mentioned above seems to be almost the same with that of the dispersion of gas in liquid.

The synchronized drop formation process may be very promising for producing fine uniformly-sized emulsion droplets, and also control of drop size is very easy since it is only necessary to vary the ac frequency.

3 EXPERIMENT

Experimental apparatus is shown in figure 1. Organic liquid (kerosene, styrene monomer, or other non-conductive liquid) flows out of sample chamber to nozzle through needle valve due to nitrogen gas of 1 atm pressure. The liquid flow rate is calculated by the weight reduction of the sample chamber between a time interval using electronic balance. A vessel is consisted of plexiglas in order to observe from outside of the bottle, which includes distilled water as a dispersion medium. Ac/dc voltage is applied between the nozzle and the earth electrode. The ac and the dc high voltage source are composed of high voltage, variable frequency transformer (Sato et al., 1988) and Fluke Model 410B power supply, respectively. Using oscilloscope, voltage is measured through high voltage probe, and electric current is calculated by the voltage drop between the resistor inserted in the earth line.

Disintegration phenomena are observed by means of TV camera, monitor and video tape-recorder using stroboscope illuminating synchronously with the applied

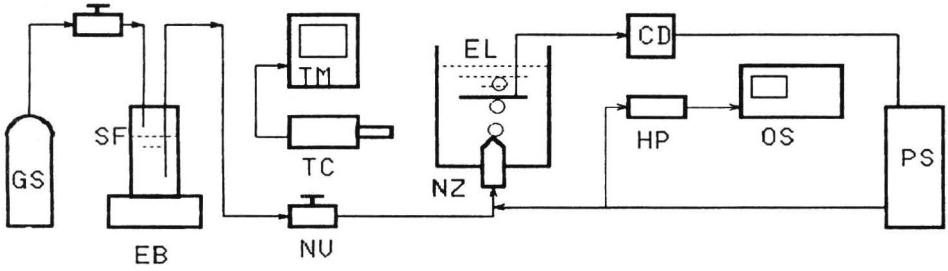

Fig. 1. Schematic diagram of experimental apparatus.

CD: Current Detector	EB: Electronic Balance	EL: Earth Electrode
GS: Nitrogen Gas Holder	HP: High Voltage Probe	NV: Needle Valve
NZ: Nozzle	OS: Oscilloscope	PS: AC/DC Power Supply
SF: Sample Feeder	TC: TV Camera	TM: TV Monitor

ac signal. One can readily decide whether the drop formation is in synchronization with ac frequency or not, since the image of the forming drops can be frozen by the strobe light during synchronous state.

Two types of nozzles were used as: (a) stainless steel capillary nozzle of 0.23 mm inside diameter with complete electrical insulation except the nozzle tip; (b) orifice type nozzle having one opening of 30~100 μm diameter in the stainless steel plate with and without electrical insulation. The capillary and the orifice type nozzles were used for applying dc and ac voltage, respectively.

The diameter of the droplets was measured by means of video image for larger diameter above 30 μm in a case of applied ac voltage, and by scanning electron microscope for very fine beads around 1 μm after polymerization of styrene monomer droplets in a case of dc dispersion state.

4 RESULTS

The proposed methods have a special feature that all kinds of electrically non-conductive organic liquids can be dispersed to uniformly-sized droplets in distilled water in the wide diameter ranges with no additives, which has been impossible by means of the prevalent methods. In the present study, the mechanism of the droplet formation can be divided into two categories as mentioned above; (a) synchronized formation with the cycle change of ac voltage; (b) cloudy droplet formation due to applied dc voltage.

4.1 *Synchronized formation under applied ac voltage*

(i) *Droplet formation in synchronization with ac frequency using orifice type insulated plate nozzle.* As the ac voltage increases, forming frequency of droplet is gradually increases until the voltage reaches to the lower limit of synchronous region. Within a synchronous region, droplet forming frequency becomes equal to the applied ac frequency, where the droplet diameter is determined only by the

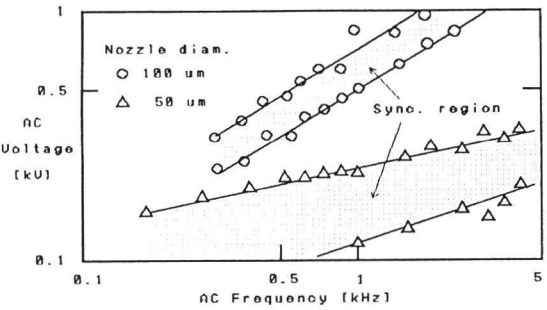

Fig. 2. Synchronous regions of uniformly-sized droplet formation between ac frequency and voltage, where kerosene of the flow rate of 0.51 ml/min is dispersed in distilled water medium.

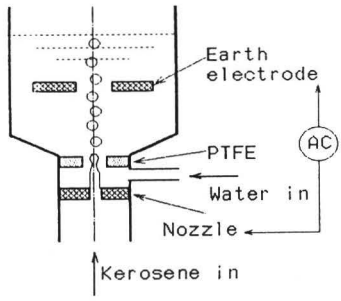

Fig. 3. Schematics of convergent electric field type nozzle.

liquid flow rate and ac frequency. Figure 2 shows synchronous region between applied ac frequency and voltage where two kinds of orifice type nozzle (stainless steel plate having diameters of 100 and 50μm with electrical insulation) were used. Kerosene was dispersed in distilled water medium and resulted droplet diameter was 50~100μm (using 100μm nozzle) and 30~80μm (using 50μm nozzle), respectively. From the figure, smaller size of droplet can be obtained using smaller diameter of the nozzle with operating larger ac frequency and lower voltage. However, as the nozzle diameter is reduced the nozzle will be easily clogged with small particles.

(ii) *Convergent electric field type nozzle.* Schematics of convergent field type arrangement of orifice type nozzle, an insulating plate and earth electrode is shown in figure 3. Where the orifice is same as used in figure 2 (without insulation), and the insulating plate is made of 200μm thick PTFE having 400μm diameter hole. Kerosene flows out of the orifice and distilled water flows through the hole surrounding the kerosene jet, in which the electric field is concentrated into the hole. For example, uniformly-sized kerosene droplets of 180μm diameter were obtained in distilled water using 100μm diameter nozzle, where the flow rate of kerosene and distilled water was 0.13 and 0.42 ml/min, respectively, and ac frequency was 700 Hz. There observed a wide frequency range of synchronous region and undetectably small electric current (less than 1μA), especially the lower limit of synchronizing voltage was only 5.2 V (100 to 1000 V as above mentioned case). Mechanism of the synchronous formation would be electrical shrinking force due to applied ac potential generated by the convergent field in the insulating plate hole. There are some superior characteristics on the proposed method as: (a) consumed energy and nozzle erosion is very small because of low operating voltage; (b) one

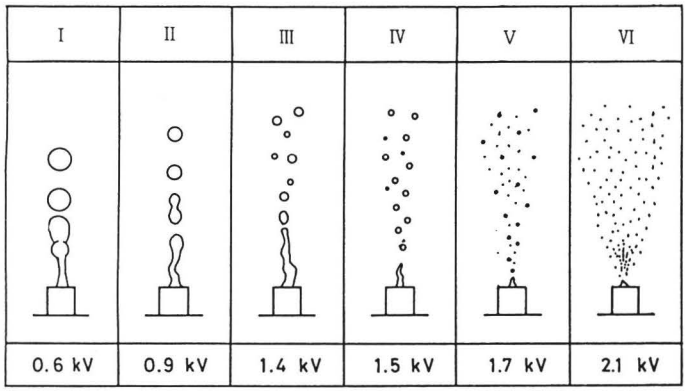

Fig. 4. Illustrations of disintegration pattern of kerosene in distilled water with varying applied dc voltage.

can use any kind of liquid as the medium other than distilled water (distilled water has to be used as the surrounding liquid of the jet); (c) one can produce smaller droplets from the thinner liquid jet due to the contraction effect of the liquid flow into the hole.

4.2 *Cloudy droplet formation by dc voltage*

Using dc voltage, extremely fine droplets can be obtained in distilled water which is about 0.9μm diameter and has a fairly uniform in size. The disintegration pattern is shown illustratively in figure 4. When an applied dc voltage is increased, the forming droplet diameter decreases which is similar to the case of applied ac voltage. As the voltage becomes 2.1 kV, a great many micro-sized droplets flow out like a cloud, then nothing will be seen inside the bottle covered with the cloud. The droplets are too small to measure by the microscope, so styrene monomer was used instead of kerosene, which was dispersed and then polymerized to solid beads to be able to observe using scanning electron microscope.

The size distribution of the droplet diameter produced by the present method and ultrasonic emulsifier is shown in figure 5. The ultrasonic method has a widely spread frequency distribution from a small size to 30μm. On the other hand, the proposed dc voltage method can produce fairly uniform droplets having a very sharp distribution of 0.9μm of average diameter. Although it might be somewhat a little problems that the distilled water (containing no electrolyte) should be used as medium liquid in the dc voltage method, the easy control of the droplet diameter will be studied in near future.

5 CONCLUSIONS

The electrically insulating liquid droplets having a uniform diameter were produced directly in the immiscible liquid medium under applied ac or dc voltage.

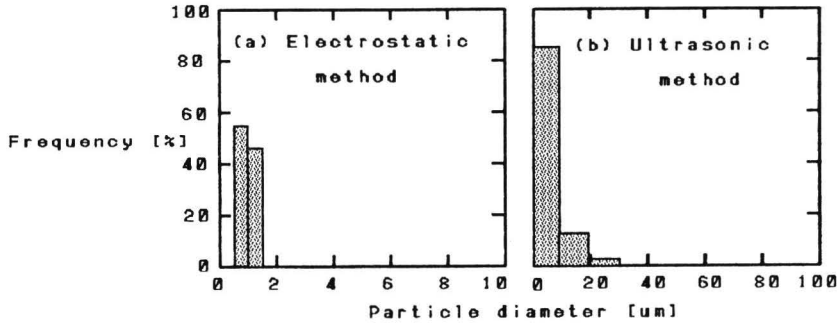

Fig. 5. Comparison of droplet size distributions between the proposed method (a) and the ultrasonic method (b).

The essentially uniform kerosene droplets of 30 to 300μm diameter were obtained by means of applied ac voltage in synchronization with its frequency. Fairly uniform styrene beads of average diameter of 0.9μm were formed in distilled water by applied dc voltage. Both methods can be applied adequately to many industrial and laboratory use alternatively of a larger or smaller diameter emulsions as each purpose of applications.

6 ACKNOWLEDGEMENT

The author would like to thank Professor Senichi Masuda for his valuable suggestions; and also to acknowledge Professor M. Sadakata and T. Sakai for their valuable discussions, and Dr. M. Saito, Mr. K. Kimura, J. Furukawa, R. Yamamoto, S. Kato and C. Katsuyama for their help with the experiments.

7 REFERENCES

Sakai, T., Sadakata, M., Sato, M. and Kimura, K., 1989. Production of concentric dual uniform size droplets from coaxial smooth jet by applied ac electric field. *JCLASS'89*, No. 12.

Sato, M., 1980. The formation of gas bubbles synchronized with ac potential., *J. Phys. D: Appl. Phys.*, vol. 13, pp. L1 - 2.

Sato, M., Miyazaki, S., Kuroda, M. and Sakai, T., 1981. The synchronized formation of uniform size bubble under applied ac potential. *Kagaku Kogaku Ronbunshu*, vol. 7, pp. 115 - 119.

Sato, M., Miyazaki, S., Kuroda, M. and Sakai, T., 1983. Formation of uniformly sized bubbles in synchronization with an ac frequency. *Int. Chem. Eng.*, vol. 23, pp. 72 - 77.

Sato, M., 1984. The production of essentially uniform sized liquid droplets in gaseous or immiscible liquid media under applied ac potential. *J. Electrostatics*, vol. 15, pp. 237 -247.

Sato, M., Miyazaki, H., Sadakata, M. and Sakai, T., 1988. Production of uniformly-sized liquid droplets under applied ac field by means of rotating multi-nozzle system. *ICLASS'88*, No. B3-1, pp. 161 - 165.

Solvent Extraction 1990, T. Sekine (Editor)

© 1992 Elsevier Science Publishers B.V. All rights reserved

FORMATION OF SINGLE CHARGED DROPS FROM A LAMINAR LIQUID JET IN ELECTRIC FIELDS

T.HIBIKI*, M.YAMAGUCHI and T.KATAYAMA
Department of Chemical Engineering, Osaka University, Toyonaka 560, Japan

ABSTRACT

Formation of single charged drops from a laminar liquid jet in a continuous liquid phase in various electric fields is studied theoretically and experimentally. Relations between growth rate of the interfacial wave of the jet and its wave number in the electric fields are derived from the Lagrangian equation of motion for the jet. The effects of the electric fields on the dynamic characteristics of the jet are analyzed numerically. The liquid-liquid systems used in experiments are water-cyclohexane, -hexane and -silicone oil. The jet length, jet radius and drop diameter decrease with the voltage. The experimental drop diameters agree well with those calculated by using maximum growth rate of the wave and the wave number for all the systems used.

INTRODUCTION

Recently, the effectiveness of the application of an electric field to contacting operations for the dispersion of the liquid in another liquid phase has been demonstrated. The application is mainly classified into four types, (A) application to dispersion of the liquid, (B) application to stirring and mixing of the liquid, (C) application to demulsification, (D) application to promotion of heat or mass transfer. In case of (A), the form of dispersion from a nozzle is classified into three types, (a) formation of single drops, (b) formation of single drops from a jet, (c) spraying formation. Estimation of the drop diameter is important for the design of contactors. With the revolution of the industrial technique, the formation of uniform charged drops of uniform size is important. Therefore, formation of single drops from a jet is essential to this technique. In this paper, the formation of single charged drops from a laminar liquid jet in liquid-liquid systems in electric fields, which are formed by three configurations of (1) a flat electrode arranged parallel above a flat one, (2) a nozzle electrode in the center of a cylindrical one, and (3) a nozzle electrode arranged vertically above a flat one, have been studied theoretically and experimentally.

*)Present address;Research Reactor Institute, Kyoto University, Kumatori-cho, Sennan-gun ,Osaka 590-04, Japan

2.Theory

2.1 Linear stability theory for a laminar liquid jet in electric fields

Consider an infinite jet of radius a_j of an incompressible, inviscid dielectric liquid in an electric field. In order to study the stability of the jet, an axisymmetric wave on the interface of the jet is assumed to be presented by

$$r=a_j+a\cdot\cos(kz+\omega) \tag{1}$$

If the amplitude of this wave is a function of time, the relation between the growth rate of the wave and the wave number can be derived from the Lagrangian equation of motion for the jet. The change in the potential energy of the system caused by the deformation of the jet is given by the sum of the change in the interfacial energy and the change in the electrical energy. The change in the potential energy and the kinetic energy of the jet are derived from a perturbation analysis of the interfacial wave. From the Lagrangian equation of motion, the growth rate of the wave for each of three kinds of electric field is given by Equations (3)-(5), respectively.

$$a=\alpha\cdot\exp(pt) \tag{2}$$

(1) a flat electrode arranged parallel above a flat one[1,6]

$$p^2=\frac{xI_1(x)}{\rho_d a_j^2 I_0(x)}\left[\frac{\sigma(1-x^2)}{a_j}-\frac{(\varepsilon_c-\varepsilon_d)^2E^2I_1(x)K_0(x)}{\{\varepsilon_d I_1(x)K_0(x)+\varepsilon_c I_0(x)K_1(x)\}}\right] \tag{3}$$

(2) a nozzle electrode in the center of a cylindrical one[4]

$$p^2=\frac{xI_1(x)}{\rho_d aj^2 I_0(x)}\left[\frac{\sigma(1-x^2)}{a_j}+\frac{(\varepsilon_c-\varepsilon_d)\varepsilon_c V^2}{\varepsilon_d a_j^2\{\ln(R/a_j)\}^2}\right] \tag{4}$$

(3) a nozzle electrode arranged vertically above a flat electrode[2]

$$p^2=\frac{xI_1(x)}{\rho_d a_j^2 I_0(x)}\left[\frac{\sigma(1-x^2)}{a_j}+\frac{4(\varepsilon_c-\varepsilon_d)\varepsilon_c V^2}{\varepsilon_d a_j^2[\ln\{4(H^2-z_0^2)/a_j^2\}]^2}\right] \tag{5}$$

$$x=ka_j \tag{6}$$

The first term in the right-hand side of Equations (3)-(5) represents the change in the interfacial energy, and the second term the change in the electrical energy. If V=0, Equations (3)-(5) are identical with Rayleigh's equation[7]. The wave number is determined from Equation (6) by using the value of x for which the growth rate, given by Equations (3)-(5), is maximized. From the calculation of Equations (3)-(5), the jet is stabilized by applying the voltage when the dielectric constant of the continuous phase is greater than that of the dispersed phase. In this case, the maximum growth rate of the interfacial wave of the jet and its wave number decrease with applied voltage[2,4].

2.2 Estimation of diameter of drop from a laminar liquid jet

The formation of drop from the jet is modeled by the following two assumptions based on experimental observations.

Assumptions:

1) The wave number k_m is the same all the way from the exit of the nozzle to the breakup point of the liquid jet. The wave number is derived from a model of modified segment[1]. $k_m \simeq 2 \cdot k_{max}$.

2) The relation between a moving length of the interfacial wave and time is $z=v_j t$.

Boundary condition:

The amplitude of the wave becomes equal to the jet radius at the breakup point.

Then, Equation (1) becomes Equation (7).

$$r=a_j[1+\exp\{p_{max.}(t-\ell/v_j)\}\cdot\cos(k_m v_j t+\omega)] \qquad (7)$$

Thus, if the jet length and jet radius are known, the volume of the drop can be calculated by integrating Equation (7) from the breakup point to the tip of the jet. The equivalent spherical diameter of the drop is used as a drop diameter.

3.Experiments**

The experimental apparatus is shown in Figure 1. The nozzle electrode (o.d. 1mm, i.d. 0.6mm) (1) set in the center of a copper cylindrical electrode (2) of diameter 20cm inside an acrylic cylinder. The cylindrical electrode was grounded, and the nozzle electrode was connected to the positive terminal of a high-voltage generator (3). The application of

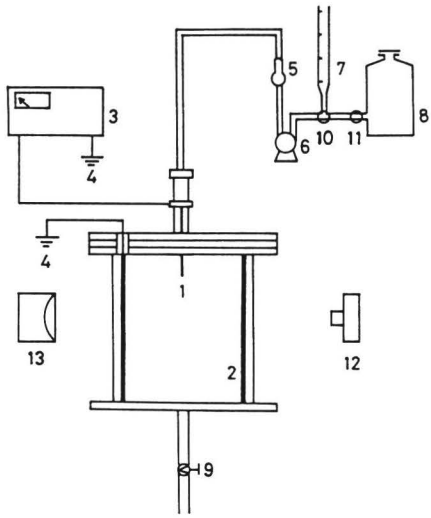

1:Nozzle
2:Cylindrical copper electrode
3:High voltage generator
4:Ground
5:Damper
6:Micro-tube pump
7:Burette
8:Dispersed phase reservoir
9:Needle valve
10:Three-way cock
11:Two-way cock
12:Camera
13:Stroboscope

Figure 1 Schematic diagram of experimental apparatus.

**)In this paper, experiments, results and discussion are described about the case of a nozzle electrode in the center of a cylindrical one as an example of electrode arrangement.

a voltage to the nozzle electrode set up an electric field. The dispersed phase flowed from a micro-tube pump (6) through the nozzle, forming a liquid jet. The drops which formed when the jet broke up were collected into a drop-collector at the center of the lower part of acrylic cell. Using the needle valve (9), the collected drops were steadily removed so as not to disturb the flow in the cell. The profiles of the jet and the drops were photographed using the camera (12) and the stroboscope (13). After enlarging the film, the jet length, jet diameter and drop diameter were measured. The flow rate of the dispersed phase was measured using the burette (7). The dispersed phase was distilled water saturated with the continuous phase, which was cyclohexane, hexane, or silicone oil saturated with distilled water. The experiments were conducted by varying the flow rate of the dispersed phase and the applied voltage.

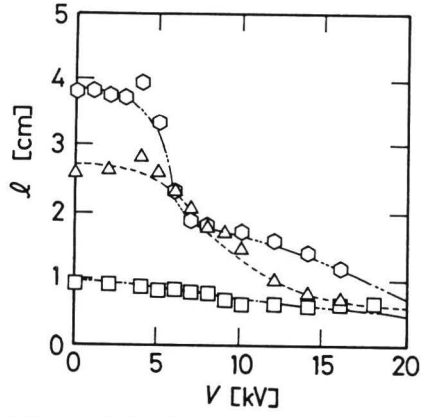

Key	Line	Continuous phase	v_N[cm/s]
□	——	hexane	89.8
△	------	cyclohexane	90.4
⬡	—·—	silicone oil	89.4

Figure 2 Relation between jet length and applied voltage.

4.Results and discussion

4.1 Jet length

Figure 2 shows an example of the relation between the applied voltage and the jet length. The lines on the figure have been drawn smoothly through the experimental points. The jet length decreased continuously with the voltage. It is explained as follows. The faster the maximum growth rate of the wave becomes, the faster the jet breaks up. That is, the jet length is in inverse proportion to the maximum growth rate. According to Equation (4), the maximum growth rate increases with the voltage. Therefore, the jet length decreases with the voltage.

4.2 Jet radius

Figure 3 shows an example of the relation between the applied voltage and the jet radius. The lines on the figure have been drawn smoothly through the experimental points. The jet radius decreased continuously with the voltage as the jet diameter is contracted by the electric force.

4.3 Drop diameter

Figure 4 shows an example of the relation between the applied voltage and the drop diameter. The lines on the figure were calculated using Equations (4) and (7). The calculated lines of water-cyclohexane, -hexane and -silicone oil system have been drawn until 8kV, 8kV and 7kV, respectively. That is why an axisymmetric jet isn't postulated as the whipping action arose over the voltage. The drop diameter decreased continuously with the voltage. It is explained as follows. As the drop diameter is calculated from integrating the form of the wave from the breakup point to the tip of the jet, the drop diameter is in proportion to wave length (or in inverse proportion to wave number). From the calculation of Equation (4), the wave number, which maximizes the growth rate of the wave, increases with the voltage. Therefore, the drop diameter decreases with the voltage.

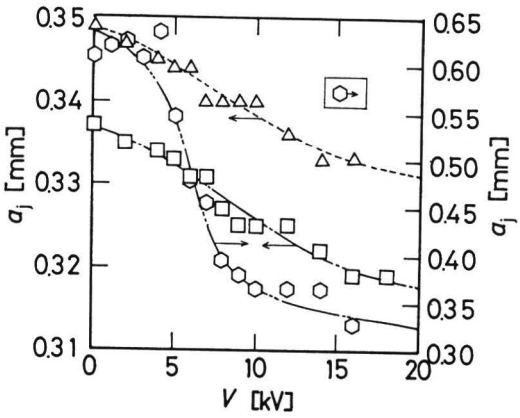

Figure 3 Relation between jet radius and applied voltage. The keys are the same as described in Figure 2.

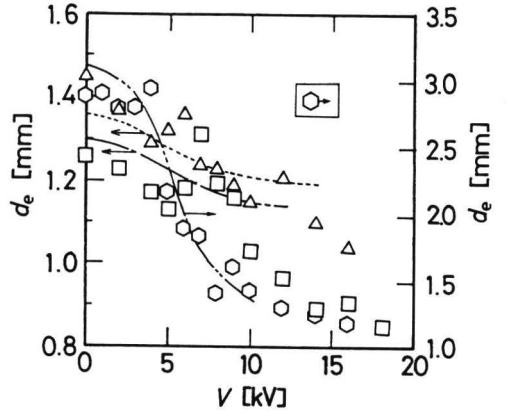

Figure 4 Relation between drop diameter and applied voltage. The keys are the same as described in Figure 2.

These lines are fairly good representations of the dependence of the drop diameter on the electric force. The drop diameter could be estimated within an error of ±10% for all the systems and arrangements of electrode[1,3,5].

5 CONCLUSIONS

The formation of single charged drops from a laminar liquid jet in electric fields were studied, and the following results were obtained.

(1) The equations of growth rate of the wave were derived from the linear stability theory. The drop diameters calculated from the equations and modified

segment model agreed well (within ±10%) with the experimental drop diameters.
(2) The jet length, jet radius and drop diameter decreased with the applied voltage.

6 NOMENCLATURE

a=amplitude of interfacial wave[m], a_j=jet radius[m], d_e=equivalent spherical diameter of drop[m], E=uniform electric field strength;V/L[V/m], H=distance between nozzle tip and flat electrode[m], $I_n(x)$=modified Bessel function of the first kind of order n[-], $K_n(x)$=modified Bessel function of the first kind of order n[-], k=wave number[1/m], k_m=modified wave number;$2\cdot k_{max.}$[1/m], ℓ=jet length[m], p=growth rate of wave[1/s], R=radius of cylindrical electrode[m], r=r-direction coordinate[m], t=time[s], V=applied voltage[V], v_j=jet velocity[m/s] v_N=average velocity of dispersed phase in nozzle[m/s], x=dimensionless wave number;ka_j[-], z=z-direction coordinate[m], z_0=distance between tip of jet and flat electrode[m], α=constant in Equation (2)[m], ε=dielectric constant[F/m], ρ=density[kg/m^3], σ=interfacial tension[N/m], ω=phase of interfacial wave[-]

<Subscripts>

c=continuous phase, cal.=calculated value, d=dispersed phase, exp.=experimental value, max.=value at maximized p

7 REFERENCES

1) Hibiki,T.,M.Yamaguchi and T.Katayama:Kagaku Kogaku Ronbunshu,**14**,476(1988)
2) Hibiki,T.,M.Yamaguchi and T.Katayama:Kagaku Kogaku Ronbunshu,15,269(1989)
3) Hibiki,T.,M.Yamaguchi and T.Katayama:Kagaku Kogaku Ronbunshu,15,1153(1989)
4) Hibiki,T.,M.Yamaguchi and T.Katayama:Kagaku Kogaku Ronbunshu,16,694(1990)
5) Hibiki,T.,M.Yamaguchi and T.Katayama:Kagaku Kogaku Ronbunshu,16,700(1990)
6) Nayyar,N.K. and G.S.Murty:Proc. Phys. Soc.,75,369(1960)
7) Rayleigh,J.W.S.:Proc. London Math. Soc.,10,4(1878)

Solvent Extraction 1990, T. Sekine (Editor)

© 1992 Elsevier Science Publishers B.V. All rights reserved

COMPUTER-ASSISTED SELECTION OF EQUIPMENT FOR LIQUID-LIQUID EXTRACTION

W. GOETTERT, E. BLASS
Chair A for Chemical Engineering, Technical University of Munich, Arcisstr. 21, 8000 Munich 2 (FRG)

ABSTRACT
The selection of equipment for an unit operation is a task which requires a lot of experience. For the case of liquid-liquid extractors an expert system is in development by the authors. The system architecture will be discussed. The expert system is connected to a simulation module which allows the design of the most important extraction columns. Results of column simulations and parameter studies will be presented.

1. INTRODUCTION

The selection of suitable equipment for an unit operation is a common problem during process-synthesis (Blass, 1986). To choose from the various available types of apparatus the one which fulfills the task as safely and economically as possible requires a lot of experience.

Liquid-liquid extraction is a good example for an unit operation for which a lot of different types of equipment have been developed (Blass et al., 1986). Most of them can still not be designed by rigorous methods. Therefore, for the final design and selection of an extractor one has to rely on laboratory experiments, rules of thumb, and heuristics. In order to compile the knowledge connected with liquid-liquid extraction equipment and to allow a more systematic approach to the selection problem an expert system is in development by the authors. This expert system is supposed to be a prototype for similar problems in process synthesis.

2. OVERVIEW OF EXTRACTION EQUIPMENT

For liquid-liquid extraction many different types of equipment have been developed, which can roughly be divided into mixer-settlers, centrifugal extractors, and countercurrent columns of various kinds. Fig. 1 presents a subset of all commercial extractors.

Each of the three classes is made up of many different extractor types. The column types e.g. can be separated in the ones with or

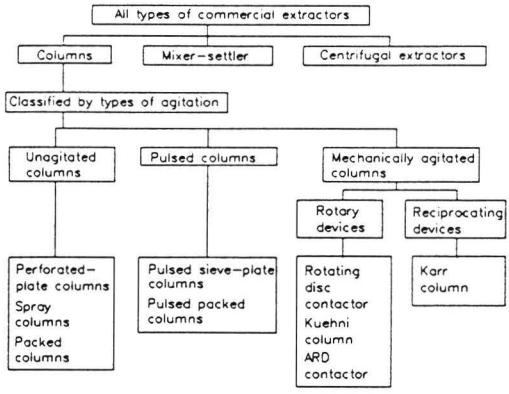

Fig. 1: Overview of commercial extractors

without mechanical agitation. The energy input can be supplied by pulsating the liquid phases, different kinds of mixers or reciprocating plates. Unagitated columns with sieve-plates or packings are also known.

3. THE SELECTION OF EXTRACTORS

Several approaches to the problem how to select extractors have been published. Reissinger (1978) presented a flow diagram which has originally been suggested by Hanson and can be used to find favourable solutions according to the given conditions of operation. Mueller (1972) ordered the extractors and the criteria in a matrix and gave a rating of their suitability. Pratt (1983) developed a similar but much more detailed matrix.

4. DESIGN OF AN EXPERT SYSTEM FOR THE SELECTION OF EXTRACTORS

4.1 Object oriented knowledge representation

As stated in the previous chapter, the extraction equipment can be ordered in a hierarchy. Following the tree from the root to the leaves the equipment becomes more and more specialized. A rotating disc contactor (RDC) shares most of its characteristics with mechanically agitated columns but some are quite different: RDCs are easier to assemble than the other agitated columns and have a lower energy input.

The object oriented knowledge representation with its concept of classes and more specialized subclasses is the ideal way of hand-

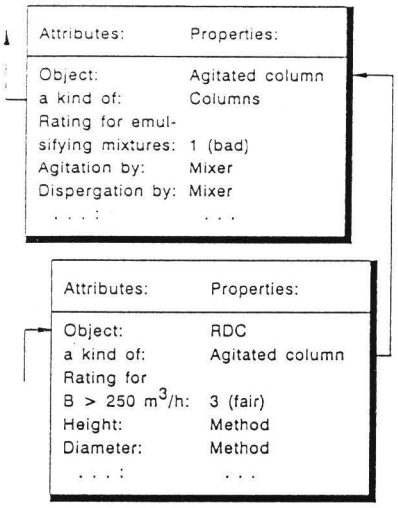

Fig. 2: Object oriented representation of extraction columns

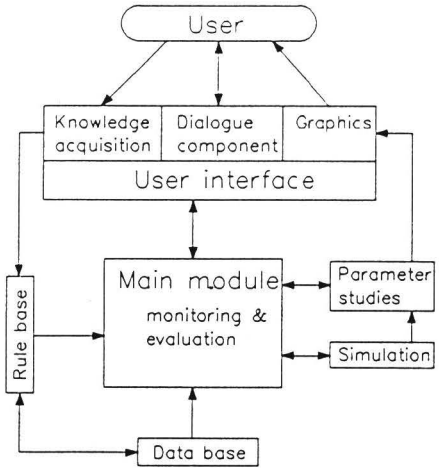

Fig. 3: Structure of the expert system

ling hierarchically structured data. Showing a small part of the knowledge base fig. 2 gives an impression of how to represent extraction columns as objects. Furthermore, the object oriented knowledge representation allows to attach "methods" to the definition of a class. In the case of extraction columns a method could provide routines for computing the dimensions, the mass-transfer coefficient or the drop size as a function of the energy input.

4.2 Production rules

Besides the object oriented knowledge representation ordinary production rules are used in the expert system. Most of these rules evaluate the physical properties of the feed and infer the suitability of the column classes to process the given mixture. Rules should be prefered which negate the suitability of a class, since they substantially reduce the time for the inference process. Examples for production rules are:

- **If** the feed mixture tends to emulsify,
  then an extractor with low or no energy input should be choosen.

4.3. Details of implementation

An expert system, which is to assist the engineer in the task of selecting a suitable extractor, should not only incorporate the heuristic knowledge of an expert in the field of liquid-liquid

extraction but also known methods of design. Although it is not possible to rely completely on the available mathematical models, they nevertheless give an indication of the working point. The results of a numerical simulation facilitate the planning of experiments, especially if parameter studies have been made in order to identify sensitive variables of the mathematical model. Fig. 3 shows the structure of the expert system.

The expert system is implemented using a commercial shell (Nexpert Object[(c)]). The shell allows an object-oriented knowledge representation and has a very comfortable user interface. Fig. 4 shows the capabilitiy of Nexpert Object to present the objects in a network style. Nexpert Object is connected to the simulation module which is programed in C. The simulation module incorporates the mathematical models for the most important extraction columns.

5. THE MODULE FOR PARAMETER STUDIES

Parameter studies are a means to determine the sensitivity of the mathematical model to small changes of the input variables. The model sensitivity S_i is defined as the first derivative of the model output Y with respect to an input variable x_i:

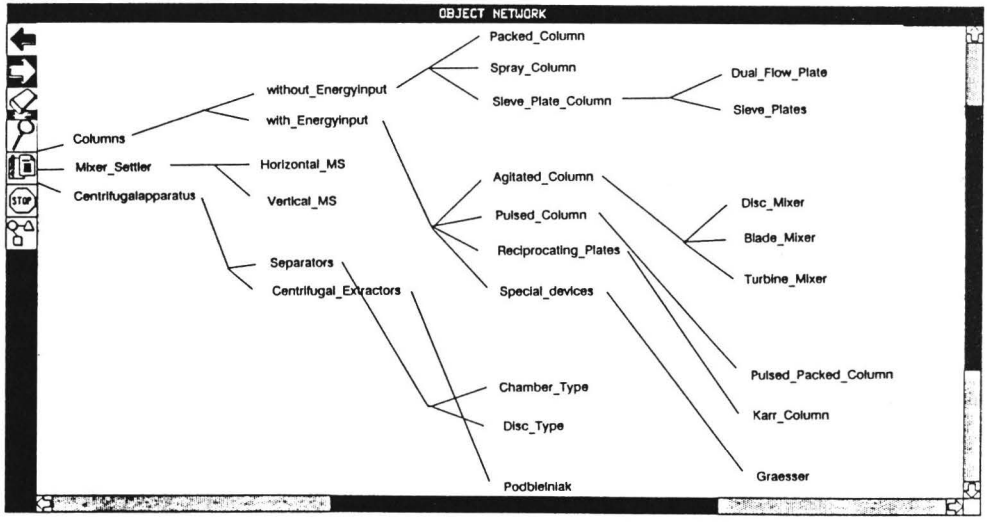

Fig. 4: Network representation in Nexpert Object[(c)]

$$S_i = \frac{\partial Y}{\partial x_i} \tag{1}$$

Therefore, the model sensitivity could be determined numerically by changing an input variable by a small step width and calculating the change of the model output.

Parameter studies can help to plan experiments: the more sensitive parameters should be determined experimentally to higher accuracy. One could also use parameter studies to estimate the flexibility of the extraction column, which is its behaviour when the conditions of operation - e.g. the composition of the feed or the ratio of solvent to feed - are changing. If unstable conditions are to be expected, an extractor with larger flexibility should be selected.

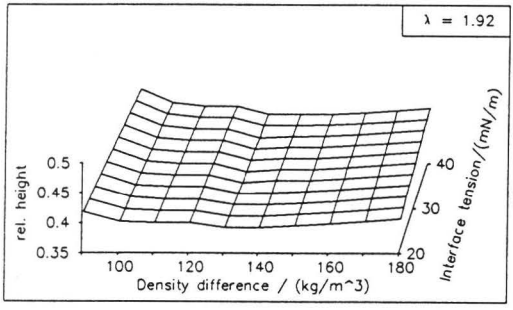

Fig. 5: Parameter study of a Kuehni-column

6. RESULTS OF PARAMETER STUDIES

Fig. 5 shows the effect of the density difference and the interface tension on the height of a Kühni-column. The height is calculated with respect to the result obtained at a density difference of 140 kg/m^3 and an interface tension of 30 mN/m.

Each calculation in the parameter field represents the complete design of an extraction column. With decreasing density difference the superficial velocities at the flood point of the column become lower, thereby increasing the mean residence time of the phases. The result is a higher enrichment of the solute and a lower column height.

7. CONCLUSIONS

An expert system is a way to assist the engineer in selecting the suitable equipment for liquid-liquid extraction. The expert system is connected to a simulation module which incorporates the mathematical design methods for extraction columns. Parameter studies with the simulation module help to estimate the reaction

of a column to changing conditions of operation and to plan experiments, which will usually be necessary despite a numerical design.

8. NOTATION

S	Sensitivity
x	Input variable
Y	Output variable

9. REFERENCES

Blass, E., Methodical development of chemical engineering processes, Ger. Chem. Eng. 9 (1986), pp. 127-135

Blass, E., Goldmann, G., Hirschmann, K., Mihailowitsch, P., Progress in liquid-liquid extraction, Ger. Chem. Eng. 9 (1986), pp. 222-238

Reissinger, K.-H., Selection criteria for liquid-liquid extractors, Chem. Engng. 6(11) (1978), pp. 109-118

Mueller, E., Ullmanns Encyklopädie der Technischen Chemie, vol. 2, 4th edn., Verlag Chemie Weinheim (1972), p. 565

Pratt, H.R.C., Selection, pilot testing and scale-up of commercial extractors, in Handbook of solvent extraction, John Wiley & Sons, New York (1983), pp. 475-495

Solvent Extraction 1990, T. Sekine (Editor)

© 1992 Elsevier Science Publishers B.V. All rights reserved

BREAKAGE AND COALESCENCE RATES OF DROPLETS IN KARR COLUMNS

FAN ZHENG, WANG DIANXIA and LI XIMING
Institute of Chemical Metallurgy, Academia Sinica, P.O. Box 353, Beijing, P. R. China.

ABSTRACT

Breakage and coalescence rates of droplets in reciprocating plate extraction columns were investigated by step change in mixing intensity, mean drop size were measured by lazer light transmission technique combined with local holdup measurement. Batch and countercurrent flow experiments with mass transfer and no mass transfer occurring showed that the dispersion mechanisms are different. The Monte Carlo simulation of digital computer was used to treat the experimental data, models of breakage and coalescence rates were obtained.

1 INTRODUCTION

Reactions or mass transfer occurring in liquid-liquid system are of major importance in industrial process. The problem of predicting drop size distributions through the population balance equation is traced to that of determining the breakage and coalescence rates of droplets under conditions prevailing in the countercurrent extraction contactors. Rational design of liquid-liquid extraction equipment needs not only the knowledge of dynamic equilibrium properties of the dispersion, but also the dynamic dispersion characteristics of droplets. The rate of mass transfer or reaction between phases are greatly effected by dispersion properties. Simulation and population balance equations can be employed to describe dispersion properties and predict rate process. Valentas[1] described the population balance equations, many researchers studied some functions in the equations. A few literatures are concerned with dispersion properties in reciprocating plate column(RPC). Jares[2], Sovova[3] Bapat[4]and Fan[5] investigated characteristic functions of dispersion model in a RPC.

In the present context, it is of interest to investigate the droplets breakage and coalescence in batch system ($\Delta \rho = 0$), countercurrent flow system with no mass transfer and the effect of mass transfer on dispersion properties.

2 EXPERIMENTAL DETAILS

2.1 Equipment

(i) Instruments

Experiments were carried out by unstable state method, the strong points

are the measurement of holdup and mean drop size on line. A local holdup-meter[6] based on the conductivity of mixtures was developed. Mean drop sizes were measured by a lazer parallel light transmission technique[7] based on light transparency:

$$\ln(I_0/I) = 1.5xl/d_{32} \quad (1)$$

(ii) Equipment

Batch experiments were carried out in a glass tank 0.1m in diameter, 0.11m in height with 3 plates. The detail was presented in previous paper[8].

Continuous countercurrent flow experiments were carried out in a squre reciprocating plate column with working height of 1.12m, the cross sectional area of $0.02\times0.1m^2$. The stainless steel plates with voidage of 32, 42.7 and 53.5 % and hole diameters of 6, 8 and 10 mm were spaced at 30～50 mm intervals. The frequencies were 2.0～15.0 1/s, the amplitutes were 3 ～ 9 mm. The dynamic interfacial tension with mass transfer were measured by drop- weight method. The mass transfer during drop formation was determined by single drop method in an empty glass column with diameter of 50 mm and height of 300 mm. The experimental temperature was kept at 25±0.2 ℃. The arrangement of equipment was shown in Fig.1.

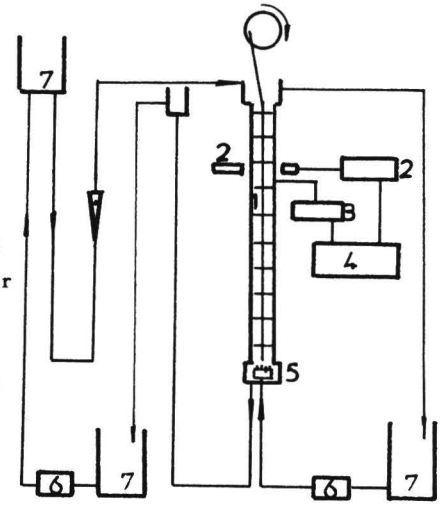

Fig. 1. Arrangement of equipment
1.RPC; 2.drop size analyser; 3. holdup-meter; 4.micro-computer; 5.distributor; 6.pump; 7.tank.

2.2 Materials

For the batch experiment, two systems having the same densities between two phases were used: xylene 81.6%$_{(v)}$ + CCl_4 18.4%$_{(v)}$, aqueous phase contained 0.002 mol/l Na_3PO_4; the second, toluene 82.6%$_{(v)}$+CCl_4 17.4%$_{(v)}$. For the continuous countercurrent flow experiment, kerosence (dispersed phase), water (continous phase) and acetic acid (solute) were used. In the measurements of the dynamic interfacial tension with mass transfer, four systems were used:

(a) kerosene - acetic acid - water,

(b) kerosene / n-octylalcohol $(50/1)_v$ - acetic acid - water,

(c) kerosene / n-octylacohol $(30/1)_v$ - acetic acid - water,

(d) n-octane - acetic acid - water.

2.3 Method

The experiments were carried out by step change in mixing intensity. The effects of the factors, including frequency of reciprocating plate, amplitude, voidage in the plates, hole size, plate spacing, and system properties, on the drop breakage and coalescence rates were investigated. The parameters of

breakage and coalescence rate were obtained by Monte-Carlo simulation method which simulated the random events by means of randon sampling and carried out statistic processing[9]. The experimental data were collected by a micro-computer.

3 RESULTS AND DISCUSSION

3.1 Batch experiment

The experiments should be carried out at $\Delta\rho=0$ since there is no liquid flow in to or out of the reciprocating plate tank. Therefore, the breakage of drops deponds on the relative velocity between drop and perforated plate, and the coalescence of drops is related to the relative velocity between drops. Assume that the zone where the equilibrium position of plate $\pm A$ is the breakage zone, and outside this zone where the probability of drop breakage is rather small can be considered as a coalescence zone. Then, the breakage rate equals the collision frequency of drops with hole edge times the probability of breakage after collision. The probability of drop breakage can be determined by the breakage conditions of drops and the law of drop motion in the tank. According to the analysis of the surface energy of drops and the drop velocity relative to plate, the breakage rate can be obtained:

$$Rb(d)=66.0(1-\Phi)^2\Phi\,(d_h/H)^{0.5}(1+x)^{-2.0}(2Af/H)$$
$$(d/d_h)^3[1-(d_{cr}/d)^{4/3}]^{0.5}n(d) \qquad (2)$$

The coalescence rate of drops can be expressed by the collision frequency times coalescence efficiency. The collision of drops can dealt with like gas molecules; the coalescence efficiency is proportional to the collision energy and inversely proportional to the surface energy.

From the process simulation by Monte- Carlo method and optimum calculation by Simplex method, the coalescence rate was obtained:

$$Rc(d_i,d_j)=5.18\times10^{-10}(d_i+d_j)^{13/6}(d_id_j)^{1/2}(\rho_d/\rho)^{1/2}$$
$$[(1-\Phi^2)/\Phi^2]^{2/3}(2Af)^2/H^{2/3} \qquad (3)$$

3.2 Countercurrent flow effects on drop breakage and coalescence rates

The breakage and coalescence mechanism of drops in continuous flow RPC is different from batch system. In the case, three effects should be considered: (a) the effect of flow for two phases, (b) the shear action near the holes in the plate, and (c) turbulence pressure fluctuation of fluid in the breakage zone (Kolmogoroff theory). The coalescence of drops is caused by (a) coalesence between drops and (b) coalescence between plate and drops by assuming that there is a thin layer of dispersed phase on the surface of plate. The coalescence takes place when contact time between drop and plate is greater than a critical value[10]. Resulting from simulation of experimental data and optimization calculation of parameters, it can be seen that (a) the effect of countercurrent flow on the breakage of drops can be neglected, (b) the action of turbulence pressure on breakage is about 80%, and the action of the shear stress is about 20% only. Therefore, the effect of turbulence

is more important. (c) the coalescence between drops and plate is about 65%, and the coalescence between drops is about 35%.

3.3 The effects of mass transfer on breakage and coalescence rates

The effect of polydispersivity on mass transfer has been investigated theoretically and experimentally[11,12]. Oppositely, one may ask mass transfer how to effect the drop breakup and coalescence rate. The breakage and coalescence of drops are strongly relative to the surface energy of two phases, and the surface energy is affected by the surface turbulence caused by mass transfer. Consequently, the effect of mass transfer on polydispersion nature can be dealt with the effect of mass transfer on interfacial tension. The effects of interfacial tension on the breakage and coalescence have been considered in previous works[8].

(i) The effect of mass transfer on interfacial tension

The effectiveness of mass transfer may be regarded as independent of the rate processes themselves which are the difference of concentration between two phases, the initial concentration of solute, mass transfer coefficient and its transfer direction.

The mass transfer direction effects on the interfacial tension is shown in Fig. 2.

System:
n-octone--acetic acid--water

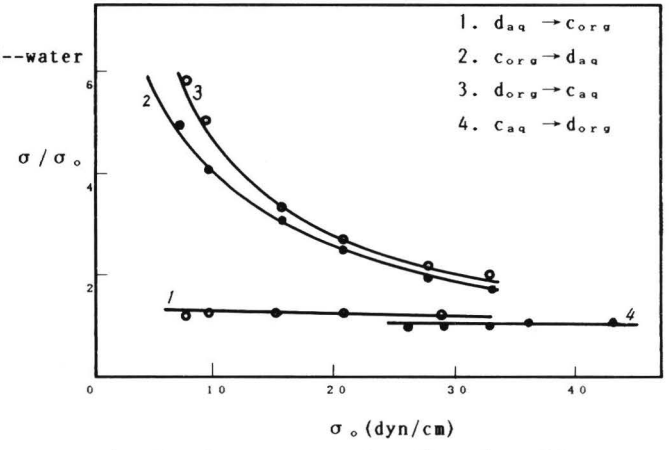

Fig. 2. The mass transfer direction effects on the interfacial tension

It can be seen that the dynamic interfacial tension is approximatly equal to that at equibrium state and the ratio σ / σ_0 does not change with the concentration if a solute transfers from aquaous phase to organic phase, no matter which phase is dispersed one. However, the difference between dynamic interfacial tension and static (equilibrium) one becomes greater when a solute transfers from organic phase to aquaous phase. The reason might result from that the solubility of acetic acid in organic phase is small.

The mass transfer coefficients during drop formation can be calculated: the total quantity of mass transfer should be the sum of that during drop formation, during drop rising in continuous phase and during drop coalescence.

$$M_T = M_F + M_R + M_C \tag{4}$$

where $M_T = V(C_0 - C_f)$ (5)

$M_F = K\ a\ \Delta C_F\ t_F$ (6)

$M_R = F_R\ a\ t_R$ (7)

$F_R = V(\Delta\ [HA_C]\ /\ t_R)\ /a$ (8)

The value of $(\Delta\ [HA_C]\ /\ t_R)$ can be obtained from the slop of C_R vs. t_R. C_R and t_R were determined from the different rising height of drops. Then the mass transfer coefficient during drop formation can be calculated:

$$K = [V\ (C_0 - C_f) - F_R\ a\ t_R]\ /\ a\ \Delta C_F\ t_F \tag{9}$$

Because the drops were taken away immediately in the top of the column by a vacuum collector, the quantity of mass transfer during coalescence can be neglected. In terms of experimental data, the relationship of interfacial tension with mass transfer occurring can be expressed by (organic phase→ aqueous phase) :

$$\sigma / \sigma_0 = 1 + 0.0275\ K^{-0.702}\ \Delta C^{-0.701} C_0^{1.53} \tag{10}$$

(ii) The rates of drop-breakage and -coalescence in RPC

Assume that the drop breakage is caused by both the turbulent fluctuation of fluid and the shear action of the holes in the plate, and the drop coalescence between drops occurs in the regions under the plate (light organic phase was dispersed phase), based on theoretical analysis and optimization in terms of the data from the unstable state experiments, the rates of breakage and coalescence can be indicated as follows:

$$R_b(d) = [\ k_t\ (\varepsilon^{2/3}\ d^{5/3}\ \rho_d\ /\sigma)^{1.3}(\ \varepsilon/d^2\ )^{1/3} + k_h\ (\rho_d d^2 f^2 A/\sigma\ )\ (\Phi\ dA/d_h)]\ [An(d)/H] \tag{11}$$

$$R_c(d_i, d_j) = k_c\ \rho_d\ \varepsilon^{2/3} Af(d_i+d_j)^{-1/3}[1-\Phi\ (1-2d_i d_j/d_h(d_i+d_j))^2]\ d_i d_j n(d_i) n(d_j)\ /H\sigma \tag{12}$$

The parameters are given in following table.

direction	k_h	k_t	k_c ($\times 10^6$)	Δd ($\times 10^2$)
no mass transfer	0.630	0.511	2.16	1.36
c→d	0.457	0.531	0.103	1.89
d→c	0.229	0.232	3.56	1.13

It can be seen that the drop coalescence is accelerated when mass transfer from d → c. The simulations of mean drop size vs. time in unsteady state were carried out by means of Monte-Carlo simulation technique. It was shown that this method is flexible and simplicity.

The mean drop size can be expressed as follows:

$$d_{32} = k_d \sigma^{0.6} / \varepsilon^{0.4} \rho_d^{0.2} \tag{13}$$

no mass transfer: $k_d = 0.231$

d → c: $k_d = 0.486$

c → d: $k_d = 0.184$

4 CONCLUSION

Drop breakage and coalescence processes can be investigated successfully by the Monte-Carlo simulation technique. The unstable state experiments can be carried out conveniently by local holdup-meter and lazer drop size analyzer. Mass transfer and its direction would effect on the liquid-liquid dispersion properties.

NOMENCLATURE

A---amplitude of reciprocation, m; a---interfacial area, m^2; C---concentration, $kmol\,m^{-3}$; d_i, d_j---drop diameter of the ith,jth class respectively, m; d_{32}---Sauter diameter, m; d_h---hole diameter of plate, m; d_{cr}---critical drop diameter, m; F---mass transfer rate, $m\,s^{-1}$; f---frequency of plate reciprocation, s^{-1}; H---stage spacing, m; I, I_0---light transparent intensity with and without dispersed phase respectively, s^{-1}; K---mass transfer coefficient, $m\,s^{-1}$; k_c, k_d, k_h, k_t---constants; l---light travelling length, m; M---quantity of mass transfer, kmol; Mc---quantity of mass transfer during coalescence, kmol; $n(d_i), n(d_j)$---drop number of size d_i, d_j; $R_b(d)$ and $R_c(d_i, d_j)$---the rate of drop breakage and coalescence respectively, s^{-1}; t---time, s; V---volume of drop, m^3; x---volumetric holdup. GREEK LETTERS: ΔC---concentration driving force for mass transfer, $kmol\,m^{-3}$; Δd---simulation deviation, m; Δ[HAc]---concentration change of drop during rising, $kmol\,m^{-3}$; ε---energy dissipation rate, $m^2 s^{-3}$; ρ---density, $kg\,m^{-3}$; σ, σ_0---interfacial tension and that at equilibrium respectively, $N\,m^{-1}$; Φ---plate free area. SUBSCRIPTS: c---continuous phase; d---dispersed phase, F---drop formation; f---final; o---initial, R---drop rising, T---total.

REFERENCES

[1] Valentas, K. J., et al. Ind. Eng. Chem. Fundls., 5, 271 (1966)
[2] Jares, J., et al., CHISA. Congress (1984)
[3] Sovova, H., et al., Czech. Chem. Commun., 47, 2393 (1982)
[4] Bapat, P. M., Chem. eng. Sci., 38, 2003 (1983)
[5] Fan, Z. et al., World Congress III of Chem. Eng., Tokyo, Japan (1986) p747
[6] Wang, I. and Fan, Z., Chinese Pat. 87202957
[7] Zhao, S., et al., Chinese Pat. 87210361
[8] Cao, S. and Fan, Z., ISEC. (1986) Volume 3, p437
[9] Rod, V., et al., Trans. Inst. Chem. Engr., 60, 48 (1981)
[10] Davies, G. A., et al., Recent Advances in L-L Extraction, C. Hanson ed., (1971) p495, Pergamon Press, Oxford
[11] Pratt, H. R. C., Solvent Extraction & Ion Exchange, 2 (4 & 5) 521 (1984)
[12] Das, P. K., et al., AIChE.J.,33 (11) 1899 (1987)

ACKNOWLEDGMENT

Partial fincial support by the National Science Foundation of China (R850079) is acknowledged.

10. LIQUID MEMBRANES

Solvent Extraction 1990, T. Sekine (Editor)

© 1992 Elsevier Science Publishers B.V. All rights reserved

NEW SURFACTANTS FOR METAL EXTRACTION BY LIQUID SURFACTANT MEMBRANES

F. Nakashio, M. Goto and K. Kondo*
Department of Organic Synthesis, Kyushu Univ., Fukuoka 812, Japan

ABSTRACT

New amphoteric surfactants which possess an acceleration effect and give a stable emulsion were prepared for metal extraction by liquid surfactant membranes (henceforth LSM). Copper extraction by LSM using the amphoteric surfactants was carried out in a stirred tank and the W/O emulsion was demulsified by a continuous electrical coalescer.

The amphoteric surfactants formed a stable emulsion at low concentration which is about one-tenth the corresponding concentration of Span 80 or Polyamine. By using the amphoteric surfactants, the extraction rate was increased about ten times as compared with the nonionic and cationic surfactants. The acceleration effect is considered to be caused by an electrostatic interaction between copper ion and hydrophilic phosphoric-group of the amphoteric surfactants. The increase of the extraction rate leads to shortening the operation time in the LSM process. Furthermore, the emulsion made of the amphoteric surfactant could be efficiently demulsified by an electrical coalescer.

1. INTRODUCTION

In the development of the metal separation processes using liquid surfactant membranes (henceforth LSM), it is very important to elucidate the effect of surfactant on the behavior of the W/O emulsion in the LSM's process, that is, the break-up and swelling rates of the W/O emulsion droplets, the permeation rate of metal through the LSM and the demulsification rate of the W/O emulsion by an electrical coalescer.

Since the discovery of LSM by Li [1], the effect of surfactant on the behavior of the W/O emulsion was studied by many investigators [2-5]. However, in most of papers, the commercial surfactants such as Span 80 and Polyamine were used. These commercial surfactants are a mixture of more than one compound.

In order to obtain more definite informations concerning the effect of the surfactants on the behavior of the W/O emulsion in the LSM's process, it is necessary to use a pure surfactant. In the LSM's process, the following conditions are required as a suitable surfactant; (1) lowering of the break-up rate of the W/O emulsion droplets in a mixer, (2) lowering of the swelling rate of the W/O emulsion droplets due to osmotic pressure, (3) enhancement of the permeation rate of metal through LSM, keeping high selectivity for metal

+K. Kondo is now at Dept. of Chem. Eng., Doshisha Univ., Kyoto 602.

Nonionic Surfactant

N-1) $2C_nGE$

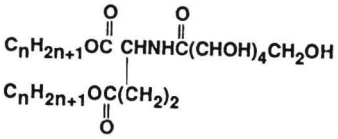

(n = 8 - 18)

N-2) $2C_{18}\,\Delta^9GE$

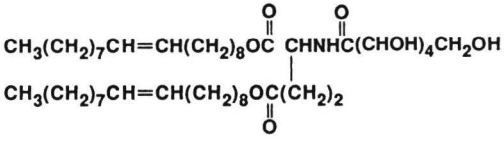

Cationic Surfactants

C-1) $2C_nQA$

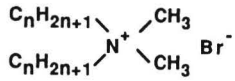

(n = 12 - 18)

C-2) $2C_{18}\,\Delta^9$ GE C_2 Q A

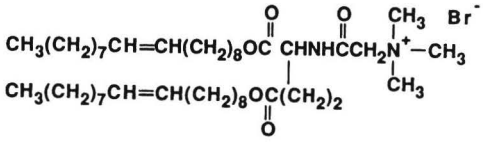

Anionic Surfactants

A-1) 2 $C_{18}\,\Delta^9$ SA

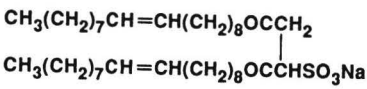

A-2) 2 $C_{18}\,\Delta^9$ P A

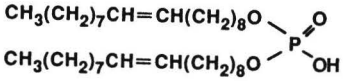

A-3) 2 $C_{18}\,\Delta^9$ CA

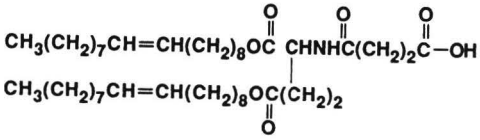

Amphoteric Surfactants

Am-1) 2 C_{18}GE C_2 QA C_2 PA

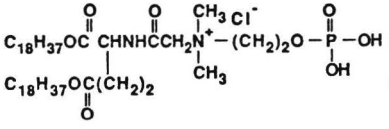

Am-2) 2 $C_{18}\Delta^9$ GE C_2 QA C_2 PA

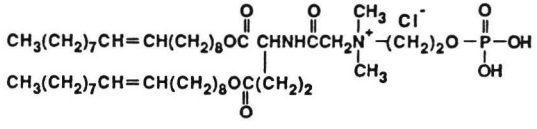

Fig. 1 New surfactants developed for LSM's process

to be separated. (4) the W/O emulsion prepared is easily demulsified by an electrical coalescer, (5) the surfactant is chemically stable and safe compounds and synthesized easily and cheaply. Considering these conditions, a number of new surfactants used in the LSM'process for metal extraction were developed, as shown in previous papers [5-10]. It was found that the dioleyl glutamic acid ribitol($2C_{18}\Delta^9GE$) forms very stable W/O emulsion [4-6], but the permeation rate of copper through this LSM containing $2C_{18}\Delta^9GE$ is strongly lowed [6]. However, the permeation rate of copper through this LSM is increased by a small amount of an anionic surfactant [8].

In this study, a further advanced amphoteric surfactants which has two long alkyl chains were developed and the break-up and swelling of emulsion, metal permeation rate and demulsification were investigated.

2. Experimental

Figure 1 shows the structure of surfactants synthesized in our laboratory.

The experimental apparatus used for copper extraction with LSM is a batch-type stirred cell equipped with four stainless steel baffles. The inner diameter and the depth of this cell are 10 cm and 15 cm, respectively. The experimental procedure is the same as that described in previous papers [4-8]. The experimental conditions are listed in Table 1.

The experimental apparatus for the demulsification by a continuous electric coalescer [10] is shown in Fig. 2. The experimental conditions are listed in Table 2.

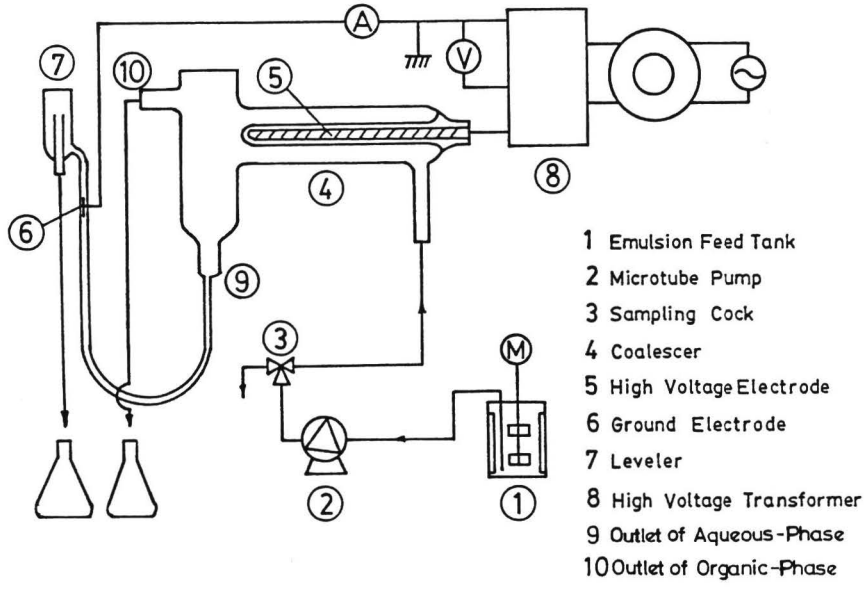

Fig. 2 Experimental apparatus for demulsification of W/O emulsion

TABLE 1
Experimental conditions for copper extraction by LSMs

1)	Volume of each phase in a Mixer	
	External aq. phase	$V°_{we} = 0.7 \times 10^{-3} m^3$
	Emulsion phase	$V°_E = 0.1 \times 10^{-3} m^3$
	Org. phase in Emulsion (n-heptane)	$V_{org} = V°_E/2$
2)	Concentration of each component	
	Copper nitrate in external aq. phase	$C_{Cu0} = 3$ -10 mol $\cdot m^{-3}$
	Hydrogen ion in external aq. phase	pH = 2.0 , 2.5
	Extractant (Purified LIX65N ; HNBPO)	$C_{HR0} = 50$ mol $\cdot m^{-3}$
	Surfactants	Cs = 1-100 mol $\cdot m^{-3}$
	Sulfuric acid in internal aq. phase	$C°_H = 500$ mol $\cdot m^{-3}$
	Break-up Tracer in internal aq. phase	$C°_{Ni,i} = 5$ mol $\cdot m^{-3}$
3)	Stirring speed	n = 5 s^{-1}
4)	Temperature	T = 303 °K

TABLE 2
Experimental conditions for demulsification

Volume ratio of internal aqueous solution to organic solution in W/O emulsion	$V°_{wi}/V_{org} = 1$
Internal aqueous solution	$C_H = 1000$ mol/m^3 (sulfuric acid) (containing 100 mol/m^3 copper sulfate)
Applied Voltage	E = 1 - 15 kV (60 Hz)
Mean residence time of the emulsion in the coalescer	θ = 60 - 540 s

3. Results and discussion

3.1 Break-up of the W/O emulsion droplets

In order to evaluate the emulsion stability, the break-up rate constant, k_b, is defined as follow:

$$\ln(1-\varepsilon) = -k_b t \qquad (1)$$

where ε is the degree of break-up, which is obtained by the amount of break-up tracer released from the internal aqueous solution of the W/O emulsion droplets into the external aqueous solution. Figure 3 shows a typical experimental result concerning the relation between the break-up rate constant, k_b, and the surfactant concentration, Cs, for various surfactants. From the results, It is found that the surfactants $2C_{18}\Delta^9GE$ and $2C_{18}\Delta^9GEC_2QAC_2PA$ formed very stable W/O emulsion by using a small amount of surfactant, compared with the commercial surfactants. Furthermore, there is the critical point of the surfactant concentration, Csc. In the range of lower surfactant concentration than Csc, the W/O emulsion becomes very unstable, but in the range of higher concentration than Csc, the W/O emulsion becomes stable and the break-up rate is kept constant. In the previous paper[6], it was found that this critical point corresponds to the concentration required to form the monolayer at the interface between the organic and the aqueous phase in the emulsion, however not for the commercial surfactants.

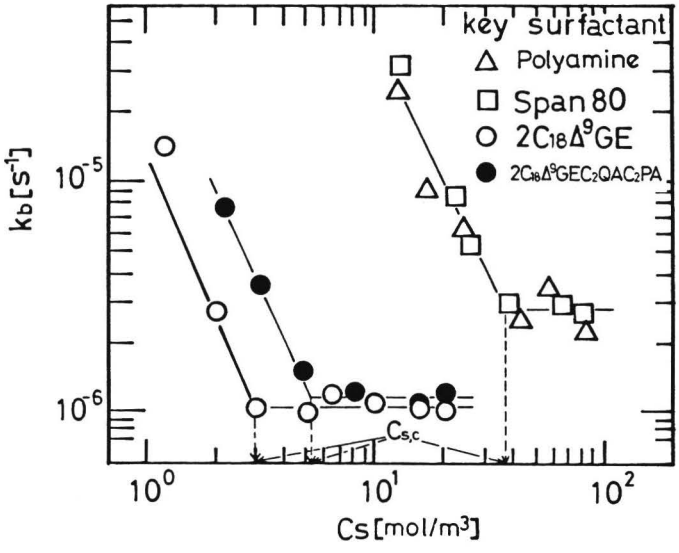

Fig. 3 Relation between break-up rate constant and surfactant concentration

Figure 4 shows a typical result concerning the relation betwee the break-up rate constant, k_b, and the alkyl chain length of the surfactant, where n is the number of carbon atoms in the alkyl chain. From the results, it is found that the surfactants having two oleyl chains forms a more stable W/O emulsion as compared with the other surfactants having saturated alkyl chains.

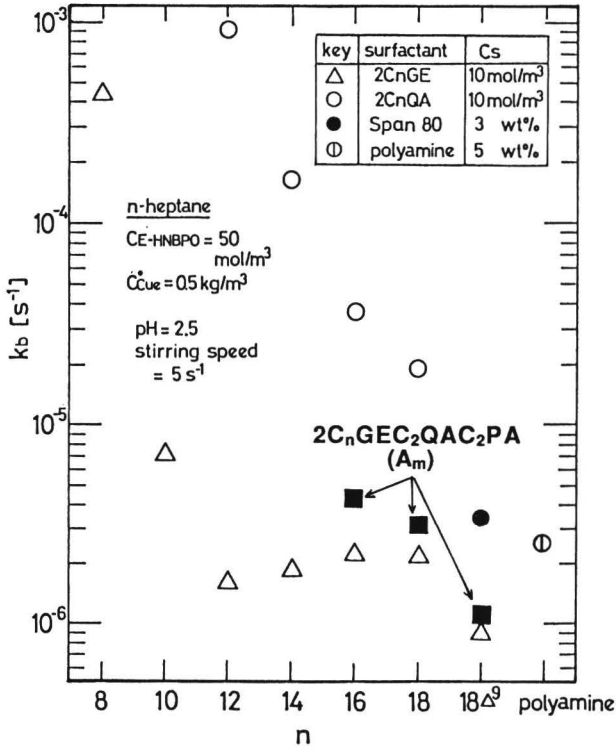

Fig. 4 Effect of alkyl chain length of surfactants on break-up of LSM

3.2 Swelling of W/O emulsion droplets

The swelling of the W/O emulsion phase is represented by the increase of the water content in the emulsion phase, Y (= Vwi/Vwi°). Figure 5 shows a typical experimental result concerning the effect of surfactant on the swelling of the W/O emulsion phase. From these results, it is found that only Span 80 strongly affects water permeation compared with other surfactants, and that in the initial period, e.g., ten minutes period, the effect of swelling is not too large. These results suggest that in the metal separation process using LSM, it is required to make up the LSM system having rapid rate of metal extraction, that is, the separation of metal finishes in the period of ten minutes.

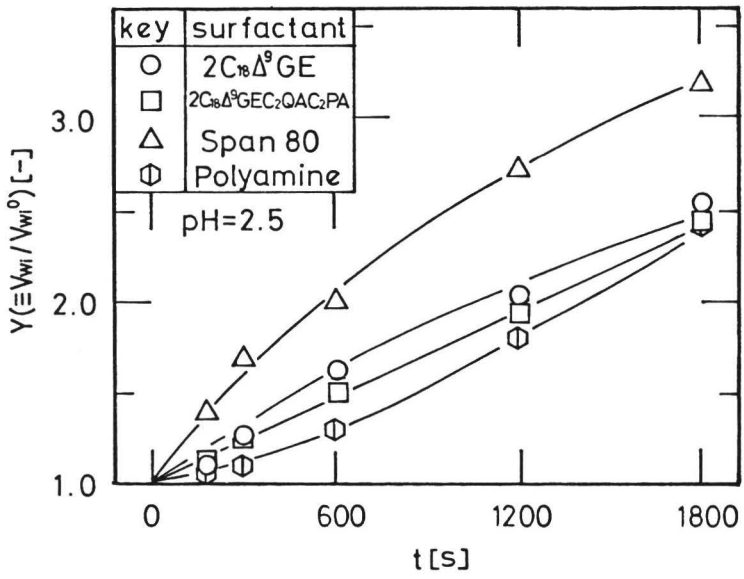

Fig. 5 Effect of surfactants on swelling of W/O emulsion

3.3 Permeation rate of metal through LSM

As described in the previous paper [7], the interface of the organic and the aqeous phase seems to be completly covered with the surfactant and the amount of the extractant, HR, at the interface seems to be very small, because the adsorption equilibrium constant of the surfactant is very large compared with the value of the extractant. It is suggested that the permeation rate of copper through the LSM is affected by the properties of the surfactants used.

The permeation rate of copper through LSM is obtained from the experimental results of copper extraction by LSM, by measuring the copper concentration in the external aqueous solution in a mixer. Figure 6 shows a typical experimental result concerning the effect of surfactant on the the copper extraction by LSM containing purified LIX 65N. The extraction rate of copper by LSM is strongly affected by the properties of surfactants, especially, the hydrophilic part of the surfactants. As expected [8,9], the extraction rate of copper by LSM containing amphoteric surfactant $2C_{18}\Delta^{9}GEC_2QAC_2PA$ (Am-2) is very large compared with the nonionic surfactants such as Span 80, the surfactant $2C_{18}\Delta^{9}GE$ and Polyamine. The main reason for this result is considered to be an electrostatic interaction between copper ion and hydrophilic phosphoric-group of the amphoteric surfactant. Using Kelex 100 as a copper carrier, the similar experimental results to the case of purified LIX 65N are obtained.

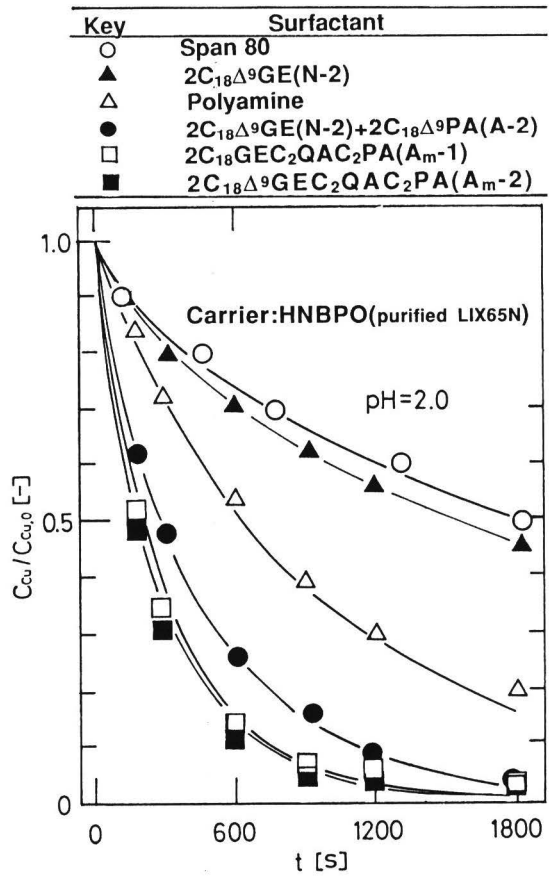

Fig. 6 Effect of surfactants on permeation rate of copper through LSM

In the previous paper [7], it was found that the copper extraction rate with LSM in a mixer is represented by the following equations.

$$-V_{We}\, dC_{Cu}/dt = (6V_E/d_E)\, k_f'\, C_{Cu}/C_H \qquad (2)$$

where V_{We} and V_E are volume of the external aqueous and the W/O emulsion phases, respectively, d_E is mean diameter of the W/O emulsion droplets, C_{Cu} and C_H are concentrations of copper and hydrogen ion in the external aqueous phase, respectively, and k'_f is extraction rate constant.

As shown by solid lines in Fig.6, the experimental results are simulated by Eq.(2), taking account of the change of C_H which is obtained from mass balance. The extraction rate constant, k'_f, is obtained for each surfactant, as shown in Table 3. It is found that the extraction rate constant in the case of new surfactant is about three or ten times larger than the case of commercial surfactants such as Polyamine or Span 80.

TABLE 3
Extraction rate constant for each surfactant

Surfactant	Extractant	dp [μm]	dE [mm]	k'f [mol/m²·s]
Span 80	HNBPO (purified LIX65N)	4.6	0.279	2.8×10^{-6}
Polyamine		7.5	0.338	7.8×10^{-6}
N - 2		4.7	0.308	2.5×10^{-6}
Am - 1		4.3	0.312	2.2×10^{-5}
Am - 2		4.1	0.303	2.8×10^{-5}
Span 80	Kelex 100	4.3	(0.28)	7.4×10^{-6}
Polyamine		5.6	(0.34)	2.1×10^{-5}
N - 2		4.1	(0.31)	6.5×10^{-6}
Am - 2		4.0	(0.30)	1.5×10^{-4}

( ) estimate

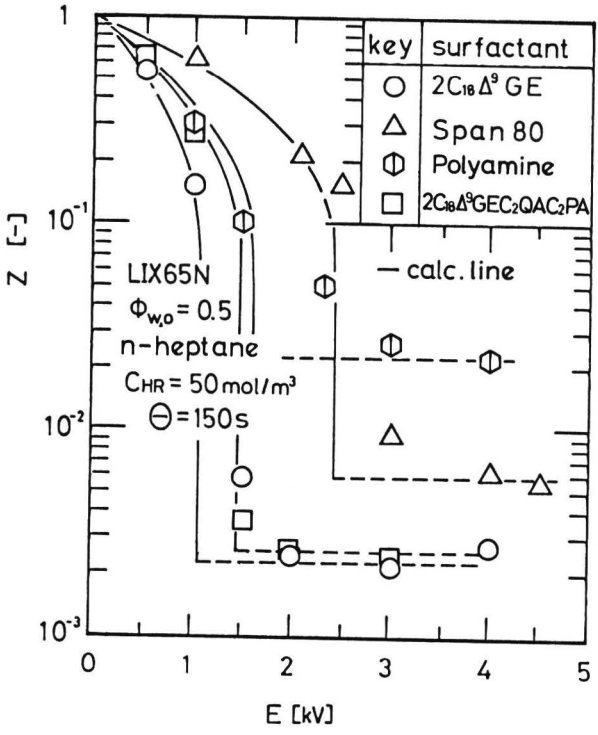

Fig. 7 Effect of surfactants on demulsification of W/O emulsion

3.4 Demulsification of the W/O emulsion by electrical coalescer

In a previous paper [5,10], a continuous electrical coalescer shown in Fig.2 was developed. Figure 7 shows a typical experimental result, which was obtained under the condition shown in table 2 . The value of Z is the water content of organic phase at the outlet of the coalescer. For example, Z = 0.01 corresponds to degree of demulsification = 99%. From the results, it is found that the emulsion made of new surfactant is easily demulsified in the continuous coalescer by applying one or two kilovolts and in a few minutes.

4. Conclusion

New amphoteric surfactant $2C_{18}\Delta^{9}GEC_2QAC_2PA$ is a very suitable surfactant for the separation of copper by liquid surfactant membranes from acidic aqueous solution, from the following viewpoints: (1) stability of W/O emulsion in a mixer, (2) rapid permeation rate of copper (this means that swelling is prevented), (3) demulsification of the emulsion in the continuous electrical coalescer.

5. REFERENCES

1 N.N.LI, US Pat.,3410794 (Nov.12, 1968)

2 J.Draxler and R.Marr, Emulsion liquid membranes, Chem.Eng.Process, 20 (1986) 319.

3 B.A.Mikucki and K.Osseo-Asare, The liquid surfactant membrane process: Effect of the emulsifier type on copper extraction by LIX65N-LIX63 mixture, Hydrometallurgy, 16 (1986) 209.

4 F.Nakashio and M.Goto, Role of surfactants in separation process using liquid surfactant membranes, Hyomen (Surface), 27 (1989) 1.

5 F.Nakashio, M.Goto and K.Kondo, Role of surfactants in the behavior of emulsion liquid membranes - Development of new surfactants, J.Membrane Sci., 38 (1988) 249.

6 M.Goto, M.Matsumoto, K.Kondo and F.Nakashio, Development of new surfactant for liquid surfactant membrane process, J.Chem.Eng.Japan, 20 (1987) 157.

7 M.Goto, K.Kondo and F.Nakashio, Extraction kinetics of copper with liquid surfactant membranes containing LIX65N and nonionic surfactant, J.Chem.Eng.Japan, 22 (1989) 71.

8 M.Goto, K.Kondo and F.Nakashio, Acceleration effect of anionic surfactants on extraction rate of copper with liquid surfactant membranes containing LIX65N and nonionic surfactant, J.Chem.Eng.Japan, 22, (1989) 79

9 M.Goto, K.Kondo and F.Nakashio, Development of amphoteric surfactant for liquid surfactant membrane in metal extraction process, J.Chem.Eng.Japan, 22, (1989) 99.

10 M.Goto, J.Irie, K.Kondo and F.Nakashio, Electrical demulsification of W/O emulsion by continuous tubular coalescer, J.Chem.Eng.Japan, 22, (1989) 401.

Solvent Extraction 1990, T. Sekine (Editor)
© 1992 Elsevier Science Publishers B.V. All rights reserved

RETARDATION OF THE TRANSPORT OF Eu(III) THROUGH SUPPORTED DI(2-ETHYLHEXYL)-PHOSPHORIC ACID-KEROSENE LIQUID MEMBRANE

Tsung-Min HUNG and Chau-Jen LEE
Department of Chemical Engineering, National Tsing Hua University
Hsinchu, Taiwan 30043, R.O.C.

ABSTRACT
Hung, T.M. and Lee, C.J., 1990. Retardation of the transport of Eu(III) through supported di(2-ethylhexyl)phosphoric acid-kerosene liquid membrane. ISEC'90

The permeation of Eu(III) with supported liquid membrane containing di(2-ethylhexyl)phosphoric acid (HDEHP) diluted in kerosene was studied. The existence of acetate may affect the permeation of Eu(III). In the presence of potassium chloride and sodium acetate, the Eu(III) ions transfer was retarded owing to a surplus of acetate ions on feed-membrane interface. This effect may be attributed to the phenomenon of concentration polarization of acetate ions.

INTRODUCTION

Supported liquid membrane (SLM) technique has attracted much attention as an effective method for selective separation and concentration of metal species from dilute solution (Danesi, 1984-85). Some studies (Novikov et al., 1987; Chiarizia et al., 1987) relating to the separation of lanthanides and actinides have been carried out in SLM system. In the SLM system using di(2-ethylhexyl)phosphoric acid (HDEHP) as carrier, the kinetics of Eu(III) permeation and its mass transfer mechanism have been studied by Danesi et al.(1982) and Nishiki et al.(1983). The extraction reaction between Eu(III) and HDEHP can be expressed as

$$Eu^{3+} + 3\ \overline{(HDEHP)_2} \rightleftharpoons \overline{Eu(DEHP)_3(HDEHP)_3} + 3\ H^+ \qquad (1)$$

where the bar indicates organic species. The forward and reverse reactions occur at feed-membrane interface and membrane-strip interface, respectively.

Acetate ions substantially play a role of accelerating the extraction equilibria in liquid surfactant membrane system (Gu et al.,1986). In this work, the effect of acetate existing in aqueous feed solution on the permeation of Eu(III) through SLM was investigated. During the permeation experiment, the transmembrane conductivity (TMC) was measured because it could reflect the circumstances of membrane.

Correspondence concerning this paper should be addressed to Dr. C.J. Lee,
T.M. Hung is now with the Institute of Nuclear Energy Research, Lung-Tan, Taiwan, ROC

2 EXPERIMENTAL

2.1 Reagents and membranes

The europium oxide (Shin-etsu Co., Japan) of 99.9% purity (minimum) was used in the experiment. The europium chloride solution was prepared by dissolving the europium oxide in hydrochloric acid. Analytical grade hydrochloric acid, potassium chloride, sodium acetate and ammonia solution were used in this study. HDEHP (Union Carbide Co., USA) with a purity of 95% was used without further purification. High grade kerosene (Union Chemical Works Ltd., Taiwan) was washed with weak acid solution, and used as diluent. All aqueous solutions were saturated with kerosene prior to use.

Celgard 2500 (Celanese Plastics, Charlotte, NC), a microporous polypropylene film, was used as the solid support. The thickness of film is 25 μm with a nominal porosity of 45% and an effective pore size of 0.04 μm. The Celgard 2500 film was impregnated with HDEHP dissolved in kerosene.

2.2 Apparatus and procedure

The permeation apparatus used is schematically shown in Fig. 1. The whole body of cell is made of acrylic plastics. The membrane, with two 2 mm thick polyethylene gaskets, was clamped between two 212 ml jacketed cells. The geometric area of membrane was 25.5 cm^2. The actual volumes of feed and strip solutions were 207 ml and 209 ml. Two platinum wires, embedded in gaskets and extended into the solution for 10 mm long, were fixed on the opposite sides of membrane for 4 mm apart. The terminals of the Pt electrodes were connected to the conductometer (METROHM E518) with a recorder.

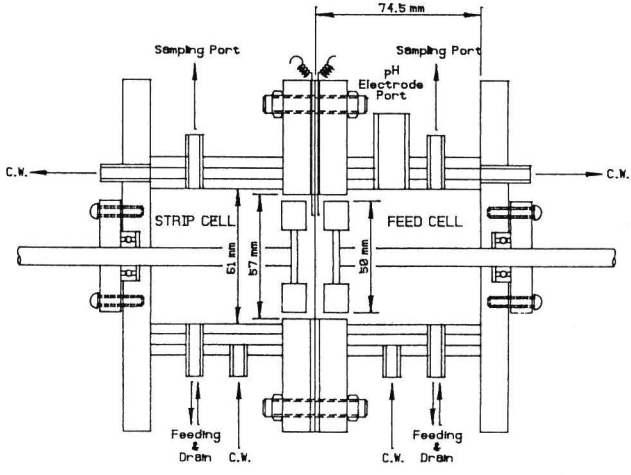

Fig. 1. The schematic permeation apparatus

After the membrane was clamped between the two-half cells, the respective degassed aqueous solutions were carefully transferred into each cell from the feeding port by gravity force. The stirrers were started as soon as both cells were filled. The rotating speed of stirrer was kept at 150 rpm. In all experiments, the stripping solution was 1M of hydrochloric acid. The experiments were performed at 25±0.3 ^{o}C by circulating cooling water through the jacketed chambers of cell. Samples, 30-80 µl each, were taken with microsyringe periodically and analyzed with UV spectrophotometer at 580 nm for europium concentration.

3 RESULTS AND DISCUSSION

3.1 Preliminary test on TMC

Two platinum wires assembled on the opposite sides of membrane as the electrodes, were used to measure the transmembrane conductivity. The electric resistance R between the electrodes comprised of aqueous feed resistance R_f, aqueous strip resistance R_s, and membrane resistance R_m. By the definition of conductivity, the transmembrane conductivity can be expressed as

$$k = \frac{c}{R_f + R_m + R_s} \qquad (2)$$

where c is the cell constant. In the SLM system, the solid membrane resistance is constant and the liquid membrane resistance varies with the composition of organic phase and the permeability rate of metal ions. Owing to much higher dielectric constants of both solid and liquid membranes than that of aqueous films, R_f and R_s may be neglected in eqn. (2). Therefore, the transmembrane conductivity is linearly related to the membrane resistance. As both cells were filled with the same aqueous solutions (0.002M Eu^{3+}, 0.5M KCl and 0.1M CH_3COONa) and stirring rate were kept at 150 rpm, the TMCs of different membrane conditions were measured. The results were shown in relative value in Table 1. All conductivities were compared to that of tap-water without membrane.

TABLE 1

Relative conductivity test

Case	Relative Conductivity
(a) Without Celgard 2500	1
(b) Dry Celgard 2500 with pin hole	1
(c) Dry Celgard 2500	0.52
(d) Celgard 2500 impregnated with 0.8F HDEHP in kerosene	0.74 - 0.6

Comparing to the TMC of dry polypropylene microporous membrane, the TMC of carrier-immobilized membrane was higher because the organic solution was in place of air in the micropore. The TMC of carrier-immobilized membrane rapidly increased to 0.74 during the beginning few minutes, and gradually decreased to 0.6 during the following 1.5 hours, and then stayed constant. After three hours running, the membrane was taken out for inspection. A thin layer of gel-like substance was found on both faces of the membrane. The gel-like coating was not soluble in dilute acid. The similar coating was formed on the surface (face to aqueous feed) of porous graphite sheet of 0.3 mm thickness which containing 0.8F HDEHP solution for Eu(III) permeation test. Referring to Harada's study (Harada et al., 1971), the gel-like coating could be Eu-HDEHP polymer. Once the polymer formed, the TMC gradually decreased.

3.2 Effect of acetate on Eu(III) permeation

3.2.1 Case I

When the feed solution comprised europium chloride (0.002M) and sodium acetate, the permeation of Eu(III) through SLM was illustrated in Fig. 2. There is little change of the Eu(III) permeability in the range of acetate content from 0.003M to 0.2M. Under the limiting condition of low permeable ion concentration, the relationship between logarithmic C/C_0 and time is linear (Danesi et al., 1982) and may be described by

$$\ln \frac{[Eu^{3+}]}{[Eu^{3+}]_0} = - \frac{Q}{V} P t \qquad (3)$$

where subscript "o" denotes the initial concentration, Q is the effective membrane area, V is the volume of feed solution, and P is the permeability coefficient. The linear relationship implies that the permeability coefficient is constant and the permeation process is controlled by aqueous diffusion. From the data shown in Fig. 2, the constant permeability coefficient was obtained as $4.35 \pm 0.25 \times 10^{-3}$ cm/s which was of the same order of magnitude as Danesi's (1982). This indicates that the assumption of fast interfacial

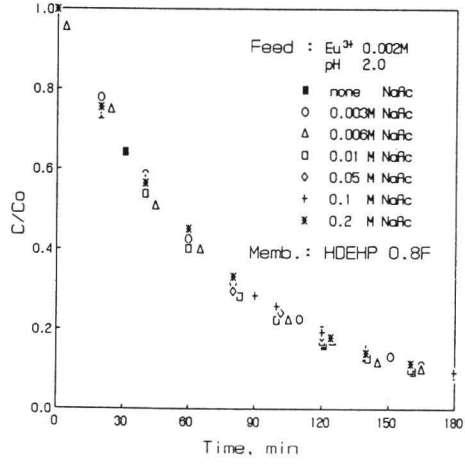

Fig. 2. The effect of acetate on the permeation of Eu(III)

reaction is still valid even in the presence of acetate in the aqueous feed.

3.2.2 Case II

The results of experiment with moderate Eu(III) (0.005M) in feed solution which also contained electrolyte (0.5M KCl) and sodium acetate, were shown in Fig. 3. These curves (as shown in Fig. 3) obviously exhibit the influence of acetate on the permeability of Eu(III) through SLM. The permeation rate of Eu(III) decreased with increasing acetate content. It is worth to note that the curve of 0.1M acetate was quite different from the other three. Especially, the concentration of Eu(III) in feed was rapidly reduced beyond the second operation hour. It was neither the permeation of ions was speeded nor the liquid membrane broke down. In fact, a layer of europium acetate precipitate coated on the feed-membrane interface, which was found after inspecting the support film at the end of experiment. This coating could be dissolved with distilled water that was different from the gel-like layer mentioned in section 3.1. During the formation of precipitate on the membrane surface, the retardation of Eu(III) transport through SLM was also reflected on the response of TMC, as shown in Fig. 4. The conductivity began to drop at the second operation hour, as well as the Eu(III) concentration in feed began to decrease abnormally.

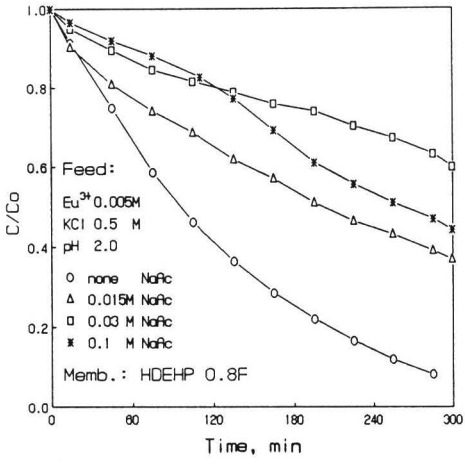

Fig. 3. The effect of acetate on the permeation of Eu(III) in the presence of electrolyte KCl

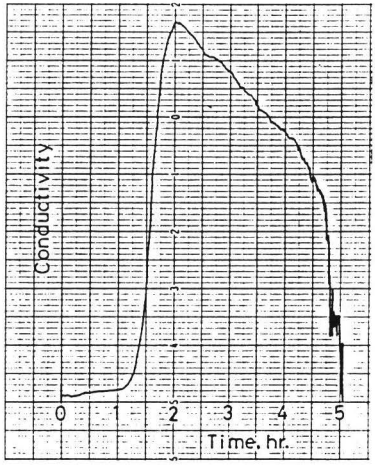

Fig. 4. Transmembrane conductivity vs. time for the case of 0.1M NaAc in Fig. 3.

It is expected that the added acetate replaces the coordinated water molecules surrounding the Eu(III) ions to form a more labile complex. Both

labile complex and acetate ion with weak surface activity were favorable for approaching to the hydrophobic membrane interface. It is beneficial to interfacial chemical reaction for liquid surfactant membrane system (Gu et al., 1986), but produces much resistance for diffusion-controlled SLM system. As Eu(III) ions permeated through the liquid membrane, a surplus of acetate ions remained on the membrane interface and resulted in the occurrence of concentration polarization. The effect of concentration polarization was simultaneously enhanced by rough porous surface of hydrophobic film and by the presence of potassium chloride. The different influence of acetate on the permeation of Eu(III) between Case I and Case II may be attributed to (1) both aqueous and membrane diffusions are simultaneously rate-controlling factors for Case II, and (2) a salting-out effect occurs in the presence of potassium chloride.

4 REFERENCES

Chiarizia, R. and Danesi, P.R., 1987. Sep. Sci. Technol., 22: pp. 641-659.
Danesi, P.R., Horwitz, E.P. and Rickert, P., 1982. Sep. Sci. Technol., 17: pp. 1183-1192.
Danesi, P.R., 1984-85. Sep. Sci. Technol., 19: pp. 857-894.
Gu, Z.M., Wasan, D.T. and Li, N.N., 1986. J. Membr. Sci., 26: pp. 129-142.
Harada, T., Smutz, M. and Bautista, R.G., 1971. Proc. ISEC 71, paper 29: pp. 950-956.
Nishiki, T. and Bautista, R.G., 1983. Metallurgical Transactions B, 14B: pp. 25-31.
Novikov, A.P. and Myasoedov, B.F., 1987. Solv. Extr. Ion Exch., 5: pp. 117-127.

Solvent Extraction 1990, T. Sekine (Editor)

© 1992 Elsevier Science Publishers B.V. All rights reserved

MODELLING AND APPLICATION OF A PILOT-SCALE SUPPORTED LIQUID MEMBRANE UNIT FOR URANYL NITRATE EXTRACTION

D.L. HOFMAN[1] , W.M. CRAIG[2] and J.J. SMIT
Potchefstroom University, c/o P.O. Box 1754 Rivonia 2128, South Africa.

ABSTRACT

Pollution legislation dictates the removal of uranyl nitrate from effluents. Supported liquid membrane (SLM) technology promises favorable attributes to attaining this goal, especially due to its environmental compatibility, ie the complete eradication of secondary pollution. A fundamental investigation into the theory, dynamics and general requirements to effect proper extraction of uranyl nitrate from effluents was carried out. A dynamic differential equation which relates the extraction rate of uranyl nitrate to other system variables is developed. A pilot-plant was designed to confirm the predictions of the model.

1 INTRODUCTION

Supported liquid membranes (SLM's), and to a lesser extent emulsion membranes, have been identified for use in the nuclear industry because their simplicity is suited to glove box operation, and the comparatively low extractant inventory cuts the operating costs dramatically. Research has been restricted to proving the technology, and the main thrust has been in the recovery of fission products (Danesi(1983)), and to a lesser extent uranium (Akiba et.al.(1987)). The advantages displayed by SLM's have been highlighted by Hofman etal (1987 and 1988).

2 THEORY

The mechanism by which a ion is transported from the feed to the strip can be described by the generalised mechanism shown in fig 1. Increasing the Reynolds Number in the aqueous phases by stirring or by increasing flows reduces the boundary layer thicknesses, and hence minimises the boundary layer resistances. Care must be taken not to induce so much turbulence so as to cause the extractant held in the pores of the solid support to be washed out. The diffusion rate of the extractant-metal complex across the SLM can be optimised by ensuring the viscosity of the extractant/ diluent solution is suitably low. A minimum viscosity is required to ensure that the capillary forces holding the extractant/diluent in the solid supports's pores is sufficient. The diameter of the pores also effects the diffusion rate. The rate of the chemical reactions are determined by the system selected.

---

1. SASOL, PO Box 5486, Johannesburg 2000, South Africa.
2. Mintek, Private Bag X3015, Randburg 2125, South Africa.

Traditionally tri-butylphosphate (TBP) is used as an extractant for extracting uranyl nitrate from aqueous streams. The solubility of TBP in water makes it unsuitable for usage in an SLM. In order to reduce the solubility of TBP, it was decided to try increase the carbon chain length. Tri-n-octylphosphate (nTOP) was found to yield the best transfer rates and showed the best SLM life. Longer chain phosphates were not suitability soluble in the diluents tested. Their higher viscosity was also a problem.

The chemical reactions at the feed-SLM interface are:

$$UO_2(NO_3)_2 + 2nTOP = UO_2(NO_3)_2(nTOP)_2 \quad (1)$$

$$HNO_3 + nTOP = HNO_3(nTOP) \quad (2)$$

The diluent used was kerosene. Hofman et.al.(1987) tested a number of diluents. The less viscous diluents were found to wash out of the SLM under the slightest pressure gradients across the SLM yielding low SLM lives. The transfer rates of the more viscous systems were lower the kerosene system. Hofman et.al.(1987) found PVDF to be the most mechanically suitable solid support under acid and radiation conditions. Good results were obtained with weak nitric acid and sodium carbonate solutions. The sodium carbonate strip solution was chosen over the nitric acid because the higher pH of the carbonate solution enhances the acid transfer across the SLM. As the stripping of the uranium is dependant on the presence of acid in the organic phase (eqn 4) the sodium carbonate strip also enhances the uranium transfer.

At the SLM-strip interface the chemical reactions are:

$$2HNO_3(nTOP) + UO_2(NO_3)_2(nTOP)_2 + 4Na_2CO_3 = Na_4UO_2(CO_3) + 4nTOP + H_2O + CO_2\ 4NaNO_3 \quad (3)$$

$$2HNO_3(nTOP) + Na_2CO_3 = 2nTOP + H_2O + CO_2 + 2NaNO_3 \quad (4)$$

3 EXPERIMENTAL

The mechanism of uranium transfer across an SLM was studied in a modified Lewis Cell (fig 2). Having selected a solid support, extractant and diluent, the only variable which can effect the diffusion across the SLM is the extractant concentration. Tests showed that the K_d for the extraction of uranium increased with increasing nTOP concentration, but reached a plateaux above an nTOP concentration of 2,5%. It was therefore decided that an nTOP concentration of 5% would be used throughout this work to ensure that extractant concentration would not be rate limiting. The effects of the stirrer speed, the feed uranium concentration, the feed acid concentration and the strip carbonate concentration on the transfer rates of uranium and acid across the SLM were investigated. The results of these experiments were used to develop a model describing the transfer of uranium and acid across an SLM. A laboratory scale hollow fibre SLM unit was used to test the model.

4 RESULTS

Figure 3a shows the effect of stirrer speed on the transfer rates of

uranium and acid. Initially the uranium transfer rate increases with increasing stirrer speed. At high stirrer speeds the transfer rate is constant. This suggests that at low stirrer speeds (thick boundary layers) the boundary layer resistance is rate controlling. As the Reynolds Number increases (higher stirrer speeds) the resistance to transfer due to the boundary layer diffusion is no longer rate controlling. The stirrer speed had no effect on the acid transfer rate. As a result the stirrer speed of all subsequent runs was 300 RPM ensureing no boundary layer effects.

The uranium feed concentration had no effect on the acid transfer rate. This result was expected as the acid is extracted by the nTOP and stripped by the sodium carbonate strip solution independently of the uranium in the feed (eqns 2 and 4). The uranium transfer rate increased with an increase in the feed uranium concentration as expected from eqns 1 and 3.

The uranium and acid transfer rates increase with increasing feed acid concentration (fig 3b). The effect of the feed acid concentration on the acid transfer rate is expected from equations 2 and 4. The acid forms part of the uranium stripping mechanism (eqn 3) and hence effects the uranium transfer rate. Figure 3b indicates a minimum feed acid concentration required for uranium transfer to take place.

Both the acid and uranium transfer rates show low values at low strip sodium carbonate concentrations. Once the carbonate concentration exceeds 2% the transfer rates of both the acid and the uranium remain constant with increasing carbonate concentrations. This suggests that the stripping reaction is not rate limiting in the presence of excess sodium carbonate.

5 SLM Model

5.1 LEWIS-TYPE CELL MODEL

From the Lewis type cell results it was found that the aqueous boundary layer resistances to the transfer of uranium and acid are not rate limiting if the Reynolds Number is sufficiently high. These two resistances can be omitted from a model if the Reynolds numbers are kept above a minimum. The transfer mechanism presented in fig 1 now becomes a three resistance model:

The extraction reaction rates can be written as (refer to eqns 1 and 2):

$$J_U = (V/A)\, k_1\, U_f\, T^2 \qquad J_H = (V/A)\, k_2\, H_f\, T \qquad (5\&6)$$

Ficks Law describes the diffusion of the uranium-nTOP and acid-nTOP complexes across the SLM:

$$J_U = (D_U/d)\,(U_f - U_s) \qquad J_H = (D_H/d)\,(H_f - H_s) \qquad (7\&8)$$

The stripping reaction rates are written as (refer to eqns 3 and 4):

$$J_U = (V/A) k_3 H_s^2 U_s C^4 \qquad J_H = (V/A)(2k_3 H_s^2 U_s C^4 + k_4 H_s^2 C) \qquad (9\&10)$$

The distribution coefficients for the extraction reactions are:

$$K_{dU} = U_f/U_f \qquad K_{dH} = H_f/H_f \qquad (11\&12)$$

Combining equations 5, 7, 9 and 11 and equations 6, 8, 10 and 12 yields:

$$J_U = (D_U/d)\left[K_{dU}U_f - \frac{k_1U_fT^2}{(k_3C^3/k_4)(k_2H_fT-2k_1U_fT^2)}\right] \quad (13)$$

$$J_H = (D_H/d)\left[K_{dH}H_f - \left(\frac{k_2H_fT-2k_1U_fT^2}{k_4C}\right)^{0.5}\right] \quad (14)$$

As observed in the Lewis Cell work, equation 13 predicts that a minimum acid concentration is required for uranium transfer to occur. The minimum occurs because acid is necessary in the SLM phase for the uranium to be stripped (eqn 3). At low acid concentrations only sufficient acid to drive the acid strip reaction (eqn 4) is present in the SLM phase.

For the system under investigation, the various system parameters could be measured from the Lewis-type cell tests. Equations 13 and 14 become:

$$J_U = 4.52\times10^{-6}U_f - \frac{6.506U_fT^2/C^3}{602H_fT - 2U_fT^2} \quad (15)$$

and $$J_H = 1.28\times10^{-16}H_f-(7.97\times10^{-34}H_fT/C-5.31\times10^{-36}U_fT^2/C)^{0.5} \quad (16)$$

5.2 HOLLOW FIBRE SLM MODEL

The model can be applied to a hollow fibre SLM system. The total mass of uranium permeating across the SLM per unit time is:

$$M_U = J_U N 2\pi R dz \quad (17)$$

A mass balance over the fibres yields:

$$M_U = u\pi R^2 N(U_i-U_o) \quad (18)$$

Combining equations 17, 18, and 15, and assuming a linear concentration gradient down the length of the hollow fibre:

$$\frac{uR(U_i-U_o)}{2} = 4.52\times10^{-6}L\frac{(U_i+U_o)}{2} + 0.506\frac{TL}{C^3}\frac{U_i-U_o}{2T(U_i-U_o)-602(H_i-H_o)} - 0.506\frac{TL}{C^3}\frac{602(U_iH_o-H_iU_o)}{(2T(U_i-U_o)-602(H_i-H_o))^2}\ln\frac{602H_o-2TU_o}{602H_i-2TU_i} \quad (19)$$

Similarly equation 20 can be derived for the acid transfer:

$$uR(H_i-H_o)/2 = 1.28\times10^{-16}L(H_i+H_o)/2 - \{3/(2L)/[5.31\times10^{-36}(U_i-U_o)T^2/C - 7.97\times10^{-34}(H_i-H_o)T/C]\} * \{(7.97\times10^{-34}TH_o/C-5.31\times10^{-36}T^2U_o/C)^{1.5}-(7.97\times10^{-34}TH_i/C-5.31\times10^{-36}T^2U_i/C)^{1.5}\} \quad (20)$$

This model was compared to results from a laboratory scale hollow fibre SLM unit. The model was accurate to within 5% of the measured values.

6 PILOT SCALE TEST

In order to test SLM's under plant conditions, a pilot scale hollow fibre SLM system (fig 4) was used. The feed solution was gravity fed through the tubes of the hollow fibre bundle, while the strip solution was pumped counter-current through the shell. The flowrates were regulated so as to maintain no pressure differential across the SLM. The unit was run batch wise.

The unit was used to treat batches of effluent over a period of 2 months without indications that the extractant was being washed out of the SLM. This

SLM lifetime is consistent with the tests carried out by Hofman (1987) and Craig (1986) where it was found that flat sheet SLM's operated continuously, with no decrease in efficiency, for over 2500 hours.

The uranium transfer rates predicted by the model are within 10% of the measured uranium transfer rates (fig 5). The predicted raffinate uranium concentration is within acceptable agreement with the measured values.

7 CONCLUSIONS AND RECOMMENDATIONS

The model developed can be used with confidence to design an SLM unit for recovering uranium. The method used for developing the model can be applied to any system. The pilot scale tests confirmed that SLM technology can be applied to the removal of uranyl nitrate from effluents. The major problem to date with SLM technology has been instability due to the extractant being washed out of the solid support. This paper has highlighted that by careful system selection this problem can be eliminated.

8 REFERENCES

Akiba, K. and Kanno, T., 1983, Transport of Uranium VI Through A Supported Liquid Membrane Containing Lix 63, Sep.Sci.Technol., **18**(9).

Craig, W.M., Hofman, D.L., Buchalter, E.M., Birkil, R.S. and Smit, J.J., 1986. Cesium Extraction From Reactor Pool Water Using Supported Liquid Membranes. Radwaste'86. Cape Town.

Craig, W.M., Portwig, G. and Buchalter, E.M., 1988. Supported Liquid Membrane Pilot Plant For The Extraction Of Uranium From A Waste Effluent. 5th National Meeting. SA Inst. of Chem.Eng.

Danesi, P.R., Horwitz, E.P., and Rickert, P.G., 1983, Rate And Mechanism Of Facillitated Americium(III) Transport Through An SLM Containing A Bifunctional Organophosphorous Mobile Carrier, J.Phys.Chem., **87**(23).

Hofman, D.L., Craig, W.M., Buchalter, E.M., Birkil, R.S. and Smit, J.J., 1987. Supported Liquid Membrane Technology Applied To The Recovery Of Useful Isotopes From Reactor Pool Water. Chem.Eng.R.& D., **65**(5).

Hofman, D.L., Buchalter, E.M. and Smit, J.J., 1988. The Kinetics Of The Extraction Of Uranium Using Supported Liquid Membranes. 5th National Meeting. SA Inst. of Chem.Eng.

9 NOMENCLATURE

A	SLM area (m^2)
C	Carbonate concentration (mass %)
d	SLM thickness (m)
R	Radius of hollow fibres (m)
D	Diffusion coefficient (m^2/s)
H	Acid concentration in the aqueous phase (mol/l)
H	Acid concentration in the SLM phase (mol/l)
J	Transfer rate (gU/m^2s or mol H^+/m^2s)
k_1-k_4	Rate constants defined by eqns 5,6,9 & 10
K_d	Distribution coefficient
L	Length of the hollow fibre bundle (m)
N	Number of hollow fibres in bundle
T	nTOP concentration (vol %)
U	Uranium concentration in the aqueous phase (gU/l)
U	Uranium concentration in the aqueous phase (gU/l)
V	Volume of Lewis-type cell (m^3)
u	Velocity through the hollow fibre (m/s)
z	distance (m)

SUBSCRIPTS

f	feed
s	strip
U	uranium
H	acid
i	inlet
o	outlet

Figure 1 Generalised SLM Mechanism

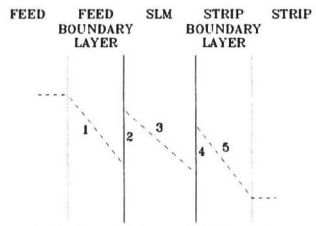

1 Diffusion of the metal through the feed boundary layer
2 Chemical reaction of the metal with the extractant
3 Diffusion of the metal-extractant through the SLM
4 Chemical reaction with the strip solution
5 Diffusion of the metal through the strip boundary layer

Figure 2 Lewis Type Cell

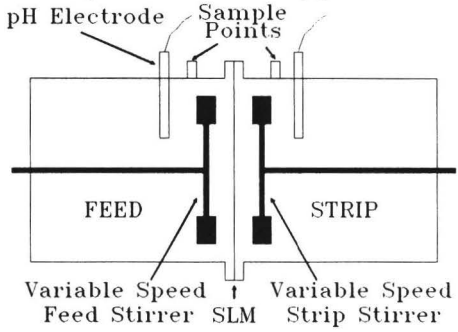

Figure 3(a)
Stirrer Speed Effect

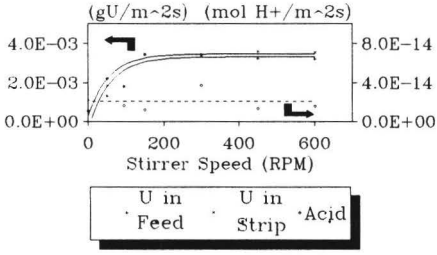

FIGURE 3(b)
Feed Acid Conc Effect

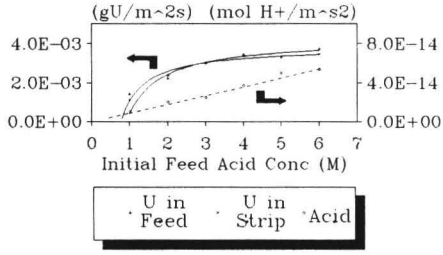

Figure 4 Pilot Hollow Fibre SLM Unit

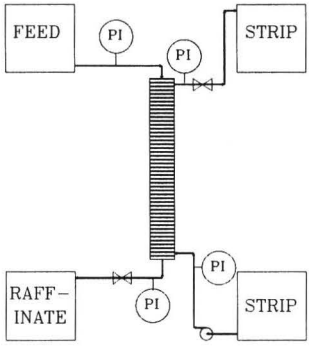

Figure 5 Pilot SLM Results

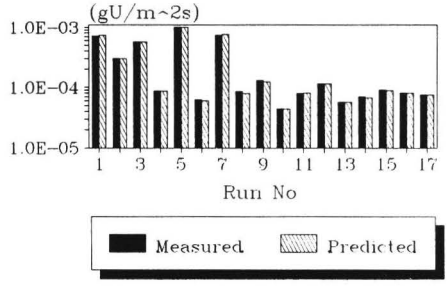

Solvent Extraction 1990, T. Sekine (Editor)
© 1992 Elsevier Science Publishers B.V. All rights reserved

RECOVERY OF URANIUM(VI) FROM WET PROCESS SULFURIC ACID BY AN EMULSION-TYPE LIQUID MEMBRANE TECHNIQUE

Tetsuji HIRATO, Kazuya KOYAMA, Yasuhiro AWAKURA and Hiroshi MAJIMA
Department of Metallurgy, Kyoto University, Sakyo-ku, Kyoto, Japan 606

ABSTRACT

The applicability of an emulsion-type liquid membrane process using tri-n-octylamine (TNOA) as extractant to concentrate U(VI) from sulfuric acid solutions was investigated. Among various agents tested, Na_2CO_3 performed best in the stripping of sulfato-complexes of U(VI) in the internal phase. The emulsion containing ECA 4360J as surfactant was more stable than that containing Span 80. The results of a batch-type extraction experiment of U(VI), to simulate a two-stage counter current extraction, suggest that the U(VI) concentration in the final raffinate can be lowered to below 1 g m^{-3} when a feed solution containing 1 kg m^{-3} U(VI) is treated. The emulsion containing ECA 4360J performed adequately with repeated use of the organic phase recovered from the liquid membrane process. However, extraction with emulsion containing Span 80 decreased gradually with repeated use of the organic phase.

1 INTRODUCTION

An ion exchange method is currently used for the purification and the concentration of dilute U(VI) solution, while a solvent extraction method is used for the purification of concentrated U(VI) solution. However, a liquid membrane method has recently received attention, since it is applicable to both dilute and concentrated solutions. The potential practical applications of a liquid membrane method include nuclear waste processing and hydrometallurgical recovery of uranium.

In this study, the authors examine the applicability of liquid membranes of the emulsion type to acidified dilute uranyl sulfate solutions, which are found in the current hydrometallurgy of uranium concentrates. Tri-n-octylamine (TNOA) is used as an extraction agent. In this case, uranyl sulfate anions are extracted according to the following reaction (Babcock et al., 1980)

$$4R_3N(org) + 4H^+(aq) + UO_2(SO_4)_3^{4-}(aq) = (R_3NH)_4UO_2(SO_4)_3(org) \quad (1)$$

where R_3N denotes TNOA.

2 EXPERIMENTAL PROCEDURES

The extractant used in this study was TNOA. Either sorbitan monooleate (Span 80) or ECA 4360J was used as surfactant. These reagents were diluted appropriately with commercially supplied kerosene. All aqueous solutions were prepared

by using de-ionized water having a specific resistivity of 5×10^6 ohm cm. Emulsions were prepared by mixing the organic phase with the internal aqueous solution, using a homogenizer. Acidic uranyl sulfate feed solution, containing 1.15 kg m^{-3} U(VI) and 33 kg m^{-3} H_2SO_4, was used in most experiments in this study. The volume ratio of internal phase / organic phase / external phase, denoted as $W_I/O/W_E$, was 1/1/10.

Extraction experiments were performed using a mixing cell consisting of a glass separable flask and a Teflon stirrer. Four hundred ml of feed solution was placed in the mixing cell, which was maintained at a constant temperature, usually 298 K. Then, separately-prepared emulsion was added to the feed solution to commence the extraction experiment. Aliquots of the aqueous phase were withdrawn periodically for U(VI) analysis. The concentration of U(VI) in the aqueous phase was determined by means of colorimetry using hydrogen peroxide or thiocyanate.

Emulsions were demulsified with an electrostatic coalescer. A glass separatory funnel was equipped with a rectangular glass tube of length, 5 cm, and cross section, 1 cm x 1 cm. Two platinum electrodes were positioned along opposite walls of the glass tube. 40 ml of water-in-oil emulsion was charged to the glass vessel, and a high voltage d.c. electrostatic field was applied in pulses to these electrodes. Aqueous phase recovered by the demulsification was continuously discharged from the bottom of the glass tube. The volume of aqueous phase recovered was measured periodically to calculate the percent demulsification.

3 EXPERIMENTAL RESULTS AND DISCUSSION

3.1 Extraction of U(VI) from aqueous sulfuric acid solution

The extraction rate of U(VI) increased with increasing TNOA concentration or with decreasing surfactant concentration in the organic phase. On the other hand, the stability of emulsion decreased with increasing TNOA concentration or with decreasing surfactant concentration. The breakdown of emulsion during extraction was more significant with Span 80 than with ECA 4360J. The recommended concentration of TNOA is thought to be between 0.02 and 0.03 kmol m^{-3}, and the concentration of surfactant, 5 wt% Span 80 or 2 wt% ECA 4360J. The mechanical entrainment of external solution was more significant with Span 80 than with ECA 4360J. An increase in H_2SO_4 concentration in the external aqueous phase resulted in a decrease in the extraction rate and the maximum percent extraction of U(VI). The degree of extraction of sulfate and bisulfate ions increased with increasing initial H_2SO_4 concentration. These competing extraction processes probably lead to a decrease in the extraction rate of U(VI).

Several extraction experiments were carried out to identify a suitable internal phase. Various stripping agents, which are commonly used in conventional

solvent extraction with TNOA, were considered. The organic phase used in these experiments, was 0.02 kmol m^{-3} TNOA - 5 wt% Span 80 - kerosene solution. Figure 1 shows the results of extraction of U(VI) with various internal aqueous phases. Desired results, both in the percent extraction as well as the stability of the emulsion, were obtained when Na_2CO_3 was used as the stripping agent in the internal phase. The best result was achieved with 2 kmol m^{-3} Na_2CO_3. Similar results were observed when using 0.02 kmol m^{-3} TNOA - 2 wt% ECA 4360J - kerosene solution as the organic phase.

With Na_2CO_3 and $(NH_4)_2CO_3$, the percents extracted were high, while that with HCl was low. When Na_2CO_3 or $(NH_4)_2CO_3$ solution is used as the internal aqueous solution, the driving force of extraction is the difference in pH between the internal and the external phases. On the other hand, when HCl is used as the stripping agent, an anion exchange-type extraction mechanism prevails in which Cl^- and U(VI) are the participating anions. Since a portion of the TNOA in the liquid membrane combines with HCl, the TNOA concentration effective in the extraction of U(VI) anions decreases, and in turn, the extraction rate decreases. Therefore, in the liquid membrane process with TNOA, it is more efficient to use a pH driving-type internal phase than an anion exchange-type phase.

Batch-type extraction experiments were conducted to simulate two-stage counter current extraction. Based on the results of Fig. 1, which show that the emulsion is stable under the experimental conditions for about 20 min, an extraction time of 10 min was selected for each extraction. Since the concentration of U(VI) in the raffinate derived from conventional solvent extraction is below 1 g m^{-3}, this concentration was set as a target.

Firstly, the extraction conditions under which the U(VI) concentration in the final raffinate in two-stage extraction becomes lower than 1 g m^{-3}, were examined. A fresh emulsion was prepared for an extraction experiment in which feed solutions of various U(VI) concentrations were selected. These concentrations represent the U(VI) concentrations in the raffinate of the first stage. The U(VI) concentrations in the external solutions before and after the extraction are shown in TABLE 1(A). The U(VI) concentration after the extraction corresponds to that of the raffinate of the second stage. The results suggest that if the U(VI) concentration in the feed solution of the second stage, which is the raffinate of the first stage, is below 0.1 kg m^{-3}, the U(VI) concentration in the raffinate of the second stage can be lowered to below 1 g m^{-3}.

The extraction conditions under which the U(VI) concentration in the raffinate of the first stage becomes lower than 0.1 kg m^{-3}, were examined. A fresh emulsion was contacted with an external solution containing 0.1 kg m^{-3} U(VI) and 33 kg m^{-3} H_2SO_4 for 10 min, to prepare an emulsion loaded with U(VI) and H_2SO_4. The loaded emulsion was introduced in the next extraction experiment. TABLE 1(B) shows the results with the loaded emulsions. The U(VI) concentration

TABLE 1. Experimental results of U(VI) extraction to simulate two-stage counter current extraction.

	TNOA (kmol m^{-3})	Surfactant	Na_2CO_3 (kmol m^{-3})	U(VI) (kg m^{-3})	
				Initial	Final
(A)	0.02	5 wt% Span 80	2.0	0.115	0.0011
	0.02	5 wt% Span 80	2.0	0.051	0.0003
	0.02	2 wt% ECA 4360J	1.5	0.111	0.0011
(B)	0.02	5 wt% Span 80	2.0	0.58	0.07
	0.03	5 wt% Span 80	2.0	1.15	0.05
	0.02	2 wt% ECA 4360J	1.5	1.15	0.09

in the raffinate after this extraction corresponds to that of the first stage extraction in the two-stage extraction. The U(VI) concentration was lowered to less than 0.1 kg m^{-3} either by treating a feed solution in which the initial U(VI) concentration was below 0.58 kg m^{-3} with emulsions containing 0.02 kmol m^{-3} TNOA or by treating 1.15 kg m^{-3} U(VI) feed solution with 0.03 kmol m^{-3} TNOA. Similar results were obtained when ECA 4360J was used as surfactant.

Thus, it is believed that the emulsion-type liquid membrane process is effective in concentrating U(VI) in the treatment of feed solutions in which the U(VI) concentration is below 1 kg m^{-3}, under the experimental conditions of this study.

The concentration of U(VI) in the internal solution following extraction is expected to be about ten times higher than that in the original feed solution, when the volume ratio of $W_I/O/W_E$ is 1/1/10. The concentration of U(VI) in the recovered internal solution was found to be 11.0 kg m^{-3} after the extraction in which 1.15 kg m^{-3} U(VI) aqueous solution was used as the feed solution.

3.2 Demulsification and recycle of organic phase

The effect of applied voltage on the demulsification of emulsion was studied in the voltage range, 5 to 25 kV. Figure 2 shows the relationship between the percent demulsification and the demulsification time. Both the initial rate of demulsification and maximum percent demulsification increase with increasing applied voltage. At 2 kV, demulsification was barely detectable. The maximum percent demulsification attained was 98 % in 15 min, but the recovered organic phase was turbid.

The demulsification rate decreased with an increase in surfactant concentration. Demulsification was more difficult with ECA 4360J than with Span 80, when compared at the same concentration level.

In order to examine the demulsification behaviour of emulsion used in the extraction process, the following experiment was performed. Emulsion prepared

with 1.0 kmol m^{-3} Na_2CO_3 solution as an internal aqueous phase and 0.02 kmol m^{-3} TNOA - 2 wt% ECA 4360J - kerosene solution as an organic phase, was subjected to U(VI) extraction for 20 min. After the extraction, the emulsion was separated from the external aqueous phase and then treated in the demulsification experiment. The demulsification rate of used emulsion was much greater than that of fresh emulsion. An evolution of gas bubbles was detected when used emulsion was demulsified. By contacting the gas bubbles with an aqueous solution of calcium hydroxide, the solution became turbid, and this suggests that the evolved gas was CO_2. The pH in the internal phase is lowered by H^+ ions transported with U(VI) and sulfate ions, and the decrease in pH is favorable to the evolution of CO_2 gas in the internal phase. The formation of CO_2 gas bubbles seems to enhance the breakup of emulsion.

In order to operate an emulsion-type liquid membrane process, it is necessary to recycle the organic phase recovered after extraction. It is important to examine the effects of demulsification on the extraction-stripping ability of the recycled organic phase. In the following experiments, the emulsion was demulsified after each extraction at an applied voltage of 15 kV for 30 min.

Figure 3(a) shows the results of U(VI) extraction with a recycled organic phase, which contains 0.02 kmol m^{-3} TNOA and 5 wt% Span 80. 1.5 kmol m^{-3} Na_2CO_3 aqueous solution was used as the internal phase. In this figure, "1st run" denotes the extraction with a fresh emulsion, and "2nd run", the extraction with emulsion prepared with organic phase recovered from the 1st run. The percent extraction of U(VI) decreases with an increase in the number of extractions. On the other hand, Fig.3(b) shows the results when 2 wt% ECA 4360J was used as surfactant instead of Span 80. No significant change in the percent extraction is detected among runs. Therefore, it is believed that the organic phase containing ECA 4360J as surfactant can be used repeatedly to prepare an emulsion after a cycle of the liquid membrane process.

CONCLUSIONS

The applicability of an emulsion-type liquid membrane process using TNOA as extractant to concentrate U(VI) from sulfuric acid solutions was investigated. Among various agents tested, Na_2CO_3 performed best in the stripping of sulfato-complexes of U(VI) in the internal phase. The emulsion containing ECA 4360J as surfactant was more stable than that containing Span 80. The results of a batch-type extraction experiment of U(VI), to simulate a two-stage counter current extraction, suggest that the U(VI) concentration in the final raffinate can be lowered to below 1 g m^{-3} when a feed solution containing 1 kg m^{-3} U(VI) is treated. The emulsion containing ECA 4360J performed adequately with repeated use of the organic phase recovered from the liquid membrane process. However, extraction with emulsion containing Span 80 decreased gradually with

repeated use of the organic phase.

REFERENCE

Babcock, W.C., Baker, R.W., LaChapelle E.D. and Smith, K.L., 1980. Coupled transport membranes III: The rate-limiting step in uranium transport with a tertiary amine. J. Membrane Sci., 7: 89-100.

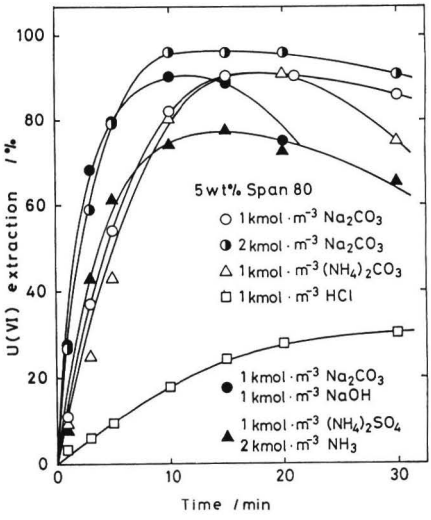

Fig.1 Effect of various internal aqueous solutions on the extraction of U(VI).

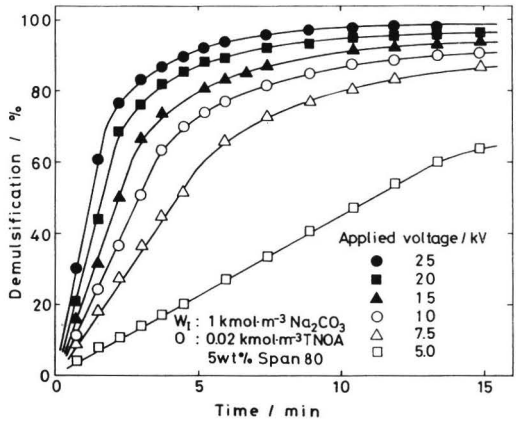

Fig.2 Effect of applied voltage on demulsification.

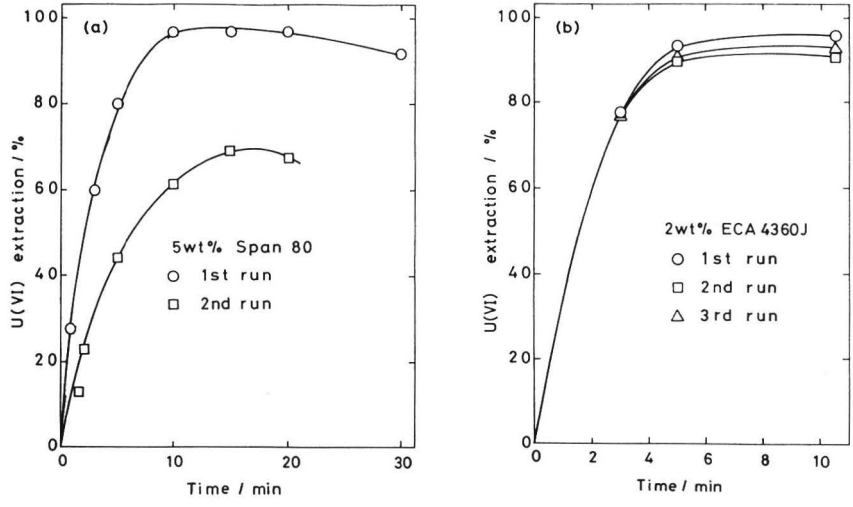

Fig.3 Extraction of U(VI) using a recycled organic phase containing (a) Span 80 or (b) ECA 4360J.

Solvent Extraction 1990, T. Sekine (Editor)

© 1992 Elsevier Science Publishers B.V. All rights reserved

LEAKAGE SUPPRESSING OF W/O EMULSION USING HIGH VISCOUS SOLVENT

SHINYA OKAZAKI, MASANAO IMAI AND MASARU SHIMIZU
Dept. of Chemical Engineering, Div. of Chemical & Biological Science,
Faculty of Engineering, Tokyo University of Agriculture and Technology.
24-16 2-chome Nakamachi, Koganei, Tokyo 184, JAPAN

ABSTRACT
OKAZAKI SHINYA, IMAI MASANAO AND SHIMIZU MASARU, 1990. LEAKAGE SUPPRESSING OF W/O EMULSION USING HIGH VISCOUS SOLVENT, Proc. ISEC '90.

The stability of W/O emulsion droplets was evaluated to investigate the effect of apparent W/O emulsion viscosity and organic phase viscosity, liquid membrane thickness, osmotic pressure difference and energy dissipation rate per unit mass of fluid by a tracer technique. The suppression of leakage was affected by the organic phase viscosity rather than the apparent W/O emulsion viscosity. The dependence of each factor was correlated as follows:

$$Kb=3.0\times10^{-19}\Delta^{-1.0}\mu_0^{-0.8}\varepsilon^{\alpha}\Delta\pi^{0.9} \quad (\Delta\pi>10^6)$$

where $\alpha=2.2\times10^{-8}\Delta\pi+0.8$

$$Kb=8.0\times10^{-13}\Delta^{-1.0}\mu_0^{-0.8}\varepsilon^{0.8} \quad (\Delta\pi<10^6)$$

1. INTRODUCTION

Extraction processes using liquid membrane with a mobile carrier are an attractive method for separation and concentration of metals. In particular, emulsion liquid membrane is very interesting because of a large interfacial area and very thin liquid membrane. The main problem is that the separation efficiency decreased due to the break-up of the W/O emulsion droplets. Therefore, it is important to develop more stable W/O emulsion droplets. Previous investigations (Akiba et al.,1984, Boyadzhiev et al.,1977, Goto et al.,1987, Imai et al.,1987, Kinugasa et al.,1989, Kondo et al.,1979, Li.,1971, Takahashi et al.,1981) reported that the leakage of tracer was caused by the break-up of W/O emulsion droplets and tracer permeation through the membrane due to various factors, i.e. type and concentration of surfactant, the agitating rate and swelling of ones.

The purpose of this study is to discuss the effect of apparent W/O emulsion viscosity and organic phase viscosity on the suppression of leakage, liquid membrane thickness, type and concentration of tracer and energy dissipation rate per unit mass of fluid.

2. EXPERIMENTAL APPARATUS AND PROCEDURE

The organic phase of emulsion liquid membrane was kerosene containing the surfactant Span 80. Liquid paraffine was blended to prepare the W/O emulsion having a viscous organic phase. The tracer mainly used was HCl which was one of the most typical acids used in extraction of metals. Furthermore, various acids and bases; H_3PO_4, H_2SO_4, HNO_3 and NaOH, and metallic salts; $Zn(NO_3)_2$, $ZnSO_4$ and $Al_2(SO_4)_3$, were used to investigate the effect of the tracer. The W/O emulsion was prepared by the following two methods using homogenizer at an agitating rate of $117sec^{-1}$ for 600 sec.

1) Method A: The W/O emulsion was prepared by addition of liquid paraffine at a constant volume fraction of inner aqueous phase (ϕ_w).

2) Method B: The W/O emulsion was prepared by changing of ϕ_w under a constant fraction of liquid paraffine (ϕ_p).

The W/O emulsion viscosity (μ) and organic phase viscosity (μ_0) were measured by a rotational viscometer (Tokyo Keiki Co. Type E) in the lower shear rate region, and the viscometer of capillary tube was used in the higher shear rate region. The leakage fraction was measured by EDTA titration method when the tracer was metallic ion, and ionic electrode or pH meter (Toyo Seisakusho Co.) when the tracer was an acid or base.

Figure 1 shows a schematic diagram of the experimental apparatus. A stirred tank with four baffle plates and the impeller were made of acrylic resin. The impeller was a six-bladed fan turbine. The diameter of the stirred tank(D) was 0.12m, and the diameter of impeller(Di) was 0.08m, 0.06m and 0.04m. The impeller was installed in the center of liquid depth and a torque meter (Yamazakiseiki Co.) was attached to the agitating axle. The energy dissipation rate was adjusted by the agitating rate and diameter of the impeller. The temperature was kept at 298K.

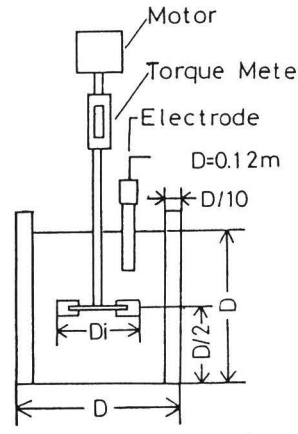

Fig.1 Experimental apparatus.

3. RESULTS AND DISCUSSION

The flow curves of W/O emulsion obeyed a non-Newtonian type fluid behavior in the lower shear rate region and a Newtonian type behavior in the higher shear rate region. Therefore, the apparent W/O emulsion viscosity was determined from the data in a high shear rate region.

The leakage fraction, θ, is defined by Eq.(1).

$$\theta = \frac{(Co - Coi) \cdot Vo}{Ci \cdot Vi} \quad (1)$$

The leakage rate, assumed to be proportional to $(1-\theta)$, is expressed as Eq.(2) (Boyadzhiev et al.,1977, Goto et al.,1987).

$$\frac{d\theta}{dt} = Kb \cdot (1-\theta) \quad (2)$$

Integrating Eq. (2) under the initial conditions (t=0, θ=0), Eq. (3) is derived as

$$\ln(1-\theta) = -Kb \cdot t \quad (3)$$

where, Kb is defined as the leakage rate constant.

Figure 2 shows the effect of ϕ_P on the change in leakage fraction with agitating time, according to Eq. (3). The Kb values were determined from these slopes of the liner relationship obtained. However, in a system with a higher ϕ_w or at a larger osmotic pressure difference, the slopes were changed to a further large at a certain agitating time. The Kb values in this study were determined from the region.

Figure 3 shows the effect of initial liquid membrane thickness (Δ) on Kb using method B. The value for Δ was obtained by Eq. (4).

$$2\Delta = \frac{dp}{\phi_w^{1/3}} - dp \quad (4)$$

The Kb values at each agitating rate

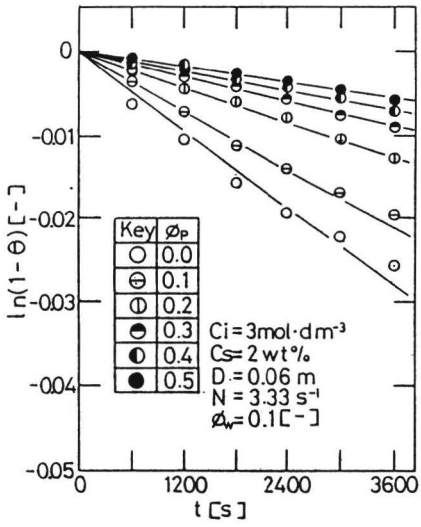

Fig.2 Effect of ϕ_P on the change of leakage fraction with agitating time.

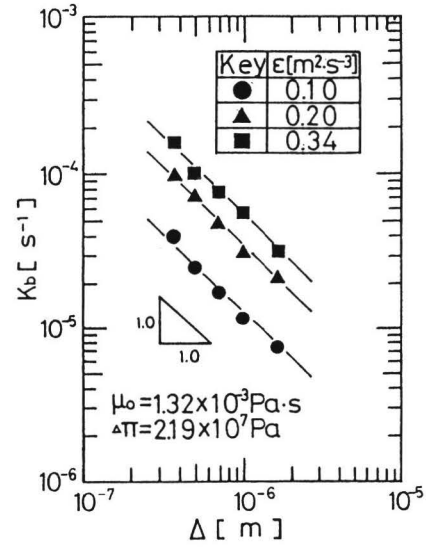

Fig.3 Effect of Δ on Kb.

showed an inversely proportional relationship to Δ. The higher ϕ_w system induced unstable W/O emulsion droplets with thinner liquid membranes. For these W/O emulsion droplets, the water permeation was induced, causing the W/O emulsion droplet to easily and consequently split with mechanical agitating energy.

Figure 4 shows the effect of μ on $Kb \cdot \Delta$ where μ was varied either by a change in ϕ_P(method A) or ϕ_w(method B). The $Kb \cdot \Delta$ values remained constant when ϕ_w was varied, but decreased when ϕ_P was varied. Hence, the data could not be arranged by the apparent W/O emulsion viscosity.

Figure 5 shows the effect of μ_0 on $Kb \cdot \Delta$ using method A and method B. The $Kb \cdot \Delta$ values were plotted by parallel straight lines with a slope of 0.8. Therefore, the stability of W/O emulsion droplets was not affected by the apparent W/O emulsion viscosity but by the organic phase viscosity. A higher μ_0 formed more stable W/O emulsion droplets because the water permeation into the inner aqueous phase was prevented. Li reported that the addition of glycerol in the O/W/O emulsion system induced the more thickness liquid membrane (Li, 1971).

Figure 6 shows the effect of ε on $Kb \cdot \Delta \cdot \mu_0^{0.8}$. The value of ε was obtained from Eq. (5).

$$\varepsilon = \frac{2\pi \cdot N \cdot Tr}{\rho_C \cdot Vo} \qquad (5)$$

When $\Delta\pi > 10^6$, the slope increase reflects a greater dependence of ε on $Kb \cdot \Delta \cdot \mu_0^{0.8}$ with increasing $\Delta\pi$. When $\Delta\pi < 10^6$, ε was

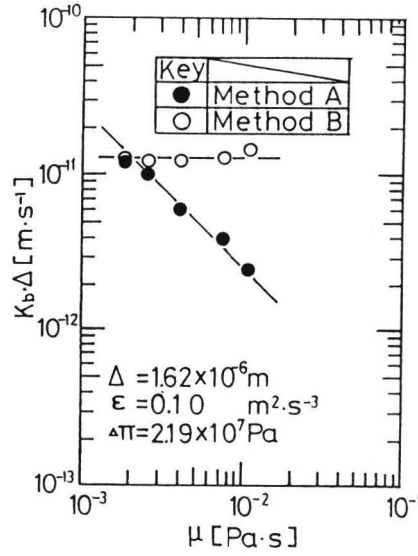

Fig.4 Effect of μ on $Kb \cdot \Delta$.

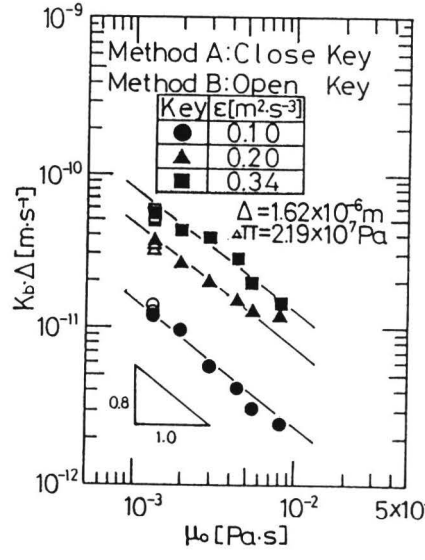

Fig.5 Effect of μ_0 on $Kb \cdot \Delta$.

constant dependence of $Kb \cdot \Delta \cdot \mu_0^{0.8}$. The Kb values were correlated by an expression relating between ε and $\Delta\pi$ as follows:

$$Kb \propto \Delta^{-1.0} \cdot \varepsilon^{\alpha} \cdot \mu_0^{-0.8} \quad (6)$$

were $\alpha = 2.2\times10^{-8}\Delta\pi + 0.8$ $(\Delta\pi > 10^6)$ and $\alpha = 0.8$ $(\Delta\pi < 10^6)$. The osmotic pressure difference gave a constant dependence to the leakage when $\Delta\pi < 10^6$. However, when $\Delta\pi > 10^6$, the slope became steeper with increasing $\Delta\pi$ because the water permeation was caused due to the higher osmotic pressure difference, consequently, the W/O emulsion easily broke down.

Figure 7 shows the dependence of $\Delta\pi$ on $Kb \cdot \Delta \cdot \varepsilon^{-\alpha} \cdot \mu_0^{0.8}$ when $\Delta\pi > 10^6$. The leakge increase with $\Delta\pi$ was not related to the kind of tracer. However, some tracers, such as HNO_3 and NaOH, have been found to remarkably weaken the stability of W/O emulsion droplets. The Kb data was proportional to $\Delta\pi^{0.9}$. All data was correlated as follows:

$\Delta\pi > 10^6$;

$$Kb = 3.0\times10^{-19}\Delta^{-1.0}\mu_0^{-0.8}\varepsilon^{\alpha}\Delta\pi^{0.9} \quad (7)$$

where $\alpha = 2.2\times10^{-8}\Delta\pi + 0.8$

$\Delta\pi < 10^6$;

$$Kb = 8.0\times10^{-13}\Delta^{-1.0}\mu_0^{-0.8}\varepsilon^{0.8} \quad (8)$$

When the volume fraction of W/O emulsion was less than 0.13, The Kb values were not infulenced.

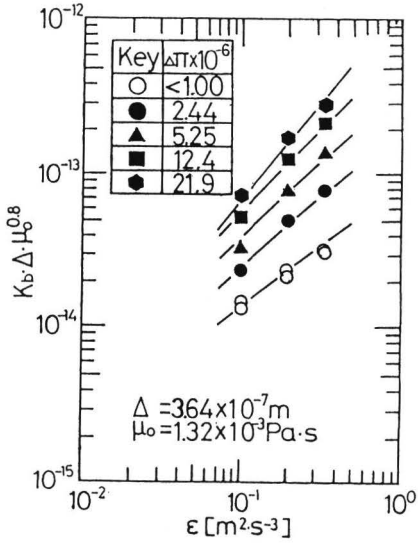

Fig.6 Effect of ε on $Kb \cdot \Delta \cdot \mu_0^{0.8}$

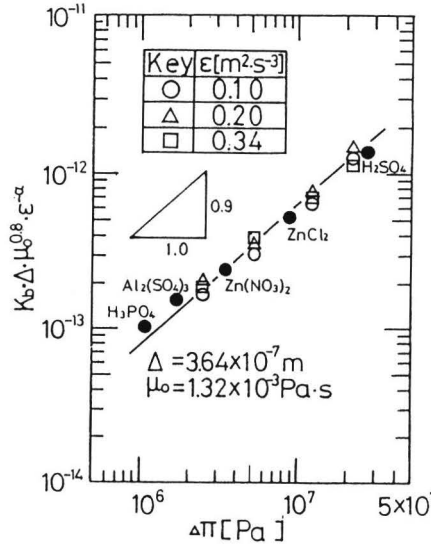

Fig.7 Dependence of $\Delta\pi$.

4. CONCLUSION

The stability of W/O emulsion droplets was investigated to determine the effect

of the organic phase viscosity, liquid membrane thickness, osmotic pressure difference and energy dissipation rate per unit mass of fluid. The following conclusions can be made from the results in this study:

1) The stability of W/O emulsion droplets was not affected by the apparent W/O emulsion viscosity but by the organic phase viscosity.

2) The leakage was increased with the volume fraction of inner aqueous phase, which affected a liquid membrane.

3) The leakage was affected by the osmotic pressure difference. The type of tracer had no effect on the leakage.

4) The dependence of each factor was correlated in Eqs (7) and (8).

5. NOMENCLATURE

Ci	$[mol \cdot m^{-3}]$	: tracer concentration in inner aqueous phase
Co	$[mol \cdot m^{-3}]$	: tracer concentration in outer aqueous phase
Coi	$[mol \cdot m^{-3}]$	: initial tracer concentration in outer aqueous phase
D	[m]	: diameter of stirred tank
Di	[m]	: diameter of impeller
Kb	$[s^{-1}]$	: leakage rate constant defined by Eq. (3)
N	$[s^{-1}]$	: agitating rate
Tr	[J]	: torque
Vi	$[m^{-3}]$	: initial volume of inner aqueous phase
Vo	$[m^{-3}]$	: initial volume of outer aqueous phase
t	[s]	: agitating time
Δ	[m]	: initial liquid membrane thickness
α	[-]	: power term of $\Delta\pi$
ε	$[m^2 \cdot s^{-3}]$	: energy dissipation rate per unit mass of fluid
θ	[-]	: leakage fraction of inner aqueous phase
μ	[Pa·s]	: apparent W/O emulsion viscosity
μ_0	[Pa·s]	: organic phase viscosity
$\Delta\pi$	[Pa]	: osmotic pressure difference between inner and outer aqueous phase
ρ_c	$[Kg \cdot m^{-3}]$	: density of outer aqueous phase
ϕ_P	[-]	: volume fraction of liquid paraffine in organic phase
ϕ_w	[-]	: volume fraction of inner aqueous phase in W/O emulsion

6. REFERENCE

Akiba, K., Takahashi, T. and Konno, T., 1984. Extraction of uranium(VI) by emulsion liquid membrane containing 5,8-diethyl-7-hydroxy-6-dodecanone oxime: Bull.Chem.Soc.Japan.,57,2618-2621

Boyadzhiev, L., Spundzhiev, T. and Benzenshek, E., 1977. Modeling of carrir-mediated extraction: Separ.Sci.,12,541-551

Goto, M., Matsumoto, M., Kondo, K. and Nakashio, F., 1987. Development of new surfactant for liquid surfactant membrane process: J.Chem.Eng.Japan, 20,157-164

Imai, M. and Furusaki, S., 1987. Leakage of the inner water phase into the outer water phase in W/O/W emulsion: Kagaku kougaku Ronbunshu,13,561-566

Kinugasa, T., Watanabe, K. and Takeuchi, H., 1989. Effect of organic solvents on stability of liquid surfactant membranes: J.Chem.Eng.Japan,22,593-597

Kondo, K., Kita, K., Koida, I., Irire, J. and Nakashio, F., 1979. Extraction of copper with liquid surfactant membranes containing benzoylacetone: J.Chem.Eng.Japan,12,203-209

Li,N.N., 1971. Separation of hydrocarbons by liquid membrane permeation: Ind.Eng.Chem.Process Des.Develop.,10,215-221

Takahashi, K., Ohtsubo, F. and Takeuchi, H., 1981. A study of the stability of (W/O)/W-type emulsions using a tracer technique: J.Chem.Ehg.Japan,14,416-418

Solvent Extraction 1990, T. Sekine (Editor)

© 1992 Elsevier Science Publishers B.V. All rights reserved

MEMBRANE EXTRACTION OF ACTINIDES

B.F. MYASOYEDOV, A.P. NOVIKOV, and M.N. MIKHEEVA
V.I.Vernadsky Institute of Geochemistry and Analytical Chemistry, USSR Academy of Sciences, Kosygin str. 19, Moscow (USSR).

ABSTRACT
Myasoyedov, B.F., Novikov, A.P., and Mikheeva, M.N. 1990. Membrane extraction of actinides.

Some results are presented of studies of mass-transfer kinetics of transuranium elements trough bulk, emulsion, and supported liquid membranes containing carriers of various classes. The radiation stability of membranes as well as the effect of interface phenomena on transport kinetics of actinides in different oxidation states are discussed.

The most worthwhile trends in the development of liquid membrane methods and their application in the analytical chemistry of radionuclides and in radiochemical productions, from our point of view, are:

(a) Constructing highly selective and sensitive modules for sensors used in continuous analytical control.

(b) Developing efficient purification methods of individual radionuclides.

(c) Developing ecologically safe and rapid pertractors for deep purification of wastes from radiotechnical plants.

(d) Developing research methods of physico-chemical properties of superheavy short-lived isotopes.

A number of these problems can be solved in the general context of studies on quasi-equilibria and transport characteristics of liquid membranes as well as their application in chemical technology and biotechnology. Other ones have their own features, first of all, related to the fact that the methods using rather thin, though not always stable, membranes can be utilized for extraction, separation and preconcentration of radioactive substances.

The problem of the membrane stability is essential in developing specific schemes and processes. A number of techniques are known of preparing liquid membranes. These are impregnation, emulsion, film, and bulk methods. Stability parameters of these membranes are being thoroughly studied and have been described in literature. We shall discuss only certain results of studies on

radiation stability of various membrane types.

The effect of radiation on normal functioning of a membrane is determined by two factors: the radiolysis of the extractant carriers and the destruction of the structures that provide stabilization (radiolysis of the surfactants in the emulsion membrane extraction, destruction of the polymer fibers and films used in solid-supported membranes). As for the film and bulk membranes, the radiative-chemical processes in these membranes and those in ordinary extraction systems are supposed to be identical.

Our studies have shown the emulsion membranes to be the most sensitive to irradiation. The latter seems to be due to the fact that in the transfer process in emulsion membranes a significant accumulation of organic complexes of extracted substances in surface-adjacent and microheterogenic layers is observed (Yurtov et al., 1988). In this case the radiation effect upon the emulsifier of surfactants is significantly higher than that at uniform distribution of alpha-radioactive isotopes in organic phase. Thus, for example, the demulsification speed of the emulsion with the most often used sorbitanmonooleate (Span-80) emulsifier, increases by 8-10 times at a radiation dose accumulated in organic phase of 100 Gr. This indicates the relatively low radiation stability of the surfactants as compared to di-2-ethylhexylphosphoric acid (HDEHP) for which the decomposition at radiation dose 2×10^6 Gr is 5-7 % (the total concentration of HMEHP and H_3PO_4). Such a low radiation stability of emulsions appears to be accounted for high radiative-chemical yield of alcohols upon decomposition of high-molecular surfactants. Alcohols are known to promote demulsification of emulsions.

At the same time, the emulsion membrane extraction appears to be a very efficient and rapid method of isolation and preconcentration of trace amounts of radionuclides. Hence, this method can be very successfully applied for group extraction of transplutonium elements (TPE) from solutions of such a strong complexon as diethylenetriamin pentacetic acid (DTPA) which is known to be used in purification stages of trivalent TPE from rare-earth elements in talspick process. Meanwhile, the emulsion containing HDEHP, Span-80 and HNO_3 extracts more than 90% of TPE from DTPA solution, while in ordinary extraction the extraction extent is not higher than 2-3%. Application of emulsion membrane extraction by redox process scheme is also possible.

Methods are known in which redox reactions are used to increase the efficiency of extraction of elements, e.g. uranium from phosphoric acid (Kendzi et al., 1982). The combination of the membrane and redox processes appears to be not less efficient in separation of heavy actinide elements, which, as a rule, have several quite stable oxidation states. For instance, the emulsion membrane extraction can be very efficiently applied to separate americium and curium, the two transplutonium elements with the most close chemical properties (see Fig. 1). In this case americium is extracted after oxidation to Am (IV) in the form of

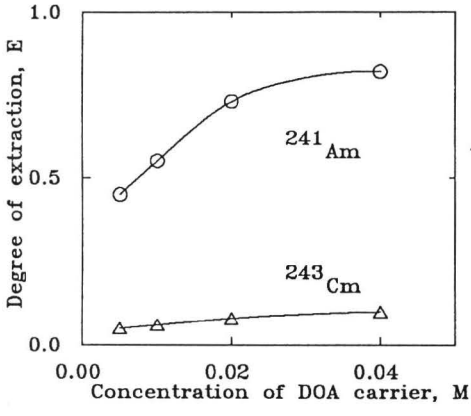

Fig. 1. Separation of Am(IV) and Cm(III) during emulsion membrane extraction. Composition of the phases: FEED - 1.5 M H_2SO_4, $5x10^{-3}$M PW; MEMBRANE - 4% Span-80, CCl_4, DOA; STRIP - 1 M H_2SO_4, H_2O_2.

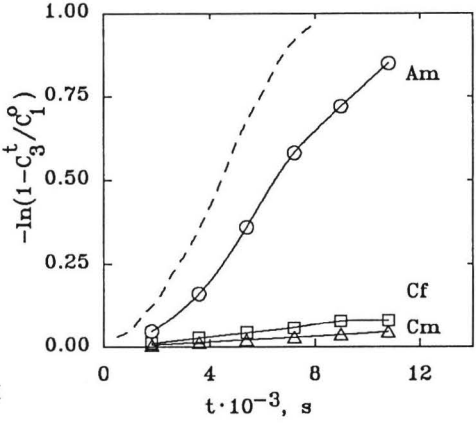

Fig. 2. Semilogarithmic plot of Am(VI) and Cm(III) concentration vs time, through SLM, [HDEHP] = 0.5 M. FEED: 2 M H_3PO_4, [Am] = $1.1x10^{-4}$ M, [Cm] = $5.6x10^{-6}$ M; STRIP: 1,1 M $HClO_4$, H_2O_2. The dashed line was calculated assuming that no reduction of Am(VI) takes place in the membrane.

phosphortungstate anion complexes. Di-n-octyl amine was used as a carrier, and Span-80 was used as an emulsifier. Re-extraction was carried out into nitrate solution after americium reduction to Am(III).

Separation of actinide elements by redox processes with solid-supported hollow film and fiber membranes is even more convenient. Although these processes are usually slower, the absence of dispersion and coalescence problems, small losses of radioactive

solutions, and the possibility of complete automation and remote control make their development rather auspicious in respect to the problems of radiochemistry. Besides, due to small specific surface of membranes very important become the interfacial phenomena and processes which are not characteristic for extraction by emulsion technique.

Certain kinetic problems arise, as a rule, in the following cases:

(a) the extracted ionic forms of a given element are unstable in the required oxidation state and easily reduced (oxidized) in membrane phase;

(b) the extracted compounds of a given element in appropriate oxidation state are so stable that can not be easily reduced (oxidized) in the accepting aqueous phase;

(c) certain compounds that formed during oxidation (reduction) process have limited solubility that leads to formation of a inter-phase layer;

(d) using high concentrations of complexing reagents in aqueous phases reduces the speed of chemical reactions by which extracted complexes are formed.

Unfortunately, all these phenomena in one or another form are revealed in the course of developing particular schemes and methods of extraction and separation of actinide elements.

The first case is the most characteristic of heavy transplutonium elements that have high standard oxidation potentials of Me(III)/Me(IV), Me(V)/Me(VI) couples. For instance, many traditional extractants, such as primary and tertiary amines, quaternary ammonium bases, neutral organophosphorous compounds, and even acids readily reduce americium (VI) and (IV).

Secondary amines which can be used as carriers of americium (IV), anionic phosphor-containing complexes, and purified HDEHP in Am(VI) extraction are the exceptions. However, in these cases the rate of trans-membrane transfer is noticeably lower than that calculated assuming absolute stability (see Fig. 2). Nevertheless, under optimal conditions presented in Fig. 2 this method can be successfully used to separate americium from trivalent curium and californium or to determine concentrations of various ionic forms of americium in solutions. The chemistry of heavy actinides having been studied unsatisfactorily makes this very important. It is necessary to emphasize that the similar task can not be accomplished by solvent extraction, because at highly developed

interfacial surface, when a potential is not continuously applied to the releasing aqueous phase, the reduction processes are significantly more rapid.

Interfacial redox reactions between ionic forms of actinides are usually slow upon formation of stable complexes with extractant-carrier, and are the rate-determining stages of the whole membrane extraction process. For example, when extracting Np(VI) through a HDEHP membrane (Fig. 3), the rates of Np(V) oxidation to Np(VI), extraction of Np(VI) into the membrane and even that of diffusion of extracted complex in the membrane are significantly higher than the rate of neptunium reduction by such reagents as $NaNO_2$, hydrazine, and H_2O_2. Besides, for the last two reagents the neptunium reduction to Np(IV) in the strip solution is characteristic, that accounts for the peaks on the kinetic curves (Fig. 3), since Np(IV) forms stable complexes with HDEHP.

As a result, in practice, the re-extraction stages have to be accomplished into the solution of complexing reagent which binds the required ionic form of extracted element eliminating the reduction stage.

In spite of the above-mentioned difficulties the combination of redox processes with transfer through liquid membranes during separation is a very convenient way to achieve deep purification of elements having relatively stable oxidation states (Fig. 3).

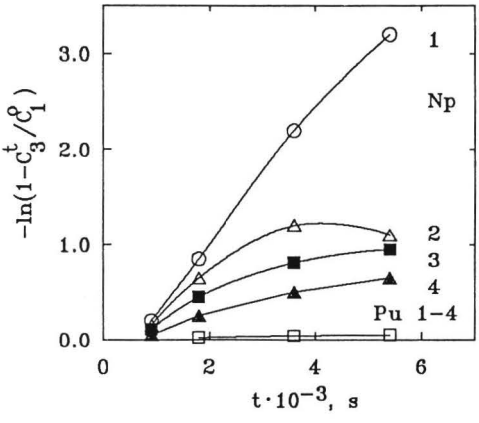

Fig. 3. Semilogarithmic plot of Np(VI) and Pu(IV) concentrations vs time, through SLM, [HDEHP] = 0.1 M. FEED: 1 M HNO_3, 10^{-4} M PW; STRIP: 1 - $(NH_4)_2CO_3$; 2 - 1 M HNO_3, N_2H_4; 3 - 1 M HNO_3, H_2O_2; 4 - 1 M HNO_3, $NaNO_2$.

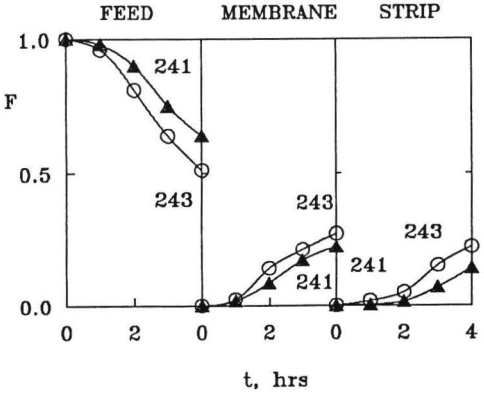

Fig. 4. Electromembrane separation of americium isotopes.
$F = [Me]^t_i/\Sigma[Me]^o_i$.

The latter can be explained by the fact that redox reactions between macro and microelements take place in actinide solutions that complicates the use of traditional extraction schemes.

In some cases the transport of actinides through liquid membranes under conditions of different redox potentials for aqueous and membrane phases is followed by kinetic isotope effects of oxidation and disproportionation reactions (especially for Me(V) ionic forms). Thus, in the process of americium (III) oxidation to americium (VI) and the extraction of the latter by membrane containing HDEHP, trans-membrane flow is enriched by heavier isotopes of americium (Fig. 4). It is known, for the systems under consideration, that the kinetic isotopic effect in the Me (V) disproportionation reactions for $^{241/243}Am$ and $^{238/212}Pu$ couples has a quite significant value of about 1.02 ± 0.01. This makes it possible to perform enrichment by traditional method using extraction-chromatographic columns (Nikitenko, 1989).

Yet, the membrane processes in this case are more convenient since they are performed in the cells of small volume without significant losses of very radiotoxic substances.

The data on separation and isolation of actinides by membrane extraction presented in this report indicate, to our mind, that this trend has its prospects. It especially concerns the development of new efficient and rapid isolation methods of heavy elements having short half-lifes. To solve these problems, the electro-dialysis membrane processes with extremely thin (less than 20 um) liquid membranes and so called "dynamic" membranes can successfully compete with traditional thin-layer chromatography and sorption.

REFERENCES

Kendzi, Ya., Kadano, M., Yuko, En., and Hirosi, H., 1982. Extraction of uranium from phosphoric acid. Pat. No 57-122785, Japan.

Nikitenko, S.I. 1989. Kinetic isotope effects in reactions of actinides. In: Actinides-89 International Conference, September 24-29, Tashkent, USSR. Abstracts, p. 377.

Yurtov, E.V., Golubkov, A.S., Guseva, T.V., Koroleva, M.Yu., and Grabovskaya, E.I., 1988. Peculiarities of liquid membrane extraction in multiple emulsion. In: Proc. Intern. Solv. Extr. Conf., Moscow, USSR. 3: 15-18

Solvent Extraction 1990, T. Sekine (Editor)

© 1992 Elsevier Science Publishers B.V. All rights reserved

TRANSPORT OF LANTHANOIDS THROUGH LIQUID MEMBRANES CONTAINING D2EHPA AS A CARRIER

Y. HIRASHIMA[+], S. KOHRI, and G. ADACHI
Department of Applied Chemistry, Faculty of Engineering, Osaka University, Yamadaoka, Suita, Osaka 565 (Japan)
[+]Development Division, The Taiyo Mining & Industrial Co., Shin-Meikai Bldg., 4 Kaigandori, Chuo-ku, Kobe 651-01 (Japan)

ABSTRACT

The transport rate was independent of the stirring rates of the aqueous phases, and of the HCl concentration in the receiving phase when it was higher than 1 M. The rate exhibited a maximum at a certain carrier concentration. The results observed in this investigation were reasonably explained assuming that the diffusion of the lanthanoid complex across the membrane controls the transport rate of the lanthanoid. The transport rate was generally larger for higher lanthanoids. The separation factors observed in this investigation were comparable to those for usual solvent extraction.

1 INTRODUCTION

Separation of individual lanthanoids is generally difficult because of their close similarity to each other in chemical properties. Solvent extraction and ion exchange processes are now mainly used in practical lanthanide separation. More efficient processes are required because lanthanides are not provided at sufficiently cheap prices. Application of liquid membrane transport to the separation of several metals has been investigated (Danesi, 1984;Novikov and Myasoedov). We report here the investigation of the transport of lanthanides through a supported liquid membrane (SLM) and discussion on the possibility of the separation of lanthanides by means of SLM transport. Di(2-ethylhexyl)phosphoric acid (D2EHPA), which is an excellent extractant for lanthanide separation, was used as a carrier.

2 EXPERIMENTAL

Di(2-ethylhexyl)phosphoric acid (D2EHPA, Union Carbide Co.) was purified by successive washing with aqueous sodium carbonate and hydrochloric acid solutions. A supported liquid membrane (SLM) was prepared by soaking a microporous polypropylene film in a solution of D2EHPA in SHELLSOL 71 (a 100% paraffin solvent, Shell Chemical Co.) for 20 min or longer. The SLM was rinsed with deionized water

before it was used for transport experiment. The polypropylene film was Duragard 2400 (trade name of Celgard 2400 in Japan; thickness: 25um, porosity: 0.38, pore size: 0.02um) kindly supplied by Polyplastic Co..

The transport cell used in this investigation is illustrated in Fig. 1. Two compartments (200 cm^3 each) for the source and receiving phases were made of glass and were separated with a SLM. The surface area of the SLM was 10.46 cm^2. The source phase solution (I) was an aqueous solution of hydrochloric acid (0-0.5 M) and lanthanide chloride (0.005-0.2 M). The receiving one (II) was an aqueous hydrochloric acid solution (0-3 M). The two solutions were stirred at 240 rpm unless otherwise specified. One-milliliter portions of samples were taken from the receiving phase at different time intervals. The concentration of a lanthanide was determined by EDTA titration with Xylenol Orange as an indicator.

The lanthanide concentration in the receiving phase increased linearly over a eight-hour transport duration. The linear increase means that the transport was constant and therefore the average of the amount of a lanthanoid during 8 hours was generally used for calculating the transport rate. The transport rate (J) of a lanthanide was defined as the amount(mol unit) of the element transported per a second and a square meter.

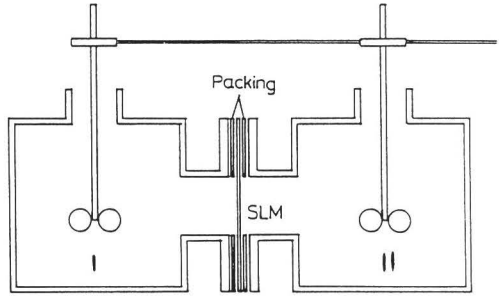

Fig. 1. Apparatus for SLM transport.

3. RESULTS AND DISCUSSION

D2EHPA extracts a tervalent lanthanide ion (Ln^{3+}) through a cation exchange reaction expressed by Eq. 1.

$$Ln^{3+}_{(aq)} + m(HX)_{n(org)} \underset{\text{Stripping}}{\overset{\text{Extraction}}{\rightleftharpoons}} LnX_3 \cdot 3HX_{(org)} + 3H^+_{(aq)} \quad (1)$$

(HX:D2EHPA, aq:aqueous phase, org:organic phase)

In the liquid membrane transport a lanthanoid ion is taken from the source phase to the membrane (extraction) and released from the membrane to the receiving phase (stripping) via the cation exchange reaction. The lanthanide transferred to the membrane

moves toward the membrane-receiving phase interface (I_{mr}) across the membrane by diffusion. Hydrogen ions are transported in the reverse of the lanthanide.

The transport rate of a lanthanide was nearly constant irrespective of varying stirring rate of either of the aqueous source and receiving phases. This result means that the diffusion in the aqueous phases was not the rate-controlling step of the transport. Therefore, the controlling step is in the extraction into the membrane, stripping from the membrane or the diffusion across the membrane.

The increase of HCl concentration in the receiving phase enhanced the transport rate of Pr at the lower HCl concentration region (<1 M) as is expected from Eq. 1, but affected the rate little at the higher concentration region (Fig. 2). The increase of the rate with the HCl concentration can be explained to be due to the promotion of stripping but the leveling is unexplainable. This result can be explained as follows assuming that the diffusion across the membrane is the controlling step. At the lower HCl concentration region the lanthanoid concentration at the interface I_{mr} of the membrane is decreased with the the increase in the HCl concentration, but the decrease becomes less

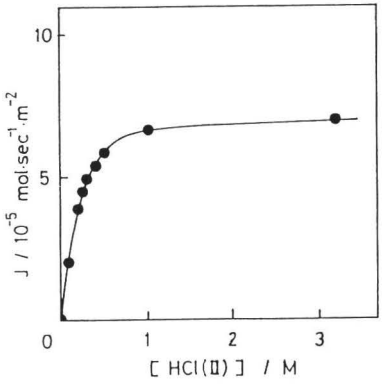

Fig. 2. Transport rate (J) of Pr vs. HCl concentration in the receiving phase. I:0.04 M $PrCl_3$+0.1 M HCl, SLM:1 M D2EHPA, II:HCl.

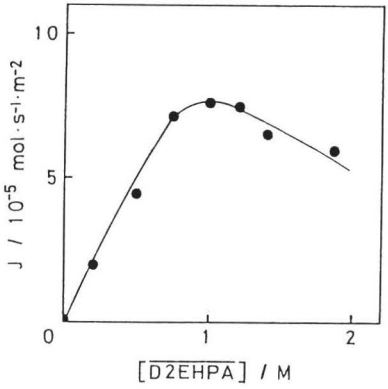

Fig. 3. Transport rate (J) of Pr vs. carrier concentration in the SLM. I:0.04 M$PrCl_3$+0.1 M HCl, SLM:D2EHPA I:3 M HCl.

significant in the higher HCl concentration region because the lanthanoid concentration already approaches closely to zero. These phenomena lead to the considerable increase of the concentration gradient across the membrane in the lower HCl concentration region and to the less prominent increase in the higher concentration region. Hereafter the concentration of HCl in the receiving phase was fixed to be 3 M.

Figure 3 shows that the transport rate of a lanthanoid exhibited a maximum at about 1 M of D2EHPA concentration (C_{HX}) in the membrane solution when the concentration was varied. The increase of the rate with the increase in the D2EHPA concentration is natural because the increase of the concentration promote the extraction of a lanthanide from the source phase and/or because the concentration of the lanthanide at the source phase-membrane interface (I_{sm}) of the membrane is increased. The increase of the lanthanide concentration at the interface means the increase of the lanthanide concentration gradient across the membrane, therefore that of the diffusion rate. The decrease of the rate in the higher carrier concentration region was caused by the inhibition of stripping or by the decrease of the diffusion coefficient due to the increase of the viscosity (η) of the membrane solution. The plot of C_{HX}/η against C_{HX} gave a curve similar to that in Fig. 3. The result is reasonably explained by assuming that the diffusion across the membrane controlled the transport and that the lanthanide concentration at the membrane side of the interface (I_{sm}) was proportional to C_{HX} since the diffusion coefficient is inversely proportional to the viscosity of the solution in most cases and since the concentration gradient should be proportional to the lanthanide concentration at I_{sm} considering that the concentration at I_{mr} is nearly zero.

As is shown in Fig. 4 the decrease of the acid concentration ($C_{H,s}$) in the source phase increased the transport rate in agreement with the expectation from Eq. 1 but unexpectedly decreased the transport rate in the lower acid concentration region, where gelatinous materials were observed in the source phase and on the surface of the membrane support. The occurrence of gelatinous materials has been reported also in the usual solvent extraction of lanthanides with D2EHPA (Hirashima et al., 1980). The unexpected decrease of the transport rate is considered to be caused by the decrease of the effective surface area of the SLM due to the deposition of the gelatinous materials.

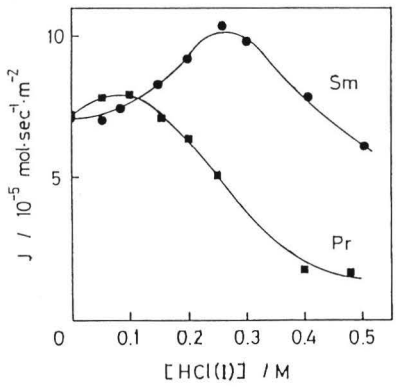

Fig. 4. Transport rates (J) of Pr and Sm vs. HCl concentration in the source phase. I:0.04 M $PrCl_3$(■) or $SmCl_3$(●), SLM:1 M D2EHPA, II:3 M HCl.

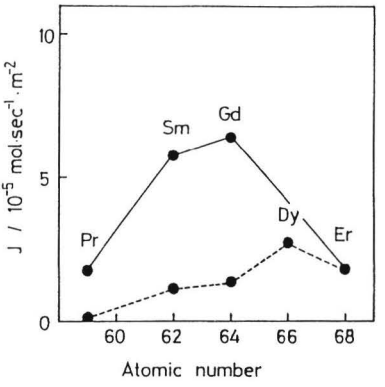

Fig. 5. Transport rates of some lanthanides. II:3 M HCl: (—●—)-I:0.04 M $LnCl_3$+0.4 M HCl, SLM:1 M D2EHPA, (-·●·-)-I:0.01 M $LnCl_3$+0.4 M HCl, SLM:0.25 M D2EHPA

The transport rate was increased quasi-linearly with increasing lanthanide concentration in the source phase in the lowest concentration region, and the increase gradually became less remarkable in the higher concentration region.

The observed phenomena above described were all explained by assuming that the diffusion of the lanthanide complexes across the membrane controlled the transport. Explanation based on the other controlling steps were inconsistent with either of the phenomena.

Fig. 5 shows that the transport rate was generally larger for heavier lanthanides. The exceptional decrease for some heaviest elements were caused by the occurrence of the gelatinous materials mentioned above.

The separation factors between observed for some two-lanthanide systems are given in Table 1. The separation factors were calculated from the ratios of the transport rates. The value obtained here were comparable to those for solvent extraction systems as is shown in Table 1, suggesting the possibility of the application of SLM transport to separation of lanthanides.

TABLE 1

Separation factors for some two-lanthanide systems.

Systems	Pr-Nd	Nd-Sm	Sm-Eu	Eu-Gd	Gd-Tb	Tb-Dy	Dy-Ho	Ho-Er	Er-Yb
SLM	1.36	6.29	2.00	1.30	1.58	1.15	1.12	1.33	2.60
Solvent Extraction	1.7	5.0	2.2	1.6	3.2	2.0	2.1	2.1	6.3

4. REFERENCES

Danesi, P.R., 1984. Sep. Sci. Technol., 19: 857.
Hirashima, Y., Kodera, H. and Shiokawa, J., 1982. Nippon Kagaku Kaishi, 627
Novikov, A.P. and Myasoedov, B.K., 1987. Solv. Ext. Ion Exch., 5: 117

Solvent Extraction 1990, T. Sekine (Editor)

© 1992 Elsevier Science Publishers B.V. All rights reserved

STUDY OF A PALLADIUM MASS ACCELERATE TRANSFER THROUGH A SOLID SUPPORTED LIQUID MEMBRANE CONTAINING KELEX100

E. Anticó[a], M. Hidalgo[a], A. Masana[a], V. Salvadó[a],
M. Muñoz[b], M. Valiente[b].

a Unitat de Química, Estudi General Girona (UAB) 17071 Girona (Spain).
b Unitat de Química Analítica, Universitat Autònoma Barcelona, 08193 Bellaterra (Spain)

ABSTRACT

By taking advantage of the SCN^- catalytic effect on the extraction of Pd(II) by Kelex100 (7-(4-ethyl-1-methyloctyl)-8-quinolinol) a liquid supported membrane has been developed to extract Pd(II) from chloride solutions.

Chemical parameters such as concentrations of Kelex100, SCN^- and stripping agents were varied to determine their influence in the Pd(II) permeation. Different complexing agents of Pd(II) were studied for the stripping solutions, e.g. thiocyanate, thiosulfate and thiourea. Thiocyanate and thiourea were the most effective.

Dodecanol and non ionic surfactants e.g. Span80, were incorporated, as organic modifiers. Such addition decreases the permeability of Pd(II).

INTRODUCTION

Solvent extraction of Pd(II) from chloride media has been the subject of several studies. A number of different reagents have been employed as extractants for palladium, i.e. alkyl and aryl phosphines (Mojski, 1979 and Walker et al., 1986), alkylamines (Masana et al., 1989), dialkyl sulphides (Cote et al., 1989), as well as chelating reagents as 8-hydroxyquinoline derivatives (Ma et al., 1984) and hydroxyoximes (Inoue et al., 1986). Among these agents 7-(1-vinyl-3,3,5,5-tetramethylhexyl)-8-quinolinol, pre-1976 Kelex100, has shown a good selectivity for Pd(II) (Ma et al.., 1984). The main drawback of this process concerns with the slow extraction rate.

By taking advantage of the SCN^- effect on the extraction of Pd(II) by Kelex100 (Al-Bazi et al., 1986) a solid supported liquid membrane (SSLM) has been developed to extract Pd(II) from chloride solutions containing small amounts of thiocyanate.

A previous study on the characterization of the extraction equilibrium of Pd(II)-SCN^--Kelex100 system has shown to form several organic metal species (Masana et al., 1990).

EXPERIMENTAL

Reagents and solutions

Kelex100 was kindly supplied by Schering España,S.A. (Barcelona, Spain) and was purified as described by Al-Bazi and Freiser (1986). Organic solutions were prepared dissolving Kelex100 in isopropylbenzene, cumene. A Kelex100 concentration of 0.1 mol.dm^{-3} was fixed.

A stock solution of Pd(II), pH=1, was prepared from $PdCl_2$ (Spanish Society of Precious Metals) dissolved in HCl and standaridzed gravimetrically with dimethylglyoxime. The metal ion concentration was kept constant at 3.0 10^{-5} mol.dm^{-3}, in the feed solution, and sodium thiocyanate ranging from 10^{-4} to 10^{-3} mol.dm^{-3} was added. Ionic strength was adjusted at 1.0 mol.dm^{-3}, with NaCl.

The receiving phase contained sodium thiocyanate or thiourea, as stripping agents, and NaCl to keep the same ionic strength that feed solution.

The pH in both feed and stripping solutions was 2.5.

SSLM description and procedure

The membrane consisted of a lipophilic polymeric support, a flat-sheet Millipore GVHP, impregnated by the organic solution containing Kelex100 as a carrier.

The permeation experiments were carried out in a two compartment membrane cell as described elsewhere (Salvadó et al., 1989).

Pd(II) permeation was monitored by periodically withdrawing samples of the feed solution and analyzing the metal content spectrophotometrically.

RESULTS AND DISCUSSION

The experimental data were collected in the form of permeability defined by:

$$P = -\frac{d[Pd(II)]}{dt}\frac{V}{Q}\frac{1}{[Pd(II)]}$$

where Q and V are the effective membrane area and the volume of feed solution (190 ml.), respectively.

Various Pd(II) complexing agents were used in the stripping solutions, e.g. thiocyanate, thiosulfate or thiourea. Thiourea and thiocyanate were the most effective. Results are collected in Fig.1. Under these conditions a yellow-orange precipitate on the feed side was observed during the experiment, on the membrane and on the teflon stirrer blades.

Once the liquid membrane was designed, the influence of various chemical parameters were investigated, ie. feed thiocyanate concentration, Kelex100 concentration in the membrane phase, pH of the stripping solution and several modifiers of the liquid membrane (dodecanol, tri-n-laurylamine (TLA), sorbitan

monoleate (SPAN) and polyethylene glycol dioleate (DOPEG)). Fig.2 shows the effect of SCN^- concentration on the Pd(II) permeability.

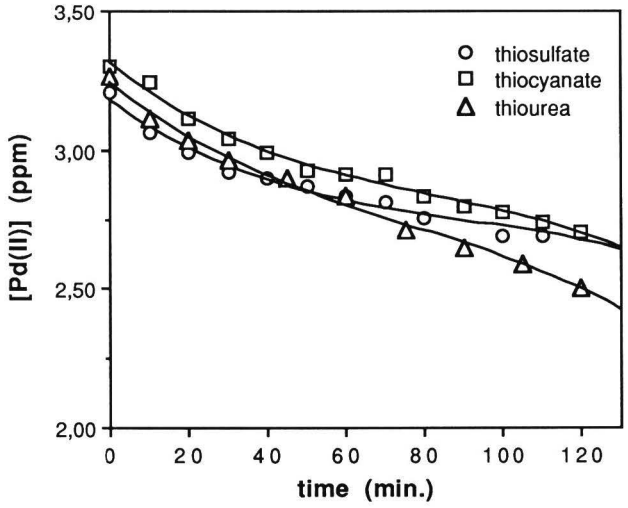

Figure 1. Influence of different stripping agents.
Feed: [NaSCN]= 1.0E-04 M.

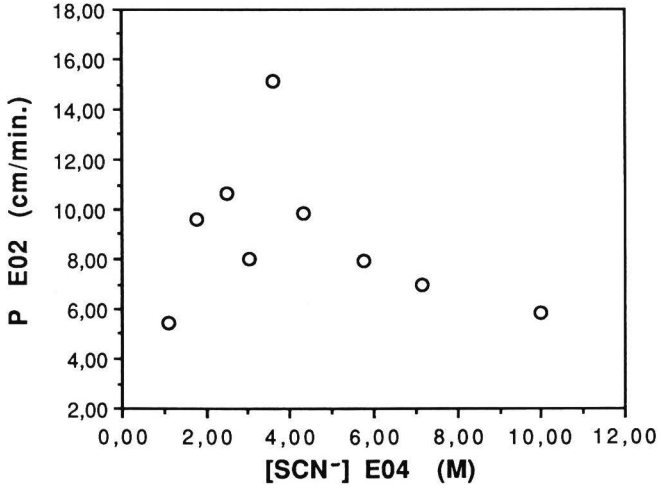

Figure 2. Membrane permeability vs. thiocyanate concentration in the feed solution. Stripping: [NaSCN]= 0.1 M.

A maximum value of permeability was found when the SCN^- concentration was $3.6\ 10^{-4}$ mol.dm^{-3}. A similar effect was observed on the metal liquid-liquid distribution coefficient (Masana et al., 1990). The effect of modifiers is shown in Fig.3 and 4

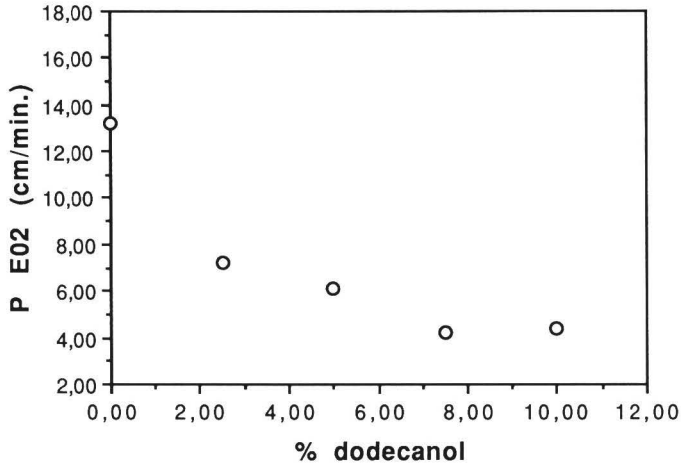

Figure 3. Influence of dodecanol concentration on the palladium(II) permeability. Feed: [NaSCN]= 3.6E-04 M. Stripping: [NaSCN]= 0.1 M.

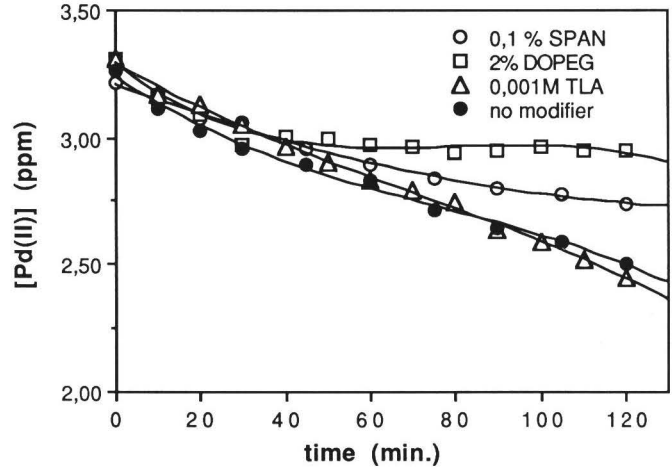

Figure 4. Effect of the presence of some organic modifiers.
Feed: [NaSCN]= 1.0E-04 M. Stripping: [thiourea]= 0.2 M.

As seen dodecanol and non ionic surfactants have a negative effect on the process. On the other hand, TLA does not change the system.

The formation of a solid phase at the feed side of the membrane has been reported in a liquid-liquid system Pd(II)-SCN^--dioctylsulphide (Cote et al., 1989). In this case the authors attributed to $Pd(SCN)_2$ the solid formed. In our case, to obtain information on the nature of the precipitate, infra-red and NMR spectra were obtained. The infra-red spectra suggest a Pd(II)-Kelex complex. A comparison between the IR spectra of Kelex100 and the precipitate reveals, for the precipitate, the supression of a pic at 3600 cm^{-1} (probably the O-H of Kelex100 which may participates in the Pd(II) complex) besides the pic at 1100 cm^{-1} region atributed to the presence of a metal chelate (Charles et al., 1956). Furthermore, corresponding NMR spectra shows substantial differences, i.e. the aromatic protons in the region 6-8.5 ppm for Kelex100 are found split for the precipitate.

In order to avoid the formation of the solid phase a bulk membrane was designed. The experiments were performed in a cell shown in Fig.5.

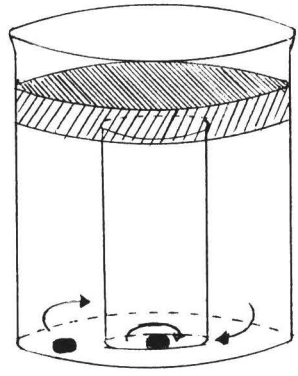

Figure 5. Cell used in the bulk liquid membrane experiments

A larger volume (25 ml.) of the organic membrane phase keeps the extracted metal complex in solution. However, as expected, the mass transfer process is faster for the solid supported liquid membrane (Fig.6).

Acknowledgements. The authors would like to acknowledge many helpful discussions with Prof. Henry Freiser and Dr. Sargon Al-Bazi from the Department of Chemistry of the University of Arizona.
This work has been carried out with the financial support of the Spanish Commission for Research and Development CICYT, Project num. MAT88-752.

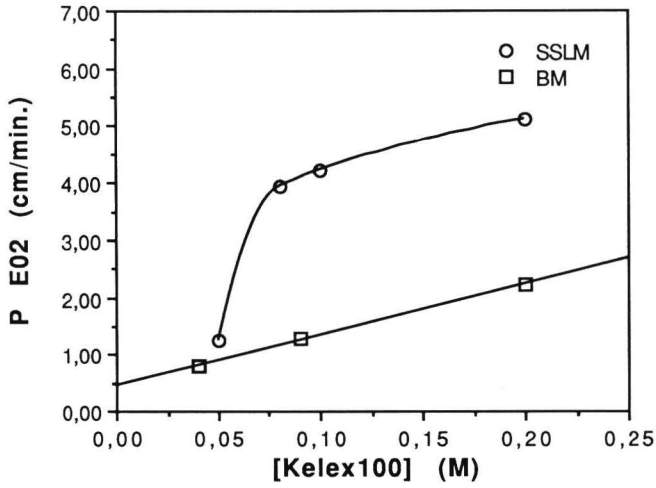

Figure 6. Comparison of the two membrane configurations: a bulk membrane (BM) and a solid supported liquid membrane (SSLM). Feed: [NaSCN]=1.0E-04 M. Stripping: [thiourea]= 0.2 M.

REFERENCES

Al-Bazi, S.J. and Freiser, H., 1986. Trans-effect in extraction kinetics: Palladium extraction by 7-(1-vinyl-3,3,5,5-tetramethylhexyl)-8-quinolinol.Solvent Extraction and Ion Exchange, 4(6):1121-1137.

Charles, R.G., Freiser, H., Friedel, R., Hilliard, L.E. and Johnston, W.D., 1956. Infra-red absorption spectra of metal chelates derived from 8-hydroxyquinoline, 2-methyl-8-hydroxyquinoline, and 4-methyl-8-hydroxyquinoline. Spectrochimica Acta, 8:1-8.

Cote, G., Ganguly, K.M. and Bauer, D., 1989. Influence of thiocyanate ions on the kinetics and thermodynamics of palladium(II) extraction with Dialkyl Sulphides. Hydrometallurgy, 23:37-45.

Inoue, K. and Maruuchi, T., 1986. Solvent extraction of palladium with SME 529: equilibria and kinetics. Hydrometallurgy, 16:93- 104.

Ma, E. and Freiser, H., 1983. Solvent extraction equilibria and kinetics in the palladium(II)-hydrochloric acid-7-(1-vinyl- 3,3,5,5-tetramethylhexyl)-8-quinolinol system. Inorg. Chem., 23:3344-3347.

Masana, A., Hidalgo, M., Salvadó, V., Muñoz, M. and Valiente, M., 1989. Separation of palladium (II) from aqueous chloride solution using tridodecylammonium chloride in toluene as extractant. Analytical Sciences, 5:201-205.

Masana, A., Hidalgo, M., Salvadó, V., Muñoz, M., Valiente, M. and Freiser, H., 1990. The effect of chemical catalysts on the solvent extraction reactions of Pd(II) by Kelex 100 from chloride solutions. In preparation.

Mojski, M., 1978. Extraction of gold, palladium and platinum from chloride, bromide and iodide solution with di-n-octyl sulphide (DOS) in cyclohexane. Talanta, 25:163-165.

Salvadó, V., Masana, A., Hidalgo, M., Valiente, M. and Muhammed, M., 1989. A study of the permeation of gold(III) through Cyanex 471x solid supported membranes (SSLM). Analytical Letters, 22(11&12):2613-2626.

Walker, R.D. and Bautista, R.G., 1986. Liquid-liquid extraction of palladium(II) from the $PtCl_4$-HCl-H_2O-xylene-Cyanex 471 system. ISEC'86, Munich, p. 107.

Solvent Extraction 1990, T. Sekine (Editor)

© 1992 Elsevier Science Publishers B.V. All rights reserved

A PHOSPHINE SULFIDE SYSTEM FOR THE SOLVENT EXTRACTION AND LIQUID MEMBRANE PROCESS OF GOLD (III)

V. Salvadó[1], M. Hidalgo[1], A. Masana[1], M. Muñoz[2], M. Valiente[2] and M. Muhammed[3].

1- Química (E.G.G.). Pça. Hospital, 6. 17071 Girona (Spain).
2- Química Analítica (U.A.B.) 08193 Bellaterra (Spain).
3- Dept. of Inorganic Chemistry. The Royal Institute of Technology (K.T.H.). S-10044 Stockholm (Sweden).

ABSTRACT

Triisobutylphosphine sulphide in aromatic solvents (toluene, cumene) has been employed to extract Gold (III) from chloride solutions. The study includes the characterization (speciation) of the extraction reactions, the design of a liquid membrane system and its implementation in different configurations of solid supported liquid membranes. Solid supported liquid membranes in two different type of support: laminar membrane and hollow fibers were studied. Different materials were analyzed as laminar membrane support.

1 INTRODUCTION

Gold may exists in polymetallic sulfide ores at very low concentrations. Processing of these materials is mainly carried out by using acidic chloride solutions where gold is present as Au(III)-chloride complexes (Johnson, 1981).

The use of liquid membranes for the extraction of gold has been reported before (Izatt, 1987). In this case, a macrocycle crown ether was employed as membrane carrier.

The solvent extraction of Gold (III) from acidic chloride media by organic solutions containing triisobutylphosphine sulfide, Cyanex 471, has been reported (Salvadó et al., 1990) to be sucessful. By taking advantage of this results we have undertaken the present work.

The main objectives are to design and develop a SSLM system for the permeation of Au(III) from aqueous chloride solutions by using different type and geometries of solid supports, i.e. flat sheets and hollow fibers. In our case, these polymeric supports were impregnated by organic solutions of Cyanex 471 (triisobutylphosphine sulfide) in cumene as a carrier.

2 EXPERIMENTAL

2.1. Reagents and solutions.

Stock Au(III) solutions were prepared from solid $HAuCl_4$ (Johnson Matthey, 49.9% of gold). Solutions containing Au(III) in the range 10 to 65 ppm in aqueous total chloride 1.0 mol.dm^{-3} were employed as feed solutions.

Cyanex 471, triisobutylphosphine sulfide, kindly supplied by American Cyanamide Co., was purified by recrystallization from ethanol-water mixture. Organic solutions of Cyanex 471 in cumene,

isopropylbenzene (Merck A.R.), ranging from 10 to 200 mmol.dm^{-3} were used as liquid membrane materials.

Aqueous solutions containing mixtures of NaSCN and NaCl at total ionic strength of 1.0 mol.dm^{-3} were prepared and used as stripping solutions. The SCN^- concentration was varied from 0.1 to 1.0 mol.dm^{-3}.

2.2. Apparatus and procedure.

The experiments were carried out by using two different geometries of solid supports for the liquid membranes, i.e. flat sheets and hollow fibers. In the case of laminar supports we employed a two compartment membrane cell provided with a circular window (Fig. 1a). A constant membrane area of 12,57 cm^2 was used througout the experimental study. In a set of experiments the stirring speed of the feed solution was varied from 700 to 1300 rpm while for the stripping solution was kept constant at 700 rpm.

When capillar solid support were used, a continuous recycling process was carried out as shown in Fig. 1b where the feed and stripping solutions are in two separated cells and the hollow fiber impregnated with the organic solution is placed in the stripping compartment, the feed solution circulates through the hollow fiber by a impulsion peristaltic pump.

In both systems, at given time intervals, samples of 1 cm^3 of the feed solution were analyzed by A.A.S. in order to determine the gold permeability.

Experiments were carried out in a termostated room at 25±1 ^{0}C.

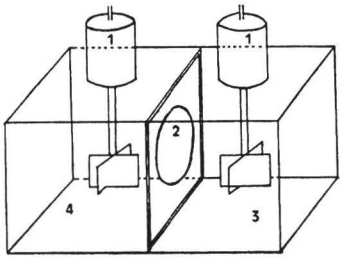

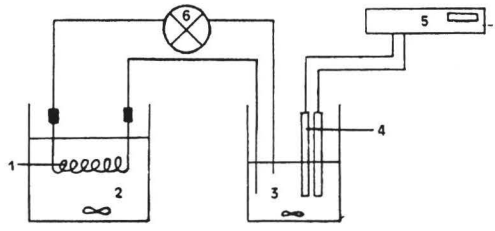

a) Laminar membrane:
1. stirring motors, 2. membrane, 3. feed compartment, 4. stripping compartment.

b) Hollow fiber:
1. hollow fiber, 2. stripping solution, 3. feed solution
4. glass electrode, 5. voltimeter, 6. peristaltic pump.

Fig. 1. Experimental scheme for the membrane systems.

3 RESULTS AND DISCUSION

From a previous study (Salvadó et al., 1990) the solvent extraction of gold by triisobutylphosphine sulfide has been explained by considering the following reactions:

$$Au^{3+} + 3\,Cl^- + TIBPS_{org} \rightleftharpoons AuCl_3.TIBPS \; ; \quad \log \beta_{11}=34{,}96 \qquad (1)$$

$$Au^{3+} + 3\,Cl^- + 2\,TIBPS_{org} \rightleftharpoons AuCl_3.2TIBPS \; ; \quad \log \beta_{12}=42.36 \qquad (2)$$

where TIBPS stands for the extractant. The extraction proceeds via a solvating type mechanism.

The permeability data are expressed in the form of gold permeability, where P is defined by:

$$P = \frac{-d[Au^{3+}]}{dt} \frac{V}{A} \frac{1}{[Au^{3+}]} \qquad (3)$$

where V is the volume of the aqueous feed solution and A represents the effective membrane area.

In the case of hollow fibers the permeability was obtained by applying the equation:

$$P = \frac{-d[Au^{3+}]}{dt} \frac{V}{A} \frac{\phi}{(\phi+1)} \frac{1}{[Au^{3+}]} \qquad (4)$$

where ø is defined as : $\phi = [Q_T / P L \varepsilon N R]$ (Danesi, 1984)

Q_T (cm^3/sec): total flow rate
N: number of fibers
L (cm): hollow-fiber length
R(cm): hollow fiber internal radius
ε : porosity

Different parameters affecting the liquid membrane performance have been studied by determining the permeability at the different conditions.

3.1. Hydrodynamic behavior of the system.

For the laminar support, the dependence of the gold permeability on the stirring speed of the feed solution was studied for the various membrane supports used. In the case of the tubular support, the linear velocity of the feed solution was varied. through the hollow fiber. Fig. 2 shows the results of the different experiments with the two geometries. It is observed that for Millipore flat support, the gold permeability is constant in the range studied, while for Accurel and Celgard 2500 supports the permeability decreases below 1000 r.p.m. On the other hand, the behavior of the Accurel hollow fiber follows the corresponding laminar support, having smaller values of permeability.

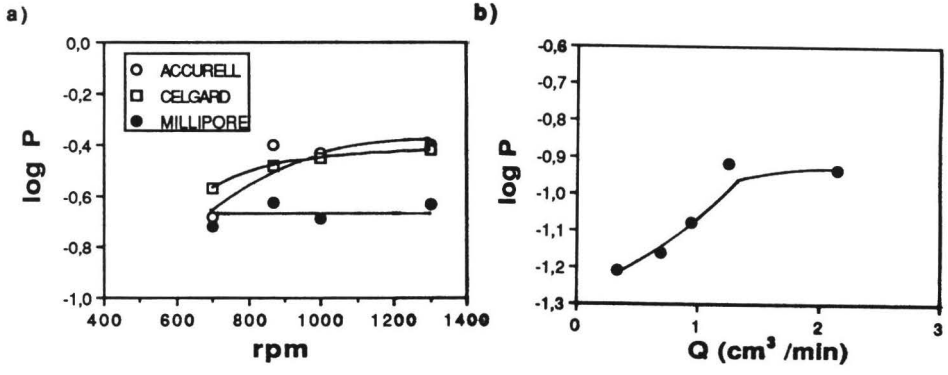

Fig. 2. Influence of hydrodynamic conditions. a) Laminar membrane, b) hollow fiber. [Au(III)] = 12 ppm, 1 M HCl.

3.2. Effect of the feed acidity.

The HCl concentration of the feed solution was varied between 0.2 10^{-3} to 1.0 mol.dm^{-3} for a set of experiments (Fig. 3) while the other variables were kept constant for the two different geometries. The obtained results show no influence of the acidity on the gold permeation as expected from the solvating mechanism on the extraction of gold (III) by TIBPS.

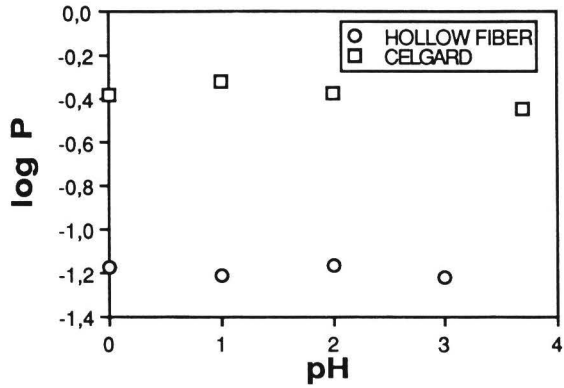

Fig.3. Effect of feed acidity. [Au(III)] = 12 ppm, [Cyanex 471] = 0.1 M.

3.3. Influence of carrier concentration.

Separate experiments were carried out where only the organic extractant (Cyanex 471) concentration was varied between 10 to 200 mmol.dm^{-3}. In these experiments, Celgard 2500 and Accurel (laminar and hollow fiber) supports were used. As observed in Fig. 4, the permeability is constant in the studied range for the different supports.

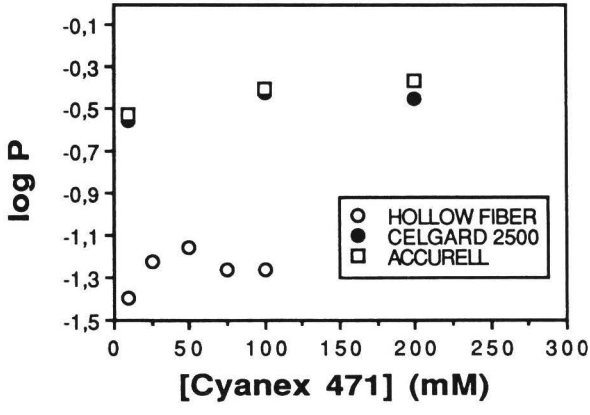

Fig 4. Effect of carrier concentration on the Au(III) permeability. [Au(III)] = 12 ppm, 1M HCl.

3.4. Influence of the gold concentration.

In this study, initial Au(III) concentration of the feed solution was varied. The results collected in Fig. 5 show no variation of the permeability within the range 10 to 65 ppm of gold.

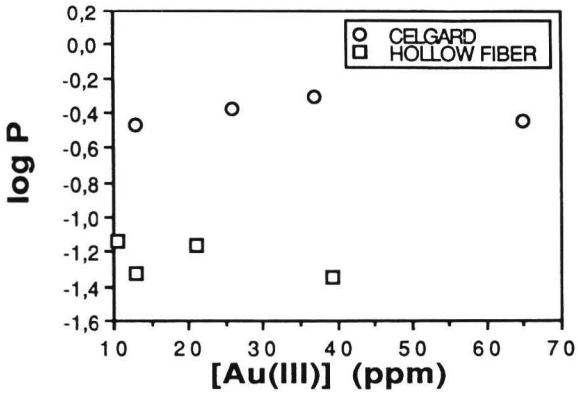

Fig. 5. Influence of feed gold concentration. [Cyanex 471] = 0.1 M.

Such behavior may indicates that Au(III) permeation is controlled by aqueous resistance (Danesi, 1984-85).

The gold permeability data have been analyzed by applying the model developed by Danesi (1984) and Muhammed et al. (1987) which assumes a linear difussion gradient and a fast interfacial extraction between the organic carrier and the aqueous extractable species. In this case the following theoretical expression for the permeability can be used:

$$P = \frac{K_d}{K_d \Delta_a + \Delta_o} \qquad (5)$$

where K_d is the distribution ratio of the permeating species at the feed side and Δ_a and Δ_o are diffusional resistences defined by : $\Delta_a = d_a / D_a$ (thickness of aqueous boundary diffusion layer / aqueous diffusion coefficient)

$\Delta_o = d_o / D_o$ (thickness of organic boundary diffusion layer / organic diffusion coeficient of the metal permeating species)

From the experimental data we observe that the variation of the chemical conditions do not influence the Au(III) permeation (Figs. 4 and 5). On the other hand, the distribution coefficient of Au(III), K_d, has been determined and found to have a very high value (10,000) in our experimental conditions. Under such conditions, eq. 5 becomes:

$$P = \frac{1}{\Delta_a} \qquad (6)$$

In our case, the transport of Au(III) is mainly dependent on Δ_a (thickness feed aqueous layer), and the type of solid supports and its geometries have a very low influence in the gold mass transfer. Table I contains the values of Δ_a calculated for the different supports used.

4 CONCLUSIONS

The results obtained from the different experiments show the mass transfer of gold (III) through the liquid membrane to proceed via a facilitated transport of the Au(III)-TIBPS extractted species. The independence of this process with the pH of aqueous feed verifies the solvating characteristics of the carrier.

From the speciation of the extraction system the species $AuCl_3$.2TIBPS may be the main responsible of the gold (III) transport.

On the other hand, under the hydrodynamic conditions studied, the aqueous resistance at the hollow fiber is found to be much higher than those obtained for the flat supports. This effect may be explained by the differences on the effectiveness of the agitation in the two configurations. It is also observed that the differences in pore size affects slightly to the mentioned resistance.

TABLE I. Obtained Δ_a values for the different supports.

	Thickness (μm)	Porosity (%)	Pore size (μm)	Δ_a (min.cm^{-1})
Millipore GVHP (Teflon)	125	75	0.2	4.8
Accurel (polypropilene)	48	50	0.1	2.6
Celgard 2500 (polypropilene)	25	45	0.04	3.0
Accurel R-52 OD/ID 1.2/1.8	600	75	0.1	18.1

Acknowledgements. Financial support was given by CICYT, MAT88-752.

5 REFERENCES

Danesi, P.R., 1984-85. Separation of metal species by supported liquid membranes. Sep. Sci. Tech., 19(11-12): 857-894.

Danesi, P.R., 1984. A simplified model for the coupled transport of metal ions through hollow-fiber supported liquid membrane. J. of Membrane Sci., 20: 231-248.

Izatt, R.M., Bruening, R.L. and Christensen, J.J., 1987. Liquid Membranes, Theory and Applications. A.C.S. Symp. Series 347. W.D.C.

Johnson, P.R., 1981. Gold and Silver leaching. Recovery and Economics. AIME.

Muhammed, M., Fernández, L. and Aparicio, J., 1987. The role of Feed Metal Concentration in the Coupled Transport of Zinc through a Bis-(2-ethylhexyl) phosphoric Acid Solid Supported Liquid Membrane from Aqueous Perchlorate Media. Sep. Sci. Tech. 22(6): 1577-1595.

Salvadó, V., Hidalgo, M., Masana, A., Muñoz, M., Valiente, M. and Muhammed, M.,1990. Extraction of Gold (III) from Hydrochloric Acid solutions by Triisobutyl Phosphine Sulfide in Toluene. Solv. Ext. and on Exch. 8(3) (in press).

Solvent Extraction 1990, T. Sekine (Editor)

© 1992 Elsevier Science Publishers B.V. All rights reserved

SEPARATION OF ALKALI METAL CATIONS BY POLYMER-SUPPORTED LIQUID MEMBRANES USING IONIZABLE CROWN ETHERS [1,2]

JERZY STRZELBICKI [3], BOZENA STRZELBICKA, ELZBIETA LUBBOCH, RICHARD A. BARTSCH
Department of Chemistry and Biochemistry, Texas Tech University
Lubbock, Texas 79 409-1061, USA

ABSTRACT

Strzelbicki, J., Strzelbicka, B., Lubboch, E. and Bartsch, R. A., 1990. Separation of alkali metal cations by polymer-supported liquid membranes using ionizable crown ethers. Proceedings of the International Solvent Extraction Conference 1990, Kyoto, Japan, July 16 - 21, 1990.

sym-(Decyl)dibenzo-16-crown-5-oxyacetic acid (**1**) and *sym*-(decyl)dibenzo-16-crown-5-oxymethylphosphoric acid monoethyl ester (**2**) were tested as ion carriers for selective transport of alkali metal cations through polymer-supported liquid membranes. Influence of an ionizable group, temperature, organic membrane solvent, and the pH of the aqueous source solution on metal cation permeation was investigated. It was found that sodium cation was selectively transported from the aqueous mixture of Li^+, Na^+, K^+ and Rb^+. Selectivity and rate of permeation were strongly influenced as well by the molecular structure of an ion carrier as by process variables. The highest selectivity was obtained with **1**. The permeation rate increased with increasing temperature and it was slower if n-octyl 2-nitrophenyl ether was used as solvent in the organic phase compared to n-pentyl 2-nitrophenyl ether. No remarkable influence of the pH of the source solution on Na^+ transport rate from basic solutions was found.

INTRODUCTION

Crown carboxylic acids with the dibenzo-16-crown-5 polyether ring generally exhibit selective complexation of Na^+ over other alkali metal cations (Strzelbicki and Bartsch, 1981a,b, 1982, Strzelbicki et al., 1982, Charewicz et al., 1982, Bartsch et al., 1984). It has been found that *sym*-(octyl)dibenzo-16-crown-5-oxyacetic acid is much more selective than its structural isomers 2-[(*sym*-dibenzo-16-crown-5)oxy]decanoic acid and *sym*-bis[4(5)*tert*-butylbenzo]16-crown-5-oxyacetic acid in separation of alkali metal cations by liquid-liquid extraction and by transport through liquid membranes (Strzelbicki and Bartsch, 1981b, Charewicz et al., 1982, Bartsch et al., 1984). With high selectivity, *sym*-(decyl)dibenzo-16-crown-5-oxyacetic acid (**1**) has been used to separate Na^+ from aqueous alkali metal chloride mixtures by transport through polymer supported liquid membranes (PSLM) (Brown et al.,

[1] This paper was presented at the ISEC'90 by Prof. Dr. Karl Schügerl of the Institute of Technical Chemistry, University of Hannover (West Germany). *[2] This research was supported by the Division of Chemical Sciences of the Office of Basic Energy Sciences of the U. S. Department of Energy.* *[3] The paper was written during the stay of J.S. in the Institute of Technical Chemistry, University of Hannover as the Alexander von Humboldt Foundation Fellow.*

1990). In this technique, porous polypropylene loaded with an organic solution of an ion carrier separates two aqueous solutions. Selective metal ion transport from the aqueous source phase into the aqueous receiving phase may be achieved if the ion carrier in the membrane exhibits different affinities toward the source phase cations. In this paper influence of the type of an ionizable group, the pH of the source solution, temperature and the organic solvent in the membrane solution on cation transport through PSLM employing two ionizable crown ethers **1** and **2** are presented.

2 EXPERIMENTAL

2.1 Procedure and apparatus

The cell used for the transport experiments is shown in Fig. 1. The cell was constructed from two glass O-ring joints. The membrane was placed between the half-cells and clamped. The membrane was sealed by contact with the ridges of the O-ring joints. The average area of the membrane in contact with the aqueous solutions was 5.62 cm^2. The receiving phase (40 ml) was a 1.0 M aqueous solution of HCl and the source phase (40 ml) was an aqueous solution of LiCl, Na^+, KCl and RbCl (200 mM each). The pH of the source phase was stabilized using Na_2HPO_4 and HCl (in the pH range 2.0 to 8.0), and Na_2CO_3 and HCl (in the pH range 9.0 to 11.2) or NaOH (for pH 12.4). The initial pH of the source phase decreased very slightly by the end of transport experiment (by no more than 0.05 pH units).

Although both the aqueous source and receiving phases were stirred at 400 rpm (with Model CA constant speed motors from Hurst Industries; Princeton, Indiana), it was found that stirring of the aqueous phases had no influence on the cation transport process. The membrane was prepared by soaking a disc of the porous polypropylene sheet in the crown carboxylic acid solution. The excess of the solution was wiped off with a tissue. All experiments were conducted in triplicate. Cells were immersed in a thermostated bath and operated over a period of 4 days. Samples were taken from the receiving phase approximately every 24 hours and the alkali metal cation concentrations were determined by ion chromatography (a Dionex Model 10 ion chromatograph). From the set of three experiments, an average was calculated. Reproducibility was usually within ±20 % (standard deviation). After completion of the experiment, the final pH of the source phase was measured using a Fisher Scientific Accumet Model 825 MP pH meter with a Corning X-EL glass body combination electrode. Control experiments was also carried out in which porous polypropylene discs were soaked with solvent only.

2.2 Reagents

Synthetic route to *sym*-(decyl)dibenzo-16-crown-5-oxyacetic acid (**1**) and *sym*-(decyl)dibenzo-16-crown-5-oxymethylphosphoric acid monoethyl ester (**2**) will be published (Brown et al., 1990 and Strzelbicki et al., 1990, respectively). Pentyl 2-nitrophenyl ether was prepared from pentyl bromide by a reported synthetic method (Organic Syntheses, 1949) Sources of other chemicals include: Aldrich (Milwaukee, Wisconsin): RbCl; Fisher (Fair Lawn, New Jersey): KCl, KOH, NaCl, NaOH, Na_2CO_3, Na_2HPO_4 and HCl; Fluka

(Ronkonkoma, New York): 2-nitrophenyl octyl ether; MCB (Norwood, Ohio): LiCl. Porous polypropylene Accurel^R 0.2 was obtained from Enka AG (Wuppertal, West Germany).

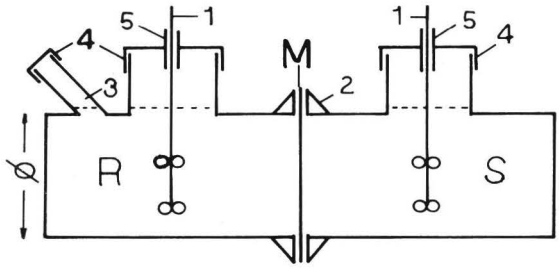

Fig. 1. Experimental cell for polymer-supported liquid membrane transport measurements (R - receiving solution, S - source solution, M - supported membrane, 1 - glass stirrer, 2 - O-ring joint, 3 - glass tube for samples collecting, 4 - rubber cap, 5 - glass tube).

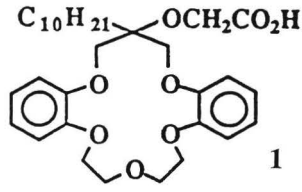

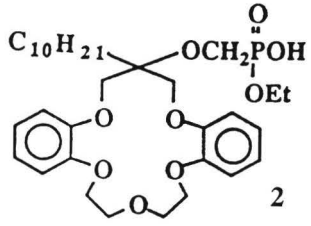

3 RESULTS AND DISCUSSION

3.1 Transport through PSLM at various pH of the source solution

Results of experiments for alkali metal cation separation from source solutions of the various pH by means of the PSLM employing **1** and **2** are presented in Figs. 2 and 3, respectively. For both ion carriers, permeation of Na^+ from acidic source solutions increased with the decreasing acidity. In the pH range close to the neutral solutions, the Na flux reached the plateau region in which it remained virtually constant in spite of the increasing pH. For **2**, the beginning of the plateau region of the curve illustrating the dependence between the Na flux and the source solution pH was shifted towards more acidic solutions by about 1.5 pH units compared with **1**. This shift can be of remarkable importance in practical applications since the PSLM involving **2** can be efficiently used for alkali metal separation from neutral solutions.

Selectivity of AMC separation using **1** was much higher compared to **2**. **1** did not transport Rb^+ or Li^+. Also, no K^+ was transported by **1** at pH lower than 8. Above this pH value, Na/K concentration ratio in the receiving solution was 50 ± 10.

2 transported K^+ in the full investigated range of the pH 2 to 12.4. Initially, Na/K concentration ratio in the receiving solution increased with the increasing pH of the source solution but in the pH range 6 to 12.4 this ratio was practically constant at about 28. The best separation selectivity of Na^+ from Li^+ was achieved at pH 8.9 ([Na]/[Li] in the receiving solution of 220). For lower values of the pH, Na/Li concentration ratio decreased to 111 and for the higher pH values this ratio decreased as well (to 173).

Thus, the ionizable group of a crown ether functioned not only as the source of protons exchangeable to alkali metal cations to provide electroneutrality of complexes transported

through the organic membrane. This group influenced also remarkably properties of those complexes and thus changed the course of the PSLM process and its selectivity.

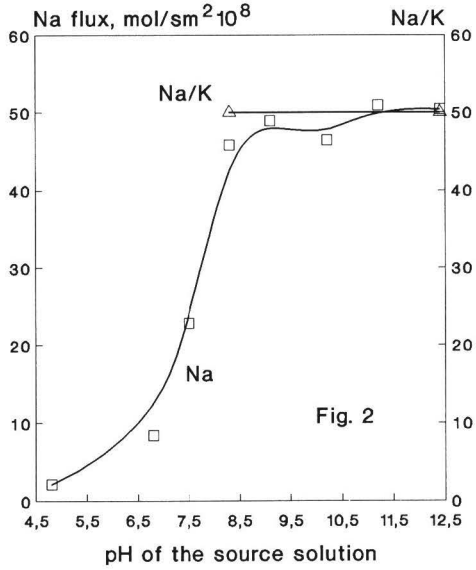

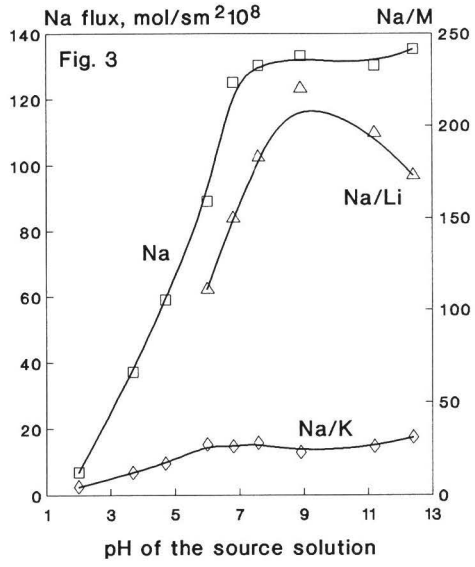

Fig. 2. Flux of Na^+ (left Y-axis) and Na/K concentration ratio in the receiving solution (right Y-axis) vs the pH of the source solution in separation of alkali metal cations by polymer-supported liquid membranes containing 4.4 mM **1** in n-pentyl 2-nitrophenyl ether (source solution: 200 mM Li^+, Na^+, K^+ and Rb^+ (each); receiving solution: 1.0 M aqueous HCl).

Fig. 3. Flux of Na^+ (left Y-axis) and concentration ratio of Na^+ vs other alkali metal cation in the receiving solution (Na/M on the right Y-axis) at various pH of the source solution in separation of alkali metal cations by polymer-supported liquid membranes containing 10 mM **2** in n-pentyl 2-nitrophenyl ether (for source and receiving solutions see Fig. 2).

3.2 Influence of the organic solvent

Series of experiments were done with the PSLM containing **2** dissolved in n-pentyl 2-nitrophenyl ether (PNPE) or n-octyl 2-nitrophenyl ether (ONPE) (Figs. 3 and 4, respectively). These organic solvents were chosen for the membrane solution since they provided a longtime stability of the membrane. That was not the case when other organic solvents of higher volatility or higher water solubility were used.

The shape of the curve illustrating the Na flux vs. the pH of the source solution was for both PNPE and ONPE similar though in the system with ONPE the beginning of the plateau region of the curve was shifted toward more acidic solutions by about 1 pH unit. The Na flux through the membrane containing ONPE was approximately 2.4-fold lower compared to the system with NPNE if the plateau region is concerned. The decrease of the Na flux resulted most probably from higher viscosity of ONPE (Brown et al., 1990).

Remarkable differences were also found in the selectivity of alkali metal cation separation by the PSLM with both solvents. Selectivity of the process with ONPE was

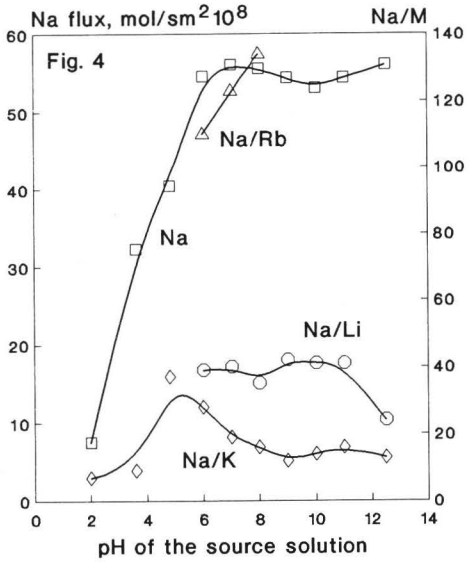

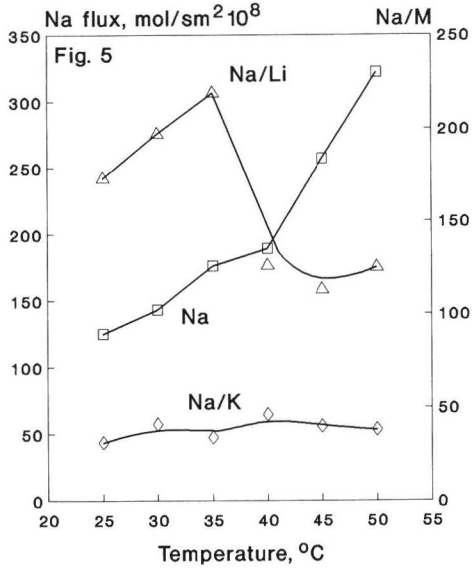

Fig. 4. Flux of Na^+ (left Y-axis) and concentration ratio of Na^+ vs other alkali metal cation in the receiving solution (Na/M on the right Y-axis) at various pH of the source solution in separation of alkali metal cations by polymer-supported liquid membranes containing 10 mM **2** in n-octyl 2-nitrophenyl ether (for source and receiving solutions see Fig. 2).

Fig. 5. Flux of Na^+ (left Y-axis) and concentration ratio of Na^+ vs other alkali metal cation in the receiving solution (Na/M on the right Y-axis) at various temperatures in separation of alkali metal cations by polymer-supported liquid membranes containing 10 mM **2** in n-pentyl 2-nitrophenyl ether (for source and receiving solutions see Fig. 2).

apparently worse than in case of PNPE. Rb^+ was transported through the membrane containing ONPE in the pH range 6.0 to 8.0 (Na/Rb concentration ratio in the receiving solution of 110 to 134) and the selectivity of Na/Li separation was clearly worse (Na/Li concentration ratio in the receiving solution of 35 to 42 in the pH range 6.0 to 11). Also, Na/K separation was worse and the curve illustrating the dependence between Na/K concentration ratio in the receiving solution vs. the pH of the source solution were differently shaped for ONPE and PNPE.

The differences in the course of alkali metal cations separation by the PSLM containing ONPE and PNPE are striking taking into account relatively small difference in the molecular structure of these two solvents (alkyl chain of PNPE is shorter by 3 $-CH_2-$ units). Though, the resulting change of the solvent properties (in the first place surface activity and viscosity) influenced remarkably the permeation.

3.3 Separation by PSLM at various temperature

The temperature effect was studied over the temperature range 25 to 50 °C for the PSLM containing **2** and PNPE (Fig. 5). There are two sections on the curve illustrating the Na flux as a function of the temperature. First, the Na flux increased relatively slowly (1.25 to

$1.89 \cdot 10^{-6}$ mol/sm^2) when temperature increased from 25 to 40 °C. Further temperature increase to 50 °C brought a sharp increase of the Na flux from 1.89 to $3.22 \cdot 10^{-6}$ mol/sm^2. Currently, no clear explanation can be provided for this phenomenon. It might result from the jumping change in the organic solvent properties, structural changes of the porous polypropylene or change in the chemical reaction mechanism.

Na/Li separation selectivity changed remarkably with temperature as well. For the temperature increase from 25 to 35 °C, Na/Li concentration ratio in the receiving solution increased from 173 to 219. Further temperature increase to 40 °C caused the decrease of this concentration ratio to 126 and this ratio remained virtually stable in spite of the following temperature increase to 50 °C. The change of the Na/Li concentration ratio in the receiving solution with the temperature suggested that Na-**2** and Li-**2** complexes were formed in chemical reactions of different type which responded differently to the change of physical parameters.

In contrast to Na/Li separation, separation of Na from K was very similar in the investigated temperature range 25 to 50 °C and the Na/K concentration ratio in the receiving solution was 38±5.

4 CONCLUSIONS

The results which are recorded and discussed above establish that structural changes within the organic phase complexing agents and the type of solvent used may produce significant variations in the selectivity and efficiency of competitive alkali metal cation transport across polymer-supported liquid membranes. The other process variables like the pH of the source solution and temperature influence this separation process as well.

5 REFERENCES

Bartsch, R. A., Charewicz, W. A. and Kang, S. I., 1984. Separation of metals by liquid surfactant membranes containing crown ether carboxylic acids. J. Membrane Sci., 17: 97-107.

Brown, P. R., Pugia, M. J., Hallman, J. L., Whaley, L. X., Desai, D. K. and Bartsch, R. A., 1990. J. Membrane Sci., in preparation.

Charewicz, W. A., Heo, G. S. and Bartsch, R. A., 1982. Comparison of highly lipophilic crown ether carboxylic acids for transport of alkali metal cations from aqueous solutions into chloroform. Anal. Chem., 54: 2094-2097.

Organic Syntheses, Collective Volume 3, 1946. Willey, New York, 2nd Edition, pp 140-141.

Strzelbicki, J. and Bartsch, R. A., 1981. Extraction of alkali metal cations from aqueous solutions by a crown ether carboxylic acid. Anal. Chem., 53: 1894-1899.

Strzelbicki, J. and Bartsch, R. A., 1981. Solvent extraction of alkali metal cations from aqueous solutions by highly lipophilic crown ether carboxylic acids. Anal. Chem., 53: 2251-2253.

Strzelbicki, J. and Bartsch, R. A., 1982. Transport of alkali metal cations across liquid membranes by crown ether carboxylic acids. J. Membrane Sci., 10: 35-47.

Strzelbicki, J., Heo, G. S. and Bartsch, R. A., 1982. Solvent extraction of alkali metal cations from aqueous solutions by crown ether carboxylic acids. Sep. Sci. Techn., 17: 635-643.

Strzelbicki, J., Strzelbicka, B., Lubboch, E. and Bartsch, R. A., 1990. Comparison of *sym*-(decyl)dibenzo-16-crown-5-oxyacetic acid and *sym*-(decyl)dibenzo-16-crown-5-oxymethylphosphoric acid monoethyl ester as alkali metal cation carriers in transport across polymer-supported liquid membranes. Influence of ionizable group, temperature, organic membrane solvent, and pH of the source phase. Anal. Chem., in preparation.

Solvent Extraction 1990, T. Sekine (Editor)

© 1992 Elsevier Science Publishers B.V. All rights reserved

CROWN ETHERS IN SEPARATION OF ALKALI METAL CATIONS[1]

JERZY STRZELBICKI[2,3], BOZENA STRZELBICKA[3], KARL SCHÜGERL[2] and RICHARD A. BARTSCH[3]

[2] Institute of Technical Chemistry, University of Hannover, Callinstraße 3, D-3000 Hannover 1, West Germany

[3] Department of Chemistry and Biochemistry, Texas Tech University, Lubbock, TX 79409-1061, USA

ABSTRACT

Strzelbicki, J., Strzelbicka, B., Schügerl, K. and Bartsch, R. A., 1990. Crown ethers in separation of alkali metal cations. Proceedings of the International Solvent Extraction Conference 1990, Kyoto, Japan, July 16 - 21, 1990.

Results are presented on separation of alkali metal cations (AMC) using a proton-ionizable and a neutral crown ether. *sym*-(Decyl)dibenzo-16-crown-5-oxyacetic acid was used as a selective ion-carrier in separation of Na^+ from a mixture of Li^+, Na^+, K^+ and Rb^+ by means of hollow fiber supported liquid membranes. Selectivity of the permeation was very high. No Rb^+ was transported in the system and Na/Li and Na/K selectivity coefficients reached 80 and 42, respectively. Expensive and/or commercially unavailable compounds involved and complicated operation were disadvantages of this process. In separation of AMC by liquid-liquid extraction, mixtures of dicyclohexano-18-crown-6 with di(2-ethylhexyl)phosphoric acid or with di(2-ethylhexyl)monothiophosphoric acid were used for complexation of AMC and their transfer into an organic phase. Selectivity of one stage liquid-liquid extraction was lower compared to liquid supported membrane process. On the other hand, reagents used in solvent extraction are commercially available, relatively inexpensive and the process is simple to perform.

INTRODUCTION

One of the possible use of crown ethers is separation of alkali metal cations. Specific complexation of a metal cation by a crown ether involving both geometrical adjustment and binding of a metal cation by donor atoms of a crown ether cavity makes it possible to separate metal cations of similar physico-chemical properties which differ with an ion diameter. A complex of a neutral crown ether with a metal cation exhibits usually high lipophilicity but its transfer into a low polar organic phase involves also transfer of a counter-ion (usually a "hard" inorganic anion like Cl^-, NO_3^- or SO_4^{2-}) and thus the maximal organic phase concentration of a metal is often too low for many practical applications.

To increase a metal concentration in an organic phase containing a neutral crown

[1] *This research was supported by the Division of Chemical Sciences of the Office of Basic Energy Sciences of the U. S. Department of Energy (for J.S., B.S. and R.A.B.) and by the Alexander von Humboldt Foundation (West Germany) (fellowship for J.S.).*

ether, a lipophilic organic acid can be added to this phase. The acid can exchange the proton for a metal cation and an electroneutral and lipophilic metal cation-neutral crown ether-deprotonized organic acid complex can be concentrated in the organic phase to high degree. Disadvantage of this method is relatively high solubility of an organic acid in the low acidic, neutral and basic aqueous solutions and thus loss of an extractant and contamination of the aqueous phase. Similarly, a neutral crown ether of low lipophilicity can be lost from the organic phase. Also, not all mixtures of a neutral crown ether and an organic acid can effectively complex a metal cation. Most often, laborious and time consuming investigation has to be carried out in order to find suitable composition of an extractants mixture.

A high metal concentration in a low polar organic phase can be achieved in the presence of a proton-ionizable crown ether, as well. The crown ether molecule incorporates a cavity and a pendant ionizable group which after deprotonization can provide electroneutrality of a complex with a metal cation. Properties of a proton-ionizable crown ether are most often very different compared to properties of a mixture of the corresponding neutral crown ether and organic acid.

Crown ethers have found application in separation techniques like solvent extraction and liquid membranes. In this paper results of two different applications of crown ethers for alkali metal separation are presented. First, *sym*-(decyl)dibenzo-16-crown-5-oxyacetic acid (**1**) was used as the Na^+ carrier in separation of AMC by hollow fiber supported liquid membranes. Secondly, mixture of dicyclohexano-18-crown-6 (DC18C6) with di(2-ethylhexyl)phosphoric acid (DEHPA) or with di(2-ethylhexyl)monothiophosphoric acid (MTDEHPA) were used for separation of alkali metal cations by liquid-liquid extraction.

2 EXPERIMENTAL

2.1 Procedure for separation using a hollow fiber module

Experiments were carried out using an Enka Lab Module type MD 020 CP2N (Enka AG, Wuppertal, West Germany) containing 40 hollow fibers (~1.5 mm of internal diameter, 50 cm of active length, ~0.5 mm of wall thickness, 1000 cm^2 of a total area). The porous fibers were loaded with a 10 mM solution of **1** in 2-nitrophenyl octyl ether and they were a supported liquid membrane between a receiving solution (flowing inside fibers) and a source solution (flowing outside fibers) (see Izatt et al., 1989 for an outline of a module).

The receiving solution (100 ml) was a double-distilled water and its pH was regulated using a 5 M aqueous hydrochloric acid. A source phase (130 ml) was an aqueous solution of 200 mM LiCl, NaCl, KCl and RbCl (each) and its pH was kept constant by addition of a 2.8 M aqueous tetramethylammonium hydroxide.

The source and the receiving solutions flowed counter-currently. Both solutions were pumped using peristaltic pumps (Barnant Co., Barrington, IL) with Barnant pump heads (Models 7016-00 and 7018-00). The pH regulating solutions were added using Sage Instrument Model 341A syringe pumps coupled with Suntex (Taiwan) digital pH controllers (Model PC-305).

The separation process was carried out for 4 days and samples were periodically (at least every 24 hr) withdrawn from the receiving solution to determine alkali metal concentration using an ion chromatograph (Dionex Model 10).

2.2 Procedure for solvent extraction

In the extraction experiments, an organic phase (5 ml) and an aqueous phase (5 ml) were shaken vigorously in separatory funnels for 5 min. The aqueous phase contained 3.25 mM (each) K^+, Rb^+ and Cs^+ (as sulphates) and Na_2SO_4 (the Na^+ concentration varied in the range 32.5 to 200 mM). Solutions of 1.0 M NH_4OH and 0.5 M H_2SO_4 were used for pH regulation. The organic phase was a cyclohexane solution of 70 mM DC18C6 and 100 mM DEHPA or MTDEHPA.

After shaking was stopped, the phases were separated and the equilibrium pH of the aqueous phase was measured. Concentration of alkali metals in the aqueous phase was determined using a Perkin-Elmer atomic absorption spectrophotometer Model 373 (flame emission and/or absorption) and thereafter a metal concentration in the organic phase was calculated. In many cases (particularly at the high Na_2SO_4 concentration), a metal concentration was determined as well in the aqueous phase after extraction as in the aqueous phase after stripping (using equal volume of an aqueous 1.0 M NH_4OH). In some systems different results were obtained for the Cs concentration in those two determinations and the concentration in the aqueous phase after extraction was higher compared to the concentration in the stripping solution. It indicated that stripping of Cs was slower than its extraction or a 1.0 M ammonium hydroxide was not enough strong stripping agent.

2.3 Reagents

Synthesic route to *sym*-(decyl)dibenzo-16-crown-5-oxyacetic acid (**1**) will be published (Brown et al., 1990). Sources of other chemicals include: Aldrich: RbCl, Cs_2SO_4 and dicyclohexano-18-crown-6; Baker (Phillipsburg, New Jersey): $MgCl_2$; Bayer AG (Leverkusen, West Germany): H_2SO_4; Fisher (Fair Lawn, New Jersey): KCl, NaCl and HCl; Fluka: 2-nitrophenyl octyl ether and Rb_2SO_4; Hoechst AG (West Germany): Hostarex PA 216 (di(2-ethylhexyl)phosphoric acid) and Hoe F 3787 (di(2-ethylhexyl)monothio-phosphoric acid); MCB (Norwood, Ohio): LiCl and $CaCl_2$; Riedel de-Haen (Seelze, West Germany): Na_2SO_4, NH_4OH and cyclohexane; Southwestern Analytical Chemicals (Austin, Texas): tetramethylammonium hydroxide.

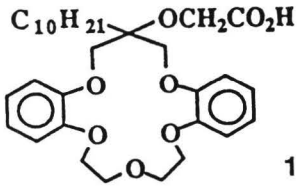

1

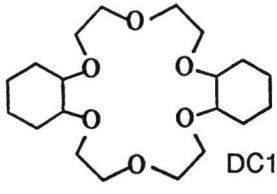

DC18C6

3 RESULTS AND DISCUSSION

3.1 Separation using hollow fibers

Two series of experiments were undertaken using the hollow fiber module. Results are presented in Table 1 and 2 as the Na flux and selectivity coefficients (given as [Na]/[M] concentration ratio in the receiving solution) vs. the pH of the receiving solution (Table 1) or the source solution (Table 2).

First, the pH of the receiving phase was changed in the range 0 to 5 while pH of the source phase was constant (pH 10) (Table 1). No remarkable influence of the pH in the range 0 to 4 on the sodium flux was found. The pH change influenced only the selectivity of permeation. The best selectivity was achieved at pH 1 ([Na]/[Li] and [Na]/[K] concentration ratios in the receiving solution was 63 and 32, respectively). At pH 5, Na flux decreased sharply, most probably due to insufficient or too slow decomplexation of the Na-**1** complex. Also selectivity of permeation at that pH value was worse than at lower values of the pH.

The second series of experiments was carried out at constant pH of the receiving solution (pH 1) while the source solution pH was changed in the range 8 to 12 (Table 2). In that case no remarkable influence of the pH change on the Na flux was found in the broad pH range 9 to 12. The highest Na flux was found at pH 11 ($2.7 \cdot 10^{-7}$ mol/m^{2}s) and the best selectivity at pH 9 ([Na]/[Li]=80, [Na]/[K]=42). At pH 8, however, Na flux decreased sharply most probably due to insufficient and/or too slow formation of the Na-**1** complex.

The experiment was also performed with the source solution (pH 9) containing $CaCl_2$ and $MgCl_2$ (at concentration of 100 mM each) in addition to alkali metal chlorides. pH of the receiving solution was kept constant at 1. Selectivity of separation of Na^+ from Li^+ and K^+ was worse than from the source solutions containing only alkali metal chlorides, but still the Na concentration in the receiving solution was 35 and 21-fold higher than Li and K concentration, and 541 and 88-fold higher than Mg and Ca concentration, respectively.

TABLE 1
Separation of AMC from the source solution of pH 10 using the hollow fiber module.

Receiv. phase pH	Na flux mol/m^{2}s 10^8	[Na]/[Li]	[Na]/[K]
0	23	27	23
1	24	63	32
2	22	49	25
3	22	44	28
4	20	25	25
5	0.85	14	19

TABLE 2
Permeation of AMC into the receiving solution of pH 1 using the hollow fiber module.

Source phase pH	Na flux mol/m^{2}s 10^8	[Na]/[Li]	[Na]/[K]
8	0.79	24	22
9	20	80	42
10	24	63	32
11	27	58	35
12	26	44	25

3.2 Separation by liquid-liquid extraction

For the Na^+ concentration of 32.5 and 130 mM (i.e., 16.25 and 65 mM Na_2SO_4) in the initial aqueous phase, a white suspension appeared in that phase in a broad range of the pH

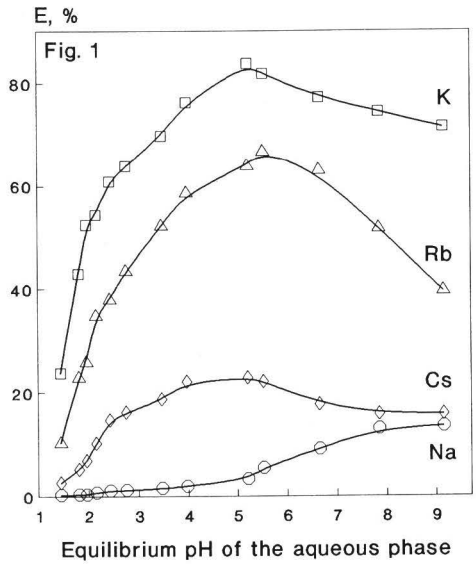

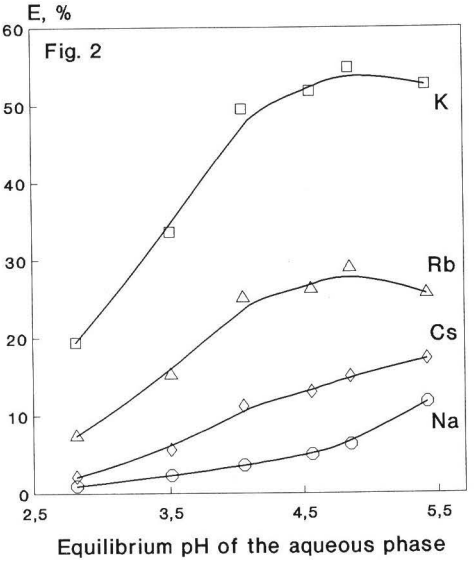

Fig.1. Percentage of metal extracted (E,%) from an aqueous 3.25 mM K^+, Rb^+ and Cs^+ and 200 mM Na^+ into a cyclohexane 70 mM DC18C6 and 100 mM MTDEHPA vs. the equilibrium pH of the aqueous phase.

Fig.2. Percentage of metal extracted (E,%) from an aqueous 3.25 mM K^+, Rb^+ and Cs^+ and 200 mM Na^+ into a cyclohexane 70 mM DC18C6 and 100 mM DEHPA vs. the equilibrium pH of the aqueous phase.

and it was stable within long time (sometimes more than one day). Most probably, the suspension was formed by DEHPA and MTDEHPA which at a low total concentration of inorganic salts are well soluble in aqueous solutions (in particular in basic and neutral ones) and at the concentration exceeding their CMC they can form a colloidal suspension.

With a 100 mM sodium sulphate, separation of phases was good and fast (<1.5 min) and therefore those systems could be suitable for practical applications. Good and fast phase separation was obviously connected with the increase of the total inorganic salt concentration in the aqueous phase and the "salting-out" effect (Ritcey and Ashbrook, 1984).

Percentage of extraction of AMC from the aqueous solution containing 3.25 mM K^+, Rb^+ and Cs^+ (as sulphates) and 200 mM Na^+ (as Na_2SO_4) into a 70 mM DC18C6 and 100 mM DEHPA or MTDEHPA are illustrated in Figs.1 and 2. Taking into account the cavity diameter of DC18C6 of 2.8-3.2 Å (estimated basing on examination of a Corey-Pauling-Kortun space-filling model) and ionic diameters of Na^+, K^+, Rb^+ and Cs^+ of 1.96, 2.66, 2.98 and 3.30 Å, respectively (Morf et al., 1979), K^+ should form the most stable complex with DC18C6. Indeed, K^+ was always extracted the most efficiently (Figs. 1 and 2). Rb^+ was the second one in the selectivity order. Extractabilities obtained for a mixture of DC18C6

with MTDEHPA (Fig.1) showed this mixture as apparently better extractant agent toward K^+ and Rb^+ compared with the DC18C6/DEHPA mixture. Maximal extractability of K^+ increased from 55 % for the extraction system with DEHPA (Fig. 2) to 81 % for MTDEHPA (Fig. 1). The respective increase of the Rb^+ extractability was 29 to 63 %. Thus, organic acids, namely DEHPA and MTDEHPA, functioned in the extraction system not only as a source of protons which could be exchanged by alkali metal cations but they influenced remarkably properties of a complex transferred into the organic phase.

Results achieved for the DC18C6/MTDEHPA mixture are comparable or surpassed results obtained for some ionizable crown ethers (Strzelbicki and Bartsch, 1981a,b, Strzelbicki et al., 1982) which were designed and synthesized for separation of alkali metal cations. The important advantage of DC18C6, DEHPA and MTDEHPA is their commercial availability.

4 CONCLUSIONS

The liquid supported membranes containing the proton-ionizable crown ether was found as highly selective technique for separation of Na^+ from a mixture of alkali metal ions. However, it seems the process can find, at present, only limited practical applications in very special cases. Nevertheless, the liquid supported membranes can be broadly applied in the future since demand for new and more efficient technologies grows in spite that they usually are more and more complicated.

Liquid-liquid extraction process for separation of alkali metal cations by the neutral crown ether and the organic acid is a simple technique and can be readily adopted for industry though its selectivity is lower than in case of liquid membranes. Selectivity of extraction may be improved in a multistage process as well as by use of other (e.g., more lipophilic) extractants.

5 REFERENCES

Brown, P. R., Pugia, M. J., Hallman, J. L., Whaley, L. X., Desai, D. K. and Bartsch, R. A., 1990. J. Membrane Sci., in preparation.

Izatt, R. M., Roper, D. K., Bruening, R. L. and Lamb, J. D., 1989. Macrocycle-mediated cation transport using hollow fiber supported liquid membranes. J. Membrane Sci., 45: 73-84.

Morf, W. E., Ammann, D., Bissig, R., Pretsch, E. and Simon, W., 1979. Cation selectivity of neutral macrocyclic and nonmacrocyclic complexing agents in membranes. In: R. M. Izatt and J. J. Christensen (Editors), Progress in Macrocyclic Chemistry. Willey-Interscience, New York , Vol. 1, p. 9.

Ritcey, G. M. and Ashbrook, A. W., 1984. Solvent Extraction. Principles and Applications to Process Metallurgy. Elsevier, Amsterdam , Part I, p. 237.

Strzelbicki, J. and Bartsch, R. A., 1981. Extraction of alkali metal cations from aqueous solutions by a crown ether carboxylic acid. Anal. Chem., 53: 1894-1899.

Strzelbicki, J. and Bartsch, R. A., 1981. Solvent extraction of alkali metal cations from aqueous solutions by highly lipophilic crown ether carboxylic acids. Anal. Chem., 53: 2251-2253.

Strzelbicki, J., Heo, G. S. and Bartsch, R. A., 1982. Solvent extraction of alkali metal cations from aqueous solutions by crown ether carboxylic acids. Sep. Sci. Techn., 17: 635-643.

Solvent Extraction 1990, T. Sekine (Editor)

© 1992 Elsevier Science Publishers B.V. All rights reserved

SEPARATION OF COBALT AND NICKEL IONS WITH 2-ETHYLHEXYL PHOSPHONIC ACID MONO-2-ETHYLHEXYL ESTER DISSOLVED IN KEROSENE

TING-CHIA HUANG and TEH-HUA TSAI
Department of Chemical Engineering, National Cheng Kung University, Tainan, Taiwan 70101, R.O.C.

ABSTRACT

The extraction equilibria of cobalt and nickel ions between lithium nitrate solution and 2-ethylhexyl phosphonic acid mono-2-ethylhexyl ester (HEHEHP) dissolved in kerosene are studied at 25.0±0.1°C. The experimental results indicated that the distribution ratio of each metal is increased with increasing the HEHEHP concentration in the organic phase as well as the pH value of aqueous solution. However, the distribution ratio is independent of the metal ions concentration at constant pH value and HEHEHP concentration. The equilibrium constants of cobalt and nickel are found to be 5.76×10^{-6} and 5.66×10^{-7} $m^3/kmol$, respectively.

Polyvinylidene difluoride membrane impregnated with HEHEHP in kerosene solution as the supported liquid membrane, have been used for the investigations of the permeation and separation of cobalt and nickel ions, from lithium nitrate solution to nitric acid solution through the supported liquid membranes. The permeabilities of metal ions are found to be dependent on the stirring rate, pH value of feed solutions, and carrier concentration in supported liquid membrane.

The experimental data also show that the separation factor increases with increasing the stirring rate and pH value of feed solution. However, the separation factor decreases with the concentration of HEHEHP in the organic phase.

1 INTRODUCTION

The separation of cobalt and nickel ions from aqueous solution is rather difficult due to their similar chemical nature. The 2-ethylhexyl phosphonic acid mono-2-ethylhexyl ester (PC-88A, abbreviated as HEHEHP or simply HA), has been found to be with a greater selectivity for cobalt over nickel than the well known extractant HDEHP for cobalt-nickel separation (Ritcey, et al., 1975; Preston, 1982; Dreisinger and Cooper, 1984; Matsuyama et al., 1987).

In this work, a systematical studies of the extraction equilibrium of cobalt and nickel with HEHEHP are undertaken. Then, the permeations of cobalt and nickel through supported liquid membrane containing HEHEHP as carrier are studied. Finally, the separation factors of cobalt and nickel in this system are obtained.

2 EXPERIMENTAL

2.1 Reagents and Membranes

HEHEHP used in this work was the product of Daihachi Chemical Ind. Co., Ltd., Osaka, Japan. The other chemicals were analytical pure reagent grade.

The porous membrane used was Durapore membrane made of polyvinylidene difluoride (PVDF), the product of Millipore Co., U.S.A. It is hydrophobic with a mean pore size of 0.45μm, a typical porosity of 70%, and a nominal mean thickness of 125μm.

2.2 Determination of equilibrium distribution ratio

The distribution ratios of metal ions between the organic phase and the aqueous phase, D_M, were measured at 25.0±0.1°C by the procedures described in our previous paper (Huang and Tsai, 1989a).

2.3 Measurement of permeation rates

The permeation rates of metal ions through SLM were performed at 25.0±0.1°C following the procedures described in our previous paper (Huang and Tsai, 1989b).

3 RESULTS AND DISCUSSION

3.1 Liquid-liquid Extraction

Assuming that cobalt and nickel cations are extracted as an m-merized complex into the slightly loaded organic phase, the extraction of Co(II) and Ni(II) with HEHEHP can be represented by the following general equations:

$$m\ M^{2+} + m(n+1)\ \overline{H_2A_2} \rightleftharpoons \overline{(MA_2 \cdot n(HA)_2)_m} + 2m\ H^+ \quad (1)$$

$$K_{ex} = [\overline{(MA_2 \cdot n(HA)_2)_m}]\ [H^+]^{2m} / [M^{2+}]^m / [\overline{H_2A_2}]^{m(n+1)} \quad (2)$$

where K_{ex} is stoichiometric equilibrium constant, M is cobalt or nickel, H_2A_2 is dimeric form of HEHEHP and the bar indicates the species in the organic phase.

The distribution ratio of cobalt or nickel is given by

$$D_M = [\overline{M(II)}] / [M(II)] = m\ [\overline{(MA_2 \cdot n(HA)_2)_m}] / [M^{2+}] \quad (3)$$

Combining eqns. (2) and (3), we can obtain the concentration of metal-HEHEHP complex in the organic phase as

$$[\overline{M(II)}] = m\ K_{ex}\ [M^{2+}]^m\ [\overline{H_2A_2}]^{m(n+1)} / [H^+]^{2m} \quad (4)$$

In eqn. (4), $[\overline{H_2A_2}]^{m(n+1)}$ is approximately kept constant at constant concentrations of HEHEHP and low distribution ratios. Thus, the slope of the plot of $\log [\overline{M(II)}]$ vs. $\log [M^{2+}][H^+]^{-2}$ gives the degree of aggregation of the metal-HEHEHP complex in the organic phase, m.

The experimental results are plotted in Fig. 1 for 0.005 kmol/m^3 $[\overline{H_2A_2}]$ and 1.0 kmol/m^3 (Li,H)NO_3 at 25°C. Figure 1 indicates linear relationship with unit slopes (m = 1) for both cobalt and nickel ions. Thus, eqn. (4) can be simplified to

$$D_M\ [H^+]^2 = K_{ex}\ [\overline{H_2A_2}]^{n+1} \quad (5)$$

Then, a plot of $\log D_M[H^+]^2$ vs. $\log [\overline{H_2A_2}]$ gives a straight line with a slope of n+1. The results are shown in Fig. 2 for various HEHEHP concentrations and 1.0 kmol/m^3 (Li,H)NO_3 at 25°C. For cobalt, a straight line of slope 1.99 is obtained, i.e. n=1, indicating that the complex is $\overline{CoA_2 \cdot (HA)_2}$. For nickel, a straight line of slope 2.79 is obtained, i.e. n=2, indicating that the complex is $\overline{NiA_2 \cdot 2(HA)_2}$.

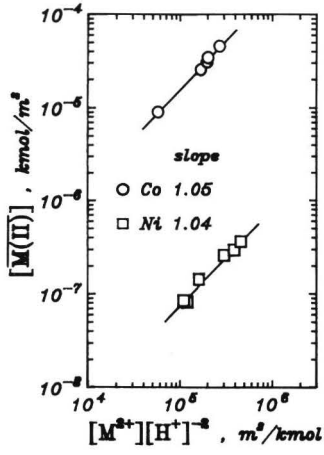

Fig. 1. Plots of log $[\overline{M(II)}]$ vs. log $[M^{2+}][H^+]^{-2}$ at equilibrium for cobalt and nickel at 25°C.

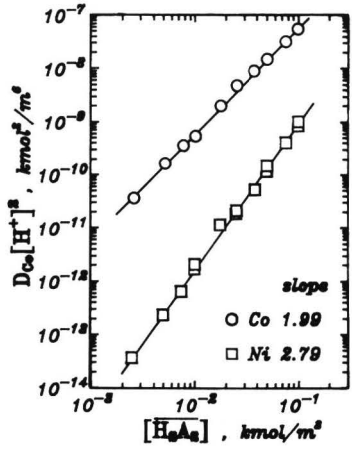

Fig. 2. Plots of log $D_M[H^+]^2$ vs. log $[\overline{H_2A_2}]$ for various HEHEHP concentrations in kerosene at 25°C.

Therefore, the extraction stoichiometries of cobalt ion and nickel ion with HEHEHP can be represented by the following reactions, respectively.

$$Co^{2+} + 2\ \overline{H_2A_2} \rightleftharpoons \overline{CoA_2 \cdot (HA)_2} + 2\ H^+ \qquad (6)$$

$$Ni^{2+} + 3\ \overline{H_2A_2} \rightleftharpoons \overline{NiA_2 \cdot 2(HA)_2} + 2\ H^+ \qquad (7)$$

From the experimental data, the extraction equilibrium constants for cobalt and nickel between HEHEHP dissolved in kerosene and 1.0 kmol/m^3 (Li,H)NO_3 solution at 25°C are calculated to be $K_{ex,Co} = 5.76 \times 10^{-6}$ and $K_{ex,Ni} = 5.66 \times 10^{-7}$ m^3/kmol, respectively. From eqn. (5), we can obtain the equations of distribution ratios of cobalt and nickel, respectively, i.e.

$$\log D_{Co} = -5.24 + 2\ pH + 2 \log [\overline{H_2A_2}] \qquad (8)$$

$$\log D_{Ni} = -6.25 + 2\ pH + 3 \log [\overline{H_2A_2}] \qquad (9)$$

3.2 Supported Liquid Membrane Permeation

The transport of cobalt and nickel through supported liquid membrane containing HEHEHP as mobile carrier is illustrated similarly our previous paper (Huang and Juang, 1987). Such a process is called "counter-transport", because it is able to transport metal ion from a low-concentration solution to a higher concentration solution. The driving force is the concentration gradient of hydrogen ion.

When the quasi-steady state is reached, the permeation rate of metal-HEHEHP complex through the membrane can be derived to be

$$J = [M(II)]_f \Big/ \left(\frac{1}{k_a} + \frac{[H^+]}{k_1\ [\overline{H_2A_2}]} + \frac{[H^+]^2}{\overline{k}_c\ K_{ex}\ [\overline{H_2A_2}]^{n+1}} \right) \qquad (10)$$

where $k_a=D_a/\delta_a$, $\bar{k}_c=\bar{D}_c/\delta_m$. D_a, δ_a, k_a are diffusivity, aqueous film thickness and mass transfer coefficient of metal in the aqueous solution. $\bar{D}_c$, δ_m, $\bar{k}_c$ are diffusivity, membrane thickness and mass transfer coefficient of the metal-HEHEHP complex in the membrane phase.

In the membrane transport process, the permeability, P, is defined as

$$P = J / [M(II)]_f \tag{11}$$

Substituting eqn. (10) to eqn. (11), the total resistance of permeation can be expressed as

$$\frac{1}{P} = \frac{1}{k_a} + \frac{[H^+]}{k_1 [\overline{H_2A_2}]} + \frac{[H^+]^2}{\bar{k}_c K_{ex} [\overline{H_2A_2}]^{n+1}} \tag{12}$$

where the three terms on right side of eqn. (12) represent aqueous film resistance, interfacial chemical resistance and membrane diffusion resistance, respectively.

From mass balance, the permeability can be evaluated by the following equation

$$\ln ([M(II)]_f / [M(II)]_f^0) = - A P t / V \tag{13}$$

where $[M(II)]_f^0$ and $[M(II)]_f$ are the metal concentrations at time 0 and t, respectively. The plot of $\ln ([M(II)]_f/[M(II)]_f^0)$ vs. t gives a straight line with a slope of -PA/V, where A = 9.62 cm^2 and V = 220 ml in this experiment.

The membrane separation factor of cobalt and nickel in supported liquid membrane is defined as the ratio of the permeation coefficients of cobalt and nickel, i.e.

$$\alpha_{SLM} = P_{Co} / P_{Ni} \tag{14}$$

The influences of stirring rate of the aqueous feed solutions on the permeabilities of cobalt and nickel are shown in Fig. 3. The results indicate that the thickness of the aqueous boundary diffusion layers reaches its minimum value when stirring rate larger than 250 r.p.m. Therefore, 300 r.p.m. is selected as the operation condition in majority cases.

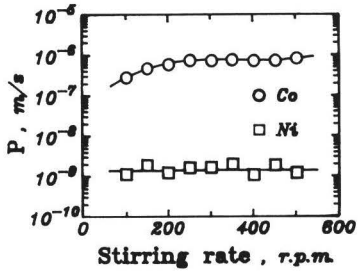

Fig. 3. Effect of stirring rate on permeation coefficient. Feed: $[Co^{2+}]_f$ $=[Ni^{2+}]_f$=0.034 kmol/m^3, $[LiNO_3]$=0.864 kmol/m^3, pH=5.0. SLM: $[\overline{H_2A_2}]$=0.05 kmol/m^3. Strip: 1.0 N HNO_3.

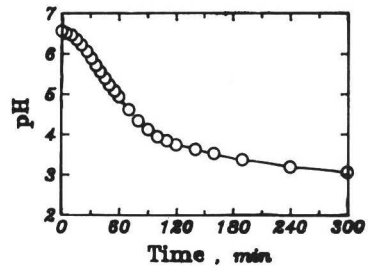

Fig. 4. Plot of pH versus time on the SLM operation at 25°C. Feed: $[Co^{2+}]_f$ $=[Ni^{2+}]_f$=0.034 kmol/m^3, $[LiNO_3]$=0.864 kmol/m^3, 300 r.p.m. SLM: $[\overline{H_2A_2}]$=0.10 kmol/m^3. Strip: 1.0 N HNO_3, 300 r.p.m.

During the counter-transport, hydrogen ions in strip solution will across SLM to feed solution. Then the pH value of feed solution will decrease and causes the permeation rate decrease. This phenomena is shown in Fig. 4.

For the sake of keeping constant permeation rate, the pH stat is applied to control pH value of feed solution. The dependence of permeabilities on the acidity of the aqueous feed solution are shown in Fig. 5. It indicates that the permeation coefficients increase with increasing the pH value of aqueous feed solution. The permeation coefficient of cobalt ion increases faster than that of nickel ion with pH value of solution increasing. Therefore, the membrane separation factor is increased with the pH value increasing, as can be seen from Fig. 6.

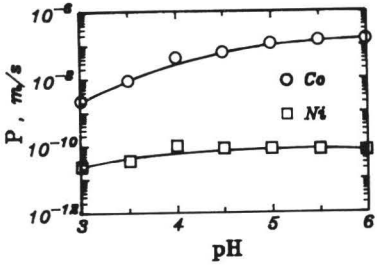

Fig. 5. Effect of pH value in the aqueous feed solution on the permeation rate. Feed: $[Co^{2+}]_f=[Ni^{2+}]_f$ =0.0034 kmol/m^3, $[LiNO_3]$=0.9864 kmol/m^3, 300 r.p.m. SLM: $[\overline{H_2A_2}]$=0.05 kmol/m^3. Strip: 1.0 N HNO_3, 300 r.p.m.

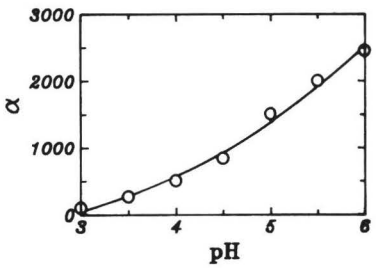

Fig. 6. Effect of pH value in the aqueous feed solution on the separation factor. Feed: $[Co^{2+}]_f$= $[Ni^{2+}]_f$=0.0034 kmol/m^3, $[LiNO_3]$=0.9864 kmol/m^3, 300 r.p.m. SLM: $[\overline{H_2A_2}]$ =0.05 kmol/m^3. Strip: 1.0 N HNO_3, 300 r.p.m.

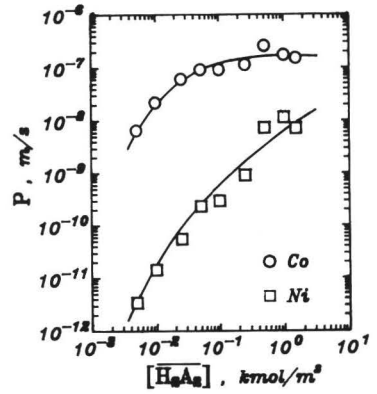

Fig. 7. Effect of $[\overline{H_2A_2}]$ in the membrane solution on the permeation rate. Feed: $[Co^{2+}]_f=[Ni^{2+}]_f$=0.034 kmol/m^3, $[LiNO_3]$=0.864 kmol/m^3, pH= 5.0, 300 r.p.m. SLM: $[\overline{H_2A_2}]$=0.005~1.55 kmol/m^3. Strip: 1.0 N HNO_3, 300 r.p.m.

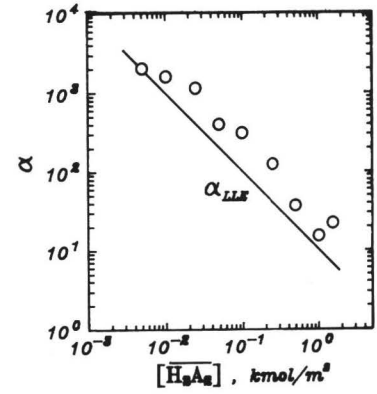

Fig. 8. Effect of $[\overline{H_2A_2}]$ in the membrane solution on the separation factor. Feed: $[Co^{2+}]_f=[Ni^{2+}]_f$=0.034 kmol/m^3, $[LiNO_3]$=0.864 kmol/m^3, pH= 5.0, 300 r.p.m. SLM: $[\overline{H_2A_2}]$=0.005~1.55 kmol/m^3. Strip: 1.0 N HNO_3, 300 r.p.m.

Figure 7 shows the effect of carrier concentration in SLM on the permeabilities of cobalt and nickel. In general, the permeabilities increase with the carrier concentration increase. Since the permeation coefficient of cobalt ion is greater than that of nickel ion at same carrier concentration, and the permeation coefficient of nickel ion increases faster than that of cobalt ion with carrier concentration increasing. Therefore, the membrane separation factors decrease with the carrier concentration increasing, as shown in Fig. 8. By defining the liquid-liquid extraction separation factor, α_{LLE}, as the ratio of the distribution ratios of cobalt and nickel, and then introducing the eqns. (8) and (9), it obtains

$$\alpha_{LLE} = D_{Co} / D_{Ni} = 10.2 / [\overline{H_2A_2}] \quad (15)$$

The effects of carrier concentration, $[\overline{H_2A_2}]$, on α_{LLE} calculated from eqn. (15) is also shown in Fig. 8.

4 CONCLUSIONS

The distribution ratios of cobalt and nickel between lithium nitrate solutions and HEHEHP dissolved in kerosene are studied. As a result, the distribution ratios of cobalt and nickel are dependent on the concentration of HEHEHP in kerosene and the pH value of aqueous solution. However, the separation factor of liquid-liquid extraction, α_{LLE}, is inversely proportional to the concentration of HEHEHP in kerosene, and independent on the pH value of aqueous solution.

When SLMs are used to separate cobalt and nickel, a mass transfer model take into account aqueous film diffusion, interfacial chemical reaction and membrane diffusion has been derived to describe the permeation of metal ions. The permeabilities of cobalt and nickel increase with both the HEHEHP concentration and the pH value of aqueous feed solution increasing. The membrane separation factor depends on the $[\overline{H_2A_2}]$ as well as pH value of the aqueous feed solution.

5 REFERENCES

Dreisinger, D.B. and Cooper, W.C., 1984. The solvent extraction separation of cobalt and nickel using 2-ethylhexyl phosphonic acid mono-2-ethylhexyl ester. Hydrometallurgy, 12(1), 1-20.

Huang, T.C. and Juang, R.S., 1987. Transport of zinc through a supported liquid membrane using di(2-ethylhexyl) phosphoric acid as a mobile carrier. J. Memb. Sci., 31(2&3), 209-226.

Huang, T.C. and Tsai, T.H., 1989a. Extraction of nickel(II) from sulfate solutions by bis(2-ethylhexyl)phosphoric acid dissolved in kerosene. Ind. Eng. Chem. Res., 28(10), 1557-1562.

Huang, T.C. and Tsai, T.H., 1989b. Studies on the separation of metal ions in aqueous solution by supported liquid membrane. National Science Council Monthly, 17(11), 1291-1314.

Matsuyama, H., Katayama, Y., Kojima, A., Washijima, I., Miyake, Y. and Teramoto, M., 1987. Permeation rate and selectivity in the separation of cobalt and nickel by supported liquid membranes. J. Chem. Eng. Japan, 20(3), 213-220.

Preston, J.S., 1982. Solvent extraction of cobalt and nickel by organophosphorus acids: I. Comparison of phosphoric, phosphonic and phosphinic acid systems. Hydrometallurgy, 9(2), 115-133.

Ritcey, G.M., Ashbrook, A.W. and Lucas, B.H., 1975. Development of a solvent extraction process for the separation of cobalt from nickel. CIM Bull., 68(753), 111-123.

Solvent Extraction 1990, T. Sekine (Editor)

© 1992 Elsevier Science Publishers B.V. All rights reserved

SUPPORTED LIQUID MEMBRANES FOR CHROMATE RECOVERY. EXPERIMENTAL STUDY.

A.I. ALONSO, M.I. ORTIZ, A. IRABIEN*.
Dpto. Ingeniería Química. Fac. Ciencias, UPV-EHU, Apdo. 644-48080 Bilbao. Spain.

ABSTRACT

In this work the application of hollow fibre supported liquid membranes to chromium (VI) recovery coming from industrial wastes (electroplating and metal coating processes) has been investigated.

After selection of the experimental system the influence of the initial concentration of chromium (VI) as well as the influence of the stripping agent and its concentration on the extraction yield have been studied from the results of continuous and batch experiments.

INTRODUCTION

Liquid membranes offer an alternative to metal recovery from aqueous effluents coming from industrial processes. The treatment of waste waters containing Cr(VI) is one of the major concerns in the Basque Country due to the large volume of electroplating and metal coating industries.

Since the work of Hochhausser and Cussler (1975) where they stated the active transport of the metal ion with emulsion liquid membranes, more efforts have been done on the modelling of the previous system of Cr(VI), Salazar et al. (1989, 1990). More recently Verhaege (1985) studied the application of different extractans to the recovery of chromium from electroplating rinse water by solid supported liquid membranes. A comparison between TBP and secondary amines (ADOGEN 382, ADOGEN 283) showed best results with the latter extractants. Loiacono et al. (1986) reported some experimental results on the recovery of Cr (VI) with flat supported liquid membranes.

In this work the viability of chromium recovery from aqueous effluents using hollow fibre supported liquid membranes has been stated, lowering its concentration below the standard levels (<7.5 ppm). Aliquat 336, a quaternary ammonium salt has been selected for the process due to the results reported with this extractant in ELM processes (Salazar et al., 1989, 1990). The influence of the stripping agent concentration on the extraction yield has been evaluated.

MATERIALS

A schematic diagram of the experimental set-up is shown in Fig.1. The laboratory module is formed by one hydrophobic microporous polypropylene hollow fibre(Accurel; ENKA, AG) inserted in a glass shell. The fibre was firmly epoxi-bonded to the ends of the permeation shell. The shell is

*Author to whom correspondence should be adressed.

a 4 mm inner diameter and 30 cm long glass tube with lateral openings at both ends allowing circulation of the stripping solution.

Feed and strip phases circulate in a cocurrent flow mode. Both phases are pumped by peristaltic pumps, leading to a satisfactory flow control.

Impregnation of the organic membrane, Aliquat 336:30%-kerosene was carried out by pumping the organic extractant through the fibre bore for one hour. The organic membrane passed rapidly through the porous wall of the fibre and was collected in the outer shell.

Samples of feed and stripping solutions were analyzed after dilution in an Ion Chromatograph Dionex Series 2000i, provided with a CS5 colum.

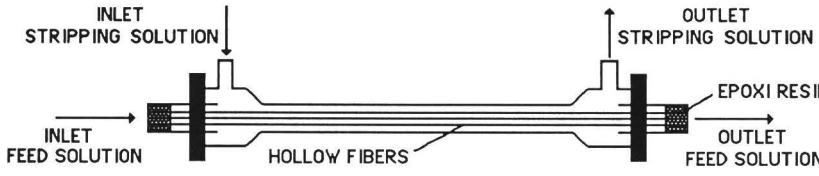

Fig. 1. Diagram of the experimental set-up

RESULTS

Being the aim of the present work to state the viability of the recovery of Cr(VI) from electroplating and metal coating rinse waters using hollow fibres supported liquid membranes, continuous and batch experiments have been performed studying the influence of the variables on the final extraction efficiency.

Two different sets of continuous experiments were performed in order to evaluate the influence of the chromium (VI) concentration in the feed solution in the range 100 ppm $\leq$Cr (VI) $\leq$ 2500 ppm and of the stripping agent type and the concentration working with NaCl and NaOH respectively; flow rates of the aqueous phases were 5 ml/h. The organic membrane was 30% of Aliquat 336 disolved in kerosene. Aqueous solutions were equilibrated with the organic phase previous to each run and the pH of the feed solution was adjusted to an initial value of pH=11 in all cases.

Tables 1, 2 and 3 show the results of the first and second sets of experiments, observing that: (i) under the experimental conditions investigated it is possible to obtain a high efficiency of extraction lowering the concentration of Cr(VI) in the feed aqueous phase down to 1 ppm, (ii) if NaCl is used as stripping agent, its concentration has no influence on the extraction yield, allowing to neglet the contribution of the stripping phase resistance on the kinetic control of the process and (iii) experiments performed with NaOH showed a dependence of the extraction efficiency on its concentration; however it was not possible to work with a NaOH concentration higher than 2M due to the complex behaviour of the organic phase.

TABLE 1

Influence of the concentration of Cr (VI) in the feed solution on the extraction yield, stripping agent NaCl 1M.

CONCENTRATION (ppm)			EXTRACTION
$Cr(VI)_{FEED}$	$Cr(VI)_{EXT}$	$Cr(VI)_{STR}$	YIELD
2500	1926	700	0.27
1000	490	550	0.52
100	1	98	0.98

TABLE 2

Influence of the concentration of NaCl in the stripping solution on the extraction yield; initial Cr(VI) conc. in the feed solution 1000 ppm

	CONCENTRATION (ppm)		EXTRACTION
NaCl	$Cr(VI)_{EXT}$	$Cr(VI)_{STR}$	YIELD
0.5 M	528	607	0.54
1 M	490	550	0.52
1.5 M	495	746	0.57

TABLE 3

Influence of the concentration of NaOH in the stripping solution on the extraction yield; initial concentration of Cr (VI) 1000 ppm

	CONCENTRATION (ppm)		EXTRACTION
NaOH	$Cr(VI)_{EXT}$	$Cr(VI)_{STR}$	YIELD
0.5 M	761	290	0.23
1 M	522	478	0.49
1.5 M	365	589	0.63
2 M	309	646	0.71

Batch experiments were performed in order to evaluate the influence of Cr(VI) concentration in the feed solution on the extraction and stripping processes. Feed and stripping solutions flowing at 52 ml/h and 120 ml/h respectively were recycled continuously; volumes of both phases were 100 ml and 50 ml in all cases. The pH of the feed solution was adjusted initially to pH=11 and a solution of NaOH 2M was used as stripping agent.

The results of these batch experiments are shown in figures 1, 2 and 3.

From these data it is concluded the viability of the recovery of chromium coming from electroplating rinse waters with hollow fibre supported liquid membranes. It is possible to reduce the concentration of the metal in the feed solution below 1 ppm; however the complexity of the system makes necessary a more detailed study of the influence of the variables leading to the modelling and optimization of the process, which is now under development.

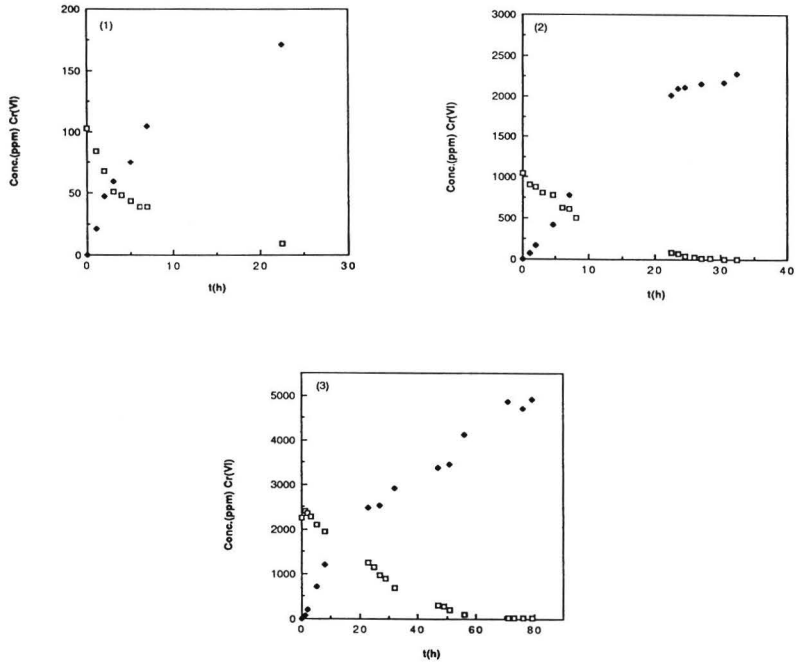

Fig. 1, 2, 3 : Batch experiments. Cr(VI) concentration in the feed (¤) and strip (◊) solutions vs time.Initial concentration of Cr(VI); Fig.1: 100 ppm, Fig.2: 1000 ppm, Fig.3: 2500 ppm.

REFERENCES

Hochhauser, A.M., Cussler E.L., 1975. Concentrating chromium with liquid surfactant membranes. AIChE J., 17, 1300.

Loiacono O., Drioli E., Molinari, R., 1986. Metal ion separation and concentration with supported liquid membranes. Journal of Membrane Science 28, 123-138.

Salazar, E., Ortiz, M.I. and Irabien, A., 1989. Recovery of Cr(VI) with emulsion liquid membranes in mechanically stirred contactor. 7th International Conference "Chemistry for Protection of the Environment". Lublin, Poland 4-7- Sept.

Salazar, E., Ortiz, M.I. and Irabien, A., 1990. Recovery of Cr (VI) with emulsion liquid membranes in mechanically stirred contactor. Influence of membrane composition on the yield of extraction. Extraction'90 10-14 Sept. Caithness U.K.

Verhaege M.A., 1985. Elimination and recovery of chromium from electroplating rinse waters by a solid supported liquid membranes. International Symposium on recycle and Secondary Recovery of Metals. 1-4 Dec. Florida. USA.

ACKNOWLEDGEMENTS

This work has been finantially supported by the Basque Government under Project 069.310-0014/89 and Research Grant (A. I. Alonso).

Solvent Extraction 1990, T. Sekine (Editor)

© 1992 Elsevier Science Publishers B.V. All rights reserved

MATHEMATICAL MODELLING OF PHENOL RECOVERY USING SUPPORTED LIQUID MEMBRANES.

A.M. URTIAGA, M.I. ORTIZ, A. IRABIEN*.
Dpto. Ingeniería Química. Fac. Ciencias, UPV-EHU, Apdo. 644-48080 Bilbao. Spain.

ABSTRACT

The use of hollow fibre supported liquid membranes for the recovery of phenol from aqueous effluents has been investigated. Kerosene and mixtures of kerosene with methyl isobutyl ketone have been used as organic membranes. Fully developed one-dimensional laminar flow mass transfer has been described with the steady-state mass conservation equation, identifying the governing wall Sherwood number and its dependency with the distribution coefficient of phenol.

INTRODUCTION

In this work phenol separation using extractive hollow fibres supported liquid membranes has been studied. The aqueous effluent containing phenol circulates inside the lumen of the hollow fibre and enters the reactive section in fully developed, one-dimensional, laminar flow. Axial diffusion can be neglected.

The stripping phase is a caustic solution circulating along the external wall of the fibre. Phenol reacts with the stripping solution to give sodium phenolate, a strong electrolyte non-soluble in the organic phase. The transport of phenol from the inner aqueous phase to the stripping phase is caused by a concentration gradient. The concentration of the solute in the stripping phase is zero as it reacts instantaneously with the sodium hydroxide to give sodium phenolate.

Solute transport takes place through the walls of the fibre containing the organic membrane. The membrane mass transfer coefficient (permeability coefficient) depends on the distribution coefficient of the solute between the membrane and aqueous phases, thus,

$$k_w = k_{wo} \cdot m_D \qquad (1)$$

where m_D is the distribution coefficient of the solute and k_{wo} is a parameter mainly depending on the physical and structural characteristics of the employed system.

The steady-state dimensionless diffusion equation describing phenol transport reduces to:

$$\frac{\partial^2 C^*}{\partial r^{*2}} + \frac{1}{r^*}\frac{\partial C^*}{\partial r^*} = \frac{v^*(r^*)}{2}\frac{\partial C^*}{\partial z^*} \qquad (2)$$

*Author to whom correspondence should be adressed.

where the dimensionless variables are defined as follows:

$C^* = C(r,z)/C_o$ $\quad r^*=r/R$ $\quad z^*= z/(R.Pe)$ $\quad z^* =z.D/(2v.R^2)$

$u(r^*) = u(r)/v$ $\quad Sh_w = r\ .\ k_w/D = r(K_{wo}.m_D)/D$

The dimensionless boundary conditions for this problem are:

B.C.1 $C(r^*) = 1,$ $\quad z^* = 0,$ $\quad$ all r^* (3)

B.C.2 $\partial C^*/\partial r^* = 0,$ $\quad r^*=0,$ $\quad$ all z^* (4)

B.C.3 $-\partial C^*/\partial r^* = Sh_w.C(r^*),$ $\quad r^*=1,$ $\quad$ all z^* (5)

Analytical solutions have been published for heat and mass transfer systems (Sideman et al., 1964/65; Davis and Parkinson, 1970). The resulting fluid bulk concentration can be expressed as:

$$C_m = \sum_{n=1}^{\infty} E_n.\exp(-\lambda^2_n.z^*) \qquad (6)$$

Davis and Parkinson (1970) calculated and listed the eigen values (λ_n) and parameters, E_n corresponding to several wall Sherwood numbers.

In this work phenol transport through supported liquid membranes has been modeled, testing the mass transfer model in conditions of small wall Sherwood numbers ($Sh_w \leq 1$) and high wall Sherwood numbers ($Sh_w=6$); simulated results with the obtained parameters agree very well with experimental results.

MATERIALS

A full description of the experimental set-up, materials and procedure used has been published elsewhere (Urtiaga et al., 1990).

RESULTS AND DISCUSSION

Two different sets of experiments have been performed using kerosene and mixtures kerosene-MIBK (17.5% MIBK) as organic membranes respectively, and changing the flow rate of the feed solution in the range $0.866\ ml/hr \leq F \leq 11.67 ml/hr$; in the latter set of experiments aqueous solutions were equilibrated with MIBK to prevent losses of the membrane due to the solubility of this compound. The initial concentration of phenol in the first case was 5gr/l, and in the second case it was 60 ppm lowering this concentration to 29 ppm.

Distribution coefficients for phenol were $m_D=0.2175$ between water and kerosene and a variable parameter dependant on phenol concentration between water and mixtures kerosene-MIBK.

However when the initial concentration of phenol was kept below 100 ppm in the latter case a constant distribution coefficient could be assumed m_D=6.23.

Experimental values of the dimesionless bulk concentration at different z* are shown in table 1, fluid bulk concentrations were calculated by application of eq.(6) for different values of Sh_w in the range of the dimensionless axial length, table 2.

TABLE 1

Results of the experiments performed with kerosene as organic membrane.

F(ml/hr)	v(cm/s)	z*	C*exp	$C_m$exp
1.1465	11.67	0.2176	0.836045	4.180225
0.7136	4.68	0.5428	0.713577	3.567878
0.5622	3.54	0.7393	0.562176	2.810880
0.3097	1.674	1.5166	0.309715	1.548575
0.1228	0.925	2.7450	0.122771	0.613855
0.1053	0.866	2.9317	0.105334	0.526670

Comparison between experimental and simulated results was made on the basis of the weighted standard deviation, figure 1. The value of the wall Sherwood number corresponding to the lower standard deviation was: $Sh_w = 0.21$

From the definition of $Sh_w = r.k_{wo}.m_D$, the parameter k_{wo} was calculated, resulting $k_{wo} = 3.2119 \times 10^{-4}$ cm.s^{-1}

TABLE 2

Simulated results of the bulk fluid concentration as a function of Sh_w and z*, using kerosene as organic membrane.

	C_m		
z*	Sh_w0.1	Sh_w0.19	Sh_w0.20
2.9317	0.325871	0.128933	0.116829
2.7450	0.349984	0.146889	0.133936
1.5166	0.559756	0.346335	0.329296
0.7393	0.753528	0.596066	0.581381
0.5428	0.812327	0.683747	0.671318
0.2176	0.919852	0.858030	0.851682

C_m			
$Sh_w0.21$	$Sh_w0.22$	$Sh_w0.23$	$Sh_w0.30$
0.105952	0.096168	0.087361	0.415923
0.122223	0.111623	0.102021	0.050919
0.312852	0.297539	0.283096	0.192742
0.567177	0.553436	0.540140	0.447619
0.659217	0.647432	0.635953	0.553864
0.845432	0.839276	0.833214	0.787826

Simulated results using the latter value of k_{wo} for the case of a mixed membrane, 17.5% MIBK - 82.5% kerosene showed good agreement with experimental results, table 3, checking the validity of the proposed model and parameters.

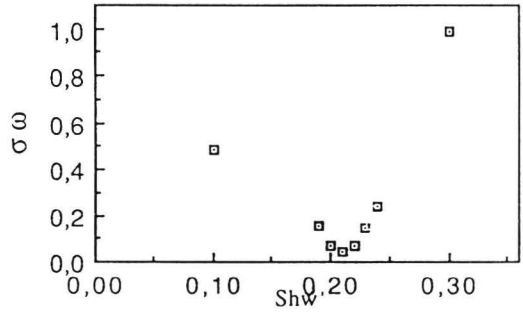

Figure 1. Results of the experiments performed with kerosene as organic membrane weighted standard deviation of the experimental results for different wall Sherwood numbers. The corresponding Sh_w=0.21.

TABLE 3

Experimental and simulated results of the experiments performed with a mixture of MIBK-Kerosene as organic membrane.

		C_m			
z*	$C_m$exp	Sh_w 3.33	Sh_w5	Sh_w6	Sh_w10
0.106075	0.483544	0.550250	0.502210	0.483810	0.445080

REFERENCES

Davis, H.R.; Parkinson, G.V., 1970. Mass transfer from small capillaries with wall resistance in the laminar flow regime. Appl. Sci. Res., 22, 20-30.

Sideman, S.; Luss, D.; Peck, R.E., 1964/65 Heat transfer in laminar flow circular and flat conduits with (constant) surface resistance. Appl. Sci. Res., Section A, vol. 14, 157-171.

Urtiaga, A.M.; Ortiz, M.I.; Irabien, A., 1990 Phenol recovery with supported liquid membranes I. Chem. E. Symp. Series No. 119, in press.

Solvent Extraction 1990, T. Sekine (Editor)

© 1992 Elsevier Science Publishers B.V. All rights reserved

SEPARATION OF CADMIUM FROM ZINC IN A CHLORIDE MEDIA BY A SUPPORTED LIQUID MEMBRANE

Y.C. HOH, C.Y. LIN, T.M. HUNG and T.M. CHIU
Institute of Nuclear Energy Research, CAEC, P.O. Box 3-7, Lung-Tan 32500, Taiwan, R.O.C.

ABSTRACT

Separation of cadmium from zinc in chloride solution with a supported liquid membrane was studied experimentally. Alamine 336 mixed with S-100 was used as the carrier. In the preliminary shake-out test, the separation efficiency was evaluated. It was shown that Alamine 336 mixed with S-100 has a higher selectivity for cadmium than zinc. The results indicated that the optimum feed aqueous pH and chloride ion concentration is equal to 1 and 0.5M, respectively. The permeation rates for cadmium and zinc were investigated by a flat sheet supported liquid membrane. The carrier Alamine 336 in S-100 was impregnated onto the supporting membrane and amonium acetate was served as the stripping phase. The diffusivity of cadmium in the liquid membrane was determined as 5.21×10^{-11} m^2/s. The separation and concentration of cadmium with hollow fiber module were performed by continuous reciuculating mode. The separation efficiencies and the concentration factors were reported.

INTRODUCTION

Supported liquid membrane (SLM) has been recently proposed as a potential technique for selective separation and concentration of metal ions. Uphill transfer, i.e., against the concentration gradient, is the main feature of SLM. This facilitated transport through SLM has been used in the studies of actinides and lanthanides separation (Danesi et al., 1985; Buchalter et al., 1987), the recovery of metal values (Danesi, 1984) as well as the separation and concentration of bio-substances.

The purpose of this study was to separate cadmium from zinc in a chloride media by supported liquid membrane. Not so many literatures on this topic were available. Danesi et al.(1983) reported the transfer rate of Cd(II) and Zn(II) from aqueous feed chloride solutions to ammonium acetate strip solution through a SLM. Trilaurylammonium chloride was the mobile carrier and triethylbenzene was the diluent. The influence of the stirring speed, feed chloride concentration, and the mobile carrier concentration was studied. Drioli et al.(1989) also studied the transport of Cd(II) through SLM. The carrier concentration, Cd(II) ion concentration in the feed and strip solutions, pH, mixing speed and temperature were selected as the experimental parameters. They concluded that the coupled transport in SLM is a promising technology for the recovery and separation of cadmium ion from aqueous solutions.

In this study, a tertiary amine, Alamine 336, was used as the mobile carrier

and S-100 was used as the diluent. Shake-out tests were used to study the Cd(II) and Zn(II) extraction equilibrium data; microporous flat sheet and hollow fiber membranes have been utilizied as supports to study the coupled transport characters and the separation efficiency of the above two metals.

2 EXPERIMENTAL

2.1 Reagents and membranes

A commercial tertiary amine, Alamine 336, 99% pure (Henkel Co.), was used as the membrane carrier. A S-100 solvent which contains greater than 95% of aromatic compound, supplied by Chinese Petroleum Co. was used as the organic diluent. $CdCl_2$, $ZnCl_2$, HCl, and CH_3COONa were analytical grade reagents.

The polymeric flat sheet support was Celgard 2500 microporous polypropylene with a 45% nominal porosity, 25μm in thickness and an effective pore size of 0.04 μm. The hollow fiber support was Enka's product. The pore size was 0.2 μm and the I.D. and O.D. was 1.8 and 2.2 mm, respectively. The effective surface area was 0.1 m^2 per cartridge.

The organic solution used as liquid membrane has been prepared by mixing an appropriate ratio of carrier with S-100. The liquid membrane was absorbed in the microporous polymer by soaking the flat sheet or filling the fibers lumen with the organic solution of the carrier and maintaining it for a sufficient time.

The SLM cell consists of two chambers which were made of acrylic, each one containing a parallel chamber having a volume of 450 ml. The impregnated membrane supporter was sandwiched by the chambers mentioned above. The contact surface area between the membrane and the solution was 35.2 cm^2. The stirring speed of each chamber was kept at 400 min^{-1}.

For the hollow fiber system, the feed aqueous solution and the strip solution were in the lumen and shell side, respectively. The two solutions were recycled during the experiments.

3 RESULTS AND DISCUSSION

3.1 Equilibration

The extraction stoichiometry of metal ions by Alamine 336 can be possibly represented by

$$MCl_{2|a} + 2\ ALMHCl_{|o} \rightleftharpoons (ALMHCl)_2MCl_{2|o} \qquad (1)$$

where M represents Cd(II) or Zn(II) ion and ALMHCl denotes the acidified Alamine 336. The subscripts a and o represents the aqueous and organic phase,

respectively. Shake-out test described by Hoh and Wang(1981) was employed to study the extraction and stripping equilibria. Figure 1 indicated the effect of ALMHCl concentration on the extraction percentages and distribution coefficients. It indicated that the extraction percentages for both metals increase rapidly with ALMHCl concentration increasing. The extraction of Cd(II) is superior to Zn(II). Figure 1 also showed that the distribution coefficient of cadmium is far better than zinc. An apparent separation effect was achieved.

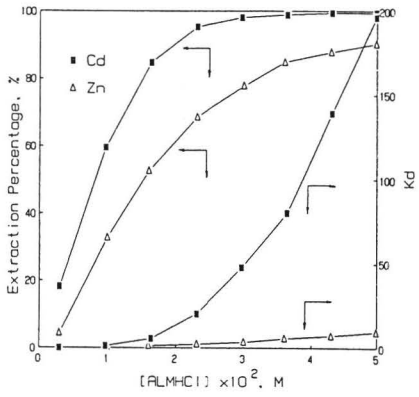

Fig. 1. Extraction percentage vs. initial concentration of Alamine 336 in S-100. Aqueous phase: $[Cd^{++}]$=0.005M (or $[Zn^{++}]$=0.005M), $[Cl^{-}]$=0.5M, pH=1; a/o=1.

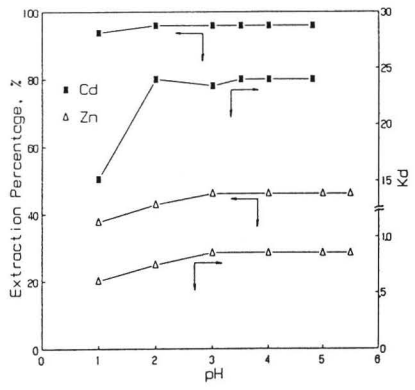

Fig. 2. Influence of pH in aqueous phase on extraction. Aqueous phase: $[Cd^{++}]$=0.023M, (or $[Zn^{++}]$=0.005M), pH=1. Organic phase:0.023M Alamine 336 in S-100. a/o=1.

Figure 2 indicated that the aqueous acidity does not affect too much on the extraction percentage and distribution coefficient. However, the chloride ion level in the aqueous phase did affect the extraction equilibria significantly as shown in Fig. 3. Especially in the range of 0.1 to 0.5M of chloride ion concentration, the extraction efficiency of Cd(II) was much higher than Zn(II). This could be attributed to the degree of formation of $CdCl_2$ is higher than $ZnCl_2$. In order to separate Cd(II) from Zn(II), the optimum chloride ion concentration in the aqueous phase was better kept below 0.5M. Figure 4 indicated a plot of log K_d against log [ALMHCl] for Cd(II) and Zn(II). Linear relationship with slope of 1.965 and 1.88 for Cd(II) and Zn(II) respectively, was obtained. The results showed that for cadmium extraction, the stoichiometry number is quite approach to 2:1 as indicated in Eq.1. However for zinc extraction, the presence of complexes with a ratio of 1:1 or 3:1 was possible.

3.2 Flat-sheet supported liquid membrane studies

Facilitated transport of metal ions through SLM can be represented by

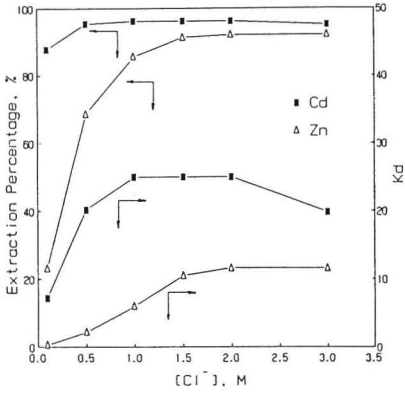

Fig. 3. Influence of Cl^- concentration on extraction.
Aqueous phase: $[Cd^{++}]$=0.005M, (or $[Zn^{++}]$=0.005M), pH=1.
Organic phase: 0.023M Alamine 336 in S-100. a/o=1.

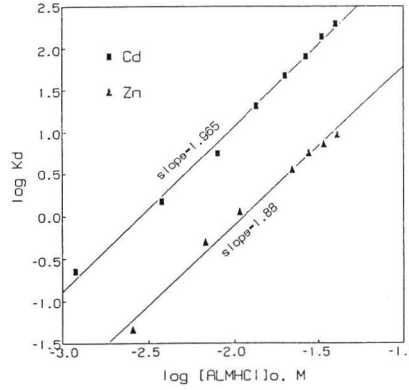

Fig. 4. Logarithmic plot of distribution vs. free ALMHCl at equilibrium.

permeation coefficient. Danesi et al.(1983) indicated that under the assumption of fast interfacial reaction occurred, the permeation coefficient can be expressed by

$$P = \frac{K_d}{K_d\triangle_a + \triangle_o} \tag{2}$$

where K_d is the distribution ratio of the metal species between the liquid membrane and the aqueous feed solution . $\triangle_a = d_a/D_a$, $\triangle_o = d_o/D_o$, d_a = aqueous film thickness, d_o = membrane thickness, D_a = aqueous diffusion coefficient of metal species and D_o = membrane diffusion coefficient of the complex. Equation 2 indicated that for the same system, the permeation rate is influenced by agitation speed. The preliminary results showed that within the stirring speed range of 150 to 600 min^{-1}, the permeation coefficient is a constant. This implied that within the agitation speed range, the ultimate value of d_a is reached. In order to ensure the d_a is an ultimate value, an agitation speed of 400 min^{-1} was selected in this study. When the feed cadmium ion concentration was low enough resulted $K_d\triangle_a >> \triangle_o$, permeation coefficient was inversely proportional to $\triangle_a$. The feed cadmium ion concentration with respect to time has a linear relationship as shown

$$\ln \frac{C}{C_o} = -\frac{Q}{V} P\, t \tag{3}$$

where C = feed metal concentration at time t, C_o = feed metal concentration at zero time, Q = effective membrane area and V = feed solution volume. Figure 5 was a plot of ln (C/C_o) against reaction time. A linear relationship was

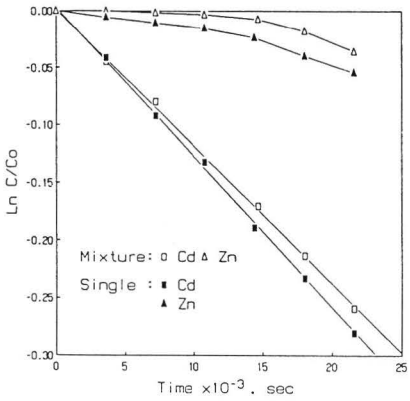

Fig. 5. Variation of Cd, Zn concentration with time in flat sheet SLM system.
Feed: $[Cd^{++}]$=0.003M and/or $[Zn^{++}]$=0.003M, [HCl]=0.1M.
Strip: 0.1M CH_3COONH_4.
Membrane: 0.023M Alamine 336 in S-100.
Agitation speed: 400 min^{-1}

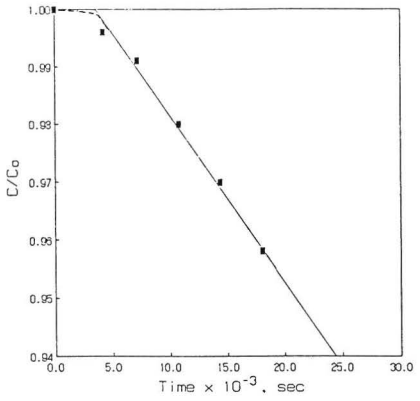

Fig. 6. Variation of Cd concentration with time in flat sheet SLM system.
Feed: $[Cd^{++}]$=0.045M, $[Cl^{-}]$=0.5M, [HCl]=0.1M.
Strip: 0.2M CH_3COONH_4, 0.3M NaCl
Membrane: 0.023M Alamine 336 in S-100.
Agitation speed: 400 min^{-1}

obtained for a single metal ion. For the cadmium case, a permeation coefficient of 2.5×10^{-4} cm sec^{-1} was obtained by using eqn. 3 and Fig. 5. Due to the degree of formation of zinc was much smaller than cadmium ion, the Δ_o in eqn. 2 could not be neglected. This implied that the mass transfer rate of cadmium ion is controlled by the aqueous film resistance. However, for zinc case, the mass transfer rate was controlled by the aqueous film and membrane resistances. This phenomena favored to the separation of cadmium from zinc. Figure 5 also indicated that at the second operation hour, the mole ratio of Cd to Zn in the stripped solution reaches to 47.7. This implied that very good separation efficiency was achieved. However, the separation efficiency decreased with time increasing and the mole ratio decreased to 10.8 at the fifth operation hour. At relatively high feed aqueous metal ion concentration, K_d value can be approximately represented by $[ALMHCl]_i/2C$ (Danesi, 1984), substituting this approximation into eqn. 2 gives

$$C = C_o - \frac{[ALMHCl]_i}{2\Delta_o} \frac{Q}{V} t \qquad (4)$$

where subscript i denotes the initial concentration. Figure 6 showed that after the induction time (Danesi et al., 1983), the plot C/C_o against t gives a slope of -2.79×10^{-6}, and the diffusion coefficient of 5.21×10^{-7} cm^2 sec^{-1} can be calculated from this slope. Danesi et al.(1983) defined that an induction time is the time require to reach a time independent interfacial resistance. This value was the diffusion coefficient of $(ALMHCl)_2CdCl_2$ in S-100 diluent. This value was smaller than Danesi's result(1983) where triethylbenzene was used as the diluent.

3.3 Hollow fiber supproted liquid membrane studies

The hollow fiber supported liquid membrane studies were operated in a recycling mode. Figure 7 indicated the results. Within 8 hours operation, 43.5%

Fig. 7. Variation of Cd and Zn concentration with time in hollow fiber system.
Feed: $[Cd^{++}]$=92.5ppm,
$[Zn^{++}]$=95ppm,
[HCl]=0.1M,
volume=8 liters,
flow rate= 2.5 l/min
Strip: 0.1M CH_3COONH_4,
volume=4 liters,
flow rate= 1.95 l/min
Membrane: 0.023M Alamine 336 in S-100.

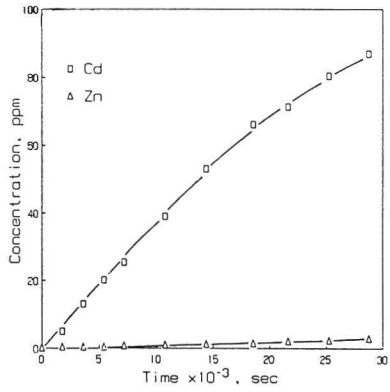

of Cd and 1.4% of Zn were permeated from the feed to the strip phase. However, as the results indicated in the flat SLM studies, the separation efficiency for the hollow fiber system also decreased with time increasing. For the operation time of 2, 4 and 8 hours, the mole ratio of Cd to Zn was equal to 29.7, 28.1 and 18.1, respectively.

4 REFERENCES

Buchalter, E.M., Hofman, D.L., Craig, W.M., Birkill, R.S. and Smit, J.J., Chem. Eng. Res. Des., 65 (1987) 381-385.
Danesi, P.R., Chiarizia, R. and Castagnola, A., J. Membr. Sci., 14 (1983) 161-174.
Danesi, P.R., Cianetti, C. and Violante, V., J. Membr. Sci., 14 (1983) 175-186.
Danesi, P.R., Sep. Sci. Technol., 19 (1984) 857-894.
Danesi, P.R., Chiarizia, R. and Rickert, P., Solv. Extr. Ion Exch., 3 (1985) 111-147.
Drioli, F., Loiacono, O., Molinari, R. and Pantano, G., Chimicaoggi, april, (1989) 25-30.
Hoh, Y.C. and Wang, W.K., J. Chem. Tech. Biotechnol., 31 (1981) 345-350.

Solvent Extraction 1990, T. Sekine (Editor)

© 1992 Elsevier Science Publishers B.V. All rights reserved

FTIR-ATR AND SOLVENT EXTRACTION STUDIES ON POTENTIOMETRIC RESPONSES OF NEUTRAL CARRIER TYPE LIQUID MEMBRANES

Masao SUGAWARA, Xiao Ming LIN, Kayoko UMEZAWA, Mohamed M. A. SHRIADAH, Seiichi NISHIZAWA and Yoshio UMEZAWA

Department of Chemistry, Faculty of Science, Hokkaido University, Sapporo, 060, (JAPAN)

ABSTRACT

Permselective ion transport at the surface of poly(vinyl chloride) supported neutral carrier liquid membranes, contacted with solutions of different kinds of metal salts was investigated by FTIR-ATR spectroscopy. When the PVC supported membranes containing dibenzo-18-crown-6 and bis[(benzo-15-crown-5)-4'-methyl] pimelate respectively were contacted with KCl aqueous solution, selective transport of K^+ ions into the interfacial region of the membrane was evidenced by the change in IR spectra through complexation of K^+ ions with neutral carriers. The cation permselectivity was correlated with almost zero extractability of liquid/liquid extraction of the corresponding bulk solvent extraction systems. A general empirical relation between potentiometric response slopes of liquid membranes and extractability of metal salts in a series of bulk extraction systems was also deduced.

INTRODUCTION

The cation permselective features of the so-called neutral carrier liquid membranes have been investigated mainly by electrodialysis[1,2], radiotracer[1,2] and different electrochemical techniques[3,4]. FTIR-ATR(Attenuated Total Reflectance) technique has some interesting features for the same purpose. The depth from the surface into which IR beam penetrates can be changed by use of several different internal reflectance elements(IRE) and different angle of incidence. For example, the observable depth around 1000 cm^{-1} region is 0.66 μm using a Ge 45° IRE with an incidence angle of 45°, 2.0 μm using a ZnSe 45° or KRS-5 45° IRE with an incidence angle of 45° and 1.4 μm using a KRS-5 45° with an incidence angle of 60°. This suggests that by FTIR-ATR technique one can observe a rather shallow part of around 0.1 mm thickness in the membranes, i.e., boundary phase of the membrane and depth profile of the membrane. Actually, by using this technique some studies on complex formation of neutral carriers with metal ions at the membrane

surface have been started [5,6]. In contrast to this interfacial technique, liquid/liquid solvent extraction offers an information about bulk partition processes of electroneutral species, in the present case, an ion-pair complex between a metal ion-neutral carrier complex cation and its counter anion. In the present study, we investigated metal ion-neutral carrier complex formation at the boundary phase of PVC supported liquid membranes contacted with aqueous metal solution by FTIR-ATR measurements in order to compare the results with liquid/liquid solvent extraction behavior and also with potentiometric responses to metal ions.

EXPERIMENTAL

FTIR-ATR spectra were recorded on a FTIR instrument of a Perkin-Elmer 1720X with Ge-45° and ZnSe-45° or KRS-5-45° IRE under nitrogen atmosphere. Sample membranes containing bis[(benzo-15-crown-5)-4'-methyl] pimelate(abbreviated hereafter as bis(benzo-15-crown-5)) or dibenzo-18-crown-6 were studied by immersing them into either 0.1 M KSCN or 0.1 M KCl solution with continuous stirring. After immersion, the membranes were touched softly with Kimwipe and placed on the IRE for ATR measurement. Dummy membranes containing the same amount of PVC and solvent but no neutral carriers were also measured to obtain the difference spectra between sample membranes and dummy membranes.

Extractability of a metal salt from an aqueous solution into an organic solvent containing a neutral carrier was determined as follows. Two ml of 10^{-3} or 10^{-4} M solution of a metal salt is shaken with 2 ml of neutral carrier saturated organic solution for 30 min, and then the concentration of unextracted metal ions in the aqueous phase was determined by atomic absorption spectroscopy. Extractability was calculated by the following equation;

Extractability(%) = (Concentration of extracted metal)/(Concentration of metal before extraction) x 100

Potential measurements were made with PVC supported liquid membrane electrodes in conjunction with a double junction Ag/AgCl reference electrode containing 3 M potassium chloride solution in the inner compartment and 1 M lithium acetate solution in the outer compartment. The electrode potential was measured with a Denki Kagaku Keiki ion-meter COM 10. The cell assembly used was as follows; Ag/AgCl reference electrode/inner solution/PVC supported liquid membrane//sample solution/1 M lithium acetate/3 M KCl/Ag/AgCl

reference electrode. Ionic strength was adjusted at 0.1 M with LiCl or NaF.

RESULTS AND DISCUSSION

(1)FTIR-ATR spectroscopic measurements

The ATR spectra of dibenzo-18-crown-6(**1**) complex with potassium thiocyanate showed large difference from that of free (**1**) as shown in Fig. 1a. The difference spectrum of the PVC membrane containing (**1**) showed the identical spectrum with that of the powder sample (**1**). We have chosen two adjacent peaks, i.e., 996 cm^{-1} due to the free (**1**) and 956 cm^{-1} due to the K^{+}-(**1**) complex , as shown by arrows

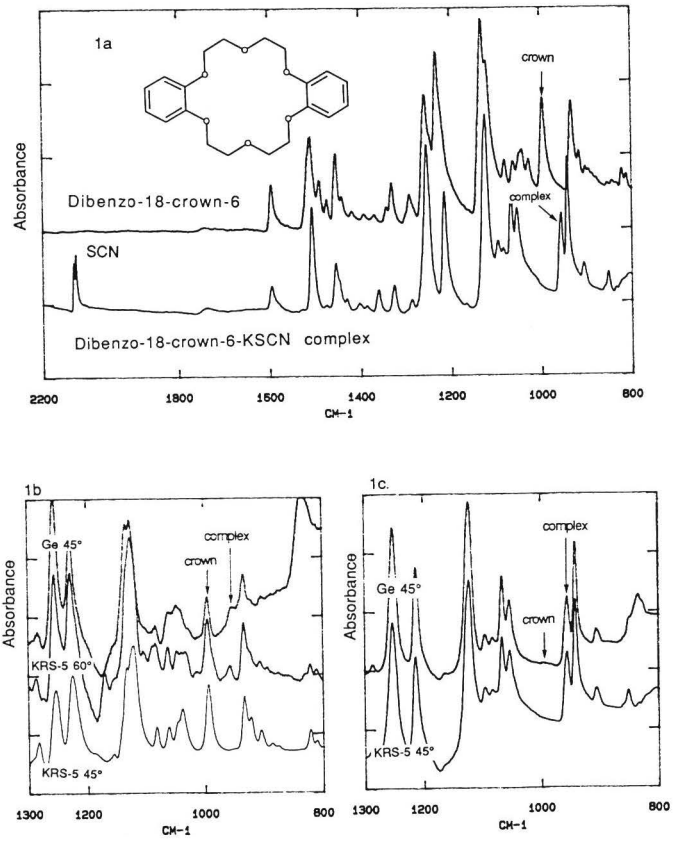

Flg. 1a. ATR spectra of dibenzo-18-crown-6 and its complex with KSCN.
1b. Difference spectra of ATR spectra of dummy membrane and membranes containing crown immersed in 0.1 M KCl solution for 1h.
1c. Difference spectra of ATR spectra of dummy membrane and membranes containing crown immersed in 0.1 M KSCN solution for 1h.

in Fig. 1a respectively, to estimate the degree of complex formation at the boundary region of the membrane. The depth profile of the K^+-(**1**) complex and free crown(**1**) in the membranes after immersion of the membrane into an aqueous KCl solution clearly showed that the K^+-(**1**) complex in the membrane phase decreased with increase in the depth, while the free crown(**1**) increased with the increase in the depth, as shown in Fig. 1b. The chloride peak is IR-inactive. But the membranes immersed into KSCN aqueous solution showed only potassium-(**1**) complex peak (free crown(**1**) peak was not observed), as shown in Fig 1 c. A SCN peak at 2055 cm^{-1} was also observed(The data are not shown in Fig. 1c.). This shows that the membrane extracts not only K^+ ions but also SCN^- ions. In Table 2 is given the peak height ratio of K^+-crown complex to free crown for (**1**) and bis(benzo-15-crown-5) membrane systems. When the membrane was contacted with KCl solution, the ratio decreased with the increase

Table 1
Slopes of log C vs. potential plot for PVC membranes based on dibenzo-18-crown-6, bis(benzo-15-crown-5),and bathocuproine and the extractability of the corresponding membrane systems.

Neutral carrier	Slope(mV) (Range, M)	Solvent[a]	K salt	Extractability %
Dibenzo-18-crown-6	45 (10^{-3}-10^{-1})	DOS	KCl[b]	0[d]
			KCl[b]	0[e]
	33 (10^{-3}-10^{-1})	DOS	KSCN[b]	8[d]
			KSCN[b]	24[e]
Bis(benzo-15-crown-5)	53 (10^{-4}-10^{-2})	DOS	KCl[b]	6[d]
			KCl[b]	5[e]
	49 (10^{-4}-10^{-2})	DOS	KSCN[b]	13[d]
	- 15 (10^{-1}-2x10^{-1})		KSCN[b]	25[e]
	40 (10^{-4} - 2x10^{-3})		KPic[b]	31[e]
	- 39 (10^{-1} - 2 x10^{-1})			
Bathocuproine	28 (10^{-6} - 10^{-4})	DOP	$CuSO_4$ [c]	7[d]
	35 (10^{-6} - 10^{-5})	DOP	$Cu(NO_3)_2$[c]	18[d]
	- 20 (10^{-4} - 10^{-3})			
	- 44 (10^{-5} - 10^{-3})	DOP	$Cu(ClO_4)_2$[c]	88[d]

(a) DOS: dioctyl sebacate, DOP: dioctyl phthalate. (b) Ionic strength I = 0.1 M with lithium chloride. (c) Ionic strength I = 0.1 M with sodium fluoride. (d) Extraction from 10^{-4} M potassium salt. (e) Extraction from 10^{-3} M potassium salt.

Table 2
Absorption peak height ratio of FTIR-ATR and FTIR transmittance spectra.

Neutral carrier	Peak height ratio[a]		Condition
Dibenzo-18-crown-6			
	I_{SCN}/I_{crown}[f]	0.1[b]	Transmittance
		0.7[b]	ATR (Ge 45°)
		0.6[c]	ATR (Ge 45°)
	$I_{complex}/I_{crown}$[g]	0.4[e]	ATR (Ge 45°)
		0.3[e]	ATR (KRS-5 45°)[j]
		0[e]	ATR (KRS-5 45°)
		∞[d]	ATR (Ge 45°)
		∞[d]	ATR (KRS-5 45°)
Bis(benzo-15-crown-5)			
	I_{SCN}/I_{crown}[h]	0.3[d]	Transmittance
		1.0[d]	ATR (Ge 45°)
		1.0[d]	ATR (ZnSe 45°)
	$I_{complex}/I_{crown}$[i]	0.9[e]	ATR (Ge 45°)
		0.7[e]	ATR (ZnSe 45°)
		1.4[d]	ATR (Ge 45°)
		1.3[d]	ATR (ZnSe 45°)

(a) Dependence of absorption peak intensity of ATR spectra on wave number was corrected. (b) Membranes immersed into 0.1 M KSCN solutions for 1 h. (c) K^+-dibenzo-18-crown-6 complex. (d) Membranes immersed into 0.1 M KSCN solution for 30 min. (e) Membranes immersed into 0.1 M KCl solution for 30 min. (f) $I_{SCN}/I_{crown} = I_{2055}/I_{1506}$, 2055 cm^{-1}: SCN^-, 1506 cm^{-1}: benzene nucleus. (g) $I_{complex}/I_{crown} = I_{956}/I_{996}$, 996$cm^{-1}$: free crown peak, 956$cm^{-1}$: new peak due to K^+-crown complex formation. (h) $I_{SCN}/I_{crown} = I_{2057}/I_{1517}$, 2057 cm^{-1}: SCN^-, 1517 cm^{-1}: benzene nucleus. (i) $I_{complex}/I_{crown} = I_{1047}/I_{1059}$; 1059 cm^{-1}: =C-O-C symmetric stretching (aromatic), 1047 cm^{-1}: new peak due to K^+-crown complex formation. (j) 60° incidence angle.

in the depth for both membranes. But with the membrane contacted with KSCN solution, the ratio is much larger than with the membrane contacted with KCl solution and it remained almost constant even with increasing depths. This results show that the K^+-crown complex formed from the SCN media penetrates into the deeper boundary region of the PVC membrane, owing to the permeation of the counter SCN^- ions, while the K^+-crown complex from the chloride media remains in a shallower interfacial region.

These FTIR-ATR results are related to the data for solvent extraction obtained in the present work(Table 1): The PVC membranes immersed into KSCN aqueous solution extracted more potassium ion, corresponding to a moderately high extractability of KSCN salt in our bulk solvent extraction experiment. Although KCl was negligibly extracted in the bulk solvent extraction(see Table 1), FTIR-ATR spectra of the PVC membrane showed that potassium ions formed a complex with the crown compound at the phase boundary region. This may indicate permselective transport of K^+ ions, i.e., $C_{K^+} \gg C_{Cl^-}$ into the interfacial region of the PVC liquid membrane occurred through complex formation with the membraneous crown.

We also examined a membrane containing bathocuproine, but by immersing it into copper(II) solutions, FTIR-ATR spectra exhibited no change, although complex formation in the PVC membrane was detected visually by appearance of yellow color of copper(II)-bathocuproine complex on the surface of the PVC membrane.

(2)Potentiometric Response and Extractability

We have measured the potentiometric response of PVC supported liquid membranes based on dibenzo-18-crown-6, bis(benzo-15-crown-5) and bathocuproine in the media containing hydrophilic anions, i.e., Cl^- and SO_4^{2-} and in the media containing hydrophobic anions, i.e., SCN^- and picrate. The log C vs. potential plots for the PVC membrane based on the bis(benzo-15-crown-5) are shown in Fig. 2. The results are correlated to the extractability data obtained in the present work as given in Table 1. From the comparison of the potentiometric response slope with the bulk extractability for all the systems examined(see Table 1), an empirical correlation is deduced, in which the systems are classified into three groups as summarized in Table 3. The Nernstian response of PVC supported neutral carrier liquid membranes is encountered in the case of the non-extractable media. In the extractable media, the anionic

response is induced. This empirical rule demonstrates that the bulk partition phenomena of metal salts are correlated to the interfacial selective cation transport phenomena,i.e., cation permselectivity as observed by FTIR-ATR, of PVC supported neutral carrier membranes and consequently, to potentiometric Nernstian and non-Nernstian responses of the liquid membrane.

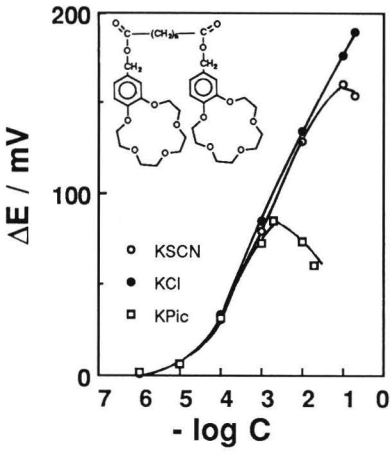

Fig. 2 Log C vs. potential plot for bis(benzo-15-crown-5)-DOS membrane in different kinds of potassium salts.

Table 3
An empirical correlation between potentiometric slope response of PVC supported neutral carrier membrane and extractability of the corresponding system.

Slope Response	Extractability
1) Nernstian	~ 0 %
2) Cationic at low concentration, but anionic at high concentration.	partly extracted
3) Anionic	strongly extracted

REFERENCES

1) Morf, W.E., and Simon, W., 1986. Cation-Response Mechanism of Neutral Carrier Based Ion-Selective Electrode Membranes. Helv. Chim. Acta, 69: 1120.
2) Thoma, A.P., Viviani-Naer, A., Arvanities, S., Morf, W.E., and Simon,W.,1977. Mechanism of Neutral Carrier Mediated Ion Transport through Ion-Selective Bulk Membranes. Anal. Chem., 49: 1567.
3) Armstrong, R.D., and Todd, M., 1988. Exchange of K^+ and Na^+ between Water and PVC in Its Presence of Different Ionophores. J. Electroanal. Chem., 248: 131.
4) Lindner, E., Niegreisz, Zs., Toth,K., Pungor, E., Berube,T.R., and Buck, R.P. 1989. Electrical and Dynamic Properties of Non-plasticized Potassium Selective Membranes. J. Electroanal. Chem., 259: 67.
5) R.Kellner, G.Fischbock, G.Gotzinger, E.Pungor, K.Toth, L.Polos, and E. Lindner, 1985. FTIR-ATR Spectroscopic Analysis of Bis-Crown-Ether based PVC-Membrane Surfaces. Fresenius' Z. Anal. Chem., 322: 151.
6) Lin, X.M., Umezawa, K., Okazaki, S., and Umezawa, Y., 1989. Studies on Host-Guest Interaction at Membrane Interface by FTIR-ATR I.PVC Supported Liquid Membrane. Abstract of Japan Society for Analytical Chemistry Meeting, Summer Session, Hokkaido Branch, P 48.

Solvent Extraction 1990, T. Sekine (Editor)

© 1992 Elsevier Science Publishers B.V. All rights reserved

POTENTIOMETRIC RESPONSE OF SYNERGISTIC EXTRACTIVE LIQUID MEMBRANES

Yasoo ITOH[1], Hideo AKAIWA[2], Masao SUGAWARA[3] and Yoshio UMEZAWA[3]
[1]Hokkaido Institute of Public Health, 060 Sapporo (Japan)
[2]Department of Applied Chemistry, Faculty of Engineering, Gunma University, 376 Kiryu (Japan)
[3]Department of Chemistry, Faculty of Science, Hokkaido University, 060 Sapporo (Japan)

ABSTRACT

Few liquid membranes containing chelating agents are known to respond potentiometrically to metal ions. However, we have found that Nernstian responses of chelate extractive liquid membrane systems for metal ions are induced by the addition of conventional synergists. For example, the poly(vinyl chloride)(PVC)-supported dioctyl(or dibutyl) phthalate membrane containing thenoyltrifluoroacetone(Htta) exhibited no potentiometric response to Ca^{2+} and Mg^{2+} ions, whereas the membrane containing both Htta and tributyl phosphate(TBP) showed potentiometric Nernstian response to Ca^{2+}($10^{-3.5}$-10^{-1} M) and Mg^{2+}($10^{-2.5}$-10^{-1} M) ions. The effect of synergists has been observed also for other chelate extractive liquid membranes.

1 INTRODUCTION

Needless to say, solvent extraction is based on distribution of an electroneutral solute between two liquid phases, and the solute passes through the liquid/liquid interface in the extraction process. The solvent extraction of metal ions is classified roughly into two systems, ion-pair extraction and chelate extraction, depending on the species that are partitioned between two phases, i.e., charged metal complexes and electroneutral metal chelate compounds. On the other hand, generation of membrane potential of the liquid membrane ion-sensor is related to the selective permeation of charged species across the liquid membrane/solution interface, though the mechanism is not clarified completely. The cation permselectivity of liquid membrane has been proved experimentally to be a very important factor for the potentiometric response of those sensors(Thoma et al.,1977, Fiedler, 1977, Doyle et al., 1982). Umezawa(1986) and Sugawara et al.(1990) found an empirical correlation between the potentiometric response of the poly(vinyl chloride)(PVC)-supported liquid membranes containing various neutral carriers and the extractabilities of respective primary cations in the bulk extraction, demonstrating that the Nernstian response to metal ions was developed in the media in which corresponding metal salts or ion-pairs were little extracted into the organic phase. For the chelate extractive

liquid membrane systems, on the contrary, the cation permselectivity of liquid membranes containing chelating agents can not formally be expected, because the electroneutral species is transported into the organic phase in ordinary chelate extraction. In fact, few liquid membranes containing chelating agents are known to respond potentiometrically to metal ions. However, we have found that the Nernstian responses of chelate extractive liquid membrane systems to metal ions are induced by the addition of conventional synergists employed in the synergistic extraction systems. In this work, we present the effect of synergists on the potentiometric response of chelate extractive liquid membrane systems in comparison with synergistic extraction systems.

2 EXPERIMENTAL

2.1 Reagents

All the chemicals used were of analytical reagent grade. Chelating agents tested were thenoyltrifluoroacetone(Htta), benzoyltrifluoroacetone(Hbfa), dithizone(Hdz) and 8-quinolinol(Hox). Synergists used were tributyl phosphate(TBP), pyridine(py), 2-methylpyridine(2-Mepy), 4-methylpyridine (4-Mepy) and tributylphosphine oxide(TBPO). Dioctyl phthalate(DOP) and dibutyl phthalate(DBP) were employed as a membrane solvent. Solutions of metal ions(1 M)were daily prepared by dissolving a weighed amount of metal chloride or sulfate, and diluted whenever needed. Distilled-deionized water was used throughout.

2.2 Preparation of liquid membranes

The PVC-supported chelate extractive membranes were prepared as follows: an appropriate amount of chelating agent, 1.5 g of membrane solvent and 0.75 g of PVC powder($n \fallingdotseq 1100$) were dissolved in 10 ml of tetrahydrofuran (THF). The solution was poured into a flat-bottomed glass petri dish(90 mm i.d.) and allowed to evaporate THF for 48 h at room temperature. Blank membranes containing no chelating agents were also prepared. Among the synergists examined, TBP was directly incorporated into the liquid membrane, whereas the other water-soluble synergists were added into the aqueous sample solution.

2.3 Potentiometric measurements

All the potentiometric measurements were carried out with an Orion ionalyzer model 701A, in conjunction with a TOA recorder model FBR-251A, at room temperature, under stirring the sample solution by means of a magnetic stirrer. A 20 mm diameter disk cut out of the prepared membrane was fixed on one end of a glass tube(15 mm i.d.x120 mm length) with an adhesive Teflon tape. Three milliliters of inner filling 0.1 M NaCl solution was put into the

glass tube. The electrochemical cell of the following type was used for potential measurement:

Ag/AgCl | 3 M KCl || 0.1 M NaCl || sample solution || liquid membrane || 0.1 M NaCl || 3 M KCl | AgCl/Ag.

Sample solutions contained usually 0.1 M NaCl and a pH-adjusting buffer (acetate or borate) or HCl. The metal ion concentration was changed from lower to higher concentration by stepwise addition of a small volume of metal salt solution with a micropipette.

2.4 Solvent extraction

To a 2 ml of aqueous solution containing a known amount of metal ion in a 10-ml stoppered test tube were added 2 ml of an organic solution of chelating agent. The chemical compositions of aqueous and organic phases were the same as used for the potentiometric measurements, except that the organic phase contained no PVC. The mixture was vigorously shaken for 30 min. After the phases were allowed to separate, the metal ion remaining in the aqueous phase was determined by atomic absorption spectrometry and the pH was measured.

3 RESULTS AND DISCUSSION

The potentiometric response of chelate extractive liquid membrane systems to a metal ion was induced by the addition of an appropriate synergist. A typical example is shown in Fig. 1. While no significant response to Ca^{2+} was observed with PVC-supported Htta-DOP membrane as well as TBP-DOP membrane, the DOP membrane containing both Htta as a chelating agent and TBP as a synergist exhibited the potentiometric response to Ca^{2+}($10^{-3.5}$-10^{-1} M) with a slope of about 40 mV/decade. This liquid membrane system responded also to Mg^{2+} and Sr^{2+}. The results obtained for other systems were listed as well in Table 1. Among the chelating agents tested, only Hox gave an unsuccessful result. The sample solution contacted with the Hox-DOP membrane became turbid with an increase in metal ion concentration during the potentiometric measurement. This is because significant amount of Hox in the membrane phase distributed into the sample solution and the water-insoluble electroneutral chelate with Cu^{2+} or Ni^{2+} was formed. Similar phenomena were occasionally observed with some other liquid membranes containing relatively high concentration of chelating agents.

Effect of concentration of synergist and chelating agent on the potentiometric response was examined with the Htta-py-Ni^{2+} system. In this system, the synergist, py was added to aqueous sample solution. As is shown in Fig. 2a and 2b, the potentiometric Nernstian response to Ni^{2+} was developed with an increase in py concentration and an increase in Htta concentration in

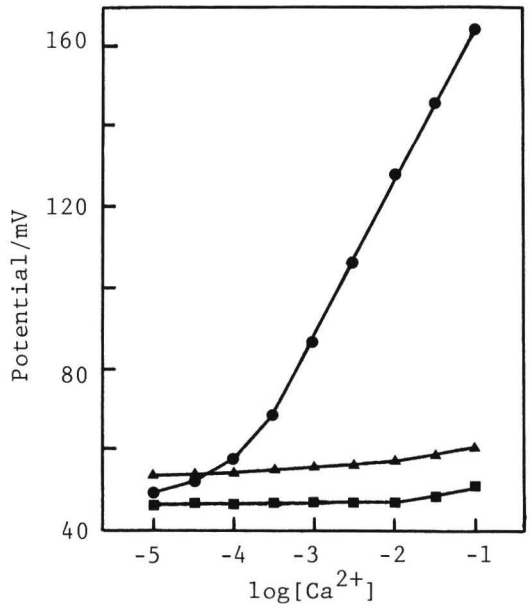

Fig. 1. Potentiometric response of Htta-TBP synergistic extractive liquid membrane to Ca^{2+}. ●; Htta-TBP-DOP, ▲; Htta-DOP, ■; TBP-DOP membrane. pH 6.8, $[Htta]_{memb}$ = 0.6 M, $[TBP]_{memb}$ = 0.44 M.

TABLE 1

Potentiometric response of synergistic extractive liquid membranes.

Chelating agent	Synergist	Membrane solvent	Metal ion	pH	Synergist present		Synergist absent
					Slope (mV/decade)	Range (M)	Slope (mV/decade)
Htta(0.6)	py(0.05)	DOP	Co^{2+}	5.8-6.9	27	10^{-5}-10^{-2}	0
Htta(0.6)	py(0.05)	DOP	Cu^{2+}	4.5-5.0	29	10^{-5}-10^{-3}	0
Htta(0.15)	py(0.05)	DOP	Ni^{2+}	5.5-6.5	29	$10^{-4.5}$-10^{-3}	0
Htta(0.6)	py(0.05)	DOP	Zn^{2+}	6.8	19	10^{-4}-10^{-2}	0
Htta(0.6)	py(0.05)	DBP	Co^{2+}	6.6	17	10^{-5}-10^{-2}	0
Htta(0.6)	2-Mepy(0.05)	DBP	Co^{2+}	6.9	10	10^{-3}-10^{-2}	0
Htta(0.6)	4-Mepy(0.05)	DBP	Co^{2+}	6.7	16	10^{-5}-10^{-2}	0
Htta(0.6)	TBP(0.44)	DOP	Ca^{2+}	5.0-7.2	40	$10^{-3.5}$-10^{-1}	0
Htta(0.6)	TBP(0.44)	DOP	Mg^{2+}	6.7	23	$10^{-2.5}$-10^{-1}	0
Htta(0.6)	TBP(0.44)	DOP	Sr^{2+}	5.5-6.7	30	10^{-3}-10^{-1}	0
Htta(0.6)	TBP(0.44)	DBP	Ca^{2+}	5.0	30	10^{-3}-10^{-1}	5
Hbfa(0.6)	TBP(0.44)	DOP	Ca^{2+}	4.8-8.8	37	10^{-3}-10^{-1}	0
Hbfa(0.6)	TBP(0.44)	DOP	Mg^{2+}	8.8	22	10^{-3}-10^{-1}	0
Hbfa(0.6)	TBP(0.44)	DOP	Sr^{2+}	6.5	26	$10^{-2.5}$-10^{-1}	0
Hbfa(0.6)	TBP(0.44)	DBP	Ca^{2+}	6.0	35	10^{-4}-10^{-1}	0
Hbfa(0.6)	TBPO(0.01)	DOP	Co^{2+}	6.8	30	10^{-4}-10^{-1}	0
Hdz(2.8×10^{-3})	TBPO(0.01)	DOP	Co^{2+}	7.0	15	10^{-3}-10^{-1}	4

Values in parentheses indicate concentrations(molarity) of respective components in liquid membrane or sample solution.

the DOP membrane. Thus, the magnitude of response to Ni^{2+} depends on the concentrations of both Htta and py, suggesting that the coexsistence of Htta and py is necessary for generating potentiometric Nernstian response of this system.

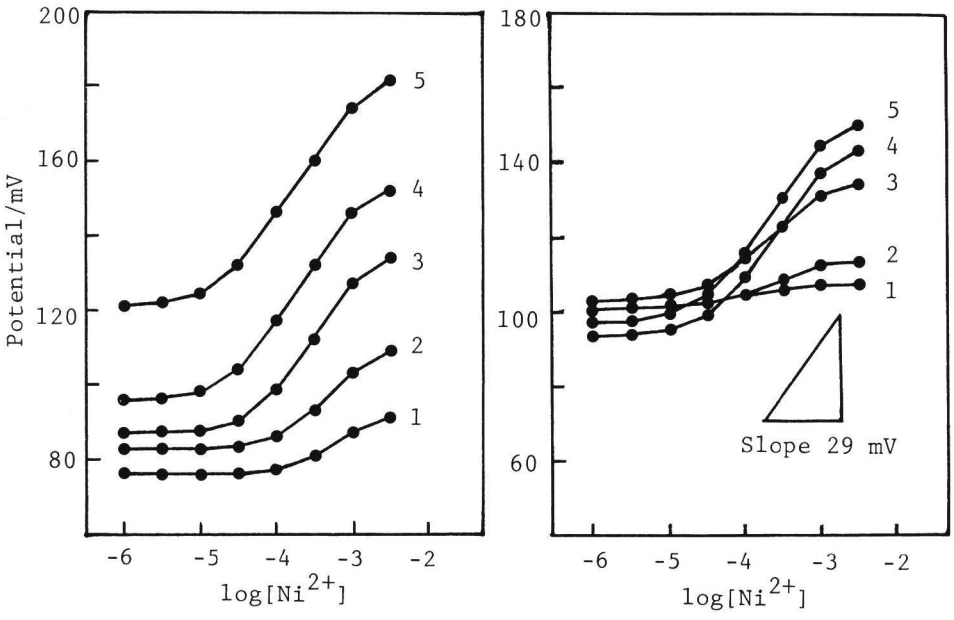

Fig. 2. Effect of concentrations of Htta and py on the potentiometric response of synergistic extractive liquid membrane to Ni^{2+}. (a)$[Htta]_{memb}$ = 0.15 M. pH 5.5. [py] = 1; 0.005 M, 2; 0.01 M, 3; 0.02 M, 4; 0.05 M, 5; 0.1 M. (b)[py] = 0.03 M. pH 5.5. $[Htta]_{memb}$ = 1; none, 2; 0.006 M, 3; 0.015 M, 4; 0.03 M, 5; 0.06 M. The triangle shows a slope of 29 mV/decade.

The solvent extraction experiments employing DOP and DBP as extracting solvents were achieved to confirm whether the synergism could be observed in those solvents. The results are given in Table 2. In all the extraction systems examined, pH values of half-extraction of metal ions in the presence of a synergist shifted to lower pH values than those in the absence. This shows effect of the synergists on the extraction of metal chelates. Analysis of synergistic extraction equilibrium was made for the Htta-py-Ni^{2+} system using DOP as an extracting solvent. The extracted species was found to be $Ni(tta)_2(py)_2$ from conventional slope analyses.

TABLE 2

The pH values of half-extraction of metal ions in various extraction systems.

Chelating agent	Synergist	Metal ion	Solvent	pH value of half-extraction	
				synergist present	synergist absent
Htta(0.6)	TBP(0.44)	$Ca^{2+}(10^{-3})$	DBP	3.8	5.5
Htta(0.6)	py(0.05)	$Co^{2+}(10^{-3})$	DOP	2.8	3.6
Htta(0.06)	py(0.05)	$Ni^{2+}(3x10^{-3})$	DOP	3.1	4.2
Hbfa(0.6)	TBP(0.44)	$Ca^{2+}(10^{-3})$	DOP	3.4	5.5
Hbfa(0.6)	TBPO(0.01)	$Co^{2+}(10^{-3})$	DOP	3.1	3.8
Hdz($2.8x10^{-3}$)	TBPO(0.01)	$Co^{2+}(10^{-3})$	DBP	3.6	3.9

Values in parentheses indicate concentrations(molarity) of respective components in organic or aqueous phase.

The potentiometric and solvent extraction results obtained above clearly show that synergistic extractive liquid membranes, as confirmed by a shift in the half-extraction pH, respond in a Nernstian or sub-Nernstian manner to metal ions when a synergist is present either in sample solution or in liquid membrane. The potentiometric response is the result of interfacial charge transfer process and solvent extraction is the bulk process. Owing to this methodological difference, the both methods may detect different kinds of species that are participated in charge separation and bulk extraction processes, respectively.

The generalization of the present approach will be useful not only for development of liquid membrane ion-sensors based on chelating agents, but also for clarification of mechanism of synergistic extraction.

4 REFERENCES

Doyle, B., Moody, G.J. and Thomas, J.D.R., 1982. Radiotracer studies on ion-selective electrode membranes containing metal complexes of a nonylphenoxy-poly(ethyleneoxy)ethanol in poly(vinyl chloride) matrices. Talanta, 29: 257-262.

Fiedler, U., 1977. Optimization of a sodium ion-selective electrode for use in serum measurements. Anal. Chim. Acta, 89: 101-109.

Sugawara, M., Lin, X.M., Umezawa, K., Shriadah, M.M.A., Nishizawa, S. and Umezawa, Y., 1990. FTIR-ATR and solvent extraction studies on potentiometric response of neutral carrier type liquid membranes. The proceedings of ISEC '90, Kyoto (Japan).

Thoma, A.P., Viviani-Nauer, A., Arvanitis, S., Morf, W.E. and Simon, W., 1977. Mechanism of neutral carrier mediated ion transport through ion-selective bulk membrane. Anal. Chem., 49: 1567-1572.

Umezawa, Y.,1986. Fundamental studies on membranes and interfaces for specific recognition of ions and molecules. Bunseki Kagaku, 35: 559-573.

Solvent Extraction 1990, T. Sekine (Editor)

© 1992 Elsevier Science Publishers B.V. All rights reserved

SEPARATION OF RHENIUM AND MOLYBDENUM BY LIQUID SURFACTANT MEMBRANES

JERZY STRZELBICKI, WOLFGANG DEGENER and KARL SCHÜGERL
Institute of Technical Chemistry, University of Hannover, Callinstraße 3, D-3000 Hannover 1 (Federal Republic of Germany)

ABSTRACT

Strzelbicki, J., Degener, W. and Schügerl, K., 1990. Separation of rhenium and molybdenum by liquid surfactant membranes. Proceedings of the International Solvent Extraction Conference 1990, Kyoto, Japan, July 16 - 21, 1990.

Separation of Re from solutions containing a high excess of Mo by liquid surfactant membranes using diisotridecylacetamide, diisotridecylamine, tri(n-octyl/n-decyl)amine and tri(n-octyl/n-decyl)methylammonium chloride is described. Diisotridecylacetamide was found as the most selective ion-carrier which transported more than 99 % of Re from the feed solution into the receiving solution and only inconspicuous amounts of Mo were found in the receiving solution. Influence of various process parameters (ion-carrier concentration, composition of the feed and receiving solution, stability of emulsion) is presented and discussed.

INTRODUCTION

Dialkylacetamides, alkylated amines and quarternary ammonium salts were found to be selective complexones of Re(VII) and Mo(VI) oxyanions in liquid-liquid extraction (Karagiozov and Vasilev, 1978, Zhou et al., 1982, Kähler and Gock, 1988). Liquid surfactant membranes (LSM) is an alternative separation technique to liquid-liquid extraction. The LSM exhibit some advantages like better utilization of a complexing agent (an ion-carrier), fast rate of metal ion transfer and often unique selectivity. In many cases, LSM were found as very efficient technique for separation and/or concentration of metal ions, e.g., for concentration of ReO_4^- using alkylated quarternary ammonium salts (Strzelbicki et al., 1984).

In this paper separation of Re and Mo by LSM using diisotridecylacetamide (**1**), tri(n-octyl/n-decyl)methylammonium chloride (**2**), diisotridecylamine (**3**) and tri(n-octyl/n-decyl)amine (**4**) is described.

2 EXPERIMENTAL

2.1 Procedure

First, an emulsion was prepared by mixing an organic solution (15 ml) with an aqueous receiving solution (15 ml) for 4 min at 20,000 rpm using a homogenizer (Janke & Kunkel IKA-Werk, Staufen, FRG). The organic solution contained an emulsifier: Paranox 100 and an ion carrier dissolved in kerosene (Essol D80). The aqueous solution was a solution of KOH or/and NaOH (K^+ was an indicator of emulsion breakage) and $NaNO_3$ (a regulator of ionic strength).

10 min after the emulsion was prepared it was stirred with 330 ml of an aqueous feed solution in the beaker (16 cm high and 60 mm in internal diameter) using a Heidolph motor Model RZR-2000 (Kleinfeld Labortechnik, Hannover, FRG) with a three-blade propeller-like stirrer. The feed solution contained 1000 ppm Mo (as $(NH_4)_6Mo_7O_{24}$), 100 ppm Re (as NH_4ReO_4) and H_2SO_4 (usually at concentration of 1.75 M). Those Re and Mo concentrations were chosen as close to composition of some real industrial solutions (Gock et al., 1987).

During the LSM process samples were taken from the feed solution and they were filtrated to separate the emulsion from the feed solution. Concentrations of Re (colorimetrically - Thierig and Umland, 1968 - using a Beckman spectrophotometer Model DU-65) and Mo (using a Perkin-Elmer atomic absorption spectrophotometer Model 373) in the feed solution was determined. Also concentration of K (by AAS) in that solution was determined and thereafter degree of emulsion breakage was calculated.

After the LSM process, the emulsion was broken using an electrocoalescer of our own construction and concentration of Re and Mo in the receiving solution was measured.

2.2 Reagents

Sources of chemicals include: Aldrich (Milwaukee, USA): NH_4ReO_4; Bayer (Leverkusen, FRG): H_2SO_4; Centre de Recherches Esso (Mont Saint Aignan, France): Paranox 100; Esso (FRG): kerosene - Essol D80; Henkel (Düsseldorf, FRG): Alamine 336 [tri(n-octyl/n-decyl)amine] (**4**) and Aliquat 336 [tri(n-octyl/n-decyl)methylammonium chloride] (**2**); Hoechst (FRG): diisotridecylacetamide (**1**) and Hoe F 2562 (diisotridecylamine) (**3**); Merck (Darmstadt, FRG): $(NH_4)_6Mo_7O_{24}$; Riedel de-Haen (Seelze, FRG): KOH, NaOH and $NaNO_3$.

3 RESULTS and DISCUSSION

3.1 Optimal H_2SO_4 concentration in the feed solution

In the extraction system water-diethyl benzene, the best separation of Re and Mo by dialkylacetamide was found at a 1.75 M sulphuric acid in the aqueous phase (Zhou et al., 1982). This finding was confirmed by our experiments with liquid surfactant membranes using a kerosene solution of **1** as a membrane phase. Three experiments were carried out with H_2SO_4 concentration in the feed solution of 1.25, 1.75 and 2.25 M. At 1.75 M H_2SO_4 no removal of Mo from the feed solution was observed while Re was almost entirely removed from that solution (>99%) after 15 min of the process. In the systems with 1.25 and 2.25 M H_2SO_4, concentration of Mo in the feed solution decreased and therefore separation of metals was less effective.

Results from liquid surfactant membrane experiments were in contrast with test extraction experiments involving a solution of diisotridecylacetamide in kerosene as the organic phase. After extraction, Mo/Re concentration ratio in the organic phase was 6.9 (at 1.75 M H_2SO_4). So, in spite of apparent similarity of these two processes, specific differences between liquid-liquid extraction (thermodynamically controlled process) and liquid

membranes (kinetically controlled process) can result in very different selectivities of separation.

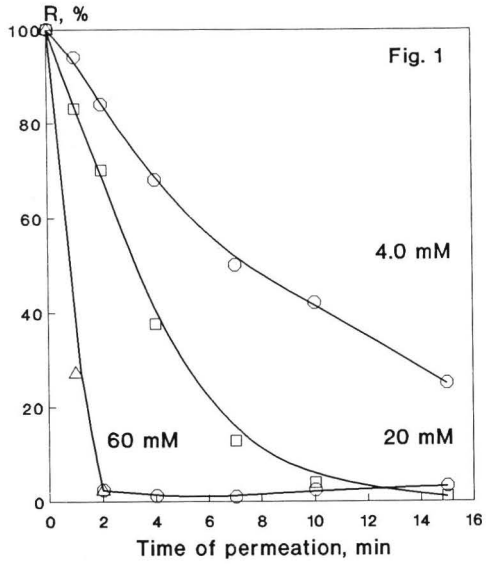

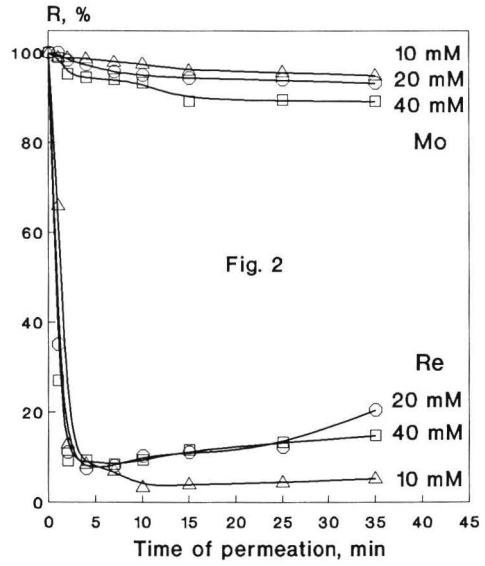

Fig. 1. Percentage of Re remaining in the source solution (R, %) vs. time of permeation in the LSM process at various concentrations of **1** in the membrane solution (organic solution: **1** at concentrations shown in the Figure and 5.0 v/v % Paranox 100 in kerosene; receiving solution: aqueous 0.1 M NaOH; source solution: 100 ppm Re, 1000 ppm Mo and 1.75 M H_2SO_4).

Fig. 2. Percentage of metal remaining in the source solution (R, %) vs. time of permeation in the LSM process at various concentrations of **2** in the membrane solution (organic solution: **2** at concentrations shown in the Figure, 3.0 v/v % Paranox 100 and 3.0 v/v % n-decanol in kerosene; receiving solution: aqueous 1.0 M (Na/K)OH; for the source solution see Fig. 1).

3.2 Separation by LSM at various ion carrier concentrations in the membrane solution

The experiments were done with 4.0, 20 and 60 mM **1** (Fig. 1) and with 10, 20 and 40 mM **2** (Fig. 2).

With the decreasing concentration of **1** in the membrane phase, permeation decreased very remarkably. At 4.0 mM **1**, only about 75 % of Re was removed from the feed solution after 15 min of the LSM process. With 20 and 60 mM **1**, removal of Re was higher than 99 % but the lowest Re concentration in the feed solution was achieved after 15 and 7 min, respectively.

For **2**, apparent differences were found in the course of process only within the first minute of the process when with the increasing concentration of **2** the permeation rate increased. For longer times, no differences in the Re permeation were found for all three concentrations of **2** and transport of Re from the feed solution was fast and efficient (80.8 to 82.6 % within 4 min). Efficiency of permeation of Re facilitated by **2** was clearly lower than in

case of 20 and 60 mM **1**.

To explain different permeation of Re through LSM with **1** or **2**, affinity of these complexones toward perrhenate, complexation and decomplexation rates, surface activity of complexones (see also 3.5) and diffusion conditions should be discussed.

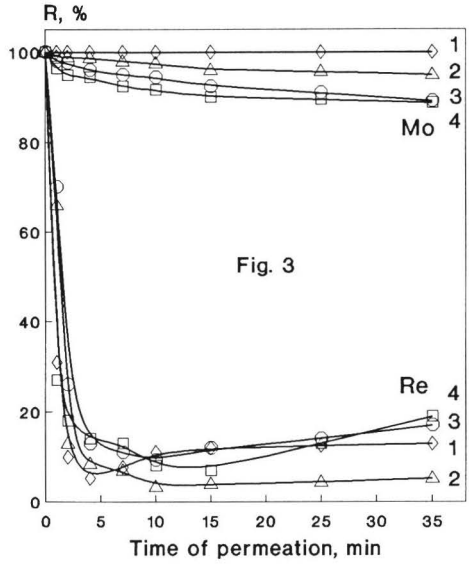

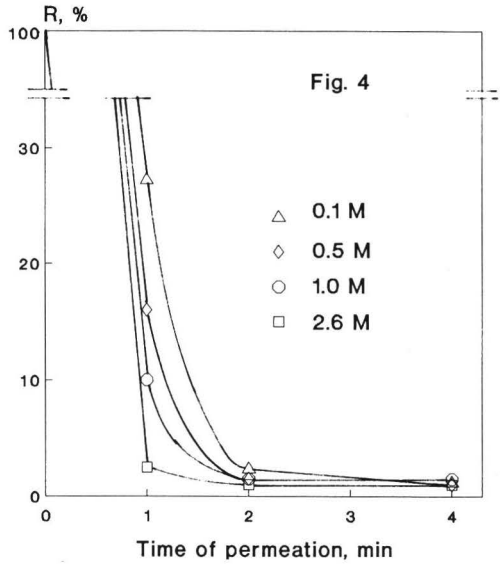

Fig. 3. Percentage of metal remaining in the source solution (R, %) vs. time of permeation through the LSM containing various ion carriers **1** - **4** (the organic solution: 10 mM ion carrier, 5.0 v/v % Paranox 100 and 3.0 v/v % n-decanol in kerosene; the receiving solution: aqueous 1.0 M (Na/K)OH and 1.5 M $NaNO_3$; for the source solution see Fig. 1).

Fig. 4. Percentage of Re remaining in the source solution (R, %) vs. time of permeation in the LSM process at various concentrations of NaOH in the receiving solution (the organic solution: 60 mM **1** and 5.0 v/v % Paranox 100 in kerosene; the receiving solution: aqueous NaOH at concentration indicated in the Figure; for the source solution see Fig. 1).

3.3 Separation of Re and Mo using various ion carriers

Four ion carriers **1** - **4** were tested in separation of Re and Mo by LSM (Fig. 3). The ion carrier concentration was kept constant at 10 mM. Permeation of Re in all four systems was comparably fast and efficient. Important differences were found in Mo permeation.

1 did not practically removed Mo from the feed solution (Mo concentration in the receiving solution after the LSM process was not higher than 200 ppm). All the other three compounds transported Mo to a different extend. E.g., in the system with **4**, already after 5 min 5.6 % of Mo was removed from the feed solution and it corresponded to the concentration of about 1200 ppm Mo in the receiving solution. Thus, **2** - **4** provided clearly worse separation of Re and Mo than **1**.

In the presence of **2** - **4**, sulphuric acid was fast transported from the feed solution into the receiving one. 1.0 M hydroxide in the receiving solution was neutralized, and after 35 min

of the process that solution became strongly acidic (pH < 1) and therefore decomplexation of Re and its release into the receiving solution was impeded or not possible at all (a lack of "driving force" in the LSM process).

For **1**, concentration of NaOH in the receiving solution as low as 0.1 M was sufficient for almost entire recovery of Re from the feed solution. That hydroxide concentration provided only transportation of no more than 50 % of Re through LSM containing **2** - **4**.

Faster H_2SO_4 and Mo(VI) anions transportation by **2** - **4** than by **1** may result from different complexation mechanism of anions by alkylated amines and quarternary ammonium salts (liquid anion exchangers) compared to alkylated acetamides (chelating agents). In particular, for divalent anions the different complexation mechanism may be of great importance.

3.4 Influence of the composition of the receiving solution

Potassium and/or sodium hydroxide was a decomposing agent of a metal ion - ion carrier complex at the receiving-organic solutions interface. In the liquid-liquid extraction experiments, 1.0 M aqueous NaOH was found as suitable for entire stripping of Re and Mo from the organic phase containing **1**. For LSM with **1**, 0.1 M NaOH provided suitable conditions for effective permeation of Re but with **2** - **4**, 1.0 M hydroxide had to be used (see 3.3). Some more experiments were done to determine influence of the composition of the receiving solution on the course of Re and Mo permeation.

A series of experiments was performed in the NaOH concentration range 0.1 to 2.6 M in the presence of **1** (Fig. 4). Some differences were observed only at the beginning of the process: after the first minute of the process 72.8, 84, 90 and 97.5 % of Re was recovered from the source solution at 0.1, 0.5, 1.0 and 2.6 M NaOH, respectively. For the second minute the respective values were as follows: 97.6, 98.5, 98.5 and >99 %. For longer time always more than 99 % of Re was transported.

The NaOH concentration in the receiving solution influenced remarkably the volume of that phase after proceess. After 15 min of the process, the resulting volume of the receiving phase was 11, 9, 4 and 2 ml in the system with 2.63, 1.0, 0.5 and 0.1 M NaOH, respectively. The decreasing volume of the receiving solution resulted most probably from the osmosis of water from the receiving solution (the lower concentrated solution) into the feed solution (the higher concentrated solution). The decreasing volume of the receiving phase led to concentrating Re in that phase to high degree. E.g., permeation of 99 % Re into the receiving solution in the LSM system with 0.1 M NaOH resulted in concentration of Re in that solution higher than 16,000 ppm.

Dependence between the final volume of the receiving solution and the total concentration of inorganic salts was found also for LSM containing 10 mM **2**, 3.0 v/v % Paranox 100 and 3.0 v/v % n-decanol. Initially, the receiving solutions contained 1.0 M (Na/K)OH and $NaNO_3$ at concentration of 0.0, 1.0, 1.5, 2.0 and 3.0 M. After the process (35 min) the final receiving phase volumes were 5, 11, 18, 19 and 25 ml, respectively.

Thus, by change of the composition of the receiving solution the course of separation by LSM could be controlled.

3.5 Stability of emulsion and its breaking by electrocoalescence

Emulsions stabilized with Paranox 100 were stable and during the LSM process their breaking degree was usually in the range 1.6 to 2.8 %. With the increasing Paranox 100 concentration, stability of emulsion increased. Span 80 was not suitable emulsifier to stabilize emulsion under experimental condition. This emulsifier most probably decomposed during the process and in some cases an emulsion was almost entirely broken within 10 to 15 min.

No clear dependence was found between stability of emulsions and structure of ion-carrier used or its concentration.

Emulsions containing **2** - **4** could be relatively easy broken by electrocoalescece. At 20.5 kV most of an emulsion was broken within 6 to 10 min. Emulsions containing **1** were much more resistible: at 22.5 kV only a part of an emulsion was broken within 30 min. It indicated that surface activity of **1** differs remarkably from that of **2** - **4**.

4 CONCLUSIONS

The experiments with the separation of Re from the solutions containing high excess of Mo by liquid emulsion membranes have shown potential usefulness of the process. Re could be selectively removed from the feed solution, transported into the receiving solution and concentrated there. Selectivity of the LSM process surpassed that of the liquid-liquid extraction under comparable process conditions.

5 ACKNOWLEDGEMENTS

This research was supported (fellowship for J.S.) by the Alexander von Humboldt Foundation (FRG). Authors would like to thank to Hoechst AG, in particular to Dr. Pfüller and Dr. Scholz of the Hoechst Division in Gendorf, FRG for synthesis and gift of diisotridecylacetamide.

6 REFERENCES

Gock, E., Kähler J. and Friedrich, J., 1987. Aktivierende Mahlung - erste Verfahrensstufe für die direkte ammoniakalische Drucklaugung rheniumhaltiger Molybdänitkonzentrate. In: Seminar Stofftrennung und Stoffanreicherung, November 23 - 24, 1987, Goslar, FRG, p.47.

Kähler, J. and Gock, E., 1988. Rheniumextraktion aus Molybdatlösungen. Erzmetall, 41: 132-137.

Karagiozov, L., and Vasilev, C., 1978. Separation of molybdenum and rhenium by extraction with mixtures of trioctylamine and Aliquat 336 followed by selective stripping. Hydrometallurgy, 4: 51-55.

Sato, Y., Valenzuela, F., Tsuneyuki, T., Kondo., K. and Nakashio., F., 1987. Extraction equilibrium of molybdenum(VI) with 2-ethylhexyl phosphonic acid mono-2-ethylhexyl ester. J. Chem. Eng. Jap., 20: 317-321.

Strzelbicki, J., Charewicz, W. A. and Mackiewicz, A., 1984. Permeation of chromium(VI) and rhenium(VII) oxyanions through liquid organic membranes facilitated by quarternary ammonium chlorides. Separation Sci. Techn., 19: 321-336.

Zhou, T., Zhoung, X., Ma, R., Huang, Z., Qu, M., and Zhou, Z., 1982. The amide type extractant A101 and its application to the separation of nobium and tantalum, and molybdenum and rhenium. Hydrometallurgy, 8: 379-388.

Solvent Extraction 1990, T. Sekine (Editor)

© 1992 Elsevier Science Publishers B.V. All rights reserved

EXTRACTION OF URANIUM FROM HEAP LEACHING SOLUTIONS BY LIQUID SURFACTANT MEMBRANES

D. HARTMANN*, D. PAREAU**, A. CHESNE**, G. DURAND**

* COGEMA/SEPA B.P. 71 87250 Bessines, FRANCE
* Ecole Centrale de Paris, LCNI, 92295 Chatenay-Malabry, FRANCE

ABSTRACT

A pilot scale liquid surfactant membrane process, designed to purify and concentrate uranium from heap leaching solutions, has been developed. The process is based on a carrier-mediated transport of uranium by a tertiary amine, and stripping by a mixture of sodium carbonate and sodium hydroxide.

During batch experiments, membrane composition had been previously adjusted in order to promote uranium transfer, using a volumetric ratio of external phase to internal phase of 40.

In a laboratory pulsed column (with flowrates up to 10 l/h), operating parameters have been optimized, through hold-up measurements, by establishing a relationship between the emulsion's residence time in the column and the depletion of uranium in the external phase.

Pilot scale testing of the complete process has been performed using a 10 cm diameter by 1 m height pulsed column. Treatment of a leach solution containing 240 mg/l of uranium with a flowrate of 116 l/h, has yielded an extraction recovery of 97 %.

Crud formation does not hinder uranium transfer. Small amounts of iron contaminating the internal phase are easily removed by filtration. A pure solution of uranyl carbonate containing over 5 g/l of uranium is recovered, which is ready for yellow-cake precipitation.

INTRODUCTION

Most of low-grade ores are treated by heap leaching for economical reasons. In the case of uranium, heap leaching has been employed for a long time. In France, it yields solutions containing usually around 200 mg/l of uranium. Uranium is then concentrated and purified by ion exchange or/and solvent extraction.

Liquid membranes represent an alternative to these techniques for the recovery of metals from dilute solutions. A number of applications, using either surfactant or supported liquid membranes, led to the build-up of pilot facilities, concerning metals such as : copper [Subramanian, 1980 ; Bart et al., 1986], chromium [Kitagawa et al., 1977], zinc [Melzner et al., 1984], indium [Guerriero et al., 1988] and uranium, from both phosphoric acid [Hayworth et al., 1983 ; Dickens et al., 1984] and sulfuric acid leaching solutions

[Babcock et al., 1983]. However, the recovery of zinc seems to be the only example for which an industrial facility was set up [Draxler et al., 1986].

We have designed a liquid surfactant membrane process to purify and concentrate uranium from sulfuric acid heap leaching liquors [Hartmann, 1989]. Chemical and physical parameters of the system were preliminary studied with the objective of optimizing uranium transfer from synthetic solutions.

The aim of this work was to bring into operation a continuous process, first by studying uranium transfer in a laboratory pulsed column, and then by testing the complete process at pilot scale.

EXPERIMENTAL

1. Solutions

Previous experiments have led to the following conditions :

* external aqueous phase :
  - synthetic sulfuric acid solution containing 200 mg/l U.
  - or heap leaching solution (U, Fe, Al, SiO_2,...).
* membrane :
  - tridodecylamine (MERCK) or Hostarex A327 (HOECHST) as carrier
  - ECA 4360 (EXXON) as surfactant
  - dodecane (PROLABO) or Isopar L (EXXON) as diluent.
* internal aqueous phase : Na_2CO_3 1 M - NaOH 0.1 M (pH = 12.6).

2. Liquid - liquid contactors

* Laboratory pulsed column (mechanical pulsation) :
  - inner diameter : 2.5 cm
  - active height : 1 m
  - 40 plates (disks and crowns) with 25 % free area
  - distance between plates : 2.4 cm.
* Pilot scale column (pneumatic pulsation) :
  - inner diameter : 10 cm
  - active height : 1 m
  - 20 plates (disks and crowns) with 25 % free area
  - distance between plates : 4.5 cm.

RESULTS AND DISCUSSION

I. LABORATORY STUDY

I.1. Influence of the flowrates of the two phases

The flowrates of the continuous aqueous phase (q_c) and dispersed emulsion phase (q_d) were varied, with a constant q_c/q_d ratio (= 10).

The intensity of pulsation was kept constant (110 cm/min). The aqueous feed solution is a synthetic one. The results are summarized in the following table.

TABLE 1

Values of hold-up (ß), emulsion's residence time (t_d) and uranium concentration in the raffinate (C_f) at steady state for different total specific throughputs (TST) ; q_c/q_d = 10 and a.f = 110 cm/min.

TST ($lh^{-1}cm^{-2}$)	ß (%)	t_d	C_f (mg/l)	Symbol
1.5	9.4	4 min 23 s	6.4	△
1.8	16.5	6 min 25 s	2.5	◇
2.0	20.3	7 min 7 s	2.1	▽
2.24	29.5	9 min 14 s	1.3	□

Assuming a plug flow of the continuous phase and taking an average value for E.a along the column length, a mass balance leads to the following equation :

$$\text{Ln}\frac{C_0}{C_f} = \frac{E_a}{ß} \times \frac{q_d}{q_c} \times t_d$$

E : mass transfer coefficient
a : external interface area a = 6 ß/D
D : diameter of emulsion globules

The plot of this relationship gives a straight line (Figure 1). The ordinate for t_d = 0 is different from zero because the plug flow model cannot be applied when the column height approaches zero.

The best uranium transfer is obtained for D ≈ 2 mm, which corresponds to E = 1.8 x 10^{-3} cm/s.

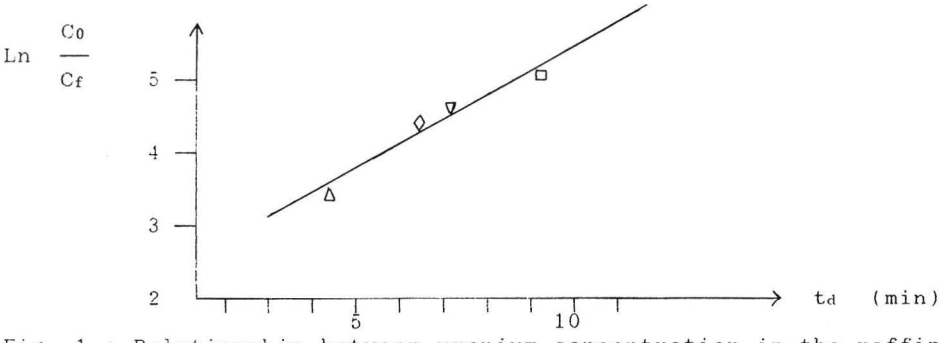

Fig. 1 : Relationship between uranium concentration in the raffinate (C_f) and emulsion's residence time in the column (t_d) at steady state for different total specific throughputs.

I.2. Influence of flowrates' ratio

The q_c/q_d ratio was varied beyond 10 in order to increase the uranium concentration factor, while maintaining an acceptable uranium extraction. Optimal conditions found with a flowrates' ratio of 10 were conserved, i.e. TST = 2.24 $lh^{-1}cm^{-2}$ and a.f = 110 cm/min.

TABLE 2

Values of hold-up (ß), emulsion's residence time (t_d) and uranium concentration in the raffinate (C_f) at steady state for different flowrates' ratios.

q_c/q_d	ß (%)	t_d	C_f (mg/l)	[U] in the Internal Phase (g/l)	Concentration* Factor
10	29.5	9 min 14 s	1.3	6.44	32.2
12	23.2	8 min 35 s	1.8	7.10	35.5
15	11.5	5 min 14 s	12	8.54	42.7

* The concentration factor is defined as [U] in the internal phase/C_0.

An increase of uranium concentration factor is observed when higher q_c/q_d ratios are used. However, ratios exceeding 12 lead to incomplete uranium extraction. In France, the specification for industrial waste streams is 1.8 mg/l of uranium.

A better depletion of uranium in the external phase could probably be obtained with q_c/q_d = 15 by using a higher column.

I.3. Influence of emulsion phase ratio (O/A)

A higher uranium concentration factor was tested by increasing the O/A ratio of the emulsion. The other operating parameters were : q_c/q_d = 10, TST = 2.24 $lh^{-1}cm^{-2}$ and a.f = 110 cm/min.

TABLE 3

Values of hold-up (ß), emulsion's residence time (t_d) and uranium concentration in the raffinate (C_f) at steady state for different emulsion O/A ratios.

O/A	ß (%)	t_d	C_f (mg/l)	[U] in the Internal Phase (g/l)	Concentration Factor
3	29.5	9 min 14 s	1.3	6.44	32.2
4	10.5	3 min 18 s	13	7.83	39.1
5	9.8	5 min 3 s	15	10.1	50.5

The uranium concentration factor increases when using higher emulsion O/A ratios, especially between O/A = 4 and O/A = 5, but the

extraction of uranium falls for O/A ≥ 4. This is due to an important decrease of the hold-up resulting from a reduced emulsion density.

II. PILOT OPERATION

II.1. Experiments with an industrial solution

The composition of the feed solution is as follows :

[U] = 240 mg/l [Fe] = 1.83 g/l [SiO_2] = 89 mg/l pH = 1.60.

The solution was clarified over a sand column and filtered through a 2 µm cartridge for complete elimination of suspended solids. The total specific throughput was reduced to 1.5 $lh^{-1}cm^{-2}$ (q_c = 116 l/h, q_d = 11.6 l/h), hence preventing loss by entrainment of the smallest emulsion globules to the external phase output.

With a pulsation intensity of 117 cm/min, a uranium extraction recovery of 98 % was obtained at steady state from a synthetic solution (C_f = 4.1 mg/l, ß = 11.4 %, t_d = 5 min 50 s). These operating parameters were maintained for the next experiments.

The influence of the industrial solution pH on uranium transfer and importance of crud formation was studied. The results are summarized in the following table.

TABLE 4

Values of uranium concentration in the raffinate (C_f), uranium concentration in the internal phase and quantity of crud for different initial pH values of a heap leaching solution.

Feed Solution pH	1.60	1.50	1.30	1.10
C_f at Steady State (mg/l)	24	8.1	12	27
Uranium Extraction Recovery (%)	90	97	95	89
[U] in the Internal Phase (g/l)	5.41	5.55	5.51	5.22
Amount of Dried Crud (g/m^3 of feed solution)	379	118	98	74

At pH 1.50, no significant loss in uranium recovery is observed with the industrial solution. The small difference is due to crud formation at the external area of emulsion globules during transfer. Though cruds occupy an important volume before settling because they are swollen by solvent, they do not affect uranium transfer significantly for pH < 1.50. Moreover, the crud solid content remains very

limited.

The amount of crud decreases when the feed solution is acidified ; however below pH 1.3, uranium transfer is slower due to the formation of amine bisulfate in the membrane.

Cruds contain a lot of Fe, SO_4, PO_4 and small quantities of U, Ca and SiO_2. They are probably generated by the interaction between low solubles salts and the surfactant.

II.2. Electrostatic coalescence

The apparatus, designed by COGEMA/SEPA, has flat, parallel and horizontal electrodes, according to recommendations found in the literature [Hsu et al., 1985]. The characteristics of the coalescer are : active volume = 1 l, distance between the electrodes = 2 cm, thickness of polycarbonate insulator = 1 mm.

A complete coalescence was obtained with the following conditions:

- electrical parameters : alternative current, 2 500 V, 50 Hz
- emulsion flowrate : 16 l/h, corresponding to 3 min 45 s of residence time in the coalescer.

At 50 Hz, the minimum voltage required for a good coalescence lies between 2 000 and 2 500 V. For different voltages above 2 500 V, we noticed a favorable influence of low frequencies in the 25 - 1 000 Hz range. Initial problems encountered with the adhesion of the insulator to the electrodes were successfully overcome.

REFERENCES

Babcock, W.C., Chidlaw, M.B., Kelly, D.J. and LaChapelle, E.D., 1983. US Bureau of Mines Report No. 203-83.

Bart, H.J., Wachter, R. and Marr, R., 1986. Proc. Int. Solv. Extr. Conf., Munich, III : 901-905.

Dickens, N., Rose, M. and Davies, G.A., 1984. In " I. Chem. E. Symposium Series No. 88 " : 69-81.

Draxler, J. and Marr, R., 1986. Chem. Eng. Process., 20 : 319-329.

Guerriero, R.and Meregalli, L., 1988. Hydrometallurgy, 20 : 109-120.

Hartmann, D., 1989. Doctor Thesis, Ecole Centrale de Paris, France.

Hayworth, H.C., Ho, W.S., Burns, W.A. and Li, N.N., 1983. Sep. Sci. Technol., 18 (6) : 493-521.

Hsu, E.C. and Li, N.N., 1985. Sep. Sci. Technol., 20 (2,3) : 115-130.

Kitagawa, T., Nishikawa, Y., Frankenfeld, J.W. and Li, N.N., 1977. Environ. Sci. Technol., 11 (6) : 602-605.

Melzner, D., Tilkowski, J., Mohrmann, A., Poppe, W., Halwachs, W. and Schugerl, K., 1984. Hydrometallurgy, 13 : 105-123.

Subramanian, K.N., 1980. Proc. of the Liquid Membrane Seminar at UMIST, Manchester.

Solvent Extraction 1990, T. Sekine (Editor)

© 1992 Elsevier Science Publishers B.V. All rights reserved

SEPARATION OF GOLD FROM ITS HYDROCHLORIC SOLUTION WITH THE LIQUID SURFACTANT MEMBRANES

Yan Nian-Xi
Department of Chemistry
Suzhou University, Suzhou 215006, China

Shi Ya-Jun and Su Yuan-Fu
Chemical Engineering Research Centre
East China University of Chemical Technology, Shanghai 200237, China

ABSTRACT

The separation of gold from its hydrochloric solution with the liquid surfactant membranes was studied by using polyamine E644 as the surfactant, N503, DBC or DIBK as the carrier and sodium sulfite or oxalic acid as the internal reagent.Results show that all the carriers can be used to extract the gold effectively, while N503 gives the best results. When sodium sulfite was used as the internal reagent, the extraction rate was much faster than when oxalic acid was used. The extraction rate increases with the decrease in PH in the external phase. Finally, the diffusion-reaction model for Type II Facilitated transport in the liquid surfactant membranes was tested by the experimental data.

INTRODUCTION

The liquid surfactant membranes have been widely investigated as a novel technique for separating and/or concentrating metal ions, chemical and biological species as well as for waste water treatment (1-6). In recent years, many authors have reported their studies on the recovery and the enrichment of valuable metals and the removal of trace contaminants from waste water.

The process for metal ion extraction by the liquid surfactant membranes can be facilitated by utilizing the Type II Facilitated Transport, i.e., the carrier-mediated transport. In this type of facilitated transport, the carriers incorporated into the membrane carry the extracted species across the membrane to the receiving phase. Compared with the solvent extraction, the liquid surfactant membranes is characterized by being rapid in separation, high in efficiency, low in power consumption and adoptable to diverse uses.

In this paper, by using the carrier-mediated transport mechanism, the extraction of gold from the hydrochloric solution with the liquid surfactant membranes is studied and the diffusion-reaction model for Type II Facilitated Transport is tested with the experimental data.

EXPERIMENTAL

The experimental procedure was the same as described in the previous paper (2). The W/O emulsion was prepared as follows. At first, the mixed membrane solution of 100 ml containing solvents, surfactants and carriers was introduced into a stirrier of ϕ60 mm, h 90 mm , with four baffles and two six-blade turbines, then at the speed of 1500rpm, the internal phase solution of 50 ml was added into the stirrer. After stirring for 20 minutes, the W/O emulsion was obtained.

The extraction experiment was carried out in a stirrer of ϕ 90 mm, h 150 mm, with a six-blade turbine. First added into the stirrer was the

Au-containing solution of 405 ml, then the above mentioned W/O emulsion of 135 ml was dispersed in the solution by agitation. Samples for analyzing the concentration of gold in the external phase were periodically removed from the bottom of the stirrer and analyzed by an atomic absorption spectrophotometer (AA-646, made by Shimadzu Corporation). The gold concentration in the external phase was expressed as the dimensionless form:

$$h = \frac{C_e}{C_{eo}}$$

where C_{eo} and C_e are the initial and instantaneous concentration of gold in the external phase.

RESULTS AND DISSCUSION

For the extraction of gold, the W/O emulsion must be sufficiently stable to ensure the complete extraction. The stability of the emulsion is affected by many factors, such as surfactants, internal reagents, carriers and their concentration and the viscosity of the membrane solvents, etc. As indicated in the previous paper (7), polyamine E644 can be used as the surfactant, kerosene as the membrane solvent. In this paper, we have chosen the carriers and the internal reagents.

The effect of carriers

Fig.1 shows the effect of carriers N503, DBC and DIBK on the concentration of gold in the external phase with 0.5M sodium sulfite as the internal reagent. It can be seen that all of them can extract gold effectively, while N503 gives the best results

The effect of N503 concentration on the gold extraction rate is shown in Fig.2. The increase in the concentration from 1% to 2% has a little influence on the extraction rate. This is because the carrier reacts with the auric ions at the outer interface of the membrane to form the complexes which diffuse from the outer interface to the inner interface where the complexes react with the internal reagent to release the carrier. Therefore, even the lower concentration of the carrier in the membrane can extract the metal specise effectively. Since the increase in the carrier concentration decreases the emulsion stability, unnecessary high concentration of the carriers must be avoided.

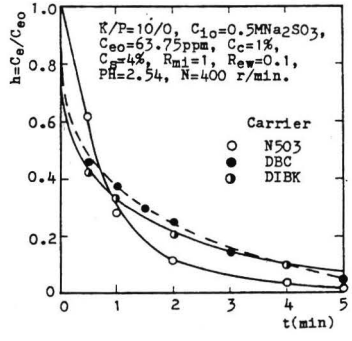

Fig.1 Comparison of carriers

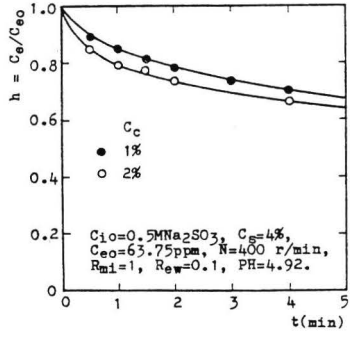

Fig.2 Effect of concentration of N503

The Effect of the Internal Reagent

The effect of the internal reagent on the gold extraction is shown in Table 1. It can be seen that when sodium sulfite is used as the internal reagent, the extraction rate is much faster than when oxalic acid is used no matter which carrier is used.

The extraction rate increases with the increase in the concentration of sodium sulfite as shown in Fig.3.

Table 1 Comparison of the internal reagent

Carrier	Internal	C_e(ppm)					
		0	2	4	6	8	10
DIBK	0.5MNa_2SO_3	65.8	10.0	2.27	1.36	0.90	1.82
DIBK	5%$H_2C_2O_4$	64.1	36.7	30.0	24.2	17.5	15.0
DBC	0.5MNa_2SO_3	65.8	5.91	0.90	0.90	0.90	1.36
DBC	5%$H_2C_2O_4$	64.1	21.7	6.7	5.8	5.0	6.7

K/P=10/0, C_S=4%, C_C=1%, R_{mi}=2, R_{ew}=1/3,
N=400 r/min, C_H=1NHCl

Effect of PH in the external phase

Fig. 3 and Fig.4 shows the effect of PH in the external phase on the extraction rate. It can be seen that the concentration of gold in the external phase decreases with the decrease in PH. Gold exists in chloride solutions mainly as the complex anions $AuCl_4^-$. In N503 or DIBK molecules, there are oxygen atoms which have unpaired electrons, so they tend to combine with protons in acidic solution and then react with $AuCl_4^-$. Thus, the carriers N503 or DIBK extract gold on the outer interface of the emulsion droplets in the following reaction:

$$RH^+ + AuCl_4^- \longrightarrow RH^+AuCl_4^-$$

It is obvious that the decrease of PH favours the above reaction and in turn, promotes the extraction rate.

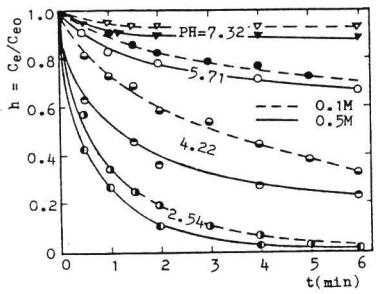

Fig.3 Effect of concentration of internal reagent and PH on h(N503)

C_{eo} = 63.9ppm, C_S = 4%, C_C = 1%, R_{mi} = 1, R_{ew} = 0.1, N = 400 r/min.

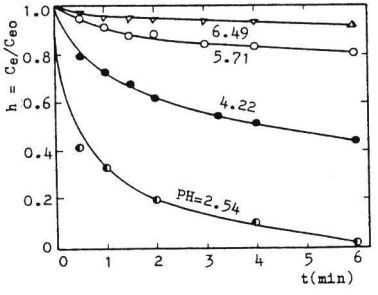

Fig.4 Effect of PH on h(DIBK)

C_{eo} = 63.9 ppm, C_S = 4%, C_C = 1%, R_{mi} = 1, R_{ew} = 0.1, N = 400 r/min, C_{io} = 0.1M Na_2SO_3/0.5M NaOH

Reuse of the emulsion

Generally, the equivalent ratio of the internal reagent to the extracted species is greater than one to lower the load in the demulsification. Therefore, the W/O emulsion must be recycled. In the experiments, the used W/O emulsion was reused to treat the fresh gold-containing solution. In this way, the W/O emulsion was repeatedly used for four times, and the typic results are shown in Fig.5. It can be seen that the remains of gold in the external phase increase after the W/O emulsion is reused, but when the extraction time is longer than six minutes, all the remains are almost the same. The attenuation of the emulsion is inevitable because its ageing leads to an increase in its viscosity. On the other hand, since the W/O emulsion undergoes the repeated coalescence and redispersion, the amount of the external phase water entrained in the W/O emulsion increases, which leads to the increase in the volume ratio of water in the emulsion (2). This also results in the increase in the viscosity of the emulsion. The viscoser the W/O emulsion, the slower the extraction rate. Therefore, much more excessive equivalent ratio ought to be avoided in the liquid surfactant membranes

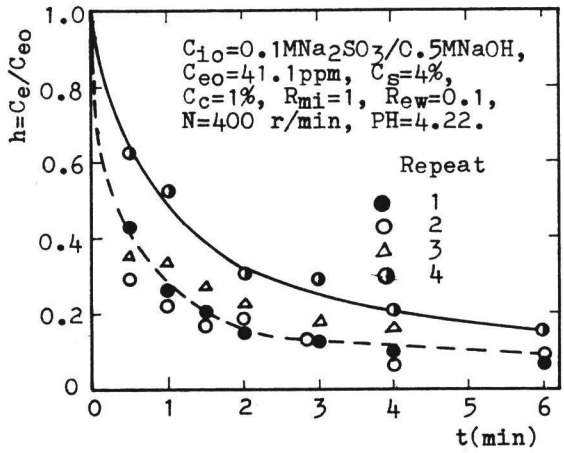

Fig.5 Reuse of the W/O emulsion

Extraction from the industrial gold-containing solution

Apart from the gold, the industrial solution contains silver, platinum, palladium, copper, iron, etc. In order to enhance the purity of gold, the selectivity of the extraction process is very important. Using N503, DBC, DIBK or MIBK as the carrier respectively, the results listed in Table 2 show that all the carriers extract gold selectively, while N503 give the fastest extraction rate and the best selectivity

Examination of the diffusion-reaction model

The diffusion-reaction model for Type II facilitated transport in the liquid surfactant membranes developed by the present authors (8) is tested by the experimental data on the extraction of gold. The results are shown in Fig.6. It can be seen that the experimental data are in good agreement with the model predictions

Table 2 Extraction from the industrial solution

Carriers	t (min)	C_e(ppm)						
		Au	Pt	Pd	Ag	Cu	Pb	Fe
N503	0	64.1	46.9	20.8	15.4	76.9	892	12.7
	2	1.7		20.3	15.2	76.8	875	12.1
	4	1.7	43.6	19.5	15.0	76.8	882	12.6
	6	0.8	40.7	18.7	14.6	76.8	875	12.2
	8	1.7	42.6	18.7	14.6	75.8	875	12.3
	10	0.8	42.6	18.0	14.6	75.8	869	12.3
DBC	0	65.8	42.9	20.7	12.1	78.0	761	13.3
	2	5.9	33.2	20.0	12.6	74.8	744	11.0
	4	0.9	35.1	21.0	12.2	73.0	737	11.8
	6	0.9	29.3	20.0	12.4	74.8	744	11.0
	8	0.9	29.3	19.0	12.4	73.6	737	10.7
	10	1.3	31.2	19.0	12.4	73.6	744	11.0
DIBK	0	65.8	42.9	20.7	12.1	78.0	761	13.3
	2	10.0	39.0	21.0	12.2	74.2	736	11.4
	4	2.3	29.3	21.0	12.4	75.3	746	11.0
	6	1.4	29.3	22.5	12.2	74.2	743	11.8
	8	0.9	31.2	20.0	12.2	74.2	743	11.0
	10	1.9	31.2	19.0	12.2	74.8	743	11.4
MIBK	0	64.1	42.9	20.9	14.4	76.9	893	13.5
	2	6.7	43.8	19.0	13.3	76.0	897	13.8
	4	1.0	42.8	19.0	13.3	76.0	883	13.8
	6	1.7	41.3	15.6	13.8	73.9	890	13.3
	8	1.0	41.3	16.4	13.8	73.2	869	13.8
	10	1.0	41.3	15.9	13.6	75.4	869	12.8

C_{io}=0.5M Na_2SO_3, C_s=4%, C_c=1%, C_H=1N HCl, N=400 r/min, R_{mi}=2, R_{ew}=1/3.

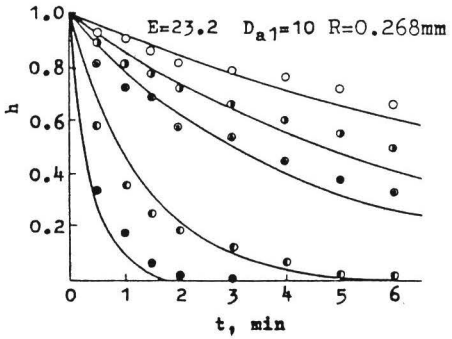

Fig.6 Test of the model predictions

	○	◑	●	◐	●
pH	5.71	4.92	4.22	2.54	1.05
B_i	6.87	5.49	3.93	2.75	2.29
D_{a2}	0.0425	0.0631	0.078	0.205	0.543
ε	0.208	0.260	0.362	0.518	0.622

R_{ew}=0.1, R_{mi}=1, C_s=4%, C_c=1%
N=400 rpm, T : 303K

CONCLUSIONS

The liquid surfactant membranes are useful to extract gold from its hydrochloric solution with polyamine E644 as the surfactant, N503, DBC or DIBK as the carrier and sodium sulfite as the internal reagent. Among the carriers, N503 gives not only the fastest extraction rate but also the best selectivity. The extraction rate increases with the decrease in PH in the external phase. The experimental data are in good agreement with the model predictions.

NOTATION

Bi — $kR/\alpha De$, Biot Module
Cc — carrier concentration in membrane phase, wt.%
Ce — solute concentration in the external phase, $kmol/m^3$
Ci — concentration of the internal reagents, $kmol/m^3$
C_H — hydrogen ion concentration in external phase, $kmol/m^3$
Cs — surfactant concentration in membranes, wt.%
Da1 — $k_r R^2/De$, Damkohler Module
Da_2 — $k_f R/\alpha D_e$, Damkohler Module
D_e — diffusivity in globules, m^2/s
E — three times of the equivalent ratio
h — C_e/C_{eo}, dimensionless concentration of gold in external phase
k — mass transfer coefficient in external phase, m/s
k_f — rate constant of forward extraction reaction, m/s
k_r — rate constant of backward extraction reaction, 1/s
N — stirring speed, r/min
R — radius of the emulsion globules, m
R_{ew} — volume ratio of emulsion phase to external phase
Rmi — volume ratio of membranephase to internal phase
t — time, min
Ve,Vi — volume of external and internal phase, respectively, m^3

Greek Letters

α — distribution coefficient between external and membrane phase
ε — perturbation parameter

Subscript

o — initial value

REFERENCES

1. Casamatta, G,, Bouchez, D. and Angelino, H., Chem. Eng. Sci., 33, 145(1978).
2. Yan Nianxi and Shi Yajun, J. Chem. Eng. Chinese Universities,1,65(1986).
3. Nishiki, T. and Bautista, R. G., AIChE J., 31(12), 2093(1985).
4. Shimidzu, T. and Okushita, H., J. Membr. Sci., 27, 349(1986).
5. Volkel, W., Bosse, J., Poppe, W., Halwachs, W. and Schugerl, K., Chem. Eng. Commun., 30, 55(1984).
6. Teramoto, M., Sakuramoto, T., Koyama, T., Matsuyama, H. and Miyake, Y., Sep. Sci. Technol., 21(3), 229(1986).
7. Yan Nianxi, Shi Yajun and Su Yuan-Fu, Stability of the W/O/W emulsions in liquid surfactant membranes, presented at the sixth symposium on separation science and technology for energy applications, Oct.22-26, 1989, Knoxville, Tennessee, USA.
8. Yan Nianxi, Shi Yajun and Su Yuan-Fu, Study on the liquid surfactant membranes, presented at the 2nd International Conference on Separation Science and Technology/39th Canadian Chemical Engineering Conference, Oct.1-4, 1989, Hamilton, Ontario, Canada.

Solvent Extraction 1990, T. Sekine (Editor)

© 1992 Elsevier Science Publishers B.V. All rights reserved

RECOVERY OF CHROMIUM (VI) FROM SULFURIC ACID SOLUTION BY LIQUID SURFACTANT MEMBRANE

Y. MORI, M. TANIGAKI and the late W. EGUCHI
Department of Chemical Engineering, Kyoto University,
Yoshida-Honmachi, Sakyo-ku, Kyoto 606 (Japan)

ABSTRACT

We deal with the recovery of chromium from a waste water containing sulfuric acid by both batch and continuous liquid surfactant membrane (LSM) operations, and investigate the proper condition of LSM process, the possibility of recycle use of the organic phase as the liquid membrane phase, and the prediction of the chromium concentration by a proposed transport model.

Chromium in the external feed solution was successfully transported and concentrated into the internal stripping solution containing lithium hydroxide through the organic phase of kerosene with 2-ethylhexyl alcohol and polyamine (Exxon Chem., ECA4360J) without any extractant. The recycle of the organic phase did not change the function of LSM, and the continuous operation using mixer-settler type extractors worked as a LSM process together with the developed continuous demulsifier by a.c. high electrostatic field.

A model for the chromium transport was presented, in which extraction of chromium, leakage of stripping phase, entrainment of feed phase, and permeation of water were taken into account. The experimental results on the continuous operation were found to be satisfactorily simulated by the proposed model with the experimental parameters from the batch data.

INTRODUCTION

This paper shows a series of our research works on the recovery of chromium (VI) from a waste water by liquid surfactant membrane (LSM) process. The proper condition of LSM operation, first, is investigated in batch experiments. Second, the transport model is proposed for the prediction of the chromium concentration. Finally, the continuous operations of LSM process are tested by one stage's and three stages' mixer-settler type apparatus, and the results are compared with the values calculated by the transport model.

1 BATCH OPERATION

1.1 *Experimental Procedure*

The stirred vessel used is 85 mm in inner diameter, 130 mm in height with four baffles of 8 mm in width and a water jacket. Stirring was carried out by a turbine impeller of 40 mm in diameter, located at 55 mm from the bottom of the vessel, with four flat blades whose width is 10 mm.

Water-in-oil (W/O) emulsions were prepared by a ultrasonic homogenizer using one part of the organic liquid membrane phase (kerosene with carrier, surfactant and modifier), and one part of the stripping solution (a 500 mol/m^3

LiOH aqueous solution). The 50 mL of emulsion was poured into the 450 mL of 50 mol/m^3 H_2SO_4 solution in the vessel using a pipette at 300 rpm stirring speed. The stirring speed was increased to 400 rpm, and 50 mL of a 50 mol/m^3 H_2SO_4 solution containing $K_2Cr_2O_7$ (1000 g/m^3 chromium) was introduced in the vessel. The time was taken to be the start of the experimental run.

Samples of the external aqueous chromium solution (feed phase) were taken periodically during the experiment. After 30 minutes of operation, the inner stripping solution was separated from the settled emulsion by an electrostatic coalescer operated at 8 kV a.c. of 1.8 kHz, reported by Mori *et. al* (1986). The concentrations of chromium, potassium and lithium in the feed and the stripping solutions were measured by atomic absorption method.

1.2 *Search for an Adequate LSM System for Chromium Removal*

Tertiary amine often are used as the carrier for the solvent extraction of chromium (VI). Figure 1 shows the time course change of chromium concentration in the feed phase, using Span 80 as the surfactant. The conditions of Run A are almost same as those employed by Hochhauser *et. al* (1975), that is the organic phase is kerosene with 4 vol. % tridodecyl amine, 2 vol. % Span 80 and 19 vol. % hexachlorobutadien. The chromium concentration in the feed phase decreased rapidly, as shown in Fig. 1, in a similar manner as reported by Hochhauser *et. al* (1975). The chromium concentration in the stripping phase after 30 minutes of LSM operation, however, was only 23 g/m^3, which indicated that most of chromium stayed in the organic phase. Run B is for a kerosene solution with 4 vol. % tri-*n*-octyl amine (TOA) and 5 vol. % Span 80 as the organic phase. Although chromium concentration in the feed phase decreased rapidly, the emulsions were completely broken in the early stage of the experimental run, as can be seen from the lithium concentration in the feed phase.

Figure 2 shows the results with polyamine (Exxon Chem., ECA4360J) instead of Span 80 as the surfactant. In Run C (polyamine + TOA), the chromium concentration in the feed phase decreased quickly to less than 1 % of the initial level. Chromium, however, was concentrated into the stripping phase only to 87 g/m^3 after LSM operation, and the formation of the gel-like chromium complex in the organic phase was observed. This gel was found to disappear when 2-ethylhexyl alcohol (EHA) was added to the organic phase. Run E is the operation with added EHA as a modifier in the organic phase. The behavior of the chromium concentration was very complex, and the concentration in the stripping phase after LSM operation was still low, approximately 130 g/m^3, although the gel-like complex disappeared.

Kerosene solution with EHA only did not form emulsion, and had no ability of chromium extraction. The emulsion made from a kerosene solution with polyamine did not transport chromium, as shown in Run F in Fig. 2. Chromium

transport, however, occurred when kerosene with EHA and polyamine but with no extracting reagent is used as the organic phase, as shown in Run G. The percent extraction reached 98 %, and chromium was concentrated approximately 1000 g/m^3 in the stripping phase. Finally we reached to the suitable condition of LSM operation, which is the usage of the organic phase of kerosene with 12 vol. % EHA and 2 vol. % polyamine, as reported by Mori *et. al* (1987).

1.3 *Transport Model*

The detailed study on the chromium extraction mechanism in the above system related that the overall extraction rate of chromium is expressed by the concentrations of $HCrO_4^-$ ion and the hydrogen ion in the feed phase (Mori *et. al* (1990)). In the case of the feed solution of 50 mol/m^3 H_2SO_4, however, the extraction rate can be approximated to be proportional to the first power of the total chromium concentration. The transport model includes the effects of the leakage of the stripping phase due to the breakage of the organic phase, the entrainment of the feed phase caused by the stirring and the permeation of water due to the difference in the total ionic concentration between the both aqueous phases.

The above transport model for batch operation can be expressed as follows; For chromium,

$$- d (V_I [Cr]_I)/dt = \{ k [Cr]_I - k_b [Cr]_{III} + k_t [Cr]_I \} a V_T \quad (1)$$

for lithium or potassium,

$$d (V_I [M]_I)/dt = \{ k_b [M]_{III} - k_t [M]_I \} a V_T \quad (2)$$

for the volume of the stripping phase,

$$dV_{III}/dt = \{ k_p (C_{III} - C_I) - k_b + k_t \} a V_T \quad (3)$$

where [ ] denotes concentration of specific ions and M refers to either lithium or potassium ions. C denotes for the total ion concentration. Subscripts I and III stand for the feed and the stripping phases. k stands for the overall extraction rate coefficient of chromium, and k_b, k_t and k_p are the rate coefficients of the leakage, the entrainment and the water permeation, respectively. V_T is the total volume and a is the specific surface area of the emulsion.

The value of the four parameters, k, k_b, k_t and k_p were determined to be 6.4×10^{-6} m/s, 3×10^{-10} m/s, 2×10^{-10} m/s and 3.6×10^{-15} $m^4s^{-1}mol^{-1}$, respectively. The time course changes of the metal concentrations and the water content of the emulsion, calculated with these rate constants, satisfactorily agreed with the observed ones as partly shown in Fig. 3 (Run G). The discrepancy between the model and the experimental data after ten minutes is considered to be due to the existence of chromium (III) in the feed phase, which can not be extracted by this LSM system.

1.4 *Recycle use of emulsion and the organic phase*

As a preliminary study for the continuous LSM operation, the possibility of the recycle use of the organic phase was investigated. Run G, H and I in Fig. 3 show the results for the first, the second and the third usage of the organic phase, respectively. These experimental results show that the recycle use does not affect the function of the LSM much, although the chromium concentration level became somewhat higher.

Run J shows the result of the LSM operation with the recycle use of the emulsion, which had been used in the former LSM experiment, and separated from the feed phase at the settler. This situation would simulate the emulsion recycle operation without demulsification, or of the multi-stages' mixer-settler operation without any treatment in each stage. The chromium concentration level in the feed phase was again somewhat higher compared with the case with a fresh emulsion. From the above preliminary experiments, it can be concluded that the present LSM system can be operated continuously.

2 CONTINUOUS OPERATIONS

2.1 *Experimental Procedure*

Figure 4 shows the flow diagram of the three stages' counter current mixer-settler LSM system, and the developed continuous electrostatic demulsifier. Keys D1, D2 and D3 show the flow dividers of the emulsion, which were used in experiments with emulsion recycle to concentrate chromium further into the inner stripping phase. The volumes of the mixer vessel V1, V2 and V3 are 550 mL, and the flow rate of the feed phase to the vessel V1 from tank FS was 50 mL/min. The overall ratio of the emulsion and feed rates was one to ten.

2.2 *One Stage Operation*

Figure 5 shows the continuous operation results using one stage mixer-settler (V3 and S3 in Fig. 4), with the mean residence times of ten minutes for both the feed solution and the emulsion. Chromium concentration in the feed phase decreased to 20 g/m^3 from 100 g/m^3 and it was concentrated to 800 $\sim$ 1000 g/m^3 in the stripping phase. No significant difference is noticed between the use of the new organic phase and that of the reused one. When the emulsion divider was used, the chromium concentration in the stripping phase increased up to 1500 $\sim$ 1900 g/m^3, approximately, double of the level in Fig. 5.

The continuous operation model can be introduced by the batch LSM model and considering the distribution of the residence time of the feed solution and the emulsion in the vessel. The lines in Fig. 5 were the concentrations calculated from the continuous operation model using the rate constants determined earlier and the condition of complete mixing in the vessel. The experimental data agreed well with the calculated value.

2.3 *Three Stages Operation*

Table 1 shows the result of 8 hours of continuous operation for the three stages' mixer-settler. Run L is for the counter current flow at the same conditions as in Fig. 5. The removal of chromium from the feed solution was 98.5 %, but the concentration in the stripping phase was less than for the one stage operation, because of the swelling of the emulsion. Run M is for the increased residence times of both the feed solution and the emulsion. The chromium concentration in the feed phase become lower, but that in the stripping phase also decreases due to the emulsion swelling. When the emulsion dividers was used (Run N), the chromium concentration in the stripping phase increased almost double of the value for Run L. The residence time of emulsion in the vessel may have a significant effect on the concentration of chromium.

Run O in Table 1 is for the parallel flow type instead of the counter current flow. The removal ratio was a little bit worse than that of the counter current case, because the chromium leakage caused by the emulsion breakage to the feed solution was higher. But the level of the concentrated chromium in the stripping solution was almost same as that of the counter current operation.

REFERENCES

Hochhauser, A.M. and Cussler, E.L., 1975. Concentrating chromium with liquid surfactant membranes. *AIChE Symp. Ser.*, 71: 136-142.

Mori, Y. and Eguchi, W., 1986. Coalescence of water-in-oil emulsion in a.c. high voltage field. *World Cong. III of Chem. Eng.*, 3: 235-238.

Mori, Y., Uemae, H., Hibino, S. and Eguchi, W., 1987. Composition conditions of surfactant liquid membrane for recovery and concentration of chromium (VI) contained in aqueous sulfuric acid solution. *Kagaku Kogaku Ronbunshu*, 13: 412-420.

Mori, Y., Shimokawa, K., Katho, H., Tanigaki, M. and Eguchi, W., 1990. Prediction model of the recovery of chromium (VI) from sulfuric acid solution by batch type liquid surfactant membrane operation, *in preparation.*

Table 1

Chromium concentrations (g/m^3) of the feed and the stripping phases and water content (vol. %) in the emulsion during three stages' LSM operations.

Run	feed phase at S1	feed phase at S2	feed phase at S3	stripping phase at S1	water content of emulsion st S1
L	30.0	6.8	1.5	700	68.0
M	18.5	2.8	1.1	600	69.0
N	28.0	6.7	2.5	1300	70.0
O	32.0	8.2	3.4	600	-

L : The experimental conditions are same as those in Fig. 5. The residence time is 10 minutes.

M : Both flow rates of the feed solution and the emulsion are decreased. The residence time is 15 minutes.

N : The emulsion streams of same flow rate were produced at the dividers.

O : Parallel flow type. Other conditions are same as Run L.

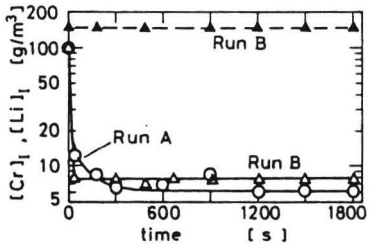

Fig. 1 Time course changes of concentrations of chromium (○,△) and lithium (▲) in the feed phase with Span 80 as the surfactant.

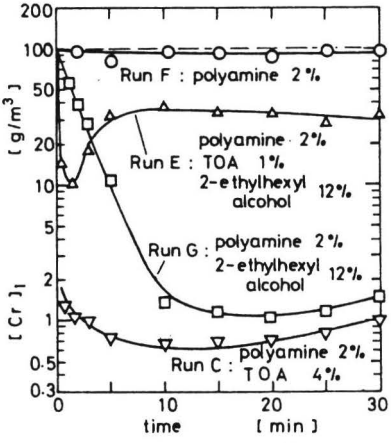

Fig. 2 Time course changes of chromium concentration in the feed phase with polyamine as a surfactant.

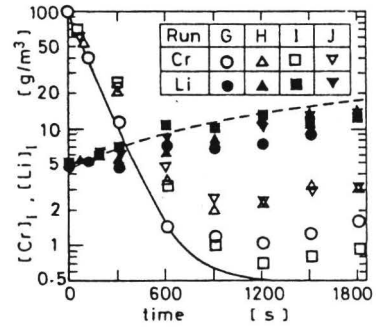

Fig. 3 Effects of the reuse of the organic phase or emulsion on LSM operation. Runs G, H, and I are the first, second and third use of the organic phase, respectively. Run J is for the recycle use of the emulsion without demulsification.

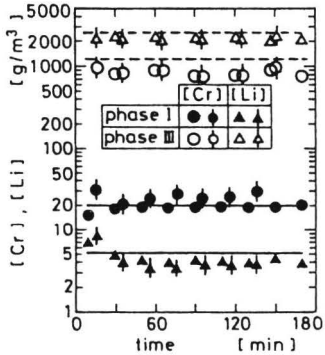

Fig. 5 Comparison of the experimental results between the fresh organic phase (normal keys) and the reused organic one (keys with vertical line) at one stage's continuous operation.

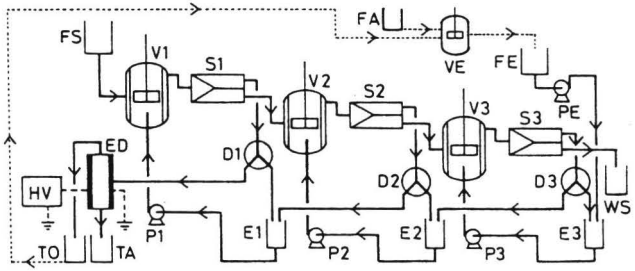

Fig. 4 Flow diagram of the three stages' counter current mixer-settler LSM system. (FS : tank for fresh feed solution, WS : tank for treated feed solution, FA : tank for stripping phase, VE : emulsifier, FE : fresh emulsion tank, V1, V2, V3 : mixers for extraction, S1, S2, S3 : settlers, E1, E2, E3 : tanks for emulsion feed, D1, D2, D3 : emulsion divider, PE, P1, P2, P3 : pump to send emulsion, ED : demulsifier, HV : high voltage generator, TA :demulsified stripping phase containing concentrated chromium, TO : tank for the organic phase).

Solvent Extraction 1990, T. Sekine (Editor)

© 1992 Elsevier Science Publishers B.V. All rights reserved

MEMBRANE BEHAVIOUR IN CHROMATE RECOVERY USING EMULSION LIQUID MEMBRANES.

SALAZAR, E., M.I. ORTIZ, A. IRABIEN*.
Dpto. Ingeniería Química. Fac. Ciencias, UPV-EHU, Apdo. 644-48080 Bilbao. Spain.

ABSTRACT

Membrane behaviour is one of the most important factors affecting metal recovery with emulsion liquid membranes. After selection of the membrane components, extractant, solvent and stabilizer, a careful investigation must be performed in order to choose properly the surfactant that allows to obtain the highest yield of extraction and recovery of the metal.

In this work several surfactants have been added, SPAN-80, BRIJ-72, BRIJ-92 and PARANOX 106 to the organic membrane used for chromium (VI) recovery in a batch ELM process using Aliquat 336 as extractant disolved in kerosene and n-decanol as stabilizer. The membrane behaviour with each surfactant has been analyzed.

INTRODUCTION

Since the first work of Hochhauser and Cussler (1975) several papers have been published reporting the viability and modelling of chromium (VI) recovery from aqueous effluents with emulsion liquid membranes, (Salazar et al 1989, 1990a, 1990b).

ELM offer high transport rates due to the large mass transfer area per unit volume, allowing simultaneous separation and concentration of the metal under practical conditions. The fundamentals of the recovery of Cr (VI) with ELM consist on the transport of the CrO_4^{2-} anion through its reaction with a quaternary ammonium salt Aliquat 336, and breakage of the formed complex in the stripping side (a caustic solution). Aliquat 336 is disolved in kerosene and n-decanol is added to avoid losses of the extractant due to its solubility in the aqueous phases. In order to allow the recycling of Cr (VI) to the industrial process, high ratios between the feed and stripping aqueous phases are needed (Ao/Ai=100/1, 50/1) making necessary an analysis of the membrane behaviour and related variables.

The surfactant has a very important role in the formulation of the organic membrane as it is related to its stability as well as to other phenomena such as water transfer due to osmosis. On the other hand mass transfer resistance to the metal transport usually increases with concentration of the surfactant.

In this work the influence on the behaviour of the liquid membrane for chromium (VI) recovery of common surfactants, SPAN-80, PARANOX-106, BRIJ-72 and BRIJ-92 has been studied.

*Author to whom correspondence should be adressed.

MATERIALS

The materials, set-up and experimental procedure have been reported elsewhere (Salazar et al., 1990a).

RESULTS

Experimental conditions are listed in table 1

TABLE 1

Experimental conditions

Cr(VI) = 50 mg/l	t_r = 10 min	Extractant = 3% V_o
$\omega_{stirrer}$ = 300 rpm	A_o/A_i = 50/1-100/1	stabilizer = 5% V_o
$NaOH_{str}$ = 0.2-1.0 N	O/A_i = 2/1-3/1	surfactant = 3%-7% V_o

After membrane formation it was put into contact with the feed solution in a batch stirred contactor and the process was allowed to run out for 10 minutes. The organic membrane and the feed solution were settled and separated. The volume of the inner stripping solution was measured and the Cr (VI) concentration was analyzed by atomic absorption spectrometry and ion exchange chromatography.

Results of water permeation, extraction yield and Cr (VI) concentration in the stripping phase for the experiments performed with the studied surfactants are shown in table 2. Replicate experiments were performed (three for each surfactant), so that mean values are reported.

TABLE 2

Experimental results: *SPAN-80=7%V_o; NaOH=0.2N **Surfactant=5%V_o; NaOH=0.2N; ***PARANOX-106=1.5%V_o; NaOH = 1N.

	*SPAN-80 A_o/A_i: 50/1	**BRIJ-72 A_o/A_i: 50/1	**BRIJ-92 A_o/A_i: 50/1	***PARANOX 106 A_o/A_i: 100/1
ΔV_i	10%	6%	40%	20%
extraction yield (%)	89	96	97.1	96.9
Cr (VI) at the stripping phase (g/l)	1.9	1.226	1.00	3.945

In the experiments performed with SPAN-80 the aqueous phases were titrated with HCl obtaining the conclusion that the surfactant reacted with the NaOH of the stripping phase. This reaction lowered the concentration of the surfactant and therefore accelerated the membrane breakage.

Water transport from the outer to the inner aqueous phase was significant in the experiments performed with SPAN-80, BRIJ-72 and BRIJ-92. The emulsifying capacity of these two last surfactants was so high that they took out water from the external aqueous phase, growing up the traped aqueous phase volume and diminishing the concentration of the stripped Cr (VI).

The behaviour of PARANOX-106 was the most interesting for a practical use because the water transport was minimized,it did not react with the stripping agent and the stability of the emulsion allowed to reach a high extraction of Cr (VI) from the feed solution and a high concentration in the stripping phase.

Two different sets of experiments have been performed, a study of the influence of the surfactant concentration on the behaviour of the liquid membrane (the rest of the variables were kept constant) and the analysis of the influence of the carrier concentration on the rate and on the yield of Cr (VI) extraction (keeping the rest of the variables at constant values).

Experimental conditions of the two sets of experiments are listed in table 3.

TABLE 3

Experimental conditions

w_{stirr} = 300 rpm	t_e = 10 min	t_r = 10 min
A_o/A_i = 100/1	O/A_i=3	Cr (VI) = 20 mg/l
NaOH = 1.0 N	Stabilizier = 5% V_o	
1st SET: surfactant = 1-5%V_o	Extractant = 0.5%V_o	
2nd SET: Extractant = 0.25-3%V_o	Surfactant = 5%V_o	

Results of water permeation, extraction yield and Cr (VI) concentration in the stripping phase after 10 minutes of operation for the two sets of experiments are shown in tables 4 and 5 respectively.

TABLE 4

Experimental results using different surfactant (PARANOX 106) concentration.

	SURFACTANT (% V_o)				
	1.0	1.5	2.0	3.0	5.0
ΔV	10%	30%	56.7%	120%	160%
Extraction yield (%)	95.8	92.6	97.0	97.6	98.2
Cr (VI) in the stripping phase (g/l)	1.525	1.236	1.005	0.690	0.543

TABLE 5

Experimental results using different extractant (Aliquat 336) concentration.

	EXTRACTANT (%V_o)			
	0.25	0.50	1.0	3.0
ΔV	226.7	160	188	193.3
Extraction yield (%)	82.1	98.2	97.5	98.2
Cr (VI) in the stripping phase (g/l)	0.386	0.543	0.578	0.426

The evaluation of the results of the first set of experiments indicates that the water transport across the organic membrane is closely related to the surfactant concentration. As result the chromium (VI) concentration in the inner aqueous phase could be dramatically lowered.

The relationship between the water trnsport and the surfactant concentration is shown in Figure 1.

The influence of the extractant concentration on the overall yield of the ELM process is negligible, it modifies only the rate of Cr (VI) separation from the aqueous external phase.

The surfactant used, PARANOX 106, is alkaline and could be ionized to produce an anionic polar group that may react with the carrier Aliquat 336 to form an oil-soluble salt in the membrane. This reaction could remove the extractant from the membrane giving lower extraction rates. In this work this effect has not been observed.

Finally it has been selected the best membrane composition: stabilizier=5%, surfactant=1.5%, extractant=0.5%, and it has been applied to the metal separation process for different Cr (VI) concentrations in the aqueous external phase. Cr (VI)=20-80 mg/l.

Figure 2 represents the extraction yield vs Cr (VI) concentration in the external aqueous phase.

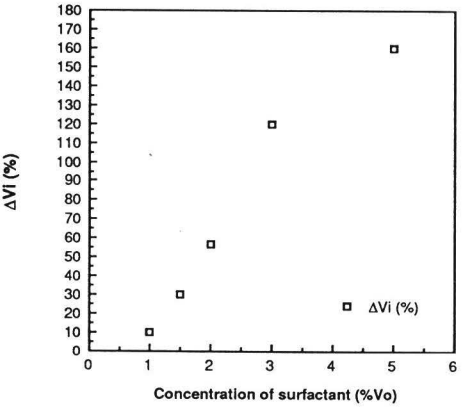

Figure 1. Water transport vs surfactant concentration

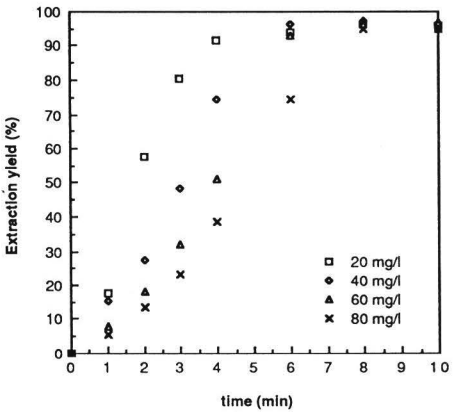

Figure 2. Extraction yield vs Cr(VI) concentration

REFERENCES

Hochhauser, A.M., Cussler, E.L., 1975, Concentrating Chromium with liquid surfactant membranes, AIChE, Symp. Ser., 71(152).

Salazar, E., Ortiz, M.I., Irabien, J.A., 1989, Recovery of Cr (VI) with emulsion liquid membranes in mechanically stirred contactors, 7th International Conference "Chemistry for Protection of the Environment", Lublin (Poland).

Salazar, E., Ortiz, M.I., Irabien, J.A., 1990a, Recovery of Cr (VI) with ELM in mechanically stirred contactors. Influence of membrane composition on the yield of extraction, EXTRACTION'90 Caithness, United Kingdom.

Salazar, E., Ortiz, M.I., Irabien, J.A., 1990b, Recovery of Cr (VI) with ELM in mechanically stirred contactors. Influence of surfactant on the yield of extraction, CHISA'90, Prague, Czechoslovak.

ACKNOWLEDGEMENTS

This work has been finantially supported by the Basque Government under Project 069.310-0014/89 and Research Grant (E. Salazar).

Solvent Extraction 1990, T. Sekine (Editor)

© 1992 Elsevier Science Publishers B.V. All rights reserved

HIGHLY SELECTIVE SEPARATION OF ORGANIC SOLUTES BY AQUEOUS LIQUID SURFACTANT MEMBRANES:

ULBRICH, M.; MARR, R.; DRAXLER, J.;
Institute of Chemical Engineering and Environmemtal Technology
University of Technology Graz, Inffeldgasse 25, 8010 Graz, Austria

ABSTRACT:
For the realization of highly selective separations the unwanted transport of components with a low solubility in the aqueous membrane has to be minimized. The emulsion breakup and the transport by solubilization in surfactant micelles are the main reasons for the unwanted transport. After a separate measurement of the emulsion breakup and the mass transfer area it was possible to investigate the influences of various parameters on the diffusional monomer transport and the micelle facilitated transport through the membrane. On the basis of the results of the separate measurement of emulsion breakup and transmembrane transport it is shown with the test mixture of toluene and n-heptane, how various parameters influence the selectivity of the toluene n-heptane separation.

1. INTRODUCTION:

The interest in aqueous liquid membranes for the separation of hydrocarbons was comparably low since Li (1968,1971) proposed it about 20 years ago. But during the last five years many research groups (Goswani et al.,1985; Plucinski et al.,1985; Son-ki Ihm et al.,1987; Kato et al.,1987) have investigated nearly all parameters, which influence the mass transfer through aqueous liquid membranes.

Due to the concentration difference between the feed phase (phase I) in the emulsion and the receiving phase (phase III), the more membrane soluble compounds permeate preferentially out of the emulsion into the receiving phase. Membrane insoluble compounds should remain almost completly in the emulsion, but there are two mechanisms, which are responsible for the unwanted transport of the generally non permeating compounds. On the one side the emulsion breakup during the permeation results in a nonselective mixing of the feed phase with the receiving phase (Krishna et al.,1987) and on the other side the solubilization of normally non water soluble compounds in surfactant micelles enables their transport through a surfactant membrane (Plucinski, 1988).The key to reach highly selective separations of organic solutes by aqueous liquid membranes is to investigate these phenomena.

2. EXPERIMENTAL:

2.1. Materials:

Usually feed phase I contained an equimolar mixture of toluene and n-heptane. The concentration of the emulsion breakup tracer hexadecane in the breakup experiments was 40 g/l. All chemicals used for the feed phase were of minimum 99% purity and were supplied by Merck.

The aqueous membrane phase II consisted of distilled water and various surfactants. The nonionic surfactant Tween 20 was supplied by Merck. The anionic surfactant sodium dodecyl sulfate (SDS) from Merck and the cationic surfactant dodecyltrimethylammonium bromid (DTAB) from SIGMA were both of 99% purity. The sodium alkyl sulfates decyl sulfate (SDeS), dodecyl sulfate (SDS), tetradecyl sulfate (STS), hexadecyl sulfate (SHS) and octadecyl sulfate (SOS) were test samples of the Henkel KGaA with a minimum 99% purity. The receiving phase III always consisted of dodecane with 99% purity.

2.2. Procedure:

The organic feed phase was emulsified in the aqueous surfactant membrane solution with a high speed stirrer Ultraturax T 50 of IKA (Janke & Kunkel) at 7500 rpm for 20 minutes. 15 minutes after emulsification 200 ml of the oil-in-water emulsion were contacted with 400 ml receiving phase in a glas agitator vessel at 250 rpm.

3. MASS TRANSFER EVALUATION:

As shown in Fig.1 the whole mass flow N is divided in a part due to emulsion breakup N_{Break} and a part due to a more or less selective diffusional transport by monomers and surfactant micelles N_{Dif}

$$N = N_{BREAK} + N_{Dif} \qquad (1)$$

The mass flow by emulsion breakup was measured with hexadecane as a breakup tracer in the feed phase. Hexadecane guarantees a neclectable membrane transport by solubilisation, but even at small concentrations it acts as a mass transfer barrier according to the emulsion degradation theory of Higuchi (1962). Nevertheless, by carrying out two identical experiments with and without hexadecane it was possible to measure the exact emulsion breakup in one experiment and the unaffected mass transport in a second experiment.

For the description of the mass flow by diffusional transmembrane transport N_{Dif} we made the following assumptions:

1. The main mass transport resistance lies in the aqueous membrane and the surfactant layers at the oil-water interfaces.
2. The mass flow is proportional to the emulsion drop surface A_{III}.

3. The partition equilibrium is reached for both oil water interfaces with a constant partition coefficient m.
4. The membrane concentration at the feed droplet interface C_{MI} is a mean value across a emulsion drop.

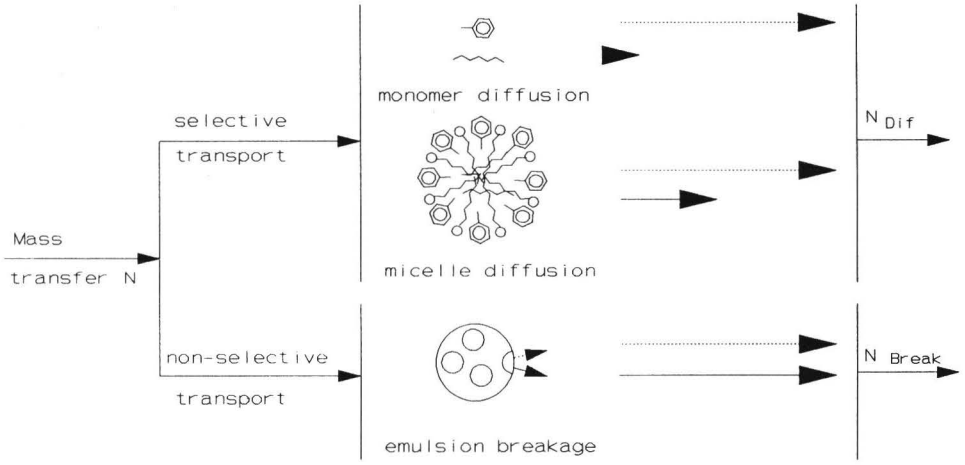

Fig. 1. Schematic diagram of the mass transport mechanism for aqueous surfactant membranes.

With the above assumptions we may put up the simple steady state equation for a feed component A

$$N_{Dif\,A} = K_A\, A_{III}\ (\ CMI_A - CMIII_A\ ) \qquad (2)$$

The overall mass transfer coefficient for the membrane K_A could be calculated from measureable variables:

$$K_A = \frac{N_A - N_{Break\,A}}{A_{III}\ (\ CI_A - CIII_A\ )} \qquad (3)$$

The surface of the emulsion drops A_{III} was evaluated with a photographic method.The selectivity of the toluene-heptane separation was estimated by the ratio of the overall mass transfer coefficients K_{tol}/K_{hep} and the selectivity ß, which includes the mass transfer by emulsion breakup.

$$ß = \frac{CIII_{tol}\ \ CI_{hep}}{CI_{tol}\ \ CIII_{hep}} \qquad (4)$$

4. RESULTS AND DISCUSSION:

4.1. Effect of surfactant kind and permeation time :

For sufficient stable emulsions the K_{tol}/K_{hep} ratio for different surfactants is shown in Fig.2.

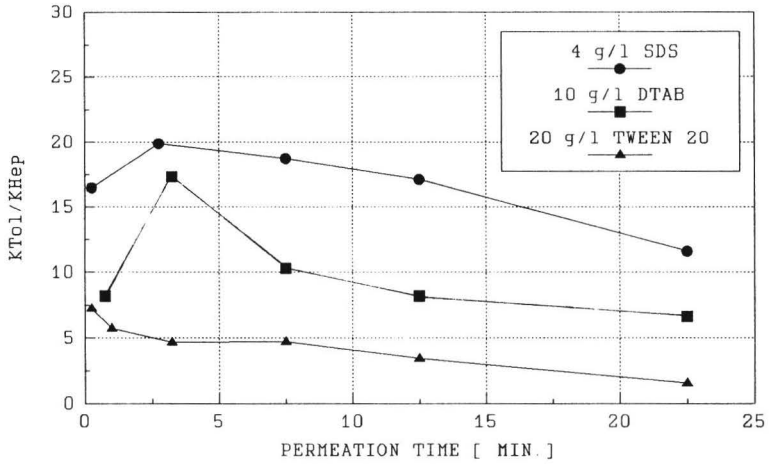

Fig.2. Overall mass transfer coefficient ratio K_{tol}/K_{hep} for various surfactants. (Φ = 0,583 ; $VIII^0/V_E^0$ = 2 ; T = 20 °C)

With 4 g/l SDS in the membrane phase the lowest amounts of heptane diffuse mostly by monomer diffusion through the membrane and result in the highest K_{tol}/K_{hep} ratios. The very effective solvating nonionic surfactant Tween 20 forms at concentration of 20 g/l many micelles, which carry a lot of heptane through the membrane. The cationic surfactant DTAB shows a much higher heptane transport rate as SDS but due to the high toluene transport rate the K_{tol}/K_{hep} ratio is comparable high.

4.2. Effect of the surfactant chain length of sodium alkyl sulfates:

The overall mass transfer coefficient for toluene K_{tol} increases considerably while the K_{hep} slighty decreases with increasing hydrophilic chain length of the surfactant in the membrane phase.

Whereas the increasing K_{tol} values could be explained with higher micelle transport rates, because of the low CMC's of long chain alkyl sulfates the slightly decreasing heptane transport is difficult to explain. A possible explanation for the reduced heptane transport might be a steric hindrance in the surfactant layer at the interface. The resulting increase of the K_{tol}/K_{hep} ratio and the selectivity ß is shown in Fig. 3.

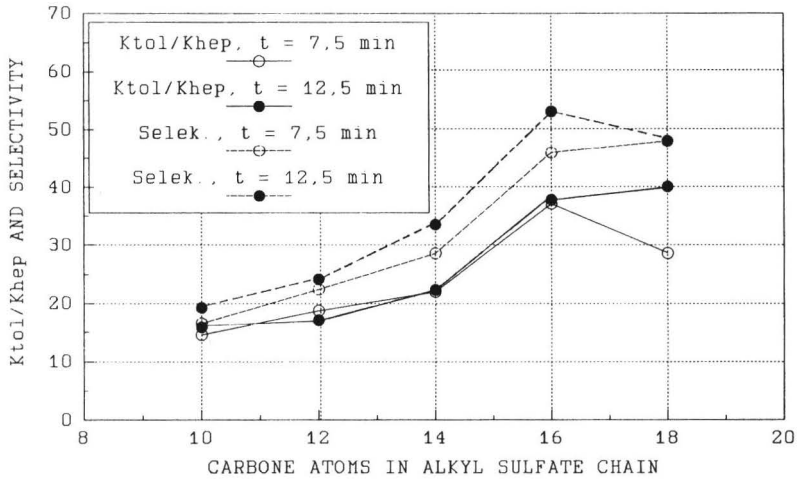

Fig.3. K_{tol}/K_{hep} ratio and the selectivity ß for sodium alkyl sulfates with different chain length. (Φ = 0,583; $VIII^0/V_E^0$ = 2; T = 20°- 45°C, c_S = 4 g/l).

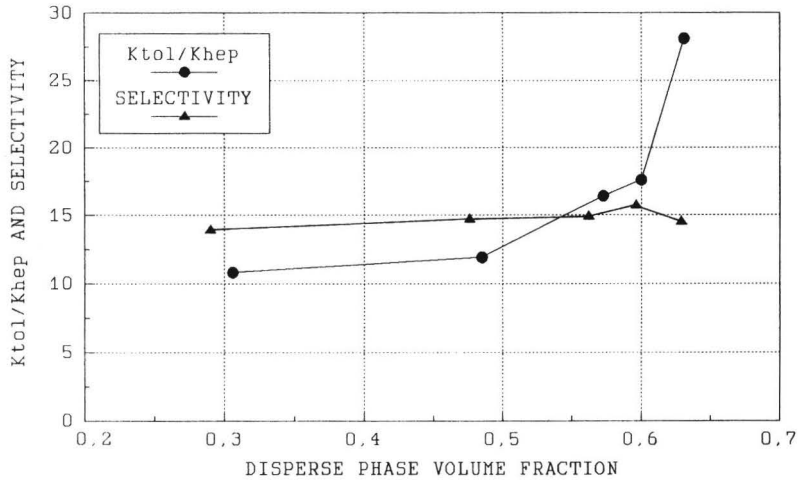

Fig. 4. K_{tol}/K_{hep} ratio and selectivity ß for various disperse volume fractions Φ in the emulsion. ($VIII^0/V_E^0$ = 2 ; T = 20°C; c_S = 4 g/l SDS)

4.3. Effect of the disperse phase volume fraction in O/W-emulsion:

Contrary effects of the disperse phase volume fraction Φ on the overall mass transfer coefficients of toluene and heptane are responsible for the steep increase of the K_{tol}/K_{hep} ratio at high Φ values, shown in Fig.4. At higher

disperse phase contents of the emulsion the increasing oil water interface needs more adsorbed surfactant and the remaining surfactant in the bulk of the membrane forms fewer micelles. Because the heptane transport needs these surfactant micelles the K_{hep} value decreases with increasing Φ. The toluene transport depends, at a surfactant concentration slightly above the CMC, more on the monomer diffusion and the thinner aqueous membrane at higher Φ values is responsible for a lower mass transfer resistance and a higher K_{tol} value. The selectivity ß decreases at high disperse phase volume fractions, because of the great increase of the emulsion breakup. The optimal disperse phase volume fraction for 4 g/l SDS lies around Φ = 0,6.

5. CONCLUSION:

The separate investigation of emulsion breakup and selective transmembrane transport gave new insights into the transport by monomer diffusion and by surfactant micelle diffusion. It was shown that beside the ability to stabilize the oil-in-water emulsion, the solvating properties and the permeability of the interface film of the surfactants have to be considered for a careful surfactant selection for an optimal separation by aqueous membranes. The fundamental results of this study are the basis of a modeling of the mass transfer and of the realization of a highly selective separation of hydrocarbons with aqueous surfactant membranes.

REFERENCES:

Casamatta, G.,Chavarie, C.,Angelino,H.,1978.Hydrocarbon separation through a liquid water membrane: modeling of permeation in an emulsion drop. AIChE Journal,Vol.24,No.6,945-49.

Goswami, A.N., Rawat, B.S.,1985. Studies on the permeation of aromatic hydrocarbons through liquid surfactant membranes. J.Memb.Sci.,24,145-68

Higuchi, W.I. and Misra,J.,1962. Physical degradation of emulsions via the molecular diffusion route and the possible prevention thereof. J.Pharm.Sci. 51,459-66

Kato,S. and Kawasaki,J.,1987. Enhanced permeation of hydrocarbons through liquid membranes by liphophilic surfactants. J.Chem.Eng.Japan,Vol.20,No.2, 140-45

Krishna, R., Goswami, A.N., Sharma, A.,1987. Effect of emulsion breakage on the selectivity in the separation of hydrocarbon mixtures using aqueous surfactant membranes.J.Memb.Sci.,34,141-54

Li, N.N.,1968. U.S. Patent,3,410,794,

Li, N.N.,1971. Permeation through liquid surfactant membranes. AIChE Journal, Vol.17, No. 2, 459-63.

Plucinski,P., 1985. The influence of solubilization upon the permeation of aromatic hydrocarbons through liquid membranes. J.Memb.Sci., 23, 105-109.

Plucinski, P., Szust, J., 1988. An Approach to the mathematical description of the permeation of hydrocarbons through liquid membranes. J.Memb.Sci., 38, 261-79.

Son-Ki Ihm, Yeon-ho Jeong and Yang-Soo Won, 1987. Experimental investigation of the oil/water/oil liquid-membrane separation of toluene and n-heptane. J.Memb.Sci., 32,31-57.

Solvent Extraction 1990, T. Sekine (Editor)

© 1992 Elsevier Science Publishers B.V. All rights reserved

NEWLY DEVELOPED WAY TO IMPROVE SEPARATION SELECTIVITY IN LIQUID MEMBRANE PERMEATION FOR HYDROCARBON SEPARATION

R. EGASHIRA and J. KAWASAKI
Dept. of Chem. Eng., Tokyo Inst. of Tech.,
Meguro-ku, Tokyo 152 (JAPAN)

ABSTRACT

The simulation of permeation and separation in an emulsion drop by a Multi-layer liquid membrane model suggested the simple way to improve the separation selectivity of this technique. Batch experiments of permeation confirmed this suggestion.

1 INTRODUCTION

It has been pointed out that the separation selectivity of emulsified liquid membrane is lower than that of an ideal flat liquid membrane (Kato and Kawasaki, 1986, 1987). There are no reports which account for the reason of this fact. In this work, permeation and separation in emulsion drops were simulated by a Multi-layer liquid membrane model. This led to suggestion of the simple way to improve the separation selectivity, which was confirmed qualitatively by the experimental data.

2 SIMULATION OF SEPARATION BY MULTI-LAYER LIQUID MEMBRANE MODEL

2.1 Permeation mechanism within an emulsion drop

Inner oil phase is divided by aqueous membrane phase in emulsion drops. Hydrocarbons permeate, therefore, through the inner oil phase itself and the aqueous membrane phase alternately toward the outer oil phase.

The characteristic permeation path was simulated by an one-dimensional Multi-layer liquid membrane model, as shown in Figs.1(a) and (b). The left end of the model emulsion in Fig.1(a) corresponds to the core of an actual emulsion drop and the right one to the interface between aqueous membrane phase and outer oil phase. It was assumed that the inner oil phase was divided into oil layers of same thickness by membrane lay-

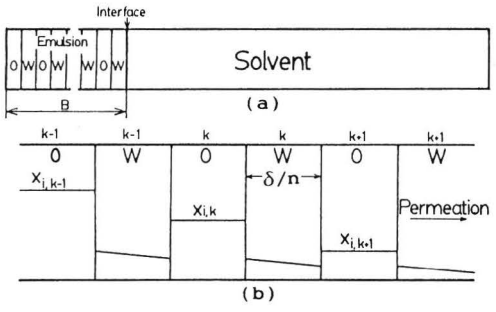

Fig.1. Schematic diagram of one-dimensional Multi-layer liquid membrane model.

ers of constant thickness.

2.2 Procedure and conditions of calculation

The equations of mass ballances are written as follows;

$$dE/dt = -dR/dt \tag{1}$$

$$d(Ey_i)/dt = -d(Rx_i)/dt \tag{2}$$

$$\sum_{k}^{n} R_k = R \tag{3}$$

$$\sum_{k}^{n} (R_k x_{i,k}) = Rx_i \tag{4}$$

The controlling resistance is assumed to exist in the aqueous membrane layers, the equations of transfer rates are represented as follows;

$$\frac{d(R_1 x_{i,1})}{dt} = \frac{\rho D_i H_i}{\delta/n} A(x_{i,2} - x_{i,1}) \tag{5}$$

$$\frac{d(R_k x_{i,k})}{dt} = \frac{\rho D_i H_i}{\delta/n} A(x_{i,k-1} + x_{i,k+1} - 2x_{i,k}) \quad (2 \leq k \leq n) \quad (R_{n+1}=E,\ x_{i,n+1}=y_i) \tag{6}$$

$$\frac{d(Ey_i)}{dt} = \frac{\rho D_i H_i}{\delta/n} A(x_{i,n} - y_i) \tag{7}$$

The initial condition is;

$$t=0;\quad x_{i,k}=x_{i0}\ (1 \leq k \leq n),\ y_i=0 \tag{8}$$

These equations were solved numerically by 4th Runge-Kutta Method under the conditions as summarized in Table 1.

TABLE 1

Conditions of calculation

Feed	benzene	m-xylene	n-hexane	n-nonane
mass fr.	0.20	0.20	0.55	0.05
Membrane	water			
Solvent	iso-Octane			

Total volume	400 cm^3
Volume fraction of emulsion	0.25
Volume fraction of oil in emulsion	0.5 ($\therefore$ $\delta=B/2$)
Contact area	2000 cm^2
Number of membrane layer	1, 2, 5, 10, 20, 50

2.3 Results and discussions

The concentrations of the more permeable components (benzene and m-xylene) decreased and those of the less permeable components (n-hexane and n-nonane) increased with the layer number as shown in Figs.2(a) and (b). These

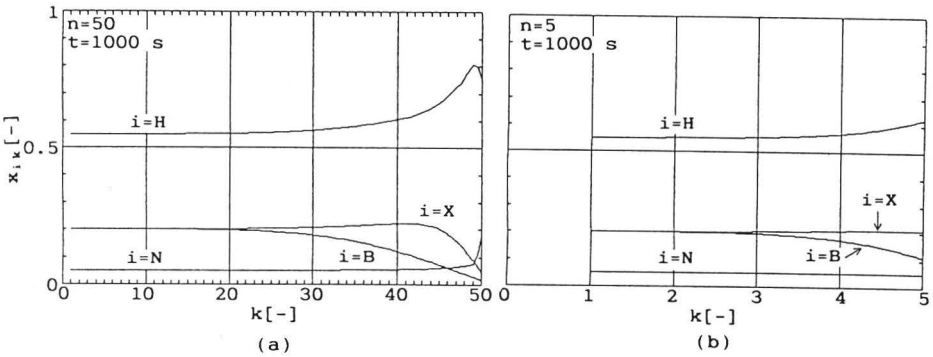

Fig.2. Concentration profiles of hydrocarbons in emulsion drop. (a) n=50. (b) n=5.

profiles, typical in bulk separation, were more obvious in the case with the larger number of the layers.

The permeation coefficient was calculated by following equation.

$$d(Ey_i)/dt = P_i A(x_i - y_i) \qquad (9)$$

Figures 3(a) and (b) show that the permeation coefficients of benzene (the most permeable component) decreased sharply with time and those of n-hexane (the less permeable component) increased at the first and decreased slowly after reaching a maximum. These tendencies were observed more prominently, especially in the case with the larger number of the membrane layers. The permeation coefficient in the case with the larger number of the layers was higher than that with the smaller number of the layers.

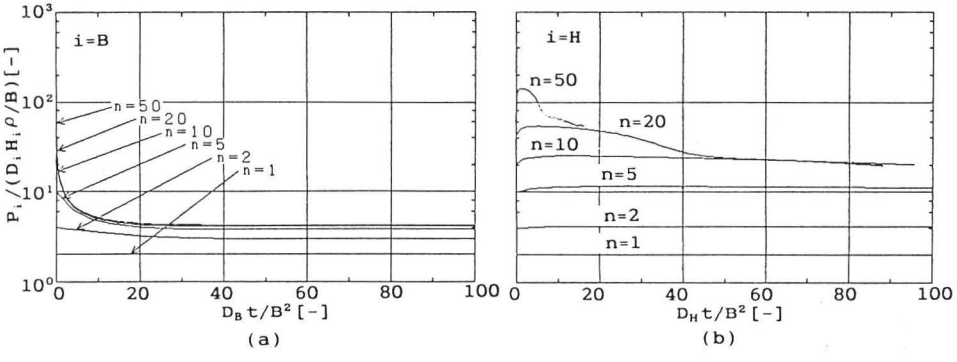

Fig.3. Permeation coefficients of (a) benzene and (b) n-hexane.

The separation selectivity of component i relative to component j was defined as follows;

$$\beta_{ij} = P_i / P_j \qquad (10)$$

The separation selectivity of benzene to n-hexane decreased with the number of the membrane layers (Fig.4).

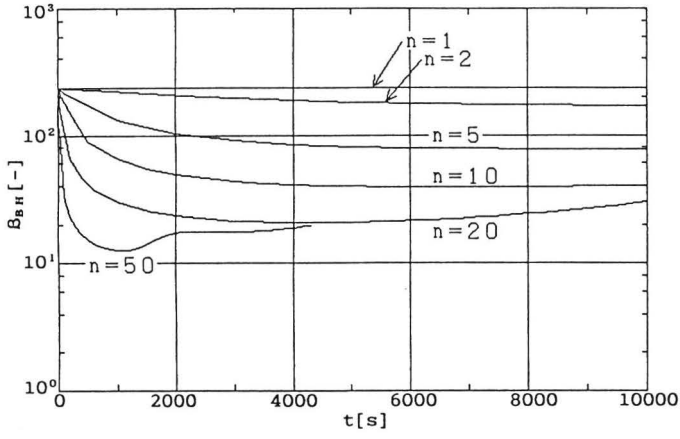

Fig.4. Separation selectivities of benzene relative to n-hexane.

The number of the membrane layers in model emulsion might correspond to that of the inner oil droplets in an actual emulsion drop. It was suggested, therefore, that the separation selectivity would be improved by decreasing the number of inner droplets in an emulsion drop.

3 BATCH PERMEATION IN STIRRING VESSEL

3.1 Experimental apparatuses and conditions

Two kinds of emulsifiers were employed to vary the diameter of the oil droplet in emulsion. The diameter of the droplet in emulsion prepared by the high speed homogenizer (H.S.H.) was about 2×10^{-6} m (Case A) and that by the

TABLE 2

Experimental conditions

Feed	benzene-m-xylene-n-hexane(-n-nonane)				
mass fr.	I	0.20	0.20	0.55	0.05
	II	0.10	0.10	0.75	0.05
	III	0.05	0.05	0.85	0.05
Membrane	water (0.8 vol.fr.)-glycerol (0.2 vol.fr.)-saponin (0.002 mass fr.)				
Solvent	iso-Octane				

Total volume	400 cm^3
Volume fraction of emulsion	0.25
Volume fraction of oil in emulsion	0.50
Stirring velocity	7.5, 10, 12.5, 15 1/s
Temperature	30 °C

stirring vessel (S.V.) was 2×10^{-5} m (Case B). The emulsion after permeation run was demulsified thermally. Inner and outer oil phases were analyzed by the gas chromatograph. The experimental conditions were summarised in Table 2. N-nonane was used as the tracer to measure the rate of membrane breakage. Iso-octane was used as both solvent and the tracer to detect mechanical entrainment.

3.2 Results and discussions

The transfer rate of permeates i was defined as follows (Kawasaki et al., 1987);

$$\frac{d(Ey_i)}{dt} = P_iA(x_i - y_i) + \frac{x_i}{x_N} \cdot \frac{d(Ey_N)}{dt} - \frac{y_i}{y_O} \cdot \frac{d(Rx_O)}{dt} \qquad (11)$$

The volumetric permeation coefficients of permeates (P_iA), calculated by eq. (11), are shown in Fig.5. The P_iA decreased with time. The larger the stirring velocity, the larger the P_iA. The P_iA in Case A were larger than those in Case B. These were observed similarly in the cases with other feed compositons.

Figure 6(a) shows that the separation selectivities of benzene and m-xylene to n-hexane, calculated by eq. (10), in Case B were higher than

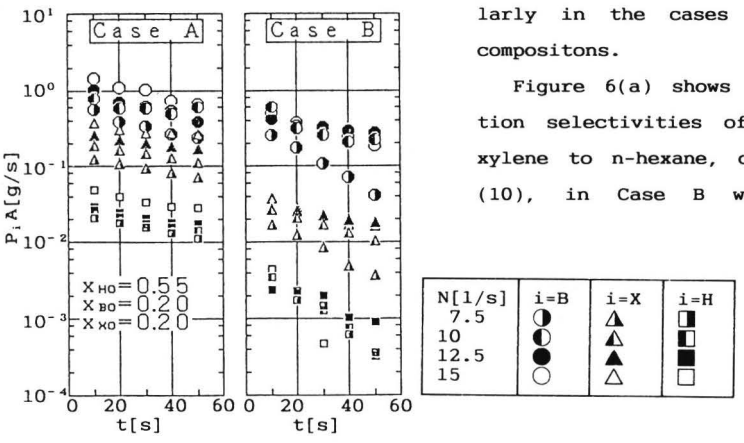

Fig.5. Volumetric permeation coefficients of permeates.

those in Case A. Figure 6(b) also shows that the selectivities in Case B were higher and closer to those in an flat liquid membrane than those in Case A. These results meant that the larger the diameter of the inner oil droplet in an emulsion drop, the higher the selectivity. This ensured the suggested simple way to improve the separation selectivity with decrease of the number of the inner droplets in an emulsion drop. The selectivities increased somewhat with decrease of the diameter of emulsion drops by increasing the stirring

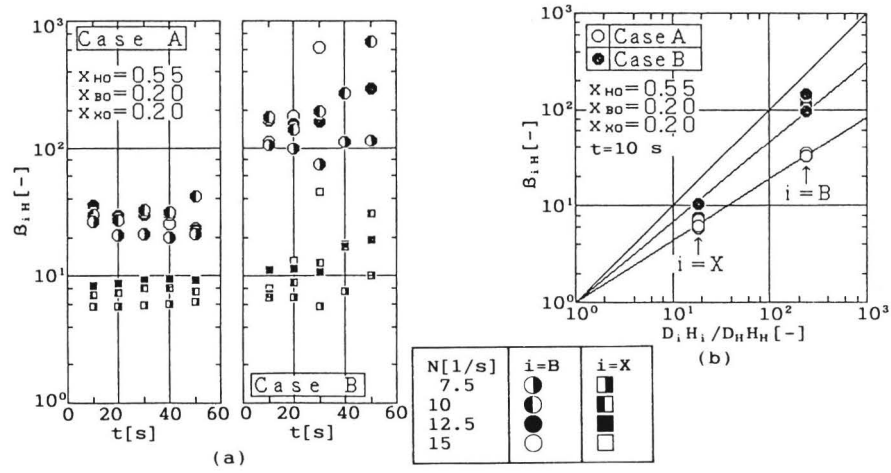

Fig.6. Separation selectivities relative to n-hexane. (a) Time course. (b) Correlation with separation selectivity of a flat liquid membrane (D_iH_i/D_HH_H).

velocity, although it is not so clear in Fig.6(a). This was also one of the confirmations of above suggestion.

4 CONCLUSIONS

The simulation by a simple one-dimensional model predicted that the separation selectivity would be improved by decreasing the number of the inner oil droplets in an emulsion drop, which could be confirmed by a series of batch experiments of permeations. This would be the easy way of improvement of the separation selectivity in this separation technique.

5 NOMENCLATURE

A: Contact area [cm^2], B: Radius of emulsion drop [cm], D: Diffusivity [cm^2/s], H: Distribution coeffcient [-], k: Layer number [-], N: Stirring velocity [1/s], n: Number of membrane layers [-], P: Permeation coefficient [$g/(s\cdot cm^2)$], t: Time [s], x: Mass fraction in raffinate phase [-], y: Mass fraction in extract phase [-], $\beta_{i,j}$: Separation selectivity of component i relative to component j, δ: Total thickness of liquid membrane [cm], ρ: Density of membrane liquid [g/cm^2].

Subscript B: Benzene, H: n-Hexane, i,j: Component i or j, N: n-Nonane, O:iso-Octane, X: m-Xylene, 0: Initial.

6 REFERENCES

Kato, S. and Kawasaki, J., 1986. Separation of aromatic hydrocarbons contained in naphtha by liquid membrane permeation.: Sekiyu Gakkaishi, 29: 404-411.

Kato, S. and Kawasaki, J., 1987. Separation of aromatic hydrocarbons contained in reformate and kerosine by liquid membrane permeation.: Sekiyu Gakkaishi, 30, 1-6.

Kawasaki, J., Suzuki, T., Kato, S., Toyoda, I. and Kondo, I., 1987. Rates of permeation and membrane stabilities in separation of hydrocarbons by liquid membrane.: Kagaku Kogaku Ronbushu, 13: 487-493.

Solvent Extraction 1990, T. Sekine (Editor)

© 1992 Elsevier Science Publishers B.V. All rights reserved

ENERGY REQUIREMENT FOR LIQUID MEMBRANE PROCESS TO SEPARATE BINARY HYDROCARBON MIXTURES

J. KAWASAKI, S. PUAJINDANETR and R. EGASHIRA

Deparatment of Chemical Engineering, Tokyo Institute of Technology,

2-12-1, O-okayama, Meguro-ku, Tokyo, 152 (Japan)

ABSTRACT

The process considered in this work consisted mainly of a multi-staged stirred permeator with extract reflux, a distillation tower with ideal stages and a mechanical demulsifier. The hydrocarbon feeds were binary mixtures of benzene and n-hexane, both of which permeated externally from the internal feed (or raffinate) into the external solvent (or extract) phase through the aqueous emulsified membrane. As an extract solvent, n-octane was selected because the boiling point differences between the solvent and permeates are satisfactorily large to result in easy distillation. Amounts of energy required for several separation problems were estimated under specified stage numbers of the permeator and distillator. Numerical values of volumetric coefficients of permeation were calculated with the aids of results of batch-wise permeation tests conducted by a small scale permeator. Effects of main operation variables, reflux ratios in the permeator and the distillator, on energy requirment are discussed in terms of product purities.

1 INTRODUCTION

There have been recently some remarkable developments in improved separation efficiency (Goswami and Rawat, 1984, Kato and Kawasaki, 1987a) and in a new demulsification technique (Kato and Kawasaki, 1987b, 1988) for the LMP process to separate hydrocarbons. Although not only better understandings of permeation mechanism but also further improvements in separation efficiencies are required, development of a possible and more substantial flow sheet and calculation of energy required in the process, are expected in the present stage.

It is rather straight forward to select the extract solvent in the LMP process to separate hydrocarbons. The low solubility in water and large boiling point differences between the selected solvent and permeates will be requested in the first screening. The possible solvent is therefore

a hydrocarbon or a mixture of hydrocarbons with large boiling point differences with permeates. The latter factor made fortunately the calculation procedure of the whole LMP process much simpler: two sets of simultaneous equations for the permeator and distillation tower were solved separately, although the process considered in this work seems to be very complicated.

2 PROCESS AND CALCULATION

2.1 Process

The process considered in this work is shown schematically in Fig.1. It consisits of two emulsifiers(EM1, EM2), a multi-stage permeator(P) with reflux,a settler(S),a demulsifier(DEM) and a conventional distillation tower(D).A binary mixture of benzene and n-hexane was selected as a model mixture. N-octane was selected as a solvent because the boiling point differs substantially from those of permeates. A part of distillate is re-emulsified by EM2 and recycled into the permeator as a reflux. A part of the raffinate obtained from the mechanical demulsifier was recycled into the demulsifier to promote effective demulsification (Kato and Kawasaki, 1987b, 1988).

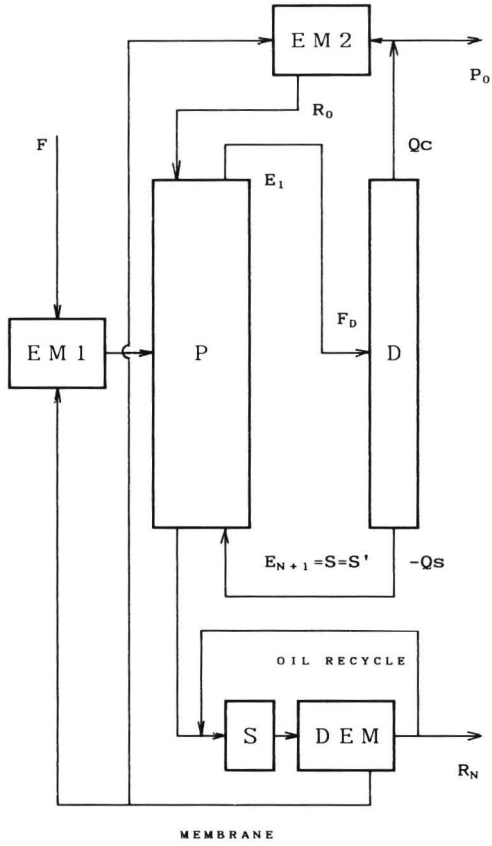

D : DISTILLATOR, DEM : DEMULSIFIER
EM1, EM2 : EMULSIFIER
P : PERMEATOR, S : STIRRED VESSEL

Fig.1 Liquid membrane process

2.2 Fundamental Equations

Fundamental equations for the permeator are summarized as follows.
Material balance for the nth stage of permeator is,

$$E_n y_{n,i} + R_n x_{n,i} = E_{n+1} y_{n+1,i} + R_{n-1} x_{n-1,i} \quad (1)$$

$$(+ F x_{F,i} \ ; \text{ if } n = n_e + 1) \quad (1')$$

If the effects of membrane break-up and mechanical entrainment are negligible, then, the peremation rate is,

$$E_n y_{n,i} - E_{n-1} y_{n-1,i} = P_i a V (x_{n,i} - y_{n,i}) \quad (2)$$

Mole fraction constraints for raffinate and extract streams are,

$$\sum_{i=1}^{3} x_{n,i} = 1 \quad (3)$$

$$\sum_{i=1}^{3} y_{n,i} = 1 \quad (4)$$

Material balance around distillation tower is,

$$E_1 y_{1,i} = (P_0 + R_0) x_{0,i} + S' y_{0,i} \quad (5)$$

and mole fraction constraint for the product is,

$$\sum_{i=1}^{3} x_{0,i} = 1 \quad (6)$$

Reflux ratio for the permeator is defined as,

$$r_P = R_0 / P_0 \quad (7)$$

Equations for the distillator are not shown here because they are conventional. Each stage of the distillator was assumed to be ideal and thermally insulated.

2.3 Calculation

As boiling point differences between permeates and the extract solvent were fairly large, ideal or complete separation was expected between these components in the distillation tower: only permeates from the top and the pure solvent from the bottom of the tower. Correspondingly the extract solvent was introduced into the permeator without containing any perme-

ates practically, which was confirmed in the following calculation. These made calculation simpler substantially than expected and therefore two sets of simultaneous equations, one for the permeator and another for the distillator, were solved separately.

In the numerical calculation for the distillator, the boiling point calculation and matrix methods were employed. Activity coefficients in liquid phase were estimated generally by Wilson's equation but only those for the combination of n-hexane-n-octane were done by the ideal solution approximation.

The amount of energy supplied into the reboiler of distillation tower for the specified searation was approximated roughly to be the amount of energy required for the whole process because the lack of informations on the power consumption in the stirred permeator and in the mechanical demulsifier.

2.4 Process Specifications

Process specifications are summarized in TABLE 1. General strategy to solve the problem is not for a design problem but for an operation problem : flow rates of products and their compositions, and amounts of energy supplied to the reboiler and that removed from condenser were calculated for the specified feed conditions, numbers of the enriching and stripping stages,and reflux ratios for both the permeator and distillation tower, as given in the TABLE. Volumetric coefficients of permeation were obtained in batch permeation runs in a strirred vessel.

TABLE 1

Specification of process

Feed	Benzene - n-Hexane $F = 51.2$ kg/h, $x_{FB} = 0.5$, $\phi_o = 0.5$
Solvent	n-Octane $S = 310.5$ kg/h (pure)
Permeator	$n_e = 4$, $n_s = 10$, $r_P = 3$, $P_B a = 0.195$, $P_H a = 0.010$ kg/(min lit) with reflux
Distillator	$n_e = 10$, $n_s = 10$, $r_D = 2.63$, adiabatic, ideal stages
Demulsifier	mechanical, with reflux, perfect demulsification

3. RESULTS AND DISCUSSIONS

The calculated results are summarized in TABLES 2(a) and (b). Reflux of the permeator was really effective. Therefore both species contained in the feed were obtained in fairly high purities : 0.94 for benzene and 0.92 for n-hexane, respectively. Yields for these components are 0.97 and 0.89, respectively. It was furher observed that the distillation tower separates permeates (mainly benzene) and solvent almost completely. The amount of energy required was 519 kcal/kg-feed (=1.23 $\times 10^5$ kJ/h) to the reboiler, although comparison between this result and energy in the conventional extraction process was not undertaken in this work.

TABLE 2 (a)

Results of calculation : Flow rates and compositions

Flow		F	P_o	R_N	F_D	R_o	S
rate [kmol/h]		0.6919	0.3550	0.3369	4.143	1.065	2.723
composition [mole fr.]	benzene	0.500	0.9402	0.0857	0.3229	0.9402	0.0000
	n-hexane	0.500	0.0577	0.9157	0.0198	0.0577	0.0007
	n-octane	0.0000	0.0022	0.0000	0.6573	0.0022	0.9993

Both purities of products and yields could be improved further with higher reflux ratios for the permeator and the distillator, in which energy required will increase to some extent. The possible improvements for these will be expected also through seaching optimum combinations of reflux ratios and numbers of stages of both the enriching and stripping sections of permeator and distillation towers.

TABLE 2 (b)

Results of calculations : Yields and required energy

Fractional yield	Y_B = 0.965 Y_H = 0.892
Energy to be supplied in reboiler	$-Q_s$ = 1.23 $\times 10^5$ kJ/h = 519 kcal/kg-feed
Energy to be removed in partial condenser	Q_c = 5.26 $\times 10^4$ kJ/h = 222 kcal/kg-feed

4 CONCLUDING REMARKS

With the reflux of the permeator, fairly high purities and yields for

both components could be obtained. Optimum combination of reflux ratios and numbers of stages should be searched to discuss the LMP process more substantially, because it was observed that the reflux ratios affected most strongly not only the separation efficiency, yields of permeates, but also the energy required, as easily estimated. Informations on the power required in the multistage stirred permeator and that in the mechanical demulsifier in terms of recycle ratios, both of which were neglected in the present work, were further requested together with development of the method for scaleing up of the permeator.

5 NOMENCLATURE

a	: specific surface area	[1/m]
E	: flow rate of extract	[kg/h], [kmol/h]
F	: feed rate	[kg/h], [kmol/h]
P	: Permeation coefficient	[kg/(m^2·h)]
R	: flow rate of raffinate	[kg/h], [kmol/h]
r	: reflux ratio	[-]
S	: flow rate of solvent	[kg/h], [kmol/h]
V	: volume of a permeation stage	[m^3]
x	: mass fraction in raffinate (for permeator)	[-]
	or mole fraction in liquid (for distillator)	[-]
Y	: fractional yield	[-]
y	: mass fraction in extract (for permeator)	[-]
	mole fraction in vapor (for distillator)	[-]

<Subscript>

- B : benzene
- c : partial condenser
- D : distillator
- e : enriching section
- H : n-hexane
- i : component i
- n : number of stage
- O : n-octane
- P : permeator
- s : still or stripping section

6 REFERENCES

Goswami, A.N.and Rawat, B.S., 1984. Permeation of hydrocarbons through liquid surfatant membranes and formation of liquid crystalline structures. J. of Membrane Sci., 20: 261-272.

Kato, S. and Kawasaki, J., 1987. Enhanced permeation of hydrocarbons through liquid membranes by lipophilic surfactants. J. of Chem. Eng. Japan., 20:140-145.

Kato, S.and Kawasaki, J. A new technique for the mechanical demulsification of O/W emulsions. J. of Chem. Eng. Japan., 20: 232-237.

Kato, S.and Kawasaki, J. Continuous demulsification of O/W emulsions by a mechanical technique. J. of Chem. Eng. Japan., 21: 321-323.

Solvent Extraction 1990, T. Sekine (Editor)

© 1992 Elsevier Science Publishers B.V. All rights reserved

MODELING OF MASS TRANSPORT WITH SIMULTANEOUS DIFFUSION AND CHEMICAL REACTION IN LIQUID MEMBRANE SYSTEMS

Jae Hyung Yoo, Hyun Soo Park, In Suk Suh

Korea Atomic Energy Research Institute, P.O.Box 7, Daeduk Danji, Daejon, 302-353 (Korea)

ABSTRACT

A Model of general use for the interpretation of mass transport within emulsion drops in liquid surfactant membrane processes is presented. This model is focused on the mass transfer rate at the internal surfaces around encapsulated droplets inside the drops, which can be enhanced by a fast chemical reaction. Since the mass transfer rate at the internal boundaries is a major rate controlling step in the emulsion-type membranes, both the diffusivity of permeating species and the internal mass transfer rate are simultaneously considered as rate determining parameters in the model. The model predictions are compared with the experimental results for an aniline separation process.

1 INTRODUCTION

In most of the liquid surfactant membrane processes, a species diffusing through membrane is stripped into the internal phase by a fast chemical reaction. This reaction takes place at the surfaces of the internal droplets containing adequate chemical reagents and thereby enhances the overall mass transport rate. While a number of mathematical models have been reported in the literature, most of them can be applicable to somewhat limited cases or only specific component systems. In this study, however, a general model was established, which can be applied to wider varieties of the liquid membrane systems. Both diffusivity in the membrane phase and internal reaction rate were simultaneously taken into account in the present model for describing the mass trasport behavior more closely to the actual phenomena. The effectiveness of this model was validated by comparing the model predictions with the experimental results for the extraction of aniline.

2 ANALYTICAL MODEL

2.1 Description of Model

The following assumptions were made to express model equations adequately.

- The mass transfer resistance in the external phase can be negligible for well-agitated systems.
- The highly viscous emulsion phase prevents the occurance of internal circulation within the emulsion drops.
- Coalescence or redispersion of the emulsion drops can be ignored during agitation.
- The drop dispersed system is assumed to be monodisperse with drops of average size. (Sauter mean diameter is used as the average drop size)

The governing equations can be obtained from the differential mass balances for the simultaneous diffusion and chemical reaction. The irreversible reaction between diffusing species and internal reagent at the surfaces of internal droplets can be represented by

$$A + bB \longrightarrow \text{Products}$$

Let A and B be diffusing species and internal reagent respectively, then the mass transfer rate into the internal phase is described as

$$N_A = K\ E\ S\ C_{Ai} \tag{1}$$

where K,E,S, and C_{Ai} are, respectively, pure mass transfer coefficient in the abscence of reagents, enhancement factor, interface area and concentration of A at the surface of internal phase. On the other hand, the disappearance rate of B is given by

$$-\frac{1}{b}\frac{dC_B}{dt} = K\ E\ a\ C_{Ai} \tag{2}$$

where a denotes the interface area per unit volume of emulsion phase.

The differential equation for C_A thus becomes

$$\frac{\partial C_A}{\partial \theta} = \frac{1}{\eta^2}\frac{\partial}{\partial \eta}\left(\eta^2 \frac{\partial C_A}{\partial \eta}\right) - \xi\ C_A \tag{3}$$

$$t = 0 \quad C_A = 0 \quad (0 \leq \eta < 1) \tag{4}$$

$$\eta = 1 \quad C_A = Cs \tag{5}$$

$$\eta = 0 \quad \frac{\partial C_A}{\partial \eta} = 0 \tag{6}$$

where

$$\xi = \frac{K\,E\,a\,R^2}{m\,De}, \quad \theta = \frac{De\,t}{(1-\phi)R^2}, \quad \eta = \frac{\gamma}{R} \tag{7}$$

De, m, ϕ and R represent effective diffusivity in the membrane phase, distribution coefficient, volume fraction of the internal phase in the emulsion, and drop radius, respectively. Since the reaction rate is faster in the outer region than in the inner region of an emulsion drop, B in the outer region will be completely consumed after a certain time, τ, has elapsed, that is, the diffusing species is no more received into the internal phase. Therefore, the following condition holds for ξ :

$$\xi = \text{finite}\ (t<\tau)\ ;\ \xi = 0\ (\tau \leq t) \tag{8}$$

In equation (3), ξ is thus the only parameter which determines the internal mass transfer rate, dominating the overall mass transport kinetics. In batch-type operations, the solute concentration in the external phase decreases with time, and thus the surface concentration Cs is not constant. For this reason, another equation for the solute concentration, Ce, in the external phase must be simultaneously solved with equations (3) through(8). The equation for Ce can be expressed as :

$$-\frac{dCe}{d\theta} = \frac{3(1-\phi)\,Vd}{Ve}\left[\frac{\partial C}{\partial \eta}\right]_{\eta = 1} \tag{9}$$

$$\theta = 0 \quad Ce = Ceo \tag{10}$$

The external and dispersed emulsion phase volumes are Ve and Vd, respectively.

2.2 Model predictions

In this study, the model equations (3)-(10) were numerically solved by means of the orthogonal collocation technique (Finlayson, 1980, pp.73-78). When six orthogonal collocation points were taken in the calculation, this method gave an approximate solution which was in good agreement with the exact solution.

Fig.1 and Fig.2, respectively, show the typical calculation results for C_A and C_B within an emulsion drop, and the effect of ξ on the decreasing rate of Ce in the

external phase. These calculations were done with arbitrary conditions.

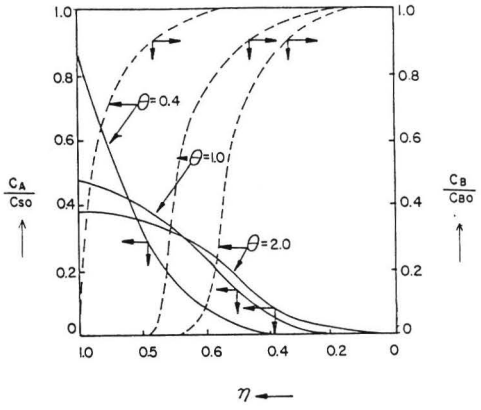

Fig. 1. Typical concentration profiles of A and B inside emulsion drop

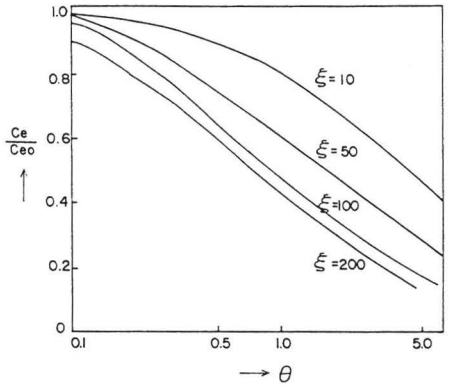

Fig. 2. Prediction of mass transport rate (decreasing rate of Ce) with various ξ

3 COMPARISON WITH EXPERIMENTAL RESULTS

The effective diffusivity of aniline was assumed to be

$$De = \frac{Dm\ (1 + 1.5\ \phi^{2/3})}{1\text{-}1.5\ \phi + 1.5\ \phi^{2/3}} \qquad (11)$$

where Dm is the molecular diffusivity in the oil-membrane phase. This correlation was obtained using the experimental results of the amine extraction studies (Teramoto et al., 1981). If aniline can diffuse in the internal phase in the form of $PhNH_2$ as well as $PhNH_3^+$, the diffusional resistance will be greatly reduced because the concentration of $PhNH_3^+$ is much higher than that of $PhNH_2$. The experimental conditions adopted in the earlier study (Yoo, 1985) are summarized in table 1.

TABLE 1. Experimental Conditions

De = 1.85×10^{-5} cm²/sec	R = 0.05 cm
Ceo = 500 ~ 2000 ppm	Ve = 850 mℓ
Ceo = 0.2 mol/ℓ (HCl)	Vd = 150 mℓ
m = 0.85	ϕ = 0.3 ~ 0.5

The key parameter, ξ, was evaluated by the curve fitting technique from the experimental result of Ce/Ceo vs. θ. As shown in Fig.3 and Fig.4, the model predictions based on the estimated value of ξ are in fairly good agreement with the experimental results. With smaller ϕ as shown in Fig.3, the overall mass transport rate was decreased as expected in the model because ξ is proportionally reduced with the decrease of a. The effect of Ceo is remarkable in Fig.4, which suggests that internal mass transfer resistance be important. Since the internal reagent in the outer region of an emulsion drop is consumed sooner with higher Ceo, this makes greater resistance for the mass transport into the emulsion drop.

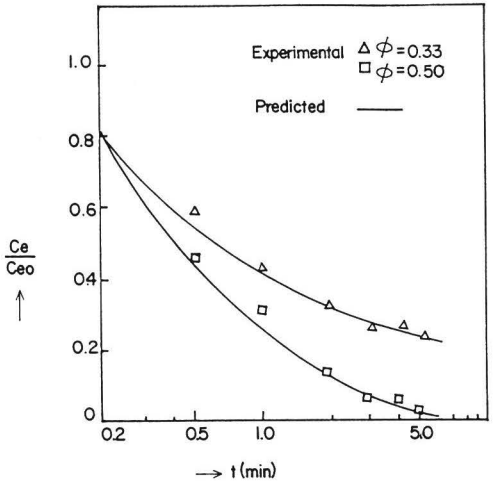

Fig. 3. Comparision between model predictions and experimental data; Effect of ϕ

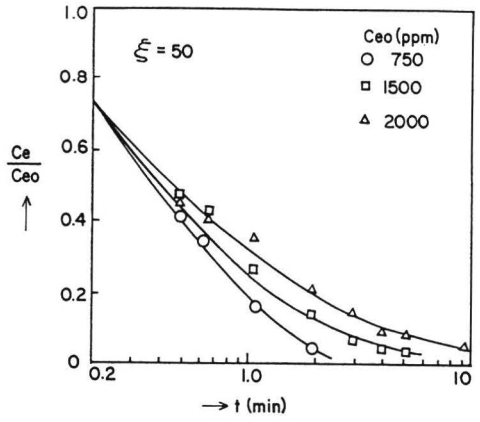

Fig.4. Comparison between model predictions and experimental data; Effect of Ceo

4. CONCLUSIONS

A general model was presented for the interpretation of mass transport kinetics in the liquid surfactant membrane processes. Both diffusion in the membrane phase and internal chemical reaction are simultaneously incorporated in this model. The model predictions were validated to mirror well the mass transport behavior through the emulsion-type membrane.

5. REFERENCES

Teramoto et al., 1981. Extraction of Amine by W/O/W Emulsion System, J.Chem. Eng. Japan, Vol.14, No.2, pp.127

Bruce A. Finlayson, 1980. Nonlinear Analysis in Chemical Engineering. MGRAW-HILL Book CO., New York, pp.73-78

J.H.Yoo, 1985. Analysis of an Agitated Column for liquid-surfactant Membrane process. Doctorate Dissertation, Korea University

Solvent Extraction 1990, T. Sekine (Editor)

© 1992 Elsevier Science Publishers B.V. All rights reserved

THE EFFECTS OF W/O EMULSION PROPERTIES IN ELECTROSTATIC DEMULSIFICATION KINETICS

T. HANO, T. OHTAKE, M. MATSUMOTO, F. HORI AND F. NAKASHIO*
Department of Environmental Chemistry and Engineering, Oita University, Oita, 870-11(Japan)
*Department of Organic Synthesis, Kyushu University, Fukuoka, 812(Japan)

ABSTRACT

The contribution of water- and oil-phase properties in the electrostatic demulsification was investigated in batch and continuous demulsifiers by using W/O emulsions prepared with various aqueous and organic solutions. The demulsification rates changed with the surfactant and diluents in addition to the drop size and hold-up of the water phase. When the same surfactant was used, the rates decreased in proportion to the 3.2 power of the viscosity of the oil phase. The distinct correlations between the rates and other physical properties like density, electric conductivity, dielectric constant and interfacial tension were not observed. The contribution of the water-phase properties could be represented well by the ionic strength. The demulsification kinetics obtained in a batch operation was found to be valid in a continuous operation. Stirring the emulsion during the operation was effective for the demulsification.

INTRODUCTION

The liquid surfactant membranes have been investigated in the fields of hydrometallurgy, wastewater treatment, and fermentation. In this separation process, W/O emulsion must be demulsified after extraction in order to recover the components concentrated in the inner water phase and to re-utilize the oil phase containing surfactants and carriers. The electrostatic method, in which high A.C. or D.C. voltage is applied to accelerate the coalescence of fine water drops and their growth to larger drops, is considered to be most economic(Joos et al., 1985; Kriechbaumer and Marr, 1985).

The demulsification kinetics is affected by both emulsification and demulsification conditions. Table 1 lists the preparation conditions and properties of emulsions which may influence the demulsification rate. In addition, the demulsification behavior is affected by various operating conditions such as applied voltage, frequency, stirring rate, temperature and electrode distance. Because of many parameters to be examined, a few papers have reported the contribution of some of these factors keeping other conditions constant (Fujinawa et al., 1984; Kataoka and Nishiki, 1986; Yamaguchi et al., 1985). In the parameters listed in Table 1, the coalescence and falling processes of water drops are greatly affected by the viscosity of surroundings. In the previous paper, we proposed the following rate equation(Hano et al., 1988);

TABLE 1

List of emulsion preparing conditions and properties

Phase	Conditions	Properties
Water phase	Electrolytes concentration	Density, Ionic strength Electric conductivity Dielectric constant
Emulsion	Agitation speed of homogenizer Water-phase holdup	Drop size, Holdup Apparent viscosity Interfacial tension
Oil phase	Surfactant concentration Carrier concentration	Density, Viscosity Electric conductivity Dielectric constant

$$dV_w/dt = 4.18\times10^5\exp(-22500/RT)\mu_{oil}^{-3.2}d_w^{3.5} \times (6.5 + 3.93N)\exp(-19.6\phi_w)\exp(-0.111C_s)$$

However, this equation was derived by using the W/O emulsions composed of aqueous copper sulfate solution and a mixture of kerosene and liquid paraffin containing Span 80 as a surfactant. The aim of the present work is, therefore, to examine the validity of the above kinetic equation for the emulsions prepared under various conditions. Continuous demulsification was also carried out and compared with a batch operation.

1. EXPERIMENTAL

1.1 Demulsification apparatus and operation

The batch and continuous demulsifiers used in this study are the same as those in the previous papers(Hano et al., 1988, 1990). The copper disk electrode was set at the bottom and grounded. The glass sealed electrode was filled with saturated aqueous sodium chloride solution into which a copper wire was immersed. A.C. 15kV of 60 Hz was applied between the two electrodes in all experiments. The demulsification rate, dV_w/dt, in a batch operation was evaluated at the point of 50% demulsification where the water layer was formed at nearly constant velocity. In a continuous operation, both the water and oil phases separated were drawn out at the same rate since the water-phase holdup of the emulsion studied was 50%. The demulsification rate in this case was defined as the drawing out rate of the water phase.

1.2 Preparation of emulsion

The original W/O emulsion in a batch run was prepared by mixing 40 cm^3 kerosene solution containing 2 wt% Span 80 and 80 cm^3 aqueous solution of 20 mol/m^3 copper sulfate with a homogenizer at 83 s^{-1}. The emulsion for the run was

prepared by mixing 120 cm^3 original emulsion with 40 cm^3 solution of kerosene and liquid paraffin containing 2 wt% Span 80. The standard sample prepared by this method contained water drops of 5.33 μm average diameter and had 50% water-phase holdup. The viscosity of the oil phase was altered by changing the composition of oils used to dilute the original emulsion. In the experiments to examine the effects of the oil-phase properties, several organic solvents were employed instead of kerosene and liquid paraffin. The contribution of the water-phase properties was investigated by using emulsions prepared with aqueous solutions of various electrolytes. The feed emulsions in a continuous operation were prepared in the same way as in a batch run.

2. RESULTS AND DISCUSSION

2.1 Effects of oil-phase properties on demulsification rates

Figure 1 is a time-course of batch demulsification at various temperature. After initial induction period, demulsification proceeded with a constant rate. The rise of the operating temperature clearly contributed to promote the demulsification. In the previous papers(Hano et al., 1988, 1990), the effects of oil-phase properties were discussed primarily in terms of the viscosity by changing the mixing ratio of kerosene and liquid paraffin. In order to see if the same dependence(-3.2 power) held in other solvents, the effects of viscosity were examined for the emulsions prepared by various organic solvents with or without adding liquid paraffin. In this case, water-drop size also varied and the demulsification rates increased according to the 3.5 power. Therefore, the demulsification rates divided by the 3.5 power of drop diameter were plotted in Fig. 2. Almost all emulsions studied followed the same correlation as for the emulsions prepared with kerosene and liquid paraffin, although some aromatic hydrocarbons exhibited a little deviation. Table 2 lists the demulsification rates and various physical properties of the oil phase which have been pointed

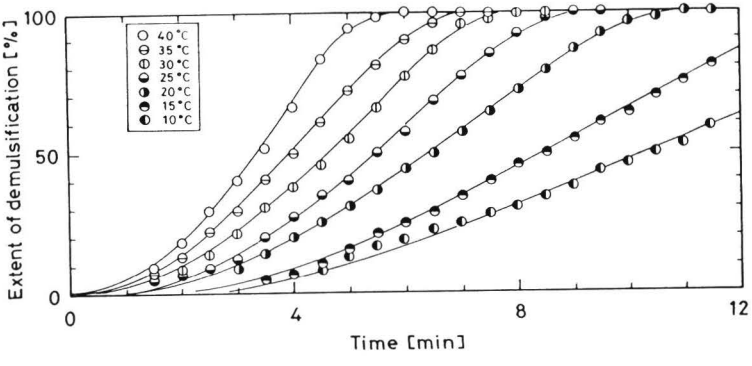

Fig.1 Time-course of batch demulsification at various temperatures

out to affect the kinetics. It is difficult to find the distinct relation between the rates and other physical properties like density(ρ), electric conductivity(C) and dielectric constant(ε). There was also no marked difference in the interfacial tension between aqueous electrolytes solutions and various organic solutions which involved 5 wt% Span80. These findings supported that the contribution of the oil phase could be expressed by the viscosity. Figure 3 examined the effects of water-phase holdup on the demulsification rate. The same dependence was obtained for all emulsions of different viscosity, which confirmed the validity of the rate equation proposed in the previous study. Figure 4 plotted the viscosity-dependence at various agitation rate in the demulsifier. Stirring the contents was found to accelerate the coalescence of water drops.

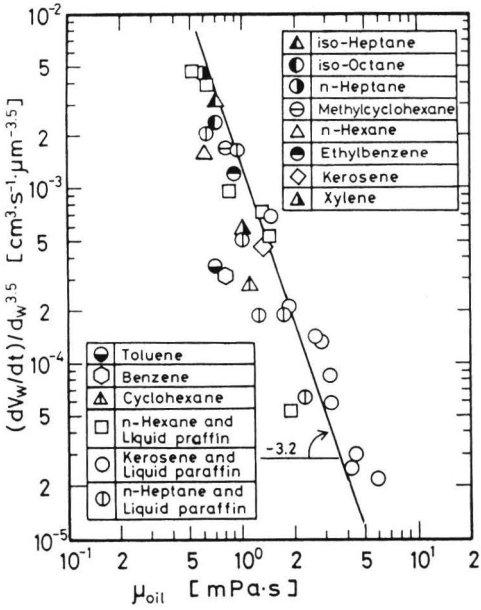

Fig.2 Effect of oil-phase viscosity

2.2 Effects of water phase properties on demulsification rates

The emulsions those water phase was prepared with different electrolytes

TABLE 2 Demulsification rates and some physical properties of the oil phase

Oil phase	ρ	ε	C	rate
n-Hexane	0.660	1.90	138	156
n-Heptane	0.684	2.10	125	439
iso-Heptane	0.674	1.97	71.5	319
iso-Octane	0.692	1.95	122	239
Cyclohexane	0.778	2.04	37.6	20.3
Benzene	0.879	2.30	34.7	31.1
Toluene	0.862	2.40	51.4	35.8
Xylene	0.868	2.41	64.6	59.2
Etylbenzene	0.866	2.52	9.4	113
Kerosene	0.793	2.11	79.7	46.8
Mixture of kerosene and liquid paraffin	0.870	2.14	44.8	8.57

ρ = density [g·cm^{-3}], ε = dielectric constant [-]
C = electric conductivity [nS],
rate = $(dV_W/dt)/d_W^{3.5}$ [10^{-5}cm^3·s^{-1}·μm$^{-3.5}$]

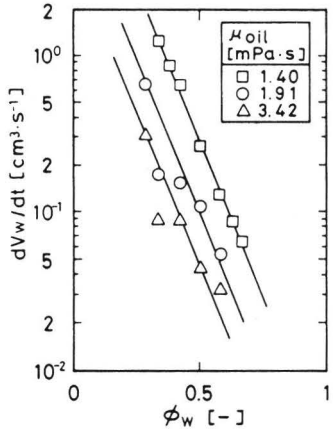

Fig.3 Effects of water-phase holdup

exhibited the same viscosity dependence, but the demulsification rates differed even at the same electrolyte concentration(Hano et al., 1990). An increase in electrolyte concentration accelerated the demulsification, and electrolyte of higher charge showed faster rates at the same concentration. An aqueous glucose solution gave very low and constant rates regardless of the concentration. These findings demonstrate that the presence of charged species in the water phase is essential for electrostatic demulsification. Figure 5 plotted the demulsification rates divided by the 3.5 power of the drop diameter against the ionic strength of water phase. The rates increased approximately in proportion to the 0.4 power of the ionic strength, although there was some scatter. Therefore, the contribution of the water phase may be represented by the ionic strength as pointed out by Kriechbaumer and Marr(1985).

2.3 Comparison of batch and continuous demulsification

The performance of the continuous demulsifier was studied by using a standard emulsion prepared with aqueous copper sulfate solution and mixture of kerosene and liquid paraffin containing Span 80. Figure 6 compared the viscosity dependence of the demulsification rates for batch and continuous operations. They exhibited almost the same demulsification behavior. Consequently, the basic demulsification kinetics obtained in batch operations can be applied to continuous operations.

CONCLUSION

The contribution of water- and oil-phase properties to the kinetics of electrostatic demulsification was investigated with W/O emulsions prepared under various conditions. The viscosity of oil phase was the most important parameter which controlled the demulsification rates. If the same surfactants was used, the rates decreased in proportion to the 3.2 power of the viscosity. There was no distinct correlation between the demulsification rates and electric properties of the oil phase. The contribution of water phase properties could be represented by the ionic strength. The demulsification kinetics observed in batch operations were found to be valid in continuous operations, too.

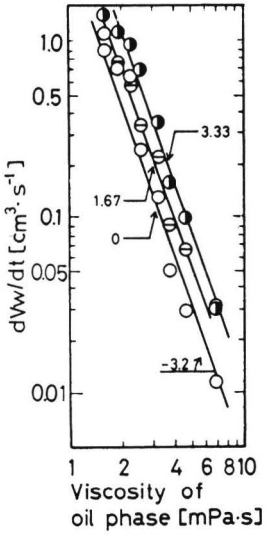

Fig.4 Effect of stirring the emulsion (parameter: agitation rate [s^{-1}])

NOMENCLATURE

C_s surfactant concentration [wt%]
d_w water-drop diameter in W/O emulsion [m]
N agitation speed of demulsifier [s^{-1}]

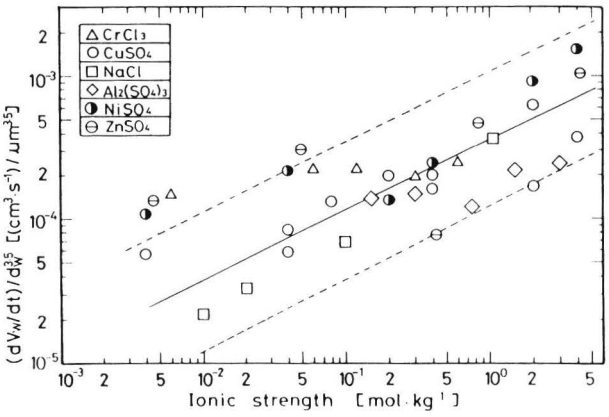

Fig.5 Correlation of the demulsification rates and ionic strength of of the water phase

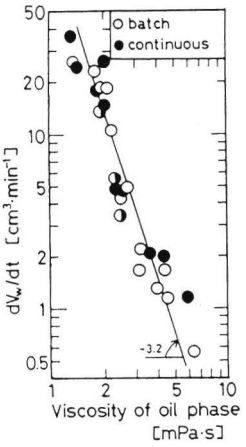

Fig.6 Comparison of batch and continuous operations

R gas constant [J/(mol·K)]
T temperature [K]
t time [s]
V_w volume of water phase separated [cm^3]
μ_{oil} oil-phase viscosity [mPa·s]
ϕ_w water-phase holdup [-]

REFERENCES

Fujinawa, K., Morishita, M., Hozawa, M., Imaishi, N. and Ino, H., 1984. Demulsification of W/O emulsion by use of high voltage of A.C. fields: J. Chem. Eng. Japan, 17:632-636.

Hano, T., Ohtake, T. and Takagi, K., 1988. Demulsification kinetics of W/O emulsion in an A.C. electric field: J. Chem. Eng. Japan, 21:345-351.

Hano, T., Ohtake, T., Hori, F. and Nakashio, F., 1990. Kinetic study of electrostatic demulsification -Contributions of oil and water phases properties: Water Treat., 5:202-213.

Joos, F.M., Snaddon, R.W.L. and Johnson, N.A., 1985. Electrostatic droplet growth in a neutrally buoyant emulsion: IEEE Trans. Ind. Appl., IA-21: 1366-1371.

Kataoka, T and Nishiki, T., 1986. Experimental study of electrical demulsification in liquid surfactant membranes: Kagaku Kogaku Ronbunshu, 12:16-22.

Kriechbaumer, A. and Marr, R., 1985. Emulsion breaking in electrical fields. In: D.O. Shah(Editor), Macro- and Microemulsions(ACS Symp. Ser. 272), Amer. Chem. Soc, New York, p.381.

Yamaguchi, M., Kobayashi, A., Ohbori, K. and Katayama, T., 1985. A method of continuous phase separation of water in oil emulsion by applying D.C. electric field: Kagaku Kogaku Ronbunshu, 11:729-734.

Solvent Extraction 1990, T. Sekine (Editor)

© 1992 Elsevier Science Publishers B.V. All rights reserved

IMMOBILIZED ENZYMES IN LIQUID MEMBRANE PERMEATION PRODUCTSEPARATION AND PRODUCTBRUSHING IN BIOTECHNOLOGY

W. PREITSCHOPF and R. MARR
Institute of Chemical Engineering and Environmemtal Technology
University of Technology Graz, Inffeldgasse 25, 8010 Graz/Austria

ABSTRACT

α-Chymotrypsin was immobilized in liquid surfactant membranes. These enzyme emulsions were employed in liquid membrane permeation (LMP) to investigate the suitability of such a process for down stream processing of fermentation broths. Emulsification, permeation and emulsion splitting was carried out and it could be shown that biochemical requirements as well as those of a LMP process can be met.

1. INTRODUCTION

Biotechnological processes exhibit specific problems due to biological constraints which limit their commercialization. One of these problems is low product concentration in a complex fermentation broth. Another is inhibition of product formation by the fermentation product itself. Having these problems in mind down stream processing for biotechnology has to meet the needs of concentrating, selectivity and continous product removal.

Liquid membrane permeation (LMP) processes with water-in-oil type emulsions have shown to be suitable tools for product separation from fermentation broths (Boey et al., 1987). Immobilization of enzymes in the aqueous interior phase of W/O-emulsions leads to enzyme emulsions. Such enzyme emulsions can be used in LMP-processes (Scheper et al., 1987) where they provide a driving force for the separation due to the biochemical reaction in the interior phase of the W/O-emulsion. In addition the selectivity of the process can be enhanced and separation is combined with derivatisation of the fermentation product.

In Figure 1 a flow sheet for the separation and simultan derivatisation of fermentation products using enzyme emulsions is shown. Like in conventional LMP processes an emulsifier, an extractor and

a coalescer are needed. Additionally an UF-module is necessary for a process with enzyme emulsions to separate the enzyme from the product solution.

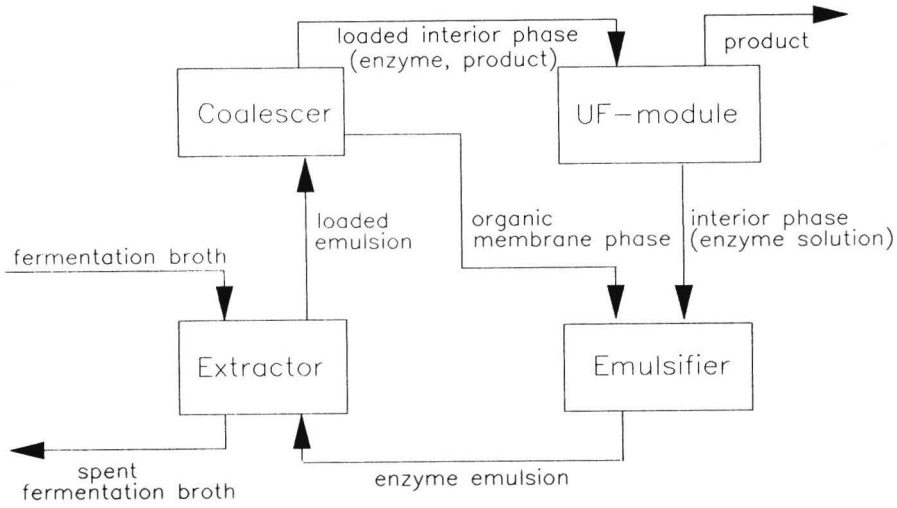

Figure 1: Separation and derivatisation of fermentation products employing a LMP process with enzyme emulsions

The aim of this study was to investigate the main stages (emulsification, permeation, emulsion splitting) of a LMP process based on enzyme emulsions. In addition the compatibility of membrane components (carrier, surfactant and diluent) with the enzyme was tested. As a model system the cleavage of L-phenylalanin methyl (PME) ester by α-chymotrypsin was used.

2 RESULTS AND DISCUSSION

2.1 Emulsification

Enzyme emulsions have been prepared by high shear stress using an ultra turrax (IKA/Germany). The organic membrane consisted of a nonionic surfactant (ECA from Paramins Laboratories/France), an anion exchanger (Aliquat 336/Henkel) and an aliphatic diluent (Shellsol T/Shell) commonly used in solvent extraction. During emulsification the temperature was kept below 10 °C. After emulsification the emulsion was partially broken by centrifugation at 20.000xg. Activity of α-chymotrypsin was determined in the aqueous phase. Figure 2 shows

the deactivation at different rpm-rates and emulsification times. It can be seen that high rpm-rates are crucial on enzyme activity. Employing only 8.000 rpm relatively high enzymatic activity is retained. Enzyme emulsions (without Aliquat 336) prepared at 8.000 rpm were used for permeation. It can be seen in figure 4 that these enzyme emulsions are enzymatically active.

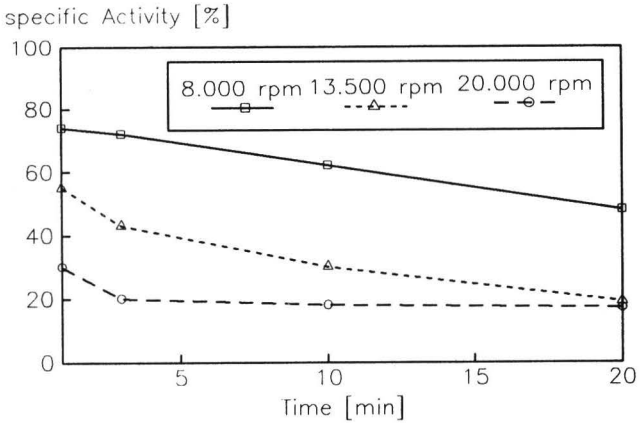

Figure 2: Deactivation of chymotrypsin by shear stress

2.2 Enzymatic activity and membrane components

The aqueous interior enzyme solution is in close contact with the organic membrane phase during a LMP process. To estimate deactivation of the enzyme by membrane components of technical purity we tested different membranes. In the experiments 20 ml of aqueous α-chymotrypsin solution (1mg/ml in buffer at pH=6.5) were stirred with 20 ml of organic membrane phase. The enzyme solution was then assayed for activity.

Figure 3 shows the time course of deactivation with different membrane components. SST is an aliphatic hydrocarbon, ECA is a polyamine surfactant, Aliquat 336 is a quaternary ammonium salt (an anion exchanger) and D2EHPA (a cation exchanger) is bis(2-ethylhexyl) posphoric acid. It can be seen from figure 3 that membrane components of technical purity deactivate the enzyme to a large extent (20 - 50 % within 6 hours). D2EHPA seems to be absolutely unsuitable since it deactivates the enzyme totally within one hour.

2.3. Permeation

To test the operational stability of the enzyme emulsions and to see the effect of different amounts of enzyme immobilized in the interior phase permeations were carried out.

The membrane phase consisted of 5 % ECA in Shellsol T . The

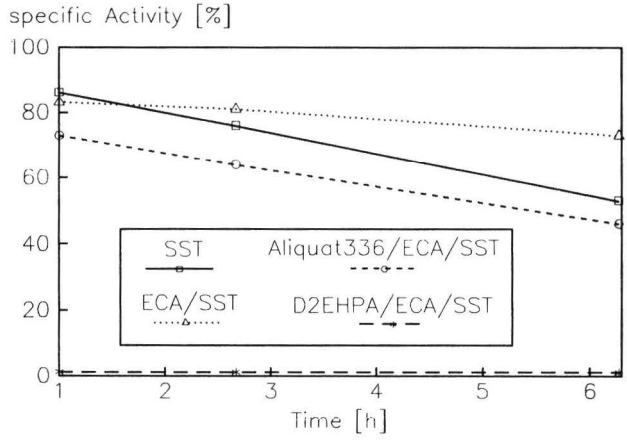

Fig. 3: Chymotrypsin activity when contacted with membrane components

interior phase was an α-chymotrypsin solution of different concentrations in buffer at pH = 6,5. The ratio membrane/interior phase was 3/1 in both cases. For emulsification the ultra turrax (8.000 rpm, 5 min) was used. 80 ml of these emulsions were dispersed into 160 ml of PME solution (pH = 6,5) and PME, L-phenylalanin and protein were monitored in the continous phase during the permeation. Neither L-phenylalanin nor protein could be detected in the outer phase indicating that the emulsion was sufficiently stable during the time of permeation.

The effect of using differnt α-chymotrypsin concentrations in the interior phase of the emulsion can be seen in figure 4. When high enzyme concentrations are used the separation of PME is controlled by the transport across the organic liquid membrane. Using only little amounts of enzyme the overall separation is strongly determined by the biochemical reaction inside the enzyme emulsions.

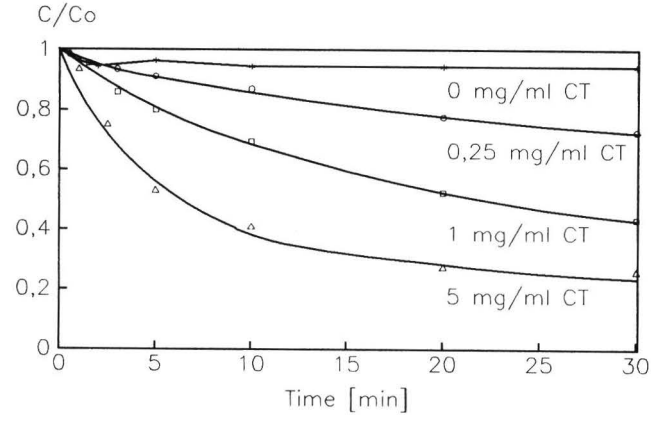

Fig.4: Permeation with enzyme emulsions of different enzyme concentrations

2.4 Splitting of enzyme emulsions

To investigate the effect of the splitting process an enzyme emulsion was prepared with the ultra turrax (8.000 rpm, 5 min). Two different membrane phases were used. One contained 5 % ECA and 3 % Aliquat 336 in Shellsol T, the other only contained the surfactant (5 % ECA) and Shellsol T. The emulsion (10 ml) was placed in a simple electrocoalescer and alternate current of different wave shapes (sinus, square) were applied for 2 minutes. With this simple electrocoalescer it was possible to recover 70 to 80 percent of the initial enzyme activity after emulsification and splitting. Taking into account the deactivation due to the emulsification step the splitting process seems to have little or no deaktivating effect on the enzyme.

3 SUMMARY

To investigate the suitability of a LMP process employing enzyme emulsions for down stream processing in biotechnology α-chymotrypsin was immobilized in the interior phase of a W/O-emulsion. The cleavage of L-phenylaline methyl ester by this model enzyme emulsion was used to study the key steps of such a process.

Emulsification was performed by using an ultra turrax. Even though deactivation of the enzyme at high rpm-rates took place it was possible to produce sufficiently stable emulsions, which retain high enzymatic activities at lower shear stress.

Components of the organic liquid membrane of technical purity showed large deactivation of the enzyme within several hours.

Using an electrostatic coalescer for emulsion splitting it was shown that only little deactivation of the enzyme occurs during this process step.

4 REFERENCES

Boey, S.C; Garcia del Cerro, M.C.; Pyle, D.L.; 1987, Extraction of citric acid by liquid membrane extraction, Chem. Res. Des., 65, 218 - 223

Scheper, T.; Likidis, Z.; Makryaleas, K.; Nowottny, C.; Schügerl, K.; 1987, Three different examples of enzymatic bioconversion in liquid membrane reactors, Enzyme Microb. Technol., 9, 625 -631,

Solvent Extraction 1990, T. Sekine (Editor)

© 1992 Elsevier Science Publishers B.V. All rights reserved

MEMBRANE TRANSPORT OF ALKALI METALS BY CROWN ETHERS

T. MURAI, K. NAKAMURA, S. NISHIYAMA, S. TSURUYA, and M. MASAI
Department of Chemical Engineering, Faculty of Engineering, Kobe University, Nada, Kobe, 657 (Japan)

ABSTRACT

The membrane transport of alkali metal ions (Na^+, K^+) by crown ethers as mobile carriers was studied in a bulk liquid membrane cell. Crown ethers used here were dibenzo-18-crown-6(DB18C6), dicyclo-18-crown-6(DC18C6), 18-crown-6(18C6), benzo-15-crown-5(B15C5) and 15-crown-5(15C5). The influence of certain transport variables, inorganic or organic counter anions, crown ethers and additives were also studied. The relative size of alkali ions to the size of the crown ether cavity and the substituted groups in the crown ether were one of the main factors controlling the transport rate. The importance of the counter-anion influence on the transport rate was clarified using organic and inorganic counter-anions. Organic counter-anions such as ethyl orange anions were more effective for enhancing the transport rate of alkali metal ion than inorganic counter-anions. The hydrophobic character of the counter-anion was discussed in connection with the transport rates.

INTRODUCTION

Since the early studies by Pederson (1), it has been reported that crown ether ligands complex most strongly those alkali metal cations whose ionic radii best match the radius of the cavity formed by the polyether ring. Crown ethers of varying cavity sizes nave been synthesized in hopes of selectively binding metal cations of different radii (2,3). The development of selective receptor molecules for cationic substrates led to their use as carrier agents for inducing selective transport through artificial membranes. Macrocyclic ligands such as crown ethers have been used as cation transport carriers in hydrophobic ligand membranes (3-10). Much attention has been given to the nature of the carriers which display a broad range of binding features. Thus, transport rates have been reported to markedly depend on the carrier in a given set of conditions. However, only a few reports have been published concerning the effect of the counter-anion, which compensates the electric neutrality of the metal-crown ether cation complex, on the transport rates of cations using macrocyclic crown ether carriers(4,7). We report here our results concerning the effect of the counter-anion on the rate of cation transport.

2 EXPERIMENTAL

2. 1 Extraction equilibrium

The measurements of extraction equilibria were similar to those previously reported [22]. Twenty milliters of chloroform containing crown ether (1-10 mmol/l) and 20 cm^3 of an aqueous solution containing KCl (10 mmol/l) and ethyl orange(EO; 4-[[4-(diethylamino) phenyl]-azo]-benzene sulfonic acid sodium salt) were introduced into a 50 cm^3 glass sample tube, which was then stoppered and immersed in a thermostated bath (298 ± 0.2 K). The

concentrations of extracted potassium ion were measured by atomic absorption spectrophotometry.

2.2 Transport of alkali metal cation

The measurements of the transport of alkali metal cations through a liquid membrane were performed using a U-tube type bulk liquid membrane cell immersed in a thermostated bath (303±0.2 K). The aqueous phases (source and receiving phases) and the organic bulk membrane phases were stirred by mechanical and magnetic stirrers, respectively. An organic solvent (70 cm^3 for K^+ and 60 cm^3 for Na^+) including the crown ether of interest was used as a bulk liquid membrane. Both the volume of the source phase (aqueous solution of an alkali metal ion and counter-anion) and the receiving phase (deionized water) were 70 cm^3. A sample of the receiving phase was withdrawn at specified time intervals and the concentration of the transported cation was determined by atomic absorption spectrophotometry. When the amounts of cation transported were small, the increase in cation concentration in the receiving phase was linear with time.

3 RESULTS

It has been reported [14-19] that an equilibrium can be established between an aqueous phase of an alkali metal ion (M^+), a picrate ion (A^-) and a benzene (or chloroform) phase of a crown ether and that the stoichiometry of the extraction species and its equilibrium constant for the extraction (Kex) can been described by eqs. (1) and (2), respectively. To investigate the complexation and the stoichiometry of the K^+ - 18C6 - EO^- ($CHCl_3$ solvent),

$M_a^+ + L_o + A_a^- \rightleftharpoons M^+LA^-_o$ (1) (M^+, cation; A^-, counter-anion; L,crown ether;

$Kex = [\,M^+LA^-\,]_o / ([\,M^+\,]_a[\,L\,]_o[\,A^-\,]_a)$ (2) subscripts a, aqueous phase; o, organic phase)

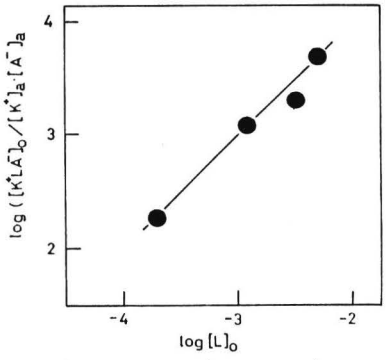

Fig. 1. The relationship between log $[M^+LA^-]_o/[M^+]_a[A^-]_a$ and log $[L]_o$: KCl-18C6-ethyl orange[EO^-]-$CHCl_3$ system; [KCl] = 10 mM; [EO^-] = 1.0 mM; [18C6] = 1.0-10.0 mM.

the equilibrium concentration of the extracted species (K^+-18C6-EO^-) was measured by varying the initial concentration of the 18C6. The relationship between log $[\,MLA\,]_o$ / ($[\,M^+\,]_a[\,A^-\,]_a$) and log $[\,L\,]_o$ was found to be a straight line with a slope of unity as illustrated in Fig. 1. (The slope in Fig. 1, calculated by the least-squares method, was 1.07). From these results, the composition of the extracted chemical species with the EO^- anion is considered

to be similar to that with picrate [14], methanil yellow [20], or methyl orange [20] as the counter-anion, at a crown ether:metal ion:counter-anion ratio of 1:1:1.

Using ethyl orange (EO^-) as a counter anion, the influence of the crown ether as a carrier on the transport rates of K^+ and Na^+ ions through a chloroform membrane was studied (Table 1). The transport rates of Na^+ ion were larger than those of K^+ ion when a 15 ring-crown ether, such as 15C5 and B15C5, was used as a carrier. On the other nand, 18 ring-crown ethers (18C6, DC18C6, and DB18C6) were found to favor the transport of K^+ ion over that of Na^+ ion. The fit between the cavity of the crown ether and the size of the alkali metal ion is considered to be an important factor for the transport of alkali metal ions by a crown ether carrier. Also, the crown ethers with substitution groups had the smaller transport rate when compared to those without the corresponding substitution groups. This might be due to the delocalization of the lone pair electrons on the oxygen atoms in the crown ether with substituted groups [22].

TABLE 1. Transport rate of K^+ and Na^+ by crown ether using a EO^- counter-anion[a].

Crown ether	Transport rate ($mol \cdot l^{-1} \cdot h^{-1} \times 10^4$)	
	K^+	Na^+
15C5	0.24	0.39
B15C5	0.21	0.22
18C6	1.26	0.27
DC18C6	1.17	0.23
DB18C6	0.88	0.19

[a] Transport conditions: $[M^+]$=10.0 mM, $[EO^-]$=10.0 mM, [L]=1.0 mM.

It has been reported that an additive such as tributyl phosphate [16] or trioctyl phosphine oxide (TOPO) [16,20] promoted the extraction rate of an alkali metal ion with the crown ether carrier. In contrast to the extraction of an alkali metal ion, the transport rate of a K^+ ion through the liquid membrane containing an 18C6 carrier was found to be retarded by the addition of TOPO or triphenyl phosphine oxide (TPPO) (The transport rate without an additive ($mol \cdot l^{-1} \cdot h^{-1}$),1.78; with TOPO, 0.61; with TPPO, 0.53). This might be in part due to the higher difficulty in the back-extraction of the K^+-18C6-PA^- complex from the organic liquid membrane to the aqueous receiving phase because of the increase in the hydrophobicity of the complex interacting with the TOPO or TPPO molecule.

To study the effect of the counter anion on the transport rate of alkali metal ions by a crown ether carrier, some of the inorganic and organic anions were used as counter anions for the potassium ion transport by a 18C6 carrier. The results are shown in Fig. 2, in which the logarithms of the transport rate of K^+ ion were plotted as a function of the enthalpy of hydration of the each inorganic anion (ΔH_{hyd}). The transport rates of K^+ ions had a tendencey to decrease with an increase in the enthalpy of hydration of an inorganic anion when used as a counter anion, though the relationship between log transport rate of K^+ and ΔH_{hyd} was not a straight line.

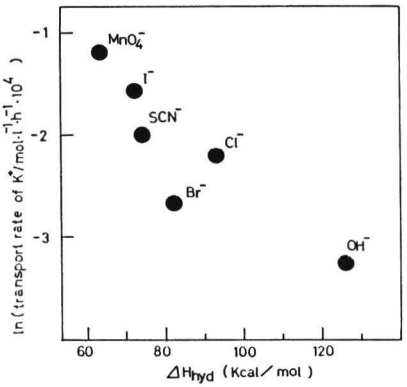

Fig. 2. The relationship between log (transport rate of K^+ /mol·l^{-1}·h^{-1}·10^4) and ΔH of anion hydration: [K^+ salt] = 10 mM; [18C6] =1.0 mM.

The effect of an organic anion on the transport rate of K^+ and Na^+ ions by a crown ether carrier was studied using crown ether (18C6,DC18C6, and DB18C6)-K^+-$CHCl_3$ systems (Table 2) and crown ether (18C6,and 15C5)-Na^+-$CHCl_3$ systems (Table 3), respectively. The use of an organic counter anion caused an ca 10-100 times increase in the transport rate of K^+ and Na^+ ions, in comparison with the case of the inorganic counter-anion usage. Though picrate anion, which has been used as an effective counter-anion, showed the largest transport rates of K^+ and Na^+ ions, regardless of the crown ether used as a carrier, other counter anions such as ethyl orange (EO^-) were found to also act as an effective counter-anion for the transport of alkali cations by a crown ether carrier. Table 4 shows the effect of nitrophenol derivatives including picric acid as a counter anion on the transport rate of K^+ and Na^+ cation by the 18C6 carrier. The transport rates with di- and mono-nitrophenols, which were of comparable orders, were found to be ca one-tenth of these with picric acid.

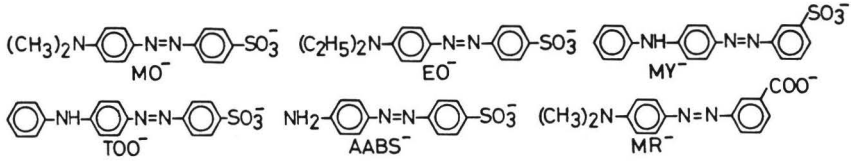

TABLE 2. Effect of counter-anions on the transport rate of K^+ ion[a].

Counter-anion	Transport rate (mol·l^{-1}·h^{-1} × 104)		
	18C6	DC18C6	DB18C6
Picrate (PA^-)	1.78	1.38	0.61
Trinitrobenzene sulfonate ($TNBS^-$)	0.35	0.32	0.22
p-Aminoazobenzoene sulfonate ($AABS^-$)	0.34	0.30	0.20
Ethyl orange (EO^-)	1.26	1.17	0.88
Tropaeolin OO (TOO^-)	1.12	0.73	0.35
Methyl orange (MO^-)	0.78	0.70	0.52
Methanil yellow (MY^-)	1.22	0.84	0.70
Methyl red (MR^-)	0.50	0.28	0.24

[a] Transport conditions: [K^+]=10.0 mM, [A^-]=1.0 mM, [L]=1.0 mM.

TABLE 3. Effect of counter-anions on the transport rate of Na^+ ion[a].

Counter-anion	Transport rate ($mol \cdot l^{-1} \cdot h^{-1} \times 104$)	
	18C6	15C5
Picrate (PA^-)	0.95	1.72
Trinitrobenzene sulfonate ($TNBS^-$)	0.24	0.23
Ethyl orange (EO^-)	0.47	0.84
Methanil yellow (MY^-)	0.31	0.49
p-Aminoazobenzoene sulfonate ($AABS^-$)	0.09	0.20

[a] Transport conditions: $[Na^+]$=100.0 mM, $[A^-]$=1.0 mM, [L]=10.0 mM.

TABLE 4. Transport rate of K^+ and Na^+ by 18C6 using nitrophenol derivatives as counter-anion[a].

Nitrophenol derivative	pKa	Transport rate ($mol \cdot l^{-1} \cdot h^{-1} \times 104$)	
		K^+	Na^+
Picric acid (PA)	0.3	1.06	0.95
2,4-dinitrophenol (DP)	4.1	0.10	0.10
o-nitrophenol (OP)	7.2	0.11	0.10
m-nitrophenol (MP)	8.4	0.08	0.09
p-nitrophenol (PP)	7.1	0.13	0.09

[a] Transport conditions: $[K^+]$=10.0 mM, $[Na^+]$=100.0 mM, $[A^-]$=1.0 mM, [18C6]=1.0 mM for K^+ transport and 10.0 mM for Na^+ transport.

4 DISCUSSION

The transport of an alkali cation through a bulk liquid membrane containing a crown ether has been accepted [6,8] that at the first step, the mobile crown ether carrier reacts at or near the membrane interface with an alkali cation, and almost simultaneously, this alkali cation-crown ether complex reacts with a counter anion to form an ion pair. Thus, the stability of the alkali metal cation-crown ether-counter anion complex, which has been reported to depend primarily upon how well an alkali cation fits the cavity surrounded by the crown ether ring, has been considered a primary factor leading to the transport of the alkali cation, like in the extraction of an alkali metal ion by crown ether carriers [21]. Only a few studies on the effect of counter anion on the transport rate of alkali cations by crown ether carrier have been reported [11,22]. So far, picrate anion has been frequently used as an organic counter-anion for the extraction[14] and/or transport[9] of alkali metal ions by crown ether carriers. To determine the substitutes for picrate anion as an counter-anion and to study the effect of the organic counter-anion, the use of organic anions such as different types of dyes has been used as a counter-anion in this study. As evidenced from Fig. 2, the smaller the enthalpy of hydration of the inorganic anion, the higher the transport rate of K^+ cation increased using the inorganic anion as a counter-anion. Thus, the results show that the hydrophobicity of the inorgainc anion used as a counter-anion is one of the factors governing the transport rate of the alkali cations. This suggestion may be useful for interpreting the results of Tables 2 and 3. Ethyl orange (EO^-), methyl orange (MO^-), tropeaolin OO (TOO^-), and p-aminoazobenzene sulfonic acid ($AABS^-$) anions have the same

azobenzene framework except for the amino substituent groups. The transport rates of K^+ and/or Na^+ cations using EO^- ,TOO^- and MO^- were found to be larger than those using $AABS^-$, regardless of the crown ether carriers. These differences in the transport rates may be caused by the differences between substituted amino groups attached to the azo benzene framework in these anions, in which EO^-, TOO^-, MO^- and $AABS^-$ anions have diethyl, phenyl, dimethyl, and no substituted groups, respectively. Thus, the organic anion with more hydrophobic groups favors the transport of alkali cations by the crown ether carrier. These results obtained in Tables 2 and 3 show that the hydrophobicity of the organic anion used as a counter-anion in the transport of alkali metal ions through a bulk liquid membrane containing a crown ether is one of the important factors governing the transport of alkali metal ions.

The transport rates of K^+ and Na^+ ions through a liquid membrane including 18C6 were compared using nitrophenol derivatives as an organic counter anion (Table 4). Although the transport rate with 2,4-dinitrophenol was expected to put it in the region between those with picric acid (trinitrophenol) and mononitrophenol, judged from the pKa values of their nitrophenol derivatives. The transport rate with 2,4-dinitriphenol was almost similar to those with mononitrophenol. This may be interpreted by the ease of intramolecular chelation of 2,3-dinitrophenol. The formation of an intramolecular chelate ring in the 2,4-dinitrophenol molecule will weaken the ionic interaction with the alkali metal ion.

5 REFERENCES

1. Pedersen C.J., J. Am. Chem. Soc. **89**, 2495, 7017 (1967), *ibid*, **92**, 391 (1970).
2. Frensdorff H.K., J. Am. Chem. Soc. **93**, 600 (1970).
3. Christensen J.J., Eatough D.J., and Izatt R.M., Chem. Rev. **74**, 351 (1974).
4. Lamb J.D., Christensen J.J., Izatt S.R., Bedke K., Astin M.S., and Izatt R.M., J. Am. Chem. Soc. **102**, 399 (1980).
5. Worg K.H., Yagi K., Smid J., J. Membr. Biol. **18**, 379 (1974).
6 Caraccio F., Cussler E.L., and Evans D.E., AIChE J. **21**, 160 (1970).
7. Christensen J.J., Lamb J.D., Izatt S.R., Starr S.E., Weed G.C., Astin M.S., Stiff B.D. and Izatt R.M., Chem. Rev. **100**, 3219 (1978).
8. Reusch C.F., Cussler E.L., AIChE J. **19**, 736 (1973).
9. Kobuke Y., Hanji K., Horiguchi K., Asada M., Nakayama Y., and Furukawa J., J. Am. Chem. Sco. **98**, 7414 (1976).
10. Newcomb M., Toner J.L., Helgeson R.C., and Cram D.J., J. Am. Chem. Soc. **101**, 4941 (1979).
11. Christensen J.J., "Bioenergetics and Thermodynamics: Model Systems" (ed by A. Braibanti), D. Reidel Publishing Co. Dordrecht, p. 111, 1980.
12. Frendorff K.K., J. Am. Chem. Soc. **93**, 4684 (1971).
13. Eisenman G., Ciani S.M., and Szabo G., J. Membr. Bio., **1**, 294 (1969).
14. Sadakane A., Iwashida T., and Toei K., Bull. Chem. Soc. Jpn. **48**, 60 (1975).
15. Takeda Y. and Goto H., Bull. Chem. Soc. Jpn. **52**, 1920 (1979).
16. Takeda Y., Bull. Chem. Soc. Jpn. **53**, 2393 (1980).
17. Hasegawa Y., Wakabayashi H., Sakuma M., and Sekine T., Bull. Chem. Soc. Jpn. **54**, 2472 (1981).
18. Takeda Y., Wada Y., and Fujiwara S., Bull. Chem. Soc. Jpn. **54**, 3727 (1981).
19. Sekine T. J., Synth. Org. Chem. Jpn. **41**, 633 (1983).
20. Tanigawa M., Nishiyama S., Tsuruya S., and Masai M., Chem. Eng. J. **39**, 157 (1988).
21. Kolthoff I.M., Anal. Chem. **51**, 1R (1979).
Rais J., and Selucky P., Radiochem. Radioanal, Lett. **6**, 257 (1971).

Solvent Extraction 1990, T. Sekine (Editor)

© 1992 Elsevier Science Publishers B.V. All rights reserved

RARE EARTH RECOVERY USING PSEUDO LIQUID MEMBRANES

Z. GU
Institute of Atomic Energy, P. O. Box 275, Beijing, Peoples Republic of China
J.D. NAVRATIL* and H. CHENG
Department of Mineral Processing and Extractive Metallurgy, The University of New South Wales, P. O. Box 1, Kensington NSW 2033 Australia

ABSTRACT

Although liquid membranes have several advantages over conventional liquid-liquid extraction, problems such as membrane instability remain. In order to solve these problems, we have combined an electrostatic field with the principle of liquid membranes and developed a novel reactor system for rare earth recovery. Our cylindrical reactor, filled with extractant and diluent, is divided by means of a perforated cylinder into an outer annular extraction cell and an inner stripping cell. Below the extraction and stripping cells are two settlers for the aqueous solutions. The design of the reactor permits the organic solution to flow freely through the special perforated cylinder and the added feed and strip solutions, outside and inside the perforation, respectively, to be completely separated. The simple process which has high efficiency, low energy and reagent consumption, and small leakage offers a new hydrometallurgical technology for rare earth recovery.

INTRODUCTION

Liquid membranes have evolved in the past two decades as an exciting new separations technology (1). They can be divided into two types: supported liquid membrane (SLM) and liquid surfactant membrane (LSM). SLM is made by impregnating porous solid membranes (e.g., hollow fibers) with a carrier liquid membrane material (e.g., solvent extractant and diluent). LSM is essentially the double-emulsion liquid membrane system. The extraction reaction for both systems takes place at the interface between the membrane phase and feed solution, while at the same time a stripping reaction occurs at the interface between the membrane phase and

---

*Present address: Chemical Waste Management, Inc., Geneva Research Center, 1950 S. Batavia Ave., Geneva, IL 60134-3310 USA.

stripping phase.

Liquid membranes have several advantages over conventional liquid-liquid extraction. The process is continuous since concurrent extraction and stripping takes place in a single stage rather than in two separated stages as required by liquid-liquid extraction. In this way the chemical equilibrium which is inherent in solvent extraction is not necessary. This non-equilibrium character of liquid membranes results in the reduction of separation stages, the saving of reagents as well as the lowering of capital costs.

However, liquid membranes have some unsolved problems. The main problem of SLM is the poor stability of the membrane due to the loss of extractant carrier sorbed in the microporous membrane. The LSM process is complicated since the introduction of surfactant into the membrane system brings two additional stages of emulsion preparation and emulsion breaking besides the separation stage.

2 PSEUDO LIQUID MEMBRANES

In order to solve these problems, Gu (1988) combined an electrostatic field with the principle of liquid membranes and developed a new type of separation method which he named "electrostatic pseudo liquid membrane" (ESPLIM). ESPLIM retains the main advantages of SLM and LSM and overcomes the above mentioned shortcomings, such as the complicated process of LSM and instability of SLM.

The principle of ESPLIM is shown in Figure 1. A reaction tank is filled with extractant and diluent, and it is divided into an extraction cell and a stripping cell by a perforated plate. The organic solution can flow freely through the perforated plate while the added feed and strip aqueous solutions at both sides of the plate are completely separated. There are settlers for the aqueous solution below the extraction cell and the stripping cell. These two settlers are separated by a partition.

During operation, a high voltage electrostatic field is applied simultaneously across the extraction cell and the stripping cell. Under the electric field, the feed solution added to the extraction cell and the stripping solution added to the stripping

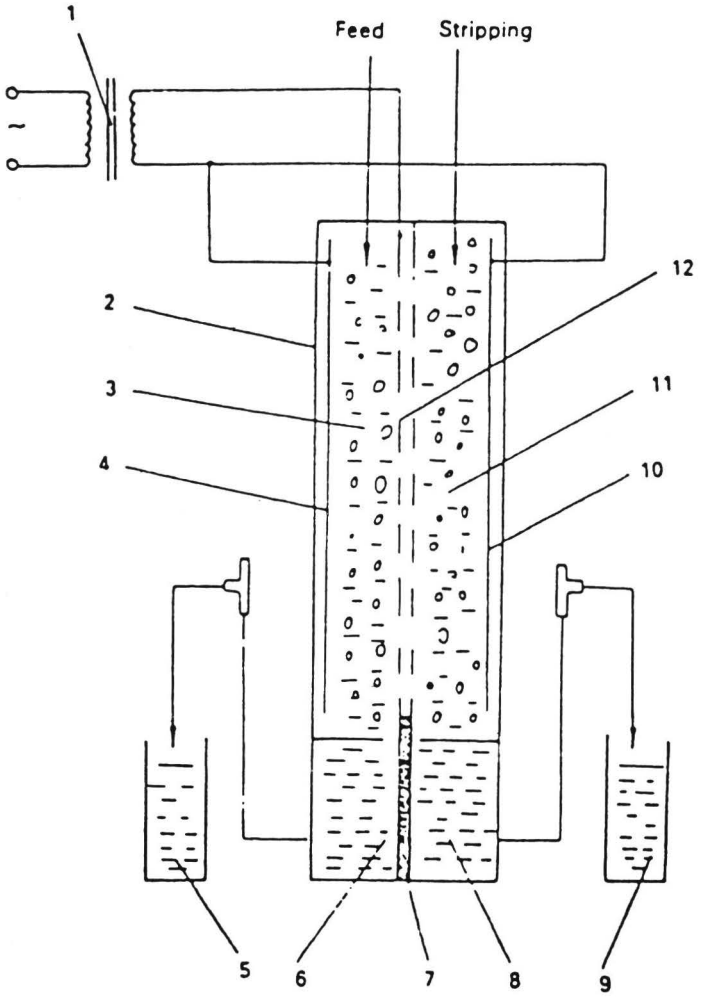

Fig. 1. Schematic diagram of ESPLIM. (1) H.V. power supply; (2) reactor tank; (3) extraction cell; (4) and (10) H.V. electrodes; (5) raffinate tank; (6) extraction settler; (7) solid partition; (8) stripping settler; (9) concentrate tank; (11) stripping cell; (12) perforated Teflon plate.

cell are dispersed into numerous droplets in the continuous organic phase. In the extraction cell, the solute in the aqueous droplets is extracted into the organic phase. The complex formed in the extraction cell, driven by its own concentration gradient, diffuses through the perforated plate into the stripping cell. The extractant is regenerated after the solute is stripped off in the stripping side. The concentration gradient of the extractant then actuates itself to diffuse back to the extraction cell through the perforated plate. The aqueous droplets in the extraction cell and stripping cell sink under gravity in the organic phase and finally go outside the electrical field at the bottom of the reaction tank where they separate from the organic phase.

ESPLIM offers the same advantages as liquid membrane systems, such as higher rate of mass transfer, fewer separation stages and lower extractant inventory. Furthermore, it possesses some unique features, such as simple processing, simple operation and low capital and energy costs. It also avoids the problems of membranes such as instability and has an order of magnitude higher flux (10^{-7} mol/cm^2-s) than SLM (Gu, 1990).

Gu's (1988) experimental work to demonstrate the principle of ESPLIM has shown that 99% extraction of Co^{2+} was achieved after the aqueous droplets containing 1000 ppm Co^{2+} merely passed through a 100 mm high electrostatic field with the duration of only 4 seconds. At the same time, the Co^{2+} concentration in the stripping solution increased sharply from zero to nearly 20,000 ppm. The consumption of electric power was only 2 watts.

The extraction of Eu^{3+} was demonstrated using ESPLIM. From the feed solution containing 780 ppm Eu^{3+}, the extraction percentage reached 95, while the Eu^{3+} was enriched 60 times in the stripping cell. The results in Table 1 show the effects of the electrostatic field in the ESPLIM process on the extraction of europium. The dispersion of the feed solution and the stripping solution by the electrostatic field in the organic phase directly affects the results of extraction and stripping. On the other hand, oscillation and recirculation of aqueous droplets in the electrostatic field are beneficial to the renewal of the interface and mass transfer is thus accelerated. The voltage required to

achieve good dispersion results is changeable according to the particular reaction tank used and the treatment method of the electrode.

Table 1. Effect of electric field voltage on europium extraction with P5709.

Voltage (kV)	Dispersion of the aqueous droplets	Extraction percentage of Eu^{2+},(%)
3.2	Worst, sinking in large drop	71.9
3.4	Worse, sinking in large drop	74.8
3.6	Bad, sink in small drop	77.8
3.8	Common, droplets oscillation	95.6
4.0	Good, droplets oscillation	96.3

3 FUTURE WORK

The effects of voltage of the electrostatic field on our test systems are being evaluated in cylindrical and rectangular reaction tanks. The cylindrical reactor, filled with extractant and diluent, is divided by means of a perforated cylinder into an outer annular extraction cell and an inner stripping cell. Below the extraction and stripping cells are two settlers for the aqueous solutions. The design of the reactor permits the organic solution to flow freely through the special perforated cylinder and the added feed and strip solutions, outside and inside the perforation, respectively, to be completely separated. The cylindrical reactor has less material requirements and three times more interfacial surface area than the rectangular reactor of equal volume. Besides the effect of reactor size and configuration, the perforation size of the separator plate is also being investigated.

Like liquid membranes, the ESPLIM process in which extraction and stripping are coupled inside the reaction tank is a non-equilibrium process. Under steady state conditions, the complex concentration is far below saturation, resulting in the very large driving force for mass transfer. Thus we are exploring the following additional factors in a specific reaction tank: 1) Concentration of extractant, 2) diluent type and density, 3) solute concentration,

4) flow ratios and 5) temperature.

The use of an ultrasonic field in place of an electrostatic field will be tested in the reaction cells as well as the absence of dispersion fields. Various sizes of droplets and aerosols will also be formed by physical means.

4 CONCLUSIONS

Work so far has shown that ESPLIM is a highly efficient and very simple separation process. While maintaining the advantages of liquid membranes, ESPLIM overcomes some shortcomings existing in liquid membrane technology. It avoids the procedures of emulsification and demulsification which are indispensable for LSM, thus remarkably simplifying the process. The use of a perforated plate (instead of porous solid membrane which is used as membrane support in SLM) leads to the significant reduction of resistance to mass transfer and elimination of the problem of membrane instability. It is expected that ESPLIM can potentially be competitive in the fields of hydrometallurgy.

5 REFERENCES

Gu, Z., Hua Gong Xue Bao (in Chinese), 6, 1988, 667.
Gu, Z., submitted to J. Membrane Science, 1990.
Lonsdale, H.K., "The growth of membrane technology", J. Membrane Sci., 10, 1982, 81.
Strathmann, H., "Membrane separation processes", J. Membrane Sci., 9, 1981, 121.
Way, J.D., Noble, R.D., Flynn, T.M., and Sloan, E.D., "Liquid membrane transport: a survey", J. Membrane Sci., 12, 1982, 239.

Solvent Extraction 1990, T. Sekine (Editor)

© 1992 Elsevier Science Publishers B.V. All rights reserved

MEMBRANE EXTRACTION FOR SEPARATION OF LONG-CHAIN UNSATURATED FATTY ACIDS

Y.MATSUBA, Harima Chemicals, Inc., Kakogawa 675, Japan;
Y.KITAMURA, T.TAKAHASHI, Dept. of Applied Chem., Okayama Univ., Okayama 700, Japan

ABSTRACT

A solvent extraction process has been developed for the fractional separation of long-chain unsaturated fatty acids. Acetonitrile (10wt% water) and n-heptane were used as solvents. Two feeds were used; a mixture of oleic and linoleic acid, and a cod oil fatty acid containing about 9wt% EPA and 2wt% DHA. The liquid-liquid equilibria data for these systems suggest that multistage extraction can separate fatty acids by their degree of unsaturation. A dispersion-free membrane extraction was then examined for this purpose, because polyunsaturated fatty acids act as emulsifiers to cause flooding in dispersion systems. The extractor consisted of a 5m long microporous tube inserted in an outer shell equipped with a center feed tap. The experimental results showed that this membrane process can be successfully applied to the purification of EPA and DHA. In addition, the efficiency of the extractor was evaluated in terms of the number of theoretical stages.

1 INTRODUCTION

Liquid-liquid extraction is one of the available processes for fatty acid separations (Pryde, 1979). Conventional dispersion-type extractors, however, have a critical problem for the purification of polyunsaturated fatty acids such as EPA and DHA, because they act as emulsifiers; the emulsification causes flooding in the dispersion system. Membrane extraction is a new separation technique especially suitable for biochemical studies (Frank et al., 1985, Dahuron et al., 1988). The most superior feature of this process is its dispersion-free nature, in which problems arising from phase dispersion can be eliminated.

The purpose of this study is to apply the membrane extraction to the fractional separation of long-chain unsaturated fatty acids. We first show that the extraction with acetonitrile (10wt% water) and n-heptane is effective for the separation of fatty acids on a theoretical basis. The applications of the membrane extractor using a microporous tube are then presented.

2 EXPERIMENTAL

2.1 Materials

All organic chemicals were reagent grade and used as received. A mixture of oleic and linoleic acid was prepared by blending of the reagents. Cod oil fatty acid was prepared by hydrolysis of cod oil followed by distillation. The GLC compositions of these feeds are listed in Tables 1 and 2.

TABLE 1

Feed composition of oleic-linoleic mixture

Composition [wt%]						
C16:0	C16:1	C18:0	C18:1E	C18:1	C18:2	Others
1.3	0.5	0.8	2.1	47.9	42.7	4.7

C18:1 : Oleic C18:2 : Linoleic

TABLE 2

Feed composition of cod oil fatty acid

Composition [wt%]										
C14:0	C16:0	C16:1 n-7	C16:2 n-4	C16:4 n-3	C18:0	C18:1 n-11	C18:1 n-9	C18:1 n-7	C18:2 n-6	C18:3 n-3
3.9	2.2	11.0	1.0	1.0	0.8	1.9	19.3	6.9	1.3	0.8
C18:4 n-3	C20:1 n-11	C20:1 n-9	C20:4 n-3	C20:5 n-3	C21:5 n-3	C22:1 n-11	C22:4 n-6	C22:5 n-3	C22:6 n-3	Others
2.7	9.7	2.7	0.2	8.5	0.3	4.8	0.4	0.3	2.1	18.2

C20:5 n-3 : EPA C22:6 n-3 : DHA

2.2 Apparatus

Fig.1 schematically shows the membrane extractor, which consisted of a 5m long hydrophobic microporous tube inserted in an outer shell with a small clearance. The inner tube was POREFLON TB-32 of 2mm ID and 3mm OD with a 1μm pore size. The shell was a PTFE tube of 4mm ID and 6mm OD. A feed tap was set at the center of the shell. Both ends of the shell were sealed with PTFE T-joints. The apparatus was used as a bundled coil of about 50cm diameter.

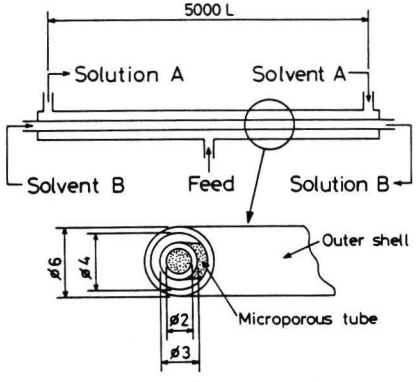

Fig.1. Experimental apparatus (membrane extractor using a microporous tube).

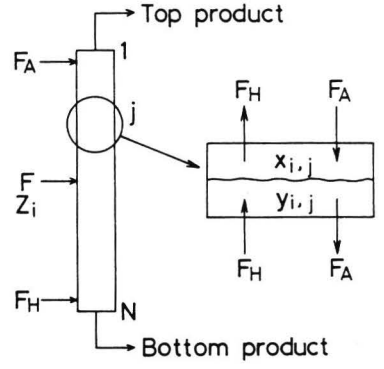

Fig.2. Fractional extraction model consisting of N theoretical stages.

Two types of pumps were used; one was a dual-plunger type HPLC pump for solvent supply and the other was a syringe pump for feed supply.

2.3 Procedures

All experiments were carried out with the double solvent countercurrent flow using acetonitrile (10wt% water) and n-heptane at 20°C. Fatty acid mixtures were fed in two ways. One is the "center feed" supplied into the center of the shell, and the other is the "end feed" supplied into the shell end as acetonitrile solutions. The composition of fatty acids were measured using a Shimadzu model GC-15A gas chromatograph equipped with a capillary column.

The key operation of this process is a pressure control between two liquid phases. Excess pressure in the n-heptane phase may cause emulsification due to the leakage of n-heptane through the pores. By setting the outlet level of the acetonitrile phase higher than the other by 5-10cm, no emulsion was formed throughout all the experiments.

3 RESULTS AND DISCUSSION

3.1 Applicability of extraction process

The liquid-liquid equilibria for the present system has been previously correlated (Matsuba et al.,1989a,1990). For a multicomponent system, the i-component concentration in the acetonitrile phase, y_i, is given as

$$y_i = y_i^{\circ} X_i \qquad (1)$$

where y_i° is the solute concentration in the acetonitrile phase for the pure i-component system, which is given as a function of total solutes concentration in the n-heptane phase, and X_i is the solvent-free i-component mole fraction in the n-heptane phase.

Fig.2 shows the theoretical stage model consisting of N theoretical stages. Two solvents are supplied to the top and the bottom, while the fatty acids are fed into the center of the column. Concentration profiles developed in a steady state are calculated from a set of nonlinear simultaneous equations based on material balance. The equation for the j-stage is written as

$$F_A y_{i,j-1} - F_H x_{i,j} - F_A y_{i,j} + F_H x_{i,j+1} = -FZ_i \quad (j = \text{feed stage})$$
$$= 0 \quad (j \neq \text{feed stage}) \qquad (2)$$

where F_A and F_H represent the flow rate of the acetonitrile and the n-heptane phase, respectively, x_i is the i-component concentration in the n-heptane phase, F is the feed rate, and Z_i is the mole fraction of the i-component in the feed. The detailed strategy for the calculation resembles that for the multicomponent distillation proposed by Wang et al.(1966).

Fig.3 shows the calculated results for the oleic-linoleic separations under the feed conditions listed in Table 1. The linoleic acid purity* (C18:2 purity) increases up to about 90wt% with increasing number of theoretical stages, N, whereas the C18:2 recovery* decreases with N. To alleviate a drastic

*Purity means weight fraction in acetonitrile phase product, and recovery means weight ratio based on acetonitrile phase product to feed mixture. Both of these values are on a solvent-free basis.

decrease of recovery in large N regions, operations with higher solvent ratios will be employed, because the C18:2 purity is less sensitive to F_A/F_H.

The separation of cod oil fatty acids listed in Table 2 were also numerically examined. The results are shown in Fig.4, where EPA and DHA are accounted for as one component because they indicate almost equal partition coefficients in the present system. A distinction from the above system was observed in the recovery curve versus N. In the preceding system the C18:2 purity can not increase without any recovery loss in C18:2, but in this system both the purity and the recovery of EPA+DHA simultaneously increase with N. This result suggests that fractional extraction is rather favorable for the separation of polyunsaturated fatty acids.

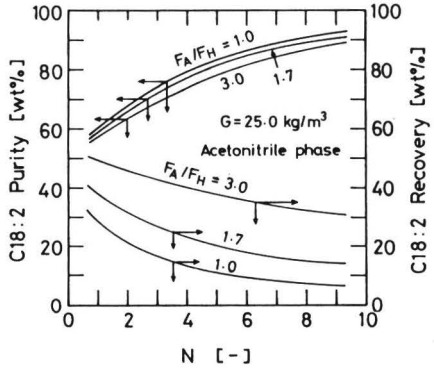

Fig.3. Calculated results for C18:1 -C18:2 separation using a fractional extraction model.

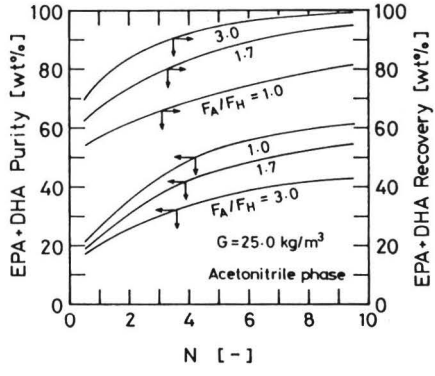

Fig.4. Calculated results for EPA+DHA purification using a fractional extraction model.

3.2 Membrane extraction of fatty acids

Fig.5 shows the variations in the purity and recovery of C18:2 with solvent flow rates under the condition of $F_A=F_H$. As can be seen, the C18:2 purity decreases with increasing solvent flow rates, while on the contrary the recovery increases. The "center feed" makes the C18:2 recovery higher than the "end feed", but unfortunately it's always accompanied with some decrease in the C18:2 purity. This depression, however, is gradually diminished at the low solvent flow rates below 0.5×10^{-8} m^3/s, i.e. the benefit of the "center feed" appears in the lower flow regions.

The separation of polyunsaturated species is the main subject of this study. A basic discussion has been made on countercurrent extractions of cod oil fatty acid (Matsuba et al.,1989b). In the present study, we demonstrate additional features of the membrane extractor. Fig.6 shows the variations of the purity and recovery of EPA+DHA with solvent flow rates. In the "end feed" the EPA+DHA purity gradually decreases with solvent flow rates, while the recovery increases up to about 75wt%. In the case of the "center feed", the

recovery curve has a minimum point around $F_A=F_H=1.2\times10^{-8}$ m^3/s. At the flow rates below the minimum point, both the purity and the recovery of EPA+DHA are simultaneously boosted. Such phenomena are due to their large partition coefficients to the acetonitrile phase; the EPA and DHA are easily recovered from the n-heptane to the acetonitrile phase in the stripping section.

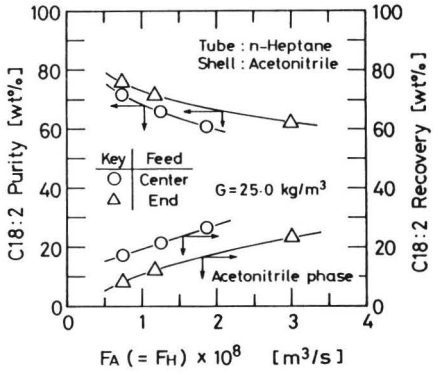

Fig.5. Experimental results for C18:1 -C18:2 separation ("center feed" into acetonitrile phase).

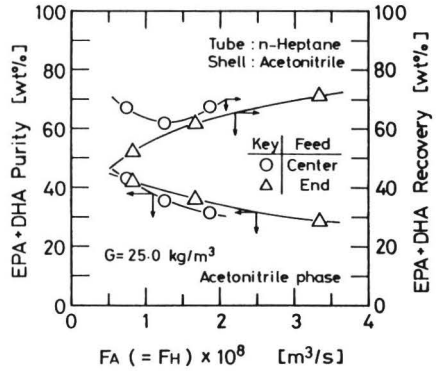

Fig.6. Experimental results for EPA+DHA purification ("center feed" into acetonitrile phase).

Fig.7 shows the results for the "center feed" into the n-heptane phase. The minimum point in the recovery curve is also observed in this case. But the "center feed" can improve neither the purity nor the recovery of EPA+DHA. Therefore, only the "center feed" into the acetonitrile phase is valid for the EPA+DHA purification.

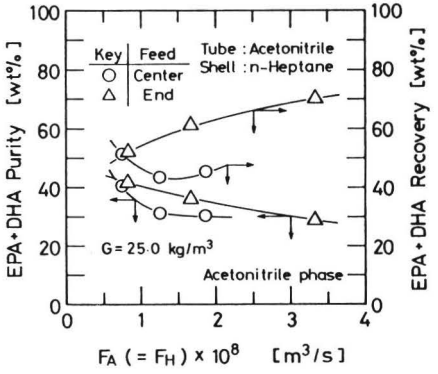

Fig.7. Experimental results for EPA +DHA purification ("center feed" into n-heptane phase).

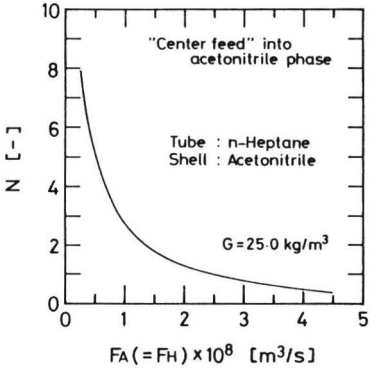

Fig.8. Variation of number of theoretical stages with solvent flow rates in fractional membrane extractor.

From the comparison between the calculation (Figs.3,4) and the experimental results (Figs.5,6), the efficiency of the membrane extractor was estimated in terms of the number of theoretical stages,N. Fig.8 shows the evaluation of

N for the "center feed" into the acetonitrile phase. The steep increase in N is observed in the region below 1.0×10^{-8} m^3/s, i.e. the membrane extractor exhibits high separation performance in such low flow regions. On the other hand, N becomes less than 1 in the region above 2.5×10^{-8} m^3/s. As described in a previous study (Matsuba et al.,1989b), the membrane used in this study is insufficient in its mass-transfer ability because of its thickness. If better materials were used, the dependence of N on the flow rate could be altered to offer higher separations. This will be a primary subject to be explored in the future. Further discussion on a mass transfer model is also necessary in order to propose a method for designing the fractional membrane extractor.

4 CONCLUSIONS

These experimental results led us to the conclusion that the membrane extractor is successfully applicable for the fractional extraction of long-chain unsaturated fatty acids based on their unsaturation, especially for the purification of polyunsaturated species such as EPA and DHA. The "center feed" scheme improves the recovery of unsaturated fatty acids to the acetonitrile phase compared to the conventional countercurrent flow ("end feed") method.

NOMENCLATURE

F	feed rate, mol/s
F_A	acetonitrile flow rate, m^3/s
F_H	n-heptane flow rate, m^3/s
G	weight ratio of total solutes to total solvents supplied to an extractor, kg/m^3
N	number of theoretical stages
X	solvent-free mole fraction in n-heptane phase
x	solute concentration in n-heptane phase, mol/m^3
y	solute concentration in acetonitrile phase, mol/m^3
y°	solute concentration in acetonitrile phase for pure component system, mol/m^3
Z	mole fraction in feed
Subscripts	
i	i-component
j	j-stage

REFERENCES

Dahuron, L. and Cussler, E.L., 1988. Protein extractions with hollow fibers. AIChE J., 34: 130-136.

Frank G.T. and Sirkar K.K., 1985. Alcohol production by yeast fermentation and membrane extraction. Biotech. Bioeng. Symp. Ser., 15: 621-631.

Matsuba, Y., Takahashi, T. and Kitamura, Y., 1989a. A correlation of liquid-liquid equilibria for long-chain unsaturated fatty acids. Kagaku Kogaku Ronbunshu, 15: 208-213.

———, 1989b. Separation of long-chain unsaturated fatty acid by solvent extraction with microporous tube. Kagaku Kogaku Ronbunshu, 15: 451-457.

———, 1990. Liquid-liquid equilibria of cod oil fatty acids-acetonitrile (10wt% water)-n-heptane system, Kagaku Kogaku Ronbunshu, 16: 404-407.

Pryde, E.H., 1979. Fatty Acids. The American Oil Chemists' Society-Champaign, Illinois, pp. 125-156.

Wang, J.C. and Henke, G.E., 1966. Tridiagonal matrix for distillation. Hydrocarbon Process., 45: 155-163.

Solvent Extraction 1990, T. Sekine (Editor)

© 1992 Elsevier Science Publishers B.V. All rights reserved

AFFINITY SEPARATION OF PROTEIN BY GEL-MATRIX MEMBRANE

H. KURAHASHI*, M. IMAI and M. SHIMIZU
Department of Chemical Engineering, Tokyo University of Agriculture and Technology, Tokyo 184, Japan
*Department of Chemical Engineering, University of Tokyo, Tokyo 113, Japan

ABSTRACT

KURAHASHI, H., IMAI, M. and SHIMIZU, M., 1990. Affinity separation of protein by gel-matrix membrane. Proc. ISEC'90

Distribution of a protein between an affinity membrane and an aqueous phase was investigated using agarose gel-matrix containing immobilized Cibacron Blue 3G-A. Alcohol dehydrogenase was distributed in an affinity membrane of various gel concentrations, containing immobilized ligand. The distribution equilibrium depended on the pH in the aqueous phase. The effective ligand concentration was obtained for various gel concentrations.

1 INTRODUCTION

Biospecific affinity, which has a high selectivity for biological components, is one of the most useful separation principles in advanced bioindustries. A gel-matrix has been commonly used for biomaterials in separation processes. However, channelling or compaction has been found to occur in chromatographical operations using gel-matrix bead (Katoh et al., 1980).

Separation of biomaterials using an affinity membrane, which is a gel-matrix immobilized ligand, is anticipated to perform a high selectivity separation in moderate conditions without channelling or compaction occurring. The gel-matrix is composed of an inner aqueous phase and gel-matrix fiber and the biological components are macromolecules. Therefore, the gel-matrix type and its concentration are considered to affect the diffusion coefficient in the gel-matrix (Ackers and Steere, 1962), the performance in affinity chromatographical separation (Katoh et al., 1980), and the distribution behavior.

This present study describes the effect of pH on the distribution equilibrium and the effect of the gel concentration on the distribution between the affinity membrane and the aqueous phase. Finally, an experimentally obtained effective ligand concentration was proposed.

2 MATERIALS AND METHODS

2.1 Materials

The Chemicals were obtained from the following suppliers: Cibacron Blue 3G-A from Sigma Chemical Co., St. Louis, MO; Alcohol dehydrogenase from yeast (E.C.1.1.1.1) and NAD from Oriental Yeast Co., Ltd., Tokyo; and Agarose from Wako Chemical Co., Tokyo,(Type S). All other chemicals used were of analytical-grade. The chemicals were used without further purification.

2.2 Preparation of Affinity membrane

Agarose solution was heated at 90℃. Agarose gel membrane was cast on a plate glass with 0.06cm side runners using an acrylic-resin blade at room temperature. After gelating the surface, the membrane was immersed in water at 20℃ for 24h to ensure that gelation was complete. The membrane diameter is 7.2cm and the thickness is ca. 0.06cm.

The agarose gel membrane was added to a beaker containing 130ml of 1.9×10^{-3} $g\cdot cm^{-3}$ Cibacron Blue 3G-A (CB), and $0.01mol\cdot cm^{-3}$ Na_2CO_3. The beaker was shaken in a water bath at 45 ℃. The coupled amount of dye was estimated spectrophotometrically (Bouriotis and Dean, 1981), after hydrolysis of the gel in 0.1M HCl for 20min at 90℃.

2.3 Distribution of ADH between membrane and aqueous phase

The affinity membrane was equilibrated with 50mM sodium phosphate buffer solution containing 0.2mM EDTA and 5mM 2-mercaptoethanol. The membrane was added to a beaker containing various amounts of Alcohol dehydrogenase (ADH) in 20ml of the same buffer solution. The beaker was shaken in a water bath for 24h in order for the system to come to equilibrium at 25℃. The amount of protein in the aqueous phase was determined by measuring the optical adsorption at 280nm. The amount of ADH bound to the membrane was calculated from the total amount of ADH present at the beginning of experiment less the amount remaining in the aqueous phase at equilibrium.

The distribution experiments using ADH or NAD with agarose gel membrane (with no affinity ligand attached) were carried out using the same procedure as that with the affinity membrane. The experimental results for the membrane and aqueous phases were determined under various experimental conditions.

3 RESULTS

3.1 Effect of pH on the ADH distribution

The pH dependence on D_{ML} is shown in Figure 1. The distribution ratio D_{ML} was defined as the ratio of the concentration of ADH per unit volume of the membrane and the concentration of ADH in the aqueous phase at equilibrium.

The values of D_{ML} decreased markedly over a pH range of 6 to 8.2. The decrease in D_{ML} can be explained by electrostatic interaction between ADH and CB. As Cibacron Blue has a negative charge (Lascu et al., 1984) and ADH was

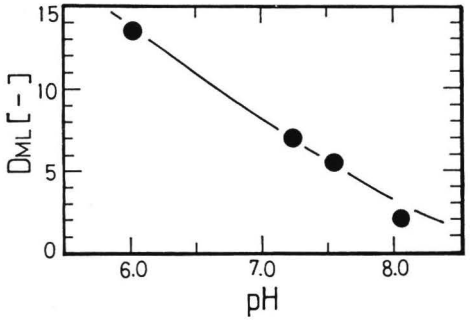

Fig.1. Effect of pH on the distribution ratio of ADH, $[CB]_t = 2.5\times10^{-6}$ mol·cm^{-3}-memb., C_G=6wt%.

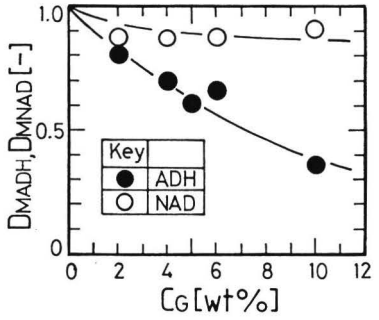

Fig.2. Effect of gel concentration on D_{MADH} and D_{MNAD}, $[CB]_t$=0 mol·cm^{-3}-memb., pH=7.25.

distributed at pH>pI.

The effect of KCl addition to the aqueous phase on the distribution ratio D_{ML} was measured. The distribution ratio decreased with increasing KCl concentration.

3.2 Effect of ligand concentration and gel concentration on ADH distribution

Within the affinity membrane, ADH molecules are considered to exist in a free state and a ligand bound state. The distribution ratio of free ADH (D_{MADH}), was determined using agarose membrane containing no ligand. Figure 2 shows the plot of D_{MADH} against the gel concentration for the agarose gel membrane at pH=7.25. The affinity distribution ratio is given by Eq.(1).

$$D_{MA} = D_{ML} - D_{MADH} \quad (1)$$

In Figure 3, the variation in the affinity distribution ratio with the

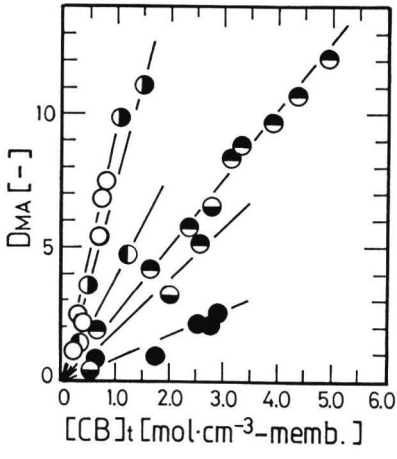

Key	C_G [wt%]
○	2
◑	4
◐	5
◑	6
◑	8
●	10

Fig.3. Relationship between D_{MA} and $[CB]_t$ for various gel concentrations, pH=7.25.

immobilized ligand concentration is shown for various gel concentrations at pH 7.25. The value of D_{MA} was proportional to the total ligand concentration coupled to agarose gel-matrix membrane for various gel concentrations. At the same ligand concentration, D_{MA} decreased with increasing gel concentration. The gel concentration and the ligand concentration are effective factors on the affinity distribution.

4 DISCUSSION

ADH has a total of four binding sites, each with equal ligand binding ability (Vallee, 1955). However, in the case of membrane immobilized ligand, only one molecule of ADH is considered to bind to one molecule of CB attached to the gel-matrix. On the basis of this assumption, the apparent dissociation constant ($mol \cdot cm^{-3}$-memb.) is defined by Eq.(2).

$$K \equiv \frac{[ADH][CB]}{[ADH \cdot CB]} = \frac{[ADH][CB]_t}{[ADH \cdot CB]} - 4[ADH] = \frac{4 D_{MADH}}{D_{MA}}[CB]_t - 4 D_{MADH} Ce \qquad (2)$$

where [ADH] is the concentration of free ADH within the membrane, [ADH·CB] is the concentration of bound ADH to immobilized CB, [CB] is the concentration of immobilized CB unbound to ADH, the subscript t represents the value of the total concentration. They are expressed in units of $mol \cdot cm^{-3}$-memb. Ce is the concentration of ADH in the aqueous phase at equilibrium ($mol \cdot cm^{-3}$-aq.).

In this study, since Ce was less than 10^{-8} $mol \cdot cm^{-3}$-aq., the term on the right side of Eq.(2) can be neglected. Therefore, the affinity distribution ratio, D_{MA} can be redefined by Eq.(3).

$$D_{MA} = \frac{4 D_{MADH}}{K_M}[CB]_t \qquad (3)$$

The relationship between D_{MA} and $[CB]_t$ was found to agree well with Eq.(3). The values of the apparent dissociation constants (K_M) were calculated using Eq.(3) with the experimental values of D_{MA} and D_{MADH}. K_M increased with increasing gel concentration. If the interaction between the affinity ligand and ADH at each gel concentration is assumed to be identical, the extrapolated apparent dissociation constant, which was extrapolated to zero gel concentration, would be equal to the dissociation constant between immobilized CB and ADH within the affinity membrane. The extrapolated value of K_M was $1.5 \times 10^{-7} mol \cdot cm^{-3}$-memb.

In the affinity membrane, it is considered that ADH molecules may come into contact with a part of CB molecules attached to gel-matrix fiber due to the steric hindrance of the gel-matrix. The effective ligand concentration

normalized by the total ligand concentration is given by:

$$\alpha(C_G)=\frac{\text{concentration of CB that is able to contact with ADH}}{\text{total CB concentration}} \quad (4)$$

The values of $\alpha(C_G)$ were calculated by Eq.(5) assuming that the gel-matrix is uniform and the ligands coupled uniformly to agarose gel-matrix.

$$\alpha(C_G)=D_{MADH}/D_{MCB} \quad (5)$$

The value of D_{MCB} is required to calculate $\alpha(C_G)$, but could not be measured because of the coupling to agarose gel-matrix. Therefore, the value measured for NAD, which has a similar molecular weight, was used for D_{MCB} (Fig.2).

The values calculated from the experimental results are written as follows:

$$\alpha(C_G)=K_M(C_G=0)/K_M(C_G) \quad (6)$$

The calculated curves of $\alpha(C_G)$ are shown in Figure 4. The solid line was calculated from experimental values of K_M. The broken line was calculated using Eq.(5). The values of effective ligand concentration calculated from the experimental results are less than the values calculated using Eq.(5). At a gel concentration less than 6wt% the values of $\alpha(C_G)$ calculated from the experimental results were found to decrease with increasing gel concentration. Beyond this concentration the value of $\alpha(C_G)$ remained relatively constant. On a large scale the gel-matrix can be considered uniform. However, from the perspective of the molecular size of ADH, this matrix cannot be considered uniform. Furthermore, the attachment of CB to the gel-matrix may be non-uniform. Thus, the effective ligand concentration is considered to depend on the

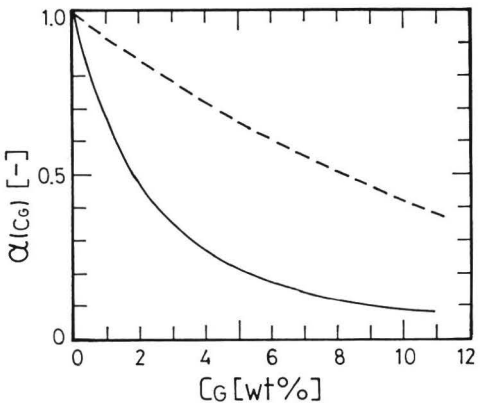

Fig.4. Relationship between $\alpha(C_G)$ and the gel concentration, pH=7.25. The solid line is calculated from experimental data. The broken line is calculated by Eq.(5).

gel-matrix structure and the size of the biomolecules. It is suggested that the choice of the gel-matrix and its concentration affects the affinity distribution in separation methods using a gel-matrix medium.

4 CONCLUSION

Distribution of ADH between the ligand immobilized gel-matrix membrane and the aqueous phase was studied using CB bound agarose gel. The distribution equilibrium was dependent upon pH. The distribution ratio was proportional to the ligand concentration and depended on the gel concentration. The effective ligand concentration was calculated from the experimental data for various gel concentrations and was found to decrease with increasing gel concentration.

5 NOTATION

$[ADH]$ = concentration of free ADH within the affinity membrane [$mol \cdot cm^{-3}$-memb.]
$[ADH \cdot CB]$ = concentration of ADH bound to immobilized CB [$mol \cdot cm^{-3}$-memb.]
$[Cb]$ = concentration of immobilized CB unbound to ADH [$mol \cdot cm^{-3}$-memb.]
$[CB]_t$ = total concentration of immobilized Cb within the adffinity membrane [$mol \cdot cm^{-3}$-aq.]
Ce = concentration of ADH in the aqueous phase at equilibrium [$mol \cdot cm^{-3}$-memb.]
D_{MA} = affinity distribution ratio of ADH between the affinity membrane and the aqueous phase, defined by Eq.(1) [-]
D_{MADH} = distribution ratio of ADH between the agarose gel membrane and the aqueous phase [-]
D_{MCB} = distribution ratio of Cb between the agarose gel membrane and the aqeous phase (denoted as D_{MNAD} in this study) [-]
D_{ML} = distribution ratio of ADH between the affinity membrane and the aqueous phase [-]
D_{MNAD} = distribution ratio of NAD between the agarose gel membrane and the aqueous phase [-]
K_M = apparent affinity constant, defined by Eq.(2) [$mol \cdot cm^{-3}$-memb.]
$\alpha(C_G)$ = effective ligand concentration normalized by the total ligand concentration [-]

6 REFERENCE

Ackers, G.K. and Steere, R.L., 1962. Restricted diffusion of macromolecules through agar-gel membranes. Biochim. Biophys. Acta, 59: 137-149.

Bouriotis, V. and Dean, P.D.G., 1981. Use of triazine dyes in the affinity chromatographic purification of alkaline phosphatase from calf intestine. J. Chromatogr., 206: 521-530.

Katoh, S. and Sada, E., 1980. Rates of mass transfer in affinity chromatography. J. Chem. Eng. Jap., 13: 151-154.

Lascu, I., Porumb, H., Porumb, T., Abrudan, I., Tarmure, C., Petrescu, I., Presecan, E., Proinov, I. and Telia, M., 1984. Ion-exchange properties of Cibacron Blue 3G-A Sepharose (Blue Sepharose) and the interaction of proteins with Cibacron Blue 3G-A. J. Chromatogr., 283: 199-210.

Vallee, B.L., 1955. Zinc and metalloenzymes. Adv. Protein Chem., 10: 317-384.

Solvent Extraction 1990, T. Sekine (Editor)

© 1992 Elsevier Science Publishers B.V. All rights reserved

ENZYME-LIKE CATALYTIC BEHAVIORS OF THE ENANTIOSELECTIVE HYDROLYSIS IN LIQIUD MEMBRANE SYSTEMS

R. Ueoka, Y. Matsumoto, K. Goto, and Y. Kato
Department of Industrial Chemistry, Faculty of Engineering, Kumamoto Institute of Technology, Ikeda 4-22-1, Kumamoto 860, Japan

ABSTRACT

The dramatically beautiful effect of ionic strength on the enantioselective hydrolysis of p-nitrophenyl-D(L)-phenylalaninates by the tripeptide benzyloxycarbonyl-L-phenylalanyl-L-histidyl-L-leucine was observed in the liquid-membrane system composed of 59 mol% double-chain surfactant (ditetradecyldimethylammonium bromide) and 41 mol% single-chain one (hexadecyltrimethylammonium bromide) in mild conditions (pH 7.6, 25 °C). In particular, the exclusively preferential cleavage of the L-isomer (k_2 = 1400 $M^{-1}s^{-1}$) but without the detectable cleavage of the D-isomer (k_2 = 0) was attained in the ionic strength of 0.02.

INTRODUCTION

The stereoselective hydrolytic-cleavage of amino acid esters has recently attracted considerable attention in connection with understanding the origins of the stereoselectivity observed with proteolytic enzymes (Fendler, 1982).

In the course of our study on the enantioselective catalysis in the vesicular systems (Ueoka et al., 1981) and the organized assemblies of micellar and vesicular surfactants (Ueoka et al., 1984a), we emphasized that the stereochemical control could be established by temperature regulation (Ueoka et al., 1984b) and by changing the composition of the coaggregates (reaction field) (Ueoka et al., 1984c).

Most recently, the authors have found appropriate systems to control the stereoselectivity of hydrolysis. That is, the enantioselectivity for the hydrolytic cleavage of the enantiomeric substrates having a long acyl chain by the active tripeptide having Phe, His, and Leu units was well correlated with the apparent mean hydrodynamic diameter of coaggregates composed of synthesized double-chained vesicular surfactants and single-chained micellar ones (Ueoka et al., 1988).

In this study we report on the dramatically beautiful effect of ionic strength (μ) on the enantioselective hydrolysis of p-nitrophenyl-D(L)-phenylalaninates (D(L)-S_{12}) by the tripeptide benzyloxycarbonyl-L-phenylalanyl-L-histidyl-L-leucine (Z-PheHisLeu) in the coaggregates (liquid-membrane system) composed of 59 mol% double-chain surfactant (ditetradecyldimethylammonium bromide : $2C_{14}Br$) and 41 mol% single-chain one (hexadecyltrimethylammonium

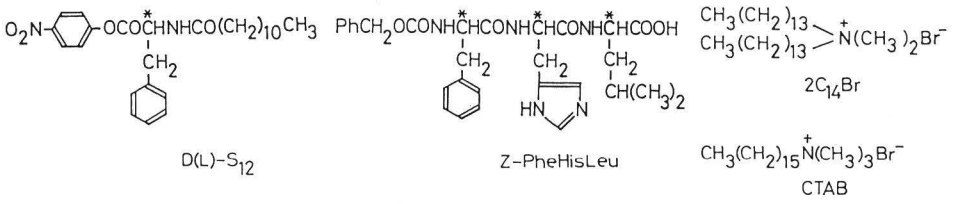

bromide : CTABr) at pH 7.6 and 25 °C.

2 EXPERIMENTAL SECTION

2.1 Materials

The enantiomeric substrates (D(L)-S_{12}) were prepared from N-(benzyloxycarbonyl)-D(L)-phenylalaninate by the esterification of the COOH group with p-nitrophenol and dicyclohexylcarbodiimide, followed by hydrobromination of the NH_2 group, and then acylation of the $NH_2 \cdot HBr$ group with dodecanoic anhydride (Ueoka et al., 1988). Satisfactory results of elemental analyses were obtained for D(L)-S_{12}. D-S_{12}: mp 105.8-107.0 °C. Anal. Calcd for $C_{27}H_{36}N_2O_5$: C, 69.21; H, 7.74; N, 5.98. Found: C, 69.32; H, 7.94; N, 5.98. L-S_{12}: mp 106.5-108.0 °C. Anal. Found: C, 68.98; H, 7.77; N, 5.96.

The surfactant $2C_{14}Br$ was prepared by reaction of the N,N-dimethyltetradecylamine and tetradecyl bromide in refluxing ethanol in the presence of sodium carbonate and purified by recrystallizations from ethyl acetate as described previously (Okahata et al., 1979). Satisfactory elemental analysis was obtained for $2C_{14}Br$. Anal. Calcd for $C_{30}H_{64}NBr$: C, 69.44; H, 12.46; N, 2.70. Found: C, 69.40; H, 12.39; N, 3.00.

Z-PheHisLeu was obtained from Bachem and was used without purification.

Commercially available hexadecyltrimethylammonium bromide (CTAB) was recrystallized from an anhydrous ethanol-ether mixture.

2.2 Light-Scattering Measurements

The dynamic light-scattering measurements were performed with a clipping type photon correlation, a He-Ne laser light source (632.8 nm), and a microcomputer that used a cumulant program and could directly afford the apparent hydrodynamic radii (R_h^{app}) of the liquid membrane composed of double- (A) and single- (B) chain surfactants as shown in Fig. 1. The R_h^{app} values have maximum errors of ±6%.

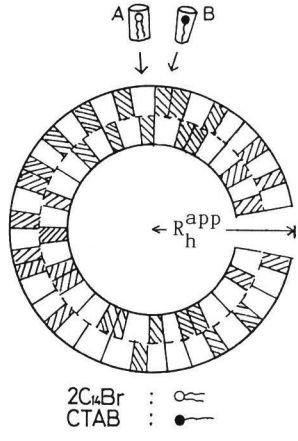

Fig. 1. Schematic representation of the liquid membrane composed of double- (A) and single- (B) chain surfactants.

2.3 Kinetic Measurements

Rates of p-nitrophenol liberation from p-

nitrophenyl esters were measured at 400 nm with a Hitachi 150-20 UV spectrophotometer. The reaction obeyed the usual pseudo-first-order rate law, and the apparent second-order rate constant (k_2) for the hydrolysis of an ester substrate was evaluated by eq 1.

$$k_2 = (k_t - k_s)/[\text{catalyst}]_0 \quad (1)$$

where k_t and k_s refer, respectively, to the observed first-order rate constants for the hydrolytic cleavage (hydrolysis) of D(L)-S_{12} with and without a catalyst and $[\text{catalyst}]_0$ indicates the initial catalyst concentration. The clear stock solutions were prepared by dissolving both catalyst and surfactant in Tris-KCl buffer with sonication (Braun Sonic Model B 3200 apparatus, 90 W) at 50 °C for 1 h.

3 RESULTS AND DISCUSSION

3.1 Control of Reaction Field: Size and Morphology of Coaggregates

The radii (R_h^{app}) of the coaggregates after being allowed to stand for 1 day (usual preparation time for kinetics) and 4-8 days (equilibrium time) are shown in Fig. 2. The particle size of the coaggregates composed of 59 mol% $2C_{14}Br$ and 41 mol% CTABr gradually increased with time in the region of lower ionic strengths (μ = 0.01-0.08) and we obtained stable particles having a constant size after being allowed to stand for 8 days at room temperature. On the other hand, no-time dependent R^{app} changes were observed in the region of higher ionic strengths (μ = 0.1-0.2). This means that the large coaggregates remain very stable for at least 10 days.

With respect to the morphology of the coaggregates (59 mol% $2C_{14}Br$ / 41 mol% CTABr), the presence of single- and double-walled vesicles, which reflects the morphology after being allowed to stand for 1 day at room temperature, was proved by electron microscopy as shown in Fig. 2. We found that the size of the coaggregates (59 mol% $2C_{14}Br$ / 41 mol% CTABr) after being allowed to stand for 1 day in the condition of μ = 0.08 (R_h^{app} = 840 Å) is about 2 times as large as that in the condition of μ = 0.02 (440 Å) on the basis of the dynamic light-scattering (dls) data and, interestingly, the relative size in the

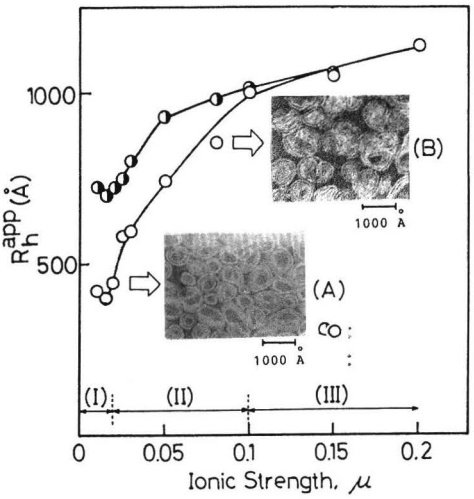

Fig. 2. R_h^{app} of the liquid membrane vs. ionic strength. Electron micrographs, negatively stained with uranyl acetate, for μ = 0.02 (A) and μ = 0.08 (B).

conditions of μ = 0.08 and 0.02 was in good agreement with the observed particle radii by electron microscopy (Fig. 2).

In the coaggregates (59 mol% $2C_{14}Br$ / 41 mol% CTABr), the fluorescence intensity originating from 1-(4-trimethylammonio) phenyl-6-phenyl-1,3,5,-hexatriene iodide placed in the pseudo-hydrophobic domain near the membrane surface, (Prendergast et al., 1981) where the enantioselective hydrolysis in this study presumably takes place, decreased to 60% of the original one as the ionic strength (μ) was lowered from 0.08 to 0.02 at 25°C as shown in Fig. 3. Such a change in the microenvironment property may come from an increase in repulsive interaction among the cationic head moieties of the amphiphiles ($2C_{14}Br$+CTABr) as the ionic strength is decreased.

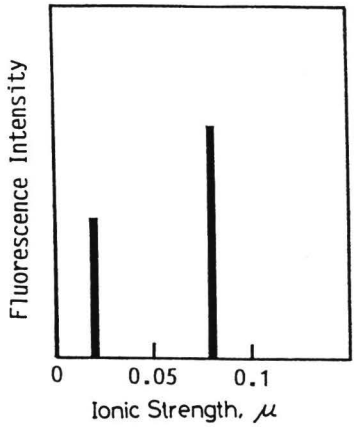

Fig. 3. Fluorescence intensity vs. ionic strength for the liquid membrane.

When the observed facts (electron microscopy, dls, and fluorescence measurements) are put together, we can group the regions into three classes (regions (I), (II), and (III)) as shown in Fig. 2. The coaggregates (59 mol% $2C_{14}Br$/41 mol% CTABr) with the high ionic strength (region (III) : $\mu \geqq 0.1$) were large (1000-1100 Å) and stable (not time dependent) vesicles rigidly packed (Ueoka et al., 1986), although those with the low ionic strength (region(I) : $\mu \leqq 0.02$) were small and unstable (390-440 Å after being allowed to stand for 1 day and 720-730 Å after 8 days of the equilibrium time) vesicles and loosely packed. On the other hand, in the middle ionic-strength range of 0.025-0.08 (region(II)), the particles should be unstable (time and ionic-strength dependent) vesicles with radii of 590-840 Å after 1 day and 720-980 Å after 8 days of the equilibrium time.

3.2 Control of Stereoselectivity

L- or D-S_{12} was cleavaged by the active tripeptide (Z-PheHisLeu) in pure micelles, pure vesicles, or coaggregates composed of micellar and vesicular surfactants (Ueoka, 1984c, 1988). Second-order cleavage rate constants (k_2, $M^{-1}s^{-1}$) for the hydrolysis of D(L)-S_{12} by Z-PheHisLeu in the $2C_{14}Br$ (59 mol%) / CTABr (41 mol%) coaggregates are summarized in TABLE 1. The control of stereoselectivity responding to ionic strength is a most attractive feature indeed! In particular, a remarkably high enantioselectivity (k_2^L/k_2^D = 1000) and the exclusively preferential cleavage of the L-isomer (k_2 = 1400 $M^{-1}s^{-1}$) but without the detectable cleavage of the D-isomer (k_2 = 0) was attained in the ionic

TABLE 1

Rate Constants (k_2, $M^{-1}s^{-1}$) and Enantioselectivity (k_2^L/k_2^D)[a]

Ionic Strength (μ)	1 day[b]			4-8 days[b]		
	L-S_{12}	D-S_{12}	L/D	L-S_{12}	D-S_{12}	L/D
0.01	1100	30	37	1800	31	58
0.015	1100	1.4	790	1600	28	57
0.02	1000	1.0	1000	1400	0	∞
0.025	1200	11	110	1800	36	50
0.05	1200	15	80	1500	73	21
0.08	1100	21	52	1400	71	20
0.10	1200	43	28	1300	81	16
0.15	1200	68	18	1200	63	19
0.20	1100	52	20	1300	72	18

[a]The rate constants have maximum errors of ±4%. Conditions: 25 °C, pH 7.6, 0.01-0.20 Tris-KCl buffer (μ = 0.01-0.20), 3% (v/v) CH_3CN-H_2O, [Z-PheHisLeu] = 5×10^{-5} M, [D(L)-S_{12}] = 1×10^{-5} M, [$2C_{14}Br$] = 1×10^{-3} M, [CTABr] = 7×10^{-4} M.

[b]The days correspond to those as shown in Fig. 2.

strength (μ) of 0.02 for the catalytic solution after being allowed to stand for 1 day and for that after 8 days, respectively. It is also worthy to note that the enantioselectivity was gradually enhanced as the ionic strength decreased in the range of μ = 0.20-0.02 (regions II and III) and was finely inverse to the radii of coaggregates. In this sense, we can consider kinetically regions (II) and (III) to be the same reaction fields, although the former might be more unstable when compared with the latter.

We should pay close attention to the fact that the stereoselectivity was optimized around a kind of fluctuation of membranes or morphology-change which should occur in a specific condition (μ = 0.02) between regions (II) and (I) as well as at temperatures and compositions close to phase boundaries and that this might be related to the activation of native enzymes at the boundary between stable and unstable regions.

4 CONCLUSIONS

The beautiful steric control for the enantioselective hydrolysis responding to the ionic strength deserves particular attention. That is, the enhancement of enantioselectivity was fairly amplified along with the diminishing in size of coaggregates composed of 59 mol% $2C_{14}Br$ and 41 mol% CTABr in the ionic-strength (μ) range from 0.20 to 0.02, although the enantioselectivity was sharply depressed from μ = 0.02 to 0.01. As a result, an ideal catalytic discrimination of the L-isomer (L-S_{12}) from the D-isomer (D-S_{12}) was attained in the 0.02 M Tris-KCl buffer (μ = 0.02).

In the light of the results shown in Fig. 2 and 3 and TABLE 1, it is plausible to conclude that the exclusively preferential molecular-recognition of the specific L-S_{12} substrate (not nonspecific D-S_{12}) by the LLL-tripeptide catalyst (Z-PheHisLeu) having some flexibility (Rebek, 1987) for the enhancement of enantioselectivity may be held in the loosely oriented molecular assemblies (small and unstable vesicles) in the ionic strength of 0.02, which produced high (k_2^L/k_2^D = 1000) or perfect (k_2 = 1400 $M^{-1}s^{-1}$ and k_2 = 0) enantioselectivity. This distinctive behavior might be related to "the induced fit theory" (Jencks, 1969) in enzyme regulations. It is very important that stereochemical control of the enantioselective hydrolysis of amino acid esters could be established by changing the ionic strength in this study.

5 ACKNOWLEDGMENT

We are grateful to Professor Yukito Murakami of Kyushu University for providing electron micrographs and helpful discussions and Dr. Masanori Cho of Kumamoto Institute of technology for providing dinamic-light scattering data.

6 REFERENCES

Fendler, J.H., 1982. Membrane Mimetic Chemistry, John Wiley & Sons. New York.

Jencks, W.P., 1969. Catalysis in Chemistry and Enzymology. McGraw-Hill.

Okahata, Y., Ando, R., and Kunitake, T., 1979. Catalytic Hydrolysis of p-nitrophenyl Esters in the Presence of Representative Ammonium Aggregates. Specific Activation of a Cholesteryl Nucleophile Bound to a Dialkylammonium Bilayer Membrane. Bull. Chem. Soc. Jpn., 52: 3647-3653.

Prendergast, F.G., Haugland, R.P., and Callahan, P.J., 1981. 1-[4-(Trimethylamino)phenyl]-6-phenylhexa-1,3,5,-triene: Synthesis, Fluorescence Properties, and Use as a Fluorescence Probe of Lipid Bilayers. 20: Biochemistry, 7333-7338.

Rebek, Jr.,J. 1987. Model Studies in Molecular Recognition. 235: Science, 1478-1484.

Ueoka, R., Matsumoto, Y., Ninomiya, Y., Nakagawa, Y., Inoue, K., and Ohkubo, K., 1981. Stereoselective Deacylation of Long-chain p-Nitrophenyl N-Acylphenylalanates by Palmitoyl-L-histidine in a Bilayer System. Chem. Lett., 785-788.

Ueoka, R., Matsumoto, Y., Nagamatsu, T., and Hirohata, S., 1984a. Isokinetic Discrimination of Artificial Membrane Systems in the Enantioselective Hydrolysis. Tetrahedron Lett., 25: 1363-1366.

Ueoka, R., Matsumoto, Y., Nagamatsu, T., and Hirohata, S., 1984b. Marked Temperature Effect on the Enantioselective Hydrolysis in Artificial Membranes. Chem. Lett., 583-586.

Ueoka, R., Matsumoto, Y., and Ihara, Y., 1984c. Dramatically Enhanced Enantioselective Hydrolysis of Amino Acid Esters with Tripeptide Nucleophile by Controlling the Reaction Field at Room Temperature. Chem. Lett., 1807-1810.

Ueoka, R., Matsumoto, Y., Yoshino, T., Hirose, T., Kikuchi, J., and Murakami, Y., 1986. Enzyme-like Enantioselective Catalysis in the Specific Coaggregate System of Vesicular and Micellar Surfactants. Chem. Lett., 127-130.

Ueoka, R., Matsumoto, Y., Moss, R.A., Swarup, S., Sugii, A., Harada, K., Kikuchi, J., and Murakami, Y., 1988. Membrane Matrix for the Hydrolysis of Amino Acid Esters with Marked Enantioselectivity. J. Am. Chem.Soc., 110: 1588-1595.

Solvent Extraction 1990, T. Sekine (Editor)

© 1992 Elsevier Science Publishers B.V. All rights reserved

STUDY ON THE SWELLING OF EMULSION LIQUID MEMBRANE

LI Weixuan, DAI Xing and SHI Yajun
Chemical Engineering Research Centre
East China University of Chemical Technology, Shanghai 200237 (China)

ABSTRACT

The water permeation and entrainment swelling by precisely estimating and measuring of two types of emulsion with the density method have been studies. The reasonable assumptions and formulae have been proposed and confirmed by particle sizer instrument for calculating the total swelling ratio. Experimental results also indicate that if Span-80 is used as a surfactant, the entrainment swelling ratio can not be neglected. Its value can be obtained from an experiment in which the concentration of inner aqueous phase is equal to that of outer aqueous phase and thus, the value equals to the swelling ratio. If E644 is used as a surfactant, the entrainment swelling ratio can be neglected.

INTRODUCTION

Artificial membrane has been a topic of great interest in recent years because of their potential applications, such as recovery of purification of metal ions, removal of phenol from waste water etc., one of the most intriguing classes of artificial membrane is the liquid membrane. Liquid membrane technology means those processes in which a simultaneous extraction/stripping process takes place across a selective liquid separating phase.

At present, the wide commercial application of liquid membrane in separation processes has not yet been achieved mainly due to three important problems, the swelling and the stability of emulsion liquid membrane and the breakdown of emulsion. In this paper, the swelling of liquid membrane has been studied. Martin and co-workers [1] first found that when Cu^{2+} could be extracted by liquid membrane technique, the total swelling ratio of emulsions was 50-100%. Up to now, the systematic studies of the subject have just been started. The previous work covered the study on mechanism of the water permeation and entrainment swelling and investigating various factors which affect the swelling [2-4]. However, the past few years, it seems that the estimation and measurement of two types of swelling were still uncertain and this may give some severe errorsin swelling data obtained by experiments and data treatment methods.

The method of measuring the changes of volume of emulsion to determine

the process swelling has two defects. One is that the volume of emulsions can not be measured precisely due to trapping corner of the mixing vessel and wall adhesive phenomenon, so it causes substantial error; and the other is that with this method, the total swelling ratio may be known but the concrete values of entrainment and water permeation swelling ratio can not be obtained. In this paper, therefore, the objective is to find a way of precisely estimating, measuring two types of emulsion and investigating effective factors preliminarily.

EXPERIMENTAL

1. Preparation of the original W/O/W emulsions

According to the phase ratio and components, certain amount of inner aqueous phase was added to the oil phase, followed by 3 min. homogenization (Supersonic Mixing Device, Shanghai Supersonic Device Corporation, China).

The multiple emulsions were prepared by dropwise addition of the above emulsion to the outer aqueous phase at a constant stirring rate over a certain period. The phase was allowed to settle, then added the emulsions into density bottle to scale its weight or made samples to measure inner aqueous droplet's size.

2. Analytical methods

For measurements of swelling ratio, density method and particle sizer method were used. Because the measurement region of the BI-90 particle sizer instrument (BI-90 Particle Sizer, Breakhaven Instruments, U.S.A.) is 0.005-5μm, and diameter of entrainment aqueous droplets is much bigger than 5μm (e.g. 200μm), the volume average diameter measured does only mean that of inner aqueous droplets.

RESULTS AND DISCUSSION

I. Calculation formulae of swelling

When emulsions and outer aqueous phase were mixed at a constant stirring rate, in general, their volumes had had obvious changes, we called this phenomenon as: swelling. Swelling not only dilutes the material in inner aqueous phase, but also causes unexpected changes of the properties of emulsions (e.g. viscosity, density and Roi, etc.), which makes it more difficult to design and to operate of equipment. So swelling is an important factor which has influence on the possibility of using liquid membrane technique in wide commercial application.

There are two different types of swelling: swelling caused by entrainment during the dispersion which is called as: entrainment swelling; and the swelling caused by the osmotic pressure difference acting

cross the oil phase layer separating the inner and outer aqueous phase, created by the difference of concentration of electrolytes.

According to definition:

$$\eta_t = \eta_1 + \eta_2 = \frac{V_i - V_{io} + V_1}{V_{io} + V_m} = \frac{(\varepsilon - 1) + V_1/V_{io}}{1 + \phi} \tag{1}$$

$$d_o = \frac{V_m d_m + V_{io} d_{io}}{V_m + V_{io}} = \frac{\phi d_m + d_{io}}{1 + \phi} \tag{2}$$

$$d = \frac{V_m d_m + V_{io} d_{io} + V_1 d_s + (V_i - V_{io}) d_w}{V_m + V_i + V_1} = \frac{\phi d_m + d_{io} + \frac{V_1}{V_{io}} d_s + (\varepsilon - 1) d_w}{\phi + \varepsilon + V_1/V_{io}} \tag{3}$$

From (2) and (3), (1) yields:

$$\eta_t = \frac{d - d_o}{d_s - d} + \frac{\varepsilon - 1}{1 + \phi} \cdot \frac{d_s - d_w}{d_s - d} \tag{4}$$

$$\eta_1 = \frac{d - d_o}{d_s - d} + \frac{\varepsilon - 1}{1 + \phi} \cdot \frac{d - d_w}{d_s - d} \tag{5}$$

$$\eta_2 = \eta_t - \eta_1 = \frac{\varepsilon - 1}{1 + \phi} \tag{6}$$

Discussion of formulae:

1. If there is no osmotic gradient acting across the oil phase layer, there is no water permeation swelling, $\varepsilon = 1$, $\eta_2 = 0$.

$$\eta_t = \eta_1 = \frac{d - d_o}{d_w - d} \tag{7}$$

2. Two swelling types exist:

a. If outer aqueous phase is pure water:

$$d_s = d_w, \quad \eta_t = \frac{d - d}{d_w - d}, \quad \eta_2 = \eta_t - \eta_1 \tag{8}$$

b. If it is electrolyte, from (5) and (6):

$$\eta_2 = \frac{\varepsilon - 1}{1 + \phi} = \frac{(d - d_o) - \eta_1 (d_s - d)}{d_w - d} \tag{9}$$

$$\eta_t = \eta_1 + \eta_2 = \frac{(d - d_o) + \eta_1 (d_w - d_s)}{d_w - d} \tag{10}$$

And $\varepsilon = V_i/V_{io} = (D_i/D_{io})^3$, its value can be obtained by BI-90 particle sizer instrument, so from (9), η_2 can be known, then η_1 and η_t can also be obtained. From (9) and (10) it is shown that if entrainment swelling ratio η_1 is known, η_t and η_2 can also be known.

3. When the entrainment swelling ratio can be neglected, $\eta_1 = 0$, from (10):

$$\eta_t = \eta_2 = \frac{d - d_o}{d_w - d} \tag{11}$$

II. The entrainment swelling

TABLE 1

The entrainment swelling ratio, when the surfactant is E644
20° C; Rew=1/3; Roi=2; 4% E644-K/P=4; N=500 r.p.m.

t, min. / η_1% / aq. phase	5	10	20	30
H_2O	0	0	-	-
2NHCl	0.462	0.462	0.528	0.502
2NNaCl	0.394	0.338	0.380	0.394
2NNaOH	0.612	0.669	0.556	0.781

If the inner and outer aqueous phases were both pure water or electrolytes with same concentration, there was no osmotic pressure difference. The total swelling ratio measured was only entrainment swelling ratio. From Table 1, it was shown that if E644 was used as a surfactant, the entrainment swelling ratio was smaller than 1%, and it changed little with the stirring time. From Figure 1, it was shown that if Span-80 was used as a surfactant, the entrainment swelling ratio increased largely, and it also changed little with the stirring time, and when the inner and the outer aqueous phases were both pure water the entrainment swelling ratio was much bigger than when they were both HCl; and the entrainment swelling ratio did not change with the changes of concentration of HCl. As mentioned above that the entrainment swelling took place at the intial stage of stirring. Different surfactant had different influence on the entrainment swelling and different sensibility to electrolytes.

If E644 was used as a surfactant, electrolytes only gave little influences on the double-electro-layer at the surfaces of entrainment droplets. If Span-80 was used as a surfactant, that effect was obvious that the effective thickness of double-electro-layer thinned due to electrolytes, so the stability of dispersion system (entrainment droplets) decreased and the entrainment swelling ratio decreased much.

If E644 was used as a surfactant, the entrainment swelling ratio could be neglected. From (11), it may be known that $\eta_1 = \eta_2 = \frac{d - d_o}{d_* - d}$ substituted it into (6) and ε can be written as:

$$\varepsilon = 1 + (1+\phi)\eta_2 = 1 + (1+\phi)\frac{d - d_o}{d_* - d} \tag{12}$$

If Span-80 was used as a surfactant and the inner and the outer aqueous phases were all electrolytes, the entrainment swelling ratio can

not be neglected; it may be assumed that it may agree with curved line 2 (Figure 1), that is $\eta_1 = \eta''$, and from (9) and (10), η_2 and η_1 can be obtained and

$$\varepsilon = 1 + (1+\phi)\eta_2 = 1 + (1+\phi)\frac{(d-d_o) - \eta''(d_s - d)}{d_w - d} \tag{13}$$

In addition, the transport of water across the oil phase took place as a consequence of the osmotic pressure imbalance created by the presence of electrolyte. This was reflected by a shift in the size distribution of the inner aqueous drops, determined by particle sizer instrument, the average diameter of drops in inner aqueous phase before and after swelling's taking place can be known, thus ε (measured) can be obtained:

$$\varepsilon = V_i/V_{io} = (D/D_{io})^3 \tag{14}$$

III. The comparison of (cal.) and (measured)

From Figure 2, it was shown that the two values of calculated from (13) and measured by particle sizer instrument are approximately equal. So the assumption mentioned above were reasonable.

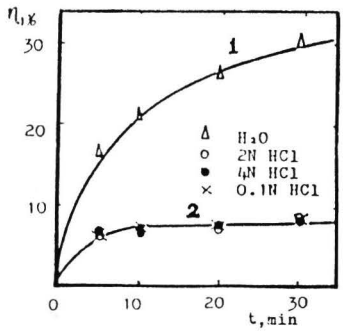

Fig. 1 The entrainment swelling ratio, When the surfactant is Span-80

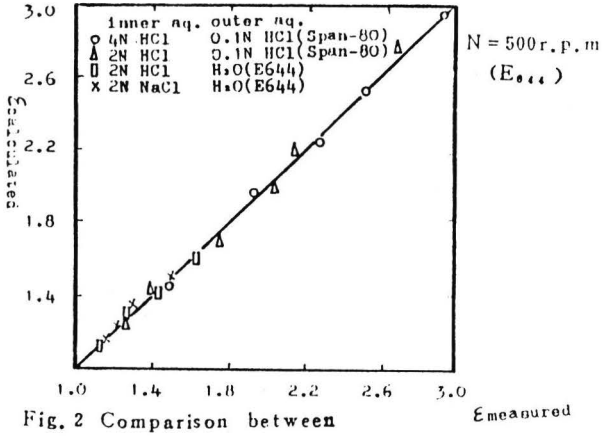

Fig. 2 Comparison between ε calculation and ε measurement

From Figure 3, it was shown that the water permeation swelling ratio increased with the concentration gradient of electrolytes across the oil phase layer.

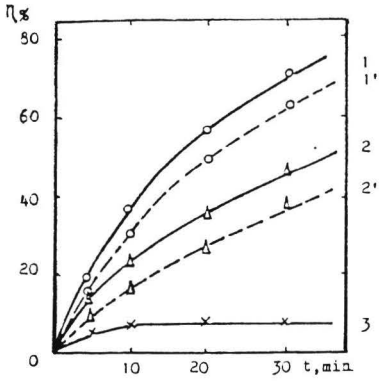

Fig. 3 The changes of swelling rate with time

full lines: $\eta_1 \sim t$ dotted lines: $\eta_2 \sim t$

1, 1' - inner aq. phase: 4N HCl, outer aq. phase: 0.1 N HCl;

2, 2' - inner aq. phase: 2N HCl, outer aq. phase: 0.1 N HCl;

3 - $\eta'' - t$ ($\eta'' = \eta_1$).

20° C, Rew = 1/3; Roi = 2;
5% Span-80 - K/P = 4/1;
N = 400 r.p.m.

CONCLUSIONS

1. The reasonable assumptions and formulae have been proposed and confirmed by particle sizer instrument. It indicates that measuring swelling data with the density method is precise and reliable. If Span-80 is used as a surfactant, the entrainment swelling ratio can not be neglected. Its value may be obtained by an experiment in which the concentration of inner aqueous phase is equal to that of outer aqueous phase, thus the value equals to the swelling ratio.

2. The entrainment swelling takes place at the initial stage of stirring. The water permeation swelling ratio increases with the stirring time's and osmotic pressure's increasing.

LIST OF SYMBOLS

η''	pure entrainment swelling ratio	V_m	volume of oil phase
η_t	total swelling ratio	d_w	density of pure water
η_1	entrainment swelling ratio	d_m	density of oil phase
η_2	water permeation swelling ratio	ε	V_i/V_{io}
V_o	volume of outer aqueous phase	ϕ	V_m/V_{io}
V_i	volume of inner aqueous phase		
d	density of emulsion liquid		
d_o	density of initial emulsion liquid		
d_a	density of outer aqueous phase		
d_{io}	density of initial inner aqueous phase		
D_i	volume average diameter of droplets of inner aqueous phase in emulsions		
D_{io}	volume average diameter of droplets of inner aqueous phase in initial emulsions		
V_{io}	volume of initial inner aqueous phase		
V_1	volume of entrainment droplets		

REFERENCES

1. Martin, T.P., et al., Hydrometallurgy, 2, 315 (1977)
2. Garti, N., et al., J. Colloid and Interface Sci., 104, 587 (1985)
3. Nakashio, F., et al., Preprint of the 14th Autumn Meeting of Soc. of Chem. Eng., Japan, H 214 (1980)
4. Matsumoto, S., et al., J. Colloid and Interface Sci., 77, 555 (1980)

11. SUPERCRITICAL AND NEW EXTRACTION SYSTEMS

Solvent Extraction 1990, T. Sekine (Editor)

© 1992 Elsevier Science Publishers B.V. All rights reserved

EXTRACTION OF XANTHINES FROM COCOA NUT SHELLS WITH CARBON DIOXIDE

G. BRUNNER, U. ZWIEFELHOFER, A. SIMON
TECHNISCHE UNIVERSITÄT HAMBURG-HARBURG
Eißendorfer Straße 38, D-2100 Hamburg 90

Summary:

The extraction of theobromine and caffeine from cocoa nut shells was studied in a laboratory extraction plant using supercritical carbon dioxide as solvent. Both xanthines can be removed from the shells. Theobromine is less readily extracted than caffeine. Water content of the solid material and the gas is an important parameter for the extraction beside solvent ratio and pressure. Diffusion coefficients are calculated from the experimental extraction curves.

Introduction:

Materials containing xanthines like caffeine, theophylline and theobromine are important raw materials for producing extracts which are consumed as beverages or for stimulating purposes. There are incentives to remove the xanthines to produce caffeine and caffeine free coffee or tea which led to systematic investigations of the decaffeination processes with supercritical gases as solvents /1/. Similar reasons led to a study of the extraction of theobromine.

This investigation was designed to yield a systematic approach to the extraction of theobromine from cocoa nut shells. So far data are available only from the patent literature /2/. Parameters of the investigation were chosen according to the extraction of caffeine from raw coffee beans and from black tea leaves.

Apparatus:

The investigation was carried out in a 2-vessel-plant (4 l/ 2 l) with gas recirculation. Extraction was achieved by the supercritical gas flowing upward in a fixed bed of about 100 g of the plant material placed into an internal vessel within the 4 l autoclace with a perforated bottom and sieve plates below for gas distribution. The extracted components were separated from the gas in the second vessel by high pressure absorption in water, which was supplied by a metering piston pump, and at a somewhat reduced pressure (extraction pressure minus 10 MPa). Gas circulation was held up by a membrane compressor. Pressure was held constant during the experiments by a second membrane compressor and measured by pressure transducers and indicated by bourdon gauges. Temperatures in the plant were maintained by thermostats and heating jackets surrounding the vessels. The connecting lines were insula-

ted by neoprene rubber tubes. Temperatures were measured by Ni-CrNi thermocouples. Gas flow rate was determined by a coriolis-force type gas flow meter. All values were registered by computer.

Method:

The plant material was accordingly prepared, i.e. in most cases humidity adjusted to about 40 wt.-%. In some cases the material was ground and divided into fractions of different particle size. The material was placed into the heated extraction vessel. After closing the vessel the gas was pumped into the extraction vessel up to the desired pressure for the extraction and then the gas cycle was opened. Extraction time was counted from that moment. During the experiments samples were taken from the gas (about 20 l gas at STP) downstream of the extraction and downstream of the precipitation of the extract through steel capillaries and heated needle valves and subsequently analysed. The capillaries were flushed with about 10 ml of water to dissolve precipitated material. The nonvolatile compounds of the sample were absorbed in water in a sample trap. Samples were also taken from the absorbing liquid in the second autoclave. The amount of absorbing liquid was determined every 30 min by total removal from the absorption vessel. The aqueous samples were filtered (0,45 µm) and analysed for xanthines by HPLC on a RP 18 column and a UV-detector at 272 nm. Xanthine concentration in the solid material was determined by grinding 1 g and cooking it with 1 g MgO in 100 g H_2O for 2.5 h. The liquid was filtered (0.45 µm) and analysed as stated above.

Materials:

Cocoa nut shells was the material used throughout the investigation. After fermentation, drying and roasting of the cocoa beans the shells are removed mechanically from the beans. The size of the resulting pieces of the shells ranges from < 0.5 mm to more than 10 mm. They are between 0.1 and 0.3 mm thick. The main components of the shells are listed in Table 1.

Table 1: Main components of cocoa nut shells

Components	Bean	Shell	
		literature value	this work
		wt.-%	
water	5.0	11	8
fat	54	2 - 4	3 - 19
caffeine	0.2	0.1	0.06 - 0.12
theobromine	2 - 4	1 - 2	0.8 - 1.2
proteines	12.0	11	n.d.
cellulose	9.0	26	n.d.
ash	2.6	8	n.d.

n.d. - not determinded

The xanthines theobromine and caffeine are originally not part of the shells. During the fermentation process, lasting for several days, the xanthines diffuse into the shell but do not penetrate into the cell matrix.

The structural formulae of both the xanthines are shown in Fig. 1. The methyl group missing in position 1 in the theobromine molecule changes physical properties substantially compared to caffeine:
Melting point: caffeine 236 °C; theobromine : 350 °C.
Sublimation: caffeine: 180 °C; theobromine: 290 °C.

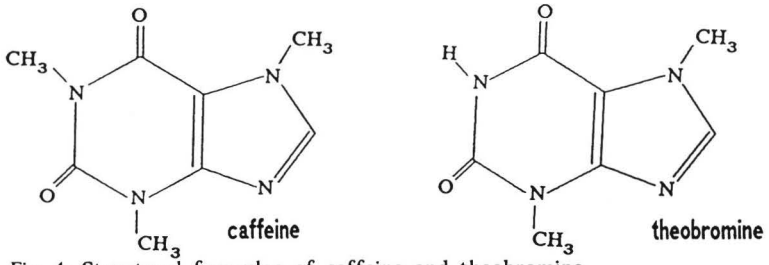

Fig. 1: Structural formulae of caffeine and theobromine

Results:

For an initial comparison, the extraction of caffeine from coffee beans and black tea leaves is shown in Fig. 2 together with the extraction of theobromine from cocoa nut shells. The process conditions pressure, temperature and solvent ratio are given in each case.

Caffeine is extracted fastest from tea, though the tea leaves contain the highest percentage of caffeine (about 3.1 wt.-%). This is probably due to the

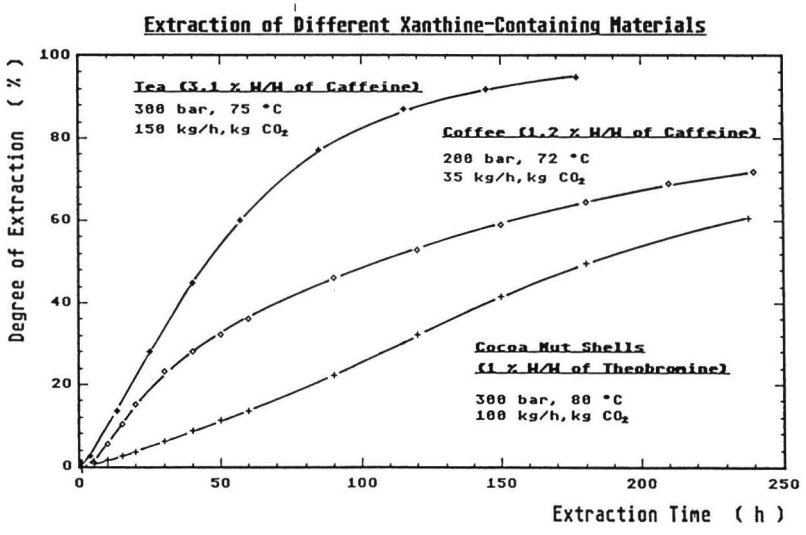

Fig. 2: Extraction of xanthines from various materials by means of supercritical carbon dioxide

small particle size and the destruction of the cell matrix during the harvesting process. Coffee beans have an intact cell matrix, diffusion paths are relatively long and the caffeine partially is bound to chlorogenic acid so that the extraction process is slower than with tea. Theobromine from cocoa nut shells is extracted at the lowest rate of the materials compared, though the theobromine content of 1 wt.-% is comparable to that of coffee beans and particle size in one dimension is comparable to that of tea leaves.

There are several important parameters of the extraction process which can influence the rate of extraction like the water content of the material, the solvent ratio, temperature and pressure. These have been studied in this investigation and the results are presented below.

Water content of the material:

The initial water content of coffee beans and tea leaves is significant for the rate of extracting caffeine /6/. During the extraction of theobromine from cocoa nut shells therefore the initial water content was varied between 8 wt.-% and 50 wt.-%. In Fig. 3 the extraction curves are shown for the different initial water contents.

During the experiments the water content of the cocoa nut shells did not remain constant. It changed from an initial water content of 15 wt.-% to 40 wt.-% after an extration of 4 hours. In the experiment with 44 wt.-% initial water concentration the water content dropped to 10 wt.-% at the end of the extraction due to lack of water in the extraction vessel during the experiment. The water content of the solid did not influence the total extracted amount of caffeine and theobromine significantly, but the rate of extraction.

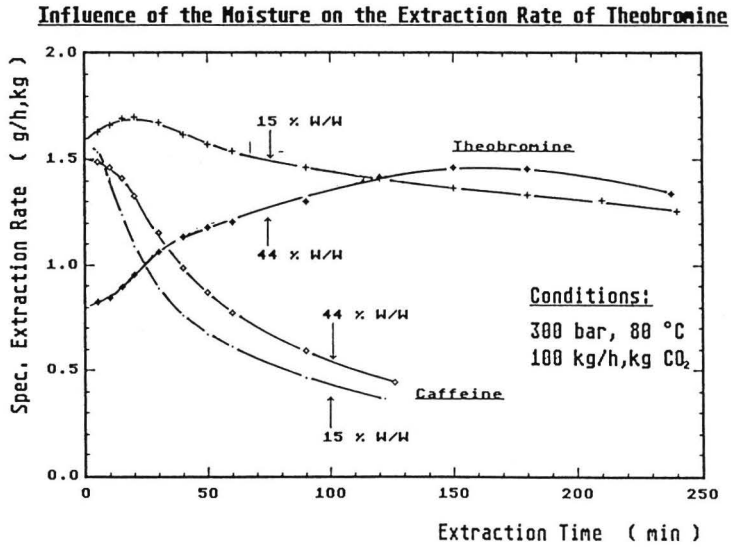

Fig. 3: Extraction rate at different initial water content of the solid material

The influence of the water content is revealed by the extraction rate shown in Fig. 3. For theobromine the rate of extraction decreases with increasing water content. During the first two hours of the experiment the mean rate of extraction at a water content of 15 wt.-% is significantly higher than that for an initial water content of 44 wt.-%. It decreases with time since water in the extraction system was transported by humid carbon dioxide to the solid and enhanced its water content during the whole experiment. On the other hand, the rate of extraction constantly increased during the experiment with the initial water concentration of 44 wt.-% since in this case the water content of the solid decreased during the experiment.

Caffeine is extracted much better than theobromine. Extraction rate for caffeine at the beginning of the extraction is nearly as fast as that for theobromine though the initial concentration of caffeine is only 10 % of that of theobromine. The reason for this phenomenon may be a low solubility of theobromine in carbon dioxide.

To study the influence of water content of supercritical carbon dioxide on the extraction rate an experiment with dry CO_2 and cocao shells of normal water content (about 8 %) was carried out. The result is compared in Fig. 4 to an extraction with humid CO_2.

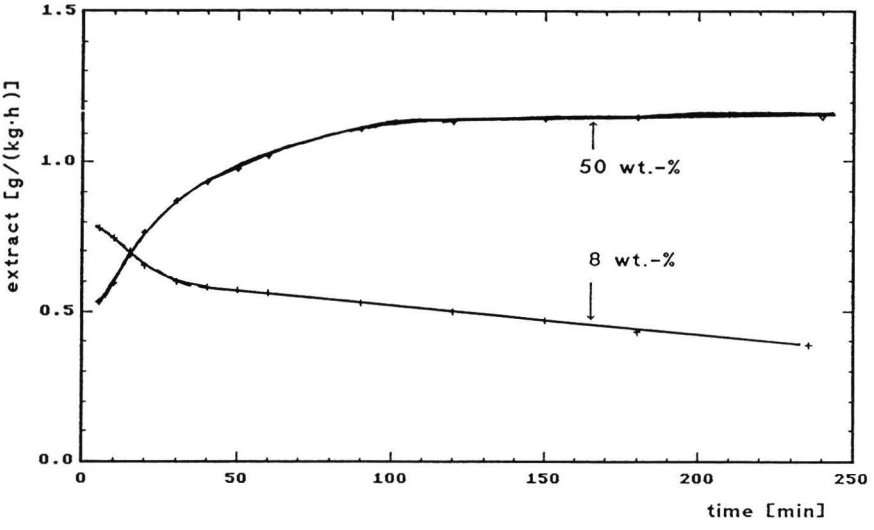

Fig. 4: Extraction rate of theobromine for dry and humid carbon dioxide

The extraction rate of the theobromine from the dry shells using dry carbon dioxide is significantly lower than that observed for water containing shells and gas. Dry carbon dioxide however did not extract any caffeine.

Solvent ratio:

The influence of the solvent ratio on the extraction of theobromine is shown in Fig. 5. With increasing solvent ratio the degree of extraction, which can be achieved in a certain time of extraction also increases. The effect is higher for solvent ratios below 100 kg/(kg·h) than for higher solvent ratios. Enhancing the solvent ratio by a factor of two from 50 to 100 kg/(kg·h) results in an increase of the degree of extraction by a factor of two. An increase in the solvent ratio from 100 to 300 kg/(kg·h) causes only an increase in degree of extraction by a factor of 1.3.

With a certain amount of gas equal or different quantities of theobromine can be extracted depending on the range of the solvent ratio. For solvent ratios below 100 kg/(kg·h), the residence time of the gas in the bed of solid particles is greater than 3 min. In this range of the solvent ratio with a given quantity of gas equal quantities of theobromine are extracted independent on the solvent ratio. The relation between quantity of gas and extracted theobromine is nearly linear. The concentration of theobromine in the gas is about 15 mg theobromine/ kg CO_2 at 30 MPa and 80 °C. At higher solvent ratios the concentration of theobromine in the gas decreases with increasing solvent ratio so that with a certain amount of gas a smaller quantity of theobromine is extracted.

For caffeine a concentration in carbon dioxide of 17 mg caffeine/kg CO_2 (30 MPa, 80 °C) is observed for solvent ratios lower than 100 kg/(kg·h). The equilibrium solubility for pure caffeine in CO_2 under these conditions is reported to be 4.1 mg/g /3/. Therefore the maximum achievable concentration during the extraction must not be taken for the equilibrium solubility of the extracted compound. The rate of extraction increases significantly with increasing solvent ratios, even at values far higher than 100 kg/(kg·h) (Fig. 5).

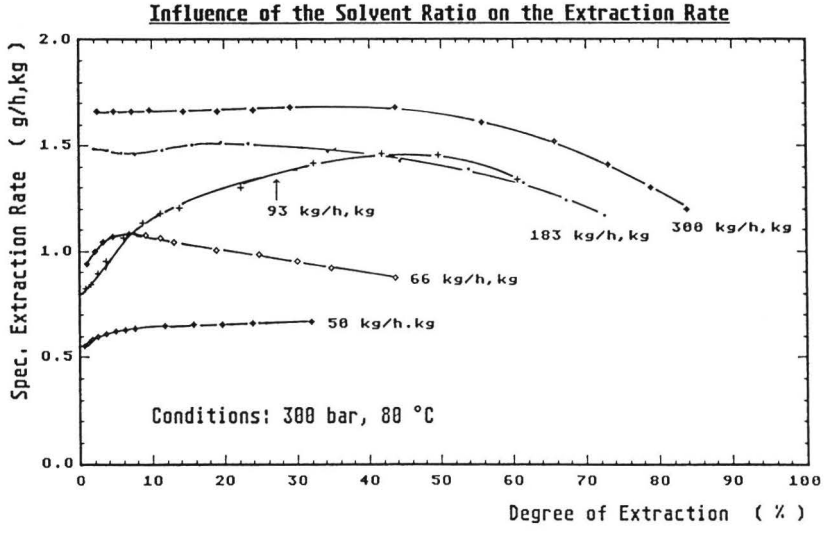

Fig. 5: The influence of the solvent ratio on the rate of extraction

Pressure and temperature:

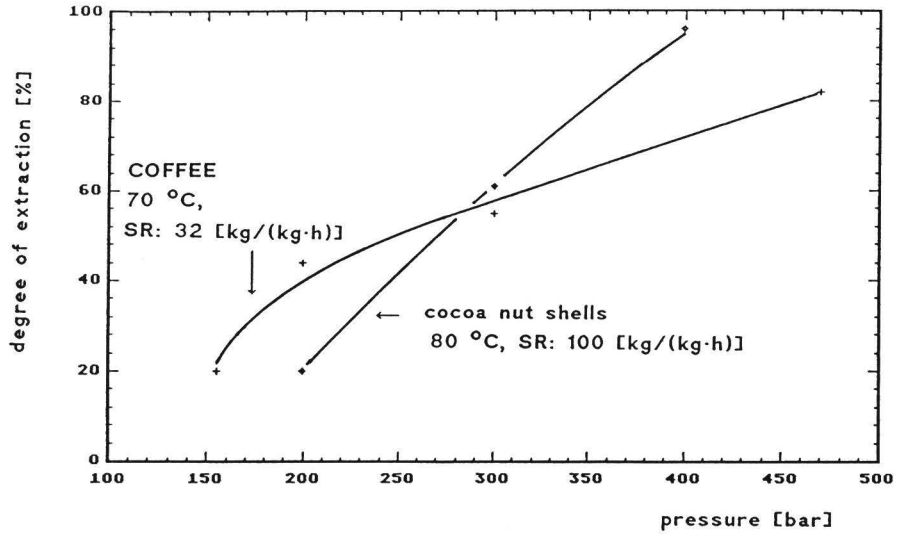

Fig. 6 : The extracted quantity of theobromine after 4 hours of operation, expressed as degree of extraction in dependence of extraction pressure.

The extraction pressure is of significant importance for the quantity of theobromine extracted in a certain time interval. In Fig. 6 the degree of ex-

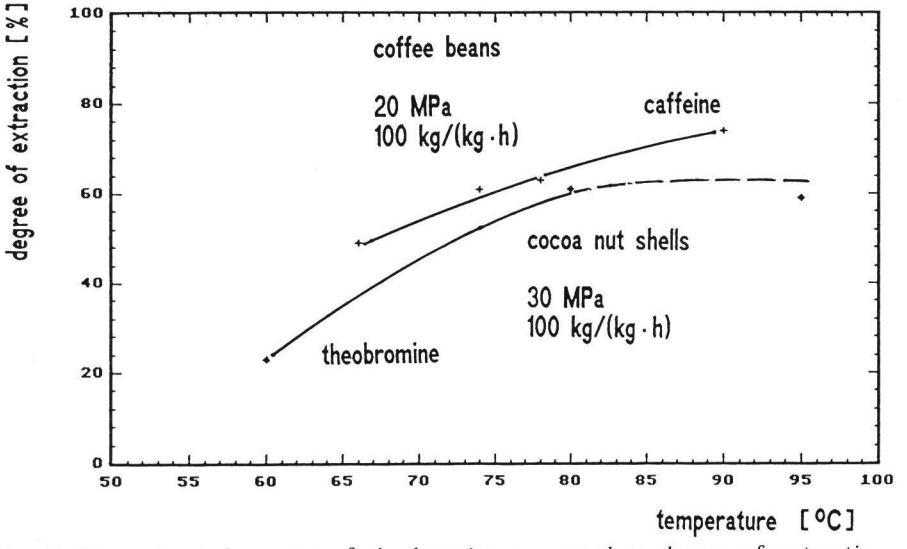

Fig. 7: The extracted amount of theobromine expressed as degree of extraction as a function of extraction temperarture

traction for a certain period of operation (4 h) is plotted against the pressure at which the extraction is carried out. To double the extraction pressure means to increase the amount extracted by a factor of 5. For comparison the dependence of the extraction of caffeine from coffee beans has been added /6 /. Though conditions of the extraction differ slightly it can be concluded that the pressure dependence is less pronounced for the extraction of caffeine than for the extraction of theobromine.

The temperature dependence of the extraction of theobromine from cocoa nut shells is shown in Fig. 7. Up to about 80 °C the rate of extraction increases with temperature. The extraction rates in the temperature range of 80 to 95 °C are nearly equal. The reason for this may be that the water content of the solid decreased in both cases from the initial content of 44 and 50 wt.-% rsp. to 10 and 4 wt.-% rsp. at the end of the 4 hours of extraction.

Particle size of the cocao nut shells:

During the investigation the cocoa nut shells were fed into the extraction autoclave as delivered from the separation process. For investigating the influence of particle size, the shells were ground and divided by sieveing into several fractions, from which two fractions, 0.5 mm - 1.0 mm and 2.8 - 3.55 mm, were employed in extraction experiments. The extraction results shown in Fig. 8 make clear that the original shell particles are the best material for an extraction. This is due to the drastically changed density of the bulk material.

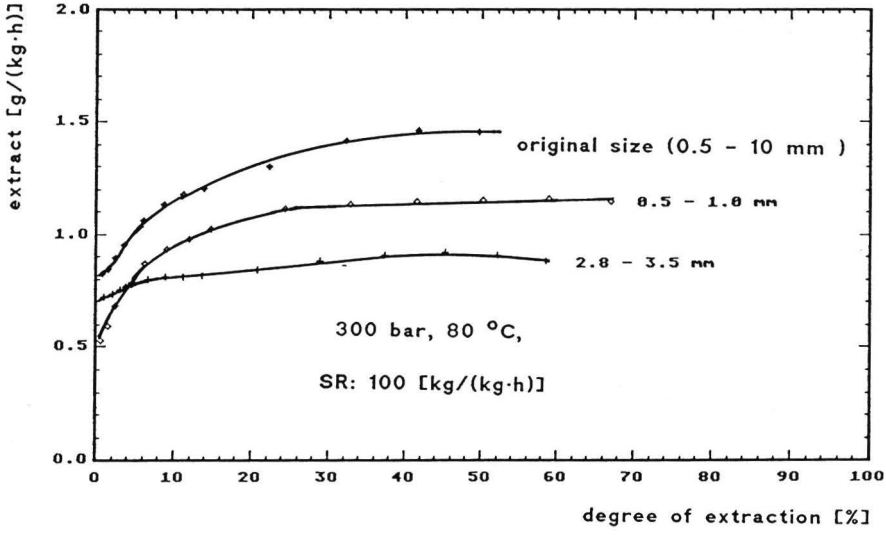

Fig. 8: Extraction rate of theobromine in dependence of degree of extraction for different particle sizes

The bulk density of the cocoa nut shells as delivered from the separation process amounts to 150 kg/m^3. It is enhanced due to crushing to about 450 kg/m^3. The bed of shell pieces is in this case made up from layers of small flat plates which are tightly stacked, while before crushing there were greater pieces of cylindrical geometry which made the layers of particles far less dense and accessible for the extracting gas.

Discussion:

The negative influence of water on the extraction rate of theobromine is probably due to the low solubility of theobromine in water. If the solubilites of caffeine and theobromine in water are compared as done in Table 2, the small affinity of theobromine for water is evident.

Table 2: Solubiility of caffeine and theobromine in water /5 /.

temperature [°C]	theobromine [g/l]	caffeine [g/l]
20	0.6	20
80	-	380
100	6.7	590

The solubility of theobromine in water at 20 °C is lower by a factor of 30 and at a temperature of 100 °C by a factor of 90 than that of caffeine. Theobromine forms no hydrates with water as does caffeine.

The mechanism of the extraction of the xanthines from solid material seems to be mainly determined by the diffusion in the solid phase. Yet an analysis of the data of the caffeine extraction showed that diffusion is not the only mass transport resistance. If diffusion is the only mass transport resistance then the extraction can be modelled by Fick's law:

$$\frac{\partial c}{\partial t} = D \cdot \frac{\partial^2 c}{\partial x^2},$$

with D for the diffusion coefficient, c for the concentration of substance in the solid and t for the time. This equation can be integrated /4/. For the geometrical shape of a plate of thickness l an equation for the amount extracted M_t related to the original amount of substance M_∞ is obtained:

$$1 - \frac{M_t}{M_\infty} = \sum_{n=0}^{\infty} \frac{8}{(2n+1)^2\ \pi^2} \cdot \exp\left[-\frac{D \cdot (2n+1)^2 \cdot \pi^2 \cdot t}{4 \cdot l^2}\right]$$

The right hand side of the equation represents the σ-function. The diffusion

coefficient as defined by the above equation can easiliy be found by a plot of the extraction curve and the σ-function. If the model is applicable the extraction curve is parallel to the σ-function, if not other transport mechanisms beyond diffusion are also of significant influence. From the difference d between the two curves the diffusion coefficient can be calculated:

$$D = 4 \cdot l^2 \cdot 10^{-d}$$

In Table 3 the diffusion coefficients obtained by this method are listed for the extraction of theobromine and caffeine from cocoa nut shells and for several experiments. Calculated diffusion coefficients depend mainly on solvent ratio. This indicates significance of mass transport resistance at the interface gas-solid.

Table 3: Diffusion coefficients for the extraction of xanthines with carbon dioxide at 30 MPa and 80 °C

solvent ratio [kg/(kg·h)]	particle size [mm]	Theobromine D [cm^2/s]	Caffeine D [cm^2/s]
50	0.5 - 10	$4.37 \cdot 10^{-9}$	$6.32 \cdot 10^{-8}$
183	"	$1.32 \cdot 10^{-8}$	$1.12 \cdot 10^{-7}$
304	"	$1.74 \cdot 10^{-8}$	$2.23 \cdot 10^{-7}$
299	0.5 - 1.0	$2.40 \cdot 10^{-8}$	$2.42 \cdot 10^{-7}$
100	2.8 - 3.55	$8.33 \cdot 10^{-9}$	$9.59 \cdot 10^{-8}$

Separation of the theobromine extract from the gas:

Separation of the theobromine from the gas was achieved during this investigation under constant conditions through a depressurization to 180 bar and an absorption with water at a ratio of 0.1 - 0.2 l H_2O/kg CO_2 at a constant temperature of 70 °C. Conditions for this separation will be investigated in a subsequent study more thoroughly. In all experiments theobromine was absorbed from the gas to a concentration below the detection limit of the applied analytical method of about 1 ppm. In the absorbing water the mean concentration of theobromine was about 0.2 g/l with maximum concentrations of 0.4 g/l at the beginning of an extraction.

Literature:

1. Brunner, G.: Stofftrennung mit überkritischen Gasen (Gasextraktion), Chem.-Ing.-Tech. **59**, 12 (1987)
2. Margolis, G.: EP 0 061 017 B1 ; September 19, 1984: Removal of Xanthine Stimulans From Cocoa
3. Gährs, H.J., E. Marnette: Verfahrenstechnik **17**, 554 (1983)
4. Crank, J.: The Mathematics of Diffusion, 2nd ed., Oxford 1973
5. Cammenga, H. K., H. Bothe: Coffein, Theophyllin und Tehobromin. Research report of the Institut für Physikalische Chemie, Technische Universität Braunschweig
6. Brunner, G.: Decaffeination of Raw Coffee by Means of Compressed Nitrous Oxide, Proc. Int. Symp. on Supercritical Fluids, Vol. 2, p. 691 - 698; Nice 1988

Solvent Extraction 1990, T. Sekine (Editor)

© 1992 Elsevier Science Publishers B.V. All rights reserved

CHROMATOGRAPHIC MEASUREMENT OF VAPOR-LIQUID EQUILIBRIUM RATIOS OF ORGANIC SOLVENTS IN SUPERCRITICAL CO_2 + POLY(VINYL ACETATE) SYSTEM

KOJI HATTORI , NING-HE WANG , SHIGEKI TAKISHIMA and HIROKATSU MASUOKA
Department of Chemical Engineering , Hiroshima University
Higashi-Hiroshima 724 , Japan

ABSTRACT

For the application of supercritical fluid extraction to the removal of impurities (solvent, monomer etc.) from polymer, phase equilibrium data of the supercritical fluid + organic solvent + polymer system are needed. In this work chromatographic method with an open tubular column was used to measure vapor-liquid equilibrium ratios (K-values) of the organic solvent at infinite dilution in the supercritical fluid + polymer system. Infinite dilution K-values on weight fraction basis were obtained from measurement of solute retention volume in conjunction with the solubility of CO_2 in the polymer which was measured by piezoelectric-quartz sorption method. Experiments were carried out for benzene and toluene in the CO_2 + poly(vinyl acetate) system at temperatures of 313.2 and 333.2K and pressures up to 8MPa. K-values of both benzene and toluene had a minimum around 4MPa. Moreover, K-values were predicted by Schotte equation of state. Pure component parameters and binary parameters needed in the prediction were determined by fitting the properties of each component and VLE data of each binary system, respectively. The agreement between measured and predicted K-values was good qualitatively but not enough quantitatively.

1 INTRODUCTION

The removal of volatile substances, such as an unreacted monomers, reaction by-products and solvents, from polymers is important operation in their manufacture. The authors (Sasaki et al.1988) have carried out experimental work of separation of organic solvents from polymers using supercritical fluid extraction technique. To examine the mechanism of above separation process the vapor-liquid equilibrium ratios of solvent in SC-CO_2 and polymer system are needed.

2 MEASUREMENT PRINCIPLE

For the measurement of the vapor-liquid equilibrium of a ternary system containing a nonvolatile material, chromatographic method is available because this method does not need the composition analysis and material balance.

Martin et al.(1941) developed an expression relating the retention volume of a solvent i ,V_{Ri} to its partition coefficient by using a theoretical plate model for the column.

$$V_{Ri}=V_g+V_L/H_i \qquad (1)$$

where V_g is the free gas volume of the column , V_L is the volume of fixed polymer phase in the column. H_i is the equilibrium partition coefficient of the solvent between two phases , (conc. of i in the vapor phase divided by conc. of

i in the polymer phase.)

For the system containing polymer , weight fraction basis K-value is convenient. From Eq.(1) , weight fraction basis K-value of the solvent i at infinite dilution , K_i^{∞} is expressed in terms of its retention volume by referring to the study of Stalkup et al. (1963)

$$K_i^{\infty} = \left(\frac{w_i^V}{w_i^P}\right)^{\infty} = \frac{m_P}{\rho_o(V_{Ri}-V_g)M_o(1-w^P{}_o)} \qquad (2)$$

where w_i^V and w_i^P are the weight fractions of the solvent in vapor and polymer phases, respectively. ρ_o and M_o denote molar density and the molecular weight of the carrier gas (CO_2), respectively. V_g is free gas volume of the column and m_P is the weight of polymer in the column. Retention volume of the sample ,V_{Ri} is defined as the product of the retention time of the sample and the carrier gas volumetric flow rate expressed at column conditions of temperature and pressure. The solubility data of CO_2 into polymer, $w^P{}_o$ were obtained from the work of Wang et al. (1990).

3 EXPERIMENTAL

In this study , open tubular column coated with polymer on its inner wall directly , was used because of its low pressure drop and ease of measuring the polymer weight and the free gas volume.

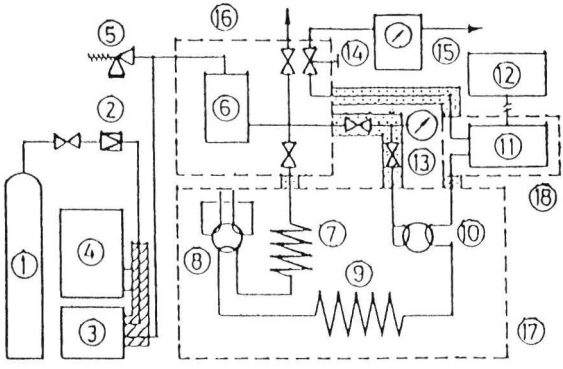

Fig.1 Schematic Diagram of Experimental Apparatus

Schematic diagram of high-pressure chromatographic apparatus used in this study is shown in Fig.1. After CO_2 as the carrier gas was pumped into a buffer tank in an air bath by a liquid pump (JASCO 880-PU), the carrier gas passed through a six-way valve as the sample injector and then through a open tubular column. The carrier gas passed through a UV detector (JASCO MULTI-320) located in an air bath and then through a needle valve where it was expanded down to atmospheric pressure. This needle valve was used to control the flow rate of the carrier gas. The carrier gas finally passed through a wet gas meter and its flow rate was measured. Vapor of the organic solvent as the sample was injected into

the carrier gas by switching the six-way valve. Retention time was measured as the time between the sample injection and detection.

Open tubular columns were made of stainless steel tubes (I.D.= 0.5mm) and weights of coated polymer were about 20 ~ 60 mg. Coating was carried out based on Dynamic Coating Method (Saito et al. 1974). PVAc solution (15 wt%) for the coating was made by dissolving PVAc in benzene. The solution placed in a solvent tank was flowed through the columns with nitrogen at pressure of about 3.5Kg/cm^2. The polymer weights in the columns were determined by the difference in the weights between the uncoated and coated columns.

4 RESULTS AND DISCUSSION

The relationship between the flow rate of CO_2 and the retention volume for benzene at 313.2K and pressures up to 5MPa is shown in Fig.2. As shown in this diagram, the dependence of flow rate on retention volume is observed. At the relatively lower pressures, instantaneous equilibria of the system were not performed because the retention volumes depend on the flow rates of the carrier gas which shows the existence of mass transfer resistance in polymer phase. The retention volumes were extrapolated to zero flow rate to obtain the equilibrium values. At pressures above 6MPa (Fig.3), flow rate dependence of the retention volume vanished and instantaneous equilibria were performed because large quantity of CO_2 dissolved into the polymer which made the polymer soften.

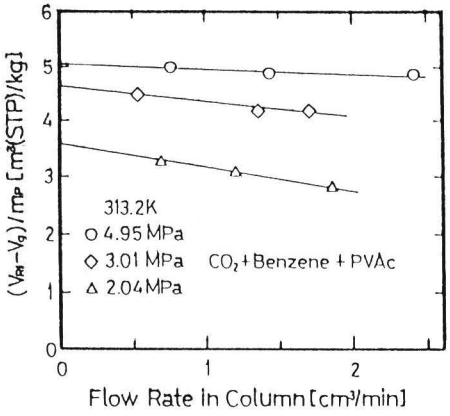

Fig.2 Effect of Flow Rate on Retention Volume of Benzene in the Low-Pressure Range

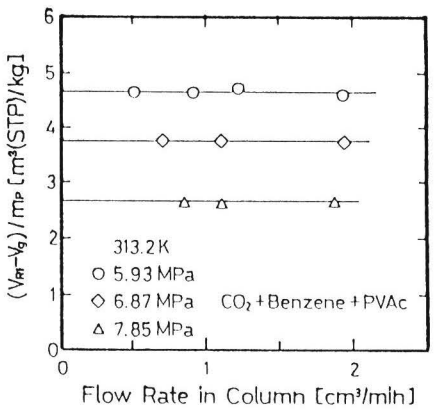

Fig.3 Effect of Flow Rate on Retention Volume of Benzene in the High-Pressure Range

Figures 4 and 5 show K-values of benzene and toluene based on Eq.(2), respectively. The K-values at each temperature and of each sample had a minimum around 4 or 5MPa. Above these pressures, K-values increased because of increase of the solvent power of CO_2. K-values at 333.2K, at which the vapor pressure of the sample is higher than that at 313.2K, were larger than those at 313.2K. But the two isotherms crossed around 7MPa. It seems that the solvent power of CO_2

prevails over the vapor pressure of the solvent. Additionally, K-values of benzene, which has higher vapor pressures than toluene has, were larger than those of toluene at same temperature and pressure. Above-mentioned behavior of the K-values is not unusual and has been also reported by Stalkup et al. (1983) in their studies of high-pressure vapor-liquid equilibrium for low molecular weight systems.

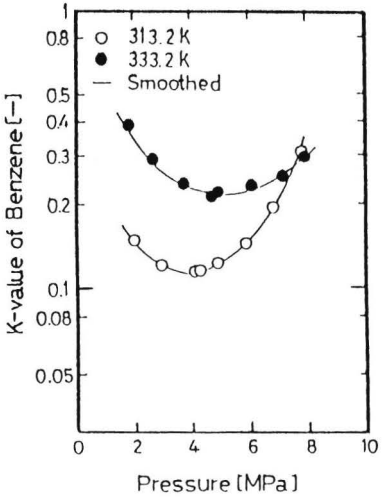

Fig.4 Infinite-Dilution K-value of Benzene in CO_2+PVAc System

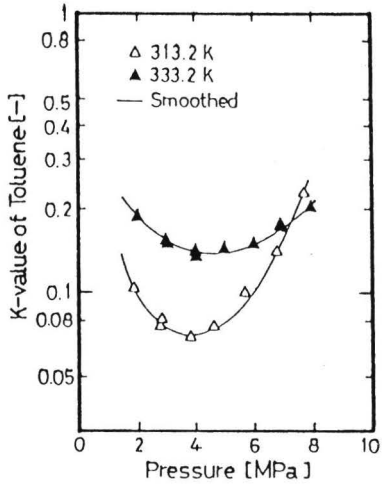

Fig.5 Infinite-Dilution K-value of Toluene in CO_2+PVAc System

5 PREDICTION USING EQUATION OF STATE

To describe the ternary phase equilibrium behavior, we adopted the Schotte equation of state (1982) where

$$\frac{\tilde{P}\tilde{v}}{\tilde{T}} = \frac{RT^*}{P^*Mv^*}\left(1-\frac{1}{\tilde{v}^{1/3}}\right) + \frac{1}{\tilde{v}^{1/3}-1} - \frac{1}{\tilde{v}\tilde{T}} \tag{3}$$

$$\tilde{P} = P/P^* \ ; \ \tilde{v} = v/v^* \ ; \ \tilde{T} = T/T^* \tag{4}$$

where $\tilde{P}$, $\tilde{v}$ and $\tilde{T}$ are reduced properties of pressure, volume, and temperature, respectively, and P^*, v^* and T^* are the characteristic parameters of the particular compound, and R is gas constant. For the mixture , the mixing rules given in the original work of Schotte were extended to multicomponent system.

$$P^* = \Sigma\Sigma\psi_i\psi_j P^*_{ij} \tag{5}$$

$$\frac{1}{Mv^*} = \Sigma\Sigma\psi_i\psi_j\frac{1}{(Mv^*)_{ij}} \tag{6}$$

$$T^* = \frac{P^*}{\Sigma \psi_i P^*_i / T^*_i} \tag{7}$$

$$\psi_i = \frac{w_i v^*_i}{\Sigma w_j v^*_j} \tag{8}$$

$$P^*_{ij} = (1-k_{ij})(P^*_i P^*_j)^{1/2} \tag{9}$$

$$\frac{1}{(Mv^*)_{ij}} = \frac{1}{2}\left(\frac{1}{M_i v^*_i} + \frac{1}{M_j v^*_j}\right) \tag{10}$$

where ψ_i, w_i and M_i are the volume fraction, mass fraction and molecular weight for component i, respectively.

The characteristic parameters for each substance were determined by correlating the P-v-T data or saturated properties of the substance using Eq.(3) and are shown in Table 1, and the binary interaction parameters(k_{ij}) in Eq.(9) were determined by correlating the phase equilibrium data of binary systems. The k_{ij}s are shown in Table 2.

TABLE 1

Characteristic Parameters in Schotte EOS

Substance	P*[MPa]	v*[cm³/g]	T*[K]
CO_2	328.3	0.6425	2175+1826(1-Tr)+2775(1-Tr)²
Benzene	308.7	0.9519	6293-12419(1-Tr)+26453(1-Tr)²
Toluene	520.3	0.9063	5163-3599(1-Tr)+4716(1-Tr)²
PVAc	378.8	0.7449	11275-10.40T

Tr = T/Tc ; T: temperature [K] , Tc: critical temperature [K]

TABLE 2

Interaction Parameters in Schotte EOS

System	kij	
	313.2K	333.2K
CO_2+PVAc[a)]	-0.0385	-0.0521
CO_2+Benzene[b)]	0.0857	0.0913
CO_2+Toluene[c)]	0.0496	0.0605
Benzene+PVAc[d)]	0.0199	0.0167
Toluene+PVAc[d)]	-0.0059	-0.0066

a) Wang et al. (1990)
b) Gupta et al. (1982)
c) Kim et al. (1986)
d) measured by the piezoelectric-quartz sorption method in this work

The predicted results of the K-values of benzene and toluene in CO_2 + PVAc system are shown in Figs.6 and 7. Prediction was good qualitatively, but not

enough quantitatively. It seems that one of the primary factors for the unsatisfactory prediction of the ternary K-values is the imperfection of the correlation for CO_2 + solvent systems. Therefore, further examination is required to improve the accuracy of the prediction.

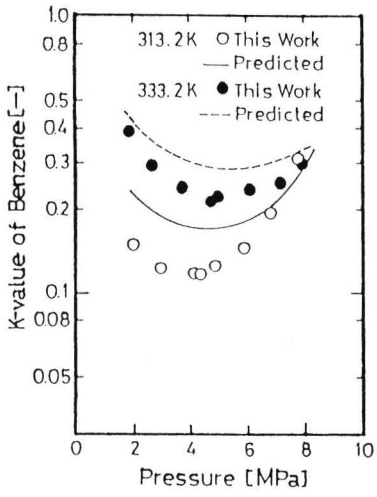

Fig.6 Infinite-Dilution K-value of Benzene in CO_2+PVAc System

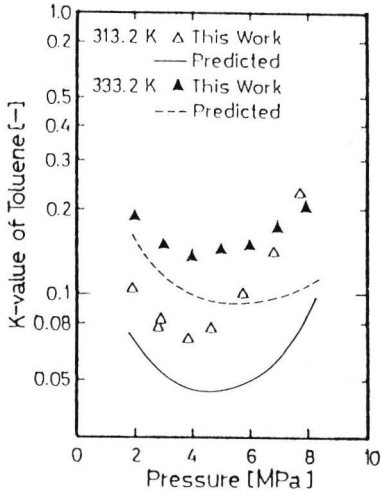

Fig.7 Infinite-Dilution K-value of Toluene in CO_2+PVAc System

6 CONCLUSIONS

High-pressure chromatographic method was used to measure the K-values of benzene and toluene in CO_2 + PVAc system at 313.2K and 333.2K. The K-values obtained in this work had the behavior similar to the those of many other systems not containing polymer.

It was also tried to predict the K-values using Schotte EOS, but the agreement was only qualitative.

7 REFERENCES

Gupta,M.L., Li,Y.H., Hulsey,B.J. and Robinson Jr.,R.L.,1982. J.Chem. Eng.Data, 27:55.

Kim,C.H., Vimalchand,P. and Donohue,M.D.,1986. Fluid Phase Equilibria, 31:299.

Martin,A.J.P and Synge,R.L.M.,1941. Biochem.J., 35:1358.

Saito,H. and Fukukawa,O.,1974. Japan Analyst, 23:339.

Sasaki,M, Takishima,S. and Masuoka,H.,1988. Proceedings of International Symposium on Supercritical Fluids, Nice, France:711.

Schotte,W.,1982. Ind.Eng.Chem.Process Des.Dev., 21:289.

Stalkup,F. and Kobayashi,R.,1963. AIChE J., 9:121.

Wang,N.H.,Takishima,S. and Masuoka,H.,1990. Kagaku Kogaku Ronbunshu, 16:931.

Solvent Extraction 1990, T. Sekine (Editor)

© 1992 Elsevier Science Publishers B.V. All rights reserved

APPLICATION OF LIQUID-LIQUID EXTRACTION OF LANTHANOID ELEMENTS TO CENTRIFUGAL PARTITION CHROMATOGRAPHY

K. AKIBA, Y. ISHIBASHI and S. NAKAMURA
Research Institute of Mineral Dressing and Metallurgy, Tohoku University, Katahira-2, Aoba-ku, Sendai 980 (JAPAN)

ABSTRACT
Akiba, K., Ishibashi, Y. and Nakamura, S., 1990. Application of liquid-liquid extraction of lanthanoid elements to centrifugal partition chromatography.

Extraction of lanthanoid elements (M) by 2-ethylhexyl 2-ethylhexylphosphonic acid (EHPA; HA) proceeds via the reaction, $M^{3+}_{aq} + 3(HA)_{2,org} \rightleftarrows M(HA_2)_{3,org} + 3H^{+}_{aq}$. This liquid-liquid extraction has been modified to a centrifugal partition chromatography (CPC). An organic solution containing EHPA was held as a stationary phase and an aqueous mobile phase was passed through the stationary phase. The retention volume (V_R) is related to the distribution ratio (D) of the desired lanthanoid element, $V_R = V_m + D \cdot V_s$, where V_s and V_m are the volumes of the stationary and mobile phases, respectively. The addition of water-soluble alcohols enhanced the resolution of adjacent bands. The mutual separation of mixed lanthanoids, Sm-Eu-Gd, was accomplished by employing the ethylene glycol-water mixture as the mobile phase. The separation process in CPC essentially corresponds to that in liquid-liquid extraction.

INTRODUCTION

Solvent extraction is a powerful technique for the group separation of lanthanoid elements, however, it requires multistage processes for the mutual separation of neighboring lanthanoids (Goto, 1968).

Centrifugal partition chromatography will be accessible for the separation of chemically similar materials (Murayama et al., 1982). This new partition chromatography employing a liquid phase as a stationary phase without any solid support materials may be essentially comparable to liquid-liquid extraction (Araki et al., 1988). The stationary and mobile phases can be easily changeable according to their own requirement based on the extraction equilibria.

Previously we proposed the possibility of the mutual separation of lanthanoid series elements employing 2-ethylhexyl 2-ethylhexylphosphonic acid in kerosene as the stationary phase (Akiba et al., 1988). Physicochemical properties of the stationary and mobile phases will affect the elution behavior of individual elements.

The present study deals with some chromatographic parameters by changing aqueous mobile phases containing water soluble alcohols. The mutual separation of lanthanoids was demonstrated for the mixture of Sm-Eu-Gd.

2 EXPERIMENTAL

2.1 Liquid-liquid extraction

2-Ethylhexyl 2-ethylhexylphosphonic acid (EHPA; HA) was washed with a sodium hydroxide solution to remove acidic impurities. The aqueous solution containing lanthanoid ions was equilibrated with a kerosene solution of EHPA. The distribution ratio (D) was obtained by γ-counting of $^{152,4}Eu$ or by determining the concentrations of lanthanoids by ICP-AES.

2.2 Centrifugal partition chromatography (CPC)

A centrifugal partition chromatograph (Sanki Engineering Ltd.) was used by arranging 6 or 12 partition cartridges (30E), in which each cartridge was composed of 54 microcells. The apparatus was operated at 40°C by rotating at 800 rpm unless otherwise noted. The EHPA solution in kerosene was held as the stationary phase into the series of microcells. After the mixture of 0.001 M (mol dm^{-3}) each lanthanoid had been loaded, the aqueous mobile phase controlled to desired pH was pumped through the partition cartridges at a flow rate of 3 cm^3 min^{-1}. The elution stream was monitored at 650 nm via a post-column reaction with 0.014% Arsenazo III.

The chromatographic parameters, the number of theoretical plate N, the separation factor α_c and the resolution R_s, were evaluated from the retention volume V_R and the bandwidth W as:

$$N = 16(V_R/W)^2 \tag{1}$$

$$\alpha_c = (V_{R,2} - V_0)/(V_{R,1} - V_0) \tag{2}$$

$$R_s = 2(V_{R,2} - V_{R,1})/(W_2 + W_1) \tag{3}$$

where V_0 is the elution volume of an unretained component.

3 RESULTS AND DISCUSSION

3.1 Liquid-liquid extraction

The extraction behavior of europium as a representative lanthanoid element was examined from aqueous solutions of different compositions. As shown in Fig. 1, the plots of log D against pH gave the straight lines with slopes close to 3 for 0.1 M $(H,Na)NO_3$ and 0.1 M $(H,Na)Cl_2CHCOO$ solutions keeping the ionic strength 0.1. The log-log plot of D vs. $[(HA)_2]$ was also found to be a straight line with a slope of 2.8. The extraction equilibrium can be expressed as:

$$M^{3+}_{aq} + 3\ (HA)_{2,org} \rightleftharpoons M(HA_2)_{3,org} + 3\ H^+_{aq} \tag{4}$$

where M denotes the lanthanoid element and $(HA)_2$, the dimer of EHPA.

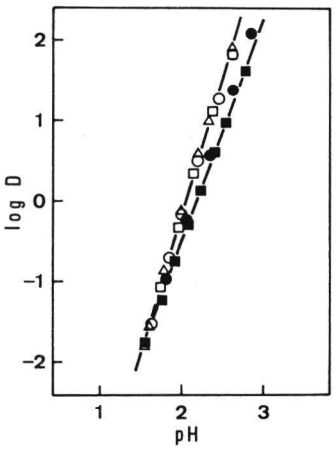

Fig. 1. Distribution ratio of Eu. 0.01 M $(HA)_2$ in kerosene; (○) HNO_3, (●) 0.1 M $(H,Na)NO_3$, (△) HCl, (□) $Cl_2CHCOOH$, (■) 0.1 M $(H,Na)Cl_2CHCOO$; 25°C.

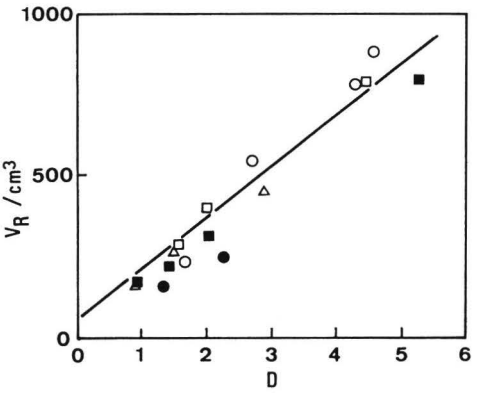

Fig. 2. Relation between the retention volume and the distribution ratio for Eu. CPC: 6 cartridges, 25°C; stationary phase: 0.01 M $(HA)_2$ in kerosene. The mobile phases correspond to the aqueous phases in Fig. 1.

3.2 Application to CPC

The elution behavior of europium was preliminarily investigated by employing 0.01 M $(EHPA)_2$ in kerosene as the stationary phase. The retention volumes obtained for different mobile phases are plotted against the D values in Fig. 2. The retention volume was found to increase with the D value as:

$$V_R = V_m + D \cdot V_s \qquad (5)$$

where V_s and V_m are the volumes of the stationary and mobile phases, respectively. The number of theoretical plate was found to increase with the V_R value and relatively large N values were obtained in 0.1 M $(H,Na)Cl_2CHCOO$ solution compared with other systems, and then this solution having buffer action was employed as the mobile phase in the subsequent experiments.

3.3 Aqueous mobile phase containing alcohol

The aqueous mixed solvent is expected to improve the separation of chromatographic bands (Akiba et al., 1988). The effect of water miscible alcohols added to the aqueous mobile phase on elution behavior has been investigated at 40°C. As Fig. 3 shows, the retention volume of europium

increased with an increase in alcohol content up to 30% v/v of methanol and ethylene glycol, but was nearly constant in the range to 20% v/v ethanol. More higher content of these alcohols brought about partial loss of the stationary phase owing to an increase in mutual solubility.

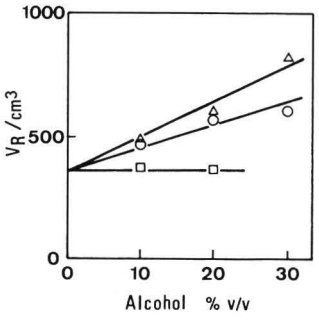

Fig. 3. Effect of the alcohol content on the retention volume. CPC: 12 cartridges; 0.02 M $(HA)_2$; 0.1 M $(H,Na)Cl_2CHCOO$; (○) EG, (△) MeOH, (□) EtOH at pH 1.90.

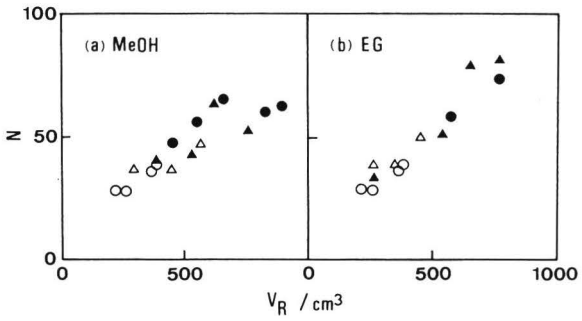

Fig. 4. Relation between the number of theoretical plates and the retention volume. (○) Water alone, (△) 10%, (▲) 20%, (●) 30% alcohol.

3.4 Number of theoretical plate

Variations in the number of theoretical plate are illustrated in Fig. 4 for water-alcohol mixed mobile phases. The N values for methanol or ethylene glycol mixtures increased with V_R values, while the mobile phase containing ethanol or 1-propanol little enhanced the N values.

3.5 Separation factor

Variations in the separation factor are shown as a function of alcohol content in Fig. 5. The mixture with methanol yielded nearly constant α_c values, however, α_c values slightly fell with increasing ethanol content. On the contrary, ethylene glycol mixtures greatly enhanced the α_c values. The separation factors α_D evaluated from the distribution ratios in liquid-liquid extraction are close to α_c values, indicating comparable separation processes.

3.6 Resolution

The resolution of the elution peaks of Sm and Gd is given in Fig. 6. The R_s values increased with pH values and also with alcohol contents. The high resolution in ethylene glycol mixtures was resulted from the high values of α_c and N. In the case of methanol mixtures, the resolution was improved by

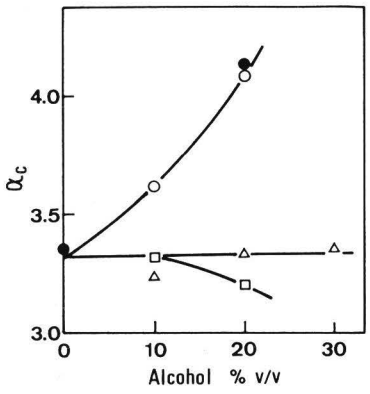

Fig. 5. Effect of the alcohol content on the separation factor for Gd-Sm. (○) EG, (△) MeOH, (□) EtOH; (●) α_D for EG.

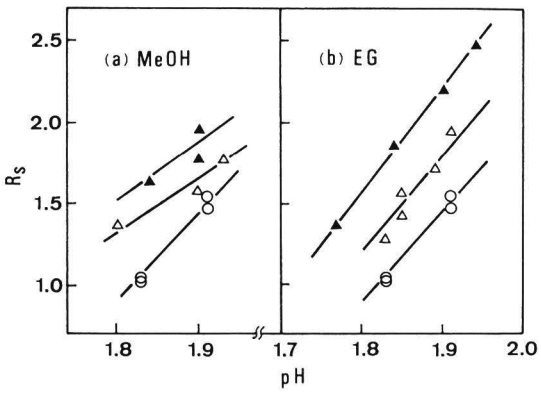

Fig. 6. Resolution for Sm-Gd as a function of pH. (○) Water alone, (△) 10%, (▲) 20% alcohol.

increasing N remaining unaltered α_c, and the ethanol mixtures sparingly contributed to increase in R_s values. The ethylene glycol mixtures are thus the most suitable of the mixed mobile phases tested.

Such elution behavior may be associated with hydrophobic properties of alcohols used. The stable stationary phase was obtained in the case of less hydrophobic ethylene glycol, yielding high values of N and α_c; while the stability of the stationary phase decreased with increasing hydrophobic properties and the values of N and α_c were little improved or rather decreased.

3.7 Separation of Sm-Eu-Gd mixture

Mutual separation of the mixture of Sm-Eu-Gd, one of the most difficult mixtures for complete separation, was carried out under optimum conditions.

The plot of the retention volume against the D value is shown in Fig. 7 for 20% v/v ethylene glycol-water system. The plot gave a linear line in accord with that expected from eqn. (5), employing V_s = 164 cm^3 and V_m = 56 cm^3 obtained experimentally. Thus the partition process in CPC is comparable to liquid-liquid extraction in these mixed aqueous systems.

A typical chromatogram obtained for the mixture of Gd-Eu-Sm is illustrated in Fig. 8. These lanthanoids yielded individual peaks with relatively high N values; N = 60 for Sm, 79 for Eu and 83 for Gd. A quantitative separation of adjacent lanthanoids, Sm and Eu was accomplished with good resolution, R_s = 1.58, in which α_c (= 2.46) is close to α_D (= 2.51). The separation of Eu and Gd with the minimum α_D (= 1.70) was also adequate as α_c = 1.69 and R_s = 1.08.

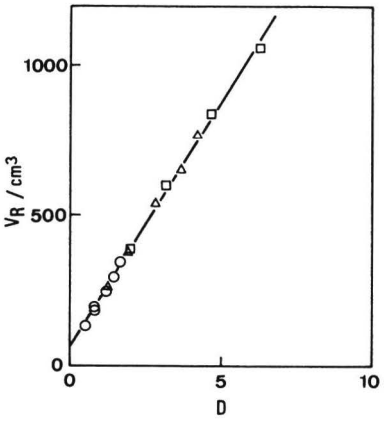

Fig. 7. Relation between the retention volume and the distribution ratio. (○) Sm, (△) Eu, (□) Gd. The solid line was predicted from eqn. (5).

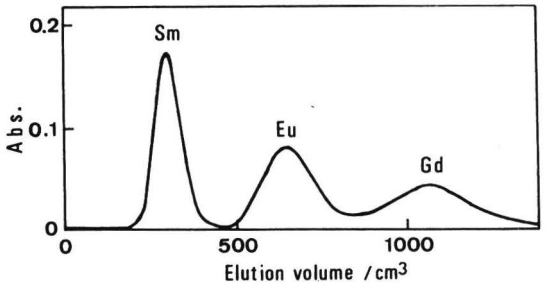

Fig. 8. Mutual separation of Sm, Eu and Gd. pH 1.94.

Thus the mutual separation of a series of lanthanoid elements will be achieved by controlling pH of the aqueous mobile phase to optimize the distribution ratio of desired elements.

4. ACKNOWLEDGMENT

This study was supported by a Grant-in Aid on Special Research of the Ministry of Education, Science and Culture.

5. REFERENCES

Akiba, K., Sawai, S., Nakamura, S. and Murayama, W., 1988. Mutual separation of lanthanoid elements by centrifugal partition chromatography. J. Liq. Chromatography, 11: 2517-2536.

Araki, T., Okazawa, T., Kubo, Y., Ando, H. and Asai, H., 1988. Separation of lighter rare earth metal ions by centrifugal counter-current type chromatography with di(2-ethylhexyl)phosphoric acid. J. Liq. Chromatography, 11: 267-281.

Goto, T., 1968. Separation factor for the extraction systems, YCl_3-$ErCl_3$-HCl, YCl_3-$HoCl_3$-HCl and some lanthanide chlorides-hydrochloric acid with 1 M di(2-ethylhexyl)phosphoric acid in n-heptane. J. Inorg. Nucl. Chem., 30: 3305-3315.

Murayama, W., Kobayashi, T., Kosuge, Y., Yano, H., Nunogaki, Y. and Nunogaki, K., 1982. A new centrifugal counter-current chromatograph and its application. J. Chromatography, 239: 643-649.

Solvent Extraction 1990, T. Sekine (Editor)

© 1992 Elsevier Science Publishers B.V. All rights reserved

UTILIZATION OF THIRD-PHASE-FORMATION IN SOLVENT EXTRACTION SYSTEMS EMPLOYING AMINE EXTRACTANTS

J. HARTL and R. MARR
Institute of Chemical Engineering and Environmental Technology
University of Technology Graz, Inffeldgasse 25, A-8010 Graz, Austria

ABSTRACT

The process using the third-phase-formation is a modification of reactive extraction. The separation of organic acids can yield higher enrichment by an additional utilization of solubility properties of the extracted compound in the solvent. Selectivity enhancement is under consideration.

1 INTRODUCTION

Removal of high polar organic solutes such as carboxylic and hydroxycarboxylic acids from diluted aqueous solutions is one of the most difficult problems in downstream processing. Liquid-liquid reactive extraction is a technology that can be used, the more when thermolabile substances are concerned. Research is done on the extraction of acetic, lactic, citric and many more acids (Siebenhofer and Marr, 1983; Wennersten, 1983; Schügerl et al., 1986; Bauer et al., 1989) and also the product separation and product brushing of amino acids is under examination (Schügerl and Degener, 1989). High distribution coefficients within selective extraction are needed to get satisfactory product enrichment and purity. A possibility to enhance enrichment is the usage of third-phase-formation in solvent extraction.

2 PROCESS DESCRIPTION

The idea of the process is a new variant of reactive extraction. An additional utilization of solubility properties while extraction is thought to enhance selectivity together with enrichment.

For the separation of biological produced carboxylic acids as well as hydroxycarboxylic acids from their fermentation broth this process employs the ion-pair forming high-molecular weight aliphatic amines. Mainly secondary and tertiary amines with straight or branched alkyl-chains of together more than 18 carbon atoms are used. Primary amines show too high solubility in water, what is the more a problem when dealing with three phases of graduate polarity.

These amine-extractants form together with an inert diluent the organic, water insoluble receiving phase. The diluent, preferably a medium fraction of alkanes, must be added to decrease the viscosity and the density of the mixture,

as well as to keep the solubility losses of the amine and the extracted acid-amine ion-pair low.

The substance of primary interest for the process development and in this paper is lactic acid. Besides, also the extraction of formic, acetic, propionic and other acids is of interest.

Extraction of carboxylic and hydroxycarboxylic acids with alkylamines gives alkylammonium salts preferably soluble in the organic phase. At high loadings in inert diluents molecular associates of these salts are formed. Dependent on the characteristics of the amine, of the extracted acid and of the organic solvent, these ionic aggregations separate from the organic phase and form an intermediate layer.

The 'Third Phase', as it is called, contains the acid in high concentration because of the reduced volume. It shows high viscosity and intermediate polarity and density. Phase disengagement can be supported by centrifugation.

Reextraction is carried through by means of solutions of alkaline salts or alkali hydroxides. Another possibility is to drive out the acid with a stronger one, like formic acid, followed by a distillative regeneration.

A process flowsheet in a schematic form is given in Figure 1.

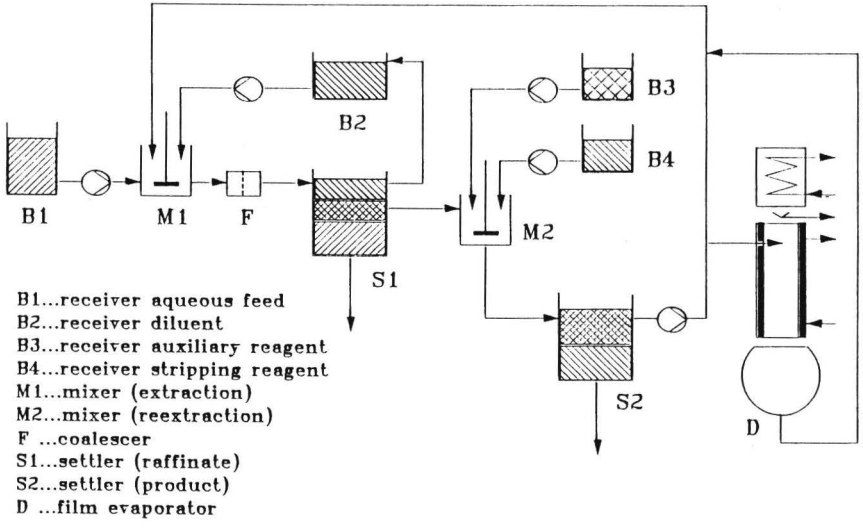

Fig.1. Process flowsheet of the third-phase-extraction

3 EXPERIMENTAL WORK

The prerequisite for employing this type of extraction process is the occurence of a third phase. Therefore different amine extractants in a preassumed concentration (50 vol%) doing well for the extraction had to be tested together

with the mentioned acids. As diluent Shellsol T (SST) was used.

Different ratios of the amine and SST were used for equilibrium curve estimation. The dependence of the extraction efficiency on different feed concentrations of the acids was measured.

Solvent developing experiments were performed in separation funnels. Equilibrium data were gained from contacting the phases in stirred beakers. Almost in every experiment the organic phase volume was 30 ml and the phase ratio was 1. The contact time was about one hour to ensure equilibrium. For pH regulation hydrochloric acid or potassium hydroxide was used.

Acid concentrations were determined by potentiometric titration with potassium hydroxide. For the third phase and the upper organic phase isopropanol was used as solvent. HPLC-analyses was employed, when a mixture of carboxylic acids couldn't be analytical separated by titration.

4 RESULTS

The following amine-extractants were tested: tri-n-butylamine, tri-n-hexylamine, tri-n-octylamine, tri-2-ethylhexylamine, tri-iso-octylamine (Adogen 381), tri-n-octyl/decylamine (Hostarex A327), trilaurylamine (Alamine 304), di-dodecyl/tridecylamine (Amberlite LA-2) and di-iso-tridecylamine (HOE F2562).

The tests showed that tri-n-butylamine is salted-in in water because of the high mutual solubility of the formed alkylammoniumlactate and water. Tri-n-hexylamine performed well in this test but it turned out that there also will be high solubility losses of the extractant. Tri-n-octylamine had about the same extraction efficiency as Hostarex A327. The latter proved to be best considering extraction efficiency together with phase disengagement and third-phase-formation.

TABLE 1

Third-phase-formation for acid extractions with 50 vol% extractant in SST. The aqueous feed concentration was 2 mol/l.

extractant \ acid	$C_3H_6O_3$	CH_2O_2	$C_2H_4O_2$	$C_3H_6O_2$	HCl
tributylamine		---	---	---	
trihexylamine	+	+	+	+	+
tri-n-octylamine	+	+	+	+	+
tri-2-ethylhexylamine		+			+
tri-iso-octylamine	+	+	+		+
tri-n-octyl/decylamine	+	+			+
trilaurylamine				---	---
di-dodecyl/tridecylamine	+	+			
di-iso-tridecylamine	+				

\+ third-phase-formation --- not investigated

In Table 1 third-phase-formation is qualitatively shown for lactic acid ($C_3H_6O_3$), formic acid (CH_2O_2), acetic acid ($C_2H_4O_2$), propionic acid ($C_3H_6O_2$) and

hydrochloric acid (HCl). The aqueous feed concentration was 2 mol/l. Generally the performed experiments showed that n-alkylamines are doing better in this procedure than iso-alkylamines. Furthermore, too long alkyl chains cause emulsification. Phase disengagement with the secondary alkylamines was worse to the systems with tertiary amines.

In Figure 2 the equilibrium curves for acetic acid (500 mmol/l) and different concentrations of Hostarex A327 (30-60 vol%) in Shellsol T are plotted. Figure 3 shows the same for lactic acid (500 mmol/l). The extraction efficiency is given in percent extracted, refering to the initial aqueous phase concentration, $c_{aq,0}$.

$$\% \text{ extraction} = 100\ (1 - c_{aq}/c_{aq,0}) \qquad (1)$$

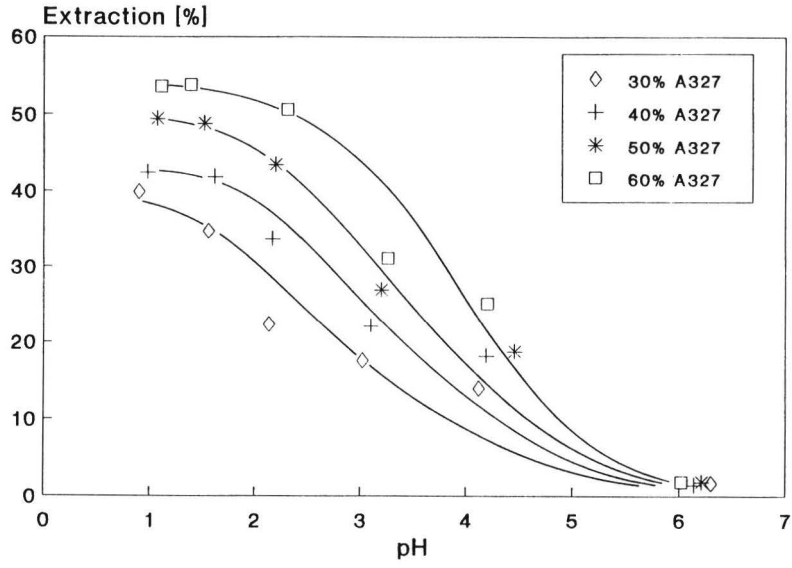

Fig.2. Extraction equilibria for acetic acid (500 mmol/l); organic phase: A327 in SST

The figures demonstrate increasing separation with decreasing pH and an optimum at the low pH of 1.5 or 2, respectively. But also the volume of the third phase and the coextraction of hydrochloric acid, which was used to adjust pH, increases. Therefore an optimum has to be found which could be around the unaffected extraction at a pH nearby 3 or 2.5, respectively.

The dependence of the extraction efficiency on different feed concentrations of acetic and lactic acid is shown in Figure 4. It also shows the volume of the third phase formed with lactic acid. Again, in this experiments the organic phase volume was 30 ml (50 vol% A327 in SST) and the phase ratio was 1.

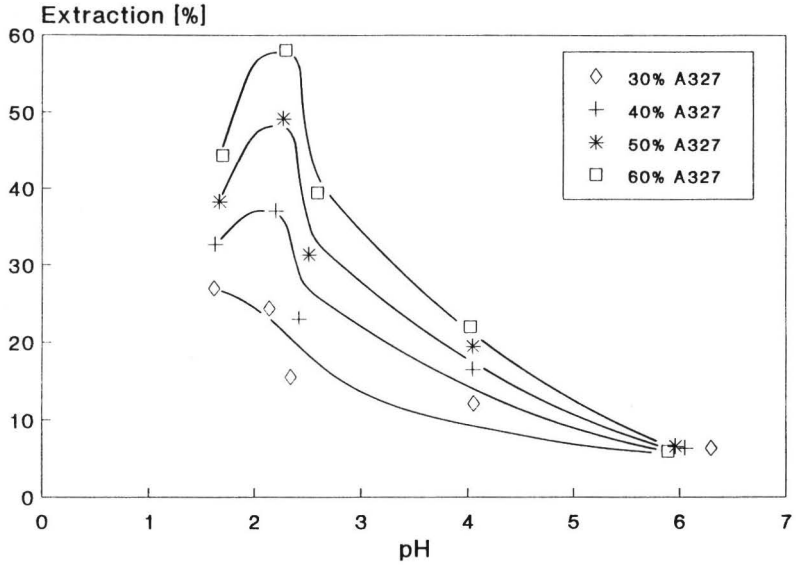

Fig.3. Extraction equilibria for lactic acid (500 mmol/l); organic phase: A327 in SST

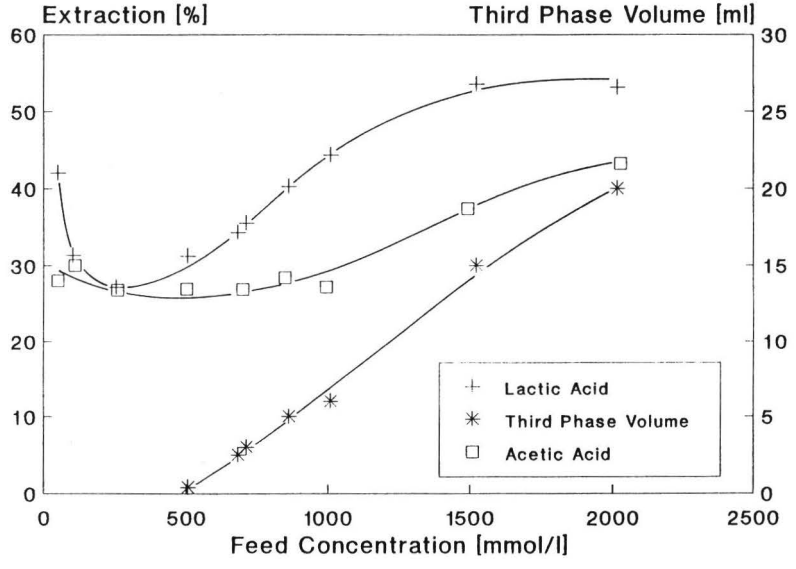

Fig.4. Extraction efficiency and third phase volume for different feed concentrations of lactic and acetic acid; organic phase: 50 vol% A327 in SST

It can be seen, that both the decreasing pH with increasing acid concentration of the aqueous phase and the growth in polarity of the organic phase due to the ion-pair formation enhance the extraction efficiency.

When using Hostarex A327 a third-phase-formation only occured with formic acid or lactic acid, respectively. The extraction of acetic acid or propanoic acid produced no intermediate layer. What caused the assumption that there could possibly be some selectivity in coextracting acetic and lactic acid because of the partition of the organic phase. Preliminary experiments on this item exhibited only a partly consent. So far, it could be seen, that the partition of the acids in two organic phases is slightly dependent on the concentration ratio of the acids in the feed solution.

The concentration of the extracted acid in the third phase was about the same for different feed concentrations and different concentrations of extractant in the solvent. But it strongly varied with the species of extractant used. Even if the separation is not as good as in conventional systems, there could always be obtained a highly concentrated third phase with acid contents of about 1-2 mol/l when Hostarex A327 was used. Employing Tri-n-hexylamine as extractant, the third phase was concentrated up to 3 mol/l for lactic acid and up to 4 mol/l for acetic acid. Too high solubility losses, as already mentioned, are matter of an objection for the usage of the latter without the necessity of a further cleaning step.

5 CONCLUSION

With reactive extraction an effective tool to separate polar organic substances, like fermentation produced carboxylic acids, is offered. In some special cases, when the conventional extraction procedure provides only small distribution coefficients and enrichment is the main criteria for an application, the new third-phase-extraction process might do help in achieving satisfactory concentrations. Investigations will go on to overcome the seen obstacles and to provide higher yield.

REFERENCES

Bauer, U., Marr, R., Rückl, W., Siebenhofer, M., 1989. Reactive Extraction of Citric Acid from an Aqueous Fermentation Broth. Ber. Bunsenges. Phys. Chem. 93: 980-984.

Schügerl, K. and Degener, W., 1989. Gewinnung niedermolekularer organischer Verbindungen aus komplexen wäßrigen Gemischen durch Extraktion. Chem.-Ing.-Tech. 61/10: 796-804.

Schügerl, K., Hänsel, R., Schlichting, E., Halwachs, W., 1986. Reaktivextraktion. Chem.-Ing.-Tech. 58/4: 308-317.

Siebenhofer, M. and Marr, R., 1983. Acid Extraction by Amines. ISEC'83, Denver, Col., Proc.18e.

Wennersten, R., 1983. The Extraction of Citric Acid from Fermentation Broth Using a Solution of a Tertiary Amine. J. Chem. Tech. Biotechnol. 33B: 85-94.

Solvent Extraction 1990, T. Sekine (Editor)

© 1992 Elsevier Science Publishers B.V. All rights reserved

HIGH-PRESSURE PHASE BEHAVIOR FOR BINARY MIXTURES OF INDOLE, PYRAZINE, PYRIMIDINE, AND QUINOXALINE WITH CO_2, C_2H_4, C_2H_6, AND CHF_3

Seiichi Yamamoto†, Kazunari Ohgaki, and Takashi Katayama
Department of Chemical Engineering, Faculty of Engineering Science, Osaka University, Toyonaka, Osaka 560 (Japan)

ABSTRACT
Yamamoto, S., Ohgaki, K., and Katayama, T., 1990. High-pressure phase behavior for binary mixtures of indole, pyrazine, pyrimidine, and quinoxaline with CO_2, C_2H_4, C_2H_6, and CHF_3.

High-pressure phase behavior for 16 binary mixtures consisting of indole, pyrazine, pyrimidine, and quinoxaline with CO_2, C_2H_4, C_2H_6, and CHF_3 has been investigated in the temperature range from 210 to 350 K and pressures up to 30 MPa. The observed phase boundaries correspond to critical loci and three-phase coexistence lines with critical end points and quadruple points.

The pressure-temperature relations along the boundaries are determined by straightforward visual observation through an equilibrium view cell. The systems are grouped into four different types of pressure-temperature diagram. The transitional patterns of pressure-temperature diagram are briefly discussed in terms of the characteristic interactions and the magnitude of size-asymmetry between unlike molecules.

1 INTRODUCTION

Recently the idea of utilizing substances in their supercritical states has received much attention. The application of supercritical fluid solvents is based on the experimental observation that many gases exhibit enhanced solvating power when compressed to conditions above the critical point. To utilize fully the unique solvent characteristics of supercritical fluid solvents, it is necessary to understand phase behavior of mixtures of supercritical fluids and solutes. However, in spite of extensive studies, experimental data concerning the phase behavior of the mixtures are still lacking at present. The present study lays emphasis primarily on elucidating experimentally the high-pressure phase behavior of binary mixtures which are composed of a supercritical fluid and a solid solute.

Even when restricted to nonpolar or moderately polar nonelectrolyte components, binary mixtures can display a variety of phase behavior. Recently, Luks (1986) has summarized systematic evolution in the phase behavior of binary mixtures using six typical types of phase diagrams. They are shown schematically in Fig. 1 in the language of pressure-temperature projections.

---

†Present address: Mechanical Engineering Research Laboratory, Kobe Steel, Ltd., Kobe 651-22 (Japan)

With increasing asymmetry between unlike molecules, the phase behavior evolves from type "A" to type "F".

In the present study, 16 binary mixtures which are composed of indole, quinoxaline, pyrazine, and pyrimidine as the first component (solute: subscript 1) and CO_2, C_2H_4, C_2H_6, and CHF_3 as the second component (solvent: subscript 2) are selected. And high-pressure phase behavior for those mixtures has been investigated in the temperature range from 210 to 350 K and pressures up to 30 MPa. The above supercritical fluid solvents are selected since they possess their critical temperatures near the room temperature and are, therefore, candidates for practical processes. Experimental data of phase boundaries for the above binary mixtures have not been previously reported.

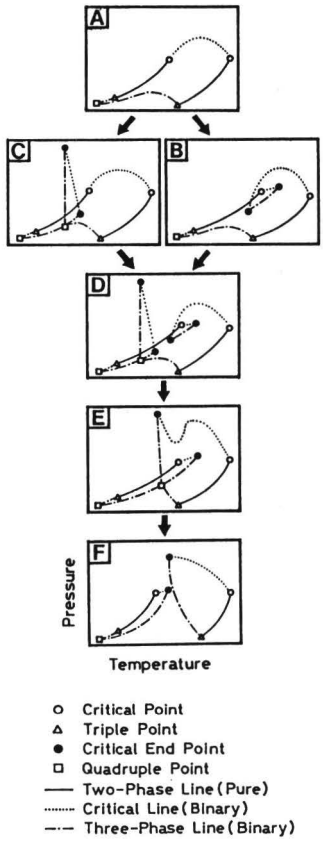

Fig. 1. Six types of phase behavior for binary mixtures shown as pressure-temperature projections.

2 EXPERIMENTAL

A detailed description of the experimental apparatus and the procedure is given in previous papers (Yamamoto et al., 1989; Yamamoto, 1990; Yamamoto et al., 1990). The pressure-temperature relations along phase boundaries are determined by straightforward visual observation through an equilibrium view cell.

3 RESULTS AND DISCUSSION

3.1 High-pressure phase behavior of binary indole systems

All the four indole systems investigated show type "F" phase behavior. The low temperature branch of the three-phase S_1-L-G line for each system which lies slightly below the vapor-pressure curve of pure solvent terminates at the first critical end point (FCEP, S_1-L=G), where the gaseous and liquid phases are critically identical in the presence of solid indole. Here the symbols S, L, and G represent solid, liquid, and gaseous phases, respectively. The pressure-temperature (p-T) trace of the high temperature branch of the S_1-L-G line originating at the triple point of indole is shown for the four systems in Fig. 2. Each of the S_1-L-G lines in the figure should terminate at the second critical end point (SCEP, S_1-L=G). However, this point could not be observed for the mixtures owing to the pressure limitation of the equilibrium

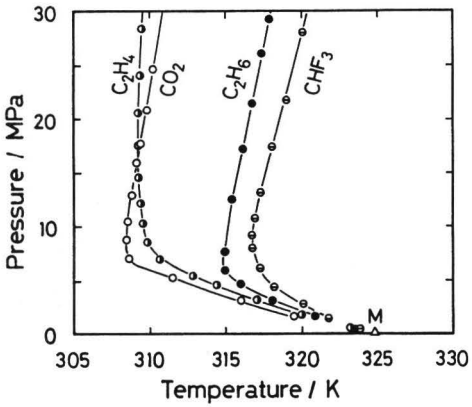

Fig. 2. Pressure-temperature trace of the high temperature branch of the three-phase S_1-L-G line for four binary mixtures containing indole (M: triple point of indole).

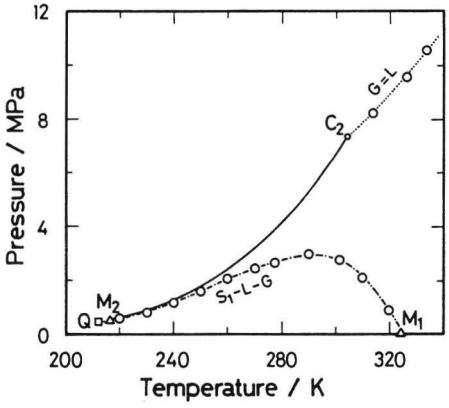

Fig. 3. Pressure-temperature projection of the high-pressure phase boundaries for the pyrazine + CO_2 system (C_2: critical point of CO_2, M_1: triple point of pyrazine, M_2: triple point of CO_2, Q: quadruple point, solid line between C_2 and M_2: vapor-pressure curve of CO_2).

cell used. It must be located at a pressure higher than 30 MPa for each system. All the systems show a temperature minimum in the three-phase coexistence curve. When the system has the minimum, a single liquid region called the liquid window appears in an isotherm at a temperature which is greater than the temperature minimum of the S_1-L-G line but still less than the SCEP temperature (McHugh et al., 1984; Cheong et al., 1986). The maximum values of the freezing point depression are 16.5, 15.7, 9.9, and 8.2 K for the binary mixtures of indole with CO_2, C_2H_4, C_2H_6, and CHF_3, respectively. This indicates that the solubilities of the gases in liquid (indole) decrease in that order.

3.2 High-pressure phase behavior of binary pyrazine systems

The p-T trace of the phase boundaries for the pyrazine + CO_2 system is shown in Fig. 3. The mixture was identified to display type "A" phase behavior. The L=G critical locus commences at the critical point of CO_2 with a positive slope. In the vicinity of the critical point, any L-L-G equilibrium line is not experimentally detected. On the other hand, the S_1-L-G line begins at the triple point of pyrazine, proceeds toward lower temperatures through a pressure maximum, and terminates at the quadruple point corresponding to the S_1-S_2-L-G equilibrium. No liquid-liquid immiscibility was observed before the onset of crystallization of CO_2 in the liquid phase.

The phase behavior of the pyrazine + C_2H_4 system was identified to belong to the category of type "F". This is because the triple point temperature of pyrazine (324.3 K) and the critical temperature of C_2H_4 (282.4 K) are fairly separated. The values of p and T at the SCEP of the system were evaluated to

be 9.91 MPa and 304.1 K, respectively, by means of extrapolation of both the L=G critical locus and the S_1-L-G line which were determined experimentally.

The p-T trace of the phase boundaries for the pyrazine + C_2H_6 system is shown in Fig. 4. The mixture was revealed to show type "E" phase behavior. The characteristic feature of the system is that the quadruple point temperature (313.5 K) is higher than the critical temperature of light component, C_2H_6 (305.4 K). The phase behavior of this system is undoubtedly type "E", but one can say that it is close to type "F" behavior.

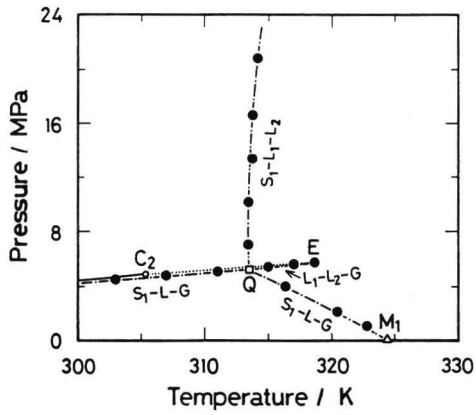

Fig. 4. Pressure-temperature projection of the high-pressure phase boundaries for the pyrazine + C_2H_6 system (C_2: critical point of C_2H_6, E: UCEP, M_1: triple point of pyrazine, Q: quadruple point).

For the pyrazine + CHF_3 system, the phase behavior at temperatures above the ice-point is quite similar to that of the pyrazine + CO_2 system. No liquid-liquid immiscibility was observed at as low as 220 K. Since the solubility of solid (pyrazine) in the liquid CHF_3 decreases with decreasing the temperature, the binary three-phase S_1-L-G line nearly coincides with the vapor-pressure curve of pure CHF_3 at around 220 K. Consequently, the liquid-liquid immiscibility is likely not to appear in lower temperatures. Hence, the system was identified to have type "A" phase behavior. The S_1-L-G line will encounter the quadruple point corresponding to the S_1-S_2-L-G equilibrium at a temperature near the triple point of CHF_3.

3.3 High-pressure phase behavior of binary pyrimidine systems

Both the pyrimidine + CO_2 and + CHF_3 systems were identified to have type "A" phase behavior. And both the pyrimidine + C_2H_4 and + C_2H_6 systems were revealed to show type "E" phase behavior. The S_1-L_1-L_2 line of the pyrimidine + C_2H_4 system which commences at the quadruple point has a negative slope on the p-T diagram, while that of the pyrimidine + C_2H_6 system has a positive slope.

3.4 High-pressure phase behavior of binary quinoxaline systems

The experimental p-T trace of the phase boundaries for the quinoxaline + CO_2 system is shown in Fig. 5. The system was identified to have type "B" phase behavior. An L_1-L_2-G line is observed with a range of 11.5 K in the vicinity of the critical point of CO_2. Here the critical locus is divided into

two parts. The p-T trace of the phase boundaries of the system at temperatures lower than the ice-point is similar to that of the pyrazine + CO_2 system (see Fig. 3).

The quinoxaline + C_2H_4 system were identified to have type "F" phase behavior. And both the quinoxaline + C_2H_6 and + CHF_3 systems were revealed to show type "E" phase behavior. The characteristic behavior of the latter is that the S_1-L_1-L_2 line has a distinct minimum in temperature.

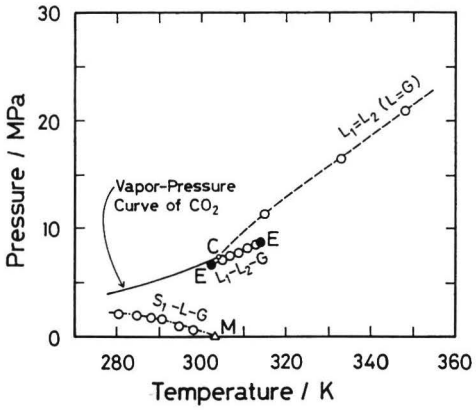

Fig. 5. Pressure-temperature projection of the high-pressure phase boundaries for the quinoxaline + CO_2 system (C: critical point of CO_2, E: critical end point, M: triple point of quinoxaline).

3.5 Transitional patterns of pressure-temperature diagram

In Table 1, the types of phase behavior for the 16 binary mixtures investigated are summarized, according to the arbitrarily defined classification of phase behavior which is depicted as in Fig. 1. In the table the temperature difference ΔT, which is defined as $\Delta T \equiv T_{m,1} - T_{c,2}$, where $T_{m,1}$ is the melting point of solute and $T_{c,2}$ is the critical temperature of solvent, for each mixture is also given. A binary mixture possesses a unique value of ΔT. The classification of phase diagrams is, on the whole, dependent on the value of ΔT. In other words, ΔT is a primary index for determining the types of phase behavior for binary mixtures. When the ΔT value is larger than 20 K, the type of phase behavior is usually "F". However, for both the pyrazine + CO_2 and + CHF_3 systems type "A" phase behavior is observed, in spite of the large values of ΔT (20.1 and 25.0 K, respectively). These findings would reflect some characteristic interactions between unlike molecules such as the strong affinity between CO_2 and Lewis base.

TABLE 1

Temperature difference ΔT and type of phase behavior for 16 systems investigated

System (1)+(2)	Type of Phase Behavior	ΔT/K
Indole + CO_2	F	21.8
Indole + C_2H_4	F	43.6
Indole + C_2H_6	F	20.6
Indole + CHF_3	F	26.7
Quinoxaline + CO_2	B	- 0.9
Quinoxaline + C_2H_4	F	20.9
Quinoxaline + C_2H_6	E	- 2.1
Quinoxaline + CHF_3	E	4.0
Pyrazine + CO_2	A	20.1
Pyrazine + C_2H_4	F	41.9
Pyrazine + C_2H_6	E	18.9
Pyrazine + CHF_3	A	25.0
Pyrimidine + CO_2	A	-11.2
Pyrimidine + C_2H_4	E	10.6
Pyrimidine + C_2H_6	E	-12.4
Pyrimidine + CHF_3	A	- 6.3

$\Delta T \equiv T_{m,1} - T_{c,2}$

4 CONCLUSIONS

Pressure-temperature relations of high-pressure phase boundaries were experimentally determined for 16 binary mixtures, which were composed of indole, quinoxaline, pyrazine, and pyrimidine as the solute and CO_2, C_2H_4, C_2H_6, and CHF_3 as the solvent. The phase boundaries were determined by straightforward visual observation through the windows of the high-pressure view cell. The observed phase boundaries included the critical lines (L_1=L_2, L=G), the three-phase equilibrium lines (S_1-L_1-L_2, S_1-L-G, L_1-L_2-G), the critical end points (S_1-L=G, L_1-L_2=G, L_1=L_2-G), and the quadruple points (S_1-S_2-L-G, S_1-L_1-L_2-G).

The systems were grouped into four different types of pressure-temperature diagram. The transitional patterns of pressure-temperature diagram were briefly discussed in terms of the characteristic interactions and the magnitude of size-asymmetry between unlike molecules.

Based on the knowledge of the phase borders obtained in the present study, we can easily acquire, although qualitatively, the phase equilibrium state maintained at an arbitrary pressure and temperature. For example, some schematic pressure-composition isotherms can be drawn according to the pressure-temperature relations of the phase boundaries. This overall information about the phase boundaries is, therefore, quite important in understanding high-pressure phase behavior.

5 REFERENCES

Cheong, P. L., Zhang, D., Ohgaki, K., and Lu, B. C.-Y., 1986. High pressure phase equilibria for binary systems involving a solid phase. Fluid Phase Equilibria, 29: 555-562.

Luks, K. D., 1986. The occurrence and measurement of multiphase equilibria behavior. Fluid Phase Equilibria, 29: 209-224.

McHugh, M. A., Seckner, A. J., and Yogan, T. J., 1984. High-pressure phase behavior of binary mixtures of octacosane and carbon dioxide. Ind. Eng. Chem. Fundam., 23: 493-499.

Yamamoto, S., Ohgaki, K., and Katayama, T., 1989. Phase behavior of binary mixtures of indole or quinoxaline with CO_2, C_2H_4, C_2H_6, and CHF_3 in the critical region. J. Supercrit. Fluids, 2: 63-72.

Yamamoto, S., 1990. High-pressure phase equilibria for binary mixtures of supercritical fluids and solids. Doctoral dissertation, Osaka University.

Yamamoto, S., Ohgaki, K., and Katayama, T., 1990. High-pressure phase behavior of eight binary mixtures of pyrimidine or pyrazine with CO_2, C_2H_4, C_2H_6, or CHF_3. J. Chem. Eng. Data, 35: 310-314.

Solvent Extraction 1990, T. Sekine (Editor)

© 1992 Elsevier Science Publishers B.V. All rights reserved

CORRELATION OF SOLUBILITIES OF COAL LIQUEFACTION PRODUCTS IN SUPERCRITICAL CARBON DIOXIDE AND SOLUBILITY ENHANCEMENTS USING EQUATION OF STATE

YOSHIO IWAI, HIROSHI YAMAMOTO*, TAKASHI SHIMIZU, AND YASUHIKO ARAI
Dept. of Chem. Eng., Kyushu Univ., Fukuoka 812, Japan
*Nippon Zeon Co., Ltd., Kawasaki 210, Japan

ABSTRACT
Iwai,Y., Yamamoto,H., Shimizu,T. and Arai,Y., 1990. Correlation of solubilities of coal liquefaction products in supercritical carbon dioxide and solubility enhancements using equation of state.

The solubility behavior in the supercritical region is essentially important in process design of supercritical fluid extraction. An entrainer is often used to enhance the solubilities of high boiling components in the gas phase. The cubic equation of state having three constants, recently proposed by Yu et al., was applied to correlate the solubilities of coal liquefaction products (solid components) in supercritical CO_2 and the solubility enhancements by entrainers. Conventional mixing rules were adopted for calculation of cross factors a_{ij}, b_{ij}, and c_{ij}. Binary parameters k_{ij} for calculation of a_{ij}, and l_{ij} for b_{ij} and c_{ij} were used. The binary parameters k_{ij} and l_{ij} (i.e. cross factors a_{ij}, b_{ij}, and c_{ij}) were determined to represent well the solubility data. Further, they were correlated with pure component properties of supercritical CO_2 and solid components such as critical volume, solid volume, number of atoms in molecule except for hydrogen, and solubility parameter. By using the empirical equations for calculation of the binary parameters k_{ij} and l_{ij}, the solubilities of solid components in supercritical CO_2 were calculated with good accuracy.

INTRODUCTION

Separation methods for coal liquefaction products have received considerable attention recently for use as the raw materials of fine chemicals. The supercritical fluid extraction is showing promise as a separation method. Correlation methods for solubilities are important in the design of a supercritical extraction process. In the present work, the cubic equation of state proposed by Yu et al. (1987a,b) was applied to correlate the solubilities of coal liquefaction products (solid components) in supercritical carbon dioxide and solubility enhancements by entrainers. The parameters of the equation of state were correlated using pure component properties. The solubilities of solid components can be calculated with good accuracy by using the generalized parameters.

2.EQUATION OF STATE

The solubilities of solid component in supercritical gas, y_i, can be

calculated by the following equation.

$$y_i = \frac{p_i^{sat}}{p} \cdot \frac{1}{\phi_i^G} \exp\left\{\frac{v_i^S(p-p_i^{sat})}{RT}\right\} \quad (1)$$

where p is the pressure, T is the temperature, p_i^{sat} and v_i^S are the saturation vapor pressure and solid-state molar volume of solid, respectively, and ϕ_i^G is the fugacity coefficient of solid component in supercritical gas. To evaluate ϕ_i^G, the following cubic equation of state proposed by Yu et al. (1987a,b) was adopted.

$$p = \frac{RT}{v-b} - \frac{a}{v(v+c)+b(3v+c)} \quad (2)$$

where a, b, and c are pure component parameters that can be calculated by using the values of critical pressure p_C, critical temperature T_C, and the Pitzer's acentric factor ω. They are shown in the previous paper(Arai et al., 1990). To apply eqn.(2), the following mixing rules for constants a, b, and c were used.

$$a=\Sigma\Sigma\, y_i y_j a_{ij},\quad a_{ij}=(1-k_{ij})(a_i a_j)^{0.5} \quad (3)$$

$$b=\Sigma\Sigma\, y_i y_j b_{ij},\quad b_{ij}=(1-l_{ij})(b_i+b_j)/2 \quad (4)$$

$$c=\Sigma\Sigma\, y_i y_j c_{ij},\quad c_{ij}=(1-l_{ij})(c_i+c_j)/2 \quad (5)$$

where k_{ij} and l_{ij} denote the characteristic parameters between unlike molecule i and j. When eqns.(2)-(5) are utilized, the fugacity coefficient ϕ_i^G can be thermodynamically derived. As discussed previously(Iwai et al., 1989),

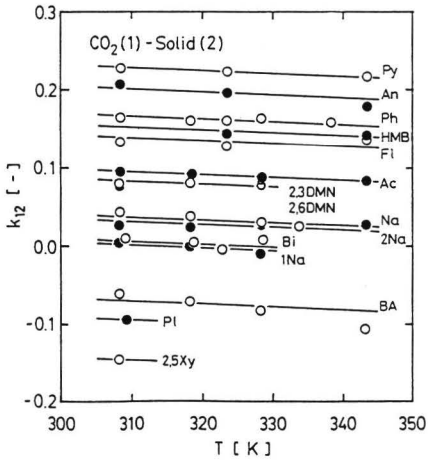

Fig.1. Temperature dependence of k_{12}. (Abbreviations are identical in Table 1)

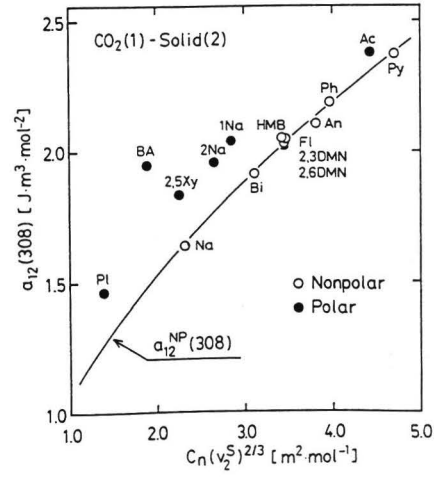

Fig.2. Correlation of $a_{12}(308)$. (Abbreviations are identical in Table 1)

the conventional mixing rules with k_{ij} and l_{ij} introduced into both attraction and size terms give good correlation.

3.CORRELATION OF BINARY SYSTEMS

The binary parameters k_{12} and l_{12} (i.e., cross parameters a_{12}, b_{12}, and c_{12}) were calculated to give good representation of the data of solubilities of solid components(2) in supercritical CO_2(1). Then, they were correlated with pure component properties. The parameter b_{12} can be correlated by the next equation.

$$b_{12} = 3.097\times10^{-5}+4.388\times10^{-5}(v_2^S/v_{C,1}) \quad (6)$$

where $v_{C,1}$ is the critical molar volume of CO_2. The binary parameter l_{12} can be calculated from eqns. (4) and (6). It was assumed that l_{12} was independent of temperature.

As shown in Fig.1, the slope of k_{12} is approximately -3.656×10^{-4} for all systems. The parameter a_{12} at 308 K, $a_{12}(308)$, can be correlated by the next equation.

$$a_{12}(308)= a_{12}^{NP}(308) + a_{12}^{PH}(308) \quad (7)$$

where $a_{12}^{NP}(308)$ is the contribution of dispersion forces and $a_{12}^{PH}(308)$ is the

TABLE 1

Prediction performance for solubilities of solids in supercritical CO_2

Solid(2)	(Abbreviation)	T(K)	N*	Dev(%)**	Ref.
Acridine	(Ac)	308-343	46	16.37	4,15
Anthracene	(An)	308-343	30	51.47	2,7,9
Benzoic acid	(BA)	308-343	55	14.94	4,10,15
Biphenyl	(Bi)	309-328	39	28.18	12
2,3-Dimethyl-naphthalene	(2,3DMN)	308-328	20	14.68	10,13
2,6-Dimethyl-naphthalene	(2,6DMN)	308-328	15	8.11	10
Fluorene	(Fl)	308,323	23	19.06	7
Hexamethylbenzene	(HMB)	323,343	20	26.14	7
Naphthalene	(Na)	308-334	108	17.59	12,17
1-Naphthol	(1Na)	308-328	18	18.20	16
2-Naphthol	(2Na)	308-343	48	26.14	4,15,16
Phenanthrene	(Ph)	308-338	28	17.88	3,7,10
Phenol	(Pl)	309	25	56.82	18
Pyrene	(Py)	308-343	22	17.22	7
2,5-Xylenol	(2,5Xy)	308	8	9.84	6

* Number of data

** $(100/N)(\Sigma|y_2(calc)-y_2(exp)|/y_2(exp))$

contribution of polar and hydrogen bonding forces. As shown in Fig.2, using results of nonpolar systems, $a_{12}^{NP}(308)$ can be correlated by

$$a_{12}^{NP}(308) = 1.0659\ (C_n\ (v_2^S)^{2/3})^{0.5184} \tag{8}$$

where C_n is the number of atoms except for hydrogen in solid molecule. Then, $a_{12}^{PH}(308)$, that is $a_{12}(308)-a_{12}^{NP}(308)$, can be correlated by

$$a_{12}^{PH}(308) = 3.0712\times10^{-2}\ (\delta_2^{PH}\ v'^S_2)^{3.7645} \tag{9}$$

where δ_2^{PH} is the contribution of polar and hydrogen bonding forces to the solubility parameter calculated by the van Krevelen's method(1976) and $v'^S=v^S$ except for benzoic acid ($v'^S=2v^S$ for benzoic acid). For binary system, a_{12} can be calculated by eqns.(3), (7), (8), (9) and the temperature dependence of k_{12}. The pure component properties in eqns.(6)-(9) are listed in the previous paper(Arai et al., 1990). The calculation results of the solubilities of solid components in supercritical CO_2 are good as shown in Fig. 3 and Table 1.

4. PREDICTION OF MIXED SOLIDS SYSTEMS

To predict the system CO_2(1)-solid component(2)-solid component(3), the parameters k_{23} and l_{23} were set to zero and a_{12}, b_{12}, c_{12}, a_{13}, b_{13}, and c_{13} were calculated by the method shown above. The calculation results are shown in Fig.4 and Table 2.

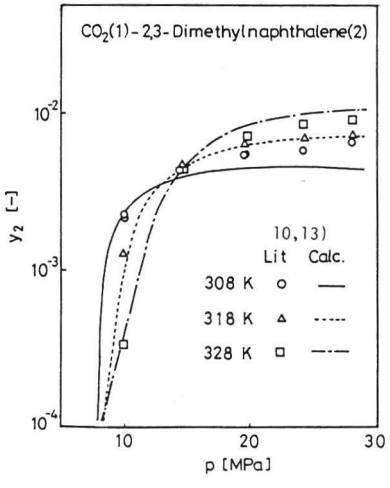

Fig.3. Solubilities of 2,3-Dimethylnaphthalene in supercritical CO_2.

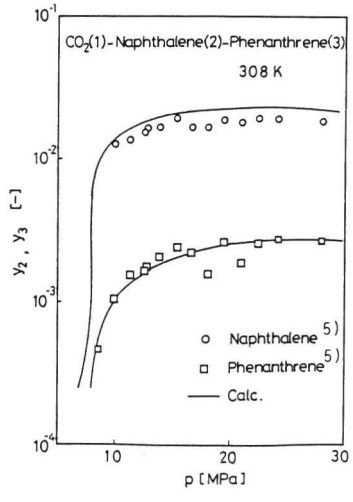

Fig.4. Solubilities of mixed solids in supercritical CO_2.

5. ENTRAINER EFFECT

The parameters $a_{23}(308)$ for the systems of CO_2(1)-solid component(2)-entrainer(3) can be correlated by the following equation.

$$a_{23}(308) = 0.63715(v_2^S v_3^L \delta_2 \delta_3)^{1.2358} + 1.718 (v'^S_2 v_3^L \delta_2^{PH} \delta_3^{PH})^{0.5826} \quad (10)$$

where v_3^L is the molar volume of entrainer in liquid state. The calculation results of solubility enhancements by entrainers are shown in Fig.5 and Table 3. In the calculations the parameters k_{13} and l_{13} were determined to give good representation of vapor-liquid equilibria for the system of CO_2(1)-entrainer(3). They are listed in Table 4. The parameter l_{23} are assumed to be zero. As shown in Fig.5 and Table 3, the calculation results are good.

6.CONCLUSIONS

The binary parameters contained in the equation of state proposed by Yu et al. were generalized by pure component properties. By using the parameters, the solubilities of coal liquefaction products in supercritical CO_2 can be calculated well. Furthermore, the solubility enhancements by entrainers can be correlated with good accuracy.

ACKNOWLEDGMENT

We gratefully acknowledge the financial support provided by Toray Science Foundation.

TABLE 2

Prediction performance for solubilities of mixed solids in supercritical CO_2

Mixed solids	T(K)	N	Dev(%)*	Ref.
An-2Na	308	6	41.54	2
BA-HMB	308	6	20.86	2
BA-Ph	308	5	15.78	11
2,3DMN-2,6DMN	308	9	8.56	11
	318	9	6.10	11
2,3DMN-Na	308	5	14.62	11
2,3DMN-Ph	308	5	15.55	11
	318	5	31.10	11
2,6DMN-Ph	308	5	13.87	11
Na-Ph	308	23	15.69	5,11
Na-Pl	308	11	32.84	5

*$\{(100/N)(\Sigma|y_2(calc)-y_2(exp)|/y_2(exp)) + (100/N)(\Sigma|y_3^2(calc)-y_3^2(exp)|/y_3^2(exp))\}/2$

Abbreviations are identical in Table 1

TABLE 3

Prediction performance of solubility enhancements by entrainers at 308 K

Solid(2) -Entrainer(3)	N	Dev(%)	Ref.
Ac-Acetone	7	8.91	4
-Methanol	8	14.56	4
An-Methanol	5	46.40	2
BA-Acetone	7	27.67	4
-Methanol	10	3.03	4
-Octane	5	30.42	4
HMB-Acetone	10	42.83	4
-Methanol	5	37.18	4
-Octane	6	26.25	3
-Pentane	6	38.44	3
-Undecane	4	30.99	3
2Na-Methanol	17	36.01	2,4
Ph-Octane	18	6.80	3
-Pentane	6	6.51	3
-Undecane	4	2.93	3

TABLE 4

Binary parameters for CO_2(1)-Entrainer(3) systems at 308 K

Entrainer	k_{13}	l_{13}	Ref.
Acetone	0.013	-0.018	8
Methanol	0.088	0.101	14
Octane	0.114	0.000	19
Pentane	0.139	0.077	1
Undecane	0.000	0.000	-

UNITS OF PARAMETERS

$a(J \cdot m^3 \cdot mol^{-2})$, $b,c(m^3 \cdot mol^{-1})$, $v(m^3 \cdot mol^{-1})$, $\delta(J^{0.5} \cdot m^{-1.5})$

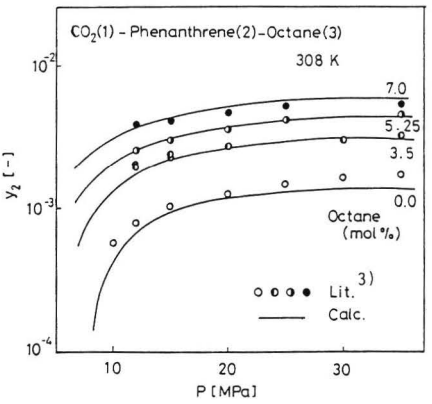

Fig.5. Solubility enhancements by entrainer.

REFERENCES

Arai,Y., Iwai,Y., Shimizu,T. and Fukuda,T., 1990. Vapor Pressures and Critical Properties of Coal-Derived Components. J. Fuel Soc. Japan, 69: 281-286.

Iwai,Y., Lu,B.C.-Y., Yamamoto,H. and Arai,Y., 1989. Correlation of Solubilities in Supercritical Fluids and Entrainer Effect Using Equation of State - Examination of Mixing Rules -. Kagaku Kogaku Ronbunshu, 15: 676-681.

van Krevelen,D.W., 1976. Properties of Polymers. Elsevier.

Yu,J.M. and Lu,B.C.-Y., 1987a. A Three-Parameter Cubic Equation of State for Asymmetric Mixture Density Calculation. Fluid Phase Equil., 34:1-19.

Yu,J.M., Lu,B.C.-Y. and Iwai,Y., 1987b. Simultaneous Calculations of VLE and Saturated Liquid and Vapor Volumes By Means of a 3P1T Cubic EOS. Fluid Phase Equil., 37:207-222

Data Sources

1. Besserer,G.J. and Robinson,D.B.,1973. J.Chem.Eng.Data,18:416
2. Dobbs,J.M. and Johnston,K.P.,1987. Ind.Eng.Chem.Res.,26:1476
3. Dobbs,J.M., Wong,J.M. and Johnston,K.P.,1986. J.Chem.Eng.Data,31:303
4. Dobbs,J.M., Wong,J.M., Lahiere,R.J. and Johnston,K.P.,1987. Ind.Eng.Chem.Res.,26:56
5. Gopal,J.S., Holder,G.D. and Kosal,E.,1985. Ind.Eng.Chem.Proc.Des.Dev.,24:697
6. Iwai,Y.,Yamamoto,H., Tanaka,Y. and Arai,Y.,1990. J.Chem.Eng.Data,35:174
7. Johnston,K.P., Ziger,D.H. and Eckert,C.A.,1982. Ind.Eng.Chem.Fund.,21:191
8. Katayama,T.,Ohgaki,K.,Maekawa,G.,Goto,M. and Nagano,T.,1975. J.Chem.Eng.Japan,8:89
9. Kosal,E. and Holder,G.D.,1987. J.Chem.Eng.Data,32:148
10. Kurnik,R.T., Holla,S.J. and Reid,R.C.,1981. J.Chem.Eng.Data,26:47
11. Kurnik,R.T. and Reid,R.C.,1982. Fluid Phase Equil.,8:93
12. McHugh,M.A. and Paulaitis,M.E.,1980. J.Chem.Eng.Data,25:326
13. Moradinia,I. and Teja,A.S.,1986. Fluid Phase Equil.,28:199
14. Ohgaki,K. and Katayama,T.,1976. J.Chem.Eng.Data,21:53
15. Schmitt,W.J. and Reid,R.C.,1986. J.Chem.Eng.Data,31:204
16. Tan,C.-S. and Weng,J.-Y.,1987. Fluid Phase Equil.,34:37
17. Tsekhanskaya,Yu.V., Iomtev,M.B. and Mushkina,E.V.,1964. Russ.J.Phys.Chem.,38:1173
18. van Leer,R.A. and Paulaitis,M.E.,1980. J.Chem.Eng.Data,25:257
19. Whiting,W.B. and Prausnitz,J.M.,1982. Fluid Phase Equil.,9:119

Solvent Extraction 1990, T. Sekine (Editor)

© 1992 Elsevier Science Publishers B.V. All rights reserved

Supercritical Extraction of Alcohol form Aqueous Solution Using Only Carbon Dioxide

Tatsuru Suzuki, Naoki Tsuge and Kunio Nagahama
Dept. of Ind. Chem., Tokyo Metropolitan University
Fukasawa 2-1-1, Setagaya-ku, Tokyo 158, Japan

ABSTRACT

Using a newly developed flow-type apparatus for supercritical fluid extraction (SFE), vapor-liquid equilibrium (VLE) data for the CO_2 - alcohol - water system were measured at 313K and 333K under 10MPa. Ethanol or 2-propanol was selected as an alcohol. Measurements were made with emphasis on solubility of alcohol and water in CO_2 rich-phase at fixed aqueous liquid compositions on CO_2 free basis.

As a result of the VLE measurements, it was found that the azeotropes of both alcohol aqueous solutions were broken at 333K and 10MPa. It suggests dehydrated ethanol and 2-propanol are able to be obtained from aqueous mixtures using a conventional multicontacting column with CO_2-SFE alone.

1. Introduction

Supercritical fluid extraction has been expected as a new energy saving process for the dehydration of alcohol. In the last decade, phase equilibrium data for the CO_2 - alcohol (particularly ethanol) - water systems have been measured by several workers [Paulaitis et al. (1981), Kuk et al. (1983), Gilbert et al. (1986), Nagahama et al. (1988), DiAndreth et al. (1989), Furuta et al. (1989), Inomata et al. (1989, 1990) and de la Ossa et al. (1990)]. Recently, Furuta et al. (1989) suggested in terms of phase equilibrium data that suitable operation condition for the dehydration of ethanol in aqueous solution using supercritical CO_2 was 333K and 10MPa.

In this work, a flow-type apparatus for SFE has been newly developed, and VLE data for the CO_2 - alcohol - water systems have been measured at 313K and 333K under 10MPa. Either ethanol or 2-propanol was selected as an alcohol. Obtained data were compared with literature data. Possibility of the dehydration of aqueous alcohol solution using CO_2-SFE alone was confirmed for ethanol and 2-propanol systems.

2. Experimental

2.1 *Apparatus*

A schematic diagram of the experimental apparatus is shown in Figure 1. The apparatus is the same as that used for the measurement of solubilities of alcohol in supercritical CO_2 [Suzuki et al. (1990)].

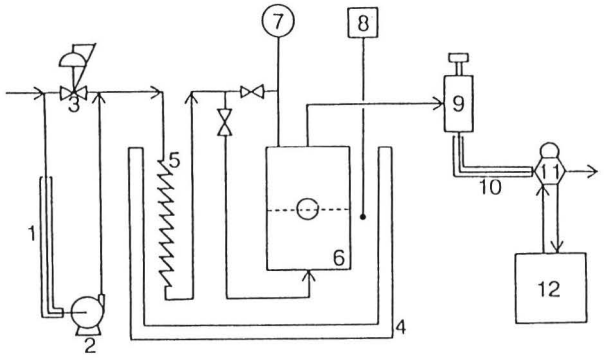

Figure 1 Schematic Diagram of the Experimental Apparatus

2.2 *Procedure*

Alcohol + water liquid mixture of known composition was fed into a high pressure cell, and the air in it was replaced by CO_2 gas. The cell was immersed in a constant temperature water bath controlled to be ±0.05K. CO_2 was charged into the cell up to the desired pressure using a cooler, a high pressure pump, a back pressure regulator and a pre-heating coil. After attainment of equilibrium, vapor mixture sample under high pressure was flashed through a heated metering valve and a heated tube, and low pressure sample was directly introduced to a gas chromatograph (GC) for vapor composition (y) analysis with a heated 6-way valve. System temperature and pressure were measured using a calibrated quartz thermometer and a calibrated digital pressure gauge, and their accuracies of the measurements were less than ±0.01K and ±0.01MPa, respectively.

The flow rate of the flashed vapor sample was about 7 cm^3/min. After these operations, a part of liquid sample left in the cell was taken out and its composition was analyzed by GC. Then liquid composition on CO_2 free basis (X) was determined as the average of compositions before and after measurements, although differences between them were very small. Accuracies of the composition analysis for vapor and liquid in mole fraction were less than ±0.0002 and ±0.001, respectively.

3. Results and Discussion

3.1 *CO_2 - ethanol - water system*

Vapor composition diagrams of the CO_2 - ethanol - water system at 313K and 333K under 10MPa are shown in Figures 2 and 3, also XY diagrams for the ethanol - water mixture on CO_2 free basis are given in Figures 4 and 5, respectively. The obtained experimental data are listed in Table 1. Several published ternary data and also binary data for CO2 - water [Wiebe.

TABLE 1

Experimental data for the CO_2(1) - alcohol(2) - water(3) system

X_2	X_3	y_1	y_2	y_3
CO_2 - ethanol - water system at 313.5K and 10.1MPa				
0.048	0.952	0.9845	0.0105	0.0050
0.138	0.862	0.9624	0.0293	0.0083
0.180	0.820	0.9650	0.0262	0.0087
0.281	0.719	0.9457	0.0427	0.0116
0.347	0.653	0.9288	0.0575	0.0137
0.445	0.555	0.9145	0.0672	0.0183
0.554	0.446	0.8708	0.0981	0.0311
CO_2 - ethanol - water system at 333.6K and 10.1MPa				
0.046	0.954	0.9859	0.0083	0.0058
0.099	0.901	0.9803	0.0135	0.0062
0.190	0.810	0.9773	0.0162	0.0055
0.382	0.618	0.9721	0.0223	0.0056
0.571	0.429	0.9680	0.0263	0.0057
0.796	0.204	0.9609	0.0353	0.0038
0.895	0.105	0.9552	0.0432	0.0016
CO_2 - 2-propanol - water system at 333.7K and 10.1MPa				
0.047	0.953	0.9740	0.0175	0.0085
0.096	0.904	0.9605	0.0293	0.0102
0.321	0.679	0.9572	0.0325	0.0103
0.481	0.519	0.9524	0.0387	0.0089
0.673	0.327	0.9503	0.0417	0.0080
0.776	0.224	0.9473	0.0455	0.0072
0.915	0.085	0.9455	0.0516	0.0028

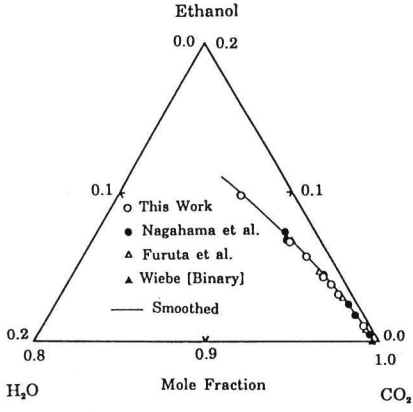

Figure 2 Ternary VLE for the CO_2 - Ethanol - Water system at 313.5K and 10.1MPa (Vapor Phase)

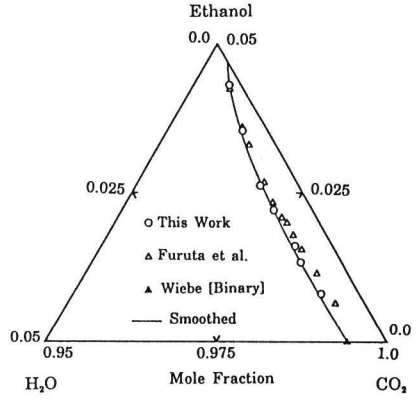

Figure 3 Ternary VLE for the CO_2 - Ethanol - Water system at 333.6K and 10.1MPa (Vapor Phase)

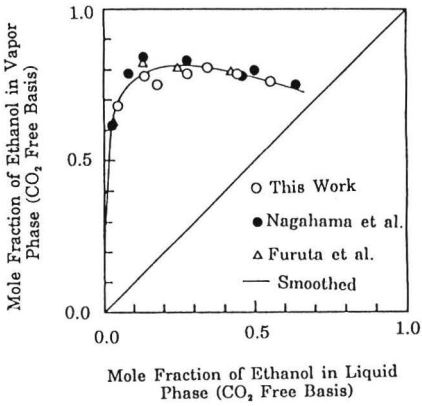

Figure 4 VLE Composition diagram for the CO_2 - Ethanol - Water System (313.5K-10.1MPa)

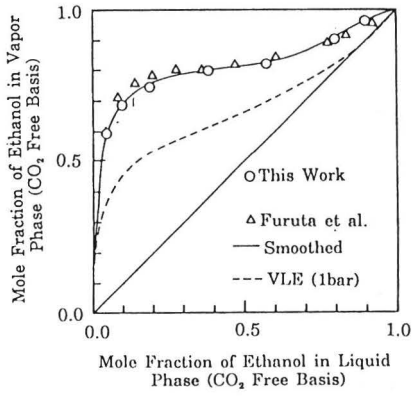

Figure 5 VLE Composition diagram for the CO_2 - Ethanol - Water System (333.6K-10.1MPa)

(1941)] at 313K were compared, and agreement with these data is very good for the vapor composition (Figures 2 and 3). Taking vary small solubility of ethanol and water in the vapor phase into account, XY diagram (Figure 4) also shows good agreement.

Figure 6 shows solvent selectivity for ethanol to water and solubility of ethanol in the CO_2 rich phase. Where they are defined as:

$$\text{selectivity} = (Y_2 / X_2) / (Y_3 / X_3) \quad (1)$$

$$\text{solubility in vapor} = \text{Alcohol (g)} / CO_2\ (100\text{g}) \quad (2)$$

To concentrate dilute aqueous ethanol mixture, lower temperature SFE is recommended because both selectivity and solubility are larger than those of higher temperature. But increasing X_2, selectivity at lower temperature goes smaller than that at higher temperature, and ends at the plait point (X=Y). The existence of the plait point makes impossible to dehydrate ethanol further. For complete dehydration of alcohol, it is necessary that there may be at least no plait point for the ternary system at the condition of interest. At 333K and 10MPa, there is 2-phase region for the CO_2 - ethanol binary system (Figure 3). It results in no plait point for the ternary system and gives XY diagram which shows possibility of complete

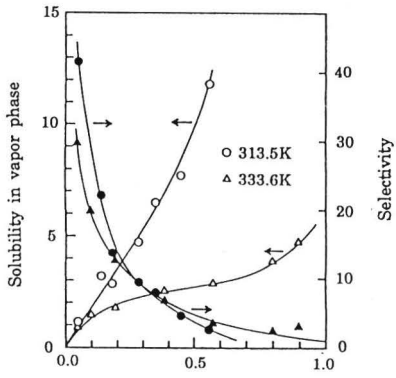

Figure 6 Solubility and Selectitity of Ethanol for the CO_2 - Ethanol - Water System under 10.1MPa

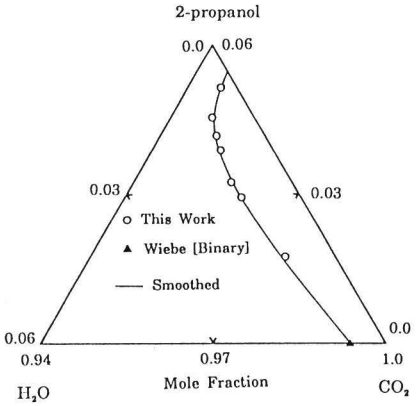

Figure 7 Ternary VLE for the CO_2 - 2-propanol - Water system at 333.7K and 10.1MPa (Vapor Phase)

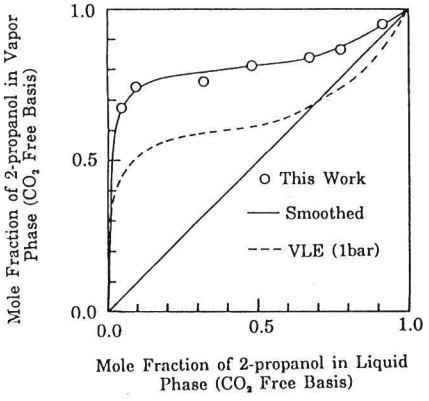

Figure 8 VLE Composition diagram for the CO_2 - 2-propanol - Water System (333.7K-10.1MPa)

dehydration of aqueous ethanol mixture (Figure 5), as was reported by Furuta et al. (1989).

3.2 *CO_2 - 2-propanol - water system*

For the CO_2 - 2-propanol - water system at 333K under 10MPa, vapor composition diagram and XY diagram are shown in Figures 7 and 8. Experimental values are listed in Table 1. Because of the complicated phase behavior around 313K and 10MPa [DiAndreth et al. (1989)], the VLE measurement was too difficult to get reliable data using our simple flow technique. Figure 9 shows solvent selectivity for 2-propanol to water and solubility of 2-propanol in the CO_2 rich phase. They exhibit similar behavior to the ethanol system at 333K and 10MPa. At atmospheric pressure, the azeotropic composition for the 2-propanol - water binary system exists at water richer end than that for the ethanol -water binary system, therefore, it is more difficult to dehydrate 2-propanol aqueous solution than ethanol one using distillation. Nevertheless, it is also possible to dehydrate 2-propanol completely using supercritical CO_2 only at 333K and 10MPa. This observation has not been reported in previous paper.

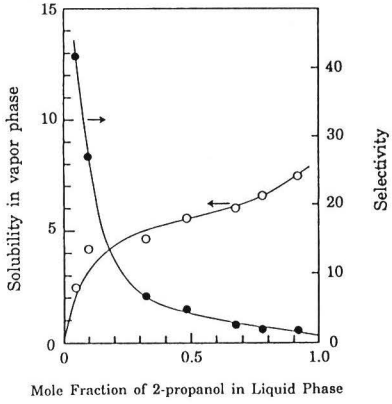

Figure 9 Solubility and Selectitity of 2-propanol for the CO_2 - 2-propanol - Water System at 333.7K and 10.1MPa

5. Conclusion

The flow-type of apparatus for SFE has been newly developed and VLE for the CO2 - alcohol (ethanol or 2-propanol) - water ternary systems were measured at 313K and 333K under 10MPa.

The experimental method is very simple and useful to determine the optimum condition of supercritical fluid extraction with high accuracy.

It was found that the complete dehydration of ethanol or 2-propanol aqueous solution was possible using CO_2 alone at 333K and 10MPa, where no ternary plait point exists.

6 Nomenclature

X : mole fraction of liquid phase on CO_2 free basis
y : mole fraction of vapor phase
Y : mole fraction of vapor phase on CO_2 free basis

subscripts

1 : CO_2
2 : alcohol (ethanol or 2-propanol)
3 : water

7 References

de la Ossa, E.M., Brandani, V., Del Re, G., Di Giacomo, G. and Ferri, E., 1990. *Fluid Phase Equilibria*, 56, 325-340

Diandreth, J.R. and Paulaitis, M.E., *Chem. Eng. Sci.* 1989, 44(5), 1061-1069

Furuta, S., Ikawa, N., Fukuzato, R. and Imanishi N., 1989. *Kagaku Kougaku Ronbunshu*,15(3), 519-525 ; 1990. *Private Communication*

Gilbert, M.L. and Paulaitis, M.E., 1986. *J. Chem. Eng. Data*, 31, 296-298

Inomata, H., Arai, K., Saito, S., Ohba, S. and Takeuchi, K., 1989. *Fluid Phase Equilibria*, 53, 23-30

Inomata, H., Kondo, A., Arai, K. and Saito, S., 1990. *J. Chem. Eng. Japan*, 23(2), 199-207

Kuk, M.S. and Montagna, J.C., 1983. In: *Chemical Engineering at Supercritical Fluid Conditions*, 101-111, Paulaitis M. E. et al. (eds.), Ann Arbor Science, USA

Nagahama, K., Suzuki, J. and Suzuki, T., 1988. *Proc. Int. Symp. on Supercritical Fluids*,Vol.1, 143-150, october 17-19, Nice, France.

Paulaitis, M.E., Gilbert,M.L. and Nash, C.A., 1981. *2nd World Congress of Chem. Eng.*, Montreal, Canada

Suzuki, T., Tsuge, N. and Nagahama, K., 1990. *To be published*

Takishima, S., Saiki K., Arai, K. and Saito, S., 1986. *J. Chem. Eng. Japan*, 19(1), 48-56

Wiebe, R., 1941. *Chem. Rev. 29, 475-481*

Solvent Extraction 1990, T. Sekine (Editor)

© 1992 Elsevier Science Publishers B.V. All rights reserved

SEPARATION OF POLYUNSATURATED FATTY ACID FROM VEGETABLE OIL BY SUPERCRITICAL FLUID EXTRACTION AND CHROMATOGRAPHY

NOBORU IKAWA, SATOSHI FURUTA, RYUICHI FUKUZATO, NOBUYUKI IMANISHI
CHEMICAL TECHNOLOGY RESEARCH LABORATORY, KOBE STEEL, LTD., 3-18, WAKINOHAMA-CHO 1-CHOME, CHUO-KU, KOBE (JAPAN)
HIDEAKI KAWANA, MASATA MITSUIKI, HIROHISA SUZUKI
CENTRAL RESEARCH LABORATORIES, AJINOMOTO CO., INC., 1-1, SUZUKI-CHO, KAWASAKI-KU, KAWASAKI (JAPAN)

ABSTRACT

A new separation method based on supercritical fluid extraction (SFE) and chromatography (SFC) is being developed for separation and enrichment of triglycerides, which consist of polyunsaturated fatty acids from vegetable oil. Supercritical carbon dioxide is used as a solvent for extraction and/or the mobile phase for chromatography. The solubility of perilla oil is measured at 313K and at pressures from 20 to 40MPa. The effects of the pressure and linear velocity are discussed for the height equivalent to a theoretical plate (HETP) and the loading capacity for supercritical fluid chromatography.

1 INTRODUCTION

The use of supercritical fluid as the solvent for the extraction and/or separation process has recently become a reality in the food, flavor and pharmaceutical industries, since carbon dioxide, as a supercritical fluid, has advantages such as its non-toxicity, low cost , lack of reactivity and its ability to be completely removed from the product.

According to recent studies in the food industry, on the other hand, the oil balance of polyunsaturated fatty acid's n-3/n-6 ratio in food affects people's health. The shift of the oil balance to the n-6 side, with the changing of the majority of people's diet from fish to meat in Japan and especially in Europe and America, increases the incidence of such diseases as allergies, myocardial infarction, hypertension and thrombosis. Therefore, to produce healthful food containing these n-3 polyunsaturated fatty acid such as α-linolenic acid, eicosapentaenoic acid and docosahexaenoic acid which are mainly contained in fish and vegetable seeds, the separation or purification of these acids is getting important.

For the above reasons, we pay particular attention to α-linolenic acid which is considered to have affects on preventing or curing the diseases caused by an excess intake of n-6 polyunsaturated fatty acid. Polyunsaturated fatty acid is regarded as unstable and difficult to be separated with simple SFE only due to

the difference in the total numbers of double bonds of triglycerides. Therefore, the purpose of this study is to propose a safe and economical separation process by using the combined SFE and SFC system, which are explained by McHugh(1986) and Smith(1988), respectively. In this paper, we will discuss the basic characteristics of SFE and SFC for the separation of polyunsaturated fatty acid.

2 EXPERIMENTAL

2.1 Material

In this study, perilla oil is selected as the raw material. Its triglyceride composition which was measured by HPLC with a UV detector (wave length: 220nm) is shown in Table 1. The triglyceride which contains three linolenic acids is called "trilinolenin" (LnLnLn), and the triglyceride which contains two linolenic acids and one linoleic acid is called "dilinolenil monolinoleil glyceride" (LnLnL). The purpose of this study is to investigate the process of separating trilinolenin from other triglycerides.

TABLE 1

Triglyceride composition of Perilla oil(area%)

LnLnLn	LnLnL	LnLL	LnLnO	LnLO	others
31.9	14.9	18.5	9.5	5.5	19.7

Ln:linolenic acid L:linoleic acid O:oleic acid

2.2 Apparatus

As mentioned before, though we will finally construct the combination system of SFE and SFC for separation of trilinolenin, in this paper SFE and SFC are studied separately.

(i) Supercritical fluid extraction. Fig.1 shows a schematic diagram of the SFE apparatus. The major components of this apparatus are a CO_2 pump, an entrainer pump, one extractor and two separators. The entrainer pump allows addition of water or ethanol as an entrainer into CO_2. The extractor and two separators are connected directly in order to operate a continuous extraction and a two stage separation process under high pressure. The control systems of temperature and pressure for each vessel are separated, and, moreover, the same extract can be sampled individually by using the line connected with the metering valve 10. The solubility of perilla oil in CO_2 is calculated from a weight of oil in the receiver and a gas volume of CO_2.

(ii) Supercritical fluid chromatography. Fig. 2 shows a schematic diagram of the SFC used in this study. It contains a CO_2 pump, entrainer pump, injector, packed column, UV detector and back-pressure regulator. The operating pressure is controlled by the back-pressure regulator, and the flow rate is controlled by the pumps. The sample, a 10% perilla oil and 90% acetone solution, is loaded with the injector, and the separation pattern is observed by the UV detector. The packed column is 4.6mm i.d. X 250mm length packed with 5μm Superpak SIL-C18 produced by JASCO in Japan.

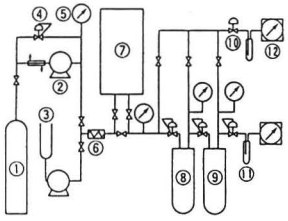

1 CO_2 cylinder
2 Liquid pump
3 Liquid tank
4 Pressure regulator
5 Pressure gauge
6 Static mixer
7 Extraction vessel
8 Separator-1
9 Separator-2
10 Metering valve
11 Receiver
12 Flow meter

Fig.1 Schematic diagram of supercritical fluid extraction apparatus.

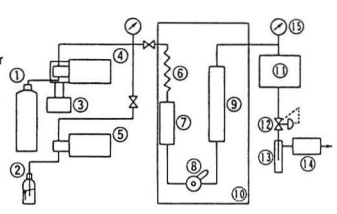

1 CO_2 cylinder
2 Liquid tank
3 Cooling unit
4 CO_2 pump
5 Liquid pump
6 Preheater
7 Mixer
8 Injector
9 Packed column
10 Air bath
11 UV detector
12 Pressure regulator
13 Receiver
14 Flow meter
15 Pressure gauge

Fig.2 Schematic diagram of supercritical fluid chromatography apparatus.

3 RESULT AND DISCUSSION

3.1 Supercritical fluid extraction

Solubility of perilla oil in CO_2 is shown in Fig. 3. The solubility increases with pressures at a constant temperature of 313K, which is similar to the data for soybean oil shown by Stahl(1984), and the value is changed by about two orders under the pressure ranges from 10MPa to 40MPa. When changing the separation pressure and/or temperature, it seems that the selectivity of the extracted oil in CO_2 changes drastically. Table 2 shows the result of extraction and a two stage saparation under high pressure. The solubility was controlled by temperature change at the first separator and by pressure change at the second separator. The composition of triglyceride does not change remarkably at both stages. However, the composition of lipids, especially diglyceride, is concentrated in separator 2. According to these results, triglyceride of perilla oil can be purified, but it seems difficult to separate each triglyceride with respect to the number of double bonds.

3.2 Supercritical fluid chromatography

Fig. 4 shows the chromatogram of the perilla oil obtained by supercritical fluid chromatography. In this chromatogram, trilinolenin was identified with a

peak number 1 by comparing the retention time of the standard reagent, and a

TABLE 2

Extract composition of perilla oil

	Lipid(area%)			Triglyceride(area%)			
	Trigly.	Digly.	others	LnLnLn	LnLnL	LnLL	others
perilla oil (raw material)	96.2	2.6	1.2	31.9	14.9	18.5	34.7
separator 1 (extract)	96.4	2.1	1.5	31.2	15.2	18.5	35.1
separator 2 (extract)	91.5	7.6	0.9	31.8	14.8	18.1	35.3

Extracted at 313K, 40MPa. Separated at 353K,40MPa and 313K,8MPa
Total extraction yield is 46% of perilla oil.

peak number 2 is corresponding to dilinolenil monolinoleil glyceride by its retention time and peak shape. The trilinolenin is completely separated from other components with respect the number of double bonds.

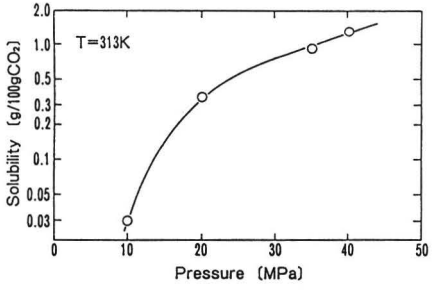

Fig.3 Solubility of Perilla oil in CO_2 v.s. Pressure.

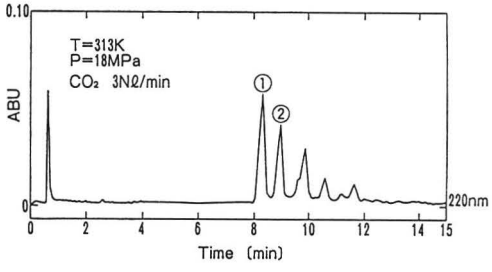

Fig.4 Chromatogram of the perilla oil obtained by the supercritical fluid chromatography. The packed column 4.6mm i.d.×250mm with 5μm Superpack SIL-C18.

The basic equation describing the separation in chromatography defines the resolution, Rs, between any two compounds and/or height equivalents to a theoretical plate, HETP. They are calculated by using the following equations, where w is peak width, t is retention time of each peak, Z is column length, and subscript is the peak number.

$$Rs = 2(t_2-t_1)/(w_1+w_2) \qquad (1)$$

$$HETP = Z(w/t)^2/16 \quad (2)$$

Fig. 5 shows the relation between linear velocity, u, and HETP of peak 1 (trilinolenin peak) and peak 2. In the case of the trilinolenin peak, the optimum value of u, which is relatively small, exists for each pressure, and the HETP decreases as the pressure increases. Moreover, the HETP increases rapidly with an increasing u at 15MPa, but this tendency declines as the pressure increases. Considering that a small HETP means good column efficiency, higher pressure is a suitable condition for separation of trilinolenin with

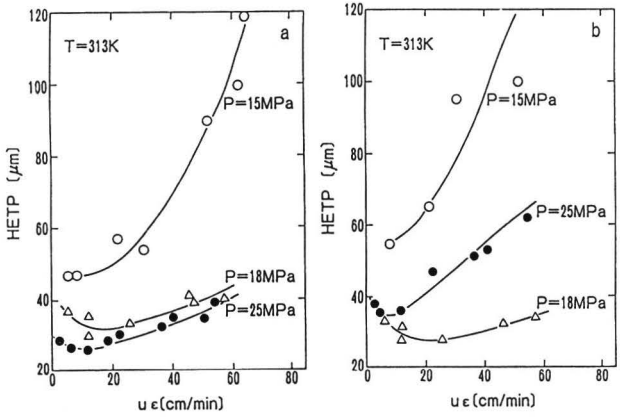

Fig.5 Effect of pressure for HETP v.s. u : a Peak 1, b Peak 2

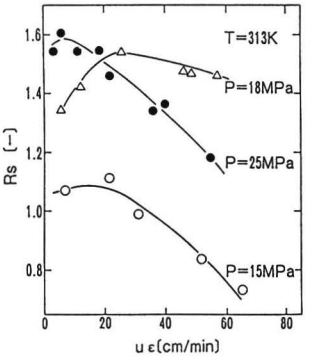

Fig.6 Effect of pressure for Rs v.s. u.

SFC. In the case of peak 2, the effect of u on HETP is similar to that of peak 1, but the pressure effect is different. If the tendency is similar to peak 1, the data at 25MPa should be located below the 18MPa data, but actually it is situated between 15MPa and 18MPa data. It seemes that the peak number 2 is divided into two peaks with respect to the difference of the linoleic acid position in a triglyceride, because the peak shape sharpenes as the pressure increase. Fig. 6 shows the relation of Rs between peak 1 and 2, and u. Optimum u values exist for each pressure, and Rs values increase with pressure. It is noted that good separations are achieved at more than 18MPa.

Fig. 7 and Fig. 8 show the effect of loading volume on HETP and Rs, respectively. HETP rapidly increases, and Rs slightly decreases as the loading volume increases. To separate any two components, Rs should be more than 1.0. Thus the maximum loading capacity of this column is regarded as about 1.5 mg at 313K and 19MPa for the column of 4.6mm i.d. X 250mm length, which was packed with 5μm Superpack SIL-C18.

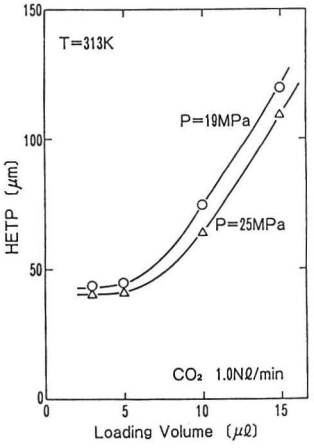

Fig.7 Effect of pressure for HETP v.s. Loading volume.

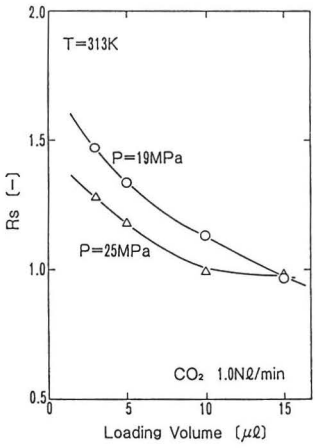

Fig.8 Effect of pressure for Rs v.s. Loading volume.

4 CONCLUSIONS

In this paper, the preliminary data was measured for the separation process of polyunsaturated fatty acid corresponding to the double bond number of polyunsaturated fatty acid by using a combined SFE and SFC process. In the SFE, the solubility of perilla oil increased as the pressure increased, and the possibility of purifing the triglyceride existed. On the other hand, trilinolenin, which consists of three α-linolenic acids, was completely separated from other triglycerides with SFC. It was noted that good separation conditions were obtained at more than 18MPa.

5 ACKNOWLEDGMENT

We would like to thank the Japanese Research and Development Association for High Separation System in Food Industry for its support and approval of this presentation.

6 REFERENCES

McHugh, M.A. and Krukonis, V.J.,1986. Supercritical Fluid Extraction: Principles and Practice. Butterworths

Smith, R.M., 1988. Supercritical Fluid Chromatography. The Royal Society of Chemistry.

Stahl, E., Quirin, K.W., Glatz,A., Gerard, D. and Rau, G., 1984. New Developments in the field of High-Pressure Extraction of Natural Products with Dense Gases., Ber. Bunsenges. Phys. Chem., 88: 900-907.

Solvent Extraction 1990, T. Sekine (Editor)

© 1992 Elsevier Science Publishers B.V. All rights reserved

SUPERCRITICAL FLUID EXTRACTION OF FLAVOURS FROM MILKFAT

A.B. DE HAAN and J. DE GRAAUW
Delft University of Technology, Laboratory for Process Equipment,
Leeghwaterstraat 44, 2628 CA DELFT, The Netherlands

J.E. SCHAAP, H.T. BADINGS
NIZO(Dutch Institute for Dairy Research), P.O. Box 20, 6710 BA EDE
The Netherlands

ABSTRACT
A process for the extraction of flavours from milkfat with supercritical carbon dioxide, operating at 45 °C, is presented. The designed process uses two steps (140 and 125 bar) to concentrate the flavours 1000 times and is capable of extracting 90% of the flavours from 10,000 ton milkfat/year. An economical evaluation indicated that the manufacturing prices of the flavour extract would be around $125,-/kg

1 INTRODUCTION

About 98% of the constituents of milkfat are triglycerides with a carbon number varying from 26 to 54 (Mulder et al., 1974). The remaining 2% contains small concentrations (ppm level) of many components (lactones, ketones, aldehydes) that provide milkfat with its characteristic flavour (Badings, 1984). These natural flavour components are of great interest to the flavour and food industry, but have to be extracted at low temperatures (40-80 °C) without contaminating the remaining milkfat.

The objective of this study was to design a process for the production of a flavour extract from milkfat with supercritical carbon dioxide in which the flavour components are concentrated about 1000 times. In a previous paper it was shown that supercritical carbon dioxide is a suitable solvent for extracting flavours from milkfat (Haan et al., 1990). Concentration factors varying from 20 to 50 have been measured at carbon dioxide densities of 600 to 700 kg/m^3 and 45 °C. Furthermore, it has been observed that the Kremser equation could be used to model the extraction process. This paper presents a design and an economical evaluation of a commercial process, that operates at 45 °C, capable of extracting 90% of the flavours from 10,000 ton milkfat/year and concentrating these flavours about 1000 times.

2 EXPERIMENTAL

A more detailed description of the used equipment and experimental procedure is given elsewhere (Haan et al., 1990). Fig. 1 shows a simplified flow diagram

of the used equipment, suited for extraction at pressures between 100 and 600 bar and temperatures from 25 to 90 °C. The extraction column, with a length of 1m and an inside diameter of 35 mm, was packed with 5 mm metal rashig rings with a specific surface area of 1000 m^2/m^3. The feed entered the top of the column and was extracted countercurrently with the supercritical carbon dioxide. After extraction the remaining raffinate was drawn off from the bottom of the column. The pressure of the carbon dioxide leaving the top of the column was reduced below the critical pressure of carbon dioxide (50-60 bar) to condense the extract in the separator. Hereafter, the gaseous carbon dioxide was condensed before increasing the pressure again to the extraction pressure. All experiments were performed under conditions where equilibrium between the feed and extract existed.

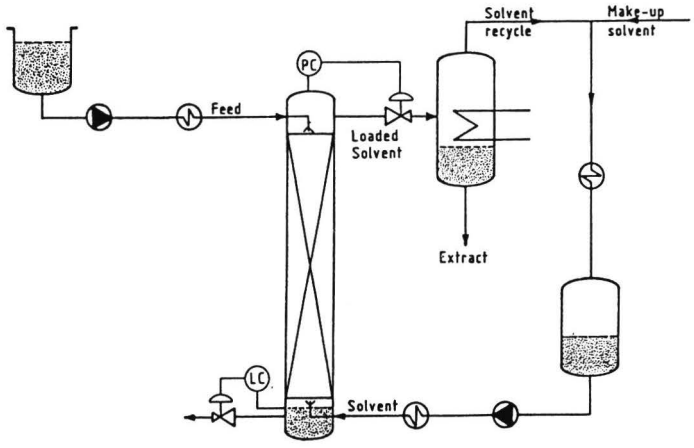

Fig. 1. Flowsheet of the used supercritical extraction equipment.

3 OPERATING CONDITIONS

During the design of the process we used the d12-lactone as the reference component which should be extracted for 90% and concentrated 1000 times. The concentration factor of the d12-lactone as a function of the carbon dioxide density and the temperature is plotted in Fig. 2. It can be seen that for the d12-lactone concentration factors around 50 can be achieved at 45 °C and a carbon dioxide density of about 600 kg/m^3. This means that the d12-lactone can only be concentrated 1000 times when a concentration factor of 20 is obtained during the first stage. Furthermore 95% of the d12-lactone should be extracted during the first stage to achieve an overall extraction efficiency of 90%

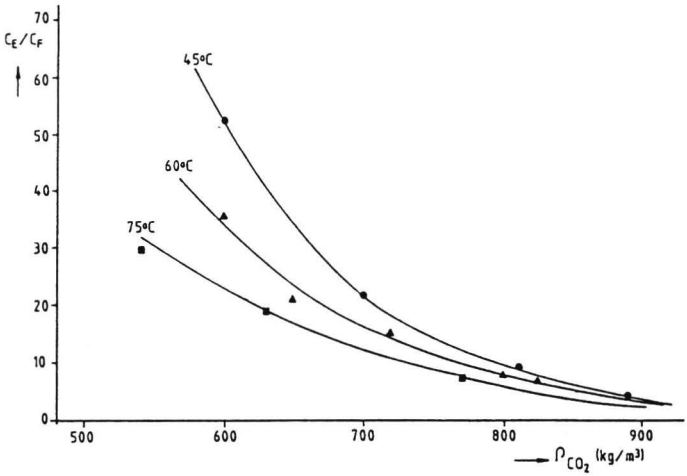

Fig. 2. Concentration factor of the d12-lactone (concentration in the extract/ concentration in the feed) as a function of the carbon dioxide density and the temperature.

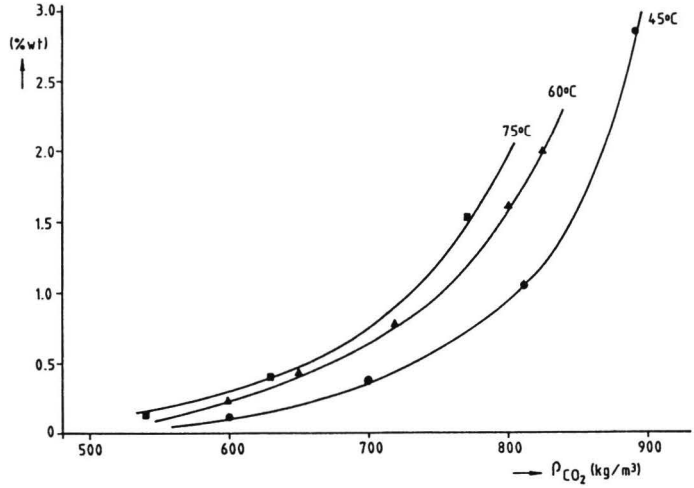

Fig. 3. Solubility of the milkfat components (extract content) as a function of the carbon dioxide density and the temperature.

after two stages. For these reasons the pressure of the first stage, operating at 45 °C, is limited to 140 bar at which a carbon dioxide density of 700 kg/m^3 is obtained. From Fig. 3, that shows the solubility of the milkfat components (extract content) in supercritical carbon dioxide as a function of the carbon dioxide density and the temperature, it is seen that at 140 bar and 45 °C an extract content of 0.35 wt% is achieved. Optimization calculations indicated

that for a solvent to feed ratio of 13, 95% of the d12-lactone could be extracted and concentrated 21 times with 13 theoretical plates. Under these conditions a minimum in the combination of operating and investment costs was obtained.

During the second stage, operating also at 45 °C the pressure is limited to 125 bar at which a carbon dioxide density of 620 kg/m^3 and an extract content of 0.12 wt% are obtained. Under these conditions 95% of the d12-lactone could be extracted and concentrated 48 times with a solvent to feed ratio of 16.5 and 13 theoretical plates.

4 FLOWSHEET DESCRIPTION

A flowsheet of the designed process is shown in Fig. 4. It is seen that only one column is used for both extraction stages because the use of a second column required considerable extra investment costs. Using the scaling rules for packed columns modified for supercritical extraction conditions, the column, equipped with 13 mm metal rashig rings (a=370 m^2/m^3), was calculated to have an internal diameter of 0.8 m, packed bed height of 18 m, shell thickness of 5 cm and total height of 24 m. During the first stage the milkfat is extracted countercurrently with the supercritical carbon dioxide at 140 bar and 45 °C to concentrate the flavours 21 times. The remaining raffinate contains about 25 wt% carbon dioxide and is expanded in three stages from the extraction pressure to 50, 20 and 1 bar to recover the dissolved carbon dioxide. The supercritical carbon dioxide leaving the top of the column is expanded isothermally to 50 bar to collect the extract. This extract contains about 17 wt% carbon dioxide and is expanded to 1 bar before storage. The gaseous carbon dioxide from the separators is condensed at 50 bar and 15 °C and recycled to the column. After one or two weeks the column is cleaned with supercritical carbon dioxide and the collected extract from the first stage is extracted again at 125 bar and 45 °C to achieve a total concentration factor of 1000. This second stage requires only 5% of the time used for the first stage.

5 ECONOMICAL EVALUATION

An economical evaluation of the designed process has been made by calculating the annual operating costs, including investment, production, maintenance, labour and overhead costs. The total investment costs were calculated from the base costs of the equipment made from or cladded with stainless steel as shown in Table 1. It is seen that the designed process, with a capacity of 10,000 ton milkfat/year, requires an investment of 3.2 million dollars. The resulting

investment costs contribute for 42% to the total annual costs while the production costs contribute for only 22%. Against a manufacturing price of \$125,-/kg 9,000 kg of extract will be produced from the milkfat. Although this manufacturing price is quite high, these kind of price levels are encountered more often in other supercritical extraction processes where spice or flavour extracts are produced.

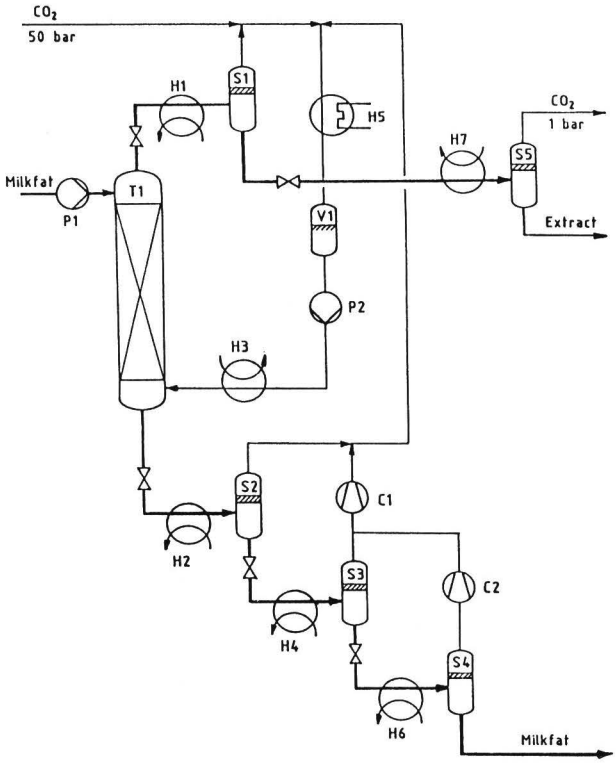

Fig. 4. Flowsheet of the designed process for the extraction of flavours from milkfat with supercritical carbon dioxide.

6 CONCLUSIONS

It appeared that two extraction stages are required to concentrate the flavour components 1000 times. A process was designed capable of extracting 90% of the flavours from 10,000 ton milkfat/year. The designed process operates at 45 °C and 140 bar during the first and 45 °C and 125 bar during the second stage. For both stages the same equipment was used to reduce the required

investment costs. The presented economical evaluation indicated that the manufacturing price of the flavour extract would be around $125,-/kg, which is not unusual for supercritical flavour or spice extracts.

TABLE 1

Estimated costs ($1,000) of the designed process for the extraction of flavours from milkfat.

Equipment	Base* Equipment Cost	Direct** Installation Factor	Installed Equipment Cost
Column	215	3.0	645
Packing	25	1.0	25
Heat Exchangers	180	2.3	415
Pumps	295	1.7	500
Compressors	80	1.6	130
Separators	70	3.0	210
CO_2-Storage	50	1.4	70
Cooling Machine	335	1.0	335
Storage Tanks	50	1.4	70
Direct Equipment Cost			2,400
Engineering, Contingency etc.			800
TOTAL INVESTMENT COST			3,200
Annual Investment Cost			480
Production Cost			250
Maintenance			95
Labor			175
Overheads			125
TOTAL ANNUAL COST (9.000 KG EXTRACT/YEAR)			1,125

* (Dutch Association of Cost Engineers, 1989)
**(Guthrie, 1974)

7 ACKNOWLEDGEMENTS

We would like to thank A. de Leeuw, F.W.R. Soeterbroek and C.J. Batenburg for performing the experiments and calculations reported in this paper.

8 REFERENCES

Badings, H.T., 1983. In: P. Walstra and R. Jenness (Editors), Dairy Chemistry and Physics. John Wiley & Sons, New York, 336 pp.

Dutch Association of Cost Engineers, 1989. WEBCI/WUBO Costing Manual. (14th Ed.) Leidschendam, The Netherlands

Guthrie, K.M., 1974. Process Plant Estimating Evaluation and Control. Craftsman Book Company of America, Solana Beach, California

Haan, A.B. de, Graauw ,J. de, Schaap ,J.E. and Badings ,H.T., 1990. Extraction of flavors from milkfat with supercritical carbon dioxide. J. Supercrit. Fluids, 3: 15-19

Mulder, H., and Walstra, P., 1974. The Milkfat Globule. Pudoc, Wageningen

Solvent Extraction 1990, T. Sekine (Editor)

© 1992 Elsevier Science Publishers B.V. All rights reserved

DEBINDERING FROM MOLDED FINE CERAMICS BY SUPERCRITICAL CARBON DIOXIDE

S. TAKISHIMA[1], H. NAGASAKI[1], H. MASUOKA[1], Y. MUKAI[2] and T. SAKAI[2]
[1]Department of Chemical Engineering, Hiroshima University, Saijo, Higashi-Hiroshima 724 (Japan) [2]Machinery and Electronics Technology Research Center, The Japan Steel Works, Ltd., 6-1, 1-Chome, Funakoshi-Minami, Aki-Ku, Hiroshima 736 (Japan)

ABSTRACT

The supercritical fluid extraction technique was applied to the debindering process of molded fine ceramics. From results of extraction experiments of several waxes from molded ceramic samples, paraffin wax was selected as a main binder component, because of its high extraction yield. In addition, binder extraction experiments were carried out from ceramics samples molded by paraffin wax, stearic acid and one of five thermoplastic resins. More than 70% of initial quantities of paraffin wax and stearic acid were extracted in two hours in the extraction conditions around 340 K and above 20 MPa. The samples containing more than 2.8 wt% of polyethylene or polypropylene showed no defects after the debindering. Moreover, the bending strength of the sintered samples was as high as that of the samples produced by the conventional methods.

1 INTRODUCTION

The injection molding technique of fine ceramics has come to be recognized as one of the most efficient methods for the mass production of complex shapes. Since this technique, however, requires a relatively large amount of binders to impart fluidity to the ceramics powder, the binders should be removed afterwards through techniques such as thermal decomposition. The debindering process requires the most time of the processes composing the entire manufacturing cycle and a great deal of energy to avoid defects such as the expansion and cracking.

Yokawa and Nakajima (1988) applied the supercritical fluid (SCF) extraction technique to the debindering process of molded fine ceramics. They found that the SCF debindering reduced debindering process time to a great extent. Optimum combinations of binder components for the SCF debindering process, however, have not become clear yet. In this work, binder extraction experiments were carried out from molded fine ceramics to investigate optimum binder combinations and optimum operation conditions for the SCF debindering process considering extraction yields of the binder components and soundness of the debindered samples.

2 SELECTION OF A LOW-MOLECULAR WEIGHT BINDER COMPONENT

Firstly, extraction experiments of several waxes from molded ceramic samples were carried out to select a low-molecular weight binder component.

2.1 Sample preparation and experimental procedure

Melting point temperatures of waxes used in this work are shown in Table 1. Al_2O_3 powder having about 0.6 μ m mean diameter and a relatively narrow particle size distribution (Showa Denko Co., AL-160SG-4) was molded into a tablet shape with 15 mm diameter and 5 mm thickness using one of these waxes. The contents of the waxes in the samples were about 20 wt%.

TABLE 1

Melting point temperature, T_m, of waxes

wax		T_m[K]
paraffin wax	(PW-A)	320
paraffin wax	(PW-B)	328
paraffin wax	(PW-C)	342
microcrystalline wax	(MCW)	352
polyethylene wax	(PEW)	380
bees wax	(BW)	336

An apparatus of vapor-flow type was used for the extraction experiments. The apparatus mainly consists of the following three parts; a liquefied CO_2 feed system, an extraction cell installed in an air bath and an expansion valve with a cold trap. Extraction of the waxes was carried out by the following procedure. The molded samples were placed in the extraction cell and CO_2 was introduced up to a desired pressure by a pump. Vapor phase was allowed to flow through the cell at a constant flow rate (about 5 l(STP)/min) for two hours. Finally, CO_2 in the cell was discharged to the atmospheric pressure at the same flow rate.

2.2 Results and discussion

Figure 1 shows the pressure dependence of extraction yields of the waxes at 343.2 K. The extraction yields increased with an increase in pressure above 10 MPa. This is because increasing pressure enlarges the solubilities of the waxes in supercritical CO_2. Paraffin waxes with relatively low melting point temperatures (PW-A and PW-B) were almost completely extracted at pressures greater than 20 MPa. The extraction yields of the other waxes were lower than those of paraffin waxes.

Figure 2 shows the temperature dependence of the extraction yields of the waxes at 20 MPa. PW-A and PW-B showed high extraction yields compared with the other waxes. From these results, PW-A was selected as a main binder component in this work.

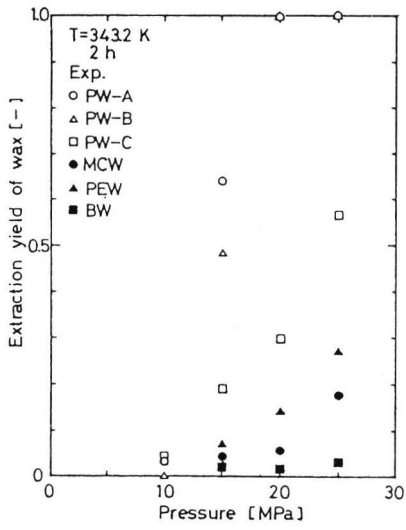

Fig. 1. Pressure dependence of extraction yields of waxes at 343.2K.

3 SELECTION OF A HIGH-MOLECULAR WEIGHT BINDER COMPONENT

Next, a high-molecular weight binder component was selected from the results of binder extraction experiments of samples molded by mixed binders.

3.1 Sample preparation and experimental procedure

Compositions of molded samples are shown in Table 2. Stearic acid was used as a lubricant. One of five thermoplastic resins was added as a high-molecular weight binder component, which was needed in order to keep debindered samples in shape. Molded samples for the bending strength test with 3.7x5.0x 65.6 mm were prepared by the injection molding. Binder extraction experiments were carried out by the same procedure as mentioned above. Since the thermoplastic resins were hardly extracted by supercritical CO_2, the extraction yield was defined as the ratio of the mass of extracted binders to that of PW-A and stearic acid initially contained in each sample.

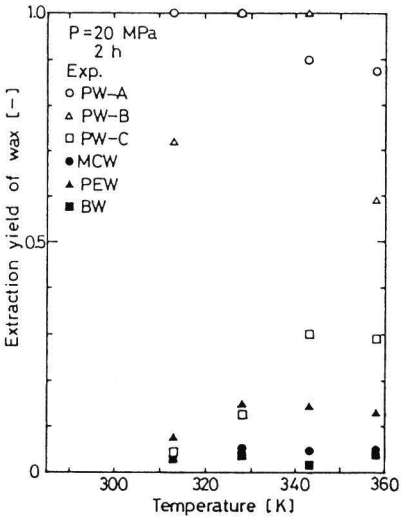

Fig. 2. Temperature dependence of extraction yields of waxes at 20MPa.

3.2 Results and discussion

Figure 3 shows the dependence of the extraction yields on polymer concentrations at 343.2 K and 20 MPa. More than 70% of the initial quantities of PW-A and stearic acid was extracted in two hours. The extraction yields slightly decreased with an increase in the polymer content. This may be due to the decrease in the diffusion coefficients of the low-molecular weight binder components in the molded samples.

The pressure dependence of the extraction yields for the sample D at 343.2 K is represented in Fig. 4. The extraction yields dramatically changed with a pressure of around 15 MPa. How-

TABLE 2

Composition of molded samples [wt%]

component	A	B	C	D
Al_2O_3	87.0	87.0	87.0	87.0
PW-A	9.9	9.3	8.0	6.0
stearic acid	2.2	2.2	2.2	2.2
thermoplastic resin (PE,PP,PAE,PVA,PS)[a]	0.9	1.5	2.8	4.8

[a] PE:polyethylene, PP:polypropylene, PAE:acrylic ester copolymer, PVA:poly(vinyl alcohol), PS:polystyrene

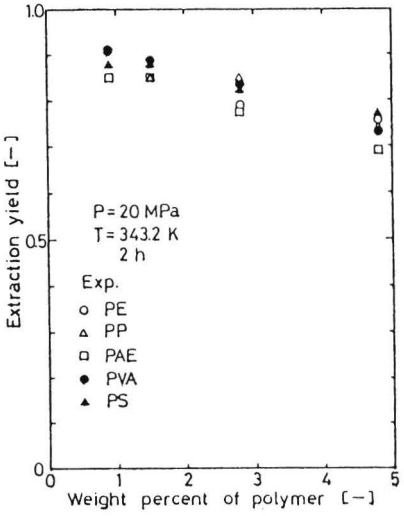

Fig. 3. Dependence of extraction yields of low-molecular weight binder components on polymer concentration at 343.2K and 20MPa.

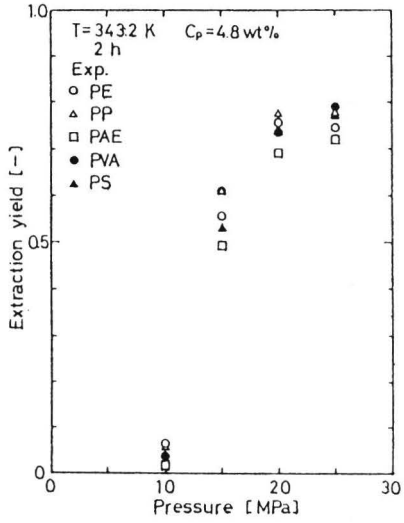

Fig. 4. Pressure dependence of extraction yields of low-molecular weight binder components at 343.2K.

ever, the extraction yields became almost constant above 20 MPa.

The temperature dependence of the extraction yield for the sample D at 20 MPa was shown in Fig. 5. The extraction yields were almost constant above 340 K, while these somewhat decreased when the temperature was lowered below 340 K.

The soundness of the debindered samples corresponding to those shown in Figs. 3 to 5 is listed in Table 3. In this table, the soundness of debindered samples was judged into four ranks; ◎: no defect was observed and easy to handle, ○:no defect was observed but difficult to handle, △:some small defects were observed, and ×:some large defects were observed or the sample was broken. It was found that the soundness of the

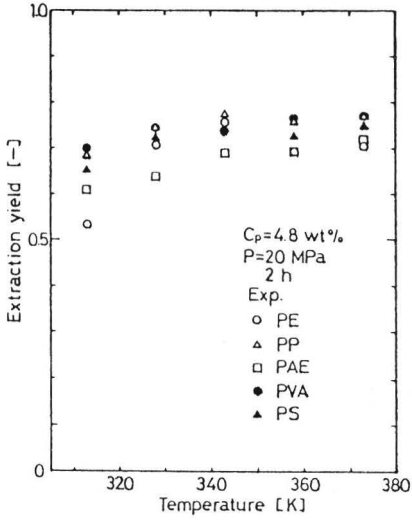

Fig. 5. Temperature dependence of extraction yields of low-molecular weight binder components at 20MPa.

TABLE 3

Soundness of debindered samples

	(T=343.2K, P=20MPa) C_p [wt%]				(T=343.2K, C_p=4.8wt%) P [MPa]				(P=20MPa, C_p=4.8wt%) T [K]				
polymer	0.9	1.5	2.8	4.8	10	15	20	25	313	328	343	358	373
PE	×[a]	△	◎	◎	○	◎	◎	◎	◎	◎	◎	◎	◎
PP	×	×	◎	◎	○	○	◎	◎	◎	◎	◎	◎	◎
PAE	△	△	△	○	×	○	○	△	△	○	○	○	△
PVA	×	×	○	○	×	○	○	○	×	△	○	○	○
PS	×	×	×	△	×	○	△	○	○	○	△	○	○

[a] as for the explanation of keys, see text

debindered samples was improved with an increase in polymer content. Samples containing more than 2.8 wt% of PE or PP showed no defect after the debindering. This may be due to the lower melting point temperatures and the lower glass-transition temperatures of these polymers, as well as molecular structures similar to that of paraffin wax. The relationship between the soundness of the debindered samples and pressure was unique. The samples debindered at 10 MPa, where binders were scarcely extracted, caused large defects. The soundness of the debindered samples was improved with an increase in extraction yield. This was considered to be due to the development of micro pores in the debindered samples caused by the extraction of the low-molecular weight binder components. If the micro pores did not develop enough, decompression operation resulted in defects such as expansions and cracks in the debindered samples. The change in temperature had no significant effect on the soundness of the debindered samples.

4 BENDING STRENGTH TEST OF SINTERED PRODUCTS

Finally, the debindered samples were sintered and their bending strength was compared with that of samples produced by different methods.

4.1 Sample preparation and experimental procedure

The sample molded using PW-A, stearic acid and 4.8 wt% of PE (sample D in Table 2) were used for the bending strength test. Ten pieces of the samples were debindered by supercritical CO_2 at 313.2 K and 20 MPa for four hours. The extraction yields were about 0.7. In order to compare the bending strength of sintered products debindered by different methods, the debindering of these molded samples by the conventional thermal decomposition method was also carried out. The thermal decomposition debindering was performed by heating the samples up to 793 K at the heating rate of 20 K/h. The debindered samples were sintered by heating from the room temperature to 1273 K at 200 K/h and from 1273 K to

TABLE 4

Results of bending strength test for sintered samples

debindering method[a]	binder[b]	debindering time [h]	bending strength [$10^8 N/m^2$] min.	max.	av.	Weibull coefficient[-]
SFE	for SFE	4	3.6	4.3	3.9	23.3
TD	for SFE	24	3.0	4.1	3.7	10.2
TD	for TD	60	3.1	4.9	4.2	8.3

[a] SFE:supercritical fluid extraction, TD:thermal decomposition
[b] for SFE:sample D in Table 2 (PE is used as a thermoplastic resin)
for TD :sample in which totally 13wt% of PE, PP and acrylic resin are used as binder(Saito et al., 1987)

1873 K at 150 K/h and by keeping at 1873 K for two hours. The bending strength and Weibull coefficients of the sintered products were obtained according to JIS R1601-1981.

4.2 Results and discussion

Table 4 lists the results of the bending strength test of the sintered products. In this table, the values for samples produced by the conventional methods with a conventional binder combination (Saito et al., 1987) are also added. The bending strength of the samples debindered by supercritical CO_2 was almost the same as that of those debindered by the thermal decomposition method. In addition, a considerably higher value of Weibull coefficient was obtained.

5 CONCLUSIONS

The supercritical fluid extraction technique was applied to the debindering process of molded fine ceramics. Paraffin wax with melting point temperature of 320 K, stearic acid and one of five thermoplastic resins were used as binder components. From the extraction experiments using supercritical CO_2, it was found that the debindering process time could be reduced to a great extent, and that the molded samples containing more than 2.8 wt% of polyethylene or polypropylene showed no defects after the debindering. In addition, the bending strength of the sintered samples was as high as that of those debindered by the conventional methods.

6 REFERENCES

Saito,K., Arakida,Y. and Inoue,M., 1987. Fain seramikkusu no shashutsu seikei gijutsu, Nikkan Kogyo Shinbunsha.
Yokawa,S. and Nakajima,N., 1988. Chourinkai bainda jokyo ni yoru seramikkusu no seizo. Kagaku Kogaku, 52, pp.513-515.

Solvent Extraction 1990, T. Sekine (Editor)

© 1992 Elsevier Science Publishers B.V. All rights reserved

NEW HOMOGENEOUS LIQUID-LIQUID EXTRACTION BY PHASE SEPARATION AND PHASE TRANSFORMATION WITH FLUOROCARBON SURFACTANT AND QUATERNARY AMMONIUM SALT

S. IGARASHI and T. YOTSUYANAGI
Department of Molecular Chemistry and Engineering, Faculty of Engineering, Tohoku University, Sendai 980 (Japan)

ABSTRACT
Igarashi, S. and Yotsuyanagi, T., 1990. New homogeneous liquid-liquid extraction by phase separation and phase transformation with fluorocarbon surfactant and quaternary ammonium salt.

An oily and transparent water-immiscible the 2nd. liquid phase containing ion-pair of perfluorooctanate($PFOA^-$) and quaternary ammonium ion(Q^+) and solute was formed at room temperature from homogeneous aqueous solution containing $PFOA^-$ and solute by addition of Q^+ salts. Q^+ salts mixture of tetrabutylammonium bromide(TBA) and tetraethylammonium bromide(TEA) {[TBA]:[TEA]=1:$2\frac{1}{2}$ was most effective. The volume of the 2nd. phase was constant over the pH range of 5.5-12.2, but it depends on kinds and concentrations of Q^+ ions. The 2nd. phase formed at room temperature(20-26 °C) made phase transformation at 30° C and the volume of the high temperature phase decreased to less than 1/10 of that of the low temperature one within 30 sec. By the combined use of phase separation and the phase transformation, 500-fold concentration (i.e. 100 $cm^3 \longrightarrow$ 0.2 cm^3) was possible within 20 min. The solute, for example, Ni(II)- and Co(III)-maleonitrildithiolato anionic complexes, Fe(II)-1,10-phenanthoroline cationic complex, and porphyrin compounds such as chlorophyll were quantitatively extracted.

1. Introduction

A homogeneous liquid-liquid extraction is a method which extracts a solute in homogeneous solution to a 2nd. phase formed from the solution by the phase separation. A typical method of such system based on the solubility change depending on temperature of propylene carbonate in water (above 70° C, it forms homogeneous solution), was first reported by Murata and Ikeda [1].

We have found that neutralization of perfluorooctanate ion ($PFOA^-$) in aqueous water-miscible organic solvent solutions (such as those of acetone, dioxane and THF) induces a new type of phase separation, which provides a small volume of an oily and transparent water-immiscible liquid phase, from a large volume of the aqueous solutions. By this finding, a new homogeneous liquid-liquid extraction based on pH dependent phase separation was reported [2,3]. Recently, an another type of phase separation with quaternary ammonium ion (Q^+) as a counter ion of $PFOA^-$ was studied in order to avoid the strongly acidic condition (pH < 0.6), which was essential in our previous method [2,3]. On the course of these studies, we have found the phenomena that the volume of the 2nd. phase remarkably changed depending upon not only the kinds of Q^+ ion and

the concentration of $PFOA^-$ and Q^+ pair, but also upon temperature. The details of such phase separation with Q^+ ion and temperature dependent phase transformation will be discussed in this paper. Based on these findings, a new concentration method by combined use of the phase separation and the phase transformation has been developed.

2.Experimental

2.1 Reagents

Perfluorooctanoic acid (HPFOA) was used as received from Tokyo Kasei Kogyo Co., LTD. A 0.1 mol dm^{-3} aqueous solution of $PFOA^-$ was prepared by neutralizing $PFOA^-$ with 0.2 mol dm^{-3} aqueous lithium hydroxide solution. Quaternary ammonium solutions were prepared by dissolving their GR grade reagents with distilled water.

2.2 Apparatus

A Horiba M-5 pH meter and Hitachi Model 124 double-beam recording spectrophotometer were used. A Karl-Fischer titrator(Mitsubishi Kasei Co., Type KF-01) was used for the measurement of water content in the water-immiscible phases. Temperature of all solutions was controlled by the use of a coolnics circulator CTR-22WS(Yamato-Komatsu Co.,).

2.3 Procedure

Eighty cm^3 of sample solution(pH 7.0) containing the solute {e.g. porphyrin compound such as TTMAPP(DOJINDO Laboratories)} and 5 cm^3 of 0.1 mol dm^{-3} $PFOA^-$ aqueous solution is taken into a 100 cm^3 cylindrical glass vial fitted with plastic cap. Then, Q^+ solution {3 cm^3 of 1 mol dm^{-3} tetrabutylammonium bromide(TBA) and 6 cm^3 of 1 mol dm^{-3} tetraethylammonium bromide(TEA) aqueous solutions} is added to sample solution and mixed. The mixture is allowed to stand for 30 min at 25 °C. After phase separation, the glass vial is put into hot water bath (above 30° C, i.e. 70° C) for 1 min. Volume of the precipitated phase(organic phase) is determined by using 0.1 cm^3 micro-syringe or 1 cm^3 syringe. Further, the concentration of solute(e.g. TTMAPP) in water phase and/or organic phase is spectrophotometrically determined.

3. Results and discussion

3.1 Phase separation phenomena with Q^+

(a) Selection of Q^+ ion: By the addition of quaternary ammonium ions of benzyltriethylammonium, phenyltriethylammonium, and tetraalkyl(Cn) ammonium salts such as butyl(C_4:TBA) and pentyl(C_5) to an aqueous solution containing $PFOA^-$, oily and transparent 2nd. phases were formed, however, neither of Q^+ ion having trimethyl group and straight-chain alkyl(Cn)(i.e. $C_6 \sim C_{19}$) did gave any

phase separation. On the course of search for more effective Q^+, we found that the use of mixture of TBA and TEA gave more rapid phase separation compared with the use of TBA only. The optimum molar ratio of TBA and TEA was in the range of (1:1) to (1:5). So that the mixture of TBA : TEA = 1 : 2 was selected as an experimental condition described below. (b) Effect of $PFOA^-$ concentration: The volume of 2nd. phase increased with increasing $PFOA^-$ concentration. (c) A pH condition: The relationship between pH and volume of 2nd. phase is shown in Fig.1. The phase separation was observed over the pH range of 5.5 to 12.2 and the constant volume of 2nd. phase was obtained. (d) Phase separation time: The 50-fold concentration (i.e. 100 cm^3 to 2.0 cm^3) was achieved within 20 min at 25° C after addition of $PFOA^-$ and Q^+ to sample solution. (e) Back-extraction: The back-extraction of concentrated solute (e.g. TTMAPP) from the organic phase to homogeneous system was successfully done by the addition of strong acid or anionic surfactant such as sodium dodecylsulfate in higher concentration than Q^+ ion. Moreover, $PFOA^-$ in the 2nd. phase changed into the solid HPFOA by addition of acid, and it suggests that PFOA may be able to recover by such method.

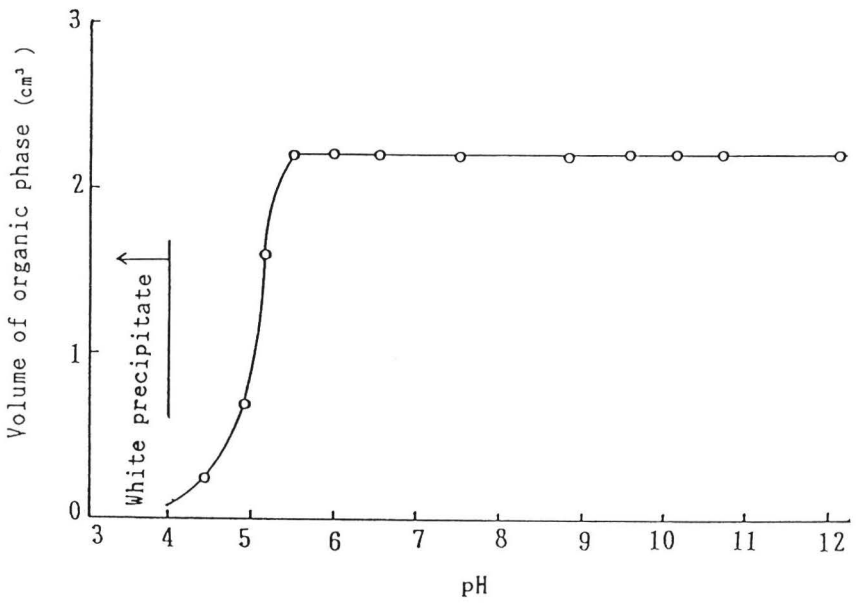

Fig.1 Relationship between pH and the volume of organic phase.

Condition: $[PFOA]_T = 5.0 \times 10^{-3}$ mol dm $^{-3}$, $[TBA]_T = 3.0 \times 10^{-2}$mol dm^{-3}, $[TEA]_T = 6.0 \times 10^{-2}$ mol dm $^{-3}$, at 25 ℃.

3.2 Temperature dependent phase transformation

The volume of the 2nd. phase formed by the use of TBA only gave remarkably change depending upon temperature (16 °C to 30 °C). The relationship of the volume of the 2nd. phase, TBA concentration, and temperature are shown in Fig.2. By the use of the mixture(1:2) of TBA and TEA, the gentle slope curves compared with those of TBA only were obtained (Fig.3). In the condition of Q^+ ion concentration {i.e. $[TBA]_T = 3 \times 10^{-2}$ mol dm^{-3}, $[TEA]_T = 6 \times 10^{-2}$ mol dm^{-3}}, the constant volume (about 2 cm^3) of the 2nd. phase was obtained in the temperature range of 20° C to 26° C. The 2nd. phase was transformed into the 3rd. liquid phase having a smaller volume (i.e. about 0.2 cm^3) within 30 sec at above 30 °C (Fig.4). The amounts of water in the each phase were measured by the coulometric titration with Karl Fischer's reagent. The amounts of water in the 2nd. phase was more than 90 wt %, however, that in the 3rd. phase was less than 45 wt %.

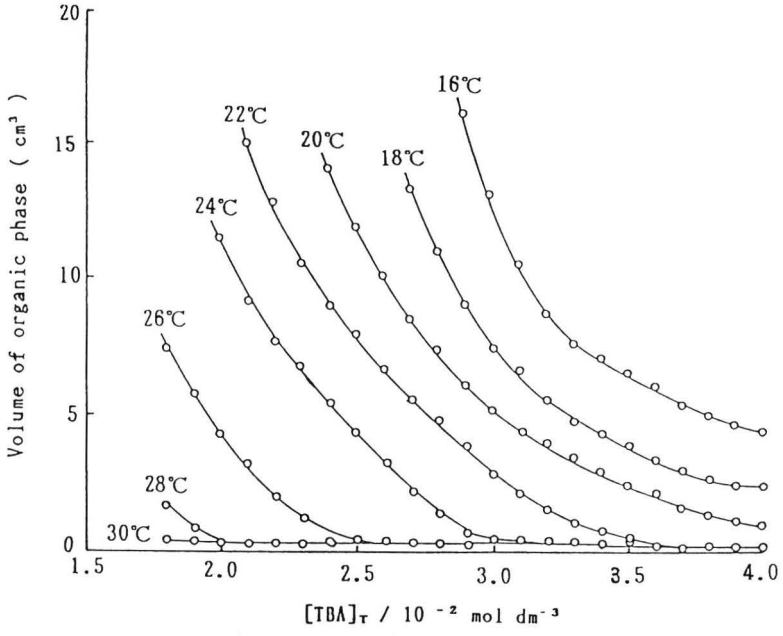

Fig.2 The relation of the volume of organic phase and the concentration of quaternary ammonium salt at various temperatures: TBA system.

Condition: $[PFOA]_T = 5 \times 10^{-3}$ mol dm^{-3}

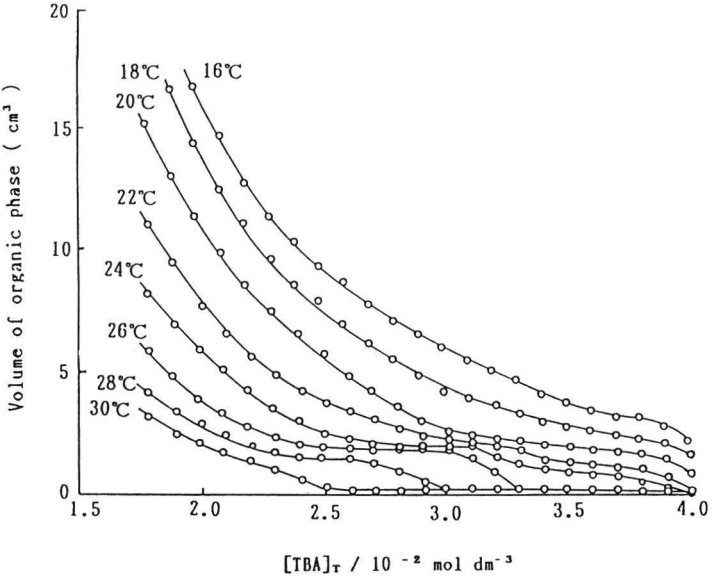

Fig.3 The relation of the volume of organic phase and the concentration of quaternary ammonium salt at various temperatures: TBA and TEA mixture system.

Condition: $[PFOA]_T = 5 \times 10^{-3}$ mol dm $^{-3}$, $[TEA]_T = 2[TBA]_T$

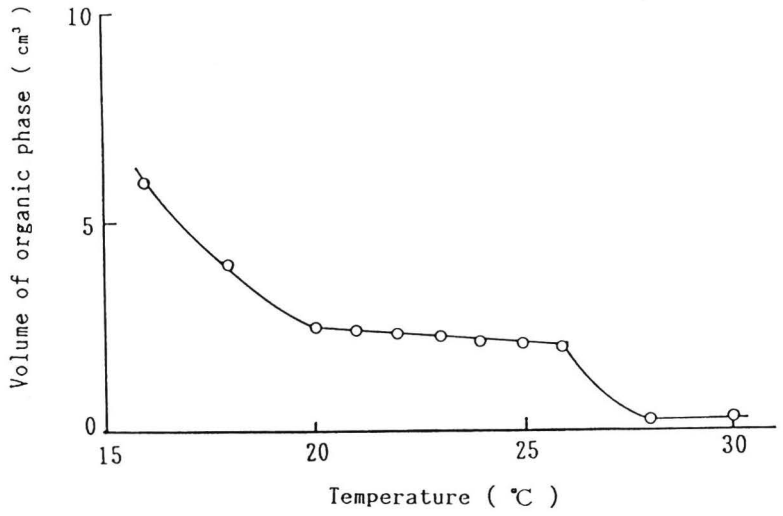

Fig.4 The relationship between temperature and the volume of organic phase.

Condition: $[PFOA]_T = 5.0 \times 10^{-3}$ mol dm^{-3}, $[TBA]_T = 3.0 \times 10^{-2}$ mol dm^{-3}, $[TEA]_T = 6.0 \times 10^{-2}$ mol dm^{-3}

3.3 Application

By the combined use of procedures for the phase separation and the phase transformation, 500-fold concentration (i.e. 100 cm^3 to 0.2 cm^3) was made possible within 20 min. Ni(II)- and Co(III)-maleonitrildithiolato anionic complexes, V(V)-desferioxamine B and Fe(II)-1,10-phenanthoroline cationic complexes, and porphyrin compounds such as water-soluble porphyrin compounds (TTMAPP, Pb(II)-TTMAPP complex, and Cu-, Fe-chlorophyllin) and hemogrobin and chlorophyll in vivo were quantitatively extracted and concentrated.

REFERENCES

1. Murata,K. and Ikeda,S., 1969. Homogeneous liquid-liquid extraction method. Bunseki Kagaku, 18: 1135.
2. Igarashi,S. and Yotsuyanagi,T., 1988. A Novel Homogeneous liquid-liquid extraction by pH dependent phase separation with fluorocarbon ionic surfactant. Proceedings of Symposium on solvent extraction(Tokyo),p.175.
3. Igarashi,S. and Yotsuyanagi,T., 1989. A New homogeneous liquid-liquid extraction method with fluorocarbon ionic surfactant - Preconcentration of porphyrin compound by pH dependent phase separation -. PACIFICHEM '89 (Hawaii), Anal.2B-02.

Solvent Extraction 1990, T. Sekine (Editor)
© 1992 Elsevier Science Publishers B.V. All rights reserved

DIVIDING INTO LAYERS AS EXTRACTION METHOD. ON THE EXAMPLE OF SOME SALT-WATER SYSTEMS

J.M.SCHWARTZ and M.M.KURSINA
Institute of Inorganic Chemistry of Latvian Academy of Sciences, Latvia, USSR

ABSTRACT
Schwartz J.M. and Kursina M.M., 1990. Dividing into layers as extraction method. On the example of some salt-water systems.

The formation of two liquid phases (dividing into layers) in the systems: inorganic salt - a liquid completely soluble in water organic extractant - boric acid - water is considered from the point of view of possibility of boric acid concentrating in the phase, enriched with organic component, and of application of this type systems for the extraction of boric acid. As the examples phase equilibria and solubilities of the components in the systems: $MgSO_4$ - polyethylenglycol-1000(1500,15000) - H_3BO_3 - H_2O and $MgSO_4$ - 3-methyl-1,3-butanediol - H_3BO_3 - H_2O, 25°C are considered. The description method for the distribution of the components in the stratification field, regarded as extraction system, is proposed. It consists in constructing the "ray of extraction" in two projections on the rectangular state diagram of one of phases.

Under the ray of extraction the locus that forms with increase of boric acid concentration in "organic" phase, is meaned.

The ray of extraction begins in the according point of analogical system without boric acid.

INTRODUCTION

In this study we propose a new method of extraction, which is based on the formation of located region of two liquid phases (stratification) in the systems: inorganic salt - completely soluble in water organic component - the extractible substance - water. In one of phases the extractible substance is concentrated by stratification, but in other - the inorganic salt - the outsalter. As an example the isothermic sections at 25°C of systems: polyethyleneglycol (PEG-1000,1500,15000) - $MgSO_4$($FeSO_4$) - H_3BO_3 - H_2O) were investigated.

2 THEORY AND METHOD

One of the liquid phases in the region of stratification is regarded as the extract, the second one - as the raffinate, but two solid components - as the extracted substance and the outsalter. In our case PEG is the extractant, the upper phase, the so

caled "organic phase", in which boric acid is concentrated, is the extract, the second phase, in which the salt is concentrated, is the raffinate. Boric acid is the extracted substance, $MgSO_4$ or $FeSO_4$ - the outsalters. This made possible to regard the region of stratification as a extraction system. As a method of description for the distribution of components in such systems we propose a modified method of "ray of extraction". The classical ray of extraction, proposed by Nikolaev [1] , is the locus on the state diagram water phase at the increasing volume of extractant. In our case the ray of extraction is the locus on the state diagram of "organic" or "water" phase by increasing the concentration of extracted component (H_3BO_3). When the solubility of one of the components in this phase is negligible, the ray of extraction is a line. When all the components are soluble in both phases, the rays of extraction are represented as two projections on the transangular envelop of state diagram of one of the phases (Fig. 1).

Each point of the ray of extraction is characterized by partition coefficients of all the components. For the sake of convenience we propose to write in one projection $\mathcal{D}$ of two components (one in parentheses), but $\mathcal{D}$ of two others - in the second.

The begining of coordinates usually is the 100% of H_2O. On the ordinate axis consequently upward and downward the weight percents of components A and B are placed, on the abscissa - component C - the extracted substance. The initial point of the ray of extraction in each of projection is the point of consequent three-component system without extractible substance. The end point is the point of crystallization of component C (extracted substance, C_1 and C_1^1). The locus of endpoints of rays of extractions gives the projections of the line of crystallization of component C (C_2-$\mathcal{D}$ and C_2^1-$\mathcal{D}^1$). The points $\mathcal{D}$ and $\mathcal{D}^1$ - are the projections of the invariant-point $\mathcal{D}$, where components B and C are both crystallized. The lines $a_o\mathcal{D}$ and $b_o\mathcal{D}^1$ - are the projections of the line of crystallization of component B. The rays of extraction can be straight lines or curves, which is conected with distribution of components in each particular case.

As an example the phase equilibria and solubility in the systems PEG-1000(1500,15000) - $MgSO_4$($FeSO_4$) - H_3BO_3 - H_2O at 25°C were investigated.

The investigation is carried out by the isothermal method. The time of equilibrium is established experimentally on the refrac-

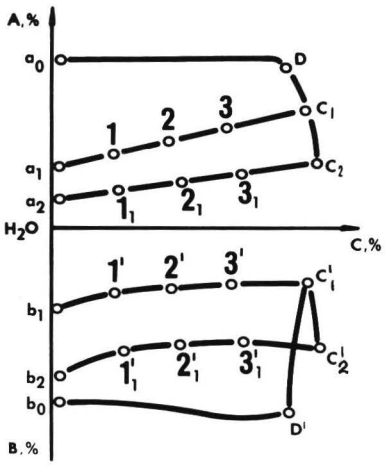

Fig. 1. The method of representation of ray of extraction in four-component system, with soluble components.

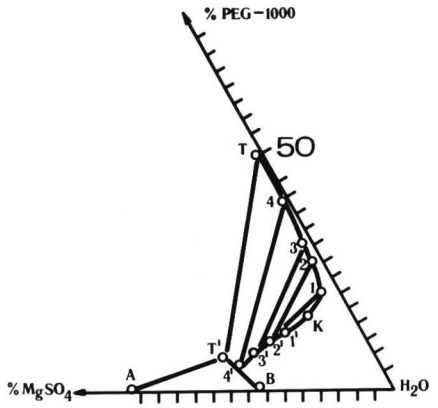

Fig. 2. The state diagram of the system $MgSO_4$-PEG-1000 - H_2O, 25°C

tion index of one of phases. The contents of phases is established by chemical analysis: $MgSO_4$ is determined by Mg^{+2} complexonometric titration with EDTA, H_2O - by method of K.Fisher and as a loss of weight heating till 110°C, H_3BO_3 - by alkalymetric titration in presence of glycerol with pH-metric determination of end point. The polyethyleneglycol content is calculated as a difference.

3 RESULTS AND DISCUSSION

The system $MgSO_4$ - PEG-1000 - H_2O, 25°C. The system has a region of stratification . The points T and T^1 on the state diagram (Fig. 2) are the triple points, where $MgSO_4 \cdot 7H_2O$ is crystallized in the presence of two liquid phases. The conodes T-T^1, 1-1^1, 2-2^1 and so on are the locia of summary contents.Both of liquid phases contain much water, but the essential part of PEG-1000 is concentrated in the upper phase (so called "organic" phase), whereas $MgSO_4$ - in the lowest phase. The concentration of PEG-1000 in the upper phase is in 2-6 degrees greaterthan in lowest one, but the concentration of $MgSO_4$ in upper phase is changed from 0,16 to 4,67%. By stratification the water is redistribated between the phases, while the concentration of $MgSO_4$ in the lowest phase increases from 15,27 to 26,69% till saturation and crystallization of $MgSO_4 \cdot 7H_2O$. The field of stratification is

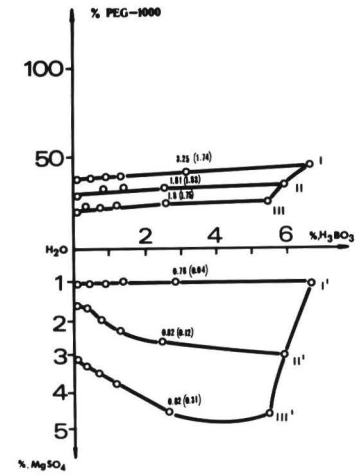

Fig. 3. The rays of extraction in the system PEG-1000 - $MgSO_4$ - H_3BO_3 - H_2O, 25°C ("organic" phase).

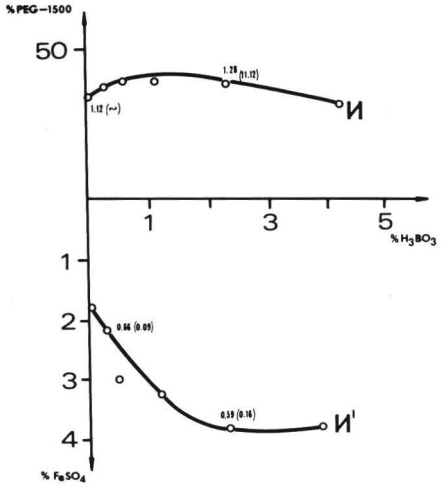

Fig. 4. The ray of extraction in the system $FeSO_4$ - PEG-1500 - H_3BO_3 - H_2O, 25 °C ("organic phase).

conserved till pH 10, even when little residue of $Mg(OH)_2$ is formed.

System PEG-1000 - $MgSO_4$ - H_3BO_3 - H_2O, 25°C. The boric acid at great initial concentration untill cryctallization is distributed between the both phases with partition coefficient more than 1. At small initial concentration all of boric acid is extracted in upper phase. The increasing of PEG-1000 shifts the limit of complete extraction of boric acid at the side of its greater concentrations. The rays of extraction in the system of coordinates H_3BO_3 - PEG (Fig. 3.) are rectilinear and parallel. In the coordinates H_3BO_3 - $MgSO_4$ only one of the rays of extraction is rectilinear (I^1), it is parallel to the abscissa axis, the concentration of $MgSO_4$ does not change and is small (0,99%). At the ray III^1 the concentration of $MgSO_4$ at the beginning increases linearly, but further the ray becomes leaning. The ray II^1 is S-type. Hereupon the concentration both of ② and of $MgSO_4$ change. The rays of extraction end in those points where the boric acid is crystallized. They form the line of crystallisation of boric acid. The systems PEG-15000 - $MgSO_4$ - H_3BO_3 - H_2O, 25°C also were investigated to inquire into the influence of polymer molar weight on the extraction of boric acid.

In the system with PEG-1500 the region of complete extraction of boric acid in the upper phase is shifted toward lower concen-

trations of boric acid, but in the system with PEG-15000, the latter is practically completely concentrated in the upper phase.

The system $FeSO_4$ - PEG-1500 - H_2O, 25°C also posesses the region of stratification, which is located at pH 1,11-7,0. In the system $FeSO_4$ - PEG-1500 - H_3BO_3 - H_2O (25°C) one ray of extraction, which starts in the point of summary concentration PEG - 25%, $FeSO_4$ - 5% and H_2O - 70% (Fig. 4.) is presented. In all the investigated region the boric acid is distributed between the both phases with a partition coefficient 1,12-1,80. The concentration of PEG-1500 in the lowest phase is not more than 2,6%. The regions of the complete extraction of boric acid in the upper phase are not observed.

4 PRACTICAL APPLICATION

The effect of stratification can be used in extraction of boric acid from brines, which contain $MgSO_4$ and $FeSO_4$ ($\sim$1 mol/l and 0,3 mol/l conseqvently). This is verified by addition of PEG to the brine till the stratification and separation of the upper layer, in which 2/3 of the total boric acid is concentrated. The procedure can be repeated three times.

5 CONCLUSIONS

1. The phase equilibria and solubility in the systems $MgSO_4$ ($FeSO_4$) - PEG-1000(1500,15000) - H_3BO_3 - H_2O (25°C) have been investigated. It is shown that the field of stratification is formed in these systems.

2. The field of stratification is regarded as an extraction system, which is described by means of the modified method of ray of extraction, where the ray of extraction means the locus that is formed at the increase of boric acid concentration. It is represented as two lines in two projection of the rectangular develop of state diagram of one of phases.

3. The stratification in two liquid phases by addition of PEG to brines, containing H_3BO_3, $MgSO_4$ and $FeSO_4$, is proposed for use in extraction of boric acid.

6 REFERENCES

1. Nikolaev A.V., Kurnakova A.G. Journ. Inorg. Chem. (Russ.) 1958, V.3. N 4. - p. 1037-1043.

12. SPECIAL APPLICATIONS: PETROCHEMICALS, BIOTECHNOLOGY

Solvent Extraction 1990, T. Sekine (Editor)

© 1992 Elsevier Science Publishers B.V. All rights reserved

HOLLOW FIBER FOR LIQUID-LIQUID EXTRACTION

S. R. WICKSRAMASINGHE, MICHAEL J. SEMMENS† and E. L. CUSSLER
Department of Chemical Engineering and Materials Science, †Civil and Mineral Engineering, University of Minnesota, Minneapolis, Minnesota 55455 (USA)

ABSTRACT

Current hollow fiber contactors are often designed to maximize mass transfer per volume. Such designs make sense for applications in heart-lung machines but not for commercial membrane separations. For commercial separations, better designs minimize the cost per mass transferred. The implications of minimizing the cost per mass transferred, explored here for simple contactor designs, can show optimum fiber sizes around 100-200 μm. At smaller fiber sizes, pumping costs are excessive; at larger fiber sizes, membrane costs are unnecessarily high.

INTRODUCTION

This paper will explore better designs for hollow fiber membrane contactors for liquid-liquid extraction. Hollow fiber membrane contactors allow dramatically improved performance when compared with conventional equipment (Zhang & Cussler (1985), Kiani *et al.* (1984)). They permit a more complete product recovery than conventional equipment, including centrifugal extractors. As a result, these contactors should find major future applications, beginning with antibiotic extraction (Prasad and Sirkar (1989)).

Existing hollow fiber contactors owe their high performance to their very large surface area per volume. This area per volume is typically around 50 cm^2/cm^3, and may be as high as 300 cm^2/cm^3. As a result, the solvent and feed phases can be contacted at high speed even if their densities are identical. In addition, the use of hollow fiber contactors avoids loading constraints like channeling and flooding. As a result, these hollow fiber modules offer advantages over conventional equipment.

There are two common types of liquid-liquid extractors: mixer-settlers and extraction towers. In mixer-settlers, the feed and solvent are mixed to give a dispersion, and then this dispersion is allowed to separate. Fast mixing gives a large surface area per volume but can produce stable emulsions which are difficult to break. Slow mixing, while avoiding stable emulsions gives a small surface area per volume and hence a slow separation. Like mixer-settlers, extraction towers can have a large surface area per volume, but their performance is affected by backmixing and flooding. Furthermore, both mixer settlers and extraction towers become difficult to operate as the densities of the feed and solvent become similar.

In hollow fiber liquid extraction, the pressure of a membrane resistance will reduce the rate of mass transfer compared to conventional equipment. Nevertheless, any reduction in the rate of mass transfer due to the membrane resistance is a small price to pay considering the huge surface area per volume possible (D'Elia *et al.* (1986)).

These features mean that hollow fiber module designs may be far from optimal but still

attractive. These sub-optimal designs often ignore maximizing the mass transfer coefficients, which is another major factor in determining module performance. These mass transfer coefficients are within a factor of five of those in conventional equipment, and are hard to change dramatically compared to the surface area per volume. As a result, early workers sensibly concentrated on the area per volume, where big gains were easier to achieve.

Recently module designers have turned to achieving better performances by increasing the mass transfer coefficients. These more mature designs are especially effective for blood oxygenators. These devices which serve as artificial lungs during surgery, increasingly use hollow fibers. The fibers are frequently arranged in geometries which allow easy manufacture and cross flow of blood outside the oxygen containing fibers. The easy manufacture is usually achieved by yarn winding machines; the cross flow increases the mass transfer coefficient.

Improved designs of hollow fiber contactors for commercial extraction will probably be different to those for blood oxygenators since the objective is different. For blood oxygenators, the objective is to maximize the oxygen transferred per module volume. This objective minimizes the module's priming volume and hence reduces the number of units of blood needed in the operation. This in turn reduces the risk of transfusions of infected blood.

Improved designs of hollow fiber contactors for extraction have a different objective. They try to minimize the cost per mass transferred. This new minimization is different to that desired in blood oxygenators. After all, in antibiotic recovery, priming volume is not a major concern.

In this paper, consideration is given to optimizing the design of hollow fiber contactors which minimize the cost per mass transferred. This study uses existing correlations for mass transfer coefficients and friction factors, as explained in the next section of the paper. Subsequent sections, discuss the implication of these results in commercial module design.

2 THEORY

2.1 General Considerations

The contactor designs developed in this paper assume that mass transfer can be influenced by resistances in either the feed or in the product, as well as by membrane permeability.

The microporous hollow fiber membranes used in this study were developed in the early 70's and consist of small tubes with internal diameters ranging from 50-400 μm. The fibers are made of the same polymeric materials commonly used for microporous flat membranes, such as polyolefins and cellulose esters. Properties like membrane thickness and porosity are similar to those of the corresponding flat membranes.

Many current microporous hollow fiber modules are designed like small shell-and-tube heat exchangers. Each consists of a glass or plastic shell containing a bundle of fibers (see Figure 1). At each end of the shell, the fibers are embedded in a potting material, often a polyurethane or an epoxy. Two distinct phases flow independently in the module. One phase flows inside the lumen of the fibers the other outside the fibers. While many hollow fiber modules have a

parallel flow configuration, some experiments using a cross flow configuration have also been reported (D'Elia *et al.* (1986); Prasad *et al.* (1986); and Yang & Cussler (1986)).

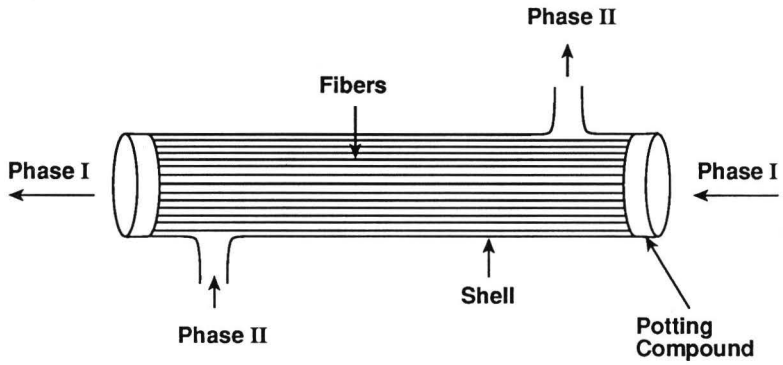

Fig. 1. Hollow Fiber Module. In this figure, the shell side fluid is shown flowing parallel to the tube side fluid.

When comparing hollow fiber liquid extraction to conventional extraction, the following characteristics must be considered:

(1) the increased mass transfer due to the larger fiber surface area per unit volume;
(2) the greater range in flow rates without channelling and flooding;
(3) the decreased mass transfer rate due to diffusion across the membrane;
(4) the cost of the fibers; and
(5) the larger pressure drop in the modules;

The first two characteristics have been demonstrated in earlier efforts (D'Elia *et al.*(1986)), but the last three merit more discussion here.

The decreased mass transfer rate due to the membrane diffusion is buried in the usual expression for mass transfer:

$$N = K\Delta C \tag{1}$$

where N is the solute flux, ΔC is the overall solute concentration difference, and K is the overall mass transfer coefficient. The overall coefficient, K, which is usually independent of concentration, results from three contributions, one from each of the individual mass transfer coefficients (see Figure 2). If the pores are filled with Phase I as is shown in Figure 2, the solute concentration is a continuous function with respect to distance from the bulk phase I solution to the right hand wall of the membrane. The concentrations at the right hand wall of the membrane are assumed to be in equilibrium. If phase I is taken as the reference phase, the overall mass transfer coefficient is given by

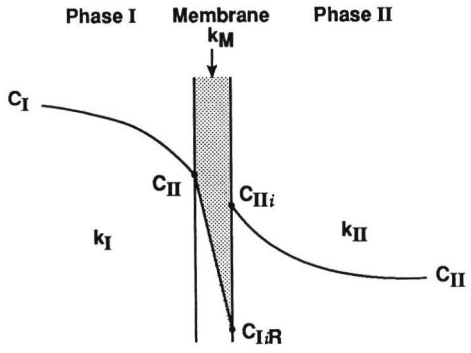

Fig. 2. Variation of Solute Concentration Across the Membrane

$$\frac{1}{K} = \frac{1}{k_1} + \frac{1}{k_M} + \frac{1}{mk_{II}} \tag{2}$$

The membrane mass transfer coefficient, k_M, is not a function of flow rates in either bulk phase, but depends upon the membrane material and the membrane thickness. The mass transfer coefficients, k_I and k_{II}, are functions of flow, and can be estimated using mass transfer correlations. For example, if Figure 2 represents a hollow fiber with k_I being the mass transfer coefficient for mass transfer through the boundary layer inside the fibers, then k_{II} is the mass transfer coefficient for mass transfer through the boundary layer outside the fibers.

To design a hollow fiber module, we first estimate the three individual mass transfer coefficients to determine the overall mass transfer coefficient and, hence, the flux across the membrane.

The mass transfer coefficient inside the fibers:

$$Sh = 1.62Gr^{0.33} \tag{3}$$

Equation (3) is a theoretical result obtained by Lévêque (1928). Many investigarors (Yang & Cussler (1986), Semmens *et al.* (1989), and Prasad and Sirkar (1988)) have used the Lévêque solution. The Lévêque solution is a limiting case of the more general Graetz solution (Graetz (1883 and 1885) and Knudsen & Katz (1958)). Prasad and Sirkar (1988) pointed out that the applicability of the Lévêque solution depends on the value of the Graetz number. For fiber lengths less than 35 cm the Lévêque solution is valid.

The following correlations are often used to describe the mass transfer coefficient outside

the fibers.

$$Sh = 1.25\left[Re\ d_e/\ell\right]^{0.93} Sc^{0.33} \tag{4}$$

$$Sh = \beta\left[d_e(1-\phi)/\ell\right] Re^{0.6} Sc^{0.33} \tag{5}$$

Equation (4) was developed by Yang and Cussler (1986) for a packing fraction, ϕ, of 0.25. ϕ is generally a function of the diameter to pitch ratio which is commonly used in heat exchanger analyses. Equation (5) developed by Prasad and Sirkar (1988) is similar in form. The major differences are the lower power to which the Reynolds Number is raised and the inclusion of ϕ as a parameter in the correlation. We expect both correlations to give similar results as long as ϕ is around 0.25 as in the case here. Here Equation (4) is used to describe the shell side mass transfer coefficient.

We now turn to the last two characteristics of hollow fibers given above, which are the fiber cost and the large pressure drop. Larger pressure drops increase the pumping cost, which is expected to be the largest operating cost. We will consider the sum of these costs in the modeling which follows.

2.2 Modeling

We begin by defining a performance index, η, as

$$\eta = \frac{\text{TOTAL COST}}{\text{MASS TRANSFERRED X TIME}} \tag{6}$$

The aim is to minimize η. The TOTAL COST is assumed to be

$$\text{TOTAL COST} = \text{MEMBRANE COST} + \text{PUMPING COST} \tag{7}$$

The pumping cost includes the cost associated with pumping the two liquid phases. We therefore expect

$$\begin{aligned}\eta = \Bigg[&\frac{\text{MEMBRANE COST}}{\text{AREA X LIFE}}\text{X MEMBRANE AREA} \\ &+ \left\{\frac{\text{COST}}{\text{ENERGY}}\text{X FEED POWER}\right\}_{\text{LIQUID 1}} \\ &+ \left\{\frac{\text{COST}}{\text{ENERGY}}\text{X FEED POWER}\right\}_{\text{LIQUID 2}}\Bigg] / \Big[\text{MASS TRANSFERRED}\Big]\end{aligned} \tag{8}$$

This may be expressed in symbols as:

$$\eta = \frac{\left\{a_f + b_f\left[1/2 f \rho_1 v_1^3\right] + b_f\left[1/2 f f \rho_2 v_2^3\right]\right\}\pi n d \ell}{Q_1 c_1\left[x_O - x_\ell\right]}. \tag{9}$$

In this equation Q_1 is the feed phase flow rate, c_1 is the feed phase concentration and x_O and x_ℓ are the entrance and exit mole fractions of the solute in the feed . Thus $Q_1 c_1[x_O - x_\ell]$ represents the mass transferred. The number of fibers is represented by n and the length of

the fibers by ℓ. The term $(\pi n d \ell)$ represents the total membrane area available and a_f is the membrane $\frac{cost}{area\ x\ life}$. The membrane cost per time is given by $a_f \pi n d \ell$. The cost per unit of energy for pumping the feed phase is represented by b_f, the friction factor for the feed is f, the density of the feed is ρ_1, and the feed velocity is v_1. Thus the term $b_f[1/2 f \rho_1 v_1^3]\pi n d \ell$ gives the pumping cost for the feed. In an analogous manner ff is the friction factor for the solvent phase, ρ_2 is the density and v_2 the velocity of the solvent. Thus the term $b_f[\frac{1}{2} ff \rho_2 v_2^3]\pi n d \ell$ gives the solvent phase pumping cost.

Equation (9) contains six unknowns: the number of fibers, n; the friction factor within the fibers, f; the friction factor outside the fibers, ff; the feed velocity, v_1; the solvent velocity, v_2; and the inside diameter of the fibers, d. The fiber length is specified. These six unknowns are constrained by five equations: two liquid flow constraints, one mass transfer equation, and two friction factor correlations. These are discussed next.

The two flow constraints are

$$Q_1 = \frac{\pi}{4} d^2 n v_1, \tag{10}$$

$$Q_2 = \frac{n d_O^2}{2}\left\{\sqrt{3}\xi^2 - \frac{\pi}{2}\right\} v_2. \tag{11}$$

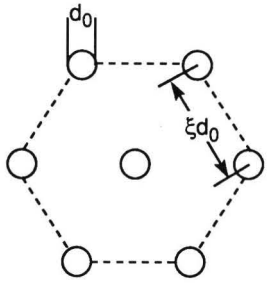

Fig. 3. Arrangement of Hollow Fibers

Equation (10) states that the volumetric flow Q_1 equals the feed velocity multiplied by the cross sectional area for flow. While Equation (11) is parallel it is somewhat more elaborate. To see why, we consider Figure 3. The fibers are assumed to be arranged in a hexagonal grid, with the center to center spacing equal to ξd_O. The fibers will touch when $\xi = 1$.

To derive Equation (11), we first recognize that the area of each hexagon is given by

$$\frac{3}{2}\left(\xi d_O\right)^2 \cot\left(30^\circ\right) = \frac{6}{4}\left(\xi d_O^2\right)\sqrt{3} = \frac{3}{2}\sqrt{3}\left(\xi d_O\right)^2. \tag{12}$$

There are three fibers per hexagon. Thus the area available for solvent flow is

$$\frac{n}{3}\left[\frac{3}{2}\sqrt{3}\left(\xi d_O\right)^2 - 3\pi\left(\frac{d_O}{2}\right)^2\right] = \frac{n d_O^2}{2}\left[\sqrt{3}\xi^2 - \frac{\pi}{2}\right], \tag{13}$$

where d_O is the outside diameter of the fibers. When n is large, the deviations from hexagonal symmetry caused by the fibers at the wall of the module are minor. The mass transfer constraint is described by:

$$\frac{K_1 a c_1 \ell}{L_2 H} = \frac{1}{HL_2/L_1 - 1} \ell n \left(\frac{y_O - m x_O}{y_\ell - m x_\ell} \right). \tag{14}$$

In Eq. (14), K_1 is the overall mass transfer coefficient based on the feed phase, a is the interfacial area per unit volume, L_2 is the solvent flux, m is the partition coefficient, L_1 is the feed flux, and y_O and y_ℓ are the exit and entrance solvent phase solute concentrations respectively. The friction factor correlations are similarly straightforward. Since the flow within the fibers is laminar, the friction factor f is given by

$$f = \frac{16}{Re} = 16 \left(\frac{\nu_1}{d v_1} \right), \tag{15}$$

if the feed is inside the fibers. As the flow outside the fibers is slow, the friction factor is given by

$$ff = \frac{113}{\xi^{2.6}} \left(\frac{\nu_2}{d v_2} \right) \tag{16}$$

if the solvent phase is outside the fibers.

Thus, we have five constraints (Eq. 10-11 and 14-16) for the six unknowns (n, f, ff, v_1, v_2, and d) in Eq. 9. We can therefore calculate the contactor's performance η if we choose a value for one unknown. In our calculations, we choose d, and then find η.

To do so, however, we must also estimate the overall mass transfer coefficient K_1. As explained above, K_1 is composed of three individual mass transfer coefficients. However, this study is restricted to two limiting cases.

The first case is one where the major resistance to mass tranfer lies in the feed. Thus it is the mass transfer coefficient inside the fibers that dominates. Accordingly, the solvent phase mass transfer coefficient i.e. the mass transfer coefficient outside the fibers is neglected. Generally, the individual mass transfer coefficients for the two phases are similar. The extent of extraction of a solute is determined by the partition coefficient of the solute. It is this partition coefficient that determines whether the mass transfer resistance in the solvent or the feed phase dominates (see Equation (2)). Changes in pH lead to changes in the partition coefficient (Prasad & Sirkar (1989)). By ensuring that the phase in which the solute is more soluble wets the pores of the fibers the membrane resistance is minimized.

The second limiting case considered is the opposite to the first. Here it is the solvent phase mass transfer coefficient that dominates. Thus the mass transfer coefficient inside the fibers is neglected.

3 RESULTS

The general considerations given above allow calculation of the performance of hollow fiber membrane contactors. The results obtained for the first limiting cases, the extraction of a

solute from a feed where the major mass transfer resistance lies in the feed phase, are given in Figures 4 and 5. These results show that an optimum fiber diameter exists which minimises η, the COST/MASS TRANSFERRED. The curves in the figures were obtained by calculating η for various values of d. Parenthetically, the method of Lagrange mulitpliers verified that the optimum fiber diameters are in the 50-250 μm range consistent with Figures 4–5. Fibers used commercially also fall in this range. A description of the method of solution of Equations 9–11 and 14–16 is given by Wickramasinghe *et al. (accepted).*

We can easily explain why the minima in Figures 4–5 occur and why costs increase if the fiber diameter is decreased or increased.

At very small fiber diameters, much less than the optimum, η may be shown to vary with d^{-4}. Smaller fiber diameters give rise to higher pumping costs of both phases. As the fiber diameter decreases, the cross sectional area for flow inside the fibers is reduced. Thus the velocity of the feed is increased, as is the pumping cost. Because cross sectional area available for flow outside the fibers is given by $\left[\frac{nd_0^2}{2}[\sqrt{3}\xi 2 - \frac{\pi}{2}]\right]$, reducing the fiber diameter also reduces the area available for flow outside the fibers. Thus the velocity of the solvent increases and the pumping cost increases accordingly.

For large fiber diameters, membrane costs dominate η. As the fiber diameter increases, the surface area for mass transfer also increases. Therefore, though the pumping costs decrease, the membrane cost increases as the fiber diameter increases. At large fiber diameters, Figures 4 and 5 show that η varies linearly with d. This is consistent with Equation (9) for, if the pumping costs can be neglected, the equation collapses to

$$\eta = \frac{\{a_f\}\pi n d \ell}{Q_1 c_1 [x_0 - x_\ell]} \tag{17}$$

which clearly shows the linear dependence of η on d. Not surprisingly, Figure 4 also shows that increasing the membrane cost decreases the optimum fiber diameter.

Figure 5 shows that, as the fiber length is increased, so does the optimum fiber diameter. Increasing the length of the fibers increases the pumping costs. Therefore one needs larger fiber diameters before the membrane cost starts to dominate, hence pushing the optimum fiber diameter to larger values. The value of η at the optimum fiber diameter also increases because it costs more to pump a fluid further. Finally, all the curves tend to the same straight line at larger fiber diameters where the membrane costs become significant.

Turning to the second limiting case it is necessary to predict the mass transfer coefficient outside the fibers. Using the correlation developed by Yang and Cussler (Equation 4), we obtain Figures 6 and 7. A detailed description of the method of solution of Equations 9–11 and 14–16 is given by Wickramasinghe *et al. (accepted).* Comparing Figures 6 and 7 to 4 and 5, we see that the curves are similar. At small fiber diameters where the pumping costs dominate, we again find that η varies with d^{-4}. At larger fiber diameters where the membrane costs dominate, η is proportional to d. An optimum fiber between 200 and 1000 μm exists which minimizes the COST/MASS TRANSFERRED.

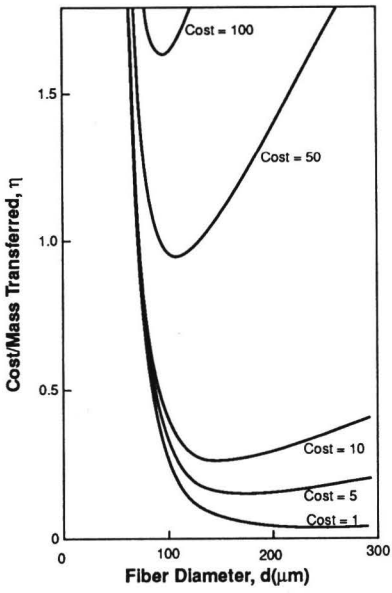

Fig. 4. Variation of membrane cost from \$100 $m^{-2}yr^{-1}$ to \$1 $m^{-2}yr^{-1}$ for case 1 where the mass transfer resistance in the feed dominates. As can be seen η of increases at small fiber diameters due to large pumping costs and large fiber diameters due to large membrane costs.

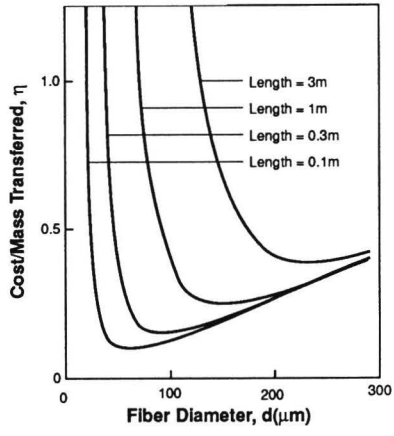

Fig. 5. Variation of fiber length from 3 to 0.1 m for case 1 where the mass transfer resistance in the feed dominates. As the fiber length increases the optimum fiber diameter increases since it cost more to pump a fluid further.

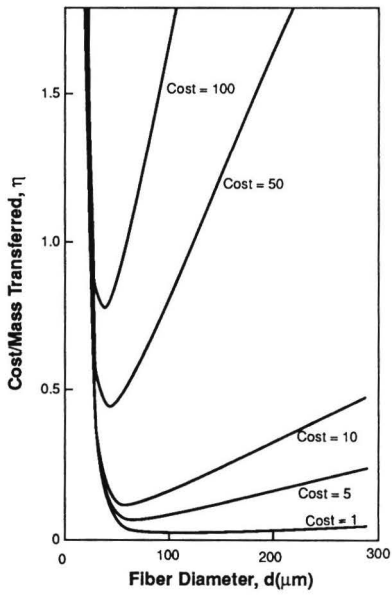

Fig. 6. Variation of membrane cost from \$100 $m^{-2}yr^{-1}$ to \$1 $m^{-2}yr^{-1}$ for case 2 where the solvent phase mass transfer resistance dominates. Using the Yang and Cussler correlation to describe the mass transfer coefficient outside the fiber produces curves similar to those in Figure 4.

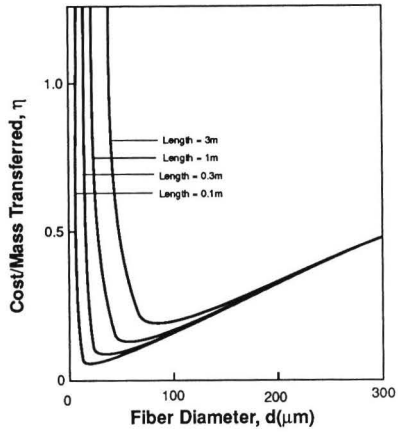

Fig. 7. Variation of fiber length from 3 to 0.1 m for case 2 where the solvent phase mass transfer resistance dominates. Using the Yang and Cussler correlation to describe the mass transfer coefficient outside the fibers produces curves similar to those in Figure 5.

4 DISCUSSION

The work above shows how the cost per mass transferred in a hollow fiber contactor can be dramatically influenced by the design of that contactor. In particular, the work shows that choosing fibers of too large a diameter leads to excessive membrane costs. Choosing fibers of too small a diameter leads to excessive pumping costs. Interestingly, optimal diameters center around a few hundred microns, which is the size of commercially available hollow fibers.

The accuracy of the estimates in the figures above is variable. Designs for the extraction of a solute where the major mass tranfer resistance is in the feed stream, evaluated in Figures 4–5, are the most dependable. In this case, the mass transfer is limited by diffusion within the lumen of the fibers. This lumen diffusion is well understood, both from theory and from experiment. Moreover, differences in manufacturing the modules rarely alter the flow in the lumen

Designs for the extraction of a solute where the major mass transfer resistance is in the solvent stream, given in Figures 6–7, are less reliable. There are two reasons for this reduced reliability. First, the mass transfer coefficient outside the fibers becomes important. Correlations for this external mass transfer coefficient are less well known, especially because the analogy between heat and mass transfer seems weak. More complete correlations for this case would help.

The second reason why Figures 6–7 are less reliable is that the flow on the shell side of the container is less well defined. Uniform flow is difficult to achieve and flows outside the fibers routinely show major channeling. Because of this channeling, we often find commercial modules with mass transfer coefficients ten to eighty times smaller than those expected from the mass transfer correlations. Reassuringly, we do find coefficients in good agreement with all correlations when we build laboratory scale modules with carefully spaced fibers to minimize channelling.

Thus our designs provide a best possible limit when mass transfer is dominated by flow outside the fibers. These designs are restricted to modules where the two phases are flowing countercurrently, in a shell-and-tube geometry.

5 ACKNOWLEDGEMENTS

This work was principally supported by the Hoechst-Celanese Corporation. Other support came from Bend Research, Inc., and from the National Science Foundation (grant CTS 8912634).

6 BIBLIOGRAPHY

Catapano, G., Bergins, M., Papenfuss, H. D., Rintelen, T. and Baurmeister, U. (1990), Mass Transport in Cross Wound Hollow Fiber Devices with Extra-luminal Flow (ELF), Proceedings of the 1990 International Congress on Membranes and Membrane Processes, Chicago, U.S.A.

D'Elia, N. A., Dahuron, L. and Cussler, E. L., (1986), Liquid-liquid Extraction with Microporous Hollow Fibers. *J. Membr. Sci.*, **29**, 309–319.

Graetz, L., (1883), Über die Wärmeleitungsfähigkeit von Flüssigkeiten. *Ann. Phys. Chem.*, **18**, 79–94.

Graetz, L., (1885), Über die Wärmeleitungsfähigkeit von Flüssigkeiten. *Ann. Phys. Chem.*, **25**, 337–357.

Kiani, A., Bhave, R. R. and Sirkar, K. K., (1984), Solvent Extraction with Immobilized Interfaces in a Microporous Hydrophobic Membrane. *J. Membr. Sci.*, **20**, 125–145.

Knudsen, J. G. and Katz, D. L., (1958), Fluid Dynamic and Heat Transfer. McGraw-Hill, New York, N.Y.

Lévêque, M. A., (1928), Les Lois de la Transmission de Chaleur par Convection. *Ann. Mines*, **13**, 201-299.

Prasad, R., Bhave, R. R., Kiani, A. and Sirkar, K. K., (1986), Further Studies on Solvent Extraction with Immobilized Interfaces in a Microporous Hydrophobic Membrane. *J. Membr. Sci.*, **26**, 79-97.

Prasad, R. and Sirkar, K. K., (1988), Dispersion-Free Solvent Extraction with Microporous Hollow Fiber Modules. *AIChE J.* , **34**(2), 177–188.

Prasad, R. and Sirkar, K. K., (1989), Hollow Fiber solvent Extraction of Pharmaceutical Products: A Case Study. *J. Membr. Sci.*, **47**(3), 235–259.

Semmens, M. J., Ren, Qin and Zander, A., (1989), Using Microporous Hollow-Fiber Membranes to Separate VOC's from Water. *J-Am. Water Works Assoc.*, **81**(4), 162–167.

Wickramasinghe, S. R., Semmens, M. J. and Cussler, E. L., Better Hollow Fiber Contactors, *J. Memb. Sci.* accepted.

Yang, M. C. and Cussler, E. L., (1986), Designing Hollow Fiber Contactors. *AIChE J.*, **32**, 1910–1916.

Zander, A. K., Semmens, M. J. and Narbaitz, R. M., (1989), Removing VOC's by Membrane Stripping. *J-Am. Water Works Assoc.*, **81**(11), 76–81.

Zhang, Qi and Cussler, E. L., (1985), Microporous Hollow Fibers for Gas Absorption I. Mass Transfer in the Liquid. *J. Membr. Sci.*, **23**, 321–332.

7 NOMENCLATURE

Roman Letters

a	interfacial area per unit volume	K	overall mass transfer coefficient
a_f	membrane cost per unit area	k	individual mass transfer coefficient
b_f	pumping cost per unit energy	ℓ	length of fibers
c	concentration	L	molar flux
ΔC	concentration difference	N	molar flux
d	inside diameter	n	number of fibers
d_0	outside diameter	Q	volumetric flow rate
f	friction factor	v	velocity
ff	friction factor outside the fibers	x	mole fraction of solute in the liquid
m	partition constant or Henry's Law constant	y	mole fraction of solute in the gas

Greek Letters

ϵ	porosity
η	defined by Equation (7)
μ	viscosity
v	kinematic viscosity
ϕ	packing factor
ρ	density
τ	tortuosity
ξ	defined in Figure 3

Subscripts

i	interfacial property
ℓ	length
M	membrane property
R	defined in Figure 2.1
O	evaluated at $z = 0$
I, 1	phase I property
II, 2	phase II property

Dimensionless Numbers

$Gr = \frac{d^2 v}{D\ell}$	Graetz number
$Re = \frac{\rho v d}{\mu}$	Reynolds number
$Sc = \frac{v}{D}$	Schmidt number
$Sh = \frac{kd}{D}$	Sherwood number

Solvent Extraction 1990, T. Sekine (Editor)
© 1992 Elsevier Science Publishers B.V. All rights reserved

EXTRACTION OF AMINO ACIDS AND PEPTIDES BY REVERSED MICELLES

S. FURUSAKI and K. KISHI
Department of Chemical Engineering
The University of Tokyo, Tokyo 113, Japan

ABSTRACT
Furusaki, S. and Kishi, K., 1990. Extraction of amino acids and peptides by reversed micelles. Proc. ISEC'90

Extraction of amino acids and peptides by reversed micelles was investigated using AOT as a micelle-forming surface active agent. The distribution between organic and aqueous phases was measured at various pH. The concentration of the amino acids and peptides inside the micellar aqueous core was much higher than the concentration in the bulk aqueous phase. The effects of hydrophobicity, electric charge and molecular weight of the peptides on the partition equilibrium were investigated and found to affect partitioning significantly.

1 INTRODUCTION

Separation of bioproducts from bioreactors is one of the important steps in bioprocesses. Liquid extraction is a prospective method for large scale separation of bioproducts because of its simpleness in operation. Recently, solubilization and extraction of proteins using reversed micelles has been investigated (Martinek et al., 1978; Luisi et al., 1979; Dekker et al., 1984; Goklen et al., 1985) and found to have good prospects, particularly for the application to crude but quick separation of bioproducts.

Since amino acids and low-molecular weight peptides have electrical charge depending upon pH, they are able to be extracted by reversed micelles. However, reports on extraction of amino acids or low-molecular weight peptides have been very few in number. Thus, it is the purpose of the present study to clarify behavior of the reversed-micellar extraction for low-molecular weight peptides in particular, comparing with the cases for amino acids or proteins.

2 MATERIALS AND METHODS

2.1 Reagents

Sodium di-2-ethylhexyl sulfosuccinate, i.e. AOT®, was used as a surfactant. It was a product of Nakarai Chemical Co., Kyoto. Isooctane and L-arginine(Arg) were analytical-grade reagents by Wako Pure Chemical Co., Tokyo. L-Tyrosine(Tyr) was a product of Kyowa Hakko Kogyo, Ltd., Tokyo. Peptides are the products of Sigma Chemical Co., St. Louis, MO. The reagents were used without further purification.

2.2 Experimental Methods

The extraction equilibrium was measured with a 100-cm^3 Erlenmeyer flask. The organic solvent was isooctane and the prescribed amount of AOT was added to it. To mix the organic and aqueous phases, a four-blade turbine of 2-cm diameter was used at ca. 600rpm. To separate the two phases, the macro-emulsion was centrifuged. The measuring time was about one hour which was sufficient to reach equilibrium. Temperature was regulated at 300K.

Amino acids were analyzed by the ninhydrine method. Peptide analysis was carried out by liquid chromatography using octadecyl silica gel (ODS) as the adsorbent. Water content in the organic phase was determined by the Karl-Fischer method.

3 RESULTS

3.1 Extraction behavior

The extraction of amino acids, peptides and protein (cytochrome C) was carried out. The aqueous and organic (isooctane) phases were brought into contact each in equal volumes. An example is shown in Fig.1. It has been observed that proteins are extracted effectively at pH lower than pI of the protein but the pH dependence of the amino acid extraction is not so sensitive as the case of the protein extraction (Hatton, 1987).

3.2 Extraction equilibrium of amino acids

Extraction of Arg and Tyr was studied (Furusaki et al., 1990) as functions of pH and ionic strength. The equilibrium could be expressed by the Freundlich-type equation. The number of Arg molecules extracted in a micelle was in the range 5-70, and the ratio of AOT molecules to Arg molecules in the micelles was between 4 and 12. Thus, Arg was not extracted in a congested manner inside the micelles. However, the Arg concentration in

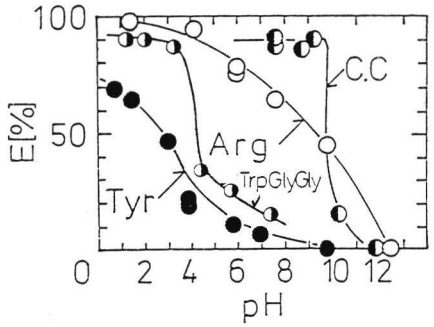

Fig.1. Effect of pH on extraction of amino acids and protein.
C_{AOT}=157mM, I=0.1M.
C.C.=cytochrome C

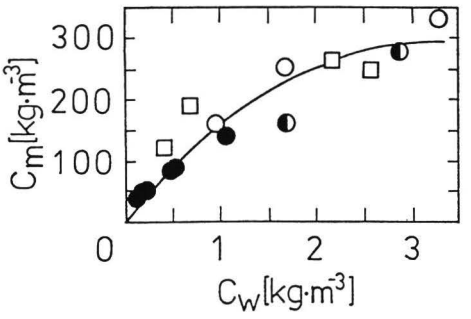

Fig.2. Concentration of Arg in the inner aqueous phase. I=0.1M (●),0.2M(□),0.5M(○),1.0M(◐)

the inner aqueous phase became much higher than that in the external aqueous phase (Fig.2).

3.3 Extraction equilibrium of low molecular-weight peptides

An example of the equilibrium of the reversed micelle extraction for low molecular-weight peptides is shown in Fig.3. It is expressed by the Henry-type equation in this experimental condition. (Concentration in this case was much lower than the case of the amino acid extraction in 3.2.) The extraction seems favorable for lower molecular weight compounds. The effect of the electric charge is seen in Fig.4.

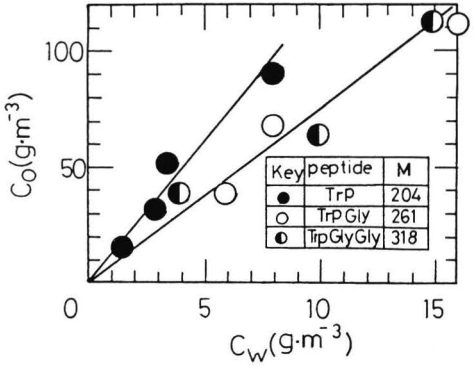

Fig.3. Distribution of Trp and Trp-derivative peptides.
Effect of molecular weight.
pH=1.2, C_{AOT}=50mM, I=0.1M.

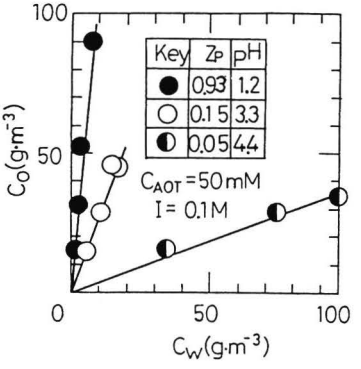

Fig.4. Distribution of Trp.
Effect of the electric charge.
C_{AOT}=50mM, I=0.1M.

As expected, molecules with large positive charge are extracted more preferably. Thus, molecular size and electrical charge are found to affect the partitioning equilibrium.

The effect of electric charge and hydrophobicity of peptides was investigated. The electric charge was calculated assuming that the amino acid residual groups were dissociated independently (Eq.(1), Fig.5).

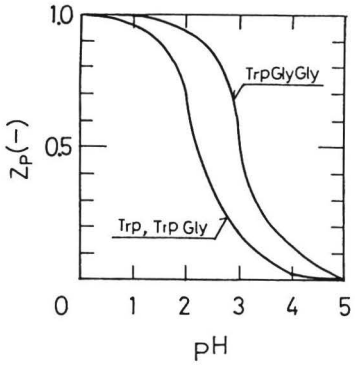

Fig.5. Variation of electric charge with pH.

$$Z_p = \sum_{i_p} \frac{n_{i_p}}{1 + 10^{pH - pK_{i_p}}} - \sum_{i_n} \frac{n_{i_n}}{1 + 10^{pK_{i_n} - pH}} \qquad (1)$$

Here, the each summation was done for all positive and negative residues, respectively, using the dissociation constants (Hayashi, 1971) for amino acids.

Several methods to express hydrophobicity have been proposed in previous literatures (Tanford, 1962; Nozaki et al.,1971; Hopp et al., 1981) using the free energy of solution from the aqueous phase to the organic phase. Rekker proposed in his book (1977) a similar index to express the hydrophobicity of peptides. His index (Rekker, 1977) was higher for more hydrophobic peptides. In this paper, we use his hydrophobicity index because of its simplicity. The hydrophobicity of peptides can be calculated as a sum of the hydrophobicity index assigned to the comprizing amino acids, if the peptide chain is shorter than 11 (Okuyama, 1981).

The effect of the electric charge density, Z_P/M, and the hydrophobicity of peptides on the distribution coefficient is shown in Fig.6 for some peptides. Peptides with high electric charge density and high hydrophobicity are extracted more

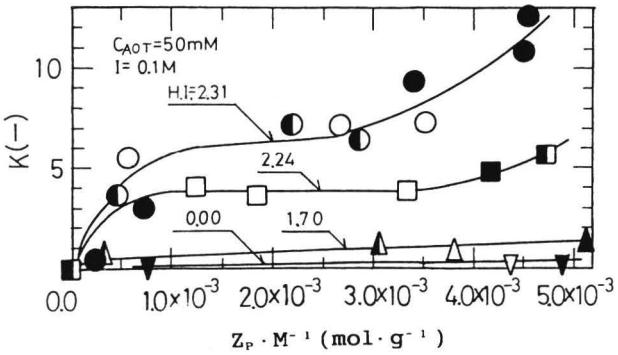

Key	peptide	Key	peptide
●	Trp	▲	Tyr
○	TrpGly	△	GlyTyr
◐	TrpGlyGly	◭	TyrGlyGly
◧	Phe	▽	GlyGly
■	PheGly	▼	GlyGlyGly
□	PheGlyGly		

Fig.6. Effect of the electric charge and hydrophobicity on the partition coefficient.

easily into the AOT microemulsion phase than those with low charge and low hydrophobicity. It seems that hydrophobic peptides tend to locate at the interface of the aqueous and organic phases. Thus, they are easily entrapped by the reversed micelles. The figure shows the plateau region where the distribution coefficient is not affected by the variation of the electric charge density. This nature is different from the extraction of amino acids.

4 CONCLUSION

Extraction of amino acids and peptides was studied using reversed micelles formed with AOT in isooctane. Equilibrium behavior was affected by electrical charge of the extracted materials. Ionic strength and AOT concentration in the organic phase also affected the equilibrium. In the case of peptides, the hydrophobicity affected significantly to the extraction characteristics.

5 NOTATION

C	$g \cdot m^{-3}$, $kg \cdot m^{-3}$	concentration
C_m	$kg \cdot m^{-3}$	concentration in the inner aqueous phase of reversed micelles
C_o	$g \cdot m^{-3}$, $kg \cdot m^{-3}$	concentration in the organic phase
C_w	$g \cdot m^{-3}$, $kg \cdot m^{-3}$	concentration in the aqueous phase
E	%	extraction yield
H.I.	——	hydrophobicity index
I	M	ionic strength
K	——	distribution coefficient

K_{in}	M	dissociation constant for the negatively charged in-th kind of amino acid fragment
K_{ip}	M	dissociation constant for the positively charged ip-th kind of amino acid fragment
M	$g \cdot mol^{-1}$	molecular weight
n_{in}	——	number of negatively charged fragments of the in-th kind of amino acid
n_{ip}	——	number of positively charged fragments of the ip-th kind of amino acid
pK	——	(-log K)
Z_P	——	average election charge

6 REFERENCE

Furusaki, S., Kishi, K., 1990. Extraction of amino acids by reversed micelles. J. Chem. Eng. Japan, 23: 91-93.

Goklen, K.E., Hatton, T.A., 1985. Protein extraction using reversed micelles. Biotechnol. Prog., 1: 69-74.

Hatton, T.A., 1987. Extraction of proteins and amino acids using reversed micelles. In: ACS Symp. Ser. No.342, Ordered Media in Chemical Separations, pp. 170-183.

Hayashi, K., 1971. Electrical property of Proteins (in Japanese). Univ. Tokyo Press, Tokyo, p.143.

Hopp, T.P. and Woods, K.R. 1981. Prediction of protein antigenic determinants from amino acid sequences. Proc. Nath. Acad. Sci., 78: 3824-3828.

Luisi, P.L., Bonner, F.J., Pollegrini, A., Wiget, P., Wolf, R., 1979. Micellar solubilization of proteins in aprotic solvents and their spectroscopic characterization. Helv. Chim. Acta, 62: 740-753.

Martinek, K., Levashov, A.V., Klyachko, N.L., Berezin, I.V., 1978. Catalysis by water-soluble enzymes in organic solvents. Stabilization of enzymes against denaturation through their inclusion in reversed micelles of surfactant. Dokl. Akad. Nauk SSSR (trans. in English) 236: 951-953.

Nozaki, Y. and Tanford, C. 1971. The solubility of amino acids and two glycine peptides in aqueous ethanol and dioxane solutions. J. Biol. Chem., 10: 2211-2217.

Okuyama, T. and Sasagawa, T. 1981. Systematic analysis of brain peptides. (in Japanese) In: Kagaku no Ryoiki, Zokan No.133. (Biomedical Chromatography), Nankodo, Tokyo, p.57-77.

Rekker, R.F. 1977. The Hydrophobic Fragmental Constant. Elsevier, Amsterdam, p.301.

Tanford, C. 1962. Contribution of hydrophobic interactions to the stability of the globular conformation of proteins. J. Am. Chem. Soc., 84: 4240-4247.

van't Riet, K., Dekker, M., 1984. Preliminary investigation on an enzyme liquid-liquid extraction process. Proc. 3rd Eur. Cong. Biotechnol. vol 3. 540-544.

Solvent Extraction 1990, T. Sekine (Editor)

© 1992 Elsevier Science Publishers B.V. All rights reserved

SOLUBILIZATION OF CELLS IN ORGANIC SOLVENTS BY REVERSE MICELLES

N. PFAMMATTER, M. FAMIGLIETTI, A. HOCHKÖPPLER and P. L. LUISI[1*]
Institut für Polymere, ETH-Zürich, CH-8092 Zürich, (Switzerland)

ABSTRACT

This paper will briefly review the solubilization of microorganisms in organic solvent by reverse micelles. We will consider chronologically the papers dealing with this subject, whereby the case of yeast will be considered separately. In each example we will describe the basic solubilization experiments, the viability of the cells (including preliminary experiments in petrol), and the applications or application ideas which have been till now described.

INTRODUCTION

By using reverse micellar solutions, or water-in-oil microemulsions, it is in fact possible to solubilize microorganisms in organic solvents and to obtain a clear, thermodynamically stable, liquid, without significant light scattering in the near uv-region. Actually this lack of turbidity of the micellar solution containing cells permits to use the expressions "solution" and "solubilization". The question, why it is so, is not a trivial one. Actually, the difference in density between the cells and the solvent is larger in the organic solvent than in water - which should favor the sedimentation of the cells. Perhaps an important reason of the stability of the cell-containing micellar solutions lies in the fact, that cells often tend to be better separated from each other in this organic solution, because of the effect of the surfactant. In addition, the larger viscosity of the micellar solution may also inhibit sedimentation of cells. The lack of light scattering could be due to a favorable optical matching with the refracting index of the solvent.

It is also important to remark that the expression "solubilization **by** reverse micellar solution " is more correct, than the expression "solubilization **in** reverse micelles" . At this stage we do not know whether the structure of reverse micelles is maintained, and whether we can talk about reverse micelles hosting microorganisms in the water pool- as for the case of other biopolymeres described by Luisi (1985), Luisi and Magid (1986), Martinek et al. (1986), Luisi et al. (1988) and Battistel et al. (1990).

The activity of cells in the new environment can be expressed with the biotechnological term "viability", a measure of the capability of cells to survive. Viability can be evaluated by the classic technique of plating out on Petri dishes small aliquot of micellar solutions opportunely diluted with aqueous physiological solution - in other words, viability of cells in micellar solutions is referred to standard "aqueous" conditions. Recently, a polarographic method for testing the activity of cells directly in the organic medium has been proposed, which is based on the determination of oxygen consumption (respiration) by a Clark electrode directly in the micellar solution (Hochköppler et al. 1989).

[1*] to whom correspondence should be addressed

No experimental part will be reported in this review. The readers are kindly referred to the original literature cited here.

2. THE SOLUBILIZATION OF BIOLOGICAL MATERIALS IN ORGANIC SOLVENTS

The first successful experiments to solubilize bacteria by reverse micellar solutions (or water-in-oil microemulsions at larger water content), were carried out in Zurich, with E. coli and Acinetobacter calcoaceticus, using Tween 85 (polyoxyethylen sorbitan trioleate) (about 10%) as surfactant in isopropylpalmitate (IPP) as solvent and 3-4% (v:v) water solution containing nutrient medium. (Haering et al., 1985). Later the same group (1987), solubilized also Corynebacterium in the same system. **Tab. 1** gives a survey of these experiments. A clear organic micellar system containing up to 10^7-10^8 cells/ml (overall concentration), can be prepared under the described conditions. (In water this cell concentration afford a turbid suspension). As Haering et al. (1987) pointed out , see **Fig. 1**, the viability depends on the type of cell, and also on several external parameters.

TABLE 1 Survey of the experiments in reverse micellar solution

MICROORGANISM	SYSTEM	W_0[1]	VIABILITY[2]	REFERENCES
A.calcoaceticus E.coli C.equi	Tw 85/IPP	28	65 1	Haering et al.(1985)
A.calcoaceticus	Tw 85/IPP or IPP/Hexadecane	28	90	Haering et al.(1987)
B.cereus (spores) S.cerevisiae	Phospholip./ Toluene	-	>0.1 (100) >0.1	Darszon et al.(1988)
Mitochondria (Soybean)	AOT/Isoactane	> 10	n.d.	Hochköppler and Luisi (1989)
S.cerevisiae	Tw 85/IPP Aso/IPP Aso/Hd	14	40 90 (5. Gen.)[3] 60 90 (2. Gen.)	Pfammatter et al. (1989)
S.cerevisiae	Aso/crude oil crude oil	14	95 90	Fig. 6
P.alcaligenes B.subtilis Arthrobacter	Aso/crude oil	14	15 100 40	
Cyanobacteria	TW 85/Sp80/ IPP or Hexadecane	14	n.d.	Fig. 3

[1] W_0 = $[H_2O]/[Surfactant]$
[2] Viability in percent after 24 hours
[3] referred to the meaning of generation, see text. (1.number => 1.Generation)

Although stability was not so good with the E. Coli strain, (Haering at al. 1985), the experiments lead to the conclusion that the cells in reverse micelles in this case seem capable of protein biosynthesis.

The group of Darszon (1988) showed the transfer of bacteria (Bacillus cereus), spores from the same bacilli and baker's yeast into a ternary system composed of toluene, phospholipids

(essentially asolectins) and a low amount of water.

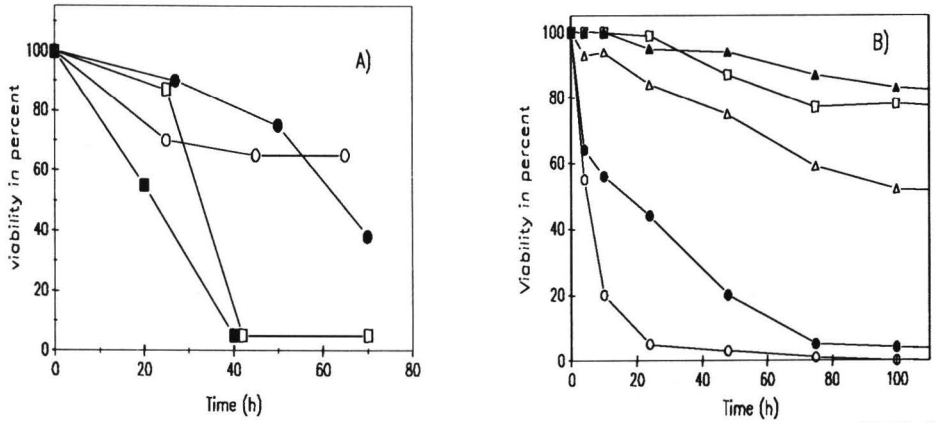

Figure 1 Influence on the viability of cells solubilized by Tw 85 in a micellar solutions. **(A)** Acinetobacter cal. in IPP (□, ○), and in a mixture of IPP/HD 7:2 (■, ●) as a function of the handling method: (●, ○) keeping them standing and (■, □) shaking. **(B)** Dependance of Baker's Yeast in IPP on watercontent. (W_0 = [H_2O]/[surfactant]). (○) => W_0 = 7, (●) => W_0 = 11, (△) => W_0 = 14, (□) => W_0= 20, (▲) => W_0= 25.

The solubilization technique was actually slightly different from that used in Zurich. The authors could show that the electron chain of yeast and bacteria preserved its functional integrity in the ternary system. In such a system, however, only one out of 10^4 yeast cells were viable after 24 hrs. In contrast, the viability of spores was not affected up to 30 days.

In the same year, a paper (Hochköppler et al. 1988) reported on the solubilization of mitochondria (extracted from soybean nodules) in AOT/isooctane water-in-oil microemulsions.

Preliminary light scattering experiments have shown that the dimensions of the organelles in the micellar solutions are not significantly altered with respect to water. The same information is also given by studies with the electron microscopy **(Fig.2)**.

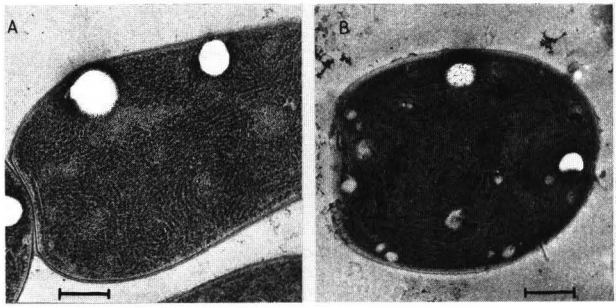

Figure 2. TEM pictures of Cyanobacteria: A) in growth medium, and B) solubilized in 76 mM Tw /IPP, w_0 = 14, after 24 hours. The bar corresponds to 3 μm. (Enlargement 18'000 times).

Until now, all attempts to solubilize cells or organelles in the organic media were carried out empirically. The first attempt to follow a more systematic pattern was accomplished in the case of Cyanobacteria. (Familietti et al., in prep.)

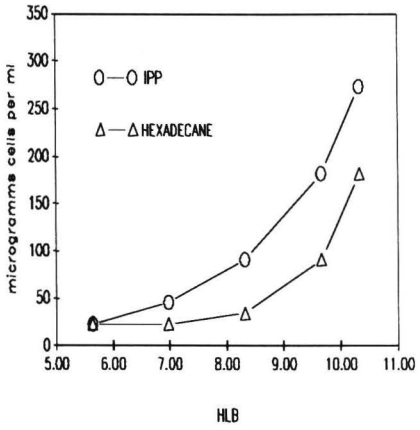

Figure 3 Influence of the HLB on the amount of Cyanobacteria to get clear solutions. (cells added with 15µl growth medium in 2 ml micellar solution.)

Recognizing that the matching between the structure of the cell surface and the hydrophobicity of the surfactant system may be an important factor to affect the solubilization, the influence of the HLB (Hydrophilic /Lipophilic Balance) of the surfactant system on the extent of solubilization was studied.

From **Fig. 3** it is apparent that indeed the HLB (determined by varying the relative proportion of the two co-surfactant, Tween 85 and Span 80) has an important influence on the solubilization, which increases remarkably for a HBL value above 8-9.

This may be one way to answer the question, if it is possible to find conditions under which the viability of cells in the organic medium extend to periods of several days or even several weeks. Then this question is important thinking of biotechnological applications.

A first positive answer in this direction could be reached during the work with yeast cells. In the following section, we will consider the case of yeast cells in some more detail.

3. BAKER'S YEAST AND FIRST EXAMPLES OF APPLICATIONS

Yeast cells are larger than most of the bacteria mentioned until now, but the solubilization is successful, (Pfammatter et al. 1989) in different solvent/surfactant systems.

The viability is affected by a series of parameters, such as w_o, nature of surfactant system, nutrient medium, and mechanical conditions (See **Fig. 1** and also **Tab. 1**).

In this case a polarographic method was used to determine the activity and concentration of cells directly in the organic milieu. (Hochköppler et al. 1989). In particular, the question was raised, of whether there is a linearity between cell concentration and activity even beyond the limit of solubility, where the solution becomes a cloudy suspension (**Fig. 4**).

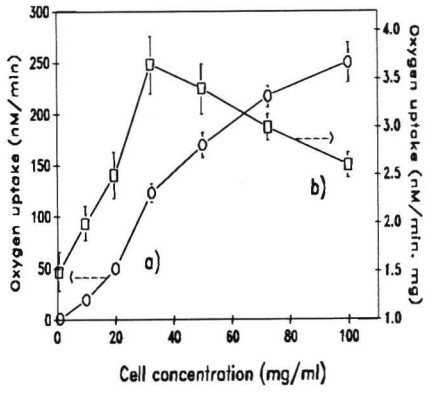

Figure 4. Dependence of the cell concentration on the oxygen uptake in 100 mM Tw 85/IPP, w_0=14: a) Absolute O_2 consumption; b) Consumption normalized to the cell concentration (per mg fresh cells)

Polarographic methods have been used also to monitor the activity of plant cells. In the paper dealing with Rumex obtusifolius, Hochköppler et al. (1990) describe that under the micellar conditions the plant cells give not the normal photosynthetic response as in water, but the light induces the consumption of oxygen in the presence of ascorbate. The activity is higher at high w_o and this indicates that the water content in the water pools affects the cellular activity in the ascorbic acid reaction.

Pfammatter et al. (1989) showed that in the system asolectin/IPP, over 20% of yeast's survival can be obtained after 9 days and cells are sensitive to the kind and amount of nutrient present in the aqueous component. In this paper the interesting observation was made, that the viability can be considerably improved by working with yeast cells obtained from parent cells which had already experienced the micellar environment. One can define actually a "second generation" a "third generation " and so on.

Let us consider now briefly some of the applications. The first successful attempt has been described by Fadnavis et al. (1989): yeast cells cross-linked with glutaraldehyde to minimize the protein extraction by reverse micelles have been used to catalyze the enantioselective hydrolysis of aminoacid derivatives.

Later on Fadnavis et al. (1990) show some results with yeast cells immobilized on calcium alginate beads. While the free cells are completely destroyed within a few hours, the immobilized cells are able to survive for several days. In this way, the authors were able to utilize yeast cells for the synthesis of peptide bonds. This is analogous to peptide synthesis catalyzed by proteases solubilized in reverse micellar solution, described by Lüthi et al (1984), and Pessina et al. (1988).

An elegant organic chemistry application of yeast cells suspended in organic solvent has been offered by Haag et al (1989). The reaction studied was the reduction of β-ketoesters and ester hydrolysis to yield optically active products. The system used was IPP containing asolectins as surfactants. In this case yeast cells were suspended in the organic medium without adding water, and yields surpassed those reported in aqueous media.

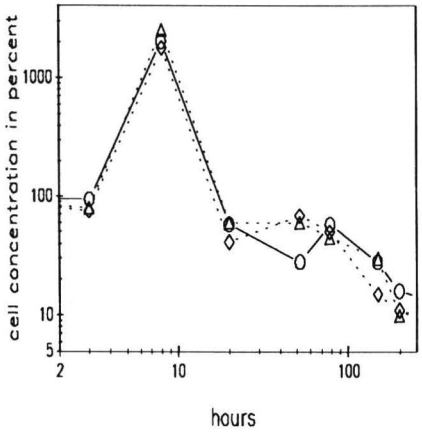

Figure 5 Cell growth at high cell concentrations: Yeast cells in Tw 85/IPP, w_0= 14 prepared with nutrient medium. (3 independent trials)

Do cells reproduce in the microemulsion system? Preliminary data indicate the growth of pseudomonas in a micellar system consisting of Tw 85/IPP (or Hexadecane).

Similar results (see **Fig. 5)** have been obtained in our group in the case of yeast. (Böhler 1989).

It has also been found that petrol, it can work as a solvent which permits the micellar solubilization of bacteria. We were able for

example to solubilize in it several types of cells, and **Fig. 6** shows some typical viability data.It is also interesting to notice that in crude oil we were able to solubilize bacteria without the help of additional surfactants (however, a certain amount of water was necessary). Most probably, there are enough molecules in petrol that display the capability of acting as surfactants.

We are presently investigating model reactions for the biodegradation of sulfur-containing products in crude oil. One of such model reaction is the degradation of dibenzothiophene.

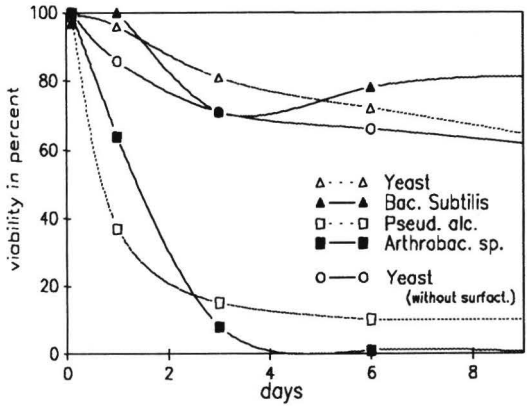

Figure 6 Viability of different cells in Asolectin/crude oil (50mg/ml). W_0=14. (Symbol legend in the graph)

4. REFERENCES

Battistel, E., Imre, E.V., Luisi, P.L., 1990. Solubilization and Structural Properties of Nucleic Acids in Reverse Micelles. In: Morton Rosoff (Ed), Controlled Release of Drugs: Polymers and Aggregate Systems.

Böhler, C., 1989. ETH diplomawork

Darszon, A., Escamilla, E., Gomez Puyou, A., Tuena de Gomez Puyou, M.,1988. Biochem. Biophys. Res. Comm., 151: 1074-1080.

Fadnavis, N.W., Prabhakar Reddy, N., Bhalerao, U.T., 1989. J. Org. Chem., 54: 3218-3221.

Fadnavis, N.W., Deshpande, A., Chauhan, S., Bhalerao, U.T., 1990. Submitted for publication.

Haag, T., Arslan, T., Seebach, D., 1989. Chimia, 43: 351-353.

Haering, G., Luisi, P.L., Meussdoerffer, F., 1985. Biochem. Biophys. Res. Comm., 127: 911-915

Haering, G., Pessina, A., Meussdoerffer, F., Hochkoeppler, A., Luisi, P.L., 1987. Ann. N.Y. Acad. Sci., 506: 337-344.

Hochkoeppler, A., Luisi, P.L., 1989. Biotechn. Bioeng., 33: 1477-1481.

Hochkoeppler, A., Pfammatter, N., Luisi, P.L., 1989. Chimia, 43: 348-350.

Hochkoeppler, A., Luisi, P.L., 1990. Biotech. Bioeng., in press.

Luisi, P.L., 1985. Angew. Chem., 97: 449-460

Luisi, P.L., Giomini, M., Pileni, M.P., Robinson, B.H., 1988. Biochim. Biophys. Acta, 947: 209-246.

Luisi, P.L., Magid, L.J., 1986. Crit. Rev. Biochem. (CRC), 20: 409-474.

Lüthi, P., Luisi, P.L., 1984. J. Am. Chem. Soc., 106: 7285-7286.

Martinek, K., Levashov, A.V., Kljachko, N., Khmelnitski, Y.L., Berezin, I.V., 1986. Eur. J. Biochem., 155: 453-468

Pessina, A., Lüthi, P., Luisi, P.L., 1988. Helvetica Chimica Acta, 71: 631-641.

Pfammatter, N., Guadalupe, A.A., Luisi, P.L. 1989, Biochem. Biophys. Res. Comm. 161. 1244-1251.

Solvent Extraction 1990, T. Sekine (Editor)

© 1992 Elsevier Science Publishers B.V. All rights reserved

SEPARATION AND CONCENTRATION OF PROTEINS WITH LIQUID-LIQUID EXTRACTION USING REVERSED MICELLES

T. NISHIKI, I. SATO and T. KATAOKA
Department of Chemical Engineering, University of Osaka Prefecture,
804 Mozu-Umemachi 4-cho, Sakai, Osaka 591 (Japan)

ABSTRACT
Nishiki, T., Sato, I. and Kataoka, T., 1990. Separation and concentration of proteins with liquid-liquid extraction using reversed micelles.

Protein extractions using Aerosol OT (AOT)-isooctane reversed micelle solutions have been studied to explore the potential for separating and enriching proteins with the reversed micellar extraction. The effects of pH, ionic strength and chlorides in a bulk aqueous phase, and AOT concentration in an organic phase on the partitioning of lysozyme and myoglobin and the solubilization of water were examined in detail. Lysozyme could be enriched into the reversed micellar phase up to thirty times the aqueous feed concentration. Lysozyme in the reversed micellar phase was efficiently stripped with potassium chloride solutions, whose concentration was 1-2 kmol/m^3 and pH was 11-12. The results indicated that the separation of two proteins and the concentration of lysozyme are capable.

1. INTRODUCTION

In biotechnology there is a need for efficient methods that can separate and concentrate proteins continuously and that can be scaled up easily. A liquid-liquid extraction utilizing reversed micelles may serve these purposes. It has been demonstrated that under certain conditions proteins can be transferred from an aqueous phase to a reversed micellar phase or vice versa (Dekker et al., 1986, 1989). There have been also some papers (Goklen and Hatton, 1987; Abbott and Hatton, 1988; Kuboi et al., 1990) on the factors affecting the partitioning of proteins between a bulk aqueous phase and a reversed micellar phase. However, the investigation of reversed micellar protein extraction is still in its infancy.

In the present paper, the effects of pH, ionic strength and cation type in a bulk aqueous phase, and surfactant concentration in an organic phase on the partitioning of proteins and the solubilization of water by reversed micellar extraction are presented. It is shown that lysozyme can be highly enriched into a reversed micellar phase. The conditions for stripping lysozyme from a reversed micellar phase to an aqueous phase are also examined.

2. EXPERIMENTAL

2.1 Materials

Anionic surfactant bis(2-ethylhexyl) sodium sulfosuccinate (AOT) was obtained from Kishida Chemical Co. In all experiments, AOT was used after drying for about 15 hours at 105°C. Organic solutions were prepared by dissolving the desired amount of AOT in isooctane. Proteins used in this study were lysozyme (MW 14,300, pI 11.1) from egg white and myoglobin (MW 17,000, pI 8.2) from equine muscle which were obtained from Sigma Chemical Co. The pH of aqueous solutions was adjusted with either hydrochloric acid or potassium hydroxide solutions. The ionic strength of aqueous solutions was adjusted using chlorides such as NaCl, KCl, $CaCl_2$ and $BaCl_2$. The salts and isooctane were guaranteed reagent grade.

2.2 Procedures

Known volumes of aqueous protein solution and organic AOT solution were contacted in a magnetically agitated Erlenmeyer flask for 15 minutes. The resulting mixture was centrifuged and the two phases were then separated. The protein concentration in each phase was determined from the UV absorption at 280 nm (Shimadzu UV-260 spectrophotometer). The percent of protein extracted to the organic phase was then calculated. The pH value of the aqueous phase was measured with a pH meter. The water content in the organic phase was determined by the Karl-Fischer titration.

Stripping experiments were performed by mixing known volumes of lysozyme-solubilized organic solution and aqueous solution for 30 minutes. After centrifugation, the phases were separated and analyzed similarly by the above methods.

3. RESULTS AND DISCUSSION

3.1 Extraction

(1) Effect of pH Aqueous feed solutions containing 1 mg/cm^3 of lysozyme were contacted with 50 mol/m^3 AOT solution at volume ratios of 1:1 and various pH values. Fig. 1 shows the percent extraction, E, of lysozyme with varying pH for each chloride. The degree of lysozyme extracted to the reversed micellar phase is affected by pH values and a pH range for 100% extraction is changed by the cation.

The result for myoglobin extraction

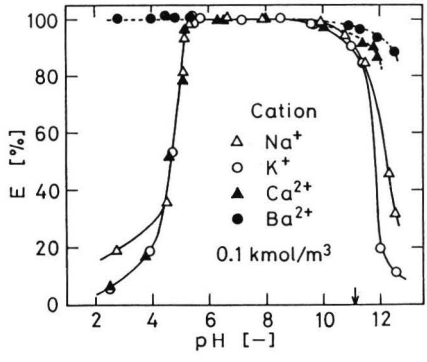

Fig. 1. Effect of pH on lysozyme extraction. C_{aqi}=1 mg/cm^3, [AOT]=50 mol/m^3.

is similarly shown in Fig. 2. About 30% of myoglobin is extracted from 0.1 kmol/m^3 KCl solution at pH=6, while no myoglobin is extracted at pH values above 8. It is expected from the results that a mixture of lysozyme and myoglobin can be separated by adjusting the pH of protein solution to about 8. Myoglobin is thoroughly extracted from 0.1 kmol/m^3 $BaCl_2$ solution at pH=5.3.

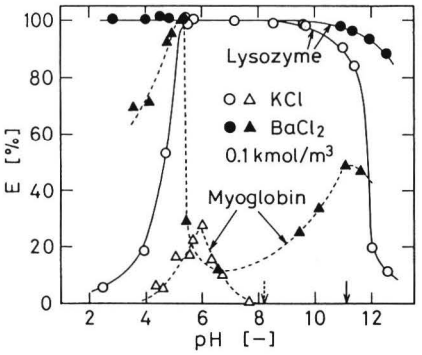

Fig. 2. Effect of pH on myoglobin extraction. C_{aqi}=1 mg/cm^3, [AOT]=50 mol/m^3.

(2) Effect of ionic strength

Fig. 3 shows the effect of ionic strength, I, on lysozyme extraction. In this case, aqueous solutions were adjusted to pH values at which 100% extraction is capable for respective chloride of 0.1 kmol/m^3. The extraction of lysozyme is affected by the concentration of K^+ or Ba^{2+}, but is almost independent of that of Na^+ or Ca^{2+}, whose ionic diameter is smaller than that of K^+ and Ba^{2+}.

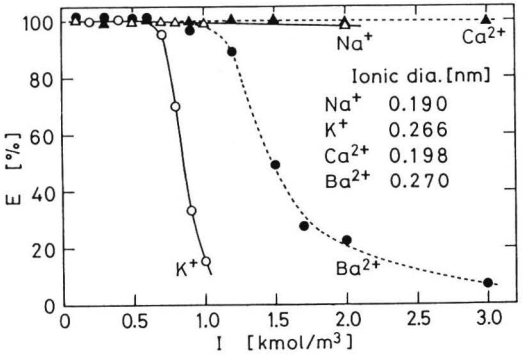

Fig. 3. Effect of ionic strength on lysozyme extraction. C_{aqi}=1 mg/cm^3, [AOT]=50 mol/m^3.

The water contents, W_o, solubilized in the organic phase are plotted against I in Fig. 4. W_o is defined as the molar ratio of water to AOT. The solubilization of water is higher for smaller cation. The change in the solubilization with I is remarkable for univalent cation in comparison with divalent cation.

(3) Effect of volume ratio of aqueous to organic phase In order to examine the extent to which lysozyme can be concentrated in the micellar phase, 1 mg/cm^3 lysozyme solution and 50 mol/m^3 AOT solution were contacted at volume ratios greater than 1. Fig. 5 shows the plots of the lysozyme concentration of micellar phase, C_{org}, versus $C_{aqi}(V_{aq}/V_{org})_i$ and W_o versus $C_{aqi}(V_{aq}/V_{org})_i$, which corresponds to the amount of lysozyme in the aqueous feed solution. For 0.1 kmol/m^3 KCl lysozyme is enriched in the micellar phase up to 14 times the aqueous feed concentration. Similar behaviors are observed between the change in

C_{org} and that in W_o with $C_{aqi}(V_{aq}/V_{org})_i$ for 0.1 kmol/m^3 KCl and NaCl, respectively, but W_o values for 0.1 kmol/m^3 $BaCl_2$ is nearly constant regardless of C_{org} values.

The effect of AOT concentration, [AOT], on lysozyme extraction is shown in Fig. 6. It is seen from the result that the extent of lysozyme concentrated in the micellar phase increases with an increase in [AOT]. The maximum concentration of lysozyme in 100 mol/m^3 AOT solution is about two times that for 50 mol/m^3 AOT. Thus, the reversed micellar solution in which lysozyme concentration is about thirty times that in the aqueous feed solution is obtained at one extraction step.

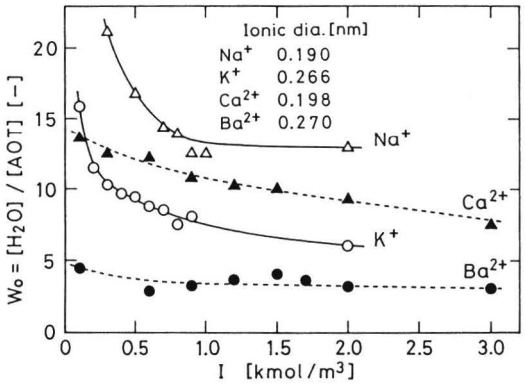

Fig. 4. Effect of ionic strength on the solubilization of water. Lysozyme extraction C_{aqi}=1 mg/cm^3, [AOT]=50 mol/m^3.

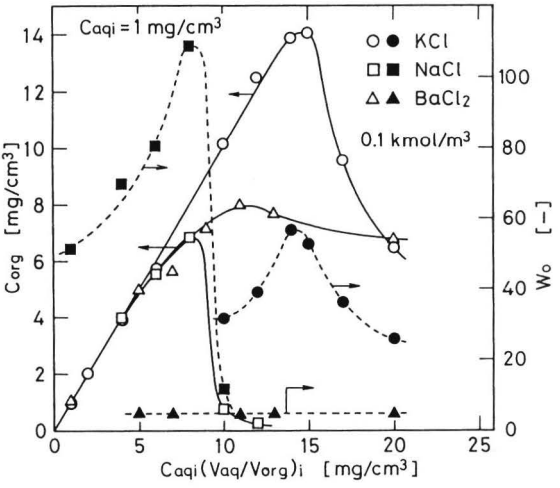

Fig. 5. Effect of volume ratio on lysozyme extraction and the solubilization of water. [AOT]=50 mol/m^3.

3.2 Stripping

(1) Effect of pH

Reversed micellar solutions solubilized lysozyme in the concentration of 1 mg/cm^3 were contacted with 1 kmol/m^3 KCl solution at volume ratios of 1:1 and various pH values. Fig. 7 shows the percent of lysozyme, E_b, stripped to the aqueous phase with varying pH. For AOT concentrations of 50 and 200 mol/m^3, there is no difference in the change in E_b with pH. About 95% of lysozyme in the micellar phase can be stripped to the aqueous phase at pH=11-12.

(2) Effect of ionic strength The effect of ionic strength, which was adjusted with chlorides, on lysozyme stripping is shown in Fig. 8. Potassium

chloride is good as the chloride by which lysozyme can be stripped efficiently and its optimum concentration is 1-2 kmol/m^3.

(3) Effect of volume ratio of organic to aqueous phase

Stripping experiments were carried out by varying volume ratios of organic to aqueous phase greater than 1 for various lysozyme concentrations, C_{orgi}, in the organic phase. The aqueous concentrations, C_{aq}, of lysozyme stripped from the micellar

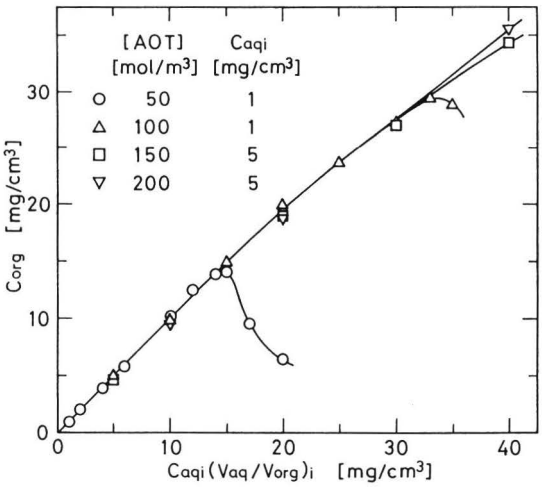

Fig. 6. Effect of AOT concentration on lysozyme extraction. [KCl]=0.1 kmol/m^3.

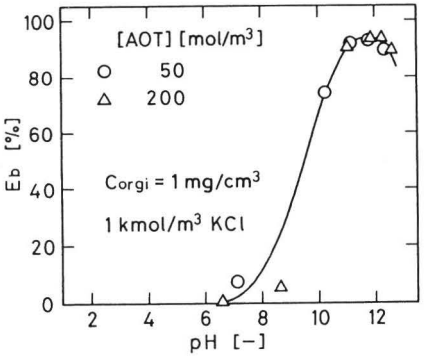

Fig. 7. Effect of pH on lysozyme stripping.

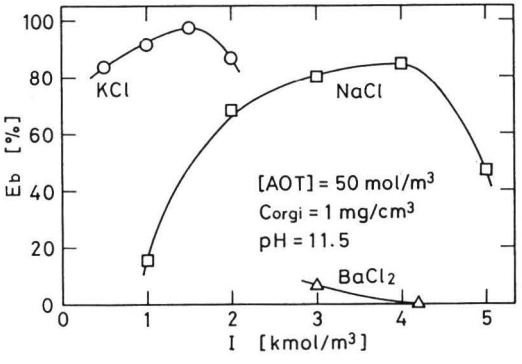

Fig. 8. Effect of ionic strength on lysozyme stripping.

phase are plotted against $C_{orgi}(V_{org}/V_{aq})_i$ in Fig. 9. Lysozyme of about 23 mg/cm^3 and 29 mg/cm^3 are respectively recovered from 50 and 200 mol/m^3 AOT micelle solutions to the aqueous phase.

4. CONCLUSION

To explore the potential for separating and enriching proteins with the reversed micellar extraction, extraction and stripping experiments of lysozyme and myoglobin were performed using AOT-isooctane reversed micelle solutions.

The effects of pH, ionic strength, cation type, and AOT concentration on the

partitioning of the proteins were clarified. The separation of two proteins is possible by adjusting the pH and potassium chloride concentration in the aqueous phase. It is respected that lysozyme can be enriched about twenty-five times the aqueous feed concentration by a extraction step followed by a stripping step.

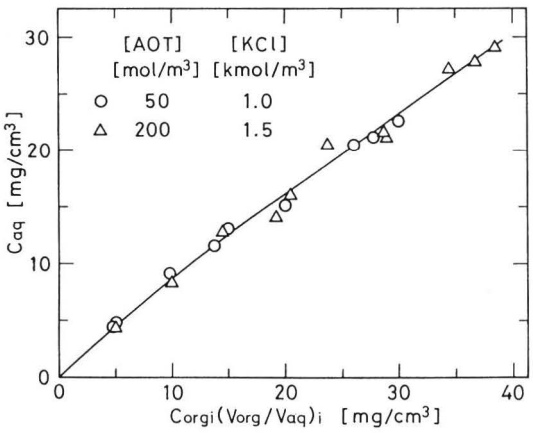

Fig. 9. Effect of volume ratio on lyzozyme stripping.

REFERENCES

Abbott, N.L. and Hatton, T.A., 1988. Liquid-liquid extraction for protein separations. Chem. Eng. Progr., Aug: 31-41.

Dekker, M., Van't Riet, K., Weijers, S.R., Baltussen, J.W.A., Laane, C. and Bijsterbosch, B.H., 1986. Enzyme recovery by liquid-liquid extraction using reversed micelles. Chem. Eng. J., 33: B27-B33.

Dekker, M., Riet, K.V., Bijsterbosch, B.H., Wolbert, R.B.G. and Hilhorst, R., 1989. Modeling and optimization of the reversed micellar extraction of α-amylase. AIChE J., 35: 321-324.

Goklen, K.E. and Hatton, T.A., 1987. Liquid-liquid extraction of low molecular-weight proteins by selective solubilization in reversed micelles. Separ. Sci. Technol., 22: 831-841.

Kuboi, R., Hashimoto, K. and Komasawa, I., 1990. Separation of proteins with reverse micellar liquid membranes. Kagaku Kogaku Ronbunshu, 16: 335-342.

Solvent Extraction 1990, T. Sekine (Editor)

© 1992 Elsevier Science Publishers B.V. All rights reserved

BIOSELECTIVE AQUEOUS TWO-PHASE PARTITION, -RELATIVE MERITS OF POLYMER AND PARTICLE DERIVATIVES-

J.G.HUDDLESTON, A.LYDDIATT, R.KUBOI*,
R.SUZUKA*, W.WANG* AND I.KOMASAWA*
Biochemical Recovery Group, School of Chemical Engineering,
University of Birmingham, Edgbaston, Birmingham B15 2TT, UK.
*Department of Chemical Engineering, Osaka University,
Toyonaka, Osaka 560, JAPAN.

ABSTRACT
The exploitation of bioselective interactions in tandem with aqueous two-phase systems(ATPS) has been attempted as a means of elevating or lowering partition coefficients to enhance product fractionation, comparing of ATPS containing affinity polymer or particulate affinity-derivatives. Bio-mimetic dyes and hydrophobic functions have been coupled to PEG polymers or conventional chromatographic media such as Sepharose and Sephadex. Partitioning and adsorption behavior of these derivatised particles have been quantitatively examined in the context of measurable characters of pH, composition(tie-line length) and hydrophobicities of phase systems and particles.

1. INTRODUCTION

Conventional approaches to protein purification by partition in aqueous two phase systems generally exhibit rather low selectivity. With a few exceptions purification factors of between two and twenty. The parameters governing partition, molecular weight of polymers, pH and salt addition tend to influence the behavior of whole classes of proteins in limited stage extraction procedures(Hustedt,1986). Only proteins having highly unusual surface properties differing significantly from contaminants can be purified to homogeneity by this method(Huddleston,1990). In addition it is difficult to quantitatively predict the partitioning behavior of complex feed stocks and process design proceeds heuristically(Kula,1986).

The technique of affinity partitioning by exploiting specific or near specific interaction of bio-molecules greatly enhances the selectivity of the method(Johansson,1985). By emphasizing one particular force controlling partition the predictability of even quite complex systems may by enhanced.

In conventional approaches to affinity partition where the ligand is covalently attached to one of the polymers, problems of ligand retention and recycling may be anticipated. Thus solid phase affinity partitioning in which the ligand is attached to a porous or non porous particulate solid may offer significant advantage.

Successful application of solid phase affinity partition requires the use of particles having appropriate surface chemistry to ensure a one sided partition. Partition of soluble ligands is not absolute in this sense.

The choice of ligand to be used in solid phase affinity partitioning depends on the application. In PEG/Salt systems, prefered for reasons of economy, choice may be limited by ionic strength and the strength of the affinity interaction as shown in Fig.1. It has already been shown that antibody-antigen interactions may be utilized on partitioned solid phases for the purification of monoclonal antibodies from murine hybridoma cell culture(Huddleston,1990). Weaker interactions may be hindered by the presenced of salt. The picture is complicated by the mixed (hydrophobic/electrostatic) nature of many biospecific interactions. The present paper addresses in particular the exploitation of hydrophobic interactions in PEG/potassium phosphate(PK) systems.

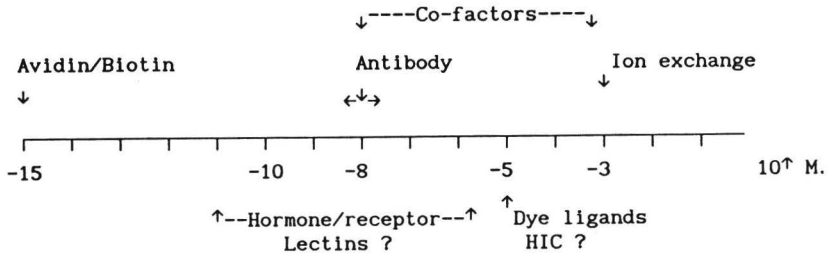

Fig.1 Overall interaction strength which may be effective in PEG/Salt systems

2. EXPERIMENTAL

Aqueous Two-phase systems composed of PEG 4000/Potassium Phosphate (PK) were prepared and characterised by a hydrophobic factor as described previously(Kuboi,1990). Protein concentration was measured by UV spectrophotometry at 280nm or by the pyrogallol red method (Micro-TP Test Wako).

Sepharose 4B(0.060-0.140mm, Pharmacia) and Sephadex G-100(0.040-0.120mm, Pharmacia) particles were derivatised with hydrophobic ligands such as Procion Blue MX-R, 1,4 diaminobutane, 1,8 diaminooctane and 1,12 diaminododecane. These were prepared, either by coupling ligands via CNBr-activated Sepharose or directly to Sepharose and Sephadex to yield ligand concentrations of 1 to 2mg/g gel. Derivatised particles and their notation are summarised in Table

1. Particles were mixed in aqueous two-phase systems containing papain (Sigma type III) and partitioning behaviour and binding capacity estimated. Particles were collected into mini-columns, washed with 2M ammonium sulfate in 1/15M phosphate buffer pH 6 and eluted in 10mM phosphate buffer.

Table 1

Partitioning of particles in ATPS (PEG/Phoshate)

systems PEG [wt%] / PK [wt%]	12 / 12	10 / 14	14 / 14	17 / 14	23 / 14
HF [mol/kJ]	0.079	0.126	0.159	0.174	0.255
⊿PEG [kg/m³]	343	364	415	453	497
PB-CNBr-S4B	U	U	U	U	U
C12-S4B	U L	U	U	U	U
C8 -S4B	B L	U	U	U	U
C4 -S4B	B L	U	U	U	U
S4B	B	B	B	B L	B L
PB-Sed	B	B	B	B	B

System Polyethyleneglycole 4000 / Potassium Phosphate ; PEG/PK
Key U ; UPPERSIDE-INTERFACE
L ; LOWERSIDE-INTERFACE
U L ; INTEFACE BOTH SIDE
B L ; BOTTOM & LOWERSIDE-INTERFACE

B ; BOTTOM

Particles
Procion-Blue-(CNBr activated Sepharose 4B) ; PB-CNBr-S4B
ω-amino dodecyl amine - Sepharose 4B ; C12-S4B
ω-amino octyl amine - Sepharose 4B ; C8 -S4B
ω-amino butyl amine - Sepharose 4B ; C4 -S4B
Sepharose 4B ; S4B
Procion-Blue - Sephadex G-100 ; PB-Sed

3. RESULTS AND DISCUSSION

Adsorbents for use in solid phase affinity partitioning must satisfy the following conditions for effective separation of enzymes in the resulting three phase system;

a) complete control of partitioning to either top or bottom phase,b) suitable binding capacity and selectivity for the enzyme in ATPS, c) mild elution resulting in high yield of active enzyme.

3.1. Partitioning of adsorbents

The relationship between the surface hydrophobicity of the particles,(HFS), the estimated hydrophobicity of the systems (HF), and their partitioning behavior was examined. Assuming similar ligand surface density the HFS of

the particles would be expected to follow the series;

PB-CNBr-S4B > C12-S4B >C8-S4B >C4-S4B> S4B

This corresponds to the tendency of the particles to partition favourably to the PEG-rich upper phase.

The results of partitioning derivatised particles in various phase systems of differing hydrophobicity (HF) are shown in Table 1. The most hydrophobic particle is PB-CNBr-S4B which shows complete preference for the PEG phase, whilst the particle S4B partitions to the bottom phase when the HF is smaller than 0.174 and subsequently in the range of HF larger than ca.0.17 partitions to the PEG phase. The Table clearly shows that particles tend to partition to PEG phases more easily when either their surface hydrophobicity (HFS) increases or when the HF of the phase system increases.

Partitioning of particles to either phase can thus be controlled easily and quantitatively by reference the HF of the system and the HFS of the particle. HFS can be varied by selection of particles and ligands. The system HF can be varied by increasing the difference in concentration of PEG between upper and lower phases principally by increasing the concentration or molecular weight(M.W.) of the polymers or by increasing the pH in PEG/PK systems and also by addition of certain salts(Kuboi,1990).

3.2. Binding capacity of adsorbents

Initial studies on the adsorption of papain in single phase systems showed that for the alkyl and PB derivatised adsorbents capacity increased with salt concentration and pH and that the capacity was not reduced by the presence of PEG. When the particles were partitioned in aqueous two phase systems capacity of these adsorbents increased with increasing concentration of polymers and salts which coincides with increasing preference of the particles for upper phases. Initial rates of adsorption were rather rapid and 80-97% of equilibrium capacity was bound within 20mins at a papain concentration of 0.45mg/ml.

Fig.2 shows the effectiveness of the adsorbents partitioned in PEG/PK systems at fairly low polymer/salt concentration. Up to 50% of papain may be recovered using 1g gel/16g of ATP system.

Recovery of bound papain is shown in Table 2. Recovery was effected after washing with 2M (NH4)2SO4 to remove weakly bound protein and elution completed with 10mM phosphate buffer pH 6. Recovery of bound papain was acheived with little loss of papain activity. However, the most hydrophobic adsorbents showed lower recoveries indicating that detergent treatment may be required to effect complete recovery of bound papain.

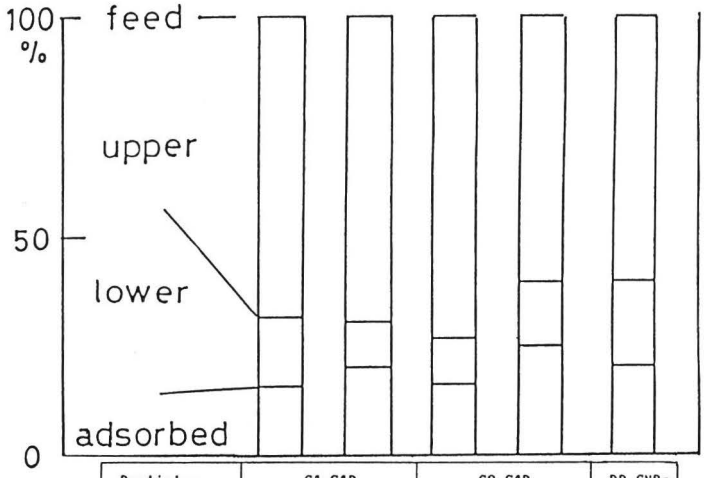

Particles	C4-S4B		C8-S4B		PB-CNBr -S4B
System PEG [wt%] PK [wt%] pH	12 12 6.0	17 14 6.0	12 12 6.0	17 14 6.0	12 12 6.0
Partitioning of particles	B	U	B	U	U
Adsorbed concentration [mg/g gel]	0.30	0.37	0.31	0.48	0.41

Fig.2 Binding capacity of particles in ATPS (PEG/PK system) for Papain
Papain ca.2.0-2.4mg; 1g gel/16g system
stiiring 120rpm-20min, centrifuge 3000rpm-2min

Table 2 Elution of partitioned adsorbents at low ionic strength

Prticle	Papain adsorbed [mg/g]	Papain eluted [mg/g]
C4-S4B	1.96	0.80
C8-S4B	1.77	0.66
C12-S4B	3.28	0.32

Additional work on the use of particles derivatised with dye-ligands has also been conducted for other enzymes. Initial results indicate that these

may be effective in PEG/salt systems in bringing about changes in partition in some cases. Increases in partition coefficient were observed with soluble ligands in the case of ADH(Kuboi,1990) but no change was observed for phosphofructokinase when ligands were used in solid or liquid form either in top or bottom phases(Huddleston,1990).

4. CONCLUSION.

The modification of particle surface properties for use in solid phase affinity partitioning has been shown to be effective in the control of their phase preference in accordance with their surface hydrophobicity(HFS) and the hydrophobicity of the system(HF). The effectiveness of such adsorbents in hydrophobic solid phase affinity partitioning has also been demonstrated.

Further elucidation is required of the types of affinity interaction which may be effectively utilised in PEG-salt systems. Solid phase affinity partitioning may offer advantages over affinity partitioning involving soluble polymer bound ligands, principally the ability to retain and recycle expensive ligands. Other advantages may acrue from application of the technique at an early stage in protein recovery sequences. Such early application of high resolution steps may offer economy in shortening process sequences. In addition it may be possible to minimise unwanted interactions in aqueous two-phase systems which may be expected to compromise direct early application of affinity adsorbents.

5. ACKNOWLEDGMENT

This work was partly supported by the British Council, Tokyo (the UK-Japan collaboration fund).

6. REFERENCES

Albertsson,P.A.,1986. Partition of Cell Particle and Macromolecule,John Wiley.

Huddleston,J.G. etal., 1989. Separations Using Aqueous Phase Systems(eds., Fisher,D. etal.) p.309, Plenum Press, London.

Huddleston,J.G. etal., 1990. I.Chem.E.Symp.Ser., No.118.

Hustedt,H. etal., 1986. Biotechnol.Letters, 8, 791.

Johansson,G., 1985. Partition in Aqueous Two Phase Systems(eds., Walter,H. etal.) p.161, Academic Press, New York.

Kuboi,R. etal., 1990. Kagaku Kogaku Ronbunshu, 16, 755.

Kula,M-R., 1986. Comprehensive Biotechnology(eds., Moo-Young,M. etal.) Vol.2, p.451, Pergamon Press.

Solvent Extraction 1990, T. Sekine (Editor)

© 1992 Elsevier Science Publishers B.V. All rights reserved

EXTRACTION OF PENICILLIN ACYLASE USING PEG/K_3PO_4 AQUEOUS TWO-PHASE SYSTEM

Shen Zhong-yao, Rong Guo, Bo Lu
Department of Chemical Engineering, Tsinghua University, Beijing, P. R. China

ABSTRACT

The extraction of penicillin acylase (PA) by using PEG/K_3PO_4 aqueous two-phase systems is described in this paper. The effect of the average molecular weight (AMW) of PEG and the concentrations of PEG and K_3PO_4 on the partition behaviours of PA and other proteins was investigated. The optimal extraction system involved 12% PEG-2000 and 13.8% K_3PO_4 with a volume ratio of 0.55. The partition coefficients were 0.77 and 52.51 for PA and proteins, respectively. A yield of 96.3% for PA in the bottom phase and a yield of 96.3% for proteins in the top phase were obtained. The results demonstrated that the purified factor and the activity yield of PA were 43.4 and 133.5%, respectively.

The release of PA from E. coli AS 1.76 by the method of solvent-osmotic pressure was studied. The optimal condition was 0.1g cell/ml phosphate buffer, 10% butyl-acetate and 0.2g/ml sucrose. The operation time was about 150 minutes. The release efficiency of nearly 100% was obtained.

INTRODUCTION

The microbial penicillin acylase, that hydrolyses penicillin into 6-APA and a side-chain acid has been investigated extensively (1-9). In this paper, the extraction of penicillin acylase by using aqueous two-phase system is reported. The main factors influencing the extraction are the type, average molecular weight and concentration of the polymer, the kind and concentration of the salt, pH, ionic strength and temperature (10).

The penicillin acylase from E. coli AS 1.76 is an intracellular enzyme. At least 20 methods of releasing enzyme from microbial cells have been presented (11). A detailed description of a solvent-osmotic pressure method for releasing PA is given in this paper.

EXPERIMENTS

E. coli AS 1.76 cells were cultured in a fermenter of 5 litres. After being centrifuged at 3780g for 30min., the cells were washed with 0.05M phosphate buffer at pH 7.7. Then the solution was mixed with butyl-acetate and sucrose completely for a certain time to release PA. The extraction was carried out in a 10ml centrifugal tube. Solutions of K_3PO_4 and PEG of known concentrations were mixed with the enzyme solution and distilled water to give a total weight of 10g. After being mixed for about 1 min., the mixture was centrifuged in a centrifuge (5 min., 1650g) for a rapid phase separation. All experiments were carried out at room temperature.

ANALYSIS METHODS

The penicillin acylase activity (A_{PA}) was assayed by an improved NIPAB method. The enzyme activity was calculated as follows:

$$A_{PA}\,(u/ml) = (OD*K) / (t*V) \quad (1)$$

where, OD is the absorbance of the sample at 405nm, K is the μmol of 6-nitrol-3-aminobenzoic acid (NIAB), when the absorbance changes for 1.0. Under the conditions of this work, K was equal to 0.617. The reaction time t was 10 min. the sample volume V was 0.2ml. Under the above conditions, the amount of the enzyme to produce 1 mol NIAB per min. is defined as one unit of activity. The amount of proteins and the concentration of PEG were determined according to the Bradford assay (13) and assay (14), respectively.

RESULTS AND DISCUSSION

1. THE RELEASE OF INTRACELLULAR ENZYME PA.

The high release efficiency of PA was obtained by using a solvent-osmotic pressure method. The release efficiency was calculated as follow:

Release Efficiency = (the A_{PA} after the release treatment) / (the A_{PA} in the initial fermentation broth) (2)

The influences of the concentrations of cell, butyl-acetate and sucrose on the release efficiency were shown in Fig. 1. The optimal cell concentration was determined at 0.1g/ml. The release efficiency can reach to 100% when the concentrations of butyl-acetate and sucrose are more than 10% and 0.2g/ml, respectively. The release of enzyme is an intra-diffusion controlled process. The operation time also has an important effect on the enzyme release. In Fig. 2, with an increasing operation time, the release efficiency shows a rapid increase at first, then level off. The release efficiency of 100% can be obtained when the operation time is more than 120min. It is also shown that the release is very low if only one of the two chemicals is added. The release mechanism of the intracellular enzyme by the solvent-osmotic pressure method can be explained as follows: since butyl-acetate is able to solve the lipids in the E. coli cell wall and membrane, it makes the cell more permeable. The sucrose added decreases the osmotic pressure of the solution, that the hydrophilic PA and other proteins in the cell membrane are released.

2. THE EXTRACTION OF PENICILLIN ACYLASE BY USING AN AQUEOUS TWO-PHASE SYSTEM.

The partition coefficient K, the extraction yield Y and the phase ratio R are three main parameters in the extraction. They are defined as follows:

$$K_i = C_{it} / C_{ib} \quad (3)$$

$$R = V_t / V_b \quad (4)$$

$$Y_{it} = (\text{amount of i in the top phase}) / (\text{the initial amount of i}) * 100\% \quad (5)$$

$$Y_{ib} = (\text{amount of i in the bottom phase}) / (\text{the initial amount of i}) * 100\% \quad (6)$$

Where C_{it} and C_{ib} are the concentrations of substance i in the top phase and the bottom phase, respectively. The V_t and V_b are the volumes of the top phase and the bottom phase, respectively, in equilibrium.

In the PEG / K_3PO_4 aqueous two-phase system, the PA is always partitioned in the bottom, phosphate rich phase, the reciprocal of the partition coefficient, $1/K_{PA}$, was used to present the partition behaviour. Fig. 3 demonstrates that an increase of the

average molecular weight of PEG (AMW) leads to a rapid increase in $1/K_{PA}$ at first, then levels off. The similar tendency is observed in the partition coefficient of other proteins K_P and the extraction yield of PA Y_{PA}. It is shown that more than 96% for Ypa in the bottom phase and 93% for Y_P in the top phase can be obtained with the optimal concentrations of PEG and K_3PO_4.

TABLE 1
The extraction yield of penicillin acylase and other proteins in the different average molecular weights of PEG / K_3PO_4 system

MW	400	600	800	1000	2000	4000	6000	11000	20000
PEG (%)	10	10	10	10	12	10	10	12	8
K_3PO_4	22	22	16.3	13.8	15.1	13.8	13.8	15.7	16.3
Y_{PA} (%)	96.8	97.5	96.3	96.4	98.3	97.2	97.0	98.2	97.2
Y_P (%)	94.0	94.2	96.0	97.4	93.2	94.7	95.7	95.1	93.5

The influence of potassium phosphate concentration on the PEG-2000/K_3PO_4 aqueous two-phase system was given in Fig. 4. The partition coefficient is mainly a function of the surface properties on the involved substances, the interfacial characteristics and the electrical potential difference of the two phases (15). with the increase of the potassium phosphate concentration the interfacial tension difference shows an increasing tendency. It causes the decrease in the partition coefficients of PA, i. e. the increase in $1/K_{PA}$. Since most proteins are negatively charged at pH 9-11 in the experiments mentioned, an increase in the potassium phosphate concentration gives rise to a higher electrical potential difference, and leads to an increase in partition coefficient of proteins. The salting out of hydrophobic group in PEG leads to a decrease in the solubility of proteins in the top phase while increasing the salt concentration (16). It will cause K_P to decline, So the influence of salt concentration on the partition coefficient of K_P is complex.

Another important factor in the extraction is the PEG concentration. The results in the PEG-2000/K_3PO_4 system were shown in Fig. 5. Increasing the PEG concentration may cause an increase in interfacial tension and a decline of the partition coefficient of the substance involved. Meanswhile, the decrease of partition coefficient of the potassium phosphate leads to an increase in the electrical potential difference of the two phases, therefore the partition coefficient of negatively charged proteins is raised.

For a defined AMW of PEG the volume ratio is determined by the concentrations of PEG and K_3PO_4. Since PEG is a nonionic surfactant, it is able to combine with water molecules to form hydrated-PEG molecules. For a given concentration of K_3PO_4, the volume ratio will increase with an increase of the concentration of PEG, because more molecules can be combined in the top phase (see Table 2). In contrast to PEG, with the increase of the concentration of K_3PO_4 the volume ratio decreases (see Table 3).

TABLE 2
The volume ratio in the PEG/K_3PO_4 system with PEG 18%

K_3PO_4 (%)	5.0	6.3	7.5	10.0	11.3
R	5.46	1.90	1.31	1.00	0.91

TABLE 3
The volume ratio in the PEG/K_3PO_4 system with K_3PO_4 8.8%

PEG (%)	10	14	16	18	20	22
R	0.60	0.77	0.95	1.18	1.26	1.40

3. THE OPTIMAL CONDITIONS IN THE AQUEOUS TWO–PHASE EXTRACTION

The results presented in Table 1 show that the separation of penicillin acylase and other proteins achieved well in all PEG/K_3PO_4 aqueous two–phase systems with nine different average molecular weights of PEG. However, it will cause difficulty for phase separation if the molecular weight is too high. PEG of a high molecular weight is also more expensive. Therefore, a PEG with a good separation efficiency and a suitable average molecular weight should be chosen in the extraction. the extraction system of PEG–2000 and K_3PO_4 were determined according to Fig. 6 and Table 4. the optimal concentration of PEG–2000 was 12% and that of K_3PO_4 was 13.8%. The results of penicillin acylase separation were shown in Table 5. The volume ratio was 0.55. The total activity yield of PA which was partitioned in the bottom phase was 133.5%. the purified factor was 43.4. a yield of 96.3% for other proteins in the top phase was obtained.

TABLE 4
The influence of PEG concentration in PEG–2000/K_3PO_4 system with K_3PO_4 13.8%

PEG–2000(%)	10	12	14	16
R	0.423	0.550	0.596	0.714
1/Kpa	9.18	12.92	13.75	5.10
Kp	61.6	52.51	55.79	50.2
Ypa(%)	95.6	96.3	95.9	87.7
Yp (%)	96.3	96.3	97.1	97.3

TABLE 5
The results of PA separation by PEG–2000/K_3PO_4 system

Purification step	Volume (ml)	Total Proteins (μg)	Total activity (u)	Specific activity 810 (u/mg)	Purified factor	Recovery Proteins (%)	Rate PA (%)
Initial ferm. broth	1.9	16137.3	0.197	0.122	1.0	100.0	100.0
Top phase	2.90	15582.0	0.010	0.0064	0.05	96.6	5.1
Bottom phase	5.80	495.6	0.263	5.3	43.4	3.1	133.5

The experiments show that it is possible to use the aqueous two–phase system presented above for an efficient separation of penicillin acylase.

ACKNOWLEDGE

The authors gretefully acknowledge the financial support from the National Natural Scientific foundation Committee of China.

REFERENCE

1. Vandamme, E.J. and Voets, J.P., 1974, Advance in Appl. Microbiol, 17:311–361.
2. Ford, J.H., 1974, Anal. Chem., 19:1994.
3. Boyer, G.E. and Everett, P. M., 1949, Anal. Chem., 21:670.
4. Ivashkiv, E., 1964, Anal. Chem., 36:2506.
5. Nata, T., 1971, Agr. Biol. Chem., 35:1678.
6. Kutzbach, C., 1974, Hoppe–Soylers, Z. Physiol. Chem., 355:45.
7. Sun Wangru, 1980, Acta Microbiologica Sinica (China), 20:(4)407–414.
8. Zhang Shuzheng, 1984, Enzyme Production Industry, Scien. Press.
9. Jiao Qinghua, 1986, Acta Microbiologica Sinica (China), 26: (3)254–259.
10. Kula, M.R., 1979, Appl. Biochem. Bioeng., Academic Press Inc., Vol. 2:71–95.
11. Zhang Shuzheng, 1987. The Research and Technology of Enzymology (1).
12. Jiao Qinghua, 1986, Acta Bioeng. (China) 2: (2), 68–70.
13. The Experimental Techniques in Biochemistry (China), 1988, Tsinghua Univ.
14. Tan Tianwei and Shen Zhongyao, A New Assay for PEG(to be published).
15. Albertsson, P.A., 1971, Partition of Cell Particles and Macromolecules.
16. Zhao GuoXi, 1984, Physical Chemistry of Surfactants, Beijing Univ. Press.

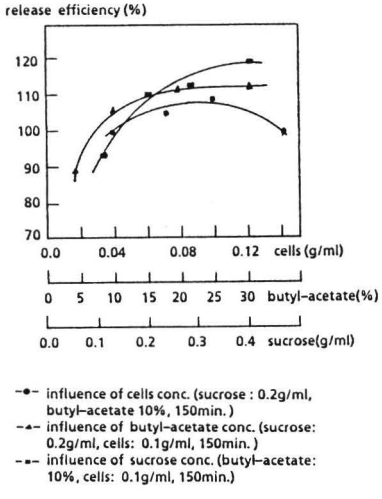

-●- influence of cells conc. (sucrose : 0.2g/ml, butyl-acetate 10%, 150min.)
-▲- influence of butyl-acetate conc. (sucrose: 0.2g/ml, cells: 0.1g/ml, 150min.)
-■- influence of sucrose conc. (butyl-acetate: 10%, cells: 0.1g/ml, 150min.)

Fig. 1 The results of solvent –osmotic pressure method of releasing penicillin acylase from E. Coli AS 1.76 cells.

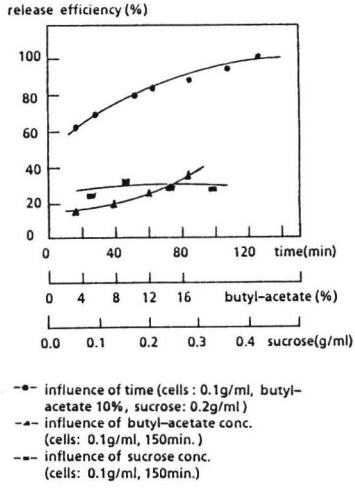

-●- influence of time (cells : 0.1g/ml, butyl-acetate 10%, sucrose: 0.2g/ml)
-▲- influence of butyl-acetate conc. (cells: 0.1g/ml, 150min.)
-■- influence of sucrose conc. (cells: 0.1g/ml, 150min.)

Fig. 2 The effects of time, butyl-acetate and sucrose conc. on the release efficiency

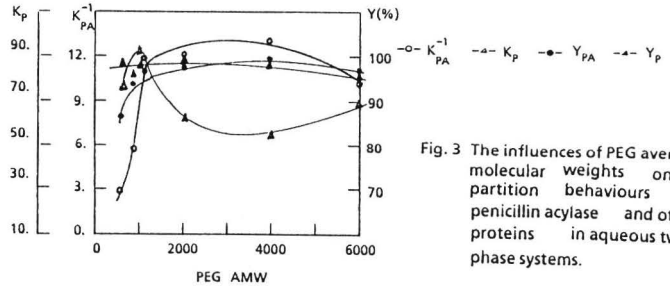

Fig. 3 The influences of PEG average molecular weights on the partition behaviours of penicillin acylase and other proteins in aqueous two-phase systems.

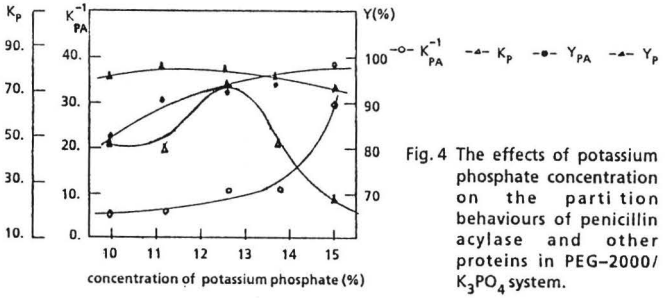

Fig. 4 The effects of potassium phosphate concentration on the parti tion behaviours of penicillin acylase and other proteins in PEG-2000/K_3PO_4 system.

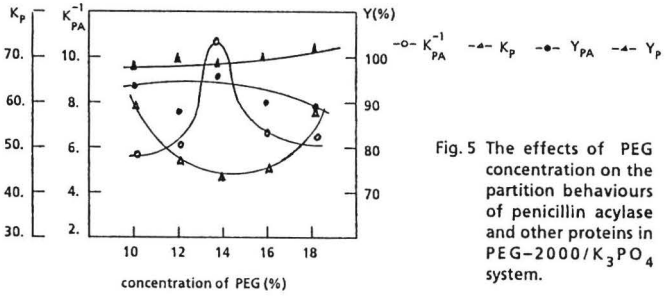

Fig. 5 The effects of PEG concentration on the partition behaviours of penicillin acylase and other proteins in PEG-2000/K_3PO_4 system.

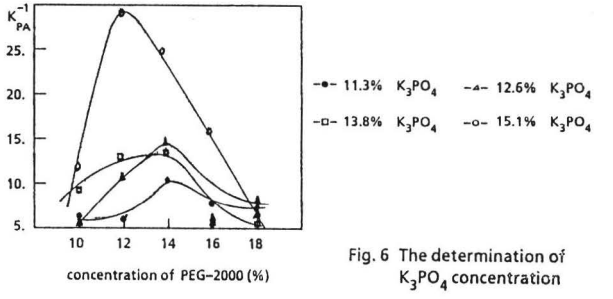

Fig. 6 The determination of K_3PO_4 concentration

Solvent Extraction 1990, T. Sekine (Editor)

© 1992 Elsevier Science Publishers B.V. All rights reserved

IMMUNOAFFINITY PARTITION OF A PROTEIN IN AQUEOUS TWO PHASE SYSTEM

Ken-ichi Suga, Suteaki Shioya and Takeshi Hirasawa
Dept. of Fermentation Technology, Osaka University, Suita, Osaka 565, Japan

ABSTRACT

Immunoaffinity partition in aqueous two-phase system is one of the interesting separation processes for bioactive polymers because the separation of the objective protein from other biopolymers can be achieved with high selectivity and high affinity under mild conditions. In this paper, the availability of the immunoaffinity partition in aqueous two-phase system is discussed based on several basic experimental studies and some of key factors to optimize the process operation conditions are investigated.

1 INTRODUCTION

In many cases, the cost for separation and purification of product from crude product is dominant in the total cost of the whole production. In recent years, the aqueous two-phase system has been applied in various areas of biotechnology. Aqueous two-phase systems are obtained by mixing solutions of two water soluble polymers. The most prominent feature of these phase systems are that both phases are water rich. Therefore, this system is useful for separation of bioproduct. The immunoaffinity partition in aqueous two-phase system (abbreviated as ATPS) is one of interesting separation processes for bioactive polymers because it can separate the objective protein from other biopolymers at high selectivity and high affinity under mild conditions. In this paper, the availability of the immunoaffinity partition in ATPS is discussed based on several basic experimental studies and some of key factors to optimize the process operation condition are investigated.

2 MATERIALS AND METHOD

2.1 Proteins

For basic study, we employed bovine pancreatic ribonuclease A (RNase A) as a model protein to be separated from contaminant proteins such as bovine serum albumin (BSA) and/or fetal calf serum (FCS). These proteins, RNase A and BSA were purchased from Sigma Co. Ltd. and FCS was from Hyclone Co. Ltd.

Monoclonal anti-RNase A antibody was purified from the culture broth of hybridoma cell line 3A21. Purification was done initially by condensation through membrane and then by column chromatography using hydroxylapatite.

2.2 Protein Assays

Protein concentration of BSA, RNase A and FCS were determined by absorbance at 280nm for BSA, FCS and at 277.5nm for RNase A, respectively in case of the solution containing single protein. For measurement of antibody concentration, indirect enzyme-linked immunosorbent assay (ELISA) was utilized. Goat anti-IgG was used as secondary antibody with alkaline-phosphatase(TAGO INC.).

Measurement of absorbance was done by using the microplate reader (MPR-A4, TOSOH).

2.3 Preparation of PEG-Antibody

We employ the Abuchowski method (Abuchowski et al., 1976) for joining PEG-protein involving activation of the PEG5000 by forming the cyanuric chloride derivative followed by reaction with lysine subunits of the protein. The modified antibody by substitution of PEG into amino group on the antibody is named hereafter as PEG-Ab or modified Ab by PEG.

2.4 Modification Ratio of antibody by PEG

To estimate the ratio of antibody modified by PEG, the number of amino-groups substituted can be determined by use of TNBS-sodium sulfite method (Habeeb, 1966). This method is to measure the spectrophotometric absorbance of the TNBS-amino complex which was produced from free-amino group of antibody (unmodified amino group) and TNBS. The modification ratio is defined as the ratio of number of modified amino-groups of PEG-Ab to number of free amino-groups of antibody before modification.

3 RESULTS AND DISCUSSION

3.1 Two-phase systems

First, 10%(w/w)PEG 6000 and 8% potassium phosphate were used for two-phase system. Then PEG 6000 from 3.5% to 5% and dextran T500 from 5.5% to 9.5% were also used.

In PEG/PP system, all proteins were partitioned to the top (PEG-rich) phases, whereas in PEG/dextran system, all proteins have the tendency to be partitioned to the bottom (dextran-rich) phases. When the antibody was modified by PEG, the objective protein binds with the antibody and is carried to the top phase since the protein coupled antibody quantitatively distributes to the upper phase. This means that the objective protein is partitioned to the top phase by the PEG modified antibody. Then the other contaminant proteins such as BSA and FCS are partitioned to the bottom phase. From this viewpoint, PEG/dextran system is selected for our ATPS and the experiment were focused on the system.

3.2 Partition of Proteins

(i) Effect of modification ratio of Ab

Figure 1 shows the effect of substitution ratio of amino group of antibody on the partition ratio of PEG-Ab in the top phase at pH 7.2. Here, partition ratio P is defined as the ratio of the amount of the protein in the top phase to the total amount of the same protein in the system. As seen in the figure, the substitution ratio of less than 30% doesn't increase the partition ratio. However, when the substitution ratio becomes more than 40%, the partition ratio remarkably increases to be almost 100%. The reason of marked increase of partition ratio is not clear at this stage. It is probably because the local concentration of PEG bound to the Ab is higher than average concentration of PEG in the top phase. Further investigation will be needed.

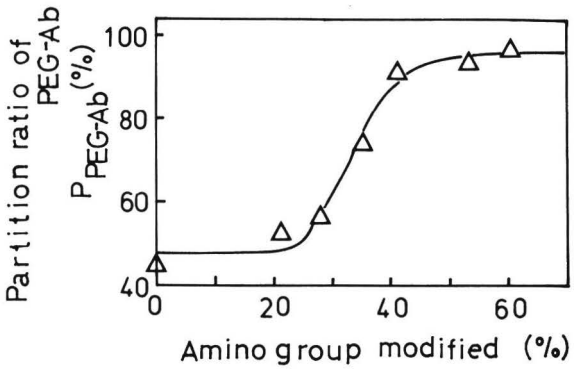

Fig. 1. Effect of modification ratio on partition of PEG-Ab in ATPS

(ii) Effect of pH

Figure 2 shows the effect of pH on the partition of PEG-Ab. As seen in the figure, the partition ratio is almost independent on pH but dependent on the substitution ratio of antibody.

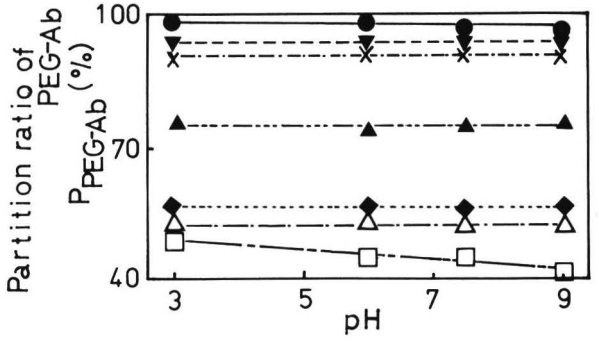

Fig. 2. Effect of pH on partition of PEG-Ab
Symbols; modification ratio of antibody □,0%; △,21%; ◆,28%; ▲,35%; ×,41%; ▼,53%; ●,60%.

3.3 Concentration of PEG and dextran in ATPS

Using various polymer concentrations, partition of PEG-Ab to the top phase was experimentally investigated. Figure 3 shows the relationship between tie-

line length (Walter et al., 1985) and partition ratio P. The longer the tie-line length is, the larger the partition ratios P of PEG and PEG-Ab are. The partition ratio P of PEG-Ab is always larger than native Ab or PEG6000 against any tie-line length. However, the effect of the tie-line length on the partition ratio P is not so prominent under more than 14.7 % of tie line length (4.2 % of PEG 6000 and 7.1 % of dextran T500).

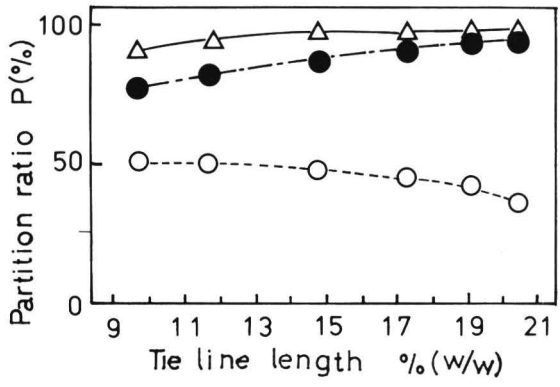

Fig. 3. Relationship between partition ratio P and tie-line length
Symbols: ○,native-IgG; ●,PEG6000; △,PEG-Ab. 60% modification ratio

3.4 Affinity Constant

(i) Effect of pH

Figure 4 shows the effect of pH on the affinity constant K for antibody-antigen equilibrium. At neutral pH at 7, K has the maximum which is about hundred times larger than that at pH 4 or at pH 10. However, it should be noticed that even at pH 4 or 10, K is order of 10^6 which is still large enough.

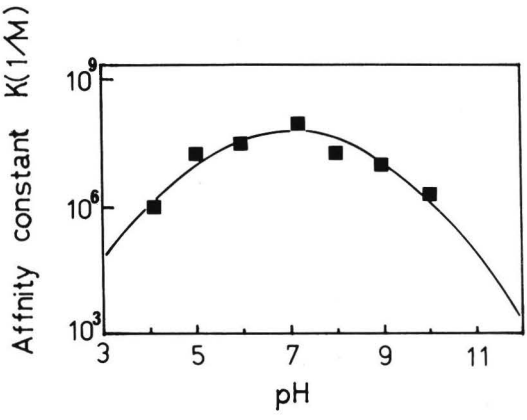

Fig. 4. Effect of pH on affinity constant K

(ii) Effect of modification ratio of antibody With biospecific ligands covalently coupled to one of the phase-forming polymers PEG it will be possible to shift the partition equilibrium of selected components within the phase system. However, it should be confirmed that the affinity constant K is still high even after the modification by substitution of amino group of antibody by PEG. Figure 5 shows the effect of substitution ratio of amino groups of antibody

on the affinity constant K. A exponential decrease of K was found as substitution ratio increases. However, even at 60% substitution ratio which is the maximum in our experiments, K is still high and about 8×10^6 M^{-1}.

3.5 Optimal Condition of pH and Modification Ratio

As stated above, we investigated the effect of pH and modification ratio of antibody on the partition ratio of protein. These quantitative relationships can be utilized for investigation of optimal conditions of pH and modification ratio for the maximum partition of objective protein RNase A to the top phase in the ATPS. We assume : 1) The partition ratio of PEG-Ab is controlled by the modification(substitution) ratio of antibody as shown in Fig.1. 2) The equilibrium between antibody and antigen exists independently in each phase. 3) Unbound protein is distributed to each phase depending on pH. Under these assumptions, we derived a mathematical model based on mass balance and equilibrium equations. An example of calculation is shown in Fig. 6. Figure 6 shows the effect of pH and modification ratio on the partition of RNase A. Where the ratio of binding sites of antibody to the objective protein RNase A concentration is 1.0. From Fig. 6, pH in the range of 4 to 10 is not so significant for increasing the par tition coefficient D but

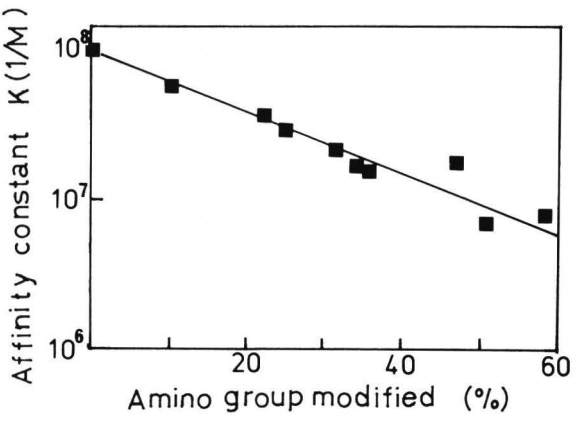

Fig. 5. Effect of modification ratio on affinity constant K at pH 7.2

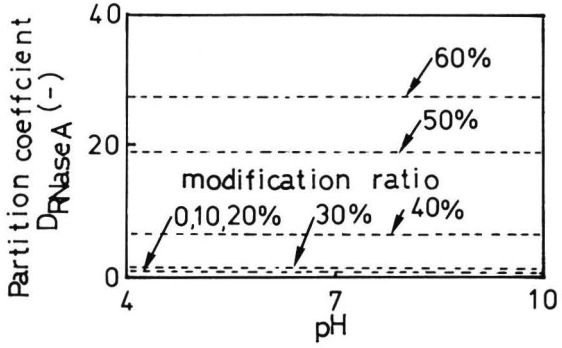

Fig. 6. Effect of pH and modification ratio on partition of RNase A
(binding site of PEG-Ab)/(RNase A conc.)=1.0

modification ratio is most dominant for increasing the partition coefficient D. Because the partition of PEG-Ab to the top phase is most significant for maximization of D and other factor, e.g., affinity constant is not so significant if it is relatively large such as the order of 10^6.

3.6 Partition of RNase A in Immunoaffinity ATPS

According to the above considerations, the partition of RNase A in this immunoaffinity ATPS was performed experimentally. The result of experiments and simulations are shown in Table 1. The simulation data are listed in the parentheses. The experimental data coincided well with the calculated ones.

In conclusion, the most significant point for maximizing the partition of the objective protein using immunoaffinity ATPS is to increase the modification ratio of antibody. Probably, the conclusion will be valid for other immunoaffinity ATPS.

TABLE 1 Partition of RNaseA in immunoaffinity ATPS

	pH 5.0 (simulation)	pH 7.0 (simulation)
D_{RNaseA} (-)	24.1 ± 9.4 (27.2)	22.9 ± 10.9 (27.2)
P_{RNaseA} (%)	95.3 ± 1.8 (96.5)	94.6 ± 2.5 (96.5)

PEG6000 4.2%, DextranT500 7.1%, 0.05M KCl
(antibody binding sites : RNaseA = 1:1)

References

Abuchowski,A., van Es,T. and Palczuk,N.C. 1976. J. Biol. Chem., 252, 3578-3581
Albertsson,P.A., 1960. Partition of cell particles and macromolecules, Almqvist & Wiksell, Stockholm; Wiley, New York
Habeeb,A.F., 1966. Anal. Biochem., 14, 328-336
Kunitz,M., 1946. J. Biol. Chem., 164, 563-568
Walter,H., Brook,D.E. and Fisher,D., 1985. Partitioning in aqueous two-phase system, Academic Press, Orlando

Solvent Extraction 1990, T. Sekine (Editor)

© 1992 Elsevier Science Publishers B.V. All rights reserved

RECOVERY OF ASPARTIC ACID FROM AQUEOUS SOLUTIONS BY EXTRACTION WITH TOMAC IN XYLENE

L. HANDOJO, W. DEGENER, and K. SCHÜGERL
Institut für Technische Chemie, Universität Hannover, Callinstr. 3, D-3000 Hannover, F.R.G.

ABSTRACT

The separation of aspartic acid from asparagine and lysine as well as the thermodynamic equilibria and kinetics of extraction of aspartic acid and coextraction of hydroxyl anions with TOMAC in xylene as the stripping phase are investigated in a stirred cell and mathematically modelled. The degrees of extraction and mass transfer coefficients are evaluated as a function of the pH-value, the solute, carrier concentrations, phase ratio, and Reynolds numbers. This dependence on the process variables is simulated with the aim to develop a model.

INTRODUCTION

Amino acid production from protein wastes could be an economical process, if effective separation techniques of amino acids from the hydrolysates are at our disposal. Presently, chromatographic separation is used. In special cases, carrier extraction could be more effective and economical. Therefore, in our laboratory, the separation of different amino acids by carrier extraction is investigated.

One of the basis of the separation of amino acids is the difference in their basic and acidic character. The former are extracted at low pH-values with cationic extractants and the latter at high pH-values with anionic extractants. In the present paper, aspartic acid (with acidic character) is separated from arginine and lysine (with basic character) at high pH-values with an anionic extractant trioctylmethlyammoniumchloride TOMAC in xylene.

2 MATERIALS AND METHODS

L-aspartic acid, L-arginine and L-lysine (Fluka, analytic degree), trioctlylmethylammoniumchloride (>97% pure, Fluka), xylene (>97% for synthesis, isomere mixture, Merck), cyclohexane (>99% for synthesis, Merck), n-butlyacetate (>98% for synthesis, Merck), diisopropylketone >98% for synthesis, Merck), isoamylacetate (>99% for synthesis, Merck) were used.

The concentrations of amino acids in the mixtures were determined with HPLC (Spectra Physics) by reversed phase chromatogaphy and OPA-precolumn derivatisation on a resolved TM column (C_{18}, Waters). After separation of the amino acids, their concentrations were determined by a polarimeter (Type 241, Perkin Elmer). The chloride ion concentration was measured by a Cl^--ion selective electrode (Type 157203, Ingold).

The thermodynamic data were evaluated at definite initial pH-values. The end (equilibrium) pH-values were determined as well. Factional 2^n design (with initial pH-value 10-14), mole ratio acid-to-carrier (0-10), volume of the aqueous phase (10-20 ml), volume ratio aqueous-to-organic phase (1-2) were used as variables.

The kinetic investigations were carried out in the stirred cell with two turbine stirrers. The temperature and pH-value were controlled, and the amino acid and Cl^--ion concentrations were monitored during the extraction. (For more details, see dissertation of L. Handojo, University of Hannover, 1988).

3 RESULTS

Equilibrium

At high pH-values only aspartic acid (pK_1 = 2.09 (COO^-), pK_2 = 9.83 (NH_3^+), pK_3 = 3.86 (side chain)) is extracted by TOMAC, arginine (pK_1 = 2.17, pK_2 = 9.04, pK_3 = 12.48) and lysine (pK_1 = 2.75, pK_2 = 8.95, pK_3 = 10.49) are not extracted at all. The extractions of amino acid $[AH_n]_w$ and hydroxide ion $[OH^-]_w$ with quaternary ammonium chloride $[Q^+Cl^-]_o$ in the organic phase is given by:

$$[A^-]_w + n\,[Q^+Cl^-]_o \;=====\; [Q^+_nA^{n-}]_o + n[Cl^-]_w \qquad (1)$$

$$[OH^-]_w + [Q^+Cl^-]_o \;=====\; [Q^+OH^-]_o + [Cl^-]_w, \qquad (2)$$

where $[Q^+_nA^-]$ and $[Q^+OH^-]_o$ are the carrier amino acid/ion pair and the carrier hydroxide/ion pair. The extraction (2) is an undesired coextraxtion of the OH^--ion.

The degree of extraction E of the animo acid is defined as

$$E = \frac{[Q^+_nA^{n-}]_{o,eq}}{[A]_{w,i}}\ 100\ [\%] \qquad (3)$$

the equilibrium constant K_A for the reaction (1)

$$K_A = \frac{[Q^+{}_n A^{n-}]_{o,eq}\,[Cl^-]^n_{w,eq}}{[Q^+Cl^-]^n_{o,eq}\,[A^{n-}]_{w,eq}} \qquad (4)$$

and for the reaction (2)

$$K_H = \frac{[Q^+OH^-]_{o,eq}\,[Cl^-]_{w,eq}}{[Q^+Cl^-]_{o,eq}\,[OH^-]_{w,eq}}\,, \qquad (5)$$

where indices i and eq mean initial and equilibrium value.

The partition coefficients P of amino acid (A) and hydroxide ion (H) are given by

$$P_A = \frac{[Q^+A^{n-}]_{o,eq}}{[A]_{w,eq}} \qquad (6)$$

$$P_H = \frac{[Q^+OH^-]_{o,eq}}{[OH^-]_{w,eq}} \qquad (7)$$

Figures 1 and 2 show the degree of amino acid extraction and the amount of OH^--ion as a function of the equilibrium pH-value of the aqueous phase at different carrier concentrations. With increasing pH-value, the degree of extraction of the amino acid increases, passes a maximum and diminishes because of the increasing coextraction of OH^--ions, which is enhanced considerably above a pH of 12.

In Figures 3, 4, and 5, the logarithm of the equilibrium constant, the partition coefficient P_A, and the logarithm of the partition coefficient P_H are plotted as a function of the equilibrium pH-value.

These functions can be described by the following relationships:

$$E = 45.81\ pH - 1.99\ pH^2 + 5.3\ MR - 0.363\ MR^2\,, \qquad (8)$$

where MR is the mole ratio of the carrier to the amino acid.

The amount of coextracted OH^--ion is given by:

$$(C_{OH})_{coex} = 2.07 - 5.42.10^{-3}\ C_{OH} + 3.84\ MR + 12.10^{-3}\ C_{OH}\cdot MR \quad (mmol/l), \qquad (9)$$

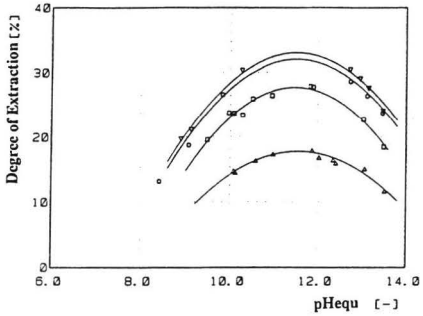

Fig 1 Degree of Extraction as a function of pH equ
A = 40 mmol/l, Carrier:
△ 40 mmol/l, □ 120 mmol/l
▽ 280 mmol/l, ○ 360 mmol/l
—— calculated

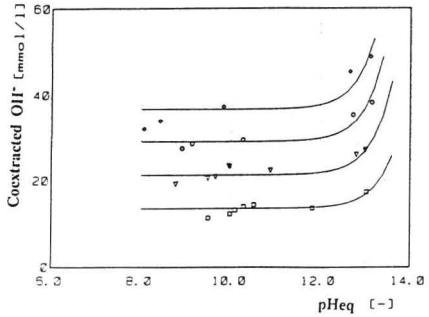

Fig 2 Coextracted OH^- as a function of pHequ, Carrier:
□ 120 mmol/l,▽200 mmol/l
○ 280 mmol/l,◇360 mmol/l
—— calculated

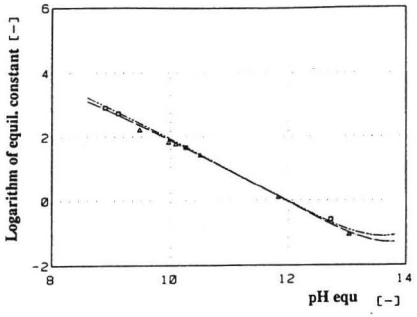

Fig 3 Logarithm of equil. constant as a function of pHeq. Carrier:
△ 120 mmol/l,□280 mmol/l
—·— calculated for 120 mmol/l
—·--·— calculated for 280 mmol/l

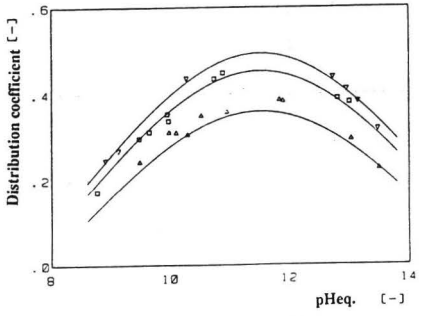

Fig. 4 Distribution coefficient as a function of pHeq.
Carrier: △ 120 mmol/l
□ 200 mmol/l,▽280 mmol/l
—— calculated

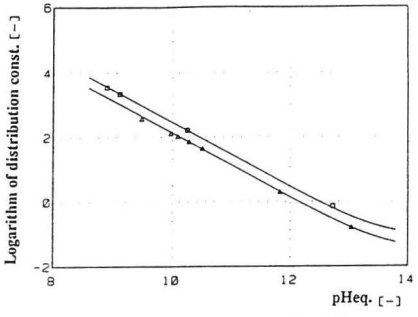

Fig. 5 Logarithm of distribution const. as a function of pHeq
Carrier: △ 120 mmol/l
□ 280 mmol/l, —— calculated

where C_{HO} is the concentration of the OH^--ion.

The amount of chloride ion in the aqueous phase can be calculated by

$$(C_{Cl})_w = 2\ (C_A)_{ex} + (C_{OH})coex + 12 \quad (mmol/l)\ , \tag{10}$$

where $(C_A)_{ex}$ (mmol/l) is the extracted amino acid.

Kinetics

The rate-determining step of the extraction is the mass transfer across the liquid/liquid interface. The overall mass transfer coefficients K_{LA} of the amino acid and K_{LH} for the hydroxide ion depend on the pH-value, the mole ratio as well as on the Reynolds number Re_w in the aqueous phase. Re_w is independent of the amino acid concentration. The Reynolds number of the organic phase Re_o decreases, and the Schmidt number of the organic phase Sc_o increases with increasing carrier concentration.

The relationship between the overall mass transfer coefficient K_{LA}, the particular mass transfer coefficients of the solute k_A, and the ion pair k_{QA} is given by:

$$\frac{1}{K_{LA}} = \frac{1}{k_A} + \frac{1}{m_A\ k_{QA}}, \tag{11}$$

where m_A is the distribution coefficient of A.

Analogoue for the OH-transfer, the following relationship is valid:

$$\frac{1}{K_{LH}} = \frac{1}{k_H} + \frac{1}{m_H\ k_{QH}}\ , \tag{12}$$

At a high pH-value (e.g., pH 10), m_H is very large (m_H = 80), therefore, $k_H \approx K_{LH}$ (= 12.43 cm/min). k_{OH} can also be calculated from eq. (12). The following relationships hold true:

$$k_{QH} = 0.151\ Re^{0.53}\ Sc_{QH}^{-0.41} \tag{13}$$

$$k_H = 3.0\ Re^{0.53}\ Sc_H^{-0.41} \tag{14}$$

The ratio of the coefficients 3.0/0.151 = 19.88 is about equal to the ratio of the molecular weights of QH to H (22.7).

By means of the knowledge of the relationship of the coefficients in eq.(15) and (16):

$$k_A = a\ Re_W^{0.53}\ Sc_A^{-0.41} \tag{15}$$

$$k_{QA} = b\ Re_o^{0.53}\ Sc_o^{-0.41}\ , \tag{16}$$

where a/b = 6.7, k_A and k_{QA} can be calculated from K_{LA}, Re_o, Sc_A, Re_W, and m_A:

$$k_A = 0.457\ Re_W^{0.53}\ Sc_A^{-0.41} \tag{17}$$

$$k_{QA} = 0.0688\ Re_o^{0.53}\ Sc_{QA}^{-0.41} \tag{18}$$

CONCLUSIONS

Aspartic acid was completely separated from arginine and lysine at high pH-values by the anionic extractant TOMAC in xylene as the stripping phase. The extraction was impaired by the coextraction of OH^--ions. The dependence of the particular mass transfer coefficients of aspartic acid, OH^--ion, and their carrier complexes on the process variables were evaluated and modelled.

Solvent Extraction 1990, T. Sekine (Editor)

© 1992 Elsevier Science Publishers B.V. All rights reserved

REGENERATION OF CARBOXYLIC ACID EXTRACTS

C. J. KING, J. N. STARR, L. J. POOLE and J. A. TAMADA
Department of Chemical Engineering and Lawrence Berkeley Laboratory, University of California, Berkeley CA 94707-9989 (U. S. A.)

ABSTRACT

Extraction is attractive for recovery of carboxylic acids from aqueous solution. For low-volatility acids (e.g., succinic, lactic, fumaric, and many others) regeneration is challenging, since distillation of the extract is not an option. Four different approaches to regeneration have been explored experimentally, analyzed and contrasted. These are (1) back extraction following a temperature increase, (2) back extraction following a change in diluent composition, (3) back extraction into an aqueous solution of a volatile tertiary amine, with the resultant trialkylammonium salt being concentrated and decomposed thermally, and (4) crystallization of a low- or moderate-solubility acid (e.g., succinic, fumaric, adipic) following evaporation of co-extracted water and some diluent. Method #3 is effective for recovery of carboxylic acids from strongly basic extractants. Method #4 is particularly effective when used with certain appropriate solvents or diluents, e. g., ketones.

1. INTRODUCTION

Solvent extraction is an effective method for recovery of carboxylic acids from aqueous solutions, such as fermentation broths and waste streams. Trialkylamines (e.g., trioctylamine) are attractive extractants because they offer high equilibrium distribution ratios, chemical specificity, and regenerability (Ratchford, et al., 1951; Ricker, et al., 1980). Other basic extractants, such as phosphine oxides and phosphates, can also be attractive. For certain acids extraction with more conventional solvents is effective. For example, the equilibrium distribution ratio for extraction of fumaric acid from water into methyl isobutyl ketone (MiBK) found in our work is 1.4.

Organic diluents and modifiers are commonly used with an amine extractant in the solvent mixture to control density, viscosity, emulsification and/or phase-segregation tendencies. The diluent can also strongly affect extraction equilibria, for reasons explicable through chemical interactions (Tamada, et al., 1990; Tamada and King, 1990a).

It is necessary to follow extraction with a regeneration step, to recover the carboxylic acid product and to reclaim the solvent mixture for recycle. For sufficiently volatile acids, e.g., acetic (Ricker, et al., 1980), the extract can be fed to a distillation sequence to produce the anhydrous acid as well as the

solvent for recycle. Regeneration is more complicated for low-volatility carboxylic acids, such as dicarboxylic and hydroxycarboxylic acids. Although evaporation can be used for sufficiently volatile solvents, it is not energy-efficient because all the solvent must be vaporized, and there is no means for separating the desired acid from other low-volatility components.

2 SWINGS OF TEMPERATURE AND/OR DILUENT COMPOSITION

Baniel, et al. (1981) have described regeneration of amine extracts of carboxylic acids by back extraction of the acid to an aqueous phase following a shift of the extraction equilibrium, obtained by changes in either temperature (temperature swing) in diluent composition (diluent swing). Amine extraction with temperature-swing regeneration is used commercially for the manufacture of citric acid by fermentation.

Tamada, et al. (1990) and Tamada and King (1990ab) have explored and interpreted the factors which govern shifts in extraction equilibria when temperature and diluent composition are changed. Important factors include the tendency of the diluent to solvate or form hydrogen bonds with the amine-carboxylic acid ion pair or complex, and the tendency toward stoichiometric overloading (complexation with more than one carboxylic acid per amine) for the particular acid and diluent.

For extraction of succinic acid by Alamine 336 (mixed trialkylamines with C_8 to C_{10} alkyl groups; Henkel Corp.) with mixtures of chloroform and n-heptane as diluent, forward extraction equilibria are much more favorable for high proportions of chloroform in the diluent. Thus diluent-swing regeneration can be carried out effectively if the more volatile chloroform is distilled from the extract after forward extraction and before back extraction. Tamada, et al. (1990b) noted that for this system the overall concentration factor, CF (the ratio of acid concentration in the initial aqueous feed to acid concentration in the aqueous back extract) is greater for diluent swing than for temperature swing in the case of low feed concentrations of succinic acid. The situation is reversed for higher concentrations of succinic acid in the feed. Diluent-swing and temperature-swing can be used together to gain still greater CF.

3 pH SWING

Back extraction of a carboxylic acid is greatly favored if the pH of the aqueous solution is increased above the pK_a of the acid; however, the carboxylate salt is produced. If the carboxylic acid is the desired product, it is necessary that another acid be added in additional steps. The process thereby consumes both an acid and a base (for pH control), and produces a salt as a by-product.

3.1. Regeneration by Back Extraction with a Volatile Aqueous Base

Extending a concept put forward by Urbas (1983,1984) in a different context, an aqueous solution of a volatile base can be used for back extraction. The resulting aqueous solution of the carboxylate salt can then be heated and concentrated by evaporation, thermally decomposing the carboxylate salt to yield the carboxylic acid product and a vapor containing the free base and water vapor, suitable for condensation and recycle. The most obvious volatile aqueous base is ammonia, but ammonium and primary and secondary alkylammonium carboxylates form amides irreversibly upon heating. Tertiary amines do not have this drawback. The most volatile tertiary amine is trimethylamine, TMA.

We have examined the use of aqueous solutions of TMA for back extraction of succinic, fumaric and lactic acids from Alamine 336 in MiBK (Poole and King, 1989, 1990). Typical results are shown in Figure 1, where the solid curve represents the prediction of a complexation model based upon experimental data for forward extraction from water (Tamada, et al., 1990), coupled with simple modeling of the aqueous phase using reported pK_a values for the acid and the amine. Notice from Figure 1 that the back extraction is essentially stoichiometric, recovering one mole of the difunctional acid per two moles of amine. This reflects the much greater basicity of the ionizing aqueous TMA than of the organic Alamine 336.

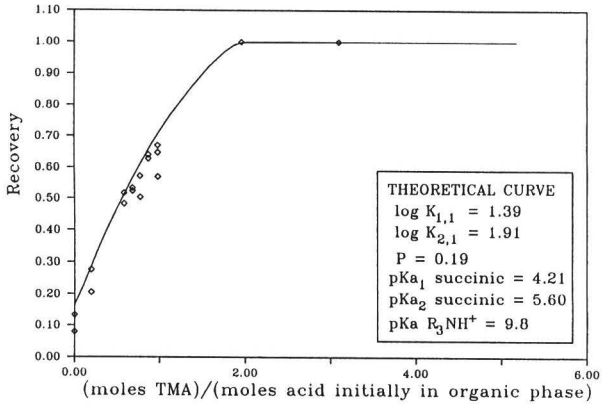

Fig. 1 Equilibria for Back Extraction of Succinic Acid from 0.3 mol/L Alamine in MiBK into Aqueous Solutions of Varying TMA Concentration.

It is desirable to carry the back extraction out in a single stage or in a cocurrent arrangement, to minimize loss of TMA to the solvent phase, which is small as long as TMA is not present in stoichiometric excess over the acid (Poole and King, 1989, 1990).

Recovery of fumaric and succinic acids from the aqueous TMA carboxylate solution has been demonstrated experimentally (Poole and King, 1989, 1990). Heating and evaporation concentrate the solution, following which the TMA carboxylate decomposes with release of TMA vapor and precipitation of the carboxylic acid. The crude solid carboxylic acid product was purified by repeated dissolution and evaporative recrystallization. Recrystallization from acetone (once) followed by MiBK (three times) gave 77% recovery of succinic acid containing less than 0.01 mole TMA/mole acid. Recrystallization from acetone (once) and MiBK (once) gave 81% recovery of fumaric acid, containing 0.05 moles TMA/mole acid. Recovery of lactic acid was found to be more difficult, because lactic acid is much more soluble in water, the concentrate becomes highly viscous due to self-association of lactic acid, and the equilibrium shifts towards the acid-amine complex as the concentration increases.

The maximum concentration of carboxylate achievable in the aqueous TMA back extract depends upon the concentration of TMA in that stream. TMA is commercially available in 25% w/w, or 3.95 mol/L, aqueous solution. The overall concentration factor (CF) achievable for 3% w/w (0.25 molar) initial aqueous succinic acid solution is therefore 3.95/0.25 = 7.9, which exceeds the CF typically attainable by temperature or diluent swing (Poole and King, 1989).

The high basicity of aqueous solutions of low-molecular-weight amines makes this method of regeneration useful for strongly basic extractants, such as higher-molecular-weight amines. Many fermentations producing carboxylic acids operate best at pH values close to or above the pK_a of the acid. A strongly basic extractant can give effective extraction at pH values equal to or somewhat above the pK_a of the acid being extracted. It is difficult to regenerate such extractants by ordinary means, and back-extraction into an aqueous solution of a low-molecular-weight tertiary amine provides a viable avenue.

4 PRECIPITATION OF LOW-SOLUBILITY ACIDS FROM THE EXTRACT

Recovery of carboxylic acids by precipitation from the extract is a possibility for carboxylic acids of low to moderate solubility and could be brought about by evaporation of solvent or diluent, temperature swing, and/or diluent swing. Precipitation of the acid by evaporation of the diluent in amine extractant systems is hampered by the fact that higher acid concentrations shift the equilibrium toward the acid-amine ion pair or complex.

4.1. Enhancement of Acid Solubility Due To Co-extracted Water

Solubilities of carboxylic acids in certain solvents and diluents increase markedly in the presence of co-extracted water. Experimental data for the system fumaric acid-cyclohexanone-water are shown in Figure 2. The lower points show

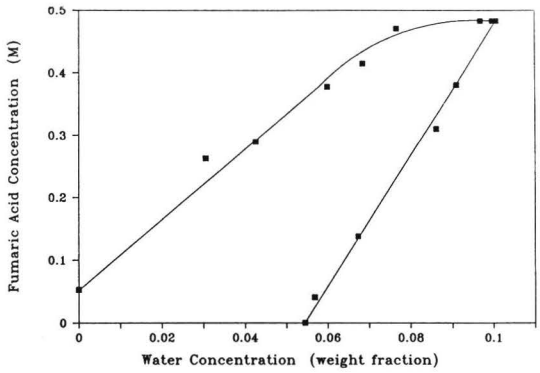

Fig. 2. Equilibria in the fumaric acid (FA)-Cyclohexanone (CH)-water system. Upper curve: FA in CH Phase in Equilibrium with Solid FA, for Varying Amounts of Water in the System. Lower Curve: FA in CH Phase in Equilibrium with an Aqueous Phase, for Varying Amounts of FA in the System.

concentrations of fumaric acid in the cyclohexanone phase in equilibrium with an aqueous phase, for varying amounts of fumaric acid in the system. The upper points show concentrations of fumaric acid in the cyclohexanone phase in equilibrium with a solid fumaric acid phase, for varying amounts of water in the system. The solubility of fumaric acid in the cyclohexanone increases by a factor of eight, from 0.0520 to 0.482 mol/L, in the presence of co-extracted water. Similar effects have been found for adipic and succinic acids and for fumaric acid in methylcyclohexanone (7.1), MiBK (5.6), 1-octanol (1.56), and di-n-butyl ether (1.64) as solvents, where the figures in parentheses indicate the factor of increase in acid solubility due to co-extracted water in each case.

4.2. Regeneration by Crystallization Due to Evaporation of Co-extracted Water

This phenomenon is the basis for a simple regeneration process where the extract is subjected to evaporative crystallization (Starr and King, 1990). Water has a high activity coefficient in organic solvents. Therefore, for solvents such as MiBK, cyclohexanone and methylcyclohexanone the co-extracted water can be removed by evaporation or stripping, with concomitant vaporization of relatively little of the ketone. Removal of the water lessens the solubility and causes the acid to precipitate.

In one test experiment, evaporation of 14% of a water-saturated extract of fumaric acid in MiBK precipitated 39% of the fumaric acid, while evaporation of 18% of an anhydrous 98% saturated solution of fumaric acid in MiBK caused precipitation of only 1.6% of the fumaric acid. It should be possible to enhance these recoveries through judicious choice of solvent.

5 CONCLUSIONS

Two novel methods of regeneration each have particular advantages for recovery of extracted carboxylic acids. Back extraction with an aqueous solution of a low-molecular-weight tertiary amine gives nearly stoichiometric recovery of acid and is suitable for regeneration of strongly basic extractants. Product recovery and regeneration are accomplished through decomposition of the trialkylammonium carboxylate. For certain solvents, such as ketones, the solubilities of carboxylic acids are greatly enhanced in the presence of co-extracted water. Stripping of that water consumes little energy and can cause precipitation of a large fraction of the extracted acid. This method of regeneration has been shown to be effective for recovery of adipic, fumaric and succinic acids from ketone extracts.

6 ACKNOWLEDGEMENT

This work was supported by the Assistant Secretary for Conservation and Renewable Energy, Office of Energy Research, Energy Conversion and Utilization Technologies (ECUT) Division, U. S. Department of Energy, under Contract DE-AC03-76SF00098, and by two National Science Foundation Graduate Fellowships.

7 REFERENCES

Baniel, A. M., Blumberg, R. and Hajdu, K., 1981. Recovery of acids from aqueous solutions. U. S. Patent No. 4,275,234.

Poole, L. J. and King, C. J., 1989. Regeneration of amine carboxylic acid extracts. Report No. LBL-28614, Lawrence Berkeley Laboratory, Berkeley CA.

Poole, L. J. and King, C. J., 1990. Regeneration of carboxylic acid-amine extracts by back-extraction with an aqueous solution of a volatile amine. Ind. Eng. Chem. Res., in press.

Ratchford, W. P., Harris, E. H., Fisher, C. H. and Willits, C. D., 1951. Extraction of lactic acid from water solution by amine-solvent mixtures. Ind. Eng. Chem., 43: 778-781.

Ricker, N. L., Pittman, E. F. and King, C. J., 1980. Solvent extraction with amines for recovery of acetic acid from dilute aqueous solutions. J. Separ. Process Technol., 1 (2): 23-30.

Starr, J. N. and King, C. J., U. S. patent application in progress, with patent rights to University of California.

Tamada, J. A., Kertes, A. S. and King, C. J., 1990. Extraction of carboxylic acids with amine extractants. I. Equilibria and law-of-mass-action modeling. Ind. Eng. Chem. Res., in press.

Tamada, J. A. and King, C. J., 1990a. Extraction of carboxylic acids with amine extractants. II. Chemical interactions and interpretation of data. Ind. Eng. Chem. Res., in press.

Tamada, J. A. and King, C. J., 1990b. Extraction of carboxylic acids with amine extractants. III. Effect of temperature, water co-extraction and process considerations. Ind. Eng. Chem. Res., in press.

Urbas, B., 1983. Recovery of acetic acid from a fermentation broth. U. S. Patent No. 4,405,717.

Urbas, B., 1984. Recovery of organic acids from a fermentation broth. U. S. Patent No. 4,444,881.

Solvent Extraction 1990, T. Sekine (Editor)

© 1992 Elsevier Science Publishers B.V. All rights reserved

REACTIVE-EXTRACTION OF L-PHENYLALANINE FROM AN ENZYMATIC SOLUTION

H.-J. Bart, R. Marr, U. Bauer, H. Reisinger
Institut für Thermische Verfahrenstechnik und Umwelttechnik
Technische Universität Graz, Inffeldgasse 25, A-8010 Graz (Austria)

ABSTRACT
Bart, H.-J.; Marr, R.; Bauer U.; Reisinger H.; 1990. Reactive extraction of L-phenylalanine from an enzymatic solution

This work presents the fundamental data for the separation of L-phenylalanine out of an aqueous enzymatic solution by a continuous reactive extraction separation process. It is shown that reactive extraction is a useful means of separating L-phenylalanine and that it meets both demands made on a separation technology; selective separation and upconcentration of the product.

INTRODUCTION

L-phenylalanine is an amino acid with the structure: $C_6H_5-CH_2-CHNH_2-COOH$. It can be produced by all four "classic" methods of amino acid production (Präve, 1984): 1) chemical synthesis, 2) protein hydrolysis, 3) enzymatic processes and 4) fermentation.
Chemie Linz AG produces L-phe by way of enzymatic transamination shown by the following equation:

$$R-CH_2-CO-COOH + HOOC-CH_2-CHNH_2-COOH \;\text{=====}\; R-CH_2-CHNH_2-COOH + CO_2 + CH_3-CO-COOH \quad (1)$$

PPA L-asp L-phe PA

A L-phe concentration of about 150 mmol/l is reached.
In the reaction solution there are L-phenylalanine (L-phe), L-aspartic acid (L-asp), phenylpyruvic acid (PPA), pyruvic acid (PA), magnesium chloride, enzymes and unidentified impurities. Pyruvic acid and phenylpyruvic acid can be separated by physical extraction with butylacetate. To separate L-phe from the remaining reaction solution reactive extraction is to be used.

The economic importance of L-phe lies in its use in the dipeptide aspartam (1-methyl-N-aspartyl-L-phenylalanine) which is more than 150

times sweeter than saccharose and raised the world production of L-phe from 50 t/a in 1981 to 5800 t/a in 1987 (Thien, 1988).

REACTIVE EXTRACTION

To extract carboxylic acids by reactive extraction tertiary amines with organic chains of 6 to 12 carbon atoms are commonly used (Schügerl, 1989). But with these amines only anions can be extracted. As shown in figure 1 L-phe is charged at each pH; it is a cation (an ammonium ion) at a low pH, it is a zwitterion at a moderate pH and it is an anion (a carboxylic ion) at a high pH.

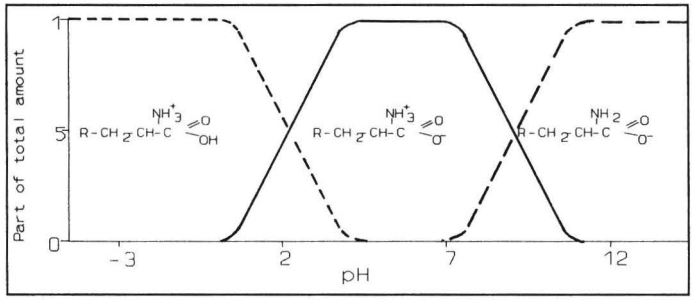

Fig. 1. Speciation of L-phenylalanine

Tertiary amines are only stable in the acidic milieu and cannot be used for reactive extraction of amino acids. L-phe can be extracted in its cationic form by DEHPA at a low pH or in its anionic form by quaternary amines at a high pH (Schügerl, 1989). As shown in equation 2 an aqueous anionic L-phe can be solubilized in an organic phase by a reaction with a quaternary organic ammonium sulfate:

$$2\ R\text{-}CH_2\text{-}CHNH_2\text{-}COO^-_a + [R_3NCH_3]_2SO_{4o} \equiv\equiv\equiv 2\ [R\text{-}CH_2\text{-}CHNH_2\text{-}COO][R_3NCH_3]_o + SO_4^{2-}{}_a \quad (2)$$

The sulfate ion is exchanged by the L-phe anion. As pKa2 of L-phe is 9.13 a pH of much more than 9.13 is needed that most of L-phe is in its anionic form (that the equilibrium is on the left side of the following equation):

$$R\text{-}CH_2\text{-}CHNH_2\text{-}COO^- + H^+ \;=====\; R\text{-}CH_2\text{-}CHNH_3{}^+\text{-}COO^- \quad (3)$$

EXPERIMENTS

All extraction experiments were done with reaction solutions from Chemie Linz AG as synthetic solutions showed to have other charac-teristics.The reaction solutions were treated with butylacetate to remove PA and PPA. Extraction was done in 100 ml vessels with magnetic stirrer of 400 rpm at a constant pH. After the extraction the phases were allowed to settle and the aqueous phase was analysed for the L-phe and the L-asp concentration by HPLC with reversed phase column, OPA (ortho-phthaldialdhyde) derivatisation and UV-detection.

RESULTS

Siebenhofer (1983) found rules for the optimal composition of the organic extraction phase for the reactive extraction of carboxylic acids by tertiary amines:

1) According to the specific separation problem, the maximum concentration of amine should be used,but this maximum must not be higher than 30 to 40 volume% as there are hydrodynamic restrictions.
2) The amount of modifier should be approximately the same as the amount of the reactive component.

These rules were confirmed by our experiments also for the extraction of L-phe by quaternary amines. Beside the extractant a diluent proved to be necessary which had to raise the interface tension to the aqueous phase and to lower the density and viscosity of the organic phase. Also the solubility of the extractant in the aqueous phase is lowered by this aliphatic diluent to only some ppm. As the quaternary amine and especially the complex formed by the extracted L-phe and the amine has no good solubility in the diluent a modifier has to be added to form one homogeneous organic phase. As diluent a kerosene and as modifier a long chained alcohole is used. According to the rules of Siebenhofer an organic phase composition of 30 vol% extractant, 25 vol% modifier and 45 vol% diluent proved to be best. Such a high amount of modifier would not be necessary to form an integrated organic phase, for that purpose 5 to 10 vol% would be enough. The amount of modifier is so high because the modifier also improves the extraction equilibrium.

At a pH of more than 10 the magnesium of the reaction solution precipitates forming magnesiumhydroxide. This precipitate disturbs the extraction. As there is no precipitate at a pH of 9.7 this pH is preferred to the highest possible pH of about 12.5 though there is worse extraction equilibrium (see equation 2 and 3). The distribu-

tion equilibrium between an organic phase of 30 vol% quaternary amine, 25 vol% alcohol and 45 vol% kerosene and the aqueous reaction solution is shown in figure 2a. A separation of L-phe out of the aqueous phase down to low concentrations in the raffinate seem to be possible by only few separation steps.

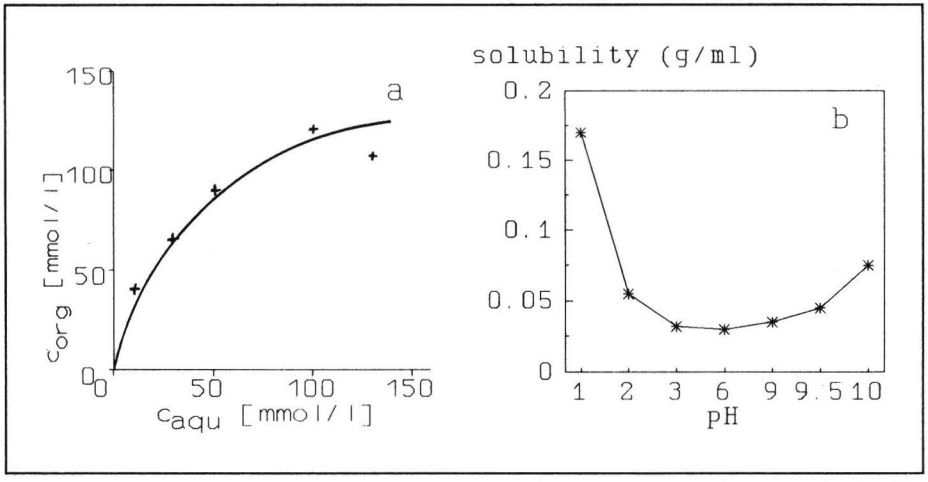

Fig. 2. (a) Distribution equilibrium of L-phe between an organic phase (30% carrier, 25% modifier, 45% diluent) and an aqueous phase at a pH of 9.7. (b) Solubility of L-phe versus pH.

As we have some components in the organic phase with high boiling points and L-phe has such a high decomposition point of 283 degrees celsius, too, there is no distillation possible to separate the L-phe out of the organic phase. But L-phe can be separated out of the organic phase by contacting it with an aqueous phase of low pH. As can be seen from equation 2 and 3 at a low pH the L-phe anion reacts with a proton to L-phe zwitterion, the equilibrium is completely driven to the right side of equation 3 and consequently to the left side of equation 2. L-phe gets insoluble in the organic phase.
As shown in figure 2b L-phe has no good solubility in the aqueous phase in its zwitterionic form, too. That leads to a precipitate of L-phe at the border area between aqueous and organic phase when the organic phase is contacted with an aqueous phase of moderate pH, for example with a solution of acetic acid. The phase separation after the reextraction step must be supported by centrifugation, with the advantage that a big part of the reextracted L-phe could be separated

directly as precipitate.

If reextraction is done by an aqueous phase of low pH, for example by a sulfuric acid solution, most L-phe can be separated out of the organic phase and solubilized in the aqueous phase (figure 3a) as L-phe has a much higher solubility in its cationic form at the low pH than in its zwitterionic form at a moderate pH (figure 2b). A concentration of up to 400 mmol/l L-phe can de reached (figure 3b).

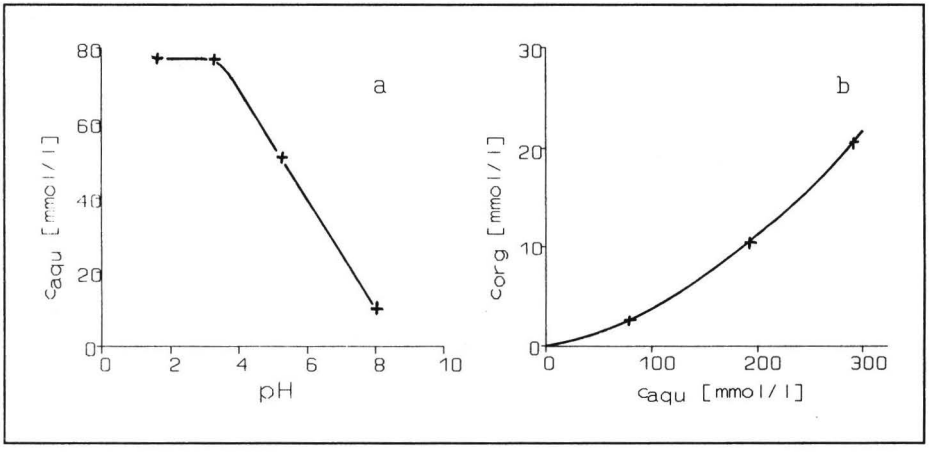

Fig. 3. (a) Solubility of L-phe in aqueous sulfuric acid versus pH. (b) Distribution equilibrium of L-phe between organic extraction phase and aqueous sulfuric acid at a pH of 3.

The extraction/reextraction by organic phase with an amine extractant and by sulphuric acid as stripping phase was done four times with the same organic phase. It was found that some L-phe remained in the organic phase after reextraction even when the organic phase was contacted with much sulphuric acid.

The remaining L-phe reduces the capacity of the organic phase for the next extraction and therefore it possibly gets necessary that the organic phase has to be washed after reextraction with additional sulphuric acid.

As we did not start a continuous extraction/reextraction we could not explore if this remaining L-phe in the organic phase reaches a summit at a certain concentration or if the organic phase is loaded with more and more L-phe after each cycle.

After reextraction L-phe can be cleaned by further steps. When raising the pH to the isoelectric point (pI = 5.48) it precipitates.

The precipitate can be filtrated, recrystallized again and washed with ethanol.

The whole process of L-phe separation with sulphuric acid reextraction is shown in a flow sheet in figure 4.

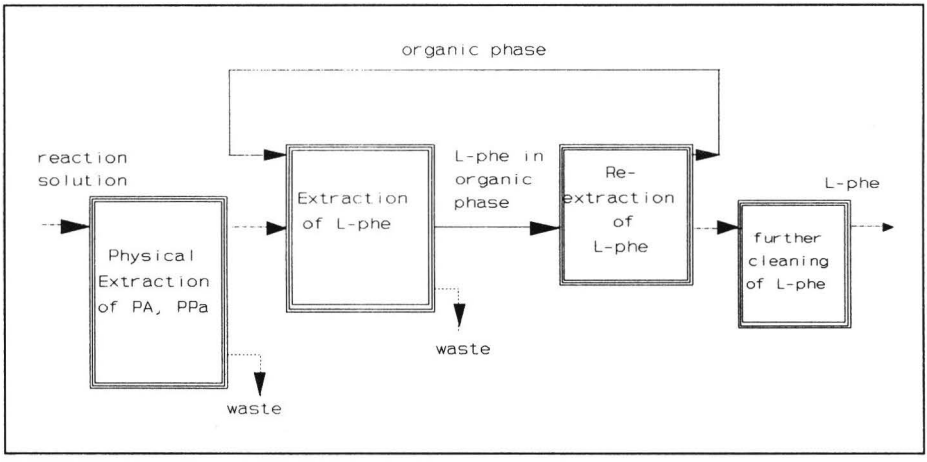

Fig. 4. Flowsheet of continuous L-phe separation

CONCLUSIONS

Further investigations of the reactive extraction of L-phe out of a reaction solution are left to be done. Nevertheless this work is an essential step in direction of the application of reactive extraction in the separation of L-phe out of reaction solutions in industrial processes. It was found that reactive extraction meets both demands made in a separation process:

1) The product is separated selectively (only small amounts of other compounds are coextracted);

2) the product is upconcentrated from about 150 mmol/l to 400 mmol/l.

REFERENCES

Präve, P. et al., 1984.Handbuch der Biotechnologie, R. Oldenburg Verlag, München-Wien, 2nd Ed., p.458.

Schügerl, K. et al., 1989. Chem.Ing.Tech., 61 Nr.10, 796

Siebenhofer, M., 1983. Verfahrensentwicklung für die Extraktion mit chemischer Reaktion am Beispiel der Carbonsäureextraktion, Dissertation, Techn. Univ. Graz.

Thien, M.P., 1988. Separation and Concentration of Amino Acids Using Liquid Emulsion Membranes, Thesis, MIT.

Solvent Extraction 1990, T. Sekine (Editor)

© 1992 Elsevier Science Publishers B.V. All rights reserved

EXTRACTION OF AMINO ACID WITH ORGANOPHOSPHORUS EXTRACTANT

M.TERAMOTO, Y.MIYAKE, H.MATSUYAMA and H.NARA
Department of Chemistry and Materials Technology, Kyoto Institute of Technology, Matsugasaki, Sakyo-ku, Kyoto 606 (Japan)

ABSTRACT

Extraction of amino acids and their related compounds with di(2-ethylhexyl)-phosphoric acid(D2EHPA) dissolved in benzene was studied. Distribution ratio of amino acid D was proportional to the fraction of amino acid in the form of zwitterion. The exponent m in the relation $D \propto [D2EHPA]^m$ was in the range from 1.7 to 2.0 for alanine(Ala), valine(Val), leucine(Leu),isoleucine(Ile), phenylalanine(Phe) and tryptophan(Trp) while m was 4 for lysine(Lys). Correlation of D with the hydrophobic scale suggested that D is mainly determined by the solubility of amino acid in the organic phase. The value of D for Phe is discussed in relation to the D values of β-phenetylamine and 3-phenylpropionic acid.

1 INTRODUCTION

It has been reported that amino acids such as lysine(Yagodin et al.,1986), Trp (Teramoto et al., 1988) and Phe(Teramoto et al., 1988, Itoh et al., 1990) can be separated and concentrated by emulsion liquid membranes (ELM) containing di(2-ethylhexyl)phosphoric acid(D2EHPA) as a carrier. Although extraction equilibrium is important as a basis of the separation of amino acid by ELM, very few studies have been performed on the extraction equilibria of amino acids (Teramoto et al., 1988). In this paper, a series of experiments on the extraction of various amino acids and their related compounds with D2EHPA dissolved in benzene was carried out to elucidate their extraction behavior.

2 EXPERIMANTAL

D2EHPA was kindly offered by Daihachi Chemical Industry Co., Ltd.. Amino acids used were Gly, L-Ala, L-Val, L-Leu, L-Ile, L-Phe and L-Trp. β-phenetylamine (1-amino-2-phenylethane, β-PhA), 3-phenylpropionic acid (PhPA) and phenylalanine ethyl ester (PheEt) were also used to discuss the distribution ratio of Phe by considering the effect of substituent on the distribution ratio. Benzene was used as a diluent.

Extraction equilibria were measured by the usual procedure at 298K. Ionic strength was adjusted at 0.1M with NaCl, and pH with HCl. The solute extracted in the organic phase was stripped with 1M HCl solution, and amino acids were analyzed by Ninhydrin method or the HPLC or the UV spectrophotometry. β-PhA, 3-PhPA and PheEt were determined by the HPLC or the UV spectrophotometry.

3 RESULTS

3.1 Extraction of α-amino acids

α-amino acid changes its charge depending on pH. In low pH region, the predominant species are A^+ and A^{+-}, and the presence of A^- can be ignored.

$$A^+ \underset{+H^+}{\overset{-H^+}{\rightleftharpoons}} A^{+-} \quad (1), \qquad K_a=[A^{+-}][H^+]/[A^+] \quad (2)$$

The distribution ratio D is expressed by eqn.(3).

$$D=[\bar{C}]/[A]_T=[\bar{C}]/([A^{+-}]+[A^+])=[\bar{C}]/\{[A^{+-}](1+[H^+]/K_a)\}=D^{+-}/(1+[H^+]/K_a) \quad (3)$$

Here, $[\bar{C}]$ is the concentration of amino acid-D2EHPA complex in the organic phase and $\bar{}$ denotes the species in the organic phase. Effect of hydrogen ion concentration on the distribution ratio of α-amino acids is shown in Fig.1. It can be seen that in the range of high pH (>pK_a) where amino acid exists mainly as the zwitterion, the distribution ratio D is almost constant, and this value corresponds to D^{+-}, the distribution ratio of A^{+-} defined by $[\bar{C}]/[A^{+-}]$. In the range of low pH (<pK_a), D is inversely proportional to $[H^+]$. If the extraction reaction and its equilibrium are assumed to be expressed by eqns.(4) and (5), respectively, then eqns.(6) and (7) are derived.

$$A^{+-} + m\overline{(HL)_2} \rightleftharpoons \bar{C} \quad (4), \qquad K_{ex}{}^{+-}=[\bar{C}]/[A^{+-}][\overline{(HL)_2}]^m \quad (5)$$

$$D = K_{ex}{}^{+-}[\overline{(HL)_2}]^m/(1+[H^+]/K_a) \quad (6), \qquad D^{+-}=K_{ex}{}^{+-}[\overline{(HL)_2}]^m \quad (7)$$

Here $\overline{(HL)_2}$ is the dimer of D2EHPA. Figure 2 shows the effect of $[\overline{(HL)_2}]$ on D^{+-}. The slopes of the plots, i.e., the values of m, are between 1.7 and 2.0, suggesting that the complex is approximately expressed by $\overline{A^{+-}(HL)_4}$. The values of D^{+-} at $[\overline{(HL)_2}]=0.0726 mol/dm^3$, and the values of m and K_a are listed in Table 1. The solid lines in Fig.1 are the results calculated by eqn.(6).

3.2 Extraction of lysine

Lysine having two amino groups changes its charged state depending on pH(<pK_a') as follows.

$$A^{++} \underset{+H^+}{\overset{-H^+}{\rightleftharpoons}} A^{+-} \underset{+H^+}{\overset{-H^+}{\rightleftharpoons}} A^{+-} \quad (8), \qquad K_a=[A^{++-}][H^+]/[A^{++}] \quad (9), \qquad K_a'=[A^{+-}][H^+]/[A^{++-}] \quad (10)$$

The following equation is derived by considering eqns.(9) and (10).

$$D=D^{+-}\{1+[H^+]/K_a+[H^+]^2/(K_aK_a')\} \quad (11)$$

The plot of D vs $[H^+]$ is shown in Fig.3. It is seen that with increasing $[H^+]$, the slope approaches -2. The value of D^{+-} for each $[\overline{(HL)_2}]$ was determined so that eqn.(11) might fit the experimental data. From the slope of the plot of D^{+-} vs $[\overline{(HL)_2}]$, the value of m was determined as 4. The solid lines in Fig.3 are the results calculated by eqns.(7) and (11). The value of D^{+-} at $[\overline{(HL)_2}]=0.0726$ M is shown in Table 1.

4 DISCUSSION

4.1 Correlation of distribution ratio with hydrophobic scale

Two hydrophobic scales of amino acids which correspond to the free energy of transfer of amino acid residue from aqueous to organic phase, Δf have been proposed(Nozaki and Tanford,1971, Bull and Breese,1984). Figure 4 shows the plot of D^{+-} vs the hydrophobic scale by Nozaki and Tanford, and also that by Bull and Breese. It can be seen that the latter gives better correlation than the former. The slopes of the former and the latter plots are 0.00134 and 0.00191 mol/cal, respectively. These values are roughly equal to 1/RT=0.00169 mol/cal. If the reaction in organic phase is expressed by eqn.(12), the partition coefficient of the zwitterion, K is expressed by eqn.(13). K is related to a free energy of transfer of amino acid from the aqueous to the organic solution, ΔG (eqn.(14)). If we assume that the values of K_{ex}' change little depending on the kinds of amino acids, eqn.(15) is finally obtained since $\Delta G = \Delta f$ + const. holds. The experimental result can be explained by this relation.

$$\overline{A^{+-}} + m\overline{(HL)_2} \rightleftarrows \overline{C};\ K_{ex}' \qquad (12a)$$

$$A^{+-} + m\overline{(HL)_2} \rightleftarrows \overline{C};\ K_{ex} \qquad (12b)$$

$$K=[\overline{A^{+-}}]/[A^{+-}]=K_{ex}/K_{ex}' \qquad (13), \qquad \ln K= -\Delta G/RT \qquad (14)$$

$$\ln D^{+-} = -\Delta f/RT + \text{const.} \qquad (15)$$

Further study is necessary to examine the validity of this relation for other diluents.

4.2 Distribution ratios of 3-phenylpropionic acid, β-phenetylamine and phenylalanine ethyl ester

The plots of D vs $[H^+]$ for PhPA (denoted by RCOOH), β-PhA (RNH_2) and PheEt (RNH_2) are shown in Fig.5. The distribution ratios of these compounds are higher than that of Phe. If the extraction equilibria for RCOOH and RNH_2 are expressed by eqns.(16) and (17), respectively, distribution ratios are expressed by eqns.(18) and (19), respectively. Here D^0 is defined by $[\overline{C}]/[RCOOH]$ or $[\overline{C}]/[RNH_2]$ where RCOOH and RNH_2 represent the species having no charge.

$$K_{ex}{}^0{}_{RCOOH} = [\overline{C}]/[RCOOH][\overline{(HL)_2}]^m = D^0{}_{RCOOH}/[\overline{(HL)_2}]^m \qquad (16)$$

$$K_{ex}{}^0{}_{RNH2} = [\overline{C}]/[RNH_2][\overline{(HL)_2}]^m = D^0{}_{RNH2}/[\overline{(HL)_2}]^m \qquad (17)$$

$$D_{RCOOH} = [\overline{C}]/[RCOOH]_T = K_{ex}{}^0{}_{RCOOH}[\overline{(HL)_2}]^m/(1+K_a/[H^+]) = D^0{}_{RCOOH}/(1+K_a/[H^+]) \qquad (18)$$

$$D_{RNH2} = [\overline{C}]/[RNH_2]_T = K_{ex}{}^0{}_{RNH2}[\overline{(HL)_2}]^m/(1+[H^+]/K_a) = D^0{}_{RNH2}/(1+[H^+]/K_a) \qquad (19)$$

By using the data shown in Fig.5 and eqns.(18) and (19), the values of D^0 at $[\overline{(HL)_2}]$=0.0726M together with the values of m were determined and are shown in Table 1. The solid lines in Fig.5 are the computed results.

In order to discuss the distribution ratio of Phe in connection with those of PhPA, β-PhA, it seems reasonable to compare the values of D^0_{Phe} with D^0_{RCOOH} and D^0_{RNH2} because these values of D^0 are related to those of $K_{ex}{}^0$ through eqns.(16), (17) and (20). Here, D^0_{Phe} is defined by $[\bar{C}]/[Phe^0]$, and Phe^0 represents $PhCH_2CH(COOH)NH_2$, which is considered to be in chemical equilibrium with $PhCH_2CHCOOHNH_3^+$ as shown by eqns.(21) and (22) although the concentration of Phe^0 is extremely low.

$$K_{ex}{}^0{}_{Phe} = [\bar{C}]/[Phe^0][\overline{(HL)_2}]^m = D^0{}_{Phe}/[\overline{(HL)_2}]^m \quad (20)$$

$$PhCH_2CHCOOHNH_3^+ \rightleftharpoons PhCH_2CH(COOH)NH_2 + H^+ \ , (Phe^+ \rightleftharpoons Phe^0 + H^+) \quad (21)$$

$$K_a{}^0{}_{Phe} = [PhCH_2CH(COOH)NH_2][H^+]/[PhCH_2CHCOOHNH_3^+] = [Phe^0][H^+]/[Phe^+] \quad (22)$$

If $K_{a,Phe}$ is defined by

$$K_{a,Phe} = [PhCH_2CH(COO^-)NH_3^+][H^+]/[PhCH_2CH(COOH)NH_3^+] = [Phe^{+-}][H^+]/[Phe^+] \quad (23)$$

then the relation between $D^{+-}{}_{Phe}(=[\bar{C}]/[Phe^{+-}])$ and $D^0{}_{Phe}=[\bar{C}]/[Phe^0]$ is expressed by eqn.(24).

$$D^0{}_{Phe} = D^{+-}{}_{Phe}(K_{a,Phe}/K_a{}^0{}_{Phe}) \quad (24)$$

The exact value of $D^0{}_{Phe}$ cannot be obtained as the value of $K_a{}^0{}_{Phe}$ is not available. Since $K_a{}^0{}_{Phe}$ is considered to be larger than $K_{a,\beta\text{-PhA}}$ ($=7.6\times10^{-10}$M), $D^0{}_{Phe}$ must be less than 4.0×10^5, which was calculated from eqn.(24) by using $K_{a,\beta\text{-PhA}}$ as $K_a{}^0{}_{Phe}$. As shown in Table 1, $D^0{}_{\beta\text{-PhA}}$ is very large due to strong acid-base interaction between β-PhA and D2EHPA. $D^0{}_{PheEt}$ is also large because PheEt is hydrophobic. $D^0{}_{PhPA}$ is rather small because its interaction with D2EHPA is through hydrogen bonding. $D^0{}_{Phe}$ is between $D^0{}_{\beta\text{-PhA}}$ and $D^0{}_{PhPA}$. This result is reasonable because the contribution of carboxyl group to $D^0{}_{Phe}$ is much smaller than that of amino group, and also because carboxyl group is hydrophilic.

4.3 Relation between m and the structure of solute

The values of m (see eqn.(4)) for α-amino acids are close to 2, and m for β-PhA is also 2. This suggests that two molecules of $\overline{(HL)_2}$ coordinate to an amino group, and also that carboxyl group contributes little to m. In this respect, the result that m is 4 for Lys is reasonable since it has two amino groups. The value of m for PhPA is about unity in accordance with the value reported for lactic acid (Nicolaev et al., 1979). When n-heptane was used as a diluent, similar results were obtained (Nara, 1990). However, it was reported that the value of m for β-PhA was about 1.3 when butyl acetate was used as a diluent (Komasawa, 1987). Therefore, it seems that more polar the diluent, smaller the value of m.

5 REFERENCES

Bull, H. and Breese, K., 1984. Surface Tension of Amino Acid Solutions: A Hydrophobicity Scale of the Amino Acid Residue. Arch. Biochem. Biophys, 161: 665-670.

Itoh, H., Thien, M.P., Hatton, T.A. and Wang, D.I.C., 1990. A Liquid Emulsion Membrane Process for the Separation of Amino Acid. Biotech. Bioeng., 35: 853-860.

Komasawa, I., Satomi, M. and Tone, S., 1987. Extraction of Weakly Basic Compounds with Physiological Activity. Kagaku Kogaku Ronbunshuu, 13: 223-229.

Nara,H., 1990. Extraction of Amino Acid with Acidic Organophosphorus Extractant. Bachelor thesis. Kyoto Institute of Technology.

Nicolaev, V.M., Lebedev, V.M. and Detkin, N.A., 1979. Russ. J. Inorg. Chem., 19: 1045.

Niitsu, M. and Sekine, T., 1978. Solvent Extraction Equilibria of Acid. VI. The Extraction of Several Mono- and Dicarboxylic Acids with Trioctylphosphine Oxide in Hexane. Bull. Chem. Soc. Japan, 51:705-709.

Nozaki, Y. and Tanford, C., 1971. The Solubility of Amino Acids and Two Glycine Peptides in Aqueous and Dioxane Solutions. J. Biol. Chem., 246: 2211-2217.

Teramoto, M. Yamashiro, T., Yamamoto, A. and Matsuyama, H., 1988. Extraction of Amino Acids by Emulsion Liquid Membranes Containing D2EHPA as a Carrier. Proc. 1st Sino-Japanese Symp. on Liquid Membrane, 45-47. Submitted to J.Membrane Sci..

Yagodin, G.A., Yurtov, E.V. and Golubkov, A.S., 1986. Liquid Membrane Extraction of Amino Acids. Proc.ISEC'86, Vol.3, 677-681.

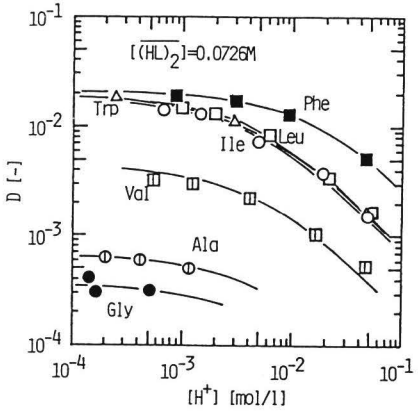

Fig.1 Plots of D vs $[H^+]$ for α-amino acids. $[\overline{(HL)_2}]$=0.0726M.

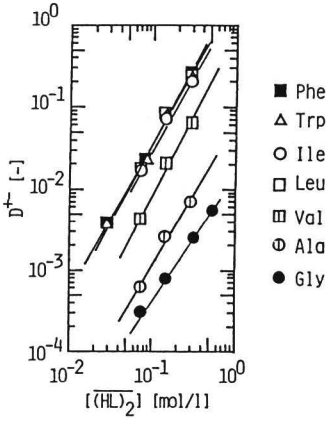

Fig.2 Plots of D^{+-} vs $[\overline{(HL)_2}]$ for α-amino acids.

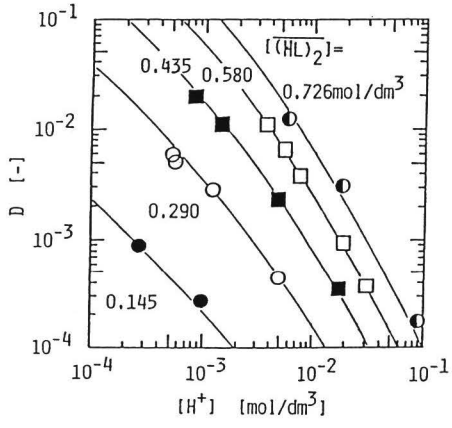

Fig.3 Plots of D vs $[H^+]$ for lysine.

Table 1 Values of pK_a, m, D^{+-} and D^0

Solute	pK_a	m	D^{+-} [a]	D^0 [a]
glycine(Gly)	2.34	1.7	3.62×10^{-4}	-
alanine(Ala)	2.34	1.7	6.34×10^{-4}	-
valine(Val)	2.32	1.9	3.71×10^{-3}	-
leucine(Leu)	2.36	1.9	1.95×10^{-2}	-
isoleusine(Ile)	2.38	1.8	1.69×10^{-2}	-
tryptophan(Trp)	2.38	1.8	1.88×10^{-2}	-
phenylalanine(Phe)	1.83	1.9	2.06×10^{-2}	$<4.0\times10^{5}$
lysine(Lys)	2.18, 8.95	4.0	1.41×10^{1}	-
β-phenetylamine(β-PhA)	9.12 [b]	2.0	-	5.8×10^{6}
3-phenylpropionic acid(PhPA)	4.0	1.0	-	1.2×10^{1} [c]
phenylalanine ethyl ester(PheEt)	-	1.8	-	$<1.6\times10^{7}$

[a] Values at $[\overline{(HL)_2}]=0.0726$ M.

[b] Komasawa, 1987.

[c] The value of D^0_{PhPA} is obtained by subtracting the physical partition of PhPA from its total partition. The physical distribution ratio of PhPA, D_{phys} in benzene is expressed by $D_{phys}=[\overline{RCOOH}]+2[\overline{(RCOOH)_2}])/[RCOOH]=[\overline{RCOOH}]x(1+2K_{dim}[\overline{RCOOH}])/\{[RCOOH](1+K_a/[H^+])\}$ (Niitsu et al., 1978). Dimerization constant K_{dim} was determined as 30 M^{-1} by vapor pressure osmometry, and partition coefficient $P=[\overline{RCOOH}]/[RCOOH]$ and pK_a were determined as 6.3 and 4.0, respectively, so that the above equation might fit the experimental result of D_{phys}.

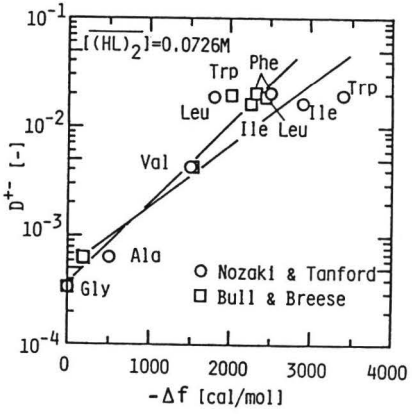

Fig.4 Plots of D^{+-} vs hydrophobic scale for α-amino acids.

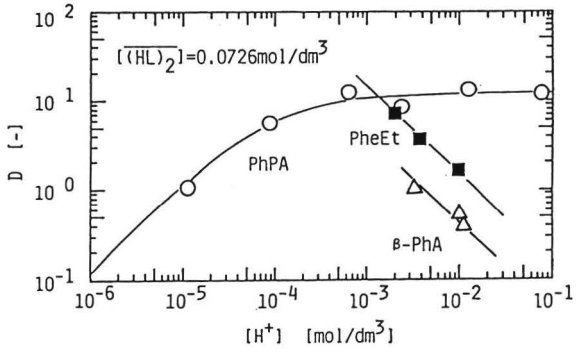

Fig.5 Plots of D vs $[H^+]$ for 3-phenylpropionic acid(PhPA), β-phenetylamine(β-PhA) and phenylalanine ethyl ester(PheEt).

Solvent Extraction 1990, T. Sekine (Editor)

© 1992 Elsevier Science Publishers B.V. All rights reserved

A NEW SEPARATION PROCESS OF CHLOROACETIC ACIDS BY EXTRACTION

H. TETZLAFF, S. RITTNER
Hoechst AG, Frankfurt/Main , FRG

ABSTRACT

A continuous liquid - liquid - extraction (LLX) process for the separation of mono- and dichloroacetic acid is presented. The acids are separated by multi-stage Van Dijck - distribution between water and di-n-butylether. The degree of purity of the acids is determined by the number of stages of the LLX-process. Extracts and raffinates are processed by distillation, water and solvent are recirculated.

INTRODUCTION

Halogenated carboxylic acids are important intermediates for different chemical syntheses in industry. For example monochloroacetic acid (b.p. 189,4°C) is used to produce carboxymethyl cellulose, herbicids and thioglycolic acid, dichloroacetic acid (b.p. 194,5 °C) is used in the synthesis of sulfonamides. The production of halogenated carboxylic acids by chlorination of carboxylic acids usually yields mixtures of mono-, di- and trihalogenated acids. Their boiling point differences are small which means the application of fractional crystallization or extractive - or azeotropic distillation methods for their separation. One disadvantage of the distillation methods is the limited chemical stability of most of the solvents employed against the agressive and reactive halogenated carboxylic acids. The difficult separation and purification process is industrially carried out preferentially by crystallization from the melt. Fig. 1 shows the melting point diagram of the system mono/dichloroacetic acid. The melt crystallization has the disadvantage that after the purification process an eutectic mixture of e. g. mono- and dichloroacetic acid is obtained which cannot be separated into individual chloroacetic acids and for which it is increasingly difficult to make use of. As a fast, continuous and gentle alternative we applied liquid-liquid-extraction (LLX) in the separation of halogenated carboxylic acids.

RESULTS

Table 1 as an example shows the results of a solvent screening for the extraction of mono (MCE)- and dichloroacetic acid (DCE) from their aqueous solutions. Listed are the significantly different distribution coefficients of MCE and DCE for their extraction with ethers and ketones and the corresponding separation factor ß. Due to the differences in the partition coefficients the distribution of the acids between an organic phase (out of table 1) and an aqueous phase offers the possibility to separate a mixture of both acids after the method of Van Dijck [1, 2].

According to the theory of Van Dijck distribution (strictly valid only in diluted solution) it is most advantageous when the substances to be separated have approximately reciprocal distribution numbers. For a roughly 1:1 mixture of MCE and DCE resulting e. g. as a mother liquor from purifying MCE by crystallization and which is to be separated by Van Dijck distribution at a mass phase ratio of 1:1, this means, that the distribution coefficients should be reciprocal. Therefore the di-n-butylether (b. p. = 141°C) is of special interest. Although it has a slightly lower separation factor for the two acids than di-n-amylether (b. p. = 187°C) it has the advantage of commercial availability and of a boiling point allowing its distillative sparation from DCE (b. p. = 194,5°C).

One possibility to make predictions about the required conditions (stage numbers, mass ratios and concentrations) to achieve a separation of MCE/DCE mixtures in concentrated solutions are MacCabe-Thiele constructions as shown in fig. 2.

The construction shows that in equilibrium the acid-concentrations in both phases and of both acids are highest in the center stage of the distribution bed, the place were the mixture of the acids is introduced. The concentration of the purified acids in the outgoing phases is limited by the boundary condition of not exceeding the mixing gap of the 4-component system in the middle part of the distribution bed. Therefore, neglecting the interactions of MCE and DCE in the solution, the triangular diagrams (fig. 3) of the two 3-phase systems MCE/DCE-di-n-butylether-water demonstrate that it is not advisable to work at concentrations above 45 w.-% of both acids in either di-n-butylether or water.

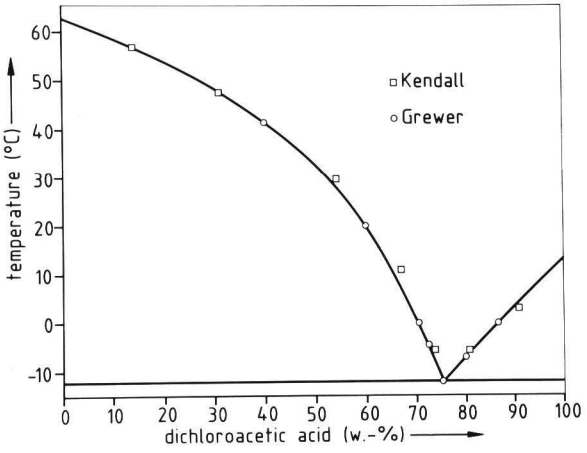

Fig 1: Melting point diagram of the system mono/dichloroacetic acid [3], [4].

TABLE 1

Distribution coefficients (K_D) and the corresponding separation factor (ß) for the extraction of MCE and DCE with ethers and ketones at room temperature from aqueous solution.

extracting agent	b.p. (°C)	K_D(MCE)	K_D(DCE)	ß
diisopropylether	66-69	1,21	5,72	4,7
di-n-butylether	141-142	0,40	2,14	5,4
diisobutylether	120	0,15	0,94	6,3
di-n-amylether	187	0,34	2,18	6,4
diisoamylether	170-172	0,25	1,73	6,9
di-n-hexylether	219-222	0,23	1,49	6,5
di-n-heptylether	256-258	0,20	1,27	6,4
methyl-tert. butyl-ether	55	4,26	17,2	4,0
dibenzylether	158-160	0,27	1,1	4,1
butyrophenon	220	0,73	2,93	4,0
valerophenon	244	0,54	2,33	4,3
diisobutylketone	169	0,91	3,80	4,2

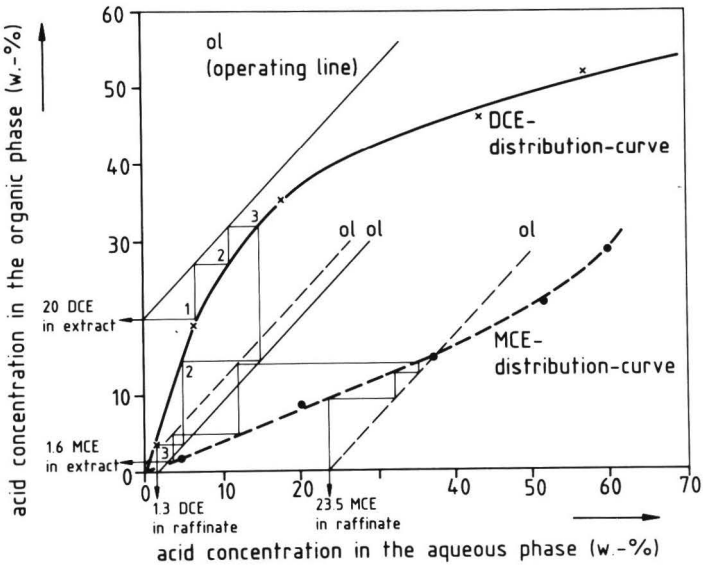

Fig. 2: MacCabe-Thiele construction of a 5-stage countercurrent distribution of MCE (54 w.-%) and DCE (46 w.-%) between di-n-butylether (1,07 parts) and water (1 part). The mixture of the acids (0,62 parts) is introduced into the third stage of the distribution bed.

This is due to the increasing miscibility of the phases and to the change in the direction of the tielines at about 50 w.-% DCE in the DCE-system. To reach as concentrated as possible extract and raffinate phases of a beforehand choosen purity a balance between stage number and mass phase ratio of the LLX-process has to be found. To do this we performed countercurrent extractions in the laboratory with Wojtech-mixer-settlers (fig. 4) at different mass phase ratios and stage numbers. For example a mixture of 46 w.-% DCE and 54 w.-% MCE (0,5 parts) was separated in this way with 15 practical mixer-settler stages by distribution between di-n-butylether (1,07 parts) and water (1,0 parts) into a di-n-butyletherphase containing

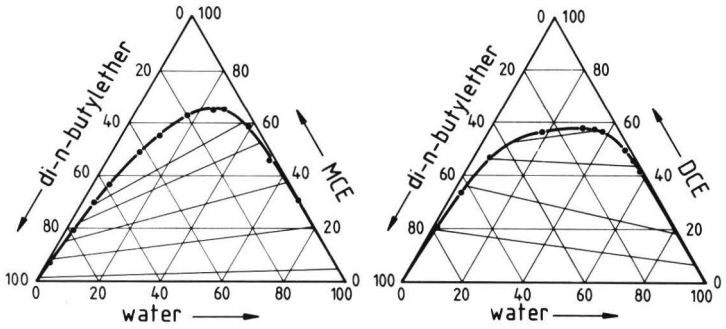

Fig. 3: Triangular diagrams of the systems MCE/DCE-di-n-butyleter-water (values given in w.-%).

17,5 w.-% DCE and 0,11 w.-% MCE and an aqueous phase containing 21,4 w.-% MCE and 0,07 w.-% DCE.

Meanwhile experiments on a technical scale in two reciprocating plate columns (type Karr, 0 = 50 mm, 3 m length) each representing one half of the distribution bed confirmed the laboratory results. Extracts and raffinates are processed by distillation, water and solvent are recirculated. DCE containing less than 0,3 w.-% MCE and MCE containing less than 0,3 w.-% DCE is produced. Fig. 5 shows schematically the whole process. The LLX-part is drawn as a multistage-distribution bed without specifying the corresponding apparatus.

REFERENCES

[1] O. Jübermann, Houben-Weyl, Methoden der organischen Chemie 4. edition, (1958), G. Thieme-Verlag Stuttgart Bd. I/1, 249-255
[2] A. Klinkenberg, Ind. Eng. Chem., 45 (3), (1953), 653-657
[3] T. Grewer, Hoechst AG, Frankfurt/Main, FRG, Applied Physics Department
[4] J. Kendall, J. Am. Chem. Sol., 36, 1722, (1914)

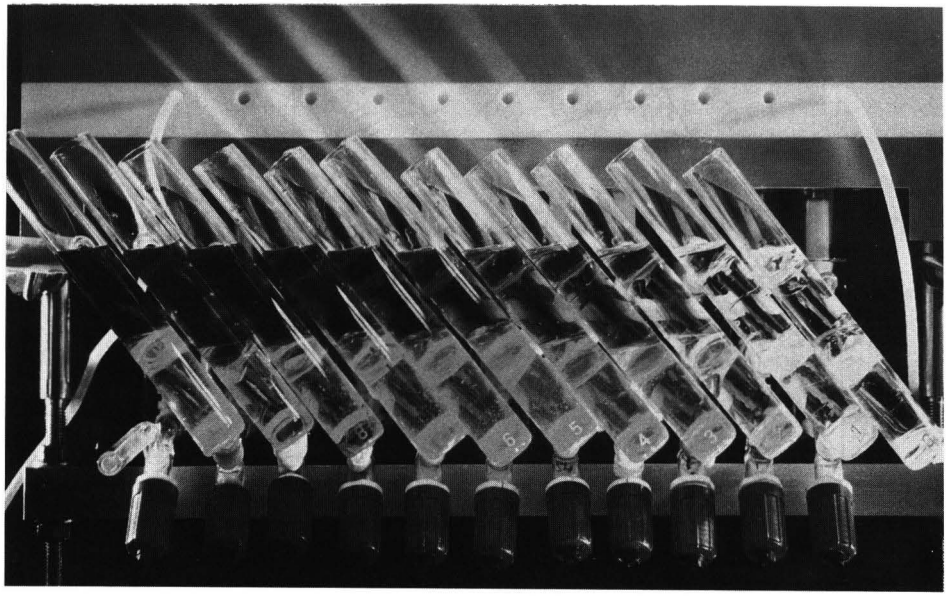

Fig. 4: Wojtech-mixer-settler filled with colored solutions for demonstration.

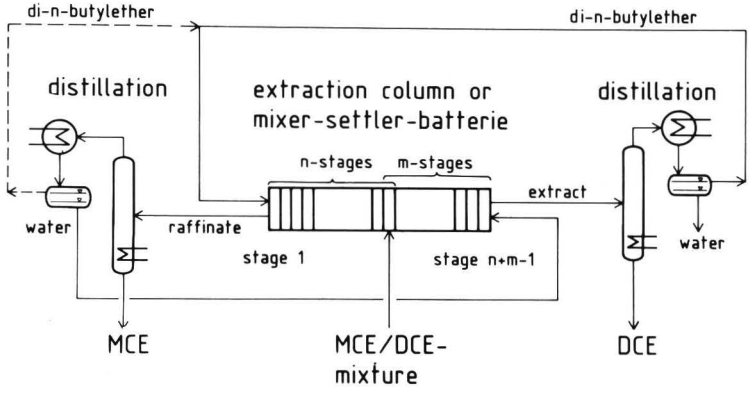

Fig. 5: Schematic drawing of the continuous LLX-separation process of MCE and DCE.

Solvent Extraction 1990, T. Sekine (Editor)

© 1992 Elsevier Science Publishers B.V. All rights reserved

PROTEIN EXTRACTION BY REVERSE MICELLES

M.E. Leser[1], G. Marcozzi[2], M. Caselli[3], P.L. Luisi[1*]
1) Institut für Polymere, ETH Zentrum, 8092 Zürich (Switzerland), 2) Eniricerche S.p.A., Via E. Ramarini 32, Monterotondo 00015 Roma (Italy), 3) Dipartimento di Chimia, Via Amendola 6, Bari, (Italy).

ABSTRACT

The good solubility power of reverse micelles for proteins and other biomolecules can be exploited for extraction and separation procedures. Two techniques to extract proteins into revese micelles are commonly used: 1) the liquid-liquid phase transfer method, and 2) the solid-liquid extraction method. Using the surfactant system AOT/water/isooctane (AOT stands for bis(2-ethylhexyl) sodium sulfosuccinate), the enzyme α-chymotrypsin can be easily transferred into the organic media and subsequently recovered again into an aqueous phase in a good yield. In this paper we report some back transfer experiments of α-chymotrypsin into 1M KCl pH 7.5. It is shown that the back transfer yield is dependent on the ionic strength which was used in the separate preceding forward extraction step. Also the enzymatic activity which was measured after this two-step extraction in the aqueous solution showed a dependency on ionic strength used for the forward transfer. In single cases almost an optimal enzymatic activity preservation was observed.

1 INTRODUCTION

In recent years, the interest in the development of new, efficient, and economic methods for the extraction and purification of proteins and other bioproducts was growing. Reverse micelles gained increased attention in this field, because they exhibit properties which open new possibilities in the separation technology of biomolecules (Kadam, 1986). Especially it was found that a great variety of proteins (i.e. enzymes) can be easily solubilized into these new organic media consisting of surfactant (up to 25-30 weight percent), water (up to 15-20%) and oil (i.e. hydrocarbon or fatty acid esters; 60 to 90%). Reverse micelles gained attention also in biotechnology because of the fact that the solubilized enzymes or other biological active species (i.e. bacteria, cells etc.) can be incorporated into the organic surfactant solutions under preservation of their biological activity (Luisi and Laane, 1986).

Reverse micellar solutions consist of spherical aggregates which are formed spontaneously by a great variety of surfactants in different organic solvents. The solutions are thermodynamically stable and transparent. The water droplets, formed in

the organic medium, are surrounded by a surfactant interfacial film. They are in general not larger than 30 nm. Using, for example, the surfactant AOT they exhibit also a remarkable monodispersity. The aggregation size is mainly influenced by the solubilized amount of water, normally referred to as w_o (w_o=[H_2O]/[AOT]), and the droplet density is determined by the amount of surfactant in solution (e.g. Eicke, 1980).

Incorporation of proteins or other biomolecules into reverse micelles can be achieved with one of these three different methods:

1) **The injection method**: Most commonly, an aqueous protein stock solution is injected into the organic micellar solution by a microsyringe and vigorously shaken till complete solubilization is achieved.

2) **The liquid-liquid phase transfer method**: The proteins are initially present in an aqueous salt solution. During equilibration with an organic micellar solution which is superimposed in a comparable volume, the proteins are transferred into the reverse micellar phase. Several years ago Luisi et al. (1977) used this transfer method for the extraction of α-chymotrypsin. The same group showed that also other proteins (i.e. trypsin, pepsin, lysozyme, horse liver alcohol dehydrogenase and others) can be extracted into micellar solutions, with a characteristic efficiency due to intrinsic properties of the proteins themselves (Luisi et al., 1979).

This finding brought about numerous following experimental and theoretical studies dealing with this extraction system (for a summary, see reviews for example of Leser and Luisi, 1990, Leodidis and Hatton, 1989, or Dekker et al., 1989). The results of all these investigations lead to the conclusion that mainly five parameters determine the extraction behaviour of the proteins: ionic strength in the aqueous phase (salt-type and concentration), pH, surfactant (type of surfactant (anionic, cationic or nonionic), co-surfactant, and concentration) in the organic phase, type of organic solvent, and temperature. The distribution of proteins in the bi-phase system was also shown to be significantly dependent on their intrinsic properties, i.e. isoelectric point (pI), molecular weight, or distribution (symmetrical or asymmetrical) of charged amino acid residues on the protein surface (Dekker et al, 1989).

3) **The solid-liquid extraction method**: This technique was used for the first time by Menger and Yamada (1979) to incorporate α-chymotrypsin into reverse micelles, and later on, also other enzymes were solubilized in this way (i.e. lysozyme (Grandi et al., 1981)). Leser et al. (1989) showed that this method can be useful for the separation of proteins, extracted from different meals. In this case the protein powder is suspended into an organic micellar solution containing already a well defined water amount, and having therefore droplets with a characteristic mean size. Moreover, this method is also suitable to solubilze water-insoluble proteins (Delahodde et al., 1984).

Once the protein is separated from a mixture by the help of reverse micelles, it must eventually be brought back into an aqueous solution (or liberated from the micellar media). This experimental configuration has been referred to as "backward transfer" (Luisi et al, 1979): a two-phase system is used in which the protein-containing micellar solution is equilibrated with an aqueous salt solution.

This paper will describe some recent backward transfer experiments using α-chymotrypsin as enzyme. This has been chosen as a model protein, since quite a few studies on its forward transfer properties have been published (i.e. Marcozzi et al., 1990, Leodidis and Hatton, 1989). We will also address the question, to what extend the enzymatic activity is maintained.

2 MATERIALS

α-chymotrypsin (EC 3.4.21.1) from bovine pancreas was obtained from Fluka, bis(2-ethylhexyl) sodium sulfosuccinate from Sigma, isooctane (analytical grade) from Merck, glutaryl-L-phenylalanine-4-nitroanilide (GPANA), analytical grade from Serva, the salts were of analytical grade.

3 METHODS

Liquid-liquid extraction: Equivalent volumes (3mL) of aqueous and micellar organic solutions were equilibrated in 10 mL tightly stoppered glass vials while stirring at 350 RPM on a mini-shaker for 15 (forward extraction, pH:5.0 20 mM acetate buffer) to 30 minutes (backward extraction). For all back transfer experiments 1M KCl 50 mM phoshate buffer pH 7.5 were used as aqueous extraction medium. Afterwards the obtained emulsion was separated again by centrifugation at about 3000-4000 RPM for 5-10 minutes. The α-chymotrypsin concentration in both phases was measured spectroscopically at 280 nm, assuming a molar extinction coefficient of 50,000 M^{-1} cm^{-1}. Further details, see Marcozzi et al., (1990).

Enzymatic assay: α-chymotrypsin activity was measured in aqueous solution using GPANA (10 mg/ml DMSO) as substrate (Erlanger et al., 1966).

4 RESULTS AND DISCUSSION

While the solubilization efficiency of proteins into reverse micelles was extensively studied so far, only a few reports dealing with the recovery of the solubilized enzymes into an aqueous phase and their enzymatic activity preservation during this process were published. The search for the conditions which favour the passage of the proteins again into the water phase can be based on the forward transfer behaviour: typically this shows a dependence of the extraction efficiency on the used salt-type and concentration as well as on pH. The basic idea is to utilize for the backward extraction conditions of pH and ionic strength under which the forward transfer does proceed only sparingly. In the case of α-chymotrypsin, an efficient back transfer would therefore take place using an acid aqueous pH (below 4) and a concentrated KCl solution ([KCl]=1M or above). Under these conditions only a minimal amount of α-chymotrypsin is

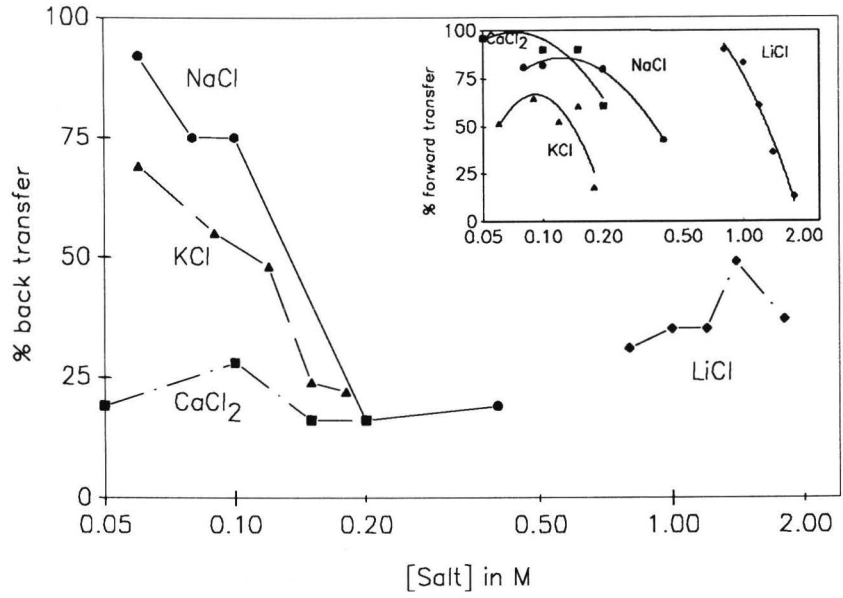

Figure 1. Extraction of α-chymotrypsin after a forward transfer (insert of Fig.1) into 50 mM AOT/water/isooctane and a subsequent, separate back transfer into 1M KCl pH 7.5 as a function of the ionic strength used in the forward transfer step. 100% in the forward transfer corresponds to the initial present enzyme concentration in the aqueous phase, 40 μM. Percentage in the back extraction is given relative to the obtained forward transfer yield; LiCl solution: back extraction into 4 M KCl pH 7.5.

extracted into the reverse micelles (Marcozzi et al., 1990). In practice, however, this strategy should be optimized in order to take into account protein denaturation at low pH and autolysis at high pH. In this work we used 1M KCl and 50 mM phosphate buffer pH 7.5. This is a good compromise between protein's stability and lower forward transfer efficiency.

Fig. 1 shows some transfer data obtained from the forward transfer of α-chymotrypsin (insert of Fig.1) and a subsequent back extraction step. The abscissa values refer to the salt concentration used in the forward transfer step. Although the back extraction is always done using an aqueous 1M KCl pH 7.5 solution, the amount of the recovered enzyme is dependent on the salt used in the preceding forward extraction. We plotted the percentage of the enzyme back extraction relative to the efficiency of the forward transfer step. The best back extraction efficiency is obtained when 0.05 to 0.1M aqueous NaCl solutions are used for the forward extraction procedure.

Although, for example, the forward extraction efficiency of α-chymotrypsin with $CaCl_2$

is similar to that obtained using NaCl, the back extraction yield is much more modest from the $CaCl_2$ micellar solutions. Moreover, no back extraction was obtained using the LiCl-forward extraction samples. Only with an aqueous 4 M KCl solution a significant back extraction is observable in this case. Notice that the forward transfer efficiency with LiCl is already observed also at a relatively high salt concentration (see insert of Fig.1). These are examples which show clearly the influence of the ionic strength used in the forward extraction process on the extraction yield obtained in the back transfer of α-chymotrypsin. These results are probably related to the fact that during the forward extraction which is governed by the salt-type used in this step, the cations distribute also specifically between the aqueous and the organic micellar phase (Caselli et al., 1990) and influence therefore the properties of both the micelle and the α-chymotrypsin (stability, interaction with micelle) in the aggregate.

A question of central importance is whether and to what extent the enzyme remains active at the end of such an extraction cycle. Fletcher and Parrott (1988) reported that only 10% of the original activity of α-chymotrypsin is retained after a forward and subsequent back extraction procedure. The authors mention that the main reason for the loss of activity is due to autolysis and not due to the phase transfer mechanism itself. Fig. 2 summarizes our results which show again a dependency of the measured enzymatic activity on the salt used in the preceding forward extraction step. The activity is given relative to the protein recovery after the backward extraction. The open symbols indicate the activity values when related to the total protein recovery (i.e. taking into account the product of the forward and the backward extraction together). In general, a much better activity preservation was observed in our work compared to the results obtained by Fletcher and Parrott. This is most likely due to a much shorter extraction time used in our work (Fletcher's extraction experiments took about 3 hours). However, so far the observed "salt effect" influencing the activity of α-chymotrypsin is not understood. Moreover it is obvious that

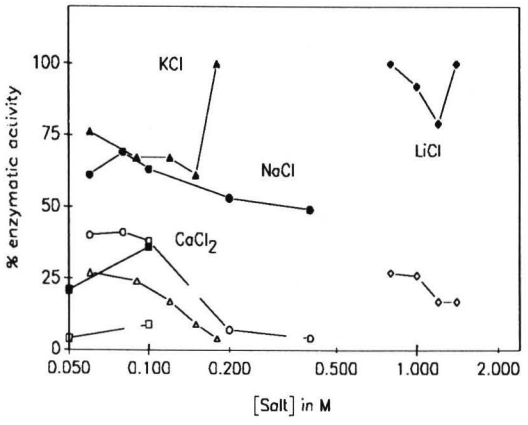

Figure 2 Activity of α-chymotrypsin after the back transfer into 1 M KCl pH 7.5. Filled symbols: activity expressed relative to the protein recovery after the back transfer; open symbols: activity expressed relative to the total enzyme recovery.

several parameters must be optimized in order to obtain a recovery of the protein which is satisfactory from both the quantitative and enzymatic point of view.

Another important point which needs further study is the upscaling. Together with the group of Renken at the EPFL in Lausanne (Switzerland) we are investigating the feasibility of the micellar extraction scheme when using larger volumes of materials.

5 REFERENCES

Caselli, M., Maestro, M., Traini, A., 1990. Surface Sci. Technol. accepted for publication.

Delahodde, A., Vacher, M., Nicot, C., Waks, M., 1984. Solubilization and insertion into reverse micelles of the major myelin transmembrane proteolipid. FEBS Lett. 172: 343.

Dekker, M., Hilhorst, R., Laane, C., 1989. Isolating Enzymes by Reverse Micelles. Anal. Biochem. 178: 217-226.

Eicke, H.-F., 1987. Aqueous nanophases in liquid hydrocarbons stabilized by ionic surfactants. In: H.-F. Eicke and D. Parfitt (Editors), Interfacial Phenomena in apolar media. Marcel Dekker, New York, Surfactant Science Series 21: pp. 41-92.

Erlanger, B.F., Edel, F., Cooper, A.G., 1966. The action of chymotrypsin on two chromogenic substrates. Arch. Biochem. Biophys. 115: 206-210.

Fletcher, P.D.I., Parrott, D., 1988. The partitioning of proteins between water-in-oil microemulsion and conjugate aqueous phases. J. Chem. Soc., Faraday Trans I, 84: 1131-1144.

Grandi, C., Smith, R.E., Luisi, P.L., 1981. Micellar solubilization of biopolymers in organic solvents.

Kadam, K.L., 1986. Reverse micelles as a bioseparation tool. Enzyme Microb. Technol. 8: 266-273.

Leodidis, E.B. and Hatton, T.A., 1989. Interphase transfer for selective Solubilization of ions, amino acids and proteins. In M.P. Pileni (Editor), Structure and Reactivity in Reverse Micelles. Elsevier, Amsterdam, pp. 270-302.

Leser, M.E. and Luisi, P.L., 1990. Application of reverse micelles for the extraction of amino acids and proteins. Chimia, in press.

Leser, M.E., Luisi, P.L., Palmieri, S., 1989. The use of reverse micelles for the simultaneous extraction of oil and proteins from vegetable meal. Biotechnol. Bioeng. 34: 1140-1146.

Luisi, P.L., Henninger, F., Joppich, M., Dossena, A., Casnati, G., 1977. Solubilization and spectroscopic properties of α-chymotrypsin in cyclohexane. Biochem. Biophys. Res. Commun. 74: 1384-1389.

Luisi, P.L., Bonner, F., Pellegrini, A., Wiget, P., Wolf, R., 1979. Micellar solubilization of proteins in aprotic solvents and their spectroscopic characterisation. Helv. Chim. Acta 62: 740-753.

Luisi, P.L. and Laane, C., 1986. Solubilization of enzymes in apolar solvents via reverse micelles. Trends Biotechnol. 4: 153-161.

Marcozzi, G., Correa, N., Luisi, P.L., Caselli, M., 1990. J. Colloid Interface Sci., submitted for publication.

Menger, F.M., Yamada, K., 1979. Enzyme catalysis in water pools. J. Amer. Chem. Soc. 101: 6731-6734.

Solvent Extraction 1990, T. Sekine (Editor)

© 1992 Elsevier Science Publishers B.V. All rights reserved

MEASUREMENT AND CORRELATION OF PHASE EQUILIBRIA OF AQUEOUS TWO-PHASE SYSTEMS AND PARTITION COEFFICIENTS OF ENZYMES

TAKESHI FURUYA, KATSUSHIGE NAKADA, YOSHIO IWAI, YASUHIKO ARAI AND KATSUHIKO TAKEUCHI*
Dept. of Chem. Eng., Kyushu Univ., Fukuoka 812, Japan
*Toyo Eng. Corp., Funabashi, Chiba 273, Japan

ABSTRACT
Furuya,T.,Nakada,K.,Iwai,Y.,Arai,Y. and Takeuchi,K.,1990. Measurement and correlation of phase equilibria of aqueous two-phase systems and partition coefficients of enzymes.

Aqueous two-phase systems provide a successful method for separating biomolecules by extraction under mild condition. Nevertheless, the phase equilibrium data of aqueous two-phase systems and the partition coefficient data of biomolecules are scarce and it is difficult to correlate them quantitatively. In the present work, the phase equilibria for the dextran-polyethylene glycol-water aqueous two-phase systems are measured. The partition coefficients of enzymes are also measured. Further, the osmotic virial equation is used to correlate the phase equilibria of the aqueous two-phase systems and the partition coefficients of enzymes.

Introduction

There is growing interest in efficient methods for the large-scale recovery and purification of bioproducts with the increasing importance of modern biotechnology. Aqueous two-phase systems provide a successful method for separating mixtures of biomolecules (Albertsson,1986,Walter et al.,1985).

To establish a separation technology using aqueous two-phase system, systematic investigations on phase separation and partition coefficient of biomolecule are needed. Further, thermodynamic framework for correlating phase equilibria and partition coefficients of biomolecules is also needed to design aqueous two-phase extraction systems.

In this study, phase equilibrium data of the dextran-polyethylene glycol-water aqueous two-phase system and partition coefficients for hydrolytic enzymes are reported. The present data are correlated using the osmotic virial equation.

2 Experimental

2.1 Materials

Polyethylene glycols (PEG) was purchased from Wako Pure Chemical Ind. as PEG 4000 (Mn:number average molecular weight=3000,lot# AWM2336). Dextran (DEX) fractions were purchased from Pharmacia Inc. as DEX T-40 (Mn=23500,lot# 07339) and DEX T-70 (Mn=36100,lot# 07340).

α-amylase (molecular weight=50000,lot# PDG0524) and β-amylase (molecular weight=50000,lot# PDK1837) were purchased from Wako Pure Chemical Ind. Glucoamylase (molecular weight=70000,lot# 91100) was purchased from Seikagaku Kogyo Co. Ltd. Pure water was purchased from Wako Pure Chemical Ind. All reagents were used without further purification.

2.2 Methods

Four two-phase systems were prepared; one contains no enzyme and other three systems contain three kinds of enzymes. Two-phase systems were made by mixing known stock solutions of PEG in water and DEX in water and then small known amount of enzyme was added. The total concentration of the polymers were adjusted as the same. The amounts of enzyme added were approximately 10, 10 and 1mg for α-amylase, β-amylase and glucoamylase, respectively. Equilib rium concentrations of PEG and DEX in aqueous two-phase systems containing such amounts of protein were quite similar to those without enzyme because protein concentration was quite small (Furuya et al.,1990).

The equilibrium phase compositions in the aqueous DEX T40-PEG4000-Water systems and the DEX T70-PEG4000-Water systems were measured using a gel-permiation liquid chromatography (GPC)., One column system (TSKGelG3000PW$_{XL}$,30cm) was used. Flow rate was 0.6ml/min and column temperature was 70^{o}C. Protein concentrations were measured spectrophotometrically with a Shimadzu UV-150 spectrophotometer at two wavelengthes of 215nm and 225nm (Sugawara et al.,1986).

Two-phases were stirred to equilibrate for 6 hours, and then were settled for 24 hours. After the phase separation was occured, each phases were withdrawn and polymer concentrations were measured by the GPC and protein concentrations were measured by the spectrophotometer. All measurements were performed at 20^{o}C ±0.2^{o}C.

2.3 Results

The experimental phase equilibrium data for the DEX T40-PEG4000-Water two-phase system are shown in Table 1 and Fig.1. Those for the DEX T70-PEG4000-Water two-phase system are also shown in Table 2 and Fig.2. The present results for the DEX T40-PEG4000-Water are found to coincide with the experimental results of Albertsson(1986) and Furuya et al.(1990). From Figs.1 and 2, it is shown that the critical point of the DEX T70-PEG4000-Water system is lower than that of the DEX T40-PEG4000-Water system.

The partition coefficient Kp of enzyme is defined here as Kp=the concentration of protein in the PEG-rich top phase/the concentration of protein in the DEX-rich bottom phase. The experimental partition coefficients for α-amylase, β-amylase and glucoamylase in the DEX T40-PEG4000-Water two-phase system are shown in Table 1 and Fig.3, and those in the DEX T70-PEG4000-Water

TABLE 1

Liquid-liquid equilibrium data for DEX T40-PEG4000-Water system and partition coefficients data of α-amylase, β-amylase and glucoamylase at 20°C

Total (wt%)			Top (wt%)			Bottom (wt%)			amylase Kp (-)		
DEX	PEG	Water	DEX	PEG	Water	DEX	PEG	Water	α-	β-	gluco
6.50	9.50	84.00	2.41	11.52	86.07	19.09	3.11	77.80	0.40	0.69	0.38
6.99	10.00	83.01	1.64	12.61	85.75	21.57	2.71	75.72	0.19	0.79	0.40
8.00	11.00	81.00	0.99	14.24	84.77	25.01	2.02	72.97	0.13	0.38	0.29
8.50	11.36	80.14	0.81	15.35	83.84	26.11	1.73	72.16	0.14	0.37	0.24
9.00	12.00	79.00	0.65	16.33	83.02	26.64	1.67	71.69	0.12	0.40	0.28

TABLE 2

Liquid-liquid equilibrium data for DEX T70-PEG4000-Water system and partition coefficients data of α-amylase, β-amylase and glucoamylase at 20°C

Total (wt%)			Top (wt%)			Bottom (wt%)			amylase Kp (-)		
DEX	PEG	Water	DEX	PEG	Water	DEX	PEG	Water	α-	β-	gluco
6.00	7.96	86.04	3.46	8.86	87.68	13.41	4.14	82.45	1.02	1.02	0.57
6.00	9.00	85.00	1.57	10.94	87.49	17.70	2.85	79.45	0.34	0.86	0.50
6.49	9.48	84.03	1.23	11.84	86.93	19.44	2.44	78.12	0.20	0.77	0.50
7.99	10.98	81.03	0.55	15.27	84.18	24.68	1.56	73.76	0.15	0.60	0.36
8.97	12.95	78.08	0.21	17.93	81.86	31.17	0.89	67.94	0.12	0.39	0.32

two-phase system are also shown in Table 2 and Fig.4. The partition coefficients obtained are lower than unity because enzymes are partitioned to the DEX-rich bottom phase.

The measurement of protein concentration in two-phase system is so difficult that the experimemtal partition coefficients are little scattered, since the measurement of protein concentration in two-phases is interfered by the presence of PEG and DEX. Although the experimental partition coefficients are scattered, there are obvious differences among the partition coefficients for α-amylase, β-

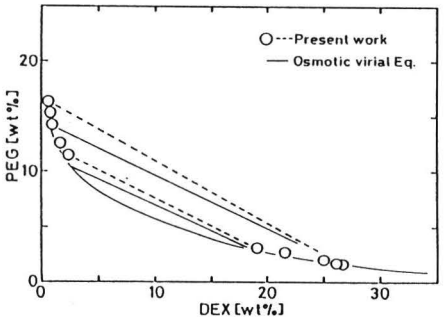

Fig.1. Experimental and calculated binodal for DEX T40-PEG4000-Water system at 20°C.

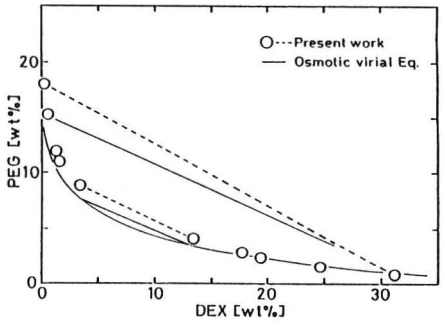

Fig.2. Experimental and calculated binodal for DEX T70-PEG4000-Water system at 20°C.

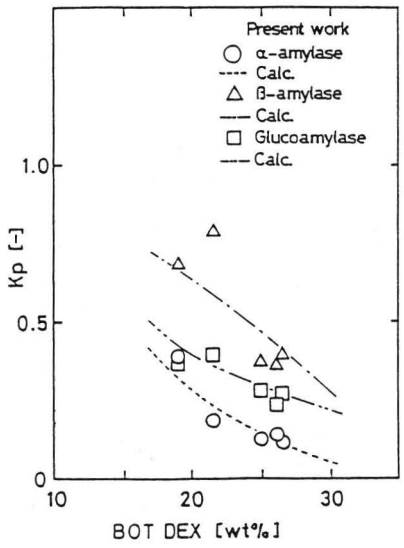

Fig.3. Experimental and calculated partition coefficients of enzymes vs. concentrations of DEX T40 in bottom phase.

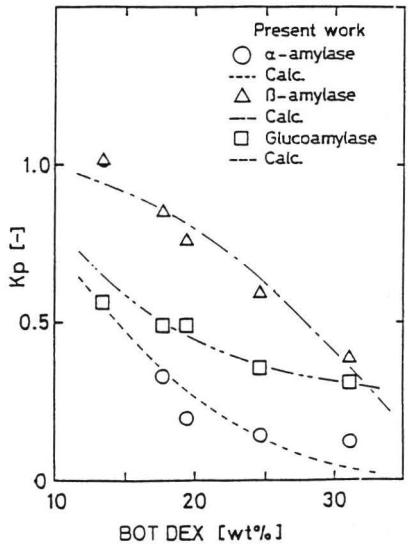

Fig.4. Experimental and calculated partition coefficients of enzymes vs. concentrations of DEX T70 in bottom phase.

amylase and glucoamylase.

3 Correlation

3.1 Osmotic virial equation

When aqueous two-phases in equilibrium with each other, the chemical potentials of component i in both phases are identical.

$$(\Delta\mu_i)^{TOP}=(\Delta\mu_i)^{BOT} \quad ; \text{ i=DEX,PEG,Water and Enzyme} \tag{1}$$

Simultaneous solution of Eq.(1) for all components gives equilibrium compositions for the two-phase systems.

The Flory-Huggins equation and the UNIQUAC equation have been applied to predict the chemical potentials(Kang et al.,1987,1988). However, the Flory-Huggins equation is not suitable for systems that have specific interactions such as hydrogen bonding (King et al.,1988). Further, the UNIQUAC equation requires many adjustable parameters.

A more suitable description of dilute aqueous two-phase systems was provided by Edmond and Ogston(1968). They developed a theory based on the osmotic virial equation truncated at the second virial coefficient term. King et al.(1988) have extended the Edmond and Ogston's equation to aqueous two-phase system with protein (four components system). According to King et al.(1988), the chemical

potentials of polymer(1)-polymer(2)-water(3)-protein(4) are written as a function of molality. Since the concentration of protein is very dilute ($m_4 \to 0$), it can be assumed that $m_4 \ll m_1$ and $m_4 \ll m_2$. Then the following four equations can be derived.

$$\Delta\mu_1 = RT(\ln m_1 + a_{11}m_1 + a_{12}m_2) \tag{2}$$

$$\Delta\mu_2 = RT(\ln m_2 + a_{22}m_2 + a_{12}m_1) \tag{3}$$

$$\Delta\mu_3 = -RTV_3\rho_3(m_1 + m_2 + (a_{11}/2)(m_1)^2 + (a_{22}/2)(m_2)^2 + a_{12}m_1m_2) \tag{4}$$

$$\Delta\mu_4 = RT(\ln m_4 + a_{14}m_1 + a_{24}m_2) \tag{5}$$

where m_i is the molality of component i, a_{ij} is the interaction coefficient between components i and j, R is the gas constant and T is the temperature, V_3 is the molar volume of water, and ρ_3 is the density of water. Interaction coefficients are directly related to the traditional second virial coefficients, A_{ij}.

$$2A_{ij} = 1000(a_{ij}/M_iM_j) \tag{6}$$

where M_i is the number average molecular weight of polymer i. And the partition coefficients is given by the following equation.

$$\ln K_p = \ln(m_4^{TOP}/m_4^{BOT}) = a_{14}(m_1^{BOT} - m_1^{TOP}) + a_{24}(m_2^{BOT} - m_2^{TOP}) \tag{7}$$

All interaction coefficients are evaluated by fitting the models to experimental data.

3.2 Results

The interaction coefficients A_{ij} are listed in Table 3. The binodals and the partition coefficients calculated by using these coefficients are shown in Figs.1,2 and Figs.3,4, respectively.

The liquid-liquid equilibria calculated agree well with the experimental data. However, small disagreement is found in the region of the PEG-rich top-phase. The partition coefficients calculated show fairly good agreement with the experimental results. Future work is required to give quantitative agreement between experimental and calculated partition coefficients.

4 Conclusions

The liquid-liquid equilibrium data for the DEX T40-PEG4000-Water, DEX T70-

TABLE 3

Binary interaction coefficients A_{ij} (ml mol/g^2) for DEX(1)-PEG4000(2)-Water(3)-Enzyme(4) system at 20°C

System	No Enzyme			α-amylase	β-amylase	glucoamylase
DEX T40-	A_{11}	6.03×10^{-4}	A_{14}	8.5580×10^{-4}	6.2122×10^{-4}	-2.8303×10^{-4}
PEG4000-	A_{22}	2.86×10^{-3}	A_{24}	2.2905×10^{-3}	1.6136×10^{-3}	-6.4316×10^{-4}
Water-	A_{12}	2.06×10^{-3}				
Enzyme						
DEX T70-	A_{11}	5.19×10^{-4}	A_{14}	7.5749×10^{-4}	5.6271×10^{-4}	-2.5138×10^{-4}
PEG4000-	A_{22}	2.86×10^{-3}	A_{24}	2.2905×10^{-3}	1.6136×10^{-3}	-6.4316×10^{-4}
Water-	A_{12}	1.93×10^{-3}				
Enzyme						

PEG4000-Water two-phase systems are reported. Further, the partition coefficients for hydrolytic enzymes, α-amylase, β-amylase and glucoamylase in the DEX T40-PEG4000-Water and the DEX T70-PEG4000-Water two-phase systems are also presented.

The osmotic virial equation is applied to correlate the liquid-liquid equilibria and the partition coefficients. Fairly good agreement was obtained between calculated and experimental results.

Acknowledgment

We greatefully acknowledge the financial support of the Grant-in-Aid for Encouragement of Young Scientists of the Ministry of Education, Science and Culture No.01750876(1989).

REFERENCES

Albertsson,P.A.,1986.Partition of Cell Particles and Macromolecules.3rd ed.,John Wiley and Sons

Edmond,E. and Ogston,A.G.,1968.An Approach to the Study of Phase Separation in Ternary Aqueous Systems. Biochem. J.,109:569-576

Furuya,T.,Iwai,Y.,Shimizu,T. and Arai,Y.,1990.Partition Coefficients of α-Amylase in the Aqueous Two-Phase System Containing Dextran and Polyethylene Glycol. Kagaku Kogaku Ronbunshu,16:830-834

Kang,C.H. and Sandler,S.I.,1987.Phase Behavior of Aqueous Two-Polymer Systems,Fluid Phase Equilibria,38:245-272

Kang,C.H. and Sandler,S.I.,1988.Effects of Polydispersivity on the Phase Behavior of Aqueous Two-Phase Polymer Systems. Macromolecules,21:3088-3095

King,R.S.,Blanch,H.W.,Prausnitz,J.M.,1988.Molecular Thermodynamics of Aqueous Two-Phase Systems for Bioseparations,AIChE J.,34:1585-1594

Sugawara,K. and Soejima,M.,1986.Tanpakushitsu no Teiryouhou,Gakkai Shuppan Center.

Walter,H.,Brooks,D.E. and Fisher,D.,1985.Partitioning in Aqueous Two-Phase Systems:Theory,Methods,Uses,and Applicatios to Biotechnology,Academic Press,Inc.

Solvent Extraction 1990, T. Sekine (Editor)

© 1992 Elsevier Science Publishers B.V. All rights reserved

CHARACTERISTICS OF ENZYMATIC NAD^+-RECYCLING REACTION IN MICROCAPSULE OF LIQUID-SURFACTANT MEMBRANE

KEIICHI KATO, NOBUYUKI YAMASAKI AND YASUO NAKASHIMA
Department of Resources Chemistry, Ehime University, Matsuyama 790 (Japan)

ABSTRACT

Characteristics of enzymatic NAD^+-recycling reaction catalysed by both alcohol dehydrogenase and malate dehydrogenase encapsulated in W/O/W emulsion were studied. Effects of various factors in preparation of the emulsion on the reaction-rate were experimentally examined. It was found that the species of organic agent of W/O/W emulsion and additive components such as soy-lecithin or bovine serum albumin, change the enzymatic reaction-rate in the emulsion. It is pointed out that the study of enzyme-containing emulsion can be applied as the model of membrane-bond enzyme or multi-enzyme system in a living cell.

1. INTRODUCTION

W/O/W emulsion can be used as a liquid-surfactant membrane microcapsule. It have been proposed by May et.al.(1972) that W/O/W emulsion can be applied to methods of enzyme immobilization. The microcapsules of encapsulated enzyme are of special interest because the microcapsules containing enzymes or other proteins may be regarded as models for the study of processes which occur in living cells.

Few investigations on preparation conditions for enzyme-encapsulation have been carried out. In this work, the effects of the preparation condition of W/O/W emulsion on enzymatic reaction in the emulsion were experimentally examined. Interesting attention was given to MDH because the enzyme is a membrane enzyme which exists in mitochondria and it is expected that the activity of enzyme may change when it is encapsulated in the emulsion. A coupled NAD^+-recycling system catalysed by MDH and YADH was chosen as the reaction system.

2. MATERIALS

Emulsifying agents of Span80(sorbitan monooleate), Tween80(polyoxyethylene sorbitan monooleate) and indigo carmine were purchased from Wako Ltd.(Japan). Crystalline YADH(A3263) and bovine selum albumin(BSA, A6793) were from Sigma Ltd.(USA). Ethanol, cholesterol

and oxalacetate were special grade from Wako Ltd.. Malate dehydrogenase from pig-heart, β-NAD^+ and β-NADH were from Boeringer Manheim Yamanouchi Ltd.(Japan; super special grade,127248,775754 and 127302,respectively). Soy-lecithin was purified by means of acetone-precipitation technique (Yamakawa,1974) from a crude sample from Wako Ltd.. Potassium phosphate buffer was 0.05M and adjusted to pH 7.50 with NaOH. Ionic strength of the solution was 0.27. EDTA was added to the buffer solution to be 0.5mM.

3.METHOD

NAD^+-recycling reaction system is shown in Scheme 1. The NAD^+-recycling was driven by adding ethanol as a substrate into the external aqueous solution of W/O/W emulsion. The enzymatic reactions were followed by measuring the extent of acetaldehyde accumulation in the external aqueous solution. In all cases, the leakage percentages of the encapsulated agents were within 1%.

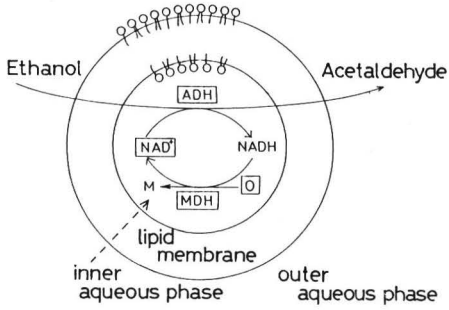

Scheme 1 Enzymatic reaction scheme of NAD^+-recycling in W/O/W emulsion. □ = encapsulated agents, O = oxalacetic acid, M= malic acid

Preparations of W/O/W emulsion of enzyme-encapsulation were carried out as follows: Thirty ml of potassium phosphate buffer containing agents to be encapsulated was slowly added dropwise to 40ml organic-agent containing Span80 in 100ml beaker under stirring by a homomixer (Tokushu Kikakogyo,Model-M) at 4000rpm(first emulsification). In usual, the used organic agent was kerosene. The weight percentage of the total of Span80 and additives on a basis of organic phase will be denoted as $\phi_{L/O}$ in this paper. Next, prepared W/O -emulsion of 40ml was added to 160ml potassium phosphate solution containing 10mM-Tween80. The added solution was then stirred by the homomixer at 3000rpm(second emulsification). Thus, W/O/W emulsion was prepared. Micrographic observation of the emulsion was made with a phase-contrast microscope(Olympus BHS-PC-A). Formation or rupture percentages of W/O/W emulsion were spectrophotometrically determined by use of indigo calmine entrapped in inner aqueous solution as tracer.

The enzymatic reaction was initiated by adding 20ml-ethanol of prescribed concentration to the 200ml W/O/W-emulsion in Erlenmeyer flask at 25 ℃. At a constant interval, the 15ml-W/O/W emulsion was sampled and centrifuged at 4500rpm. The centrifuged semi-transparent solution of 10ml was sampled and ultrafiltered(Advantec Toyo, UHP-43K). The filtered solution was heated in 98 ℃-water bath in order to stop the reaction completely. After being cooled, the sample was analyzed. Acetaldehyde concentration of the sample was spectrophotometrically determined by measuring of NADH absorbance -change caused by enzymatic reaction catalysed by YADH in a similar manner as May et.al.(1976).

4.Results and Discussion

4-1)Effect of additives to Span80 on stability of W/O/W emulsion

The effects of additive lecithin or cholesterol to Span80 on emulsion rupture are shown in Fig.1. Rupture percentage of the emulsion was determined on the basis of that just after the preparation of the emulsion. It is found from Fig.1 that the addition of lecithin or cholesterol increases the emulsion stability. This is due to the increase of mechanical strength of surfactant membrane by the addition of lecithin or cholesterol.(Matsumoto et.al.1977)

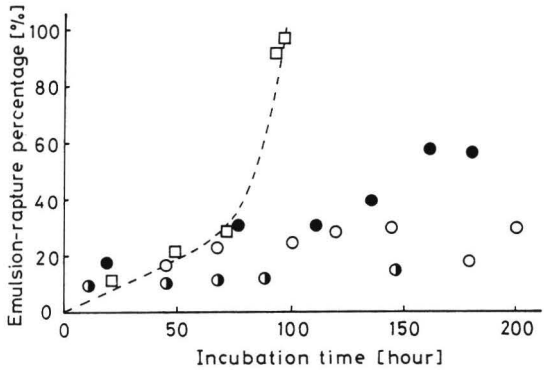

Fig.1 The effect of added lecithin or cholesterol on emulsion stability. The weight ratio of the additives to Span80 : (-□-) only Span80, (○) lecithin/Span80 =0.3, (●)cholesterol/Span80 =0.2, (◑) cholesterol /Span80 =0.5. $\phi_{L/O}$=5%.

4-2) Effect of lecithin on the NAD^+-recycling in W/O/W emulsion

The reaction experiments on the NAD^+-recycling in the emulsion containing various amount of lecithin were carried out. As shown in Fig.2, acetaldehyde production during 90 min of reaction which represents apparent enzymatic activity increases with an increase in the weight ratio of lecithin to span 80 up to about 0.07. Under

the preparation conditions, percentages of emulsion formation were almost 100%. The following reason is considerd for the activity-increase. First, the addition of lecithin increases the mechanical strength of surfactant membrane as described above. Then, the increase of the strength would prevent the activity deterioration of enzymes which is caused by shearing stress of homomixer or by the contact of enzyme with organic agent at first emulsification. Secondly, it is probable that MDH and YADH are partly inside the surfactant membrane of W/O/W emulsion and the enzyme activity is enhanced by the interaction between enzyme and lipid: MDH is membrane enzyme included in mitochondria of living cell.

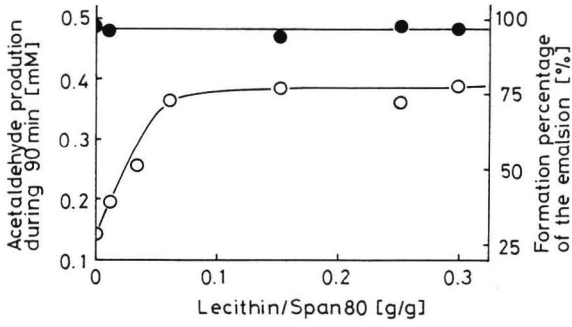

Fig.2 The effect of added lecithin to Span80 on the acetaldehyde production and emulsion formation. Concentration conditions :[ADH]=0.42 mg/l, [MDH]= 0.14mg/l, [NAD^+]= 0.027 mM, [oxal.]=0.74mM, [etha.]= 145mM. The keys :(●)formation percentage of W/O/W emulsion;(○) acetaldehyde production during 90 min interval in reaction time. $\phi_{L/O}$=40%.

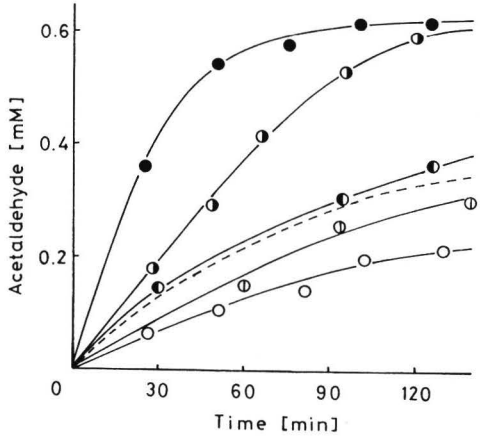

Fig.3 Time-cources of acetaldehyde production with concentrations of BSA. The concentrartion conditions were the same as those in Fig.2. The dotted line represents the time-cources in homogeneous system. The keys :(●)0.5wt.%, (◑) 0.05,(◐) 0.01, (◔)0.005,(○)0. $\phi_{L/O}$=40%, non-containig lecithin.

4-3)Effect of BSA on the NAD^+-recycling in W/O/W emulsion

In inner aqueous solution of the emulsions,BSA was dissolved. As shown in Fig.3, it is found that the enzymatic activity in the W/O/W emulsion increases with the increase of the BSA concentrations.

Bovine serum albumin has a large molecule weight and stabilizes enzyme by the steric-structure of itself. At first emulsification, BSA would ,therefore, prevent YADH and MDH from being subjected to shearing stress and contacting kerosene by surrounding the enzymes.

4-4)The effect of the organic agent of oil phase on the apparent enzymatic reaction-rate

By use of various organic agents, the experiments on the enzymatic reaction were carried out. As shown in Fig.4, the order of the apparent enzymatic reaction-rate of the emulsion is as follows : kerosene>n-hexane>n-decane. On the other hand, the distribution coefficients of ethanol and acetaldehyde were measured and the results are shown in Table 1. From the comparison of the results in Table 1 with those in Fig.4, it is obvious that the order of the enzymatic reaction-rates in Fig.4 corresponds to that of the distribution coefficients. From these results, it is found that the solubility of substrate or product in the organic agent

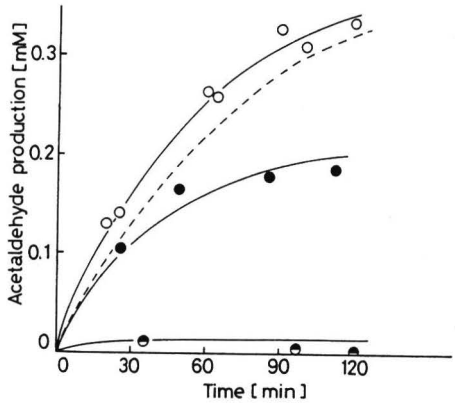

Fig.4 Time-cources of acetaldehyde production with various organic-agents of oil phase. The conditions were the same as those in Fig.2. The dotted line : homogeneous system. The keys :(○) kerosene, (●)n-hexane, (◓)n-decane.

TABLE 1.

Distribution coefficients of substrate of ethanol and acetaldehyde of product with respect to various organic agents

organic-agent	ethanol (substrate)	acetaldehyde (product)
kerosene	1.48	1.34
n-hexane	0.81	0.71
n-decan	0.81	0.22

* Note) The distribution coefficients were determined under the condition : $\phi_{L/O}$=40%, lecithin/span80=0.3 ; The used aqueous phase was pottasium phosphate buffer.

gives important effect on the apparent enzymatic reaction-rate of the liquid membrane.

4-5)Comparison of the enzymatic reaction in W/O/W emulsion system with that in homogeneous one

It is interesting to compare the enzyme activity of NAD^+-recycling reaction in W/O/W emulsion system with that in homogeneous one. Figures 3 and 4 show the comparison of the systems. In the comparison of the activities, the concentrations of the encapsulated substances in the aqueous solution system where "O"(oil phase) was removed from W/O/W were set up to be equivalent with those in homogeneous system. That is to say, the concentrations of encapsulated substances were represented as those in the total volume of both inner aqueous solution and outer aqueous one. The time-courses of acetaldehyde production in the emulsion systems become higher than that in homogeneous system (dotted line) in the high concentration-range of both lecithin and albumin. This fact is very interesting. Possible explanation for the enhancement of acetaldehyde production in W/O/W emulsion is as follows. First, the enzymatic activity would be increased by the interaction between enzyme and lipid. Secondly, it is probable that in multi-enzyme system such as MDH and ADH, complexs of enzymes allow high concentration of substrate intermediates in the microenvironment of the emulsion. Therefore, greater kinetic efficiency in the emulsion could be achieved (Srere et.al. 1973).

5.Conclusion

1)The addition of lecithin or BSA enhances enzyme-activity in W/O/W emulsion. 2)Enzymatic reaction-rate of the emulsion is related with the solubility of substance and product to oil phase.

6.REFERENCES

May,S.W. and Li,N.N.,1972. The immobilization of urease using liquid-surfactant membrane, Biochim.Biophys.Acta.,**47**,No.5 : 1179-1185

May,S.W. and Landgraff,L.M.,1976. Cofacter recycling in liquid membrane-enzyme systems,Biochim.Biophys.Acta.,**68**,No.3 : 786-792

Matsumoto,S., Kohda,M and Murata,M., 1977. Preparation of lipid vesicles on the basis of a technique for providing W/O/W emulsions, J.Colloid Interface Sci., **62**, No.1 : 149-157

Srere,P.A., Mattiasson,B. and Mosbach,K.,1973. An immobilized three-enzyme system : A model for microenvironmental conpartmentation in mitochondria, Proc.Nat.Acad.Sci.USA, **70**, No.9 : 2534-2538

Yamakawa,T.,1974. Shishitsu no Kagaku (Seikagaku jikken Koza,3) Tokyo kagaku dohjin, 19pp

Solvent Extraction 1990, T. Sekine (Editor)

© 1992 Elsevier Science Publishers B.V. All rights reserved

PHASE EQUILIBRIA OF THREE AQUEOUS TWO-PHASE SYSTEMS

MASAHIRO KATO, MASATO YAMAGUCHI, TOSHIHIRO KIUCHI, SHOICHI ITO,
and MICHIMASA NAKAMURA
Faculty of Engineering, Nihon University, Koriyama, Fukushima 963 (Japan)

ABSTRACT

Aqueous two-phase separation technology is now very attractive in engineering for purification of biological materials. In the present study, solubility curves and liquid-liquid equilibria were measured for three aqueous two-phase systems, dextran-polyethylene glycol-water at 298K, polyvinyl alcohol-polyethylene glycol-water at 308K, and ammonium sulfate-polypropylene glycol-water at 298K. An experimental method for measuring the plait point is proposed in the present study. The plait point was determined with the present experimental method for ammonium sulfate-polypropylene glycol-water system. The distribution ratios of exo-maltotetrahydrolase and maltotetraose were measured for polyvinyl alcohol-polyethylene glycol-water system; the one of invertase for ammonium sulfate-polypropylene glycol-water system.

INTRODUCTION

Aqueous two-phase systems are suitable for the purification or isolation of biological materials which would be denatured by the thermal or chemical environments encountered in typical chemical engineering separation techniques (Albertsson, 1986). The aqueous two-phase systems have recently applied for various areas of biotechnology such as large-scale enzyme purification (Kula et al., 1982), affinity purification (Johanson et al., 1985), extractive bioconversions (Tjerneld et al., 1985), continuous sacchrication of starch (Hayashida et al., 1988), and separation of papain from papaya latex (Kuboi et al., 1989). For the aqueous two-phase systems, theoretical discussions have recently been made by some researchers (Gustafsson et al. 1986; Kang et al. 1987, 1988a,b; Furuya et al. 1989; Haynes et al. 1989; Cabezas et al. 1989).

In the present study, an experimental method for measuring the plait point is proposed. The plait point of the ternary system is the most essential point on liquid-liquid equilibria. The plate point can be conventionally determined as the crossing point of conjugate line and solubility curve. The general method is some times troublesome by the extrapolation of the conjugate line to the solubility curve. The plait point can be determined by the present experimental method with interporation.

In the present investigation, solubility curves and liquid-liquid equilibria were measured for three aqueous two-phase systems, dextran-polyethylene

glycol-water at 298K, polyvinyl alcohol-polyethylene glycol-water at 308K, and ammonium sulfate-polypropylene glycol-water at 298K. The distribution ratios of exo-maltotetrahydrolase and maltotetraose were measured for polyvinyl alcohol-polyethylene glycol-water system; the one of invertase for ammonium sulfate-polypropylene glycol-water system.

EXPERIMENTAL SECTION

Solubility points were measured by the conventional cloud-point titration method. For the measurement of liquid-liquid equilibria, the calibration curves of water composition on the solubility curve were drawn using the refractive index data on the binodal curves. Next, two-liquid heterogeneous solution was settled at constant temperature. After attaining equilibrium state, the upper and lower liquid phases were taken out and their refractive indexes were measured. The experimental point of liquid-liquid equilibria was obtained as a crossing point of the experimental binodal curve and the line of fixed water composition.

An experimental method for measuring the plait point is proposed in the present study. The experimental method is schematically shown in Figs. 1 and 2. Two different binary solutions, P1 and P2, are first prepared. The another binary solution, Q, is also prepared. By adding the binary solution Q into the two solutions, P1 and P2, the phase separations are observed a little over the solubility curve. Two types, T1 and T2, are shown in the phase sepa-

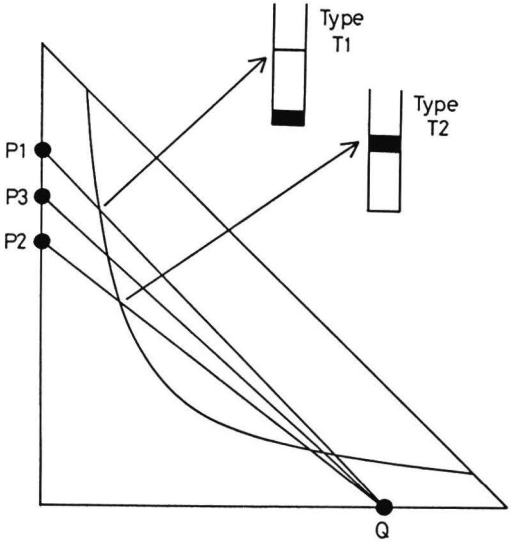

Fig. 1. Schematic experimental diagram for measuring plait points.

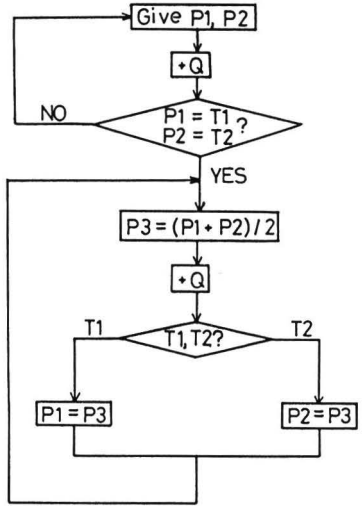

Fig. 2. Experimental flow diagram of plait points, in case of T1 with P1.

ration. A small amount of lower or upper phase appears by the phase separation, as schematically shown with T1 or T2, respectively. The plait point is between them on the solubility line when the two different types are observed. In this case, a new binary solution P3 between P1 and P2 is prepared. The type of the phase separation is further observed with the same procedure. Repeating the present experimental procedure, the plait point can be determined. The present experimental method is however essentially not applicable for the special systems having the tie line data of the same density.

Dextran, polyvinyl alcohol, and ammonium sulfate were supplied from the Wako Pure Chem. Ind. Co., Ltd. Polyethylene glycol and polypropylene glycol were supplied from the Sigma Chem. Co., Ltd. and the Katayama Chem. Ind. Co., Ltd., respectively. The average molecular weights of the polymers, dextran, polyvinyl alcohol, polyethylene glycol, and polypropylene glycol, respectively, are 100000, 22000, 8000, and 400. Invertase and maltotetraose were supplied from the Wako Pure Chem. Ind. Co., Ltd. Exo-maltotetrahydrolase was given by the Chiyoda Chem. Eng. & Constr. Co., Ltd. Distilled water was used in the experiments. The Shimazu UV-265FS spectrophotometer was used to determine the concentrations of exo-maltotetrahydrolase and invertase at static wave lengths of 282.0 nm and 259.8 nm, respectively. The concentration of maltotetraose was measured by the Hitachi L-6000 high performance liquid chromatography with the Bio-Rad Laboratories HPX-42A column of 30 cm length and with the Shodex SE-61 detector.

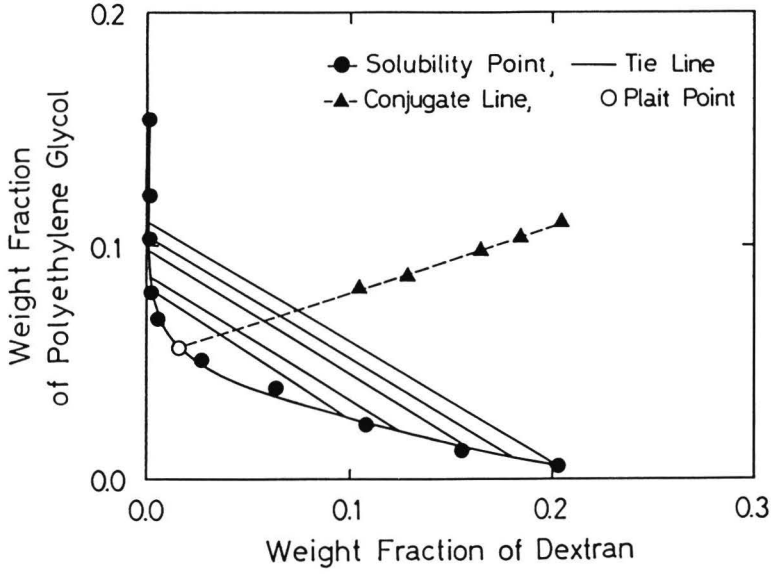

Fig. 3. Phase diagram of dextran-polyethylene glycol-water system at 298K.

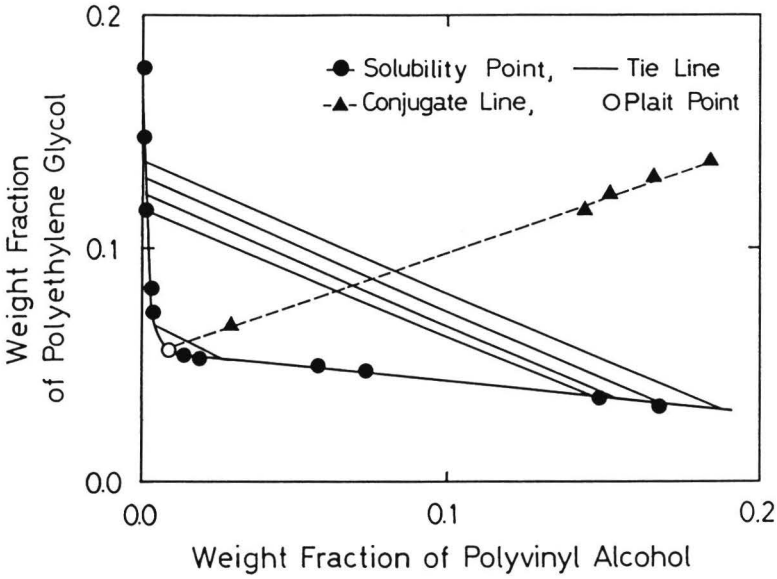

Fig. 4. Phase diagram of polyvinyl alcohol-polyethylene glycol-water system at 308K.

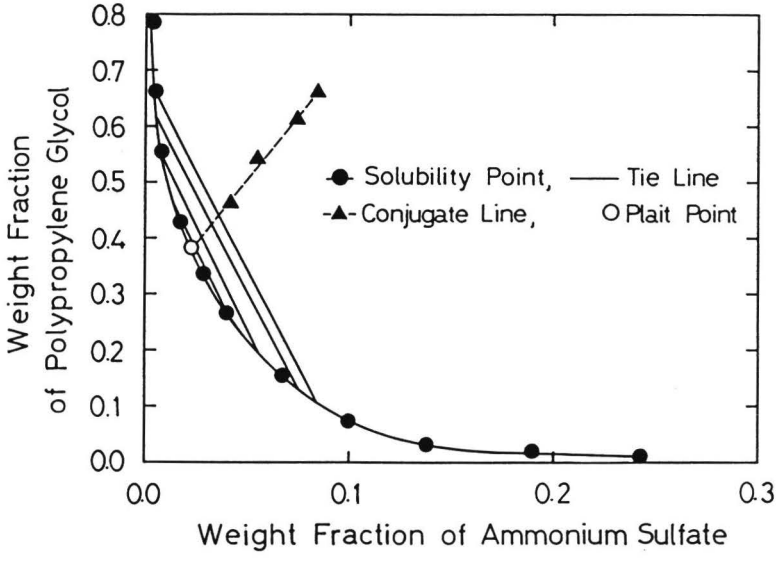

Fig. 5. Phase diagram of ammonium sulfate-polypropylene glycol-water system at 298K.

TABLE 1

Solubility data of three aqueous two-phase systems, weight fraction.

System I			System II			System III		
(1)	(2)	(3)	(1)	(2)	(3)	(1)	(2)	(3)
0.2029	0.0056	0.7915	0.1678	0.0322	0.8000	0.2425	0.0119	0.7456
0.1553	0.0122	0.8325	0.1489	0.0358	0.8153	0.1895	0.0209	0.7896
0.1080	0.0233	0.8687	0.0736	0.0476	0.8788	0.1377	0.0327	0.8296
0.0633	0.0388	0.8979	0.0578	0.0498	0.8924	0.0997	0.0742	0.8261
0.0270	0.0509	0.9221	0.0189	0.0528	0.9283	0.0673	0.1554	0.7773
0.0055	0.0685	0.9260	0.0137	0.0543	0.9320	0.0402	0.2664	0.6934
0.0023	0.0799	0.9178	0.0036	0.0727	0.9237	0.0288	0.3363	0.6349
0.0016	0.1030	0.8954	0.0031	0.0830	0.9139	0.0175	0.4292	0.5533
0.0016	0.1217	0.8767	0.0012	0.1164	0.8824	0.0082	0.5557	0.4361
0.0012	0.1542	0.8446	0.0006	0.1478	0.8516	0.0049	0.6631	0.3320
------	------	------	0.0005	0.1776	0.8219	0.0037	0.7859	0.2104

System I : Dextran(1)-polyethylene glycol(2)-water(3) at 298K
II : Polyvinyl alcohol(1)-polyethylene glycol(2)-water(3) at 308K
III : Ammonium sulfate(1)-polypropylene glycol(2)-water(3) at 298K

TABLE 2

Tie line data of three aqueous two-phase systems, weight fraction.

Upper phase			Lower phase		
(1)	(2)	(3)	(1)	(2)	(3)
Dextran(1)-polyethylene glycol(2)-water(3) system at 298K					
0.0013	0.1099	0.8888	0.2045	0.0047	0.7908
0.0014	0.1035	0.8951	0.1840	0.0074	0.8086
0.0014	0.0978	0.9008	0.1645	0.0103	0.8252
0.0015	0.0868	0.9117	0.1283	0.0184	0.8533
0.0015	0.0816	0.9169	0.1045	0.0228	0.8727
	0.0162**		0.0563**	0.9275**	
Polyvinyl alcohol(1)-polyethylene glycol(2)-water(3) system at 308K					
0.0007	0.1370	0.8623	0.1840	0.0330	0.7830
0.0008	0.1300	0.8692	0.1660	0.0350	0.7990
0.0010	0.1230	0.8760	0.1520	0.0370	0.8110
0.0012	0.1160	0.8828	0.1440	0.0380	0.8180
0.0045	0.0670	0.9285	0.0290	0.0510	0.9200
	0.0087**		0.0565**	0.9348**	
Ammonium sulfate(1)-polypropylene glycol(2)-water(3) system at 298K					
0.0050	0.6610	0.3340	0.0840	0.1080	0.8080
0.0060	0.6125	0.3815	0.0740	0.1380	0.7880
0.0090	0.5425	0.4485	0.0550	0.2025	0.7425
0.0140	0.4625	0.5235	0.0420	0.2570	0.7010
	0.0229*		0.3828*	0.5943*	

* Plait point determined with the present method with interporation.
**Plait point determined with the conventional method with extraporation.

TABLE 3

Experimental data of distribution ratios, (upper layer/lower layer).

Feed composition, weight fraction			Distribution ratio	
(1)	(2)	(3)	Enzyme	Oligosaccharide
Polyvinyl alcohol(1)-polyethylene glycol(2)-water(3) system at 308K				
0.0800	0.0800	0.8400	0.52*	1.07
Ammonium sulfate(1)-polypropylene glycol(2)-water(3) system at 298K				
0.3500	0.0400	0.6100	3.75**	----

*Exo-maltotetrahydrolase **Invertase

RESULTS

As shown in Figs. 3 to 5, solubilities and tie lines were obtained. The experimental numerical values are given in Tables 1 and 2 for solubilities and tie lines, respectively. The plait point was determined with the present method for ammonium sulfate-polypropylene glycol-water system; with the conventional method for the other two systems. Table 3, shows the distribution ratios of exo-maltotetrahydrolase and maltotetraose for polyvinyl alcohol -polyethylene glycol-water system; the one of invertase for ammonium sulfate-polypropylene glycol-water system.

ACKNOWLEDGMENTS

The authors are indebted to the wide-research fund of Nihon University. We also thank the Chiyoda Chem. Eng. & Constr. Co., Ltd. for the supply of exo-maltotetrahydrolase.

REFERENCES

Albertsson, P.A., 1986. Partition of Cell Particles and Macromolecules, 3rd. Ed., Wiley, New York.
Cabezas, H., Evans. J.D. Jr., and Szlag, D.C., 1989. Fluid Phase Equil., 53: 453.
Furuya, T., Shimizu, T., Mishima, K., Iwai, Y., Kawakami, Y., and Arai, Y., 1989. Preprint of Annual Meeting of Chemical Engineers Japan.
Gustafsson, A., Wennerstrom, H., and Tjerneld, F., 1986. Polymer, 27: 1768.
Hayashida, K., Kunimoto, K., Shiraishi, F., Kawakami, Y., Arai, Y., and Kusunoki, K., 1988. Preprint of Hiroshima Meeting of Chemical Engineers Japan.
Haynes, C.A., Blanch, H.W., and Prausnitz, J.M., 1989. Fluid Phase Equil., 53: 463.
Johanson, R.A. and Henkin, J., 1985. J. Biol. Chem., 260: 1465.
Kang, C.H. and Sandler, S.I., 1987. Fluid Phase Equil., 38: 245.
Kang, C.H. and Sandler, S.I., 1988a. Biotech. Bioeng., 32: 1158.
Kang, C.H. and Sandler, S.I., 1988b. Macromolec., 21: 3088.
Kuboi, R., Wang, W.-H., Morimatsu, K., Tone, S., and Komasawa, I., 1989. Kagaku Kogaku Ronbunshu, 15: 497.
Kula, M.-R., Kroner, K.H., and Hustedt, H., 1982. Adv. Biochem. Eng., 24: 74.
Tjerneld, F., Persson, I., Albertsson, P.A., and Hahn-Hagerdal, B., 1985. Biotech. Bioeng., 27: 1036.

Solvent Extraction 1990, T. Sekine (Editor)

© 1992 Elsevier Science Publishers B.V. All rights reserved

TRANSPORT OF PROTEINS THROUGH REVERSED MICELLAR SOLUTION LAYER AS A LIQUID MEMBRANE

T. KINUGASA*, S. TANAHASHI, K. TAKAHASHI AND H. TAKEUCHI
Department of Chemical Engineering, Nagoya University, Nagoya 464-01, Japan

ABSTRACT
Extraction of lysozyme and ribonuclease-A using reversed micellar solution formed by Aerosol OT(AOT) in isooctane was studied. Distribution equilibria of the proteins between the aqueous and organic phases were explained in terms of two effects : an electrostatic interaction and a size exclusion effect. The amount of water solubilized into the surfactant solution was correlated with concentrations of the salt and AOT. It was found that the micellar solution saturated with lysozyme has a limiting content which depends on only the water content. Furthermore, the transport of protein through the micellar solution layer was attempted and the selective separation of lysozyme to ribonuclease-A was feasible for the binary mixture.

INTRODUCTON

The development of efficient methods for the recovery of proteins and other bioproducts from fermentation broths and cell culture media is desired for an advance in biotechnology. Chromatography and electrophoresis are usefully applied to purification of high value pharmaceuticals, but are expensive and difficult to scale beyond laboratory size. Also, solvent extraction is not suitable because of denaturation in organic solvents.

Most recently, a novel extraction technique using reversed micelles (RM) has been reported as an alternative procedure (Luisi,1985; Goklen and Hatton,1987). RM is associated colloid of amphiphilic surfactants dissolved in an organic solvent. A hydrophilic core of RM solubilizes water, and then proteins can be extracted into the core water without denaturation.

In this study, distribution equilibrium of proteins into an RM solution was examined using an anionic surfactant. Solubilization of water in its surfactant solution was also studied along with the micelle size. Furthermore, the transport of protein through the RM solution layer as a liquid membrane (Armstrong and Li, 1988 ; Kuboi et al.,1990) was attempted on the separation of each protein from a binary mixture of lysozyme and ribonuclease-A.

2 EXPERIMENTAL

Distribution equilibrium : Bis-(2-ethylhexyl)sodium sulfosuccinate (Aerosol OT, or AOT) was used as the surfactant in this study. An organic solution was prepared by dissolving AOT in 2,2,4-trimethylpentane (isooctane). An aqueous

* Present address: Niihama National College of Technology, Niihama 792, Japan

solution was prepared by dissolving a protein in distilled water containing KCl for the adjustment of its ionic strength and further adjusted to a desired pH by the addition of 0.1M HCl or KOH. The protein used was lysozyme (LYS) from chicken egg white (molecular weight : M_p=14300, isoelectric point : pI=11) and ribonuclease-A (RNS, M_p=13680, pI=9.6) from bovine pancreas.

Equal volumes(10mL) of the organic and aqueous solutions were shaken in a flask for 120 minutes at 298K. After reaching equilibrium, the two phases were separated on a centrifuge, and then protein contents of the aqueous and organic phases, C_W and C_O , were determined by spectrophotometry at 280nm. Percentage extraction of proteins was obtained as E (= $C_O V_O$ / $C_{W,0} V_{W,0}$), where V_W and V_O are the volumes of the aqueous and organic phases; subscript 0 indicates the initial feed. Further, water content of the organic phase was measured by Karl-Fischer titration, and the molar ratio of the water to surfactant, W_O = [H_2O] / [AOT], was then obtained, where [ ] presents the molar concentration of species in the bracket.

Liquid membrane transport : A glass cell used for liquid membrane transport is shown in Fig.1, being equipped with two shafts having two impellers of flat blade, which were rotated at 3.8s^{-1}. Equal volumes (18mL) of aqueous feed and strip solutions were placed in the separate bottom sections and the RM solution of 18mL was located on the two aqueous phases as a liquid membrane layer. Protein is solubilized into the RM phase on the feed side, following to leave it on the strip side. The feed or strip solution was drawn from a sampling port by a constant flow pump, and then backed into the cell via a UV detector, whereby the time course of the protein content was observed from a change in the absorbance. The separation of LYS and RNS was also attempted using the liquid membrane cell, whereby each content of the proteins in the aqueous phase was determined by HPLC.

3 RESULTS AND DISCUSSION

3.1 Distribution equilibrium of protein

(i) Effects of ionic strength and pH on the extraction. Figure 2 shows the effect of the salt concentration, [KCl], on the extraction of proteins, LYS and RNS, into the RM solution, wherein the protein content of the aqueous feed was 1g/L. The extraction behavior was sensitive to [KCl]. Such behavior can be explained in terms of two effects. One is a size exclusion effect. With an increase in the ionic strength, the electrostatic repulsion between the neighboring headgroups of AOT is reduced. This con-

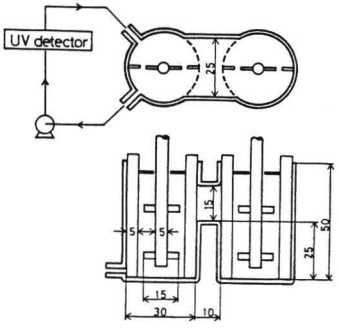

Fig.1. Details of bulk liquid membrane cell used.

tribution gives rise to the formation of smaller RM in the organic phase, and is likely to provide the exclusion effect in response to the size of protein molecule. Another is due to the decrease in electrostatic attractions between the charged groups of protein and the polar heads of the surfactant in RM. Thus, with increasing the ionic strength, the extraction of the proteins was decreased.

Stokes diameters of the proteins, calculated from the partial specific volume by use of the friction factor, are 3.8nm for LYS and 3.3nm for RNS. In Fig.3, the diameter of the RM entrapped one molecule of each protein is compared with the mean diameter obtained on a dynamic light scattering photometer, where the length of AOT molecule was assumed to be 1.1nm.

The extraction of LYS can be obviously explained in terms of the size effect. However, the result for RNS was low even when the micelle size was larger than the protein molecules. This implies that the electrostatic interaction has more significant effect in the extraction.

The effect of aqueous feed pH on the extraction of the proteins is shown in Fig.4. The extraction changed drastically at the pH value adjacent to the pI of each protein. When the aqueous feed has a pH value above its pI, the electrostatic repulsion between the negative charges of protein and the polar groups of AOT acts as a suppression in the extraction. At the lower pH, however, the extraction of LYS was reduced. It is considered that too strong attraction between protein and AOT molecules is liable to form insoluble aggregates.

(ii) Effect of water content on the solubilization of proteins. Figure 5 shows the effects of the salt and surfactant concentrations on the solubilization of water in AOT/isooctane solut-

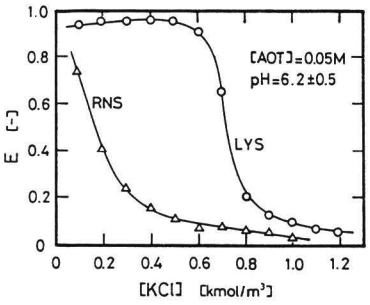

Fig.2. Effect of aqueous concentration of KCl on the extraction of lysozyme and ribonuclease-A.

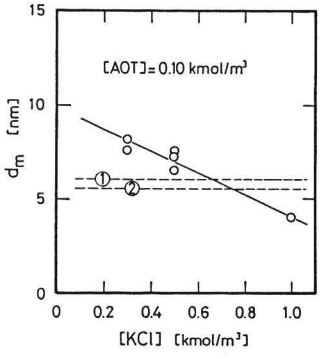

Fig.3. Plots of mean diameters of RMs against KCl concentration. Dashed lines are for an RM entrapped one molecule of LYS(1) and RNS(2).

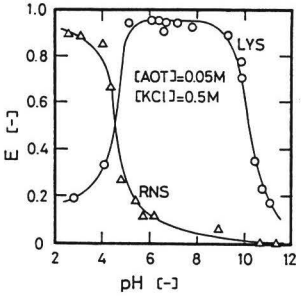

Fig.4. Effect of solution pH on the extraction of proteins.

ions in the presence of the proteins. The water content decreased with an increase in [KCl], slightly depending on [AOT]. Furthermore, we found that W_O is independent of the pH. Consequently, the water solubilization data can be correlated by

$$W_O = 9.8\,[AOT]^{0.12}\,[KCl]^{-0.34} \quad (1)$$

and the solid lines in Fig.5 represent Eq.(1).

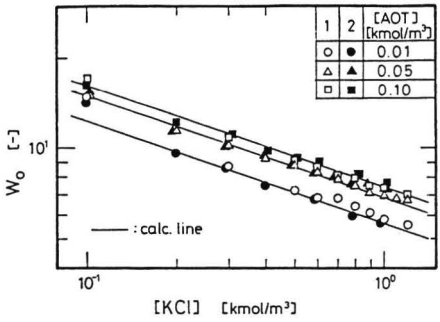

Fig.5. Effect of salt concentration on the water content of AOT/isooctane solution in the presence of proteins. 1 : lysozyme, 2 : ribonuclease-A.

The equilibrium relation in the protein extraction was examined from LYS contents of both the aqueous and organic phases, where the initial contents of the aqueous feed ranged 0.1 to 25g/L. With increasing the initial content, the organic phase in equilibrium with the aqueous phase increased in the protein content, and then went through a maximum. In the case of larger C_W, it was liable to form aggregates consisting of LYS and AOT molecules. This leads to a lowering of [AOT], and hence the value of W_O decreases.

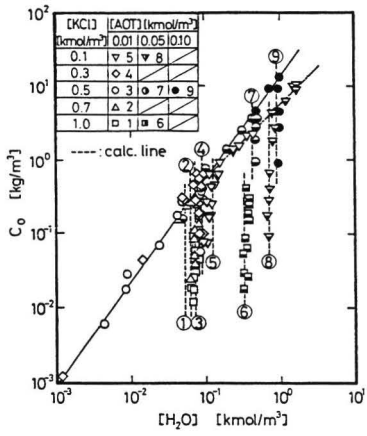

Fig.6. Relationship between LYS content and water content of the micellar solution. The aq. feeds were in 0.1-25g/L of LYS at the pH of 6.8. Dashed lines represent the water content calculated from Eq.(1).

Figure 6 shows a plot of C_O vs. [H_2O], wherein the dashed lines represent the calculated values from Eq.(1). As the value of $C_{W,0}$ increases, the organic phase increases in C_O up to a limiting value along the dashed line at each constant value of [H_2O]. However, further increase in $C_{W,0}$ permitted it to behave two different ways in response to the salt concentration. In the case of higher [KCl] (lines 1-4, 6, 7 and 9), after reaching each limiting content, the value of C_O decreases with [H_2O] along the solid line. The decrease in [H_2O] may be caused from the lowering of [AOT] due to the formation of the aggregates as mentioned above. While, for the aqueous feed with low [KCl] (lines 5 and 8 for 0.1M), the value of C_O increased, followed by a maximum along the dash-dotted line with variation of [H_2O]; then the maximal content was about twice as high as the limiting value. This implies that an RM formed in the present experimental conditions can contain

two molecules of LYS for having the dimeter of about 10nm (see Fig.3).

3.2 Liquid membrane transport

Figure 7 shows the effect of KCl concentration in an aqueous feed on the transport of the proteins during an hour operation in the bulk liquid-membrane cell, indicating that the rate of the protein transport is faster at lower [KCl], as can be expected from the results of the extraction equilibria. Also the effect of feed pH was qualitatively explained by the equilibrium relation; however, the operating conditions on the strip side affected only the rate of the back extraction from the membrane phase.

The time courses of LYS content on the feed and strip sides in the membrane cell are shown in Fig.8, where the experimental conditions favorable for the extraction were selected on the basis of the results of the distribution equilibrium. The protein content on the feed side decreased below 10% of its initial value for 5 hours, whereas the concentration rise on the strip side reached to 80% content of the feed for 10 hours, further to 90% for 20 hours, though a short time-lag was observed in the transport. As the protein was transferred from the feed to the strip side through the membrane phase, the formation of aggregates was also observed at the interface between the strip and membrane phases, which may

Key	○	△
Protein	LYS	RNS
pH_F	6.9	3.1
$[KCl]_S$	1.0M	1.0M
pH_S	11.0	6.6

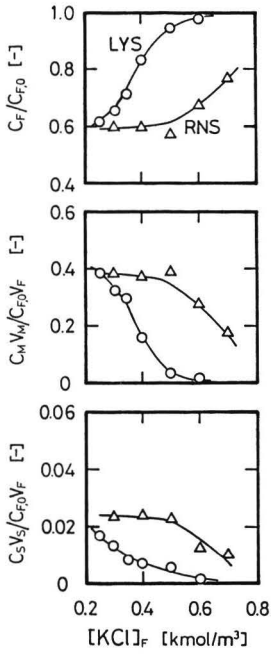

Fig.7. Effect of KCl concentration on the protein transport in an hour operation.

Table 1.
Results for the separation of the proteins from binary mixture of lysozyme(LYS) and ribonuclease-A(RNS) in 12 hours operation.

Proteins	Feed side		Strip side	
	[KCl]	pH	[KCl]	pH
	0.3M	6.8	1.0M	11.7
LYS (Single)	1.9%		85.3%	
RNS (Single)	85.2%		4.6%	
LYS (binary)	2.6%		82.6%	
RNS (Binary)	87.1%		2.9%	

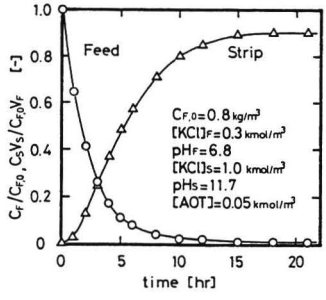

Fig.8. Time courses of LYS on the feed and strip sides in the liquid membrane cell.

be composed of the denatured proteins and AOT molecules. However, the loss of the protein, which was evaluated from a mass balance, was only about 1%.

Further study was made on the separation of LYS and RNS by use of the liquid membrane cell under the same experimental conditions as used in the lysozyme transport. Table 1 shows the results for the binary system of LYS and RNS together with those for each single system. In both the single and binary systems, a little RNS was recovered on the strip side through the membrane even in 12 hours operation; then, the separation factor of LYS to RNS attained to ca.28. This suggests that liquid membranes containing RM have a potential application for the separation and concentration of proteins from aqueous solutons.

CONCLUSIONS

The extraction of lysozyme and ribonuclease-A with reversed micellar solution was studied in AOT/isooctane system. The distribution equilibria of the proteins were explained in terms of an electrostatic interaction and a size exclusion effect. These effects depend on the concentration of KCl and pH in the aqueous solution. The water content of the micellar solution was correlated with the ionic strength and AOT concentration. Maximal content of the proteins solubilized in the micellar solution depended on only the water content. A bulk liquid membrane of the reversed micellar solution was applied to separation and concentration of the proteins. Lysozyme was separated in a high selectivity from the binary mixture with ribonuclease-A.

ACKNOWLEDGMENT

This work was supported by a Grant-in-Aid for Scientific Research (No.01550 730) from the Ministry of Education, Science and Culture of Japan. We wish to thank Dr. Toyoko Imae, Faculty of Science of Nagoya University, for the use of the dynamic light scattering photometer.

REFERENCES

Armstrong, D.W. and Li, W., 1988. Highly Selective Protein Separations with Reversed Micellar Liquid Membranes. Anal.Chem., 60:86-88.

Goklen, K.E. and Hatton, T.A., 1987. Liquid-Liquid Extraction of Low Molecular-Weight Proteins by Selective Solubilization in Reversed Micelles. Separat. Sci. Technol., 22: 831-841.

Kuboi, R., Hashimoto, K. and Komasawa, I., 1990. Separaton of Proteins with Reverse Micellar Liquid Membranes. Kagaku Kougaku Ronbunshu, 16: 335-342.

Luisi, P.L., 1985. Enzymes Hosted in Reverse Micelles in Hydrocarbon Solution. Angew. Chem. Int. Ed. Engl., 24: 439-450.

Solvent Extraction 1990, T. Sekine (Editor)

© 1992 Elsevier Science Publishers B.V. All rights reserved

PROTEIN EXTRACTION BY REVERSED MICELLES USING NEW SURFACTANTS

M. GOTO, K. KONDO+ and F. NAKASHIO
Department of Organic Synthesis, Kyushu Univ., Fukuoka 812, Japan

ABSTRACT

A surfactant plays a key role in the protein extraction by reversed micelles. In this study, extraction of some proteins by new reversed micelle was carried out using dioleyl phosphoric acid (abbreviated DOLPA) instead of conventional surfactant AOT. Large protein more than 50000 of molecular weight, which is difficult to dissolve into AOT reversed micelle, could be easily extracted by DOLPA reversed micelle. Denaturation of the proteins was depressed by using DOLPA reversed micelle because of the poor solubility of the DOLPA to the aqueous solution. Further, hybrid reversed micelle of DOLPA and AOT was investigated. It is found that extracted ratio of α-chymotrypsin was increased by use of the hybrid reversed micelle.

1. INTRODUCTION

A separation technique using reversed micelles provides an attractive alternative to conventional procedures for the separation and the purification of proteins and other biopolymers, since its aggregate in apolar solvent gives a unique environment and the promise of truly continuous operations with high volumetric capacities.

Recently, extraction behavior of many proteins using reversed micelles was investigated and a few applications of liquid membrane system have been also studied. However, in most work reported on protein extraction by reversed micelles, conventional surfactant AOT was used to form reversed micelles and little attention has been paid to search for a suitable surfactant for the protein extraction. The surfactant plays a key role in the separation process because solubilized species are stabilized by a surfactant layer in which the polar head groups point inwards, while the hydrophobic tails extend into the surrounding organic phase.

For this technology, it is necessary to develop new reversed micelle system and to clear the effect of surfactant on the extraction behavior of proteins. In a previous paper[1], we synthesized a series of dialkyl phosphoric acid surfactants. Among them, dioleyl phosphoric acid, abbreviated as DOLPA, is better than the other surfactants as regard the characteristic of protein extraction. Large proteins which is difficult to extract by AOT reversed micelle could be dissolved by the DOLPA reversed micelle. In this study, the extraction behavior of some proteins from an aqueous phase into DOLPA reversed micelles was studied in comparison with

+K. Kondo is now at Dept. of Chem. Eng., Doshisha Univ., Kyoto 602

that of the conventional surfactant AOT. Further, hybrid reversed micelle of DOLPA and AOT was also investigated.

2. Experimental

2.1 Reagent

Figure 1 shows the structure of surfactant used in the experiment. Sodium di-2-ethylhexyl sulfosuccinate (AOT) of reagent grade supplied from American Cyanamid Co., Ltd. was used without further purification. Di-2-ethylhexyl phosphoric acid(D2EHPA) delivered from Daihachi Chemical Industry Co., Ltd. was used without further purification. Dioleyl phosphoric acid(DOLPA) was synthesized as described in a previous paper[2]. Organic solvent is isooctane of analytical grade. All proteins are products of Sigma, Chemcal Co., Ltd. and used as received.

a) AOT

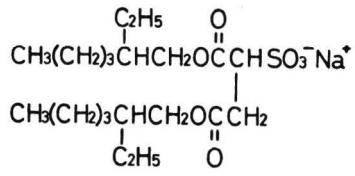

b) D2EHPA

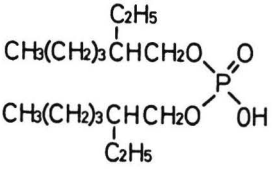

c) DOLPA

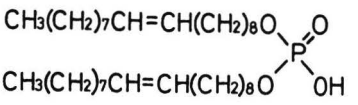

Fig.1 Surfactant structures

2.2 Protein extraction

The pH and ionic strength of the aqueous solution were adjusted using phosphate buffer solution and potassium chloride. Equal volumes(10ml) of the aqueous and organic solutions of known concentrations were shaken in a flask immersed in a thermostatted water bath(303K), and allowed to get equilibrium. The concentration of proteins was determined by UV-spectrophotometer and the water content in the organic phase was also measured by Karl-Fischer method. The mean diameter of reversed micelles was measured with a Photal(Otsuka Elec.) dynamic light scattering spectrometer(DLS-700). Measuring the concentration of P or S atom in the aqueous phase with ICP-Atomic Emission Spectroscopy(SEIKO SPS-1200VR), the distribution ratio of surfactants between aqueous and organic phase was determined.

3. Results and discussion

3.1 Water content dissolved by reversed micelles

Figure 2 shows the relation between water content dissolved by reversed micelles in isooctane and surfactant concentration. When DOLPA and AOT were used, the quantity of water dissolved in reversed micelles was constant at the low concentration of surfactant but that was increased linearly at the concentration more than about 1 mol/m^3. However, when the D2EHPA which has the same hydrophilic part of DOLPA and the same hydrophobic part of AOT was

used, the forming-ability of reversed micelles was very low compared with both of them. High concentration was necessary to form a stable reversed micelle using D2EHPA. In a previous paper[1], it was reported that the formation of reversed micelles using DOLPA can be controlled by adjusting an aqueous pH.

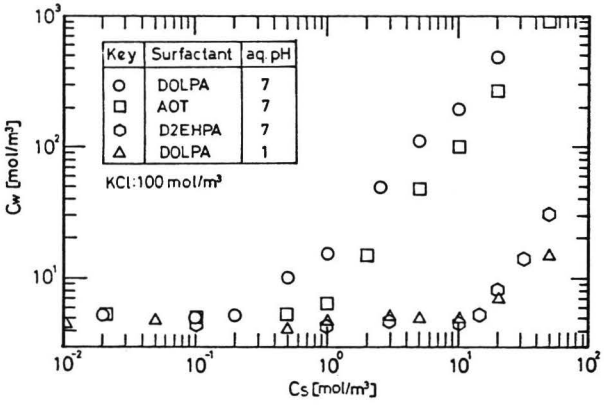

Fig. 2 Relation between water content and surfactant concentration

Under condition of low pH(pH<4), DOLPA mainly exists as a dimer in isooctane and anionic species of DOLPA forms a stable reversed micelle at the high pH(pH>6).

3.2 Distribution ratio of surfactant between aqueous and organic phase

Distribution ratio of surfactant, D, between aqueous and organic phases was defined by Equation (1).

$$D = C_{s,aq}/C_{s,org} \qquad (1)$$

Table 1 shows the distribution ratio for each surfactant at pH=1 and 7. DOLPA was scarcely dissolved in aqueous phase. Denaturation of proteins using reversed micelles is caused by complex formation with aqueous solved surfactants. From the viewpoint, DOLPA is a suitable surfactant for the protein extraction and the detail will be discussed in the next section.

TABLE 1.
Distribution ratio of surfactants between aqueous and organic phase

	surfactant		
aqueous pH	DOLPA	AOT	D2EHPA
pH=7	8.9×10^{-5}	3.0×10^{-2}	2.5×10^{-2}
pH=1	$<<10^{-4}$	2.8×10^{-2}	8.5×10^{-3}

3.3 Effect of surfactant on protein extraction by reversed micelles

Table 2 shows the results of protein extraction from an aqueous phase into reversed micelles. Mean diameter of AOT reversed micelle was 3~5nm under this experimental condition. It is difficult to dissolve large proteins into the AOT reversed micelles. In particular, reddish precipitate of hemoglobin was produced using AOT reversed micelles. The precipitate was filtered off and dried under reduced pressure. In order to clear whether the precipitate is a denaturated hemoglobin or complex of hemoglobin and AOT, we investigated the sample by elemental analysis.

TABLE 2.

Effect of surfactant on protein extraction by reversed micelles

		surfactant		
protein	**optimum pH**	**DOLPA**	**AOT**	**D2EHPA**
lysozyme	7.0	99.8%	98.9%	63.7%
myoglobin	5.9	99.2%	64.3%	67.1%
α-chymotrypsin	5.2	67.2%	49.3%	12.0%
hemoglobin	6.0	99.7%	reddish precipitate	reddish precipitate
albumin	5.6	22.3%	<<2%	0%
γ-globulin	–	0%	0%	0%

Table 3 shows the results of elemental analysis. From the result, the denaturation of hemoglobin was caused by complex formation with hemoglobin and aqueous solved AOT molecule. On the other hand, hemoglobin dissolved in the DOLPA reversed micelles was confirmed holding the higher-order structure by CD and ESR spectrum.

TABLE 3.

Results of elemental analysis

	C[%]	H[%]	N[%]
hemoglobin	50.4	7.2	15.4
AOT	53.9	8.4	
precipitate	52.1	7.7	6.3
hemoglobin +120*AOT	52.4	7.9	6.6

Figure 3 shows the change of reversed micelle diameter dissolving the lysozyme into the reversed micelles. In the case of DOLPA reversed micelles, the diameter distribution changes to the small region, however, in the case of AOT one, it changes to the large region. The observed diameters of them correspond to the rigid packed state of lysozyme. The protein in the water pool of

reversed micelles interact strongly with the hydrophilic part of surfactant.

3.4 Separation of proteins by DOLPA reversed micelles

Separation of hemoglobin and albumin using DOLPA reversed micelles was investigated. Figure 4 shows the effect of pH on the extraction of hemoglobin and albumin. Both of proteins possess almost the same molecular weight(Mw=65000). It is difficult to separate on the basis of size difference. However, it is possible to separate both of proteins utilizing the difference of isoelectric point (hemoglobin=6.8, albumin=4.9). Separation of hemoglobin and albumin was carried out adjusting the optimum pH.

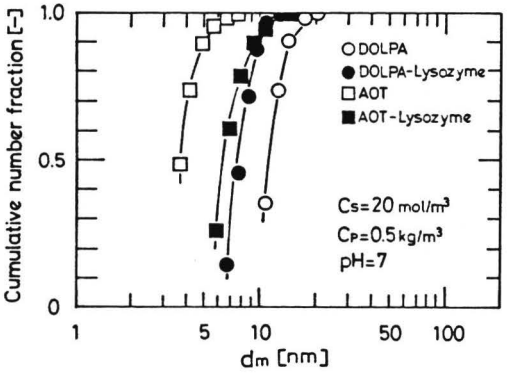

Fig.3 Change of reversed micelle diameter

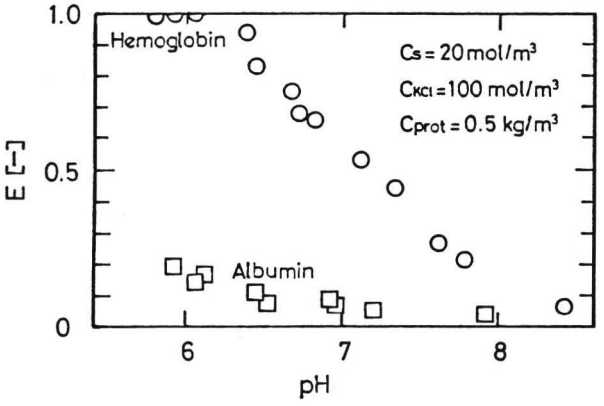

Fig. 4. Effect of aqueous pH on extraction of hemoglobin and albumin

Under this experimental condition, the optimum pH was about 6. Figure 5 shows the effect of salt concentration on the extraction of hemoglobin and albumin. Extracted ratio of proteins decreased with a increase in salt concentration, and the salt effect of NaCl was larger than of KCl.

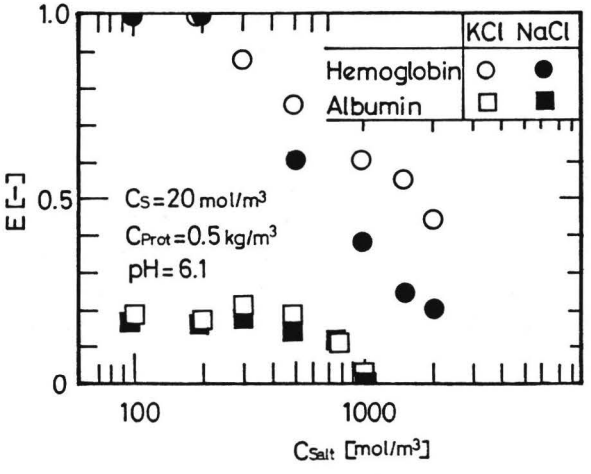

Fig. 5. Effect of salt on protein extraction

3.5 Extraction of α-chymotrypsin using hybrid reversed micelle

Extracted ratio of α-chymotrypsin by reversed micelles using AOT is about 50% at pH=6.5 and even if the DOLPA reversed micelle is used, that is about 60~70%. In this study, hybrid reversed micelles of DOLPA and AOT was applied for the extraction of α-chymotrypsin. Figure 6 shows the extraction results of α-chymotrypsin using the hybrid reversed micelles. The extracted ratio of α-chymotrypsin goes up to over 90% using the hybrid reversed micelle when the concentration ratio of DOLPA to AOT is 0.67~1.5. Mixing the DOLPA and AOT, it was confirmed that the form of reversed micelle changes from sphere to coil by measuring the angle dependence of light scattering, however, the detailed studies are now under way.

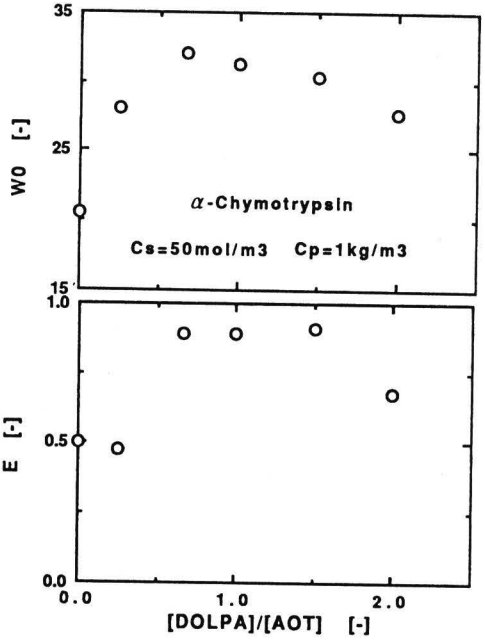

Fig. 6 Extraction of α-chymotrypsin by hybrid reversed micelle

4. Conclusion

Protein extraction by new reversed micelle using DOLPA surfactant was carried out. Hemoglobin which is difficult to extract by AOT reversed micelle, could be easily dissolved in DOLPA reversed micelle. Denaturation of proteins was depressed by using DOLPA reversed micelle. Further, hybrid reversed micelle shows the new characteristic for the protein extraction.

5. REFERENCES

1) M.Goto, K.Kondo, F.Nakashio: Protein extraction by reversed micelles using dioleyl phosphoric acid, J.Chem.Eng.Japan, 23, in press(1990)

2) M.Goto, K.Kondo, F.Nakashio: Acceleration effect of anionic surfactants on extraction rate of copper with liquid surfactant membranes containing LIX65N and nonionic surfactant, J.Chem.Eng.Japan, 22, 79(1989)

Solvent Extraction 1990, T. Sekine (Editor)

© 1992 Elsevier Science Publishers B.V. All rights reserved

SEPARATION OF PROTEINS USING AFFINITY AQUEOUS TWO-PHASE EXTRACTION IN PEG/SALT SYSTEMS

W.-H. WANG, R. KUBOI and I. KOMASAWA
Department of Chemical Engineering, Osaka University, Toyonaka, Osaka 560, (Japan)

ABSTRACT

Aqueous two-phase extraction using PEG (polyethylene glycol)/PK (phosphate) systems has not been used for affinity partition because of its high salt concentration, in spite of the advantage of low cost over PEG/Dex (dextran) systems. PEG modified with general dye ligands such as Procion Blue (PB) was however found to be effective for papain and some dehydrogenases in a PEG/PK system as well as in a PEG/Dex system. Separation of papain from papaya latex using PB-PEG in the PEG/PK system was successfully carried out. The inhibition constant of PB-PEG for papain was found to have nearly the same values in the PEG/PK system as in the PEG/Dex system, indicating the hydrophobic nature of the interaction. These results could be extended to some dehydrogenases suggesting that affinity partition in PEG/salt systems is a new potential method for the separation and purification of proteins.

1 INTRODUCTION

Aqueous two-phase systems have been extensively applied to the extraction and separation of proteins. The most efficient approach to improve the selectivity of the extraction is to utilize the biospecific interaction of a protein with an affinity ligand such as its inhibitor. Compared with the high cost of PEG/Dex systems, PEG/salt systems are cheap enough to be used at commercial scale. However,the extraction of proteins by affinity partition in PEG/salt systems has been considered to be impossible, because of the presence of salt of high concentration. Actually, it has not been investigated in detail.

In the present work, the extraction of papain by using PEG modified with affinity ligands of Gly-Gly-Tyr-Arg and Procion Blue MX-R as well as by using ionisable sulphonate bound PEG in PEG/PK and PEG/Dex systems has been studied. PB-PEG has been used for the separation of papain from crude papaya latex in the former system. The applicability of the method to some dehydrogenases has also been investigated.

2 EXPERIMENTAL

2.1 Materials

PEG4000(M.W.=3000), PEG1540(M.W.=1500) and Dex(M.W.=100000-200000) were supplied by Wako Pure Chemical LTD.. PEG4000 derivatives of peptide, Gly-Gly-Tyr-Arg (GGTA-PEG), triazine dye, Procion Blue MX-R (PB-PEG), and sodium sulphonate (S-PEG) were prepared following the procedure described

previously[6]. The proportion of modified PEG is 95mol%, 7.5mol% and about 90 mol%, respectively. Other chemicals were of analytical grade.

Crude papaya latex originated in SriLanka was dissolved in distilled water or cysteine solution and the resulting leachate liquor was used in partition. Alcohol dehydrogenase (ADH) from bakers yeast and L-glutamic dehydrogenase (GDH) from bovine liver were supplied by Sigmal Chemical Co.(U.S.A.).

2.2 Partition

The composition of the systems is 7wt% PEG4000 (including ligand-PEG) and 10wt% Dex, or 12wt% PEG4000 (including ligand-PEG) and 12wt% PK, with the exception that PEG1540 and non-bound PB were used for the affinity partition of GDH. pH was adjusted with NaOH or HCl for the PEG/Dex systems and with PK buffer for the PEG/PK systems.

After mixing by shaking, the systems were centrifuged to speed up phase separation. The activity of papain and the concentration of total protein in each phase were determined as described previously[5]. The corresponding phase solution from a two-phase system containing no protein was usually used as blank in spectrophotometry. Partition coefficient, K, is defined as the ratio of the concentration or the activity in the two phases, and separation factor as the ratio of the partition coefficient of the desired component to that of the total proteins.

3 RESULTS and DISCUSSION

The partition coefficient of a protein in an aqueous two-phase system is determined by several interactions as follows[1]:

$$\ln K = \ln K_{el} + \ln K_{hphob} + \ln K_{hphil} + \ln K_{conf} + \ln K_{lig} \qquad (1)$$

where the subscripts, el, hphob, hphil, conf and lig, denote, respectively, electrostatic, hydrophobic, hydrophilic, conformational and ligand contributions. These factors can be adjusted to alter the partition behavior effectively by using different kinds of PEG derivatives.

3.1 Effect of charged PEG

The effect of S-PEG on the partition of papain in PEG/Dex and PEG/PK systems is shown in Fig.1. 1wt% of S-PEG was added to the PEG/Dex system, and 1.5wt% to the PEG/PK system. In the PEG/Dex system without S-PEG, partition coefficient of papain activity, K_{pa}, and concentration of total protein, K_{pr}, are low and independent of pH. When S-PEG is used, they increase especially at low pH and become dependent on pH. This result can be explained by the attraction between negatively charged S-PEG concentrated in the upper phase[4] and positively charged proteins in the range of pH less than their pI. However, this effect of S-PEG is not observed in the PEG/PK system. The partition of papain and

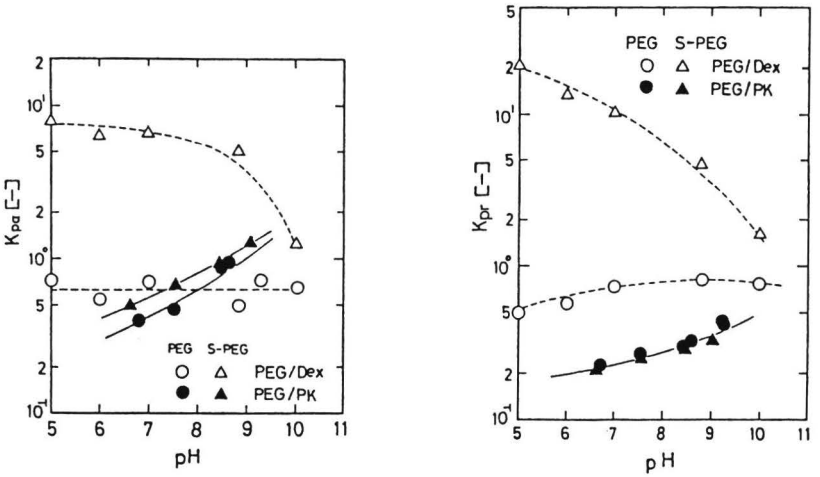

Fig.1 Effect of S-PEG on the partition coefficient of (a)papain, K_{pa}, (b)total protein, K_{pr}, in the PEG4000(7%)/Dex(10%) and PEG4000(12%)/PK(12%) systems

other proteins is insensitive to the addition of S-PEG. The electrostatic interaction between S-PEG and proteins is probably diminished by the shielding effect of the salt. This limits the practical use of charged PEG in PEG/salt systems.

3.2 Effect of an electrostatic affinity ligand

GGTA is known as a competitive inhibitor for papain and is used practically for its purification by chromatography[3]. It has been reported that residues Asp(158) and Trp(176) in the active site of papain have an electrostatic and hydrophobic interaction with the Arg and Tyr of GGTA, respectively, forming an inactive protein-inhibitor complex[3]. The inhibition constant, K_i, which is the dissociation constant of the complex can be determined by Dixon plot[2]. The influence of the systems on K_i is given in Table 1. K_i of GGTA and GGTA-PEG is about 0.2 mM in the PEG/Dex system, and about 100 times greater in the PEG/PK system than in the PEG/Dex system. The affinity of GGTA or GGTA-PEG for papain decreases dramatically in the high ionic strength environment.

The effect of GGTA-PEG on the partition coefficient and the separation

Table 1 Influence of coexistent two-phase systems on the inhibition constant of papain by GGTA-PEG (GGTA) and PB-PEG (PB) (pH:6,2~7.5)

System		GGTA	GGTA-PEG	PB	PB-PEG
PEG/Dex		0.23	0.21	0.22	0.178
PEG/PK	Upper phase	28	150	0.246	0.182
	lower phase	21	-	0.062	0.100

factor of papain, K_{pa} and K_{pa}/K_{pr}, is shown in Fig.2. In the PEG/Dex system, K_{pa} and K_{pa}/K_{pr} give 2 times greater values when 1wt% of GGTA-PEG is used. However, no change is observed in the PEG/PK system. This indicates that salts hinder the effect of GGTA-PEG as found in the case of S-PEG. Thus, the electrostatic interaction predominates over the hydrophobic for the affinity between papain and GGTA-PEG. Weak eletrostatic affinity interactions cannot be expected to occur in PEG/salt systems.

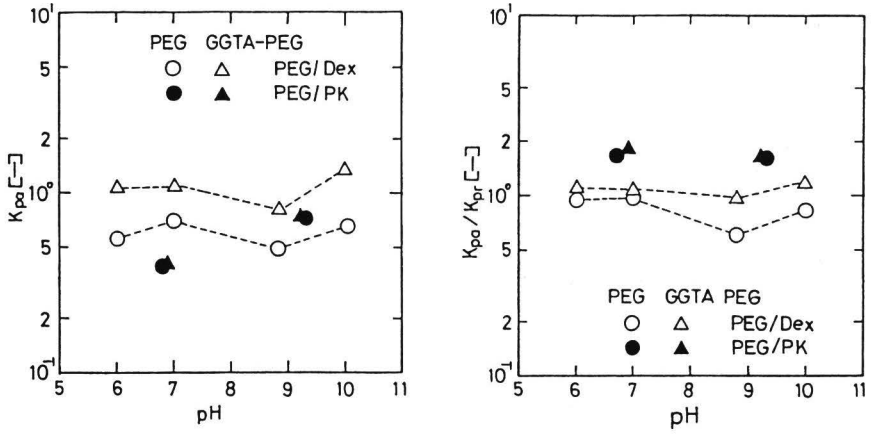

Fig.2 Effect of GGTA-PEG on (a)the partition coefficient of papain, K_{pa}, (b)the separation factor of papain, K_{pa}/K_{pr}, in the PEG4000(7%)/Dex(10%) and PEG4000/PK(12%) systems

3.3 Effect of a hydrophobic affinity ligand

Previous work has shown that PB-PEG is an inhibitor of papain[5]. The inhibition constant, K_i, of PB and PB-PEG for papain in the PEG/Dex and PEG/PK systems is also shown in Table 1. The upper phase of the PEG/PK system has almost the same values as the PEG/Dex system in contrast to GGTA-PEG. Furthermore, in the PEG/PK system, K_i in the lower phase is less than in the upper phase, indicating a stronger affinity between papain and PB-PEG (or PB) in the presence of PK. On the other hand, the distribution of PB-PEG into the upper PEG-rich phase is extreme at room temperature($K_{PB\text{-}PEG}>100$), while GGTA-PEG is more equally distributed between the two phases($K_{GGTA\text{-}PEG}=0.6\text{-}1.5$). These results indicate that PB-PEG is much more hydrophobic than GGTA-PEG, as expected from the structural formula of PB shown in Fig.3.

Fig.4 shows the effect of PB-PEG on the partition of papain from crude papaya latex at pH8.4-8.5 in the PEG/PK system. Addition of PB-PEG to the system results in an increase in the partition coefficient of papain, K_{pa}, and a decrease in that of total protein, K_{pr}, thus an increase in the separation factor of papain, K_{pa}/K_{pr}. When PB-PEG is used up to 9%, K_{pa}/K_{pr} increases from 2.7 to 15.4. PB-PEG increases the hydrophobicity of the system[5]. Thus

the ligand has a combined effect on the system, enhancing the partition of papain to the upper phase whilst promoting the partition of other hydrophilic proteins such as lysozyme and chymopapain to the lower phase. Obviously, such a hydrophobic ligand can also be exploited to achieve an effective affinity partition in PEG/salt systems.

The variation of the specific activity of papain, SA(U/mg), in the two phases, as well as its yield in the upper phase, $yield_u$(U%, g%), is shown in

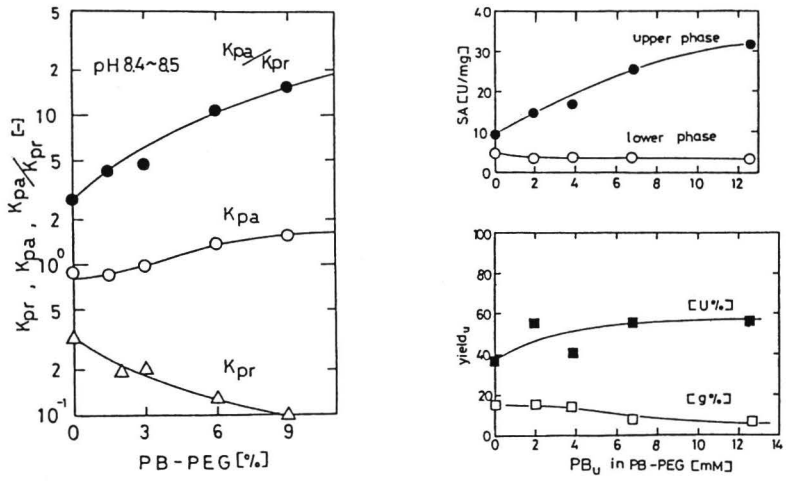

Fig.4 Effect of PB-PEG on the partition of papain in the PEG4000(12%)/PK(12%) system

Fig.5 Effect of PB-PEG on the specific activity and yield of papain in the upper phase of the PEG/PK system
(U%:Activity percentage of papain; g%:Gram percentage of total protein)

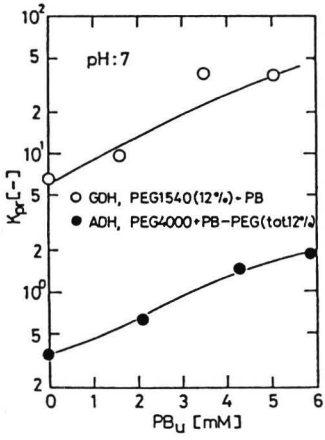

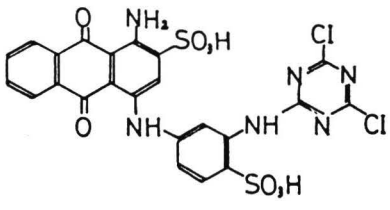

Fig.3 Structural formula of Procion Blue

Fig.6 Effect of PB-PEG or PB on the partition coefficient of ADH and GDH

Fig.5. Leachate liquor of papaya latex contains many contaminating proteins and SA is only 3-6 U/mg. The purity of papain in the upper phase, SA_u, increases with the concentration of PB-PEG. When 9wt% of PB-PEG is used, that is, $[PB_u]$=12.5mM, SA_u attains 32U/mg, which is a similar value with that of a commercial product. The recovery of the papain activity in the upper phase is 56U%, whilst the yield of total protein is 6.6g%.

The conventional purification procedure of papain from papaya latex employs fractional precipitation in a total of six steps. Results based on such a procedure have been given previously[6]. Assuming a yield of papain at the 1st step of 100%, 23.7U/mg of papain was obtained at the 6th step with a yield of 4.0U% and 0.9g%. The purity and recovery of papain obtained by the present one-step affinity partition using cheap PB-PEG is better than that with the conventional procedure. The extraction can be easily carried out continuously and at large process scale.

The applicability of PB-PEG to the affinity partitioning of dehydrogenases has also been verified. By using PB-PEG or PB in PEG/PK systems, an improvement of partition coefficient of ADH and GDH was observed, as shown in Fig.6, in which PEG1540 was used to increase the solubility of GDH. This indicates that this work could be further extended to other hydrophobic proteins or those which have hydrophobic active sites.

4 CONCLUSION

The affinity partition of papain from papaya latex has been investigated and a comparison made between PEG/PK and PEG/Dex systems. GGTA-PEG loses its affinity for papain in the former systems, indicating the importance of the electrostatic interaction between GGTA and papain. On the other hand, the hydrophobic ligand, PB-PEG, had almost the same values of inhibition constant for papain in these two systems, thus it may be used to achieve an effective affinity partition of papain in the PEG/PK system. These results could be extended to some dehydrogenases, suggesting that the use of hydrophobic affinity partition in PEG/salt aqueous two-phase systems is a new potential method for the separation and purification of proteins.

5 REFERENCE

1) Albertsson, P.A., 1977. Endeavour, 1, 69
2) Dixon, M., 1953. Biochem. J. 55, 170
3) Funk, M.O., Nakagawa,Y., Skochdopole, J. and Kaiser, E.T., 1979. Int. J. Peptide Protein Res., 13, 296-303
4) Johansson, G., 1970. Biochim. Biophys. Acta, 222, 381
5) Kuboi, R., Wang, W.-H. and Komasawa, I., 1990. Kagaku Kogaku Ronbunshu, 16, 773-779
6) Kuboi, R., Wang, W.-H., Morimatsu, K., Tone, S. and Komasawa, I., 1989. Kagaku Kogaku Ronbunshu, 15, 497-503

Solvent Extraction 1990, T. Sekine (Editor)

© 1992 Elsevier Science Publishers B.V. All rights reserved

HYDROPHOBIC EFFECT ON PARTITION OF BIOPOLYMERS IN AQUEOUS TWO-PHASE EXTRACTION SYSTEMS WITH SALTS

R. KUBOI, H. TANAKA AND I. KOMASAWA
Department of Chemical Engineering, Osaka University, Toyonaka, Osaka 560, JAPAN

ABSTRACT

The relative hydrophobicities of aqueous two-phase solutions (referred to as the separation field) were evaluated by means of a hydrophobic factor (HF) derived from the partition of various amino acids of known relative hydrophobicities. The surface hydrophobicities of proteins, HFS, were also evaluated by the ratio of their partition coefficient and the HF value of the partitioning system. The hydrophobic interaction between a solute and the HF value of the system was found to be the dominant factor in the partitioning at the isoelectric point. The addition of salt in high concentration results in changes to both the values of the HF of the separation field and the HFS of the proteins. The increase of HFS depends on molecular weight of proteins. Proteins with different surface hydrophobicities, isoelectric points and molecular weight can be separated effectively by the combined effect of hydrophobic, electrostatic and salt effects.

INTRODUCTION

In Aqueous Two-Phase Systems, the partition coefficient of proteins is influenced by several factors such as those arising from electrostatic, hydrophobic and salt effects. To effectively separate proteins by phase partitioning, it is necessary to estimate these individual effects quantitatively and to use the combined effect for separation. The electrostatic effect arises from the interaction between the protein net charge and the interfacial potential which arises from the unequal partition of salt. This area has been the subject of extensive research see for example Albertsson (1986) and Johansson (1985). Hydrophobic effects and salt effects, however, have not been systematically investigated (Shanbhag, 1975 and Zaslavsky, 1978). Relative hydrophobicities of systems and surface hydrophobicities of proteins have been quantified and reported previously (Kuboi, 1990). The present work illustrates the evaluation of the relative hydrophobicities of the fields and the surface hydrophobicities of the proteins to be separated. The effect of the addition of salt on the nature of interaction between the field and the protein has also been examined.

1. EXPERIMENTAL

Materials

Dextran(Dex)60000-70000 and Dex100000-200000 were supplied by Wako Pure Chemical Ltd. Poly ethylene glycol(PEG)1540,4000,6000,20000 (Mw=1500,3000,7500, 20000) were also supplied by Wako. Amino Acids were supplied by Ishizu Pharmaceutical Ltd. Hamburger Penta peptide(HEPP) was supplied by Tanabe Pharmaceutical Ltd. Papain, ribonuclease a, cytochrome c, BSA, ovalbumin, chymopapain, hemoglobin and alcohol dehydrogenase were supplied by Sigma Chemicals. Lysozyme and chymotrypsin were from Wako. Inorganic salts(NaCl, Na_2SO_4) were of analytical grade supplied by Wako.

Method

Systems with the following total composition,(9%)Dex, (9-13%)PEG and (0.1-2Mole/kg) salt, were used in this work. The phase systems were prepared by mixing stock solutions of 30% Dex and 30% PEG together with salt and protein solutions at room temperature. After mixing by gentle inversions the systems were centrifuged at 5000rpm for 20min. The concentration of amino acids was measured by HPLC using the OPA reaction. Peptide and proteins were measured by the ninhydrin (Akahori, 1954) and pyrogallol red (Fujita, 1983) methods, respectively. The colour developed was measured at 570nm and 600nm.

2 RESULT AND DISCUSSION

2-1 Hydrophobic effect

Fig.1 shows the partition coefficient of several amino acids in a PEG6000(9%)/Dex100000-200000(9%) system as a function of their relative hydrophobicities(RH) as defined by Tanford (1971). The linear relationship

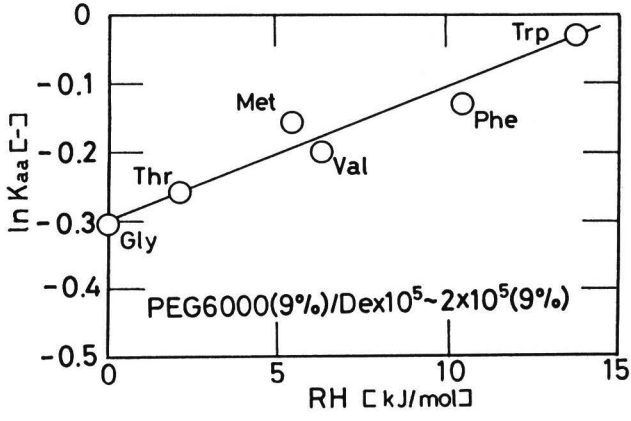

Fig.1 Dependence of partition coefficient of amino acids on RH (relative hydrophobicity defined by Tanford) in PEG6000(9%)/Dex100000-200000(9%) system.

between the logarithm of the partition coefficient of the amino acids(lnKaa) and RH can be seen. Since the slope of this line may be considered to provide a measure of the difference in the relative hydrophobicity between the two phases of this system, the slope has been defined as the hydrophobic factor(HF). The hydrophobicities of various amino acids and peptides were successfully expressed by the ratio of lnKaa (or lnKpe) to HF value of the field (Kuboi, 1990). This method was also applied to proteins such as papain, ribonuclease a and hemoglobin as shown in Fig.2, in which the data were obtained at their isoelectric points to diminish the electrostatic effect. The surface hydrophobicity of protein HFS (determined by the hydrophobic factor of solutes) was given by the ratio of lnKpr to HF value of the field. HFS values, determined in this way, for these proteins indicate that papain is the most hydrophobic protein and hemoglobin the most hydrophilic. By this definition, protein partitioning at isoelectric points can be described by eq.(1).

$$\ln Kpr = HF \times HFS \qquad (1)$$

Proteins with different HFS (surface hydrophobicity) may be separated effectively by controlling HF (the hydrophobicity of the system).

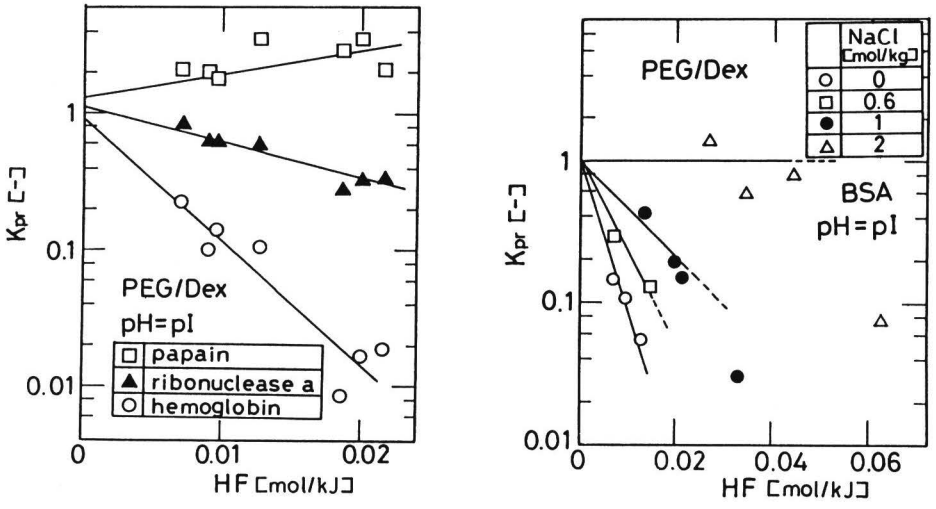

Fig.2 Effect of HF on partition coefficient of several proteins.
system:PEG1540,4000,6000,20000(9-10.8%)/Dex100000-200000(9%)
PEG1540,4000,6000(9-13%)/Dex60000-90000(9%)

Fig.3 Effect of addition of NaCl on the relationship between partition coefficient of BSA at isoelectric point and hydrophobic factor of the system.
system:PEG1540,4000,6000(9-10.8%)/Dex100000-200000(9%)
PEG4000(9%)/Dex60000-90000(9%)

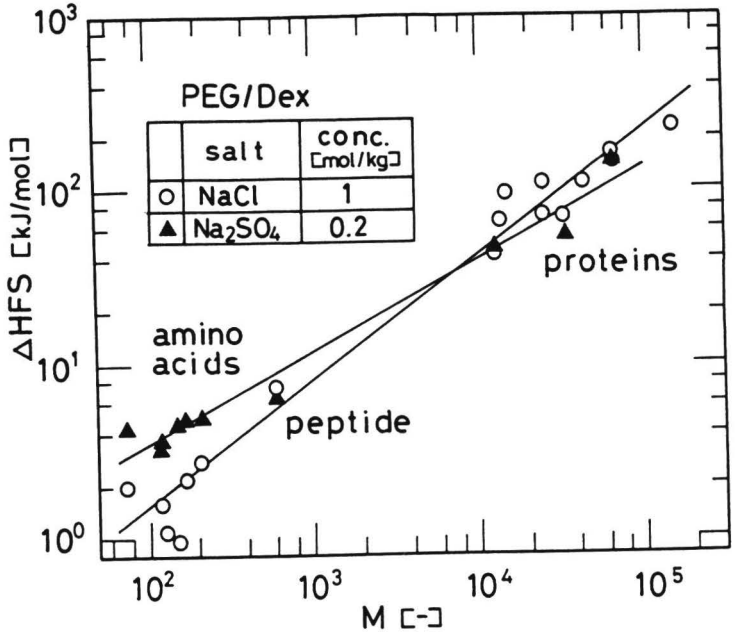

Fig.4 Increment, due to the addition of 1mol/kg NaCl and 0.2mol/kg Na_2SO_4, of surface hydrophobicity of amino acids, peptide and proteins with differing molecular weight.

2-2 Salt effect

Increases in the the concentration of salt added to aqueous two phase system have been shown to dramatically change the partition coefficient of proteins (Johansson, 1985). The effect of addition of sodium chloride on the partition of BSA is shown in Fig.3 as a function of HF. The salt clearly causes an increase in the HFS of BSA. The driving force for the increment of HFS, ΔHFS, may by caused by the entropy change of water due to the addition of salt, the increment, ΔHFS, is dependent on the molecular weight as follows.

$$\Delta HFS = AM^{2/3}(\Delta S_1 - \Delta S_2) \quad (2)$$

ΔS_1 and ΔS_2 are the entropy change in the top and the bottom phase respectively. M is the molecular weight of proteins. A is a constant. The increment, ΔHFS, caused by the addition of 1mol/kg NaCl or 0.2mol/kg Na_2SO_4 are plotted against molecular weight of amino acids, peptide and proteins in Fig.4. Straight lines with a slope of about 2/3 are seen for both salt systems. Thus, the increment of HFS by salt addition becomes greater with molecular weight of proteins. Separation of chymopapain(Mw=35000) and cytochrome c(Mw=12400) can be realized by the addition of 1mol/kg NaCl as shown in Fig.5.

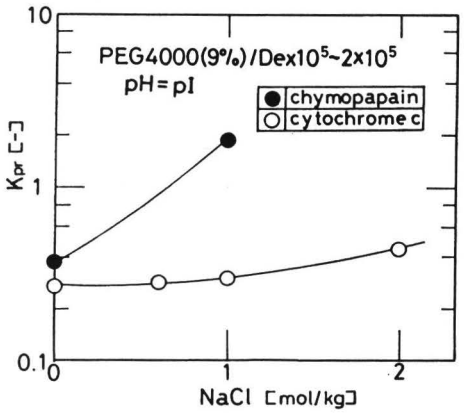

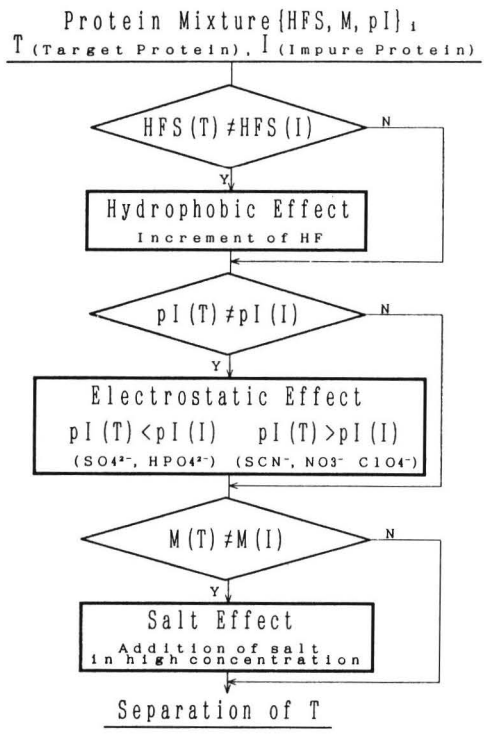

Fig.5 Effect of addition of NaCl on the partition of chymopapain and cytochrome c at their isoelectric points.

Fig.6 Scheme for separation of proteins by the combined effects of hydrophobic, electrostatic and salt addition.

3 CONCLUSION

Separation of proteins

The partition coefficient of proteins is the integral over the hydrophobic effect, Khphob., the electrostatic effect, Kel., and the salt effect, Ksalt.

$$\ln Kpr = \ln Khphob. + \ln Kel. + \ln Ksalt \quad (3)$$

To rationally design the effective separation of proteins, these effects must be used to enhance the selectivity of chosen systems for proteins. A scheme for the separation of proteins by the combined effect of these factors is shown in Fig.6. When a difference in HFS of the proteins exists, the hydrophobic effect can be used by controlling the HF of the separation field. When two proteins differ in isoelectric points, the electrostatic effect can be used by the choice of salts partitioned unequally between top or bottom phase. If two proteins differ in molecular weight, the salt effect can be used by the addition of salt in high concentration. When more than one difference in these

properties, surface hydrophobicity, isoelectric point and molecular weight exists, the combined effect can be used for the separation of proteins.

4 REFERENCES

Akahori, S. and Mizusima, M., 1954. Tanpakusitu Kgaku (Protein Chemistry) 1. Kyouritu Shuppan, 201

Albertsson, P. A., 1986. Partition of Cell Particles and Macromolecules. John Wiley, New York

Fujita, Y.,Mori, I. and Kitano, S., 1983. Bunseki Kagaku, 32, E379

Johansson, G., 1985. Partition in Aqueous Two-Phase Systems. In: H.Walter et al. (Editor), Academic Press, New York, 161-226

Kuboi, R., Tanaka, H. and Komasawa, I., 1990. Hydrophobicities and partition properties of proteins in aqueous two-phase extraction system.,Kagaku Kougaku Ronbunsyu, 16, 755-762

Nozaki, Y. and Tanford, C., 1971. The solubility of amino acids and two glysine peptides in aqueous ethanol and dioxane solutions. J. Biol. Chem., 246, 2211-2217

Shanbhag, V. P. and Axelsson, C. G., 1975. Hydrophobic interaction determined by partition in aqueous two-phase systems. Eur. J. Biochem., 60, 17-22

Zaslavsky, B. Yu, Miheeva, L. M. and Rogozhin, S. V., 1978. Possibility of analytical application of the partition in aqueous biphasic polymeric systems technique. Biochim. Biophys. Acta, 510, 160-167

Solvent Extraction 1990, T. Sekine (Editor)

© 1992 Elsevier Science Publishers B.V. All rights reserved

SEPARATION OF BIOPOLYMERS WITH REVERSE MICELLAR BULK LIQUID MEMBRANES

R.Kuboi, Y.Mori, Y.Yamada, I.Komasawa and P.L.Luisi*
Dept.of Chem.Eng., Osaka University, Toyonaka, Osaka 560, JAPAN
*Institut fur Polymere, ETH-Zentrum, CH-8092 Zurich, SWISS

ABSTRACT
Selective transport of proteins and amino acids through the reverse micellar liquid membrane from an aqueous phase to another was successfully attemted using bulk liquid membrane systems mainly composed of anionic (AOT) and cationic (CTAB) surfactants. Protein extraction model based on size exclusion effect was successfully presented. Protein - reverse micelle interaction especially hydrophobic interaction was quantified. Improvement of selectivity and activity yield of lipase after forward and backward extraction was also achieved using affinity liquid membrane systems.

1. INTRODUCTION

The partition coefficient, K, of a biopolymer in reverse micellar systems is determined by several factors as follows [4]:

$$\ln K = \ln K_{el.} + \ln K_{ster.} + \ln K_{hphob.} + \ln K_{lig.} \qquad (1)$$

where K is defined as the ratio of the biopolymer concentration in the bulk organic phase and that in the aqueous phase, and the subscripts, el., ster., hphob. and lig., denote electrostatic, steric (size exclusion), hydrophobic, and affinity ligand contributions, respectively.

Extraction of amino acids into reverse micelles(RVM) is mainly dependent on the electrostatic interaction between ionic surfactants, ex.negatively charged AOT reverse micelles, and the surface charge of solutes and also on the hydrophobic interaction between RVM and hydrophobic amino acids [8,9]. The latter interaction becomes dominating factor at their isoelectric point, pI. On the other hand, extraction of a protein into RVM at its pI is mainly influenced by the size exclusion effect, the hydrophobic interaction and the interaction with affinity ligands in RVM [3,5,7].

There is, however, no quantitative correlation on these steric, hydrophobic and affinity interaction between proteins and reverse micelles. Lack of quantitative data on these factors restrict further application of reverse micelle extraction in the down stream processing in developing bioindusty.

In this paper; 1)selective transport of proteins through the reverse micellar liquid membrane from an aqueous phase to another has been attemted using the bulk liquid membrane system mainly composed of anionic (AOT) and

cationic(CTAB) surfactants and applied to the separation of amino acid derivatives or proteins, 2)the extraction model of proteins with various molecular weights is briefly discussed based on size exclusion effect of RVM, 3)quantification of hydrophobicity, HF, of reverse micellar two-phase systems has been carried out based on the measuring method reported in the previous paper using partitioning of amino acids with known hydrophobicity, R.H.[4], 4)affinity extraction of lipase has been attempted using either a hydrophilic inhibitor or an amphiphilic bile salt as ligand to improve enzyme activity yield after forward and backward extraction.

2. EXPERIMENTAL

2.1 Liquid membrane systems

Three type of liquid membrane systems were used as shown in Fig.1. Phase transfer experiments of amino acid derivatives were carried out with liquid membrane system type-a, where an aqueous solution containing the protein mixture will be sandwiched between two microemulsion solutions, one with higher density consisting of CTAB in chloroform/n-hexanol 1:1 (v/v), the lighter consisiting of AOT in isooctane, where the CTAB is positively, while the AOT is negatively charged. Phase transfer experiments of proteins were carried out in the similar system type-b with slightly modified configulation and solvent. And finally for separation of three proteins type-c was used where forward and backward extraction take place for both AOT and CTAB membranes at the same time.

These experimental conditions such as volume of each phase, AOT or CTAB and KCl concentration, pH and the water content in the organic phases Wo (=[H2O]/[AOT],[H2O]/[CTAB]) were the same as shown in the previous works[3,9]. These vessels were gently shaken on an Minishaker or stirred by magnetic stirrer, making sure that there was no inter-mixing of phases.

2.2 Measuring method of hydrophobicity

The relative hydrophobicity of the two phases is named as hydrophobic factor, HF, can be evaluated by partitioning of various amino acids of which relative hydrophobicities, R.H., have been defined and measured by Nozaki and Tanford[4]. As described in detail for aqueous two-phase systems[4], HF is defined as the increment of ln K with the increment of the relative hydrophobicity of amino acids, RH, used, i.e. (ln K-ln KGly)/RH. Therefore HF can be easily determined by measuring partition coefficients K of several amino acids or peptides such as Val, Tyr, Phe, Trp, Phe-Phe, Phe-Trp and Trp-Trp regardless of phase systems and containing salts.

2.3 Experimental procedure

Extraction experiments were carried out mainly by contacting aqueous feed solution with given pH and concentrations of salt (NaCl or KCl), amino acids,

peptides or proteins with an equal volume (5ml) of reverse micelle containing isooctane with given AOT concentration. In the affinity extraction either phenyboric acid(PBA) or taurodeoxycholic acid(TDCA) is added as a hydrophilic inhibitor or amphiphilic ligand, respectively. The system was then gently stirred. The proteins used are shown in Table 1 with their pI and HFS. These concentrations were measured by either UV spectrophotometry (Shimadzu, UV-265FW) or HPLC (Shimadzu, LC-6A), and water content in organic micellar phase by Karl-Fischer method. The water content, Wo, was defined by the molar ratio of water to AOT. Reverse micelle size distribution was measured by the dynamic light scattering method by using DLS-700Ar(Otsuka Electr.).

3. RESULTS AND DISCUSSION

3.1 Electrostatic effect and bulk liquid membrane separation

It was clearly shown that the electrostatic interaction between AOT and the amino group and also between CTAB and the carboxyl group play the dominant role, especially when the solute molecules are small and charged (system type-a or b in Fig.1). Because the fraction extracted of peptides and proteins from aqueous phase to organic (micellar) phase , E, increase sharply with either increase (CTAB) or decrease (AOT) in pH from near the isoelectric point (pI). AOT is suitable for the extraction of the solutes with heigher pI (ex. Lysozyme, a-Chymotrypsin, +H2-Phe-OM) and CTAB for that with lower pI (ex. Lipase, Ac-Trp-O-)(data in detail shown elsewhere[3,9]).

While the maximum values of E and dE/dpH for proteins decrease with increase in molecular weight, MW, of proteins to be separated due to the steric or size exclusion effect. Extraction of solutes with low MW such as amino acid dervatives or peptides is also influenced by their hydrophobic interaction with RVM and can be separated by these combined interactions.

Finally, the mixture of the proteins was separated in the combined liquid membrane system type-c in Fig.1. As shown in Table 2, nearly pure Lysozyme and lipase were separated into the aqueous pahse 1 and 2 respectively, although E of each protein was 30% and 20%. Lysozyme was selectively transported through AOT membrane to aqueous phase 1, while lipase was CTAB membrane to aqueous phase 2.

3.2 Size exclusion effect and extraction Model

A simple scheme for extraction of proteins with various MW into micellar solution at their isoelectric points, pI, is presented on the basis of the observed reverse micelle size distribution and the following assumptions; i.e. 1) only the proteins adsorbed on aqueous bulk and organic interface may dissolve into micellar solution when they encounter with micelles of which sizes (of inner micro-water-pool, i.e. dm-2.4nm) are greater than proteins, 2)

the protein concentration at the interface is constant independently of the micellar phase condition, and 3) the effectiveness of collision which results in subsequent protein uptake is proportional to the ratio of cross sectional area for collision of the inner micro-water-pool to that of the protein, i.e. ((dm-2.4)/dp)2. With these assumptions the fraction extracted of proteins, EpI, can be expressed as the following equation:

$$EpI = \int_{dm>\overline{dp}+2.4} (Const.)(Cm)(Dm)(Rmp)((dm-2.4)/\overline{dp})^2 d(dm) \quad (2)$$

where dm, Cm and Dm are respectively micelle size, concentration and diffusion coefficient and Rmp is collision radius defined as (dm + dp)/2 . The results shown in Fig.2 were well correlated by this model(results shown elsewhere [5,7]). It has also been shown that the bell-shaped dependency of EpI on Wo corresponds to the effective micellar number[2,5], and that EpI for the similar size of proteins inclease with the surface hydrophobicity of proteins, HFS, which was quantified in our previous work[4].

3.3 Hydrophobic effect and hydrophobicity of RVM

1)Hydrophobic factor HF of RVM system

Based on the following simple corelation which was presented previously[4],

$$\ln Khphob. = HF * HFS \quad (3)$$

we assume the similar relation for RVM systems as follows;

$$\ln K'pI(amino\ acids) = HF * (R.H. + const.) \quad (4)$$

where K'pI is the corrected partition coefficients of solutes at their pI defined by the ratio of its concentration in the micro-water-pool of RVM (not the bulk organic phase) and its bulk aqeous concentration. We neglect the possible difference in the solubilization mode of hydrophobic amino acids and peptides for the simplicity, i.e. micellar-wall or water-pool solubilization. Typical results of measured K' at pI were plotted against R.H. (where the hydrophobicity scale of Gly is defined as 0) in Figs.3. Both plots show linear correlations with different slopes depending on salt concentration and salts. Hydrophobic factors HF of these phase systems were determined by these slopes for each salt concentration and the salt. The obtained HF values in RVMS are rather surprisingly in the similar range of those observed in PEG (polyethyleneglycol)/salt aqueous two-phase systems [4] showing the significance of the salt effect on the hydrophobicity.

2)Effects of salts and Wo on HF of RVM system

The effect of addition of various salts to the reverse micellar two-phase systems on HF was quantitatively examined. The effects vary with the salt type and concentration and are shown in detail in the reference[6]. Addition of salt to phase systems usually cause hydrophobicity change as shown in the aqueous two-phase systems[4]. In the case of RVM systems, it also cause the

reduction of micelle size and the water content, Wo. HF values are plotted against Wo with the salt type as a parameter in Fig.4. HF increases with decreasing in Wo, i.e. increasing in salt concentration for NaCl and Na2SO4, while it does not vary widely for LiCl. This quantitative result supports the previous qualitative description on the specific character of the micro-water-pool[8,10]. For the separation of the specific protein, therefore, Wo must be controlled carefully depending on the hydrophobicity and the size of the target protein, since both steric and hydrophobic interactions between the protein and RVM are found to be dominant factors in the partitioning of proteins at their isoelectric point. For example, in order to extract hydrophobic small protein Na2SO4 or NaCl can be added in high concentration, while hydrophilic large protein LiCl may be used in general.

3.4 Affinity extraction and activity yield

In the affinity extraction of lipase, PBA is used as a strong inhibitor (soluble only in water). Comparison of the extracted fraction of lipase with PBA and that without PBA showed that the former is even worth to the latter probably due to the conformational change caused by the strong inhibitor.

In the case of amphiphilic ligand, taurodeoxycholic acid (TDCA), which is mainly solubilized in micellar interface, comparison of the extracted fraction and activity yield of lipase with TDCA and that without TDCA showed that the former was several times larger than the latter in the range of Wo, ca. 10 to 15. It was also found that TDCA form stable mixed micelles with AOT having similar size and no effect to other proteins such as papain and chymotrypsin.

Finally, the clude lipase was separated in the bulk liquid membrane system either with AOT and AOT+TDCA membrane phase. Activity yield after forward and backward extraction was negligibly small for the usual AOT micelles. For the AOT+TDCA mixed micellar membrane, however, both the extracted fraction and activity yield of lipase from the aqueous pahse 1 to 2 was significantly improved(results in detail shown in refernce[6]).

4. CONCLUSION

1) Selective transport of proteins through the reverse micellar liquid membrane from an aqueous phase to another was successfully carried out.
2) Protein - reverse micelle hydrophobic interaction was quantified.
3) Protein extraction model based on size exclusion effect was presented.
4) Improvement of selectivity and activity yield of lipase after forward and backward extraction was achieved using AOT+TDCA affinity liquid membrane.

5. ACKNOWLEDGMENT

This work was partly supported by the JSPS collaboration fund.

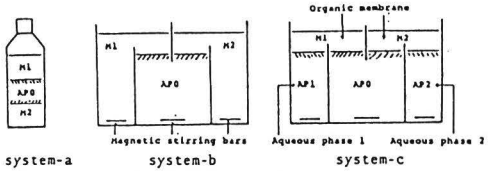

Fig. 1 Combined bulk liquid membrane apparatus

Table 1

Protein	M.W.	pI	HFS[kJ/mol]
α-Chymotrypsin	25000	9.7	-85.0
Ribonuclease-a	13700	7.8	-62.1
Lysozyme	14300	11.1	-39.3
Papain	23400	8.8	43.7
C.V.Lipase	30000	7.3	105

Table 2 Separation of three proteins in the system-c after 750 min contact

	Feed conditions				% Extracted		
Phase	Vol [ml]	KCl [M]	pH	Wo	Lys	Cyt	Lip
AP0 *1	16	0.1	9.0	–	32.1	57.7	62.3
M 1 *2	3.5	–	–	9.8	7.5	2.8	0
AP1	10	0.7	11.3	–	56.3	1.8	0
M 2 *3	3.5	–	–	5.2	0	0	9.3
AP2	10	2.0	5.0	–	0	0	21.4
DP *4	–	–	–	–	4.1	38.7	7.0

*1 Feed conc. of each protein: 50μM
*2 AOT 50mM // isooctane
*3 CTAB 200mM // n-hexanol/chloroform 4:1(v/v)
*4 denatured protein

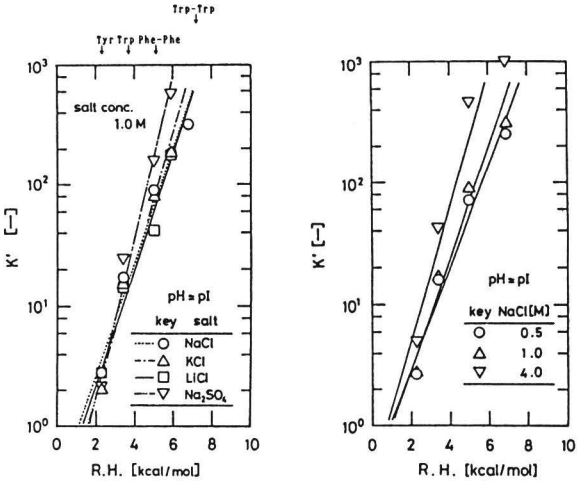

Fig.3 Effect of Relative Hydrophobicity of amino acids and peptides on their partition coefficient, as a parameter of NaCl conc. (right) and as a parameter of salt type (left).

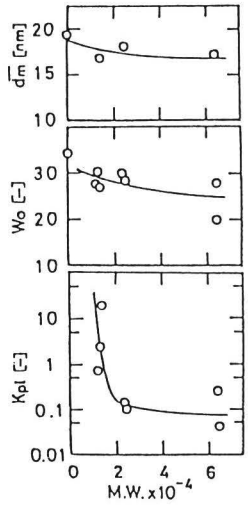

Fig 2 Effect of M.W. on dm, Wo and KpI.

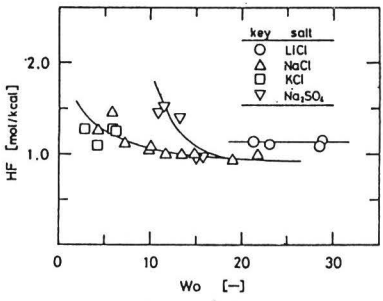

Fig.4 Correlation of Hydrophobic Factor with water content Wo.

6. REFERENCES

1) Hatton,T.A., 1987, ACS Symp.Ser.,342,170
2) Kuboi,R., Y.Mori and I.Komasawa, 1989, Kagaku Kogaku Ronbunshu,15,669
3) Kuboi,R., K.Hashimoto and I.Komasawa, 1990, ibid.,16, 335
4) Kuboi,R., H.Tanaka and I.Komasawa, 1990, ibid.,16, 755 & 1053
5) Kuboi,R., Y.Mori and I.Komasawa, 1990, ibid.,16, 763 & 1060
6) Kuboi,R., Y.Yamada, Y.Mori and I.Komasawa, ibid., in press
7) Kuboi,R., Y.Yamada, I.Komasawa and J.Chaudhuri, submitted
8) Leodidis,E.B. and T.A.Hatton, 1989, "Structure and Reactivity in Reverse Micelles", ed.M.P.Pileni, Elsevier, p.270
9) Leser,M.E. and P.L.Luisi, 1990, Chimia,44, 270
10)Luisi,P.L., 1985, Angew. Chem.,24, 439

Solvent Extraction 1990, T. Sekine (Editor)

© 1992 Elsevier Science Publishers B.V. All rights reserved

PHASE INVERSION BEHAVIOUR OF AQUEOUS TWO-PHASE SYSTEMS

I.P.T.MOORE, A.GILCHRIST, J.HAWTIN, A.W.NIENOW
R.KUBOI* AND I.KOMASAWA*
School of Chem. Eng., University of Birmingham,
Edgbaston, Birmingham B15 2TT, UK.
*Dept. of Chem. Eng., Osaka University,
Toyonaka, Osaka 560, JAPAN.

ABSTRACT
The phase inversion behavior was investigated using a conductivity probe and a video camera for the system of polyethylene glycol(PEG), molecular weight 10k(10,000)/potassium phosphate(PK) in a stirred vessel. The settling times were longer for systems which had the PEG phase as the continuous one. For a given liquid pair there was a wide range of relative volumes in which either liquid phase could be stably continuous (ambivalent region). The PEG phase, which is the more viscous, was more stable when dispersed in the salt phase than vice versa. This hysterisis effect is similar to that observed in aqueous/organic systems. There was a gradual widening of the ambivalent region with increasing solute concentrations and this effct was marked when the PEG phase was inverting to become the dispersed phase in a continuous salt phase system.

1. INTRODUCTION

Aqueous two-phase systems, which are formed by mixing two polymers or a polymer and a salt which show "incompatibility" in a solvent, have a high proportion of water(65-90wt%), very small density difference and interfacial tension (0.1-0.01dyne/cm) making a favourable environment for labile enzymes, biologically active proteins, cells and cell organelles(Kula,1982). These phase systems are capable of suspending cells and cell debris and further partitioning the desired products into one phase and cell debris or other substances into opposite phases. In these systems mixing is quite rapid and usually phase separation (settling) is a rate controlling step because of high viscosity.

It has been suggested from previous works with aqueous/organic systems that phase inversion, at which the dispersed phase inverts to become the continuous phase, can occur in a wide range of phase volume ratio and affects significantly settling time, phase separation and extraction efficiency (Gaggero,1988, Selker,1965). It is pronounced especially for the system with large or small phase viscosity ratio (which corresponds to the system for PEG/salt or PEG/dextran), since settling time can vary significantly dependent on which phase is continuous. It is, therefore, critical to ensure that the correct phase remains dispersed / continuous during operation.

The effects of stirring speed and phase composition on the phase inversion behavior of aqueous two-phase systems, PEG (polyethylene glycol) / PK (dipotassiumhydrogen phosphate), were investigated in this work using a conductivity probe and a video camera in a stirred vessel. The same equipment was previously used to study aqueous/organic systems (Gilchrist, 1989).

2. EXPERIMENTAL

The required amount of the PEG (or salt) phase, prepared from the mixture of 12wt% PEG, 12wt% PK and water (12/12wt%), was placed in a 600ml glass vessel equipped with a conductivity probe and a lamp for a video camera and set in the constant temperature (298K) water bath (Fig.1). The corresponding, opposite salt (or PEG) phase was continuously and slowly dripped in the centre of the vessel, directly above the agitator which had two blades with a diameter of 3cm and was positioned just above the bottom. Throughout the experiment the conductivity reading was recorded using chart recorder and the torque and the video were also recorded if necessary. The addition of the "opposite" phase was stopped when inversion occured showing step change in the conductivity (Fig.2). Then the stirrer was stopped to measure the settling time using the conductivity chart recording (Fig.3).

A series of experiment was carried out varying impeller speed, 300 to 700rpm, and phase composition, 10/10wt% to 15/15wt%.

Additional experiments were also made to quantify the mixing time (measuring the variation of conductivity with time after addition of a lump of "opposite" phase).

Fig.1 Experimental apparatus

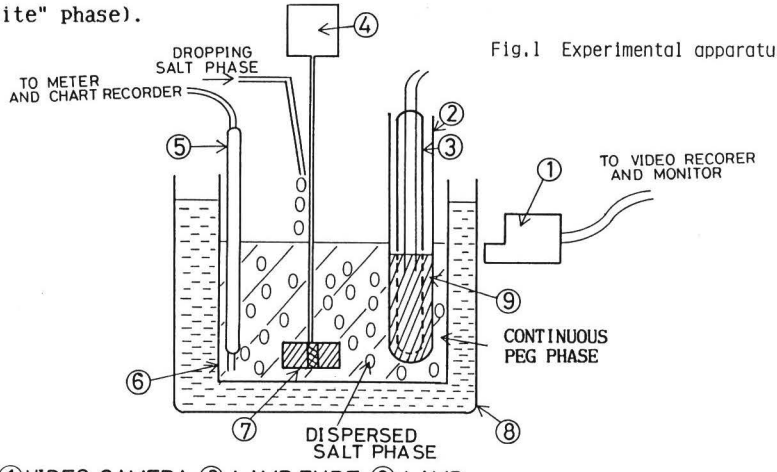

①VIDEO CAMERA ② LAMP TUBE ③ LAMP
④STIRER DRIVE MOTER WITH TORQUE & SPEED METER ⑤ CONDUCTIVITY PROBES
⑥600ml GLASS VESSEL⑦ 3cm diameter, 2 bladed STIRRER
⑧CONSTANT TEMPERATURE WATER BATH⑨ LIGHT DIFFUSER

The effect of the presence of particles was also investigated by addition of 10g of 3mm diameter plastic beads to the phase system. Phase diagram (the binodal and the tie lines) is measured by the "cloud point" and conductivity reading and shown in Fig.4 and Table 1.

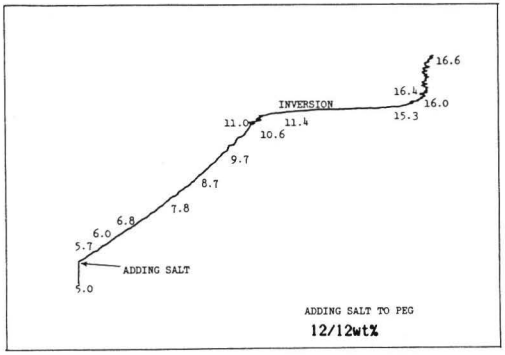

Fig.2 An example of the conductivity chart recording showing the step increase at phase inversion where the salt phase is added to the PEG phase at a stirrer speed of 405 rpm.

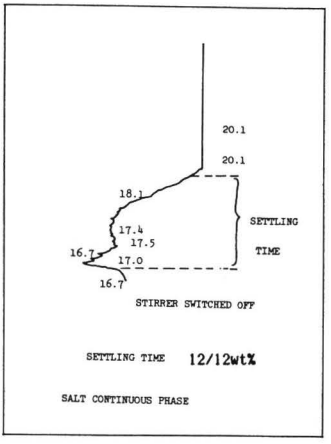

Fig.3 An example of the chart recording after stirrer switched off for the settling time measurement following the experiment shown in Fig.2

Table 1 The physical properties of the phase systems (PEG10K/PK,at25℃)

Physical property	10/10 wt% mixture		12/12 wt% mixture		15/15 wt% mixture	
	salt phase	PEG phase	salt phase	PEG phase	salt phase	PEG phase
Conductivity [ms/cm]	83.0	7.7	99.2	3.9	121.8	1.7
Refractive Index	1.3545	1.377	1.36	1.386	1.369	1.3975
Density [kg/m³]	1120	1080	1160	1090	1200	1090
Viscosity [cP]	4.0	67.5	5.0	118	4.6	285
Mass of each phase after separation [g]	625	368	645	349	646	350
wt ratio (salt/PEG phase)	1.7		1.85		1.85	

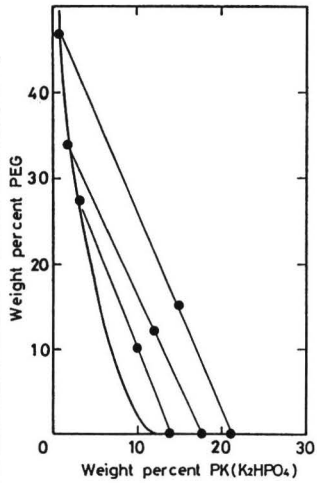

Fig.4 Phase diagram for the used PEG/salt system (PEG 10k / PK)

3. RESULTS AND DISCUSSION

3.1 Mixing time and settling time

The mixing time was measured for a stirrer speed of 500rpm, for the addition of the salt phase to the PEG phase of the 12/12wt% mixture. It was sufficiently small in the range of 3-9sec as expected. The power consumption of the stirrer motor was unaffected by phase inversion.

The results of settling times for the system with the PEG phase as the continuous one were more than 10 times longer than for the corresponding salt phase continuous systems (several mins), as shown in Table 2, because of larger resistance to both movement and coalescence of dispersed droplets. The settling time increases with increasing concentration of phase component and stirring speed prior to settling.

3.2 Visual observation

The image of dispersed droplets, recorded at a magnification of 50, showed that prior to the phase inversion the droplets were very uniform regularly shaped spheres of about 2mm of diameter. As the inversion occurred, the droplets were much more irregular in both shapes and size ranged, randomly over about 0.5 to 5mm.

3.3 Effect of stirrer speed on ambivalent region

On comparing the results for the PEG/PK systems with those for aqueous/organic systems (McClarey,1976), it can be seen that the ambivalent region becomes narrower for higher stirrer speeds in both systems as shown in Fig.5, but, the size of the region for the PEG/PK systems is larger than that for the latter one (i.e. about 30wt% as opposed to about 20wt% respectively), and also that unlike the latter one, whose ambivalent region was centered around the 50vol% line, that for the PEG/PK system was completely above the 50wt% line(where the volume fraction is approximately the same as the weight fraction).

Table 2 The effect of phase composition on phase inversion at a constant stirrer speed of 600 rpm and 25℃

Phase composition (PEG/PK)	10/10 wt%		12/12 wt%		15/15 wt%	
	(A)*	(B)**	(A)	(B)	(A)	(B)
wt fraction of PEG phase at inversion	0.750	0.820	0.650	0.860	0.544	0.863
settling time [min]	<2.5	70	2.5	>30	3.4	>>30

* (A) Addition of salt phase to PEG phase (settling time in salt cont. phase)

**(B) Addition of PEG phase to salt phase (settling time in PEG cont. phase)

The shape of the ambivalent region (shown by the decrease in the PEG weight fraction at the point of inversion) suggests that with increasing stirrer speed, the phase inversion from a continuous salt phase to continuous PEG phase becomes easier, whereas the inversion from continuous PEG phase is nearly unaffected.

3.4 Effect of viscosity ratio on ambivalent region

The ambivalent region for various hydrocarbon / sodium chloride solution phase systems, measured in the wide range of viscosity ratio (ν upper phase / ν lower phase), was shown in Fig.6. Based on this result, the estimated minimum volume fraction for the PEG phase is 0.42 and the maximum is 0.82 for the viscosity ratio of 23.0 ($=\nu_{PEG}/\nu_{salt}$, cf. $\nu_{PEG}/\nu_{dextran}\sim 0.01$), whereas the observed volume fractions at 600rpm are 0.65 and 0.86, respectively. Considering the interfacial tensions of the two types of system are very different, there is remarkably good agreement for the maximum value of the dispersed phase which can be achieved.

3.5 Effect of concentration and particles on ambivalent region

The results shown in Table 2 suggest that with increasing phase component concentration, the subsequent phase inversion becomes progressively more difficult and that this effect is more pronounced for the inversion from continuous PEG phase to continuous salt phase, than for the opposite inversion.

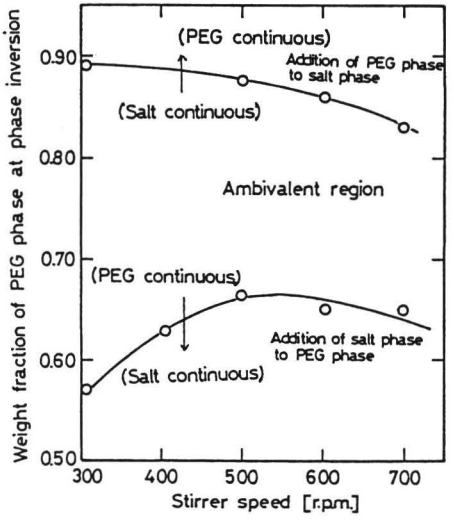

Fig.5 Variation of ambivalent region with stirrer speed (12/12wt%)

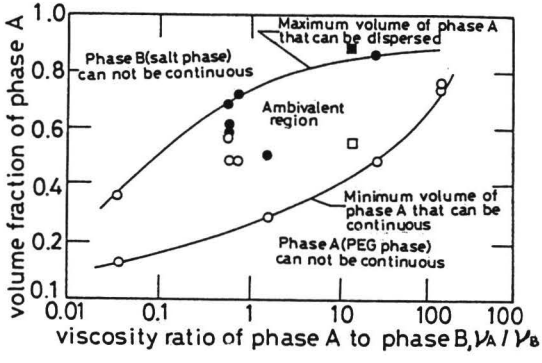

Fig.6 Comparison of ambivalent region for aqueous two phase systems with those for various organic-aqueous two phase systems.

In contrast, the effect of including particles in the phase system did not affect the phase inversion behaviour. However, the particles used were significantly larger than the average droplet size and these results may not apply to smaller particles, which could attach themselves to the droplet interface and thus influence the inversion.

4. CONCLUSION

The effects of stirring speed and phase composition on the phase inversion were investigated mainly using a conductivity probe.

1) For a given liquid pair there was a wide range of relative volumes in which either liquid phase could be stably continuous.

2) The PEG phase (the more viscous) was more stable when dispersed in the salt phase than vice versa. This hysterisis effect is similar to that observed in aqueous/organic systems.

3) Based on the mass fraction of the PEG phase at inversion, the ambivalent region, lay completely above the 50 wt% line and was about 30 wt% wide at 300rpm. The ambivalent region narrowed with increasing stirrer speed.

4) At stirrer speed 600rpm there was a gradual widening of the ambivalent region with increasing solute concentrations. This effect was more marked when the PEG phase was inverting to become the dispersed phase in a continuous salt system.

5) The presence of the plastic beads had no observable effect on the phase inversion behavior.

6) In all experiments the settling times were longer for systems which had the PEG phase as continuous one. Increasing the stirrer speed prior to settling, increased the settling time.

7) A video was used to study the droplet shapes and sizes for a PEG to salt continuous phase inversion. It showed that prior to inversion the dispersed droplets were fairly uniform, gradually increasing in size as inversion approached. After inversion the droplets were irregular in both shape and size.

5. REFERENCES

1) Gaggero, M. etal., 6th Eur.Conf.on Mixing, BHRA(1988)

2) Gilchrist, A. etal., Chem.Eng.Sci., 44, 415(1989)

3) Kula, M-R., Adv.in Biochem.Eng., 24, 73(1982)

4) McClarey, M.J. etal., AIChE Symp., 173(74), 134(1976)

5) Selker, A.H. etal., Can.J.Chem.Eng., 43, 298(1965)

Solvent Extraction 1990, T. Sekine (Editor)

© 1992 Elsevier Science Publishers B.V. All rights reserved

PROTEIN TRANSPORT BETWEEN AQUEOUS PHASE AND MICELLAR ORGANIC PHASE USING SELF-ASSEMBLED AMPHIPHILES

SOSAKU ICHIKAWA, MASANAO IMAI,
SHOJI URUSHIYAMA and MASARU SHIMIZU
Department of Chemical Engineering,
Tokyo University of Agriculture & Technology.
24-16 2-Chome Nakamachi, Koganei, Tokyo 184, JAPAN.

ABSTRACT
Ichikawa, S., Imai, M., Urushiyama, S. and Shimizu, M., 1990. Protein transport between aqueous phase and micellar organic phase using self-assembled amphiphiles. Proc. ISEC'90

Protein transport between an aqueous phase and a micellar organic phase using a self-assembled amphiphile was studied. The minimal amount of amphiphilic molecule AOT required for almost 100% transfer of the protein cytochrome-c was determined. It was found to increase with increasing initial protein concentration and ionic strength in the aqueous phase. The amount of water in the micellar organic phase containing protein was greater than in the protein-free system. The existence of water molecules accompanying protein was recognized.

1 INTRODUCTION

In recent years, highly selective, simple and economically feasible separation methods for biomaterials, are becoming more important in commercial processes. Reversed micelles, which are the self-assemblage of amphiphiles in organic solvent, provide a novel means of biomaterial extraction (Luisi et al., 1979; Göklen and Hatton, 1985; Dekker et al., 1986).

In reversed micellar extraction, the protein is transferred between the aqueous phase and micellar organic phase with the aid of amphiphilic molecules. The amphiphilic molecule is an indispensable component in this operation. However, in excess this component will result in impurity of the final product. It is necessary to add an appropriate amount of amphiphilic molecule to the organic phase.

Water transport occurs when the aqueous and micellar organic phases contact. The micro aqueous phase formed in the reversed micelle provides a hydrophilic surrounding for a protein, thus maintaining of protein's activity in the reversed micellar

organic phase. It is important to consider the transferred water in relation to transferred protein for the reversed micellar system.

The purpose of this study is to determine the minimal amount of amphiphilic molecule required for the protein transport into the reversed micellar organic phase, and to discuss the transferred water in relation to transferred protein.

2 EXPERIMENTAL

2.1 Reagents

Sodium di-2-ethylhexyl sulfosuccinate ($C_{20}H_{37}O_7Na$), AOT, was purchased from NAKARAI TESQUE INC. and used without further purification. 2, 2, 4-trimethylpentane (isooctane) purchased from KISHIDA CHEMICAL Co. was used as the organic solvent. Cytochrome-c from horse heart (commercially denoted as typeⅢ), obtained from SIGMA CHEMICAL Co., was used as a transfer protein. Distilled water was used for the preparation of the aqueous phase.

2.2 Methods

The reversed micellar organic phase was prepared by dissolving AOT in isooctane. The aqueous phase was made by adding cytochrome-c into the aqueous phase, which was adjusted to desired ionic strength with KCl beforehand. The pH was adjusted by 0.1N HCl or 0.1N NaOH accordingly.

The protein transfer between the aqueous phase and micellar organic phase was performed by mixing two phase of equal volume with a magnetic stirrer for 15 minutes. To settle the emulsion, the mixture was centrifuged for 15 minutes at 2500 revolutions per minute. The concentration of protein was measured with a spectrophotometer (HITACHI U-2000). The amount of water transferred into the reversed micellar organic phase was measured by Karl-Fischer method.

3 EXPERIMENTAL RESULTS AND DISCUSSION

3.1 Change in the minimal AOT concentration with initial protein concentration

Figure 1 shows the change in the amount of protein transferred with AOT concentration for various initial aqueous phase protein concentrations. The amount of transferred protein is defined by Eq. (1)

$$E \equiv (C_{PO} V_O / C_{Pw,i} V_w) \times 100 \quad (1)$$

where C_{PO} and $C_{Pw,i}$ are the protein concentration of the reversed micellar organic phase and the initial aqueous phase, respectively. The amount of protein transferred increased with increasing AOT concentration. Almost 100% protein transfer occurred for the range of experimental conditions selected. The AOT concentration, at which almost 100% protein transfer occurred, increased with increasing initial aqueous phase protein concentration. It was found that a minimal AOT concentration exists for almost total protein transfer and that it increased with initial protein concentration in the aqueous phase. When the AOT concentration is insufficient, a denaturated protein looking like a gel complex type substance was observed after mixing both phases.

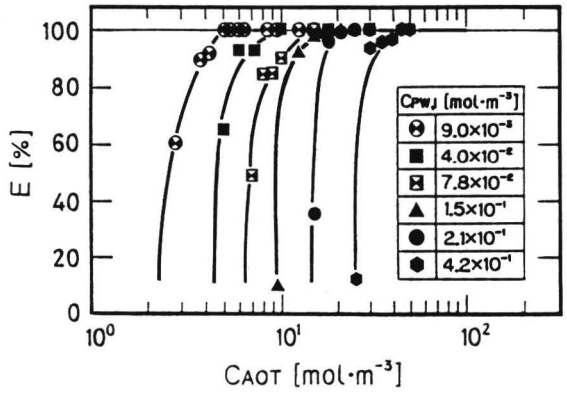

Fig. 1. Change in the amount of protein transferred with AOT concentrations. C_{KCl}=100mol·m^{-3}, pH=7.1～8.8

The amount of water transferred at the minimal AOT concentration obtained from Figure 1 was plotted in Figure 2. For the comparison, the amount of transferred water in the protein-free system was also presented (Imai et al., in preparation). The amount of water in the protein containing system was greater than in the protein-free system. From this result, it is consider that the transferred protein was accompanied by water molecules into the reversed micelle. This

accompanying water preserves the protein's activity in the reversed micelle. The number of water molecules accompanying one transferred protein molecule was calculated to be ca. 2200 from the difference in the amount of water transferred for the protein-free and protein containing systems.

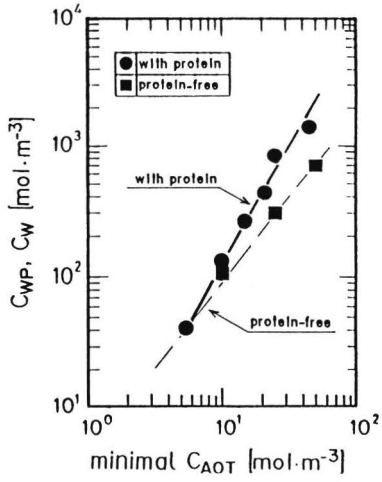

Fig. 2. Transferred water into the reversed micellar organic phase.

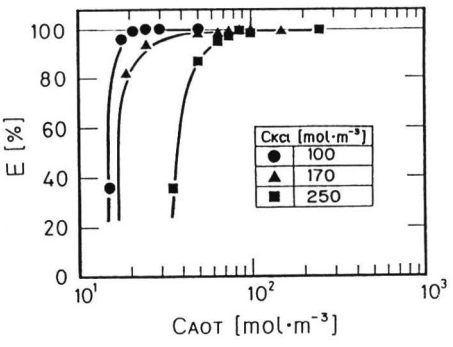

Fig. 3. Change in the amount of protein transferred (%) with AOT concentration.
$C_{Pw,i}$=2.1×10^{-1}mol·m^{-3}, pH=7.4～8.6

3.2 Change in the minimal AOT concentration with ionic strength

Figure 3 shows the change in the amount of protein transferred with AOT concentration for three ionic strengths. The initial protein concentration was 2.1×10^{-1}mol·m^{-3} in each case. The AOT concentration, at which almost 100% protein transfer occurred increased with ionic strength. The minimal AOT concentration required for almost 100% protein transfer increased with increasing ionic strength of aqueous phase.

Figure 4 shows the change in the amount of accompanying water with ionic strength. This amount decreased with increasing ionic strength. The ionic strength affects the hydrophilic surroundings of proteins transferred into the reversed micelles.

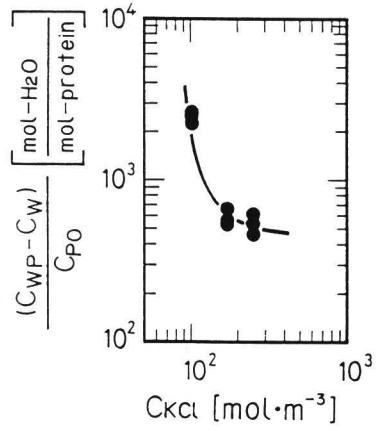

Fig. 4. Change in the number of water molecules accompanying protein.

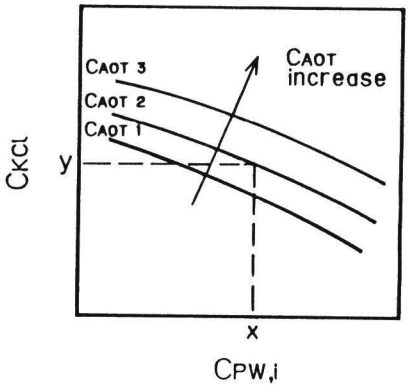

Fig. 5. Schematic diagram to estimate the minimal AOT concentration required for protein extraction.

3.3 Schematic diagram to estimate the minimal AOT concentration

From the results in Figures 1 and 3, the minimal amount of AOT required increased with an increase in initial protein concentration and ionic strength. We propose a schematic diagram to conveniently estimate the essential AOT concentration in Figure 5. For example, in the case of $C_{PW,i}$ = x and C_{KCl} = y, the minimal AOT concentration can be estimated as C_{AOT2} using this diagram.

4 CONCLUSION

The protein transport between an aqueous phase and a micellar organic phase was investigated using a self-assembled amphiphile, AOT. The minimal amount of AOT required for almost 100% protein transfer was determined. It was found to increase with increasing initial protein concentration and ionic strength in the aqueous phase. A schematic diagram was proposed to estimate the essential AOT concentration. The amount of water in the protein containing system was greater than in the protein-free system. The existence of water molecules accompanying the transferred protein was recognized.

ACKNOWLEDGMENT

The authors would like to appreciate the financial support from SANEYOSHI SCHOLARSHIP FOUNDATION.

5 NOTATION

C_{AOT}	$(mol \cdot m^{-3})$	concentration of AOT in the reversed micellar organic phase
C_{KCl}	$(mol \cdot m^{-3})$	concentration of potassium chloride in the aqueous phase
C_{PO}	$(mol \cdot m^{-3})$	concentration of protein in the reversed micellar organic phase
$C_{PW,i}$	$(mol \cdot m^{-3})$	concentration of protein in the initial aqueous phase
C_W	$(mol \cdot m^{-3})$	concentration of water in the reversed micellar micellar organic phase
C_{WP}	$(mol \cdot m^{-3})$	concentration of water in the reversed micellar organic phase containing protein
E	(%)	transferred protein percentage defined by Eq. (1)
V_O	(m^3)	volume of the reversed micellar organic phase
V_W	(m^3)	volume of the aqueous phase

6 REFERENCES

Imai, M., Kamiwatari, F. and Shimizu, M.: in preparation.

Dekker, M., Riet, K.V. and Weijers, S.R., 1986. Enzyme recovery by liquid-liquid extraction using reversed micelles. Chem. Eng. J., 33: B27-B33.

Göklen, K.E. and Hatton, T.A., 1985. Protein extraction using reversed micelles. Biotechnol. Prog., 1: 69-74.

Luisi, P.L., Bonner, F.J., Pellegrini, A., Wiget, P. and Wolf, R., 1979. Micellar solubilization of proteins in aprotic solvents and their spectroscopic characterization. Helv. Chim. Acta, 62: 740-753.

Solvent Extraction 1990, T. Sekine (Editor)

© 1992 Elsevier Science Publishers B.V. All rights reserved

SEPARATION AND ENRICHMENT OF AMINO ACIDS WITH LIQUID SURFACTANT MEMBRANE

T. HANO, T. OHTAKE, M. MATSUMOTO, D. KITAYAMA, F. HORI AND F. NAKASHIO*
Department of Environmental Chemistry and Engineering, Oita University, Oita, 870-11(Japan)
*Department of Organic Synthesis, Kyushu University, Fukuoka, 812(Japan)

ABSTRACT

The separation and enrichment of amino acids were carried out with liquid surfactant membrane(LSM) containing tri-n-octylmethylammonium chloride(TOMAC) as a mobile carrier and polyamine as an emulsifier. To clarify the extraction mechanism, the extraction equilibrium and kinetics were investigated. The extraction equilibrium constants(K_A) for various amino acids differed considerably, and could be correlated well with hydrophobicity scale of each amino acid. The permeation kinetics of amino acids through LSM was studied in a stirred transfer-cell. Mass transfer coefficients were determined based on the double-film model with an instantaneous reaction. The initial permeation rate was controlled by the mass transfer processes across the interface between the aqueous and emulsion phases.

INTRODUCTION

The liquid membrane processes which were proposed as an innovative separation technique have been applied to a variety of fields like hydrometallurgy and wastewater treatment. Recently, the application to the downstream processing of various bioproducts (amino acids(Haensel et al., 1986; Hano et al., 1990 and to be published; Teramoto et al., 1989; Thien et al., 1986, 1988; Itoh et al., 1990), organic acids(Hano et al., 1990 and to be published), antibiotics(Hano et al., 1990)) has become of interest owing to the advantages of simultaneous separation and enrichment together with the unnecessity of pretreatment. This paper discussed the recovery of amino acids with extraction.

The amino acids, which are one of the typical bioproducts, are separated and concentrated at present by ion exchange and crystallization. However, the drop of resin adsorption power results in the reduction of purification efficiency. The separation of amino acids by liquid membrane was reported initially by Behr et al.(1973), by employing an extractant since amino acids are hardly soluble in organic solvents. Two types of extractants have been employed so far. One is used at low pH range to extract amino acids cations and the other is at high pH range to extract anions. The phosphoric acid esters and quaternary ammonium salts are the typical extractants to exchange with cations and anions, respectively. In this study, tri-n-octylmethylammonium salt(abbrevated as TOMAC)(Haensel et al., 1986; Hano et al., 1990 and to be

published; Thien et al., 1986, 1988) was employed in the carrier-mediated transportation of amino acids. Since the liquid surfactant membrane (LSM) processes are composed of extraction, it is necessary to investigate the extraction equilibria and kinetics to establish the optimum recovery system. However, the extraction behavior of amino acids has not been investigated in detail. In the present study, in order to evaluate the rate-controlling step in the LSM operation, extraction equilibria of amino acids and kinetics were studied.

1. EXPERIMENTAL

1.1 Extraction equilibria

The extracion equilibrium at 298K was measured by mixing $25cm^3$ of the aqueous amino acid solution and $25cm^3$ of the kerosene solution which dissolved Capriquat^R (TOMAC), Doujindo lab.) as an extractant. The aqueous amino acids solutions were adjusted to pH11 to 12 by KOH in order to shift amino acids into anion type. The concentration of amino acids in the aqueous solution was determined by the HPLC (Japan Spectroscopic Co.) equipped with a fluorescence detector using OPA-post-labeling method. The concentration of Cl^- was measured by an ionmeter and H^+ by a pH meter. The hydrophobicity scales of isoleucine (Ile) and arginine (Arg) were determined by measuring the solubilities of these amino acids in ethanol at 298K according to the method of Nozaki and Tanford(1971).

1.2 Permeation through LSM

The W/O emulsions for the LSM processes were prepared by mixing $80cm^3$ of the oil phase and $40cm^3$ of the aqueous phase in a homogenizer at 167 s^{-1} for 10min. The oil phase was composed of 5% ECA4360J (Exxon Chemical Co.) as a nonionic surfactant, Capriquat® as an mobile carrier and kerosene as a solvent, respectively. The internal water phase was aqueous $1mol \cdot dm^{-3}$ NaCl solution. The LSM operation was performed by contacting $90cm^3$ of the W/O emulsion with $200cm^3$ of the amino acid solution in a stirred transfer-cell, and agitating both phases gently at $0.33s^{-1}$ in order to hold a free flat interface. This operation was carried out to make easy the kinetic analysis, since the extraction in an emulsion-dispersed system proceeded very quickly and accurate data of concentration change was difficult to get. Urea was added to the amino acids solution to suppress the swelling of the emulsion due to osmosis. At a prescribed time after starting the agitation, samples were withdrawm from the amino acid solution and the concentration of amino acid in the external aqueous solution was measured by HPLC.

2. RESULTS AND DISCUSSION

2.1 Extraction equilibria

Since amino acids are amphoteric, the acids turn to anions at high pH range. In discussing the extraction equilibrium, TOMAC(noted as QCl) was assumed to undergo equimolar reaction with amino acid anion and OH^- as follows(Haensel et al. 1986).

$$A^- + QCl \rightleftarrows QA + Cl^- \quad (1)$$

$$K_A = [QA][Cl^-]/[A^-][QCl] \quad (2)$$

$$OH^- + QCl \rightleftarrows QOH + Cl^- \quad (3)$$

$$K_{OH} = [QOH][Cl^-]/[OH^-][QCl] \quad (4)$$

Figure 1 shows the example of the equilibrium plots for Trp, Phe, Leu, Val and Gly (these abbrevations are explained in Table 1). Each amino acid anion was found to form the salt with TOMAC by the ratio of 1:1 because the experimental data gave a slope of nearly equal to one. OH^- was also found to form the salt with TOMAC by the ratio of 1:1, though the amount of extracted OH^- was considerably smaller than that of amino acids.

Table 1 lists the extraction equi-

Table 1 Equilibrium constants of extraction and isoelectric points for various amino acids

Amino Acids	pI	K_A
Glycine (Gly)	5.97	0.036
Alanine (Ala)	6.00	0.038
Valine (Val)	5.96	0.089
Leucine (Leu)	5.98	0.29
Isoleucine (Ile)	6.02	0.24
Methionine (Met)	5.74	0.21
Phenylalanine (Phe)	5.48	0.97
Tryptophan (Trp)	5.89	8.89
Histidine (His)	7.59	0.083
Arginine (Arg)	10.76	0.062
Serine (Ser)	5.68	0.049
Threonine(Thr)	6.16	0.071

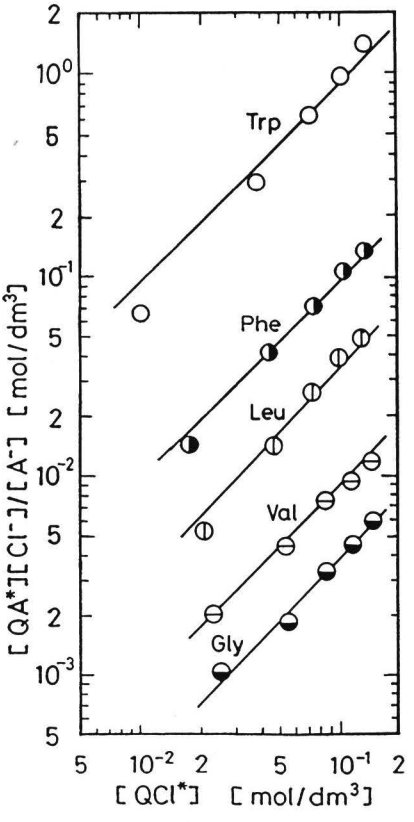

Fig. 1 Extraction equilibria of Trp, Phe, Leu, Val and Gly

librium constants, K_A, and isoelectric points, pI, of amino acids. There existed a considerable difference in K_A values. For instance, K_A of Trp was about 260 times that of Gly. These findings suggest the possibility of selective separation by the reactive extraction with TOMAC.

Thien et al.(1988) pointed out that the difference of extraction behavior was strongly related with the hydrophobicity of amino acids. The hydrophobicity scales of amino acids proposed by Nozaki and Tanford(1971) are defined as the free energy change when each amino acid transferred from water to ethanol phases. The scales are expressed as a relative value by assigning glycine as reference substance. On the other hand, the equilibrium constant K_A is related to the free energy change of extraction ($-\Delta G$) by the following equation.

$$-\Delta G = RT\ln K_A \tag{5}$$

where R and T are gas constant and temperature, respectively. Therefore, the relative difference (ΔG) of ($-\Delta G$) for each amino acid was calculated as follows by assigning glycine as a reference substance.

$$\Delta g = (-\Delta G) - (-\Delta G_{Gly}) = RT\ln(K_A/K_{A,Gly}) \tag{6}$$

Figure 2 is plots of Δg values against the hydrophobicity scales proposed by Nozaki and Tanford(1971). A good correlation could be obtained between free energy changes and hydrophobicity scales, which implied that the reactive extraction of amino acids was controlled significantly by their hydrophobicities.

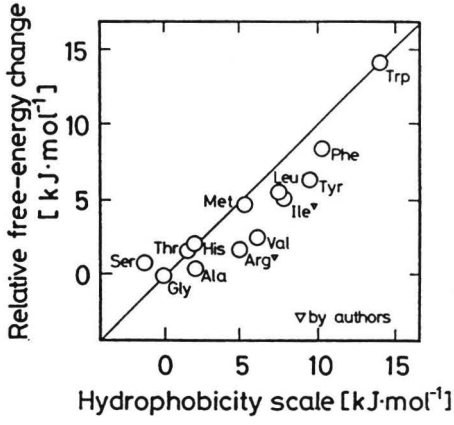

Fig. 2 Comparison of free-energy changes in the amino acid extraction with TOMAC and hydrophobicity scales

2.2 Permeation through LSM

Figure 3 is a time-course of amino acids extraction in a transfer-cell by using TOMAC as a mobile carrier. The order of initial extraction rate coincided with that of K-value. Figure 4 illustrates the effects of amino acid concentration on the extraction flux measured in a transfer-cell. The dependence on the concentration changed from the first order to zero with the increase of the concentration. The flux increased

at high agitation speeds, therefore the mass transfer across the interface clearly affected the permeation rates. These extraction behavior was analyzed according to the double-film model as Haensel et al.(1986) treated. In addition, it is assumed that the reaction at the interface proceeds instantaneously and mass transfer across the films controls the overall extraction process. Table 2 listed the mass transfer coefficients calculated by the Marquardt method. The solid lines in Figs. 3 and 4 were calculated by using these mass transfer coefficients. There was a satisfactory agreement between experimental and calculated results.

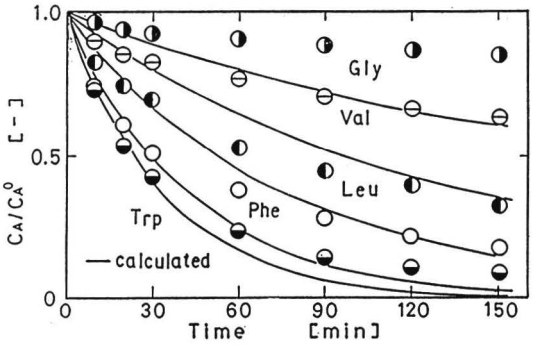

Fig. 3 Time-course of amino acids extraction in a transfer-cell

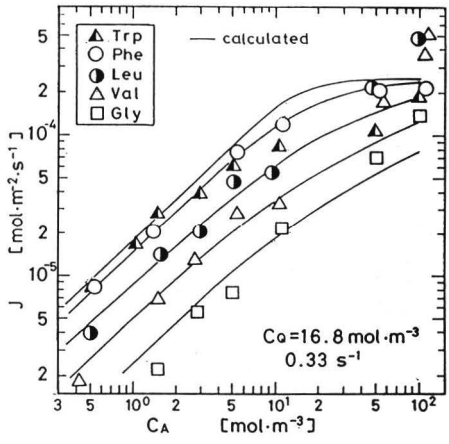

Fig. 4 Extraction flux for various amino acids

CONCLUSION

The recovery of amino acids with the LSM processes by using two kinds of mobile carrier was studied, and the following results were obtained.

1) TOMAC reacted with amino acid anions by the ratio of 1:1. There existed a considerable difference in the extraction equilibrium constants of amino acids investigated. The extraction equilibrium constants could be correlated well with the hydrophobicity scale of each amino acid.

2) The permeation of amino acids through the LSM was carried out in a transfer-cell and analyzed based on

Table 2 Transfer coefficients for various amino acids

Amino Acids	K_A	$10^5 k$ Amino acid	Amino acid-Carrier salt
Trp	8.9	1.78	1.00
Phe	0.97	1.58	1.72
Leu	0.29	0.89	0.92
Val	0.089	0.53	0.75
Gly	0.036	0.26	0.60
Carrier		1.50	
Chloride ion		3.50	

the double-film model. The order of the permeation rates coincided with that of the extraction equilibrium constants.

ACKNOWLEDGMENT

We thank Exxon Chemical Co. Ltd. for providing ECA4360J.

NOMENCLATURE

C	= concentration	$[mol \cdot dm^{-3}]$
J	= flux across the interface	$[mol \cdot cm^{-2} \cdot s^{-1}]$
K_A	= extraction equilibrium constant of amino acid anion	[-]
K_{OH}	= extraction equilibrium constant of OH^- anion	[-]
pI	= isoelectric point	[-]
k	= mass transfer coefficient	$[m \cdot s^{-1}]$

REFERENCES

Behr, J. P. and Lehn, J. M., 1973. Transport of amino acids through organic liquid membranes: J. Am. Chem. Soc., 95: 6180-6110.

Haensel, R., Halwachs, W. and Schügerl, K., 1986. Reactive extraction of d,l-phenylalanine with trioctyl-methyl-ammonium chloride(TOMAC) as a carrier-III. Equilibrium and mass transfer investigations: Chem. Eng. Sci., 41: 1811-1815.

Hano, T., Ohtake, T., Matsumoto, M., Kitayama, D., Hori, F. and Nakashio, F., Extraction equilibria of amino acids with quaternary ammonium salt: to be published in J. Chem. Eng. Japan.

Hano, T., Ohtake, T., Matsumoto, M., 1990. Extraction of fermented organic acids and penicillin with liquid membrane: Chem. Eng., 35: 585-590.

Hano, T., Ohtake, T., Mtsumoto, M., Hori, F. and Nakashio, F., 1990. Separation and concentration of fermented products by liquid surfactant membrane processes: Proc. APBioChEC'90, pp. 428-431.

Hano, T., Matsumoto, M., Ohtake, T., Sasaki, K., Hori, F. and Kawano, Y., Extraction of organic acids with tri-n-octylphosphineoxide: to be published in J. Chem. Eng. Japan.

Nozaki, Y. and Tanford, C., 1971. The solubility of amino acids and two glycine peptides in aqueous ethnol and dioxane solutions: J. Biol. Chem., 246: 2211-2217.

Teramoto, M., Nara, H., Matsuyama, H. and Miyake, Y., 1989. Extraction of amino acids with acidic organophosphorus compound: Proc. Symp. Solv. Extr., pp. 23-28.

Thien, M. P., T. Hatton, A. and Wang, D. I. C., 1986. Liquid emulsion membranes and their applications in biochemical separations: Separation, Recovery, and Purification in Biotechnology (ACS Symp. Ser. No.314), pp. 67-77.

Thien, M. P., T. Hatton, A. and D. I. Wang, C., 1988. Separation and concentration of amino acids using liquid emulsion membranes: Biotech. Bioeng., 32: 604-615.

Itoh, H., Thien, M. P., Hatton, T. A. and Wang, D. I. C., 1990. A liquid emulsionmembrane process for the separation of amino acids: Biotech. Bioeng., 35: 853-860.

Solvent Extraction 1990, T. Sekine (Editor)

© 1992 Elsevier Science Publishers B.V. All rights reserved

APPLICATION OF LIQUID MEMBRANE TECHNIQUE TO THE RECOVERY OF FERMENTED ORGANIC ACIDS

T. HANO, M. MATSUMOTO, T. OHTAKE, K. SASAKI, F. HORI and Y. KAWANO*
Department of Environmental Chemistry and Engineering, Oita University, Oita 870-11 (Japan)
*Laboratory of Applied Chemistry, Miyazaki University, Miyazaki 889-21 (Japan)

ABSTRACT

To establish a new recovery process of organic acids from the fermented broth, the liquid surfactant membrane technique was applied to separate some organic acids. Extraction equilibria of lactic acid with various extractants, that is, tri-n-octylphosphineoxide(TOPO), tri-n-butylphosphate, tri-n-octylamine and dioctylamine, were studied. Diluent effect on the extraction equilibrium of lactic acid was discussed. The separation and enrichment of various organic acids which could be produced by fermentation was conducted with liquid surfactant membrane containing TOPO as a mobile carrier and polyamine as an emulsifier.

INTRODUCTION

Liquid membrane techniques have been developed in the area of hydrometallurgy and wastewater treatment, and the substrates treated were limited to various metal ions and some simple organic compounds like phenol.

With the development of biotechnology, liquid membrane techniques have been applied to the downstream processing of the bioproducts(Boey et al. 1987, Nuchnoi et al. 1987, 1989). Most of the fermented organic acids, the representative bioproducts, exhibit the product inhibition. Therefore, the combination of liquid membrane technique with fermenter have the advantage that the acids from the fermented broth can be removed continuously and their concentration are kept to low level in the broth so as to suppress the product inhibition.

In the present paper, to clarify the fundamental mechanism of liquid membrane separation of organic acids, the extraction equilibria of lactic acid with various extractants were measured and discussed concerning the diluent effects on extraction behavior. The application of liquid surfactant membrane(LSM) to the separation and enrichment of some organic acids was examined.

1. EXPERIMENTAL

1.1 Extraction equilibria of lactic acid

Tri-n-octylphospine oxide(TOPO), tri-n-butyl phosphate(TBP), tri-n-octylamine (TOA) and di-n-octylamine(DOA) of GR grade were used as an extractant

(henceforth EXT) without further purification. Organic solution was prepared by dissolving the extractant in hexane, butyl acetate or their mixture. Aqueous solution was prepared by dissolving lactic acid in deionized water without pH adjustment. Aqueous and organic solutions of equal volumes($25cm^3$) were shaken in a flask at constant temperature(308 K) to attain equilibrium. After 24 hours, the aqueous solution was taken and the acid concentration and pH was determined by HPLC and pH meter, respectively.

1.2 Permeation of organic acids through liquid surfactant membrane

In the experiments of LSM, kerosene was selected as a diluent because hexane or butyl acetate used in extraction equilibrium study could not give stable emulsions. The membrane phase ,therefore, was composed of 5 wt% polyamine(ECA 4360J) or Span 80, 15 wt% TOPO and 80 wt% kerosene.

W/O emulsion was prepared by mixing equal volumes($15cm^3$) of the membrane phase and a receiving phase composed of aqueous sodium carbonate solution(0.5 $kmol/m^3$) in a homogenizer. The agitation time and speed were 10 min and 167 s^{-1} , respectively. 30 ml of W/O emulsion was poured into 150 ml of aqueous acid solution agitated at 5 s^{-1}. The temperature was kept 308K during the run. After pouring W/O emulsion, samples were taken from the tank at intervals and left for a while to separate into W/O emulsion and external aqueous phases. The acid concentration in the external aqueous phase was determined by HPLC.

2. RESULTS AND DISCUSSION

2.1 Extraction equilibria

Figure 1 shows the fraction of lactic acid extracted with two extractant when hexane was used as a diluent. Under the same experimental condition, the organic solution containing TOA or DOA did not extract lactic acid, even in the case that they were not diluted.

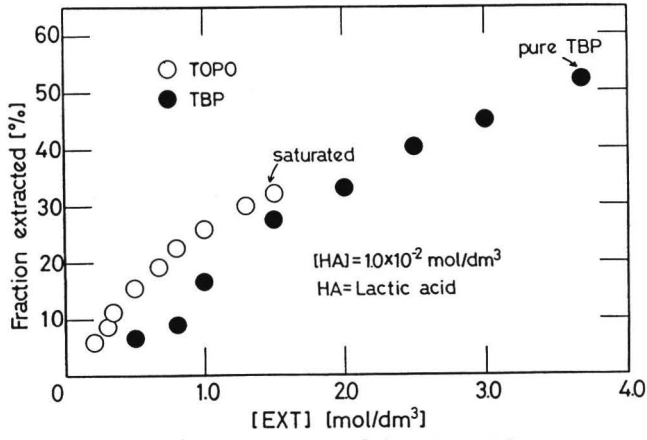

Fig.1 Extraction of lactic acid

2.1.1 Extraction of lactic acid with TOPO

The extraction of acid with TOPO, which gave the highest extraction capacity, was discussed.

In a previous paper(Hano et al. to be published in J. Chem. Eng. Japan), the extraction equilibria of weak carboxylic acids, HnA, by TOPO were represented as follows:

$$HnA + nEXT \rightleftharpoons HnA(EXT)n \quad :K \tag{1}$$

$$K = [HnA(EXT)n]/[HnA][EXT]^n \tag{2}$$

where n is the solvation number of the acid and K is the extraction equilibrium constant. Hano et al. found that the solvation numbers of the acids were the same as the numbers of carboxyl groups in each acid molecule. Rearranging Eq.(2), Eq.(3) is obtained.

$$[HnA(EXT)n]/[EXT]^n = K[HnA] \tag{3}$$

where the concentration of the undissociated acid in the aqueous solution, [HnA], is calculated from pKa value, the total concentration of acid and pH in the aqueous solution. The free extractant concentration at equilibrium, [EXT], is calculated by subtracting the fraction combined with the acid from its initial concentration.

In the previous paper(Hano et al.), the linear relation between the reactive extraction constants and physical distribution constants between diluent and water was found for a series of acids having the same number of carboxyl groups. Based on this finding, the extraction mechanism of the acid was concluded as shown in Fig. 2. This fact implies that the association constant, β, between TOPO and the acid distributed in a diluent was constant when the same diluent was used. The association constant was considered to depend on the polarity of a diluent, therefore, the diluent effect on the extraction of lactic acid with TOPO was examined by varying the mixing ratio of hexane and butylacetate.

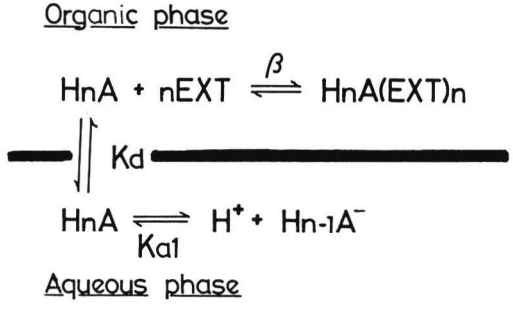

Fig. 2 Extraction mechanism of organic acid

The experimental results were plotted in Fig. 3 according to Eq.(3). Straight lines with a slope of 1 were obtained and it

was confirmed that 1:1 complex was formed in all the diluents used. The K values obtained are listed in Table 1. The K value slightly increases with increasing the fraction of butyl acetate. The increase in polarity of diluent, in general, accelerates the distribution of the acid into a diluent and suppresses the hydrogen bond formation between the acid and TOPO in a diluent. A relatively small difference in K value seems to predict the canceling out of two inverse effects each other.

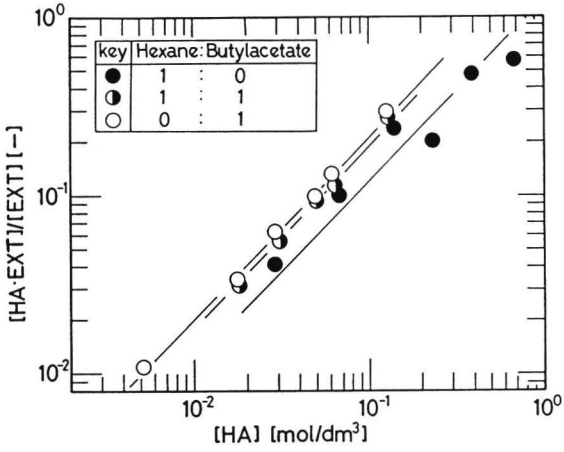

Fig. 3 Diluent effect on lactic acid extraction with TOPO

Table 1 Extraction constant of lactic acid

hexane: butylacetate	TOPO	TOA
1 : 0	1.19	-
2 : 1		143
1 : 1	1.97	673
1 : 2		914
0 : 1	2.13	11900

2.1.2 Extraction of lactic acid with TOA

Since TOA scarcely extracted lactic acid in hexane, the mixture of hexane and butylacetate was used as a diluent and the diluent effect on the extraction of lactic acid with TOA was examined. In treating the experimental data obtained with TOA, the formation of 1:1 complex was assumed. The plots according to Eq.(3) are shown in Fig.4. Lactic acid was extracted with TOA in the diluent containing butylacetate and the experimental results satisfied the above assumption of stoichiometry. The K values obtained are listed in Table 1, too. When TOA was used as an extractant, the extraction equilibrium constants remarkably increased with the fraction of butyl acetate in a diluent. The K value for TOA-butyl acetate system is about 10000 times as greater as that for

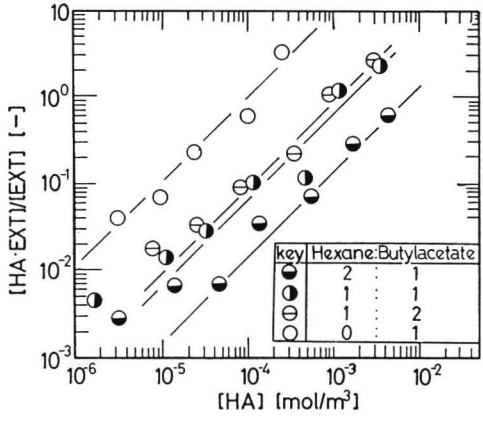

Fig.4 Diluent effect on lactic acid extraction with TOA

TOPO-hexane system. Contrary to the TOPO system, this fact indicates that association between TOA and the acid was more stabilized in a polar diluent. At the present, chemistry of association is unclear, but the association between TOA and the acid is presumed to be more ionic than that for TOPO.

2.2 Extraction of organic acids by liquid surfactant membrane

Figure 5 shows the time-course of the extraction for various carboxylic acids in the case that the emulsions were prepared with Span 80. The extents of extraction for each acid remain under 80% even after 30 min. This is because that the emulsions prepared with Span 80 are unstable at relatively high temperature (308 K). Therefore, polyamine(ECA 4360) was employed as an emulsifier in the following runs.

Figures 6 to 7 show time-courses of the extraction for monocarboxylic and dicarboxylic acids, respectively, along with extraction equilibrium constants with TOPO. The extents of extraction for each acid reached to more than 90% after 30 min. The swelling and breakage of the emulsion which are most serious problems in LSM

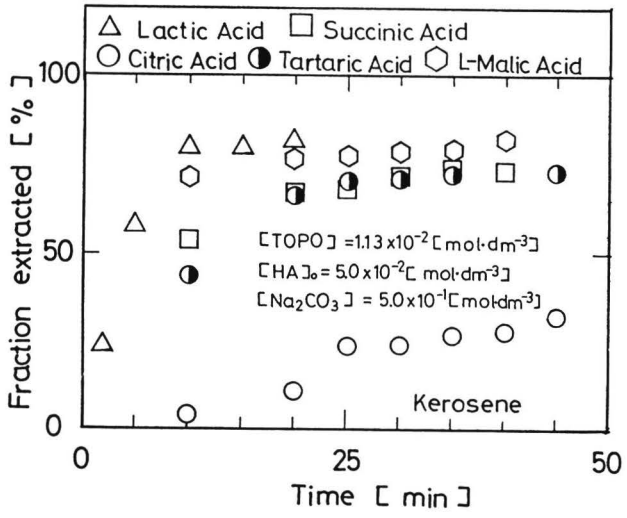

Fig.5 Extraction of organic acids with LSM prepared by Span 80

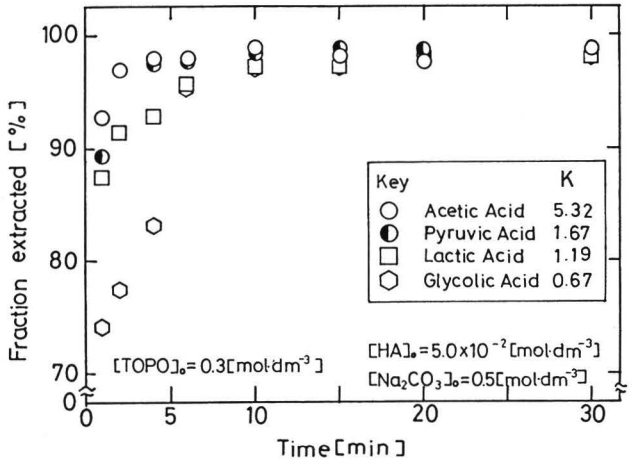

Fig.6 Extraction of monocarboxylic acid with LSM prepared by ECA 4360

operation were small in these runs. The conditions for separation of the acids were not optimized, but it seems that the permeation rates of the acids are dependent on the extraction equilibrium constant with TOPO.

CONCLUSIONS

To establish a new recovery process of organic acids from the fermented broth, the liquid surfactant membrane technique was applied to separate some organic acids. Extraction equilibria of lactic acid with various extractants, that is, tri-n-octylphosphineoxide(TOPO), tri-n-butylphosphate, tri-n-octylamine(TOA) and di-n-octylamine, were studied.

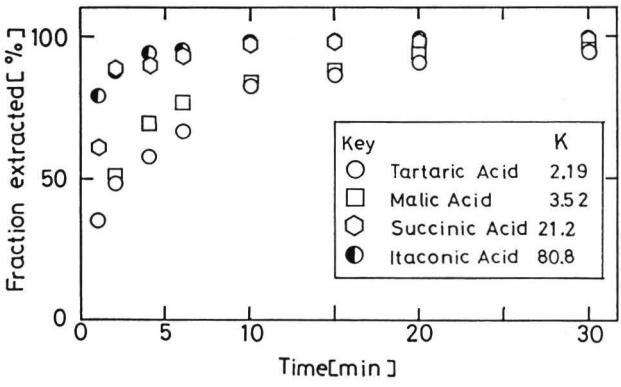

Fig. 7 Extraction of dicarboxylic acid with LSM prepared by ECA 4360

Diluent effect on extraction equilibrium of lactic acid with TOPO or TOA was discussed. The large difference was observed for TOPO and TOA in the contribution of a diluent to the association between lactic acid and an extractant.

The separation and enrichment of various fermented organic acids was conducted with the liquid surfactant membrane containing TOPO as a mobile carrier and polyamine as an emulsifier. It was found that the permeation rates of the acids were dependent on the extraction equilibrium constant with TOPO.

ACKNOWLEDGMENT

The authors express their thanks to Mr. S. Uenoyama for his valuable experimental assistance and are grateful to Hokko Chemical Industry for supplying the samples of TOPO.

REFERENCES

Boey, S.C., Garcia del Cerro, M.C. and Pyle, D.L., 1987. Extraction of citric acid by liquid membrane extraction:Chem. Eng. Res. Des., 65:218-223.

Hano, T., Matsumoto, M., Ohtake, T., Sasaki, K. and Hori, F., Extraction equilibria of organic acids with tri-n-octylphosphineoxide:to be published in J. Chem. Eng. Japan.

Nuchnoi, P., Izawa, I., Nishio, N. and Nagai, S., 1987. Extractive acidogenic fermentation by a supported liquid membrane:J. Ferment. Technol., 65:669-702.

Nuchnoi, P., Nishio, N. and Nagai, S., 1989. On-line extraction of volatile fatty acids in acidogenic chemostat culture using a supported liquid membrane:J. Ferment. Bioeng., 67:195-199.

Solvent Extraction 1990, T. Sekine (Editor)

© 1992 Elsevier Science Publishers B.V. All rights reserved

METHODS FOR CHARACTERIZATION THE HYDRODYNAMIC BEHAVIOUR OF FERMENTER BROTHS IN LIQUID-LIQUID EXTRACTORS

CHRISTOPHER JOB and ECKHART BLASS
Lehrstuhl A fuer Verfahrenstechnik, Technische Universitaet Muenchen
Arcisstrasse 21, D-8000 Muenchen 2, FRG

ABSTRACT

The liquid-liquid extraction for product separation from fermenter broths, which still contain the cells, is very advantageous. This **whole broth extraction** has hydrodynamic problems, if the broth is very viscous. In a gravity extractor the drop sedimentation and the drop separation is disturbed, if the solvent is dispersed into the broth. If the broth is dispersed, an unusable entrainment of the solvent occurs, when the broth drops coalesce. For the quantification of these effects some experimental methods were developed. The sedimentation behaviour of single drops can be calculated with the aid of single drop investigations and with a falling sphere apparatus. The sedimentation velocity and the coalescence behaviour of drop swarms can be detected with a special solvent drop column. The entrainment that occurs at the coalescence of broth drops can be measured with a special broth drop column.

With the informations received, it is possible to decide, whether the specific fermenter broth can be processed by a gravity extractor and to choose a suitable extractor design. The methods give the information to find out whether the solvent or the broth has to be the dispersed phase.

1 INTRODUCTION

If the first separation process in the downstream processing after a fermentation is the liquid-liquid extraction of the product with an organic solvent, it is advantageous to extract the product directly from the whole broth. The usage of **whole broth extraction** makes it possible to avoid cell separation that is often very difficult (Bender and Koglin, 1985), the losses of product in the filter cake or the unfavourable washing of the filter cake (Katinger et al., 1981) and it is possible to carry out the whole broth extraction in a producing fermenter as in-situ extraction (Job et al., 1990) for the increase of the productivity of the fermentation process. If the cell concentration is high the whole broth extraction is done in centrifugal fields by decanters only. There are no experiences in direct extraction by gravity extractors if the broth has a high cell concentration. The reasons lie in the special properties of fermenter broths that differ very much from the properties of fluids that are usually handled in gravity extractors: High concentrated fermenter broths are very viscous, show a pseudoplastic or plastic flow behaviour and contain a lot of surfactants and the cells that can precipitate. These properties are the reason for the fact that common liquid-liquid extractors cannot process high concentrated fermenter broths under usual operation conditions. The phenomenological analysis of the behaviour of viscous broths in the two phase system shows the following effects (Job, 1990): If the solvent is the dispersed phase, the properties of the broth hinder the drop formation, the drop sedimentation and the drop coalescence. The formation of very small drops at drop formation, drop sedimentation and drop coalescence result in an undesired entrainment of the solvent with the broth. If the broth is the dispersed phase, the drop formation is disturbed and the formation of inverse dispersions at the coalescence of the broth drops also causes an entrainment of the solvent with the broth.

For being able to decide whether an individual fermenter broth can be extracted in a gravity extractor, it is necessary to get a quantitative characterization of the behaviour of the broth by experimental methods. The calculation of the behaviour of fermenter broths is only possible, if all the influence of the properties of the broth is known, if the broth shows a special rhelogical behaviour and if the measurement of the flow behaviour at very low shear gradients succeeds with sufficient accuracy. These conditions do not exist for fermenter broths. Therefore it is necessary to develop measuring techniques for the sedimentation behaviour and the phase separation behaviour in phase systems with a fermenter broth.

2 THE MINIMUM DROP DIAMETER FOR DROP SEDIMENTATION

If the fermenter broth has a yield stress, a minimum drop diameter exists that is necessary for drop sedimentation. Smaller drops cannot sedimentate in the broth, because they cannot overcome the yield stress.

2.1 *SINGLE DROP INVESTIGATION*

The minimum drop diameter can be detected by single drop examinations. The drops must be positioned into the broth by a syringe. A glass vessel has to be used and the drops must be close to the side, so that their sedimentation can be observed. The investigation of drops with different diameters corresponding to the representation in fig. 1 leads to the smallest sedimentating drop. Probably the particles of the broth sedimentate during the measurement. This can be controlled by observing a mark of ink that is syringed into the broth.

The wall effects do not allow the quantitative measurement of the sedimentation velocity.

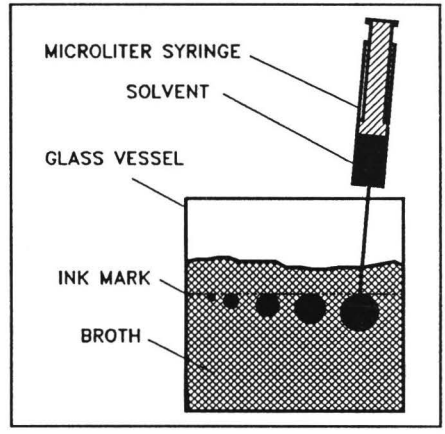

Fig. 1: Estimation of the Minimum Drop Diameter by Single Drop Investigations

2.2 *THE MINIMUM DROP DIAMETER IN DEPENDENCE OF YIELD STRESS*

Fig. 2 shows the values of minimum drop diameters in dependence of the yield stress of the broth that were measured by the method described before. The results show great differences to the diameters calculated by equations that were used by Dedegil (1987) and Zeppenfeld (1988). These equations cannnot be applied for the calculation of the minimum drop diameter.

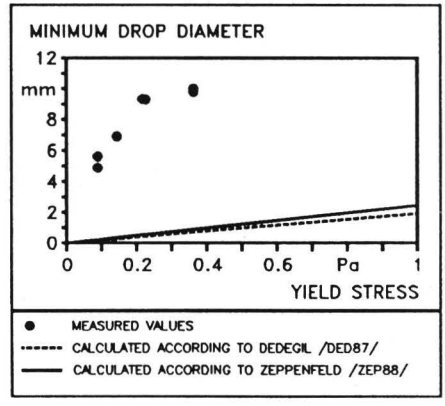

Fig. 2: Measured and Calculated Values of Minimum Drop Diameter in Dependence of Yield Stress

3 THE SEDIMENTATION VELOCITY OF SINGLE PARTICLES

Some investigations showed (Job, 1990) that the settling velocity of spheres is equal to the rising velocity of a drop if both have the same diameter and density difference to the broth and if their velocity is low. For the quantitative measuring of the rising velocity of drops an apparatus can be used that allows the estimation of the settling velocity of spheres.

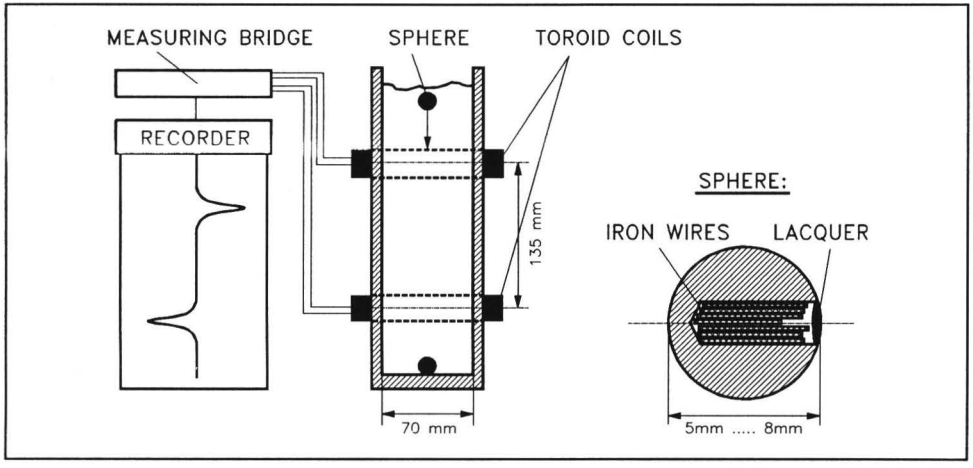

Fig. 3: Falling Sphere Apparatus for Measuring Single Particle Velocity in Non-transparent Broths

3.1 *THE FALLING SPHERE APPARATUS*

Fig. 3 shows the construction of the spheres. They are made of polyurethan or polyamid and filled with iron wires until they have the appropriate weight. This way it is possible to measure the position of the spheres in the **falling sphere apparatus** containing the non-transparent broth with two toroid coils (fig. 3), because the spheres cause a change of the brigde voltage, when they pass the coils.

3.2 *THE VELOCITY OF SINGLE SPHERES*

Fig. 4 shows the measured settling velocities of spheres in different broths in dependence of the sphere diameter. Although the broths have pseudoplastic flow behaviour the settling velocities are by approximation proportional to the square of the sphere diameter. Only the broth containing 12g/l Bentone shows a divergence. In this case the velocity is proportional to d_p^{10}. The reason being the **plastic flow behaviour of the broth. In this broth no settling occurs if the spheres have a diameter** of 5mm and smaller. A high exponent at the particle diameter is a sign for plastic behaviour of the broth.

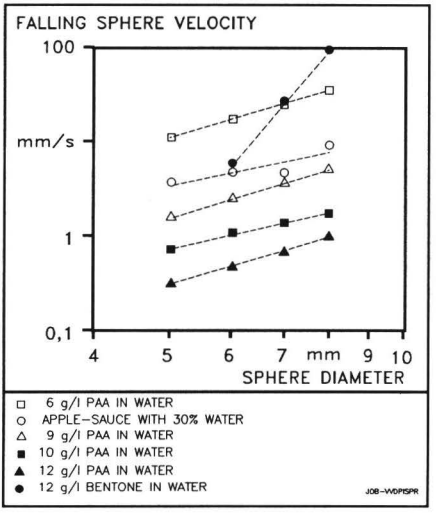

Fig. 4: Velocities of Spheres in Different Broths in Dependance of Sphere Diameter

4 THE BEHAVIOUR OF DROP SWARMS

In many cases the sedimentation behaviour of drop swarms differs from the sedimentation velocity of single drops. If experimental results with single drops and spheres, which are comparatively easy to obtain, show, that their sedimentation is good enough for liquid-liquid-extractors, it is ingenious to start the more difficult experiments for the detection of the behaviour of drop swarms. For that usage the **solvent drop column** was developed (fig. 5).

4.1 *THE SOLVENT DROP COLUMN*

The apparatus allows the setting of the drop diameter with two valves by alternate dosing of the broth and the solvent into the column. The broth and the solvent can be carried in circuit. The column diameter is 24 mm.

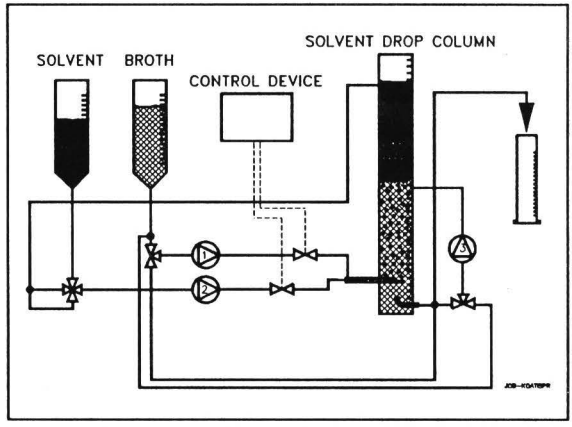

Fig. 5: Solvent Drop Column for Investigation of the Behaviour of Drop Swarms at Sedimentation and Coalescence

4.2 *THE DROP SWARM VELOCITY*

The apparatus allows the calculation of the drop swarm velocity v_s from equation (2) after the superficial velocity of the dispersed phase $\dot{v}_d$ has been measured and after the solvent hold-up ε has been read from the calibration at the column wall.

$$v_s = \dot{v}_d / \varepsilon \qquad (2)$$

Fig. 6 shows experimental results on the dependence of the drop swarm velocity from the superficial velocity of the solvent. The drop swarm velocity increases very much if the superficial velocity increases. The reason being the pseudoplastic flow behaviour of the continuous phase that is causal for a shear thinning effect and for the unequal distribution of the drops in the continuous phase. The results corroborate the tendencies that Gummalam and Chhabra (1987) calculated for the behaviour of bubble swarms in pseudoplastic fluids.

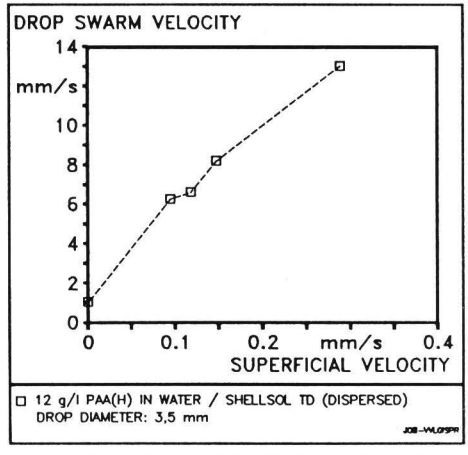

Fig. 6: Dependence of the Sedimentation Velocity of Solvent Drop Swarms from the Superficial Velocity of the Solvent

4.3 *THE COALESCENCE TIME IN DENSE DROP PACKAGE*

The **solvent drop column** is also usable for the detection of the residence time of drops in a dense drop package in a vertical separator. The coalescence time in the dense drop package t_k can be calculated with equation (3) after the height of the dense drop package h_k and the superficial velocity of the solvent in the separator $\dot{v}_d$ has been measured.

$$t_k = h_k / \dot{v}_d \qquad (3)$$

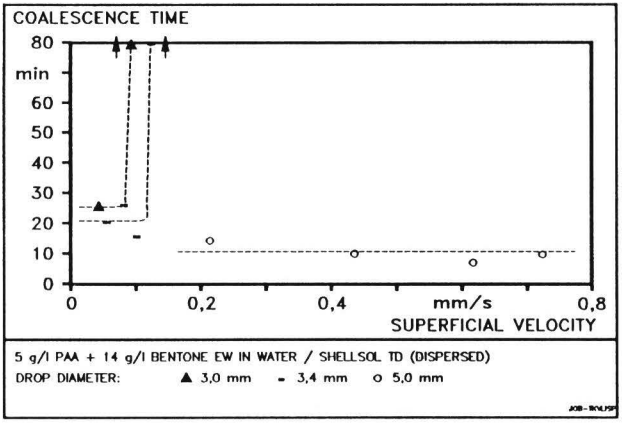

Fig. 7: Dependence of the Coalescence Time from the Superficial Velocity of the Solvent

Fig. 7 shows the dependence of the coalescence time from the superficial velocity. The coalescence time does not depend on the superficial velocity at low values. If the superficial velocity passes a critical value, sudden flooding of the separator occurs. This effect cannot be observed at separators with low viscous fluids. The flooding point will be reached at lower superficial velocities, if the solvent drops are smaller. This flooding point must be taken in consideration for the design of the separator of an extractor for fermenter broths.

5 THE COALESCENCE BEHAVIOUR OF BROTH DROPS

If the broth is dispersed into drops the drops enclose little solvent drops when they coalesce in the separator at the bottom of the extractor. This formation of an inverse dispersion causes an undesired entrainment of the solvent with the broth.

5.1 *THE BROTH DROP COLUMN*

The broth drop column has been designed for the experimental quantification of the entrainment (fig. 8). The column is made of glass and has a diameter of 16 mm. Thus it is possible to generate adequate superficial velocities of the broth with only one nozzle for drop formation. With the aid of the pulsator that is added to the nozzle the broth can be pumped in small batches into the solvent. One batch is equal to the volume of a drop. By varying the

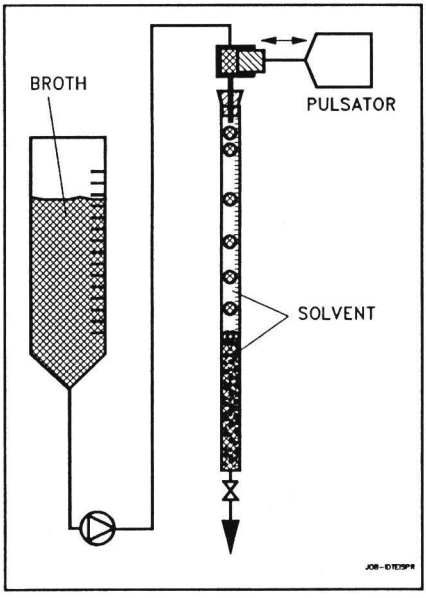

Fig. 8: Broth Drop Column for Investigation of the Behaviour of Broth Drops at Coalescence

pulse frequence it is possible to set the drop diameter on the desired value. The volumetric flow rate of the broth $\dot{V}_B$ can be measured by the calibrated feeding vessel. The solvent rests.

The entrainment ε_L' can be calculated from equation (4) with the difference in the solvent volumes $V_{L,\alpha}$ at the beginning and $V_{L,\omega}$ at the end of the measurement that must be read from the calibration on the column wall. The solvent entrainment ε_L' oscillates in spite of constant process conditions. For that reason the measuring time t_m must be long enough so that the result is statistically ensured.

$$\varepsilon_L' = \frac{1}{\frac{t_m \cdot \dot{V}_B}{V_L^{\alpha} - V_L^{\omega}} + 1} \qquad (4)$$

5.2 *THE ENTRAINMENT AT THE COALESCENCE OF BROTH DROPS*

Fig. 9 shows the dependence of the solvent entrainment form the superficial velocity of the broth. The entrainment increases when the superficial velocity increases. The diameter of the drops does not seem to have a significant influence on the entrainment.

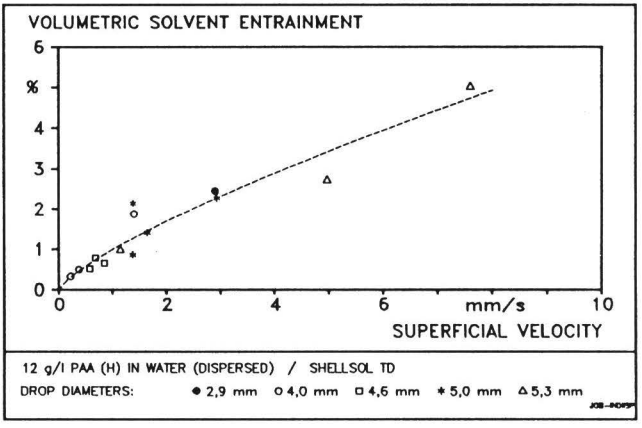

Fig. 9: Dependence of Solvent Entrainment at the Coalescence of Broth Drops from the Superficial Velocity of the Broth

6 REFERENCES

Bender, W. and Koglin, B.,1985. Mechanische Trennung von Bioprodukten. Preprints der GVC-Vortragstagung "Verfahrenstechnik der Aufarbeitung von Bioprodukten", Düsseldorf, 14.-15.10.1989: 17-28.

Dedegil, M. Y., 1987. Drag coefficient and settling velocity of particles in non-newtonian suspensions. J. of Fluids Engng., 109: 319-323.

Gummalam, S., Chhabra, R. P., (1987). Rising velocity of a swarm of spherical bubbles in a power law non-newtonian liquid. Can. J. of Chem. Engng., 65: 382-390.

Job, C., Weilnhammer, C., Blass, E., 1990. Improvement of product yield from fermentations with in-situ-extraction. Dechema-Biotechnology-Conferences, 4: in press.

Job, C., 1990. Hydrodynamische Auswahl und Auslegung von Schwerkraftapparaturen für die Direktextraktion von Fermenterbrühen. Dissertation TU München.

Katinger, H., Wibbelt, F., Scherfler, H., 1981. Kontinuierliche direkte Extraktion von Antibiotika mit Separatoren und Dekantern. Verfahrenstechnik, 15: 179-182.

Zeppenfeld, R., 1988. Verfahrenstechnik der Polysaccharidfermentationen im Rührreaktor. Dissertation TU München.

Solvent Extraction 1990, T. Sekine (Editor)

© 1992 Elsevier Science Publishers B.V. All rights reserved

A USE OF LIQUID EMULSION MEMBRANE FOR THE OPTICAL ISOMER SEPARATION OF AMINO ACID

HEUNG YONG HA and SEONG-AHN HONG
Division of Chemical Engineering, Korea Institute of Science and Technology
P.O. Box 131, Cheongryang, Seoul, 130-650 (Korea)

ABSTRACT

Enzymatic production of L-amino acid from a racemic mixture of D,L-amino acid ester was studied by a liquid emulsion membrane technique. Using a D,L-phenylalanine methyl ester as a model substrate, it was shown that the separation of racemic mixtures can be achieved by liquid emulsion membrane techniques. The enzyme immobilized in liquid membrane was also examined in terms of activity loss due to membrane phase and D-amino acid ester transferred from the external phase. Furthermore, the effect of membrane phase which consists of surfactant, carrier and organic solvent on the emulsion stability was investigated. It was found that increase of membrane viscosity greatly enhances the emulsion stability. For optimum conditions, it was possible to reuse the emulsion which consists of membrane phase and internal phase without further separation. It was concluded that emulsion stability was one of the most serious things to be optimized in terms of membrane composition for the continuous process development of this system.

INTRODUCTION

The liquid emulsion membrane (LEM) technique is a potential method of immobilizing enzymes for industrial processes. Li(1974) was the first to report on the possibility of encapsulating enzymes in LEM. Recently, three different examples of enzymatic bioconversion in LEM reactors have been demonstrated (Scheper, et al., 1987). However, more works are required to show the technical feasibility of enzyme immobilization via LEM.

In this study we elucidate some aspects related to the enzymatic production of L-phenylalanine utilizing a liquid emulsion membrane technique in a batch system i.e. the effects of some experimental variables on enzyme activity and the stability of liquid membrane.

2 EXPERIMENTAL

The membrane system was produced as follows. In the first stage the aqueous enzyme solution was emulsified in the membrane phase at high shear rates to give a stable water-in-oil emulsion. And then the emulsion was dispersed in the continuous substrate phase (external phase) with a stirrer at low impeller speeds.

The reaction was performed in a batch type reactor. The LEM solution was sampled at a given interval and the external phase was separated from the emulsion phase. And then the external phase was analysed using a high performance liquid chromatography equipped with a C18 μ-Bondapak column.

Two organic solvents with different viscosities, Kerosene and S-60NR, were tested. Span 80 was used as a surfactant and Adogen 464 as a carrier. A typical experimental condition

is listed in Table 1, unless otherwise mentioned.

3 RESULTS AND DISCUSSION

3.1 Effect of enzyme concentration

Hydrolysis of L-PheOMe was performed by α-chymotrypsin immobilized in a LEM. Fig. 1 illustrates the typical results of the batchwise reaction which show the concentration profiles of L-Phe and L-PheOMe for the different enzyme concentrations in the internal phase. As the reaction proceeds, the substrate is transported into the internal phase and its concentration in the external phase decreases, whereas L-Phe produced by enzymatic reaction in the internal phase is transported from the internal to the external phase across the membrane phase by the help of a carrier and its concentration in the external phase increases.

In Fig. 1, the results indicate that high enzyme concentration accelerates the reaction rate and thus enhances the permeation of substrate from the external to the internal phase. For an enzyme concentration of 0.2g/l in the internal phase, the reaction almost goes to completion within 3 hours. Meanwhile, the transport rate of the product from the internal to the external phase does not change much with the enzyme concentration. This result implies that the concentration gradient of the product between the internal phase and the external phase is not a main driving force for the transport of the product. As will be shown later, the transport rate of the product is mainly affected by the properties of the membrane phase such as viscosity and the carrier concentration.

It may be worthwhile to compare the enzyme activity or reaction rate in a LEM system with that in an aqueous phase system. For the enzymatic reaction in an aqueous phase, the reaction rate may be obtained by estimating the initial rate of change of the substrate. For the reaction in a LEM system, however, the situation is very complicated because of the

TABLE 1

A typical experimental condition

Internal phase :	Enzyme : α-chymotrypsin = 0.1 g/l		
	pH = 7.0 (buffer solution)		
Membrane phase :	Organic solvent :	Kerosene (S-60NR)	94 wt%
	Surfactant :	Span 80	5 wt%
	Carrier :	Adogen 464	1 wt%
External phase :	Substrate : L-PheOMe = 0.05 M		
	pH = 7 (buffer solution)		

Volume ratios of each phases : Internal / Membrane = 7/10
Emulsion / External = 1/4
(Emulsion = Internal + Membrane phase)
Emulsification : 7000 rpm for 30 min at 10 °C
Reaction : agitation = 300 rpm, 25 °C

. Analysis of the products : HPLC with a reverse phase μ-Bondapak C18 column

mass transfer limitation. As shown in Fig. 1, the concentration profile of the substrate may be divided into three regions with respect to the slopes. During the first 30 min, the slopes are very steep. After this initial period, the slope decreases and becomes almost constant for several hours. Finally, the slope is further reduced.

In a LEM, the calculation of reaction rate based on the slope of the initial period may invoke erroneous results because the rate of disappearance of the substrate in the external phase during this initial period is not the same as the rate of enzymatic reaction. However, it would be reasonable to define a reaction rate based on the slope of the second period. In this period where a steady state may be established, it is assumed that the transport rate of the substrate from the external phase into the internal phase is almost equal to the dissapperance of the substrate in the internal phase by the enzymatic reaction. The estimated reaction rates obtained from Fig. 1 and for the aqueous phase are listed and compared in Table 2. An interesting thing is that the reaction rates based on the second stages are almost the same regardless of the enzyme concentration. The enzyme activity in a LEM is about 60% of the native activity of the enzyme in an aqueous phase.

3.2 Effect of agitation

The effect of agitation stress on the enzyme activity in an aqueous phase was investigated. For an agitation speed of 7000 rpm, about 90% of the original activity was lost in 10 min and almost no activity remained with a 30 min agitation. This result is very suggestive when compared with the enzyme activity in a LEM. When the LEM is prepared, the mixutre of membrane phase and aqueous enzyme solution is agitated by a homogenizer at 7000rpm for 30 min. The enzyme in a LEM, however, retains 60% of its native activity as mentioned previously. These results indicate that the membrane phase acts as a protective barrier

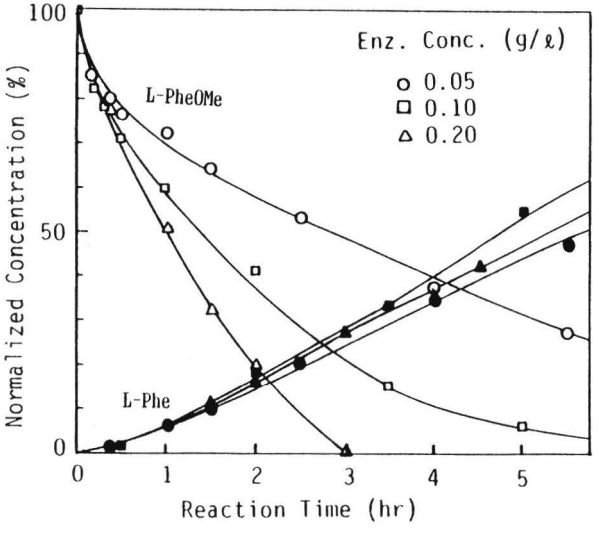

Fig. 1 Concentration profiles of L-PheOMe and L-Phe in the external phase with time during the enzymatic reaction in a LEM (S-60NR) : effect of enzyme concentration

TABLE 2

Effect of enzyme concentration on the reaction rate at pH 7 at 25 °C

Reaction System	Conc. based on the volume of each phase		Conc. based on the total volume of LEM		Initial reaction rate	Reaction rate at steady state
	Enzyme (g/l)	L-PheOMe (M)	Enzyme (g/l)	L-PheOMe (M)	(units/ mg-enz)	(units/ mg-enz)
LEM	0.05	0.05	0.00412	0.04	138.3	16.3
	0.10	0.05	0.00824	0.04	95.9	15.2
	0.20	0.05	0.03632	0.04	32.0	14.3
Aqueous	.	.	0.1	0.05	25.2	

* reaction rates are the rates of change of L-PheOMe in the initial and steady state region of the reaction and also calculated using the concentrations of enzyme and L-ester based on total volume of LEM system

for the enzyme solubilized in the internal phase of the emulsion to retain its activity from the destructive stress of agitation.

3.3 Effect of pH

Enzyme activity is dependent on the pH of the aqueous solution and shows a bell-shaped profile with respect to pH. In the aqueous phase α-chymotrypsin has a maximum activity at a pH of 7 for the hydrolysis of L-PheOMe and the same result was obtained using the enzyme immobilized in a LEM.

In a LEM, however, for the pHs other than an optimum pH of 7, enzyme did not retain its activity for a long time. At an optimum pH of 7, the enzyme activity was not deteriorated during the reaction and the reaction went to completion. At pHs of 6 or 8, the reaction did not go to completion and the conversion of the substrate leveled off in a few hours.

3.4 Effect of organic solvent

Fig. 2 shows the effect of organic solvent on the transport rate of L-Phe and the stability of LEM. The result of the same transport rate of L-PheOMe implies that the enzymatic activity in a LEM is not affected by a selection of organic solvent. The transport rate of L-Phe and the stability of LEM, however, depend on the viscosity of the organic solvent. As the viscosity of the organic solvent increases, LEM stability (LEM life time) increases and the transport rate of L-Phe decreases.

3.5 Effect of carrier concentration

Fig. 3 shows the effect of carrier concentration on the enzymatic reaction in the LEM. As can be seen from the profiles of L-PheOMe, enzyme activity is independent of the car-

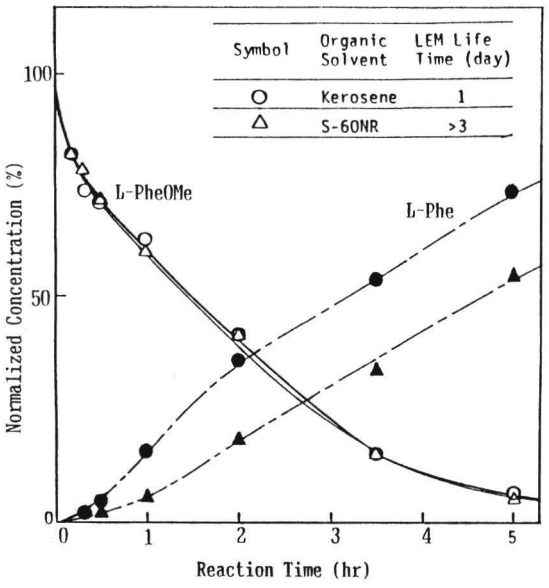

Fig. 2 Effect of organic solvent on the enzymatic reaction at pH 7 in a LEM

rier concentration. Only the transport rate of L-Phe and stability of the LEM are affected by the carrier concentration. The transport rate of L-Phe increases with carrier concentration, but above a certain value, about 1.5%, the LEM system broke down in a short time and the internal aqueous phase was eluted out. Finally, the LEM system (water-in-oil-in-water system) was divided into two immiscible water-organic phases.

3.6 Effect of D-ester

D-amino acid ester is not reactive and inhibits α-chymotrypsin activity. We examined the inhibitory effect of D-ester in an aqueous phase and confirmed that the activity of α-chymotrypsin decreases with the concentration of D-ester. With a 0.1M of racemic mixture of D,L-ester, the activity loss was as much as 30%.

To test the effect of D-ester on the enzymatic activity in a LEM, reaction was performed with D,L-ester as a substrate. The result was compared with that obtained using L-ester only. The decreasing profiles of L-ester were not changed by the presence of D-ester. However, it was observed that the presense of D-ester greatly affects the emulsion stability as well as product yield. The reason behind this observation has yet to be exploited.

3.7 Reuse of a LEM

The possibility of the reuse of a LEM was examined by checking the enzyme activity change. Experiments were performed as follows. First, prepare a LEM and carry out the reaction. Second, after the reaction goes to completion, separate the emulsion from the

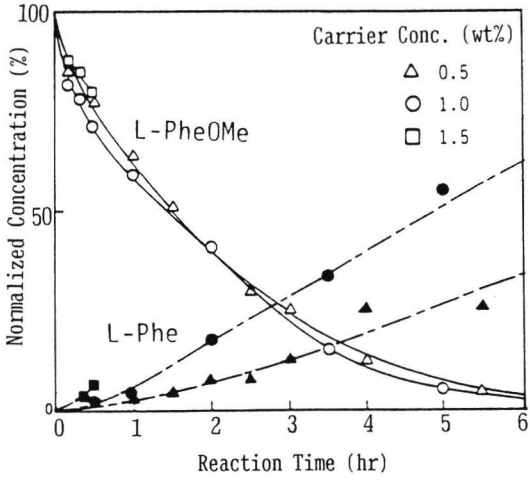

Fig. 3 Effect of carrier concentration at pH 7 in a LEM (S-60NR)

external phase. Third, prepare a new external phase with the substrate and proceed the second run by dispersing the emulsion phase separated into the new external phase.

We repeated the reaction three times by using the emulsion phase recovered. The activity of the enzyme immobilized in a LEM remained almost constant and the LEM was very stable after a reuse of LEM as many as three times.

4 CONCLUSIONS

(a) The pH of the internal phase is one of the most important variables to determine the enzyme activity in a LEM.

(b) The membrane composition (especially, viscosity of the organic solvent) must be optimized in terms of emzyme activity and emulsion stability

(c) The presence of D-ester affects the emulsion stability as well as product yield. The reason behind this result has yet to be determined.

(d) The enzyme immobilized in the emulsion keeps the reaction activity more than 3 days. Also, it is possible to reuse the emulsion separated.

(e) The enzyme in a LEM retains 60% of its native activity in spite of vigorous mixing during the emulsification step.

5 REFERENCES

Mohan, R.R. and Li, N.N., 1974. Reduction and separation of nitrate and nitrite by liquid membrane-encapsulated enzymes. Biotech. Bioeng., 16: 513-523.

Scheper, T., Halwachs, W. and Schugerl, K., 1984. Production of L-amino acid by continuous enzymatic hydrolysis of DL-amino acid methyl ester by the liquid membrane technique. Chem. Eng. J., 29: B31-B37.

Scheper, T., Likidis, Z., Makryaleas, K., Nowottny, C. and Schugerl, K., 1987. Three different examples of enzymatic bioconversion in liquid membrane reactors. Enzyme Microb. Technol., 9: 625-631

Solvent Extraction 1990, T. Sekine (Editor)

© 1992 Elsevier Science Publishers B.V. All rights reserved

RECOVERY OF LOW-MOLECULAR BIOLOGICAL PRODUCTS FROM AQUEOUS MIXTURES BY CARRIER EXTRACTION

K. SCHÜGERL, A. BRANDES, W. DEGENER, P. VON FRIELING, L. HANDOJO, Institut für Technische Chemie, Universität Hannover, Callinstr. 3, D-3000 Hannover, F.R.G.

ABSTRACT

The influence of extractant (carrier), diluent, modifier, pH-value and salt concentration on the degree of extraction and selectivity of organic acids are considered. The possible separation of chemically similar compounds is discussed.

INTRODUCTION

Plant extracts, fermentation broths, waste protein hydrolysates yield complex mixtures. The recovery of the desired products from these mixtures can be carried out by adsorption, precipitation, ion exchange chromatography, and extraction.

The product recovery by adsorption/ion exchange chromatography usually has a low capacity, the precipitation a low selectivity, the extraction by oxygen-bearing extractants (alcohols, esters) a low selectivity, low partition coefficients, and the solvent phase a high solubility in the aqueous phase. The partition coefficient and the selectivity of the solvent extraction and the extractant losses due to high solubility can be improved by the use of phosphorous-bonded, oxygen-bearing extractants and with high-molecular-weight aliphatic amine extractants in diluents of low solubility in the aqueous phase.

In the case of organic acids, the first two categories involve the solvation of acid donor bonds. In the first category, the solvation bonds are weak and nonspecific. In the second category, the solvation bonds are stronger and more specific. In the third category, ionic interactions are involved. In this poster, the use of phosphorous-bonded, oxygen-bearing and aliphatic amine extractants for organic acid recovery are discussed.

DISCUSSION

Separation of solutes with a single charged group

The aliphatic and some aromatic carboxyl acids belong to this category. On account of their acidic character, they have affinity to basic extractants (electron donators). Such extractants are, e.g., trioctylphosphinoxide (TOPO) or higher dialkylamines, e.g., N-lauryl-N-trialkylmethylamine (Amberlite LA-2), higher trialkylamines, e.g., tri-n-octlyl/tri-n-decylamine (HOSTAREX A 327). TOPO and HOSTAREX A 327 are used for the extraction of acetic acid (Ricker et al. 1979), Amberlite LA-2 for the extraction of aromatic carboxyl acids (Halwachs et al. 1983) and of penicillin G and V (Reschke et al. 1984). The selectivity of the extractants can be influenced by a modifier. E.g., the selectivities of formic acid, acetic acid, propionic acid, and butyric acid with tri-isooctylamine (Hostarex A 324) as extractant, in kerosene as diluent, considerably changes as isodecanol (modifier) is added to the solution (Siebenhofer et al. 1983).

Separation of solutes with more than one charged group which form zwitter ions

The separation of solutes with more than one charged group, which forms zwitter ions in the neutral range, is a most difficult task. Typical compounds are the amino acids.

Except for threonine, all bifunctional amino acids have their $pK_1(COO^-)$-value between 2 and 3, and their $pK_2(NH_3^+)$ value between 9 and 10. This holds true also for the trifunctional amino acids, except for cystein (pK_1 = 1.71, pK_2 =10.78) and histidine (pK_1 = 1.82).

The separation of amino acids of a basic character from those of an acidic character is fairly easy, likewise is the separation of amino acids with a polar side group from those with a nonpolar side group.

The separation of leucine and isoleucine, which have a nonpolar side group, and lysine, with a positive-charged side group (basic character), can be performed with 100 mmol/l TOMAC (trioctylmethylammonium chloride) and 6% decanol (modifier) in methylcyclohexane at pH 10 to 11. As expected, the basic amino acid remains in the aqueous phase, and the amino acids with the nonpolar uncharged side group (leucine and isoleucine) move into the organic phase. After the back-extraction with HCl- or NaCl-solutions into the aqueous phase, leucine and isoleucine can be separated by ex-

traction by an anion exchanger (200 mmol/l ALIQUAT 336 (trialkylmethylammonium chloride) in cyclohexane. Leucine moves into the organic phase and isoleucine remains in the aqueous phase.

According to an alternative method, leucine and isoleucine are extracted with tetradodecylammonium bromide, an anion exchanger, in presence of 6% decanol in xylene at pH 12. Leucine moves into the organic phase and isoleucine remains in the aqueous phase.

A comparison of the degrees of extraction of 10 mmol/l leucine and isoleucine during the extraction with tetrahexyl-, tetraoctyl- and tetradodecylammonium bromide in presence of 2%, 4%, and 6% dodecanol in xylene at pH 12.4 indicates that the degree of extraction of both components increases with an increasing alkyl chain length, however, the selectivity of leucine diminishes. Therefore, the best separation is attained with tetrahexylammonium bromide. On the other hand, the difference of the selectivities increases with increasing NaCl-concentration (Fig. 1).

Another example for the separation of an amino acid with a nonpolar side group (tryptophan), but high solubility in water, from another with a polar side group (tyrosine), but low solubility in water, is their extraction from the aqueous phase with 15 mmol/l TOMAC in xylene at pH 10 to 11. Both of them move into the organic phase. However, during back-extraction with 1.5 mol/l NaCl-solution, the degree of extraction of tryptophan is lower than that of tyrosine. This allows their separation (Kirgios et al. 1986). When increasing the NaCl-concentration, the extraction degrees of both increase. However, the difference of their selectivities is highest at 0.15 mol/l (Fig. 2).

During the extraction of arginine and lysine, amino acids of a basic character, and aspartate, of an acidic character, with 0.3 mol/l TOMAC in xylene at pH 12, only aspartate moves into the organic phase, as expected. The degree of extraction of aspartate as a function of the equilibrium pH-value passes a maximum at pH 12 because of the coextraction of the OH^--ions (Fig. 3) (Handojo 1988).

Lactic acid/lactate can be extracted from aqueous solutions with different extractants: TOPO (trioctylphosphinoxide), TBP (tributyl phosphate), LA-2 (sec. Amine), D2EHPA (diethylhexylphosphoric acid), HOSTAREX A 327 (tert. amine), ALIQUAT 336 (quaternary amine), ADOGEN 464 (quaternary amine) (Fig. 4). The extraction is carried out with TOPO, TBP, LA-2, D2EHPA and HOSTAREX at a low pH and with quaternary amines at a high pH (v. Frieling 1989).

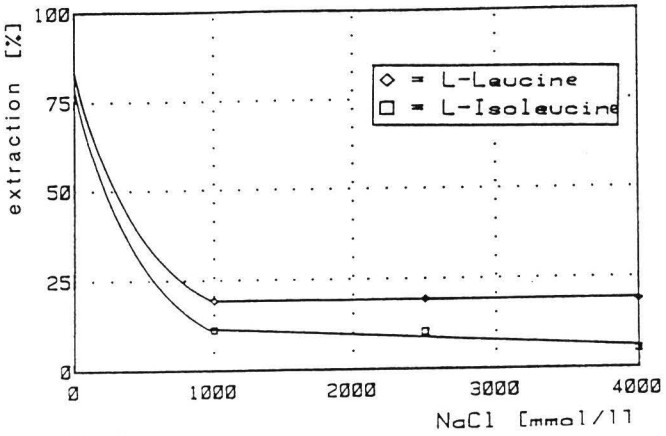

Fig. 1

Leucine/isoleucine extraction by 0.2 M Aliquat 336 (trialkylmethyl-ammonium chloride) in cyclohexane from NaCl solutions
C_0 = 10 mM

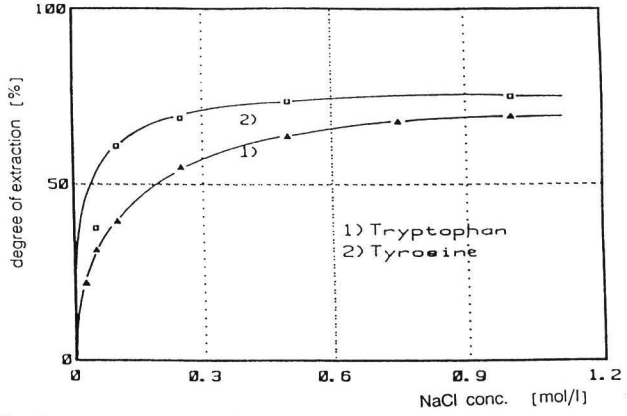

Fig. 2 Re-extraction of tryptophan and tyrosine from xylene by NaCl solution

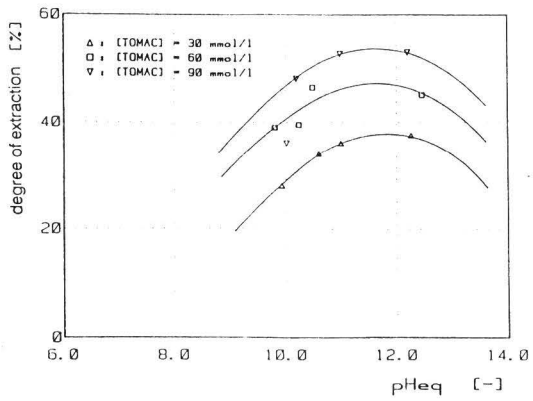

Fig. 3 Extraction of aspartic acid in the presence of arginine with TOMAC as a function of the equilibrium pH value
C_0 = 10 mM

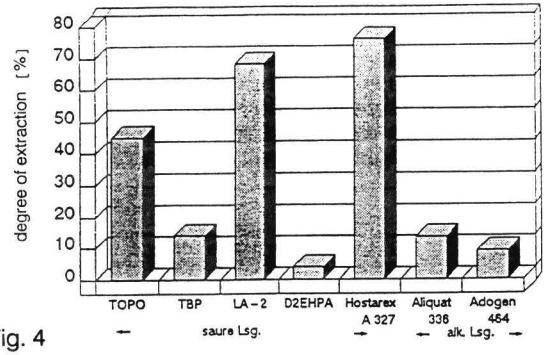

Fig. 4

Reaction of lactic acid from the organic solutions of TOPO, TBP, La-2, and D2EHPA with acidic extractants and from the organic solutions of HOSTAREX A 327, ALIQUAT 336 and ADOGEN 464 with basic extractants.

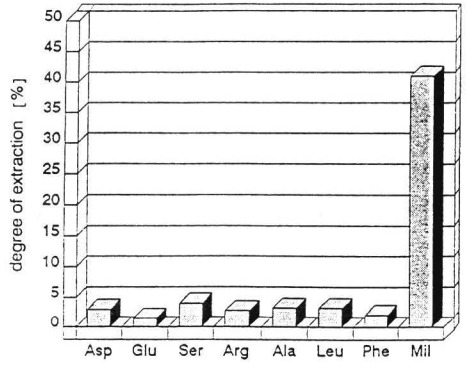

Fig. 5 Selectivity of lactic acid extraction in presence of amino acids. Extraction with Hostarex A 327 in xylene at pH 1.8 and re-extraction with 1 M NaOH.

The separation of lactic acid (pK_a = 3.86) from amino acids (pK_1 =2 to 3) is possible, based on the difference of their pK-value. If the aqueous solution of lactic acid and amino acids are extracted with 40% HOSTAREX A 327 (1:1 tri-n-octyl/tri-n-decyl-amine mixture) in presence of 10% isodecanol on 50% kerosene at pH 1.8, only lactic acid moves into the organic phase. All amino acids remain in the aqueous phase. After the back-extraction with 1 mol/l NaOH, a pure lactate solution is obtained (Fig. 5). Similar results can be obtained with TOPO and LA-2 (v. Frieling 1989).

CONCLUSION

The recovery of products from complex mixtures and the separation of chemically similar solutes by extraction is possible. However, the process development is still empirical. More investigations are necessary to pedict the optimal conditions for the separation.

REFERENCES

v. Frieling, P., 1989, Master thesis, University of Hannover

Halwachs, W., Schügerl, K., 1983. Investigation of reactive extraction on single droplets, Chem. Eng. Sci. 38: 1073-1084.

Handojo, L., 1988. Trennung von Asparaginsäure und Arginin mittels Reaktivextraktion, dissertation, University of Hannover

Kirgios, I., Rhein, H.B., Schügerl, K., 1986. Bedeutung der Koextraktion bei der Aminosäure-Aufarbeitung mit Anionenaustauschern. Chem. Ing. Techn. 58: 908-909

Reschke, M., Schügerl, K., 1984. Reactive extraction of penicillin. The chem. Eng. Journal, 28: B11-B20.

Ricker, N.L., Michaels, J.N., King, C.J., 1979. Solvent properties of organic bases for extraction of acetic acid from water. J. Separ. Proc. Technol. 1: 36-41.

Siebenhofer, M., Marr, R., 1983. Acid extraction by amines, ISEC'83

Solvent Extraction 1990, T. Sekine (Editor)

© 1992 Elsevier Science Publishers B.V. All rights reserved

SEPARATION OF MIXTURE OF VINYLTRIMETHYLSILANE AND TETRAHYDROFURAN BY EXTRACTION

Borisova I.A., Sokolov N.M., Vatskova V.G., Gorbunov A.I.

State scientific and research institute of chemistry and technology of organoelement compounds, Moscow, USSR

The problem of environment protection is very acute in the last few years. Because of this, much attention is being given to the development of oecologically pure production processes with little wastes. To determine the possibility of optimization of vinyltrimethylsilane (VTS) washing from tetrahydrofuran (THF) by water for the purpose of lowering its specific consumption and of increasing THF concentration in aqueous solutions as well as to extract it from used extractant by re - extraction, we studed liquid - liquid equilibrium in triple systems which are formed by VTS, THF, water and toluene at 293.15°K Using diagrames of equilibrium of abovementioned systems we calculate the processes of crude VTS extractive washing by water from THF and extraction of THF from water flows up to concentration 0.01% mass by toluene. The laboratory testing of calculated conditions for extractive washing of crude VTS from THF and for re-extraction of THF from generating flows of water confirmed reliability of data. Flow sheet of VTS extraction and regeneration from sewage with complete water recyclisation is developed on the basis of performed studies.

The problem of environment protection is very acute in the last few years, that is why much attention is being given to the development of ecologically pure productions with little wastes. Vinyltrimethylsilane (VTMS) is the initial product for gas-separating membranes production, which especially lately, have found broad application in various materials separation. Tetrahydrofuran (THF) is used as solvent in VTMS production, in process of crude VTMS production, its mixture with THF content of 40-60% by mass. is formed. At cleaning of crude VTMS from THF in the industrial conditions cross-flow extraction method with the use of water as extractant is applied. For VTMS production with THF content at the level of 0.1% by mass. 6-9 consecutive operations of mixing and separation are required with the ratio of initial mixture and extractant of about 1. Waste extractant is aqueous solution, the content of THF is 3-4% by mass., that is why its regeneration is not realized and waste waters, being formed, are subjected to flame detoxication.

For optimization of crude VTMS washing-off, reduction of extractant specific flow rate, increasing THF concentration in the waste extractant and consequently solvent regeneration and its return to production plant investigation of liquid-liquid equilibrium at 20°C in the system VTMS-THF-water was carried out. Position of binodal - curve of mutual solubility of components and equilibrium nodes have been determined separately using titration method and analytical method /1,2/. Diagram phase equilibrium in the indicated system is given in Fig. 1. On the basis of the obtained equilibrium data, calculation of THF distribution coefficients was performed as a ratio of its concentrations in aqueous and organic phases. Coefficient values analysis has shown, that in THF concentration change area in mixtures from 80 to 5% by mass. they make up from 0,6 to 0,43. In THF small concentration area distribution coefficient has its permanent value of 0,43.

Using obtained equilibrium data calculation was held concerning statics of continuous countercurrent washing-off process of crude VTMS from THF with water having various ratios of extractant initial mixture flow and residual concentration of THF in VTMS at the level of 0,1% by mass.

For illustration in Fig. 2 design curves of THF concentration dependence in organic and aqueous phases on number of phase contact stages at varios of initial mixture and extractant streams are shown. Thus at THF starting concentration in initial crude VTMS equal to 41% by mass. for achieving required THF residual concentration in VTMS of 0,1% by mass. 7,6 phase contact stages at initial mixture and extractant stream ratio of 0,25 and 9,2 stages at 0,33 respectively are required.

At washing of VTMS from THF with continuous countercurrent extraction it is possible to increase THF content in waste extractant - water up to 10-14% by mass. at the cost of extractant volume decreasing which makes it advisable to carry out regeneration of scarce and expensive THF.

To evaluate the possibility of extraction process application as less power intensive as compared with rectification for THF regeneration out of the waste extractant from crude VTMS, extraction treatment process investigation has been carried out concerning liquid-liquid phase equilibrium in THF-water-toluene system at 20°C with the use of the above-mentioned methods. Toluene selection as extractant has been determined by following considerations: toluene has limited solubility with water and complete solubility with THF; it is comparatively cheap and available, besides the following THF regeneration out of mixtures with toluene by rectification does not present any difficulty. Diagram of phase equilibrium in THF-water-toluene system is given in Fig.1 Calculation of THF distribution coefficient as the concentration ratio

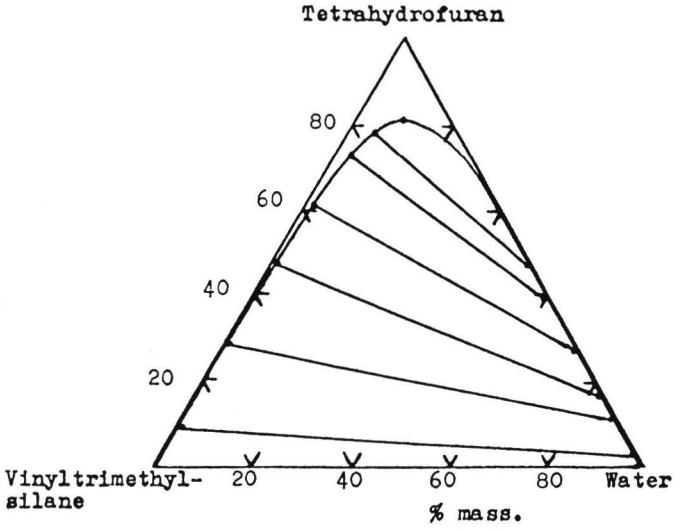

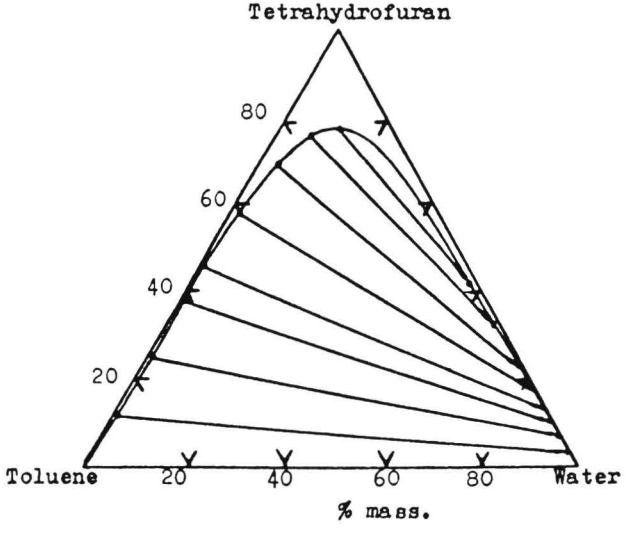

Fig.1 Liquid-liquid phase equilibrium diagrams of systems formed by vinyltrimethylsilane, tetrahydrofuran, water and toluene at 293.15° K

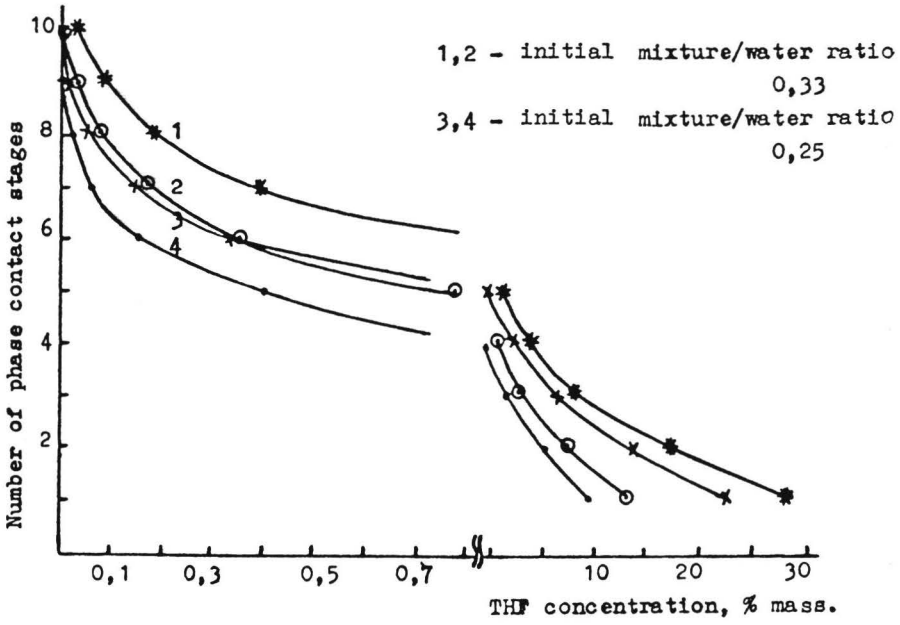

Fig.2 Dependence of THF concentration in organic (curves 1 and 3) and aqueous (curves 2 and 4) phases on number of contact stages for difference ratios flows.
THF concentration in initial mixture was 41 % mass.

of equilibrium organic and aqueous phases has shown that for THF extraction from its aqueous solutions, extraction method can be applied using toluene as extractant (THF distribution coefficient value varies from 1.92 to 3.85 for mixtures, containing THF from 70 to 1.0% by mass.

For computer calculation of THF extraction process statics from aqueous solutions mathematical modelling for THF-water-toluene system at 20° using equations NRTL /3/, UNIQUAC /4/ and Tsuboka-Katajama /5/ has been carried out. Indicated equations parameters have been calculated based on liquid-vapour equilibrium data of respective binary components. It has been found that UNIQUAC equation best approximates for this mixture dependence of component activity coefficient on liquid phase composition. Further calculation of extraction process have been carried out with the help of liquid-liquid phase equilibrium model at the 12% by mass. initial concentration in the starting mixtures. In the course of calculations ratios of initial solution and extractant streams and also phase contact stages have been changed. Calculation has shown that require

0.01% by mass. THF residual concentration in aqueous solution waste extractant is reached at 5 stages of contact phase with the ratio of initial mixture and toluene of 1.14 and at 7 stages - at 1.64 and 16 stages - at 3.0 respectively.

Thus for required treatment of crude VTMS, containing THF of 40-60% by mass. at crude and water stream ratio of 0.25-0.35 countercurrent extractor with the efficiency of 10 stages is required and for THF extraction from aqueous solutions up to its residual concentration of 0.01% by mass. (at the THF initial concentration of 10-14% by mass.) countercurrent extractor with 10 phase contact stages with initial mixture and toluene ratio of 1-2 is required. On the basis of the obtained data process scheme of crude VTMS purifecation and THF extraction from waste waters by extraction method with complete water recyclization has been developed. Indicated process block-diagram is given in Fig. 3.

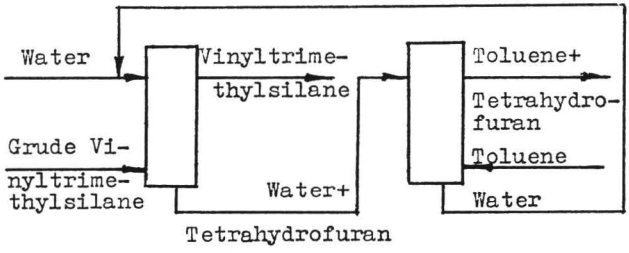

Fig. 3. Block-diagram of VTMS treatment and THF regeneration processes

References:

1. Mozhuhin A.S. et al. Liquid-vapour and liquid-liquid system equilibrium and n-propanol-water-propylpropyonate. Zh. Fiz. Khim., 1967, 41 p. 1687.
2. Alders L. Liquid-liquid extraction. Elsevier Publishing Co, Amsterdam a.o., 1955, 220 p.
3. Renon H., Prausnitz J.M. Local compositions in thermodynamic excess functions for liquid mixtures. - AIChE Journal, 1968, v. 14, N 1, p. 135-144.
4. Abrams D.S., Prausnitz J.M. Statistical thermodynamics of liquid mixtures. A new expression for the excess Gibbs energy of partly or completely miscible systems. - AIChE Journal, 1975, v. 21, N 1, p. 116-118.

5. Tsuboka T., Katajama T. Modified Wilson equtia for vapor-liquid and liquid-liquid equilibria. J. Chem. Jap., 1975, v. 8, N 3, p. 181-183.

In liquid-liquid equilibrium modelling and extraction process calculation Erlykina M.E., Zhernosek V.M. have taken part.

Author Index

Abe,H. 717
Abe,S. 123
Abe,Y. 1127
Abid,K.H. 1429
Abisheva,Z.S. 949,955
Adachi,G. 1499
Adachi,K. 1075
Aguilar,M. 159,171
Akaiwa,H. 441,1555
Akatsu,J. 723
Akiba,K. 1677
Al-Murab,S.R. 907
Albinsson,Y. 473
Alonso,A.I. 1535
Alstad,J. 491,1387
Aly,H.F. 87,219,249,729
Ami,N. 699
Angel,S.A. 1235
Anisimov,V.I. 573
Anticó,E. 1505
Aose,S. 399
Aoyagi,H. 225
Arai,Y. 177,1695,1821
Arbel-Hardad,M. 333
Arias,J.J. 515
Arm,S.T. 621
Asano,T. 799
Awakura,Y. 1481

Baba,Y. 351,805,931
Badings,H.T. 1713
Bailes,P.J. 1313,1411
Bal,Y. 919
Baluev,A.V. 291
Bart,H.-J. 1121,1339,1797
Bartsch,R.A. 1517,1523
Bauer,D. 919
Bauer,G. 491
Bauer,U. 1797
Bautz,H. 651
Beer,M. 1021
Bernard,C. 747
Beyad,M.H. 339
Blaida,I.A. 949
Blass,E. 1271,1283,1423,1447,1893
Bleyl,H.-J. 555,561
Bo,Lu 1773
Borges,T.M. 515
Borisova,I.A. 1911
Bosman,R.J. 327
Brajenović,N. 1027
Brandes,A. 1905
Breschet,C.A. 609
Bressler,E. 333
Brunner,G. 1661
Bumbálek,V. 1133
Burgess,A. 1087,1145
Burnham,R.F. 961
Byeseda,J.J. 1211,1417

Campbell,M.J. 423
Caselli,M. 1815
Cauwenberg,V. 1265
Chen,Fuming 429
Chen,Jiayong 793,853
Chen,Shao-Jin 273
Chen,Wen-Jun 273
Chen,Xiao-Xiang 1351
Cheng,Hanying 1631
Chesne,A. 411,539,1009,1567
Chikirda,N.M. 393
Chiu,Tai-Ming 1181,1543
Choppin,G.R. 61
Chung,Koo-Soon 925
Cierpiszewski,R. 817
Collard,S. 961
Condamines,N. 417
Cortina,J.L. 159
Coste,J.A. 609
Cote,G. 919
Craig,W.M. 1475
Cruz-Pinto,J.J.C. 1241
Cuillerdier,C. 417
Cusack,R.W. 1333
Cussler,E.L. 1737

D'Olieslager,W. 967
Dai,Xing 877,1655
Dai,Youyuan 1381
Dalton,R.F. 1087,1145
Dalverny,G. 747
Danilov,V.N. 527
De Graauw,J. 1713
De Haan,A.B. 1713
De Pablo,J. 171
De Schepper,A. 1115
Debreuille-Gresse,M.F. 135
Degener,W. 1217,1561,1785,1905
Delafontaine,G.L. 609
Demopoulos,G.P. 1099
Denniss,I.S. 549
Deorkar,N.V. 467
Dhaskali,G. 1009

Diamond,H. 357
Distin,P.A. 787
Dmitriev,S.N. 509
Draxler,J. 37,1121,1589
Du Preez,A.C. 883,1081
Durand,G. 411,1009,1567

Eccles,H. 741
Egashira,R. 1595,1601
Eguchi,W.(The late) 1579
El-Dessouky,S. 249
El-Sourougy,M.R. 729
Engkvist,I. 473
Ermolajeva,T.N. 527
Ertel,D. 555
Eyal,A.M. 333

Famiglietti,M. 1755
Fan,Zheng 1453
Fawcett,P. 741
Fawdry,G.P. 327
Fedorov,Yu.S. 285,759
Fei,Weiyang 1369
Fleitlich,I.Yu. 1187
Flett,D.S. 1,1127
Fournier,W. 747
Franz,G. 835
Fraux,A. 1393
Freiser,H. 69
Fu,Lichun 591
Fujinaga,K. 369
Fujine,S. 497,651,663,675
Fukuzato,R. 1707
Fumoto,H. 663
Furusaki,S. 1749
Furuta,S. 1707
Furuya,T. 1821

Galantseva,T.V. 1187
Galla,U. 555,633
Gao,Lijuan 1057
Gao,Song 1295
Garnaka,Z. 533
Gatrone,R.C. 357
Gerbish,Sh. 509
Germain,M. 539,597
Gilchrist,A. 1869
Gillet,B. 597
Glasunov,N.V. 573
Gleisberg,B. 711
Godfrey,J.C. 1393,1429
Goettert,W. 1447
Goldacker,H. 555
Gonda,K. 871
Gorbunov,A.I. 1911
Gorski,B. 711,1021
Gorski,N. 1021
Goto,K. 503,1649
Goto,M. 1459,1845
Grant,R.A. 961
Greenwood,H. 741
Grinbaum,B. 1235
Gu,Guobang 375
Gu,Zhongmao 1631
Gue,J.P. 579
Guimarães,M.M.L. 1241

Ha,Heung Yong 1899
Haberberger,F. 491
Haberland,K. 1399
Haesebroek,G. 1115
Hakushi,T. 363
Haman,J. 1133
Han,Shumin 1063
Handojo,L. 1785,1905
Hano,T. 1613,1881,1887
Harada,M. 777
Haraguchi,K. 315
Harrison,J.W. 1289
Hartl,J. 1683
Hartland,S. 1175,1259
Hartmann,D. 1567
Hasegawa,Y. 93
Hatton,T.A. 23
Hattori,K. 1671
Hawtin,J. 1869
Hayashi,S. 399,567,603,639,681
Herranz,C. 147
Hibiki,T. 1441
Hidalgo,M. 1505,1511
Hirai,T. 1015
Hirano,H. 735
Hirasawa,T. 1779
Hirashima,Y. 1499
Hirata,A. 841
Hirato,T. 1481
Ho,Kung-Liang 1181
Hochköppler,A. 1755
Hofman,D.L. 1475
Hoh,Ying-Chu 901,1181,1543
Hong,Seong-Ahn 1899
Honjo,T. 457
Honma,S. 615
Hori,F. 1613,1881,1887
Horng,Jiin-Shiung 901
Horwitz,E.P. 357
Hotoku,S. 675
Hozawa,M. 973
Hu,W.H. 321
Huang,Ching-Tsven 693
Huang,Chun-Hui 105
Huang,Ting-Chia 693,1529
Huddleston,J.G. 1767
Hufnagl,H. 1283
Hugelmann,D. 747
Hung,Tsung-Min 901,1469,1543

Hwang,Ran 925

Ibrahim,A. 729
Ichige,Y. 399
Ichikawa,S. 1875
Idegami,A. 681
Igarashi,S. 1725
Iguchi,T. 799
Ikawa,N. 1707
Ikeuchi,H. 93
Imai,M. 405,1487,1643, 1875
Imai,T. 1375
Imaishi,N. 973
Imanishi,N. 1707
Imura,H. 895
Inaba,K. 213
Inoue,K. 351,805,931
Inoue,Y. 363,669
Irabien,A. 1535,1539,1585
Ishibashi,Y. 1677
Ishikawa,I. 913
Ito,S. 1833
Itoh,Y. 1555
Iwabuchi,H. 705
Iwai,Y. 1695,1821
Iwai,Y. 1821

Jalhoom,M.G. 907
Jansons,E. 533
Jayawant,D.V. 1003
Jenkins,J.A. 621,1345
Jewad,S.K. 907
Jiang,Jincai 591
Jiang,Kaixi 1205
Job,C. 1893

Kaffrell,N. 491
Kaghazchi,T. 865
Kamidate,T. 315
Kaneko,T. 1075
Kanki,T. 799
Karr,A.E. 1333
Kartasheva,N.A. 183,261
Kasahara,I. 503
Kasai,S. 1199
Kasymova,A.S. 949
Katano,H. 231
Kataoka,T. 1761
Katayama,T. 1375,1441,1689
Kato,K. 1827
Kato,M. 1833
Kato,S. 141
Kato,Y. 1649
Kawana,H. 1707
Kawano,Y. 829,1887
Kawasaki,J. 1595,1601
Kawata,T. 567,603

Ke,Jiaxiong 1369
Khalifa,S.M. 87,219,249
Khol'kin,A.I. 1187
Khopkar,S.M. 467
Kienle,A. 1283
Kihara,S. 225,309
Kihara,T. 497,675
Kim,Chul 1253
Kim,J.D. 645
Kim,Kwang-Wook 645
Kimura,T. 723
King,C.J. 1791
Kinugasa,T. 1839
Kirgios,J. 1217
Kirou,V.I. 1247
Kishi,K. 1749
Kishida,M. 777
Kishimoto,Y. 681
Kitamori,T. 497
Kitamura,Y. 1637
Kitayama,D. 1881
Kiuchi,T. 1833
Klyguin,V.A. 573
Koga,J. 615
Kohri,S. 1499
Kolarik,Z. 207,561
Komasawa,I. 1015,1199,1767, 1851,1857,1863,1869
Komatsu,H. 657
Komatsu,Y. 521
Kondo,K. 829,1459,1845
Koppiker,K.S. 1003
Korenman,Ja.I. 527
Korotkov,I.A. 573
Koyama,K. 705,1481
Krjukov,A.I. 527
Krzyzanowska,E. 817
Kubo,N. 699
Kuboi,R. 1767,1851,1857, 1863,1869
Kubota,M. 585
Kulmuchamedov,G.K. 1187
Kunimasa,H. 1375
Kunugita,E. 1199
Kunzmann,M.W. 207
Kurahashi,H. 1643
Kursina,M.M. 1731
Kusakabe,S. 123
Kuwahara,M. 991

Lanin,V.P. 393
Larkai,S.K.L. 1411
Lee,Chau-Jen 901,1469
Lee,Yong-Kuk 1253
Legin,E.K. 279
Lei,Xia 1381
Lelyuk,G.A. 759
Leser,M.E. 1815
Leudet,A. 747
Levins,D.M. 1069

Li,Biao-Guo 105,1295
Li,Da-Ren 243
Li,Deqian 811,1039,1045,
1051,1057,1063
Li,Hui 1295
Li,Shusen 321
Li,Weixuan 1655
Li,Ximing 1453
Li,Yanli 375
Lin,Chung-Yun 1543
Lin,Xiao-Ming 1549
Liu,Daxing 1205
Liu,Fuan 165,195
Liu,He-Ping 105
Liu,Huizhou 793,853
Liu,Suying 591
Liu,Yu 363
Liu,Zhong-Qun 273
Lo,T.C. 1405
Logsdail,D.H. 1345
Long,Tiwu 375
Lorenz,M. 129
Lubboch,E. 1517
Luboshnikova,K.S. 1187
Luisi,P.L. 1755,1815,1863
Lyddiatt,A. 1767
Lyman,D.E. 339

Ma,Genxiang 1045,1051,
1057,1063
Ma,Hengli 979
Madureira,C.M.N. 1241
Maeda,M. 497,651,663,675
Maeda,S. 345
Maeda,Y. 485
Majima,H. 1481
Marcozzi,G. 1815
Markov,V.S. 261
Marr,R. 37,1121,1339,
1589,1619,1683,1797
Martinez,M. 147
Maryutina,T.A. 451
Mas,C. 835
Masai,M. 1625
Masana,A. 1505,1511
Mashkin,A.N. 759
Masson,M. 579
Masuda,Y. 231
Masuoka,H. 1671,1719
Matsuba,Y. 1637
Matsuda,M. 141
Matsuda,T. 931
Matsui,M. 309
Matsui,T. 497
Matsumoto,M. 1613,1881,
1887
Matsumoto,S. 615
Matsumoto,Y. 1649
Matsunaga,H. 937
Matsushita,T. 1033
Matsuyama,H. 1803
Mehandjiev,M.M. 237
Mehandjiev,M.R. 237
Merchuk,J.C. 1307
Messemaekers,C. 1265
Mežaraups,G. 533
Mihaylov,I. 787
Mikheeva,M.N. 1493
Miki,R. 463
Mills,A.L. 1289
Min,Yi 473
Miquel,P. 747
Miralles,N. 147,159
Mishima,K. 177
Mitsuiki,M. 1707
Miura,N. 657
Miyake,Y. 777
Miyake,Y. 823,1803
Miyauchi,T. 1223
Mizuta,M. 153
Mohite,B.S. 1093
Moore,I.P.T. 1869
Mori,K. 1075
Mori,Y. 1579,1863
Morita,Y. 585
Motomizu,S. 485
Muhammed,M. 1511
Mühl,P. 1187
Mukai,Y. 1719
Müller,U. 1301
Muñoz,M. 1505,1511
Murai,R. 111
Murai,T. 1625
Murayama,W. 717
Murphy,A. 1151
Musikas,C. 297,417
Myasoyedov,B.F. 1493
Myers,P.E. 621

Nabeshima,M. 687
Nagahama,K. 141,1701
Nagai,T. 1193
Nagasaki,H. 1719
Nagatani,M. 177
Naka,Y. 429
Nakada,K. 1821
Nakagawa,K. 315
Nakamura,K. 1625
Nakamura,M. 1833
Nakamura,S. 1677
Nakashima,Y. 1827
Nakashio,F. 805,829,1459,
1613,1845,1881
Nakata,Y. 823
Nakayama,E. 81
Nakayama,H. 111
Nam,N.T.P. 711
Nara,H. 1803
Narita,S. 669
Nash,K.L. 357

Navratil,J.D. 1151,1631
Nedungadi,K. 1259
Nemoto,S. 567,639
Nerosin,N.A. 573
Neuman,R.D. 75,165,195,201
Neumoev,N.V. 261,573
Nienow,A.W. 1869
Nikiforov,A.S. 183,261,753
Nikolotova,Z.J. 183
Nishiki,T. 1761
Nishimura,S. 1163,1169
Nishioka,H. 463
Nishiyama,S. 1625
Nishizawa,S. 841,1549
Nitsch,W. 847
Nofal,M. 87
Noirot,P.A. 135
Novikov,A.P. 1493

O'Shima,E. 429
Oda,M. 829
Ogata,T. 315
Ohgaki,K. 1689
Ohki,A. 345
Ohtake,T. 1613,1881,1887
Ohyama,Y. 111
Okamoto,F. 399
Okano,Y. 841
Okazaki,S. 1487
Omori,E. 657
Onda,N. 735
Ooka,N. 457
Ortiz,M.I. 1535,1539,1585
Oshima,M. 485
Osseo-Asare,K. 117
Ouchi,M. 363
Ozawa,M. 603,681

Pareau,D. 1009,1567
Park,Hyun-Soo 645,1607
Park,Sang Joon 201
Partridge,B.A. 621
Pashkov,G.L. 1187
Pasquiou,J.Y. 597
Patil,J.M. 1093
Pavlovich,V.B. 573
Penner,L.R. 423
Perez de Ortiz,E.S. 117, 1277
Perez Trujillo,J.P. 515
Petrich,G. 555,561
Pfammatter,N. 1755
Pfeff,M. 1301
Pfüller,P. 435
Philippe,M. 579
Phillips,C. 549
Plucinski,P. 847
Ponomareva,E.I. 949,955
Poole,L.J. 1791
Pratt,H.R.C. 1363
Preitschopf,W. 1619
Preston,J.S. 883,1081
Prochaska,K. 817
Pröll,Th. 1301
Puajindanetr,S. 1601

Qin,Wei 1381
Quan,C. 381

Rakib,M. 411
Rauscher,H. 1271
Reeve,R.N. 1393
Regueiras,P.F.R. 1241
Reisinger,H. 1797
Renard,E.V. 573
Resetarits,M.R. 1327
Rhein,H.B. 267
Rickert,P.G. 357
Ritcey,G.M. 1069
Rittner,S. 479,1809
Robinson,K.S. 1345
Rogowski,J. 491
Römer,J. 555
Rommel,W. 1423
Rong,Guo 1773
Rozen,A.M. 99,183,255, 261,753
Rushton,A. 741
Russel,J.H. 423

Saeed,M.T. 1277
Saeki,N. 405
Saitoh,T. 315
Sakagami,M. 497
Sakai,T. 1719
Sakamoto,Y. 805
Salazar,E. 1585
Salvadó,V. 171,1505,1511
Sami,T.M. 895
Sannen,L. 967
Sano,M. 1163,1169
Saoud,M. 135
Sarathy,P.K. 165
Sasaki,K. 705,783,1887
Sastre,A. 147,159
Sato,I. 1761
Sato,K. 913,985,991,997
Sato,M. 699,973,1435
Sato,T. 913,985,991,997
Savastano,C.A. 117
Savin,A.V. 393
Schaap,J.E. 1713
Schmidt,H. 1301
Schmieder,H. 555,633
Schön,J. 555,633
Schügerl,K. 267,1217,1523, 1561,1785,1905

Schwartz,J.M. 1731
Sekido,E. 231
Sekine,T. 111,123,213
Selmanchuk,N.N. 527
Sembira,A. 1307
Semmens,M.J. 1737
Sergeev,V.V. 1187
Shehata,F. 219
Shelley,P. 381
Shen,Zhong-yao 1773
Shi,Yajun 877,1573,1655
Shibata,J. 1163,1169
Shibayama,R. 1193
Shieh,Mu-Chang 693
Shimizu,M. 405,1487,1643, 1875
Shimizu,R. 567
Shimizu,T. 1695
Shin,Young-Joon 645
Shioya,S. 1779
Shishkin,S.V. 509
Shishkina,T.V. 509
Shkarin,P.Yu. 261
Shklyar,L.I. 573
Shono,A. 973
Shono,T. 1033
Shriadah,M.M.A. 1549
Simon,A. 1661
Sinegribova,O.A. 393
Skålberg,M. 491,1387
Skarnemark,G. 491,1387
Slater,M.J. 1265
Smetanin,E.Ya. 573
Smit,J.J. 1475
Sohrabi,M. 859
Sokolov,N.M. 1911
Spivakov,B.Ya. 451
Stambouli,M. 411
Starr,J.N. 1791
Steiner,L. 1175,1259
Stenns,M. 267
Stenström,S. 943
Stevens,G.W. 1363
Stieglitz,L. 651
Strzelbicka,B. 1517,1523
Strzelbicki,J. 1517,1523, 1561
Su,Yuan-Fu 243,387,1351, 1573
Suga,K. 1779
Sugai,H. 681
Sugawara,M. 1549,1555
Suglobov,D.N. 279
Suh,In-Suk 1607
Sukhanov,P.T. 527
Sun,D. 1151
Sun,Ducheng 1039
Suyitno 663
Suzuka,R. 1767
Suzuki,A. 663
Suzuki,H. 1707
Suzuki,N. 895
Suzuki,T. 823,1701
Suzuki,T.M. 937
Suzuki,Y. 189
Szilassy,I. 1139
Szymanowski,J. 765,817

Tachikawa,E. 225
Tachimori,S. 699,717
Taguchi,S. 503
Takagi,M. 345
Takahashi,K. 627,783,1357, 1839
Takahashi,T. 189,1637
Takeda,H. 567,639
Takeishi,H. 717
Takeuchi,H. 1357,1839
Takeuchi,K. 1821
Takishima,S. 1671,1719
Taldykina,S.N. 527
Tamada,J.A. 1791
Tamhina,B. 1027
Tamura,N. 603
Tanahashi,S. 1839
Tanaka,C. 681,687
Tanaka,H. 429,1857
Tanaka,M. 1033,1157
Tananaev,J.G. 183
Tani,S. 585
Tanigaki,M. 1579
Tarasova,E.G. 955
Tavlarides,L.L. 1247
Tazaki,M. 351
Temos,J. 1363
Terada,K. 457
Teramoto,M. 823,1803
Tetzlaff,H. 479,1809
Thakur,N.V. 1003
Tian,Heng-Shui 387
Tochiyama,O. 669
Togashi,A. 399
Tominaga,T. 93
Tomita,A. 799
Trautmann,N. 491
Trifonov,Yu.I. 279
Tsai,Teh-Hua 1529
Tsouris,C. 1247
Tsuboi,I. 1199
Tsuge,N. 1701
Tsukada,T. 627
Tsuruya,S. 1625

Uchiyama,G. 651,675
Ueda,Y. 567
Ueoka,R. 1649
Uesugi,K. 463
Ulbrich,M. 1589
Umetani,S. 309
Umezawa,K. 1549

Umezawa,Y. 1549,1555
Urtiaga,A.M. 1539
Urushiyama,S. 405,1875
Usuda,S. 699,717

Vadasdi,K. 1139
Valiente,M. 171,515,1505,1511
Van Rompay,P. 1265
Vatskova,V.G. 1911
Villaescusa,I. 171
Vlasov,V.S. 255
Vliegen,J. 1115
Vogelpohl,A. 129
Von Ammon,R. 835
Von Frieling,P. 1905

Wada,F. 931
Wakamatsu,S. 699
Wakui,Y. 937
Wang,Dianxia 1453
Wang,Jiading 1381
Wang,Ning-He 1671
Wang,W.-H. 1767,1851
Wang,Xiang-Tian 387
Wang,Zhonghui 1045
Warren,K.W. 1211,1417
Watahiki,M. 735
Watanabe,H. 315
Watanabe,T. 93
Watarai,H. 783
Wei,Xiufang 591
Weng,Shifu 793
Wicksramasinghe,S.R. 1737
Wolf,D. 1307
Wozniak,M. 135
Wu,Jinguang 165,195,793
Wu,Peiqiang 853
Wu,Qiuzhi 375

Xing,Miaolin 1175
Xu,Guang-Xian 105,1295

Yamada,E. 81
Yamada,H. 153
Yamada,Y. 93,1863
Yamaguchi,M. 1375,1441,1833
Yamamoto,H. 1695
Yamamoto,R. 603
Yamamoto,S. 1689
Yamamoto,T. 639,1199
Yamana,H. 657,705,735
Yamasaki,A. 189
Yamasaki,N. 1827
Yamashoji,Y. 1033
Yamazaki,Y. 315
Yan,Chun-Hua 1295
Yan,Nian-Xi 1573
Yang,Jiaoyong 1205
Yang,Liucheng 591
Yang,Xuexian 591
Yasu,S. 871
Yasukawa,R. 351
Ye,Guiqin 1369
Ye,Guoan 591
Ye,Yuxing 591
Yokoyama,H. 627
Yoneyama,K. 1327
Yoo,Jae-Hyung 645,1607
Yoshida,Z. 225
Yoshinari,T. 735
Yoshiyasu,S. 1375
Yoshizuka,K. 351,805,829,931
Yotsuyanagi,T. 49,1725
Young,J.W. 327
Yu,Shuqiu 793,853
Yu,Zhi-Jian 195
Yuan,Chengye 321,979
Yuan,Shengang 321
Yue,Santang 811
Yushmanov,V.E. 261

Zagorodnyaya,A.N. 955
Zakareia,N. 87
Zarnegar,B.M. 339
Zelentsova,L.V. 1187
Zhan,Huifang 1205
Zhang,Baoqing 1369
Zhao,Hugen 591
Zhou,Nai-Fu 75,165,195
Zhou,Zukang 853
Zhu,Lin 273
Zhu,Shenlin 1369
Zhuravleva,E.L. 509
Zi,Xiaohong 1045
Zilberman,B.Ya. 285,759
Zolotov,Yu.A. 451
Zwiefelhofer,U. 1661